VDI Wissensforum

VDI-Berichte 2354



Dritev

19th International VDI Congress

Dritev – Drivetrain for Vehicles

July 10 and 11, 2019, Bonn

Main topics:

- OEM solutions for the electrified powertrain
- Different approaches of how to increase power density
- Innovative 4-wheel-drive systems
- New ways to achieve NVH reduction
- Multi-gear transmissions in electrified powertrains
- Development optimization by improving simulation methods

https://doi.org/10.51202/9783181023549 - Generiert durch IP 216.73.216.36, am 19.01.2026, 02:19:31. © Urheberrechtlich geschützter Inhalt. Ohne gesonderte Erlaubnis ist jede urheberrechtliche Nutzung untersagt, insbesondere die Nutzung des Inhalts im Zusammenhang mit, für oder in KI-Systemen, KI-Modellen oder Generativen Sprachmodellen.

https://doi.org/10.51202/9783161023549 - Generiert durch IP 216.73.216.36, am 19.01.2026, 02:19:31. © Urheberrechtlich geschützter Inhalt. Ohne gesonderte Erlaubnis ist jede urheberrechtliche Nutzung untersagt, insbesondere die Nutzung des Inhalts im Zusammenhang mit, für oder in KI-Systemen, KI-Modellen oder Generativen Sprachmodellen.

VDI-BERICHTE
Herausgeber:
VDI Wissensforum GmbH

https://doi.org/10.51202/9783181023549 - Generiert durch IP 216.73.216.36, am 19.01.2026, 02:19:31. © Urheberrechtlich geschützter Inhalt. Ohne gesonderte Erlaubnis ist jede urheberrechtliche Nutzung untersagt, insbesondere die Nutzung des Inhalts im Zusammenhang mit, für oder in KI-Systemen, KI-Modellen oder Generativen Sprachmodellen.

Bibliographische Information der Deutschen Nationalbibliothek
Die Deutsche Nationalbibliothek verzeichnet diese Publikation in der Deutschen Nationalbibliographie; detaillierte bibliographische Daten sind im Internet unter www.dnb.de abrufbar.

Bibliographic information published by the Deutsche Nationalbibliothek (German National Library)
The Deutsche Nationalbibliothek lists this publication in the Deutsche Nationalbibliographie (German National Bibliography); detailed bibliographic data is available via Internet at www.dnb.de.

© VDI Verlag GmbH · Düsseldorf 2019
Alle Rechte vorbehalten, auch das des Nachdruckes, der Wiedergabe (Photokopie, Mikrokopie), der Speicherung in Datenverarbeitungsanlagen und der Übersetzung, auszugsweise oder vollständig.

Der VDI-Bericht, der die Vorträge der Tagung enthält, erscheint als nichtredigierter Manuskriptdruck.
Die einzelnen Beiträge geben die auf persönlichen Erkenntnissen beruhenden Ansichten und Erfahrungen der jeweiligen Vortragenden bzw. Autoren wieder. Printed in Germany.

ISSN 0083-5560
ISBN 978-3-18-092354-3

https://doi.org/10.51202/9783181023549 - Generiert durch IP 216.73.216.36, am 19.01.2026, 02:19:31. © Urheberrechtlich geschützter Inhalt. Ohne gesonderte Erlaubnis ist jede urheberrechtliche Nutzung untersagt, insbesondere die Nutzung des Inhalts im Zusammenhang mit, für oder in KI-Systemen, KI-Modellen oder Generativen Sprachmodellen.

Content

Hybrid

Advanced development of dedicated hybrid concepts – Systematic search for optimal powertrain concepts 1
M. Horn, F. Kutter, B. Vahlensieck, ZF Friedrichshafen AG, Friedrichshafen

Evaluation of the dedicated range-extender transmission powertrain concept DE-REX regarding efficiency, costs and complexity – Comparative assessment of electric and hybrid powertrain configurations based on test bench measurements. 21
A. Viehmann, J.-E. Schleiffer, S. Rinderknecht, Institute for Mechatronic Systems in Mechanical Engineering (IMS), Technical University Darmstadt

Hybridized manual transmission – Opportunities and challenges of mild hybridization 49
K. Baron, C. Rübsam, Opel Automobile GmbH, Rüsselsheim;
M. Werra, F. Küçükay, Institute of Automotive Engineering, Technical University Braunschweig

Low-cost DCT for emerging markets incl. 48 V hybridization 67
G. Hellenbroich, FEV Europe GmbH, Aachen

Modular Systems

Modular system 8G-DCT with all-wheel drive 79
A. Harsch, G. Clausen, Daimler AG, Stuttgart;
A. Rink, Daimler AG, Sindelfingen

7DCT/HDT400 – New fuel-efficient FWD DCT and hybrid transmission for up to 400 Nm 95
L. Herdle, Magna Powertrain, Untergruppenbach

Innovative 8HP modular design kit for conventional, MHEV and PHEV transmissions. 103
A. Locher, M. Ebenhoch, P. Gutmann, ZF Friedrichshafen AG, Friedrichshafen

https://doi.org/10.51202/9783161023549 - Generiert durch IP 216.73.216.36, am 19.01.2026, 02:19:31. © Urheberrechtlich geschützter Inhalt. Ohne gesonderte Erlaubnis ist jede urheberrechtliche Nutzung untersagt, insbesondere die Nutzung des Inhalts im Zusammenhang mit, für oder in KI-Systemen, KI-Modellen oder Generativen Sprachmodellen.

Simulation

Artificial intelligence in transmission control – Clutch engagement with reinforcement learning 113
A. Lampe, R. Serway, L. Große Siestrup, IAV GmbH, Berlin;
C. Gühmann, Technical University Berlin

Virtual lubrication analysis – Simulation of oil flow in gearboxes using a novel lagrangian approach 133
R. Gat, M.Ehlen, AVL Thermal and HVAC, Munich

Development of an optimization framework for the comparative evaluation of the ecoimpact of powertrain concepts 137
A. Esser, J.-E. Schleiffer, T. Eichenlaub, S. Rinderknecht,
Technical University Darmstadt

Holistic design approach for electric drives. 163
P. Fietkau, N. Lamparsky, M. Felbermaier, A. Fröhlcke, T. Conze,
Dr. Ing. h.c. F. Porsche AG, Weissach

Increasing Power Density

Potential of lightweight construction and component properties of joined spur gears. 179
C. Leonhardt, M. Otto, K. Stahl, Gear Research Centre, Technical University of Munich

Solutions for increased power density at shifting clutches 197
H. Merkel, BorgWarner Transmission Systems, Ketsch

ecoLIFE^3: An approach for a resource-efficient dimensioning of vehicle components based on a holistic optimization with real life load data –paradigm shift in transmission engineering based on big data 213
S. Foulard, COMPREDICT GmbH, Darmstadt;
S. Rinderknecht, F. Braun, P. Jardin, Institute for Mechatronics Systems in
Mechanical Engineering, Technical University Darmstadt

https://doi.org/10.51202/9783181023549 - Generiert durch IP 216.73.216.36, am 19.01.2026, 02:19:31. © Urheberrechtlich geschützter Inhalt. Ohne gesonderte Erlaubnis ist jede urheberrechtliche Nutzung untersagt, insbesondere die Nutzung des Inhalts im Zusammenhang mit, für oder in KI-Systemen, KI-Modellen oder Generativen Sprachmodellen.

Topology Optimization

1, 2 or 3 – how much it would be? Evaluating the need of multispeed electric drives coming from different perspectives 227
K. von Rueden, C. Danzer, J. Liebold, T. Mueller, T. Hirschbeck, IAV GmbH, Berlin, Gaimersheim, Gifhorn and Chemnitz / Stollberg

Optimization of multi-motor electric drive systems – What is the optimum combination in terms of efficiency and cost? 255
P. Janssen, R. Keizer, FEV Europe GmbH;
T. Rosen, FEV Consulting GmbH, Aachen

Potentials for improving the system behaviour of highspeed clutches for BEV using optimal transmission springs. 265
H. Gürbüz, S. Ott, A. Albers, Mubea Tellerfedern GmbH, Daaden,
IPEK – Institut für Produktentwicklung, Karlsruhe

Electrical Drive Concepts of the Future I

Efficiency of electric axle drive systems – Potential of multi-speed-drives 279
S. Demmerer, ZF Friedrichshafen AG, Friedrichshafen

Integrated eDrive system for various performance classes 287
T. Pullen, GKN ePowertrain, Driveline International GmbH, Technology Centre Lohmar, Lohmar

Next generation of 48V HEV. 295
W. Wenzel, M. Eglinger, BorgWarner Ludwigsburg GmbH, Ludwigsburg;
M. Li, C. Sieg, J. Hengst, F. Küçükay, Institute of Automotive Engineering,
Technical University Braunschweig

https://doi.org/10.51202/9783181023549 - Generiert durch IP 216.73.216.36, am 19.01.2026, 02:19:31. © Urheberrechtlich geschützter Inhalt. Ohne gesonderte Erlaubnis ist jede urheberrechtliche Nutzung untersagt, insbesondere die Nutzung des Inhalts im Zusammenhang mit, für oder in KI-Systemen, KI-Modellen oder Generativen Sprachmodellen.

NVH

Minimize torsional vibrations – Full isolation if necessary 313
A. Kooy, R. Seebacher, Schaeffler Automotive Buehl GmbH & Co. KG, Bühl

Effective acoustic development of electrified powertrains – Combination of simulation and evaluation methods 329
C. Möser, T. Märkle, K. Hornung, AUDI AG, Ingolstadt

NVH-challenges and solution approaches in electric drive development from the supplier's view 349
C. Dassler, M. Kurch, M. Nichols, Schaeffler Technologies AG & Co. KG, Herzogenaurach

Transmission system footprint related to fatigue, efficiency and NVH 367
A. Grunwald, GKN Driveline International GmbH, ePowertrain Technology Centre Lohmar

Transmissions Concepts

Development of a new next-generation CVT for small cars 385
S. Kurokawa, M. Kunihisa, JATCO Ltd, Atsugi, Japan;
Y. Oyama, Nissan Motor Co., Ltd, Atsugi, Japan

New next generation eight-speed automatic transmission for FWD vehicles 397
C. Kim, HYUNDAI TRANSYS, Hwaseong, Korea

Efficient 6-speed manual transmission for modern downspeeding solutions 411
H. Göbbels, S. Scholz, S. Volkmer, Volkswagen AG, Wolfsburg

https://doi.org/10.51202/9783161023549 - Generiert durch IP 216.73.216.36, am 19.01.2026, 02:19:31. © Urheberrechtlich geschützter Inhalt. Ohne gesonderte Erlaubnis ist jede urheberrechtliche Nutzung untersagt, insbesondere die Nutzung des Inhalts im Zusammenhang mit, für oder in KI-Systemen, KI-Modellen oder Generativen Sprachmodellen.

Components

Efficiency improvements in transmissions using new latching technologies in clutch & hydraulic actuation systems 427
A. Moser, F. Brezger, BorgWarner Drivetrain Engineering GmbH, Ketsch

Flexible oil management for dual-clutch transmissions. 447
M. Bahne, A. Wiesebrock, Magna Powertrain Transmission Systems, Untergruppenbach

Single vs. multi-cone synchronizers with carbon friction lining – A comparison of load limits and deterioration behavior 455
U. Stockinger, H. Pflaum, K. Stahl, FZG – Gear Research Centre (FZG), Technical University of Munich

Triple wet clutch module and actuation system, shift cylinders and park lock for modern hybrid transmissions – Architecture and technical description of a triple wet clutch unit and the related active and passive clutch and shift actuation system 471
O. Simon, Valeo Transmissions, Amiens, France;
W. Heubner, Valeo Actuation Systems, Ebern

Four-wheel

New all-wheel drive systems in Mercedes-Benz SUVs. 483
S. Stöhr, R. Koesling, V. Marx, Daimler AG, Stuttgart

Development of new hybrid AWD system for the SUV segment 501
K. Hasegawa, D. Kosaka, S. Shimizu, K. Kawabata, H. Tsukashima, Toyota Motor Corporation, Aichi, Japan

OEM Concepts for Electrical Powertrain

Volkswagen's electric drivetrains of the new modular e-drive kit (MEB) 515
P. Lück, K. Bennewitz, J. Tousen, Volkswagen AG, Wolfsburg

Volvo Cars modular electric axle drive 531
M. Jörgensson, C. Wolrath, J. Hallnéus, Volvo Car Group, Göteborg, Sweden

https://doi.org/10.51202/9783161023549 - Generiert durch IP 216.73.216.36, am 19.01.2026, 02:19:31. © Urheberrechtlich geschützter Inhalt. Ohne gesonderte Erlaubnis ist jede urheberrechtliche Nutzung untersagt, insbesondere die Nutzung des Inhalts im Zusammenhang mit, für oder in KI-Systemen, KI-Modellen oder Generativen Sprachmodellen.

Electrical Drive Concepts of the Future II

Innovative transmission concept for hyper-high-speed electromechanical powertrains 541
D. Schweigert, M. Mileti, B. Morhard, M. Sedlmair, M. Fromberger,
M. Otto, T. Lohner, K. Stahl, Gear Research Center (FZG), Technical University of Munich

GKN's ActiveConnect AWD system as an energy-efficient solution for electrified vehicles . . . 555
C. Schmahl, M. Höck, D. Ressin, M. Kesseler, GKN ePowertrain, Lohmar

Schaeffler eAxle family – future solutions for the electric drivetrain 567
A. Kinigadner, T. Biermann, Schaeffler Technologies AG & Co. KG, Herzogenaurach

https://doi.org/10.51202/9783161023549 - Generiert durch IP 216.73.216.36, am 19.01.2026, 02:19:31. © Urheberrechtlich geschützter Inhalt. Ohne gesonderte Erlaubnis ist jede urheberrechtliche Nutzung untersagt, insbesondere die Nutzung des Inhalts im Zusammenhang mit, für oder in KI-Systemen, KI-Modellen oder Generativen Sprachmodellen.

Many thanks to the Gold-Sponsors of the Congress:



www.iot.bosch.com



www.castrol.com/de



www.gkndriveline.com



www.magna.com



www.daimler.de



www.zf.com

https://doi.org/10.51202/9783161023549 - Generiert durch IP 216.73.216.36, am 19.01.2026, 02:19:31. © Urheberrechtlich geschützter Inhalt. Ohne gesonderte Erlaubnis ist jede urheberrechtliche Nutzung untersagt, insbesondere die Nutzung des Inhalts im Zusammenhang mit, für oder in KI-Systemen, KI-Modellen oder Generativen Sprachmodellen.

https://doi.org/10.51202/9783161023549 - Generiert durch IP 216.73.216.36, am 19.01.2026, 02:19:31. © Urheberrechtlich geschützter Inhalt. Ohne gesonderte Erlaubnis ist jede urheberrechtliche Nutzung untersagt, insbesondere die Nutzung des Inhalts im Zusammenhang mit, für oder in KI-Systemen, KI-Modellen oder Generativen Sprachmodellen.

Advanced Development of Dedicated Hybrid Concepts

Systematic search for optimal powertrain concepts

Dr.-Ing. **Matthias Horn**, Dipl.-Ing. **Fabian Kutter**,
Dr.-Ing. **Bernd Vahlensieck**, ZF Friedrichshafen AG, Friedrichshafen

Zusammenfassung

Im vorliegenden Beitrag werden die Marktchancen und Motivatoren für maßgeschneiderte Hybridantriebe erläutert und darauf aufbauend die technischen Ansätze hinter sogenannten dedizierten Hybridkonzepten beschrieben. Es erfolgt der Versuch einer Gruppierung verschiedener Ausprägungen von maßgeschneiderten Hybridkonzepten entsprechend ihrer E-Drive-Struktur und Radsatz-Architektur. Die bei den verschiedenen Typen von maßgeschneiderten hybriden Antriebskonzepten realisierbaren Funktionen zum Anfahren und Lastschalten werden im Detail diskutiert. Abschließend stellen die Autoren die systematische Konzeptsuche für ein exemplarisches Anforderungsszenario vor. Der Fokus liegt hierbei unter anderem auf den Konsequenzen, die sich aus den Bauraumrestriktionen bei einem im Vorderwagen quer zur Fahrtrichtung installierten hybriden Antriebssystem mit mehreren elektrischen Maschinen ergeben.

Abstract

The following paper discusses market potential and motivation for tailor-made hybrid powertrains. Technical ideas behind these dedicated hybrid concepts are described. It is shown an attempt to cluster different types of tailor-made hybrid concepts according to their e-drive structure and gear set architecture. The technical features of these different types of tailor-made hybrid concepts for vehicle launch and power shift are explained in detail. Finally the authors show the methods of systematically searching and evaluating concepts for an exemplary requirement set. They focus on the consequences of package restrictions for transversal installed hybrid powertrain systems with multiple electric machines.

https://doi.org/10.51202/9783181023549 - Generiert durch IP 216.73.216.36, am 19.01.2026, 02:19:31. © Urheberrechtlich geschützter Inhalt. Ohne gesonderte Erlaubnis ist jede urheberrechtliche Nutzung untersagt, insbesondere die Nutzung des Inhalts im Zusammenhang mit, für oder in KI-Systemen, KI-Modellen oder Generativen Sprachmodellen.

Motivation for tailor-made hybrid powertrains

Future CO_2 restrictions for vehicles show a clear trend towards 95 g CO_2/km and less in several regions of the world for 2020+. EU already set a goal to cut CO_2 emissions by 35 % for 2030 from 2021 values. Especially for large and heavy passenger cars with high driving resistances these targets can't be reached without electrification of the driveline. That's why many new battery electric and hybrid vehicles will be introduced into the market.

The growing variety of vehicles with electrified powertrain will soon be reflected in sales figures. Figure 1 shows predicted compound annual growth rates (CAGR) for vehicles with different electrified powertrain concepts. Due to these growth rates in 2030 approx. 14 % of worldwide sold vehicles will be battery electric and 32 % will have hybrid powertrains.

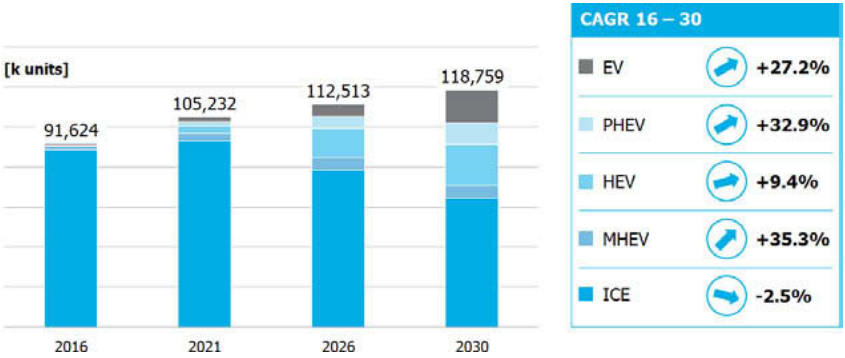


Fig. 1: Market forecast for global powertrain electrification of passenger cars (2017 data)

In the group of vehicles with hybrid powertrains the relevance of different degrees and types of hybridization is still very uncertain. The currently unclear development of the market shares makes planning for original equipment manufacturers (OEM) and suppliers difficult. To maintain sufficient flexibility, a modular approach with compatible and replaceable transmission systems seems to be the best way for the beginning of the 2020 years. Transmission kits allow appropriate degrees of electrification for different sales scenarios. [1]

Because of the increasing number of metropolitan areas with local emission-free driving concepts, end of next decade, the focus could shift more towards electric driving. Driving with internal combustion engines (ICE) will become less attractive and only implied for long distance

https://doi.org/10.51202/9783181023549 - Generiert durch IP 216.73.216.36, am 19.01.2026, 02:19:31. © Urheberrechtlich geschützter Inhalt. Ohne gesonderte Erlaubnis ist jede urheberrechtliche Nutzung untersagt, insbesondere die Nutzung des Inhalts im Zusammenhang mit, für oder in KI-Systemen, KI-Modellen oder Generativen Sprachmodellen.

travel with high power. For this time, dedicated hybrid concepts for full and plug-in hybrid vehicles have to be considered. They are led by the idea of a tailor-made hybrid transmission, use the electric machine (EM) for basic transmission functions and pursue following four goals: lower mechanical complexity, increased efficiency, reduced costs and favorable package.

Dedicated hybrid concepts satisfy especially the market demand of the electrification of multi-purpose cars for single vehicle households. They allow efficient electrical everyday commuting and driving in local emission-free zones with relatively small electric energy storages and without range anxiety. Furthermore they support the efficient use of resources and allow an intelligent end-customer orientated implementation of electro mobility.

Idea and classification of tailor-made hybrid powertrains

In order to reach the above mentioned targets of reduced mechanical complexity, increased efficiency, minimized costs and optimized package a shift of functionality has to be performed. Typically transmission gear set functions must be transferred to the electric drive unit (e-drive) of the powertrain. Dedicated hybrid concepts use their e-drive not only for electric driving but also for basic transmission functions. Pure dedicated hybrid concepts try to fulfill individual requirement sets without friction shift elements, mechanical vehicle launch element and mechanical reverse gear. Beyond that many dedicated hybrid concepts offer a reduced number of mechanical gears for ICE and hybrid driving compared to modular hybrids with an EM at the transmission input [2]. As a consequence, these dedicated hybrid concepts have a considerably reduced functionality without a fully operating e-drive. Removing the electric machine causes a loss of basic transmission functionality and there is typically no modularity with non-hybrid and mild-hybrid concept variants.

Dedicated hybrid concepts can be clustered according to different criteria. One approach – which seems to be very favorable for dedicated hybrid concepts – puts the e-drive into the centre. The first differentiating criterion of this approach is the e-drive structure represented by the number of installed electric machines. The second criterion bases on the integration of the EM into the gear set. Depending on the linking element between electric machine and gear set and the gear set architecture individual characteristic electric driving modes can be realized. For a two-wheel drive vehicle four types of dedicated hybrid concepts result. Exemplary representative functional layouts of these types are shown in figure 2.

https://doi.org/10.51202/9783181023549 - Generiert durch IP 216.73.216.36, am 19.01.2026, 02:19:31. © Urheberrechtlich geschützter Inhalt. Ohne gesonderte Erlaubnis ist jede urheberrechtliche Nutzung untersagt, insbesondere die Nutzung des Inhalts im Zusammenhang mit, für oder in KI-Systemen, KI-Modellen oder Generativen Sprachmodellen.

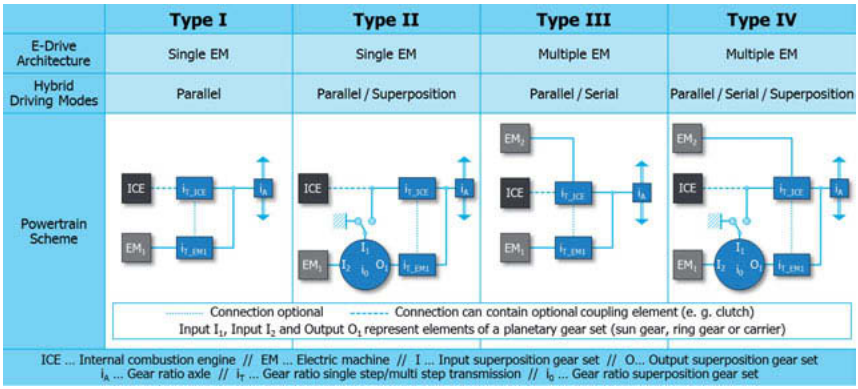


Fig. 2: Powertrain schemes for different types of dedicated hybrid concepts for two-wheel drive vehicles

The main differentiating element of dedicated hybrid concepts Type I and Type III compared to dedicated hybrid concepts of Type II and Type IV is the planetary gear set for the super positioning of rotational speeds. This planetary gear set must be directly or indirectly linked via its two input elements (sun gear, planetary carrier or ring gear) to at least two of the propulsion aggregates (ICE, EM1 or EM2). When this structural requirement is – temporarily or permanently – fulfilled the rotational speed of the planetary gear set output can be adjusted continuously variable. This functionality can be used for example for hybrid vehicle launch. The single phases of such an electro-dynamic launch (EDA) are shown in figure 3.

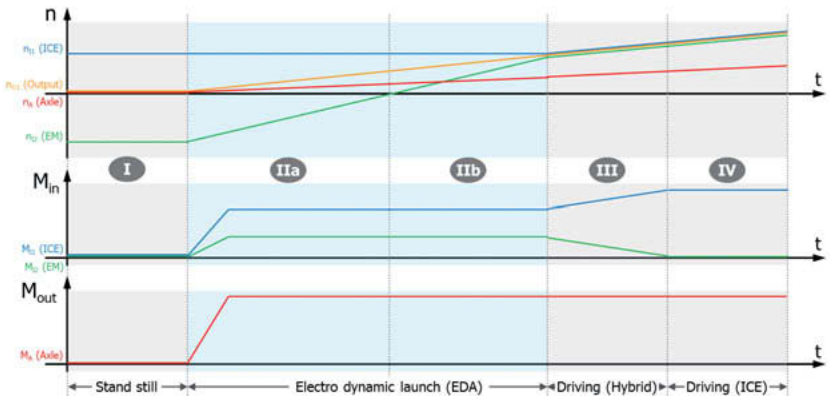


Fig. 3: Phases of a vehicle launch in electro-dynamic mode (EDA)

https://doi.org/10.51202/9783181023549 - Generiert durch IP 216.73.216.36, am 19.01.2026, 02:19:31. © Urheberrechtlich geschützter Inhalt. Ohne gesonderte Erlaubnis ist jede urheberrechtliche Nutzung untersagt, insbesondere die Nutzung des Inhalts im Zusammenhang mit, für oder in KI-Systemen, KI-Modellen oder Generativen Sprachmodellen.

The represented chart contains the rotational speeds (n_{I1}(ICE), n_{I2}(EM)) and torques (M_{I1}(ICE), M_{I2}(EM)) at the two inputs shafts of the super positioning planetary gear set and additionally the rotational speed (n_{O1}) and torque (M_{O1}) at the output shaft of this gear set. The resulting rotational speed (n_A(Axle)) and torque (M_A(Axle)) at the wheels are also shown.

During Phase I the vehicle stands still. The axle drive as well as the output shaft of the super positioning planetary gear set does not rotate. The ICE rotates with idle speed, thus the EM has to rotate in opposite direction. It operates in generator mode. At the beginning of Phase IIa the rotational speed of the electric machine is reduced and as a result the vehicle launches. The rotational speed of the EM reduces till the EM has to change the direction of rotational speed. At this moment generator mode ends. In Phase IIb the EM operates in motor mode. At the end of Phase IIb all three elements of the super positioning gear set have the same rotational speed. The vehicle launch is completed. The clutch shift element of the vehicle launch ending speed in the ICE associated part of the transmission can be closed. In Phase III the vehicle drives in parallel hybrid mode, which means ICE torque and EM torque can be changed without interdependence. After the complete reduction of the torque at the EM a mode change into ICE driving is possible (Phase IV).

The maximum performance of the EDA mode primarily depends on the performance of ICE and EM as well as the following gear ratios: EM to ICE, EM to transmission output and ICE to transmission output. Unlike electro-motoric launch (EMA) the EM temporarily runs as a generator during electro-dynamic launch (EDA), too. This allows a vehicle launch with very low SOC or even with empty battery. [2, 3]

The described super positioning of the rotational speeds can also be used for creeping with very low speed (short and long distances) and charging the electric energy storage (at standstill and at low speed).

An additional use case is electro-dynamic shifting (EDS). In this case the super positioning structure is used to shift from one driving mode into another driving mode without total traction force interruption. The phases of such an exemplary electrically supported upshift from ICE speed n to ICE speed n+1 are shown in figure 4.

https://doi.org/10.51202/9783181023549 - Generiert durch IP 216.73.216.36, am 19.01.2026, 02:19:31. © Urheberrechtlich geschützter Inhalt. Ohne gesonderte Erlaubnis ist jede urheberrechtliche Nutzung untersagt, insbesondere die Nutzung des Inhalts im Zusammenhang mit, für oder in KI-Systemen, KI-Modellen oder Generativen Sprachmodellen.

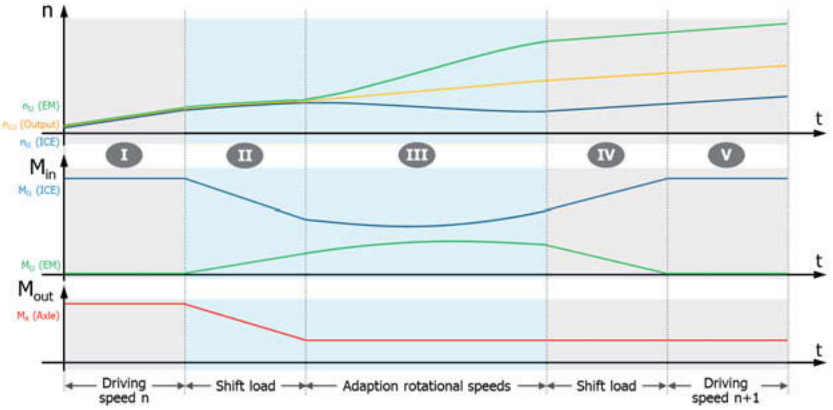


Fig. 4: Phases of an electro-dynamic power shift (EDS)

In phase I the vehicles accelerates in parallel hybrid mode. At the end of Phase I the torque of the ICE is reduced and simultaneously the torque of the electric machine is raised. As a consequence the power flow on the super positioning gear set changes. The loads at the loaded shift elements of the active gear n reduce in the ICE associated part of the transmission. At the end of Phase II the locked shift elements in the ICE associated transmission are without load. The necessary change of the locked shift elements for the required shift from ICE gear n to ICE gear n+1 can be performed while ICE and EM adapt the necessary rotational speeds and torques simultaneously. After the change of the locked shift elements load is shifted back to the ICE associated transmission and the ride can be continued in gear n+1 (Phase V).

The main functional differences of the above introduced four types of dedicated hybrid concepts are summarized in figure 5. Both the installation of a second electric machine as well as the integration of a planetary gear set for the superposition of rotational speeds create more functional freedom in terms of realizing basic transmission functions with help of the e-drive. From a functional point of view the combination of both measures generates most flexible dedicated hybrid concepts.

https://doi.org/10.51202/9783181023549 - Generiert durch IP 216.73.216.36, am 19.01.2026, 02:19:31. © Urheberrechtlich geschützter Inhalt. Ohne gesonderte Erlaubnis ist jede urheberrechtliche Nutzung untersagt, insbesondere die Nutzung des Inhalts im Zusammenhang mit, für oder in KI-Systemen, KI-Modellen oder Generativen Sprachmodellen.

	Type I	Type II	Type III	Type IV
E-Drive Architecture	Single EM	Single EM	Multiple EM	Multiple EM
Hybrid Driving Modes	Parallel	Parallel / Superposition	Parallel / Serial	Parallel / Serial / Superposition
Vehicle launch/ Creeping	Electric	Electric, hybrid (EDA)	Electric, hybrid (serial)	Electric, hybrid (serial / EDA / power-split)*
ICE load optimization	Torque mode	Torque mode & CVT mode	Torque mode & CVT mode	Torque mode & CVT mode
ICE start while electric driving	ICE start using EM_1 → EM_1 tractive force reduction	ICE start using EM_1 → EM_1 tractive force reduction	ICE start using EM_2 → No EM_1 tractive force reduction → High comfort	ICE start using EM_2 → No EM_1 tractive force reduction → High comfort
Power shift electric driving	No	No	EMS	EMS / EDS
Power shift hybrid driving	EMS / IMS	EMS / IMS / EDS	EMS / IMS	EMS / IMS / EDS
Reverse driving	Electric	Electric, hybrid (EDA)*	Electric, hybrid (serial)	Electric, hybrid (serial / EDA / power-split)*

ICE ... Internal combustion engine // EM ... Electric machine // EDA ... Electro dynamic vehicle launch // EDS ... Electro dynamic power shift
EMS ... Electro motoric shift // IMS ... Internal combustion engine motoric shift // *depending on gear set architecture

Fig. 5: Summary of individual functional options for selected powertrain functions according to above introduced four types of dedicated hybrid concepts

Systematic search for tailor-made hybrid powertrains

In order to find optimal dedicated hybrid concepts a systematic concept search has to be performed. This search must consider the whole powertrain, including ICE with its periphery, e-drive with electric energy storage and transmission with axle drive. Especially the well-considered assignment of the required functionality to the above mentioned sub-systems is very important. An intelligent allocation of single powertrain functions can extend the simplification of the propulsion aggregates. For example it is possible to shift dynamic requirements from ICE to e-drive. As a result, exhaust turbocharger, variable camshaft adjustment and exhaust after treatment can be simplified and ICE costs will be reduced. An e-drive system with two electric machines can help to simplify the belt drive. A transmission with an additional creeping gear can reduce the necessary torque of the electric machine.

ZF has created a computer-aided process and tool chain for the systematic search of dedicated hybrid concepts. The core of this development environment is a synthesis tool for the transmission of the dedicated hybrid concept. The main steps of the process and tool chain are shown in figure 6.

https://doi.org/10.51202/9783181023549 - Generiert durch IP 216.73.216.36, am 19.01.2026, 02:19:31. © Urheberrechtlich geschützter Inhalt. Ohne gesonderte Erlaubnis ist jede urheberrechtliche Nutzung untersagt, insbesondere die Nutzung des Inhalts im Zusammenhang mit, für oder in KI-Systemen, KI-Modellen oder Generativen Sprachmodellen.

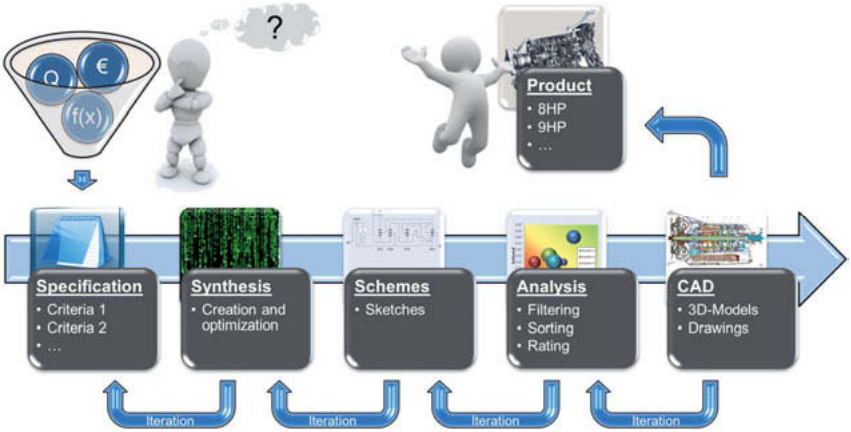


Fig. 6: Main steps for the systematic search of transmissions for dedicated hybrid concepts

The created process chain combines partly automated steps for transmission synthesis and gear set scheme creation with an expert concept rating and selection. It helps to find ideal concepts for specific use cases and customer requirements.

The holistic multi-criteria transmission system optimization considers all possible driving modes and mode transitions. This means during the synthesis process not only ICE, hybrid and electric speeds are optimized. Rather all options and limitations of the described electro-dynamic modes for vehicle launch, power shift and charging while standstills are also taken into account. In contrast to the concept search for conventional transmissions pre-defined combinations of ICEs and e-drive architectures mark the starting point of the process. The transmission gear set represents only the linking element, which helps to fulfill individual requirement sets.

In order to use the ZF synthesis tools global customer requirements have to be translated into transmission requirements in a first step. The resulting transmission requirement set must contain following groups of requirements:

- Performance and efficiency requirements
- Functional requirements
- Installation space requirements

https://doi.org/10.51202/9783181023549 - Generiert durch IP 216.73.216.36, am 19.01.2026, 02:19:31. © Urheberrechtlich geschützter Inhalt. Ohne gesonderte Erlaubnis ist jede urheberrechtliche Nutzung untersagt, insbesondere die Nutzung des Inhalts im Zusammenhang mit, für oder in KI-Systemen, KI-Modellen oder Generativen Sprachmodellen.

The single requirements differ according to the vehicle segment, target market and OEM. In order to fulfill several customer requirement sets with one multi-customer concept the single requirements have to be weighted and intelligently merged.

Set of requirements for tailor-made transmission concepts

The three groups of requirements regarding driving performance/efficiency, functionality and installation space contain various parameters. In the following paragraph some of these parameters are discussed in detail on the basis of an exemplary requirement set for a passenger car with transversal installed powertrain.

In figure 7 several driving performance parameters are summarized. Two of the most important driving performance factors are maximum electric and hybrid acceleration. In the exemplary requirement set for hybrid and electric mode the same launching performance is demanded, whereas in hybrid mode the maximum torque is available up to higher driving speeds. Hill climbing and towing capacity is a key factor, also for dedicated hybrid concepts. When the transmission has to be adapted to different vehicle categories - including SUV and SEDAN with trailers -, a charge sustaining mode for hill driving and crawling must be considered. At low battery state of charge (SOC=0) it's important to be able to maneuver fore and back – also while driving on steeper slopes. Limitations regarding towing and climbing capacity might be acceptable to meet installation space requirements.

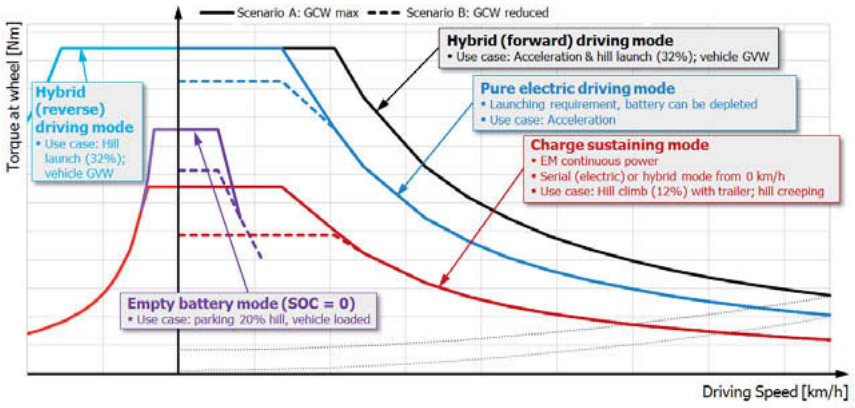


Fig. 7: Exemplary driving performance requirements for dedicated hybrid concepts

https://doi.org/10.51202/9783181023549 - Generiert durch IP 216.73.216.36, am 19.01.2026, 02:19:31. © Urheberrechtlich geschützter Inhalt. Ohne gesonderte Erlaubnis ist jede urheberrechtliche Nutzung untersagt, insbesondere die Nutzung des Inhalts im Zusammenhang mit, für oder in KI-Systemen, KI-Modellen oder Generativen Sprachmodellen.

The morphological box in figure 8 shows functional options, which has to be discussed during the systematic search of dedicated hybrid concepts.

	Option 1	Option 2	Option 3	Option 4	Option 5	Option 6	Option 7
Hybrid driving modes	Parallel	Serial	Superposition	Power-split	...		
Reverse driving modes	ICE driving	EM driving	Hybrid driving (serial)	Hybrid driving (parallel)	Hybrid driving (electro-dynamic)	Hybrid driving (power-split)	...
Shift type ICE modes	No power shift	Power shift with friction shift element	Electro-motoric power shift (EMS)	Electro-dynamic power shift (EDS)	ICE motoric power shift (IMS)	...	
Shift type EM modes	No power shift	Power shift with friction shift element	Electro-motoric power shift (EMS)	Electro-dynamic power shift (EDS)	...		
Ratio of main / add. EM modes	Shorter than shortest ICE mode	Corresponding to shortest ICE mode	Corresponding to one middle ICE mode	Corresponding to longest ICE mode	...		
ICE load optimization	Torque mode	Torque & CV mode	...				
ICE start for main / add. EM mode	No ICE mode	Reduced number of ICE modes	All ICE modes	...			
Vehicle launch / Creeping	With torque converter	With integrated launch element	Electric (motoric)	Hybrid (electro-dynamic)	Hybrid (serial)	Hybrid (power-split)	...
Battery charge while standstill	Possible	Possible with brake activation	Impossible	...			

EDS ... Electro Dynamic Shift // EMS ... Electro Motoric Shift // IMS ... Internal Combustion Engine Motoric Shift
ICE ... Internal Combustion Engine // EM ... Electric Machine // CV ... Continuous variable

Fig. 8: Morphological box with functional options for dedicated hybrid concepts with two electric machines

The key functions are shift types for ICE and EM modes, vehicle launching modes and decoupling options for the electric machine in the upper ICE gears. Dedicated hybrid concepts which can start the ICE under all conditions do not need additional conventional ICE starters. Also pure serial driving with low speed or in crawling modes might be a useful option to fulfill functional requirements. For low battery state of charge a charging mode during standstill can be important for certain vehicles.

Even though dedicated hybrid concepts are normally not modular to non-hybrid and mild hybrid concepts they have to fulfill similar installations space requirements. As long as a combination with state-of-the-art 4-cylinder ICE cannot be excluded, the dedicated hybrid transmission with e-drive must fit into a conventional transmission installation space. An example for such a front transverse installation space with its limiting elements is shown in figure 9.

https://doi.org/10.51202/9783181023549 - Generiert durch IP 216.73.216.36, am 19.01.2026, 02:19:31. © Urheberrechtlich geschützter Inhalt. Ohne gesonderte Erlaubnis ist jede urheberrechtliche Nutzung untersagt, insbesondere die Nutzung des Inhalts im Zusammenhang mit, für oder in KI-Systemen, KI-Modellen oder Generativen Sprachmodellen.

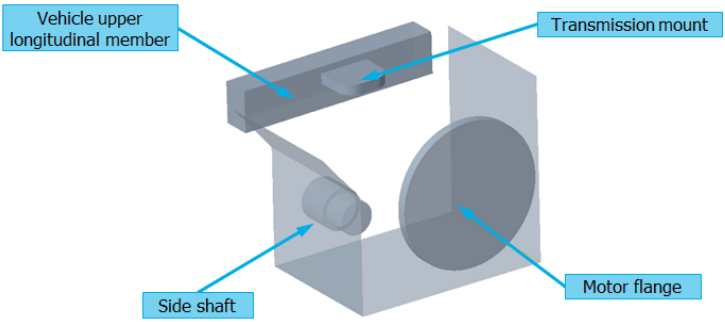


Fig. 9: Generic front transverse installation space

Rating and comparison of tailor-made hybrid powertrains

Within the above described requirement set for tailor-made hybrid powertrains „must-criteria“ and „nice-to-have-criteria” have to be distinguished. Concepts which do not fulfill all “must-criteria” have to be discarded. The „nice-to-have-criteria” can be used for the relative rating of remaining concepts.

If a requirement set includes following „must-criteria”

- serial driving in a charge-sustaining mode with high towing capacity
- electric power shift of all mode changes (EDS and/or EMS) without friction elements
- comfortable ICE start under all conditions and circumstances

only concepts with two electric machines (Type III or Type IV) will be shortlisted.

In figure 10 exemplary dedicated hybrid concepts with two electric machines are shown which were found during a systematic concept search with above mentioned „must-criteria“.

Concept A1 and Concept B1 have a planetary gear set layout. Both concepts use two planetary gear sets for the creation of individual driving modes. Concept C1 is in layshaft design. It contains one layshaft with four single spur gears. For eight shift elements five actuators are needed. C1 and C0 must be actuated separately. The seven shift elements of Concept A1 can be actuated via four actuators. The single shift element is C0, separating the ICE from transmission. Concept B1 also needs four actuators (three double used) for seven shift elements.

https://doi.org/10.51202/9783181023549 - Generiert durch IP 216.73.216.36, am 19.01.2026, 02:19:31. © Urheberrechtlich geschützter Inhalt. Ohne gesonderte Erlaubnis ist jede urheberrechtliche Nutzung untersagt, insbesondere die Nutzung des Inhalts im Zusammenhang mit, für oder in KI-Systemen, KI-Modellen oder Generativen Sprachmodellen.

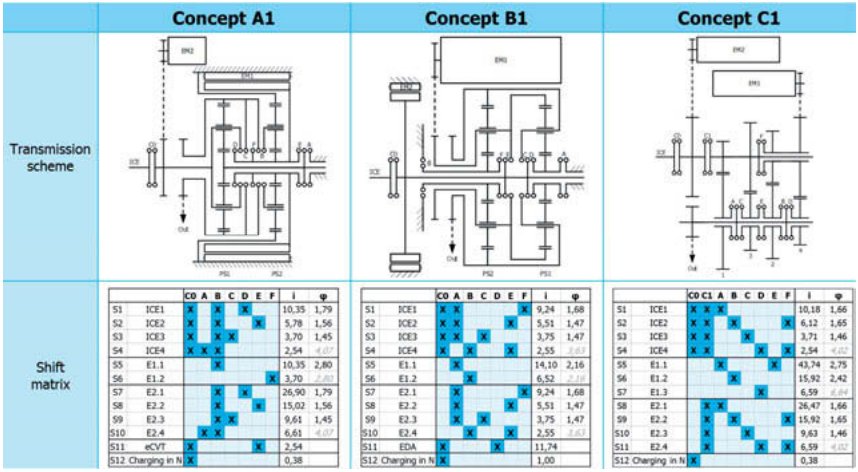


Fig. 10: Exemplary dedicated hybrid concepts with two electric machines

All concepts bring four ICE gears and do not include a reverse gear. The main electric gear of Concept A1 (E1.1) has the same ratio as the first ICE gear (ICE1). That's why Concept A1 suits for a coaxial EM with no further preratio. With concepts B1 and C1 an electric machine preratio is needed, because the gear ratio of the electric gear (without a preratio) would be the same as ICE2. With the two planetary transmission concepts the E1.1 - E1.2 gear-ratio step is 2,2 (Concept B1) and 2,8 (Concept A1). These ratio steps are determined by the i0 ratio of the two planetary gear sets, creating also the four ICE gears. Therefore E1.1 - E1.2 ratio step cannot be chosen freely. In Concept C1 the E1.2 - E1.3 ratio step is 2,4 and the same as ICE2 - ICE4 ratio step. The six different parallel hybrid modes of Concept A1 contain the four gear ratios of the ICE combined with E1.1 and ICE gear ICE3 and ICE4 in combination with E2. Concept C1 ads one to seven total parallel hybrid modes, where only ICE1, ICE2, ICE3 can be combined with E1.2. ICE1, ICE3 and ICE4 are possible with E1.3. Concept B1 with two electric gears brings five parallel hybrid modes, where only ICE1, ICE2, ICE3 can be combined with E1.1. ICE3 and ICE4 are possible with E1.2. This is acceptable because Concept B1 brings electro-dynamic power shift (EDS) to loadshift between the electric gears. Concept C1 ads one electric gear E1.1, which is only used as an electric crawling gear for hill creeping and towing, compensating the lower S1 performance of an axially parallel electric machine. To operate in serial mode, in this crawling gear the shift element C1 is open and C0 is closed. In all other modes, C1 is always closed.

https://doi.org/10.51202/9783181023549 - Generiert durch IP 216.73.216.36, am 19.01.2026, 02:19:31. © Urheberrechtlich geschützter Inhalt. Ohne gesonderte Erlaubnis ist jede urheberrechtliche Nutzung untersagt, insbesondere die Nutzung des Inhalts im Zusammenhang mit, für oder in KI-Systemen, KI-Modellen oder Generativen Sprachmodellen.

With two electric machines all concepts allow serial driving with EM2 as a generator and EM1 as driving motor. EM2 can also be used for pure electric driving, summing up with EM1 torque for an electric torque boost. Concept B1 contains a power split EDA mode (shift element D), which can be used as state-of-the-art power split mode and also for hybrid vehicle launch. The eCVT mode of Concept A has low traction force and can be used as overdrive cruising mode. Vehicle launching with concept A1 and C1 is electric only.

For dedicated hybrid concepts with two electric machines (Type III or Type IV) three topologies respectively e-drive architectures for the installation of the electric machines can be distinguished:

- Two coaxial electric machines (coaxial to motor/input shaft)
- One coaxial electric machine and one axially parallel electric machine
- Two axially parallel electric machines

In the available transverse axial installation space between the motor flange with dual mass flywheel system and the side members there is a need to place in addition to the transmission gear set two electric machines (or at least an e-machine connection for the axially parallel electric machine) and an output gear to the differential shaft. Considering these three elements and axially permute them multiplying it with the three mentioned topologies multiple different architectures result. Figure 11 gives an overview of all these possibilities.

Coaxial / Coaxial

Architecture	Front position (after DMF)	Middle position	Back position (near side member)	Exempl. concept
1.11	Output	EM1 (c)	EM2 (c)	
1.12	Output	EM2 (c)	EM1 (c)	
1.21	EM1 (c)	Output	EM2 (c)	B2
1.22	EM1 (c)	EM2 (c)	Output	
1.31	EM2 (c)	Output	EM1 (c)	
1.32	EM2 (c)	EM1 (c)	Output	

Coaxial / Axially parallel

Architecture	Front position (after DMF)	Middle position	Back position (near side member)	Exempl. concept
2.11	Output	EM1 (a)	EM2 (c)	
2.12	Output	EM1 (c)	EM 2 (a)	
2.13	Output	EM2 (c)	EM1 (a)	
2.14	Output	EM2 (a)	EM1 (c)	
2.21	EM1 (a)	Output	EM2 (c)	
2.22	EM1 (c)	Output	EM2 (a)	
2.23	EM1 (a)	EM2 (c)	Output	
2.24	EM1 (c)	EM2 (a)	Output	
2.31	EM2 (a)	Output	EM1 (c)	A1
2.32	EM2 (c)	Output	EM1 (a)	
2.33	EM2 (a)	EM1 (c)	Output	
2.34	EM2 (c)	EM1 (a)	Output	B1

Axially parallel / Axially parallel

Architecture	Front position (after DMF)	Middle position	Back position (near side member)	Exempl. concept
3.11	Output	EM1 (a)	EM2 (a)	C1
3.12	Output	EM2 (a)	EM1 (a)	
3.21	EM1 (a)	Output	EM2 (a)	
3.22	EM2 (a)	Output	EM1 (a)	
3.31	EM2 (a)	EM1 (a)	Output	
3.32	EM1 (a)	EM2 (a)	Output	

EM1 ... Electric machine 1 EM2 ... Electric machine 2 Output ... Transmission output (c) ... coaxial (a) ... axially parallel

Fig. 11: Overview of all e-drive architectures for dedicated hybrid concepts with two electric machines

https://doi.org/10.51202/9783181023549 - Generiert durch IP 216.73.216.36, am 19.01.2026, 02:19:31. © Urheberrechtlich geschützter Inhalt. Ohne gesonderte Erlaubnis ist jede urheberrechtliche Nutzung untersagt, insbesondere die Nutzung des Inhalts im Zusammenhang mit, für oder in KI-Systemen, KI-Modellen oder Generativen Sprachmodellen.

The architectures shown in figure 11 with two coaxial electric machines are only feasible in combination with planetary gear sets. There is also a need for dog-clutch actuation from inside a shaft because the accessibility is blocked by the coaxial electric machines. Important to consider within this architecture is that you cannot freely choose the electric machine outer diameter to fit with different centre distances from motor to differential shaft, without interfering with the vehicle side shafts.

Whereas axially parallel motors permit the usage of outer actuation elements they have disadvantages regarding electric efficiency due to the additional mechanical elements like a chain-drive or gear wheels. Topology three with two axially parallel electric machines makes use of the maximal axial length of the installation space for the electric machines because they do not interfere axially with each other.

To choose the perfect transmission architecture for a given set of requirements, multiple evaluation criteria have to be taken into account. First of all the asked driving performance of the e-drive and its connection to the transmission shafts must be achievable in the investigated architecture. Interference or collision with side shafts, vehicle side and cross members are hard criteria. The transmission output and differential placement needs to take into account the maximum tire side position of the side shaft.

In the following, some promising e-drive architectures listed in figure 11 are described more in detail using the introduced exemplary dedicated hybrid concepts A, B and C.

Architecture No. 2.32 shown in figure 12 has the main electric machine coaxial placed under the transmission mount near the vehicle’s left tire, considering clearance to the upper side member (b). EM2 is axially placed in parallel between EM1 and the motor flange, where clearance for the ICE-transmission screwing tools (a) has to be considered. An electric machine at the lowest point must be avoided because of cooling and oil flow issues. Inside the EM1 rotor two planetary gear sets can be placed. This architecture can be used for mixed systems (layshaft and planetary) or pure planetary transmissions. In addition architecture No. 2.32 is also feasible for concepts without EM2 and only one electric machine.

https://doi.org/10.51202/9783181023549 - Generiert durch IP 216.73.216.36, am 19.01.2026, 02:19:31. © Urheberrechtlich geschützter Inhalt. Ohne gesonderte Erlaubnis ist jede urheberrechtliche Nutzung untersagt, insbesondere die Nutzung des Inhalts im Zusammenhang mit, für oder in KI-Systemen, KI-Modellen oder Generativen Sprachmodellen.

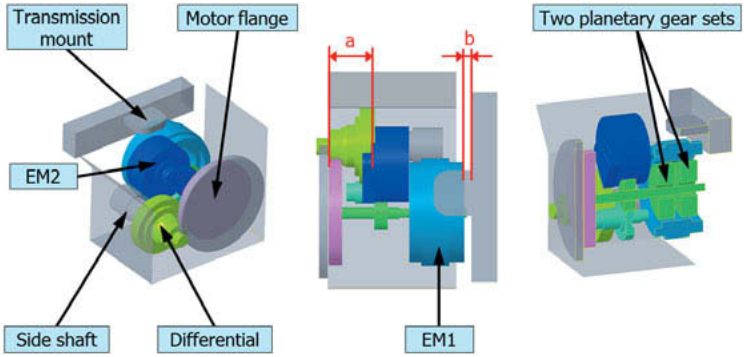


Fig. 12: Architecture No. 2.32 (EM1 coaxial, EM2 axially parallel)

As an alternative for pure planetary transmission systems with two gear sets, architecture No. 2.34 shown in figure 13 is an option.

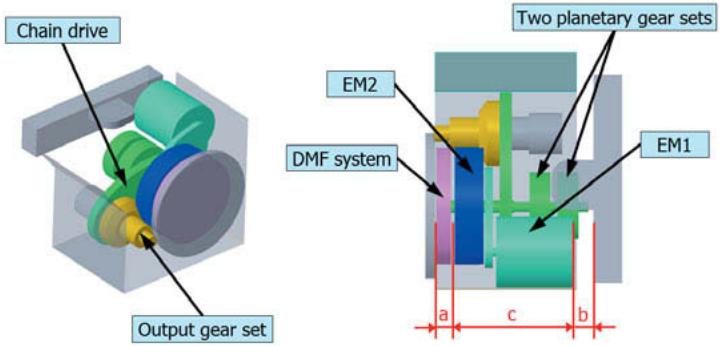


Fig. 13: Architecture No. 2.34 (EM1 axially parallel, EM2 coaxial)

EM1 is an axially parallel e-drive offering to access the shifting elements at the planetary gear sets from the outside with state-of-the-art shifting forks. The coaxial EM2 is placed axially directly after the DMF system. Therefore also within this architecture the axial length of both electric machines sums up to the maximum possible axial installation space, considering clearance to the upper vehicle side member (b) and DMF system (a). To use this architecture it is reasonable to use a chain drive with an additional output planetary gear set to realize the output gear ratio. The placement of EM1 and EM2 allows usage of state-of-the-art OEM transmission mounts.

https://doi.org/10.51202/9783181023549 - Generiert durch IP 216.73.216.36, am 19.01.2026, 02:19:31. © Urheberrechtlich geschützter Inhalt. Ohne gesonderte Erlaubnis ist jede urheberrechtliche Nutzung untersagt, insbesondere die Nutzung des Inhalts im Zusammenhang mit, für oder in KI-Systemen, KI-Modellen oder Generativen Sprachmodellen.

Layshaft transmissions require different e-drive architectures within a front transverse installation space. Architecture No. 3.11 shown in figure 14 contains two axially parallel electric machines. Both electric machines can make use of the maximum axial length between the side member (b) and the clearance for the ICE to transmission screwing tools (a). EM1 length might also be influenced by the position of the differential spur gear. Shifting elements at the layshaft or the input shaft can be accessed from the outside with state-of-the-art shifting forks.

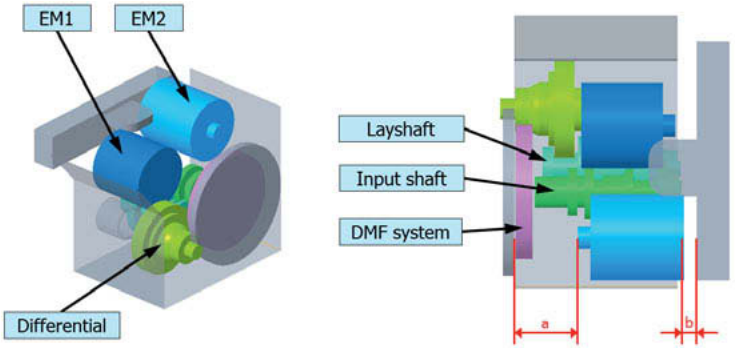


Fig. 14: Architecture No. 3.11 (EM1 axially parallel and EM2 axially parallel)

Architecture No. 1.21 shown in figure 15 is suitable for planetary gear set transmissions.

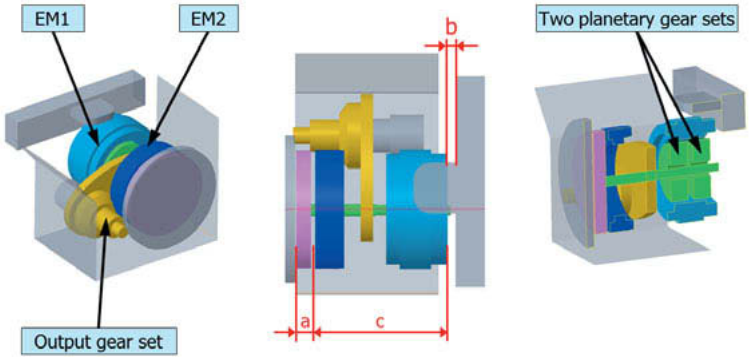


Fig. 15: Architecture No. 1.21 (EM1 coaxial, EM2 coaxial)

To make use of the maximum possible power in the given axial length, it might also be an option to use a chain drive and an additional output gear set on the differential shaft to realize

https://doi.org/10.51202/9783181023549 - Generiert durch IP 216.73.216.36, am 19.01.2026, 02:19:31. © Urheberrechtlich geschützter Inhalt. Ohne gesonderte Erlaubnis ist jede urheberrechtliche Nutzung untersagt, insbesondere die Nutzung des Inhalts im Zusammenhang mit, für oder in KI-Systemen, KI-Modellen oder Generativen Sprachmodellen.

the output gear ratio. The overall length of EM1 and EM2 (c) is limited by the clearance to the upper vehicle side member (b) and the ICE side DMF System (a). The coaxial electric machines make it difficult to use state-of-the-art electro-mechanical actuation from the outside with shifting forks to access shifting elements placed near the gear sets. Therefore there is a need for actuation from inside the transmission shafts.

The examples above show that there are several architectures which allow the installation of a dedicated hybrid powertrain with two powerful electric machines and two planetary gear sets or one layshaft into state-of-the-art front transversal installation spaces without changing the position of the ICE flange position. Of course, concepts with only one axially parallel connected electric machine allow more freedom for packaging, regarding accessibility of shifting elements, installable power and freedom for the output placement and its gear ratio. On the other hand, these concepts are more limited concerning functional and efficiency requirements compared to dedicated hybrid concepts with no friction shift elements and two electric machines.

Summary, conclusion, outlook and acknowledgements

Dedicated hybrid powertrains for plug-in hybrid and full hybrid vehicles can help to make the vision of an affordable electro mobility come true. Compared to battery electric powertrains these concepts get along with significant smaller electric energy storages and offer an unlimited mobility to the end customer. Dedicated hybrid powertrains continue the path of a modular hybridization with one electric machine at the transmission input. They offer additional approaches to increase electric driving efficiency, raise power density and reduce costs. Depending on e-drive and gear set architecture different types of dedicated hybrid powertrains can be differentiated. Concepts with two electric machines and a super positioning gear set offer the highest functional flexibility. These concepts address especially functional demanding requirement sets.

ZF has used its further developed process and tool chain for the systematic search of ideal dedicated hybrid concepts with two electric machines. On the basis of an exemplary multi-customer requirement set attractive concepts have been identified. In this paper for some of these concepts it was shown how dedicated hybrid transmissions with two powerful electric machines can be integrated into challenging installation spaces of transversal passenger cars. At the moment ZF is working on the experimental evaluation of one of these concepts.

https://doi.org/10.51202/9783181023549 - Generiert durch IP 216.73.216.36, am 19.01.2026, 02:19:31. © Urheberrechtlich geschützter Inhalt. Ohne gesonderte Erlaubnis ist jede urheberrechtliche Nutzung untersagt, insbesondere die Nutzung des Inhalts im Zusammenhang mit, für oder in KI-Systemen, KI-Modellen oder Generativen Sprachmodellen.

The authors thank following colleagues for their support in the preparation of this paper: Mr. S. Blattner, Dr. J. Kaltenbach and Mr. T. Martin.

List of references

[1] Vahlensieck, B.: Lösungen der Antriebsstrang-Elektrifizierung: integriert und modular. Vortrag: Frühjahrstagung 2018 - VDMA-EMINT (= Electronics, Micro and Nano Technologies), Friedrichshafen.

[2] Horn, M., U. Griesmeier, B. Vahlensieck: New Concepts for Plug-In Hybrid and parallel Range-Extender Transmissions. Vortrag: VDI Getriebe in Fahrzeugen 2017, Bonn.

[3] Roske, M., Speck, F.-D., Kerschl, S.: Das elektrodynamische Anfahrelement- ein Hybridantrieb mit erweiterter Anfahrfunktionalität, VDI-Tagung Getriebe in Fahrzeugen 2006, Friedrichshafen, VDI-Berichte Nr. 1943.

List of abbreviations

a	Distance a
b	Distance b
c	Distance c
e	Electrified
i	Gear ratio
i_0	Gear ratio planetary gear set
n	Rotational speed

A	Axle transmission
CAGR	Compound annual growth rate
CO_2	Carbon dioxide
CV	Continuous variable
CVT	Continuously variable transmission
DHT	Dedicated hybrid transmission
DMF	Dual mass flywheel

https://doi.org/10.51202/9783181023549 - Generiert durch IP 216.73.216.36, am 19.01.2026, 02:19:31. © Urheberrechtlich geschützter Inhalt. Ohne gesonderte Erlaubnis ist jede urheberrechtliche Nutzung untersagt, insbesondere die Nutzung des Inhalts im Zusammenhang mit, für oder in KI-Systemen, KI-Modellen oder Generativen Sprachmodellen.

DNA	Deoxyribonucleic acid
EDA	Electro-dynamic vehicle launch
EDS	Electro-dynamic power shift
EM	Electric machine
EMS	Electro-motoric power shift
EV	Electric vehicle
GCW	Gross combined weight
GVW	Gross vehicle weight
HEV	Hybrid electric vehicle
I	Input shaft
ICE	Internal combustion engine
IMS	Internal combustion engine motoric shift
M	Torque
MHEV	Mild hybrid vehicle
O	Output shaft
OEM	Original equipment manufacturer
PHEV	Plug-in hybrid vehicle
SOC	State-of-charge
SUV	Sport utility vehicle
T	Transmission
ZF	ZF Friedrichshafen AG

https://doi.org/10.51202/9783181023549 - Generiert durch IP 216.73.216.36, am 19.01.2026, 02:19:31. © Urheberrechtlich geschützter Inhalt. Ohne gesonderte Erlaubnis ist jede urheberrechtliche Nutzung untersagt, insbesondere die Nutzung des Inhalts im Zusammenhang mit, für oder in KI-Systemen, KI-Modellen oder Generativen Sprachmodellen.

https://doi.org/10.51202/9783181023549 - Generiert durch IP 216.73.216.36, am 19.01.2026, 02:19:31. © Urheberrechtlich geschützter Inhalt. Ohne gesonderte Erlaubnis ist jede urheberrechtliche Nutzung untersagt, insbesondere die Nutzung des Inhalts im Zusammenhang mit, für oder in KI-Systemen, KI-Modellen oder Generativen Sprachmodellen.

Evaluation of the Dedicated Range-Extender Transmission Powertrain Concept DE-REX regarding Efficiency, Costs and Complexity

Comparative assessment of electric and hybrid powertrain configurations based on test bench measurements

Andreas Viehmann, M.Sc., **Jean-Eric Schleiffer**, M.Sc.,
Prof. Dr.-Ing. **Stephan Rinderknecht**,
Institute for Mechatronic Systems in Mechanical Engineering (IMS),
Technical University Darmstadt

Supported by:
Federal Ministry for Economic Affairs and Energy
on the basis of a decision by the German Bundestag

Kurzfassung

Der „Doppel-E-Antrieb mit Range-Extender (DE-REX)“ ist ein innovatives DRT-Antriebskonzept. Zur Steigerung der rein elektrischen Effizienz ist der DE-REX elektrisch mehrgängig und mit zwei kleineren elektrischen Maschinen ausgeführt. Im Rahmen des abgeschlossenen DE-REX-Projekts wurde das Antriebskonzept als Gesamtantriebsstrang sowohl an einem Antriebsstrang-Prüfstand als auch in einem Versuchsfahrzeug untersucht. In diesem Beitrag werden anhand von Effizienz-Messungen am Prüfstand im NEFZ und WLTC detaillierte Analysen zur Energieverbrauchsreduktion vorgestellt. Der elektrische Energieverbrauch mit dem Mehrgang- und Mehrmotoren-Antriebskonzept kann im WLTC gegenüber einem elektrischen Festgang-Antrieb um 10,7 % reduziert werden (NEFZ: 15,2 %). Aufbauend auf den Prüfstanduntersuchungen wird eine vergleichende Bewertung von Antriebsstrangkonzepten bzgl. deren Gesamtsystemkosten durchgeführt. Für ein langstreckentaugliches Fahrzeug wird ein Kostenreduktionspotential des DE-REX von ~19 % gegenüber einem BEV mit elektrischem Festgang-Antrieb aufgezeigt. Abschließend wird die nächste Generation des Doppel-E-Antriebs vorgestellt: Der „TDT4LR“.

https://doi.org/10.51202/9783181023549 - Generiert durch IP 216.73.216.36, am 19.01.2026, 02:19:31. © Urheberrechtlich geschützter Inhalt. Ohne gesonderte Erlaubnis ist jede urheberrechtliche Nutzung untersagt, insbesondere die Nutzung des Inhalts im Zusammenhang mit, für oder in KI-Systemen, KI-Modellen oder Generativen Sprachmodellen.

Abstract

The "Two-Drive-Transmission with Range-Extender (DE-REX)" is an innovative DRT powertrain concept. To increase the pure electric efficiency, the DE-REX is equipped with a multi-speed transmission and two smaller electric motors. In the completed DE-REX project, the powertrain concept was tested both on a powertrain test bench and in a demo vehicle. This contribution presents detailed analysis of the energy consumption reduction based on test bench measurements in the NEDC and WLTC. The electric energy consumption with the multi-speed and multi-motor concept can be reduced by 10.7 % in the WLTC compared to a fixed-speed electric drive (NEDC: 15.2 %). Based on the test bench investigations, a comparative evaluation of powertrain concepts with regard to their total powertrain system costs is carried out. A cost reduction potential of the DE-REX of ~19 % compared to a BEV with electric fixed-speed transmission is shown for a vehicle suitable for long distances. Finally, the next generation of the Two-Drive-Transmission is presented: The "TDT4LR".

1. Introduction

In order to meet legal requirements concerning CO_2-Emissions, Battery Electric Vehicles (BEV) are increasingly introduced into market by OEMs. The most widespread pure electric powertrain architecture for BEVs is a combination of one high-power electric motor (EM) with a fixed-speed transmission like in the Tesla Model 3, the BMW i3 or the Volkswagen e-Golf. In the powertrain dimensioning process, the gear ratio of the fixed-speed transmission has to be chosen according to the design requirements concerning maximum vehicle speed and launch torque for example. Since the maximum speed of an EM is limited by the strength of the EM rotor due to the centripetal force for example, the gear ratio has to be as low that the maximum EM speed is reached at vehicle top speed. On the other hand, a low gear ratio for high speed operation leads to a reduced launch torque. Therefore, it would be desirable to choose the gear ratio as high as possible, because then the torque and accordingly the power rating of the EM could be reduced. The conflict of goals for the selection of the gear ratio for a fixed-speed transmission is countered by increasing the power of the EM. With a powerful EM the design requirement concerning launch torque can be met even with a comparatively low gear ratio which is selected according to the vehicle top speed requirement. On the one hand using a powerful EM has the further advantage of outstanding acceleration capabilities and extraordinary driving performance, but on the other hand, the efficiency of these powertrains is relatively low. This is because in ordinary driving situations high driving power is rarely used which means that the powerful EM is most commonly at partial load, which is associated with lower efficiency.

https://doi.org/10.51202/9783181023549 - Generiert durch IP 216.73.216.36, am 19.01.2026, 02:19:31. © Urheberrechtlich geschützter Inhalt. Ohne gesonderte Erlaubnis ist jede urheberrechtliche Nutzung untersagt, insbesondere die Nutzung des Inhalts im Zusammenhang mit, für oder in KI-Systemen, KI-Modellen oder Generativen Sprachmodellen.

In order to resolve the conflict of goals at the dimensioning of the gear ratio, multi-speed transmissions are discussed. The lowest gear ratio of the multi-speed transmission can still be chosen for high speed operation while the highest gear ratio can be chosen in order to fulfil the requirement for launch torque with a less powerful EM. Simulation-based investigations showed that the efficiency of electric powertrains can be improved with multi-speed transmissions. In order to meet the expectations of costumers on dynamic and comfortable electric driving, the gearshifts of the multi-speed transmissions have to be without interruption of traction force. In conventional multi-speed transmissions this is usually encountered by applying powershift elements like friction clutches (e.g. dual clutches) which in term are costly and burdened with a high application effort (e.g. lifetime adaption of the friction element actuation).

At the Institute for Mechatronic Systems for Mechanical Engineering (IMS) at TU Darmstadt an alternative approach for pure electric and hybrid electric powertrains was developed: the innovative, modular powertrain concept named Two-Drive-Transmission (TDT) [1]. The TDT aims at high efficiency while pure electric driving by using a multi-speed transmission consisting of two parallel subtransmissions (STM) and by installing two EMs with half power instead of one powerful EM. Instead of using friction clutches for powershift capabilities, the functional integration of the EMs in a two STM arrangement is used: while the gear in one STM is shifted, the other EM, which is coupled to the other STM, can still propel the vehicle. The working principle of torque-supported gearshifts is introduced in detail in [2].

Compared to BEVs with one powerful EM and a fixed-speed transmission, the efficiency of the TDT approach is expected to be higher. In the course of the paper, the potentials of a multi-motor and multi-speed transmission powertrain compared to a fixed-speed transmission powertrain with one EM are investigated based on measurement results in Chapter 4.

The efficiency of the electric powertrain directly correlates with the battery capacity for a fixed design requirement concerning electric range. The combination of less efficient fixed-speed transmissions with a powerful EM and the requirement for driving long distances leads to enormous battery capacities (60-80 kWh) in current BEVs. Besides the range-anxiety of the costumers of BEVs, environmental conditions (HVAC) also need to be taken into account for HV battery sizing resulting in even higher costs. Instead of using a large battery for applications with high range requirements, the TDT utilizes an Internal Combustion Engine (ICE) in a parallel-series hybrid electric powertrain configuration. The cost benefits of the hybrid TDT variants compared to long-range capable BEV and state of the art add-on hybrids in P2-configuration are discussed in Chapter 5.

The TDT approach with a very efficient electric powertrain and a parallel-series range-extender aims at providing a future-oriented powertrain solution for the Universal Hybrid Electric Vehicle

https://doi.org/10.51202/9783181023549 - Generiert durch IP 216.73.216.36, am 19.01.2026, 02:19:31. © Urheberrechtlich geschützter Inhalt. Ohne gesonderte Erlaubnis ist jede urheberrechtliche Nutzung untersagt, insbesondere die Nutzung des Inhalts im Zusammenhang mit, für oder in KI-Systemen, KI-Modellen oder Generativen Sprachmodellen.

(UHEV). Based on the IMS definition, among other things the UHEV is characterized by local emission-free electric driving for about 60-100 km and by the capability for driving long distances (> 350 km) under real driving conditions.

2. Efficiency potentials of transmissions in pure electric powertrains based on the idea of the TDT

In the course of Drivetrains in Vehicles 2014, a simulation-based evaluation of electric energy consumption of different pure electric powertrains for a C-segment vehicle was presented [3]. The design requirements were specified by a vehicle top speed of 180 km/h and a desired wheel torque for launch of 2 500 Nm. In order to meet these requirements with different powertrain architectures starting from a fixed-speed single-EM drive to a multi-speed multi-EM TDT variant, the gear ratios and the required EM power were determined and summarized in Table 1.

Table 1: Comparison of the dimensioning and electric energy consumption of different powertrain configurations for BEVs based on [3]

	$1EM_{171kW}$,1i	**$1EM_{96kW}$,1i**	**$1EM_{96kW}$,2i**	**$2EM_{48kW}$,2i**
Top speed	180 km/h	180 km/h	180 km/h	180 km/h
Launch torque	2 500 Nm	1 400 Nm	2 500 Nm	2 500 Nm
EM power	171 kW	96 kW	96 kW	2x 48 kW
Gear ratios	i = 6.4	i = 6.4	i_1 = 12 i_2 = 6.4	i_{11} & i_{21} = 12 i_{12} & i_{22} = 6.4
Energy consumption in NEDC	100 %	87.5 %	84.1 %	80.2 %

In order to fulfil the top speed requirement for an EM with a maximum speed of 10 000 rpm, the lowest gear ratio was set to 6.4. To meet the launch torque requirement with the gear ratio of 6.4 for the fixed-speed powertrain, the EM power rating was increased following a scaling approach. The calculations resulted in a necessary EM power of 171 kW. By applying a multi-speed transmission with two gears ratios, the power of the EM can be reduced to 96 kW. The reduction of the EM power is limited due to requirements regarding the power demand at vehicle top speed. The gear ratio for launch was determined to be 12. For the analysis of the different effects of the improvement in electric energy consumption, a variant with reduced EM power and fixed-speed transmission was added. This variant shows the effect of the downsizing of the EM enabled by the application of a multi-speed-transmission (note: this variant does not fulfil the launch torque requirement). In the TDT variant with two EMs with a power of 48 kW

https://doi.org/10.51202/9783181023549 - Generiert durch IP 216.73.216.36, am 19.01.2026, 02:19:31. © Urheberrechtlich geschützter Inhalt. Ohne gesonderte Erlaubnis ist jede urheberrechtliche Nutzung untersagt, insbesondere die Nutzung des Inhalts im Zusammenhang mit, für oder in KI-Systemen, KI-Modellen oder Generativen Sprachmodellen.

each, the gear ratios of both STM are equal. For the simulation-based assessment of the electric energy consumption in the New European Driving Cycle (NEDC), the fixed-speed EM drive was set as baseline configuration. Therefore, the energy consumption of the other variants refer to the one of the baseline configuration. Based on these simulation results and the further results of an optimization the specific hybrid TDT variant called Two-Drive-Transmission with Range-Extender (DE-REX) was developed [4]. The following section introduces the DE-REX powertrain.

3. DE-REX Powertrain

For the hybrid DE-REX powertrain, the power of the two identical EM and the ICE as well as the gear ratios were determined by applying a multi-criteria optimization method [5]. The partners TU Darmstadt, AKKA, Daimler and Magna GETRAG developed the DE-REX powertrain in a publicly funded project based on the results of the optimization process. Therefore, the transmission and the EM were designed, assembled and tested as components and as an entire powertrain at a powertrain test bench and in a demonstrator vehicle.

3.1 Powertrain Layout

Fig. 1 shows the schematic gearset layout of the DE-REX powertrain. Both STMs are arranged coaxial which means that the input gearing of STM1 (highlighted in yellow in Fig. 1) is supported by the main shaft of STM2 (highlighted in blue in Fig. 1). Therefore, both STMs use the same gear wheels for the 1st and 2nd gear. The clutch C0 connects the ICE to STM2. Thus, the ICE uses the gearing of EM2 in STM2 for parallel hybrid operation. The input shafts of the aggregates are coupled to the transmission output by dog clutches labelled as C11, C12, C21 and C22. Compared to powershiftable friction clutches, dog clutches are cheaper and cause less power losses in neutral position or while shifting. Fig. 2 illustrates a cut section model of the DE-REX transmission hardware. The electric motors EM1 and EM2 are two identical permanent magnet synchronous motors, which provide a maximum power of 48 kW each [6].

https://doi.org/10.51202/9783181023549 - Generiert durch IP 216.73.216.36, am 19.01.2026, 02:19:31. © Urheberrechtlich geschützter Inhalt. Ohne gesonderte Erlaubnis ist jede urheberrechtliche Nutzung untersagt, insbesondere die Nutzung des Inhalts im Zusammenhang mit, für oder in KI-Systemen, KI-Modellen oder Generativen Sprachmodellen.

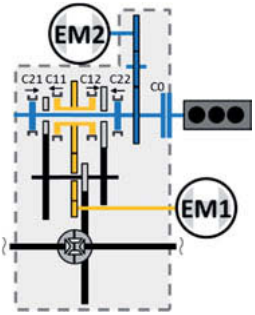


Fig. 1: Schematic layout of the DE-REX powertrain



Fig. 2: DE-REX transmission cut section model

3.2 Operation modes

The DE-REX powertrain provides eight pure electric, six parallel and two series hybrid operating modes. In this contribution, the focus is on the different pure electric driving modes. Table 2 lists the eight pure electric driving modes. The operation modes with one EM only (called “E1”; either EM1 or EM2) in the 1st or 2nd gear define the modes from no. 1 to no. 4. For the unique nomenclature of the driving modes, the prefix for the number of EMs is complemented by the label of the engaged clutch (e.g. C21 for STM2 in the 1st gear). It is expected, that the modes “E1” will be particularly efficient at low vehicle power demand, since one relatively small EM is then operated at a high specific load. In the electric modes 5 to 8, both EM propel the vehicle. The modes differ in the chosen gear in the STMs: while in mode 5 both EMs are propelling in the 1st gear, in mode 8 both EMs are using the 2nd gear. The modes numbered with 6 and 7 are mixed modes, where one EM is in the 1st and the other EM in the 2nd mode. For the “E2” driving modes 5 and 8, the torque request is split equally between the EM.

https://doi.org/10.51202/9783181023549 - Generiert durch IP 216.73.216.36, am 19.01.2026, 02:19:31. © Urheberrechtlich geschützter Inhalt. Ohne gesonderte Erlaubnis ist jede urheberrechtliche Nutzung untersagt, insbesondere die Nutzung des Inhalts im Zusammenhang mit, für oder in KI-Systemen, KI-Modellen oder Generativen Sprachmodellen.

Table 2: Mode description for pure electric driving modes in the DE-REX powertrain

Mode #	Nomenclature	Gear STM1	Gear STM2
1	E1C11	1	0
2	E1C12	2	0
3	E1C21	0	1
4	E1C22	0	2
5	E2C11C21	1	1
6	E2C12C21	2	1
7	E2C11C22	1	2
8	E2C12C22	2	2

Investigations of the gearshift quality in the DE-REX demonstrator vehicle show that gear changes with dog clutches are very comfortable and especially at partial load, a gearshift is not perceivable for the passengers [2]. Therefore, the operating strategy has the option of choosing the suitable driving mode based on the optimal powertrain efficiency without any restrictions regarding shift comfort.

3.3 Development of pure electric operating strategy

In order to develop an operating strategy for pure electric driving, the combined efficiency of the EMs and the power electronics (PE) was investigated [7]. Therefore, the DC input power $P_{\mathrm{PE,el,DC}}$ of the PE and the mechanical output power $P_{\mathrm{EM,mech}}$ at the EM shaft was measured for the entire operating range at the EM component test bench. The combined efficiency of the EM and the PE was determined by

$$\eta_{\mathrm{EM+PE}} = \frac{P_{\mathrm{EM,mech}}}{P_{\mathrm{PE,el,DC}}}.$$

Furthermore, the mechanical efficiency of the DE-REX transmission was determined in different E1 driving modes for selected operating points. Therefore, the mechanical input power $P_{\mathrm{EM,mech}}$ of the EM at the transmission input and the mechanical output power $P_{\mathrm{TM,out,mech}}$ at the transmission output was measured and the efficiency for the multitude of single-input-single-output systems was calculated by

$$\eta_{\mathrm{TM,E1CXY}} = \frac{P_{\mathrm{TM,out,mech}}}{P_{\mathrm{EM,mech}}}.$$

https://doi.org/10.51202/9783181023549 - Generiert durch IP 216.73.216.36, am 19.01.2026, 02:19:31. © Urheberrechtlich geschützter Inhalt. Ohne gesonderte Erlaubnis ist jede urheberrechtliche Nutzung untersagt, insbesondere die Nutzung des Inhalts im Zusammenhang mit, für oder in KI-Systemen, KI-Modellen oder Generativen Sprachmodellen.

For determining the efficiency of the transmission in the entire operating range for all pure electric driving modes, a model-based approach was applied [8]. The result is an estimation of the mechanical efficiency of the transmission for the feasible operating range in different pure electric driving modes. Fig. 3 shows the procedure to determine the optimal model selection and the resulting pure electric operating strategy for the DE-REX.

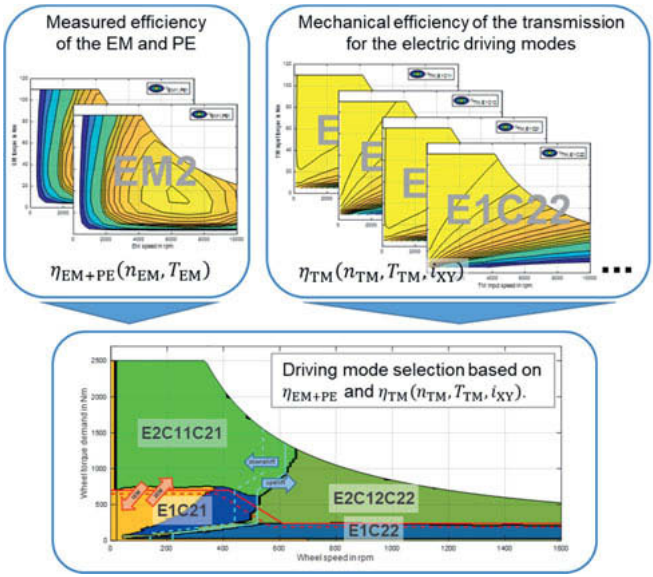


Fig. 3: Pure electric operating strategy for the DE-REX based on component efficiency analysis

In the following, the overall powertrain efficiency of EM with PE and TM in all electric driving modes was calculated depending on the transmission output speed and the requested wheel torque. A mode map showing the most efficient mode was determined. Based on this investigations, a suitable heuristic shift curve and EM selection curve was derived.

As the driving mode selection map in Fig. 3 shows, for low wheel torque demands only one EM is used. Due to the efficiency characteristics of the transmission (STM1 is more efficient in the 1st gear and STM2 is more efficient in 2nd gear), the operating strategy choses EM1 only in 1st gear at low output speed and low torque request and EM2 in 2nd gear at high output speed and low torque requests. For higher power demands, both EMs are used in the 1st or 2nd gear.

https://doi.org/10.51202/9783181023549 - Generiert durch IP 216.73.216.36, am 19.01.2026, 02:19:31. © Urheberrechtlich geschützter Inhalt. Ohne gesonderte Erlaubnis ist jede urheberrechtliche Nutzung untersagt, insbesondere die Nutzung des Inhalts im Zusammenhang mit, für oder in KI-Systemen, KI-Modellen oder Generativen Sprachmodellen.

In order to evaluate the electric energy consumption a powertrain test bench was set up at the TU Darmstadt. The following section introduces the schematic test bench layout.

3.4 Powertrain test bench

At the test bench of the Institute for Internal Combustion Engines and Powertrain Systems the entire DE-REX powertrain was set up. The powertrain test bench was used for the commissioning of the entire powertrain before integration into the demonstrator vehicle and for investigations concerning the electric energy and hybrid fuel consumption. For the sake of this paper, the powertrain test bench is used to measure the electric energy consumption in different regulatory driving cycles. Therefore, the DE-REX powertrain is tested according to a “Powertrain-in-the-Loop” approach. Fig. 4 shows the schematic layout and working principle of the powertrain test bench.

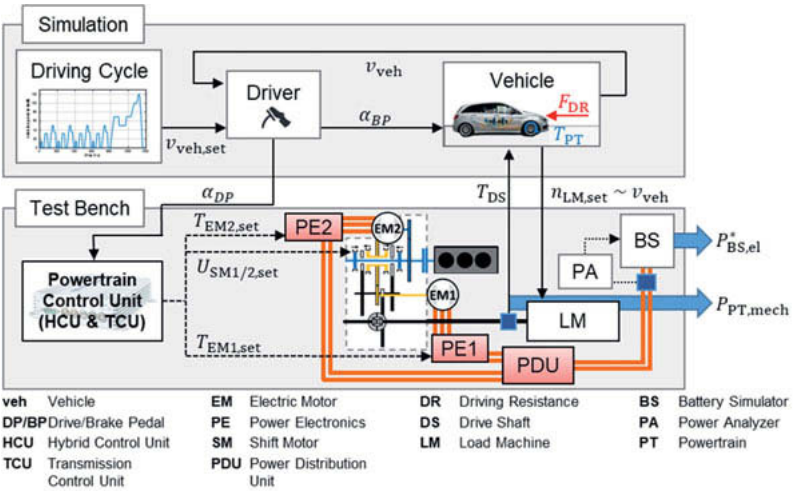


Fig. 4: Schematic layout of the powertrain-in-the-loop test bench

In the simulation environment, the velocity profile of a drive cycle $v_{\mathrm{veh,set}}$ is fed to the virtual driver module. The driver controls the vehicle speed by a virtual drive pedal position α_{DP}, which is forwarded to the central powertrain control unit. The control unit determines the optimal driving mode and coordinates the EM torques $T_{\mathrm{EM1/2,set}}$ and the shifting system $U_{\mathrm{SM1/2,set}}$ of the transmission. The entire powertrain including the PE, EM and transmission runs at the test bench. A torque flange at the output of the transmission measures the output torque T_{DS}, which

https://doi.org/10.51202/9783181023549 - Generiert durch IP 216.73.216.36, am 19.01.2026, 02:19:31. © Urheberrechtlich geschützter Inhalt. Ohne gesonderte Erlaubnis ist jede urheberrechtliche Nutzung untersagt, insbesondere die Nutzung des Inhalts im Zusammenhang mit, für oder in KI-Systemen, KI-Modellen oder Generativen Sprachmodellen.

is fed to a vehicle model in the simulation domain. In the vehicle model, the actual vehicle speed is simulated considering the actual measured torque of the drive shaft and the vehicle driving resistance F_{DR}. The vehicle data for the calculation of the driving resistance are listed in Table 3. Based on the actual vehicle speed, the corresponding output speed of the transmission is calculated which is the set value $n_{\mathrm{LM,set}}$ for the speed control of the load machine.

Table 3: Vehicle data for the vehicle model in the simulation domain

Parameter	Value	Unit
Vehicle mass	1700	kg
Air drag coefficient	0.26	-
Frontal area	2.432	m^2
Rolling friction coefficient	0.01	-
Dynamic wheel radius	0.31	m

The evaluation of the energy consumption bases on the measurement of the mechanical power at the transmission output $P_{\mathrm{PT,mech}}$ (torque and speed of the drive shaft) and the electric power measured at the battery simulator (voltage and current). The measurement of the electric power by the battery simulator $P_{\mathrm{BS,el}}$ is calibrated with a Zimmer LMG 500 power analyzer resulting in the corrected electric power $P^{*}_{\mathrm{BS,el}}$.

4. Investigation of the efficiency for pure electric modes

Based on the introduced test setup of the DE-REX powertrain at the powertrain test bench, the electric energy saving potentials of a multi-speed and multi-motor electric drive compared to a fixed-speed single-EM powertrain is investigated. The DE-REX offers the variety to use the transmission and EMs in different driving modes which are representative for a fixed-speed or a two-speed transmission with one EM. Following the configurations introduced in Table 1 based on the simulation results published in [3], for the sake of this contribution, three different configurations are tested and evaluated at the test bench:

- Fixed-speed baseline-powertrain ($1EM_{171kW}$,1i): This configuration is represented in the DE-REX powertrain by using both EMs in the 2nd gear only (mode 8 (E2C12C22)) which is equivalent with "$1EM_{96kW}$,1i" in Table 1. Since the DE-REX-EMs are less powerful (2x 48 kW) than the EM has to be for meeting the requirements (171 kW), the measured energy consumption is corrected in the data analysis based on the efficiency map of the EM using a linear scaling approach.

https://doi.org/10.51202/9783181023549 - Generiert durch IP 216.73.216.36, am 19.01.2026, 02:19:31. © Urheberrechtlich geschützter Inhalt. Ohne gesonderte Erlaubnis ist jede urheberrechtliche Nutzung untersagt, insbesondere die Nutzung des Inhalts im Zusammenhang mit, für oder in KI-Systemen, KI-Modellen oder Generativen Sprachmodellen.

- The electric two-speed-transmission ($1EM_{96kW}$,2i): For the evaluation of an electric two-speed-drive with one EM, the DE-REX is investigated in the driving modes where both EMs are used in the 1st or 2nd gear (modes 5 (E2C11C21) and 8 (E2C12C22)).
- Two-Drive-Transmission ($2EM_{48kW}$,2i): for the multi-speed multi-EM investigation, the intelligent operating strategy introduced in Section 3.2 freely choses the most efficient driving mode for the DE-REX powertrain.

Table 4 summarizes the different powertrain configurations and their representation with the DE-REX powertrain at the test bench. The following sections describe in detail the approach to illustrating the different configurations using the DE-REX test bench and the associated test bench results.

Table 4: Measurement configurations for the investigations at the test bench

	$1EM_{171kW}$,1i	**$1EM_{96kW}$,1i**	**$1EM_{96kW}$,2i**	**$2EM_{48kW}$,2i**
DE-REX driving modes	8* (scaled)	8	5, 8	1, 2, 3, 4, 5, 8
Gear shifts	none	none	Shift curve	Shift curve
1 EM vs. 2 EM operation	1 EM (represented by 2 scaled EM 50/50)	1 EM (represented by 2 EMs 50/50)	1 EM (represented by 2 EMs)	1 or 2 EM (depending on operating strategy)
Energy consumption evaluation	Scaling of measurement for $1EM_{96kW}$,1i	Test bench measurement	Test bench measurement (**corrected for recuperation shifts)	Test bench measurement (**corrected for recuperation shifts)

4.1 Baseline: Fixed-speed transmission with one powerful EM ($1EM_{171kW}$,1i)

As introduced in the previous sections, the EM in combination with a fixed-speed transmission needs a maximum power of 171 kW in order to meet the launch torque and vehicle top speed requirements. For the representation of this configuration in the DE-REX powertrain both EM with 48 kW each operate with an equal distribution of the requested torque to the EMs. The efficiency for the operating points of a 48 kW EM operated at half of the requested torque is equal to the efficiency in the operating points of a linear scaled EM with 96 kW (= 2x 48 kW) at full torque demand:

https://doi.org/10.51202/9783181023549 - Generiert durch IP 216.73.216.36, am 19.01.2026, 02:19:31. © Urheberrechtlich geschützter Inhalt. Ohne gesonderte Erlaubnis ist jede urheberrechtliche Nutzung untersagt, insbesondere die Nutzung des Inhalts im Zusammenhang mit, für oder in KI-Systemen, KI-Modellen oder Generativen Sprachmodellen.

$$\eta_{48\,\mathrm{kW}}\left(\frac{T_{\mathrm{demand}}}{2}, n_{\mathrm{EM}}\right) = \eta_{96\,\mathrm{kW}}(T_{\mathrm{demand}}, n_{\mathrm{EM}})\,.$$

Fig. 5 shows the efficiency characteristics and the operating points (OP) for the two EMs with 48 kW in the NEDC. Summing up the torque of EM1 and EM2 and transferring it to the scaled efficiency map of the 96 kW EM leads to the OPs on the right side of Fig. 5.

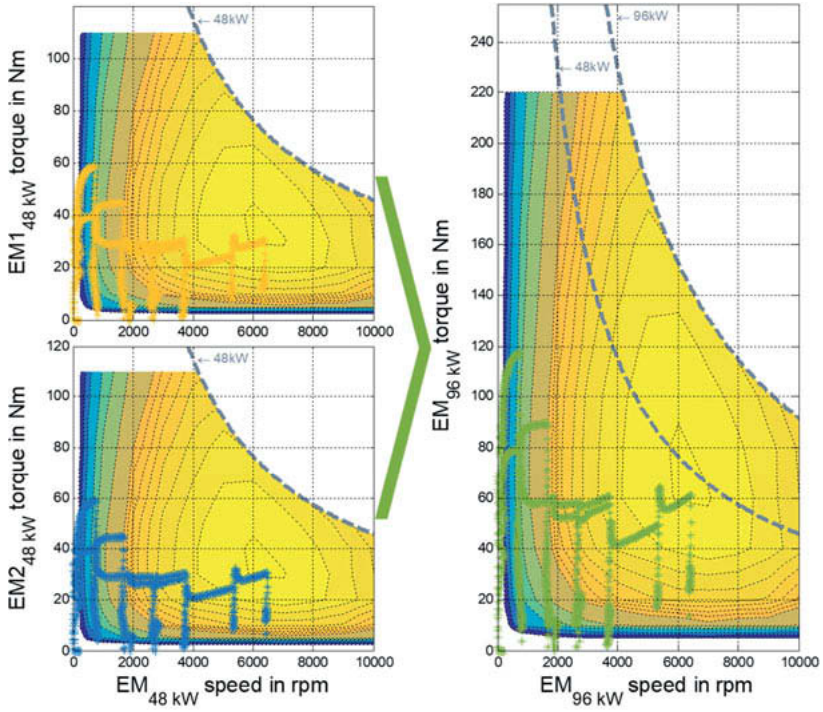


Fig. 5: Operating points of EM1 and EM2 and transfer to EM_{96kW}

By measuring the electric energy consumption with the DE-REX in mode 8 with both EM in 2nd gear the efficiency characteristics of the variant with a single 96 kW EM and a fixed-speed transmission is represented ("$1EM_{96kW}$,1i").

Fig. 6 shows the results of the test bench measurements for the NEDC. The background colors in the vehicle speed profiles indicate the selected mode according to the colors in the driving mode selection map in Fig. 3. Since this variant only uses the 2nd gear for both STM (mode 8), the speeds of the EM directly correlates with the vehicle speed and there are no gearshifts.

https://doi.org/10.51202/9783181023549 - Generiert durch IP 216.73.216.36, am 19.01.2026, 02:19:31. © Urheberrechtlich geschützter Inhalt. Ohne gesonderte Erlaubnis ist jede urheberrechtliche Nutzung untersagt, insbesondere die Nutzung des Inhalts im Zusammenhang mit, für oder in KI-Systemen, KI-Modellen oder Generativen Sprachmodellen.

Since the requested driver torque is distributed equally to the EMs, the torques of both EMs are equal for the entire driving cycle. The electric energy consumption of this configuration with a single 96 kW EM and a fixed-speed transmission denoted as “1EM$_{96kW}$,1i” in the NEDC is at 13.47 kWh/100km.

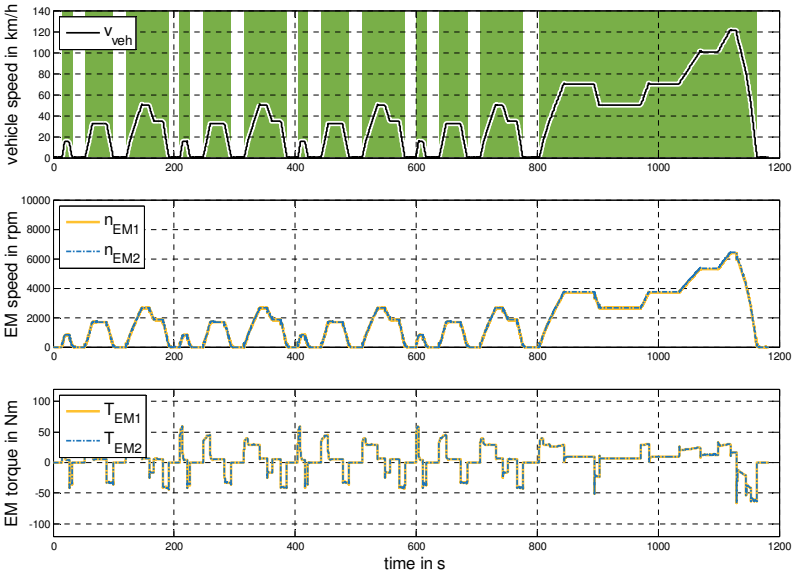


Fig. 6: Measurement results for the “1EM$_{96kW}$,1i” configuration in the NEDC:

Electric energy consumption: $E^*_{BS,NEDC}(1EM_{96kW}, 1i) = 13.47\ \frac{kWh}{100\ km}$

Scaled Electric energy consumption $E^*_{BS,NEDC}(1EM_{171kW}, 1i) \approx 15.3\ \frac{kWh}{100\ km}$

In order to transfer these results to the configuration with an EM power of 171 kW, the efficiency map of the 96 kW EM is scaled linear once again to a variant with 171 kW. Fig. 7 shows the scaling procedure and the location of the operating points in NEDC in the scaled efficiency maps for traction phases. Since the efficiency in the lower torque area decreases, the overall cycle efficiency decreases for the powerful EM and therefore, the electric energy consumption in the NEDC increases to ~ 15.3 kWh/100km.

https://doi.org/10.51202/9783181023549 - Generiert durch IP 216.73.216.36, am 19.01.2026, 02:19:31. © Urheberrechtlich geschützter Inhalt. Ohne gesonderte Erlaubnis ist jede urheberrechtliche Nutzung untersagt, insbesondere die Nutzung des Inhalts im Zusammenhang mit, für oder in KI-Systemen, KI-Modellen oder Generativen Sprachmodellen.

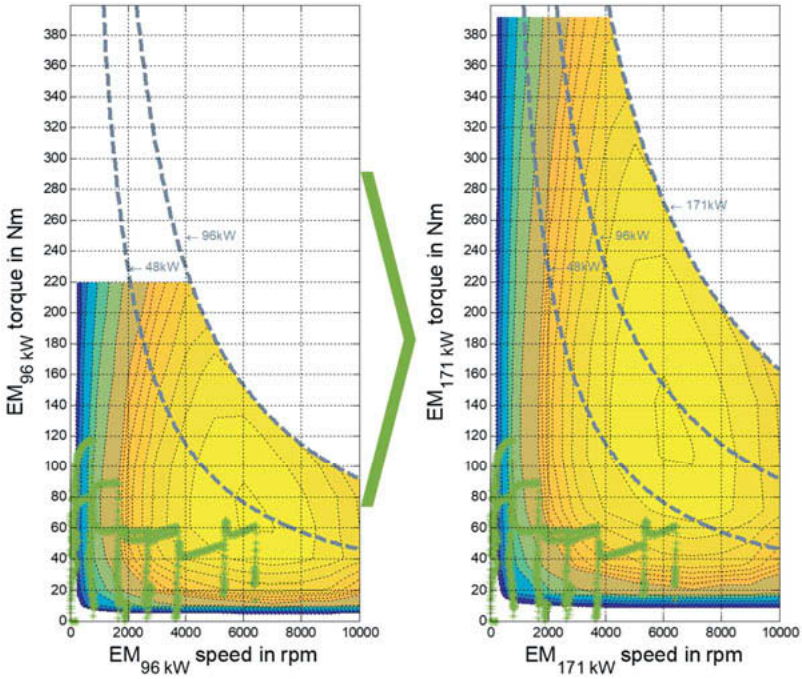


Fig. 7: Scaling procedure for the EM_{171kW} configuration and OPs in the NEDC

It has to be stated that the efficiency characteristics of a fixed-speed transmission would differ from the used DE-REX multi-speed transmission, since the DE-REX transmission has more power loss related components (e.g. additional gear stages, bearings) than a fixed-speed transmission. On the one hand, it is assumed that the efficiency of the fixed-speed transmission would then be higher than in the DE-REX transmission and therefore, the electric energy consumption could decrease. On the other hand, the dimensioning of the fixed-speed transmission has to take into account the higher maximum input power, which will lead to the necessity for larger bearings and a higher gear width for example. This would lead to higher power losses in the fixed-speed transmission compared to the DE-REX transmission, which is dimensioned for a total maximum electric input power of 96 kW. Both exemplary effects mentioned here cancel each other out to some extent, so it can be assumed that a reasonable estimation of the energy consumption is determined here for the intended comparison of different configurations in this contribution. For detailed analysis in the future work, a detailed

https://doi.org/10.51202/9783181023549 - Generiert durch IP 216.73.216.36, am 19.01.2026, 02:19:31. © Urheberrechtlich geschützter Inhalt. Ohne gesonderte Erlaubnis ist jede urheberrechtliche Nutzung untersagt, insbesondere die Nutzung des Inhalts im Zusammenhang mit, für oder in KI-Systemen, KI-Modellen oder Generativen Sprachmodellen.

power loss model for a suitable fixed-speed transmission is considered for evaluating the specific efficiency characteristics and to be able to carry out a substantiated assessment of the resulting effects on the energy consumption of the fixed-speed-transmission single-EM approach.

4.2 Electric two-speed transmission with one downsized EM (1EM$_{96kW}$,2i)

The EM can be downsized by applying a two-speed transmission. Based on the requirements for this case study, the power reduces to 96 kW and therefore is equal to the sum of both DE-REX EMs. For investigating the electric powertrain with one downsized EM with two gears, the EMs in the DE-REX powertrain are used in parallel in the 1st or 2nd gear. Based on the principle for the equivalence of the efficiency of two EMs with halved torque and the efficiency of one EM that is twice as powerful described in Section 4.1, the electric energy consumption measured with the DE-REX in mode 5 and 8 is representative for the configuration with a two-speed transmission with one single EM that is downsized compared to the baseline with fixed-speed transmission. Therefore, the operating strategy chooses the most efficient gear based on a shift curve as described in Section 3.3 and presented in Fig. 3, but without using the possibilities of single-EM operation.

Fig. 8 shows the results for the test bench measurements for the NEDC. As known from the previous baseline configuration, the speeds and the torques of EM1 and EM2 are equal. In contrast to the baseline configuration, the profiles for the EM speeds and the color highlighting in the vehicle speed profile indicate gearshifts. For launch and acceleration procedures, the powertrain uses the 1st gear in the lower vehicle speed phases. For constant speed driving situations and at higher vehicle speeds, the 2nd gear is used. Peaks in the profile of the EM torques are due to the rapid speed control of the EMs for active speed synchronisation in case of gearshift events. In the DE-REX powertrain, the gearshifts in traction phases are fully torque supported which would not be possible for a “1EM$_{96kW}$,2i” configuration with dog clutches. Therefore, the “1EM$_{96kW}$,2i” configuration would require powershiftable friction elements for shifting comfort reasons, which cause additional transmission losses which are not considered here.

https://doi.org/10.51202/9783181023549 - Generiert durch IP 216.73.216.36, am 19.01.2026, 02:19:31. © Urheberrechtlich geschützter Inhalt. Ohne gesonderte Erlaubnis ist jede urheberrechtliche Nutzung untersagt, insbesondere die Nutzung des Inhalts im Zusammenhang mit, für oder in KI-Systemen, KI-Modellen oder Generativen Sprachmodellen.

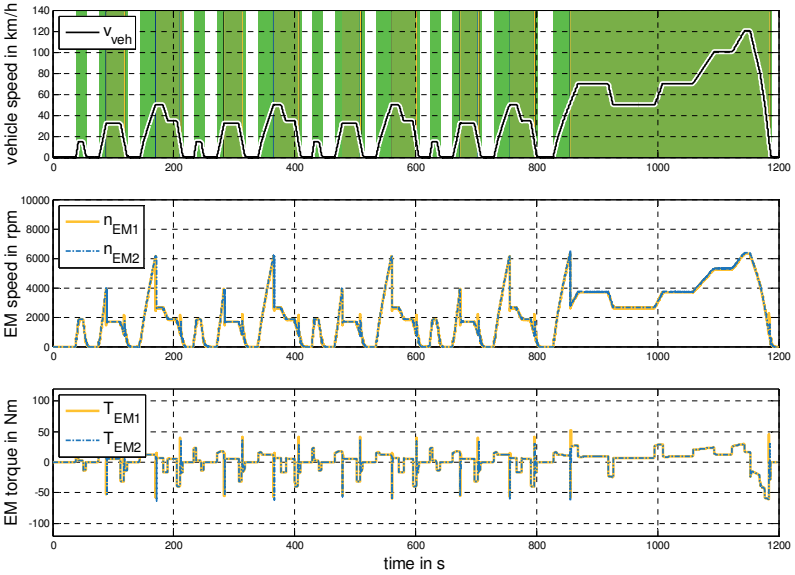


Fig. 8: Measurement results for the "1EM$_{96kW}$,2i" configuration in the NEDC:

Electric energy consumption: $E^{**}_{BS,NEDC}(1EM_{96kW}, 2i) = 13.21\ \frac{kWh}{100\ km}$

At the current development status of the transmission controls, the gearshifts in the deceleration phases are not fully torque supported by the EMs due to interdependencies of the virtual driver model and the implemented one pedal mode. The one pedal mode is necessary for the operation of the demonstrator vehicle that does not have a brake pedal that allows for brake blending. Therefore, a certain amount of energy while gear shifting in recuperation phases is dissipated in the friction brakes of the virtual vehicle. For the evaluation of the overall energy consumption in the driving cycles, it is assumed that this amount of energy can be recuperated (considering a mean powertrain energy conversion efficiency in the traction operation). The revised electric energy consumption of this configuration is 13.21 kWh/100km.

For a final evaluation of this configuration, it has to be taken into account that the structural layout of a two-speed electric transmission with one EM would differ from the investigated DE-REX layout. On the one hand, it is possible to reduce the total number of loss relevant components, but on the other hand, powershift elements (e.g. a wet dual clutch) would be necessary for shifting comfort reasons, which in turn increase the power losses. This configuration is intended to demonstrate the potential for downsizing of EMs in electric powertrains

https://doi.org/10.51202/9783181023549 - Generiert durch IP 216.73.216.36, am 19.01.2026, 02:19:31. © Urheberrechtlich geschützter Inhalt. Ohne gesonderte Erlaubnis ist jede urheberrechtliche Nutzung untersagt, insbesondere die Nutzung des Inhalts im Zusammenhang mit, für oder in KI-Systemen, KI-Modellen oder Generativen Sprachmodellen.

with the aid of multi-speed transmissions. This estimation is to some extent uncertain, but shows a distinct tendency.

4.3 TDT with intelligent mode selection (2EM$_{48kW}$,2x2i)

In the last configuration to be examined here, the potentials of the TDT powertrain concept with two small EMs and two parallel two-speed STMs are demonstrated with aid of the DE-REX powertrain test bench. An intelligent mode selection based on the efficiency maps of the EM and the transmission introduced in Section 3.3 is used for this purpose. Fig. 9 shows the results of the test bench measurements.

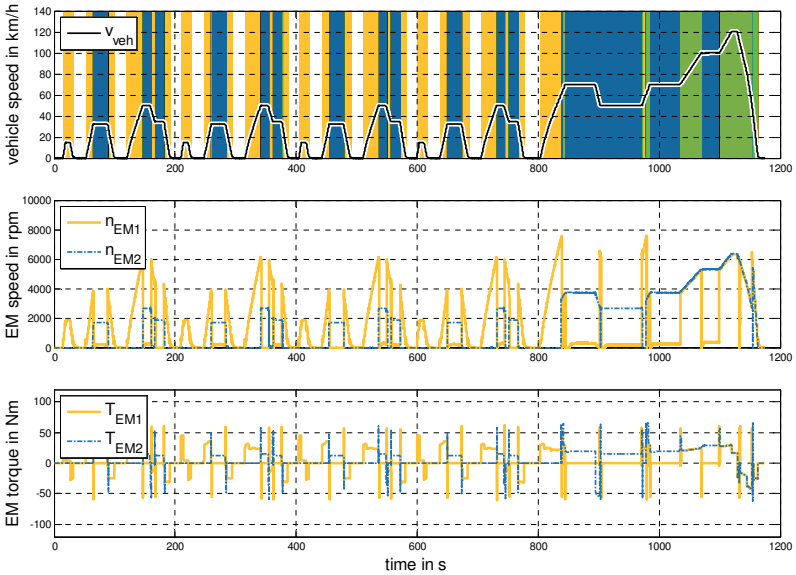


Fig. 9: Measurement results for the "2EM$_{48kW}$,2x2i" configuration in the NEDC:

Electric energy consumption: $E^{**}_{BS,NEDC}$(2EM$_{48kW}$,2x2i) = 12.97 $\frac{kWh}{100\ km}$

As indicated in the speed profile of the EMs, the operating strategy choses only EM1 for accelerating and recuperation phases in the Urban Driving Cycle (UDC) of the NEDC, highlighted in yellow in the vehicle speed profile. For constant speed phases with higher speeds than ~ 30 km/h, EM2 is used in the 2nd gear, highlighted in blue in the vehicle speed profile. At the higher speeds in the Extra-Urban Driving Cycle (EUDC), EM2 is used for constant speed driving and

https://doi.org/10.51202/9783181023549 - Generiert durch IP 216.73.216.36, am 19.01.2026, 02:19:31. © Urheberrechtlich geschützter Inhalt. Ohne gesonderte Erlaubnis ist jede urheberrechtliche Nutzung untersagt, insbesondere die Nutzung des Inhalts im Zusammenhang mit, für oder in KI-Systemen, KI-Modellen oder Generativen Sprachmodellen.

is supported by EM1 for acceleration and deceleration phases, highlighted in green. In total 87.5 % of the driving time one EM propels the vehicle and only in 12.5 % of the driving time both EMs are used. Due to predominately operation with one EM only, the particular EM torque is higher than in the other configurations investigated before. This leads to a higher specific load and therefore, to a higher EM efficiency. The evaluation of the electric energy consumption (considering the correction of the virtual brake torque while gearshifts in recuperation phase like described in the previous configuration) yields to 12.97 kWh/100km for the NEDC. The following section focuses the comparative assessment of the different configurations in the NEDC and additionally in the WLTC.

4.4 Comparative evaluation of the powertrain configurations

In the previous sections, the results for the (synthetic) NEDC were used to make the differences and peculiarities of the configurations easier to understand. Since the Worldwide harmonized Light-duty Test Procedure (WLTP) replaced the NEDC in 2018, all introduced configurations were additionally tested in the associated cycle (WLTC). Exemplary, the test bench results for the "2EM$_{48kW}$,2x2i" configuration are illustrated in Fig. 10.

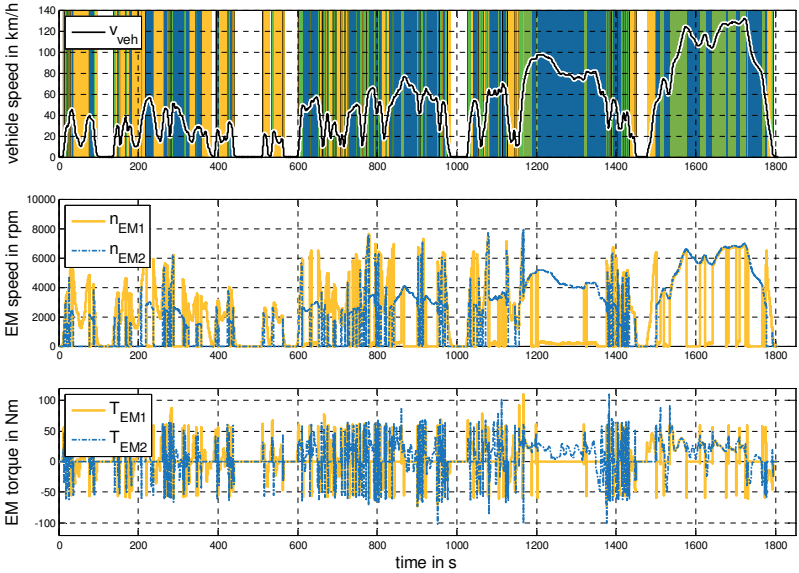


Fig. 10: Measurement results for the "2EM$_{48kW}$,2x2i" configuration in the WLTC:

https://doi.org/10.51202/9783181023549 - Generiert durch IP 216.73.216.36, am 19.01.2026, 02:19:31. © Urheberrechtlich geschützter Inhalt. Ohne gesonderte Erlaubnis ist jede urheberrechtliche Nutzung untersagt, insbesondere die Nutzung des Inhalts im Zusammenhang mit, für oder in KI-Systemen, KI-Modellen oder Generativen Sprachmodellen.

Electric energy consumption: $E^{**}_{BS,WLTC}(2EM_{48kW},2x2i) = 14.75\ \frac{kWh}{100\ km}$

Since the power demand in the WLTC is higher than in the NEDC, the operating strategy uses the two-EM operation more often (~ 21 %). Especially in the more dynamic driving phases with more frequent acceleration and deceleration phases, the driving modes are changed multiple times in order to choose the most efficient mode. Since the gearshifts are very comfortable and in partial load even not perceivable [2], the frequent mode changes have no relevance for the driving comfort.

Merging the test bench results for the different configurations for the NEDC and the WLTC leads to the comparative evaluation of the electric energy consumption shown in Fig. 11.

https://doi.org/10.51202/9783181023549 - Generiert durch IP 216.73.216.36, am 19.01.2026, 02:19:31. © Urheberrechtlich geschützter Inhalt. Ohne gesonderte Erlaubnis ist jede urheberrechtliche Nutzung untersagt, insbesondere die Nutzung des Inhalts im Zusammenhang mit, für oder in KI-Systemen, KI-Modellen oder Generativen Sprachmodellen.

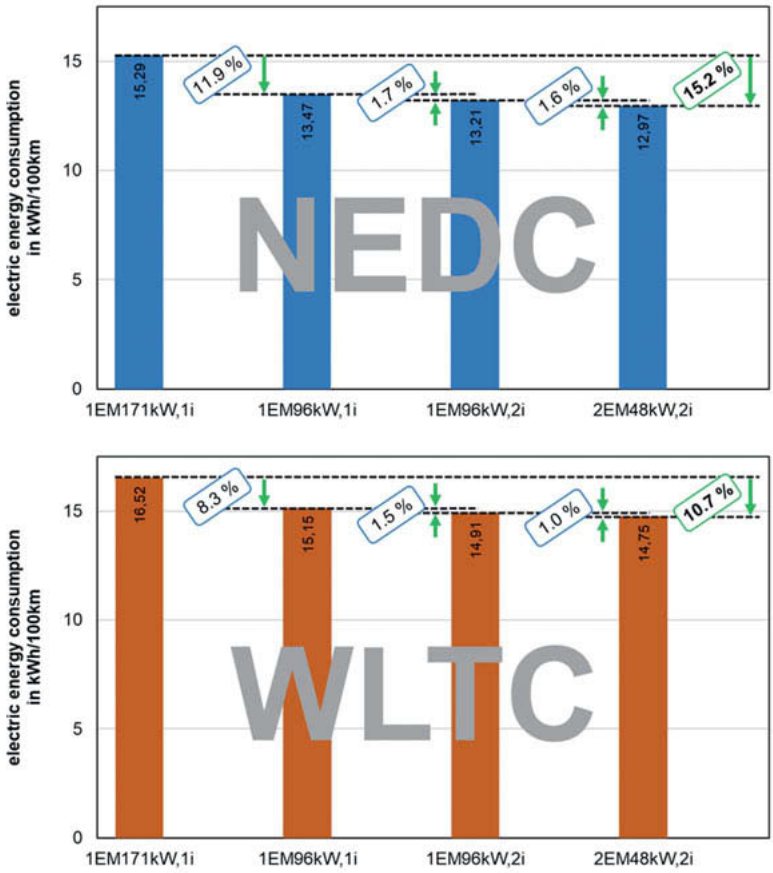


Fig. 11: Comparative evaluation of the electric energy consumption of different configurations (NEDC at the top, WLTC at the bottom)

The measurements carried out show that in both cycles the TDT approach can achieve a significant overall advantage in terms of electrical energy consumption compared to the baseline (NEDC: 15.2 %; WLTC: 10.7 %).

The greatest contribution to this total reduction in energy consumption is achieved by downsizing the EM, although this is only made possible by the use of multi-speed transmissions (NEDC: 11.9 %; WLTC: 8.3 %). The actual use of multiple speeds in cycle operation also provides a further, but smaller, contribution to the total reduction (NEDC: 1.7 %; WLTC: 1.5 %).

https://doi.org/10.51202/9783181023549 - Generiert durch IP 216.73.216.36, am 19.01.2026, 02:19:31. © Urheberrechtlich geschützter Inhalt. Ohne gesonderte Erlaubnis ist jede urheberrechtliche Nutzung untersagt, insbesondere die Nutzung des Inhalts im Zusammenhang mit, für oder in KI-Systemen, KI-Modellen oder Generativen Sprachmodellen.

The additional potential of driving with only one EM at lower loads (similar to the cylinder deactivation procedure for ICEs) is of the same order of magnitude (NEDC: 1.6 %; WLTC: 1 %). Compared to the simulation-based results, the improvements in terms of the electric energy consumption are lower for the test bench measurements. This is mainly because no standby losses of the PEs have been taken into account yet in the simulation model. In the DE-REX the PEs are standard purchased parts, which have relatively high standby-losses. For the next development generation, the PE will also be in the focus in terms of reducing energy consumption. An estimation for the WLTC based on the evaluation of the mean standby loss of the PEs and their idle times in single-EM operation (~79 % of the time in the WLTC) phases leads a further reduction in the energy consumption of about ~ 0.28 kWh/100km. This results in an improvement of about ~ 12.4 % compared to the baseline (instead of 10.7 %). The effect is even higher in the NEDC, because of the longer single-EM operation (~ 17.8 % instead of 15.2 %). Thus, the estimated overall efficiency potential for the TDT approach based on the measured test bench data is in the range of the simulations from [3].
Based on these results the impact of the energy consumption advantages on the total powertrain systems costs of the different topologies, including the HV battery, are investigated for vehicles that are capable for long-range operation.

5. Evaluation of total powertrain system costs incl. HV battery

From the system point of view, the total powertrain cost analysis has to include all significant cost drivers like the EM, PE, cooling, HV battery and for hybrid variants all ICE-related components. By following the idea of a system approach, the efficiency of the powertrain system for a given vehicle and a requirement for the pure electric range is directly linked to the costs of the entire powertrain system including the HV battery. In the following, costs of different representative vehicles with the powertrain configurations introduced in the previous chapters are investigated. Table 5 shows the representative vehicle concepts, the corresponding powertrain configuration incl. the electric energy consumption for the WLTC determined in Chapter 4 and the parameterization of the HV battery based on the requirement for the electric range of the concepts. For this case study, it is assumed that the vehicle is capable for a range of 350 km, which means that the BEV variants need a pure electric range of 350 km. For the hybrid DE-REX vehicle and a state of the art Plug-in Hybrid Electric Vehicle (PHEV), a pure electric range of 100 km is required, since for long distances the hybrid modes are used. For the PHEV variant, a parallel hybrid in P2 configuration with a six-speed dual clutch transmission (DCT) is assumed. Due to the six transmission speeds, it is supposed that the demand of electric power of the EM can be further reduced to 80 kW. The abbreviation of the different

https://doi.org/10.51202/9783181023549 - Generiert durch IP 216.73.216.36, am 19.01.2026, 02:19:31. © Urheberrechtlich geschützter Inhalt. Ohne gesonderte Erlaubnis ist jede urheberrechtliche Nutzung untersagt, insbesondere die Nutzung des Inhalts im Zusammenhang mit, für oder in KI-Systemen, KI-Modellen oder Generativen Sprachmodellen.

concepts (BEV and PHEV) are supplemented by the size of the battery in kWh. The electric energy consumption for the BEV72, the BEV65 and the DE-REX base on the test bench measurements in Chapter 4. In contrast to this, the electric energy consumption of the PHEV20 was estimated optimistically based on information for state of the art PHEV available on market.

Table 5: Powertrain configurations for the representative vehicle concepts

	BEV72	BEV65	DE-REX	PHEV20
Powertrain	1EM$_{171kW}$,1i	1EM$_{96kW}$,2i	2EM$_{48kW}$,2x2i	(P2-6G-DCT)
# of speeds	1	2	2x2	6
EM power	171 kW	96 kW	2x 48 kW	80 kW
$\mathbf{E}^{**}_{\mathbf{BS,WLTC}}$	$\sim 16.5\ \frac{\mathrm{kWh}}{100\mathrm{km}}$	$14.91\ \frac{\mathrm{kWh}}{100\mathrm{km}}$	$14.75\ \frac{\mathrm{kWh}}{100\mathrm{km}}$	$\sim 16\ \frac{\mathrm{kWh}}{100\mathrm{km}}$
Requirement for electric range	350 km	350 km	100 km	100 km
Battery capacity (80% usable)	72 kWh	65 kWh	18.5 kWh	20 kWh

For the case study, the required capacity of the HV battery is calculated based on the electric energy consumption in the WLTC and the requirement for the pure electric range. Furthermore, it is assumed that only 80% of the battery capacity is used for lifetime reasons. The result for battery calculation shows that the battery of the two-speed configuration (BEV65) is 7 kWh smaller than the fixed-speed BEV72, which in term would lead to reduced battery costs. It has to be stated that for the calculation of the battery capacity, no additional energy amount for heating, cooling or auxiliaries is considered. Detailed investigations of the influence of these additional energy consumers are presented in [9] for example. By considering these influencing factors in future work, the required battery capacity would increase even further in real driving situations. Furthermore, it was not taken into account that the required size of the battery has an influence on the total mass of the vehicle (which was fixed to 1 700 kg) and thus on efficiency. This is an optimistic estimation in terms of the efficiency for the vehicles with large batteries.

In the following, the basic principles of the component cost model are introduced. Afterwards, the costs for different representative powertrains for the introduced vehicles are evaluated.

https://doi.org/10.51202/9783181023549 - Generiert durch IP 216.73.216.36, am 19.01.2026, 02:19:31. © Urheberrechtlich geschützter Inhalt. Ohne gesonderte Erlaubnis ist jede urheberrechtliche Nutzung untersagt, insbesondere die Nutzung des Inhalts im Zusammenhang mit, für oder in KI-Systemen, KI-Modellen oder Generativen Sprachmodellen.

5.1 Powertrain system costs

The cost model for the powertrain system components bases on an IMS-approach for modeling transmission costs [10]. Based on a bottom-up approach, the costs of the transmission components are summed up to the transmission overall costs. A component-based cost model for ICEs was developed according to the same scheme. For the EM and the PE a cost model approach based on the literature was adopted [11]. For the EM costs, the costs for permanent-magnet synchronous motors (PMSM) are considered, since the EMs in the DE-REX and the used efficiency characteristics are for PMSM only. For future work, the cost model is extended to other EM types (like induction machines) as well. Based on the price for batteries estimated for Tesla batteries of 111 $/kWh [12], the costs for the battery are scaled linearly with 100 €/kWh, which is assumed to be a very progressive cost estimation.

5.2 Results of the cost modelling

For the evaluation of the powertrain system overall costs, the introduced representative vehicles are analyzed. Fig. 12 shows the results of the cost assessment. The costs of a fixed-speed transmission BEV72 (no clutches, no shifting system and only two gear stages) are the baseline and set to 100 %. As the diagram shows, the overall costs of a pure electric vehicle can be reduced significantly due to the application of a two-speed transmission. The additional costs for a two-speed transmission including a wet dual clutch, a hydraulic actuation system and additional gears in the BEV65 compared to the fixed-speed transmission in the BEV72 are overcompensated since the smaller battery and the smaller EM are substantially cheaper. In total, the costs for the BEV65 are ~ 12 % lower than the baseline BEV72.

The costs for the “$2EM_{48kW}$,2x2i” TDT powertrain in a BEV would also be in the range of the BEV65. The efficiency advantage of this TDT powertrain would lead to a slightly smaller battery and concurrently lower costs. This advantage, however, would be almost nullified by the additional costs due to the two EMs. Based on the cost model for the EM, the total costs of the two EMs with a power of 48 kW each are about 27 % higher than the costs of one EM with 96 kW. However, the realization of multi-speed transmissions based on the TDT principle allow for a more efficient powertrain at equivalent costs. Depending on specific quantity scenarios at component level, e.g. caused by modularization or manufacturing collaborations, an advantage can arise in favor of one or the other approach.

Ultimately, compared to the costs for the EM in the fixed-gear transmission BEV72, the costs for two downsized EMs with 48 kW each are about 12 % lower than the one powerful EM in the BEV72.

https://doi.org/10.51202/9783181023549 - Generiert durch IP 216.73.216.36, am 19.01.2026, 02:19:31. © Urheberrechtlich geschützter Inhalt. Ohne gesonderte Erlaubnis ist jede urheberrechtliche Nutzung untersagt, insbesondere die Nutzung des Inhalts im Zusammenhang mit, für oder in KI-Systemen, KI-Modellen oder Generativen Sprachmodellen.

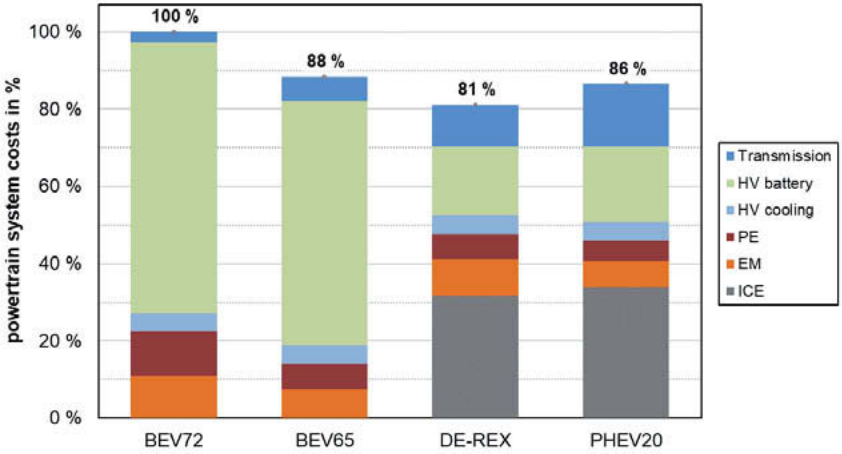


Fig. 12: Relative overall powertrain systems costs. Baseline: fixed-speed BEV

For the specific hybrid TDT variant DE-REX, the battery size and therefore, the battery costs in comparison to the BEVs with long-range capability are significantly reduced. In turn, an ICE including turbo charger, cooling system, fuel system and exhaust system is added which leads to additional costs. The total powertrain costs of the DE-REX vehicle approach are 19 % lower than the BEV72.

Finally, the costs of the DE-REX vehicle are compared to the state of the art PHEV20. Fig. 12 shows that the overall costs of the powertrain system in the DE-REX are 5 percentage points lower than the PHEV20, although two EMs and PEs are used. The greatest contribution to the cost advantages of the DE-REX results from the reduction of the transmissions cost. Instead of a complex and expensive DCT with an additional disconnect clutch for the ICE, a gearset for six forward-speeds and corresponding synchronizer systems, the DE-REX bases on a simple and cheap transmission technology. Significant cost advantages result from the reduction of gears and the usage of dog clutches. Furthermore, the ICE in the DE-REX is less powerful than in the PHEV20, which results in a slightly lower ICE costs. The consequent functional integration of the EMs combined with a smart transmission concept like in the DE-REX shows the best results in terms of overall powertrain costs for vehicles, which are able to drive locally emission-free in urban areas, and are suitable to cover longer distances as well.

https://doi.org/10.51202/9783181023549 - Generiert durch IP 216.73.216.36, am 19.01.2026, 02:19:31. © Urheberrechtlich geschützter Inhalt. Ohne gesonderte Erlaubnis ist jede urheberrechtliche Nutzung untersagt, insbesondere die Nutzung des Inhalts im Zusammenhang mit, für oder in KI-Systemen, KI-Modellen oder Generativen Sprachmodellen.

6. Next generation of the TDT: The Two-Drive-Transmission 4 Long-Range (TDT4LR)

The DE-REX powertrain showed the potential of the TDT-approach compared to pure BEV and current PHEVs in terms of driving and shifting comfort as well as in terms of efficiency and costs. For the next generation of the TDT the TDT4LR is developed at the IMS. The TDT4LR combines the basic ideas of the TDT with a new gearset layout. In the TDT4LR, there are four different gear ratios, which can be used while pure electric and hybrid driving. Compared to the actual DE-REX powertrain, the additional gear ratios in the electric and hybrid operation and the further reduced complexity of the gearset layout (only two gear stages from all input shafts to the drive shafts) leads to additional potentials in terms of reducing electric energy and fuel consumption with lower costs at the same time. Based on first assumptions, the pure electric energy consumption reduces by further 2-3 %. Combining these efficiency potentials with the further cost reduction potentials at the transmission and a further simplification of the ICE (e.g. no turbo charger) results in further reduction of the costs to 76 % of the BEV72 which means further 5 percentage points less than the actual DE-REX system.

7. Summary & Outlook

The modular TDT powertrain concept for electric and hybrid vehicles aims at high efficiency and high gearshift comfort at simultaneously low powertrain costs. Previous simulation based results showed the significant potentials of the idea of a multi-speed and multi-EM powertrain concept in terms of reducing the electric energy consumption. In the course of the publicly funded DE-REX project, a specific TDT variant was developed and investigated both at the powertrain test bench and in a demonstrator vehicle. In recent publications, the high level of shift comfort was confirmed based on measurements in the demonstrator vehicle [2]. For this contribution, the focus was to proof the efficiency potentials of the TDT based on test bench measurements with the DE-REX powertrain and to evaluate the resulting overall powertrain system cost potentials.

For the comparative evaluation of different pure electric powertrain configurations, the DE-REX powertrain was investigated in different operating modes, which are representative for the operation of an EM in other drivetrains like a fixed-speed transmission. Based on the test bench measurements, it could be shown successfully that the electric energy consumption is reduced by about 10.7% in the WLTC (NEDC: 15.2 %) by applying a TDT powertrain instead of a state of the art fixed-speed transmission with one powerful EM in a BEV.

Further potentials in terms of reducing the electric energy consumption are possible with purpose design PEs that is in the focus for the next generation of the TDT. Goals for the purpose

https://doi.org/10.51202/9783181023549 - Generiert durch IP 216.73.216.36, am 19.01.2026, 02:19:31. © Urheberrechtlich geschützter Inhalt. Ohne gesonderte Erlaubnis ist jede urheberrechtliche Nutzung untersagt, insbesondere die Nutzung des Inhalts im Zusammenhang mit, für oder in KI-Systemen, KI-Modellen oder Generativen Sprachmodellen.

design PE are low standby losses (for efficiency reasons), high overload capacity (for further increase of the shifting comfort) and low costs.

The results of the test bench measurements have a direct influence on the evaluation of the overall powertrain costs. Due to the reduced energy consumption of multi-speed BEVs, the HV battery capacity can be reduced significantly for a given electric range requirement. In the BEV variants, the costs of a two-speed single-EM as well as of a two-speed two-EM configuration are about 12 % lower than the baseline configuration with a fixed-speed transmission with a single powerful EM. Furthermore, the TDT-based hybrid DE-REX powertrain shows the highest potentials in terms of reducing costs compared to the BEVs and a state of the art PHEV. It is worth mentioning that the results of the investigations for the case study depend significantly on the chosen requirements, efficiency characteristics of the EM and the detailed consideration of the efficiency of the transmission. However, the case study confirms that the TDT concept is an attractive solution in terms of efficiency, costs and modularity for a future-oriented electric and hybrid powertrain. Furthermore, the next generation of the TDT - the TDT4LR – shows further potentials for improvements.

https://doi.org/10.51202/9783181023549 - Generiert durch IP 216.73.216.36, am 19.01.2026, 02:19:31. © Urheberrechtlich geschützter Inhalt. Ohne gesonderte Erlaubnis ist jede urheberrechtliche Nutzung untersagt, insbesondere die Nutzung des Inhalts im Zusammenhang mit, für oder in KI-Systemen, KI-Modellen oder Generativen Sprachmodellen.

8. References

[1] Rinderknecht, S., Meier, T., and Fietzek, R., “Electric Two-Drive-Transmission for E-Vehicles” in: VDI-Berichte 2130: Getriebe in Fahrzeugen 2011, ISBN 978-3-18-092130-3, 2011.

[2] Viehmann, A., König, R., and Rinderknecht, S., “Investigation in Gear Shifts in a Parallel-Series Hybrid Powertrain with Dog Clutches in a Demonstrator Vehicle” in: VDI-Berichte 2328: Dritev - Drivetrain for Vehicles 2018, ISBN 978-3-18-092328-4, 2018.

[3] Rinderknecht, S., König, R., and Schleiffer, J.-E., “Modularity Aspects for Hybrid Electric Powertrains on the Example of the Two-Drive-Transmission” in: VDI-Berichte 2218: Getriebe in Fahrzeugen 2014, ISBN 978-3-18-092218-8, 2014.

[4] König, R., An, J., Rinderknecht, S., and Binder, A., “Abschlussbericht des Projekts Doppel-E-Antrieb” doi:10.2314/GBV:861498585.

[5] König, R. and Rinderknecht, S., “Multi-Objective Optimization of the Two-Drive-Transmission for a Hybrid Electric Vehicle” in: FISITA World Automotive Congress 2014, Maastricht, Netherlands, 2014.

[6] An, J. and Binder, A., “Permanent magnet synchronous machine design for hybrid electric cars with double e-motor and range extender” in: e & i Elektrotechnik und Informationstechnik. 133(2):65–72, 2016, doi:10.1007/s00502-016-0397-7.

[7] An, J. and Binder, A., “Operation Strategy with Thermal Management of E-Machines in Pure Electric Driving Mode for Twin-Drive-Transmission (DE-REX)” in: IEEE Vehicle Power and Propulsion Conference (VPPC), Belfort, France, 2017.

[8] Shen, Y., Viehmann, A., and Rinderknecht, S., “Investigation of the power losses of the hybrid transmission DE-REX based on modeling and measurement” in: Proceedings of the Institution of Mechanical Engineers, Part D: Journal of Automobile Engineering 53:1-12, 2019, doi:10.1177/0954407019829655.

[9] Jardin, P., Esser, A., Givone, S., Eichenlaub, T., Schleiffer, J.-E., and Rinderknecht, S., “The Sensitivity in Consumption of Different Vehicle Drivetrain Concepts Under Varying Operating Conditions: A Simulative Data Driven Approach,” in: Vehicles 1(1):69–87, 2019, doi:10.3390/vehicles1010005.

[10] Schleiffer, J.-E. and Rinderknecht, S., “Verbundvorhaben Bezahlbare Elektrische REIchweite durch ModularitäT: Schlussbericht Teilvohaben TP4 "Entwurf und Simulation"”, 2016, doi:10.2314/GBV:873390571.

https://doi.org/10.51202/9783181023549 - Generiert durch IP 216.73.216.36, am 19.01.2026, 02:19:31. © Urheberrechtlich geschützter Inhalt. Ohne gesonderte Erlaubnis ist jede urheberrechtliche Nutzung untersagt, insbesondere die Nutzung des Inhalts im Zusammenhang mit, für oder in KI-Systemen, KI-Modellen oder Generativen Sprachmodellen.

[11] Propfe, B., “Marktpotentiale elektrifizierter Fahrzeugkonzepte unter Berücksichtigung von technischen, politischen und ökonomischen Randbedingungen”, 2015, doi:10.18419/opus-6897.

[12] Lambert, F., “Tesla’s Gigafactory 1 battery cells have a 20% cost advantage over LG”, Available online: https://electrek.co/2018/11/20/tesla-gigafactory-battery-cells-made-cost-advantage-panasonic-lg-report/ (accessed on March 25, 2019).

https://doi.org/10.51202/9783181023549 - Generiert durch IP 216.73.216.36, am 19.01.2026, 02:19:31. © Urheberrechtlich geschützter Inhalt. Ohne gesonderte Erlaubnis ist jede urheberrechtliche Nutzung untersagt, insbesondere die Nutzung des Inhalts im Zusammenhang mit, für oder in KI-Systemen, KI-Modellen oder Generativen Sprachmodellen.

Hybridized Manual Transmission

Opportunities and challenges of mild hybridization

Konstantin Baron, **Christian Rübsam**,
Opel Automobile GmbH, Rüsselsheim;
Matthias Werra, M.Sc. Prof. **F. Küçükay**,
Institute of Automotive Engineering,
Technical University Braunschweig

1. Kurzfassung

Die Automobilindustrie befindet sich im Umbruch. Die Hauptursachen dafür sind die Verschärfung gesetzlicher Vorgaben, aber auch neue Technologietrends, sowie eine geänderte Erwartungshaltung der Kunden an das Fahrzeug und die Mobilität. Eine Elektrifizierung des Antriebs stellt einen möglichen Lösungsansatz für diese neuen Herausforderungen dar. Während der Verbrennungsmotor nach wie vor Teil der zukünftigen Antriebe zu sein scheint, z.B. in Hybridfahrzeugen, scheint das manuelle Getriebe immer mehr aus dem Fokus der Produktentwicklung zu geraten.

Andererseits haben Opel, sowie auch andere Fahrzeughersteller, weiterhin einen hohen Anteil an manuellen Getriebe in ihrem Portfolio. Dafür gibt es triftige Gründe: hohe Effizienz, niedrige Kosten, niedriges Gewicht, bewährte Technologie und geringere Komplexität verglichen mit automatisierten Getrieben. Durch die Kombination dieser Eigenschaften mit Elektrifizierungstechnologie entsteht eine hybridisierte Version eines manuellen Getriebes, welche eine Weiterentwicklung der konventionellen Version darstellt.

2. Abstract

Today’s automotive industry is under transformation. This transformation is mainly driven by legal requirements, new technology trends, new customer preferences and their mobility behaviour. Propulsion electrification is a big contributor to solve new challenges. While combustion engine technology will be part of this future propulsion architecture e.g. in hybrids, manual transmissions are frequently claimed to become obsolete.

On the other side, Opel as well as other car manufacturers still have a high penetration of manual transmissions in their current portfolio for good reasons like high efficiency, low cost, low weight, its proven technology and lower complexity compared to automatic transmissions.

https://doi.org/10.51202/9783181023549 - Generiert durch IP 216.73.216.36, am 19.01.2026, 02:19:31. © Urheberrechtlich geschützter Inhalt. Ohne gesonderte Erlaubnis ist jede urheberrechtliche Nutzung untersagt, insbesondere die Nutzung des Inhalts im Zusammenhang mit, für oder in KI-Systemen, KI-Modellen oder Generativen Sprachmodellen.

Combination of those attributes with a propulsion electrification technology leads to a hybrid version of a manual transmission that could be the successor of the conventional version.

3. Introduction

In cooperation with the Institute of Automotive Engineering of the Technical University Braunschweig (TUB) Opel has performed an investigation to understand the hybridization impact on manual transmissions more in detail. Opel's long experience and deep knowledge in the transmission sector combined with scientific method of the university facilitated in-depth analysis for an appropriate setup, expected fuel economy improvement and new requirements for the transmission. This publication provides results and conclusions of those activities.

4. Why Hybrid Manual Transmission

Transmission volume is increasing worldwide while the manual transmission share is dropping in the same period. Nevertheless, there still will be a significant share of manual transmissions in the overall production volume and in South Asia it is even increasing [1].

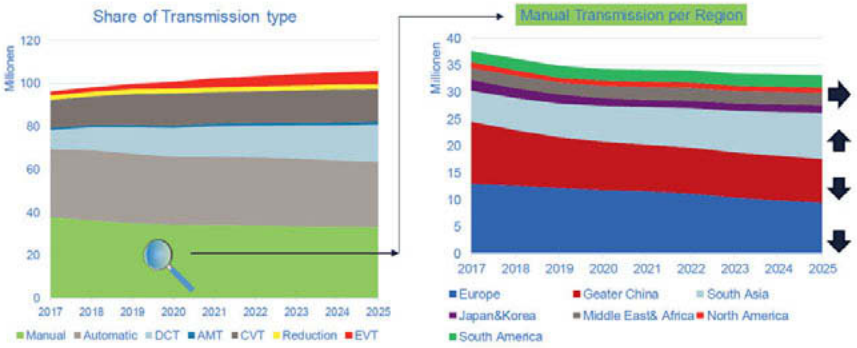


Fig. 1: Manual transmission share statistic by IHS [1]

Having this fact in mind, developing a hybrid version of a manual transmission is a good way to reduce the CO2 emissions of passenger cars [2] worldwide. This paper includes analysis results for a new type of transmission - a combination of a conventional manual transmission with a 48V electrical motor and an electric actuated clutch. Components like DC/DC converter and 48V battery are not part of the analysis described in this paper.

https://doi.org/10.51202/9783181023549 - Generiert durch IP 216.73.216.36, am 19.01.2026, 02:19:31. © Urheberrechtlich geschützter Inhalt. Ohne gesonderte Erlaubnis ist jede urheberrechtliche Nutzung untersagt, insbesondere die Nutzung des Inhalts im Zusammenhang mit, für oder in KI-Systemen, KI-Modellen oder Generativen Sprachmodellen.

Hybrid manual transmissions can improve powertrain efficiency as demonstrated in applications with hybrid automated transmissions (AT, DCT, CVT). In addition, the electrified manual transmission takes advantage of lower cost, higher efficiency and lower complexity. The new concept makes this manual transmission more attractive to customers, since it supports new comfort features that have not been feasible before with the conventional version.
Major attributes:

- Electric driving - Launch and drive by electric motor, change driving direction by electrical motor for autonomous parking
- Efficiency improvement - Recuperation during vehicle deceleration maneuver, load point shifting for combustion optimization, support combustion engine with electrical boost
- Comfort improvement - No clutch pedal (optional), torque fill during shifts (depends on topology)

Without going into details in this paper, there is an additional aspect. The introduction of 48V power grid enables the usage of new electrical components with higher efficiency like e-turbocharger, e-AC compressor or e-brake booster.

5. Concept description

The position of the electrical motor (EM) in the power-flow and thus the drivetrain topology is the fundamental aspect. A hybrid solution for a transmission requires the EM position to be at the input-shaft or output-shaft. Therefore, the options for topology can be limited to P2 or P3.
The optimum solution has to be a trade-off between different factors:

- Fuel economy (on-cycle, RDE, customer related)
- Drive quality (transition between different modes)
- Package (fit to target vehicles)
- Dimension (torque capacity, power)
- Design complexity (controls, reliability and durability)
- Cost (development, manufacturing)
- Feature support (el. driving, autonomous parking, torque fill etc.)

https://doi.org/10.51202/9783181023549 - Generiert durch IP 216.73.216.36, am 19.01.2026, 02:19:31. © Urheberrechtlich geschützter Inhalt. Ohne gesonderte Erlaubnis ist jede urheberrechtliche Nutzung untersagt, insbesondere die Nutzung des Inhalts im Zusammenhang mit, für oder in KI-Systemen, KI-Modellen oder Generativen Sprachmodellen.

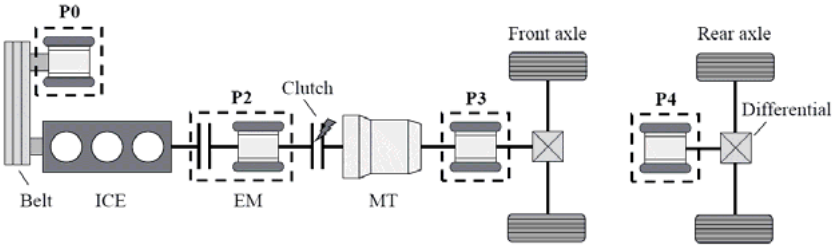


Fig. 2: Hybrid topology [2]

The major focus in this analysis is on fuel economy improvement. But also the customer satisfaction needs to be considered in the system setup.

The main area of application for manual transmissions is in the A, B- and C-segment of passenger cars. In those applications the space in the engine compartment is often limited, vehicles are front wheel driven with transversely installed transmissions. For this analysis a C-segment vehicle was selected for reference.

Therefore, the additional distance required between engine and transmission becomes an important factor for the concept selection. In this aspect, the P2 topology is critical, especially with serial connection of the EM (coaxial to transmission input shaft). Due to package limitation, a parallel connection of the EM to the transmission output shaft was selected for this analysis. In this P3 configuration, the EM is very close to the wheels resulting in low torque losses in electrical drive mode and recuperation.

To keep the complexity of the gearbox on a minimum level, only one gear step (fixed ratio) for the EM connection was considered for the analysis. A fixed ratio between wheels and EM means that the EM speed is proportional to vehicle speed hence the use of the EM in less efficient operating areas cannot be avoided with this P3 architecture. This leads to a negative impact on recuperation and e-drive performance at certain vehicle speed operation areas. In this aspect, a P2 takes advantage of various gear steps of the transmission, which enables an operation of the EM in its highest efficient areas [2].

On the other hand, specific for manual transmissions with a P2 layout, the EM cannot remain connected to the driveline during gearshifts. The EM has to be disconnected in order to prevent an increase of inertia and associated synchronization effort. As a result, there is no recuperation and electrical boost possible during gearshifts. The overall system performance is linked to driver's shifting profile - it develops into a function of the number of gearshifts to be shifted and the gearshift duration itself.

https://doi.org/10.51202/9783181023549 - Generiert durch IP 216.73.216.36, am 19.01.2026, 02:19:31. © Urheberrechtlich geschützter Inhalt. Ohne gesonderte Erlaubnis ist jede urheberrechtliche Nutzung untersagt, insbesondere die Nutzung des Inhalts im Zusammenhang mit, für oder in KI-Systemen, KI-Modellen oder Generativen Sprachmodellen.

Additional opportunity of the EM connected to the output shaft (P3) is the possibility to transfer torque to the wheels independently from gear actuation. The negative effect of propulsion torque loss during gearshifts can be reduced by EM torque applied to the wheels, resulting in higher driving comfort.

Not only the position of the EM in the power flow is an important factor but also the performance data of the electrical machine. Saving potential depends on EM recuperation performance, the higher the electrical power of the machine, the higher the potential for energy recuperation and thus for fuel saving. Fig. 3 below shows that the relation between saving potential and electrical power of EM is not linear, the sweet point for a P3 architecture is at 20kW peak (kWp). An additional increase of electrical power does not provide an appreciable saving improvement [2]. For the analysis described in this paper, an EM with a power of ~25kWp (in generator mode) was selected in order to cover the upper end of the reasonable range.

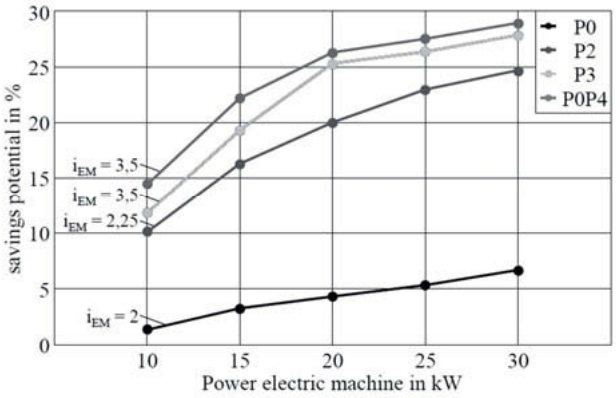


Fig. 3: Impact of different EM power on saving potential in WLTC [2]

There are more components in a hybrid vehicle which affect the entire system performance but are not further described in detail here. The 48V battery is a big contributor to the overall performance. It needs to be carefully selected to make full use of EM performance in terms of power and energy. Within this project a range between 12Ah and 20Ah has been applied to identify impact on fuel consumption on- and off-cycle.

An electrically actuated clutch (e-Clutch) is part of the setup and used to disconnect the combustion engine according to the operation strategy as required.

https://doi.org/10.51202/9783181023549 - Generiert durch IP 216.73.216.36, am 19.01.2026, 02:19:31. © Urheberrechtlich geschützter Inhalt. Ohne gesonderte Erlaubnis ist jede urheberrechtliche Nutzung untersagt, insbesondere die Nutzung des Inhalts im Zusammenhang mit, für oder in KI-Systemen, KI-Modellen oder Generativen Sprachmodellen.

6. Simulation method

The advantage in CO2 emissions (and fuel economy) of this hybrid MT compared to the conventional MT application was investigated. The official WLTC (Worldwide harmonized Light Duty Test Cycle), 3 different RDE (Real Driving Emissions) cycles and also customer related cycles (3D method - Driver, Driven vehicle, Driving environment [4]) have been considered for this analysis. Although the RDE focuses on pollutant emissions (e.g. NOx), it is a valid indication for customer related fuel economy.

The RDE can differ in terms of parameters and dynamics the cycle is based on. This is because of tolerances of RDE trips, so a RDE cycle can be more or less demanding. This leads to a different effect on the emissions and fuel consumption [3]. Fig. 4 shows three different cycles that were defined according to RDE specification and used for fuel economy simulation.

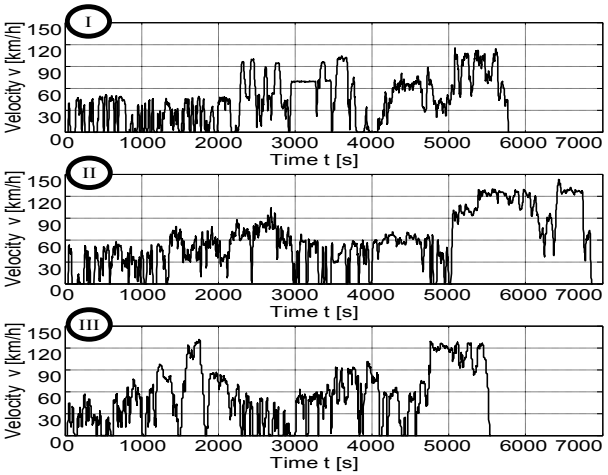


Fig. 4: Valid RDE cycle variant for the simulation [3]

The graph on top (I) represents the RDE cycle with mild vehicle speed profile. The cycle in the middle (II) shows the average case. The lowest course (III) is representative for a more demanding RDE cycle.

https://doi.org/10.51202/9783181023549 - Generiert durch IP 216.73.216.36, am 19.01.2026, 02:19:31. © Urheberrechtlich geschützter Inhalt. Ohne gesonderte Erlaubnis ist jede urheberrechtliche Nutzung untersagt, insbesondere die Nutzung des Inhalts im Zusammenhang mit, für oder in KI-Systemen, KI-Modellen oder Generativen Sprachmodellen.

The basis for the customer related cycles is the 3D method [3], which comprises 3 variations of each:

- Vehicle Load (low, medium, high)
- Driving style (mild, average, sporty)
- Road type (urban, rural, motorway)

Every 3D-combination represents one driver. Each driver uses different representative statistics, e.g. for accelerator and brake pedal position and gradient, gear shifting points as well as engine speed, to represent the different driving behaviors. Every combination of these variations adds up to 27 different customer related fuel consumption values that have been analyzed [4]. A very unique factor when modelling a hybrid MT is the gear shifting operation. While the e-clutch actuation is controlled by algorithm in an optimal way, the gear shifting is performed by the driver solely.

As part of the modelling and parametrization of the 3D model, the Institute of Automotive Engineering of the Technical University Braunschweig executed a driving clinic with 27 test persons and different road profiles using a measurement car with a state of the art manual transmission and clutch system. It was equipped with each a position and a force sensor for clutch pedal and the manual transmission gear shift lever. All clutch actuations and gearshift operations have been recorded, analysed and classified. In order to be able to reproduce the gear shifting profile and the e-Clutch actuation in the simulation model properly and in a realistic way, the launch and gear shifting operations were implemented into the simulation depending on the power requirement. This means various launch and gear shifting operations depending on the customer operating behaviour regarding the driving style have been taken into account as a basis for simulation.

Finally, a parameter study was executed to evaluate the influence on fuel consumption / CO2 emission by varying for example battery size, EM power, EM gear ratio, ambient temperature or 12V grid energy consumption. Especially the influence of the gear ratio of the electric machine was of interest for the transmission layout and design. The ratio was increased to allow the EM to be connected up to 100kph and reduced for a speed up to 180kph.

7. Operation strategy

The operation strategy in a hybrid vehicle is a major control parameter (beside battery size and EM performance) in order to achieve best fuel economy on the one side, but also to guarantee for a “charge sustaining system” on the other side. Moreover, it is also a goal to make use of the electric energy for comfort and customer facing features (like electric parking etc.). The

https://doi.org/10.51202/9783181023549 - Generiert durch IP 216.73.216.36, am 19.01.2026, 02:19:31. © Urheberrechtlich geschützter Inhalt. Ohne gesonderte Erlaubnis ist jede urheberrechtliche Nutzung untersagt, insbesondere die Nutzung des Inhalts im Zusammenhang mit, für oder in KI-Systemen, KI-Modellen oder Generativen Sprachmodellen.

operation strategy defines the coordination of torque between the combustion engine and the electric machine and the direction of electric (power) flow in any driving condition.

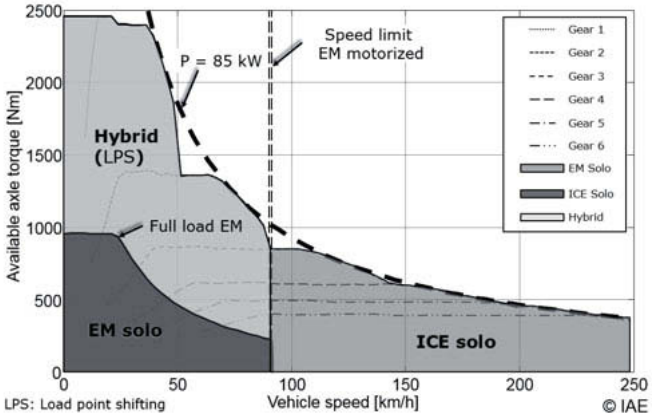


Fig. 5: Modes of operation strategy

The available torque capacity of the components used in this project and the corresponding operating modes are shown in Fig. 5. As already described in “Concept Description” chapter the gear ratio of the electric drive dictates the region were EM can be operated efficiently, in this analysis the limit is at 90kph. Above this operation speed only the combustion engine will be used for propulsion - ICE solo mode. For lower torque demands and below 90kph only EM can be used to propel the vehicle - EM solo mode. The maximum usable EM capacity depends on different factors like temperature (inverter and machine) and battery state of charge (SoC). It is obvious that there are conditions where EM solo mode is not available at all.

Since the concept is based on manual transmission, the driver needs to shift gears even in EM solo mode. Therefore, a strategy needs to be developed to guide the driver (especially when the ICE is switched off), to ensure the transmission input shaft speed never underruns nor exceeds an appropriate value. This is crucial because at any time it might be required to re-couple the ICE to the drivetrain when changing from e-drive-mode to Hybrid- or ICE mode.

The area with higher torque requests is used as a Hybrid mode, that means the combustion engine and the electric machine are working together in order to achieve the best fuel economy. This operating mode is also called Load Point Shifting (LPS).

When the required propulsion torque is low and the ICE would be operating in a low efficient operating point, the electric machine can be used as a generator to charge the battery. This

https://doi.org/10.51202/9783181023549 - Generiert durch IP 216.73.216.36, am 19.01.2026, 02:19:31. © Urheberrechtlich geschützter Inhalt. Ohne gesonderte Erlaubnis ist jede urheberrechtliche Nutzung untersagt, insbesondere die Nutzung des Inhalts im Zusammenhang mit, für oder in KI-Systemen, KI-Modellen oder Generativen Sprachmodellen.

additional torque moves the operating point of the ICE to a fuel efficient point with higher torque. On the other way around, if high propulsion power is required, the EM can work as a motor and add power. With this, the ICE torque and thus CO2 emissions can be reduced. For every ICE engine speed there exists an optimum torque regarding the efficiency. Based on the SoC, the requested torque by the driver as well as the torque capacity, the operating strategy algorithm calculates a factor called k_{opt}. This factor determines the range the ultimate torque is shifted to between the ICE's requested torque and the optimum torque regarding the efficiency. The factor k_{opt} is shown in Fig. 6.

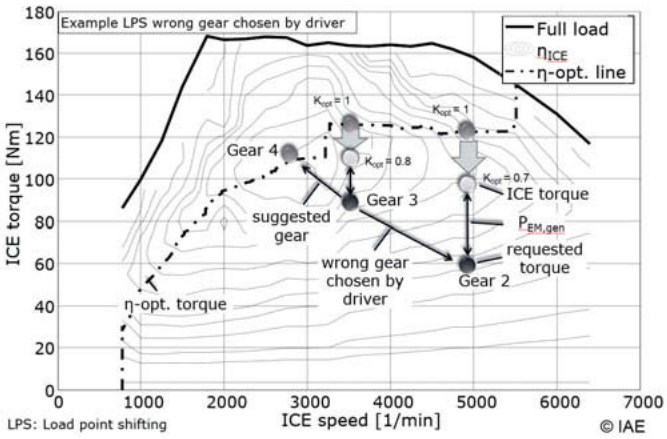


Fig. 6: Effect of load point shifting strategy

The transition process between all three modes – EM solo, Hybrid and ICE solo – is realized in combination with hysteresis in order to prevent high frequency shifting between the modes. While combined with an automatic transmission, the operating point of the ICE can be optimized not only by shifting the load but also with changing the gear, in the manual transmission application the driver might not follow the shift indication command and skip the shifting operation or even shift into a wrong gear (e.g. to high engine speed). Thus the LPS function gains more importance for fuel consumption reduction in driver's hand.

Fig. 6 shows an example where a driver selects 3rd gear. Shifting into 4th gear would move the ICE to the optimum load point and is indicated as recommended gear. Instead the 2nd gear is selected wrongly by the driver. With the Load Point Shifting functionality the engagement of the wrong gear is at least partially compensated.

https://doi.org/10.51202/9783181023549 - Generiert durch IP 216.73.216.36, am 19.01.2026, 02:19:31. © Urheberrechtlich geschützter Inhalt. Ohne gesonderte Erlaubnis ist jede urheberrechtliche Nutzung untersagt, insbesondere die Nutzung des Inhalts im Zusammenhang mit, für oder in KI-Systemen, KI-Modellen oder Generativen Sprachmodellen.

Brake blending

One major goal of a hybrid propulsion system is to make a maximum use of kinetic energy that would be wasted in a conventional powertrain during braking. Therefore, the aim is to apply generator torque at any time the driver uses the brake pedal to slow down the car.

The strategy for recuperation during breaking with an MT-hybrid basically is comparable to an AT application. Within this project, a simplified approach was used. The brake-system was calibrated in the simulation model in a way that there is a free travel in the first 15% brake pedal travel before the mechanical brakes are activated. Within this free travel the EM generating torque is applied. From driving quality perspective, this methodology is not a preferred one, but it ensures that in any maneuver the friction brakes are only active when the EM braking capacity is not sufficient to obtain the desired deceleration and thus a maximum energy recuperation is achieved.

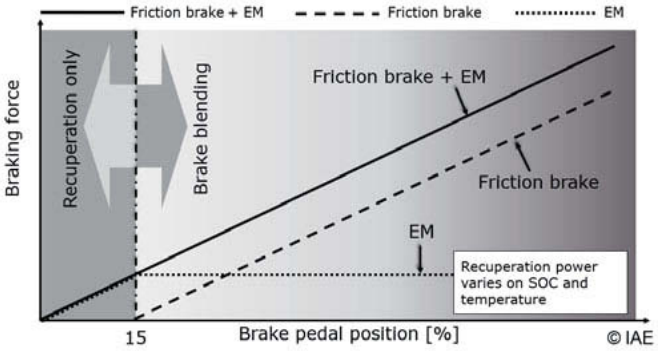


Fig. 7: Brake blending strategy

8. Fuel Consumption Results

WLTC: The simulation results in a fuel consumption for the selected base application of 5,61L/100km or an equivalent CO2 emission of 133,5g/km. This value is close to the reference base car and appears to be very realistic. The hybrid vehicle achieved with 4,43L/100km or 105,4g CO2/km a reduction of 21,1%. This relative improvement indicates a very promising capability of the mild hybrid system.

RDE: 3 RDE cycles with different power demands have been investigated. The achieved fuel consumption / CO2 reduction is varying between 11,5% (@4,46L/100km) and 22,1%

https://doi.org/10.51202/9783181023549 - Generiert durch IP 216.73.216.36, am 19.01.2026, 02:19:31. © Urheberrechtlich geschützter Inhalt. Ohne gesonderte Erlaubnis ist jede urheberrechtliche Nutzung untersagt, insbesondere die Nutzung des Inhalts im Zusammenhang mit, für oder in KI-Systemen, KI-Modellen oder Generativen Sprachmodellen.

(@6,01L/100km). Especially the cycle with higher loads is affected by the hybrid system and shows significant higher reduction capability.

Customer statistic: The 3D model, as described in chapter “Simulation method“, shows a wide spread of fuel economy results. The best improvement is obtained with a sporty driving style in an urban cycle (-36,5%), whereas the lowest absolute consumption with the hybrid can be achieved by a mild driving style on a rural road with 3,95L/100km, which is an improvement of 11,5%. As expected, the reduction of fuel consumption and CO2 on a motorway is very low, or even negative for an average driver, since the negative impact of the additional weight and friction caused by the hybrid system components predominates the limited opportunity to re-cuperate energy when driving with constant speed and only low driving dynamics.

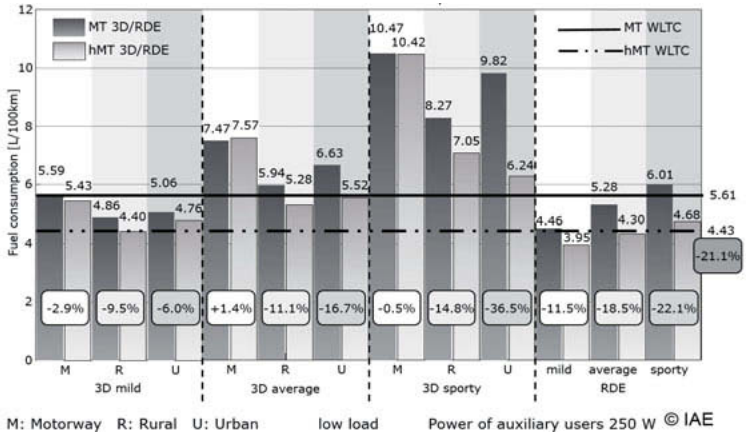


Fig. 8: Simulation result - Fuel Consumption WLTC/RDE/3D model

The influence of the EM’s gear ratio, which was investigated within a parameter study, is not a significant value but can be obtained with a relative increase of fuel consumption up to 1,59% for the selected parameter range.

9. Transmission Load Results

In order to be able to compare the transmission loads of the hMT and MT with each other and to identify the most critical driver for the gearbox, the load spectra are taken into account. Thus, the Wöhler line plays an important role when looking at the damage resulted due to loads. In order to cover a wide range of failure mechanisms in the transmission two different Wöhler lines have been used, one with low exponential and another one with high exponential. In a

https://doi.org/10.51202/9783181023549 - Generiert durch IP 216.73.216.36, am 19.01.2026, 02:19:31. © Urheberrechtlich geschützter Inhalt. Ohne gesonderte Erlaubnis ist jede urheberrechtliche Nutzung untersagt, insbesondere die Nutzung des Inhalts im Zusammenhang mit, für oder in KI-Systemen, KI-Modellen oder Generativen Sprachmodellen.

double logarithmic diagram – overrolling cycles on the x-axis and torque on the y-axis – a low exponential results in a steep Wöhler line whereas high exponentials lead to a flat line. Thus, flatter course will focus on the higher torque parts and lower impact of low torque areas while steeper courses of the Wöhler line take the lower part torque into account as well.

This sensitivity study shows, that the range the Wöhler line varies in, does not influence the statements on the most critical driver. The following Fig. 9 shows the results for the damaging of the gear input shaft.

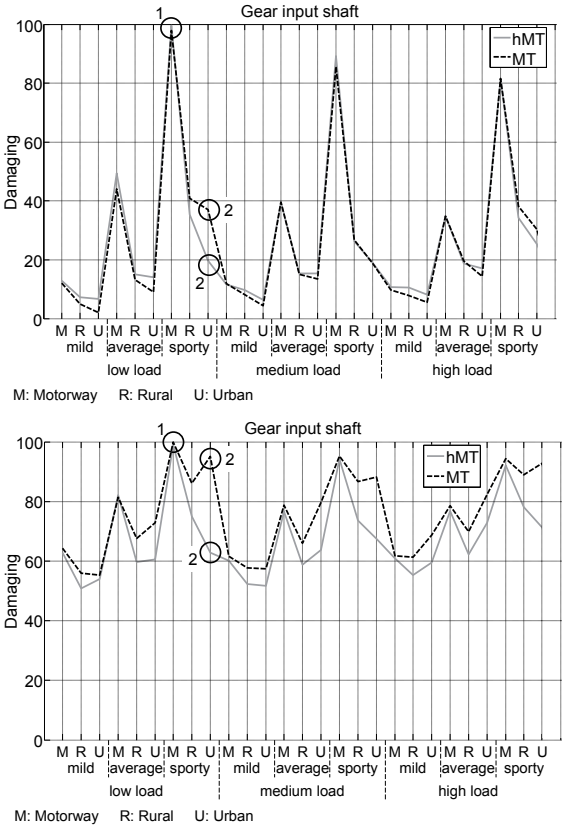


Fig. 9: Damage based on “Wöhler” curve with high exponential (left) vs low exponential (right)

https://doi.org/10.51202/9783181023549 - Generiert durch IP 216.73.216.36, am 19.01.2026, 02:19:31. © Urheberrechtlich geschützter Inhalt. Ohne gesonderte Erlaubnis ist jede urheberrechtliche Nutzung untersagt, insbesondere die Nutzung des Inhalts im Zusammenhang mit, für oder in KI-Systemen, KI-Modellen oder Generativen Sprachmodellen.

Generally, Fig. 9 shows that the minimum and maximum damaging differ in a wide percentage range for the gear input shaft. Both Wöhler lines are created in a way that the most critical driver causes a damaging of 100 %. By doing so, it is possible to directly compare the 27 different driver behaviours investigated within the 3D method with each other as well as to compare the damaging of the drivers with the two Wöhler lines. Fig. 9 shows that for both Wöhler lines the most critical driver does not change. In particular, it is the sporty driver on motorways with a vehicle with low load. Regarding the vehicle load, higher vehicle load results in lower damaging. This is due to the 3D statistics. For example, the gear shifting speed is different for a vehicle with low and high load.

In the following the most critical customer driver, marked in Fig. 9 with 1, and the driver with the highest damaging difference between the MT and hMT, marked in Fig. 9 with 2, are compared with each other in terms of their load spectra. This is shown in Fig. 10 where the overrolling cycles are calculated for 300000 km.

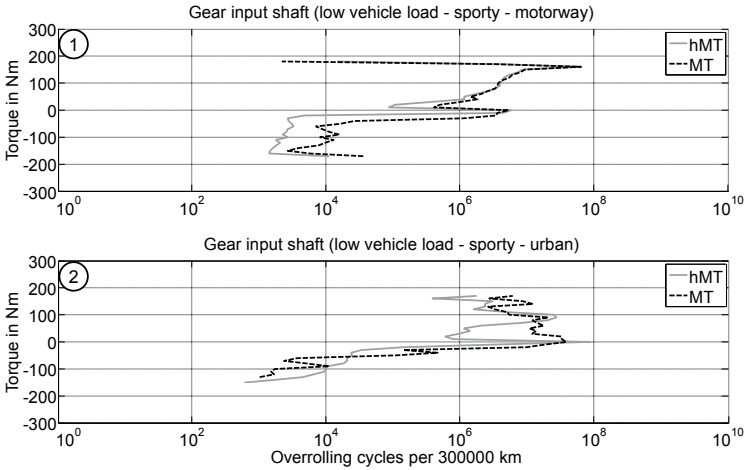


Fig. 10: Load spectra for the gear input shaft of the hMT and MT

The upper part of Fig. 10 shows the first comparison for the gear input shaft of the hMT and MT related to point 1 marked in Fig. 9. The traction load spectrum does not show any significant differences but at low torque (area between approx. 0 and 80 Nm). This is caused by launching in EV mode with the ICE turned off. Still this low torque only has a minor effect due to its low overrolling cycles compared to the Wöhler lines high cycle fatigue. Negative torque range is

https://doi.org/10.51202/9783181023549 - Generiert durch IP 216.73.216.36, am 19.01.2026, 02:19:31. © Urheberrechtlich geschützter Inhalt. Ohne gesonderte Erlaubnis ist jede urheberrechtliche Nutzung untersagt, insbesondere die Nutzung des Inhalts im Zusammenhang mit, für oder in KI-Systemen, KI-Modellen oder Generativen Sprachmodellen.

lower for the hMT due to more phases the ICE is turned off and thus not being dragged. These differences are not significant because of the low overrolling cycles.
The lower part in Fig. 10 shows the gear input shaft load spectrum with the biggest difference in damaging of the MT and hMT with point 2 marked in Fig. 9 (sporty driver, urban, low vehicle load). One reason for the differences in damaging are due to lower load for the hMT in torque range between 0 and 100 Nm at higher overrolling cycles. These are due to EV mode in urban areas so the ICE is turned off and no load is applied on the transmission input shaft. Another reason for the damaging differences is based on launching events. The hMT, when SOC is high enough, launches the vehicle in EV mode and starts the ICE when the load is too high to be applied by the EM alone. At the point of time the ICE is turned on, the vehicle has already accelerated. On the contrary, the MT launches the vehicle by the ICE only. The process of engaging the clutch takes time while the hMT, for the same launching event, has already accelerated and gained speed after the same time has passed. The sporty MT driver would accelerate the vehicle in the lower gears for a longer time to reach a certain vehicle speed at the same time the hMT does

The following Fig. 11 represents the damaging of the hMT compared to the MT with two different Wöhler lines for the gear output shaft. The most critical driver for the gear output shaft is the sporty driver in urban areas with a low load vehicle. One of the main aims of the hMT study was to identify whether the gearbox of the conventional vehicle can be used for the hMT without modifications for durability. Thus no boosting functionality was applied in the operating strategy. With the results shown in Fig. 11 the gear output shaft load behaviour is the basically the same for the hMT as it is for the MT.

https://doi.org/10.51202/9783181023549 - Generiert durch IP 216.73.216.36, am 19.01.2026, 02:19:31. © Urheberrechtlich geschützter Inhalt. Ohne gesonderte Erlaubnis ist jede urheberrechtliche Nutzung untersagt, insbesondere die Nutzung des Inhalts im Zusammenhang mit, für oder in KI-Systemen, KI-Modellen oder Generativen Sprachmodellen.

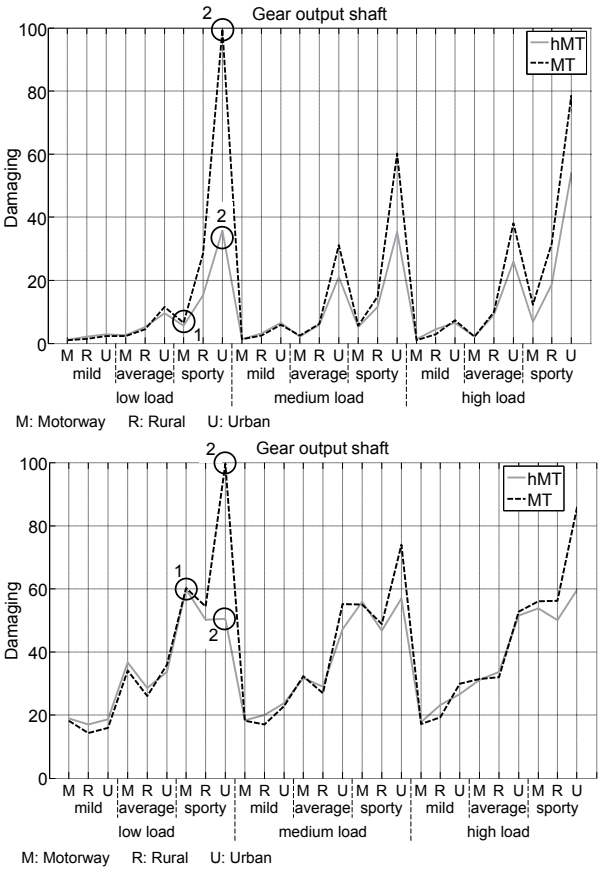


Fig. 11: Damage based on “Wöhler” curve with high exponential (left) vs low exponential (right)

Finally, the load spectra of the hMT and MT for point 1 and point 2 marked in Fig. 11 are shown in Fig. 12 (low vehicle load – sporty – motorway).

https://doi.org/10.51202/9783181023549 - Generiert durch IP 216.73.216.36, am 19.01.2026, 02:19:31. © Urheberrechtlich geschützter Inhalt. Ohne gesonderte Erlaubnis ist jede urheberrechtliche Nutzung untersagt, insbesondere die Nutzung des Inhalts im Zusammenhang mit, für oder in KI-Systemen, KI-Modellen oder Generativen Sprachmodellen.

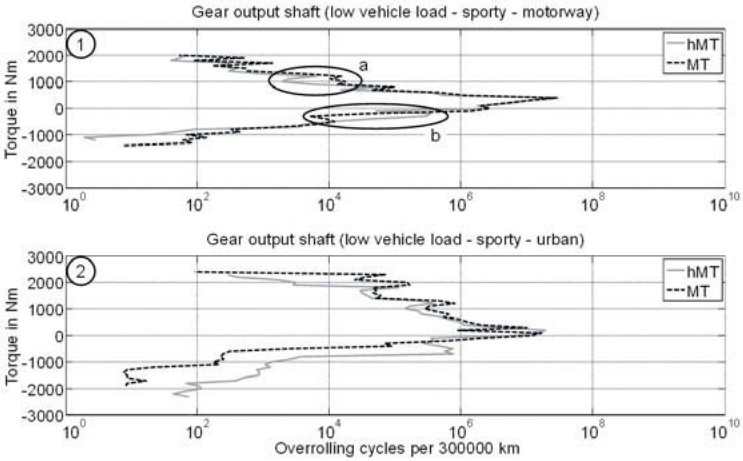


Fig. 12: Load spectra of the gear output shaft for the hMT and MT

As presented in the upper part of Fig. 12, the main differences in the load spectra can be seen in areas of negative torque at the gear output shaft between 0 and -500 Nm (Fig. 12 @b) and in the traction range between 500 and 1250 Nm (Fig. 12 @a). The differences in point 1 result from the hMT being capable of recuperation. Negative torque in the MT-application at the gear output shaft is caused by ICE dragging. The differences in point 2 are based on the process of launching events. At this point, statistically the sporty motorway driver has only very few launching events per 100 km. Still the fact of different launching process applies as already mentioned above. The lower part of Fig. 12 represent the load spectra for the sporty driver in urban areas with a vehicle with low load. Due to more launching and braking events in urban areas compared to driving on a motorway, the positive and negative torque differences are more significant. Thus the damaging differences are higher. The explanations apply as it does for the upper part of Fig. 12.

10. Conclusion

The P3 architecture for a hybrid manual transmission is a proper choice in terms of efficiency, package and effort. In combination with a 25kWp electrical motor and the applied operation strategy, the fuel consumption improvement opportunity is more than 20% in the WLTC compared to a similar conventional C-segment vehicle. The forecasted improvement in customer hand is even higher, based on statistical data used for this analysis.

https://doi.org/10.51202/9783181023549 - Generiert durch IP 216.73.216.36, am 19.01.2026, 02:19:31. © Urheberrechtlich geschützter Inhalt. Ohne gesonderte Erlaubnis ist jede urheberrechtliche Nutzung untersagt, insbesondere die Nutzung des Inhalts im Zusammenhang mit, für oder in KI-Systemen, KI-Modellen oder Generativen Sprachmodellen.

Use cases come along with hybridization do not lead to higher absolute loads. In certain operation conditions, like in generator mode, the load is different compared to a conventional manual transmission and needs to be assessed more in detail for the affected components.
Further advantage of this setup is the ability to drive electrically in both directions without the need to shift gears. Features like autonomous park assist can be supported even with a manual transmission, which makes this technology more attractive to customers. In addition, propulsion torque is possible during gear shifts, providing the opportunity for driving comfort improvement during gear shifts on manual and automated manual transmission (AMT) systems.

[1] IHS Markit statistic

[2] Werra, M.; Ringleb, A.; Müller, J.; Prof. Dr.-Ing. Küçükay: Topology Comparison of 48V drivetrains with manual transmission; TU Braunschweig, Institute of Automotive Engineering; 17th CTI Symposium

[3] Ringleb, A.; Prof. Dr.-Ing. Küçükay, F.: Representative driving cycles for Real Driving Emissions; TU Braunschweig, Institute of Automotive Engineering; Hybrid And Electric Vehicles, 14th Symposium, Braunschweig; 2017.

[4] Prof. Dr.-Ing. Küçükay, F.: Repräsentative Erprobungsmethoden bei der Pkw-Getriebeentwicklung; VDI Berichte Nr. 1175; 1995;

https://doi.org/10.51202/9783181023549 - Generiert durch IP 216.73.216.36, am 19.01.2026, 02:19:31. © Urheberrechtlich geschützter Inhalt. Ohne gesonderte Erlaubnis ist jede urheberrechtliche Nutzung untersagt, insbesondere die Nutzung des Inhalts im Zusammenhang mit, für oder in KI-Systemen, KI-Modellen oder Generativen Sprachmodellen.

https://doi.org/10.51202/9783181023549 - Generiert durch IP 216.73.216.36, am 19.01.2026, 02:19:31. © Urheberrechtlich geschützter Inhalt. Ohne gesonderte Erlaubnis ist jede urheberrechtliche Nutzung untersagt, insbesondere die Nutzung des Inhalts im Zusammenhang mit, für oder in KI-Systemen, KI-Modellen oder Generativen Sprachmodellen.

Low-cost DCT for emerging markets incl. 48 V hybridization

Dr.-Ing. **Gereon Hellenbroich**, FEV Europe GmbH, Aachen

Kurzfassung

Nach den Handschaltgetrieben und den automatisierten Schaltgetrieben sind die Doppelkupplungsgetriebe (DCT) der nächste logische Entwicklungsschritt bei den automatischen PKW-Getrieben für aufstrebende Wachstumsmärkte, da sie einerseits durch ihre Lastschaltfähigkeit den Komfort steigern und andererseits auf denselben Fertigungstechnologien basieren. Gleichzeitig werden auch in diesen Märkten hybridisierte Getriebevarianten immer wichtiger. Dabei werden niedrige Kosten der Schlüssel zum Erfolg sein, sowohl bei den Herstellungskosten wie auch bei den Gesamtkosten über Lebensdauer. Dieses Ziel kann durch kostenoptimierte Doppelkupplungs- und Aktuierungssysteme, spezielle Radsatzkonzepte und einen kostengünstigen, modularen 48 V-Hybridisierungsansatz erreicht werden. Basierend auf dem 7-xDCT-Radsatzkonzept der FEV wurde eine modulare DCT-Architektur mit einer einzigartigen Hybridisierungslösung entwickelt, welche eine Kombination aus P2.5- und P3-Funktionalität bietet und einen maximalen Gleichteileansatz zwischen konventioneller und hybridisierter Getriebevariante verfolgt. Die Getriebelänge ist dabei für beide Varianten identisch und liegt zwischen 330 mm und 355 mm, je nachdem ob ein nass- oder trockenlaufendes Kupplungssystem zum Einsatz kommt. Diese Werte stellen Bestwerte im Bereich der hybridisierten Doppelkupplungsgetriebe dar.

Abstract

Following manual transmissions and AMTs, dual clutch transmissions (DCT) are the logical next development step in automatic passenger car transmissions for emerging markets, as they offer increased comfort due to their powershift capability and share the same base manufacturing technologies. At the same time, hybrid options are also becoming an important feature for these markets. The key to success will be low costs, both in terms of manufacturing and total cost of ownership. Enablers for this are a low cost dual clutch and actuation system, a low complexity gearset and a modular, low cost 48 V hybrid option. Based on FEV's 7-xDCT concept, a modular DCT architecture was developed which includes a unique, add-on hybrid solution that offers both P2.5 and P3 functionalities with maximum commonality between the conventional and hybrid variants. The overall transmission length for both the conventional and

https://doi.org/10.51202/9783181023549 - Generiert durch IP 216.73.216.36, am 19.01.2026, 02:19:31. © Urheberrechtlich geschützter Inhalt. Ohne gesonderte Erlaubnis ist jede urheberrechtliche Nutzung untersagt, insbesondere die Nutzung des Inhalts im Zusammenhang mit, für oder in KI-Systemen, KI-Modellen oder Generativen Sprachmodellen.

hybrid variant is between 330 mm (wet clutch version) and 355 mm (dry clutch version), making it easily the most compact hybrid DCT solution available.

Introduction and market trends

Automated manual transmissions (AMT) have become popular in emerging markets, especially in India. Their additional comfort by relieving the driver from clutch pedal operation during heavy traffic is appreciated by many customers. The inherent torque interruption during gear shifts, which prevented the AMT from becoming a success in Europe, did not prevent the success of AMTs in these markets up to now. Still, customers frequently complain about the shift comfort of AMT solutions. Therefore, it has to be expected that also emerging markets will want to move to transmission solutions with powershift capability in the future.

Dual clutch transmissions (DCT) are the logical next step for these markets, as they use the same base manufacturing technologies as the current manual transmissions and AMTs. New, complex subsystems such as the dual clutch unit can be purchased from Tier-1s, at least for the first generation of products. The key to success will be low costs, both in terms of manufacturing and total cost of ownership. Existing DCT products do not fulfill this core requirement yet. In order to do so, FEV has developed a DCT concept which is focusing on simplicity and modularity.

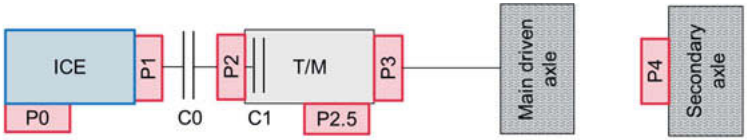
Key enablers are:

- A low cost dry dual clutch system
    - to avoid the cost of auxiliary components such as oil pumps and filter
    - to guarantee serviceability outside an OEM dealer network
- A low complexity gearset with particularly short 1st gear ratio
    - to reduce the stress on the dry dual clutch during frequent stop and go traffic
    - to improve launch and creep quality and robustness
- A simple single shift drum actuation solution for shift forks and park lock system
    - To reduce the number of actuators and corresponding follow-up costs on control unit level
- Design-protection for a future modular, low cost 48 V hybrid solution

https://doi.org/10.51202/9783181023549 - Generiert durch IP 216.73.216.36, am 19.01.2026, 02:19:31. © Urheberrechtlich geschützter Inhalt. Ohne gesonderte Erlaubnis ist jede urheberrechtliche Nutzung untersagt, insbesondere die Nutzung des Inhalts im Zusammenhang mit, für oder in KI-Systemen, KI-Modellen oder Generativen Sprachmodellen.

Hybrid architectures

When hybridizing a powertrain, different architectures with different function sets can be considered. Desirable hybrid functions do include charge at standstill, boosting, recuperation, all-electric operation (maneuvering or driving depending on available power level and battery capacity) as well as combustion engine restart from either standstill, engine-off sailing or all-electric operation. However, the available functions do depend on the architecture of the hybrid powertrain. Potential hybrid architectures are shown in Fig. 3 and range from P0 to P4:



P0: On front sinde of engine (e.g. BSG)
P1: On flywheel of engine, e.g. MB S400e
P2: On transmission input, e.g. MB E-Class, VW, BMW-ZF, HMC
P3: On transmision output
P2.5: Connected to one branch of DCT, e.g Getrag concepts (Torque split hybrid)
P4: On secondary axle, e.g. PSA

Fig. 1: Overview Hybrid Architectures

P0 and P1 architectures offer a similar function set: As the electric motor cannot be decoupled from the combustion engine, all-electric maneuvering or driving is not possible and recuperation potential is limited. The P2 and P2.5 concepts can generally provide all functions. P3 and P4 cannot perform combustion engine start from standstill and charge at standstill as the electric motor is directly coupled to the wheels. In addition, P3 and P4 architectures typically only feature a single gear ratio for the electric motor, with which the entire operating speed range of the vehicle needs to be covered. This results in a long gear ratio for the electric motor, limiting torque amplification and all-electric driving performance. Most of the described architectures can be combined with different automatic transmission concepts, while the P2.5 concept is unique to dual clutch transmissions (DCTs).

Hybridization of front-wheel drive transmissions

The vast majority of today's cars are based on front-wheel-drive platforms with transversally installed internal combustion engines, for which the integration of the hybrid components, es-

https://doi.org/10.51202/9783181023549 - Generiert durch IP 216.73.216.36, am 19.01.2026, 02:19:31. © Urheberrechtlich geschützter Inhalt. Ohne gesonderte Erlaubnis ist jede urheberrechtliche Nutzung untersagt, insbesondere die Nutzung des Inhalts im Zusammenhang mit, für oder in KI-Systemen, KI-Modellen oder Generativen Sprachmodellen.

pecially the electric motor, presents a huge challenge in packaging. For most of the applications, the powertrain length and thus the transmission length is already maxed out for the conventional, non-hybrid powertrains. It is therefore the target to develop hybrid transmission variants without increasing the transmission length. For the hybridization of torque converter based transmissions such as conventional automatic transmissions, one common solution is the replacement of the torque converter by an electric machine. Together with the addition of a disconnect clutch, such a modification will result in a P2 hybrid architecture with virtually no length increase and only minor modifications to the base transmission.

Concepts for DCT hybridization

Dual clutch transmissions (DCTs) have become hugely successful in both the Chinese and European markets during the past decade. In order for the DCTs to remain successful and based on the market trends mentioned before, cost effective and modular hybrid variants are required, preferably with the function set of either P2 or P2.5 architectures. However, compared to torque converter based transmissions, hybridization of DCT presents an unequally bigger challenge: For a P2 hybridization, the electric machine and the disconnect clutch are additional components, the dual clutch is still required and cannot be replaced like the torque converter of the automatic transmission. In order to limit the length increase, the three clutches and the electric machine need to be highly integrated, which mean a new, costly clutch development is required for the hybrid version. Sometimes, even the number of speeds needs to be reduced (e.g. from 7 to 6) in order to save length. The Volkswagen DQ400e is an example for such an approach, Fig. 4. While the length increase due to hybridization is moderate, the transmission has only low commonality with other conventional Volkswagen DCTs, featuring a unique triple clutch arrangement, unique 6-speed gear cluster and unique housings.

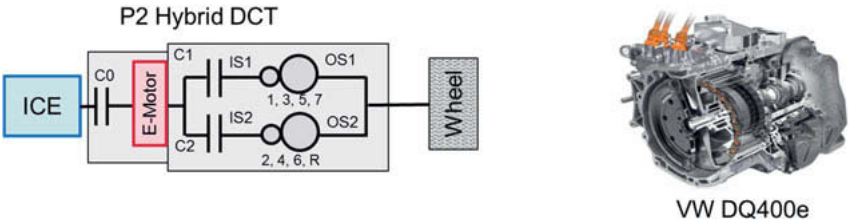


Fig. 2: Concepts for DCT hybridization: P2 hybrid

https://doi.org/10.51202/9783181023549 - Generiert durch IP 216.73.216.36, am 19.01.2026, 02:19:31. © Urheberrechtlich geschützter Inhalt. Ohne gesonderte Erlaubnis ist jede urheberrechtliche Nutzung untersagt, insbesondere die Nutzung des Inhalts im Zusammenhang mit, für oder in KI-Systemen, KI-Modellen oder Generativen Sprachmodellen.

For the P2 hybrid variant within FEV's 7DCT family [1], only the dual clutch unit is replaced by a triple clutch arrangement within the rotor of an electric machine, while the rear housing with all internals remains completely unchanged compared to the conventional version. Although this approach is more modular compared to VW's one, it also comes with a length increase of 60 mm to 70 mm compared to the conventional version. And still, a dedicated (and therefore costly) triple clutch system including electric motor has to be developed only for the hybrid version.

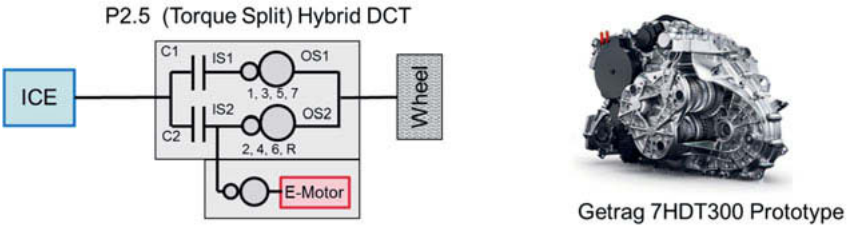


Fig. 5: Concepts for DCT hybridization: P2.5 hybrid

Another concept for the hybridization of dual clutch transmissions is the P2.5 or "Torque-Split" hybrid, for which the electric machine is arranged in parallel to the transmission and connected to one of the input shafts. One example for this architecture is the Getrag 7HDT300, Fig. 5. Theoretically, only minor hardware modifications are required on the base transmission and there is no length increase, which are the key benefits of this architecture. Especially the dual clutch unit of the transmission can remain unchanged. However, there are challenging influences on the operating strategy of the transmission

Challenges of P2.5 hybrid architectures

First of all, the electric motor must actively synchronize all gear shifts on its branch as typical synchronizer units have not been designed to deal with the additional inertia of the electric motor. In order to perform the active synchronization with the required performance, the battery must be able to boost and charge at peak power. This can be a challenge especially at cold temperatures, where most Li-Ion batteries only provide reduced boost and charge powers.

One more conflict does exist between the operation of the transmission itself and the operating strategy of the hybrid system. It is desired for the hybrid strategy to have permanent access to the electric machine for charging and boosting. This is impossible to guarantee when there is a lot of gear shifting activity, with almost no time between shifts to get into either boost or

https://doi.org/10.51202/9783181023549 - Generiert durch IP 216.73.216.36, am 19.01.2026, 02:19:31. © Urheberrechtlich geschützter Inhalt. Ohne gesonderte Erlaubnis ist jede urheberrechtliche Nutzung untersagt, insbesondere die Nutzung des Inhalts im Zusammenhang mit, für oder in KI-Systemen, KI-Modellen oder Generativen Sprachmodellen.

charge mode with the electric motor. At the same time, the frequent ramps in and out of charge mode do also increase the dynamics and torque gradients for the combustion engine, which can be an additional challenge for engine emissions.
Last but not least, the recuperation during coast down needs to be interrupted two times for the down shifts in the transmission branch to which the electric motor is connected. In order to mask these interruptions for the driver, a brake-by-wire system is mandatory.

Modified hybrid architecture proposed by FEV

In order to avoid the described challenges associated with the P2.5 hybrid architecture, FEV proposes to use a combination of P2.5 and P3 architectures. In P2.5 mode, all the described functionality is available, including torque amplification for electric driving and maneuvering by using one of the lower gears of the DCTs. In P3 mode, the electric motor is directly coupled to the wheels. In this mode, the operating point of the electric motor can be chosen independently of the operation of the DCT itself. By using the combination of both modes, all the critical operating conditions of both P2.5 and P3 architectures can be effectively avoided.
Of course, now a compact mechanical layout is required that provides the desired functionality without voiding the package boundaries of typical front wheel drive architectures. In a straight forward approach, an additional shaft (called “auxiliary” or “aux” shaft) with a synchronizer or dog clutch unit on it can be added to the transmission. An off-axis electric motor, similar to the ones used for P2.5 architectures, is connected to this shaft by means of a gear or chain drive. In one shift position, the shaft and thus the electric motor is coupled to one of the DCT’s input shafts, effectively providing the P2.5 functionality. In a second shift position, the shaft is coupled directly to the differential, effectively providing the P3 functionality by forming an additional output shaft. With this approach, typically also an additional neutral position is created for the electric motor. This neutral position can be used to decouple the electric motor completely e.g. during extended highway driving without charge demand, thus reducing spinning and friction losses. The neutral function also provides functional safety benefits, as the electric motor can be decoupled in the event of a technical defect.

https://doi.org/10.51202/9783181023549 - Generiert durch IP 216.73.216.36, am 19.01.2026, 02:19:31. © Urheberrechtlich geschützter Inhalt. Ohne gesonderte Erlaubnis ist jede urheberrechtliche Nutzung untersagt, insbesondere die Nutzung des Inhalts im Zusammenhang mit, für oder in KI-Systemen, KI-Modellen oder Generativen Sprachmodellen.

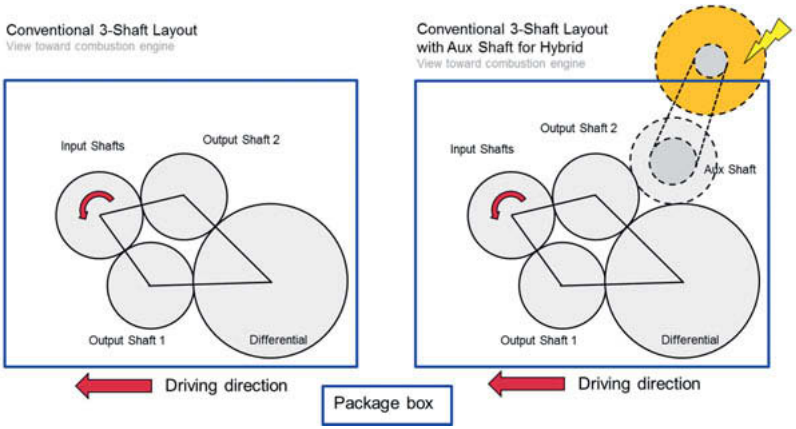


Fig. 6: Hybridization of three-shaft transmission

The left part of Fig. 6 shows a side view of a transmission with a typical three-shaft layout. Such a layout is commonly used for dual clutch transmissions with up to 7 forward speeds. However, it is visible that it is not possible to package both an auxiliary shaft and the electric motor inside the (simplified) package box. In fact, the shown position of the auxiliary shaft would also result in a conflict in terms of rotation directions. Conventional three-shaft layouts are therefore not suitable for the described approach with the auxiliary shaft.

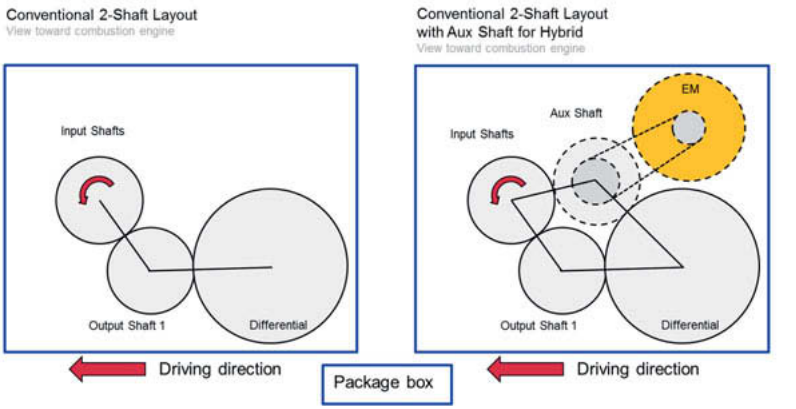


Fig. 7: Hybridization of two-shaft transmission

https://doi.org/10.51202/9783181023549 - Generiert durch IP 216.73.216.36, am 19.01.2026, 02:19:31. © Urheberrechtlich geschützter Inhalt. Ohne gesonderte Erlaubnis ist jede urheberrechtliche Nutzung untersagt, insbesondere die Nutzung des Inhalts im Zusammenhang mit, für oder in KI-Systemen, KI-Modellen oder Generativen Sprachmodellen.

The left part of Fig. 7 shows a side view of a typical two-shaft transmission layout. Such a layout can be used for DCTs up to five forward speeds, one example being the 5DCT150 of FEV [2]. As there is no second, upper output shaft, this kind of layout provides enough package space for an additional auxiliary shaft with the electric motor being placed e.g. above the differential ring gear, which is shown on the right side. However, with this layout, all speeds have to be driven through the single output shaft. Therefore and due to restrictions in overall transmission length, this kind of layout is limited to 5 forward speeds plus reverse.

FEV's 7-xDCT combined hybrid

In order to achieve the combined P2.5 and P3 functionality together with a base DCT layout of more than 5 forward speeds, the gearset architecture of the FEV 7-xDCT can be favorably applied. This architecture features a single output shaft and only three synchronizer units, but still achieves 6 to 7 forward speeds by using so-called "generated" gears [3]. A short intermediate shaft is used to optionally couple the two input shafts for the generation of speeds 1, 4 and 7. As this shaft is not linked to the differential, it can be placed below the input shaft and does not take up the space that is required for the auxiliary shaft and electric motor. Therefore, the xDCT architecture allows to package the electric motor just like a two-shaft layout does, while offering up to 7 forward speeds, for which otherwise a three-shaft layout would be necessary. Fig. 8 shows the resulting stick diagram including the auxiliary shaft for the hybrid functionality.

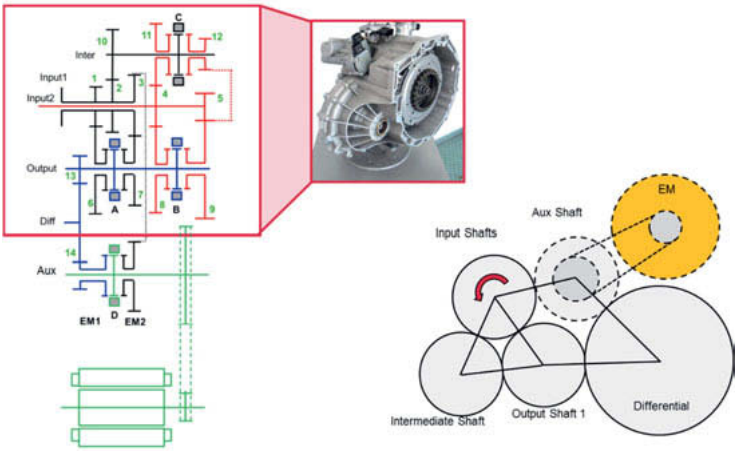


Fig. 8: 7-xDCT hybrid with P2.5 - N - P3 functionality

https://doi.org/10.51202/9783181023549 - Generiert durch IP 216.73.216.36, am 19.01.2026, 02:19:31. © Urheberrechtlich geschützter Inhalt. Ohne gesonderte Erlaubnis ist jede urheberrechtliche Nutzung untersagt, insbesondere die Nutzung des Inhalts im Zusammenhang mit, für oder in KI-Systemen, KI-Modellen oder Generativen Sprachmodellen.

The gearset part of the non-hybrid 7-xDCT (boxed area) remains completely unchanged. It is a very compact gearset with only 4 gear planes in length, resulting in an overall transmission length of 330 mm to 355 mm depending on the chosen dual clutch system, shorter than any other DCT gearset on the market. The “Aux” shaft including the shift element D, the two idler gears EM1 and EM2 and the electric motor with its connection can be modularly added to convert the conventional transmission into a hybrid variant. As the 7-xDCT only uses 3 synchronizer units, the mechanical complexity including the hybrid-specific components is not higher than the one of other conventional DCTs. Due to the generation of gears 1, 4 and 7, the original 7-xDCT layout uses a more complex power shift type (called “supported shift”, [3]) for the 3 to 4 upshift. If this is not desired, this functional drawback can be avoided easily by adjusting the gear ratios and shift schedule and thereby going down to 6 forward speeds, then with a completely conventional DCT shift schedule. For the hybrid variant, the 7 speeds can be kept as the drawbacks can be masked completely be the addition of the electric motor.

7-xDCT 48 V hybrid design details

The conventional version of 7-xDCT uses an available, electro-mechanically actuated dry dual clutch system and has been built and successfully tested as a prototype [4]. Based on the same gearset for up to 280 Nm input torque, which has proven to be both very robust and good in NVH, the 48 V hybrid version was designed. Fig. 9 shows the current design status, next to the conventional version of the transmission.

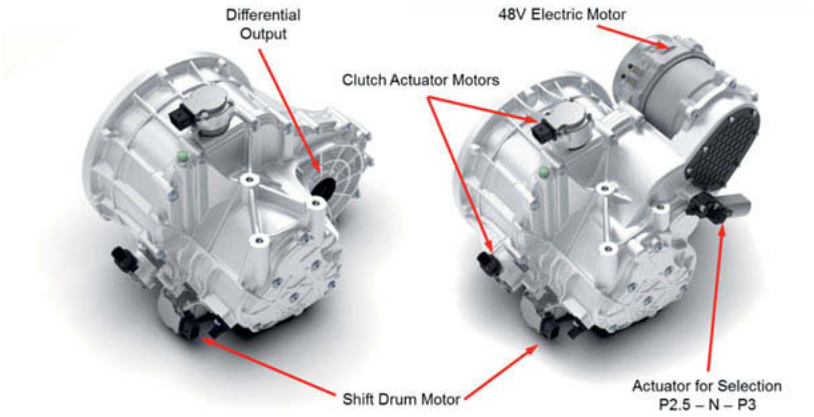


Fig. 9: 7-xDCT conventional and 48 V hybrid versions, outside view

https://doi.org/10.51202/9783181023549 - Generiert durch IP 216.73.216.36, am 19.01.2026, 02:19:31. © Urheberrechtlich geschützter Inhalt. Ohne gesonderte Erlaubnis ist jede urheberrechtliche Nutzung untersagt, insbesondere die Nutzung des Inhalts im Zusammenhang mit, für oder in KI-Systemen, KI-Modellen oder Generativen Sprachmodellen.

As explained before, the electric motor has been arranged above the differential. It is standard, stand-alone 48 Volt motor which is bolted to a modified rear housing. Also, the additional actuator motor for the P2.5-N-P3 selection is visible. With the current gear layout, the maximum total gear ratio for the electric motor in P2.5 mode is larger than 25. Even with the moderate peak torques of 48 V electric motors, this ratio ensures sufficient wheel torque for electric launching, maneuvering and low speed electric driving. In P3 mode, the total ratio is around 7, which allows to use the electric motor across the entire speed range of the vehicle.

Fig. 10 reveals more internals of the transmission. The electric motor is coupled to the auxiliary shaft by a chain drive. Compared with gear drives including an idler gear, this solution is more tolerant with regard to center distances and can help to reduce NVH challenges. The three shift forks of the conventional base transmission are actuated electro-mechanically with a single shift drum. This system can remain completely unchanged also for the hybrid variant, following the modular approach.

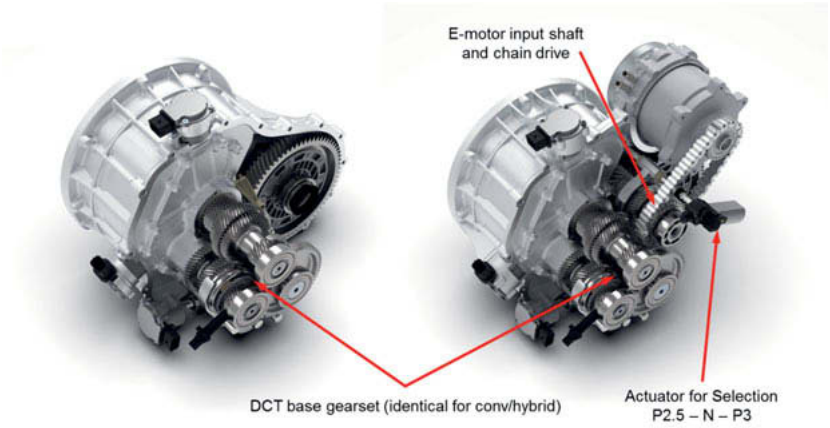


Fig. 10: 7-xDCT conventional and 48V hybrid versions, internals

The selection of the hybrid operating mode (P2.5 – N – P3) is performed by an additional, low cost, electro-mechanical actuator. As the required shift forces and number of actuations over transmission life are rather low, a low power brushed motor can be used, keeping the add-on cost for the hybrid system low.

https://doi.org/10.51202/9783181023549 - Generiert durch IP 216.73.216.36, am 19.01.2026, 02:19:31. © Urheberrechtlich geschützter Inhalt. Ohne gesonderte Erlaubnis ist jede urheberrechtliche Nutzung untersagt, insbesondere die Nutzung des Inhalts im Zusammenhang mit, für oder in KI-Systemen, KI-Modellen oder Generativen Sprachmodellen.

Fig. 11: Contains a specification overview for the hybrid version and some pictures of the available prototype hardware for the conventional version.

7-xDCT280 Hybrid Key Data	
No. of Speeds	7+R (option: 6+R with conv. shift schedule)
Torque capacity	280 Nm (ICE) plus electric motor
Ratio spread	7.06 (other values possible)
Actuation system	Full power-on-demand
Hybrid architecture	**Combined P2.5 and P3 ("Mixed")**
E-motor power	48 V stand-alone, bolt-on
E-motor total gear ratios	> 25 (P2.5 mode), appr. 7 (P3 mode)
Weight (dry)	65 kg (conventional), <90 kg (hybrid)
Installation length	**355 mm (dry clutch version)**

ICE – Internal combustion engine





Fig. 11: 7-xDCT specification overview

The overall transmission length for the hybrid variant is between 330 mm (wet clutch version) and 355 mm (dry clutch version), making it easily the most compact hybrid DCT concept available. At the same time, the combined P2.5-N-P3 functionality elegantly solves the issues typically associated with either P2.5 or P3 architectures alone, making it a unique offering in the industry.

https://doi.org/10.51202/9783181023549 - Generiert durch IP 216.73.216.36, am 19.01.2026, 02:19:31. © Urheberrechtlich geschützter Inhalt. Ohne gesonderte Erlaubnis ist jede urheberrechtliche Nutzung untersagt, insbesondere die Nutzung des Inhalts im Zusammenhang mit, für oder in KI-Systemen, KI-Modellen oder Generativen Sprachmodellen.

[1] G. Hellenbroich, I. Steinberg, D. Freiholtz, “Efficient and Industrialized Dual Clutch Transmission Family for Powertrains up to 350 Nm”, VDI transmissions in vehicles, Bonn, 2017

[2] I. Steinberg, G. Hellenbroich, D. Freiholtz, “FEV’s DCT family up-to 350 Nm for transversal, transaxle P/Ts”, FISITA 2016, Korea

[3] G. Hellenbroich, J. Ruschhaupt, C. Duindam, “FEV’s 7-xDCT – LOW-COST DRY DCT WITH SINGLE SHIFT DRUM”, CTI Transmission Symposium, Berlin 2012

[4] G. Hellenbroich, J. Ruschhaupt, S. Kirschstein “FEV’s 7-xDCT – Prototype of a New DCT Generation”, Aachen Kolloquium 2013

https://doi.org/10.51202/9783181023549 - Generiert durch IP 216.73.216.36, am 19.01.2026, 02:19:31. © Urheberrechtlich geschützter Inhalt. Ohne gesonderte Erlaubnis ist jede urheberrechtliche Nutzung untersagt, insbesondere die Nutzung des Inhalts im Zusammenhang mit, für oder in KI-Systemen, KI-Modellen oder Generativen Sprachmodellen.

Modular system 8G-DCT with all-wheel drive

Dipl.-Ing. (FH) **Alexander Harsch**,
Dr.-Ing. **Gunnar Clausen**,
Daimler AG, Stuttgart;
Dr.-Ing. **Anton Rink**,
Daimler AG, Sindelfingen

Zusammenfassung

Um die neu eingeführte Generation der Mercedes-Benz Kompaktfahrzeugfamilie (MFA2) auch triebstrangseitig auf ein neues Niveau zu bringen, wurde mit dem 8G-DCT ein neues Doppelkupplungsgetriebe entwickelt. Der Erstanlauf des 8G-DCT erfolgt mit dem ebenfalls neu entwickelten Diesel-Vierzylindermotor OM 654 in der frontangetriebenen 4x2-Variante.

Neben den technischen Highlights des kompakten Hochleistungsradsatzes sowie dem Trockensumpfkonzept des Ölhaushalts mit einer bedarfsgerechten Pumpensteuerung lag der Fokus der Entwicklung auf der hohen Modularität des 8G-DCT. Hierbei ermöglicht der konsequente modulare Aufbau die Erweiterungen des Getriebes hinsichtlich Allradfähigkeit, der zukünftigen Elektrifizierung sowie einer Erhöhung der Drehmomentkapazität. Die Erweiterung der Doppelkupplung durch eine Bestückungsvariante und der gezielte Einsatz von Hochleistungswerkstoffen ist dabei zielführend, um die Steigerung der Drehmomentkapazität des 8G-DCT zu erreichen.

Abstract

The 8G-DCT is a new dual clutch transmission developed to bring the newly introduced generation of the Mercedes-Benz compact vehicle family (MFA2) to a new level on the powertrain side. The 8G-DCT will be started for the first time with the newly developed OM 654q four-cylinder diesel engine in the front-wheel drive (4x2) variant.

In addition to the technical features of the compact high-performance wheelset and the dry sump concept of the oil household with demand-oriented pump control, the focus of development lay on the high modularity of the 8G-DCT. The consequent modular design makes it possible to extend the transmission with regard to all-wheel drive capability, future electrification and an increase in torque capacity. The extension of the double clutch by a mounting

https://doi.org/10.51202/9783181023549 - Generiert durch IP 216.73.216.36, am 19.01.2026, 02:19:31. © Urheberrechtlich geschützter Inhalt. Ohne gesonderte Erlaubnis ist jede urheberrechtliche Nutzung untersagt, insbesondere die Nutzung des Inhalts im Zusammenhang mit, für oder in KI-Systemen, KI-Modellen oder Generativen Sprachmodellen.

variant and the systematic use of high-performance materials is targeted to increase the torque capacity of the 8G-DCT.

1. History of compact cars and their drivetrains at Mercedes-Benz

In autumn 1997, Mercedes-Benz brought some fresh thinking into the compact class with a completely new concept in the A-Class [1], see figure 1. This concept combined advantages such as exemplary use of space and great variability to Mercedes standards with the agile handling of a compact car. Mercedes Benz had unit sales of around 1.1 million since 1997. In the powertrain, Mercedes-Benz introduced a 5-speed 2-shaft manual transmission and a 5-speed spur gear automatic transmission with torque converter for Mercedes-Benz specific comfort, figure 2, [2].

Featuring the intelligent sandwich concept and the distinctive one-box design, the second generation of the A-Class displayed all the outstanding characteristics of the predecessor model [1]. In addition, the A-Class introduced market-leading technical innovations, which underlined its role as a trendsetter in the compact-car segment. The two new transmissions put the final touch to the high level of dynamism and driving pleasure in the second generation A-Class [1]. Mercedes-Benz presented both the new six-speed manual transmission as well as the AUTOTRONIC - the first continuously variable transmission by Mercedes, [3]. The AUTOTRONIC transmission was the smoothest in an already very smooth line-up of transmissions from Mercedes-Benz [1], figure 2. The first-generation B-Class also celebrated its world premiere.

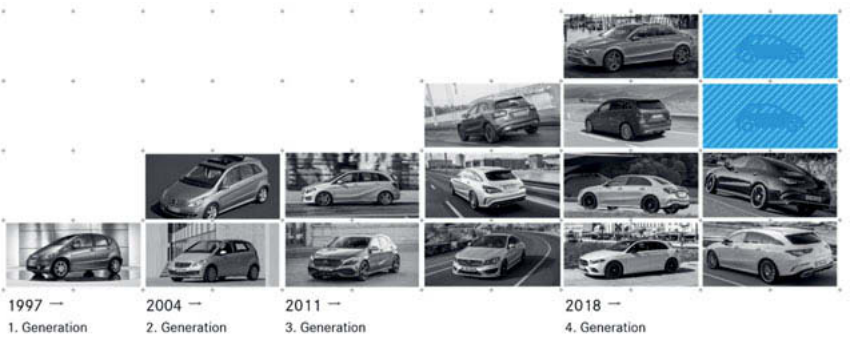


Fig. 1: History of compact cars at Mercedes-Benz

Featured with a new four-cylinder petrol engine with direct injection and turbo-charger, a new diesel engine, along with new assistance systems, technologically the second generation of

https://doi.org/10.51202/9783181023549 - Generiert durch IP 216.73.216.36, am 19.01.2026, 02:19:31. © Urheberrechtlich geschützter Inhalt. Ohne gesonderte Erlaubnis ist jede urheberrechtliche Nutzung untersagt, insbesondere die Nutzung des Inhalts im Zusammenhang mit, für oder in KI-Systemen, KI-Modellen oder Generativen Sprachmodellen.

the B-Class introduced a new compact car era at Mercedes-Benz in the year 2011 [1]. A new 7-speed three-shaft dual clutch transmission [4] and a new 6-speed 3-shaft manual transmission, figure 1 and figure 2 were available [5]. High-grade materials and finely structured surfaces, fine details, precision work-manship plus safety equipment unique to the segment raised the standard for comparison in the compact car segment [1]. In 2012, Mercedes-Benz presented the new A-Class. The company opened a completely new chapter in the compact segment: markedly emotive in design, with powerful engines ranging and extremely efficient [1]. In the fourth generation of the compact car, the three new models CLA, CLA shooting brake and GLA, a sports utility vehicle in the compact car class, started their market launches.

Now in 2018, the new Mercedes-Benz A-Class is as youthful and dynamic as ever, but grown-up and comfortable like never before [1]. It completely redefines modern luxury in the compact class, and revolutionizes interior design. New, efficient diesel and petrol engines allows power in models of the new A-Class. In addition, although Mercedes-Benz has retained the sporty appearance, the utility value has increased. Applying the new dynamic style of Mercedes-Benz to the compact class was a challenge. The almost sculptural lines of the A-Class are very typical for Mercedes [1].



Fig. 2: History of transmissions in compact cars

2. Introduction 8G-DCT

With the launch of the third generation Mercedes-Benz compact vehicle family in 2011 [1], the first in-house developed 7-speed dual clutch transmission 7G-DCT was introduced. [4] This transmission had already set high standards with regard to performance, power density and efficiency. [5]

To meet the increasing requirements regarding fuel consumption, torque capacity, weight, package and modularity, the new 8-speed dual clutch transmission 8G-DCT was developed

https://doi.org/10.51202/9783181023549 - Generiert durch IP 216.73.216.36, am 19.01.2026, 02:19:31. © Urheberrechtlich geschützter Inhalt. Ohne gesonderte Erlaubnis ist jede urheberrechtliche Nutzung untersagt, insbesondere die Nutzung des Inhalts im Zusammenhang mit, für oder in KI-Systemen, KI-Modellen oder Generativen Sprachmodellen.

as part of the next generation of Mercedes-Benz compact vehicles (MFA2 platform - market launch of the first model series in May 2018). [1]

Development targets

Particular attention was paid to the following objectives when developing the 8G-DCT: [7]

- Increase in number of gears
- Increase in maximum input torque
- High modularity to support 4x2- and 4x4-variants as well as future electrification
- Minimization of mechanical and electrical losses
- Reduction of weight through systematic lightweight design
- Compliance of the available installation space
- Enhancements in shift performance and shift comfort

Transmission design and specifications

The dual clutch transmission is designed in a classic and compact three-shaft layout. The even gears are connected to the inner one of the two radially nested clutches and the odd gears to the outer clutch. Gears 2, 4, 7, 8 are located on the upper output shaft and the gears 1, 3, 5, 6 and reverse gear are on the lower output shaft.

Intelligent nesting and use of the gear set pairs enabled an axial length of 361 mm to be achieved in the relevant area. Thanks to the compact design and the implemented lightweight design measures, the weight (including transmission oil) of the aggregate is only 84 kg. Hence this transmission sets a new benchmark with respect to size and weight in the compact car segment with such a performance capacity. [7]

https://doi.org/10.51202/9783181023549 - Generiert durch IP 216.73.216.36, am 19.01.2026, 02:19:31. © Urheberrechtlich geschützter Inhalt. Ohne gesonderte Erlaubnis ist jede urheberrechtliche Nutzung untersagt, insbesondere die Nutzung des Inhalts im Zusammenhang mit, für oder in KI-Systemen, KI-Modellen oder Generativen Sprachmodellen.

Table 1: Transmission specifications

Technical specifications of the 8G-DCT			
Gear ratio	1st	15.93	17.56
	2nd	11.18	12.32
	3rd	7.34	8.09
	4th	5.15	5.67
	5th	3.74	4.12
	6th	2.93	3.22
	7th	2.29	2.52
	8th	1.81	1.99
	Reverse	13.39	14.75
Spread		8.81	
Centre distance		188 mm	

3. Modular design and expandability of the transmission

In the development of the 8G-DCT, one main focus was set on the modular design of the transmission in order to cover all variants based on the new compact vehicle platform. In addition to the future electrification, the all-wheel drive capability and the adaptation to different model series of the platform were also taken into account.

https://doi.org/10.51202/9783181023549 - Generiert durch IP 216.73.216.36, am 19.01.2026, 02:19:31. © Urheberrechtlich geschützter Inhalt. Ohne gesonderte Erlaubnis ist jede urheberrechtliche Nutzung untersagt, insbesondere die Nutzung des Inhalts im Zusammenhang mit, für oder in KI-Systemen, KI-Modellen oder Generativen Sprachmodellen.

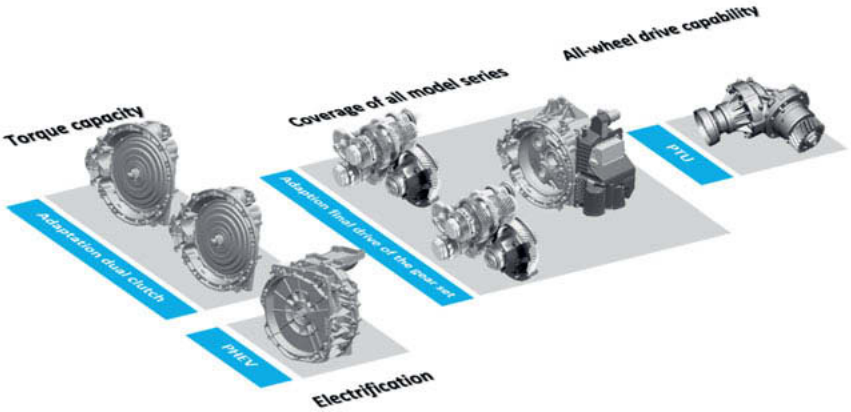


Fig. 3: Modular system 8G-DCT for the new generation of Mercedes-Benz compact cars

Due to the systematic modular design of the 8G-DCT, the transmission can meet the requirements of all model series of the compact vehicle platform. While the future-oriented design of the 8G-DCT makes it possible to electrify the powertrain, the torque capacity can be specifically increased by adapting the dual clutch. This is achieved by varying the number of friction plates and the use of high-performance materials. In order to meet the torque requirements of the various model series of the Mercedes-Benz compact cars, the axle ratio in the wheel set can be adapted to the vehicle.

The high modularity allows the all-wheel drive capability of the transmission. The power take off unit (PTU) acts as a transfer case and, in conjunction with the rear axle drive, enables the familiar 4MATIC drive to be implemented in the latest generation of compact vehicles.

With the integration of a hybrid power head between the transmission and the combustion engine it will be also possible to offer an electrified version of the 8G-DCT.

4. Dual clutch unit and mechanical pump drive

The two clutches are nested radially, hydraulically actuated and cooled on an on-demand basis. A re-design of the frictional surfaces further increased the start-off and shift performance. The mechanical main pump is driven by a chain drive connected to the dual clutch. This design offers outstanding acoustic benefits with low installation space requirements. The torque capacity of the dual clutch is scalable by varying the number of friction plates. [7]

https://doi.org/10.51202/9783181023549 - Generiert durch IP 216.73.216.36, am 19.01.2026, 02:19:31. © Urheberrechtlich geschützter Inhalt. Ohne gesonderte Erlaubnis ist jede urheberrechtliche Nutzung untersagt, insbesondere die Nutzung des Inhalts im Zusammenhang mit, für oder in KI-Systemen, KI-Modellen oder Generativen Sprachmodellen.

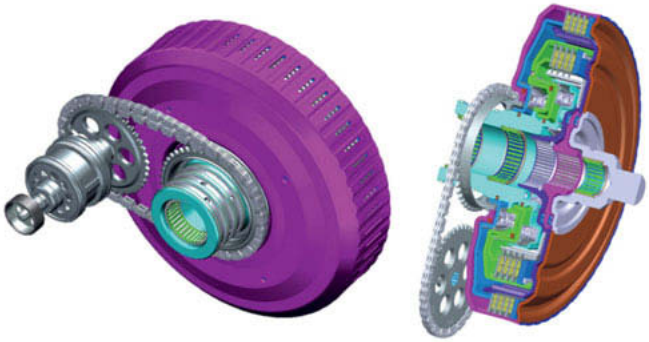


Fig. 4: Dual clutch unit and mechanical pump drive

Table 2: Specification sheet dual clutch

Technical specifications dual clutch		
Maximum torque	520 Nm	
Maximum speed	7,300 rpm	
Touchpoint	Clutch 1	~ 2.0 bar
	Clutch 2	~ 2.3 bar
Gain	50 Nm / bar	
Friction Pairings	Standard torque capacity	8
	Higher torque capacity	10
Weight	~ 8.6 kg	
Gear arrangement	Clutch 1	1, 3, 5, 7 & Reverse
	Clutch 2	2, 4, 6 and 8

5. Gear set

The compact design of the high-performance gear set was achieved by the double-use of the fixed gears 6/8 and 7/5 in the even and odd sub-transmissions respectively.

https://doi.org/10.51202/9783181023549 - Generiert durch IP 216.73.216.36, am 19.01.2026, 02:19:31. © Urheberrechtlich geschützter Inhalt. Ohne gesonderte Erlaubnis ist jede urheberrechtliche Nutzung untersagt, insbesondere die Nutzung des Inhalts im Zusammenhang mit, für oder in KI-Systemen, KI-Modellen oder Generativen Sprachmodellen.

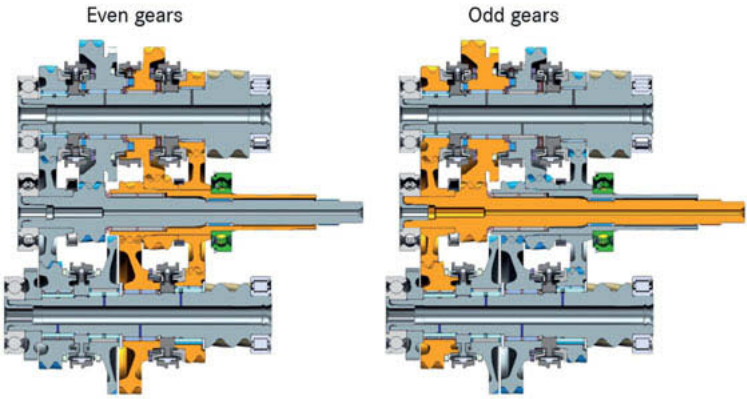


Fig. 5: Gear set layout

Another remarkable feature is the power flow of the 1st gear. The gear ratio of the 1st gear is achieved by using the gear wheel pairs 3, 4 and 2. For this purpose, the idler gears 3 and 4 are coupled and rotate together at a relative speed to the upper output shaft. [7]

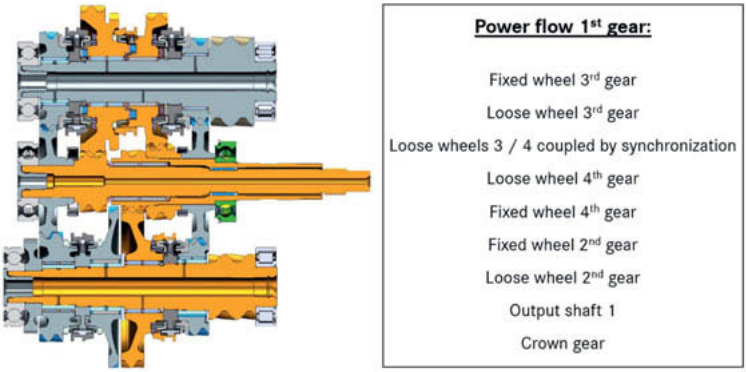


Fig. 6: Power flow 1st gear

To fulfill the requirements of the different car lines, there are used two different axle ratio variants within the 8G-DCT. For the heavy vehicles of the MFA2 family is used a shorter gear ratio to achieve an optimal driving performance. The overall gear spread remains with both variants identical (φ=8.81).

https://doi.org/10.51202/9783181023549 - Generiert durch IP 216.73.216.36, am 19.01.2026, 02:19:31. © Urheberrechtlich geschützter Inhalt. Ohne gesonderte Erlaubnis ist jede urheberrechtliche Nutzung untersagt, insbesondere die Nutzung des Inhalts im Zusammenhang mit, für oder in KI-Systemen, KI-Modellen oder Generativen Sprachmodellen.

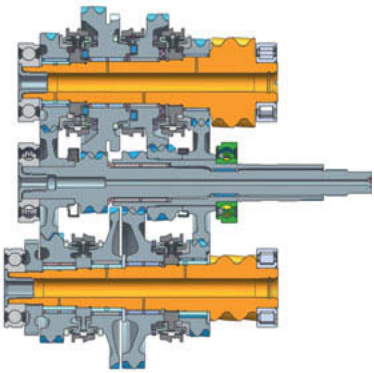


Fig. 7: Axle ratio variants realized by

Another innovation is the first serial use of the so-called DCT-type synchronization. This is characterised by the fact that the engagement teeth are dispensed, and the resulting installation space can be added to the toothing width. [7]



Fig. 8: DCT-type synchronizer (source: Hoerbiger Antriebstechnik GmbH)

6. All-wheel drive system

The 8G-DCT will be available with the all-wheel drive system 4MATIC with fully variable torque distribution [1].

This will be reached by the modular integration of a power take-off unit (PTU) in the transmission. The PTU is not integrated as an add-on component at the transmission output, unlike with comparable all-wheel-drive systems, but forms part of the main transmission. The oil system of the main transmission supplies the PTU with lubricant for oiling and cooling purposes.

https://doi.org/10.51202/9783181023549 - Generiert durch IP 216.73.216.36, am 19.01.2026, 02:19:31. © Urheberrechtlich geschützter Inhalt. Ohne gesonderte Erlaubnis ist jede urheberrechtliche Nutzung untersagt, insbesondere die Nutzung des Inhalts im Zusammenhang mit, für oder in KI-Systemen, KI-Modellen oder Generativen Sprachmodellen.

Additional seals are not required, which has a positive impact on efficiency in conjunction with reduced-friction tapered roller bearings.
The spur gear of the PTU takes up drive torque via the dual clutch transmission final drive and transfers it via an NVH-optimized bevel gear set to the propeller shaft. The gear ratio between the final drive of the 8G-DCT and the spur gear of the PTU reduces the torque to the rear axle to the level of the propeller shaft, allowing the bevelset gear ratio of the PTU to be designed in a very compact fashion. The total weight of the PTU is just appr. 10 kg, and although the unit is small in its configuration, it can reliably transfers up to 1.000 Nm of torque.

The rear axle differential operates with an integrated multiple clutch. This clutch is powered electro-mechanically. Via a crown wheel and a ball ramp, an electric motor exerts an axial force on the clutch pack to open or close the plates. The rear axle differential compensates the different paths rotational speeds of the rear wheels.
Drive torque distribution between the front and rear axles is fully variable. Depending on the driving situation, 100% of the drive torque can be directed to the front axle (e.g. when driving straight ahead with no increased slip at the front axle), or in borderline cases up to 50% can be directed to the rear axle if the friction coefficient suddenly changes. [6]



Fig. 9: Power take-off unit and rear axle differential

7. Electrification of the 8G-DCT

The 8G-DCT will be expanded by a very compact power head to enable an electrified version. Beside of the electric engine, the dual clutch as well as the disconnect clutch find place in the power head. The low-loss wet disconnect clutch is integrated within the rotor of the electric engine. The integrated permanent excited synchro machine connects high efficiency with a high power and torque density, whereby can be reached a very agile electric and hybrid drivability. [8]

https://doi.org/10.51202/9783181023549 - Generiert durch IP 216.73.216.36, am 19.01.2026, 02:19:31. © Urheberrechtlich geschützter Inhalt. Ohne gesonderte Erlaubnis ist jede urheberrechtliche Nutzung untersagt, insbesondere die Nutzung des Inhalts im Zusammenhang mit, für oder in KI-Systemen, KI-Modellen oder Generativen Sprachmodellen.

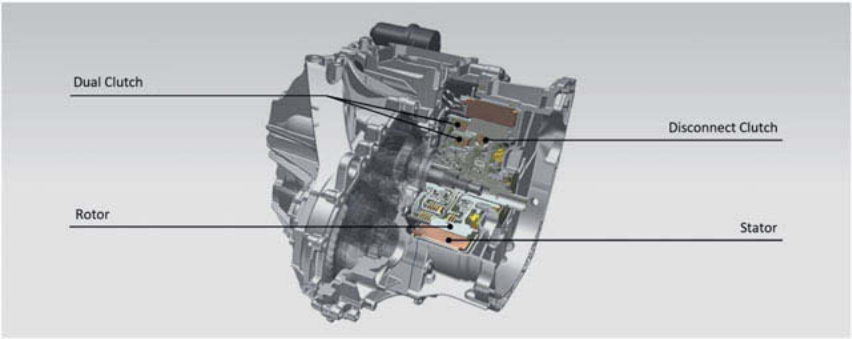


Fig. 10: The 8G-DCT hybrid transmission with integrated power head

8. Oil system / dry sump lubrication

A dry sump lubrication system has been used in the gear set chamber to reduce the oil churning losses. The oil in the gear set chamber is actively extracted via the electric tandem pump and is pumped into a reservoir formed by the transmission housing and oil pan module. Oil is pumped from this reservoir by both the mechanically driven and the electrically driven pump into the respective suction filters and subsequently supply the hydraulic control unit.

The hydraulic control unit supplies oil to the hydraulic actuators on the one hand and on the other hand all cooling and lubrication requirements are also taken care of. Due to the presence of a dry sump lubrication system, active lubrication is necessary to cool the gear meshing zones. The oil is supplied via an oil spider with multiple nozzles made of plastic. [7]

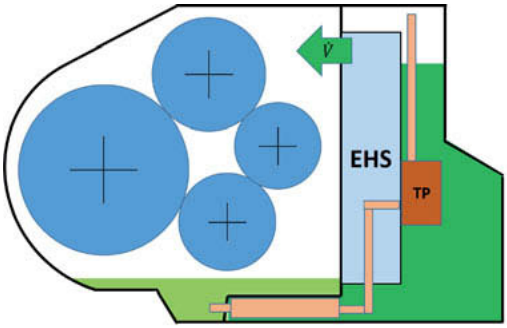


Fig. 11: Dry sump lubrication

https://doi.org/10.51202/9783181023549 - Generiert durch IP 216.73.216.36, am 19.01.2026, 02:19:31. © Urheberrechtlich geschützter Inhalt. Ohne gesonderte Erlaubnis ist jede urheberrechtliche Nutzung untersagt, insbesondere die Nutzung des Inhalts im Zusammenhang mit, für oder in KI-Systemen, KI-Modellen oder Generativen Sprachmodellen.

9. Modular lightweight design

To comply with the weight targets and for reduction of effort in the final assembly, highly integrated lightweight components have been designed and the examples are: [7]

- Gearshift module
- Oil pan module
- Park-by-Wire module



Fig. 12: Gearshift module (left), oil pan module (middle) and Park-by-Wire module (right)

Gearshift module

The hydraulically actuated gearshift module valves include shift forks, actuating pistons and position sensors as one testable unit. The hydraulic cylinder and pistons are made of high-performance plastics and meet the highest requirements for dimensional accuracy and pressure resistance.

Oil pan module

The oil pan module integrates the suction filters of the mechanical and electrical pumps, the transmission oil cooler, the pressurized oil filter, the transmission ventilator and the actual oil pan to a single unit. The oil pan base body is also made of plastic and meets the highest demands of precision.

Park-by-Wire module

The actuation unit of the park pawl is also designed as a module and assembled as a pre-tested unit in the transmission.

https://doi.org/10.51202/9783181023549 - Generiert durch IP 216.73.216.36, am 19.01.2026, 02:19:31. © Urheberrechtlich geschützter Inhalt. Ohne gesonderte Erlaubnis ist jede urheberrechtliche Nutzung untersagt, insbesondere die Nutzung des Inhalts im Zusammenhang mit, für oder in KI-Systemen, KI-Modellen oder Generativen Sprachmodellen.

10. Electro-hydraulic control unit

The electrohydraulic control unit is built of the transmission control unit (TCU), the hydraulic unit as well as the electric pump and is compact and modular at the same time. The optimized valve dynamics and valve control enable shorter shift times. A development focus lay on reducing the hydraulic power consumption by minimizing leakages.

The fully integrated transmission control unit (TCU) of the 8G-DCT is based on a printed circuit board as a circuit breaker which houses components both sides connected by means of reflow soldering. The central element is a triple-core microcontroller with integrated flash memory and RAM. [7]

The same basic control unit is used for all transmission variants.

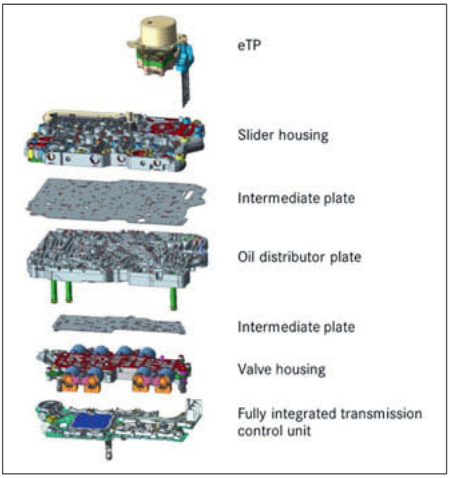


Fig. 13: Electro-hydraulic and transmission control unit

11. Software (transmission function)

The software of the new 8G-DCT has been completely revised compared to the predecessor model 7G-DCT. The result is a software module that can be used for both conventional and hybrid powertrains.

The transmission software provides the driver four drive modes. The Comfort program is preset, which optimally meets the requirements with respect to comfort, dynamics and environmental compatibility. In addition to the Comfort mode, the Eco mode provides the driver with a

https://doi.org/10.51202/9783181023549 - Generiert durch IP 216.73.216.36, am 19.01.2026, 02:19:31. © Urheberrechtlich geschützter Inhalt. Ohne gesonderte Erlaubnis ist jede urheberrechtliche Nutzung untersagt, insbesondere die Nutzung des Inhalts im Zusammenhang mit, für oder in KI-Systemen, KI-Modellen oder Generativen Sprachmodellen.

coast function. During coasting, the power flow between the engine and transmission is interrupted so that the vehicle is not decelerated by the engine's drag torque during coasting. Coasting is cancelled when the driver depresses the accelerator pedal or brake pedal. In addition, the radar data is evaluated as per the coasting strategy and used for activation and deactivation of the coasting function. In the Sport program, the shift times are shortened compared to the Comfort program and the load points are shifted to higher rpms. This allows the driver to quickly call up the maximum engine power output. The driver can activate a permanent manual program in the individual mode. In this manual program the driver determines the engaged gear via the paddle shifters on the steering wheel. The transmission control system checks the driver's gear request and prevents implausible gear shifts or operation errors. The fastest acceleration is achieved in the sport program when the launch control is activated.

System parameters of the transmission such as friction coefficients, filling times and shifter fork positions are obtained continuously and stored in the EEPROM. The software modules for dual clutch and gear shifter use this information for the control of fast and comfortable gear shifts. The individual mechanical, hydraulic and electrical components are continuously monitored. An ISO26262 certified monitoring concept guarantees the safe operation of the transmission. [7]

For all variants and car series will be used one standard software, which will be adapted customer specific.

https://doi.org/10.51202/9783181023549 - Generiert durch IP 216.73.216.36, am 19.01.2026, 02:19:31. © Urheberrechtlich geschützter Inhalt. Ohne gesonderte Erlaubnis ist jede urheberrechtliche Nutzung untersagt, insbesondere die Nutzung des Inhalts im Zusammenhang mit, für oder in KI-Systemen, KI-Modellen oder Generativen Sprachmodellen.

References

[1] Daimler Media. https://media.daimler.com

[2] Göddel, T.; Hillenbrand, H.; Hopff, C.; Jud, M.: Das neue Fünfgang-Automatikgetriebe W5A180. Sonderausgabe ATZ und MTZ, 10/1997, Seiten. 96 – 101

[3] Kiesel, J., Greiner, J., Veil, A., Strenkert, J.: Das neue CVT- Getriebe Autotronic von Mercedes-Benz, Wien: 26. Wiener Motorensymposium.

[4] Wörner, R.; Damm, A.; Eberspächer, R; Gitt, C.: Effiziente Front-Quer-Getriebe von Mercedes-Benz. ATZ 113 (2011), Nr. 12, S. 914 - 921, Wiesbaden: Springer Vieweg

[5] Henning, G.; Gödecke, T.; Damm, A.: Neue Getriebe für die neuen Kompakten. ATZ extra - Die neue A-Klasse von Mercedes-Benz (2012), S. 70 - 73, Wiesbaden: Springer Vieweg

[6] Dörr, C.; Lessi, S.; Adolph, M.; Marx, V.; Veik, F.: The drivetrain for the new Mercedes-Benz compact cars, Berlin: 17th International CTI Symposium.

[7] Harsch, A.; Kemmner, B.; Ertel, A.; Dr. Rink, A.: Die nächste Generation DCT-Getriebe für die Mercedes-Benz Kompaktfahrzeugfamilie; Berlin: 17th International CTI Symposium.

[8] Gödecke, T.; F. Ascher; D. Dickgießer; L. Engbroks; T. Schürmann, R. Voigtländer Daimler AG: EQ Power Plug-In Hybrid – EQ Power Plug-In Hybrid – Electrified from A to S, Wiener Motorensymposium, 2019

https://doi.org/10.51202/9783181023549 - Generiert durch IP 216.73.216.36, am 19.01.2026, 02:19:31. © Urheberrechtlich geschützter Inhalt. Ohne gesonderte Erlaubnis ist jede urheberrechtliche Nutzung untersagt, insbesondere die Nutzung des Inhalts im Zusammenhang mit, für oder in KI-Systemen, KI-Modellen oder Generativen Sprachmodellen.

https://doi.org/10.51202/9783181023549 - Generiert durch IP 216.73.216.36, am 19.01.2026, 02:19:31. © Urheberrechtlich geschützter Inhalt. Ohne gesonderte Erlaubnis ist jede urheberrechtliche Nutzung untersagt, insbesondere die Nutzung des Inhalts im Zusammenhang mit, für oder in KI-Systemen, KI-Modellen oder Generativen Sprachmodellen.

7DCT/HDT400

New fuel-efficient FWD DCT and hybrid transmission for up to 400 Nm

Lothar Herdle,
Magna Powertrain, Untergruppenbach

ZUSAMMENFASSUNG

Die Magna DCT Technologie begann 2008 als je ein Doppelkupplungsgetriebe in Front-quer und Inline Anordnung in den Markt eingeführt wurden.

Die Produktion der dritten Generation der Manga DCTs - das 7DCT300 - wurde Anfang 2015 aufgenommen. Dieses Jahr werden global rund 1,2 Millionen Einheiten in 4 Werken produziert.

Dieses 7-Gang Doppelkupplungsgetriebe mit ölgekühlter Kupplung, elektrohydraulischen Kupplungsbetätigung und elektromechanischen Gangaktuierung bietet die beste Effizienz in seiner Klasse und exzellente Fahrbarkeit. Ohne weitere Komponenten kann das Magna 7DCT300 für Start-Stopp-Systeme und erweiterte Segelfunktionen mit Motor aus eingesetzt werden. Darüber stellt es das Basissystem für eine skalierbare Hybridisierung.

Als konsequente Evolution des 7DCT300 wurde das 7DCT400 entwickelt, um höhere Motordrehmomente zur Abdeckung von Front-Quer-Plattformen der OEMs zu ermöglichen. Eine weitere Senkung des Verbrauchs und eine Steigerung der Leistungsdichte waren zentrale Entwicklungsziele. Mit der parallelen Entwicklung des 7HDT400 – der hybridisierten Variante – wurden maximale Synergien im Design und in der Fertigung erzielt.

Der vorliegende Bericht stellt die wesentlichen Kennwerte und Attribute des 7DCT400 und seiner Hybridvarianten dar sowie optionale Module wie Sperrdifferential und Allradanbindung – bereit für den Einsatz in verschiedensten Fahrzeuganwendungen.

ABSTRACT

Magna DCT technology was introduced in 2008 when a transversal and an inline application were launched.

The production of the third generation of Magna DCTs – the 7DCT300 - started in early 2015. In the meanwhile several OEM vehicle programs have followed in Europe and China.

This year approx. 1.2 million units will be produced at 4 plants globally.

https://doi.org/10.51202/9783181023549 - Generiert durch IP 216.73.216.36, am 19.01.2026, 02:19:31. © Urheberrechtlich geschützter Inhalt. Ohne gesonderte Erlaubnis ist jede urheberrechtliche Nutzung untersagt, insbesondere die Nutzung des Inhalts im Zusammenhang mit, für oder in KI-Systemen, KI-Modellen oder Generativen Sprachmodellen.

The front-transversal seven-speed dual clutch transmission with its wet dual clutch, electrohydraulic clutch actuation and electro-mechanic shift actuation offers best in class fuel efficiency and excellent drivability. Without any additional actuation components, the Magna 7DCT300 dual clutch transmission is dedicated for stop/start, extended sailing functions with stopped engine and is the base transmission for scalable hybridization.
As a consequent evolution of the 7DCT300, the 7DCT400 was designed to achieve higher engine torques to cover OEMs front-transversal portfolios. Further improving the overall fuel efficiency and the torque to weight ratio were key objectives. With the parallel development of the 7HDT400 - the hybrid version of the DCT – a maximum of synergies for design and manufacturing have been achieved.
This paper describes concept and main attributes of the 7DCT400 and its hybrid derivative 7HDT400 in comparison to 7DCT300. It outlines the key improvements and highlights some optional features like limited slip differential or a mechanical AWD interface, to be ready for various OEM applications.

INTRODUCTION

With the success of the 7DCT300 OEM asked for a stronger derivative of the 7DCT300. Magna started the development of a 400 Nm nominal torque variant and its hybrid version the 7DCT/HDT400.
Main development targets were a further improved efficiency, increase power density at the same package space.

EXTENDED FWD TRANSVERSE PORTFOLIO

The 7DCT/HDT400 closes the gap in the product portfolio for high torque DCTs/HDTs.
It enables OEMs to cover their passenger car lines with transversal architecture by the 7DCT/HDT family.
It replaces the Magna’s outgoing first generation 6DCT451 by a modern product and can exceed the 400 Nm input torque by e-boost through the P2.5 architecture of the 7HDT400.

https://doi.org/10.51202/9783181023549 - Generiert durch IP 216.73.216.36, am 19.01.2026, 02:19:31. © Urheberrechtlich geschützter Inhalt. Ohne gesonderte Erlaubnis ist jede urheberrechtliche Nutzung untersagt, insbesondere die Nutzung des Inhalts im Zusammenhang mit, für oder in KI-Systemen, KI-Modellen oder Generativen Sprachmodellen.

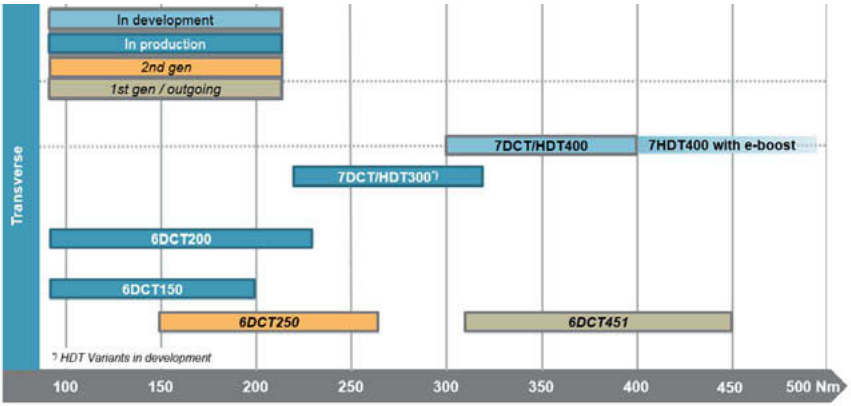


Fig. 1: The Magna's FWD TRANSVERSE DCT/HDT PORTFOLIO

PRODUCT CHANGES COMPARED TO 7DCT300

The 7DCT/HDT 300 uses the 7DCT300 a base for an evolutionary approach.

The successful concept and layout is unchanged and driven further using latest technology and advanced engineering findings of the last years.

The main focus at the development are torque capacity increase and further improvement of efficiency.

Common building blocks enable a modular & scalable concept to support OEM strategies.

The main areas of changes are

- Introduction of DC400 clutch
- Reinforcement of bearings
- Optimization of gear design and machining
- Efficiency optimization of bearings
- Suction area without churning of the oil
- Further integration step at the clutch actuator

As one result, the new transmission family can be manufactured on the same production line with the current 7DCT300.

https://doi.org/10.51202/9783181023549 - Generiert durch IP 216.73.216.36, am 19.01.2026, 02:19:31. © Urheberrechtlich geschützter Inhalt. Ohne gesonderte Erlaubnis ist jede urheberrechtliche Nutzung untersagt, insbesondere die Nutzung des Inhalts im Zusammenhang mit, für oder in KI-Systemen, KI-Modellen oder Generativen Sprachmodellen.

EFFICIENCY MEASURES

Specific examples for measure to improve the transmission efficiency are optimized gear meshes. The gear design utilized a consequent reduction of the specific sliding speed in the mesh.

A second area of improvement is a reduction of oil splash losses: A lower oil level without reducing the oil volume decreases the submergence of gears and clutch.

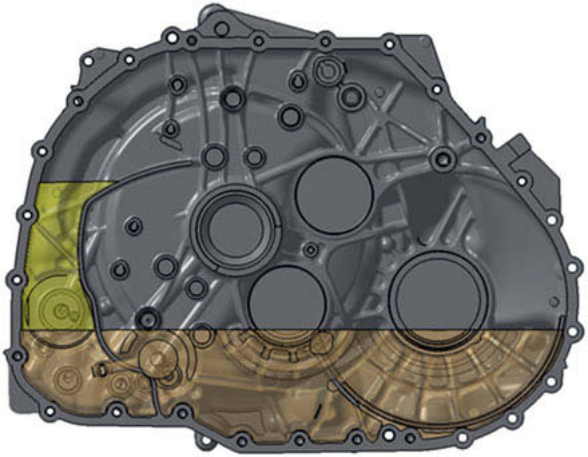


Fig. 2: Reduced of oil level

https://doi.org/10.51202/9783181023549 - Generiert durch IP 216.73.216.36, am 19.01.2026, 02:19:31. © Urheberrechtlich geschützter Inhalt. Ohne gesonderte Erlaubnis ist jede urheberrechtliche Nutzung untersagt, insbesondere die Nutzung des Inhalts im Zusammenhang mit, für oder in KI-Systemen, KI-Modellen oder Generativen Sprachmodellen.

A differential enclosure is introduced to minimize the dragged oil flow.



Fig. 3: Differential enclosure

STAND-ALONE ATTRIBUTE – BEST-IN-CLASS EFFICIENCY TRANSMISSION

The applied measures lead to system efficiency, which is considered best-in-class.

The efficiency improvement compared to the already very efficient 7DCT300 at the WLTP cycle

- DCT: 1.9 g CO2/km
- HDT MHEV (48V): 14-16%
- HDT PHEV: 19-68%

https://doi.org/10.51202/9783181023549 - Generiert durch IP 216.73.216.36, am 19.01.2026, 02:19:31. © Urheberrechtlich geschützter Inhalt. Ohne gesonderte Erlaubnis ist jede urheberrechtliche Nutzung untersagt, insbesondere die Nutzung des Inhalts im Zusammenhang mit, für oder in KI-Systemen, KI-Modellen oder Generativen Sprachmodellen.

STAND-ALONE ATTRIBUTE – BEST-IN-CLASS TORQUE-TO-WEIGHT RATIO



Fig. 4: Transverse Transmission system weight / torque diagram

Fig. 4 gives and overview of weight over torque for various transmission systems. For a fair comparison the connecting and damping element (Flex plate for torque converter transmissions, DMF for DCTs) is added.

It is obvious that the 7DCT400 outpaces its competitors in terms of power density. The 7HDT400 with only 16 kg of additional weight is only slightly above conventional transmissions systems. Since the HDT replaces components like the 12V generator the relevant weight on vehicle system level is even better.

https://doi.org/10.51202/9783181023549 - Generiert durch IP 216.73.216.36, am 19.01.2026, 02:19:31. © Urheberrechtlich geschützter Inhalt. Ohne gesonderte Erlaubnis ist jede urheberrechtliche Nutzung untersagt, insbesondere die Nutzung des Inhalts im Zusammenhang mit, für oder in KI-Systemen, KI-Modellen oder Generativen Sprachmodellen.

PRODUCT CHARACTERISTICS

7DCT400 and 7HDT400 in its mild hybrid 48V and plug in 380V version have the following characters key features:

Key features 7DCT400

- 7-speed transmission, 1 rev gear
- Center distance 197 mm
- 400 Nm nominal torque capacity
- Wet-nested dual-clutch (500 Nm dynamic torque)
- Weight FWD 74 kg (incl. oil)
- Actuation “power-on-demand”
- Park-by-wire – normally stay
- Gear ratio spread up to 7.9
- AWD optional

Key features 7HDT400 MHEV/PHEV

- 400 Nm nominal torque capacity for 197 mm center distance (add. boost with eMachine possible)
- Oil-cooled eMachine integrated in transmission
- **MHEV 48V Hybridization**
- 15 - 25 kW eMachine
- Water-cooled inverter, directly connected to eMachine
- Weight 90 kg (incl. oil, 48V inverter)
- **PHEV 380V Hybridization**
- 60 - 85 kW rare earth magnet eMachine
- Water-cooled inverter, chassis mounted
- Weight 99 kg (incl. oil, incl. inverter)

PARALLEL DEVELOPMENT OF DCT AND HDT

For the first time a fully parallel development of DCT and HDT was performed. The strategic goals were

- Reduce complexity of the product family
- Enable production at the same assembly line with the least possible change over time

The product strategy has targets such as

- Offer the customer a system with flexible configuration – DCT / HDT MHEV / HDT PHEV
- Fast adaptation to market needs possible by using installed equipment
- Scalable CO2 by 48V or Plug-in hybrids
- Scalable dynamics using eMachine boost at the different hybrid levels plus AWD option

https://doi.org/10.51202/9783181023549 - Generiert durch IP 216.73.216.36, am 19.01.2026, 02:19:31. © Urheberrechtlich geschützter Inhalt. Ohne gesonderte Erlaubnis ist jede urheberrechtliche Nutzung untersagt, insbesondere die Nutzung des Inhalts im Zusammenhang mit, für oder in KI-Systemen, KI-Modellen oder Generativen Sprachmodellen.

CONCLUSION

With the 7DCT400 and its hybrid derivatives both an efficiency improvement for conventional powertrains and a contribution to powertrain electrification is provided and expanded to higher torque and power.

The customer can chose the “right” scale of electrification which very much depends on use cases and the availability/efficiency of energy sources.

The use of hardware and software “building blocks” enables to use economy of scales while OEM specific DNA and attractive added value for car drivers is given.

[1] Gindele, J.: A comprehensive System Approach for Future Powertrain Application, CTI Symposium USA, Novi, May 2018

[2] Schweiher M.: How many Speeds do Future Powertrains Need?, Magna Drivetrain Forum, Untergruppenbach, October 2016

[3] Bahne M.; Frey, U.: CO_2 Potentials of Dual-clutch Transmission – A Technology Outlook.
In: ATZworldwide, 12/2017, pp. 18-22

https://doi.org/10.51202/9783181023549 - Generiert durch IP 216.73.216.36, am 19.01.2026, 02:19:31. © Urheberrechtlich geschützter Inhalt. Ohne gesonderte Erlaubnis ist jede urheberrechtliche Nutzung untersagt, insbesondere die Nutzung des Inhalts im Zusammenhang mit, für oder in KI-Systemen, KI-Modellen oder Generativen Sprachmodellen.

Innovative 8HP Modular Design Kit for Conventional, MHEV and PHEV Transmissions

Anton Locher, Dr. **Michael Ebenhoch**, **Patrick Gutmann**,
ZF Friedrichshafen AG, Friedrichshafen

1. Introduction

The increase of legal requirements to reduce pollutant emissions, the megatrend of electrification as well as customers' continuously increasing demand for comfort and improved vehicle performance and handling comprehensively require further development and adaptation of today's driveline technologies.

In addition, the number and changing nature of influencing factors that determine the purchasing behavior of customers are leading to an increasing volatility of the markets.

This trend must be countered with appropriate flexibility in the product portfolio of automotive manufacturers and suppliers.

Torque converter transmissions, dual clutch transmissions and continuously variable transmissions are established in the vehicles for transverse drives. However, the planetary automatic transmission continues to dominate in longitudinal drives, due to its superiority for installation in the vehicle tunnel.

Based on conventional transmission technologies, hybrid versions of longitudinal drives have now been launched in the markets as modular concepts. These concepts are faced with particular challenges due to installation space restrictions, as the electric drive also have to be accommodated in the existing vehicle architecture, in addition to the conventional drive technology.

Promising new concepts have been developed using integrated approaches, for which in particular planetary gearsets in longitudinal design show clear advantages. In conjunction with

https://doi.org/10.51202/9783181023549 - Generiert durch IP 216.73.216.36, am 19.01.2026, 02:19:31. © Urheberrechtlich geschützter Inhalt. Ohne gesonderte Erlaubnis ist jede urheberrechtliche Nutzung untersagt, insbesondere die Nutzung des Inhalts im Zusammenhang mit, für oder in KI-Systemen, KI-Modellen oder Generativen Sprachmodellen.

the necessary flexibility in the product portfolio described above, solutions that can be used to implement both, conventional automatic transmissions and hybrid drives in a modular design kit solution are to be regarded as particularly viable for the future.

The market developments and forecasts show an increase in the share of hybrid drives. However, electromobility in total is showing slow progress, due to high costs for procurement and infrastructure, an insufficient charging infrastructure and vehicle ranges that are currently still low.

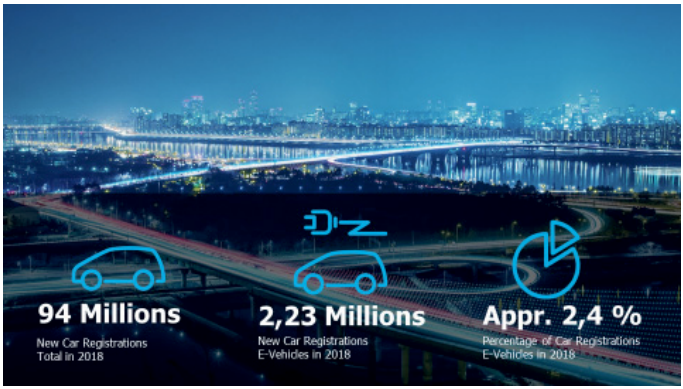


Fig. 1: New car registrations of E-vehicles worldwide

In order to optimally utilize the potential of hybrid drive technology and make it suitable for high volume production, even greater challenges in development and production have to currently be overcome in terms of installation space requirements, additional weights, additional costs and technical complexity.

Therefore, the target vision of viable future hybrid technology have to take the following challenges into account: efficient technology with a high integration capacity, flexibility, cost optimization and the fulfillment of customer mobility needs by expanding electrification.

Modular systems, such as the ZF 8HP transmission family are fundamental for fulfill these requirements.

https://doi.org/10.51202/9783181023549 - Generiert durch IP 216.73.216.36, am 19.01.2026, 02:19:31. © Urheberrechtlich geschützter Inhalt. Ohne gesonderte Erlaubnis ist jede urheberrechtliche Nutzung untersagt, insbesondere die Nutzung des Inhalts im Zusammenhang mit, für oder in KI-Systemen, KI-Modellen oder Generativen Sprachmodellen.

ZF's 8-speed modular design kit system is in the 3rd generation of volume production and offers further potential as well as new concept approaches for innovatively enhanced developments, based on the aforementioned general conditions and requirements.

2. Electrification

Electrified transmissions have been part of the 8HP transmission family since the 1st generation. Technologies currently in volume production include plug-in hybrids in the 3rd generation and transmissions with electrified pump systems on the basis of 48 V on-board supply systems, which enable unrestricted use of the transmission, when the combustion engine is switched off for sailing up into the high-speed range.

Due to greatly increasing demands for electrification of drive systems, solutions are required that enable comprehensive electrification of mild and plug-in hybrids in a modular design kit solution based on conventional core 8-speed transmissions. The objective is a full integration of the electric drive within the specified or existing vehicle installation spaces.

On this basis, the following concept for the 4th generation of 8HP transmissions was developed.

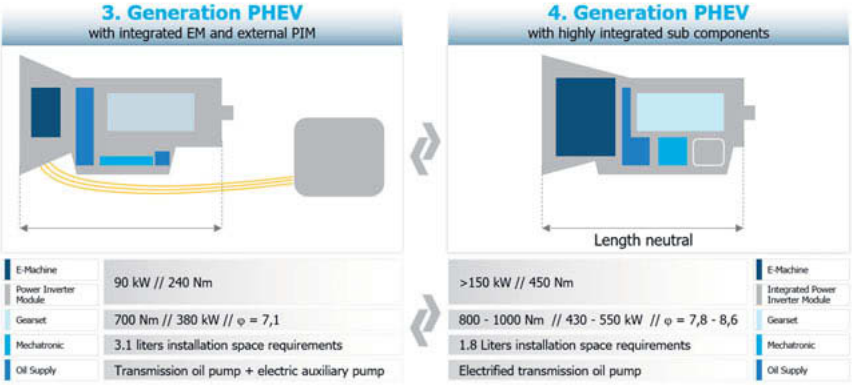


Fig. 2: Fully integrated technologies: sub-systems as an enabler

To best meet customer requirements, this system is divided into three sizes and three technologies: conventional, mild hybrid and plug-in hybrid.

https://doi.org/10.51202/9783181023549 - Generiert durch IP 216.73.216.36, am 19.01.2026, 02:19:31. © Urheberrechtlich geschützter Inhalt. Ohne gesonderte Erlaubnis ist jede urheberrechtliche Nutzung untersagt, insbesondere die Nutzung des Inhalts im Zusammenhang mit, für oder in KI-Systemen, KI-Modellen oder Generativen Sprachmodellen.

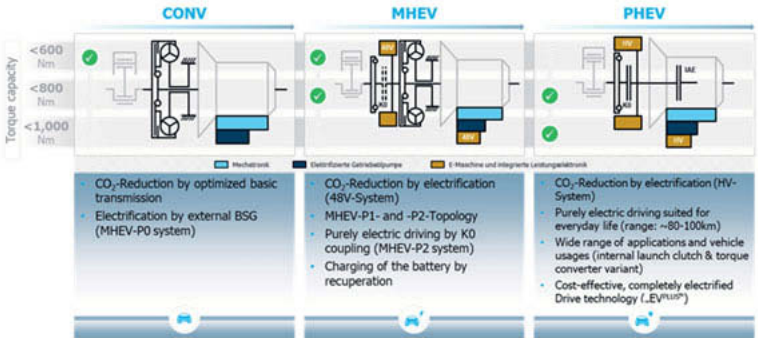


Fig. 3: Modular design kit 8HP 4th Generation

3. Package neutral integration

Derived from the requirement to generate installation space in order to package the integration of the E-machine and the power inverter module as well as carry-over the base 8-speed transmission architecture, new geometric and technical solutions were developed.

Fundamental potentials in 8HP technology are created by the following measures:

3.1 Electric drive: Power Inverter Modules and Electric Motor

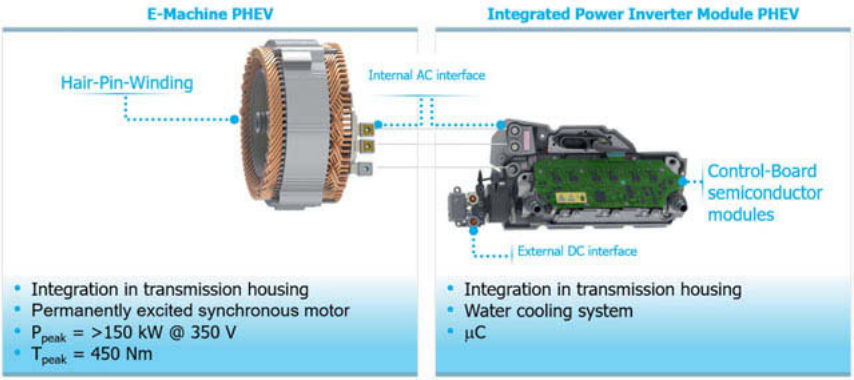


Fig. 4: Fully integrated technologies: E-Drive PHEV

https://doi.org/10.51202/9783181023549 - Generiert durch IP 216.73.216.36, am 19.01.2026, 02:19:31. © Urheberrechtlich geschützter Inhalt. Ohne gesonderte Erlaubnis ist jede urheberrechtliche Nutzung untersagt, insbesondere die Nutzung des Inhalts im Zusammenhang mit, für oder in KI-Systemen, KI-Modellen oder Generativen Sprachmodellen.

3.2 Fully integrated launch elements

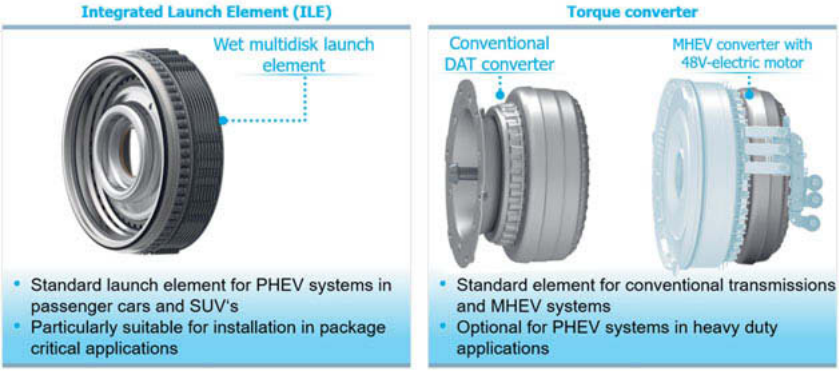


Fig. 5: Fully integrated technologies: Launch elements

3.3 Installation space optimized mechatronics with fully integrated pump system

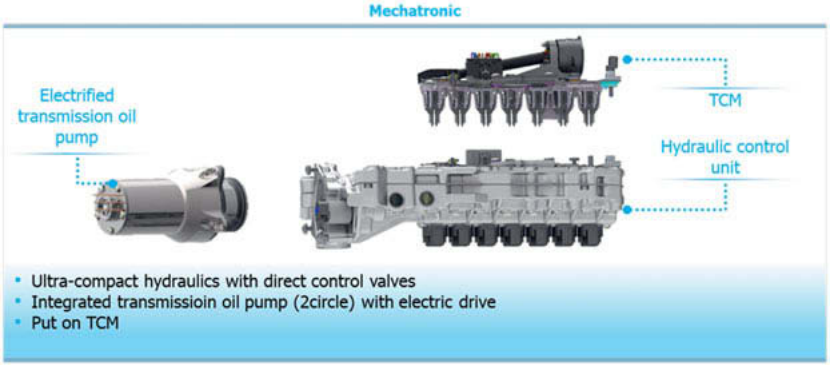


Fig. 6: Fully integrated technologies: Mechatronic

https://doi.org/10.51202/9783181023549 - Generiert durch IP 216.73.216.36, am 19.01.2026, 02:19:31. © Urheberrechtlich geschützter Inhalt. Ohne gesonderte Erlaubnis ist jede urheberrechtliche Nutzung untersagt, insbesondere die Nutzung des Inhalts im Zusammenhang mit, für oder in KI-Systemen, KI-Modellen oder Generativen Sprachmodellen.

3.4 Integrated parking lock module

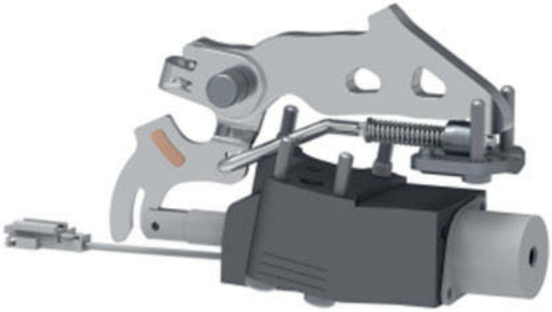


Fig. 7: Parking lock mechanics with actuators

Considering these measures in total the necessary installation space can be identified, which enables a full integration of the E-Drive, consisting of power inverter module and E-machine within the given vehicle architecture.

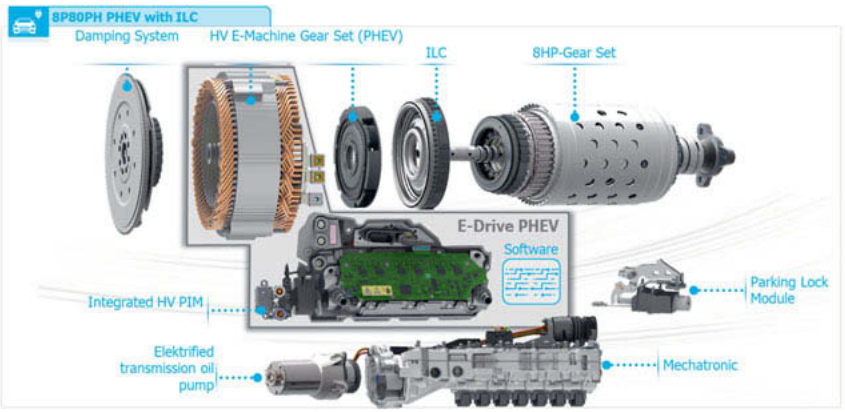


Fig. 8: Fully integrated technologies: Overview of PHEV

https://doi.org/10.51202/9783181023549 - Generiert durch IP 216.73.216.36, am 19.01.2026, 02:19:31. © Urheberrechtlich geschützter Inhalt. Ohne gesonderte Erlaubnis ist jede urheberrechtliche Nutzung untersagt, insbesondere die Nutzung des Inhalts im Zusammenhang mit, für oder in KI-Systemen, KI-Modellen oder Generativen Sprachmodellen.

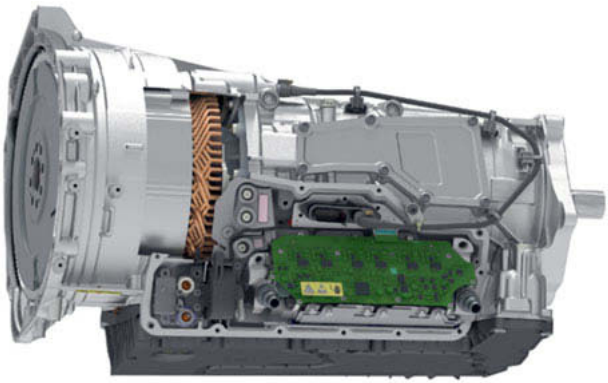


Fig. 9: Modular Design Kit 8HP 4th Generation

The hybrid drives that are thus created have an additional benefit: Minimizing the distances between power inverter module and the electric motor eliminates long, lossy and complex external wiring harness solutions and connecting cables can be completely integrated into the transmission. Accordingly, this eliminates the need to reserve installation space for power inverter module and cable routing in the vehicle compartment. We call this technology the EVPlus drive.

4. CO_2 reduction: favorable overall assessment

The increase in electric power in recuperation and boost mode as well as the increase in vehicle ranges for purely electric driving results in significant CO_2 advantages. In addition, mechanical losses in the 4th generation basic transmission were further reduced.

https://doi.org/10.51202/9783181023549 - Generiert durch IP 216.73.216.36, am 19.01.2026, 02:19:31. © Urheberrechtlich geschützter Inhalt. Ohne gesonderte Erlaubnis ist jede urheberrechtliche Nutzung untersagt, insbesondere die Nutzung des Inhalts im Zusammenhang mit, für oder in KI-Systemen, KI-Modellen oder Generativen Sprachmodellen.

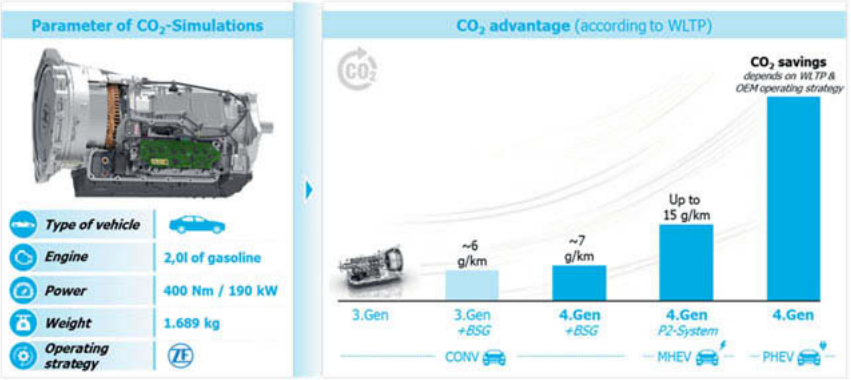


Fig. 10: CO2 savings: achieved emission reduction

Plug-in hybrids with this technology enable electric ranges from 80 to 100 kilometers. In day-to-day use with customers, it can be assumed the majority of the vehicle operations, as for example the commuter traffic in city areas and concurbations is driven purely electric. As a result, significant contributions to environmental friendliness and reduction of the local emission of pollutants in polluted urban areas are achieved. This new technology is named EVPlus.

5. Flexibility by modular design kit solutions

For the greatest possible flexibility and minimization of variants in production, carry-over solutions for all transmission derivatives need to be developed on a sub-system level.

Important individual components such as power inverter module, the parking lock module, the oil supply / hydraulics and electric motors are designed as carry-over parts for the targetted transmission design kit and transmission derivatives.

The modular design thus enables a high degree of exchange flexibility in production and enables to very quickly respond to volume shifts in the markets.

Due to the following characteristic features, high exchange flexibility is created in the modular design kit of the 4th gen.:

https://doi.org/10.51202/9783181023549 - Generiert durch IP 216.73.216.36, am 19.01.2026, 02:19:31. © Urheberrechtlich geschützter Inhalt. Ohne gesonderte Erlaubnis ist jede urheberrechtliche Nutzung untersagt, insbesondere die Nutzung des Inhalts im Zusammenhang mit, für oder in KI-Systemen, KI-Modellen oder Generativen Sprachmodellen.

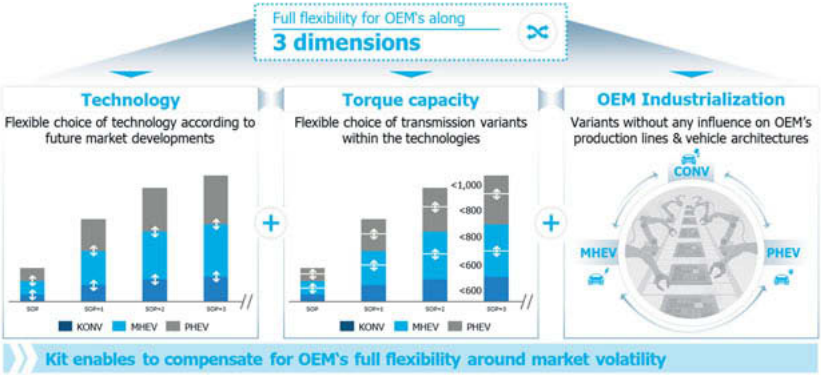


Fig. 11: Flexibility: Full flexibility within the 8HP 4. Generation

The achieved high cost efficiency enables the high volume production of the new drive technologies and is therefore the basis for a broad rollout of hybrid technology.



Fig. 12: Flexibility: Cost efficiency leads to the "EVPlus"

6. Summary: => ready for the future

In addition to the enhanced development of components and sub-systems, major challenges in geometric and electric integration, thermal management, acoustics and EMC have to be overcome in order to make the technology of highly integrated hybrid drives suitable for series volume production.

https://doi.org/10.51202/9783181023549 - Generiert durch IP 216.73.216.36, am 19.01.2026, 02:19:31. © Urheberrechtlich geschützter Inhalt. Ohne gesonderte Erlaubnis ist jede urheberrechtliche Nutzung untersagt, insbesondere die Nutzung des Inhalts im Zusammenhang mit, für oder in KI-Systemen, KI-Modellen oder Generativen Sprachmodellen.

The next generation of ZF's 8-speed transmissions has been designed consistently from the point of view of electrification and hybridization and, due to the achieved degree of integration of electrification as well as the high cost efficiency, gives the newly developed modular design kit the necessary flexibility to meet future market requirements.

As an overall assessment, in this generation the majority of the daily usage will be all-electric using the plug-in hybrid drives. As a result, electric drives will be the primary drive for plug-in hybrids in the future compared to combustion engines and will significantly reduce the fear of many drivers on their way to electrified mobility regarding limited vehicle ranges.

This technology can help us succeed in making electromobility accessible to many people – especially for those, who can only afford one car, but want to travel long distances without any problems, for example travelling on vacation by car.

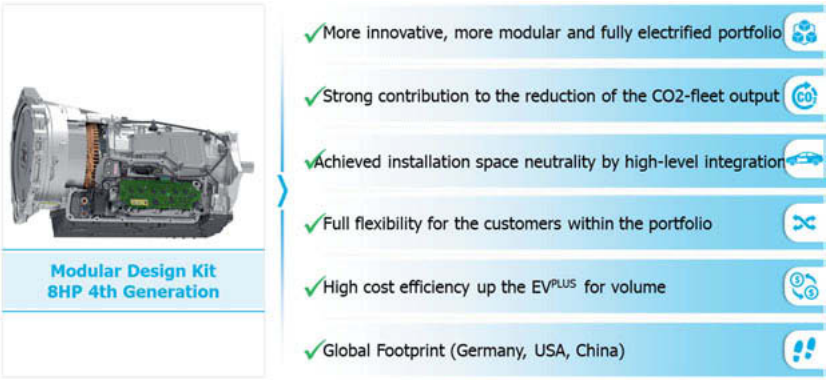


Fig. 13: 8HP 4th generation at a glance

https://doi.org/10.51202/9783181023549 - Generiert durch IP 216.73.216.36, am 19.01.2026, 02:19:31. © Urheberrechtlich geschützter Inhalt. Ohne gesonderte Erlaubnis ist jede urheberrechtliche Nutzung untersagt, insbesondere die Nutzung des Inhalts im Zusammenhang mit, für oder in KI-Systemen, KI-Modellen oder Generativen Sprachmodellen.

Artificial Intelligence in Transmission Control

Clutch Engagement with Reinforcement Learning

Alexander Lampe, **Roland Serway**,
Leopold Große Siestrup, IAV GmbH, Berlin;
Clemens Gühmann, Technical University Berlin

Zusammenfassung

Im Bereich der Softwareentwicklung für Getriebe finden überwiegend modellbasierte Steuerungskonzepte ihren Einsatz, die eine physikalische Modellierung des Systems voraussetzen. Sie haben den Nachteil, dass sie die Kenntnis über das reale System erfordern, dieses aber meist nur mit begrenzter Güte abbilden. Die Folge daraus ist ein erhöhter und damit zeitintensiver Applikationsaufwand zur Feinabstimmung des Systems. Hierbei erfordern Getriebe-Softwarefunktionen, wie der Anfahrregler für Automatikgetriebe mit Reibkupplung als Anfahrelement, einen besonders hohen Applikationsaufwand, da sie maßgeblich den Komfort des Systems mitbestimmen. Gleichzeitig erschweren nichtlineare Systemphänomene und unsicherheitsbehaftete Regelgrößen den Entwurf eines Anfahrreglers, der den Ansprüchen des Kunden gerecht wird.

Mit dem Ziel einerseits den Applikationsaufwand zu reduzieren und andererseits die Regelgüte zu erhöhen, wird ein datenbasierter Regler mit dem Reinforcement Learning (RL) Ansatz entwickelt. Die Vorteile gegenüber modellbasierten und modellprädiktiven Ansätzen wie der Modellprädiktiven Regelung (Model Predictive Control, MPC), ergeben sich dadurch, dass ein Modell des dynamischen Systems nicht zwingend notwendig ist (model-free RL) und der RL-Algorithmus erfahrungsbasiert arbeitet. Das Reglerverhalten wird dabei von einer zu minimierenden Kostenfunktion bzw. zu maximierenden Reward-Funktion abgeleitet. Das heißt, der Reinforcement Learning Regler arbeitet bezüglich einer gewählten Kostenfunktion optimal.

In diesem Artikel wird Reinforcement Learning, ein Verfahren aus dem Bereich des maschinellen Lernens, in den Kontext der Anwendung im Bereich von Automotive Embedded Systemen gestellt und diskutiert. Dabei wird unter anderem auf die Anwendbarkeit des Verfahrens im Hinblick auf die Einhaltung Funktionaler Sicherheit und auf Hardware-Anforderungen eingegangen. Der Artikel gibt außerdem einen Einblick in die Auswahlkriterien des Algorithmus

https://doi.org/10.51202/9783181023549 - Generiert durch IP 216.73.216.36, am 19.01.2026, 02:19:31. © Urheberrechtlich geschützter Inhalt. Ohne gesonderte Erlaubnis ist jede urheberrechtliche Nutzung untersagt, insbesondere die Nutzung des Inhalts im Zusammenhang mit, für oder in KI-Systemen, KI-Modellen oder Generativen Sprachmodellen.

und die Vorgehensweise bei der Festlegung wichtiger Größen. Abschließend werden erste Ergebnisse aus der Simulation, basierend auf einem einfachen Triebstrangmodell, präsentiert.

Abstract

Software development for transmissions mainly uses model-based control concepts that require physical modeling of the system. The drawback is that knowledge of the real system is needed, which can usually only be represented with limited quality, resulting in augmented, time-consuming calibration effort for fine-tuning of the system. Transmission software functions such as the start-up controller for automatic transmissions with friction clutch as start-up element play a key role in defining system comfort and thus require a particularly high calibration effort. At the same time, non-linear system phenomena and uncertain control variables make it difficult to design a start-up controller that meets customer demands.

In order to reduce calibration effort on the one hand and improve control quality on the other, a data-based controller has been developed with the reinforcement learning approach (RL). The advantages compared to model-based and model-predictive approaches such as model predictive control (MPC) result from the fact that is not strictly necessary to model the dynamic system (model-free RL) and the RL algorithm works on the basis of experience. The controller behavior is derived from minimizing the cost function and maximizing the reward function. In other words, the reinforcement learning controller operates optimally in terms of a chosen cost function.

This paper presents and discusses reinforcement learning as a machine learning process in the context of its use in automotive embedded systems, looking among others at the applicability of the method with regard to complying with functional safety and in terms of hardware requirements. The paper also gives an insight into the selection criteria for the algorithm and the procedure for stipulating important variables. Finally, initial simulation results are presented based on a simple powertrain model.

1 Introduction

There have been rapid developments in the field of machine learning recently, due to progress in inventing new algorithms and the development of more powerful hardware. Furthermore, open source frameworks encourage researchers and engineers to apply machine learning to their specific problems. Latest successes such as image recognition and the ability to play computer and board games on a human or even super-human level demonstrate the potential of machine learning algorithms in general and reinforcement learning in particular [1, 2].

https://doi.org/10.51202/9783181023549 - Generiert durch IP 216.73.216.36, am 19.01.2026, 02:19:31. © Urheberrechtlich geschützter Inhalt. Ohne gesonderte Erlaubnis ist jede urheberrechtliche Nutzung untersagt, insbesondere die Nutzung des Inhalts im Zusammenhang mit, für oder in KI-Systemen, KI-Modellen oder Generativen Sprachmodellen.

Control-theory-based algorithms such as physical model approaches are common practice in transmission control. They are model-based and therefore need a good understanding of the underlying system to create physical models. This requires techniques such as parameter estimation. In most cases, the model is simplified so that linear control methods can be used, but this comes at the cost of control inaccuracy. It also results in greater manual calibration effort to adjust the control software to physical phenomena and uncertainties not covered by the model. In automatic transmissions such as dual clutch transmissions and automated manual transmissions, clutch engagement control is one of the most demanding functions in scenarios such as vehicle start-up and maneuvering where high control accuracy is required. But clutch engagement triggers uncertainties and non-linear effects that are hard to model. Clutch engagement also has a major impact on comfort. The characteristics of the physical system combined with customer expectations lead to a high function development and calibration workload.

Data-driven models and control algorithms such as reinforcement learning have scarcely been investigated in transmission control. But their autonomous learning of a representation of the physical system eliminates the need for a physical model: they seem to be well suited for control problems such as clutch engagement control in automatic transmissions.

This paper investigates the reinforcement learning approach for solving the clutch engagement control problem while considering practical issues such as hardware and functional safety requirements. It begins with a basic introduction to machine learning and then shows which constraints must be met to comply with ISO 26262. It discusses the relationship between reinforcement learning and model predictive control, as the latter is well investigated in published research. Reinforcement learning is seen to have several advantages over model predictive control. These include lower computational demand so that the algorithm runs on standard hardware, together with more opportunities for fine-tuning control behavior. The paper then gives a basic understanding of how reinforcement learning works and what must be considered to solve the clutch engagement problem with reinforcement learning when starting from scratch. Finally, simulations illustrate the potential of this approach, showing first results for a clutch engagement controller in a simplified environment.

2 Machine Learning in Embedded Systems

This section outlines the differences between traditional programming and machine learning and why machine learning has great potential for use in embedded systems but is also questioned with regard to safety.

https://doi.org/10.51202/9783181023549 - Generiert durch IP 216.73.216.36, am 19.01.2026, 02:19:31. © Urheberrechtlich geschützter Inhalt. Ohne gesonderte Erlaubnis ist jede urheberrechtliche Nutzung untersagt, insbesondere die Nutzung des Inhalts im Zusammenhang mit, für oder in KI-Systemen, KI-Modellen oder Generativen Sprachmodellen.

2.1 Machine Learning - Strengths and Weaknesses

The machine learning approach to solving a problem differs generally from that of traditional computer programming. In traditional programming, programmers use their knowledge to write down rules which may result in a computer program that solves the intended task. Knowledge can be any kind of understanding of the problem, including for example expertise gained by experience, or technical methods which the programmer feels to be appropriate for the problem. However, the solution is always highly dependent on the programmer's knowledge and understanding, and on the *model* he or she has in mind.

On the contrary, in machine learning, knowledge is built upon data. This is done by extracting rules which then serve as a program as shown in Fig. 1. The general advantage is that there is no need to make any assumptions about the underlying problem. The solution is not bound to or restricted by the knowledge of an expert, technical specialist or programmer. This can be seen as a scaling effect in creating programs as they can be generated from data [3].

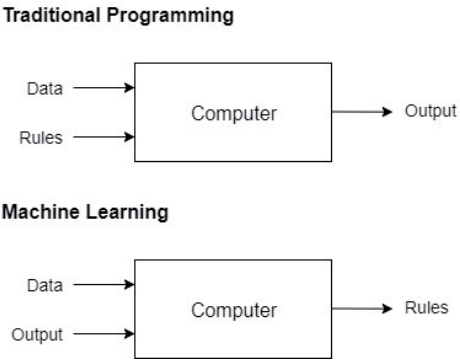


Fig. 1: Comparison of concepts: traditional programming vs. machine learning. Adopted from [3].

From that point of view, machine learning can even be used to create programs for problems where no solutions existed in the past. It also offers great potential for enhancing functionality and improving the quality of automotive applications. In particular, embedded automotive applications can benefit from machine learning algorithms, where it is hard to describe processes, physical relations and phenomena using physical models such as the clutch engagement process.

https://doi.org/10.51202/9783181023549 - Generiert durch IP 216.73.216.36, am 19.01.2026, 02:19:31. © Urheberrechtlich geschützter Inhalt. Ohne gesonderte Erlaubnis ist jede urheberrechtliche Nutzung untersagt, insbesondere die Nutzung des Inhalts im Zusammenhang mit, für oder in KI-Systemen, KI-Modellen oder Generativen Sprachmodellen.

Besides the huge potential of machine learning algorithms, they also have some drawbacks. With data being the source from which the program is created, in-depth data analysis is mandatory to ensure that the selected data represents the problem. After all, the program must offer a general solution to the problem. In other words, its results for unseen data must be as good as for the training data. Furthermore, the machine learning algorithm also has to match the data and problem. It therefore still takes a lot of effort to create programs using machine learning algorithms, but there is a shift in emphasis from writing rules to analyzing data and creating rules from data.

Machine learning algorithms need plenty of data and computational power for training (program creation). As a result, current standard embedded hardware in general and powertrain hardware in particular is not suitable for online learning. The need for program validation in particular makes online learning impractical and unsafe. However, it should be possible to move the training and validation process offline, based on the emergence of cloud-integrated vehicles.

Moreover, the way in which information is abstracted and processed by neural networks makes it hard for humans to interpret the decisions of a machine learning program. This raises issues in terms of the safety of embedded systems.

2.2 Machine Learning and Embedded Systems in the Context of Functional Safety

Machine learning is used in many day-to-day applications such as personal assistants, referral systems (advertising, audio and video on-demand services, image search), spam filtering and more besides. As previously mentioned, their common feature is that they rely on data and abstracting rules to perform their intended task. Furthermore, most machine learning applications are just services providing information, which means they do not cause injuries if they fail. They are not safety-critical. In contrast to the wide range of service applications, machine learning is rarely used in embedded systems, especially in automotive applications where safety and reliability are major factors. In the automotive sector, standards such as ISO 26262 have emerged to establish consistent and systematic processes that deal with safety-related embedded development. These standards neither specify nor restrict the use of functions but claim to be a standardized process for hazard and risk analysis which must result in precise specifications for software safety requirements. In the context of machine learning in embedded systems and ISO 26262, there are two main obstacles with regard to ensuring safety of software, as Salay [4] pointed out:

1. Lack of specification, and
2. Non-interpretability.

https://doi.org/10.51202/9783181023549 - Generiert durch IP 216.73.216.36, am 19.01.2026, 02:19:31. © Urheberrechtlich geschützter Inhalt. Ohne gesonderte Erlaubnis ist jede urheberrechtliche Nutzung untersagt, insbesondere die Nutzung des Inhalts im Zusammenhang mit, für oder in KI-Systemen, KI-Modellen oder Generativen Sprachmodellen.

Lack of specification addresses the issue that it is not completely possible to specify advanced functionality such as autonomous driving. For instance, no appropriate specification is available for the functionality of recognizing objects (pedestrians, vehicles, cyclists). Non-interpretability refers to the widely known problem that humans cannot comprehend decisions or actions by black box models such as neural networks because information processing and decision-making is encoded in the neural network.

These obstacles are primarily a hindrance to advanced functions such as perception of the surroundings in the context of automated driving, where precise requirements are hard to specify and where there are no alternatives to machine learning when it comes to safety monitoring functions. In contrast, a clutch controller operates in a state space with much smaller dimensions and has well definable operational targets. There is therefore no lack of specification, so that functional safety standards can be applied. As a consequence, safety monitoring functions can be defined and tested by strict rules using imperative programming, therefore being interpretable and standard-compliant. Finally, if it is assumed that there is strict separation between the function and safety monitoring based on actual safety standards, there are no restrictions on using machine learning algorithms in such an application. As shown in Fig 2, the safety monitoring function uses unprocessed sensor inputs and monitors the action of the machine learning controller without having any access to the internals of this function. On detecting any anomalies, the safety monitoring function disables the controller and enables a safe action that ensures a safe state.

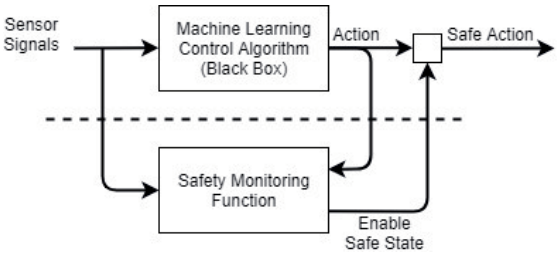


Fig. 2: Safety monitoring concept. Adopted from [5].

3 Clutch Engagement and Vehicle Start-Up

Clutch engagement in the context of a vehicle start-up is one of the most demanding functions in automatic transmissions such as dual clutch transmissions (DCT) and automated manual transmissions (AMT), due to the multiple criteria that have to be met. This section discusses these criteria and gives an overview of published investigations.

https://doi.org/10.51202/9783181023549 - Generiert durch IP 216.73.216.36, am 19.01.2026, 02:19:31. © Urheberrechtlich geschützter Inhalt. Ohne gesonderte Erlaubnis ist jede urheberrechtliche Nutzung untersagt, insbesondere die Nutzung des Inhalts im Zusammenhang mit, für oder in KI-Systemen, KI-Modellen oder Generativen Sprachmodellen.

3.1 A Multi-Objective Problem

From a historical perspective, AMTs and DCTs became an alternative to previous automated transmissions, which offer high levels of comfort during vehicle start-up and in the low-speed range thanks to the natural, smooth transmission behavior of the hydraulic torque converter. In DCTs and AMTs, this functionality must be realized with an actuated dry or wet clutch. Low-speed operation makes high demands of control accuracy because

- drivers generally tend to be more perceptive in the lower speed range;
- vehicles are usually started up and driven at low speed in safety-critical situations such as parking and maneuvering where the transmission behavior must meet the driver's expectations.

While a hydraulic torque converter is mechanically designed to fulfill these requirements, an automatic transmission with a clutch as a start-up element introduces some tricky problems with respect to control in low-speed and start-up scenarios. Generally this refers to

- highly non-linear transmission behavior (especially in systems with dry clutch) where the transmitted torque is a function of slip speed, clutch plate temperature, actuation force and other less dominant variables;
- imprecisely estimated torque of the internal combustion engine (especially near idle speed) which generally needs to be used as a controller’s state.

The targets for high-quality start-up and maneuvering control from the consumer's perspective are

- plausibility: meet the driver’s intention;
- reliability and confidence: always meet the driver’s expectation
- comfort: smooth control, avoid shocks;
- spontaneity and sportiness: give direct feedback to the driver.

These requirements are hard to fulfill with regard to the underlying non-linear transmission behavior. Some of them are conflicting: comfort needs smooth clutch operation; on the other hand, spontaneity needs fast clutch operation for an immediate response. In addition to control targets focusing on engagement quality, automatic transmissions with insufficient clutch cooling capability (as is the case with dry clutch systems for instance) can be subjected to additional friction loss constraints which must be taken into account when defining the control targets. As a consequence, the complexity of the overall problem demands great development effort to meet market requirements.

https://doi.org/10.51202/9783181023549 - Generiert durch IP 216.73.216.36, am 19.01.2026, 02:19:31. © Urheberrechtlich geschützter Inhalt. Ohne gesonderte Erlaubnis ist jede urheberrechtliche Nutzung untersagt, insbesondere die Nutzung des Inhalts im Zusammenhang mit, für oder in KI-Systemen, KI-Modellen oder Generativen Sprachmodellen.

3.2 A Discussion of Published Works

In technical terms, the above-mentioned criteria can be described as a multi-objective optimization problem. This idea has been broadly investigated for clutch engagement in general and dry clutch engagement in particular, using the approach of optimum control and model predictive control [6, 7, 8, 9, 10]. In optimum control, the fundamental equation is a cost function $J(x,u)$ as a function of states x and actions u, minimized over a finite time horizon. Assuming that x and u are scalar, a simplified representation of the cost function can be expressed as:

$$J(x_k,u)=\sum_{l=k}^{k+p}\left(q\cdot x_l^2+r\cdot u_l^2\right),$$

where q and r are scalar weight factors and p is the prediction horizon of the controller. The objective is to find a trajectory of actions $u_k,\dots,u_{k+p}$ which minimizes the cost function within the prediction horizon:

$$u=arg\min_u J(x_k,u)$$

In MPC, this optimization problem is solved for each time step k. By using the measured state x_k obtained from sensors, the feedback loop is closed, and the optimization problem is turned into a closed-loop controller. In this approach, a mathematical description of the dynamic model is mandatory as it is needed in the optimization process to calculate the state trajectories $x_{k+1},\dots,x_{k+p}$. All references mentioned use linear models of various orders to construct convex optimization problems which have only one global optimal solution. As a consequence, they are much easier to solve than non-linear problems.

In [6], a linear model with rigid bodies and no elasticities is used. The optimization goals are to reduce clutch slip while ensuring smooth clutch operation. This is achieved by defining x to represent the slip at the clutch, $x=w_{slip}$, and u as the derivative of clutch torque capacity, which is proportional to the change in vehicle acceleration when the clutch slips. In addition, a constraint $x_{k+p^*}=0$ is introduced to force the slip decrease to zero after p^* steps. This produces suboptimal and impractical solutions since the time of engagement is unknown and must be estimated as it depends on non-predictable quantities such as engine torque (driver's demand) and development of vehicle speed to meet the engine idle speed constraint, which is $\omega_{Eng,k}\geq\omega_{Eng,idle,k},\ \forall\ k$.

In general, Garofalo [7] uses a similar model and approach but introduces more constraints such as the *no-kill* condition, which takes the engine idle speed constraint into account, and the *no-lurch* condition, which reduces the induced shock at the clutch lock-up instant. This is achieved by enforcing a minimized difference between the clutch torque transmitted before the lock-up instant and after the lock-up instant, where the transmitted torque after the lock-up

https://doi.org/10.51202/9783181023549 - Generiert durch IP 216.73.216.36, am 19.01.2026, 02:19:31. © Urheberrechtlich geschützter Inhalt. Ohne gesonderte Erlaubnis ist jede urheberrechtliche Nutzung untersagt, insbesondere die Nutzung des Inhalts im Zusammenhang mit, für oder in KI-Systemen, KI-Modellen oder Generativen Sprachmodellen.

instant can be obtained from algebraic manipulation of the dynamic equations of the model. In contrast to Glielmo [6], x is defined as the difference between engine speed and a desired trajectory, $x = \omega_{Eng,ref} - \omega_{Eng}$, which must be chosen as appropriate for the no-kill condition. Dolcini [8] adds new states to the linear model with a spring and a damper at the transmission output to reflect the elasticities from the differential to the wheels. The no-lurch constraint can then be formulated in terms of the spring twisting angle at the lock-up instant, which is also obtained by algebraic manipulation of the model's dynamic equations.

In contrast to the previously mentioned approaches, Amari [9] drops the action term in the cost function and instead uses two reference speed trajectories for optimization. One acts as a reference for the desired clutch slip and the other as a reference for the desired engine speed. Those reference trajectories are updated and re-calculated in each time step. The slip speed trajectory ensures a smooth and steady reduction of the slip speed to zero which approximately fulfills the no-lurch condition at the lock-up instant. The engine speed trajectory is a function of the driver's torque demand, taking into account the engine's maximum torque characteristic as a function of engine speed and the idle speed constraint. Amari [9] solves the issue of a fixed duration for clutch engagement which is now adopted in each time step and obtained from a look-up table that maps the acceleration pedal to an estimated clutch engagement duration or number of steps p^*, respectively. The clutch engagement duration is set in limits of a minimum duration, in case of maximum acceleration demand, and infinite duration, in case of no acceleration demand.

All of the previously discussed proposals use the MPC approach where a cost function must be optimized online for each time step. In [6] and [7], constrained optimization problems must be solved. This is an expensive task in terms of computational effort with increasing hardware requirements and hardware costs. Amari [9] reduces computational costs by transforming the constrained optimization problem into an unconstrained one based on reference trajectories which implicitly satisfy the constraints. Nevertheless, the prediction horizon is still restricted since it has a major impact on computational costs.

That is why Bemporad [10] proposes offline MPC, using a multi-parameter programming solver to divide the state space into regions and to determine linear gains. This produces control actions equivalent to MPC. While Bemporad [10] uses a linear model and linear MPC, non-linear MPC can also be applied since there is no real-time requirement in offline MPC. Although in [10] suitable results are obtained by dividing the state space into three to seven regions, the question as to how many regions are necessary for non-linear MPC remains unanswered.

As stated before, a model is mandatory for MPC. Linear models are the only way of keeping computational costs for online MPC as low as possible. While the model used in MPC can be

https://doi.org/10.51202/9783181023549 - Generiert durch IP 216.73.216.36, am 19.01.2026, 02:19:31. © Urheberrechtlich geschützter Inhalt. Ohne gesonderte Erlaubnis ist jede urheberrechtliche Nutzung untersagt, insbesondere die Nutzung des Inhalts im Zusammenhang mit, für oder in KI-Systemen, KI-Modellen oder Generativen Sprachmodellen.

simpler than the real system, as shown in [7], linear MPC lacks the fine-tuning options that are in great demand for state-of-the-art solutions and high-value products.
This explains why heuristic methods are most common in current embedded software development, combining techniques such as feed-forward control, map-based control and parameter estimation which are designed to offer a high level of freedom for the purpose of calibration and fine-tuning capabilities.

4 Clutch Engagement and Reinforcement Learning

This section gives a general introduction to the idea and mechanisms of reinforcement learning and outlines the potential with regard to its application in embedded systems in terms of control. It then uses reinforcement learning to address the clutch engagement problem and presents initial results.

4.1 Reinforcement Learning and its Potential in Embedded Systems

Reinforcement learning is an area of machine learning where a program, called an agent, interacts with an environment and is trained to maximize a cumulative reward by taking appropriate actions. It has become well-known because agents can learn complex strategies to solve complex tasks that cannot be solved by any other method, such as conventional computer programming. It has attracted a lot of attention in the field of research where an agent develops its own rules and strategies when playing board games and computer games. Such applications have a great appeal for research due to the large input space: agents play computer games fed by raw pixels and have to develop long-term strategies. Agents are seen to be capable of human level or even super-human level performance in board games such as Go and chess [2] and computer games such as Dota 2 [11] and StarCraft [12]. Apart from the breakthrough in playing games, reinforcement learning also plays an important role in applications such as robotics, where the application of classic control theory is dominant [13].
To familiarize the reader with the basic concept of an agent, Fig. 3 compares a reference tracking controller and a reinforcement learning agent. As can be seen, the terminology and notation is slightly different. But in general and from the control perspective, the agent is equivalent to a controller taking actions based on the observed states, s_k and y_k. New states

https://doi.org/10.51202/9783181023549 - Generiert durch IP 216.73.216.36, am 19.01.2026, 02:19:31. © Urheberrechtlich geschützter Inhalt. Ohne gesonderte Erlaubnis ist jede urheberrechtliche Nutzung untersagt, insbesondere die Nutzung des Inhalts im Zusammenhang mit, für oder in KI-Systemen, KI-Modellen oder Generativen Sprachmodellen.

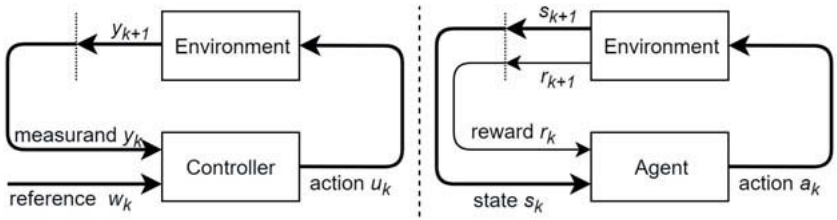


Fig. 3: Comparison of a reference tracking controller (left) and a reinforcement learning agent (right)

s_{k+1} are obtained from the environment by taking actions based on previous states, $s_{k+1} = f(s_k, a_k)$. The mapping of states s to actions a is called *policy* π of the agent, denoted $a_k = \pi_{\theta_\pi}(s_k)$. The policy π_{θ_π} is a function with parameters θ_π. In most cases this is a neural network where parameters are optimized to maximize the reward. The reward is a scalar value that the agent receives from the environment and is a function of states and actions, $r_{k+1} = f_r(s_k, a_k)$.

In more precise terms, the goal is to maximize the cumulative return G_k that is a weighted sum of the reward of the current time step r_k and all successive rewards:

$$G_k = \sum_{l=k}^{N} \gamma^{l-k} \cdot r_l = \gamma^0 \cdot r_k + \gamma^1 \cdot r_{k+1} + \gamma^2 \cdot r_{k+2} + \ldots + \gamma^N \cdot r_{N-k}$$

Both the reward and the return are scalar values. γ is a design parameter in the limits of zero and one and N is the length of an episode. γ determines the foresight of the agent. If γ is zero, the agent tries to maximize only the reward of the current time step as all successive rewards are not taken into account. For infinite episodes, γ must be less than one to ensure finite returns.

The goal in most cases is to find an optimum trajectory of actions $u_k, \ldots, u_N$ rather than an optimum action with respect to the current time step, so that γ is set to a value near one. For example, $\gamma = 0.99$ is commonly used.

The objective of maximizing the cumulative return is equivalent to minimizing a cost function. That shows a direct relation between reinforcement learning and model predictive control. MPC results in optimum trajectories of actions so that reinforcement learning should do the same. But some key differences should be pointed out. In a model-free approach, a reinforcement learning agent is trained on data and builds its own understanding of the environment and its implied rules. In comparison to MPC, this has the advantage that no model is required, and the optimality of the solution is not restricted by model accuracy. But this comes at the

https://doi.org/10.51202/9783181023549 - Generiert durch IP 216.73.216.36, am 19.01.2026, 02:19:31. © Urheberrechtlich geschützter Inhalt. Ohne gesonderte Erlaubnis ist jede urheberrechtliche Nutzung untersagt, insbesondere die Nutzung des Inhalts im Zusammenhang mit, für oder in KI-Systemen, KI-Modellen oder Generativen Sprachmodellen.

cost of *sample inefficiency*. To obtain an understanding of the environment and find an optimum policy, the agent must explore the environment to gain new information. In other words, the agent has to try different actions to find the best one. On the other hand, it should rely on the knowledge it has gained to get high rewards. This trade-off is widely known as the *exploration vs. exploitation* dilemma and is still unresolved [14].

As the state space grows, more samples of the environment are needed. In simulated environments, such as games or physical systems simulation, exploring the environment is inexpensive and mostly fast. In contrast, exploring real environments always incurs costs and can be a slow process, since the agent has to explore the environment in real time. Many researchers therefore focus on extending existing reinforcement learning algorithms or finding new ones with faster convergence to the optimum solution, thus being more efficient in terms of samples [15, 16].

Once the agent's optimum policy has been found, there is no further need for training. The agent memorizes the optimum action as a function of its state. A reinforcement learning agent is therefore better suited to embedded applications, since computation of the action is relatively cheap in comparison to MPC because MPC lacks memoization and has to solve the optimization problem for each time step all over again. Görges [17] provides a detailed view of the relationship between model predictive control and reinforcement learning.

Section 3.2 showed that all approaches use linear MPC to minimize computational costs. Cost formulation is therefore restricted to being a quadratic formulation of states and actions. By contrast, in reinforcement learning the reward r_k can be any non-linear function, thus enabling large degrees of freedom with respect to fine-tuning as is necessary for vehicle start-up and maneuvering.

4.2 The Choice of Algorithms

A huge number of reinforcement learning algorithms exists. The number is expected to grow even more due to intensive research. Algorithm selection depends on the specific problem, particularly the environment, so that there is only one subset of algorithms that can be used for the clutch engagement task. The family of reinforcement learning algorithms has two main concepts: *Q-learning* and *policy gradients*. Q-learning is used in the field where the action space is discrete or discretized so that the agent has to select one of a finite number of actions. This is achieved by trying to predict the expected return G_k as a function of states and discrete actions a_i, $Q(s, a_i)$. The optimum policy π then consists in taking the action a_i that gives the maximum expected return. In policy gradient methods, direct mapping from states to actions is learned, $a = \pi_{\theta_\pi}(s)$, for use in environments with a continuous action space. The policy is

https://doi.org/10.51202/9783181023549 - Generiert durch IP 216.73.216.36, am 19.01.2026, 02:19:31. © Urheberrechtlich geschützter Inhalt. Ohne gesonderte Erlaubnis ist jede urheberrechtliche Nutzung untersagt, insbesondere die Nutzung des Inhalts im Zusammenhang mit, für oder in KI-Systemen, KI-Modellen oder Generativen Sprachmodellen.

learned by gradient methods that push its parameters θ_π towards maximizing the expected return. Since Q-learning is not applicable to problems with a continuous action space such as the clutch engagement problem, the algorithm must be chosen from the policy gradient family. There is still a wide choice of policy gradient methods. Weng [18] gives an overview of available and most significant policy gradient algorithms and the variations, counted 16 at the time of writing. One major characteristic of the algorithm is whether it is *on-policy* or *off-policy*. On-policy algorithms require fresh data. In other words, the policy cannot be trained with data gathered with an old policy. In more precise terms, every time the policy is updated, the new policy must be used to gather new data and is then updated again. The algorithm therefore has to learn online. But this has to be avoided in embedded systems as described in Section 2.1. Off-policy algorithms can learn from old data gathered during operation [19] and should be the preferred choice for embedded applications.

4.3 Deep Deterministic Policy Gradient Algorithm in Brief

The experiments described in this paper were conducted with the deep deterministic policy gradient (DDPG) algorithm. This section gives a general idea of the algorithm. Details of the algorithm can be found in the original paper [20]. It is an off-policy algorithm and uses a buffer of fixed size to store the data gathered during execution. The buffer is used to train the agent. As the agent operates in the environment, the buffer is updated with new data. This can be a valid setup for embedded applications, where the buffer is filled during operation and training takes place offline.

The key idea is to have two neural networks: the policy network with parameters θ_π called *actor* that maps states to actions, $a = \pi_{\theta_\pi}(s)$, and an additional network with parameters θ_Q called *critic* that estimates the cumulative return G as a function of states and actions, $Q_{\theta_Q}(s,a)$. Assuming that the critic is trained to be a good approximation of the cumulative return, $G(s,a) \approx Q_{\theta_{\{\}}}(s,a)$, a can be replaced in $Q_{\theta_Q}(s,a)$ by the policy $a = \pi_{\theta_\pi}(s)$:

$$Q_{\theta_Q}(s,a) = Q_{\theta_Q}\left(s, \pi_{\theta_\pi}(s)\right)$$

The gradient of the estimated cumulative return can then be calculated with respect to the actor's parameters:

$$\frac{\partial}{\partial \theta_\pi} Q_{\theta_Q}\left(s, \pi_{\theta_\pi}(s)\right)$$

Assuming that the agent is in a state s, the gradient describes the directions in which the parameters of the actor must be changed to increase the function Q and therefore increase the (estimated) cumulative reward.

https://doi.org/10.51202/9783181023549 - Generiert durch IP 216.73.216.36, am 19.01.2026, 02:19:31. © Urheberrechtlich geschützter Inhalt. Ohne gesonderte Erlaubnis ist jede urheberrechtliche Nutzung untersagt, insbesondere die Nutzung des Inhalts im Zusammenhang mit, für oder in KI-Systemen, KI-Modellen oder Generativen Sprachmodellen.

Finally, the gradient is used to update the parameters of the actor. That is done in many iterations. At the same time, the critic is trained and improved to estimate the cumulative reward.

4.4 Experimental Setup and Results

The focus of this section is to show that clutch engagement with Reinforcement learning is technically feasible, as it is the current state of investigation. A simple longitudinal model of a powertrain is therefore used. Model uncertainties, actuator dynamics and powertrain elasticities are neglected for this study.

At the start of investigating clutch engagement with a reinforcement learning controller, various central issues have to be addressed before an agent can be trained. As described above, states are mapped to actions by the policy of the agent, which is a neural network. The training process aims to optimize the policy with respect to the cumulative rewards obtained from the environment. Since the reward function $r_k = f_r(s_k, a_k)$ is not defined at the start of the investigation, there is no pre-existing knowledge about how complex, or non-linear in particular, the policy might be. A simple reward function can be expected to result in a simple, less non-linear policy. A highly non-linear reward function requires a more non-linear policy. The design of the reward function therefore has a direct impact on the requirement for policy approximation, so that the neural network has to be selected appropriately. Furthermore, it is known that there is always a trade-off between capability of approximation and generalization. Neural networks with many neurons have higher approximation capability but can fail to generalize unseen data. As a basic rule, more data is needed to train a larger neural network as there are more parameters to be tuned. This comes at the cost of longer training time. Moreover, the state space of the environment is assumed to be large. It is therefore hard to get a good representation of data since the data is correlated in the dimension of time, as the dynamic system evolves in time and the step size between samples is small. In brief, there are many interdependencies that require a great deal of investigation and experiments on account of their effect on training performance and the ultimate optimality of the policy.

To overcome these issues and to abbreviate the investigation, a neural network was trained to imitate an existing clutch engagement controller that was developed in-house and is used in prototype vehicles. To this end, a dataset was created from measurements and simulations to train the neural network with supervised learning. Supervised learning takes far less training time than reinforcement learning so that various neural network architectures have been trained and validated in simulation and in the prototype vehicle. Finally, a neural network with three hidden layers and a total number of 90 neurons produced sufficient results with respect

https://doi.org/10.51202/9783181023549 - Generiert durch IP 216.73.216.36, am 19.01.2026, 02:19:31. © Urheberrechtlich geschützter Inhalt. Ohne gesonderte Erlaubnis ist jede urheberrechtliche Nutzung untersagt, insbesondere die Nutzung des Inhalts im Zusammenhang mit, für oder in KI-Systemen, KI-Modellen oder Generativen Sprachmodellen.

to the approximation error and generalization capability. Furthermore, and with regard to application in volume production, the neural network and larger sized networks were successfully tested to run on top of production software on standard hardware, as used in mass production. The network architecture obtained from the supervised learning investigation is used for the policy network of the agent. The network's parameters are initialized arbitrarily because the goal is to learn the policy from scratch using only the reward function. The network architecture of the critic was iteratively adjusted and has approximately four times as many neurons as the policy network.

To simulate a vehicle start-up and to excite the system, a virtual driver is required to generate engine torque trajectories. It transpired that the agent fails to learn if only simple and few engine torque trajectories are used over and over again. This is because simple trajectories generate correlated data that is poorly distributed in state space. A virtual driver generating arbitrary engine torque trajectories proved to be the solution here.

As stated before, the reward function determines how the agent should act in the optimum case. Furthermore, it defines how hard it is to solve the problem with a great impact on the convergence of the training process. The design of a reward function is named as one of the most challenging tasks. The reward function in continuous state space should be continuous and preferably differentiable, since it is estimated by the critic network. Besides, the reward function should have no local minima which could hamper the agent during exploration in the training phase as it can get stuck in a local minimum.

The reward function is kept simple as a starting point for initial investigations. Adding a negative sign to the cost function from Section 3.2 turns it into a reward function. The agent then always receives negative rewards and tries to avoid actions that result in negative rewards. On the contrary, an agent that receives positive rewards tries to find and repeat actions that give high rewards to maximize its cumulative return. But since the agent is trained to respect given constraints such as the no-kill and no-lurch condition, it is more intuitive to punish the agent in case of constraint violation than to give positive rewards if constraints are met.

Finally, the reward function consists of three terms. The first term punishes the violation of the engine speed constraint that is to ensure a minimum engine speed needed to fulfill the driver's torque demand:

$$n_{ref,k} = max(f_{n,min}(T_{Eng,k}), n_{Gear,k})$$

$f_{n,min}(T_{Eng})$ maps the engine torque demand to a minimum engine speed and is obtained from the engine's maximum torque characteristic. The maximum is used to calculate the final reference speed and captures the case in which the shaft speed on the transmission side is larger than the minimum required engine speed.

https://doi.org/10.51202/9783181023549 - Generiert durch IP 216.73.216.36, am 19.01.2026, 02:19:31. © Urheberrechtlich geschützter Inhalt. Ohne gesonderte Erlaubnis ist jede urheberrechtliche Nutzung untersagt, insbesondere die Nutzung des Inhalts im Zusammenhang mit, für oder in KI-Systemen, KI-Modellen oder Generativen Sprachmodellen.

The second term ensures that clutch actuation is smooth and punishes the change of actions:

$$\Delta a_k = a_k - a_{k-1}$$

The reward is:

$$r_k = -\left(c \cdot \left(n_{ref,k} - n_{Eng,k}\right)^2 + (1-c) \cdot \Delta a_k^2\right) \cdot e_{idle,k} ,$$

where c is used to adjust the weighting of both two terms and $e_{idle,k}$ is the third term that reinforces the punishment if the no-kill condition is violated:

$$e_{idle,k} = max\left(n_{idle,k} - n_{Eng,k}, 1\right)$$

It equals one if the no-kill condition is satisfied and is greater than one if it is violated. Using $e_{idle,k}$ as a multiplier is a trick to avoid a local minimum. It makes exploration in the region below engine idle speed highly unattractive. If the third term is used as an addend, the reward function is very sensitive to improper weighting and the agent tends to ignore the no-kill condition.

State dependencies are known from prior investigations into practice. A reduced set is used here, since the simulated environment is simpler than the real environment:

$$s_k = \left[n_{Eng,k}, n_{Gear,k}, T_{Eng,k}, T_{Dyn,k}, a_{k-1}\right]$$

T_{Dyn} is the dynamic engine torque respectively clutch cutting torque that is transmitted if the clutch is assumed to be locked. It is the same quantity that is used in MPC to fulfill the no-lurch condition. a_k is the clutch torque capacity and a_{k-1} is the action of the previous time step. It is used in the reward function to calculate Δa_k. It must therefore be accessible by the critic network to make appropriate estimates of the cumulative return.

The agent was trained using the described setup but was not able to control the clutch in any way. There was no convergence. There are two main reasons for this. Firstly, the agent tends to become instable with highly oscillating actions. Random low-magnitude noise is added to the actions during training. This is mandatory to let the agent explore the environment and try different actions.

https://doi.org/10.51202/9783181023549 - Generiert durch IP 216.73.216.36, am 19.01.2026, 02:19:31. © Urheberrechtlich geschützter Inhalt. Ohne gesonderte Erlaubnis ist jede urheberrechtliche Nutzung untersagt, insbesondere die Nutzung des Inhalts im Zusammenhang mit, für oder in KI-Systemen, KI-Modellen oder Generativen Sprachmodellen.

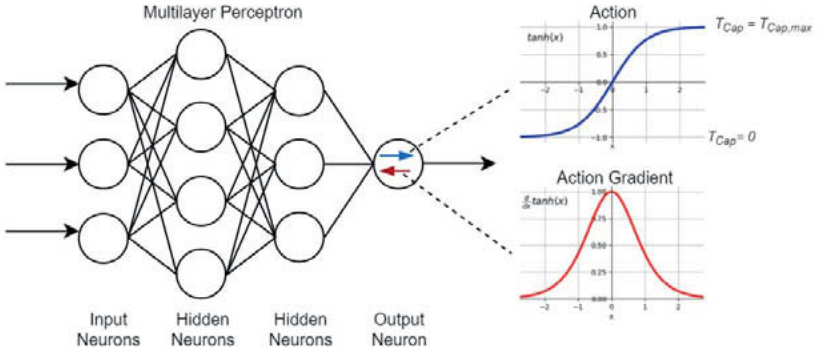


Fig. 4: Neural network with $tanh$ output activation and its derivative used for back propagation

Noisy actions excite the system and result in noisy gradients of the engine and output speed. These noisy gradients are propagated back into the policy and critic network as they are used in the calculation of the dynamic torque T_{Dyn}. As a temporary solution, the noise can be reduced by using filters. Nevertheless, this should be avoided as the environment is deterministic and noiseless and filters can conceal potential stability issues of the attempted approach. Secondly, the output of the policy network is a normalized action $a \in (-1,1)$ by applying the tangens hyperbolicus to the output layer of the network, as shown in Fig. 4. The action is then scaled to the valid clutch capacity range, $T_{Cap} \in (0, T_{Cap,max})$. The policy network's parameters are updated by back-propagating the gradient of the parameters through the network. This involves the derivative of the tangens hyperbolicus. Fig. 4 shows that the gradient vanishes near the upper and lower clutch capacity limit so that the network has poor learning capability in these areas.

This issue is overcome by slight changes to the setup. The policy is now defined to produce the derivative of the action:

$$\Delta\, a_k \;= \pi_{\theta_\pi}(s_k)$$

The derivative of the action is then scaled according to a maximum and minimum clutch torque gradient $\Delta T_{Cap} \in (\Delta T_{Cap,min}, \Delta T_{Cap,max})_{\dot{T}}$ integrated in time and fed to the environment. The result consists in far improved policy learning with the gradients no longer vanishing with low and high clutch torques. Δa_k shows better statistical distribution than a_k. In addition, the agent produces more stable results with the temporary integration of action breaking the direct feedback of noisy action through the speed gradients.

https://doi.org/10.51202/9783181023549 - Generiert durch IP 216.73.216.36, am 19.01.2026, 02:19:31. © Urheberrechtlich geschützter Inhalt. Ohne gesonderte Erlaubnis ist jede urheberrechtliche Nutzung untersagt, insbesondere die Nutzung des Inhalts im Zusammenhang mit, für oder in KI-Systemen, KI-Modellen oder Generativen Sprachmodellen.

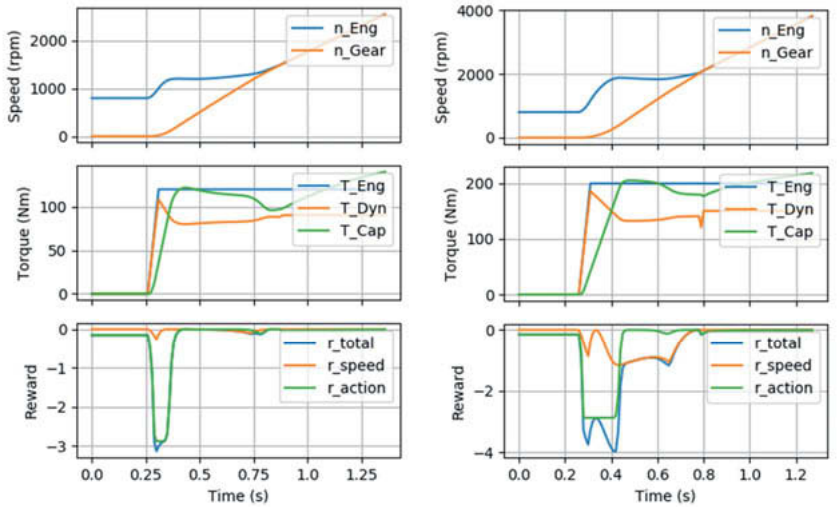


Fig. 5: Agent acting in the environment. Simulation of a vehicle start-up with a step response of 120 Nm (left) and 200 Nm (right) after 2000 episodes (trials) of training. The idle term of the reward function is not shown, as the no-kill condition is always fulfilled.

Fig. 5 shows two results for a vehicle start-up with an engine torque step of 120 Nm (left) and 200 Nm (right). Both results indicate smooth engagement. Even though the no-lurch condition is not taken into account, the lock-up instant is also smooth. In the figure on the left, the main component of the reward results from the actuation. The reference speed tracking error can be kept small. The figure on the right shows that the agent's performance is limited by the gradient $\Delta T_{Cap,max}$ due to the high engine torque increase. As a result, the engine flares and the reference speed tracking error increases. Despite the restrictions of the actuator, the agent shows stable control behavior as those restrictions are taken into account during training. Overall, the agent shows good performance for the simple start-up scenario that is comparable to results obtained from a clutch engagement controller used in practice.

5 Conclusion and Future Work

This paper has investigated the application of a reinforcement learning agent for solving an automotive embedded system control problem. Machine learning takes a different approach than traditional software development so that the paper has discussed issues such as the

https://doi.org/10.51202/9783181023549 - Generiert durch IP 216.73.216.36, am 19.01.2026, 02:19:31. © Urheberrechtlich geschützter Inhalt. Ohne gesonderte Erlaubnis ist jede urheberrechtliche Nutzung untersagt, insbesondere die Nutzung des Inhalts im Zusammenhang mit, für oder in KI-Systemen, KI-Modellen oder Generativen Sprachmodellen.

compliance of functional safety and hardware requirements. It has been shown that machine learning algorithms can be applied to safety-critical embedded systems on condition that standard-compliant safety monitoring functions are developed. In general, reinforcement learning can be used for continuous control and is well suited to multi-objective optimization problems. The approach can be applied with standard hardware under the assumption that it is trained offline.

First simulation results revealed that the agent achieved good performance in a simple environment for a vehicle start-up using a simple reward function. This is the baseline for further investigations. The aim is to run the agent in a real-world environment such as a prototype vehicle to evaluate whether the reinforcement learning approach can compete with a state-of-the-art clutch engagement controller. This includes analyzing robustness and adaptability because the long-term goal consists in creating a self-learning agent that automatically adapts to the physical system, thus reducing or even eliminating the need for manual in-vehicle calibration.

References

[1] Alom, M. Z. et al., The History Began from AlexNet: A Comprehensive Survey on Deep Learning Approaches, arXiv, 2018

[2] DeepMind, The story of AlphaGo so far, https://deepmind.com/research/alphago/, n.d.

[3] Brownlee, J., Basic Concepts in Machine Learning, https://machinelearningmastery.com/basic-concepts-in-machine-learning, 2015

[4] Salay, R.; Czarnecki, K., Using machine learning safely in automotive software: An assessment and adaption of software process requirements in ISO 26262, arXiv, 2018

[5] Arbeitskreis EGAS, Standardisiertes E-Gas Überwachungskonzept für Benzin und Diesel Motorsteuerungen, https://www.iav.com/sites/default/files/attachments/seite/ak-e-gas-v6-0-de-150922.pdf, 2005

[6] Glielmo, L.; Vasca, F., Engagement control for automotive dry clutch, Proc. American Control Conf., 2000

[7] Garofalo, F. et al., Optimal tracking for automotive dry clutch engagement, Proc. of the 15th IFAC congress, 2002

https://doi.org/10.51202/9783181023549 - Generiert durch IP 216.73.216.36, am 19.01.2026, 02:19:31. © Urheberrechtlich geschützter Inhalt. Ohne gesonderte Erlaubnis ist jede urheberrechtliche Nutzung untersagt, insbesondere die Nutzung des Inhalts im Zusammenhang mit, für oder in KI-Systemen, KI-Modellen oder Generativen Sprachmodellen.

[8] Dolcini, P.; de Wit, C. C.; Béchart, H., Improved optimal control of dry clutch engagement, IFAC Proceedings Volumes, 2005

[9] Amari, R. et al., Unified MPC strategy for idle-speed control, vehicle start-up and gearing applied to an automated manual transmission, 17th IFAC World Congress, 2008

[10] Bemporad, A. et al., Optimal Piecewise-Linear Control of Dry Clutch Engagement, 2001

[11] OpenAI, OpenAI Five, https://openai.com/five/, 2019

[12] DeepMind, AlphaStar: Mastering the Real-Time Strategy Game StarCraft II, https://deepmind.com/blog/alphastar-mastering-real-time-strategy-game-starcraft-ii/, 2019

[13] Recht, B., A tour of reinforcement learning: The view from continuous control, Annual Review of Control, Robotics, and Autonomous Systems, 2018

[14] Sutton, R. S.; Barto, A. G. (Ed.), Reinforcement learning, The MIT Press, 1998

[15] Schulman, J. et al., Proximal Policy Optimization, https://openai.com/blog/openai-baselines-ppo/, 2017

[16] Haarnoja, T. et al., Soft Actor Critic—Deep Reinforcement Learning with Real-World Robots, https://bair.berkeley.edu/blog/2018/12/14/sac/, 2018

[17] Görges, D., Relations between model predictive control and reinforcement learning, IFAC-PapersOnLine, Elsevier, 2017

[18] Weng, L., Policy Gradient Algorithms, https://lilianweng.github.io/lil-log/2018/04/08/policy-gradient-algorithms.html#what-is-policy-gradient, 2019

[19] Lapan, M., Deep Reinforcement Learning Hands-On, Packt Publishing, 2018

[20] Lillicrap, T. P. et al., Continuous control with deep reinforcement learning, arXiv, 2015

https://doi.org/10.51202/9783181023549 - Generiert durch IP 216.73.216.36, am 19.01.2026, 02:19:31. © Urheberrechtlich geschützter Inhalt. Ohne gesonderte Erlaubnis ist jede urheberrechtliche Nutzung untersagt, insbesondere die Nutzung des Inhalts im Zusammenhang mit, für oder in KI-Systemen, KI-Modellen oder Generativen Sprachmodellen.

Virtual Lubrication Analysis – Simulation of Oil Flow in Gearboxes using a novel Lagrangian Approach

- **Introduction and Objectives of Gearbox Investigation**
- **Advanced Solution based on an implicit Lagrangian Approach**
- **Lubrication Analysis – Industrial Examples**
- **Current R&D Activities – Thermal Investigation**

M.Eng. **Rohit Gat**, Dipl.-Ing **Michael Ehlen**,
AVL Thermal and HVAC, Munich

Abstract

The usage of computational fluid dynamics (CFD) to analyze liquid fluid flows in autonomous key components are of growing interest. A wide domain of application nowadays gives a huge potential in different areas. In modern transmission development one major task is to ensure lubrication and cooling of critical components (bearings, sealing's, gears engagements) in passive lubrication systems.

Cost efficient lubrication systems for state-of-the-art transmissions and gearboxes are mostly passive and driven by oil splashing due to the wheelset's rotation. To ensure the lubrication at all critical components in all operating points and conditions is a challenging task in modern gearbox development. Therefore, numerous different test scenarios have been evolved (tilt test benches, transparent housings). In an early development stage, these measurements cannot be performed due to the lack of existing prototypes. In later design stages, these measurements require expensive prototyping and instrumentation, while major design changes may already lead to a delay in the development process. Further, these testing scenarios only allow limited insight and fail to predict oil flows through channels, drains or

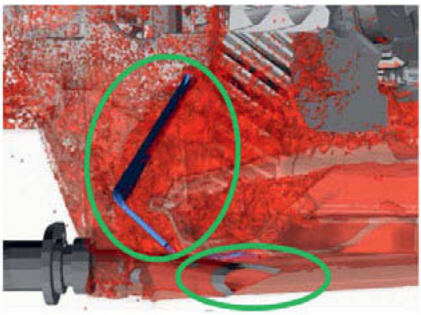


Fig. 1: Influence of baffle plates on oil flow behavior in the vicinity of the suction point during dynamic lateral acceleration profile.

https://doi.org/10.51202/9783181023549 - Generiert durch IP 216.73.216.36, am 19.01.2026, 02:19:31. © Urheberrechtlich geschützter Inhalt. Ohne gesonderte Erlaubnis ist jede urheberrechtliche Nutzung untersagt, insbesondere die Nutzung des Inhalts im Zusammenhang mit, für oder in KI-Systemen, KI-Modellen oder Generativen Sprachmodellen.

hollow drilled shafts. For these reasons a reliable and stable way to simulate these processes will help to prove a developed concept while saving time and money.

A new and innovative method is introduced to simulate various fluid management problems, which can be applied to calculate all kind of transient free surface flows in a very fast, accurate and robust way. This state-of-the-art technique solves the Navier-Stokes equations using a mesh-free approach. The point-based nature allows the computation of systems with complex moving geometries without any restrictions. In contrast to conventional mesh-based CFD, the method can handle real geometries and movements without simplifications (e.g. gears interlocking). AVL Thermal and HVAC developed a failsafe and easy workflow for various automotive fluid management applications, including the prediction of oil flows in transmissions and gearboxes. These approaches and workflows have already been proven and successfully applied, for example at various projects for OEMs.

Some of these applications are shown, such as the breakdown of the lubrication system of a Six stage dual clutch transmission (DCT, see fig. 1) above a critical tilting angle, and the virtual lubrication development of an electric axle drive (see fig. 2). Within the provided examples, the analysis possibilities and the post-processing abilities of the method are demonstrated. Visualization of the oil flow as path lines and illustration of the general oil distribution from virtual cameras are possible, as well as the determination of mass flows through ducts and channels or the highlighting of geometries or faces in contact with oil. These qualities allow a comprehensive and deep analysis of a transmission's lubrication system and its performance and limitations.

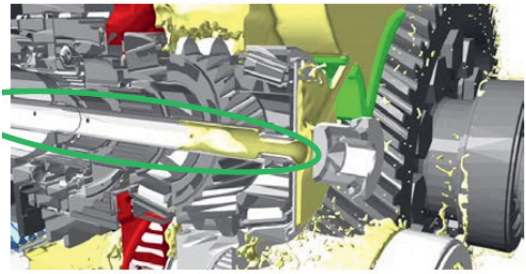


Fig. 2: Visualization of hollow shaft lubrication of an electric axle drive during operation.

For an outlook, a major task at AVL qpunkt R&D activities is the further development of the method in order to determine thermal behavior of transient free surface flows. Besides lubrication, the main demand of passive lubrication systems is to ensure the cooling of critical components (e.g. bearings, gears engagement). Models for thermal conduction and heat transfer

https://doi.org/10.51202/9783181023549 - Generiert durch IP 216.73.216.36, am 19.01.2026, 02:19:31. © Urheberrechtlich geschützter Inhalt. Ohne gesonderte Erlaubnis ist jede urheberrechtliche Nutzung untersagt, insbesondere die Nutzung des Inhalts im Zusammenhang mit, für oder in KI-Systemen, KI-Modellen oder Generativen Sprachmodellen.

(fluid-wall/wallfluid) have therefore recently been implemented to the solver. First results from proof of concept studies are promising, validation is currently ongoing at AVL qpunkt. Aim of the study is the development of a methodology which is capable to predict heat transfer coefficients from (moving) components or surfaces to the surrounding fluid in transient free surface flow applications

https://doi.org/10.51202/9783181023549 - Generiert durch IP 216.73.216.36, am 19.01.2026, 02:19:31. © Urheberrechtlich geschützter Inhalt. Ohne gesonderte Erlaubnis ist jede urheberrechtliche Nutzung untersagt, insbesondere die Nutzung des Inhalts im Zusammenhang mit, für oder in KI-Systemen, KI-Modellen oder Generativen Sprachmodellen.

https://doi.org/10.51202/9783181023549 - Generiert durch IP 216.73.216.36, am 19.01.2026, 02:19:31. © Urheberrechtlich geschützter Inhalt. Ohne gesonderte Erlaubnis ist jede urheberrechtliche Nutzung untersagt, insbesondere die Nutzung des Inhalts im Zusammenhang mit, für oder in KI-Systemen, KI-Modellen oder Generativen Sprachmodellen.

Development of an Optimization Framework for the Comparative Evaluation of the Ecoimpact of Powertrain Concepts

Arved Esser, **Jean-Eric Schleiffer**, **Tobias Eichenlaub**, **Stephan Rinderknecht**,
Technical University Darmstadt

Zusammenfassung

Der Stand der Technik in der Bewertung der lebenswegbezogenen Treibhausgasemissionen verschiedener Antriebsstrangkonzepte basiert auf der Bewertung von Eigenschaften bestehender Fahrzeuge am Markt. Diese Fahrzeuge wurden allerdings mit unterschiedlichen Zielen entwickelt und mit diversen Nutzungsprofilen betrieben. Wie die Antriebsstrangkonzepte im Vergleich abschneiden würden, wenn sie optimal auf das jeweilige Untersuchungsszenario ausgelegt würden, bleibt unklar. Die Kenntnis über diese Optimalparametrierung der Antriebskonzepte ist jedoch nötig, um einen fairen Vergleich der Technologien zu ermöglichen. Dies gilt insbesondere dann, wenn innovative Antriebsstrangkonzepte sowie zukünftige Szenarien betrachtet werden, in denen deutliche Abweichungen zu heute üblichen Parametrierungen von Fahrzeugen möglich sind. Im Rahmen des öffentlich geförderten Projekts „FahrKLang“ wurde eine Optimierungsumgebung für die vergleichende Bewertung des „Real Ecological Impact“ (REI) verschiedener Antriebsstrangkonzepte entwickelt, die in diesem Beitrag vorgestellt wird. Für jedes Untersuchungsszenario werden optimale Antriebsparametrierungen der verschiedenen Antriebskonzepte zur Minimierung des REI und eine angepasste Betriebsstrategie ermittelt, wodurch eine einheitliche Bewertungsbasis geschaffen wird. Repräsentative Fahrzyklen ermöglichen dabei eine effiziente Bewertung der Konzepte auf Basis von realen Flottenfahrdaten innerhalb der Optimierungsumgebung.

Abstract

The state of the art in the evaluation of the ecological impact of various powertrain concepts is based on the evaluation of characteristics of existing vehicles on the market. However, these vehicles were developed with different objectives and are operated with various usage profiles. The potential of the powertrain concepts, if they were optimally designed for a given parameter

https://doi.org/10.51202/9783181023549 - Generiert durch IP 216.73.216.36, am 19.01.2026, 02:19:31. © Urheberrechtlich geschützter Inhalt. Ohne gesonderte Erlaubnis ist jede urheberrechtliche Nutzung untersagt, insbesondere die Nutzung des Inhalts im Zusammenhang mit, für oder in KI-Systemen, KI-Modellen oder Generativen Sprachmodellen.

set of a scenario to be investigated, remains unclear. But the knowledge of these optimal parametrizations of the powertrain concepts is necessary to enable an unbiased comparison of the technologies, especially if future scenarios are considered in which significant deviations from current parameter sets are possible. This work is based on results of the publicly funded FahrKLang project, in which an optimization framework for the comparative assessment of the "Real Ecological Impact" (REI) of various powertrain concepts has been developed. For each investigated scenario, optimal powertrain parametrizations of the various concepts to minimize the REI and a customized operational strategy are identified, thereby creating an equal evaluation basis. Representative driving cycles enable an efficient evaluation of the concepts based on real fleet driving data within the optimization environment.

1 Introduction and Motivation

In order to determine the environmental impact of vehicle powertrain concepts, greenhouse gas emissions over the entire life cycle of a vehicle must be estimated. The vehicle production, its operation including the necessary energy supply as well as the end-of-life have to be considered. Current life cycle assessment studies use the parameters of vehicles that are already available on the market. For each powertrain concept to be investigated, characteristic component properties are assigned. Battery capacities and power ratings of energy converters are assigned to characteristic vehicles that are intended to represent whole classes of vehicles. Consumption values are often only taken into account in the form of estimations of average consumption and do not consider real driving profiles or the specific efficiency advantages of innovative concepts.

However, this approach must be questioned when the actual potential of innovative powertrain concepts to reduce greenhouse gas emissions is to be determined. The properties of vehicles already available on the market, which serve as a basis for the characteristic vehicles, were developed with different and very diverse objectives. It is not known to what extent the environmental impact of currently available vehicles has been taken into account in the design process. It remains unclear how different concepts would comparatively perform if they were optimally adapted to real driving profiles with the aim of minimizing greenhouse gas emissions.

In this contribution, the results of the publicly funded project "FahrKLang" are presented, in which an overall optimization environment for the comparative assessment of the Real Ecological Impact (REI) of powertrain concepts was developed.

After an overview of the optimization framework in Section 2, which describes the approach in more detail, descriptions of the central principles of the comparative evaluation of the REI of

https://doi.org/10.51202/9783181023549 - Generiert durch IP 216.73.216.36, am 19.01.2026, 02:19:31. © Urheberrechtlich geschützter Inhalt. Ohne gesonderte Erlaubnis ist jede urheberrechtliche Nutzung untersagt, insbesondere die Nutzung des Inhalts im Zusammenhang mit, für oder in KI-Systemen, KI-Modellen oder Generativen Sprachmodellen.

concepts follow. These include the determination of representative driving cycles from large sets of real driving data from a fleet of vehicles in Section 3 as well as the determination of key performance indicators in the operational phase by simulation in Section 4. Section 5 shows the comparative evaluation of the optimal parametrizations of different powertrain concepts determined on the basis of different evaluation scenarios. In Section 6, we give an outlook on the extent to which the approach presented and the results achieved can contribute to the development of future, innovative powertrains.

2 Optimization Framework

The dimensioning and parametrization of powertrain components has a significant impact on the evaluation of the REI of vehicles. In order to be able to compare different powertrain concepts for a specific vehicle in the sense of a benchmark, the interactions between the individual components, the impact of the users behavior on powertrain efficiency as well as sizing impacts on the different phases of the lifecycle must be taken into account. An accurate dimensioning and parametrization with the aid of a holistic overall system optimization approach is needed.

Basis for the dimensioning of the components of powertrain concepts to be compared is the evaluation of key parameters of the operational phase like consumption using real driving data from a fleet of vehicles, which are intended to represent the characteristic driving behavior of users in Germany. A cycle synthesis method, based on [1] and further described in Section 3, generates representative driving cycles. The extensive data sets are thereby reduced to a necessary minimum. This enables a computationally efficient evaluation of powertrain concepts with the aid of simulation based on real driving data.

An optimization framework was developed to determine the optimal powertrain parametrization. To achieve this, an operating strategy based on a locally optimal control approach, called Equivalent Consumption Minimization Strategy (ECMS) [2, 3], is adapted for each variant. The compressed but representative driving cycles enable the investigation of the operational phase of the necessary multitude of variants with high computing efficiency. The objective function of the optimization, which is evaluated using a genetic algorithm, is not only made up of the greenhouse gas emissions during the operational phase, but is considering the entire life cycle. The production phase, in particular, is strongly influenced by the dimensioning of the components. Fig. 1 shows the framework of the optimization environment. For each powertrain concept, the minimum greenhouse gas emissions are determined based on a representative driving cycle by an optimal dimensioning and parametrization of the respective components. In

https://doi.org/10.51202/9783181023549 - Generiert durch IP 216.73.216.36, am 19.01.2026, 02:19:31. © Urheberrechtlich geschützter Inhalt. Ohne gesonderte Erlaubnis ist jede urheberrechtliche Nutzung untersagt, insbesondere die Nutzung des Inhalts im Zusammenhang mit, für oder in KI-Systemen, KI-Modellen oder Generativen Sprachmodellen.

this way, a reliable and unbiased basis for the comparison of different powertrain concepts is created.

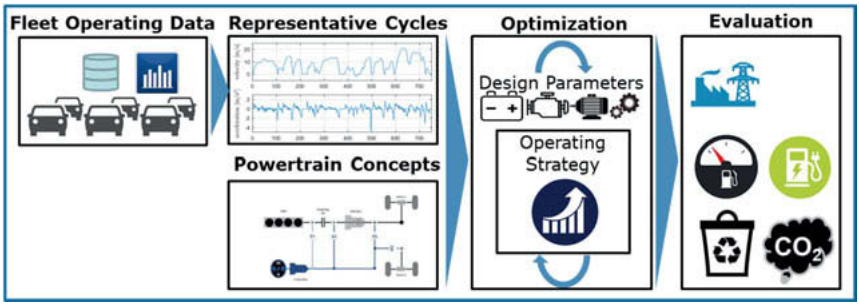


Fig. 1: FahrKLang Optimization Framework

The plausibility of the resulting vehicle parameters during the optimization process, which are set by a genetic algorithm by selection, mutation and recombination of the design parameters according to Table 1, is ensured by additional technology-neutral design constraints. The generated vehicles must be able to achieve a launch acceleration of 2,5 m/s² on a slope of 30%, accelerate to 60 km/h in 8 seconds and achieve a remaining acceleration of 0,33 m/s² at 180 km/h. Furthermore, all parametrizations of powertrain concepts that are capable of purely electric driving must achieve a purely electrical range of 60 km and a total range which is specified in a seperate table for each scenario showing the applied parameter sets. All powertrain concept parametrizations, presented in the results, fulfill these design constraints.

Table 1: Design parameters of the optimization process

N_{ICE}	Index of the internal combustion engine in the database
P_{EM}	Peak power of the electric machine
C_{Batt}	Capacity of the battery
n_{Transm}	Number of speeds in the transmission system
i_{N}	Gear ratio of the transmission speeds i_1 to i_{N}
$i_{\mathrm{EM,Hybrid}}$	Relative ratio of the connection of the electric machine for Parallel-Hybrid-Electric-Powertrains

https://doi.org/10.51202/9783181023549 - Generiert durch IP 216.73.216.36, am 19.01.2026, 02:19:31. © Urheberrechtlich geschützter Inhalt. Ohne gesonderte Erlaubnis ist jede urheberrechtliche Nutzung untersagt, insbesondere die Nutzung des Inhalts im Zusammenhang mit, für oder in KI-Systemen, KI-Modellen oder Generativen Sprachmodellen.

Based on the calculated energy demand in the operational phase as well as the masses of components resulting from the powertrain dimensioning and parametrization, equivalent CO_2 emissions over the entire life-cycle are finally determined with the help of researched emission factors for different scenarios to be investigated. The determined CO_2 emissions in the production of the vehicles are shown in Fig. 7 for an exemplary scenario.

In this contribution, three scenarios are examined and discussed in detail in Section 5, which can be described with a set of parameters for each scenario (Table 4, Table 7). In addition to evaluating the effects of changes in the total distance to be travelled without the need for a vehicle to be charged (scenario with and without the requirement for long-range capability), the effects of external factors such as emission factors for energy production or the energy density of energy storage systems are also examined by means of estimates for future enhancements (reference year 2018 vs. reference year 2030).

3 Evaluation of Fleet Driving Data

To enable a proper estimation of the REI of different powertrain concepts, real fleet driving data that depict the characteristic vehicle usage must be used as evaluation basis. Within the FahrKLang project, vehicles with the requirement of long-range capability were the main subject of research. Firstly, a detailed depiction of the driving behaviour concerning velocity and acceleration is required. Secondly, more general information about the distribution of trip distances and the total achieved mileage must be determined to enable a profound REI estimation.

Until now, there is no available data set containing extensive fleet driving data within Germany which was recorded over a longer period. Such a database would be necessary for a detailed depiction of the real usage behaviour and a real-driving based evaluation of the REI. As an estimation of this real fleet driving data, a data set that resulted from the “simTD” project [4] was used in the project, which contains recorded vehicle operation data on a 1 Hz basis from the metropolitan region of Frankfurt. The fleet consisted of different vehicles from different manufacturers that were driving in the regular traffic. The processed data set contains a total of 143.078 driven kilometres. The occurrence frequency of operating states as a function of velocity and acceleration and possible transitions between operating states are shown in Fig. 2.

https://doi.org/10.51202/9783181023549 - Generiert durch IP 216.73.216.36, am 19.01.2026, 02:19:31. © Urheberrechtlich geschützter Inhalt. Ohne gesonderte Erlaubnis ist jede urheberrechtliche Nutzung untersagt, insbesondere die Nutzung des Inhalts im Zusammenhang mit, für oder in KI-Systemen, KI-Modellen oder Generativen Sprachmodellen.

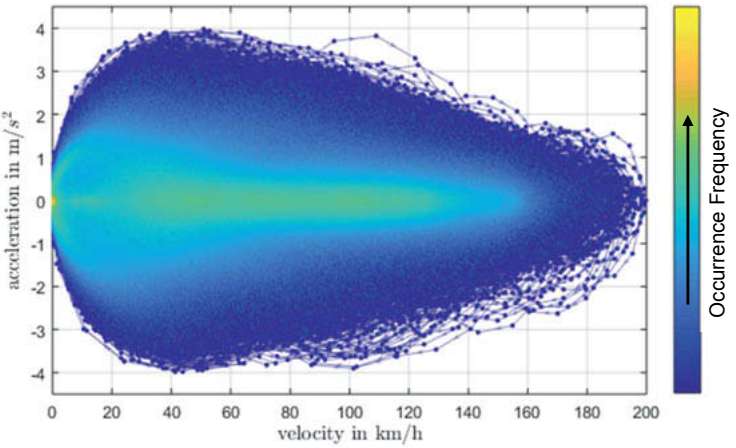


Fig. 2: Occurrence frequency of operating states of the fleet driving data as a function of velocity and acceleration. Nodes represent operating states while connections represent occurred transitions between the states.

Most frequent states are idling and cruising at constant speeds of 50 km/h and 80-120 km/h. However, the available database lacks trips with large distances travelled at once, which is why the overall driving profile from Fig. 2 was considered for the scenarios with and without the requirement for long-range capability. The occurrence frequency shows that the largest part of the driving is at moderate speeds and accelerations, but less frequent events occure at high power demands or high decelerations.

For the simulation-based evaluation of different powertrain concept parametrizations within the optimization framework, representative driving cycles of the overall fleet driving profile are required. The stochastic cycle synthesis procedure proposed in [1] is used within this study. A driving cycle is assumed to be representative if it shows the same characteristic values of the criteria set $\boldsymbol{\theta}$ as the overall fleet profile shown in Fig. 2. The criteria set $\boldsymbol{\theta}$ is composed out of six single criteria $\theta_1, \theta_{2,\ldots}, \theta_6$, where *v* is the velocity, *a* is the longitudinal acceleration and *s* is the travelled distance. The label “acc” indicates time periods of positive and zero traction forces, while “tot” stands for the total time period.

https://doi.org/10.51202/9783181023549 - Generiert durch IP 216.73.216.36, am 19.01.2026, 02:19:31. © Urheberrechtlich geschützter Inhalt. Ohne gesonderte Erlaubnis ist jede urheberrechtliche Nutzung untersagt, insbesondere die Nutzung des Inhalts im Zusammenhang mit, für oder in KI-Systemen, KI-Modellen oder Generativen Sprachmodellen.

$$\theta_1 = \frac{1}{s_{\text{tot}}} \int_{t \in \tau_{\text{acc}}}^{t_{\text{end}}} v(t)^3 \, dt \quad (1)$$

$$\theta_2 = \frac{1}{s_{\text{tot}}} \int_{t \in \tau_{\text{acc}}}^{t_{\text{end}}} v(t) \, dt = \frac{s_{\text{acc}}}{s_{\text{tot}}} \quad (2)$$

$$\theta_3 = \frac{1}{s_{\text{tot}}} \int_{t \in \tau_{\text{acc}}}^{t_{\text{end}}} a(t) v(t) m \, dt \quad (3)$$

$$\theta_4 = \frac{1}{t_{\text{end}}} \int_0^{t_{\text{end}}} v(t) \, dt \quad (4)$$

$$\theta_5 = \frac{1}{t_{\text{end}}} \int_0^{t_{\text{end}}} (v(t) - \theta_4)^2 \, dt \quad (5)$$

$$\theta_6 = \frac{1}{t_{\text{end}}} \int_0^{t_{\text{end}}} (a(t) - \bar{a})^2 \, dt \quad (6)$$

The relative error values are calculated for each criteria and the overall mean error is used as a final performance value to evaluate the quality of a driving cycle. Table 2 shows the exemplary calculation of the performance value for the first of the three chosen synthesized driving cycles, which can be seen in Fig. 4.

Table 2: Exemplary calculation of the performance value for the first of the three chosen synthesized driving cycles with a final performance value of 1,22 %.

Criteria	Single cycle value	Fleet data value	Rel. error	Criteria	Single cycle value	Fleet data value	Rel. error
θ_1	338,2156	339,6601	0,43 %	θ_4	15,7919	15,3205	3,08 %
θ_2	0,5316	0,5223	1,77 %	θ_5	129,6887	128,7599	0,72 %
θ_3	0,1749	0,1734	0,84 %	θ_6	0,3151	0,3136	0,47 %
$\boldsymbol{\theta}$							**1,22 %**

The driving cycles should be of a minimum duration since an efficient evaluation of many parametrizations of a powertrain concept is necessary within the optimization framework and the computational effort scales approximately linear with the cycle duration. At the same time, it is more difficult to satisfy all criteria in the criteria set $\boldsymbol{\theta}$, when the duration of a cycle becomes shorter. For this reason, a parameter study was performed to identify a suited cycle duration. The results are shown in Fig. 3. For all investigated cycle durations from 300 s to 1500 s, 2000 driving cycles have been synthesized to create a pareto front showing the achievable performance value for each cycle duration. The graph shows that the best cycle quality improves significantly with the cycle duration at lower durations, while the quality increases rather slowly for higher cycle durations. A cycle duration of 800 s is chosen for the final evaluation, since

https://doi.org/10.51202/9783181023549 - Generiert durch IP 216.73.216.36, am 19.01.2026, 02:19:31. © Urheberrechtlich geschützter Inhalt. Ohne gesonderte Erlaubnis ist jede urheberrechtliche Nutzung untersagt, insbesondere die Nutzung des Inhalts im Zusammenhang mit, für oder in KI-Systemen, KI-Modellen oder Generativen Sprachmodellen.

further improvements of the performance value would require a significantly higher cycle duration.

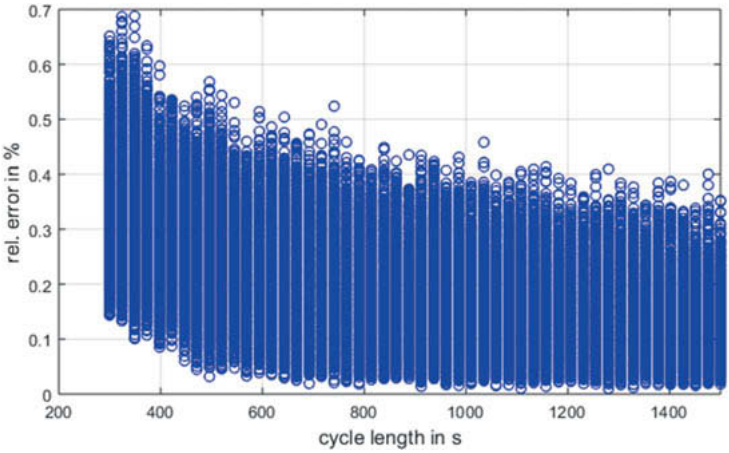


Fig. 3: Parameter study for the identification of required cycle duration. The achieveable performance value decreases with higher cycle durations.

After the final cycle duration has been determined, a more detailed study with the fixed duration of 800 s is performed. 50.000 cycles are synthesized and the resulting error distribution is shown in Fig. 4. The best cycles, shown on the right, have an error of 1-1,5 %. Regarding other uncertainties in the evaluation of the REI for different powertrain concepts, this error is considered as acceptable. Therefore using these representative driving cycles of Fig. 4 within the optimization framework enables an estimation of the REI based on the real driving profile shown in Fig. 2.

The second type of required information about trip distance distribution and mean vehicle mileage is retrieved from calculations of the DLR-VF, based on [5], that were also used in the FahrKlang project. From this source, the mean vehicle life mileage is assumed to be 158.000 km, based on the distribution of achieved mileage for a compact class vehicle.

The trip distance distribution is especially relevant for Plug-in Hybrid Electric Vehicles (PHEV). On short trips, an almost purely electrical driving is possible while the battery capacity might be insufficient for higher distances, which is why the combustion engine has to be used more often with increasing trip distances. For a proper estimation of the consumptions of PHEV

https://doi.org/10.51202/9783181023549 - Generiert durch IP 216.73.216.36, am 19.01.2026, 02:19:31. © Urheberrechtlich geschützter Inhalt. Ohne gesonderte Erlaubnis ist jede urheberrechtliche Nutzung untersagt, insbesondere die Nutzung des Inhalts im Zusammenhang mit, für oder in KI-Systemen, KI-Modellen oder Generativen Sprachmodellen.

powertrain concepts, different trip distances have to be taken into account for the simulation. The final consumption values are then computed by weighting the results with the real occurrence frequency of the different trip distances.

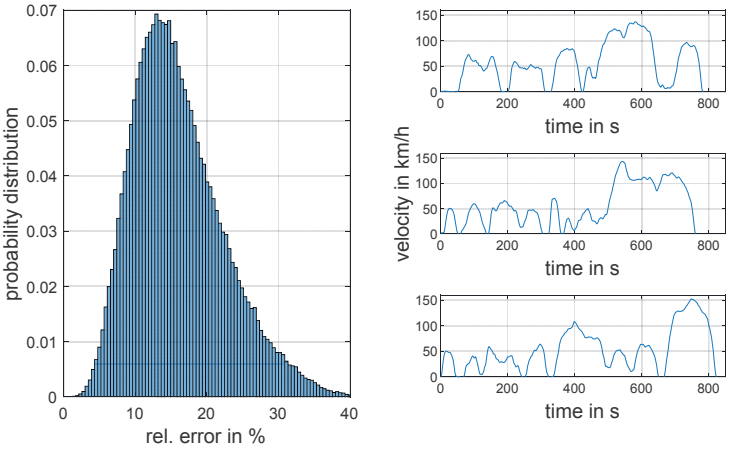


Fig. 4: Error distribution of the 50.000 synthesized cycles and the three chosen cycles.

For the scenarios with the requirement for long-range capability, which were the main investigation focus, trip distances above 100 km were considered. Three distances were chosen (150 km, 250 km and 350 km) and simulated on the representative driving cycles from Fig. 4. The weighting factors, determined from the distribution of trip distances within Germany, are 0.5 for the 150 km trip and 0.25 for the 250 km and 350 km trip.

Concerning the scenario without the requirement for long-range capability, two trip distances (75 km and 100 km) were chosen and the weighting factors were set to 0.6 and 0.4, respectively.

4 Vehicle Simulation Model

A vehicle simulation model was developed to calculate the energy consumption of variable parametrizations for multiple powertrain concepts. The energy demand and fuel consumption of each vehicle parametrization is used to estimate the ecological impact of the vehicle during operational phase. In order to ensure the comparability of different powertrain concepts, every vehicle parametrization created by the optimization algorithm shares an equal base vehicle body with predefined parameters like rolling resistance coefficient, drag coefficient or base

https://doi.org/10.51202/9783181023549 - Generiert durch IP 216.73.216.36, am 19.01.2026, 02:19:31. © Urheberrechtlich geschützter Inhalt. Ohne gesonderte Erlaubnis ist jede urheberrechtliche Nutzung untersagt, insbesondere die Nutzung des Inhalts im Zusammenhang mit, für oder in KI-Systemen, KI-Modellen oder Generativen Sprachmodellen.

mass. Only the structure and dimensioning of powertrain components is adapted to create different parametrizations of a powertrain concept.

For this reason, a generic powertrain model was created that consists of components for the energy converters (Internal Combustion Engine ICE, Electric Machine EM and Generator G), as well as the transmission and the battery. The architecture is shown in Fig. 5. Subdividing the transmission into three parts allows for a convenient differentiation in the model between parallel hybrid powertrain topologies like P2 or P3 configuration.

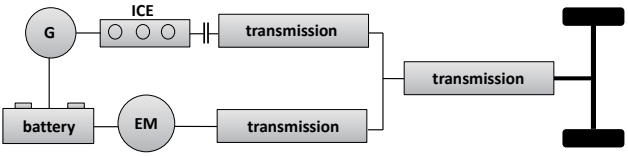


Fig. 5: Architecture of the developed generic powertrain model

Based on this architecture, the following powertrain concepts listed in

Table 3 are defined and investigated within this framework.

Table 3: Powertrain concepts investigated within this framework

ICEV-O	Conventional Vehicle with petrol engine
mHEV	Mild hybrid vehicle in P2 configuration
BEV	Battery electric vehicle with fixed gear ration transmission
BEV-2eG	Battery electric vehicle with 2-speed transmission
sREV	Series hybrid with range extender
PHEV(P2)	Parallel plug-in hybrid in P2 configuration
PHEV(P3)	Parallel plug-in hybrid in P3 configuration
PHEV(P3-2eG)	Parallel plug-in hybrid in P3 configuration with an additional dedicated 2-speed transmission for the EM

As described in Section 2, a number of powertrain parameters are being optimized in order to identify the optimal parametrization for each powertrain concept that minimizes the REI. This approach allows for an unbiased comparison of the technological potential of the different

https://doi.org/10.51202/9783181023549 - Generiert durch IP 216.73.216.36, am 19.01.2026, 02:19:31. © Urheberrechtlich geschützter Inhalt. Ohne gesonderte Erlaubnis ist jede urheberrechtliche Nutzung untersagt, insbesondere die Nutzung des Inhalts im Zusammenhang mit, für oder in KI-Systemen, KI-Modellen oder Generativen Sprachmodellen.

powertrain concepts. Therefore, methods are required to scale the components of the powertrain based on the optimization parameters. Alongside the efficiencies of the components, which mainly determine the fuel consumption and energy demand of the vehicle during the operational phase, the masses of the powertrain components have a significant impact on the total CO_2 emissions of the vehicle. They both increase the consumption of the vehicle due to an increased vehicle weight and determine the emissions during production and end-of-life phases.

The EM is scaled by means of its power. Different powers require adapted efficiency maps as well as an adapted mass which is especially relevant for the estimation of the ecological impact during production. In our approach, we define a reference permanent magnet synchronous electrical machine and apply a torque based scaling of the efficiency map to match it with the respective power

$$\frac{T_{\mathrm{EM}}}{T_{\mathrm{ref}}} = \frac{P_{\mathrm{EM}}}{P_{\mathrm{ref}}} \tag{7}$$

where T and P denote the torque and power of the reference and scaled machine, respectively. The mass of the EM as a function of power is estimated with the help of a nonlinear regression curve derived from literature data [6, 7]. This method is likewise applied to other components of the powertrain, e.g. the inverter.

Concerning the ICE, a different approach is chosen. To avoid the necessity of scaling the complex characteristics of an ICE efficiency map, a database of several engines with varying power is created. The optimizing algorithm is thus not choosing the ICE power from a continuous interval, but discrete values according to the engines in the database. Every engine is defined by its brake specific fuel consumption map including the full load characteristics and therefore its power, the type of fuel used and its mass. The mass is again estimated as a function of the ICE power by a regression curve based on collected data.

The design matching of the transmission and the engines has a great influence on vehicle consumption and the capability to fulfill the special design constraints mentioned in Section 2. Therefore, transmission ratios are also being optimized in this framework and the mass of the transmission is calculated based on an empirical correlation as a function of maximum torque, transmission ratio and gear number [8].

The vehicle simulation model is a backwards facing model of the longitudinal dynamics and consists of two processing steps. At first, the traction demand of the vehicle at the wheels required to follow the driving cycle is calculated by means of a driving resistances equation,

https://doi.org/10.51202/9783181023549 - Generiert durch IP 216.73.216.36, am 19.01.2026, 02:19:31. © Urheberrechtlich geschützter Inhalt. Ohne gesonderte Erlaubnis ist jede urheberrechtliche Nutzung untersagt, insbesondere die Nutzung des Inhalts im Zusammenhang mit, für oder in KI-Systemen, KI-Modellen oder Generativen Sprachmodellen.

taking drag, rolling resistance, grade resistance and acceleration resistance into account. Subsequently, the operating strategy chooses operating points for the energy converters to meet the traction demand at every time step that ultimately determine an overall vehicle consumption. Losses in the powertrain components are modelled with constant efficiencies for the transmissions and battery and efficiency maps for the ICE and the EM. Even though the efficiencies of the transmission and the battery are generally also dependent on the operating point or external influencing factors, the sensitivity of the REI with regard to transmission and battery efficiency is rather low and thus not considered.

An ECMS operating strategy is applied to choose locally optimal operating points for the energy converters with respect to consumption, thus deciding on gear shifting as well as the torque split between ICE and EM. The cost function J of the ECMS which is being minimized in every time step specifies an equivalent fuel mass flow rate of electrical and petrochemical energy [2, 3]. The cost ratio of electrical and petrochemical energy is defined by the equivalent cost factor s.

$$J = b_e P_{\mathrm{ICE}} + s \frac{1}{LHV} \frac{1}{\eta_{\mathrm{EM}} \eta_{\mathrm{batt}}} P_{\mathrm{EM}} \tag{8}$$

In Equation 8, b_e denotes the brake specific fuel consumption, LHV the lower heating value, and η the efficiency. For powertrain concepts with only a single energy converter, the number of degrees of freedom reduces to one since the torque can not be split upon two energy converters. Apart from that, the operating strategy can be applied to all powertrain concepts in the same fashion, which ensures the comparability of the consumption estimation of different powertrain concepts. This definition of an operating strategy also allows for additional operating modes of parallel hybrid powertrain concepts, e.g. boosting or load point shifting.

The exact value of the cost factor s is chosen for every parametrization individually in an inner iteration loop. The mild hybrid, since it does not have the option of external charging, needs to operate in charge sustaining mode. The cost factor of the plug-in hybrids, on the other hand, is set such that the whole usable electric energy of the battery is depleted at the end of a driving cycle, thus assuming an optimal user behaviour in terms of regular charging after each trip.

5 Results

Within this section, the results of the overall optimization framework for the chosen scenarios are presented. Firstly, the analysis for reference year 2018 is presented. For this reference

https://doi.org/10.51202/9783181023549 - Generiert durch IP 216.73.216.36, am 19.01.2026, 02:19:31. © Urheberrechtlich geschützter Inhalt. Ohne gesonderte Erlaubnis ist jede urheberrechtliche Nutzung untersagt, insbesondere die Nutzung des Inhalts im Zusammenhang mit, für oder in KI-Systemen, KI-Modellen oder Generativen Sprachmodellen.

year, a scenario with and without the requirement of long-range capability (350 km and 100 km range, respectively) are compared. Secondly, the results for the scenario with the requirement for long-range capability in the reference year 2030 are summarized.

5.1 Scenario without the requirement for long-range capability (100 km) in the reference year 2018

The scenario without the requirement for long-range capability in 2018 is defined by the following set of parameters shown in Table 4.

Table 4: Parameter set for the scenario without the requirement for long-range capability in 2018.

Total range	100 km
Specific emissions of energy production	578 g CO_2/kWh
Specific energy of the battery	109 Wh/kg
Total vehicle mileage	158.000 km

The parametrizations of the powertrain concepts for this scenario, determined by the optimzation framework, are summarized in Table 5. The parameters correspond to the powertrain concept parametrizations that results in a minimal REI for the investigated scenario. The battery capacities of the BEV are relatively low (~22 kWh) but sufficient for the moderate range requirement. Comparing the required electrical power of the single-speed and two-speed BEV shows that the two-speed transmission resolves conflicting design goals between maximum vehicle speed and necessary starting torque, resulting in less required power for the BEV-2eG. The reduced demand of installed power and the potential to choose the operating gear lead to a reduction of electric consumption for the BEV-2eG of ~4 % compared to the BEV.

https://doi.org/10.51202/9783181023549 - Generiert durch IP 216.73.216.36, am 19.01.2026, 02:19:31. © Urheberrechtlich geschützter Inhalt. Ohne gesonderte Erlaubnis ist jede urheberrechtliche Nutzung untersagt, insbesondere die Nutzung des Inhalts im Zusammenhang mit, für oder in KI-Systemen, KI-Modellen oder Generativen Sprachmodellen.

Table 5: Powertrain parameters of the different concepts determined by the optimization framework for the scenario without the requirement for long-range capability in 2018.

Concept	Power ICE in kW	Power EDM in kW	Battery capacity in kWh	Total mass in kg	El. consumption in kWh/100km	Fuel consumption in l/100km	Max. Torque required in Nm
ICEV-O	96	0	0	1110	0,0	5,0	1657
mHEV	96	21	2	1157	0,0	4,2	1728
BEV	0	145	22,4	1274	17,9	0,0	1903
BEV(2eG)	0	82	21,6	1260	17,2	0,0	1882
sREV	50	145	16,9	1298	16,2	0,6	1939
PHEV(P2)	50	34	14,5	1284	14,0	0,9	1918
PHEV(P3)	50	55	16,2	1285	15,6	0,5	1920
PHEV(P3-2eG)	50	39	15	1270	14,4	0,7	1897

The PHEV concepts show a large difference in maximum EM power between the series (sREV) and parallel topologies. The series hybrid is limited to use the power of the electric traction machine to satisfy the design constraints, whereas the parallel hybrids can transmit the combined power of the EM and the ICE to the wheels. The PHEV in P3 topology requires the highest amount of electrical power among the parallel PHEVs, since the purely electric city driving operation (design constraint), as well as reaching the required maximum speed, must be enabled with a single-speed transmission. The hybrids in P2 and P3-2eG topology, on the other hand, can use the multispeed transmission for the EM.

For the PHEV concepts, optimal battery capacities of ~15-17 kWh are identified which satisfy the design constraint of 60 km electrical range. With this battery capacity, the hybrid concepts are also able to achieve high electrical driving percentages on trips up to 100 km, as shown by the low petrochemical consumption in Table 5. In the case of the series hybrid, it is advantageous to increase the battery capacity in order to reduce the otherwise necessary operation of the range extender, since this leads to disadvantages in the overall electric consumption due to multiple energy conversion steps.

In terms of the total weight of the vehicles, the optimum variants of the conventional and mild hybrid vehicle are the lightest. The BEV and the PHEV have similar weights, as the BEV needs a larger battery and the PHEV has additional installed powertrain components.

The determined REI of the different powertrain concepts are illustrated in Fig. 6. A general result is that the electrification of powertrains is beneficial for the scenario without the requirement for long-range capability, since all electrified powertrains outperform the conventional ICEV. The BEV are well suited for this scenario due to the moderate battery capacities and the generally high efficiency of the powertrain. The two-speed BEV yields the best results for this scenario.

https://doi.org/10.51202/9783181023549 - Generiert durch IP 216.73.216.36, am 19.01.2026, 02:19:31. © Urheberrechtlich geschützter Inhalt. Ohne gesonderte Erlaubnis ist jede urheberrechtliche Nutzung untersagt, insbesondere die Nutzung des Inhalts im Zusammenhang mit, für oder in KI-Systemen, KI-Modellen oder Generativen Sprachmodellen.

The parallel PHEV show REI values in between the results of the BEV. The optimization environment optimizes the powertrain concepts such that synergies are used efficiently for the entire system, resulting in dedicated hybrid transmissions (DHT). For example, the parallel PHEV can only meet the high driving requirements using both traction machines. When driving at medium power requirements, the PHEV can operate using the small parametrized EM at a high specific utilization which is beneficial for a high efficiency. In addition, the available electric energy of the battery is distributed by the operating strategy using hybrid functionalities (purely electric or combustion engine driving, load-shift & boosting).

Further details on the CO_2-emissions during the production of the powertrain components are summarized in Fig. 7. The PHEV concepts have the highest number of necessary components for the powertrain. The ICEV and BEV concepts only require their corresponding components. In this scenario without the requirement for long-range capability, the glider, which gathers all components that are not part of the powertrain, has the highest impact. The production of the battery also shows a relevant amount of CO_2-emissions. In the case of higher installed battery capacities for the scenarios with the requirement for long-range capability, the emissions during the production of the battery become most relevant.

https://doi.org/10.51202/9783181023549 - Generiert durch IP 216.73.216.36, am 19.01.2026, 02:19:31. © Urheberrechtlich geschützter Inhalt. Ohne gesonderte Erlaubnis ist jede urheberrechtliche Nutzung untersagt, insbesondere die Nutzung des Inhalts im Zusammenhang mit, für oder in KI-Systemen, KI-Modellen oder Generativen Sprachmodellen.

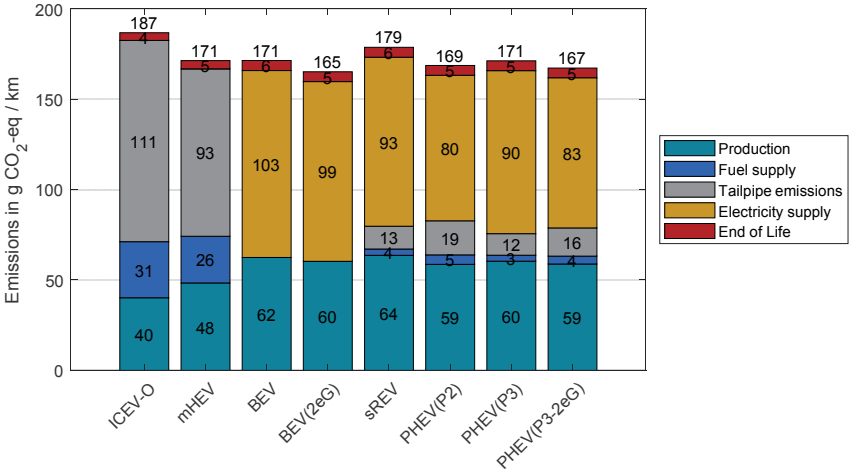


Fig. 6: Identified Real Ecological Impact of the different powertrain concepts for the scenario without the requirement for long-range capability in the reference year 2018.

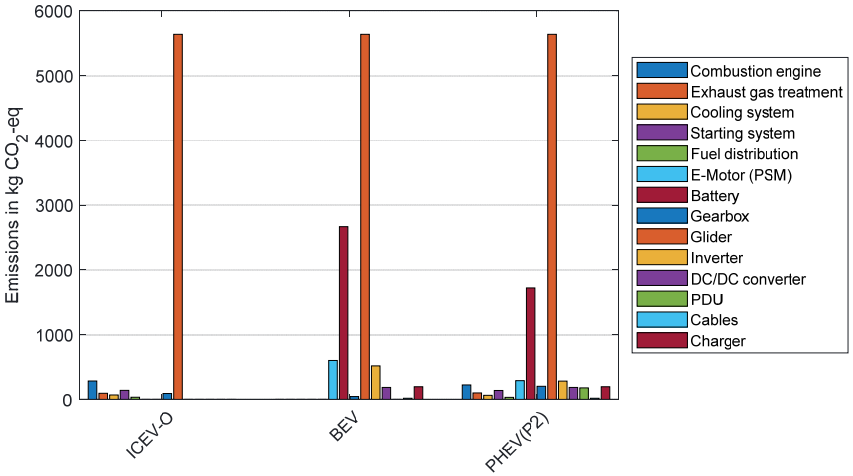


Fig. 7: CO_2-emissions in the production of vehicle components for the scenario without the requirement for long-range capability in the reference year 2018.

https://doi.org/10.51202/9783181023549 - Generiert durch IP 216.73.216.36, am 19.01.2026, 02:19:31. © Urheberrechtlich geschützter Inhalt. Ohne gesonderte Erlaubnis ist jede urheberrechtliche Nutzung untersagt, insbesondere die Nutzung des Inhalts im Zusammenhang mit, für oder in KI-Systemen, KI-Modellen oder Generativen Sprachmodellen.

5.2 Scenario with the requirement for long-range capability (350 km) in the reference year 2018

The same parameter set of Table 4 is applied to this scenario, except for an increased range requirement of 350 km. The calculated powertrain concept parametrizations, determined by the optimization procedure for the parametrization of the powertrain concepts, are summarized in Table 6. The ICEV-O and the mHEV only show minor deviations from the scenario without the requirement for long-range capability. The differences arise from the fact that the evaluation cycles and their weights between the driving cycles, as described in Section 3, differ in the scenarios with and without the requirement for long-range capability. For the BEV on the other hand, there are major differences compared to the scenario without the requirement for long-range capability. First, the required battery capacity to achieve the total range of the scenario increases significantly. This leads to a high vehicle weight and required maximum torque at the wheels. The single-speed BEV needs a high amount of installed power in order to meet the starting torque and the maximum speed requirements in combination. The two-speed BEV, on the other hand, can meet the requirements with significantly less power due to its transmission.

The series PHEV (sREV) also requires a lot of power due to its single-speed transmission. The optimization identifies an optimal battery capacity of approximately 18 kWh and relies on greater use of the range extender to charge the battery during operation, thus achieving the required range despite lower battery capacity compared to the BEV.

In the case of the parallel PHEV, there are only slight differences in the parametrization in comparison to the scenario without the requirement for long-range capability. Due to longer trip distances, the fuel consumption per 100 km increases significantly compared to the scenario without the requirement for long-range capability. At the same time, less electric energy is available per distance, which is why the electric consumption per distance is lower. As discussed in Section 4, the operating strategy ensures that the entire available battery capacity is always used.

https://doi.org/10.51202/9783181023549 - Generiert durch IP 216.73.216.36, am 19.01.2026, 02:19:31. © Urheberrechtlich geschützter Inhalt. Ohne gesonderte Erlaubnis ist jede urheberrechtliche Nutzung untersagt, insbesondere die Nutzung des Inhalts im Zusammenhang mit, für oder in KI-Systemen, KI-Modellen oder Generativen Sprachmodellen.

Table 6: Powertrain parameters of the different concepts determined by the optimization framework for the scenario without the requirement for long-range capability in 2018.

Concept	Power ICE in kW	Power EDM in kW	Battery capacity in kWh	Total mass in kg	El. consumption in kWh/100km	Fuel consumption in l/100km	Max. Torque required in Nm
ICEV-O	96	0	0	1110	0,0	5,1	1657
mHEV	96	22	2	1160	0,0	4,2	1733
BEV	0	219	90,4	1910	20,9	0,0	2853
BEV(2eG)	0	95	84,1	1842	19,4	0,0	2751
sREV	50	206	17,5	1311	7,1	3,3	1958
PHEV(P2)	50	32	14,5	1278	5,9	2,7	1908
PHEV(P3)	50	49	16,3	1283	6,6	2,6	1917
PHEV(P3-2eG)	50	33	15	1266	6,1	2,6	1891

The identified REI over the entire life cycle of the powertrain concepts are shown in Fig. 8. A comparison with the scenario without the requirement for long-range capability reveals significant differences. The BEV concepts show a major increase in their REI values. This is primarily due to the large battery capacities to meet the requirements, which lead to excessive CO_2-emissions in production and, secondly, to an increased vehicle weight, which in turn affects the consumption. Since the design requirements have to be covered with the high vehicle weight, there is also a very high electric power required, which contributes to the REI during the component production. The two-speed BEV-2eG, as before, has clear advantages over the single-speed BEV, since the required electrical power and the electric consumption can be reduced significantly (~9% compared to the BEV). This also results in a smaller required battery capacity. However, the determined REI shows that BEV concepts are not optimal for a long-range capable vehicle in the reference scenario for 2018.

The parallel PHEV and the mHEV perform best under all considered powertrain concepts. The comparison to the scenario without the requirement for long-range capability shows that the ICE of the PHEV is used much more on the now longer trip distances. This worsens the REI of the parallel PHEV compared to the short-distance scenario. Although the mHEV cannot charge external electric energy, it also has significantly lower production costs than the PHEV, and reaches the best balance with a small margin to the PHEV concepts within this scenario. As before, the P2 topology is slightly advantageous over the P3 topology and the innovative P3-2eG concept performs best for the PHEV concepts with a small margin.

https://doi.org/10.51202/9783181023549 - Generiert durch IP 216.73.216.36, am 19.01.2026, 02:19:31. © Urheberrechtlich geschützter Inhalt. Ohne gesonderte Erlaubnis ist jede urheberrechtliche Nutzung untersagt, insbesondere die Nutzung des Inhalts im Zusammenhang mit, für oder in KI-Systemen, KI-Modellen oder Generativen Sprachmodellen.

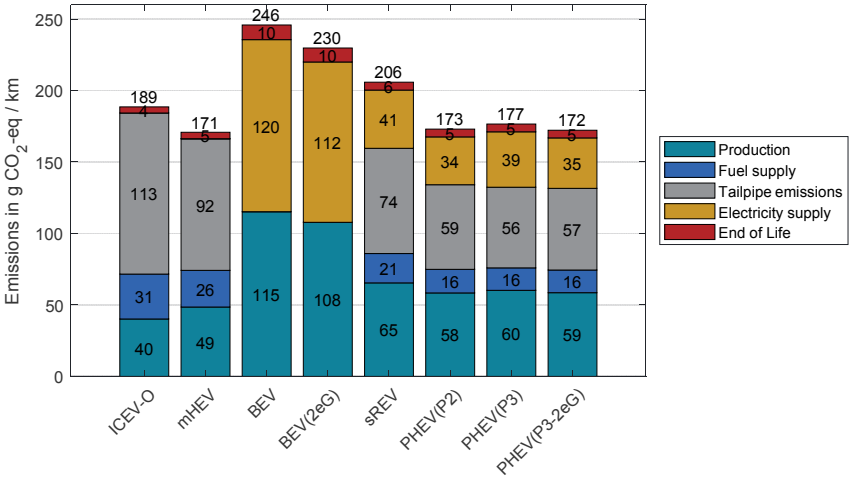


Fig. 8: Identified Real Ecological Impact of the different powertrain concepts for the scenario with the requirement for long-range capability in the reference year 2018.

The operating behaviour of the parallel PHEV in P2 topology on the first driving cycle for a trip distance simulation of 350 km is shown in Fig. 9. The simulation of operating behaviour is carried out within the optimization framework for many different parametrizations of all powertrain concepts in order to identify the minimal achievable REI.

https://doi.org/10.51202/9783181023549 - Generiert durch IP 216.73.216.36, am 19.01.2026, 02:19:31. © Urheberrechtlich geschützter Inhalt. Ohne gesonderte Erlaubnis ist jede urheberrechtliche Nutzung untersagt, insbesondere die Nutzung des Inhalts im Zusammenhang mit, für oder in KI-Systemen, KI-Modellen oder Generativen Sprachmodellen.

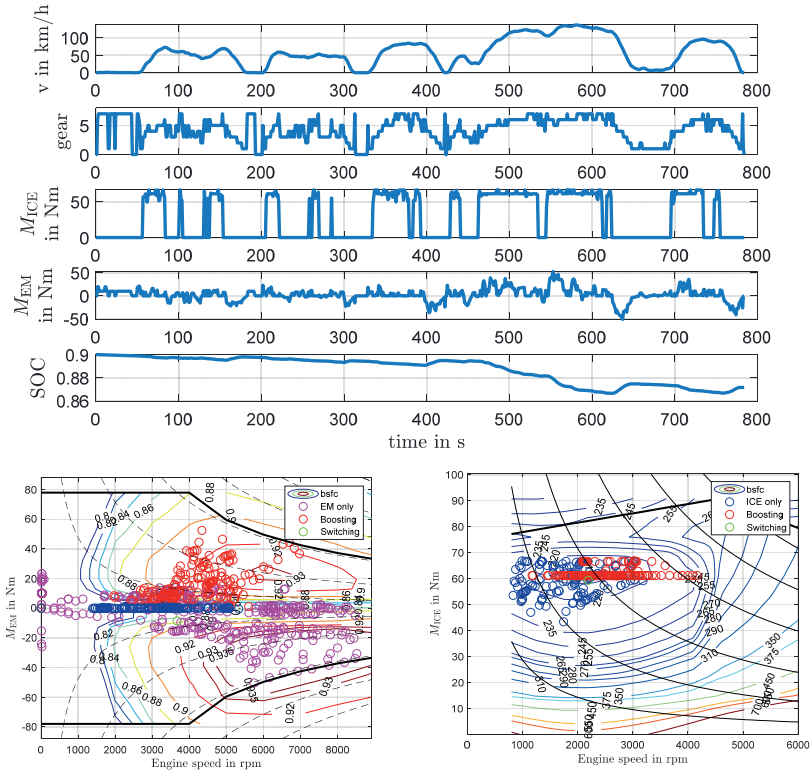


Fig. 9: Exemplary simulation of a parallel PHEV in P2 topology

https://doi.org/10.51202/9783181023549 - Generiert durch IP 216.73.216.36, am 19.01.2026, 02:19:31. © Urheberrechtlich geschützter Inhalt. Ohne gesonderte Erlaubnis ist jede urheberrechtliche Nutzung untersagt, insbesondere die Nutzung des Inhalts im Zusammenhang mit, für oder in KI-Systemen, KI-Modellen oder Generativen Sprachmodellen.

5.3 Scenario with the requirement for long-range capability (350 km) in the reference year 2030

The parameter set of this scenario is summarized in

Table 7.

Table 7: Parameter set for the scenario with the requirement for long-range capability in the reference year 2030.

Total range	350 km
Specific emissions of energy production	447 g CO_2/kWh
Specific energy of the battery	126 Wh/kg
Total vehicle mileage	158.000 km

The parameters of the powertrain concepts identified by the optimization environment are shown in Table 8. For the ICEV-O, there is no difference to the reference year 2018, as it does not benefit from the improved specific emissions of the energy production or the higher energy density of the battery, and further improvements of combustion technology or fuel properties have not been taken into account. The mild hybrid benefits only marginally, as the vehicle weight is slightly reduced due to the improved battery technology.

Table 8: Powertrain parameters of the different concepts determined by the optimization framework for the scenario without the requirement for long-range capability in 2018.

Concept	Power ICE in kW	Power EDM in kW	Battery capacity in kWh	Total mass in kg	El. consumption in kWh/100km	Fuel consumption in l/100km	Max. Torque required in Nm
ICEV-O	96	0	0	1109	0,0	5,1	1657
mHEV	96	20	2	1155	0,0	4,2	1725
BEV	0	199	87,5	1772	20,3	0,0	2647
BEV(2eG)	0	92	82,3	1721	19,0	0,0	2571
sREV	50	192	36,3	1438	14,6	1,3	2147
PHEV(P2)	50	33	14,5	1259	5,8	2,7	1880
PHEV(P3)	50	49	16,3	1262	6,7	2,5	1886
PHEV(P3-2eG)	50	32	15	1246	5,9	2,6	1862

https://doi.org/10.51202/9783181023549 - Generiert durch IP 216.73.216.36, am 19.01.2026, 02:19:31. © Urheberrechtlich geschützter Inhalt. Ohne gesonderte Erlaubnis ist jede urheberrechtliche Nutzung untersagt, insbesondere die Nutzung des Inhalts im Zusammenhang mit, für oder in KI-Systemen, KI-Modellen oder Generativen Sprachmodellen.

Significant changes, however, arise in the BEV parametrizations. Thanks to the improved battery technology, these vehicles can operate with significantly reduced weight compared to the scenario with the requirement for long-range capability from 2018. The lower weight also results in less electric power necessary to meet all design requirements, which also reduces the specific electric consumption. The improved efficiency can also further reduce the required battery capacity compared to the reference year 2018.

The series hybrid gives further interesting results. The battery capacity of the vehicle is increased compared to the reference year 2018, which reduces the need to provide electric energy by the range extender and reduces fuel consumption.

In the case of parallel hybrids, there are no significant changes in the parametrizations. The parallel operation with the ICE is significantly more efficient than the series mode of operation of the sREV and it is still worthwhile for the parallel hybrids to use this operation mode extensively in the reference year 2030. Due to the higher energy density of the battery, a little less weight leads to slightly reduced consumptions compared to the scenario with the requirement for long-range capability in 2018.

The calculated REI of the powertrain concepts are shown in Fig. 10 for scenario with the requirement for long-range capability in the reference year 2030. The BEV improve the most compared to the scenario of 2018 and the two-speed BEV achieves a comparable REI level to the ICEV-O. Despite the technological developments taken into account, the REI of the BEV concepts still suffer from high emissions that are caused by the production of the vehicles.

https://doi.org/10.51202/9783181023549 - Generiert durch IP 216.73.216.36, am 19.01.2026, 02:19:31. © Urheberrechtlich geschützter Inhalt. Ohne gesonderte Erlaubnis ist jede urheberrechtliche Nutzung untersagt, insbesondere die Nutzung des Inhalts im Zusammenhang mit, für oder in KI-Systemen, KI-Modellen oder Generativen Sprachmodellen.

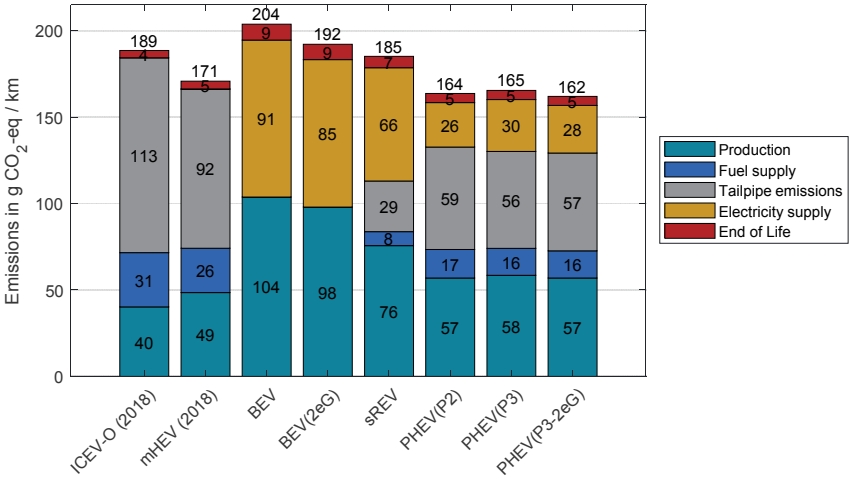


Fig. 10: Identified Real Ecological Impact of the different powertrain concepts for the scenario with the requirement for long-range capability in the reference year 2030. Technological progression in ICE technology was not considered.

As in the previous scenarios, the series hybrid has disadvantages compared to the parallel topologies. The parallel PHEV perform best in the reference year 2030 and show a significant improvement, which is mainly due to the improved electricity mix. As in the previous results, the P2 topology shows advantages over the P3 topology, due to the multispeed transmission that can be used by the electric machine. The P3-2eG topology performs best among the parallel hybrids due to the variety of operating options.

Overall, the parallel PHEV have the greatest potential to reduce the REI for the scenario with the requirement for long-range capability in the reference year 2030. Despite the moderate battery capacity, a purely electric, locally emission-free city driving and a relatively high total electrical driving percentage are achieved, since the shortest simulated trip distance with the highest electrical driving percentage has the largest weighting factor in the consumption assessment.

6 Summary and Conlusions

This work presents an optimization framework for the comparative evaluation of the Real Ecological Impact (REI) of different powertrain concepts. We show that in order to establish an unbiased comparison, multiple criteria need to be considered.

https://doi.org/10.51202/9783181023549 - Generiert durch IP 216.73.216.36, am 19.01.2026, 02:19:31. © Urheberrechtlich geschützter Inhalt. Ohne gesonderte Erlaubnis ist jede urheberrechtliche Nutzung untersagt, insbesondere die Nutzung des Inhalts im Zusammenhang mit, für oder in KI-Systemen, KI-Modellen oder Generativen Sprachmodellen.

First of all, the greenhouse gas emissions of the vehicle need to be considered over the whole life cycle, including production, operational and end-of-life phases.

Secondly, the consumption of the vehicles needs to be determined by means of real driving data. Therefore, we applied a cycle synthesis method based on real driving profiles. By that, we are able to compress big fleet data sets into computationally efficient but representative driving cycles.

Moreover, the parametrization of powertrain concepts has a significant effect on both the emissions in the production phase and the consumption during the operational phase. The comparison of existing production vehicles cannot characterize the actual potential of a powertrain concept to reduce the REI since different design goals were considered in the development of these vehicles. We created a framework that explicitly optimizes the parametrization of the powertrain concepts based on real driving data to reduce the REI of the vehicles and thus, enables to assess the actual potential of the respective powertrain concepts.

We analyzed the REI of a conventional vehicle, multiple hybrid electric vehicles with diverse powertrain topologies, and two purely electric powertrain concepts. The results are shown for scenarios with and without the requirement for long-range capability of 100 km and 350 km range, respectively. The scenario with the requirement for long-range capability is additionally investigated for a predicted scenario parameter set in the year 2030.

We identified a significant impact of the chosen scenario on the assessment of the powertrain concepts. Battery electric vehicles, today and especially in the future, have a good potential to reduce the REI in the scenario without the requirement for long-range capability, but they perform much worse in the scenarios with the requirement for long-range capability where the required large battery capacity leads to a high energy consumption due to an increased vehicle weight and particularly to high emissions during the production phase. Even for the year 2030, the predicted increase in battery density and the decreased specific emissions of energy production cannot compensate for this.

The best results of the scenario with the requirement for long-range capability are achieved by the parallel plug-in hybrids and the mild hybrid. Interestingly and in contrast to current production vehicles, all of the powertrains are optimized towards DHT that use the advantages of both energy converters and also the synergy of the combined use of the energy converters. The ICE and EM can be dimensioned smaller which reduces the emissions in the production phase. The parallel plug-in hybrids are also benefiting from the improved scenario parameters with

https://doi.org/10.51202/9783181023549 - Generiert durch IP 216.73.216.36, am 19.01.2026, 02:19:31. © Urheberrechtlich geschützter Inhalt. Ohne gesonderte Erlaubnis ist jede urheberrechtliche Nutzung untersagt, insbesondere die Nutzung des Inhalts im Zusammenhang mit, für oder in KI-Systemen, KI-Modellen oder Generativen Sprachmodellen.

regards to electric energy production and energy storage. Moreover, the parallel plug-in hybrids perform well on the scenario without the requirement for long-range capability, since the powertrains are optimized towards a high percentage of electrical driving.

In general, parallel plug-in hybrid concepts are identified to robustly achieve a good ecological potential for all investigated scenarios. Concerning the scenario with the requirement for long-range capability, the parallel PHEV perform best, even when the scenario of 2030 is considered. Still, the prediction of future REI for different powertrain concepts is linked to significant uncertainties because of the high sensitivity to external factors. The developed optimization framework allows for a proper comparison of the ecological potential of different powertrain concepts under changing boundary conditions on an equal evaluation basis and is therefore suited to be used in an agile manner, adapting to the latest predictions of boundary conditions.

7 Acknowledgements

We thank our partners in the publicly funded project FahrKLang. This article would not have been possible without their contribution to the project. In addition to the partner institutes (IWAR) and (VKM) at TU Darmstadt, the DLR Institute of Transport Research (DLR VF) is to be mentioned.

Supported by:

Federal Ministry
for Economic Affairs
and Energy

on the basis of a decision
by the German Bundestag

https://doi.org/10.51202/9783181023549 - Generiert durch IP 216.73.216.36, am 19.01.2026, 02:19:31. © Urheberrechtlich geschützter Inhalt. Ohne gesonderte Erlaubnis ist jede urheberrechtliche Nutzung untersagt, insbesondere die Nutzung des Inhalts im Zusammenhang mit, für oder in KI-Systemen, KI-Modellen oder Generativen Sprachmodellen.

8 References

[1] A. Esser, M. Zeller, S. Foulard, and S. Rinderknecht, “Stochastic Synthesis of Representative and Multidimensional Driving Cycles,” in *WCX World Congress Experience*, 2018.

[2] G. Paganelli, S. Delprat, T. M. Guerra, J. Rimaux, and J. J. Santin, “Equivalent consumption minimization strategy for parallel hybrid powertrains,” in *IEEE 55th Vehicular Technology Conference*, Birmingham, AL, USA, 2002, pp. 2076–2081.

[3] L. Serrao, S. Onori, and G. Rizzoni, “ECMS as a realization of Pontryagin's minimum principle for HEV control,” in *American Control Conference*, St. Louis, MO, USA, 2009, pp. 3964–3969.

[4] Ingo Totzke et al., “Sichere Intelligente Mobilität: Deliverable D41.1,” 2010. [Online] Available: https://www.eict.de/projekte/#project-19.

[5] infas institut für angewandte sozialwissenschaft gmbh and Deutsches Zentrum für Luft- und raumfahrt e.V. - Institut für Verkehrsforschung, Eds., “Mobilität in Deutschland 2008,” FE-Nr. 70.801/2006, 2010.

[6] A. Nordelöf, E. Grunditz, A.-M. Tillman, T. Thiringer, and M. Alatalo, “A scalable life cycle inventory of an electrical automotive traction machine—Part I: Design and composition,” (en), *Int J Life Cycle Assess*, vol. 23, no. 1, pp. 55–69, 2018.

[7] A. Balazs, *Optimierte Auslegung von Hybridantriebsträngen unter realen Fahrbedingungen*. Fakultät für Maschinenwesen, RWTH Aachen, Dissertation, 2015.

[8] Mitschke, M., Wallentowitz, H., *Dynamik der Kraftfahrzeuge*: Springer, 2014.

https://doi.org/10.51202/9783181023549 - Generiert durch IP 216.73.216.36, am 19.01.2026, 02:19:31. © Urheberrechtlich geschützter Inhalt. Ohne gesonderte Erlaubnis ist jede urheberrechtliche Nutzung untersagt, insbesondere die Nutzung des Inhalts im Zusammenhang mit, für oder in KI-Systemen, KI-Modellen oder Generativen Sprachmodellen.

Holistic Design Approach for Electric Drives

Dr.-Ing. **Peter Fietkau**, Dipl.-Ing. **Niklas Lamparsky**,
Dr.-Ing. **Michael Felbermaier**, Dr.-Ing. **Annette Fröhlcke**,
Dipl.-Ing. **Thomas Conze**, Dr. Ing. h.c. F. Porsche AG, Weissach

Zusammenfassung

Der vorliegende Beitrag beschreibt die bei der Porsche AG eingeführte Systematik zur gesamtheitlichen digitalen Antriebsentwicklung am Beispiel der mechanischen Auslegung eines Elektroantriebs. Die Komponenten und Berechnungsdisziplinen werden nicht mehr einzeln betrachtet, sondern in dreizehn sogenannten digitalen Antriebssystemen (dAS) zusammengefasst. Diese werden analog zu der Hardwareentwicklung über den Produktentwicklungsprozess weiterentwickelt, wobei sie zu definierten Meilensteinen gewisse Reifegrade erfüllen müssen. Aus mehreren dAS wird letztendlich ein digitaler Prototyp aufgebaut.

Die dAS Lastkollektive und Fahrleistungen liefern die notwendigen Auslegungsgrößen für einen neuen Antrieb. Im dAS Motor werden die Aktivteile der E-Maschine ausgelegt und das Gehäuses in Wechselwirkung mit dem Getriebe abgesichert. Im dAS Getriebe werden im ersten Schritt alle Radsatzteile nach gängigen Normen der Technik ausgelegt und anschließend das gesamte Aggregat in einem FE-System abgewälzt. Diese Simulation liefert endgültige Aussagen zu auftretenden Kräften, Betriebsfestigkeit und Akustik. In den dAS Schmierung, Thermik und Aktorik werden alle Temperaturen bestimmt und der Schmierkreislauf ausgelegt. Das dAS Antriebstrangdynamik liefert Informationen zu Triebstrangschwingungen und entwirft Regelalgorithmen zu deren Reduzierung.

Der dargestellte Prozess eignet sich, um einen Elektroantrieb gesamtheitlich digital auszulegen und abzusichern. Auftretende Wechselwirkungen werden von Beginn an systematisch berücksichtigt und es wird der gesamte Entwicklungsprozess von der Konzeptphase bis zum Start of Production (SOP) in der virtuellen Welt abgebildet.

Abstract

This paper describes the system introduced at Porsche AG for holistic digital powertrain development, using the mechanical design of an electric drive as an example. The components and simulation disciplines are no longer examined individually, but rather combined in thirteen so-called Digital Powertrain Systems (DPS). These are developed in the Product Development

https://doi.org/10.51202/9783181023549 - Generiert durch IP 216.73.216.36, am 19.01.2026, 02:19:31. © Urheberrechtlich geschützter Inhalt. Ohne gesonderte Erlaubnis ist jede urheberrechtliche Nutzung untersagt, insbesondere die Nutzung des Inhalts im Zusammenhang mit, für oder in KI-Systemen, KI-Modellen oder Generativen Sprachmodellen.

Process (PDP) as with hardware development, and must achieve certain levels of maturity at defined milestones. Ultimately, a digital prototype is built from several DPSs.
The Load Spectra DPS and Driving Performance DPS deliver the necessary design parameters for a new drive system. In the Motor DPS, the active components of the electric motor are designed and the housing is validated in interaction with the gearbox. In the Transmission DPS, the first step is to design all the parts of the gear sets in accordance with common technical standards. Next, the complete system is replicated and rotated in an FE system. This simulation supplies conclusive information on the occurring forces, service strength and acoustics. In the Lubrication, Thermal and Actuation DPSs, all temperatures are determined and the lubrication circuit is designed. The Powertrain Dynamics DPS provides information on powertrain oscillations and maps out control algorithms to reduce them.
The process described here is suitable for the holistic digital design and validation of an electric drive. Interactions that occur are systematically observed right from the start, and the entire development process is mapped virtually, from the concept phase to the Start of Production (SOP).

1. Introduction

In powertrain development today, there is a marked trend to increase the number of variants while simultaneously reducing development times and test vehicles per derivative. On the other hand, ever more powerful calculation programs and greater computing power are increasingly available. The result is a significant trend towards the digitalization of product development, i.e. greatly expanded design and simulation scopes and increasing use of virtual tests instead of real ones.
Modern electric drives combine the e-motor, inverter and gearbox in a single unit. Consequently, numerous disciplines are involved, which are in complex mutual relationships. Each component and each discipline comes with its own requirements for design, some of which contradict one another. Beyond actual powertrain development, too, various conditions and requirements have to be met, e.g. in terms of crash behavior and NVH properties. In order to face up to both these challenges and increased level of digitalization, new strategies for digital powertrain development are required.
The possibilities of virtual product development are described extensively in the literature. The basics are set out by Bauer and Dangelmaier [1], Ovtcharova [2] and Stark et al. [3]. Armbrüster et al. [4] describe an automated simulation process for FE analyses in vehicle design. Hein et al. [5] developed a holistic approach to gearing design. Hofstetter et al. [6] make use of a linked design process for gearings, bearings and housings to optimize the gearbox under

https://doi.org/10.51202/9783181023549 - Generiert durch IP 216.73.216.36, am 19.01.2026, 02:19:31. © Urheberrechtlich geschützter Inhalt. Ohne gesonderte Erlaubnis ist jede urheberrechtliche Nutzung untersagt, insbesondere die Nutzung des Inhalts im Zusammenhang mit, für oder in KI-Systemen, KI-Modellen oder Generativen Sprachmodellen.

consideration of the installation space, but do not extend this to cover the entire product development process (PDP). Fuger and Hanke [7] present a closed, integrated simulation workflow for the active components of an electric motor. Buchberger et al. [8] [9] describe the design aspects of electric drives and, in particular, an NVH development process. Similarly, Steffens et al. [10] describe an analytical method for NVH issues. A possible link to higher-level development processes in the concept phase is set out by Hirz [11]. Piechottka, Kercher et al. [12] [13] demonstrate a concept design methodology for developing powertrains on the basis of a virtual development chain. Albers et al. [14] take a similar approach.

Unlike all the above, the system introduced by Porsche AG encompasses all the phases of the PDP and all the components and simulation disciplines of the powertrain. This article describes this system by way of a practical example involving the powertrain development of a pure battery electric vehicle (BEV). The focus here is on the mechanical design.

2. Digital Powertrain Development

In order to satisfy future requirements in the trend towards virtual development, reduced development resources and increasing complexity, Porsche AG has introduced a new system of digital powertrain development, see Fig. 1.

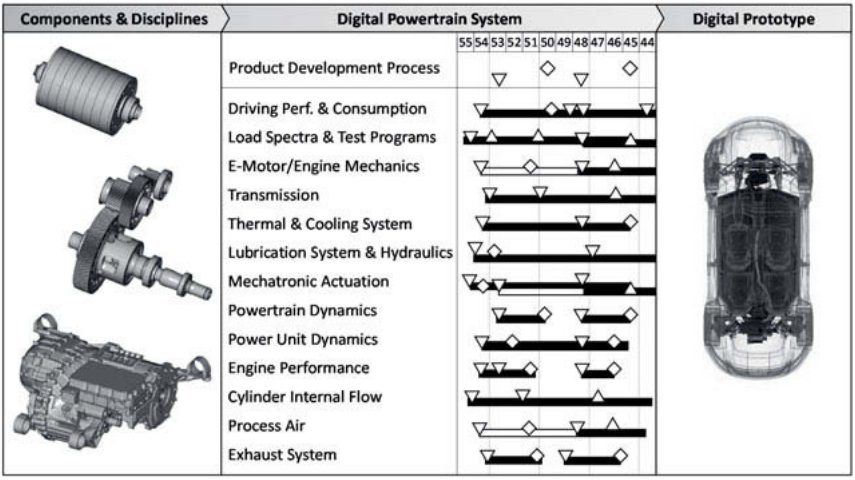


Fig. 1: Digital powertrain development

https://doi.org/10.51202/9783181023549 - Generiert durch IP 216.73.216.36, am 19.01.2026, 02:19:31. © Urheberrechtlich geschützter Inhalt. Ohne gesonderte Erlaubnis ist jede urheberrechtliche Nutzung untersagt, insbesondere die Nutzung des Inhalts im Zusammenhang mit, für oder in KI-Systemen, KI-Modellen oder Generativen Sprachmodellen.

The components and design disciplines are no longer examined individually, but rather combined in so-called Digital Powertrain Systems (DPSs). There are thirteen of these systems in total, but not all of them are relevant to BEVs. The DPSs reproduce the respective area virtually with the aid of models, and pool all the relevant information. They were generically planned in the PDP in consultation with the relevant departments. This generic model is adapted to each project and provides a schedule for tracking all virtual activities. In addition, data provision for the individual DPSs at precisely defined milestones, model build-up and the results are tracked with the aid of status sheets and regular reports are made to the management. As in hardware development, digital models also have to meet certain maturity criteria at set points in time. All input and output data are stored centrally in a simulation data management system.

A project-specific contact is named for each DPS. Moreover, there is a central coordinator for each project, who coordinates all digital scopes, acts as the interface to other departments, monitors deadlines and costs and is on all the key project committees.

From the DPSs, those that provide core information on the overall vehicle are combined to create a Digital Prototype (DPT). The status of this DPT is also tracked and reported to the management board at defined PDP milestones. This ensures that the entire development process is reflected in the virtual world, from the concept phase to the SOP. As an example, the following section discusses some very important DPSs for BEVs.

3. Driving Performance DPS and Load Spectra DPS

At the start of a project, the vehicle target values for driving performance and consumption are established. On this basis, powertrain variants can be generated and evaluated in the Driving Performance & Consumption DPS with the aid of optimization algorithms. Degrees of freedom exist here in the number of driven axles, performance, torque, number of gears and transmission ratios. In parallel, the Electric Motor DPS and Transmission DPS take account of installation space restrictions and actual hardware layouts. In this example, however, the transmission ratios and the performance and torque of the drive units were already provided by the overall vehicle department.

As the next step, load spectra are created on this basis in the Load Spectra & Test Programs DPS. Using overall vehicle simulations on defined design tracks, the mechanical loads of all powertrain components can be ascertained. Regularly throughout the project runtime, loops take place with updated input data, allowing hardware modifications, software updates and findings from measurements, etc. to be incorporated in the process. Further, limit load spectra and test bench test programs are generated in the Load Spectra & Test Programs DPS. This is also where endurance test results and field data are statistically analyzed.

https://doi.org/10.51202/9783181023549 - Generiert durch IP 216.73.216.36, am 19.01.2026, 02:19:31. © Urheberrechtlich geschützter Inhalt. Ohne gesonderte Erlaubnis ist jede urheberrechtliche Nutzung untersagt, insbesondere die Nutzung des Inhalts im Zusammenhang mit, für oder in KI-Systemen, KI-Modellen oder Generativen Sprachmodellen.

4. Electric Motor DPS

Mechanical design of the electric motor takes place in the Electric Motor/Engine Mechanics DPS. This process examines all components such as the shaft, laminated rotor core, stator, housing plus all support arms and the bearing assembly. Special attention is paid to lamination design. Here, the mechanical and magnetic properties have conflicting objectives. Mechanically, the laminations must be designed to have sufficient strength, low inertia and a low weight, and the bending natural frequency of the rotor as a whole must be as high as possible. In electromagnetic terms, however, parameters such as power density, torque fluctuations and losses are of vital importance. To resolve this conflict of interests, a combined optimization process has been introduced, see Fig. 2. Using a parametric CAD model, the magnetic and mechanical properties are determined separately and the geometrical parameters are successively optimized using an optimization algorithm. The optimum design for the relevant requirements can be defined on this basis.

Fig. 3 illustrates how the mechanical properties of stress and service life are determined for the individual optimization step.

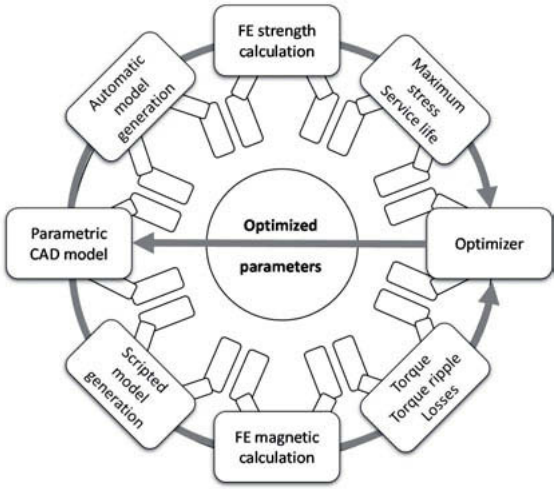


Fig. 2: Rotor design optimization

https://doi.org/10.51202/9783181023549 - Generiert durch IP 216.73.216.36, am 19.01.2026, 02:19:31. © Urheberrechtlich geschützter Inhalt. Ohne gesonderte Erlaubnis ist jede urheberrechtliche Nutzung untersagt, insbesondere die Nutzung des Inhalts im Zusammenhang mit, für oder in KI-Systemen, KI-Modellen oder Generativen Sprachmodellen.

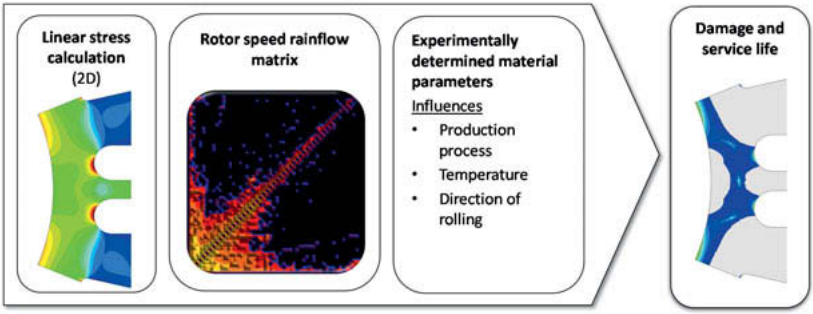


Fig. 3: Lamination service life calculation

The stresses are calculated with the aid of a 2D FE model. The primary stress originates not from the produced torque, but from centrifugal forces. The rotational speed spectrum is therefore a decisive factor and was determined in the Load Spectra DPS. The material characteristic values of the motor laminations depend on numerous influences such as thickness, bonding, production process, etc. which is why they have been validated in experiments on material samples. Service life can then be determined based on damage accumulation [15].

As well as the lamination design, the design of the interference fit assemblies between the laminated core and shaft and between the stator and housing also plays an important role, see Fig. 4. For the interference fit between laminated core and shaft, the minimum required overlap is derived from the expansion at maximum speed combined with the temperature distribution calculated in the Thermal & Cooling System DPS. Here, the interference fit must remain closed and sufficient torque must be transferable. In motors with very high speeds, additional measures may be necessary, such as a combination with positive locking elements. The maximum permitted overlap is determined at zero rotor speed, whereby the stresses must always remain below the yield strength. For the interference fit between the stator and housing, the minimum required overlap is calculated from the necessary torque transmission and the maximum temperature, while the maximum permitted overlap is derived from housing strength at minimum temperature.

In addition, further important parameters for the rotor, such as natural bending frequency, deformation during installation/first heating, protection against bursting, and the strength of the shaft itself are evaluated in the Electric Motor/Engine Mechanics DPS.

https://doi.org/10.51202/9783181023549 - Generiert durch IP 216.73.216.36, am 19.01.2026, 02:19:31. © Urheberrechtlich geschützter Inhalt. Ohne gesonderte Erlaubnis ist jede urheberrechtliche Nutzung untersagt, insbesondere die Nutzung des Inhalts im Zusammenhang mit, für oder in KI-Systemen, KI-Modellen oder Generativen Sprachmodellen.

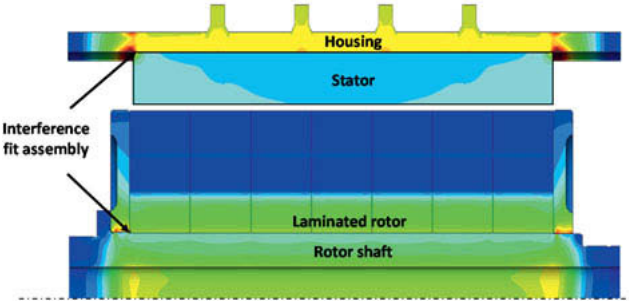


Fig. 4: Interference fit assemblies shaft/laminated rotor and stator/housing

As well as the rotor, this DPS also analyzes the entire housing including support arms. Here, not only are already designed parts checked - design proposals are also actively put forward using topology optimizations. Examples of support arms and housings can be seen in Fig. 5. A commercial tool is used for optimization. The objective function was to minimize the weight and increase dynamic stiffness to improve the acoustic properties. Interfaces to neighboring components and the maximum installation space were the set constraints. Next, the output of optimization had to be adapted to obtain a geometry suitable for casting.

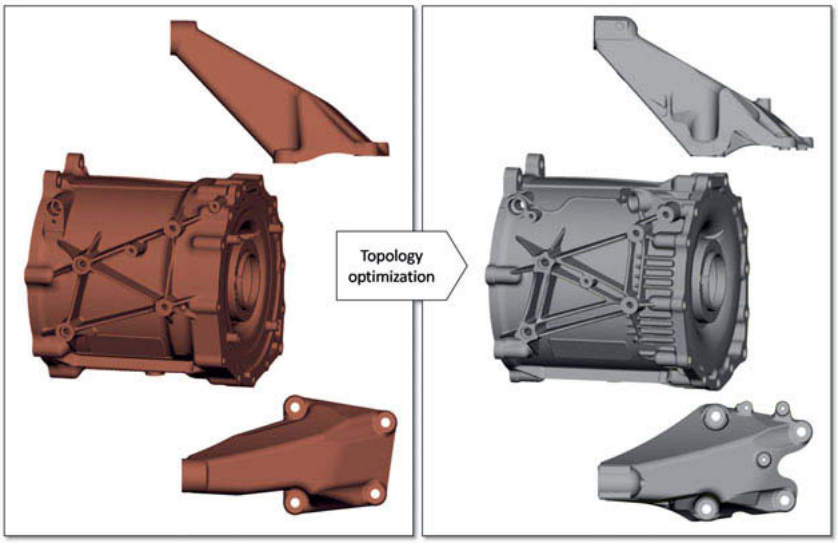


Fig. 5: Topology optimization

https://doi.org/10.51202/9783181023549 - Generiert durch IP 216.73.216.36, am 19.01.2026, 02:19:31. © Urheberrechtlich geschützter Inhalt. Ohne gesonderte Erlaubnis ist jede urheberrechtliche Nutzung untersagt, insbesondere die Nutzung des Inhalts im Zusammenhang mit, für oder in KI-Systemen, KI-Modellen oder Generativen Sprachmodellen.

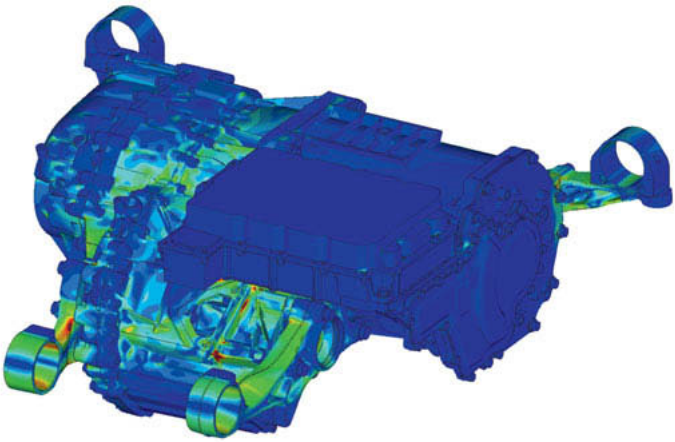


Fig. 6: Overall housing stresses

Ultimately, the complete housing is evaluated as a unit in the Electric Motor DPS. Here, there are close interactions with the Transmission DPS, which provides the loads acting on the housing from the gear set. Depending on the layout of the gear set, these loads can create relatively complex dynamic loads on the housing, e.g. when planetary gears roll off an internal gear fixed in the housing. Additional requirements arise as a result of excitation from the road, e.g. when braking on a washboard surface, and from the crash simulation. Fig. 6 contains an example for the housing evaluation showing the stresses in a complete drive unit for a given operating point, with which service life is ultimately determined by means of damage accumulation.

5. Transmission DPS

The entire gear set is designed in the Transmission DPS, based on the spectra from the Load Spectra DPS. In other words, the dimensions of all machine elements such as gearing, shafts, bearings, shaft-hub connections, shift elements and differential are established. Further, efficiency maps are simulated in this DPS, and acoustic excitation is minimized.

Firstly, gear set dimensioning is conducted in accordance with common standards and design guidelines. For this purpose, a model of the gear set, including motor rotor, is generated using commercial design software. Since housing stiffness is a factor when determining acting forces, particularly when the bearing assembly is statically overdetermined, there is an interaction with the Electric Motor DPS.

https://doi.org/10.51202/9783181023549 - Generiert durch IP 216.73.216.36, am 19.01.2026, 02:19:31. © Urheberrechtlich geschützter Inhalt. Ohne gesonderte Erlaubnis ist jede urheberrechtliche Nutzung untersagt, insbesondere die Nutzung des Inhalts im Zusammenhang mit, für oder in KI-Systemen, KI-Modellen oder Generativen Sprachmodellen.

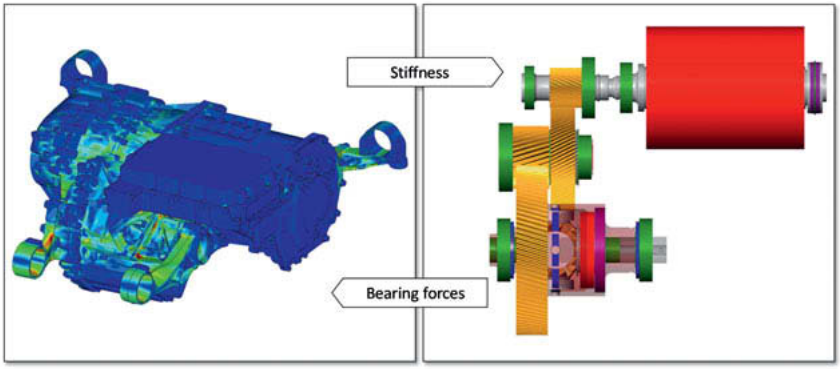


Fig. 7: FE-housing and gear set interaction

Stiffness is taken into consideration in the design software by incorporating a modally reduced FE model, see Fig. 7. The forces acting on the housing are in turn transferred back to the Electric Motor DPS. Moreover, this means that this initial model of the gear set can already provide conclusions on displacements during operation, resulting contact patterns and necessary gearing corrections. These are extremely important to service life and acoustics.

After this dimensioning process, stress/load cycle (S/N) or torque/load cycle (T/N) curves are determined for the key elements of the gear set. An example can be seen in Fig. 8, which shows a shaft, a bearing and several gear teeth with tooth root breakage and pitting as the causes of failure. By plotting these in a common diagram, component dimensioning can be compared very easily. Ideally, all lines would lie one on top of the other, because then damage of all components would be uniform. This would indicate minimum material usage and therefore minimum weight at the given proportions. In practice, however, numerous restrictions render this unachievable.

The resulting limit T/N curve for the complete drive unit can be determined by reading the minimum bearable number of load cycles for each load. With this figure, the ability to endure new load spectra can be estimated very quickly. To this aim, damage accumulation of the spectrum is calculated using the resulting limit T/N curve. In addition, static load capacity and safety factor for scuffing must be considered. The limit T/N curve is also used in the Load Spectra DPS to generate a limit load spectrum. Here, the component limits are exploited to the maximum for experimental validation, even if these limits will not be reached with the current intended usage of the drive unit.

https://doi.org/10.51202/9783181023549 - Generiert durch IP 216.73.216.36, am 19.01.2026, 02:19:31. © Urheberrechtlich geschützter Inhalt. Ohne gesonderte Erlaubnis ist jede urheberrechtliche Nutzung untersagt, insbesondere die Nutzung des Inhalts im Zusammenhang mit, für oder in KI-Systemen, KI-Modellen oder Generativen Sprachmodellen.

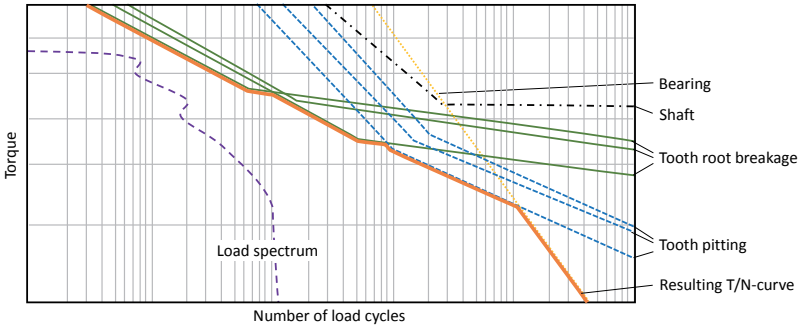


Fig. 8: Resulting limit T/N curve for different damage mechanisms

Next, the entire gear set including housing is replicated and rotated in an FE system. To do this, all parts including gears and bearings are meshed, and occurring contacts are defined. This process takes account of tolerances between the components and prevailing temperatures. This model delivers detailed information on forces and deformations during operation, while also considering interactions produced due to several gears on one shaft, forces from shift elements, changing bearing pre-loads, etc.

This enables local damage calculations, i.e. the damage is resolved locally instead of gear meshing and bearings being examined as an integral unit. Since the point of maximum stress can change due to deformation during operation, these local results may sometimes differ considerably from the integral examination based on common standards. As an example, Fig. 9 shows pitting damage on a tooth flank, tooth root damage over the width of the tooth, and the maximum pitting damage for an inner bearing race over the width of the bearing, all determined using this method. The occurring transmission error and therefore the acoustic excitation are also assessed. Depending on the results of the service life and acoustic calculation, the design is adapted, e.g. through gearing corrections, modifying the bearing geometry, or changing support structures.

An example of this kind of optimization can be seen in Fig. 10. Here, first the original geometry of a final drive gear wheel is shown. The calculated flank line error shows strong dependence on load in traction and thrust mode, which makes it impossible to achieve tooth correction that is adequate for all loads. The result is asymmetrical contact patterns with very high local damage, and major acoustic excitation due to transmission error, especially in the 1st gear mesh order.

https://doi.org/10.51202/9783181023549 - Generiert durch IP 216.73.216.36, am 19.01.2026, 02:19:31. © Urheberrechtlich geschützter Inhalt. Ohne gesonderte Erlaubnis ist jede urheberrechtliche Nutzung untersagt, insbesondere die Nutzung des Inhalts im Zusammenhang mit, für oder in KI-Systemen, KI-Modellen oder Generativen Sprachmodellen.

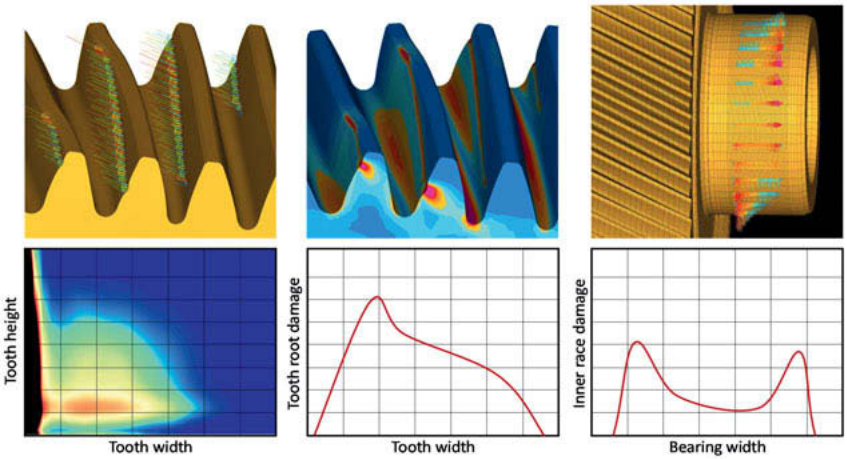


Fig. 9: Local damage calculation for tooth flank pitting, tooth root breakage and inner bearing race pitting

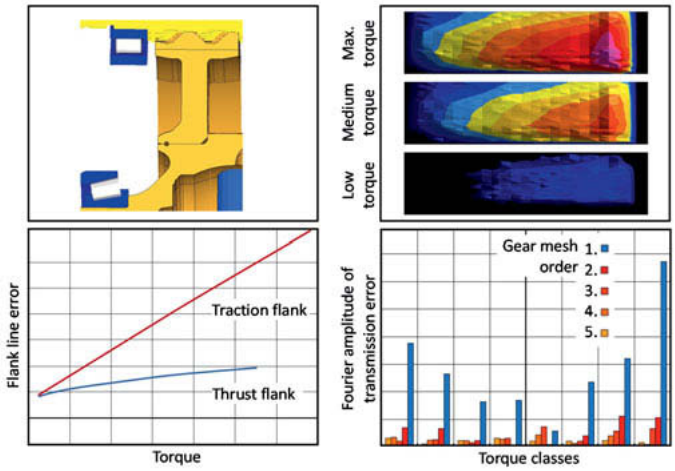


Fig. 10: Wheel body geometry, contact pattern, flank line error and transmission error for standard wheel body

https://doi.org/10.51202/9783181023549 - Generiert durch IP 216.73.216.36, am 19.01.2026, 02:19:31. © Urheberrechtlich geschützter Inhalt. Ohne gesonderte Erlaubnis ist jede urheberrechtliche Nutzung untersagt, insbesondere die Nutzung des Inhalts im Zusammenhang mit, für oder in KI-Systemen, KI-Modellen oder Generativen Sprachmodellen.

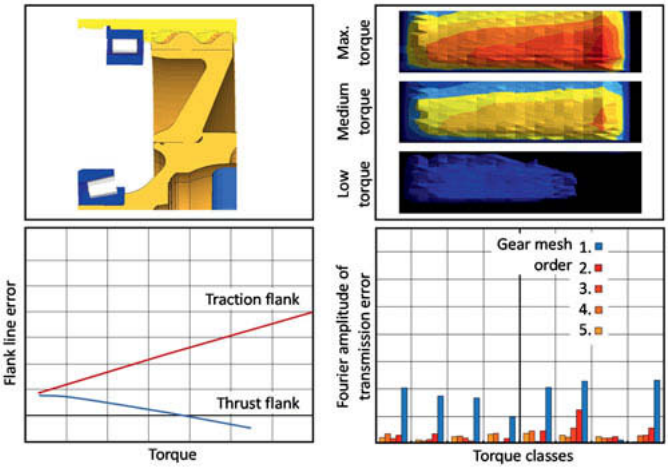


Fig. 11: Wheel body geometry, contact pattern, flank line error and transmission error for Z-shaped wheel body and β-correction

The optimization proposal made, comprising a Z-shaped wheel body, is shown in Fig. 11. This shape considerably reduces flank line errors. In combination with a moderate flank line correction, the contact pattern was improved and acoustic excitation reduced. In another optimization, welding distortion was recorded in experiments by welding the finished gear wheel body to the hub and measuring the flank error, and taken directly into consideration during production by changing the flank line correction before welding.

6. Cooling DPS, Lubrication DPS and Actuation DPS

In the Thermal & Cooling System DPS, the temperatures of all components are determined using 3D Conjugate Heat Transfer (CHT) calculations. What's more, the pressure loss characteristics of the heat exchangers and the heat output of the drive unit to the cooling system are established. The results are used in the Electric Motor DPS and Transmission DPS, e.g. for the strength and stiffness calculation, designing interference fits, determining bearing clearances, and the efficiency simulation. Furthermore, achievable continuous output and derating thresholds in different driving cycles can be forecast in coordination with the Driving Performance & Consumption DPS. Heat-up behavior is also examined. Additionally, a simplified temperature model is elaborated, which subsequently runs online on the vehicle control unit.

https://doi.org/10.51202/9783181023549 - Generiert durch IP 216.73.216.36, am 19.01.2026, 02:19:31. © Urheberrechtlich geschützter Inhalt. Ohne gesonderte Erlaubnis ist jede urheberrechtliche Nutzung untersagt, insbesondere die Nutzung des Inhalts im Zusammenhang mit, für oder in KI-Systemen, KI-Modellen oder Generativen Sprachmodellen.

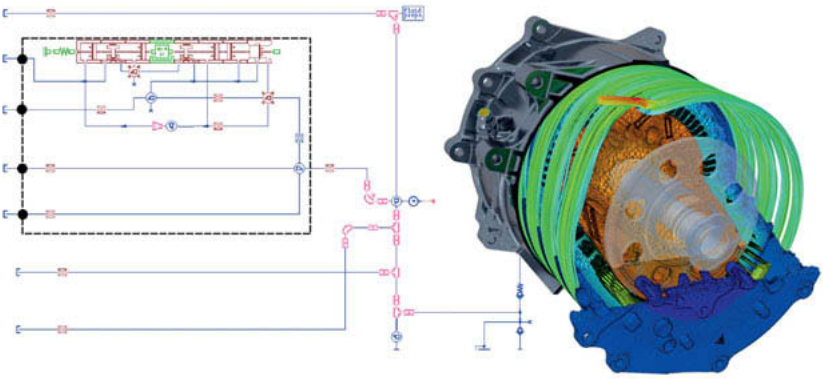


Fig. 12: 1D-hydraulic- and 3D-CHT-simulation

In the Lubrication System & Hydraulics DPS, a 1D model is used to simulate the gearbox oil circuit. This helps with designing the switching valves, measuring coolant and lubricant flow rates, dimensioning the pump and determining the required pump power in the various driving cycles. This in turn is important for the vehicle range. The oil flow rates are also included in the Thermal & Cooling System DPS, which then feeds back oil and coolant temperatures, see Fig. 12.

If necessary, a mechanical or hydraulic actuation system for shift actuation can be simulated and designed in the Mechatronic Actuation DPS using 1D models. Depending on the design, this may interact with the Lubrication System DPS and Transmission DPS, and also supplies control path models for a software- or hardware-in-the-loop simulation of the future control unit.

7. Powertrain Dynamics DPS

In this DPS, the overall powertrain is mapped in a multibody system model, and torsional vibration behavior is analyzed. This plays a vital role in electric cars, in particular, because the powertrain itself is relatively rigid, there are no separating clutches or similar, and the electric motor can deliver very high torque gradients if necessary. This can result in major oscillations in the 5–20 Hz frequency range during ABS braking, load change maneuvers, µ-split situations or when driving off at high torques. Therefore, special control algorithms that prevent these oscillations in the vehicle - or at least reduce them - are developed in this DPS [16].

https://doi.org/10.51202/9783181023549 - Generiert durch IP 216.73.216.36, am 19.01.2026, 02:19:31. © Urheberrechtlich geschützter Inhalt. Ohne gesonderte Erlaubnis ist jede urheberrechtliche Nutzung untersagt, insbesondere die Nutzung des Inhalts im Zusammenhang mit, für oder in KI-Systemen, KI-Modellen oder Generativen Sprachmodellen.

8. Overall Process and Digital Prototype

The standard scopes of the individual DPSs described here are regularly tracked in status sheets and reported to the management. The PDP contains fixed milestones at which the individual DPSs must show a certain level of maturity. This is achieved by aggregating the detailed statuses in the various DPSs, whereby a distinction is made between data provision, model build-up and results, see Fig. 13. As the final step, the statuses of the DPSs that are important for the overall vehicle are combined to create a DPT. This is a virtual image of the powertrain, which allows conclusions to be drawn about core properties and expected service life.

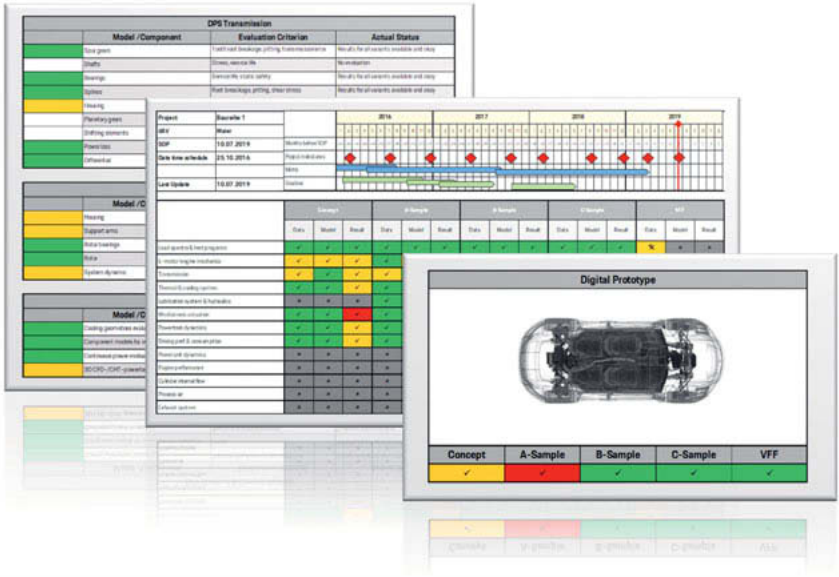


Fig. 13: DPS and DPT status report

9. Conclusion

This paper described the system introduced at Porsche AG for holistic digital powertrain development, using the mechanical design of an electric drive as an example. Virtual development is divided into several DPSs, which bring together different components and disciplines and are developed and evaluated throughout the PDP in entirely the same way as hardware development. Ultimately, a digital prototype is built from several DPSs. As well as the general

https://doi.org/10.51202/9783181023549 - Generiert durch IP 216.73.216.36, am 19.01.2026, 02:19:31. © Urheberrechtlich geschützter Inhalt. Ohne gesonderte Erlaubnis ist jede urheberrechtliche Nutzung untersagt, insbesondere die Nutzung des Inhalts im Zusammenhang mit, für oder in KI-Systemen, KI-Modellen oder Generativen Sprachmodellen.

description of the system, DPSs that are especially important for BEVs were discussed in detail and examples provided.

In conclusion, the process described here is suitable for the holistic digital design and validation of an electric drive. Therefore, most of the activities can be planned and budgeted at the start of the project. Interactions that occur are systematically observed throughout, and the entire PDP is mapped virtually from the concept phase to the start of production. This way, a high level of maturity can be achieved early on in the development process, cutting the number of recursion loops to a minimum. Virtual scopes should be further expanded in future, to enable not just components but also, increasingly, functions and software to be developed without actual hardware. This increases the level of maturity, the speed of development and the number of possible tests, while simultaneously reducing the number of real test vehicles.

10. References

[1] Bauer, W., Dangelmaier, M.: Virtuelles Engineering. In: Lindemann, U.: Handbuch Produktentwicklung. Hanser: München 2016

[2] Ovtcharova, J.G.: Virtual Engineering: Principles, Methods and Applications. International Design Conference – Design 2010, Dubrovnik 2010

[3] Stark, R., Hayka, H., Israel, J.H., Kim, M.: Virtuelle Produktentstehung in der Automobilindustrie. Informatik-Spektrum 34 (2011) 1 pp. 20–28

[4] Armbrüster, M., Straube, S.: Prozessautomatisierung und -standardisierung im Simulationsumfeld. VDI-Kongress SIMVEC, Baden-Baden 2016

[5] Hein, M., Tobie, T., Stahl, K.: Holistic approach for fatigue life design of vehicle transmissions. International VDI Congress Dritev, Bonn 2018

[6] Hofstetter, M., Hirz, M. Gintzel, M., Schmidhofer, A.: Multi-Objective System Design Synthesis for Electric Powertrain Development. 2018 IEEE Transportation Electrification Conference and Expo (ITEC), Long Beach, CA, 2018, pp. 286-292

[7] Fuger, R., Hanke, M.: An Integrated Workflow for the Simulation-Driven Development of Electric Motors and Generators. VDI-Kongress SIMVEC, Baden-Baden 2018

[8] Buchberger, R., Grieshofer, O., Puchner, K., Sereinig, R.: System optimization of electric drives in term of lightweight design, acoustics and efficiency by means of modern transmission simulation methods. International VDI Congress EDrive, Bonn 2018

[9] Buchberger, R., Grieshofer, O., Hinterberger, W., Sereinig, R.: NVH-Entwicklungsprozess für elektrische Antriebe. Automobiltechnische Zeitschrift ATZ 119 (2010) 10 pp. 26–31

[10] Steffens, C., Nussmann, C., Pilath, C.: Virtual product development techniques applied to powertrain acoustics. ATZautotechnology 6 (2006) 1 pp. 36–39

https://doi.org/10.51202/9783181023549 - Generiert durch IP 216.73.216.36, am 19.01.2026, 02:19:31. © Urheberrechtlich geschützter Inhalt. Ohne gesonderte Erlaubnis ist jede urheberrechtliche Nutzung untersagt, insbesondere die Nutzung des Inhalts im Zusammenhang mit, für oder in KI-Systemen, KI-Modellen oder Generativen Sprachmodellen.

[11] Hirz, M.: An approach of multi disciplinary collaboration in conceptual automotive development. Int. J. Collaborative Enterprise 2 (2011) 1 pp. 39–56

[12] Piechottka, H.: Methodical Synthesis and Simulation-Assisted Analysis of Electrified Vehicle Concepts. CTI Symposium, Berlin 2016

[13] Kercher, F., Piechottka, H., Bargende, M., Küçükay, F.: Optimale Antriebsstrangauslegung auf Basis einer virtuellen Entwicklungskette. In: Liebl, J., Beidl, C.: Simulation und Test 2017. Springer Fachmedien: Wiesbaden 2018

[14] Albers, A., Reichert, U., Ott, S., Radimersky, A.: Software supported development of a Battery Electric Vehicle powertrain considering the efficiency. International VDI Congress Drivetrain for Vehicles, Friedrichshafen 2016

[15] Haibach, E.: Betriebsfestigkeit. Springer: Berlin Heidelberg New York 2006

[16] Pham, T., Scholz, C., Bofinger, G., Seifried, R.: Driveline Control – Intelligent Actuator Inputs to Improve Component Protection, Performance and Comfort. International VDI Congress Drivetrain for Vehicles, Bonn 2017

https://doi.org/10.51202/9783181023549 - Generiert durch IP 216.73.216.36, am 19.01.2026, 02:19:31. © Urheberrechtlich geschützter Inhalt. Ohne gesonderte Erlaubnis ist jede urheberrechtliche Nutzung untersagt, insbesondere die Nutzung des Inhalts im Zusammenhang mit, für oder in KI-Systemen, KI-Modellen oder Generativen Sprachmodellen.

Potential of lightweight construction and component properties of joined spur gears

Christoph Leonhardt, Michael Otto, Karsten Stahl,
Gear Research Centre, Technical University of Munich

Kurzfassung

Die Verschärfung der gesetzlichen Emissionsgrenzwerte macht das Thema Leichtbau in der Automobilindustrie wichtiger denn je. In dieser Veröffentlichung wird der Leichtbauansatz eines Zahnrades in Mehrkomponentenbauweise bestehend aus einem hochfesten Zahnkranz und einem beanspruchungsgerecht konstruierten Radkörper untersucht. Dabei kommen statische Tests und Laufversuche zum Einsatz. Es stellt sich die Frage, ob durch eine Mehrkomponentenbauweise ähnliche Tragfähigkeiten wie in der integralen Bauweise erzielt werden und damit Leichtbaupotenziale ausgeschöpft werden können.

Im Rahmen der Versuche wurden verschiedene Zahnradvarianten mit unterschiedlichen Radkörpern und Fügeverfahren untersucht. Die Auswertung der Ergebnisse ergab, dass die Leichtbauzahnräder hohen statischen Belastungen von bis zu 890 Nm standhalten können, in den dynamischen Tests jedoch bei deutlich niedrigeren Belastungen ausfallen. Im statischen Test fielen die Zahnräder wegen eines Durchrutschens des Zahnkranzes auf dem Radkörper aus. Eine Variante mit formschlüssiger Zahnkranz-Radkörper-Verbindung erreichte die höchsten dynamisch ertragbaren Drehmomente, vorausgesetzt der Radkörperwerkstoff bietet eine ausreichende Festigkeit.

Das Leichtbaupotenzial, das zur Bewertung der Mehrkomponentenbauweise herangezogen wurde, wird aus der Tragfähigkeit und dem dazugehörigen Bauteilgewicht des Leichtbauzahnrades bestimmt. Ein Zahnrad mit massivumgeformten Radkörper aus Stahl hatte ein Leichtbaupotenzial von 32 % bezogen auf eine definierte Referenzvariante. Die in diesen Untersuchungen verwendeten Prototypen können die Tragfähigkeitswerte eines geschmiedeten Stegrades nach dem Stand der Technik nicht erreichen. Nichts desto trotz hat sich dieser Ansatz aufgrund höherer Flexibilität bei Werkstoffwahl und Fertigungsprozessen und damit einem zusätzlichen Kosteneinsparpotenzial als vielversprechend herausgestellt. Aus den Ergebnissen dieser Untersuchungen konnten weitere Leichtbau- und Tragfähigkeitspotenziale aufgedeckt werden.

https://doi.org/10.51202/9783181023549 - Generiert durch IP 216.73.216.36, am 19.01.2026, 02:19:31. © Urheberrechtlich geschützter Inhalt. Ohne gesonderte Erlaubnis ist jede urheberrechtliche Nutzung untersagt, insbesondere die Nutzung des Inhalts im Zusammenhang mit, für oder in KI-Systemen, KI-Modellen oder Generativen Sprachmodellen.

Abstract

Lightweight construction nowadays is a very important issue in the automotive industry. In this paper the approach of a multi-component gear design with high-strength gear rim and stress-related designed of the gear body is investigated based on static and dynamic experiments. The aim was to evaluate if this approach can compete with state-of-the-art gears built in an integrated design, where the gear is produced in one part. The experimental program includes different variants of multi-component gears such as gears with a gear body out of cut and stacked sheet metal as well as a deep-drawn and a cold forged gear body. The evaluation of the experiments showed, that the tested gears could withstand high static torques up to 890 Nm but significantly lower torques in the dynamic test. In the experiments on the static test rig the gears failed mainly by a slipping motion of the gear rim on the gear body. Variants with a form fit type connection between gear rim and gear body showed the highest torques in the dynamic tests, assuming that the gear body has a sufficient material strength.

The lightweight potential was determined by relating the load carrying capacity with the component weight of the specimen. The variant with the gear body forged into the gear rim reached the highest lightweight potential of 32 % compared to a reference variant. The multi-component gear design with the actual implementation cannot compete with state-of-the-art gears produced in an integrated design in terms of strength, but appeared to be a promising approach with further potential in load carrying capacity and lightweight potential.

1. Introduction

In the context of environmental legislation becoming more and more stringent concerning the threshold values of exhaust emission the automotive industry is looking for possibilities to reduce the vehicle weight. Efforts to increase comfort, occupant safety and driving dynamic led to rising vehicle weight, since a great number of sensors, electronic devices and cables needed to be installed. The car body has already been optimized by using high strength sheet metal and stiffness-optimized geometry.

Another potential to reduce the weight of the vehicle is located in the drive train. Rotating parts not only influence the mass of the drive train, but also can reduce the rotating inertia and therefore reduce the fuel consumption and thus emissions.

Gears are an important part of the drivetrain and transmit the power of the engine by converting the torque and the rotational speed. In state-of-the-art gearboxes, gears are mainly made of high strength case-hardened steel. The high strength of the material is needed to withstand

https://doi.org/10.51202/9783181023549 - Generiert durch IP 216.73.216.36, am 19.01.2026, 02:19:31. © Urheberrechtlich geschützter Inhalt. Ohne gesonderte Erlaubnis ist jede urheberrechtliche Nutzung untersagt, insbesondere die Nutzung des Inhalts im Zusammenhang mit, für oder in KI-Systemen, KI-Modellen oder Generativen Sprachmodellen.

the high stresses in tooth contact, whereas the stresses in other areas are comparatively moderate. A gear manufactured in one part and out of one material cannot take advantage of the most possible lightweight potential.

An alternative approach presented in this paper is to build up the gear in a multi-component design. This leads to a gear rim and a gear body, which have to be joined together. This differential design comes up with various advantages towards the integrated design. Gear rim and gear body can be manufactured using different materials, which can reduce the component costs and enable a stress-related design of the gear. Another advantage of this approach is that different manufacturing processes e.g. deep drawing or forging processes can be used, which can be a cost benefit in large-scale production.

Besides the advantages of the multi-component concept there are some drawbacks arising from the parting line between gear rim and gear body. Since the transmitted torque is at least partially transmitted by friction, an adequate interference fit pressure is needed. This leads to conflicting objectives. On the one hand the pressure should be preferably high to prevent the gear rim from slipping on the gear body. On the other hand a high interference fit pressure leads to tangential stresses in the gear rim, which can reduce the load carrying capacity of the toothing. Tooth root breakage might be an occurring damage. This trade-off can be seen in Fig. 1. where the safety factor for a gear (module 2 mm) with a tooth width of 14 mm and a rim thickness of one, two and three times module was calculated.

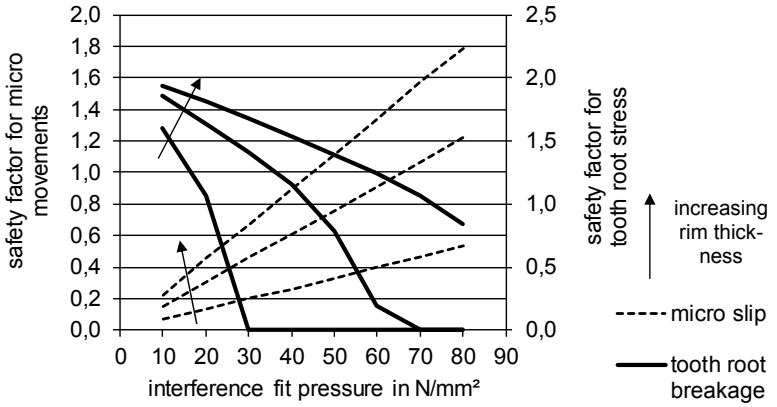


Fig. 1: Trade-off between the transmittable torque and the safety factor for tooth root breakage depending on the interference fit pressure

https://doi.org/10.51202/9783181023549 - Generiert durch IP 216.73.216.36, am 19.01.2026, 02:19:31. © Urheberrechtlich geschützter Inhalt. Ohne gesonderte Erlaubnis ist jede urheberrechtliche Nutzung untersagt, insbesondere die Nutzung des Inhalts im Zusammenhang mit, für oder in KI-Systemen, KI-Modellen oder Generativen Sprachmodellen.

The connection between gear rim and gear body can be realized as press fit and as form fit or a combination of both. Experimental investigations showed that shaft-hub connections with polygon profile can reach high torque transmitting capabilities ([1],[2]).

The research issue of this paper deals with the question, if the multi-component gear design can realize a lightweight construction potential towards the integrated state-of-the-art design. The multi-component design of a gear is not a new approach since gears in larger scale are often separated in gear rim and gear body. In these cases the reason for this differential design is mostly to save costs for the high-strength gear rim material and to simplify the handling of the large-sized parts during the manufacturing and the heat treatment process. The multi-component design for gears in automotive dimensions has not been extensively investigated.

Looking at the literature many investigations on the effect of a small gear rim thickness on the tooth root bending stress or the tooth root breakage for spur gears can be found (cf. e.g. [3], [4], [5]). Most of these investigations are based on the finite element method and crack propagation models. Some studies are focused on internal gears (cf. e.g. [6], [7]). The standard for calculation of safety factors for typical gear damages ISO 6336 [8] only takes the rim thickness into consideration but does not include the tangential stress in the tooth root caused by the interference fit pressure.

Other investigations on multi-component gears are focused on the dynamic behavior. For e.g. Nitsch [9] investigates a gear with a plastic gear body and could prove better dynamic behavior. Within the literature research no holistic investigations on the load carrying capacity, the lightweight potential and the dynamic behavior of gears in multi-component design could be found. The approach of a multicomponent design comes up with various challenges, which have to be solved to compete with the integrated design. Besides the known limitations other effects such as the slipping of the gear rim on the gear body can cause a failure. All these topics have to be considered developing a competitive multi-component gear.

In this paper the results of extensive experimental investigations on the load carrying capacity of multi-component gears in static and dynamic tests are presented. Different variants of prototypes have been tested and evaluated in terms of their load carrying capacity and lightweight potential. The presented results in this paper were obtained in the research project “Massiver Leichtbau (TP 2)” that was initiated as cooperation project with the research institutes IWT (Bremen), IFU (Stuttgart), utg (München) and FZG (München). The content of this paper is the experimental investigation of multi-component gears, further results of this research project can be found in the cited literature.

https://doi.org/10.51202/9783181023549 - Generiert durch IP 216.73.216.36, am 19.01.2026, 02:19:31. © Urheberrechtlich geschützter Inhalt. Ohne gesonderte Erlaubnis ist jede urheberrechtliche Nutzung untersagt, insbesondere die Nutzung des Inhalts im Zusammenhang mit, für oder in KI-Systemen, KI-Modellen oder Generativen Sprachmodellen.

2. Materials and Methods

The lightweight potential of a gear concept is evaluated by the weight of the gear and its load carrying capacity. Therefore many experiments on different gear variants have been conducted. The experiments were carried out on a static and a dynamic test rig.

Experimental Program

A gear design containing two components offers the implementation of different manufacturing processes. The gear rim was produced by lathing and gear hobbing. The material of the gear rim is the case-hardened steel 18CrNiMo7-6. The geometry of the toothing was inspired by automotive application and adapted to the center distance of the test rig (cf. Table 1).

Table 1: Gear geometry of the test gears

geometry value	Symbol	Value	Unit
normal module	m_n	2.0	mm
angle of pressure	α_n	20	°
center distance	a	91.5	mm
face width	b	14	mm
helix angle	β	30	°
number of teeth	z_1/z_2	38/39	-
rim thickness	s_R/m_n	1.88	-

The gear body was produced by different manufacturing methods (cf. Table 2). The first concept is a massive, cylindrical gear body made of 18CrNiMo7-6. This gear body offers no lightweight potential but is useful to generate fundamental knowledge about the joining and heat treatment process.[10]

The second variant is produced by cutting and stacking of sheet metal (sheet thickness 1.5 mm). To realize lightweight potential, a weight-optimized structure has been created. In the prototype process notches have been cut by laser. Subsequently the single sheet components are stacked and centered by pins. In industrial series production these steps can be integrated in a more cost-effective cutting process.

The third type of gear body consists of two half shells, which are manufactured by a deep-drawing process.[11]

These three concepts transmit the torque from the gear rim to the gear body by a friction type press-fit. The fourth concept in contrast is based on a combined form fit/press fit connection between gear rim and gear body. Therefore the manufacturing process of the gear body is

https://doi.org/10.51202/9783181023549 - Generiert durch IP 216.73.216.36, am 19.01.2026, 02:19:31. © Urheberrechtlich geschützter Inhalt. Ohne gesonderte Erlaubnis ist jede urheberrechtliche Nutzung untersagt, insbesondere die Nutzung des Inhalts im Zusammenhang mit, für oder in KI-Systemen, KI-Modellen oder Generativen Sprachmodellen.

integrated in the joining process between gear rim and gear body. The inner surface of the gear rim has a polygon geometry in peripheral direction and a concavely formed crowning in axial direction. The geometry of the gear body has been optimized by numerical investigations. [12],[13]

Table 2: Test specimens for experimental investigations

				
variant	1	2	3	4
joining process	joined after heat treatment/ joined after tempering	joined after heat treatment/ joined after tempering	joined after tempering	joined by forging
gear body (material)	massive (18CrNiMo7-6)	cut and stacked (DP-K780Y980T)	deep-drawn (DC04)	forged (C15, EN-AW 6082)
weight	626 g	417 g	325 g	425 g/270 g

The central process of all concepts is the joining process of gear rim and gear body. The gears connected by press fit are joined by heat. Since the multi-component design comes up with an additional joining process in contrast to the integrated design, measures have to be taken to reduce the additional effort. Hence the joining process is conducted by the heat of the heat treatment. Within the investigations two strategies have been pursued. The first approach is to join the gear rim by the heat of the case hardening process. Experiments showed that a durable joint can be reached by cooling down the gear body in liquid nitrogen to -196 °C. The gear ring joined on the gear body at 850 °C was quenched in a gas nozzle field to initiate the case hardening process. [10]. The second process is the joining after tempering.

The variants presented are manufactured with the optimum parameters for heat treatment and joining process that are determined in large pilot test series, which are not part of this paper.

In order to evaluate the lightweight potential of the different concepts, the weight of the gear has to be known. Therefore the specimens have been weighed by the analysis scale Mettler Toledo XP2004S (reading accuracy: 0.1 mg). The standard deviation of gear weight (2.3 g)

https://doi.org/10.51202/9783181023549 - Generiert durch IP 216.73.216.36, am 19.01.2026, 02:19:31. © Urheberrechtlich geschützter Inhalt. Ohne gesonderte Erlaubnis ist jede urheberrechtliche Nutzung untersagt, insbesondere die Nutzung des Inhalts im Zusammenhang mit, für oder in KI-Systemen, KI-Modellen oder Generativen Sprachmodellen.

due to variation in the manufacturing process was determined by evaluation of random samples.

Reference Gear

For the evaluation of the lightweight potential of the different gear concepts a reference has to be defined. In these investigations the variant 1 serves as reference for the evaluation of the lightweight concepts.

Experiments on static test rig

The static test was developed to conduct screening tests for a large set of parameters concerning the manufacturing process. The test design with a short execution time allows a large scope of experiments with reasonable effort.

The test gearbox is depicted in Fig. 2 and consists of a massive housing manufactured of cast iron with a center distance of 91.5 mm. The test gear meshes with a counter gear of higher load carrying capacity, in order to generate the damage on the lightweight gear. Both are mounted on shafts, which in turn are mounted with tapered roller bearings in the housing. The mesh position is chosen such that the tooth root stress reaches a maximum. The torque is produced by an asynchronous motor and a spindle lifting gear with high transmission ratio (not depicted) in combination with a lever construction.

https://doi.org/10.51202/9783181023549 - Generiert durch IP 216.73.216.36, am 19.01.2026, 02:19:31. © Urheberrechtlich geschützter Inhalt. Ohne gesonderte Erlaubnis ist jede urheberrechtliche Nutzung untersagt, insbesondere die Nutzung des Inhalts im Zusammenhang mit, für oder in KI-Systemen, KI-Modellen oder Generativen Sprachmodellen.

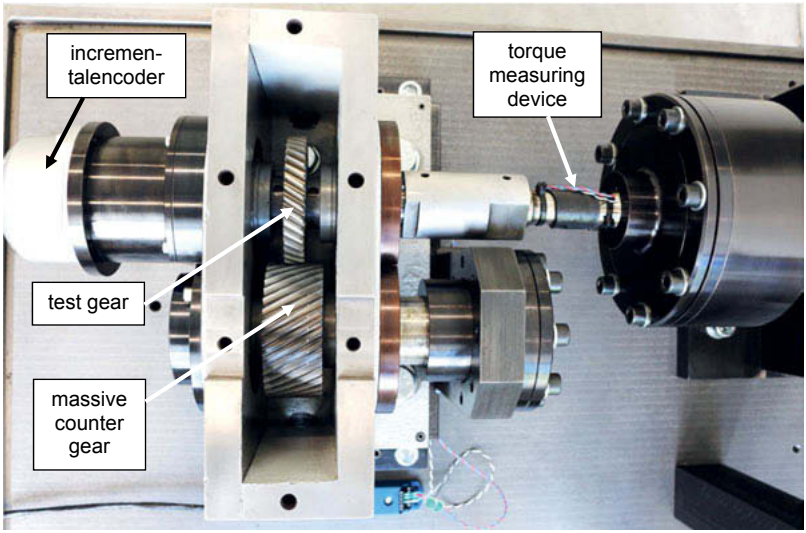


Fig. 2: Test gearbox of the static test rig

The test gear shaft is loaded with torque that can be measured by a torque measuring device. The accuracy of the applied torque measuring shafts is 1.25 % (95 % confidence interval) with regard to the nominal value (300 Nm, 600 Nm and 1000 Nm).

Having information about the deformation of the gear is essential to determine the appearance of damage. Therefore an incremental encoder (accuracy: 18000 increments per revolution) is applied to the test shaft. Because there is no torque load on the part of the shaft between the incremental encoder an the test gear, except the torque resulting from the friction in the bearings, which is comparably small, the deformation of the gear can be measured directly by means of the torsion angle.

The applied measurement equipment enables the evaluation of the maximum statically transmitted torque and the appearance of a damage in the gear. The test run is controlled by software.

The test procedure is subdivided in three phases (cf. Fig. 3). The first phase is implemented to find the offset value of the torque measuring device at zero load. Additionally the system is preloaded by a small load to eliminate the clearance in the whole system including shaft-hub connections and the tooth contact. The second phase is the actual test run. The torque applied to the test shaft is increased constantly until a damage occurs. The measurement signals in-

https://doi.org/10.51202/9783181023549 - Generiert durch IP 216.73.216.36, am 19.01.2026, 02:19:31. © Urheberrechtlich geschützter Inhalt. Ohne gesonderte Erlaubnis ist jede urheberrechtliche Nutzung untersagt, insbesondere die Nutzung des Inhalts im Zusammenhang mit, für oder in KI-Systemen, KI-Modellen oder Generativen Sprachmodellen.

dicate a damage by means of disproportionate change of torque and torsional angle. Subsequently phase three is initiated. The load is decreased until the whole system is unloaded and the test procedure is completed.

The evaluation of the measurement signals results in a value of maximum statically transmitted torque without a damage of the gear.

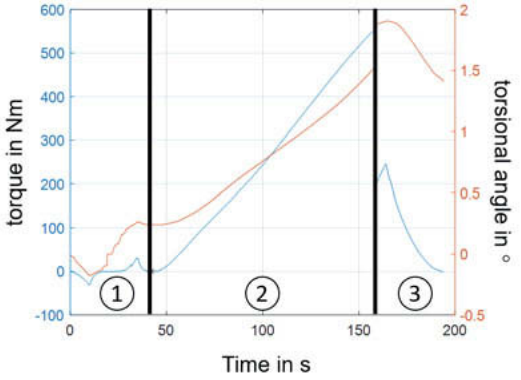


Fig. 3: Exemplary test procedure of a static test

The evaluation of the maximum statically transmitted torque without damage is performed with three samples per variant. The result is the arithmetic mean with a 95 % confidence interval. The population is assumed to be normally distributed.

Experiments on dynamic test rig

The conditions in a dynamic test are much closer to the industrial application than in a static test. In this test all teeth are loaded in a continuous mesh whereas the static test provides only one defined mesh position.

The tests are conducted on a standard FZG back-to-back test rig (cf. Fig. 4). The test rig consists of two gearboxes with the same gear ratio for each spur gear stage. The two test gears are mounted in the test gearbox. The slave gearbox consists of two massive gears with the same gear geometry but larger face width to prevent them from damage. The two gearboxes are connected by shafts. On the one side there is a hydraulic load clutch that applies controlled torque to the gears in both gear boxes, on the other side a torque measuring shaft generates an electrical signal for the documentation of the load torque. This concept enables high power circulating in the loop between the two gearboxes, whereas the electric motor only has to compensate losses of bearings, gears and oil seals. The lubrication is provided by an external oil

https://doi.org/10.51202/9783181023549 - Generiert durch IP 216.73.216.36, am 19.01.2026, 02:19:31. © Urheberrechtlich geschützter Inhalt. Ohne gesonderte Erlaubnis ist jede urheberrechtliche Nutzung untersagt, insbesondere die Nutzung des Inhalts im Zusammenhang mit, für oder in KI-Systemen, KI-Modellen oder Generativen Sprachmodellen.

supply unit with temperature control. The test run is conducted with oil injection lubrication at 60 °C. The rotational speed was 2000 rpm.

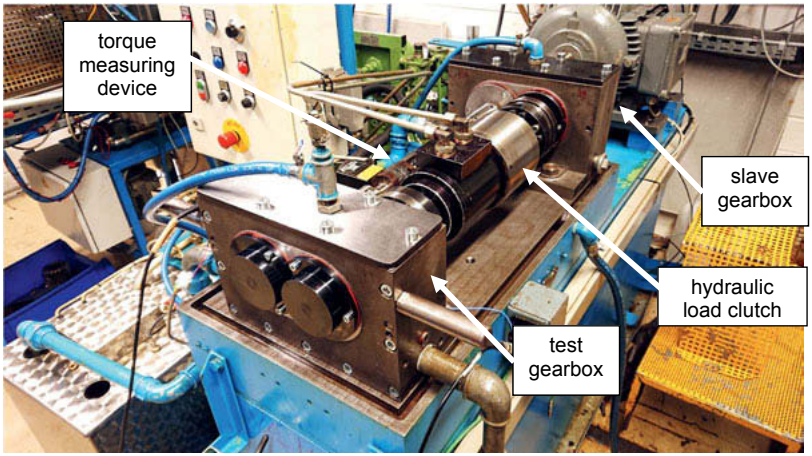


Fig. 4: Standard FZG back-to-back test rig

The tests were performed with different load levels in the fatigue strength range. The test procedure was aborted when a damage occurred or a maximum number of 200000 load cycles was reached. The result consists of a torque value with the assigned number of load cycles. In order to detect a slipping motion of the gear rim on the gear body, a control marking covering both parts was applied to each specimen by laser labeling.

3. Results

This section presents the results gained from static and dynamic tests performed with multi-component gears. The experimental results in combination with the weight of the specimens result in a lightweight potential.

Experiments on static test rig

Within the static tests all specimens showed the same damage. The gear rim slipped relatively to the gear body. In the case of the form fit gear rim/gear body connection this led to plastic deformations of the gear rim and/or the gear body.

The mean of the maximum reached torque is depicted in Fig. 5. The reference gear (variant 1) with massive gear body reaches a mean statically transmittable torque of 845 ± 122 Nm (joined after tempering) and 741 ± 197 Nm (joined after case-hardening).

https://doi.org/10.51202/9783181023549 - Generiert durch IP 216.73.216.36, am 19.01.2026, 02:19:31. © Urheberrechtlich geschützter Inhalt. Ohne gesonderte Erlaubnis ist jede urheberrechtliche Nutzung untersagt, insbesondere die Nutzung des Inhalts im Zusammenhang mit, für oder in KI-Systemen, KI-Modellen oder Generativen Sprachmodellen.

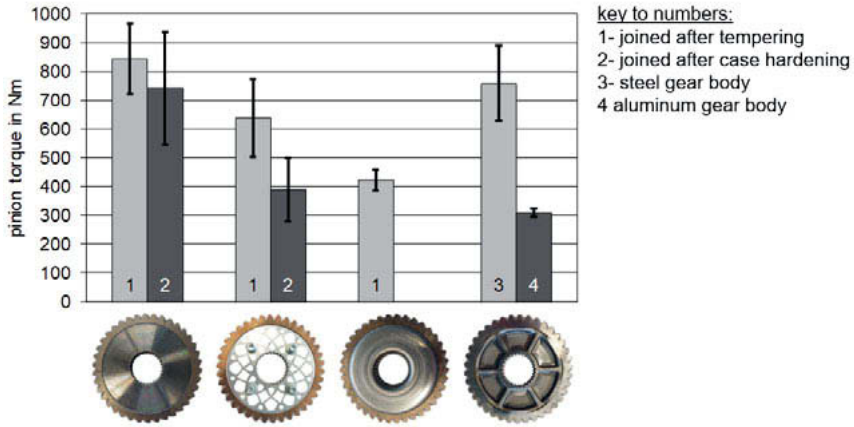


Fig. 5: Results of the static experiments

The values for the transmittable torque for the gear with stacked sheet metal gear body (variant 2) reached lower values. The evaluation of the test provides a torque of 638 ± 134 Nm (joined after tempering) and 388 ± 111 Nm (joined after case-hardening). For the gears with deep-drawn gear body joined after case hardening (of variant 3) the joining process was not feasible. The gear joined after tempering reached a mean torque of 422 ± 37 Nm. The gears joined by forging (variant 4) with steel gear body showed a torque of 759 ± 132 Nm and thus range in a similar level as the reference gear (variant 1). The same concept with aluminum gear body can withstand a much lower torque of 308 ± 15 Nm. The torque range for the individual specimens is between 303 Nm and 889 Nm. The means of the gears joined after tempering seemed to be higher than the variants joined after case-hardening. No tooth root breakage was observed.

Experiments on dynamic test rig

The type of damage in the dynamic tests occurred depending on the type of gear rim/gear body connection. In the case of a press fit the gear rim tended to slip on the gear body. Due to axial forces resulting from the helix angle (cf. Table 1) the gear ring often slipped off axially from the gear body (especially variant one). Within the variants 2 and 3 this effect could be observed in a lower extend. This behavior might appear because of the edges of the sheet metal gear bodies that act as a micro form fit in axial direction. The variant with form fit type gear rim / gear body connection (variant 4) showed a rupture of the gear rim for the steel gear body and plastic deformation of the aluminum gear body.

https://doi.org/10.51202/9783181023549 - Generiert durch IP 216.73.216.36, am 19.01.2026, 02:19:31. © Urheberrechtlich geschützter Inhalt. Ohne gesonderte Erlaubnis ist jede urheberrechtliche Nutzung untersagt, insbesondere die Nutzung des Inhalts im Zusammenhang mit, für oder in KI-Systemen, KI-Modellen oder Generativen Sprachmodellen.

The results for the dynamic tests are depicted in Fig. 6. For the reason of limited extent of this paper only selected results are presented. The reference gear (variant 1, joined after tempering) failed by the gear rim slipping off the gear body. The test was conducted with 6 samples (cf. Fig. 6a). Three samples passed the maximum load cycle value of 200000 with a load of 100 Nm without any slipping motion of the gear rim. A load of 150 N resulted in failed gears at approx. 2000 load cycles. The limited number of samples only allows the conclusion that the threshold value for the torque transmitted without slipping is between 100 Nm and 150 Nm.

For the gears with sheet metal gear bodies (variant 2 and 3) a slipping motion in circumferential direction could be observed. Since the gear rims remained on the gear body, the slipping angle between the two parts could be evaluated. Taking into account the number of load cycles, a slipping velocity depending on the applied torque can be determined, assuming a constant movement of the gear rim (cf. Fig. 6c and Fig. 6d).

The linear relationship between the pinion torque and the slipping velocity gained from linear regression analyses is depicted in the graphs with the 99 % confident interval (dashed line). It is obvious, that the slope of the slipping velocity of the gears with deep-drawn gear body is approx. three times bigger than the slope of the gear with stacked sheet metal gear body. This is due to the higher radial stiffness of the gear body produced of stacked sheet metal, which results in a difference in pressure in the contact surface between gear body and gear rim. The threshold value for slipping motion for both variants is nearly the same being approx. 80 Nm.

https://doi.org/10.51202/9783181023549 - Generiert durch IP 216.73.216.36, am 19.01.2026, 02:19:31. © Urheberrechtlich geschützter Inhalt. Ohne gesonderte Erlaubnis ist jede urheberrechtliche Nutzung untersagt, insbesondere die Nutzung des Inhalts im Zusammenhang mit, für oder in KI-Systemen, KI-Modellen oder Generativen Sprachmodellen.

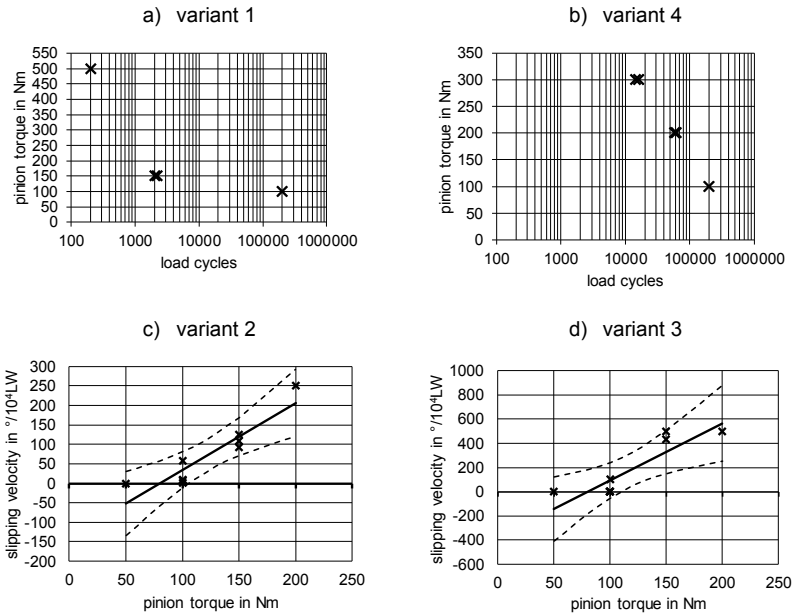


Fig. 6: Results of the dynamic experiments

The gears with forged steel gear body (cf. Fig. 6b) failed by rupture of the gear rim. The crack started in the tooth root and propagated to the parting line between gear ring and gear body. The permissible torque and the number of load cycles without failure showed an approximately linear correlation in the fatigue strength area for single logarithmic representation. A value for fatigue limit can't be derived from the data because the number of load cycles is too low and the data base too small. Evaluating the experimental results with a limit value of load cycles of 200000, the fatigue limit is located between 100 Nm and 200 Nm.

Summarizing the experimental results of the tests conducted on the dynamic test rig, the different concepts of multi-component gears failed with different types of damage. Variant 4 with form fit connection between gear rim and gear body failed with rupture of the gear rim (steel) or the plastic deformation of the gear body (aluminum). Gears with press fit connection failed by the slipping motion of the gear rim, few gear rims slipped off the gear body. The torque threshold value for the particular damage is the lowest for the variants with press fit type connection with uneven surface or low radial stiffness. The gear with massive gear body (joined after tempering) showed a higher permissible torque without failure. The tested specimens

https://doi.org/10.51202/9783181023549 - Generiert durch IP 216.73.216.36, am 19.01.2026, 02:19:31. © Urheberrechtlich geschützter Inhalt. Ohne gesonderte Erlaubnis ist jede urheberrechtliche Nutzung untersagt, insbesondere die Nutzung des Inhalts im Zusammenhang mit, für oder in KI-Systemen, KI-Modellen oder Generativen Sprachmodellen.

with form-fit type connection between gear rim and gear body showed the presumably highest values of the permissible torque without damage.

Evaluation of the lightweight potential

The preceding sections showed the results of the static and dynamic test by means of a maximum transmittable torque value without failure. To evaluate the lightweight potential, the load carrying capacity of each variant has to be brought in relation with the component weight. For reasons of comparability the maximum statically transmittable torque values serve as criterion for the load carrying capacity. The samples tested in the static test rig showed the same type of damage and resulted after evaluation in an explicit torque value.

Hence the weight of the specimen can be determined very accurate in comparison to the load carrying capacity, the weight is presumed to be a constant, whereas the determined torque is assumed to be a random variable. Under these assumptions a confident interval of 95 % was calculated. Concerning the different heat treatments, only the variants with the higher load carrying capacity were evaluated.

To enable an intuitive interpretation of the results, the lightweight potentials have been normalized to the value of the reference gear (variant 1). The results are depicted in Fig. 7.

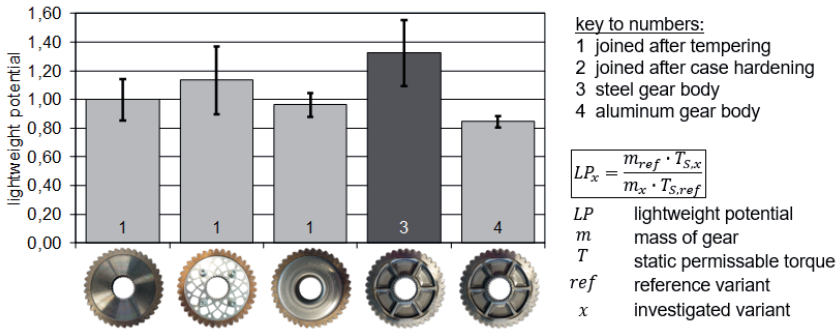


Fig. 7: Evaluation of the lightweight potential of the investigated gear concepts

The reference gear (variant 1) showed the highest statically transmittable torque, but also the highest weight. Variant 2 (stacked sheet metal gear body) had a nominal lightweight potential of +13 %. The reason could be the relative stiff gear body in combination with the reduced weight obtained by structural optimization. Due to the small sample size there is some degree of uncertainty for this value. The gear with the deep-drawn gear body showed a nominal value of -4 % lightweight potential within these experimental investigations. The variant 4, which

https://doi.org/10.51202/9783181023549 - Generiert durch IP 216.73.216.36, am 19.01.2026, 02:19:31. © Urheberrechtlich geschützter Inhalt. Ohne gesonderte Erlaubnis ist jede urheberrechtliche Nutzung untersagt, insbesondere die Nutzung des Inhalts im Zusammenhang mit, für oder in KI-Systemen, KI-Modellen oder Generativen Sprachmodellen.

combined high statically transmittable torques with low weight showed the highest lightweight potential with a significant difference (p-value < $3 \cdot 10^{-3}$, 2 sample t-test for independent samples) of +32 % referred to the reference variant. The high load carrying capacity can be attributed to the form fit type connection between gear rim and gear body.
The same variant but manufactured with aluminum gear body showed a negative lightweight potential with a nominal value of -15 %. The advantage of the form fit cannot be used, because of plastic deformation in the gear body leads to deterioration of the form fit.

4. Discussion

In the context of the investigation of a multi-component gear design with different concepts in terms of heat treatment and joining process static and dynamic tests have been conducted. Within these tests some variants showed high absolute values of the statically transmittable torque of about 890 Nm, whereas other variants showed considerably lower values. The transmittable torques without failure that were reached in the dynamic tests were considerably lower compared to the static test. The phenomenon of micro movements between gear rim and gear body led to damages of the gears at low torques. The overall limit value of torque without damage was under 200 Nm, which is less than a quarter of the maximum static values.
Evaluating the lightweight potential of the tested gears the static load carrying capacity was used for reasons of comparability. Taking into account the weight of the tested gears, the variant with cold forged gear body reached a lightweight potential of +32 % compared to the reference gear (massive gear body). The investigations showed that there is a potential to reduce the weight and probably the costs of a gear using a multi-component design.
Looking at the absolute values of dynamically transmitted torques, it becomes clear that the investigated multi-component gears cannot compete with state-of-the-art gears in integrated design concerning the load carrying capacity. This is due to the parting line between gear rim and gear ring, which is an additional weak point in the path of torque transmission.
This drawback can be faced with different measures to reinforce this weak point. An additional adhesive bond in the contact surface between gear rim and gear body can strengthen the connection between both parts. Experiments in the context of this investigations have proved the use of the appropriate forging lubricant to be an efficient measure to increase the load carrying capacity [2]. The gained load carrying capacity has a direct impact on the lightweight potential because this measure does not change the component weight significantly. Other approaches such as a glued joint or a joint between gear rim and gear body produced by laser melting yield the same effect. Another possibility to increase the load carrying capacity of the

https://doi.org/10.51202/9783181023549 - Generiert durch IP 216.73.216.36, am 19.01.2026, 02:19:31. © Urheberrechtlich geschützter Inhalt. Ohne gesonderte Erlaubnis ist jede urheberrechtliche Nutzung untersagt, insbesondere die Nutzung des Inhalts im Zusammenhang mit, für oder in KI-Systemen, KI-Modellen oder Generativen Sprachmodellen.

gear rim / gear body connection with no increase of the component weight can be the use of micro form fit, e.g. by knurling the contact surface.

The investigations showed that the first prototypes cannot reach the same load carrying capacity and lightweight potential as state-of-the-art gears. With further research and development of the implementation of this promising approach, multi-component gears can probably compete with state-of-the-art gears, which show low weight reduction potential because they have been optimized for decades. With the multi-component gear design the use of more expensive high-strength steels becomes an option because only the gear rim has to consist of this cost-intensive material. Furthermore this gear design may be suitable for applications with smaller power density or the use as idler gear or planetary gear where no resulting torque acts between gear rim and gear body but high stresses in the tooth contact.

The investigations have shown the multi-component gear design to be a highly promising approach with some drawbacks in the actual implementation but high potential to overcome these weak points.

5. Acknowledgments

Federal Ministry for Economic Affairs and Energy

The research project “Intelligent lightweight design through multi-component processes” (IGF-Nr. 18189 N) of the Research Association for steel Application (FOSTA), Heat Treatment and Material Engineering Association (AWT), Research Association for Drive Technology (FVA) and Research Association of Steel Forming (FSV) is supported by the Federal Ministry of Economic Affairs and Energy through the German Federation of Industrial Research Associations (AiF) as part of the program for promoting industrial cooperative research (IGF) on the basis of a decision by the German Bundestag. The author thanks the funders which made this research and their results possible. Furthermore the author thanks the other co-researchers Dawid Nadolski, Robert Meißner and Tim Benkert for the production and provisioning of the specimens used in these investigations.

https://doi.org/10.51202/9783181023549 - Generiert durch IP 216.73.216.36, am 19.01.2026, 02:19:31. © Urheberrechtlich geschützter Inhalt. Ohne gesonderte Erlaubnis ist jede urheberrechtliche Nutzung untersagt, insbesondere die Nutzung des Inhalts im Zusammenhang mit, für oder in KI-Systemen, KI-Modellen oder Generativen Sprachmodellen.

6. Literature Cited

[1] Leidich, E.; Reiß, F.; Schreiter, R.; Investigations of hypocycloidal shaft and hub connections. Materials Science and Engineering Technology, ISSN 0933-5137

[2] Meissner, R.; Liewald, M.; Leonhardt, C.; Otto, M.; Stahl, K.: Torsionsfestigkeit von gebauten Zahnrädern im Mehrkomponentenverfahren mittels Querfließpressen; VDI-Welle-Nabe-Tagung, Stuttgart 2018

[3] Verma, J.G.; Kumar, S., Kankar, P.K.: Crack growth modeling in spur gear tooth and its effect on mesh stiffness using extended finite element method., Engineering Failure Analysis, Volume 94, December 2018, Pages 109-120, DOI: 10.1016/j.engfailanal.2018.07.032

[4] Miyachika, K., Daing Mohamad Nafiz, B.D.I.: Effects of helix angle on root stress of thin-rimmed helical gears with various web arrangements, Proceedings of the ASME Design Engineering Technical Conference, Volume 5, 2013, Article Number V005T11A008, 2013, DOI: 10.1115/DETC2013-12852

[5] Marunic, G.: Effects of rim and web thickness on gear tooth root, rim and web stresses, Key Engineering Materials, Volume 385-387, 2008, Pages 117-120, ISSN:10139826

[6] Karpat, F.; Ekwaro-Osire, S.; Yilmaz, T.G., Dogan, O., Yuce, C: Design and analysis of internal gears with different RIM thickness and shapes, ASME International Mechanical Engineering Congress and Exposition, Proceedings (IMECE), Volume 9, 2015, DOI: 10.1115/IMECE2015-52211

[7] Kawalec, A., Wiktor, J.: Tooth-root stress calculation of internal spur gears, Proceedings of the Institution of Mechanical Engineers, Part B: Journal of Engineering Manufacture, Volume 218, Issue 9, 2004, Pages 1153-1166, DOI: 10.1243/0954405041897185

[8] ISO6336:2006-09, Calculation of load capacity of spur and helical gears

[9] Nitsch, C. H.: Dynamisches Betriebsverhalten von Werkstoffverbundrädern., TU München Diss. 2015

[10] Leonhardt, C.; Otto, M.; Stahl, K. Nadolski, D. et. al.: Lightweight gearwheel design using separate gear ring and wheel body, International Conference on Steels in Cars and Trucks, Amsterdam-Schiphol, 2017

https://doi.org/10.51202/9783181023549 - Generiert durch IP 216.73.216.36, am 19.01.2026, 02:19:31. © Urheberrechtlich geschützter Inhalt. Ohne gesonderte Erlaubnis ist jede urheberrechtliche Nutzung untersagt, insbesondere die Nutzung des Inhalts im Zusammenhang mit, für oder in KI-Systemen, KI-Modellen oder Generativen Sprachmodellen.

[11] Benkert, T. Hiller, M.; Volk, W.: Multi-component lightweight gearwheels with deep-drawn wheel body for automotive applications. Journal of Physics: Conference Series 896, S. 12083, DOI: 10.1088/1742-6596/896/1/012083

[12] Meissner, R., Liewald, M.: Numerical investigations of multi-component lightweight design for joining gearwheels by lateral extrusion; NUMIFORM 2016, Troyes Frankreich

[13] Meissner, R.; Liewald, M.: Influence of lubrication on manufacturing of Multi-component gearwheels, Forschung im Ingenieurswesen, 2017;DOI: s10010-017-0249-6

https://doi.org/10.51202/9783181023549 - Generiert durch IP 216.73.216.36, am 19.01.2026, 02:19:31. © Urheberrechtlich geschützter Inhalt. Ohne gesonderte Erlaubnis ist jede urheberrechtliche Nutzung untersagt, insbesondere die Nutzung des Inhalts im Zusammenhang mit, für oder in KI-Systemen, KI-Modellen oder Generativen Sprachmodellen.

Solutions for increased power density at shifting clutches

Dipl.-Ing.(FH) **Harald Merkel**,
BorgWarner Transmission Systems, Ketsch

Zusammenfassung

Bei modernen Fahrzeug- und Antriebskonzepten besteht die Notwendigkeit eine Vielzahl von Funktionalitäten zu integrieren. Insbesondere bei Hybrid – und Elektrofahrzeugen ist hierbei eine kompakte und gewichtsreduzierte Bauweise zwingend notwendig

BW hat nun spezielle Lösungen entwickelt um eine höhere Leistungsdichte bei schaltbaren Kupplungen darzustellen.

Hierzu wurden Reibbeläge entwickelt die einen höheren statische Reibwert bereitstellen und dadurch eine kompaktere Bauweise der Lamellenkupplung bezüglich axialem Bauraum (durch Reduzierung der Reibflächenanzahl) oder eine Reduzierung der Durchmesser der Reibelemente ermöglichen.

Um eine höhere Leistungsdiche bei thermisch hoch beanspruchten Kupplungen zu ermöglichen wurden Hochleistungsbeläge entwickelt ,die mit hohen Oberflächentemperaturen betrieben werden können und resistent gegen Hot Spot Bildung sind. Daher können die spezifischen Auslegungsparameter wie Reibleistung und Reibarbeit deutlich angehoben werden was eine kompaktere Bauweise der Lamellenkupplung ermöglicht. Diese Beläge ermöglichen daher auch Schaltungen bei sehr hohen Differenzdrehzahlen .

Das Thema Bauraum- und Gewichtsreduzierung wird durch ein innovatives Lamellendesign adressiert.Hierbei kommen Kunststoffe gepaart mit neuartigen Fertigunsverfahren zum Einsatz

Zur Übertragung sehr hoher Drehmomente im begrenzten Bauraum hat Borg Warner ein neuartiges Kupplungskonzept entwickelt bei dem eine Synchroneinheit,dargestellt durch eine Lamellenkupplung,kombiniert ist mit einer mechanischen Arretierung.Diese Bauweise führt im Vergleich mit einer konventionellen Lamellenkupplung zu einer deutlichen Bauraum und Gewichtsreduzierung.

https://doi.org/10.51202/9783181023549 - Generiert durch IP 216.73.216.36, am 19.01.2026, 02:19:31. © Urheberrechtlich geschützter Inhalt. Ohne gesonderte Erlaubnis ist jede urheberrechtliche Nutzung untersagt, insbesondere die Nutzung des Inhalts im Zusammenhang mit, für oder in KI-Systemen, KI-Modellen oder Generativen Sprachmodellen.

Abstract

Modern vehicle and drivetrain concepts face many integration problems due to the various functions within the system. Hybrid and Electric vehicles present new challenges, especially in terms of weight reduction and installation space.

BorgWarner has developed special solutions to increase the power density of shifting clutches.

New friction materials with increased static coefficient of friction have been developed to allow for a compact clutch design.

BorgWarner has also developed new high performance friction materials which can handle higher interface temperatures without sacrificing robustness against hot spotting. Thanks to these advantages, the power and energy limits of clutches can be increased.

A new friction plate design has been developed using plastic core plates and a new manufacturing concept. The design advantage is getting the same performance in a smaller packaging space with lower weight.

BorgWarner has also developed a new clutch concept that allows high torque transmission in an extremely compact installation space. The new clutch design combines a friction plate clutch with a mechanical lock device.

Introduction

Friction clutches are the most complex elements in drivetrain. The mechanism of functionality is until today not really understood. At the same time there is a tendency to go to the limits of the system by layout. This means the increased power density by installation space and mass. The consequence is an increased demand for friction performance and wear reduction by increased requirements for thermal and mechanical robustness.

As an enabler for increased power density of friction clutches there is a need for improvements in the friction materials and in the component designs.

Transmission design trends and friction material requirements

Figure 1 shows the global transmission trends and necessary friction enablers to fulfill the requirements.

Recent development of 9 to 11 speed transmission for combustion engines and transmissions for Hybrid and EV vehicles have increased a need for friction materials to handle the increased power density and increased energy levels.

https://doi.org/10.51202/9783181023549 - Generiert durch IP 216.73.216.36, am 19.01.2026, 02:19:31. © Urheberrechtlich geschützter Inhalt. Ohne gesonderte Erlaubnis ist jede urheberrechtliche Nutzung untersagt, insbesondere die Nutzung des Inhalts im Zusammenhang mit, für oder in KI-Systemen, KI-Modellen oder Generativen Sprachmodellen.

Due to reduced friction in the powertrain there are increased requirements for NVH robustness for the clutch system. To support the demand for increased power density the package size and the weight has to be reduced.



Fig. 1: Transmission trends and friction material requirements

Increased power density

Increased power density means the reduction of the installation space and reduction of the mass. To achieve these objectives there are some needs to improve the friction system.
The improvements has to be in thermal robustness and hot spot resistance. An enabler for higher power density is the increase in the static coefficient of friction. This allows the reduction in diameter or in the number of friction surfaces.
Additional weight reduction can be achieved by replacement of traditional materials.

https://doi.org/10.51202/9783181023549 - Generiert durch IP 216.73.216.36, am 19.01.2026, 02:19:31. © Urheberrechtlich geschützter Inhalt. Ohne gesonderte Erlaubnis ist jede urheberrechtliche Nutzung untersagt, insbesondere die Nutzung des Inhalts im Zusammenhang mit, für oder in KI-Systemen, KI-Modellen oder Generativen Sprachmodellen.

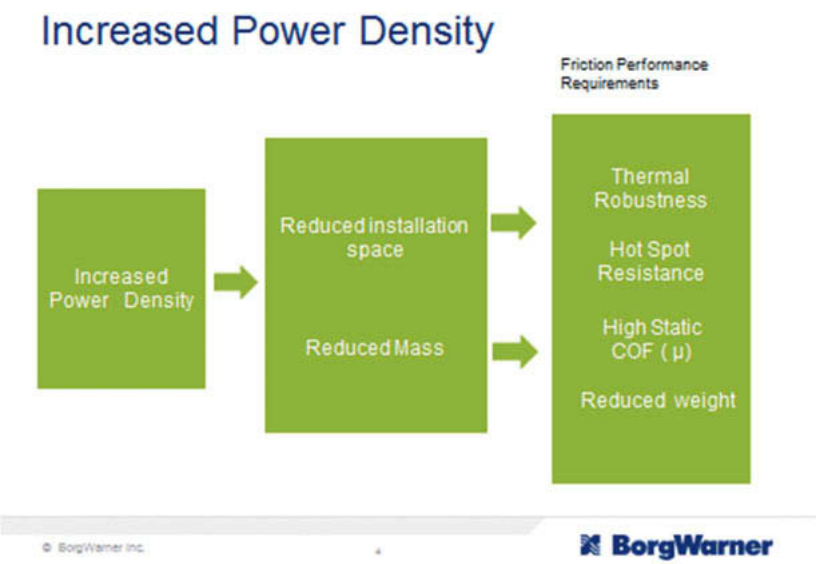


Fig. 2: Increased power density

Friction materials solutions

For different applications BW has produced special friction materials. For shifting clutches In Step AT or shift elements for EV vehicles BW developed a friction material with high static COF. For shifting clutches with extremely high shifting power the new Hot Spot resistant friction material BW5002 is available.

For launch clutch applications like DCT clutches the new friction material BW6970 is now available.

https://doi.org/10.51202/9783181023549 - Generiert durch IP 216.73.216.36, am 19.01.2026, 02:19:31. © Urheberrechtlich geschützter Inhalt. Ohne gesonderte Erlaubnis ist jede urheberrechtliche Nutzung untersagt, insbesondere die Nutzung des Inhalts im Zusammenhang mit, für oder in KI-Systemen, KI-Modellen oder Generativen Sprachmodellen.

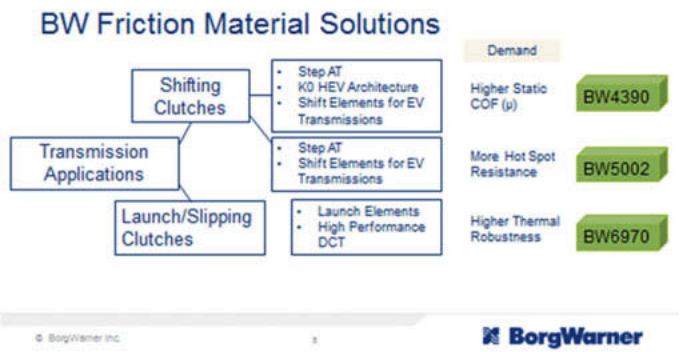


Fig. 3: BW friction material solutions

BW3490-High μfriction material



Fig. 4 BW4390 high μ friction material

Fig.5 shows the static COF of BW 4390 under different testing conditions.

The chart shows the influence of pressure, temperature and cooling oil flow on the static COF. The lowest static COF is achieved by high pressure, high temperature conditions.

https://doi.org/10.51202/9783181023549 - Generiert durch IP 216.73.216.36, am 19.01.2026, 02:19:31. © Urheberrechtlich geschützter Inhalt. Ohne gesonderte Erlaubnis ist jede urheberrechtliche Nutzung untersagt, insbesondere die Nutzung des Inhalts im Zusammenhang mit, für oder in KI-Systemen, KI-Modellen oder Generativen Sprachmodellen.

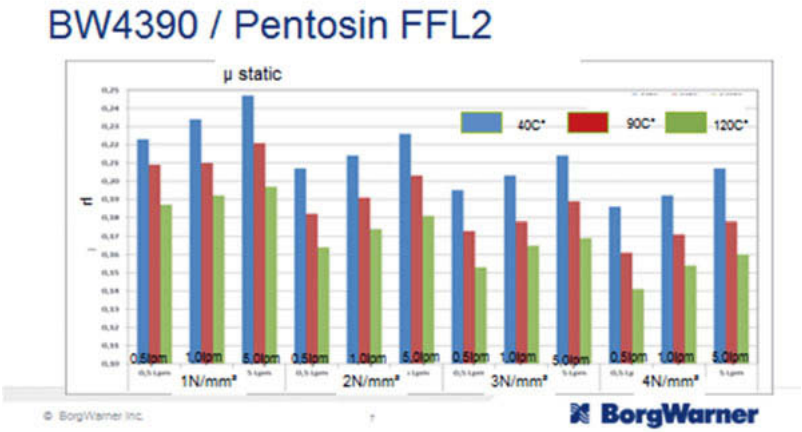


Fig. 5: BW4329

In direct comparison BW4390 shows a 25% increase in the static COF compared to a conventional friction material

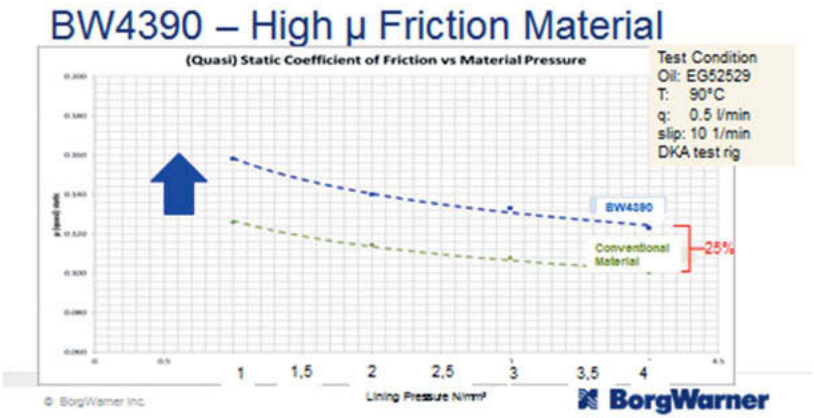


Fig. 6: BW4390 high μ friction material

https://doi.org/10.51202/9783181023549 - Generiert durch IP 216.73.216.36, am 19.01.2026, 02:19:31. © Urheberrechtlich geschützter Inhalt. Ohne gesonderte Erlaubnis ist jede urheberrechtliche Nutzung untersagt, insbesondere die Nutzung des Inhalts im Zusammenhang mit, für oder in KI-Systemen, KI-Modellen oder Generativen Sprachmodellen.

BW5002- Hot Spot Resistance

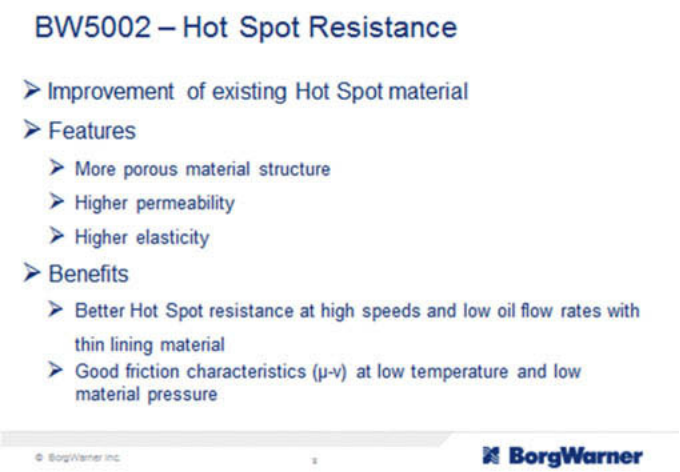


Fig. 7: BW 5002

BW 5002 has an increased pore structure compared to a standard Hot Spot material.
The pore size and the number of pores are larger than the conventional Hot Spot material.

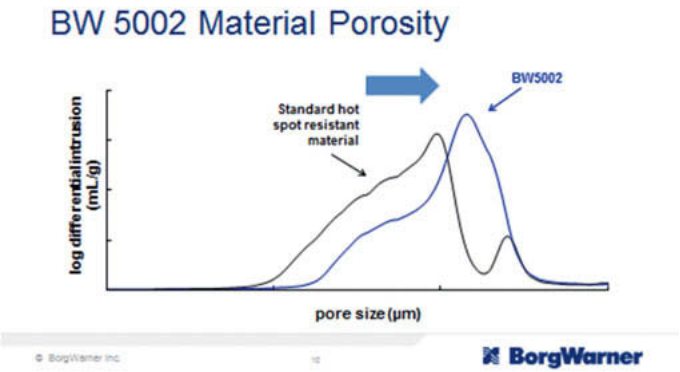


Fig. 8: BW 5002 porosity

https://doi.org/10.51202/9783181023549 - Generiert durch IP 216.73.216.36, am 19.01.2026, 02:19:31. © Urheberrechtlich geschützter Inhalt. Ohne gesonderte Erlaubnis ist jede urheberrechtliche Nutzung untersagt, insbesondere die Nutzung des Inhalts im Zusammenhang mit, für oder in KI-Systemen, KI-Modellen oder Generativen Sprachmodellen.

Elasticity is an important physical property for a hot spot resistant friction material.
Fig. 9 shows the elasticity comparison between a standard shifting clutch material, a standard Hot Spot resistant material and BW 5002

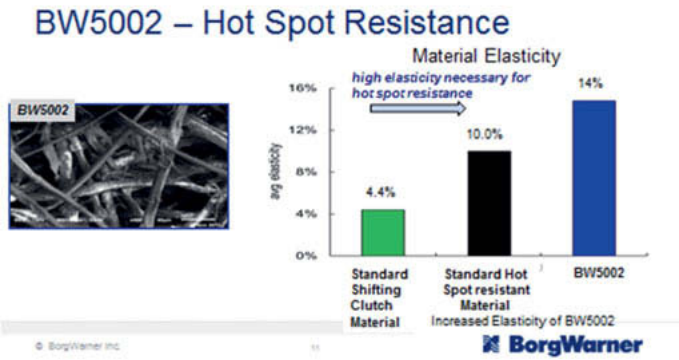


Fig. 9: Elasticity of BW5002

Compared to the standard Hot Spot material BW5002 has desirable curve shape. Also at low temperature and low pressure BW5002 shows a descending curve shape.
The Hot Spot performance is increased compared to the standard Hot Spot materials.
With the new BW5002 differential speeds at the shift event up to 97 m/s are possible.

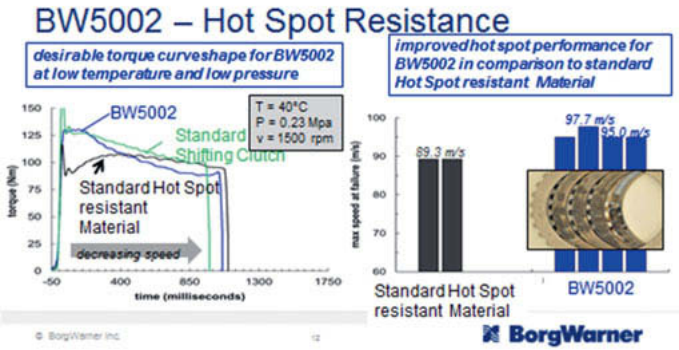


Fig. 10: Hot Spot resistance test results

https://doi.org/10.51202/9783181023549 - Generiert durch IP 216.73.216.36, am 19.01.2026, 02:19:31. © Urheberrechtlich geschützter Inhalt. Ohne gesonderte Erlaubnis ist jede urheberrechtliche Nutzung untersagt, insbesondere die Nutzung des Inhalts im Zusammenhang mit, für oder in KI-Systemen, KI-Modellen oder Generativen Sprachmodellen.

BW6970 –High Performance Friction Material

The new friction material BW6970 is developed for extremely high thermal input in the friction system. The material is developed for slipping clutch applications like WSC and DCT. Interface temperatures up to 440 C° are possible.

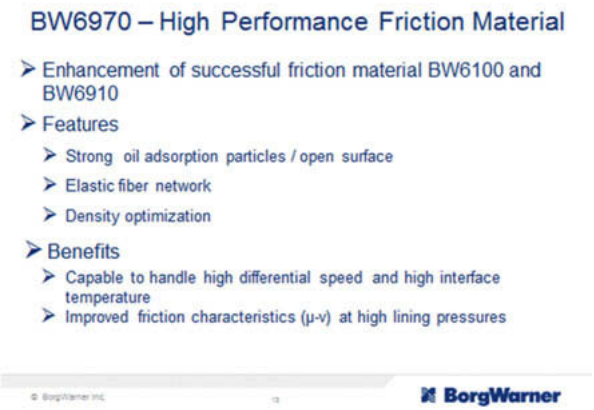


Fig. 11: BW 6970

BW6970 shows a high Elasticity and a larger porosity compared to traditional slipping clutch materials.

https://doi.org/10.51202/9783181023549 - Generiert durch IP 216.73.216.36, am 19.01.2026, 02:19:31. © Urheberrechtlich geschützter Inhalt. Ohne gesonderte Erlaubnis ist jede urheberrechtliche Nutzung untersagt, insbesondere die Nutzung des Inhalts im Zusammenhang mit, für oder in KI-Systemen, KI-Modellen oder Generativen Sprachmodellen.

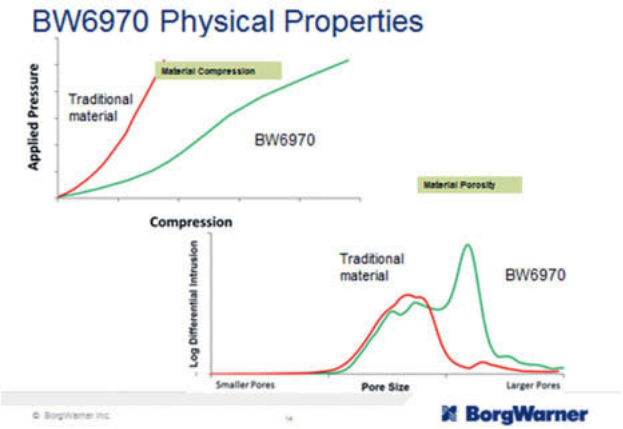
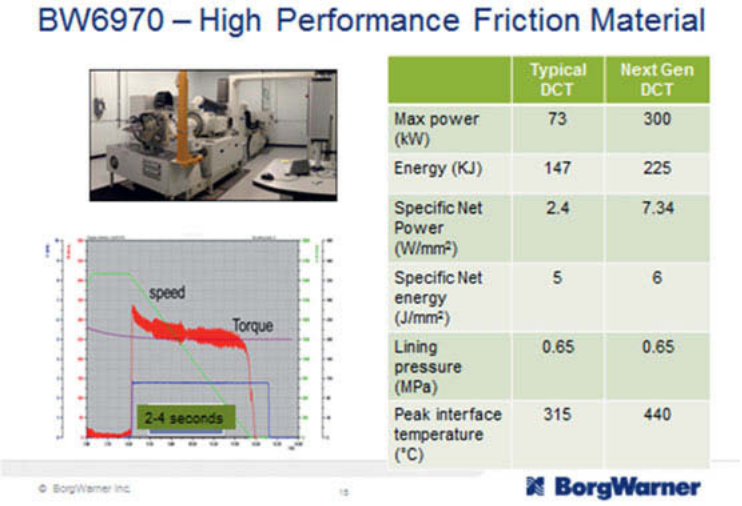


Fig. 12: Physical properties of BW6970

The High Speed Launch Test shows the friction performance of the new BW6970 compared to a traditional slipping clutch material.



	Typical DCT	Next Gen DCT
Max power (kW)	73	300
Energy (KJ)	147	225
Specific Net Power (W/mm²)	2.4	7.34
Specific Net energy (J/mm²)	5	6
Lining pressure (MPa)	0.65	0.65
Peak interface temperature (°C)	315	440

Fig. 13: Test conditions

https://doi.org/10.51202/9783181023549 - Generiert durch IP 216.73.216.36, am 19.01.2026, 02:19:31. © Urheberrechtlich geschützter Inhalt. Ohne gesonderte Erlaubnis ist jede urheberrechtliche Nutzung untersagt, insbesondere die Nutzung des Inhalts im Zusammenhang mit, für oder in KI-Systemen, KI-Modellen oder Generativen Sprachmodellen.

Compared to a traditional slipping clutch material the BW6970 shows almost not drop in the COF after 400 load cycles.

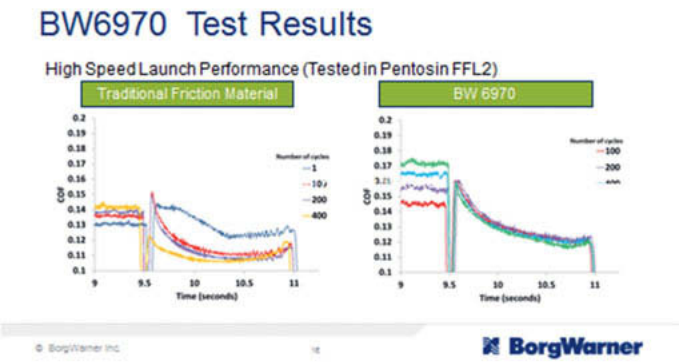


Fig. 14: BW 6970 test results

Molded Core Plate

The traditional core plate consists of a stamped metal core covered with glue and two friction linings. To produce this friction plate a lot of process steps are necessary.
Stamping ,etching, coating with glue , bonding and sizing.
The Molded friction plate consists of a plastic core with enclosed friction pads.
This is a process with significant lower process steps.
Further advantages include the significant lower weight ,inertia and shorter axial length.

https://doi.org/10.51202/9783181023549 - Generiert durch IP 216.73.216.36, am 19.01.2026, 02:19:31. © Urheberrechtlich geschützter Inhalt. Ohne gesonderte Erlaubnis ist jede urheberrechtliche Nutzung untersagt, insbesondere die Nutzung des Inhalts im Zusammenhang mit, für oder in KI-Systemen, KI-Modellen oder Generativen Sprachmodellen.

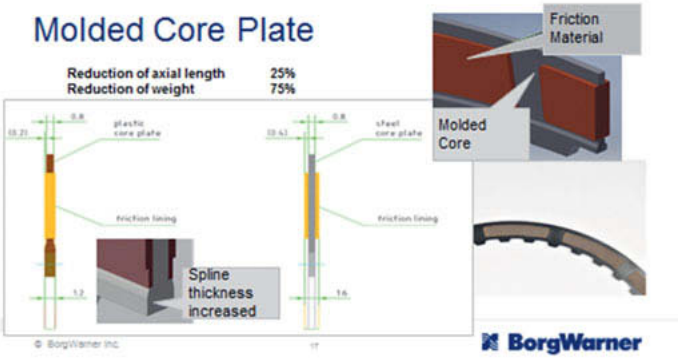


Fig. 15: Molded core plate design

Figure 16 compares the manufacturing process steps between a conventional friction plate and a molded core plate. There is significant lower amount of process steps with the molded core plate. The surface preparation and the coating of the steel core with glue can be eliminated.

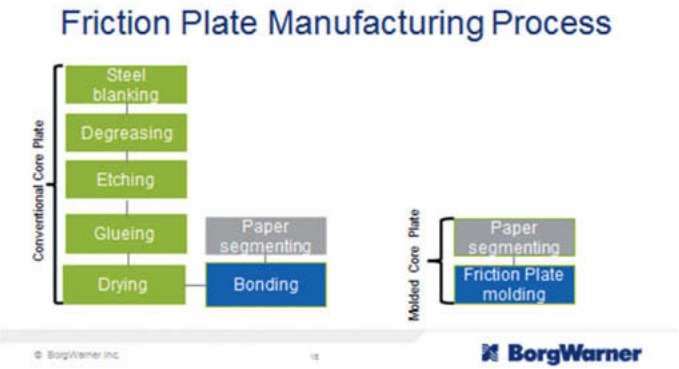


Fig. 16: Process flow comparison

https://doi.org/10.51202/9783181023549 - Generiert durch IP 216.73.216.36, am 19.01.2026, 02:19:31. © Urheberrechtlich geschützter Inhalt. Ohne gesonderte Erlaubnis ist jede urheberrechtliche Nutzung untersagt, insbesondere die Nutzung des Inhalts im Zusammenhang mit, für oder in KI-Systemen, KI-Modellen oder Generativen Sprachmodellen.

Aluminum Core Plate

Aluminum core plates are an enabler for significant weight reduction. The advantage is not only the 65% weight reduction of the core plate itself but the possibility to manufacture the mating parts like hubs or housings with aluminum without having the risk of hammering problems. Another advantage is the non magnetic characteristic of the Aluminum core plate which could be an advantage in proximity to electronics.



Fig. 17: Aluminum core plate

High Torque Low Drag System (HTLD)

The HTLD is a system which is combining a friction clutch for synchronization with a dog clutch for transmitting high torque.
The advantages are the extremely high torque density of the clutch system and the ability of the system to switch between synchronization and form closure without torque interruption.

https://doi.org/10.51202/9783181023549 - Generiert durch IP 216.73.216.36, am 19.01.2026, 02:19:31. © Urheberrechtlich geschützter Inhalt. Ohne gesonderte Erlaubnis ist jede urheberrechtliche Nutzung untersagt, insbesondere die Nutzung des Inhalts im Zusammenhang mit, für oder in KI-Systemen, KI-Modellen oder Generativen Sprachmodellen.

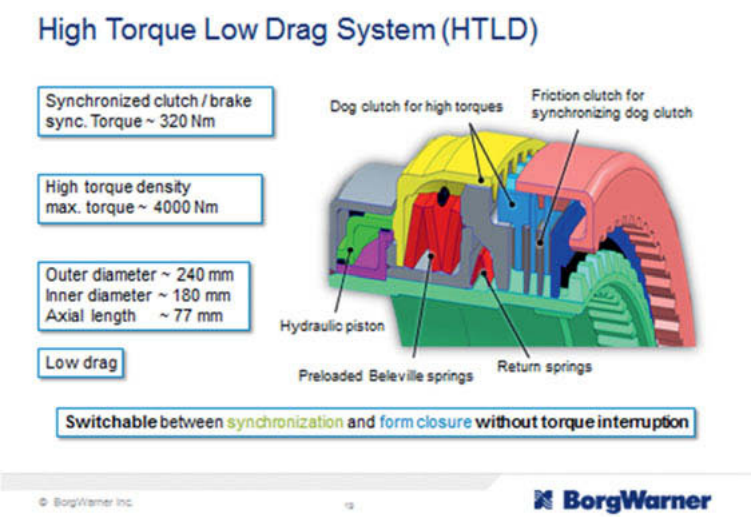


Fig. 18: HTLD clutch system

Fig. 19 shows the function of the clutch in three different modes.

1. Open clutch mode
   Friction clutch and dog clutch are not engaged .
2. Synchronization
   Piston is pressurized with 8bar, friction clutch is slipping with synchron speed
3. Dog clutch engaged
   Dog clutch is engaged at 12 bar apply pressure. Torque is transmitted by form fit

https://doi.org/10.51202/9783181023549 - Generiert durch IP 216.73.216.36, am 19.01.2026, 02:19:31. © Urheberrechtlich geschützter Inhalt. Ohne gesonderte Erlaubnis ist jede urheberrechtliche Nutzung untersagt, insbesondere die Nutzung des Inhalts im Zusammenhang mit, für oder in KI-Systemen, KI-Modellen oder Generativen Sprachmodellen.

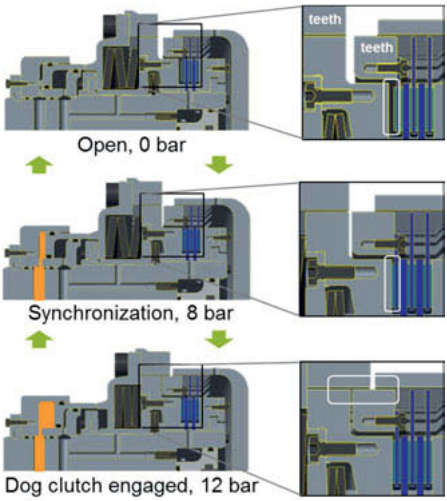


Fig. 19: Operation mode

First test results are shown in Fig 20. The system shows very low drag torque at different oil flow rates. The max drag torque was about 2.5Nm at max. oil flow.
Fig. 20 shows a disengagement of the dog clutch. What is plotted here is the switch from dog clutch engagement to controlled slip.

https://doi.org/10.51202/9783181023549 - Generiert durch IP 216.73.216.36, am 19.01.2026, 02:19:31. © Urheberrechtlich geschützter Inhalt. Ohne gesonderte Erlaubnis ist jede urheberrechtliche Nutzung untersagt, insbesondere die Nutzung des Inhalts im Zusammenhang mit, für oder in KI-Systemen, KI-Modellen oder Generativen Sprachmodellen.

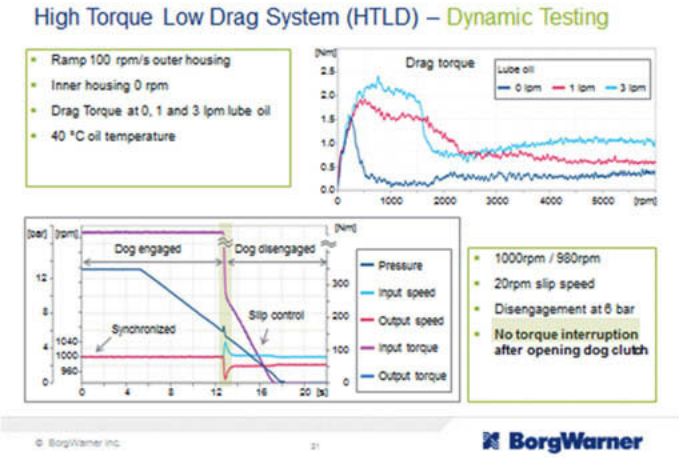


Fig. 20: Dynamic test results

Summary

New friction materials with increased thermal robustness and Hot Spot resistance and materials with higher static COF are enablers for increased power density

Alternative materials and design concepts for friction plates support weight and package size reduction

The High Torque Low Drag System (HTLD) combines a friction clutch with a dog clutch with the advantage of high torque density and low drag losses

https://doi.org/10.51202/9783181023549 - Generiert durch IP 216.73.216.36, am 19.01.2026, 02:19:31. © Urheberrechtlich geschützter Inhalt. Ohne gesonderte Erlaubnis ist jede urheberrechtliche Nutzung untersagt, insbesondere die Nutzung des Inhalts im Zusammenhang mit, für oder in KI-Systemen, KI-Modellen oder Generativen Sprachmodellen.

ecoLIFE^3: An Approach for a Resource-Efficient Dimensioning of Vehicle Components based on a Holistic Optimization with Real Life Load Data

Paradigm Shift in Transmission Engineering Based on Big Data

Dr.-Ing. **S. Foulard**, COMPREDICT GmbH, Darmstadt;
Prof. Dr.-Ing. **S. Rinderknecht**, M.Sc. **F. Braun**, M.Sc. **P. Jardin**,
Institute for Mechatronics Systems in Mechanical Engineering,
Technical University Darmstadt

Zusammenfassung

Nach dem Stand der Technik werden Fahrzeugkomponenten so ausgelegt, dass spezifische Anforderungen hinsichtlich deren Betriebslebensdauer auf Basis von standardisierten Testprozeduren erreicht werden. Allerdings werden diese Prozeduren für eine sehr begrenzte Nutzergruppe definiert, welche die durchschnittlichen Belastungsbedingungen von den Komponenten stark überschreiten. Ein solches Vorgehen reduziert drastisch die gesamte Ressourceneffizienz. Das Institut für Mechatronische Systeme im Maschinenbau der TU Darmstadt (IMS) und seine Ausgründung, die COMPREDICT GmbH, arbeiten gemeinsam an dieser Problematik und schlagen einen innovativen Ansatz für einen Gesamtprozess zum effizienten und belastungsgerechten Design bzw. Leichtbaudesign in der Automobilindustrie vor, sog. ecoLIFE^3. Die Grundidee von dieser zum Patent angemeldeten und rein softwarebasierten Methode ist, dass die gesamte Fahrzeugflotte Teil eines kontinuierlich überwachten Optimierungsproblems im Rahmen eines wissensbasierten Entwicklungsprozesses wird. Dadurch werden künftige Fahrzeugkomponenten im Rahmen einer multidimensionalen Optimierung auf Basis einer holistischen Betrachtung ausgelegt, wobei unter anderen Kosten und CO_2-Fußabdruck berücksichtigt werden. Dadurch wird ein Paradigmenwechsel in die Dimensionierung von Fahrzeugkomponenten eingeführt, für welche eine gleichbleibende bzw. sogar höhere Zuverlässigkeit im Zusammenhang mit Leichtbau und Kostenneutralität gleichzeitig erreicht werden. Dies wird anhand einer sogenannten Last- und Lebensdauerüberwachung und dem potenziellen Austausch von Komponenten für die extremsten Fahrer erreicht, wobei die dadurch entstehenden Mehrkosten durch die Ersparnisse aufgrund der kleineren Dimensionierung ausgeglichen werden können.

https://doi.org/10.51202/9783181023549 - Generiert durch IP 216.73.216.36, am 19.01.2026, 02:19:31. © Urheberrechtlich geschützter Inhalt. Ohne gesonderte Erlaubnis ist jede urheberrechtliche Nutzung untersagt, insbesondere die Nutzung des Inhalts im Zusammenhang mit, für oder in KI-Systemen, KI-Modellen oder Generativen Sprachmodellen.

Abstract

According to the state of the art, vehicle components are designed to meet specific requirements regarding their useful lifetime based on standardized testing procedures. However, these procedures are defined by a very small group of drivers who by far exceed the average loading condition of components. That reduces drastically the overall resource efficiency. The Institute for Mechatronic Systems in Mechanical Engineering of the TU Darmstadt (IMS) and its spin-off COMPREDICT GmbH are working jointly on this problem and propose an innovative approach for an overall efficient right-sizing and lightweight design process in automotive engineering, so-called ecoLIFE^3. The main idea of this patent-pending and purely software-based method is that the global vehicle fleet becomes part of a continuously monitored optimization problem within a knowledge-based development process. By that, future vehicle components are designed within a multi-objective optimization based on a holistic approach considering among others monetary costs and CO_2-footprint. In that sense, a paradigm shift is introduced in vehicle components dimensioning, for which an equal or even higher level of reliability together with lightweight design and cost-neutrality are reached at the same time. This is done by so-called load & lifetime monitoring and, eventually, replacing components for the most extreme drivers while balancing this with the monetary advantage of smaller dimensioned parts.

Motivation

For the dimensioning and the market release of automotive components, a conservative approach is generally adopted in order to guarantee a high degree of reliability and to avoid operating failures as much as possible. Usually, a hypothetical 99.9 % driver is taken as a reference, which covers theoretically 99.9 % of the usage profiles. For cost and time reasons, simulations and few field tests mainly determine these requirements. Being that, the accuracy and the validity of this reference profile are questionable. Moreover, due to limited accurate knowledge about real and high dynamic operating conditions, and besides safety factors, very demanding driving situations are considered, which do not necessarily represent the end user behaviour, and often overestimate it. As a direct result, the components developed with standard industry procedures are overdesigned for most of the users. This leads to superfluous weight, which in turn implies higher material costs and fuel consumption.

To tackle this issue, IMS and COMPREDICT have developed an innovative approach: the software-based lightweight design. This approach is based on two main aspects. First, the real

https://doi.org/10.51202/9783181023549 - Generiert durch IP 216.73.216.36, am 19.01.2026, 02:19:31. © Urheberrechtlich geschützter Inhalt. Ohne gesonderte Erlaubnis ist jede urheberrechtliche Nutzung untersagt, insbesondere die Nutzung des Inhalts im Zusammenhang mit, für oder in KI-Systemen, KI-Modellen oder Generativen Sprachmodellen.

operation loads are computed from existing vehicle data in the so-called load monitoring system through the use of virtual sensors. Second, the components are designed within the patent-pending ecoLIFE^3 procedure [1].
In this paper, the focus is set on the ecoLIFE^3 procedure and the load monitoring system is only briefly described for comprehension purpose. More information about the load monitoring system can be found in [2].

Load Monitoring System: Virtual Sensor for High-Precision Load Profiles

Purely software-based, the load monitoring system acquires the dynamic component loads with virtual sensors presenting such a level of accuracy, that they are as accurate as a dedicated sensor which would directly measure the corresponding physical quantity (e.g. torque, force, stress, strain, temperature). For the virtual sensors, COMPREDICT has developed an approach relying on sensor fusion by using stochastic approaches coupled with artificial intelligence. On this basis, highly accurate load and usage profiles are computed. The application-oriented and easily adaptable load monitoring system does not require any additional hardware and is based on already available vehicle sensors and signals running on the vehicle bus, such as a Controller Area Network (CAN). Additionally, a durability assessment can be included in the algorithms, so that a lifetime monitoring runs also in parallel. For this purpose, a high degree of accuracy is mandatory for the load determination, which is made possible with the COMPREDICT algorithms.
The idea behind the load monitoring system is to turn every single series-production car into a development car, meaning generating as accurate and as granular information as a development engineer would record with additional sensors and hardware in a test vehicle. The load monitoring system is intended for implementation in standard control units of series production cars. For such applications, the amount of generated data is kept low, and the limited computing power and storage capacity of standard Electronic Control Units (ECU) are considered, such that the system can be implemented in all vehicles without any special expense. Fig. 1 shows the basic structure of a typical load and lifetime monitoring system for transmissions.
The system relates to standard industry procedures for load spectrum and damage calculation. For instance, gearwheels are generally monitored according to a nominal stress concept coupled with a Revolutions-At-Level counting method and a linear damage accumulation according to Miner-Haibach [3]. For transmission applications, the developed algorithm for damage prediction refers to the initial specifications of the transmission manufacturer. This enables a direct comparison between the design procedure and the real operating conditions. For this, the Wöhler curves assumed during the development of the components and the underlying

https://doi.org/10.51202/9783181023549 - Generiert durch IP 216.73.216.36, am 19.01.2026, 02:19:31. © Urheberrechtlich geschützter Inhalt. Ohne gesonderte Erlaubnis ist jede urheberrechtliche Nutzung untersagt, insbesondere die Nutzung des Inhalts im Zusammenhang mit, für oder in KI-Systemen, KI-Modellen oder Generativen Sprachmodellen.

damage targets and strength limits are taken as a reference for assessing the real-time damage levels. The speed and load dependent variables are factored in the conversion of torque into stress with the same hypotheses as in the design procedure and the dynamic effects in the drivetrain are reproduced by the torque virtual sensor.

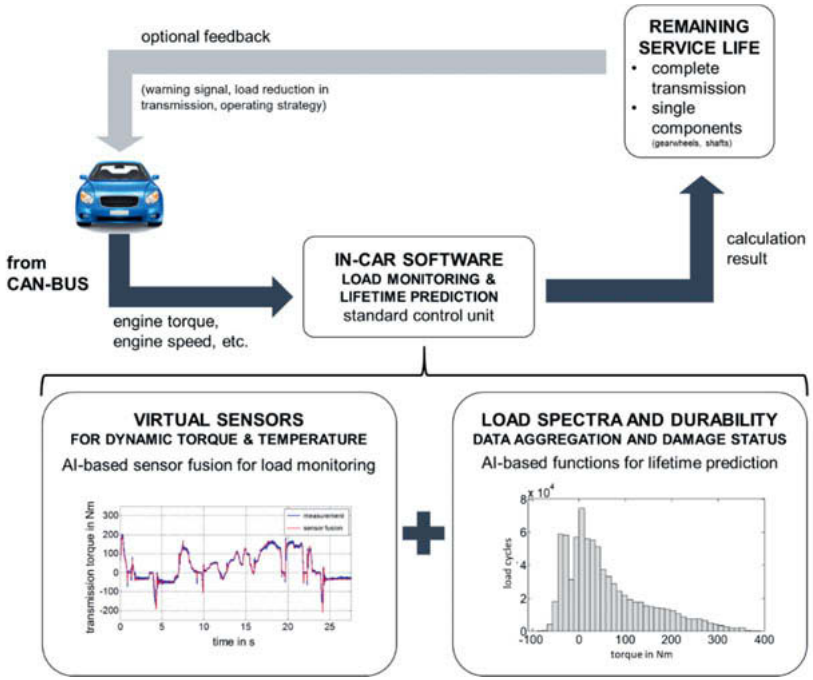


Fig. 1: General structure of a typical load & lifetime monitoring system for transmissions

Besides, an implementation of the system does not bring any additional uncertainties in comparison with today's calculation schemes, for example about the statistical dispersion of strength limits (Fig. 2). For instance, a continuous comparison between the calculated damage state resulting from the design load collectives and the calculated damage state caused by the real loads can be computed in this regard. In addition, the influence of the transmission temperature, which is also acquired with a virtual sensor, is accounted for.

The outputs of the load and lifetime monitoring system can be transmitted wirelessly or read during service inspections in order to feed the online data lake, where vehicle and fleet level data is stored.

https://doi.org/10.51202/9783181023549 - Generiert durch IP 216.73.216.36, am 19.01.2026, 02:19:31. © Urheberrechtlich geschützter Inhalt. Ohne gesonderte Erlaubnis ist jede urheberrechtliche Nutzung untersagt, insbesondere die Nutzung des Inhalts im Zusammenhang mit, für oder in KI-Systemen, KI-Modellen oder Generativen Sprachmodellen.

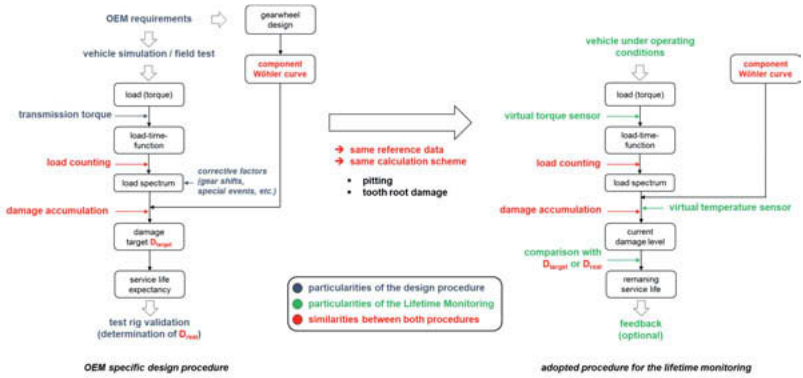


Fig. 2: OEM-specific design procedure vs. adopted procedure for the lifetime monitoring

Smart Big Data: COMPREDICT Suite and ecoLIFE³

By going beyond the vehicle level and considering a complete vehicle fleet, the possibility of a continuous optimization procedure on basis of the outputs of load & lifetime monitoring system emerges for a better control of user profile discrepancies, customer-optimized lightweight design, cost-efficiency and improved resource management. This is namely what the ecoLIFE³ approach developed at IMS and implemented by COMPREDICT aims at. The abbreviation is standing for **e**lectronic and **c**ontinuous **o**ptimization of **LIFE**time and **LI**gthweight **FE**atures based on **L**oad **I**dentification and **F**atigue **E**stimation. The basic idea of the ecoLIFE³ procedure is to involve the data generated by the load & lifetime monitoring system in the component dimensioning process, the operating strategy and the predictive maintenance of components. This way, the global vehicle fleet becomes a part of a continuously monitored optimization problem within a knowledge-based development process. For this purpose, the data generated by the load & lifetime monitoring system are transferred to external evaluation units for deep analysis (see Fig. 3).

Regarding data security and privacy, no person-related data is generated or transferred. Basically, no time series are recorded and only aggregated data are computed. The unique information is then about the usage profiles and, possibly, attained damage levels. This means that it cannot be determined, where, how or when a customer drove or why one loading condition or another was generated. However, it could certainly be deduced, if a component was aggressively loaded or not. But, from this point of view, this is the same kind of deduction which can be done today for an engine on basis of oil service intervals.

https://doi.org/10.51202/9783181023549 - Generiert durch IP 216.73.216.36, am 19.01.2026, 02:19:31. © Urheberrechtlich geschützter Inhalt. Ohne gesonderte Erlaubnis ist jede urheberrechtliche Nutzung untersagt, insbesondere die Nutzung des Inhalts im Zusammenhang mit, für oder in KI-Systemen, KI-Modellen oder Generativen Sprachmodellen.

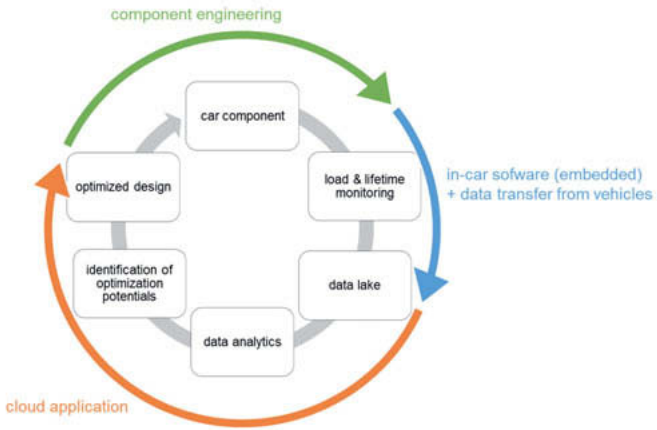


Fig. 3: Principle of the **ecoLIFE^3** concept

In the next sections, a visionary application of ecoLIFE^3 is proposed, which results in a paradigm change in the transmission development philosophy. The design will not be carried out for the typical 99.9 % driver anymore, but for a less demanding reference driver. A potential transmission replacement is knowingly accepted for drivers, who by far exceed the average usage profile, basically at the expense of the OEM. In case of a transmission replacement, the on-cost are considered in the optimization process and can be compensated or even over-compensated depending on the chosen reference driver. In any case, all end-users profit from lightweight with the related reduction of CO_2-emissions. In this context, the ecoLIFE^3 procedure is introduced to find the optimal reference driver for certain cost, weight and/or CO_2 reduction. This is done by achieving a holistic optimization of the resource deployment with respect to cost, weight, CO_2-footprint and component replacement. Furthermore, with the help of the load and lifetime monitoring system, the ecoLIFE^3 approach reaches its full potential, so that despite lighter designed transmissions a safe and failure-free operation is achieved for all users at all time. Indeed, since every single car is monitored in the field, critical states are recognized at an early stage and failure prevention is possible. In addition, the generated data can be used to estimate future maintenance plans. By following this scheme, the vehicle components can be optimized from generation to generation, which is why ecoLIFE^3 is an iterative and continuous optimization. This is a clear contrast with the traditional design strategy of vehicle components, which neither uses the real usage profiles nor represents an iterative and continuous optimization process.

https://doi.org/10.51202/9783181023549 - Generiert durch IP 216.73.216.36, am 19.01.2026, 02:19:31. © Urheberrechtlich geschützter Inhalt. Ohne gesonderte Erlaubnis ist jede urheberrechtliche Nutzung untersagt, insbesondere die Nutzung des Inhalts im Zusammenhang mit, für oder in KI-Systemen, KI-Modellen oder Generativen Sprachmodellen.

An application of ecoLIFE³ for a manual transmission

Here, an application of ecoLIFE³ is proposed for a manual transmission by targeting an optimization of weight, costs and CO_2-footprint while considering at the same time durability and quality requirements [4]. In this study, a transverse gearbox with 6 gears of a standard B-segment front-wheel vehicle is considered (Fig. 4).

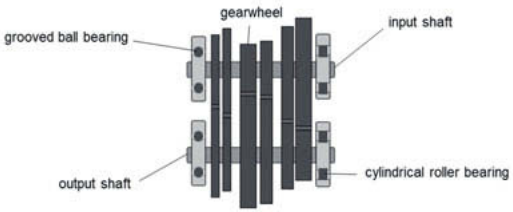


Fig. 4: Basic layout of the transverse transmission considered in this study

The gear ratios are fixed and geometry parameters of the gearwheels, the shafts, the bearings and the housing are optimized. For simplicity purpose, it is also assumed that the helix angle of the gearwheels is fixed. On this basis, a multi-objective penalty function is defined by considering the three aforementioned optimization goals and defining for each one a geometry-based model (Fig. 5 to Fig.7).

For instance, for the cost calculation referring to the gearwheels, the main aspects of the manufacturing process chain are considered from round material to case-hardening, going through sawing and gear hobbing.

https://doi.org/10.51202/9783181023549 - Generiert durch IP 216.73.216.36, am 19.01.2026, 02:19:31. © Urheberrechtlich geschützter Inhalt. Ohne gesonderte Erlaubnis ist jede urheberrechtliche Nutzung untersagt, insbesondere die Nutzung des Inhalts im Zusammenhang mit, für oder in KI-Systemen, KI-Modellen oder Generativen Sprachmodellen.

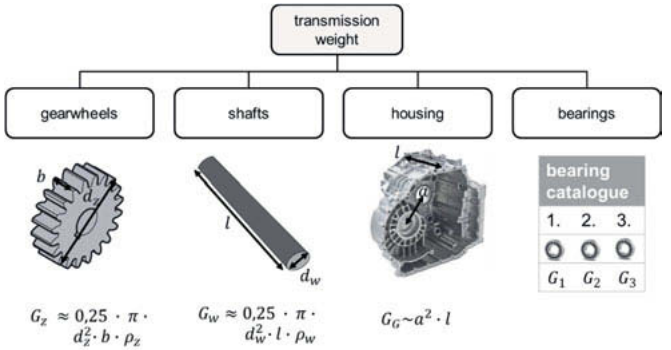


Fig. 5: Overview of the weight model

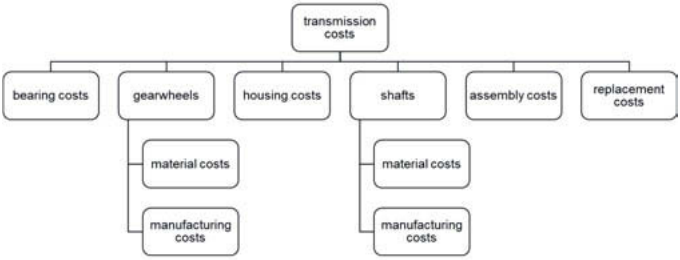


Fig. 6: Overview of the cost model

For a given manufacturing process chain, the costs are calculated for each different step according to a cost per time unit (with values realistic for mass production) and by estimating the necessary manufacturing time as a function of the gearwheel geometry.

https://doi.org/10.51202/9783181023549 - Generiert durch IP 216.73.216.36, am 19.01.2026, 02:19:31. © Urheberrechtlich geschützter Inhalt. Ohne gesonderte Erlaubnis ist jede urheberrechtliche Nutzung untersagt, insbesondere die Nutzung des Inhalts im Zusammenhang mit, für oder in KI-Systemen, KI-Modellen oder Generativen Sprachmodellen.

manufacturing costs = (manufacturing cost per time unit) x (manufacturing time)

manufacturing time = setup + recovery + allowance + main time + auxiliary process time

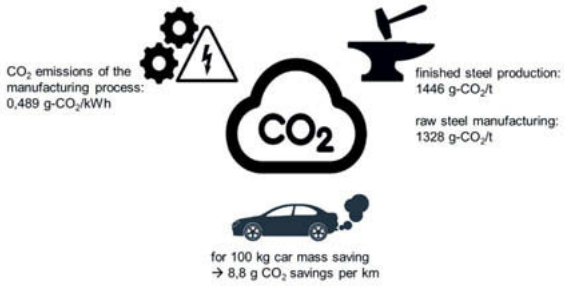


Fig. 7: Overview of the CO_2 footprint model

In this study, a comprehensive database of transmission usage profiles is considered. The database refers to 500000 vehicles with mileages between 25000 and 200000 km and lifetime between 2 and 10 years, which were generated on basis of real and publicly available GPS data from Open Street Map and through a drivetrain model for a B-segment car with the patented driveREAL method [5]. The usage profiles are determined in such a way, that they are independent of the transmission geometry. This means that they only contain information about the acting transmission torques. The conversion into stress or rather geometry-dependent loads is done within the geometry optimization process for the different components. However, the computation of the component load spectra is adapted to each component. For instance, a Revolutions-At-Level counting method is adopted for the gearwheels and a Rainflow counting for the shafts.

For the durability considerations, the equations defined by Naunheimer in [6] are adopted, so that damage calculations are done according to standard damage calculation procedures based on an estimation of the B_{10}-Wöhler curves. Then, the calculated Wöhler curves give the loading capacity of the corresponding component based on its geometry. The durability of the housing is not explicitly considered, so that only the geometry is optimized depending on the geometry of the gearwheels and the shafts. In this sense, the housing is considered as a cylinder for which the length (correlated to the shaft length) and the center distance of the transmission are the characteristic parameters. Concerning the bearings, they are assumed to be purchased parts, so that they are chosen from a supplier catalog and can only take discrete geometric values. However, a fatigue calculation is also carried out for the bearings, so that the durability requirements are also assessed during the optimization process.

https://doi.org/10.51202/9783181023549 - Generiert durch IP 216.73.216.36, am 19.01.2026, 02:19:31. © Urheberrechtlich geschützter Inhalt. Ohne gesonderte Erlaubnis ist jede urheberrechtliche Nutzung untersagt, insbesondere die Nutzung des Inhalts im Zusammenhang mit, für oder in KI-Systemen, KI-Modellen oder Generativen Sprachmodellen.

For the transmission design itself, a mileage of 250000 km or 15 years of operation time are taken as minimal requirements, depending on which condition is reached first. For the durability assessment, a damage limit of 0,3 is adopted. Being that, standard requirement targets are considered as constraints for the optimization process, such that the transmission defined by ecoLIFE^3 is fulfilling standard automotive quality requirements.

For comparison purpose, an upper-limit for the dimensioning is defined by following the design procedure proposed by Naunheimer in [6], which is known to be a rough estimation and overestimates the design requirements. Anyway, this enables to generate a baseline to assess, if the cost and weight models give plausible results. According to the proposed calculation schema, the rough estimated design of the transmission shows following properties:

- Weight: 41,5 kg
- Overall transmission cost: 450€
- Variable costs: 388€
- Fixed costs: 62€
- Replacement cost in a workshop: 300€

The weight is calculated based on the weight model described in the previous section. The overall transmission costs are estimated according to market-oriented values. The variable costs are determined with the cost model defined before. The fixed costs are then calculated as the difference between overall and variable costs and are assumed to be non-variable in the ecoLIFE^3 process. The fixed costs are relevant in case of a transmission replacement. In such a case, the fixed costs, the later optimized variable costs and the replacement costs in a workshop (experience value) are added up and considered as additional costs in the overall cost calculation. The optimization process also checks if more than one transmission replacement is necessary to fulfill the mileage and lifetime requirements, so that the overall cost calculation is also adapted in ecoLIFE^3 if this event occurs.

The first step of the ecoLIFE^3 procedure is the extrapolation of the usage profiles to the minimal quality requirements, namely 250000 km or 15 years. In this study, the extrapolation is computed based on the spectrum form factors, maximal spectrum value and spectrum size, as proposed in [7]. COMPREDICT has also developed AI-based methods to extrapolate usage profiles. But for the sake of simplicity, a standard approach was adopted here.

After the extrapolation process, the second step is the classification of the extrapolated usage profiles in order to get the true distribution of the X% drivers. For this, it is not purposeful to use the most demanding driver who is covering X% for each gear. This way, the resulting profile would cover more than the expected X%. In the best case, the least demanding usage profile covering X% of the drivers by considering the transmission as an entire system should

https://doi.org/10.51202/9783181023549 - Generiert durch IP 216.73.216.36, am 19.01.2026, 02:19:31. © Urheberrechtlich geschützter Inhalt. Ohne gesonderte Erlaubnis ist jede urheberrechtliche Nutzung untersagt, insbesondere die Nutzung des Inhalts im Zusammenhang mit, für oder in KI-Systemen, KI-Modellen oder Generativen Sprachmodellen.

be taken as a reference (Fig. 8). This is done with a genetic algorithm relying on an evolution strategy which finds the desired profile within an eight-dimensional search space. The eight dimensions refer to a duty value calculation for the six gear stages and both shafts. Duty values are enough in the present case, because only the relative difference between the usage profiles and not the specific damage value of a component is relevant. It was also assumed that all the gears have the same degree of relevance, so that no weighting factor was introduced for the different components in the loss function. Also, the bearings are not explicitly considered in the classification process. The suitable bearings are taken from a supplier catalog after determining the optimal X% driver.

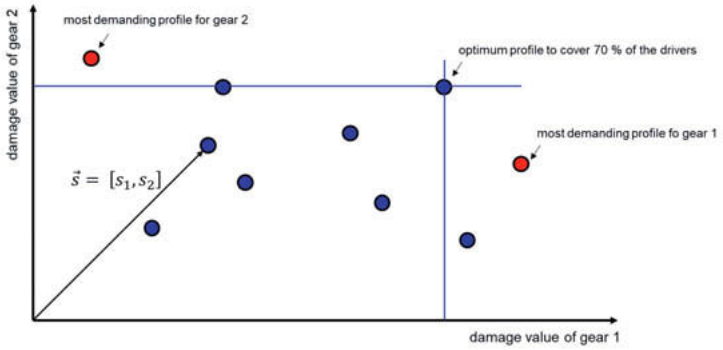


Fig. 8: Example of optimization problem for the profile classification of two different gears

Anyway, the loss function of the classification can be adapted to specific requirements, if needed. For instance, a ponderation can be adopted between the different transmission components. Also, the classification of the usage profiles can be integrated in the geometry optimization (see next step) and specific damage values instead of duty values can be considered for each component.

The last step of the procedure is the optimization of the transmission geometry with regard to the pre-defined multi-objective penalty function. This final step is achieved by finding the most favorable geometry for the transmission components. This is also done with a genetic algorithm relying on a principle similar as for the classification of the usage profiles. However, the optimization problem has three weighted simultaneous objectives (costs, CO_2-footprint and weight), three constraints (mileage, lifetime and damage level) and five geometry parameters to be optimized (see Fig. 5 to Fig. 7).

https://doi.org/10.51202/9783181023549 - Generiert durch IP 216.73.216.36, am 19.01.2026, 02:19:31. © Urheberrechtlich geschützter Inhalt. Ohne gesonderte Erlaubnis ist jede urheberrechtliche Nutzung untersagt, insbesondere die Nutzung des Inhalts im Zusammenhang mit, für oder in KI-Systemen, KI-Modellen oder Generativen Sprachmodellen.

At the end of the optimization, following results are generated (Fig. 9). In the presented results, transmission replacements are already taken into consideration for not-covered driver profiles and the corresponding impact on costs and CO_2-emissions is also included. Since it is more useful in this study to discuss about savings instead of total emissions for car emissions, the values shown in the figure for the savings of CO_2-emissions over 100000 km are calculated against a theoretical vehicle. This does not impact the results when doing relative comparisons.

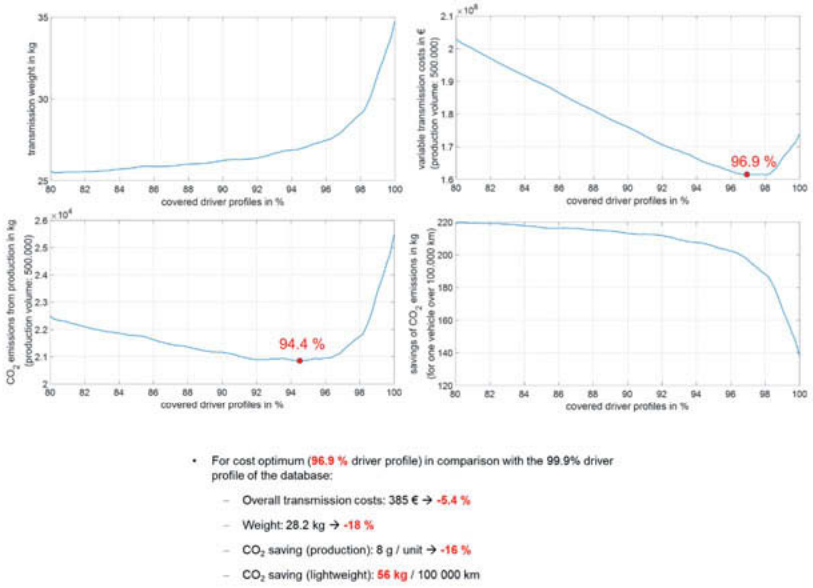


Fig. 9: Results from the ecoLIFE^3 optimization process

The first conclusion is that the ecoLIFE^3 procedure is able to truly and accurately catch the real 99.9 % driver, without needing any assumption. In practice, it can be fairly said that the current state-of-the-art for dimensioning procedures would generate a design which will cover usage profiles between this real 99.9 % and the rough estimation proposed above according to Naunheimer. Anyway, it appears that, in any case, it is not purposeful to design for 99.9 % of the drivers, even if this design relies on real field data. In other words, this means that, even if the exact distribution of the driver profiles is known, a design for the most extreme driver profiles is not advisable. Indeed, the ecoLIFE^3 approach shows that huge potentials are possible with

https://doi.org/10.51202/9783181023549 - Generiert durch IP 216.73.216.36, am 19.01.2026, 02:19:31. © Urheberrechtlich geschützter Inhalt. Ohne gesonderte Erlaubnis ist jede urheberrechtliche Nutzung untersagt, insbesondere die Nutzung des Inhalts im Zusammenhang mit, für oder in KI-Systemen, KI-Modellen oder Generativen Sprachmodellen.

regard to lightweight design and cost savings, if a less demanding profile is considered. By taking the overall cost optimum (96.9 % driver), the transmission costs can be reduced by more than **5.4 %** (385 € instead of 407 €) and the transmission weight by more than **18 %** (28.2 kg instead of 34.4 kg), when compared to the real 99.9 % driver profile. This way, **16 %** of CO_2 emissions can also be saved during the manufacturing process (8 g CO_2 savings for each produced transmission). Additionally, based on the weight saving, more than **56 kg** of CO_2 emissions can be saved for each vehicle over a mileage of 100000 km.

Even if the results of the cost optimum are compared with the real 99 % driver profile (also sometimes taken as theoretical reference), high savings can be still realized according to ecoLIFE^3: 3 % of the costs (385 € instead of 395 € overall costs for the 99 % driver profile) and 10 % of weight (28.2 kg instead of 31.5 kg overall costs for the 99 % driver profile).

The ecoLIFE^3 procedure coupled with the load and lifetime monitoring opens a new way to dimension transmissions and to manage costs and CO_2-emissions without downgrading quality standards and reliability requirements.

Towards Vehicle 5.0

The goals in automotive engineering are to make vehicles lighter, more environment-friendly and autonomous. In connection with these goals, car-to-car communication and the internet of things open new ways to process and use operating data. As of now, a lot additional knowledge can be generated by analysing operating data. The research cluster Vehicle 5.0 at TU Darmstadt, of which IMS and its spin-off COMPREDICT are foundation stones, focusses on the development of scientific methods and a knowledge-based approach to enable the continuous improvement and the intelligent operation of connected vehicles with the support of Big Data. The aim of the research cluster Vehicle 5.0 is to develop progressive methods, which aimed at introducing a paradigm shift in the automotive industry by exploiting synergies in connecting their evolutionary development with the revolutionary approaches of the data mining industry.

Conclusion and outlook

The patent-pending ecoLIFE^3 procedure opens a new design philosophy for dimensioning car components and systems. The example given here for automotive transmissions shows that huge savings can be realized with this approach in terms of costs, weight and CO_2 footprint. Originally developed at IMS, COMPREDICT is now implementing the corresponding algorithms in its software platform. IMS and COMPREDICT are jointly working on further improvements of the method. For transmission application, the next steps will be to enhance the pro-

https://doi.org/10.51202/9783181023549 - Generiert durch IP 216.73.216.36, am 19.01.2026, 02:19:31. © Urheberrechtlich geschützter Inhalt. Ohne gesonderte Erlaubnis ist jede urheberrechtliche Nutzung untersagt, insbesondere die Nutzung des Inhalts im Zusammenhang mit, für oder in KI-Systemen, KI-Modellen oder Generativen Sprachmodellen.

cess by including failure probability and distribution aspects in the optimization routine. Furthermore, other extensions of the method are the increase of model complexity, for instance, by taking the helix angle as a geometry optimization parameter and the more accurate modelling of the manufacturing process chain.

Bibliography

[1] Foulard, S.; Rinderknecht, S.; Fietzek, R.: Verfahren zur Auslegung und Dimensionierung eines Neuteils eines Kraftfahrzeugs. German Patent Reg. DE 10 2015 120 107.0 (2015)

[2] Rinderknecht, S.; Fietzek, R.; Foulard, S.: Online and Real-Time Condition Prediction for Transmissions based on CAN-Signals. SAE World Congress 2017, 04.-06. April 2017, Detroit, Michigan, USA (2017)

[3] Haibach, E.: Betriebsfestigkeit: Verfahren und Daten zur Bauteilberechnung. VDI, 2002

[4] Braun, F.: Erweiterung eines Verfahrens zur wissensbasierten Auslegung und Wartung von Fahrzeugkomponenten. Master-Thesis, TU Darmstadt, 2019

[5] Eßer, A.; Zeller, M.; Foulard, S.; Rinderknecht, S.: Stochastic Synthesis of Representative and Multidimensional Driving Cycles. SAE World Congress Experience, April 10-12, 2018, Detroit, MI, USA (2018)

[6] Naunheimer, H.: Automotive Transmissions: Fundamentals, Selection, Design and Application. Springer Berlin Heidelberg, 2007

[7] Hinkelmann, K.; Müller, C.; Masendorf, R.; Esderts, A.: Extrapolation von Beanspruchungskollektiven, Clausthal-Zellerfeld, Technische Universität Clausthal, 2011

https://doi.org/10.51202/9783181023549 - Generiert durch IP 216.73.216.36, am 19.01.2026, 02:19:31. © Urheberrechtlich geschützter Inhalt. Ohne gesonderte Erlaubnis ist jede urheberrechtliche Nutzung untersagt, insbesondere die Nutzung des Inhalts im Zusammenhang mit, für oder in KI-Systemen, KI-Modellen oder Generativen Sprachmodellen.

1, 2 or 3 – how much it would be? Evaluating the need of multispeed electric drives coming from different perspectives

Dr. **Klaus von Rueden**, Dr. **Christoph Danzer**, Jens **Liebold**,
Tim Mueller, **Tobias Hirschbeck**,
IAV GmbH, Berlin, Gaimersheim, Gifhorn and Chemnitz / Stollberg

Zusammenfassung

Um die Entwicklungsziele für 2025+ in Bezug auf CO_2-Emissionen, Leistung, Komfort, Gewicht und Kosten zu erreichen, untersuchen die Fahrzeughersteller verschiedenen Szenarien für Flottenbedarf, Modularität und Produktionskosten. In diesem Zusammenhang spielt der Antriebsstrang eine entscheidende Rolle. Grundlegende Entscheidungen haben weitreichende Konsequenzen, die im Zweifelsfall nur mit großem Aufwand korrigiert werden können. Die Komplexität der Ziele, Anforderungen und Randbedingungen ist so hoch, dass eine Optimierung mit standardisierten Methoden nicht mehr möglich ist. IAV hat in den letzten Jahren Werkzeugketten und deren Anwendungen eingeführt, mit denen die modularen Systeme einer gesamten Fahrzeugflotte aus konventionellen, hybriden und vollelektrischen Antrieben abgebildet werden können.

Ziel der Automobilhersteller ist es, mit einem modularen System aus E-Maschinen-, Getriebe- und Leistungselektronik mit möglichst wenigen Baugruppen auf die unterschiedlichsten Kundenanforderungen im Bereich der Elektromobilität reagieren zu können.

Die Frage, ob und wann Mehrgang-Antriebssysteme zur Verfügung stehen, hängt nicht zuletzt von den gewählten Randbedingungen für die Topologie des Elektromotors ab. So zeigt sich, dass permanentmagnetische Synchronmaschinen andere Anforderungen an die Getriebe stellen als beispielsweise Asynchronmaschinen. Neben der rein energetischen Betrachtung von Elektromotor, Leistungselektronik und Getriebe, ist die Fahrbarkeitsoptimierung in mehrstufigen Systemen von großer Bedeutung. Viele Hersteller arbeiten bereits an Mehrgangantrieben. Besonders bei einem Zweiganggetriebe ist Stufensprung sehr groß, was einerseits besondere Anforderungen an die Steuerung des Gangwechsels selbst stellt und andererseits bei der Konstruktion der E-Maschine berücksichtigt werden muss. Beide mit dem Fokus auf die Optimierung des Fahrkomforts. IAV nutzt spezielle hauseigene Analysetools, die auch die Konzeptentscheidung mit klaren Aussagen in der Konzeptphase mit einem digitalen Prototyp unterstützen.

https://doi.org/10.51202/9783181023549 - Generiert durch IP 216.73.216.36, am 19.01.2026, 02:19:31. © Urheberrechtlich geschützter Inhalt. Ohne gesonderte Erlaubnis ist jede urheberrechtliche Nutzung untersagt, insbesondere die Nutzung des Inhalts im Zusammenhang mit, für oder in KI-Systemen, KI-Modellen oder Generativen Sprachmodellen.

Abstract

In order to achieve the development goals for 2025+ in terms of CO_2-emissions, performance, comfort, weight and costs, vehicle manufacturers look for different scenarios for fleet requirements, modularity and production costs. In this context, the powertrain plays a crucial role. Fundamental decisions have far-reaching consequences, which in case of doubt can only be corrected with great effort. The complexity of the goals, requirements and boundary conditions are so high that optimization by means of standardized methods is no longer possible. Over the past years, IAV has introduced tool chains and their applications that can be used to represent the modular systems of an entire vehicle fleet consisting of conventional, hybrid and all-electric power trains.

Development goals, such as high starting performance and high maximum speed, can also be opposed by the drive systems. The aim of car manufacturers is to be able to respond to a wide variety of customer requirements in the segment of electric mobility with as few assemblies as possible with a modular system consisting of e-machine, transmission and power electronics. The question of whether and when multiple-drive systems are available depends not least on the selected boundary conditions for the topology of the electric motor. Thus, it is shown that permanent-magnet synchronous machines place different demands on the transmissions than, for example, asynchronous machines. In addition to the purely energetic consideration between the electric motor, power electronics, transmission and actuation system, the drivability optimization in multi-speed systems is of great importance. Many manufacturers are already working on multi-speed transmissions. Especially in a two-speed gearbox, the increment is very large, which on the one hand makes special demands on the control of the gear change itself and on the other hand must be taken into account in the e-machine design. Both with the focus on driving comfort optimization. IAV uses special in-house analysis tools, which also support the concept decision with clear statements during the concept phase, using a digital prototype.

In this presentation, different approaches to the design of electric power trains with one or more gears are shown.

https://doi.org/10.51202/9783181023549 - Generiert durch IP 216.73.216.36, am 19.01.2026, 02:19:31. © Urheberrechtlich geschützter Inhalt. Ohne gesonderte Erlaubnis ist jede urheberrechtliche Nutzung untersagt, insbesondere die Nutzung des Inhalts im Zusammenhang mit, für oder in KI-Systemen, KI-Modellen oder Generativen Sprachmodellen.

Introduction

It is known from the past that an internal combustion engine (ICE) has an unusable useful map solely for the drive in a vehicle. On the one hand, there is no torque available at zero motor speed, which is essential for starting up. On the other hand, the maximum power is usually only available in the upper quarter of the speed spectrum. High vehicle speeds are therefore only associated with high motor speeds. In addition, it is advisable to adjust the load of the engine to lower speeds and higher torques in order to minimize fuel consumption and emissions. A useful transmission spread of vehicles driven purely by ICE is therefore defined by the transmission ratio of the first gear through the required starting characteristics, especially the maximum acceleration and maximum climbing ability without or with trailer, and the maximum speed of the vehicle to be achieved. (cf. [Mit04])

This article describes the approach to the definition of purely electrical drive systems from the three points of view:

- Vehicle longitudinal performance,
- Efficiency, powertrain losses and driving range and
- Shift quality and driving comfort

Typical powertrain configurations with one or two motors is shown in *Fig. 1*.

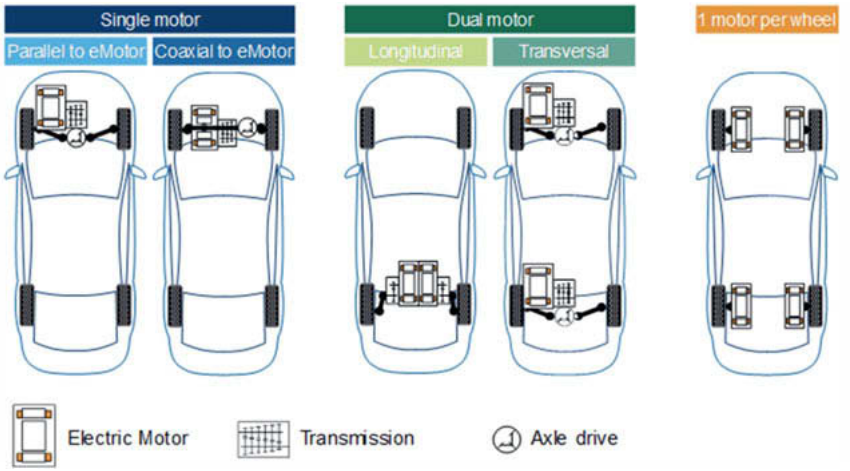


Fig. 1: Typical powertrain configurations

https://doi.org/10.51202/9783181023549 - Generiert durch IP 216.73.216.36, am 19.01.2026, 02:19:31. © Urheberrechtlich geschützter Inhalt. Ohne gesonderte Erlaubnis ist jede urheberrechtliche Nutzung untersagt, insbesondere die Nutzung des Inhalts im Zusammenhang mit, für oder in KI-Systemen, KI-Modellen oder Generativen Sprachmodellen.

The most common configuration by far is a single motor whose output shafts is running in parallel to the electric motor shaft (*Fig. 1* left), used e. g. for Nissan LEAF, BMW i3. Coaxial derivate are used to save package space especial on rear axles of convertible electric vehicles ([Pi18]). Because of its high traction power availability the transversal dual motor configuration (*Fig. 1* 4th picture) is often used in sports cars with a high acceleration demand, e. g. Tesla Model S P100D. To improve the transversal dynamic of the vehicle, both electric machines can be applied to one axle with a separate gear-set for each wheel ([Pi18]) or with an easy singular gear-set to summate the electric power on one axle drive ([Kreis18]).

Consideration of the vehicle performance

This physical law also applies to electrically powered vehicles. The balancing act between maximum motor speed on the one hand and maximum performance during starting on the other, but also efficiency and noise development during driving, has already been described several times in the literature (cf. [Alt15], [Gas17], [IAV11] & [Xu18]). The variance of the powertrain parameters is considerably greater here than with purely combustion engine drives. It is easier to define a powertrain configuration with only one, usually multi-stage, single-speed transmission than with purely ICE-powered vehicles. Thus, in addition to the maximum torque and maximum power of the electric motor, its maximum speed - within technical limits - can also be adjusted relatively easily. Both, speed and torque are necessary in order to reconcile the requirements of starting characteristics and maximum vehicle speed with a single-speed transmission. While, in accordance with the laws of growth for electrical machines, the maximum torque of electrical machines can be increased quadratic with the diameter and linearly with the length of the active parts involved in torque generation. Without any impact to the pack-age space, this increase is generally only possible with an increase in the phase current. This effect is strong non-linear declining and feasible under high thermal loads of the machine. Increasing the maximum motor speed does not pose an electromagnetic challenge. Limits are set here in the voltage applied to the inverter, i. e. either the battery voltage or a so-called DC/DC-voltage increased by means of a boost converter, or the maximum switching frequency of the connected inverter. The inverter must still be able to switch the current as close as possible to a sinusoidal shape. In the case of highly utilized electric motors based on the principle of asynchronously running rotors (induction ma-chines, IM), a strongly decreasing maximum power can often be observed with the speed. (cf. [Pi18]) The inherent feature of IM is that as the speed increases, the DC-voltage is no longer sufficient to drive the increasing counter-induced voltage and the increasing voltage drops of the currents at the inductors. As a result, the torque and thus the power must drop as the speed

https://doi.org/10.51202/9783181023549 - Generiert durch IP 216.73.216.36, am 19.01.2026, 02:19:31. © Urheberrechtlich geschützter Inhalt. Ohne gesonderte Erlaubnis ist jede urheberrechtliche Nutzung untersagt, insbesondere die Nutzung des Inhalts im Zusammenhang mit, für oder in KI-Systemen, KI-Modellen oder Generativen Sprachmodellen.

continues to rise. Typical characteristic curves for IM and PMSM are shown in *Fig. 2*. This effect is not applied to permanently exited (PMSM) or wound field synchronous (WFSM) machines.

An upshift, i. e. the change to a gear with a lower reduction ratio, will thus lead to a significantly increased acceleration with a drive with IM, an effect which does not occur with purely combustion engine drives.

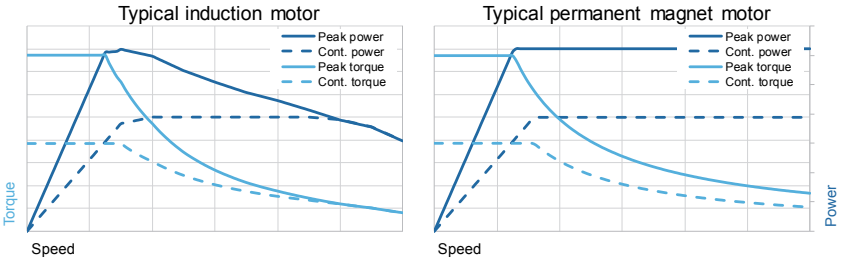


Fig. 2: Typical characteristic power and torque curves of induction and permanent magnet synchronous machines

Mechanically, the speed of the rotors is limited by the following aspects:

- maximum sliding speed of the seals on the shaft (e. g. radial shaft seals),
- maximum load on the cages of rolling bearings as a result of smooth running, sealing function and centrifugal forces,
- maximum load, e. g. on the stack of sheets or the rotor winding, due to centrifugal force and
- maximum sliding and rolling speed at the first tooth contact.

By improving the materials used, the technical limits for bearings and seals have been continuously improved in recent years. The adhesion of the lubricant to the tooth contact can also be achieved by better chemical compounds. Permanent lubrication can also be achieved by a forced supply of lubricant, for example via an additional oil pump. The additional costs are obvious. In addition, there are linearly increasing, speed-dependent losses, such as friction losses on bearings and seals or the ventilation losses of the rotating rotor.

https://doi.org/10.51202/9783181023549 - Generiert durch IP 216.73.216.36, am 19.01.2026, 02:19:31. © Urheberrechtlich geschützter Inhalt. Ohne gesonderte Erlaubnis ist jede urheberrechtliche Nutzung untersagt, insbesondere die Nutzung des Inhalts im Zusammenhang mit, für oder in KI-Systemen, KI-Modellen oder Generativen Sprachmodellen.

The technical facts described above are also interpreted differently by the state of the art. Most of all passenger cars on the market with electrically driven axles, purely electric vehicles or P4-hybrids use a single-speed transmission with a fixed reduction ratio. Some of them cannot be shifted under load. ([Alt15], [Gas17]])

From a technical point of view, multi-motor concepts are very interesting. While a distribution of the traction power over several drive axles has a positive influence on the longitudinal dynamics. With one motor per wheel, the transverse dynamics can be significantly improved by electrical "torque vectoring" and starting on different surfaces, so-called µ-split starting. The recuperation potential is also higher - especially at high speeds - if it is distributed over two axes. However, the cost of two drives per vehicle is significantly higher than the cost of a multi-stage drive concept with only one motor. The Porsche Taycan drives and Tesla's "D" models serve as examples. The wheel tor-ques required for maximum acceleration and maximum climbing ability can also be rep-resented by two smaller electric motors on one axle (see [Krei18]). This adds up the mechanical and monetary effort of two motors and inverters with a more complex gearbox and a more complex electric motor control system.

In order to protect the electric drive in P4 hybrid drives, such as the BMW 225xe iPerformance Active Tourer, against excessive speed, various coupling devices are used which mechanically decouple the electric motor from the drive wheel of the vehicle. The vehicle's maximum speed can no longer be reached with electrical support. In the case of multiple-speed drives, this is achieved by activating the neutral position, whereby the electric motor can set an undetermined speed level on the electric motor as a result of internal friction in open switching elements (cf. source [Alt15], [Gas17]). Whether the driver can be expected to shift gears by interrupting the tractive effort varies from manufacturer to manufacturer. In the BMW i8 example, the gears are only shifted in driving situations in which no tractive force moves the vehicle. ([Alt15])

The following chapters analyze the technical feasibility of gearshifts as a function of the step changes to be shifted, as well as the energy flows and efficiency of multi-speed transmissions compared to single-speed transmissions and the influence of the electric machine topology on this.

Consideration of powertrain losses

In vehicles with internal combustion engines, the trend is towards more supercharged engines with more and more gears in the subsequent transmission. The aim here is to make the most of the combustion engine map and the tractive effort offered by the combustion engine to meet

https://doi.org/10.51202/9783181023549 - Generiert durch IP 216.73.216.36, am 19.01.2026, 02:19:31. © Urheberrechtlich geschützter Inhalt. Ohne gesonderte Erlaubnis ist jede urheberrechtliche Nutzung untersagt, insbesondere die Nutzung des Inhalts im Zusammenhang mit, für oder in KI-Systemen, KI-Modellen oder Generativen Sprachmodellen.

the vehicle's tractive effort requirements. There are similar trends in the area of purely electric vehicles. But, due to the significantly lower losses of the electric drive-train with multi-speeds because of speed related losses. However, it is no longer sufficient to integrate only more gears in an electric drive. Depending on the con-figuration of the electric motor, the inverter, the battery, cooling system and subsequent transmission, both positive and negative consumption effects can occur.

Based on a modular drive unit, these individual losses of the powertrain for a 1-, 2- or 3-speed drive unit are calculated and summed up in a cycle simulation. In addition, three different vehicle classes, two different electric motor types and several drive cycles will be compared. While the strengths of the 1-speed drive lie primarily in cost efficiency and compactness, the 2- and 3-speed should provide sales arguments through efficiency, better fuel consumption and as said in the first chapter more favorable driving performance characteristics. (*Fig. 3*)

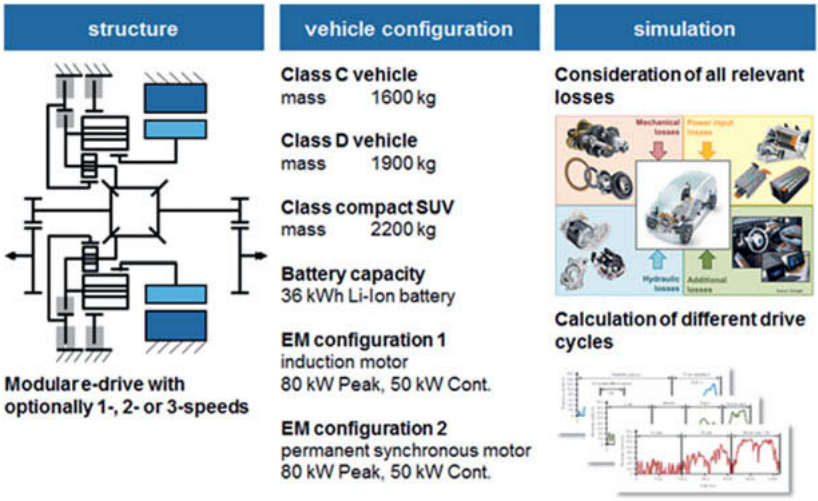


Fig. 3: Basic information about the longitudinal simulation

At the beginning, a c-class vehicle with IM with squirrel cage made of copper will regarded. As a result of the simulation, the vehicle ranges of the individual powertrains in different drive cycles are shown below. All have a $36\ kWh$ battery as a basis and must meet the minimum requirements of $30\ \%$ climbing ability and $130\ km/h$ maximum speed [IAV11].

https://doi.org/10.51202/9783181023549 - Generiert durch IP 216.73.216.36, am 19.01.2026, 02:19:31. © Urheberrechtlich geschützter Inhalt. Ohne gesonderte Erlaubnis ist jede urheberrechtliche Nutzung untersagt, insbesondere die Nutzung des Inhalts im Zusammenhang mit, für oder in KI-Systemen, KI-Modellen oder Generativen Sprachmodellen.

A more detailed comparison of the drive-units shows, that the percentage of electrical losses decreases with the number of speeds. Further the larger the road and highway section of the speed profile, the lower the mechanical losses of the multi-speed concepts because of their lower speed depended losses. In addition, the increasing power shift losses in the WLTP and Artemis cycles prove to be a disadvantage for the higher step (ratio spread 2.6) of the 2-speed transmission. Efficiency advantages of the 2-speed drive in the NEDC, which is no more frequently booked, therefore cannot confirmed in the more realistic cycle evaluations of the WLTP and Artemis. It has shown that both, in the WLTP and in the Artemis, the 3-speed-drive performs best. In addition, the range decreases in both cycles due to the increasing driving resistances and loss of components. In the WLTP, only marginal differences between the three configurations are discernible. Even in the combined Artemis cycle, there is a consumption advantage of only 2.26 % compared to the direct drive. The savings potential hardly justifies the additional expenditure for development, production and application of the more complex drive units in the cycle evaluations presented here. In this respect, the multi-speed transmissions in combination with used IM offers only advantages in terms of maximum speed and the acceleration capacity of the vehicle. A significant range advantage is eliminate.

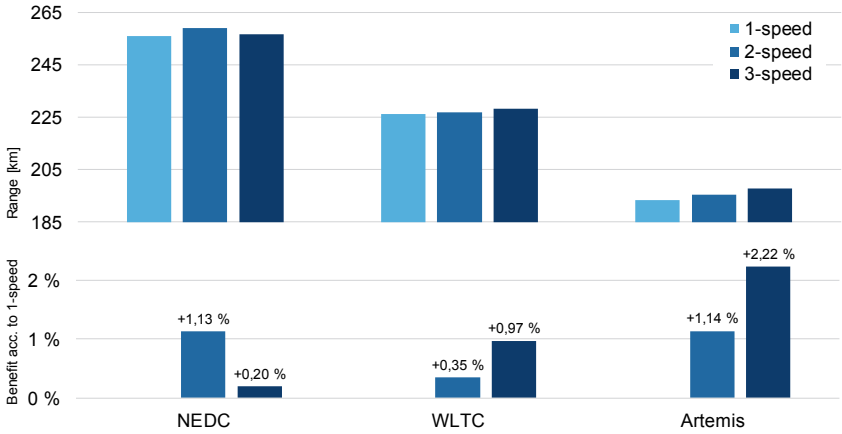


Fig. 4: Simulation results of different drive cycles using the c-class vehicle with 1-, 2- or 3-speeds and an induction motor

The tendency to change a gear based on a more efficient operating point is unexpectedly present, like shown in *Fig. 5* for the WLTP. The percentage of upper gears is over 40 %, which

https://doi.org/10.51202/9783181023549 - Generiert durch IP 216.73.216.36, am 19.01.2026, 02:19:31. © Urheberrechtlich geschützter Inhalt. Ohne gesonderte Erlaubnis ist jede urheberrechtliche Nutzung untersagt, insbesondere die Nutzung des Inhalts im Zusammenhang mit, für oder in KI-Systemen, KI-Modellen oder Generativen Sprachmodellen.

is close to the percentage of first gears. The reduction of the load-independent mechanical losses, which are reduce by the upshifts, is not sufficient to compensate the additional mechanical loss mechanisms, such as switching elements, bearings, gear meshing and rotary feedthroughs, in the multi-speed drives. Nevertheless, the main blocking point for a better energy consumption of the multi-speed-units is the efficiency map of the IM. The additional losses like stray load loss, rotor loss and copper losses in comparison to permanent magnet motors results in an efficiency map, which is more trained in high-speed ranges. Therefore, the main operating points of the drive cycles miss the map range of highest efficiency.

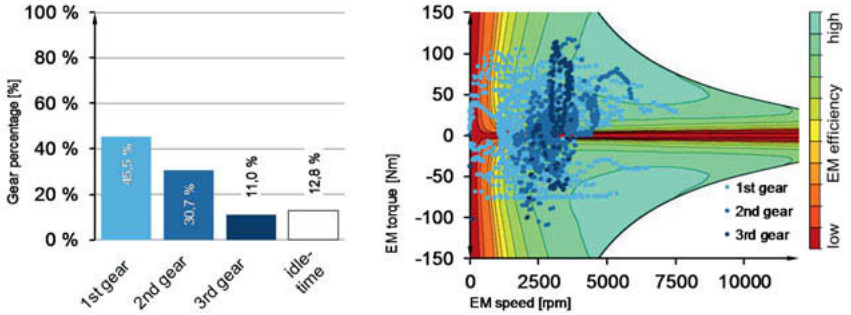


Fig. 5: Gear percentage and torque/speed points in EM efficiency map of the induction motor with using the 3-speed-configuration and a c-class vehicle in WLTP drive cycle simulation

The previous evaluations have shown that no significant range advantages can be achieve with multiple-speed drives and the chosen IM. An essential sales argument for the more complex drive configurations is lost. The aim of an electric motor optimization should therefore be to further increase the consumption advantages of the 2- and 3-speed drive. An electric motor that promises lower power losses in the drive system already in the semi-load range is more advantageous. During a gear change to higher second or third gear, the torque demand on the motor increases. Such a motor is difficult or impossible to map with the aid of an IM. In contrast, synchronous motors can designed precisely by adapting a wide range of parameters. The peak and rated power as well as the associated corner speeds have remained the same. Thanks to a high proportion of reluctance torque, the new permanently excited synchronous motor, in contrast to the IM, can maintain $80\ kW$ over the entire speed

https://doi.org/10.51202/9783181023549 - Generiert durch IP 216.73.216.36, am 19.01.2026, 02:19:31. © Urheberrechtlich geschützter Inhalt. Ohne gesonderte Erlaubnis ist jede urheberrechtliche Nutzung untersagt, insbesondere die Nutzung des Inhalts im Zusammenhang mit, für oder in KI-Systemen, KI-Modellen oder Generativen Sprachmodellen.

range (*Fig. 2*). The efficiency map of the motor in *Fig. 6* fulfils the criteria of the map characteristic. From $2.000\ rpm$ to $6.000\ rpm$, high efficiency is achieve up to the torque limit. With increasing speed, it decreases again. Even in the range of high torques, the PMSM machine is considerably better than the self-excited three-phase motor.

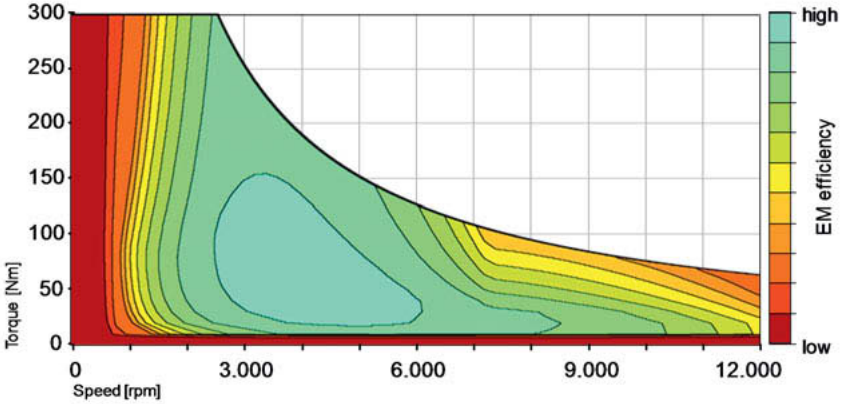


Fig. 6: Efficiency map of the optimized synchronous motor including inverter losses

Finally, the range advantage shows what an optimized drive with a permanently excited synchronous machine makes possible. *Fig. 7* shows this comparison for various vehicle variants in the WLTP cycle. In all three-column diagrams, the 3-speed drive with the longest range is at the top. The 2-speed version follows closely behind, combining the advantage of better map utilization with lower mechanical losses in one system. The additional mechanical losses due to the additional intermediate gear cannot be sufficiently compensated by the 3-speed compared to the 2-speed. The 1-speed design falls back due to increasing electrical losses in the high-speed range. In the SUV alone, there are over $5\ \%$ lower fuel consumption values in the multi-speed drives. In the D-Class vehicle, the figure for the 2-speed variant is $4.1\ \%$. A comparison of the two electric motors in the c-class vehicle also shows (*Fig. 4* center, *Fig. 6* left) that the range in the 2-speed and 3-speed configurations is increase again by approximately $3\ \%$. This also fulfils the goal of tapping further potential for multi-speed drives with the optimized electric motor.

https://doi.org/10.51202/9783181023549 - Generiert durch IP 216.73.216.36, am 19.01.2026, 02:19:31. © Urheberrechtlich geschützter Inhalt. Ohne gesonderte Erlaubnis ist jede urheberrechtliche Nutzung untersagt, insbesondere die Nutzung des Inhalts im Zusammenhang mit, für oder in KI-Systemen, KI-Modellen oder Generativen Sprachmodellen.

The full potential of the 2- or 3-speed drive is then show in the Artemis cycle, which, due to the higher performance requirements placed on the c-class vehicle, also offers more fuel consumption advantages for the multi-speed drives (*Fig. 8* left side). The 2-speed requires 7.5 % less energy, the 3-speed even 8.2 % less. The effectiveness of the characteristic map optimization of the synchronous machine can clearly see in the utilization of the efficiency map. Almost all points of the 2nd and 3rd gear are in the most fuel-efficient map range (*Fig. 8* right side).

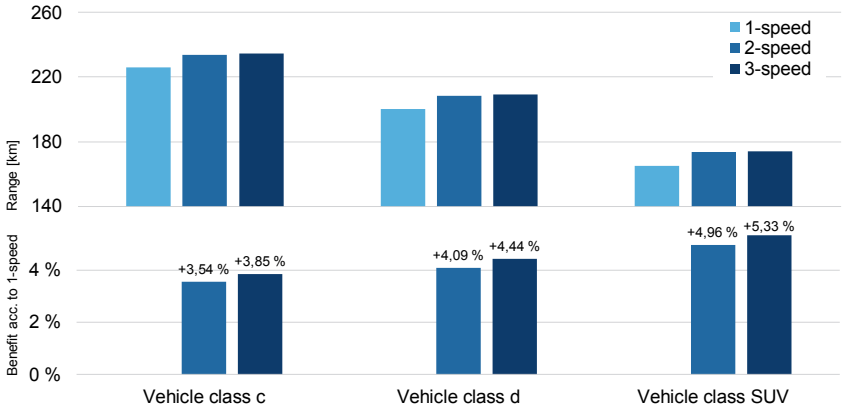


Fig. 7: Simulation results of different vehicle configurations with 1-, 2- or 3-speeds and an optimized permanent synchronous motor in a WLTP drive cycle simulation

Fig. 9 shows all losses in the Artemis cycle at the components divided into main groups. With regard to these losses, it can be clearly seen once again what a considerable proportion of the electrical losses are due to the overall drivetrain efficiency. If these can be reduce, there remains a clear advantage for the drive. It is clear to see that the mechanical losses in the multispeed drives increase due to the higher number of mechanical components. In the illustrated cycle and powertrain with 2- and 3-speed drive, however, the losses are not so high that the electrical benefit are compensated once again. The hydraulic losses can even be reduce, despite the additional actuating power for the switching elements.

In summary, the 2- and 3-speed drive in the configuration with asynchronous machine cannot sufficiently meet the requirement for more range for the electric vehicle. With a maximum consumption reduction of 2.2 %, the additional expense for the much more complex and expensive drives cannot be justified. Nevertheless, the drives are characterize by better acceleration capacity and higher top speeds.

https://doi.org/10.51202/9783181023549 - Generiert durch IP 216.73.216.36, am 19.01.2026, 02:19:31. © Urheberrechtlich geschützter Inhalt. Ohne gesonderte Erlaubnis ist jede urheberrechtliche Nutzung untersagt, insbesondere die Nutzung des Inhalts im Zusammenhang mit, für oder in KI-Systemen, KI-Modellen oder Generativen Sprachmodellen.

From a technical point of view, it is therefore advisable to individually optimize electric drives for future developments. The most important point is and remains energy efficiency and the associated range of the vehicle. If there are no significant differences here, the multispeed system loses an important sales argument. Unfavorably selected map characteristic or excessive mechanical losses can destroy the consumption advantage.

According to technical assessment, the 2-speed drive with synchronous machine best meets the evaluation criteria. The drive variant enables efficiencies of over 84 % over a wide range. In addition, the selected vehicles also achieve very good range results in all cycle calculations compared to the 3-speed drive. Due to the performance characteristics of the synchronous machine and the 2nd gear, the drive permits acceptable driving performance characteristics.

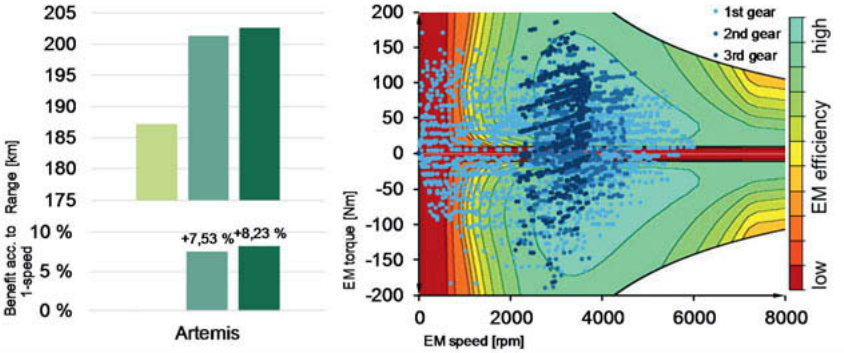


Fig. 8: Simulation results of c-class with 1-, 2- or 3-speeds and the permanent synchronous motor in an Artemis drive cycle simulation and torque/speed points in efficiency map of the optimized PMSM using the 3-speed configuration and a c-class in these simulation

The investigations in the next section will show whether the large spread of 2.6 in the 2-speed drive leads to significant loss of comfort, excessive heat input in the shift element and high shifting times in comparison to the 3-speed.

https://doi.org/10.51202/9783181023549 - Generiert durch IP 216.73.216.36, am 19.01.2026, 02:19:31. © Urheberrechtlich geschützter Inhalt. Ohne gesonderte Erlaubnis ist jede urheberrechtliche Nutzung untersagt, insbesondere die Nutzung des Inhalts im Zusammenhang mit, für oder in KI-Systemen, KI-Modellen oder Generativen Sprachmodellen.

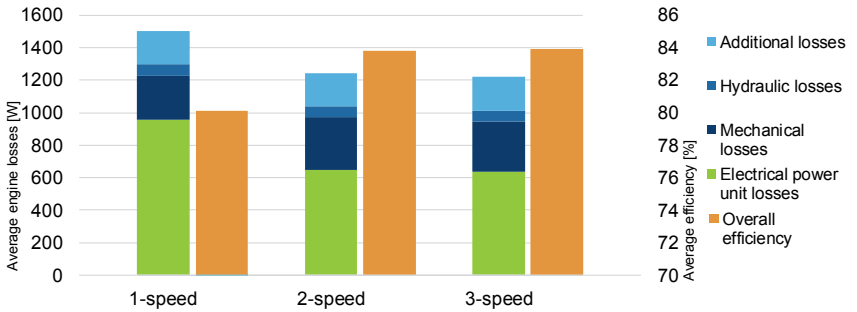


Fig. 9: Individual losses of the components of c-class with 1-, 2- or 3-speeds and the permanent synchronous motor in an Artemis drive cycle simulation

Consideration of shift quality and driving comfort

In this chapter, we will focus on the question: how many speeds an electric vehicle need from the point of controllability, comfort and durability. Therefore we will setup a digital prototype with a full physical based vehicle model and real transmission control algorithm and an objective shift evaluation in a closed loop simulation. The investigation comprise:

The combination of these aspects lead to a high number of simulation runs. Here we will show an overview of the most important perspectives.

To analyze controllability, comfort and durability we will focus on objective physical shifting criteria. The shifting comfort, respective shift quality, is considered by evaluating the power-up, power-down, coast-up and coats-down shift using an IM and a PMSM.

For the shift-quality analysis different gear steps are considered. Using the PMSM gear steps from $\varphi_{12} = 1.4$ to 3.4, using the IM the speed steps from 1.4 to 4.4 are simulated. The simulation is performed with IAVs Velodyn (Vehicle Longitudinal Dynamics). Velodyn is an add-on software for Matlab/Simulink and simplified the usage and development of vehicle powertrain models. The simulation parameters used here are vehicle data for compact class ($m = 1600\ kg$) with rear wheel drive. *Fig. 10* shows the general structure of the simulation model in IAV Velodyn. All blocks are connected by two bus systems, a signal bus and a control bus. For our simulations two different electric machines are considered, the IM and PMSM. Both with a maximum torque of $300\ Nm$ and a maximum power of $80\ kW$. One boundary condition was the usage of a power-shift transmission. Due to fast shiftable operation a double clutch transmission (DCT) was chosen with a total area of $A_C = 26749.1\ mm^2$ for each clutch.

https://doi.org/10.51202/9783181023549 - Generiert durch IP 216.73.216.36, am 19.01.2026, 02:19:31. © Urheberrechtlich geschützter Inhalt. Ohne gesonderte Erlaubnis ist jede urheberrechtliche Nutzung untersagt, insbesondere die Nutzung des Inhalts im Zusammenhang mit, für oder in KI-Systemen, KI-Modellen oder Generativen Sprachmodellen.

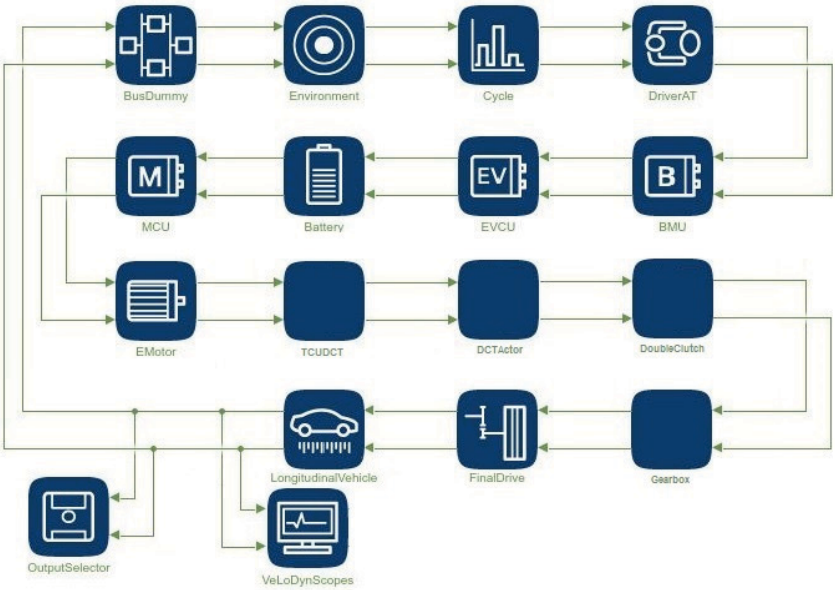


Fig. 10: Structure of the simulation model in IAV Velodyn

To evaluate the shifting process, three different criteria are used:

- First criteria is the vehicle jerk, derived from the acceleration gradient during shifting. On the one hand there is the positive acceleration gradient j_{pos} and on the other hand the negative acceleration gradient j_{neg}. The classification of j_{pos} and j_{neg} are considered to be comfortable with an ICE between $2.5\ m/s^3$ and $5\ m/s^3$. These values are empirical values. So the first criteria j_{pos_max} and j_{neg_max} are limited to $5\ m/s^3$.
- The second evaluation criteria is the limitation of friction energy penetration (heat input) into the clutches, which represents the durability aspect, The maximum friction energy is determined by using the total area of the clutch AC and the permitted specific heat input q_{AE}. The following equation shows the correlation:

$$E_{f_max} = A_C \cdot q_{AE}$$

$$q_{AE} \text{ [OBJ] } q_{AE} = 1.5\ J/mm^2 \text{ [OBJ] } q_{AE} = 2.0\ J/mm^2$$

$$E_{f_{max\ \ ps}} = A_C \cdot q_{AE_{ps}} = 26749.1\ mm^2 \cdot 1.5 \frac{J}{mm^2} = 40.27\ kJ$$

https://doi.org/10.51202/9783181023549 - Generiert durch IP 216.73.216.36, am 19.01.2026, 02:19:31. © Urheberrechtlich geschützter Inhalt. Ohne gesonderte Erlaubnis ist jede urheberrechtliche Nutzung untersagt, insbesondere die Nutzung des Inhalts im Zusammenhang mit, für oder in KI-Systemen, KI-Modellen oder Generativen Sprachmodellen.

$$E_{f_max_sbs} = A_C \cdot q_{AE_{sbs}} = 26749.1\ mm^2 \cdot 2.5 \frac{J}{mm^2} = 53.70\ kJ$$

- The third shift evaluation criteria is the shifting time. With an ICE the empirical values for the shifting time during of power up-shifts are up to 1.8 seconds (duration for torque swap and speed sync). Though, we limit the maximum shifting time t_{shift} for all investigations as boundary condition to 1.8 seconds.

Fig. 11 shows the shifting point for the gear step of 2.4. We define the shifting points that the power of the electrical machine before and after the shift is at the same value. The figure on the left side shows the IM, the right side shows the PMSM. Although the maximum power of both electrical machines is the same, the mean power during the shift using an IM is less than using the PMSM.

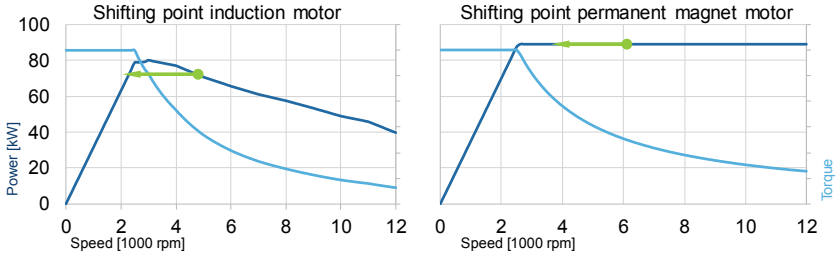


Fig. 11: Shifting points for IM and PMSM from 1st to 2nd speed

Fig. 12 illustrates an exemplary power up-shift with the gear step of 2.4 by using the PMSM, to explain the behavior of speed, torque and acceleration characteristics.
At the beginning there is the torque swap phase (from $6.4\ s$ to $6.8\ s$), where the torque of the electric machine is transferred from the off going clutch 1 to the oncoming clutch 2. The torque swap results in a drop of acceleration due to less torque at the wheel. The second phase is the speed synchronization (from $6.8\ s$ to $7.9\ s$). Here the speed of the electric machine is pulled down to the speed level of shaft 2 by the oncoming clutch. The acceleration is rising again until the oncoming clutch is closed. The target during the application is to get a homogeneous and monotonic slope of acceleration during the speed sync. The execution of the other simulations are performed analogue.

https://doi.org/10.51202/9783181023549 - Generiert durch IP 216.73.216.36, am 19.01.2026, 02:19:31. © Urheberrechtlich geschützter Inhalt. Ohne gesonderte Erlaubnis ist jede urheberrechtliche Nutzung untersagt, insbesondere die Nutzung des Inhalts im Zusammenhang mit, für oder in KI-Systemen, KI-Modellen oder Generativen Sprachmodellen.

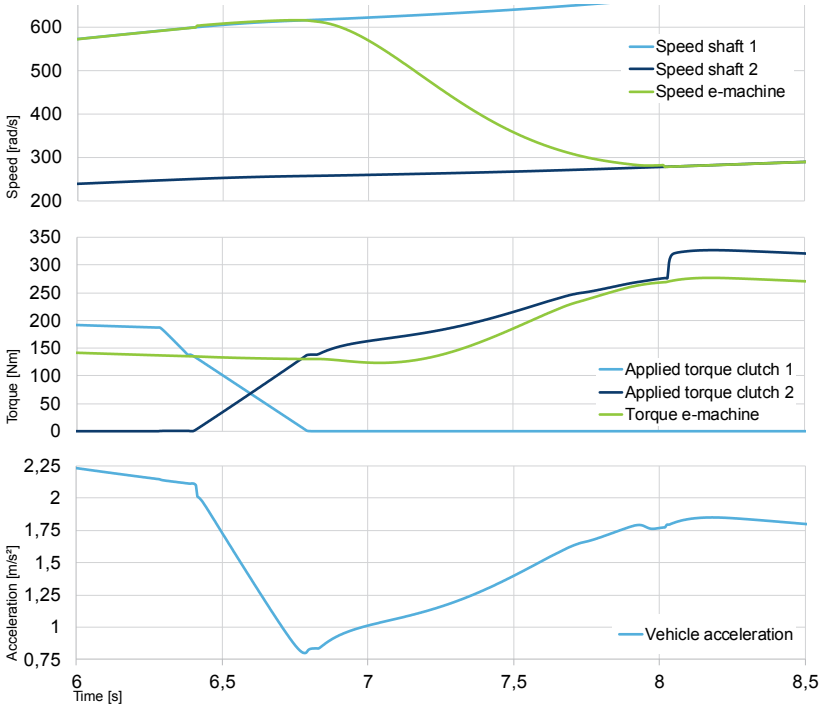


Fig. 12: Power up-shift with gear step 2.4

Fig. 13 shows an exemplary graph of a power down-shift. Here the order of torque swap and speed sync is reverse to the power up-shift. From $22.0\ s$ to $22.4\ s$ the off going clutch is opening and the speed of the PSM is rising until it has harmonized with the speed of the oncoming clutch. From $22.4\ s$ to $22.8\ s$ the torque is now handed over from the off going to the oncoming clutch. It can be seen that the acceleration is rising nearly with a constant slope up to the maximum acceleration. The target of the application was to get this constant slope in the acceleration curve.

https://doi.org/10.51202/9783181023549 - Generiert durch IP 216.73.216.36, am 19.01.2026, 02:19:31. © Urheberrechtlich geschützter Inhalt. Ohne gesonderte Erlaubnis ist jede urheberrechtliche Nutzung untersagt, insbesondere die Nutzung des Inhalts im Zusammenhang mit, für oder in KI-Systemen, KI-Modellen oder Generativen Sprachmodellen.

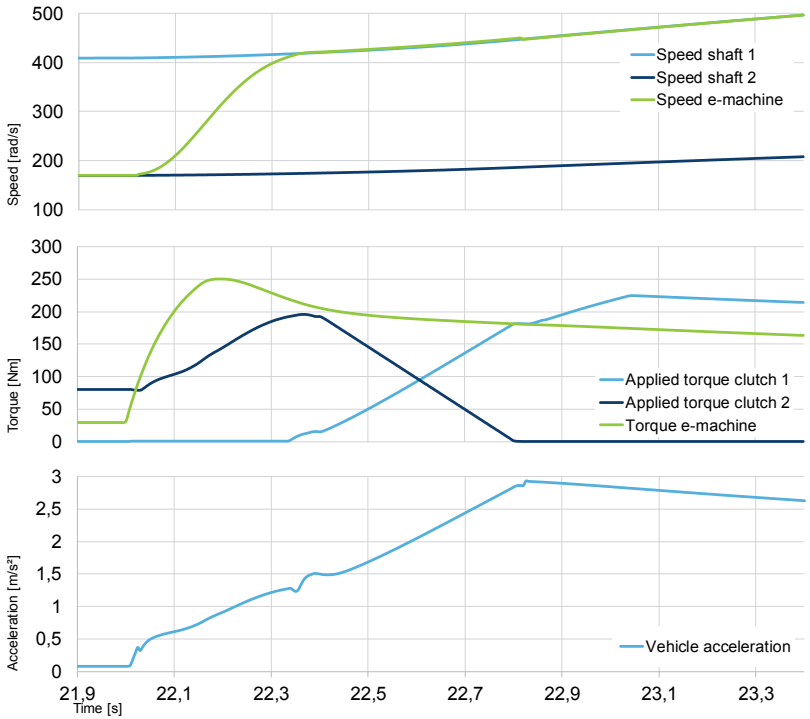


Fig. 13: Power down-shift with gear step 2.4

Fig. 14 highlights an exemplary cost up-shift. At first the off-going clutch is opened. To reduce the motor speed faster, the PSM is generating electricity and charging the battery (from $26.1\ s$ to $27.5\ s$). After the speed of PSM and oncoming clutch is identical the on-coming clutch is closing and the shift is complete. The ideal application would be that the acceleration during the shift is constant. During this coast up-shift the acceleration was between $-0.20\ m/s^2$ and $-0.25\ m/s^2$.

https://doi.org/10.51202/9783181023549 - Generiert durch IP 216.73.216.36, am 19.01.2026, 02:19:31. © Urheberrechtlich geschützter Inhalt. Ohne gesonderte Erlaubnis ist jede urheberrechtliche Nutzung untersagt, insbesondere die Nutzung des Inhalts im Zusammenhang mit, für oder in KI-Systemen, KI-Modellen oder Generativen Sprachmodellen.

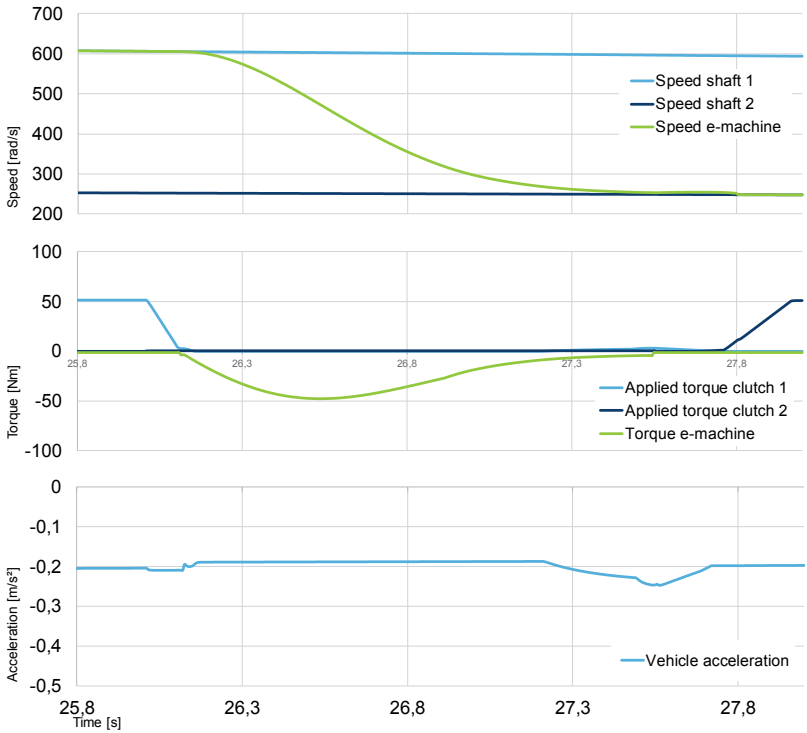


Fig. 14: Coast up-shift with gear step 2.4

Fig. 15 is showing the last shifting type, the coast down-shift. At the beginning of the shift the torque is handed over from off going to oncoming clutch ($30.10\ s$ to $30.11\ s$). After the torque swap the motor speed has to be increased to the level of the closing clutch. This is achieved by additional pressure on the closing clutch. The PSM is additionally producing moment to speed up faster. After the speed is identical the coast down-shift is completed.

https://doi.org/10.51202/9783181023549 - Generiert durch IP 216.73.216.36, am 19.01.2026, 02:19:31. © Urheberrechtlich geschützter Inhalt. Ohne gesonderte Erlaubnis ist jede urheberrechtliche Nutzung untersagt, insbesondere die Nutzung des Inhalts im Zusammenhang mit, für oder in KI-Systemen, KI-Modellen oder Generativen Sprachmodellen.

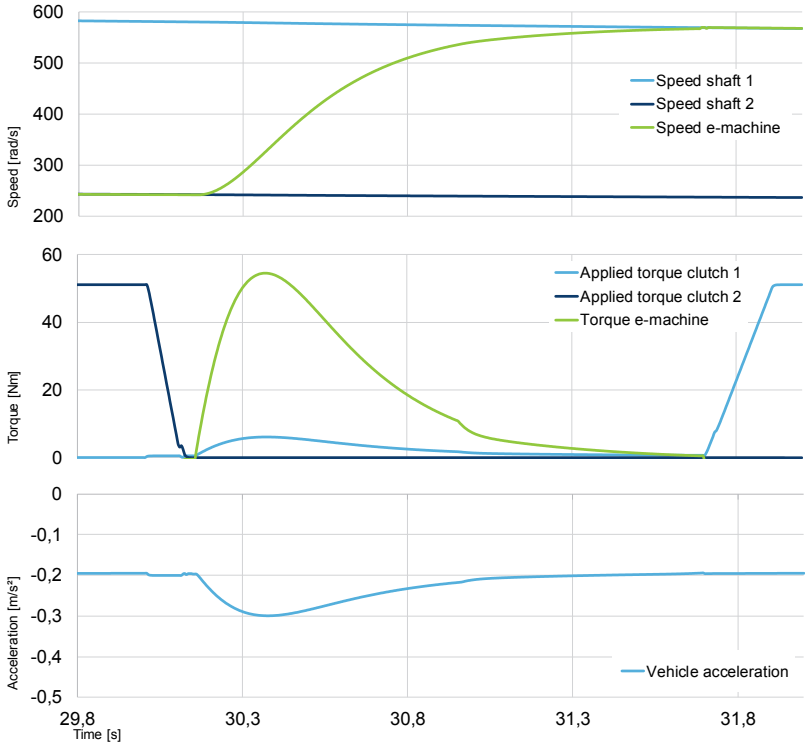


Fig. 15: Coast down-shift with gear step 2.4

For evaluating the shifting process objectively the IAV Tool Transmission Drivability Toolbox (TDT) is used. TDT is an automatized tool which determines amongst others the objectives maximal positive and negative acceleration jerk j_{neg} and j_{pos}, the frictional energy of the two clutches E_{f_K1} and E_{f_K2} during shifting and the shifting times t_{shift}, t_{trqswp} and t_{syn}.

Fig. 16 show graphically evaluation of the shifting times and the acceleration gradients. On the upper part of *Fig. 16* the yellow line bounds the time for torque swap, the purple line bounds the time for speed sync. The lower part of *Fig. 16* shows how the maximum positive (orange tangent) and negative (green tangent) jerk is determined. The following results for all gear steps are evaluated analogous.

https://doi.org/10.51202/9783181023549 - Generiert durch IP 216.73.216.36, am 19.01.2026, 02:19:31. © Urheberrechtlich geschützter Inhalt. Ohne gesonderte Erlaubnis ist jede urheberrechtliche Nutzung untersagt, insbesondere die Nutzung des Inhalts im Zusammenhang mit, für oder in KI-Systemen, KI-Modellen oder Generativen Sprachmodellen.

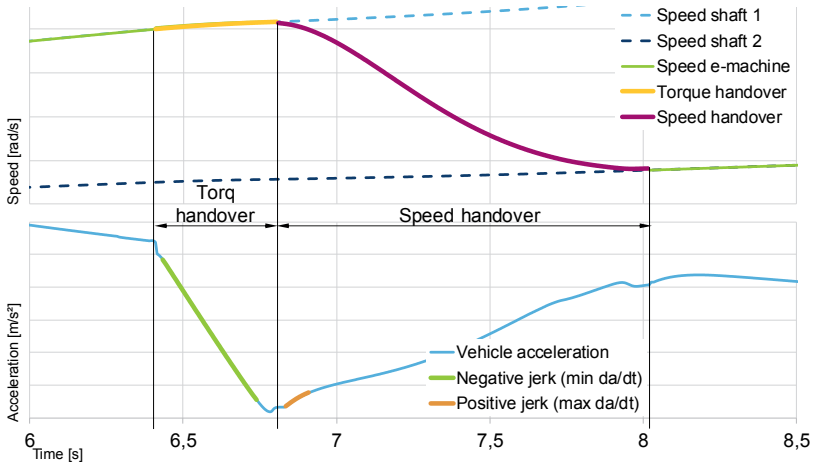


Fig. 16: Evaluation of gear step 2.4 by using TDT

Fig. 17 depict a speed step variation from $\varphi_{12} = 1.4$ to 3.4. The step $\varphi_{12} = 1.4$ is the reference for all next discussions. Shown are the positive and negative acceleration gradient, the heat input of the oncoming and off going clutch and the duration of switch, torque swap and speed synchronization. To have a good base for discussion the positive jerk for all speed steps was calibrated to the same reference value of step of $\varphi_{12} = 1.4$. This was successfully achieved for almost all step changes without one exception for $\varphi_{12} = 3.4$.

The next challenge was the calibration of the negative jerk lower than the reference $\varphi_{12} = 1.4$. This could also be realized under the impact of higher heat input into the clutch, which as a negative consequence to the durability. The middle and lower graphs show, that the heat input at the oncoming clutch increases more and more with rising speed step. The heat input at the off going clutch with a maximum of $1\ kJ$ is very low compared to the heat input at the oncoming clutch.

https://doi.org/10.51202/9783181023549 - Generiert durch IP 216.73.216.36, am 19.01.2026, 02:19:31. © Urheberrechtlich geschützter Inhalt. Ohne gesonderte Erlaubnis ist jede urheberrechtliche Nutzung untersagt, insbesondere die Nutzung des Inhalts im Zusammenhang mit, für oder in KI-Systemen, KI-Modellen oder Generativen Sprachmodellen.

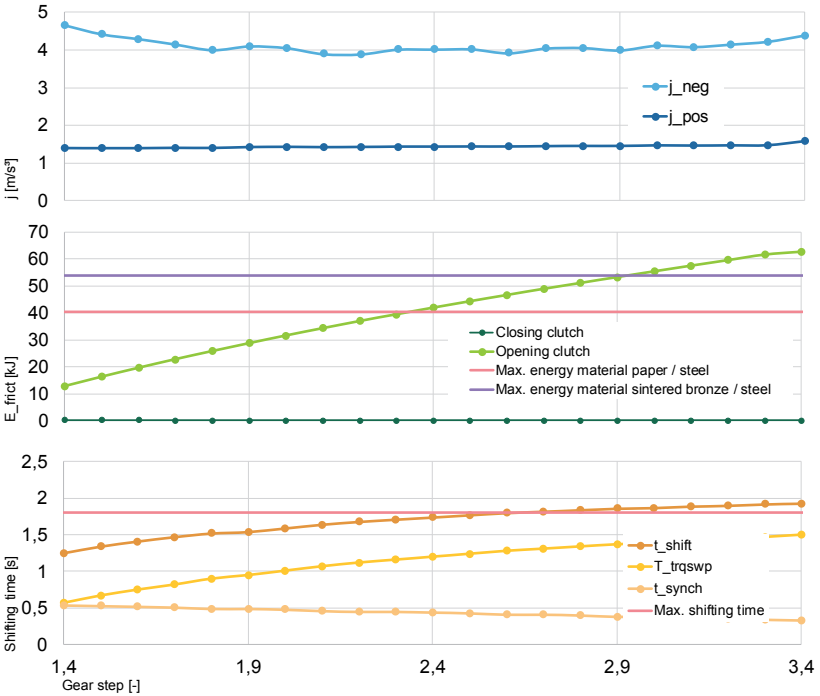


Fig. 17: Analysis of power up shift using a PMSM

The maximum friction energy, which the clutch out of paper and steel can absorb, is $40.27\ kJ$. Under these boundary conditions *Fig. 17* shows, that maximum gear steps up to 2.3 can be realized. Using a clutch out of sintered-bronze and steel would improve the absorption to a maximum energy of $53.70\ kJ$, which increases the maximum gear step to 2.9. If even higher step changes need to be realized, two options can be taken into account. Either the time of speed sync will be reduced, which results in faster shifting and increasing positive jerk, or the surface area of the clutch will be extended, what is limited by the clutch housing design. The effect of faster shifting can be seen in *Fig. 18*.

The maximum heat energy is now set to $40.27\ kJ$. The effects of this limitation results in a rising positive jerk with increasing gear step, which has at least a negative effect on the driving comfort. Though the highest gear step under consideration of a maximum positive jerk value of $5\ m\ /\ s^3$, is $\varphi_{12} = 3.4$.

https://doi.org/10.51202/9783181023549 - Generiert durch IP 216.73.216.36, am 19.01.2026, 02:19:31. © Urheberrechtlich geschützter Inhalt. Ohne gesonderte Erlaubnis ist jede urheberrechtliche Nutzung untersagt, insbesondere die Nutzung des Inhalts im Zusammenhang mit, für oder in KI-Systemen, KI-Modellen oder Generativen Sprachmodellen.

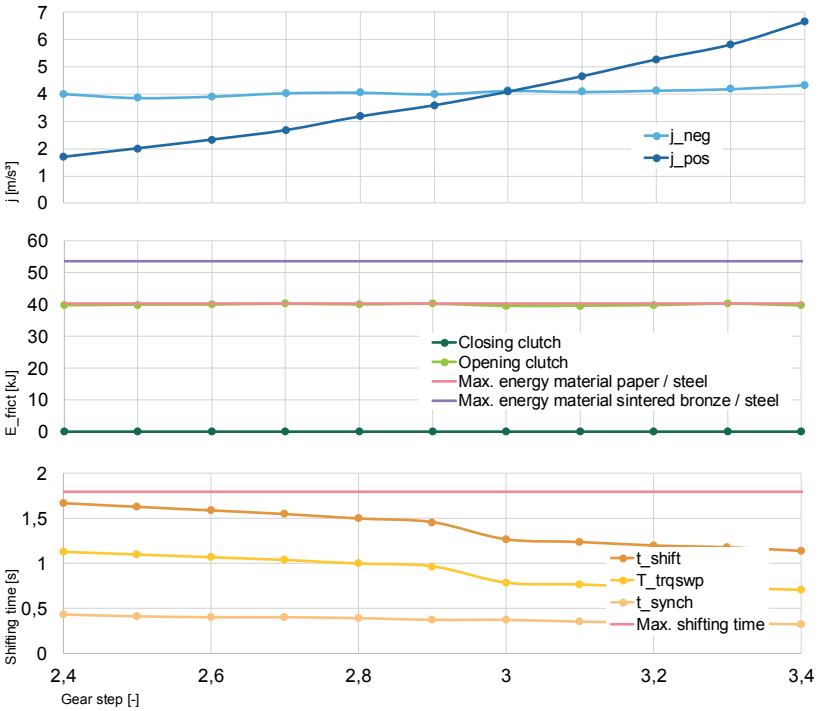


Fig. 18: Analysis of a power up shift using a PMSM with constant frictional energy

As a first conclusion out of the drivability aspects we can summarize, that the maximum gear step is limited to $\varphi_{12} = 2.3$ by using a paper/steel-clutch or 2.9 by using a sintered-bronze/steel-clutch. If a lower comfort is acceptable, even a gear step up to 3.1 is possible under consideration of the paper/steel-clutch.

Now the evaluation of an IM instead of PMSM in combination with a two-speed transmission will be discussed.

Fig. 19 shows again the positive and negative Acceleration gradient, the heat input of on coming and off going clutch and the duration of shifting, torque swap and speed synchronization for the different gear steps from $\varphi_{12} = 1.4$ to 4.4. Here the characteristic is nearly the same as with the PMSM. However, due to the lower power level during shifting a higher gear steps than be achieved with the PMSM.

https://doi.org/10.51202/9783181023549 - Generiert durch IP 216.73.216.36, am 19.01.2026, 02:19:31. © Urheberrechtlich geschützter Inhalt. Ohne gesonderte Erlaubnis ist jede urheberrechtliche Nutzung untersagt, insbesondere die Nutzung des Inhalts im Zusammenhang mit, für oder in KI-Systemen, KI-Modellen oder Generativen Sprachmodellen.

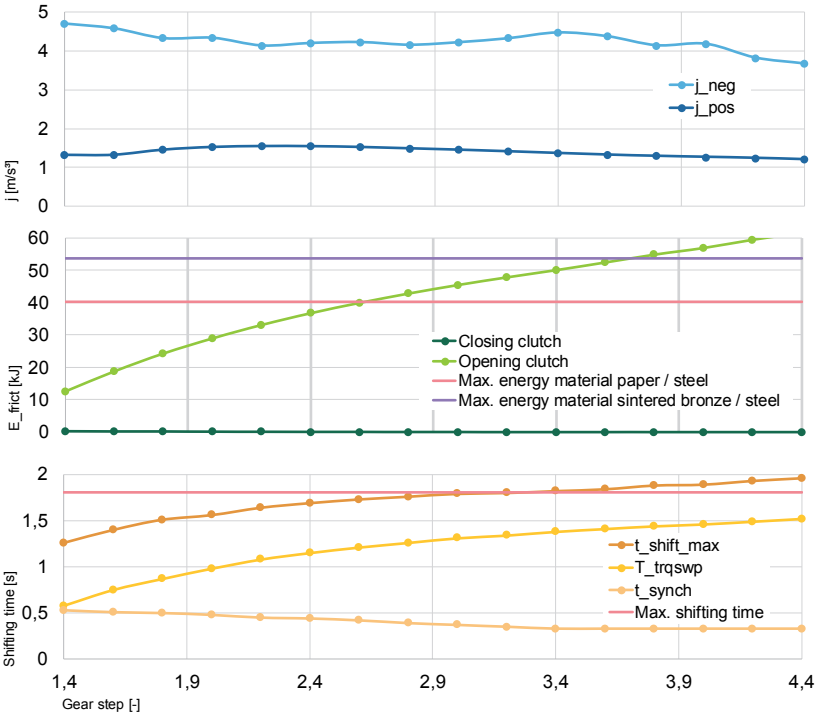


Fig. 19: Analysis of power up shift using an IM

Here the limiting friction energy of the paper/steel-clutch is reached with a gear step of $\varphi_{12} = 2.6$. Using the sintered-bronze/steel-clutch a gear step of $\varphi_{12} = 3.6$ can be achieved. Similar to the PMSM it is possible to use higher gear steps with the ASM by reducing the time of speed sync, or by enlarging the surface area of the clutch.

Fig. 20 shows the effect of reducing the synchronization phase. The allowed maximum heat energy again is set to $40.27\ kJ$. The result of the limitation is the same as using the PMSM. The negative jerk is rising with increasing gear step.

https://doi.org/10.51202/9783181023549 - Generiert durch IP 216.73.216.36, am 19.01.2026, 02:19:31. © Urheberrechtlich geschützter Inhalt. Ohne gesonderte Erlaubnis ist jede urheberrechtliche Nutzung untersagt, insbesondere die Nutzung des Inhalts im Zusammenhang mit, für oder in KI-Systemen, KI-Modellen oder Generativen Sprachmodellen.

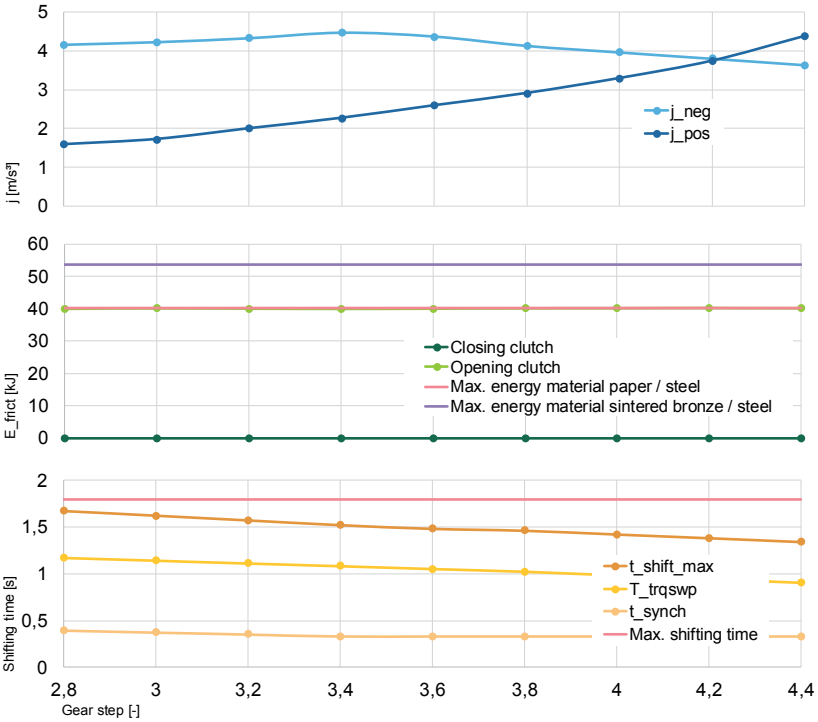


Fig. 20: Analysis of a power up shift using an IM with constant frictional energy

In summary it can be said, that the maximum step change using an ASM is at least 2.6 with a clutch consisting of paper/steel or 3.6 consisting of sintered-bronze/steel. If a lower comfort is accepted, even a gear step up to 4.4 is possible with the paper/steel pairing.

To compare 2-speed and 3-speed transmission with regard to shift quality, the *Fig. 21* explain the evaluation of the power up-shift of a 2-speed transmission with a gear step of 2.6 (blue) and the two power up-shifts of a 3-speed transmission with a gear step of 1.6 each (dark green: shift from gear 1 to 2; light green: shift from gear 2 to 3).

https://doi.org/10.51202/9783181023549 - Generiert durch IP 216.73.216.36, am 19.01.2026, 02:19:31. © Urheberrechtlich geschützter Inhalt. Ohne gesonderte Erlaubnis ist jede urheberrechtliche Nutzung untersagt, insbesondere die Nutzung des Inhalts im Zusammenhang mit, für oder in KI-Systemen, KI-Modellen oder Generativen Sprachmodellen.

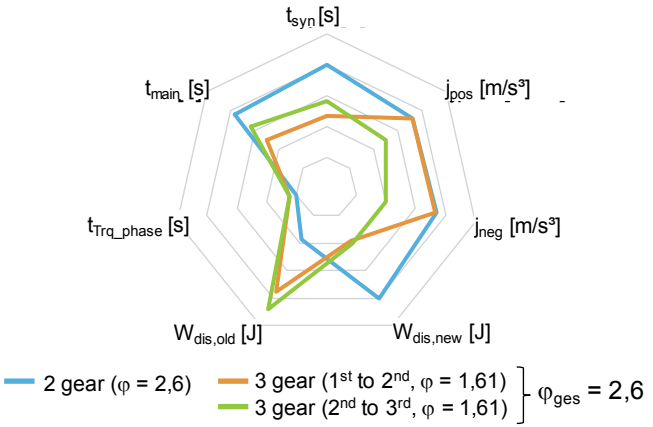


Fig. 21: Comparison of two and three gear transmission with the same total spread

It shows that j_{pos} and j_{neg} of the 2-speed version and the first shift of the 3-speed version are almost the same. However, the shifting time and frictional energy during the shift is less. The second upshift of the 3-speed transmission then is much more comfortable (less j_{pos} and j_{neg}). We can assume that the 3-speed transmission with an approximately same total spread (2.56 vs. 2.6) is at least as comfortable as the 2-speed transmission, and probably more comfortable because of the shorter main shifting time.

Conclusion and outlook – Holistic system approach

The balancing act between maximum motor speed on the one hand and maximum performance during starting on the other, but also efficiency and noise aspects can be better solved using a multi-speed transmission. In case of a single speed system (reducer) a compromise decision has to be made between the achieved output wheel torque and the maximum velocity of the vehicle. With only one ratio this will lead to a bigger electric motor and also higher losses compared with multi-speed optimized machines.

The previous evaluations have shown that no significant cruising range advantages can be achieve with multi-speed drives and the chosen IM. For a PMSM drivetrain with minimum two speeds, a significant benefit in terms of average system losses and vehicle range is reachable. The higher the ratio step, the bigger the consumption advantage of multi-speed systems. The

https://doi.org/10.51202/9783181023549 - Generiert durch IP 216.73.216.36, am 19.01.2026, 02:19:31. © Urheberrechtlich geschützter Inhalt. Ohne gesonderte Erlaubnis ist jede urheberrechtliche Nutzung untersagt, insbesondere die Nutzung des Inhalts im Zusammenhang mit, für oder in KI-Systemen, KI-Modellen oder Generativen Sprachmodellen.

result is a better utilization of the electric motor's map and lower losses of mechanical components.
Under consideration of useful material parameters, a gear step of maximum 3.1 can be achieved with a maximum jerk of $5\ m/s^3$ by using a PMSM. If an IM is applied instead of a PMSM, it is actually possible to achieve gear steps up to 4.4.

The question of whether and when multi-speed systems are available depends not least on the selected boundary conditions for the layout and topology of the electric motor, its inverter and battery, not to forget the transmission itself.
To define a suitable powertrain solution for future vehicles IAV uses an advanced development process that makes intensive use of systematic computer-aided development tools. The tool chain starts with the “Powertrain synthesis” which determines the initial boundaries for the following development steps. Further specialized tools like “Transmission synthesis” and “E-motor synthesis” find the right solutions that fulfil these requirements in a best possible way.
The growing complexity of future powertrains is currently making engineers rethink conventional development processes that focused primarily on optimization of single powertrain components. Increasing significance is being attached to interaction between individual powertrain components, particularly in hybrid powertrains with high levels of electrification as well as conventional and all-electric systems.

Finally the investigations shows that with multi-speed electric drive systems the cruising range can be extended by choosing a dedicated transmission structure with highest mechanical efficiency properties and a multi-speed individual e-motor. Those systems mostly offer an increasing potential for heavier vehicles, because the downsizing and down speeding of the electric motor due to a higher ratio step becomes more important with increasing wheel torques and vehicle velocities. Furthermore, the EM design needs to be considered with changing the transmission type from single- to multi-speeds.

https://doi.org/10.51202/9783181023549 - Generiert durch IP 216.73.216.36, am 19.01.2026, 02:19:31. © Urheberrechtlich geschützter Inhalt. Ohne gesonderte Erlaubnis ist jede urheberrechtliche Nutzung untersagt, insbesondere die Nutzung des Inhalts im Zusammenhang mit, für oder in KI-Systemen, KI-Modellen oder Generativen Sprachmodellen.

References

[Alt15] Altenrath, Th., Gassmann, Th.: “GKN Two Speed Electric Front Axle for the BMW i8”, 15th International VDI Congress Drivetrain for Vehicles, 2015

[Etas18] ETAS, “ETAS - Add-Ons - INCA-FLOW – Guided Calibration and Automation”, https://www.etas.com/en/products/inca_flow-addons.php, accessed October 2018

[Gas17] Gassmann, Th.: “GKN 2-speed Transmission Technology for Hybrid and Electric Vehicle”, 11th International CTI Cymposium, May 2017, USA

[IAV11] Schneider, E.; Fickel, F.; Cebulski, B.; Liebold, J.: “Highly integrative and flexible electric drive unit for electric vehicles”, In: ATZ - Automobiltechnische Zeitschrift, May 2011, Volume 113, Issue 5, pp 360–365

[IAV16] Hauser, M. & von Rüden, Dr. K.: „Optimiertes Fahrverhalten von Nutzfahr-zeu-gen“, In: ATZ Offhighway, November 2016, Volume 9, Issue 4, pp 36–39

[SAS16] Danzer, Ch., Vallon, M. Wukisiewitsch, W., Kratzsch, M.:„Powertrain Syn-thesis for the Design of Complex System Configurations “, In: MTZ worldwide, Sep-tem-ber 2016, Volume 77, Issue 9, pp 42–47 | Cite as

[Krei18] Kreisel, „Kreisel legt 2 Gänge zu“, http://www.kreiselelectric.com/blog/kreisel-legt-2-gaenge-zu, accessed October 2018

[Mit04] Mitschke, M.; Wallentowitz, H.: Dynamik der Kraftfahrzeuge, Berlin, Sprin-ger-Verlag, 2004

[Pi18] Pint, S.; Ardey, Dr. N.; Mendl, Dr. G.; Fröhlich, G.; Straßer, R.; Laudenbach, Dr. Th.; Doerr, Dr. J.: „The new full electric drivetrain from Audi“, 39th International Vienna Motor Symposium, 2018

[Xu18] Xu, X.; Dong, P.; Liu, L.; Zhang, H.: Progress in Automotive Transmission Tech-nology, In: Automotive Innovation, July 2018, Volume 1, Issue 3, pp 187–210

https://doi.org/10.51202/9783181023549 - Generiert durch IP 216.73.216.36, am 19.01.2026, 02:19:31. © Urheberrechtlich geschützter Inhalt. Ohne gesonderte Erlaubnis ist jede urheberrechtliche Nutzung untersagt, insbesondere die Nutzung des Inhalts im Zusammenhang mit, für oder in KI-Systemen, KI-Modellen oder Generativen Sprachmodellen.

https://doi.org/10.51202/9783181023549 - Generiert durch IP 216.73.216.36, am 19.01.2026, 02:19:31. © Urheberrechtlich geschützter Inhalt. Ohne gesonderte Erlaubnis ist jede urheberrechtliche Nutzung untersagt, insbesondere die Nutzung des Inhalts im Zusammenhang mit, für oder in KI-Systemen, KI-Modellen oder Generativen Sprachmodellen.

Optimization of multi-motor electric drive systems

What is the optimum combination in terms of efficiency and cost?

Peter Janssen, M.Sc.**, Ruben Keizer**, M.Eng.,
FEV Europe GmbH;
Tobias Rosen, M.Sc.,
FEV Consulting GmbH, Aachen

Zusammenfassung

Für Elektrofahrzeuge werden derzeit verschiedene Konfigurationen für die EDU (Electric Drive Unit) verwendet. Häufig wird ein Permanent Erregter Synchron Motor (PMSM) eingesetzt, aber auch andere E-Motor Technologien wurden erfolgreich im Markt eingeführt, beispielsweise Renault und Tesla. Fahrzeuge im mittleren bis höheren Leistungsbereich werden oft mit zwei Antrieben an vorder und hinterachse ausgestattet.

In dieser Studie wurden verschiedene Kombinationen von E-Motoren für eine Fahrzeuganwendung mit 230 kW Peak-Systemleistung und 5000 Nm Peak-Achsmoment untersucht. Die Ergebnisse zeigen, dass eine Leistungsverteilung von ca. 30% vorne und 70% hinten empfehlenswert ist. Mit einem richtig gewählten Technologiepaket können in puncto Energieeffizienz bis zu 4% gewonnen werden. Die besten Ergebnisse – sowohl in Bezug auf die Kosten als auch in Bezug auf den Energieverbrauch werden mit einer Kombination von zwei unterschiedlichen E-Motor Technologien erzielt, zum Beispiel mit einem ASM auf der Hinterachse und einem PMSM oder EESM auf der Vorderachse.

Abstract

Today´s electric vehicles are equipped with various types of electric drive units (EDU). Today the most commonly used e-motor type is the Permanent Magnet Synchronous Motor (PMSM). Other technologies are also used successfully (e.g. by Tesla, Renault). In vehicles in the mid to high-power range also the use of two EDUs is observed more often. This paper describes a study, in which different power splits and different e-motor types for a 230 kW/5000Nm (peak values) vehicle were investigated. The study shows that a split of installed power of about 30% on the front axle and 70% on the rear can be recommended.

By using a smart combination of e-motor types, for example an ASM on the rear axle and a EESM or PMSM on the front axle, energy efficiency can be increased significantly (up to 4%) compared to a 2WD version with moderate cost increase.

https://doi.org/10.51202/9783181023549 - Generiert durch IP 216.73.216.36, am 19.01.2026, 02:19:31. © Urheberrechtlich geschützter Inhalt. Ohne gesonderte Erlaubnis ist jede urheberrechtliche Nutzung untersagt, insbesondere die Nutzung des Inhalts im Zusammenhang mit, für oder in KI-Systemen, KI-Modellen oder Generativen Sprachmodellen.

Introduction

In today´s electrically-driven passenger cars many different concepts of drive systems are used. Most applications use 1-speed gearset , some applications use multi-speed solutions. The most widespread e-motor technology today is the PMSM (Permanent Magnet Synchronous Motor), but also different e-motor types such as ASM (Asynchronous Motor) and EESM (Externally Excited Synchronous Motor) are used. In high power and SUV applications also multi-EDU systems are used.

This paper describes a study in which different power levels and different e-motor technologies were analysed for a target vehicle application with a system power of ~230 kW with respect to energy consumption and cost.

Setup of solution matrix and boundary conditions

This study was carried out for a D-segment vehicle application. Total peak power and torque are kept constant over all applications at 5000 Nm maximum axle torque and 230 kW peak power. Three different electric motor types (PMSM, EESM and ASM) were considered in different power distributions front to rear axle (20%/80%, 30%/70% and 50%/50%) as well as a single EDU variant (100% RWD).

Base input data was taken from FEV´s benchmarking programs. All data for e-motor and inverter as well as reducers was measured by FEV, using FEV testing methods to ensure comparability of the measurements among the different components. The measurements were then scaled to the needed levels. The electric motor was scaled by moving the corner point up or down in the map, thus keeping the shape of the map and the power to torque ratio the same. In a second step the speed range was adjusted to keep the air gap speed of the e-motor constant in all variants.

For the reducer the method of relative efficiency was used. With this method the efficiency map is displayed over relative torque (i.e. actual torque / max torque). Figure 1 shows the scaling method both for the e-motor and for the reducer.

https://doi.org/10.51202/9783181023549 - Generiert durch IP 216.73.216.36, am 19.01.2026, 02:19:31. © Urheberrechtlich geschützter Inhalt. Ohne gesonderte Erlaubnis ist jede urheberrechtliche Nutzung untersagt, insbesondere die Nutzung des Inhalts im Zusammenhang mit, für oder in KI-Systemen, KI-Modellen oder Generativen Sprachmodellen.

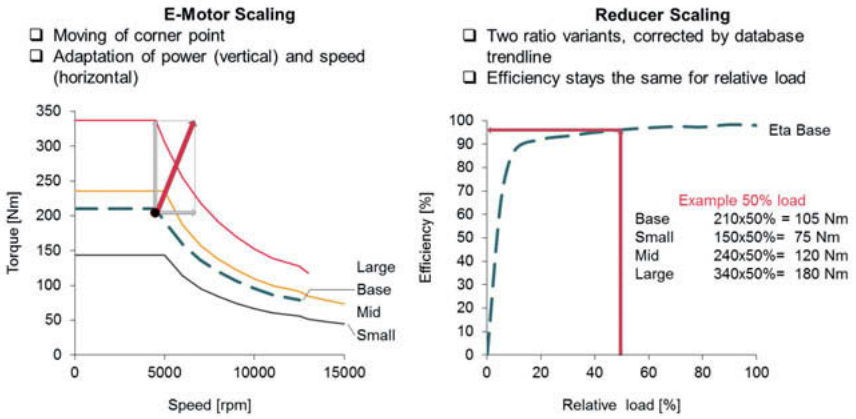


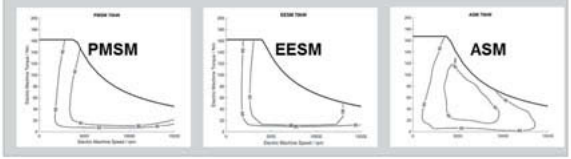
Fig. 01: Method for scaling of e-motor and reducer to achieve different EDU power levels

To cover the requested power range, two e-motor families with different diameters were defined, keeping the maximum air gap speed at 125 m/s by varying the maximum e-motor speed.

This resulted in two different transmission families. The main dimensions were kept constant within one family, and only scaled by gear width and material choice.

The overall resulting EDU specifications for this study is shown in Figure 2.

Item	EDU 1	EDU 2	EDU 3	EDU 4
Peak power [kW]	70	115	160	230
Rotor diameter [mm]	165		200	
Max speed [rpm]	15.000		12.500	
Ratio [-]	9,375		7,813	
Output Torque [Nm]	1522	2500	3478	5000



- Power range is too large to handle by active length only
- Family 1 (EDU 1&2):
  - Air gap diameter 165 mm
  - Rated speed 15.000 rpm
  - → Ratio 9,38
- Family 2 (EDU 3&4):
  - Air gap diameter 200 mm
  - Rated speed 12.500 rpm
  - → Ratio 7,81
- DC voltage 350V constant
- Three E-Motor types
  - PMSM
  - EESM
  - ASM

Stator ⌀ and length identical

Fig. 02: Table of resulting EDU variants for the study

https://doi.org/10.51202/9783181023549 - Generiert durch IP 216.73.216.36, am 19.01.2026, 02:19:31. © Urheberrechtlich geschützter Inhalt. Ohne gesonderte Erlaubnis ist jede urheberrechtliche Nutzung untersagt, insbesondere die Nutzung des Inhalts im Zusammenhang mit, für oder in KI-Systemen, KI-Modellen oder Generativen Sprachmodellen.

To eliminate undesired second order side effects and focus on driveline differences, parameters such as board net power consumption, temperature profile and voltage level were kept constant for all variants.

Regenerative braking was also kept constant for all AWD configurations, assuming a full recuperation up to 3 m/s². The variants with RWD only were limited in recuperation above 1,5 m/s², and allow only half of the recuperation potential at 3 m/s² (see Fig. 03)

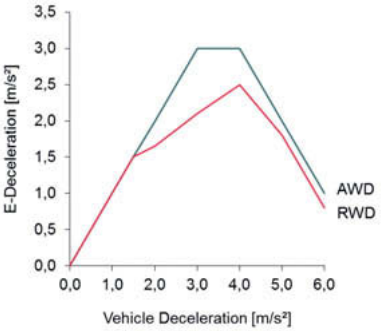


Fig. 03: Electric recuperation as a function of vehicle deceleration

Efficiency simulation results

For each configuration (EDU size and e-motor type) first the optimum torque split for lowest energy consumption was determined for all loads and vehicle speeds. Fig 04 shows an example of such a torque split optimization for one operating point, and a resulting power distribution map.

https://doi.org/10.51202/9783181023549 - Generiert durch IP 216.73.216.36, am 19.01.2026, 02:19:31. © Urheberrechtlich geschützter Inhalt. Ohne gesonderte Erlaubnis ist jede urheberrechtliche Nutzung untersagt, insbesondere die Nutzung des Inhalts im Zusammenhang mit, für oder in KI-Systemen, KI-Modellen oder Generativen Sprachmodellen.

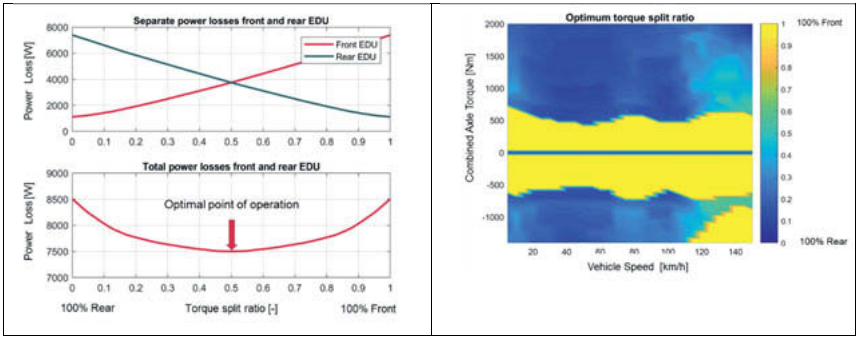


Fig. 04: Approach for optimal power distribution and example power distribution map for one given powertrain combination

The simulation study shows an optimal power distribution of ~30%/70% front to rear in RDE and a nearly constant optimal range for WLTC between 20%/80% and 30%/70% power distribution. Except for the PMSM EDU a single motor EDU is never better in efficiency compared to a dual EDU drivetrain with optimized power split. For WLTC this is caused only by EDU efficiency and for RDE cycles also by limited recuperation potential of the rear EDU. Figure 05 shows the results of all case studies observed.

https://doi.org/10.51202/9783181023549 - Generiert durch IP 216.73.216.36, am 19.01.2026, 02:19:31. © Urheberrechtlich geschützter Inhalt. Ohne gesonderte Erlaubnis ist jede urheberrechtliche Nutzung untersagt, insbesondere die Nutzung des Inhalts im Zusammenhang mit, für oder in KI-Systemen, KI-Modellen oder Generativen Sprachmodellen.

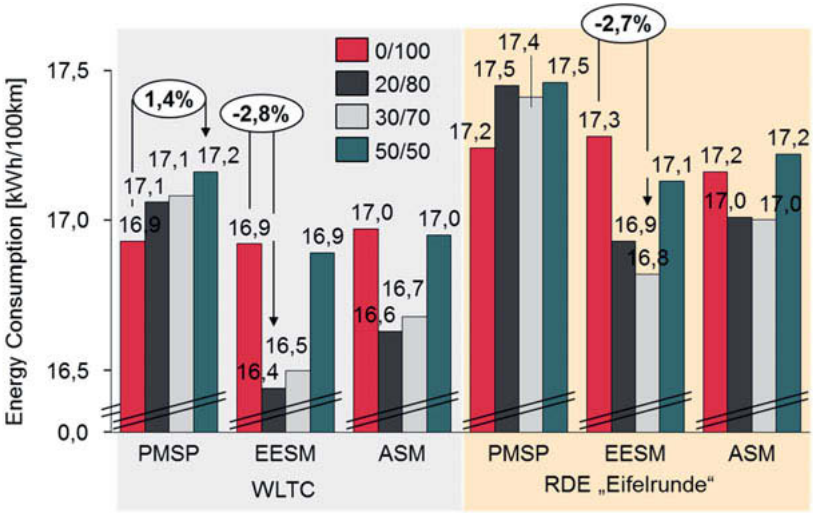


Fig. 05: Simulation results for different power distributions per different E-Motor type

In a next step, cross combinations of different e-motor types were investigated with respect to energy efficiency. For dual PMSM applications a variant using a disconnect device was also investigated. This system was driven in single motor mode up to 80% load of this first motor, and after that in energy balanced dual motor mode.

The combination of a small PMSM EDU with a large ASM or EESM EDU offers further improvement in energy efficiency. The combination of a small EESM and a large ASM results in the overall best performance in this study, although the benefit over the PMSM/ASM combination is only marginal. Compared to a vehicle with two optimally-sized PMSM EDUs, the energy efficiency improvement can be more than 4% both in WLTC and in RDE. Figure 5 shows the results of the best combinations for WLTC and RDE driving.

https://doi.org/10.51202/9783181023549 - Generiert durch IP 216.73.216.36, am 19.01.2026, 02:19:31. © Urheberrechtlich geschützter Inhalt. Ohne gesonderte Erlaubnis ist jede urheberrechtliche Nutzung untersagt, insbesondere die Nutzung des Inhalts im Zusammenhang mit, für oder in KI-Systemen, KI-Modellen oder Generativen Sprachmodellen.

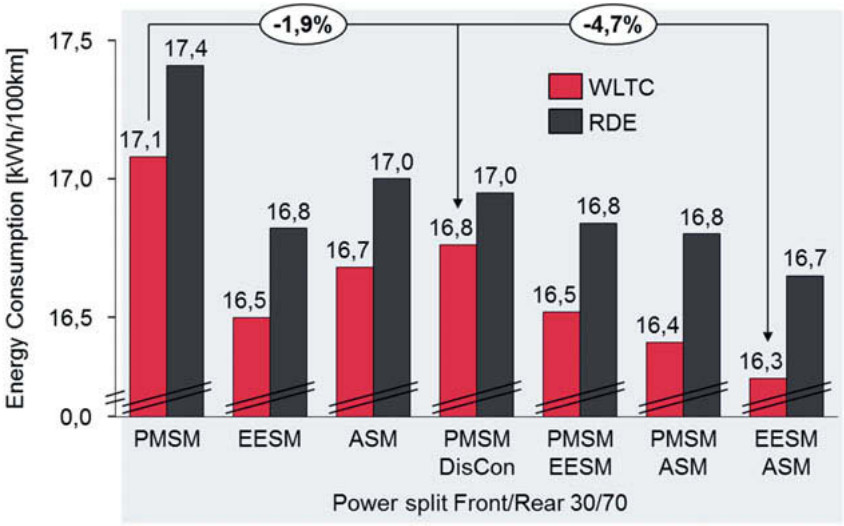


Fig. 06: Simulation results for 30% front / 70% rear power distribution and combination of e-motor types

Cost Analysis

The cost analysis was conducted under an assumed high-volume production scenario of around 250.000 units/year for each EDU variant. All e-motors of one power level have identical stator main dimensions, so that peak performance is nearly identical for PMSM and EESM type motors. The peak power of ASM motors would be slightly lower, but this e-motor type can be overloaded more extensively due to the absence of temperature sensitive materials in the rotor. So the peak power was assumed to be identical as well by exploiting the higher overload capability. For vehicles with dual EDU, only one EDU is equipped with a parking lock system. It was assumed that all systems are equipped with DC/AC inverters using 650 V IGBT semiconductors. For EESM machines an additional DC/DC converter for excitation current for the rotor was included.

For the cost study, the EDUs were structured into the four groups: system housing (3 in 1 housing), torque transfer (including parking lock), e-motor and inverter. The cost analysis is based on a generic BOM and the costs were assessed on main component level, e.g. for the e-motor:

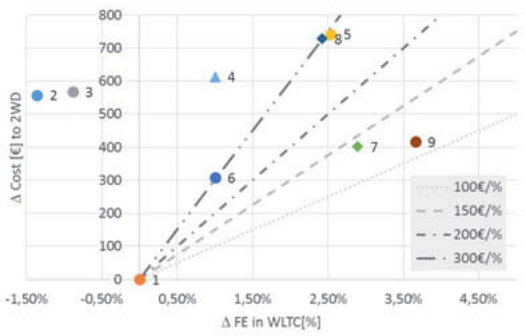
https://doi.org/10.51202/9783181023549 - Generiert durch IP 216.73.216.36, am 19.01.2026, 02:19:31. © Urheberrechtlich geschützter Inhalt. Ohne gesonderte Erlaubnis ist jede urheberrechtliche Nutzung untersagt, insbesondere die Nutzung des Inhalts im Zusammenhang mit, für oder in KI-Systemen, KI-Modellen oder Generativen Sprachmodellen.

- Rotor
- Stator
- Bearings
- Electric connection
- Sensors

The results show only a small difference in delta manufacturing cost between PMSM and EESM EDUs. The ASM has a cost advantage due to its simpler passive rotor design without permanent magnets.

Conclusions:

Figure 07 displays the results in energy efficiency versus the calculated delta cost.



Nr	Solution (F/R)
1	Baseline: RWD PMSM
2	50% PMSM / 50% PMSM
3	30% PMSM / 70% PMSM
4	30% PMSM / 70% PMSM-Disconnect
5	30% EESM / 70% EESM
6	30% ASM / 70% ASM
7	30% PMSM / 70% ASM
8	30% PMSM / 70% EESM
9	30% EESM / 70% ASM

Fig. 07: Overview of energy consumption vs. cost for different solutions

https://doi.org/10.51202/9783181023549 - Generiert durch IP 216.73.216.36, am 19.01.2026, 02:19:31. © Urheberrechtlich geschützter Inhalt. Ohne gesonderte Erlaubnis ist jede urheberrechtliche Nutzung untersagt, insbesondere die Nutzung des Inhalts im Zusammenhang mit, für oder in KI-Systemen, KI-Modellen oder Generativen Sprachmodellen.

To sum up, the following conclusions can be derived from this study:

- With a single motor PMSM vehicle as a baseline, all variants with combinations of multiple PMSMs without disconnect lead to an increase in energy consumption and an increase in cost.
- Adding a disconnection clutch feature on the largest EDU leads to an efficiency increase of nearly 2% at relatively low additional cost.
- The cheapest multi-EDU solution, which offers AWD and saves energy compared to this baseline, is a combination of ASM machines.
- The optimal combination for this application is a large ASM machine in the rear, covering 70% of the power demand in combination with a small EDU in the front delivering 30% of the power, either as EESM or PMSM.
- Best performance in cost vs. efficiency is always achieved by a small, high efficient front EDU (e.g. EESM or PMSM) in combination with a large, cheaper EDU in the rear (ASM). Like this, ratios close to 100 €/% energy saving can be obtained compared to the baseline RWD only variant.
- Considering economies of scale (low-power EDUs with higher production volume) the application of multi-EDUs in mid to high-powered vehicles offers additional features (energy efficiency,extended driving range, AWD) at little to no cost on EDU level.

https://doi.org/10.51202/9783181023549 - Generiert durch IP 216.73.216.36, am 19.01.2026, 02:19:31. © Urheberrechtlich geschützter Inhalt. Ohne gesonderte Erlaubnis ist jede urheberrechtliche Nutzung untersagt, insbesondere die Nutzung des Inhalts im Zusammenhang mit, für oder in KI-Systemen, KI-Modellen oder Generativen Sprachmodellen.

https://doi.org/10.51202/9783181023549 - Generiert durch IP 216.73.216.36, am 19.01.2026, 02:19:31. © Urheberrechtlich geschützter Inhalt. Ohne gesonderte Erlaubnis ist jede urheberrechtliche Nutzung untersagt, insbesondere die Nutzung des Inhalts im Zusammenhang mit, für oder in KI-Systemen, KI-Modellen oder Generativen Sprachmodellen.

Potentials for improving the system behaviour of highspeed clutches for BEV using optimal transmission springs

M.Sc. **Hüseyin Gürbüz**, Dipl.-Ing. **Sascha Ott**,
Univ.-Prof. Dr.-Ing. Dr. h. c. **Albert Albers,**
Mubea Tellerfedern GmbH, Daaden,
IPEK – Institut für Produktentwicklung, Karlsruhe

Kurzfassung

Im Zuge der zunehmenden Hybridisierung und vollständigen Elektrifizierung von höheren Fahrzeugklassen, gilt es neben der Entwicklung von effizienten Betriebsstrategien auch die Komponenten im Antriebsstrang weiterzuentwickeln. Darüber hinaus zeigen die in der Forschung & Entwicklung verfolgten Konzepte im Bereich der schaltbaren Hochdrehzahlantriebe für BEV, dass in zukünftigen E-Fahrzeugen variable Übersetzungen Sinn ergeben, um die Anforderungen bzgl. max. Anfahrmoment und Höchstgeschwindigkeit effizient zu erreichen. Ein zentrales Ziel ist es, durch die Komponenten einen maximalen Beitrag bei der Leistungsdichte, Regelung und Komfort in zukünftigen Antriebssträngen zu leisten und die neuen Herausforderungen im Hochdrehzahlbereich in der frühen Phase der Produktentwicklung zu berücksichtigen.

Heute im Automatikgetriebe eingesetzten Schaltelemente, Kupplungen und Bremsen, bieten auch in Zukunft ein enormes Potenzial, da sie einen großen Teil des zur Verfügung stehenden Bauraums einnehmen und einen maßgeblichen Einfluss auf das Regelungs- und Komfortverhalten des Antriebsstrangs haben.

Im Rahmen eines Konsortialprojekts mit dem IPEK- Institut für Produktentwicklung, Mubea Tellerfedern GmbH, Miba Frictec GmbH und Kaco GmbH + Co. KG wird eine „Highspeed Clutch“ für schaltbare Hochdrehzahlantriebe mit Drehzahlen bis zu 30.000min^{-1} entwickelt und als Demonstrator aufgebaut.

Dieser Beitrag stellt das innovative Kupplungskonzept vor, bei der optimale Getriebefedern eingesetzt werden, um das Systemverhalten der Hochdrehzahlkupplung positiv zu beeinflussen und die Effizienz zu maximieren. Es wird der Einsatz von Getriebefedern für Arretierungen vorgestellt, um die gespeicherte potenzielle Energie zur Kupplungsaktuierung einzusetzen. Weiterhin wird der Einsatz von Spreizfedern vorgestellt, die eine stabilen Position der Reib-

https://doi.org/10.51202/9783181023549 - Generiert durch IP 216.73.216.36, am 19.01.2026, 02:19:31. © Urheberrechtlich geschützter Inhalt. Ohne gesonderte Erlaubnis ist jede urheberrechtliche Nutzung untersagt, insbesondere die Nutzung des Inhalts im Zusammenhang mit, für oder in KI-Systemen, KI-Modellen oder Generativen Sprachmodellen.

und Stahllamellen ermöglichen und hohe Schleppverlusten im offenen Zustand der Hochdrehzahlkupplung durch Lamellentaumeln verhindern.

Abstract

In the course of the increasing hybridization and complete electrification of higher vehicle classes, it is necessary to develop efficient operating strategies as well as components in the powertrain. In addition, the concepts followed in research & development in the area of shiftable high speed drives for BEV show that variable transmission ratios make sense in future electric vehicles in order to efficiently meet the requirements with regard to maximum starting torque and maximum speed. A central goal is to use the components to make a maximum impact on power density, control and comfort in future powertrains and to take account of the new challenges in the high-speed range in the early phase of product development.

Shift elements, clutches and brakes used today in automatic transmissions also offer enormous potential in the future, as they require a large part of the available installation space and have a significant influence on the control and comfort behaviour of the driveline.

As part of a consortium project with the IPEK - Institute for Product Engineering, Mubea Tellerfedern GmbH, Miba Frictec GmbH and Kaco Co KG, a high-speed clutch for shiftable high-speed drives with speeds of up to 30,000 rpm is being developed and set up as a demonstrator. This article presents the innovative clutch concept, in which optimum transmission springs are used to positively influence the system behavior of the highspeed clutch and maximize efficiency. The use of transmission springs for mechanical latching systems is presented in order to use the stored potential energy for clutch actuation. Furthermore, the use of separation springs will be presented, which enable a stable position of the friction and steel discs and prevent high drag losses in the open state of the high speed clutch due to plate tumbling.

1. Introduction

The majority of electric vehicles available on the market have a central drive with a fixed ratio. However, the 1-speed transmission and the gear selection offer only one compromise between the maximum achievable speed and the required starting torque. For vehicles in higher vehicle segments, this topology leads to an oversizing of the electric machine or the use of several electric machines and thus to higher costs. A more efficient solution is the use of a variable gear ratio for starting and maximum speeds, so that the size of the electric machine can be reduced. Through using of more powerful electric machines and power electronics in combination with a shiftable transmission, high speed concepts make it possible to increase the

https://doi.org/10.51202/9783181023549 - Generiert durch IP 216.73.216.36, am 19.01.2026, 02:19:31. © Urheberrechtlich geschützter Inhalt. Ohne gesonderte Erlaubnis ist jede urheberrechtliche Nutzung untersagt, insbesondere die Nutzung des Inhalts im Zusammenhang mit, für oder in KI-Systemen, KI-Modellen oder Generativen Sprachmodellen.

power density. In addition, the operation of the electric machine in optimum efficiency by means of several transmission stages makes it possible to increase overall efficiency of the electric drive train. [1][2][3][4]

The systematic development of shiftable high-speed transmissions and their subsystems offers the opportunity to develop more cost-effective electric drive trains for the mass market and thus to increase the acceptance of electric vehicles. For reasons of comfort, the powershift capability of a shiftable transmission in an electric vehicle must be regarded as a fixed requirement [5].

Preliminary work, as well as other international research work, shows that in particular high speed concepts with shiftable transmissions have the potential to satisfy the necessary driving dynamic range requirements. Previous demonstrator projects have shown that the feasibility of high-speed concepts is always limited by tribological challenges [6].

In addition to the requirements for lubrication of the gear contacts and rolling bearing fatigue strength, the clutch in particular is of central importance here. Highspeed concepts using state-of-the-art drive systems, components and design methods can only be implemented today by avoiding clutch systems. This can be achieved by extreme demands on the controllability, control quality and efficiency of all drive subsystems (power electronics, electric machine). The costs for this stand in the way to the widespread use of electric vehicles. The consortium project therefore lays the foundation for establishing robust and cost-effective clutch technology in future-oriented drive trains. According to the state of the art in research and technology, existing clutch solutions are not suitable for meeting the extreme requirements with regard to freedom from drag torque, fatigue strength and controllability.

2. Consortium project “Highspeed Clutch”

The consortium project “Highspeed Clutch” was launched to demonstrate the innovative components in the field of clutch technology, also for e-mobility. In order to transfer system competence to the supplier and strengthen contributions in e-mobility, the consortium was set-up from suppliers who already supply components for conventional frictional clutches. The consortium partners Kaco GmbH & Co. KG (Kaco), Miba Frictec GmbH (Miba) and Mubea Tellerfedern GmbH (Mubea) are responsible for the development and implementation of components. The system-side consideration from the requirement determination to the validation of the clutch is ensured by the project partner IPEK - Institut for Produkct Engineering at Karlsruhe Institute for Technology (KIT) (*Fig. 1*).

https://doi.org/10.51202/9783181023549 - Generiert durch IP 216.73.216.36, am 19.01.2026, 02:19:31. © Urheberrechtlich geschützter Inhalt. Ohne gesonderte Erlaubnis ist jede urheberrechtliche Nutzung untersagt, insbesondere die Nutzung des Inhalts im Zusammenhang mit, für oder in KI-Systemen, KI-Modellen oder Generativen Sprachmodellen.

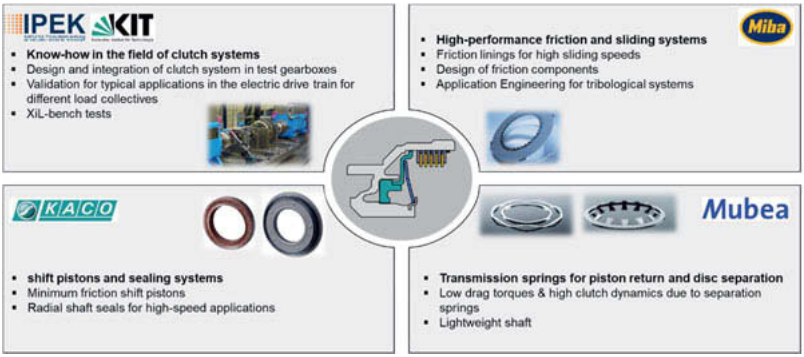


Fig. 1: Consortium of project “Highspeed Clutch”

Miba develops and manufactures the friction pairs and sliding coatings required for torque transmission for the project. Innovative actuator and sealing systems are being developed and implemented by the consortium partner Kaco in order to actuate the frictional clutch. In addition to developing and supplying technical springs for separating the friction pairs and piston return, Mubea is also the consortium leader in this project. The IPEK brings know-how from various completed and ongoing projects such as the research project " Energieeffiziente und flexibel industriell herstellbare Elektrofahrzeugantriebe - Effect360°" funded by the Federal Ministry of Education and Research (BMBF) in the field of shiftable high speed transmissions for electric drive systems into the project and creates the simulation models and test bench tests required for the accompanying and early validation of the system properties of the clutch. The aim of the consortium project is to conduct a feasibility study for multi-disc clutches in a shiftable high speed drive with 30,000 rpm for electric vehicles. Furthermore the aim is to maximize the input clutch speed and identify today's limits. In addition, the load shifting capability and control under high speed conditions are to be demonstrated in test bench tests. In the procedure, the requirements from the "Effect360°" research project are first derived for the clutch. Subsequently, the subsystems will be investigated using FEM and a test bench in order to determine today's limits and to work out the development demands. In the further course of the project, concepts will be generated to meet the identified challenges. The concepts are then evaluated and selected with regard to risk of feasibility. A continuous validation by means of FEM and physical-virtual test bench tests is carried out in order to be able to operate frontloading. After continuous validation of the subsystem, bench tests are performed at system level. Here, the IPEK XiL approach is applied, where physical-virtual test bench tests can be carried out (*Fig. 2*).

https://doi.org/10.51202/9783181023549 - Generiert durch IP 216.73.216.36, am 19.01.2026, 02:19:31. © Urheberrechtlich geschützter Inhalt. Ohne gesonderte Erlaubnis ist jede urheberrechtliche Nutzung untersagt, insbesondere die Nutzung des Inhalts im Zusammenhang mit, für oder in KI-Systemen, KI-Modellen oder Generativen Sprachmodellen.

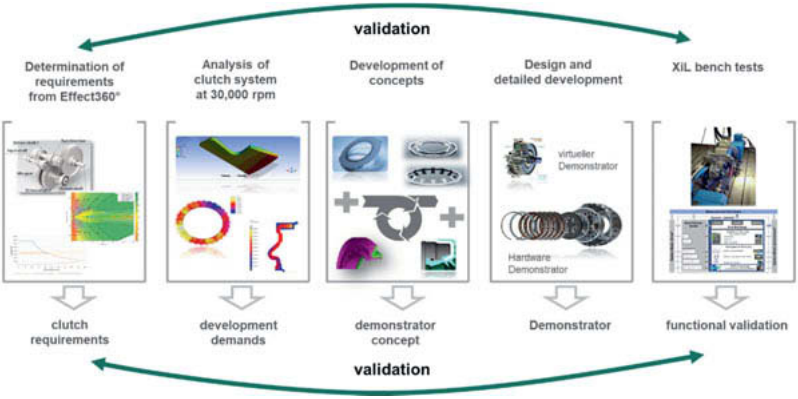


Fig. 2: Development Approach

3. Requirements for a clutch system in BEV with a highspeed drive

Compared to conventional drive trains, an electric drive train with a highspeed electric machine has changed requirements and boundary conditions for the clutches. Due to the torque characteristic curve, for example, the clutch is no longer required for starting. In addition to the higher requirements for controllability, higher losses and stresses on the clutch components are to be expected. Due to the lower number of gears (2-3 speed), the maximum differential speed for clutches in electric drive trains is significantly higher than for clutches in internal combustion engine vehicles, which lead to high sliding speeds and heat input during the synchronization process [7]. In the open state of the clutch, the high differential speeds can lead to high drag losses due to the phenomenon of multi-disc tumbling. Further challenges arise in the area of material stress, since with increasing circumferential speed the centrifugal forces reach values that can lead to plastic deformations of the components.

The frictional clutches used in powershift transmissions of conventional drives have not been developed for high-speed applications with speeds up to 30,000 rpm according to the state of the art in research and technology.

For the initial design of the frictional clutch system, the requirements and boundary conditions from the research project Effect360° are used (*Fig. 3*).

https://doi.org/10.51202/9783181023549 - Generiert durch IP 216.73.216.36, am 19.01.2026, 02:19:31. © Urheberrechtlich geschützter Inhalt. Ohne gesonderte Erlaubnis ist jede urheberrechtliche Nutzung untersagt, insbesondere die Nutzung des Inhalts im Zusammenhang mit, für oder in KI-Systemen, KI-Modellen oder Generativen Sprachmodellen.

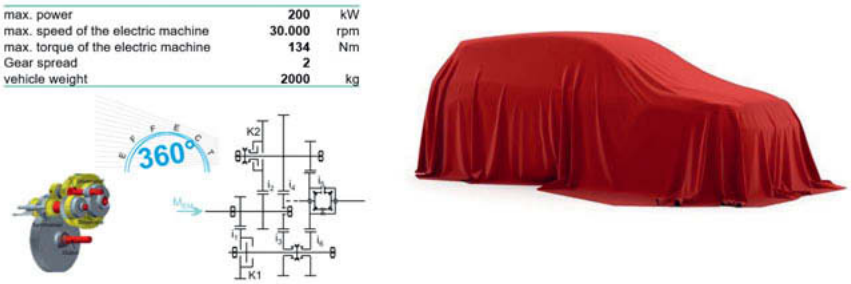


Fig. 3: Clutch requirements of research project Effect360°

The driveline, designed for higher vehicle classes, consists of a 3-speed transmission with 2 friction clutches and an electric machine with 134Nm nominal torque and 200kW power output [1]. When designing the friction system, it is noticeable that the mean sliding diameter of the friction discs must be considerably reduced due to the permitted sliding speeds. The result is an increase in the number of required discs at the given motor torque. The *Fig. 4* shows the design for paper and sintered friction linings. 12 friction plates are required for the selection of paper friction linings and 9 for sintered friction linings. The mean sliding diameter is 65mm.

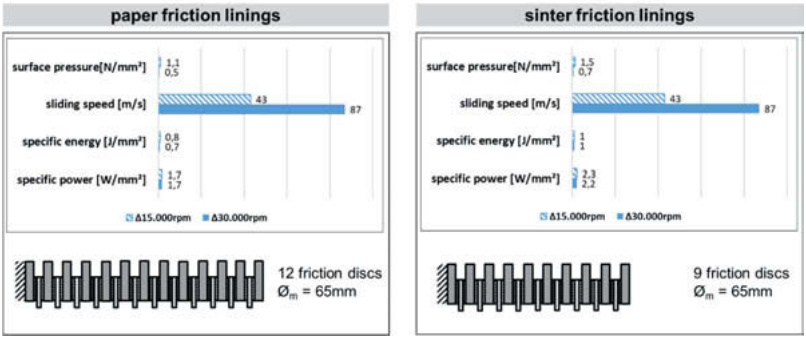


Fig. 4: Design of the friction system for a high speed drive with 30.000rpm

Furthermore, the dynamic pressures were calculated for a piston rotating with the clutch speed. Here, too, the piston diameters must be reduced in order to keep the rotational pressures low. However, the pressure for a piston with a diameter of 50mm is already 23bar [8]. The analysis of the most frequently used clutch systems today leads to the result that at high input speeds

https://doi.org/10.51202/9783181023549 - Generiert durch IP 216.73.216.36, am 19.01.2026, 02:19:31. © Urheberrechtlich geschützter Inhalt. Ohne gesonderte Erlaubnis ist jede urheberrechtliche Nutzung untersagt, insbesondere die Nutzung des Inhalts im Zusammenhang mit, für oder in KI-Systemen, KI-Modellen oder Generativen Sprachmodellen.

the axial force losses and the dynamic pressures increase very strongly and must be eliminated or compensated by measures. In the synthesis phase, a large number of countermeasures were developed for the identified challenges. Selected solution variants are shown in the *Fig. 5*.

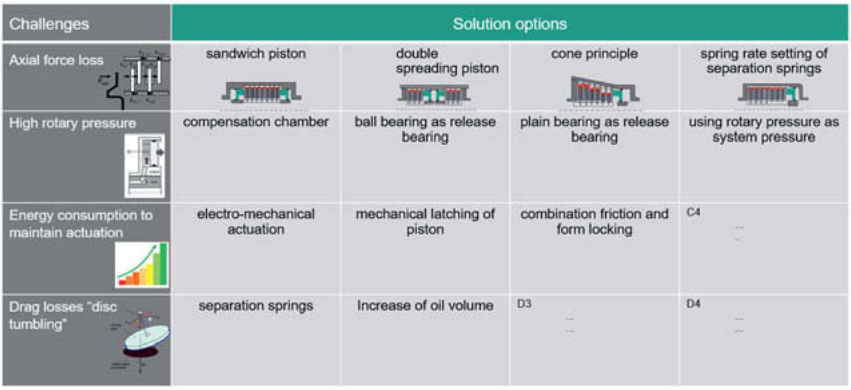


Fig. 5: Challenges and solution variants of multi-disc highspeed clutches for BEV

The first step is to compensate axial force losses caused by spline friction. To this end, concepts were developed which, for example, provides actuation from both sides (sandwich piston) or divide the disc package into two halves and spread it out from the centre (double spreading piston). A further possibility is the variable adjustment of the friction disc diameter (cone principle) or the adjustment of the spring rates of separation springs in order to allow the friction pairing furthest away from the piston side to first come into friction contact by means of a "soft spring". A further challenge lies in the area of actuation. The pressure required for torque transmission must be maintained permanently for hydraulically actuated clutches. Here, the energy requirement of today's actuation systems must be reduced to a minimum. The drag losses occurring when the clutch is open must also be minimized.
The solution variants found were evaluated with regard to feasibility, costs, control expenditure and development expenditure and a solution selection was then made.

4. Clutch design for BEV

The clutch design for shiftable highspeed drives in electric vehicles developed as part of the consortium project is shown in the *Fig. 6*. The axial force losses due to the high number of discs are compensated by actuating from both sides of the disc pack. This also ensures that

https://doi.org/10.51202/9783181023549 - Generiert durch IP 216.73.216.36, am 19.01.2026, 02:19:31. © Urheberrechtlich geschützter Inhalt. Ohne gesonderte Erlaubnis ist jede urheberrechtliche Nutzung untersagt, insbesondere die Nutzung des Inhalts im Zusammenhang mit, für oder in KI-Systemen, KI-Modellen oder Generativen Sprachmodellen.

the total stroke is divided between two pistons and that there is a high dynamic response. A further increase in clutch dynamics is achieved by the separation springs, in which the clutch clearance relevant for drag losses is set as small as possible. To avoid dynamic pressures due to the rotation of the shift piston at the clutch input speed, the concept presented here uses a plain bearing as release bearing.

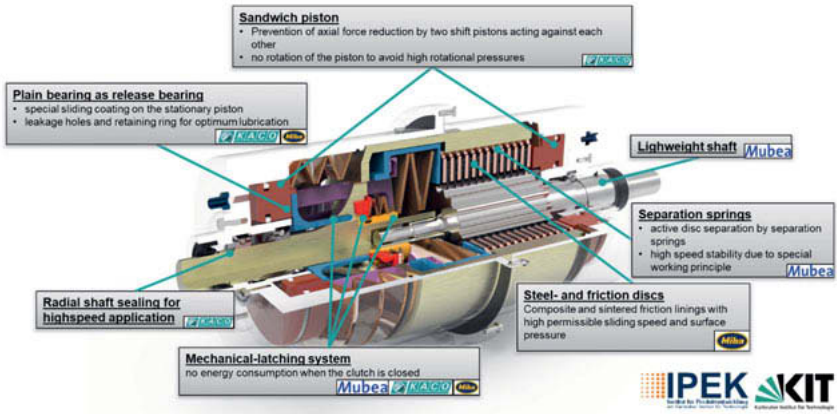


Fig. 6: Highspeed clutch for multispeed electric vehicles

Here, special sliding coatings from Miba are used. Optimum lubrication for high sliding speeds and surface pressures is achieved by means of leakage holes and retaining rings.
The circumferential speeds at the sealing systems are above 30m/s, so that radial shaft seals from Kaco developed especially for high-speed applications are used.

4.1 Innovative latching system with optimum transmission springs for highspeed applications

For torque transmission in wet multi-disc clutches with hydraulic shift pistons, a pressure must be maintained to compress and hold the discs in the axial direction. Since the actuating pressure must be maintained permanently, energy is required in addition to the actuating energy to keep the hydraulic piston closed or open. The supply lines and the pressure chambers in which the hydraulic pistons are located are permanently pressurised, which also has a negative effect on the seals. Leaks in the hydraulic medium must also be compensated. One of the central development goals in actuation is therefore to reduce the required actuating energy. One possibility is offered by mechanical latching devices, which keep the shift piston closed

https://doi.org/10.51202/9783181023549 - Generiert durch IP 216.73.216.36, am 19.01.2026, 02:19:31. © Urheberrechtlich geschützter Inhalt. Ohne gesonderte Erlaubnis ist jede urheberrechtliche Nutzung untersagt, insbesondere die Nutzung des Inhalts im Zusammenhang mit, für oder in KI-Systemen, KI-Modellen oder Generativen Sprachmodellen.

and allow the required pressure to be reduced after latching. In the latching system presented here, the pressure can be completely reduced for the first time, so that pressure is only required again when the clutch is subsequently opened. The latching unit is designed in such a way that it completely takes over the holding function in the closed or open state of the multi-disc clutch. In one latching position it maintains the contact force on the discs of the multi-disc clutch, while in the other latching position it is reset so far that no force acts on the discs so that the clutch can be opened.

The idea is based on the locking mechanism of a ballpoint pen. For this purpose, the three essential components latching crown, guidance crown and sliding sleeve are adapted for a clutch integration (*Fig. 7*).

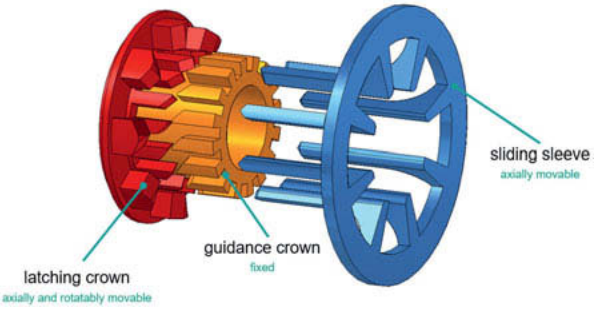


Fig. 7: Key components of the latching system

The latching crown has a ring-shaped base body which is axially movable and rotatable relative to the shaft. The base body has axially extended cams on its one end. The guidance crown is fixed and serves for axial guidance of the latching crown and sliding sleeve. Furthermore, it allows a defined rotation of the locking crown into the next tooth gap due to the adapted tooth shape. The sliding sleeve can only be moved axially from the piston.

In order to move the latching crown to the different locking positions, it is moved axially by means of the piston. Since the control surfaces are inclined in relation to the direction of rotation of the latching crown, it is rotated around its axis under axial load in such a way that it can reach the respective latching position. The locking device forms a mechanical stop which allows the required contact pressure on the discs to be maintained simply and reliably.

Fig. 8 shows the latching sequence when closing the clutch.

https://doi.org/10.51202/9783181023549 - Generiert durch IP 216.73.216.36, am 19.01.2026, 02:19:31. © Urheberrechtlich geschützter Inhalt. Ohne gesonderte Erlaubnis ist jede urheberrechtliche Nutzung untersagt, insbesondere die Nutzung des Inhalts im Zusammenhang mit, für oder in KI-Systemen, KI-Modellen oder Generativen Sprachmodellen.

First the piston has moved back so far in the open state of the clutch (1) that there is no contact on the plain bearing. Two disc spring packs are provided in the latching system. Belleville spring pack 1 is preloaded to the maximum axial force required, so that the forces required for synchronization and torque transmission can first be transmitted from the piston without deflection of the disc spring pack. The second disc spring assembly is used to keep the forces on the tooth flanks of the latching crown and guidance crown low and to allow the engagement to take place independently and at lower forces than the axial force of the clutch.

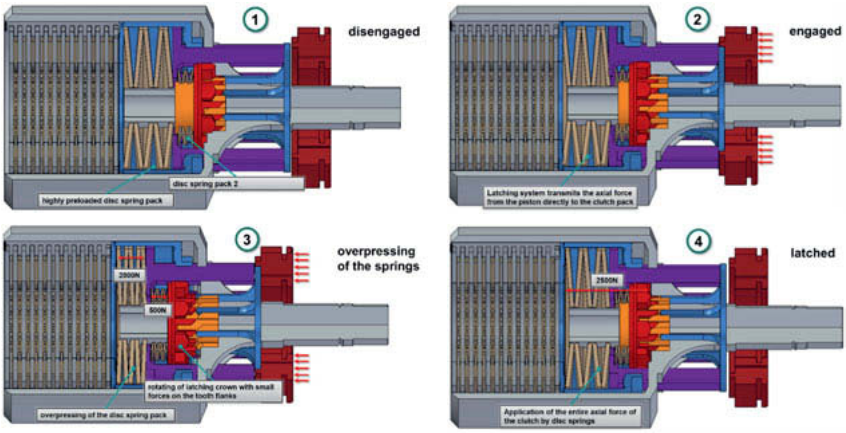


Fig. 8: Sequence of latching system

If the pressure in the piston chamber is now continuously increased, the shift piston moves axially and moves the complete latching unit in the direction of the clutch pack so that first the clearance of the clutch is closed and then the speed and torque are adjusted (2).
The pressure is then further increased in order to press over the preloaded disc springs with the finger piston and move the latching crown into the rotary position. The cam of the latching crown is pushed out of the grooves of the output shaft by the sliding sleeve. The disc spring assembly 2 and the specified tooth contour of the latching crown, guidance crown and sliding sleeve twist the locking crown and push it into the next tooth gap. In this position, the cams cannot engage in any grooves or recesses in the output shaft (3).
Due to rotation of the latching crown and springback of the disc spring pack 2, the cam now hits an end stop in the output shaft and is locked. If the piston pressure is now reduced, the

https://doi.org/10.51202/9783181023549 - Generiert durch IP 216.73.216.36, am 19.01.2026, 02:19:31. © Urheberrechtlich geschützter Inhalt. Ohne gesonderte Erlaubnis ist jede urheberrechtliche Nutzung untersagt, insbesondere die Nutzung des Inhalts im Zusammenhang mit, für oder in KI-Systemen, KI-Modellen oder Generativen Sprachmodellen.

piston moves back through disc spring pack 1 and the finger piston and latching crown are supported on the output shaft (4). The axial force required for torque transmission is now fully provided by disc spring pack 1. The piston can be moved to the initial position by a return spring so that there is also no contact on the plain bearing and it is not stressed.

4.2 Selection and design of optimum transmission springs for high speed clutches

The targeted further development of transmission springs for piston return led to the use of transmission disc springs in order to successively reduce the axial installation space of the shifting elements in recent years. Further advantages have been demonstrated with technical springs for active disc separation, so-called separating springs, which, in addition to further reducing the axial installation space (additional adoption of the piston return), also contribute to a reduction in drag losses in the open state and to an improvement in the comfort of wet-running clutches and brakes [9]. Since the transmission springs rotate with the clutch speed, changed requirements and boundary conditions arise for the transmission springs in a high-speed clutch. In contrast to the clutch components, transmission springs change their geometry depending on the operating condition of the clutch. As a result, the springs are subjected to different centrifugal forces when the clutch is closed and open. In the case of slotted disc springs, FEM calculations have shown that the tongues work comparatively like centrifugal levers at high speeds and that the spring force changes with increasing speed. However, it is possible to minimize the influence of the speed on the spring force by adjusting the distance from the centre of mass of the spring to the turning centre. With disc springs without slots, the centre of mass and the centre of turning are very close to each other, so that these type of disc springs have a high speed stability. FEM investigations and test bench trials at the IPEK - Institute for Product Engineering have already proven this design method for disc springs up to 15,000 rpm. For the design of the springs for latching, disc springs were therefore used as they allow a small installation space and a loss of force of <5% at 30,000 rpm (*Fig. 9* left).

In addition, the innovative highspeed clutch design includes separation springs that are intended to prevent high drag torques due to disc tumbling. Here the spring stiffness is designed so that the discs are held in a stable position and cannot tumble. In addition to reducing of the drag torque, this springs are also used to achieve faster opening and closing of the friction pairings and thus further increase the clutch dynamics. A high speed stability of this kind of springs is also required here, as they rotate at the clutch speed of 30000rpm. Conventional separation springs with a waveform lose spring load because the waveform is stressed by the

https://doi.org/10.51202/9783181023549 - Generiert durch IP 216.73.216.36, am 19.01.2026, 02:19:31. © Urheberrechtlich geschützter Inhalt. Ohne gesonderte Erlaubnis ist jede urheberrechtliche Nutzung untersagt, insbesondere die Nutzung des Inhalts im Zusammenhang mit, für oder in KI-Systemen, KI-Modellen oder Generativen Sprachmodellen.

centrifugal force. Here, too, a FEM-coupled design enables the separation springs to be optimally designed for high speeds. By adjusting the number of waves and material thickness, the separation springs with waveform can be used for high speeds. However, newly developed separation springs are used in the highspeed clutch concept here, which, thanks to a new operating principle, also offer very high speed stability with low space requirements. (*Fig. 9* right).

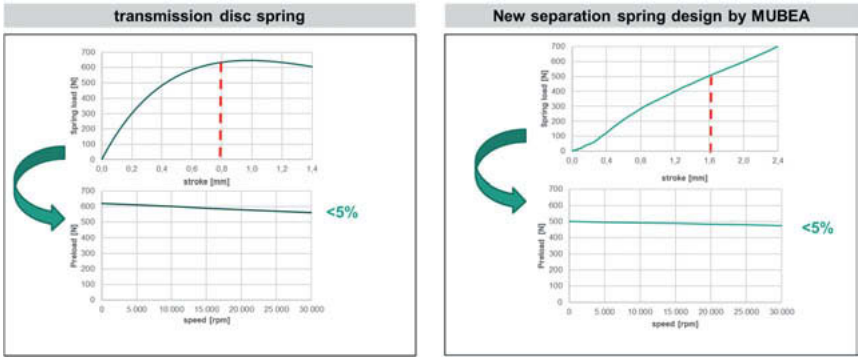


Fig. 9: Effect of speed on the spring load of a transmission disc spring and Mubea separation spring

5. Summary and outlook

This article presented the results of the analysis of the use of wet multi-disc clutches in a shiftable high speed drive with 30,000 rpm from the consortium project "Highspeed Clutch".

The design of the friction system shows that the high sliding speeds lead to average friction diameters which are below the values common in automotive applications. With a constant clutch torque, the number of friction pairings must be increased, which in turn results in a strong axial force loss due to spline friction. The analysis of the actuation with a hydraulic shift piston further shows that a rotational pressure is generated in the piston chamber which is above today's system pressure. As part of the consortium project, an innovative clutch concept was developed that offers potential in terms of efficiency and system behavior for use in a shiftable high-speed drive for electric vehicles. The efficiency is maximized by mechanical latching of the piston so that no energy is required when the clutch is closed. For this purpose, transmission disc springs were used which are suitable for high speeds and have a small installation space. Another novelty is the actuation via release bearing in the form of a plain bearing. For this purpose, leakage holes and retaining rings are specifically attached to the piston in order

https://doi.org/10.51202/9783181023549 - Generiert durch IP 216.73.216.36, am 19.01.2026, 02:19:31. © Urheberrechtlich geschützter Inhalt. Ohne gesonderte Erlaubnis ist jede urheberrechtliche Nutzung untersagt, insbesondere die Nutzung des Inhalts im Zusammenhang mit, für oder in KI-Systemen, KI-Modellen oder Generativen Sprachmodellen.

to achieve optimum lubrication in the sliding contact. In the open state innovative separation springs stabilize the entire clutch package at high speeds, ensuring optimum lubrication of the friction system and preventing disc tumbling. In addition, the separation springs are used to set a defined and small clutch clearance. In the further steps of the project, a hardware demonstrator will be set up, which will then be examined and evaluated with regard to efficiency and control behavior by XiL test bench tests.

Acknowledgement The results and conclusions on which this publication is based were developed as part of the "Highspeed Clutch" consortium project. The authors thank the consortium partners Miba Frictec GmbH and Kaco GmbH & Co. KG for providing the information published in this paper.

https://doi.org/10.51202/9783181023549 - Generiert durch IP 216.73.216.36, am 19.01.2026, 02:19:31. © Urheberrechtlich geschützter Inhalt. Ohne gesonderte Erlaubnis ist jede urheberrechtliche Nutzung untersagt, insbesondere die Nutzung des Inhalts im Zusammenhang mit, für oder in KI-Systemen, KI-Modellen oder Generativen Sprachmodellen.

[1] Reichert, U. Bause, K. und Ott, S. „Presentation of a multispeed gearbox for a BEV increasing the efficiency and power density," in 16. Internationales CTI Symposium, Berlin, 2017.

[2] Gwinner, P. Stahl, C. Rupp S. und Strube, A. „Innovatives Hochdrehzahl-Antriebsstrangkonzept für hocheffiziente elektrische Fahrzeuge," ATZ – Automobiltechnische Zeitschrift, pp. 72-75, 2017.

[3] Albers, A. Bause, K. Klingler, S. Puls, R. und Behrendt, B. „Schaltbare Getriebe für Elektrofahrzeuge am Beispiel urbaner Nutzungsszenarien," in Urbane Mobilität der Zukunft : Symposium des Innovationsclusters REM - Regional Eco Mobility 2030, Karlsruhe, 2015.

[4] Eghtessad, M. , Meier, T. Rinderknecht, S. und Küçükay, F. „Antriebsstrangoptimierung von Elektrofahrzeugen," ATZ – Automobiltechnische Zeitschrift, pp. 78-85, 01 September 2015.

[5] Gassmann, T. „GKN 2-speed Transmission Technology for Hybrid and Electric Vehicle," in 15th International CTI Symposium,, Berlin, 2016.

[6] Domian, H.-J. , Ketteler, K.-H. und Scharr, S. „elektrische Achsantriebsmodul für hohe Drehzahlen," ATZ - Automobiltechnische Zeitschrift, pp. 954-959, 14 November 2013.

[7] Albers, A. Reichert, U. Bause, K. Radimersky, A. und Ott, S. „Entwicklung einer verlustoptimierten Kupplung für ein mehrgängiges Getriebe für ein Elektrofahrzeug," in VDI Kupplungen und Kupplungssysteme in Antrieben, Ettlingen, 2017.

[8] Gürbüz, H. Ott, S. Albers, A. „Entwicklungsansätze für innovative Hochdrehzahlkupplung in E□Fahrzeugen" in Forschung im Ingenieurwesen (2019),

[9] Schulz, J. Seelakamp, C.-P. „Optimization of wet clutches in automatic transmissions by use of different types of springs," in 16th International CTI Symposium,, Berlin, 2017.

https://doi.org/10.51202/9783181023549 - Generiert durch IP 216.73.216.36, am 19.01.2026, 02:19:31. © Urheberrechtlich geschützter Inhalt. Ohne gesonderte Erlaubnis ist jede urheberrechtliche Nutzung untersagt, insbesondere die Nutzung des Inhalts im Zusammenhang mit, für oder in KI-Systemen, KI-Modellen oder Generativen Sprachmodellen.

Efficiency of Electric Axle Drive Systems

Potential of Multi-Speed-Drives

Dr. rer. nat. **Stephan Demmerer**,
ZF Friedrichshafen AG, Friedrichshafen

Zusammenfassung

Heutige Elektroantriebe haben in der Regel ein Reduziergetriebe mit einer konstanten Übersetzung. Über Zweiganggetriebe spricht man dagegen immer dann, wenn man höhere Höchstgeschwindigkeiten und zeitgleich hohe Anfahrmomente realisieren möchte. Dies ist beispielsweise bei Sportwagen oder Nutzfahrzeuganwendungen häufig der Fall.

Geht es um Effizienz, so sind Zweiganggetriebe bisher selten diskutiert worden. Ein Grund dafür ist das homogene Kennfeld des Elektroantriebs. Hier können selbst bei einer besseren Ausnutzung nur geringe Verbrauchseinsparungen erzielt werden. Betrachtet man jedoch die Auslegung des Gesamtsystems unter Berücksichtigung der E-Maschine, so lässt sich die Effizienz deutlich steigern, kurz: Ein Zweigang-Elektroantrieb kann einen signifikanten Effizienzgewinn liefern, während ein Zweigang-Getriebe in erster Linie die Performance eines Antriebs verbessert.

Abstract

Today's electric drives usually have a reduction gearset with a constant ratio. Two-speed transmissions are then in discussion, if higher maximum speeds and high starting torques should be achieved at the same time. This is often the case for sports cars or commercial vehicle applications.

For reasons of efficiency, two-speed transmissions have been rarely discussed, since the characteristic map of an electric drive is so homogeneous that only low fuel savings are achieved through better utilization of the characteristic map. However, a greater efficiency gain can be achieved in the overall system design with the involvement of the electric motor and the inverter. A two-speed electric drive can provide significant efficiency gains while a two-speed transmission manly improves the performance of a drive.

https://doi.org/10.51202/9783181023549 - Generiert durch IP 216.73.216.36, am 19.01.2026, 02:19:31. © Urheberrechtlich geschützter Inhalt. Ohne gesonderte Erlaubnis ist jede urheberrechtliche Nutzung untersagt, insbesondere die Nutzung des Inhalts im Zusammenhang mit, für oder in KI-Systemen, KI-Modellen oder Generativen Sprachmodellen.

1. Introduction

The car industry and their customers have to tackle contradicting requirements of increased performance demand on the one hand and higher efficiency on the other. E-mobility seams to offer a solution for both: zero emissions and high acceleration. But performance means not only fast acceleration values from 0 to 100 km/h, but also high gradeability for sports and outdoor activities. High top-speed and continuous power at high velocities are also required to improve electric vehicles (EVs).

Efficiency is even more important, considering that the energy storage is the costliest component of the vehicle and the charging time is an obstacle on a long range journey with a battery electric vehicle (BEV). Higher efficiency either results in a reduced size of the battery or in a higher range when keeping the existing battery size.

Two-speed transmissions or even multispeed transmissions can temper these disadvantages and help to establish BEVs on a broader base. Different car segments have different requirements: where sports cars or SUVs have a strong focus on performance, the majority of the vehicle segments focuses on efficiency and costs.

Efficiency is usually measured as fuel consumption in l/100km, means energy per distance travelled. In the case of EVs, we are talking about electric energy in kWh and we are keeping the logic of conventional vehicles. The energy consumption for EVs is measured in kWh/100km. Therefore legislation has defined that the electric energy has to be measured at the input socket at the car (see picture 1).

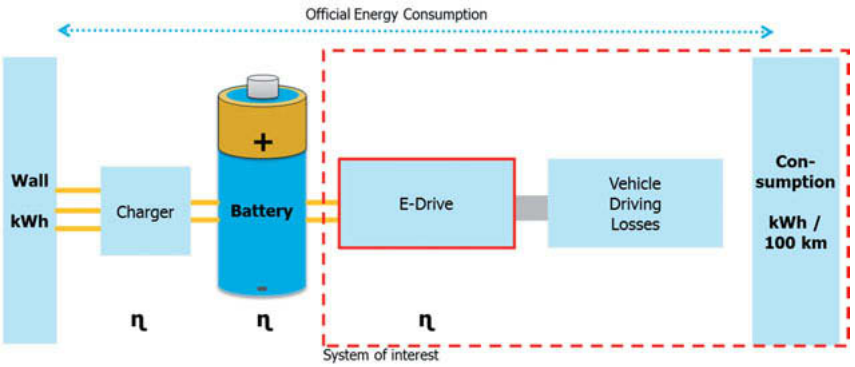


Fig. 1: Vehicle driveline and system limits. Red marked is the system in focus for two speed e-drives.

https://doi.org/10.51202/9783181023549 - Generiert durch IP 216.73.216.36, am 19.01.2026, 02:19:31. © Urheberrechtlich geschützter Inhalt. Ohne gesonderte Erlaubnis ist jede urheberrechtliche Nutzung untersagt, insbesondere die Nutzung des Inhalts im Zusammenhang mit, für oder in KI-Systemen, KI-Modellen oder Generativen Sprachmodellen.

The official values for energy consumption including the efficiency of the charging process refer to the onboard charger and the battery itself. In the case of the electric SMART, energy consumption values vary between 20.1 and 14.0 kWh/100km, only depending on the charging process and infrastructure [1].
The cycle to be used by the vehicle is the WLTC. The distance is about 23 km. The WLTP procedure exactly describes how to evaluate the energy consumption for 100 km of distance.
Efficiency is the percentage value of energy out and energy in. In the best case, without any losses, it is 100%. In conventional powertrains, the energy flow is uni-directional. For electric drivetrains, the energy is flowing forth and back: The e-drive converts electric energy into mechanical energy while driving and mechanical energy into electric energy during the recuperation phase. This restored energy will be used again for driving, and so on. The energy will pass the e-drive system several times and will be converted each time with the efficiency η. The efficiency is therefore the significant parameter several times, until the whole energy stored in the battery has been converted into driving distance. As a rule of thumb, the effect of extended range (in %) is twice as much as the improved efficiency of the drive unit (in %), assuming the same amount of energy is consumed.

$$\text{Range Extension } \Delta\text{km [\%]} \approx 2 \times \Delta\eta \text{ Efficiency Improvement } [\%] \quad (1)$$

Furthermore, greater efficiency leads to a lower consumption of electric energy and thus to a lower amount of charged energy. Lower charged energy leads to lower losses by the charger. This can be a significant value, as discussed above. So improved efficiency has multiple effects on saving energy and therefore on energy costs.

In the following we will firstly focus only on the transmission and secondly on the complete driveline with multispeed transmissions.

2. Two-speed Transmission Approach

Most requests for 2-speed engines are aimed at improving the performance of the vehicle, while the target of efficiency improvement needs a different approach. We will look at the performance first and then take a closer look at the efficiency approach.

https://doi.org/10.51202/9783181023549 - Generiert durch IP 216.73.216.36, am 19.01.2026, 02:19:31. © Urheberrechtlich geschützter Inhalt. Ohne gesonderte Erlaubnis ist jede urheberrechtliche Nutzung untersagt, insbesondere die Nutzung des Inhalts im Zusammenhang mit, für oder in KI-Systemen, KI-Modellen oder Generativen Sprachmodellen.

2.1 Performance Enhancement

The e-motor is characterized by power and torque. The transmission reduces the rotational speed and simultaneously increases the torque. Most reduction gearsets have a ratio in the range of 10, meaning 10 times higher torques and 10 times lower rpms.
Special applications require a higher top speed, which can be achieved easily by a lower ratio. But the torque is then reduced during launching. A ratio of 5 means doubled top speed and half the torque. A ratio of 20 means doubled launching torque, which can be good for high tonnage for commercial vehicles, but half the top speed.
Two speed transmissions can solve this conflict and can provide higher torque and top speed at the same time. Especially for commercial vehicles and for sports cars, this is an attractive option.

2.2 Efficiency Improvement

Another idea is to improve efficiency of the e-drive by using a two-speed transmission. The idea is similar to that of conventional combustion engines and multispeed transmissions. In the past decades, transmissions were equipped with more and more speeds, mainly to use a better point in the efficiency map. Compared to combustion engines, the efficiency map of an e-motor is much more homogeneous. The benefit of shifting to better points is very low.
We found out that especially for low torques, low weight means low performance requirements. The benefit with regard to the range only amounts to about 1-2%. The higher internal losses of a two-speed transmission and the higher costs, however, make any business case unprofitable. For commercial vehicles or even for trains, the benefit is slightly higher. In these applications, two-speed transmissions enter the market only in combination with performance enhancements.

As intermediate summary we can say that a two-speed transmission for electric drives only makes sense to enhance performance and not efficiency. To improve the efficiency, a complete system design in combination with two-speed transmissions is necessary, which will be described in the following.

3. E-Drive System Approach with Two Speeds

The idea of the system approach is that the e-motor and the inverter are designed and optimized from the beginning with the knowledge of the transmission capabilities. For example,

https://doi.org/10.51202/9783181023549 - Generiert durch IP 216.73.216.36, am 19.01.2026, 02:19:31. © Urheberrechtlich geschützter Inhalt. Ohne gesonderte Erlaubnis ist jede urheberrechtliche Nutzung untersagt, insbesondere die Nutzung des Inhalts im Zusammenhang mit, für oder in KI-Systemen, KI-Modellen oder Generativen Sprachmodellen.

high top speeds can be excluded by the e-motor, because this can be realized by the transmission. It is a completely different approach than only attaching a two-speed transmission to the existing layout of an e-motor.

3.1 Performance Enhancement

The performance can be increased by both - a two-speed transmission or higher electric power. The empowering of the e-motor is generally the cheaper and more efficient solution. But the electric power has its limitations. The maximum current of known semiconductors is limited to about 500-600 A. This leads to a power limitation in the 400V class of about 200 kW. If more power is required, a second e-motor and inverter could be added. This can be done in a smart way with a 6-phase e-motor and a doubled inverter. To avoid this effort, which would increase the costs significantly, a two-speed transmission can enhance the performance by staying with the 3-phase system. A transmission cannot increase the power, but the acceleration and the torque can be improved. In the continuous phase, the output power can also be enhanced by shifting to rotational speeds with a better output power. The costs of such a system might be lower than for a 6-phase e-motor system.
Increasing the voltage can also be an option to avoid 6 phases and two-speed transmissions to get more output performance.

3.2 Efficiency Improvement

Efficiency improvement also means cost reduction: it is possible to use a smaller battery to achieve a certain range, to reduce the costs of the vehicle. Alternatively, the range can also be extended by improving efficiency. Finally, the lower consumption of electric energy is a cost factor for everyday driving, since electricity for EVs is becoming more and more expensive.
Common layouts of e-drives are defined by performance requirements, based on which e-motors, inverters and gear ratios are defined. Within this framework, efficiency can be optimized.
Within the new mindset, efficiency is the key parameter for the layout. The e-motor and inverter do therefore not need to reach all performance requirements, like torque or maximum speed. These values can then be achieved by using a multispeed transmission (see picture 2).

https://doi.org/10.51202/9783181023549 - Generiert durch IP 216.73.216.36, am 19.01.2026, 02:19:31. © Urheberrechtlich geschützter Inhalt. Ohne gesonderte Erlaubnis ist jede urheberrechtliche Nutzung untersagt, insbesondere die Nutzung des Inhalts im Zusammenhang mit, für oder in KI-Systemen, KI-Modellen oder Generativen Sprachmodellen.

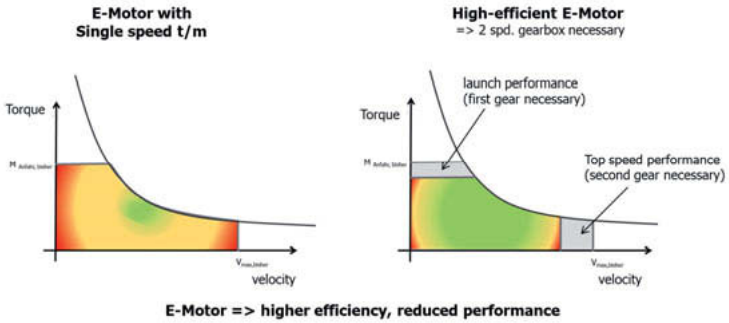


Fig. 2: Principle mindset of single-speed (left) and multispeed (right) e-motor design.

ZF has already developed two variants of an e-motor: a performance version and an efficiency version. While the performance version can provide full power of about 150 kW maximum, the efficiency version has a range benefit of +3%. The effect of a two-speed transmission leads to another 1,7% range extension, so all in all, we can almost reach a range increase of 5% with the same amount of energy. The internal losses of the two-speed transmission compared to a single-speed reduction gearset have to be tested and optimized and are not yet considered in the given numbers.

The shifting strategy with the given asynchronous motor is rather simple: below 70 km/h, the first gear is engaged, while the second gear is for higher velocities. City driving can then be realized without gearshifts.

The performance of the efficiency e-drive can be similar to the performance e-drive when using a second speed. Until 80km/h, acceleration is almost comparable, while the performance gap increases with higher rotational speeds. By shifting to the second gear, the performance gap is almost closed.

4. Modular and Scalable E-Drive Concept

ZF is developing a modular and scalable e-drive design kit, consisting of different sizes of e-motors and inverters and a modular and scalable transmission concept, that can be adjusted to different requirements.

https://doi.org/10.51202/9783181023549 - Generiert durch IP 216.73.216.36, am 19.01.2026, 02:19:31. © Urheberrechtlich geschützter Inhalt. Ohne gesonderte Erlaubnis ist jede urheberrechtliche Nutzung untersagt, insbesondere die Nutzung des Inhalts im Zusammenhang mit, für oder in KI-Systemen, KI-Modellen oder Generativen Sprachmodellen.

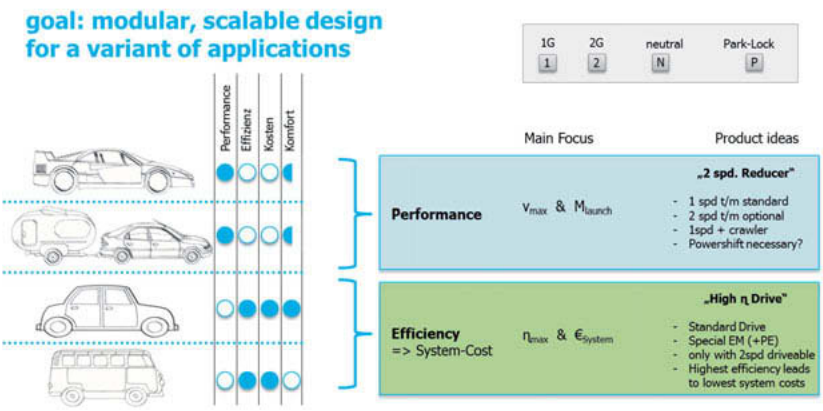


Fig. 3: Different requirements for different applications

By using a spur gear concept, different ratios can be implemented. Also modularity for single-speed and two-speed variants can be realized. Powershift can be provided, if needed. Also a neutral position and a parking lock position can be realized in a modular and scalable way for many applications (see Fig. 4).

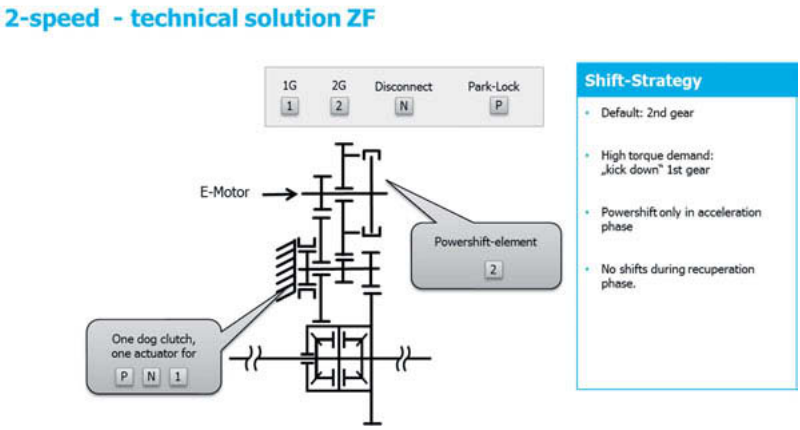


Fig. 4: ZF transmission concept

https://doi.org/10.51202/9783181023549 - Generiert durch IP 216.73.216.36, am 19.01.2026, 02:19:31. © Urheberrechtlich geschützter Inhalt. Ohne gesonderte Erlaubnis ist jede urheberrechtliche Nutzung untersagt, insbesondere die Nutzung des Inhalts im Zusammenhang mit, für oder in KI-Systemen, KI-Modellen oder Generativen Sprachmodellen.

For another e-drive layout with about 200 kW, we could downsize and reduce the length of an e-motor by 60 mm. By using a two-speed transmission, we regain performance. The transmission has an additional length of about 55 mm, so all in all, we can install the two-speed e-drive in the same installation space as the single-speed version. The weight also stays almost the same.

5. Summary

The conclusion of our investigations is, that a pure single speed can help to improve the performance in case of a specific application and a given e-motor – inverter combination. For gaining efficiency benefits, a system layout and system optimization is necessary. Only by combining e-motor layout and multispeed transmission can performance requirements be achieved and efficiency benefits be realized.

[1] SMART, official homepage: https://www.smart.com/de/de/index/smart-emobility.html 1.4.2019

[2] Hellenbroich, G. FEV; Hillmann, T. YASA; 17th CTI Symposion Berlin, Dec. 2018 Hier steht das YASA-Prinzip 2-Gang Effizienz

[3] Janssen,P.; Hellenbroich, G.; Lahey, H.-P.; FEV; ATZ 11/2018; p.56-61; 2018 Hier steht das Parksperrenthema

https://doi.org/10.51202/9783181023549 - Generiert durch IP 216.73.216.36, am 19.01.2026, 02:19:31. © Urheberrechtlich geschützter Inhalt. Ohne gesonderte Erlaubnis ist jede urheberrechtliche Nutzung untersagt, insbesondere die Nutzung des Inhalts im Zusammenhang mit, für oder in KI-Systemen, KI-Modellen oder Generativen Sprachmodellen.

Integrated eDrive system for various performance classes

Dr.-Ing. (TH) **Thomas Pullen**,
GKN ePowertrain, Driveline International GmbH,
Technology Centre Lohmar, Lohmar

Abstract

The compact fully integrated electric drive system combines an excellent power to weight ratio and a high volumetric power density. Due to the smart and optimized GKN design a scalability of the integrated system in various performance classes is achieved, despite conventional interfaces between the electric motor, high-performance electronics and transmission are consistently transferred to a common system housing structure.

By modularization of the main subcomponent assemblies an output power from 100kW up to 260kW can be realized. Software controlled active cooling of the electric motor or active lubrication of the transmission can be implemented depending on the thermal and efficiency requirements. The variation of the transmission ratio allows the adjustment of the system performance characteristics according to the vehicle specification.

In addition a performance feature like park by wire or an electronic disconnect differential at the output stage of the transmission, decoupling the transmission and electric motor from the drivetrain, can optionally be integrated. This leads to improved flexibility for the driving strategy of all-wheel and two-wheel drive configurations.

The result of the systematic integration in combination with modularization enables the reduction of complexity across the vehicle derivatives for customer platforms. Benefits are cost advantages due to volume effects, reduced development time and cost and increased robustness for customer tailored propulsion systems.

Introduction

The requirements and specifications for electric drive systems are becoming more and more extensive, as these are defined over various performance classes with the respective required functionalities for customer platform approaches. Front and rear wheel drive systems, which in combination enable electric all-wheel drive applications, should, however, be covered by one design concept in order to reduce complexity.

https://doi.org/10.51202/9783181023549 - Generiert durch IP 216.73.216.36, am 19.01.2026, 02:19:31. © Urheberrechtlich geschützter Inhalt. Ohne gesonderte Erlaubnis ist jede urheberrechtliche Nutzung untersagt, insbesondere die Nutzung des Inhalts im Zusammenhang mit, für oder in KI-Systemen, KI-Modellen oder Generativen Sprachmodellen.

In addition, the different package situations require a high volumetric power density with an optimum power-to-weight ratio, which leads to a high integration level of the main subcomponents in the design concept. Flexibility in the performance features, such as an electronic disconnect or park lock system, is furthermore essential depending on the intended use in the respective vehicle derivative.

GKN's compact, fully integrated electric drive system combines an excellent power-to-weight ratio of greater than 1.9kW/kg with a high volumetric power density of 0,3-0,35kW/dm³, see Figure 1. Due to the smart and optimized design and functional modularization of the most important sub-component assemblies a scalability of the integrated system in various performance classes is achieved, despite conventional interfaces between the electric motor, high-performance electronics and transmission are consistently transferred to a common system housing structure.

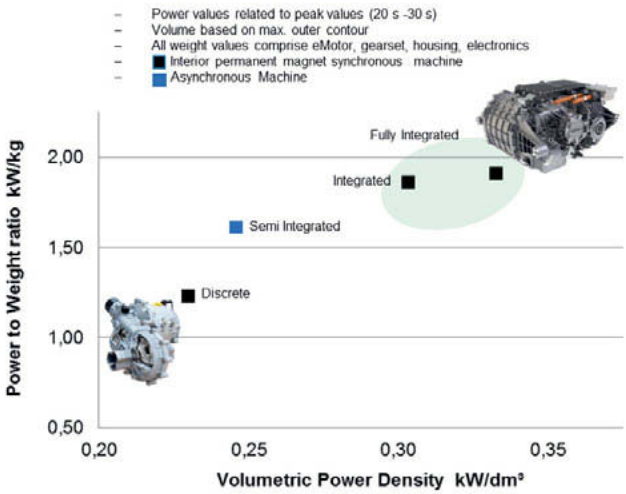


Fig. 1: Integration concepts of the electric drive systems – Source GKN

Systematic integration in combination with modularization

In order to reduce the development scope and by this the complexity of electrical drive systems for vehicle derivatives, the power range is clustered to determine the power of the electric motors. In addition, the system target weights, the maximum required transmission

https://doi.org/10.51202/9783181023549 - Generiert durch IP 216.73.216.36, am 19.01.2026, 02:19:31. © Urheberrechtlich geschützter Inhalt. Ohne gesonderte Erlaubnis ist jede urheberrechtliche Nutzung untersagt, insbesondere die Nutzung des Inhalts im Zusammenhang mit, für oder in KI-Systemen, KI-Modellen oder Generativen Sprachmodellen.

ratio depending on the vehicle speed specifications and, in particular, the most limited installation package are then used as evaluation variables to define the highest performing system in the respective cluster. The definition of High-Performers enable the best possible approach to program management, since the extensive scope is reduced to a few systems and development can therefore be carried out in the shortest possible time at reasonable costs and with a high level of quality assurance, see Figure 2.

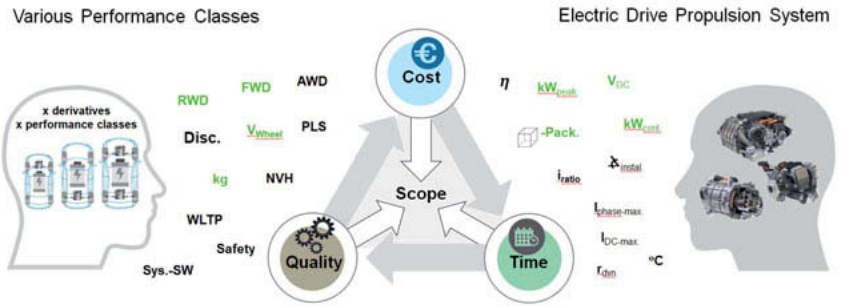


Fig. 2: Evaluation variables for clustering the requirement for electric drive systems for vehicle platforms – Source GKN

In the application example used three High-Performers were identified, two for the power ranges 140kW and 190kW in the front wheel drive and one for the power range up to 200kW in the rear wheel drive. For the two High-Performers in the high power range in particular the selected internal permanent magnet synchronous motor is required in order to achieve the power density in the limited installation package. The efficiency range of the synchronous machine is also better suited to the dynamic requirement profile when using front wheel drive systems in an all-wheel drive application. In addition, the 140kW High-Performer does not require active rotor shaft cooling of the internal permanent magnet synchronous motor, see Figure 3.

https://doi.org/10.51202/9783181023549 - Generiert durch IP 216.73.216.36, am 19.01.2026, 02:19:31. © Urheberrechtlich geschützter Inhalt. Ohne gesonderte Erlaubnis ist jede urheberrechtliche Nutzung untersagt, insbesondere die Nutzung des Inhalts im Zusammenhang mit, für oder in KI-Systemen, KI-Modellen oder Generativen Sprachmodellen.

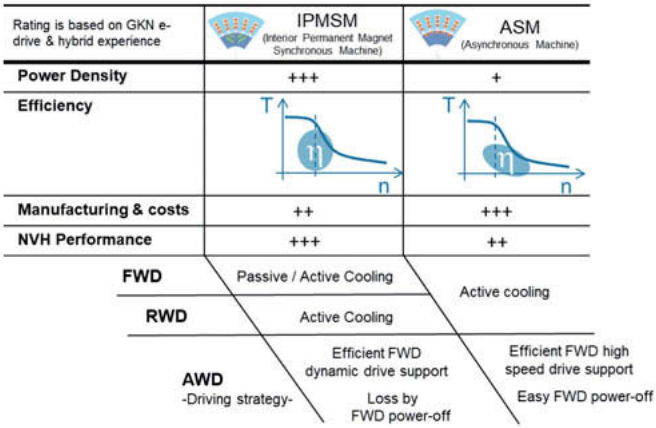


Fig. 3: Electric motor type selection and scaling in the power ranges of High-Performers – Source GKN

While maintaining a constant stator and rotor shaft outer diameter, the electric motor is power scaled by adapting the number of rotor stack stages and thus the length of the active parts. The electric motor for the rear wheel drive can be used for the 190kW High-Performer of the front wheel drive. This reduces the number of necessary drive systems used in the application example, which further reduces the complexity. Modules with constant dimensions can be defined. Figure 4 shows, based on the fix stator outer diameter, constant dimensions for the central system housing structure, the B-shield housing and the inverter housing structure.



Fig. 4: Integrated design concepts for front- and rear wheel drive High-Performers – Source GKN

https://doi.org/10.51202/9783181023549 - Generiert durch IP 216.73.216.36, am 19.01.2026, 02:19:31. © Urheberrechtlich geschützter Inhalt. Ohne gesonderte Erlaubnis ist jede urheberrechtliche Nutzung untersagt, insbesondere die Nutzung des Inhalts im Zusammenhang mit, für oder in KI-Systemen, KI-Modellen oder Generativen Sprachmodellen.

Despite constant dimensioning, the system housing is designed in such a way that the option of active electric motor rotor shaft oil cooling can be integrated. An oil pump module with an oil/water heat exchanger and suction filter can be adapted below the inverter for power ranges greater than 140kW by cutting open the system housing structure at the dedicated cast-on interface. Hardware in the loop tests were conducted to determine the oil flow rate as a function of the pump speed in the temperature range of -30°C to 95°C for pressures up to 3 bar. On this basis a PWM-control was developed, which ensures an oil flow rate with an accuracy of ± 2%. Numerical fluid dynamic investigations were conducted to optimize the design of the inner rotor shaft geometry and the oil outlet holes so that the oil flow in the rotor shaft does not break off even at a maximum rotor speed of 17.000rpm, see Figure 5. This ensures that the permissible magnet and wire temperatures in the electric motor are not exceeded at continuous power and maximum speed.

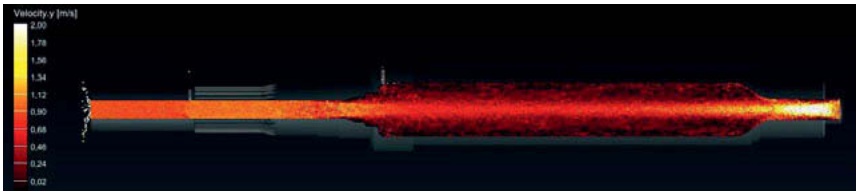


Fig. 5: CFD Result of oil flow in the rotor shaft at 17.000rpm, oil flow rate 5l/min, at 85°C – Source GKN

To optimize cost the electric motor in the power range up to 140kW can be operated without active rotor shaft oil cooling. As a result, active cooling of the gearbox is no longer applicable. To optimize the oil distribution with passive cooling, an inlet module is installed on gearbox side of the system housing. This inlet, specifically developed by numerical fluid dynamic analyses, generates oil reservoirs by rotation of the gear shafts, from which the oil supply to the bearing points and gear meshing is ensured, see Fig. 6.

https://doi.org/10.51202/9783181023549 - Generiert durch IP 216.73.216.36, am 19.01.2026, 02:19:31. © Urheberrechtlich geschützter Inhalt. Ohne gesonderte Erlaubnis ist jede urheberrechtliche Nutzung untersagt, insbesondere die Nutzung des Inhalts im Zusammenhang mit, für oder in KI-Systemen, KI-Modellen oder Generativen Sprachmodellen.

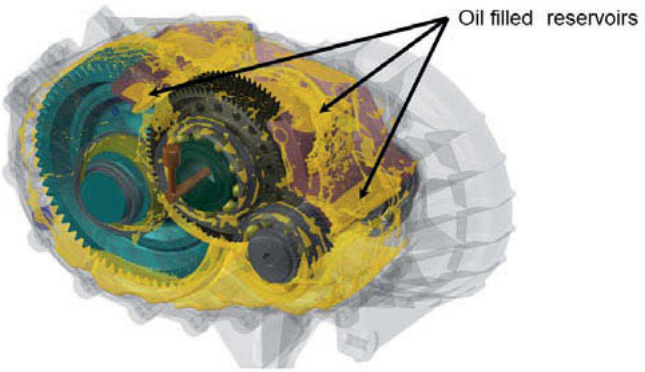


Fig. 6: CFD Result of oil distribution in the gearbox with inlet module at 50kph, at 70°C – Source GKN

In addition, such an oil distribution reduces the drag torque values so that drag torques close to active cooling can be achieved at low speeds, see Fig. 7.

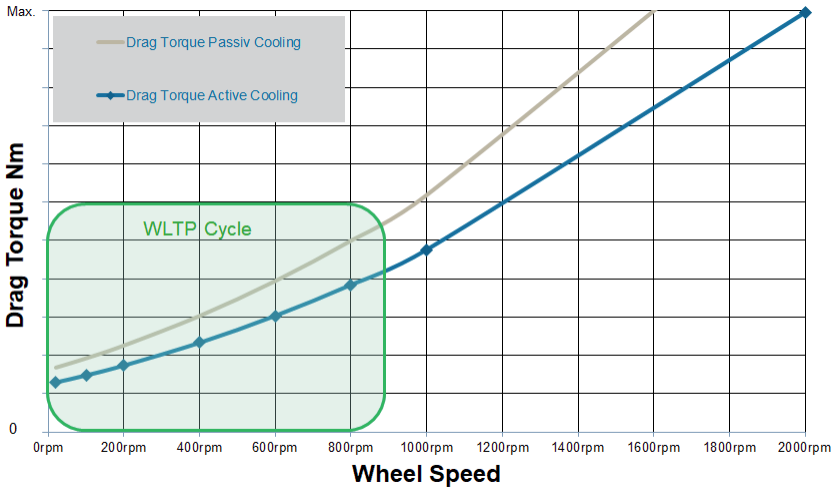


Fig. 7: Drag torque comparison for active and optimized passive gearbox lubrication – Source GKN

https://doi.org/10.51202/9783181023549 - Generiert durch IP 216.73.216.36, am 19.01.2026, 02:19:31. © Urheberrechtlich geschützter Inhalt. Ohne gesonderte Erlaubnis ist jede urheberrechtliche Nutzung untersagt, insbesondere die Nutzung des Inhalts im Zusammenhang mit, für oder in KI-Systemen, KI-Modellen oder Generativen Sprachmodellen.

In order to adjust the transmission ratio in the gearbox to lower vehicle speeds, whereby the High-Performer represents the maximum required, the interface between the electric motor and the input of the transmission is adapted. The input-pinion is exchangeable and with its splined interface, shrunk-fit onto the rotor shaft, enables a minimum eccentricity and minimum angular error. A three bearing arrangement, whereby a pilot bearing is placed onto the input pinion within the gearbox cover, reduces the misalignment at the spline interface, see Figure 8. The changeable gear on the lay-shaft also has shrunk-fit and therefore a minimum of eccentricity. Despite the modular design, this approach enables NVH and efficiency values to be improved at a position, where high speed and torque has to be transmitted.

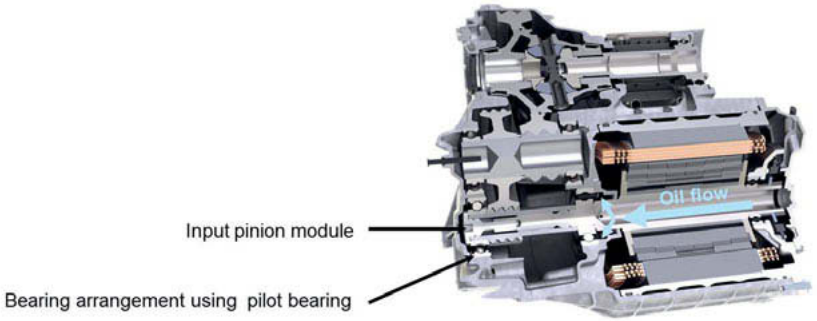


Fig. 8: Modular interface between the electric motor and the input of the transmission – Source GKN

A further performance feature, which can be integrated, is the electronic disconnect differential at the second stage of the transmission. It can decouple the transmission and electric motor at the interface to the side shafts from the road. Thus the system efficiency, considering all-wheel drive configurations, will improve by use of the electronic disconnect differential varying between connected and disconnected driving events - depending of the driving strategy.

Changes in the power electronics of the respective High-Performers are realized by varying the number of transistor modules, which means the number of modules for the High-Performer in the power range up to 140kW, are reduced due to its lower required current and voltage values. The internal cooling interface to the heat sink is defined identically. External interfaces for coolant transfer are kept identical in shape and position. A separator module

https://doi.org/10.51202/9783181023549 - Generiert durch IP 216.73.216.36, am 19.01.2026, 02:19:31. © Urheberrechtlich geschützter Inhalt. Ohne gesonderte Erlaubnis ist jede urheberrechtliche Nutzung untersagt, insbesondere die Nutzung des Inhalts im Zusammenhang mit, für oder in KI-Systemen, KI-Modellen oder Generativen Sprachmodellen.

enables the adjustment between the HV-busbar interface and the electric motor terminals, which vary in length due to the electric motor scaling. The control board of the power electronics features two motor control channels, the first for the traction motor control and a second optional channel for an actuator, e.g. for the electronic pump.

Summary

GKN developed the compact fully integrated electric drive system in a smart and optimized design concept by breaking down the scope and clustering the systems into a single modular High-Performer system that can be applied to various performance classes and by this reduces complexity in customer platform approaches. The High-Performer combines an excellent power to weight ratio and a high volumetric power density by transferring conventional interfaces between the electric motor, high-performance electronics and transmission consistently to a common system housing structure. While keeping the dimensions and interfaces of the system housing constant, the functional modularization of the most important sub-component assemblies enables output power and performance to vary.

The permanent magnet synchronous electric motor can be adapted by adjusting the number of rotor stack stages and thus the length of the active parts. While keeping the interface architecture, a high voltage separator module adjusts the connection to suit the terminals of the electric motor and the power electronics. Changes in the power electronics due to lower required current and voltage values are realized by varying the number of transistor modules. The software controlled electronic pump as key feature of the active thermal management can be implemented on demand to cool actively the electric motor and lubricate the transmission for systems in the high power ranges. An inlet module to reduce drag loss at low speeds optimizes passive transmission lubrication improving efficiency.

The replaceable input pinion with pilot bearing arrangement enables the installation of different transmission ratios according to the vehicle speed specification. Misalignment at the spline interface is eliminated improving NVH and efficiency in a position where high speeds and torques must be transmitted. The electronic disconnect differential at the output stage of the transmission, as a performance module to decouple the transmission and electric motor from the drivetrain, can optionally be integrated replacing the open differential. This leads to an improved design flexibility to match the electric drive system performance characteristics to the driving strategy of all-wheel and two-wheel drive configurations.

https://doi.org/10.51202/9783181023549 - Generiert durch IP 216.73.216.36, am 19.01.2026, 02:19:31. © Urheberrechtlich geschützter Inhalt. Ohne gesonderte Erlaubnis ist jede urheberrechtliche Nutzung untersagt, insbesondere die Nutzung des Inhalts im Zusammenhang mit, für oder in KI-Systemen, KI-Modellen oder Generativen Sprachmodellen.

Next generation of 48V HEV

Dr. **W. Wenzel**, Dr. **M. Eglinger**,
BorgWarner Ludwigsburg GmbH, Ludwigsburg;
M. Li, **C. Sieg**, **J. Hengst**, Prof. Dr.-Ing. **F. Küçükay**,
Institute of Automotive Engineering, Technical University Braunschweig

Abstract

To improve efficiency and performance at moderate costs 48V HEV play an important role. Current 48V hybrids provide a peak electrical power of approximate 20 kW. It is expected that in the next years the 48V system can offer a peak electrical power up to 35 kW. Thus, the efficiency and performance of the 48V electrified drive train can be enhanced. In this paper, different drive train topologies suitable for 48V hybridization – P0P4, P2P4 – are investigated in two driving cycles - WLTC and RDE cycle. They are compared to a high-voltage power split DHT (Dedicated Hybrid Transmission), a current P0 48V hybrid and a conventional vehicle. In order to evaluate the efficiency, the charge sustaining fuel consumption is calculated. In addition, the acceleration time in hybrid operation from 0 km/h to 100 km/h is examined to compare the performance. To estimate the powertrains, a modular simulation model developed at the Institute of Automotive Engineering (IAE) is used. Furthermore, a lossmap-based transmission loss simulation is integrated to improve the validity and accuracy of the simulation. The next generation 48V MHEV (P0P4 and P2P4) show a great potential to increase driving performance and efficiency in comparison to the current 48V MHEV (P0).

Introduction

The upcoming limits for fleet CO_2 limitation especially in Europe and China are pushing electrification of vehicles significantly. To achieve a balance between powertrain costs and lowering the CO_2 emissions, different levels of hybridization were developed and appear on the market. Besides very low electrification of an entry level of 12V dual storage hybrids [1], which already allow a small amount of brake energy recuperation and engine off coasting, so-called mild hybrids with 48V will occupy a huge portion of the market and are expected to replace conventional vehicles as a new baseline in some segments. Especially in Europe and China, a big market could be expected. 48V hybrids can improve efficiency and driving performance at moderate costs. A 48V board net, on the one hand, could be an enabler for electric climate compressor, electric air boosting devices [2] and also supports electric systems like an anti-

https://doi.org/10.51202/9783181023549 - Generiert durch IP 216.73.216.36, am 19.01.2026, 02:19:31. © Urheberrechtlich geschützter Inhalt. Ohne gesonderte Erlaubnis ist jede urheberrechtliche Nutzung untersagt, insbesondere die Nutzung des Inhalts im Zusammenhang mit, für oder in KI-Systemen, KI-Modellen oder Generativen Sprachmodellen.

roll system. On the other hand, the power levels allow brake energy recuperation levels, which cover a high share of the energy offered in the standard test cycles.

The base architecture for the first mild hybrid vehicles is the P0 architecture with maximum power during recuperation of up to 12 kW and usually a less power for electric boosting on the crankshaft. P0 applications are easy to be installed, however, the losses on the recuperation path from the wheels to the motor generator unit (MGU) are relatively high, which limits the CO_2 benefits of this approach. Engine start with a belt starter alternator is fast, so engine off coasting and extended start-stop provides benefits which might not be fully covered in the test cycle, but can be addressed by eco-innovation credits.

More advanced mild hybrid vehicles are equipped with more powerful electric Motors (EM) in different parallel architectures. The most common solution is the P2 topology where the EM is located between the internal combustion engine (ICE) and the transmission. A clutch to disconnect the ICE allows recuperation with a higher power to harvest a higher share of the available energy. The architectures P3 and P4 are characterized by low mechanical losses in the recuperation path. However, the operation point of the EM cannot be changed by a gear shift. In general, the option to disconnect the engine allows to recuperate a higher share of braking energy which improves the CO_2 potential of these applications. An evaluation of different architectures for current and future 48V HEV including 48V electrified DCT was carried out by [3].

In this paper, a further step is taken. The 48V mild hybrids are taken to the next level, which leads to additional technical possibilities. Instead of one electric motor, two motors will be used in different architectures. To limit the electric currents, the total mechanical power of the EM is limited to 35 kW in total. Even, if the recuperation potential could not be increased that much compared to a P2 system, the benefits of this advanced architecture are given by

- More electric boost
- Efficient use of both EMs (different sizing allows to use motors optimized for efficient working ranges)
- Operation of the combustion engine closer to the sweet spot by load point shift and avoiding low load operation

The objectives of the research are an evaluation of different drive train topologies suitable for next generation of 48V HEV in WLTC and RDE cycle via simulation and examination of optimal integration of two EMs in a 48V hybrid powertrain. Efficiency and driving performance of P0P4 and P2P4 are compared to a conventional internal combustion engine vehicle (ICV), a current 48V hybrid (P0) and a high-voltage power split DHT.

https://doi.org/10.51202/9783181023549 - Generiert durch IP 216.73.216.36, am 19.01.2026, 02:19:31. © Urheberrechtlich geschützter Inhalt. Ohne gesonderte Erlaubnis ist jede urheberrechtliche Nutzung untersagt, insbesondere die Nutzung des Inhalts im Zusammenhang mit, für oder in KI-Systemen, KI-Modellen oder Generativen Sprachmodellen.

Based on the evaluation of the European market, a representative vehicle is selected. Small SUVs, sometimes also named city SUV, have a big growth rate and a high market in Europe, but show significant growth rates also on other markets, e.g. China.

Modular simulation model and operating strategy

For evaluation and optimization of different powertrain concepts, a modular simulation model was developed at IAE [4]. The functional principle of the model is shown in Figure 1.

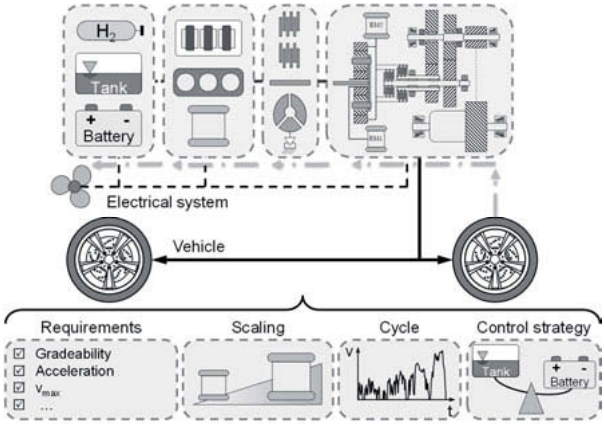


Fig. 1: Modular simulation model of the IAE

In this backward simulation model, the speeds and driving resistances on the wheel are calculated in the wheel module using the vehicle parameters and the driving cycle data. Then, the necessary output torques and speeds of the transmission module are calculated. In the transmission module, the gear ratios, as well as the mechanical connections, are defined. Furthermore, up to nine integrated EMs can be integrated into the transmission. In this way, a performance and efficiency simulation of any conventional or hybrid transmission is possible with low effort.

A model developed by [5] is used to generate transmission loss maps. It allows to model the efficiency of the transmission taking the operating mode dependent transmission efficiency into account. Apart from load-dependent losses such as the losses of bearing and gearing, independent losses such as the losses of oil pump are considered. The generated loss maps can then be integrated into the modular simulation model. During simulation, all possible com-

https://doi.org/10.51202/9783181023549 - Generiert durch IP 216.73.216.36, am 19.01.2026, 02:19:31. © Urheberrechtlich geschützter Inhalt. Ohne gesonderte Erlaubnis ist jede urheberrechtliche Nutzung untersagt, insbesondere die Nutzung des Inhalts im Zusammenhang mit, für oder in KI-Systemen, KI-Modellen oder Generativen Sprachmodellen.

binations of operating points, e.g. speeds and torques of transmission-integrated EM, are calculated within the transmission module. Based on these results, the propulsion and launch element module calculate matching operating points for the energy converters outside the transmission.

The efficiency of the EM and the ICE is calculated with loss maps. The best possible mode of operation, as well as the best operation point is selected by the optimization-based Equivalent Consumption Minimization Strategy (ECMS) developed by [4].

The ECMS can be complemented by additional drivability criteria to be closer to a real-world application. For example, the minimum operating time for the ICE is 4 s in this analysis. To simplify the evaluation, only warm operation will be taken into account. The minimum duration of one operating mode is set to 2 s. Mode shifting events are limited with an operation mode selection regulation.

Topologies

In this paper, various topologies applicable to future 48V hybrid vehicles are investigated. The configurations P0P4 and P2P4 comprise an EM connected to the rear axle providing temporary electric all-wheel-drive. The conventional powertrain, P0 powertrain and power split powertrain are integrated into a basic vehicle with front-wheel drive. The main topologies P0P4, P2P4 for MHEV and power split for HEV are shown in Figure 2.

https://doi.org/10.51202/9783181023549 - Generiert durch IP 216.73.216.36, am 19.01.2026, 02:19:31. © Urheberrechtlich geschützter Inhalt. Ohne gesonderte Erlaubnis ist jede urheberrechtliche Nutzung untersagt, insbesondere die Nutzung des Inhalts im Zusammenhang mit, für oder in KI-Systemen, KI-Modellen oder Generativen Sprachmodellen.

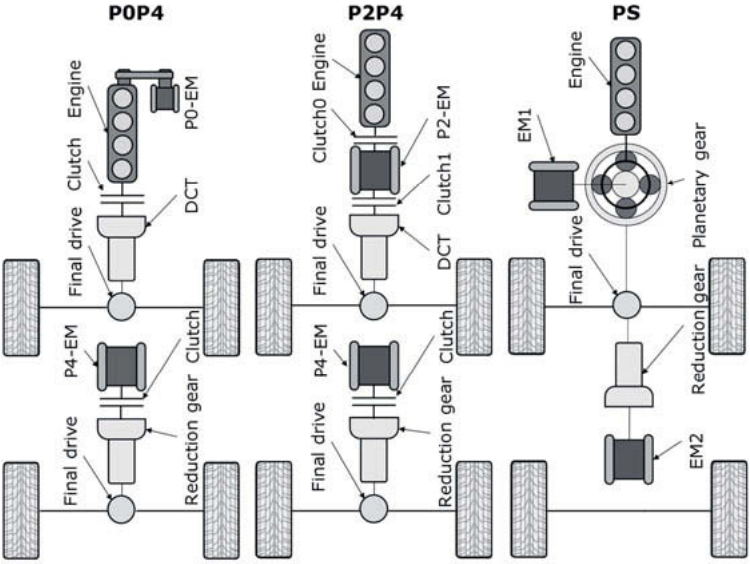


Fig. 2: Topologies of P0P4, P2P4 and power split DHT

Compared to a P0 topology, the P2 layout, comprising a separating clutch between ICE and EM, allows to disconnect the ICE while driving. Thus, the electric motor can operate independently without engine drag losses. In addition, it is possible to use all gears of the transmission during the electric drive. In the P4 hybrid, the electric motor is driving the rear axle so that electric all-wheel-drive is temporarily possible. In this paper, the P4-EM is connected to the rear axle via a disconnect clutch to avoid over-speeding at high vehicle speeds.

The power split DHT (PS-DHT), see Figure 2, as efficiency benchmark comprises an ICE connected to a planetary gear set (PGS) and two EM also connected to the PGS allowing a power split mode. These two electric motors are also connected to each other via the power electronics. A continuous variation of the gear ratio between ICE and wheel is possible, even when the battery is fully charged. The PS-DHT is characterized by a lower mechanical complexity resulting from fewer gear meshes and the absence of a launch element. However, the disadvantages are the relatively low efficiency of the electrical branch compared to the mechanical branch and the higher required electrical power.

https://doi.org/10.51202/9783181023549 - Generiert durch IP 216.73.216.36, am 19.01.2026, 02:19:31. © Urheberrechtlich geschützter Inhalt. Ohne gesonderte Erlaubnis ist jede urheberrechtliche Nutzung untersagt, insbesondere die Nutzung des Inhalts im Zusammenhang mit, für oder in KI-Systemen, KI-Modellen oder Generativen Sprachmodellen.

Vehicle parameters and energy converters

The vehicle parameters for the small SUV are based on a market research. Table 1 shows the most important vehicle parameters.

Table 1: Vehicle parameters of the small SUV

	Value	Unit
vehicle mass (incl. driver)	1600	kg
max. load	500	kg
frontal area	2.45	m²
c_D	0.30	-
$f_{Roll,0}$	0.008	-

In order to maintain the driving performance at low state of charge (SOC) and to represent a typical rightsizing approach, the ICV and MHEV architecture are combined with a boosted direct injection gasoline engine with a displacement of 1.5 L. Having high overall efficiency in mind, the selected engine uses a high compression ratio with fixed Miller valve timing, which reduces the complexity. In the ICV and the MHEV a 7-speed-DCT with wet clutchs was used. A 2.0 L naturally aspirated engine with Atkinson valve timing approach and a high compression ratio is used in the power split hybrid. In this paper, two different permanent magnet synchronous electric motors (PSM EM) are used and scaled to meet the driving performance requirements. The data of used drive machines are shown in Table 2.

Table 2: ICE parameters and basic EM parameters used for scaling

Drive machine	ICE for 48V HEV	48V EM	ICE for power split	high voltage EM
Type	1.5 L turbo-charged direct injection	PSM	2.0 L naturally aspirated Atkinson	PSM
peak power [kW]	96	15	110	75
max. torque [Nm]	205	105	180	250
max. speed [1/min]	6000	6000	6000	12000

In this paper, the total electrical power is limited to 35 kW. In WLTC, the power of the auxiliaries is set to 200 W and to 450 W in the RDE cycle. The usable capacity of the battery is 1.2 kWh and the efficiency is set to be 95 %.

https://doi.org/10.51202/9783181023549 - Generiert durch IP 216.73.216.36, am 19.01.2026, 02:19:31. © Urheberrechtlich geschützter Inhalt. Ohne gesonderte Erlaubnis ist jede urheberrechtliche Nutzung untersagt, insbesondere die Nutzung des Inhalts im Zusammenhang mit, für oder in KI-Systemen, KI-Modellen oder Generativen Sprachmodellen.

Driving performance requirements

The modular simulation model allows to define driving performance requirements for various operating states of the drive train. All possible states are shown in Figure 3. These take into account how the main energy sources interact with each other and influence the driving performance. In electrical operation (state A) the battery provides the necessary driving power. In the charging operation (state B) the battery is being charged, the ICE needs to provide the charging power as well as the necessary driving power. In the discharging operation (state C) both the battery and the ICE provide power for driving. In ICE operation (state D) the vehicle is driven only via the ICE and the battery is neither charged or discharged. State E describes a drive train state in which the operating strategy is allowed to choose the drive train state (states A – D) which leads to the maximum vehicle performance at every vehicle speed.

For the P0P4 and P2P4 architectures, the similar performance requirements are defined. In contrast, different requirements are defined for the power split. The defined performance requirements for each drive train state are listed in Table 4.

The defined maximum speed is 180 km/h in hybrid mode. The vehicle should reach a speed of 70 km/h in pure electric operation. EM should operate up to speeds of 135 km/h to be able to recuperate braking energy at high speeds in WLTC. In hybrid operation, the vehicle is expected to reach the traction limit up to 10 km/h. In electric operation, the MHEV is required to provide an acceleration of 1 m/s² in a range between 0 km/h and 20 km/h. In contrast to MHEV the power split should enable an acceleration ability with 1.75 m/s² to 20 km/h in electric operation to cover all acceleration maneuvers up to 20 km/h in WLTC. Furthermore, the vehicle is expected to provide 20 kW boost power and ensure a 3 kW charge power.

https://doi.org/10.51202/9783181023549 - Generiert durch IP 216.73.216.36, am 19.01.2026, 02:19:31. © Urheberrechtlich geschützter Inhalt. Ohne gesonderte Erlaubnis ist jede urheberrechtliche Nutzung untersagt, insbesondere die Nutzung des Inhalts im Zusammenhang mit, für oder in KI-Systemen, KI-Modellen oder Generativen Sprachmodellen.

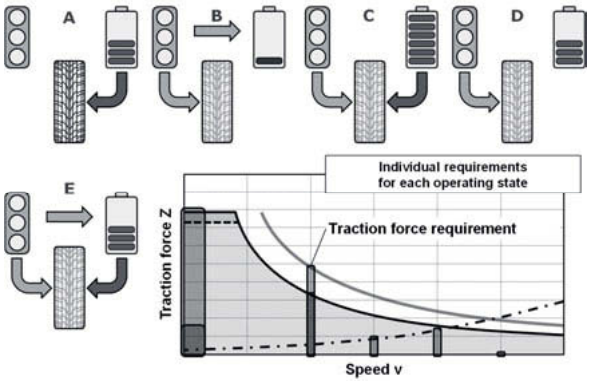


Fig. 3: Operating states of hybrid drives: (A) battery operation, (B) hybrid operation - battery charging, (C) hybrid operation - battery discharging, (D) ICE operation - no battery usage, (E) hybrid operation - arbitrary battery usage

Table 4: Driving performance requirements for different operating states

MHEV	Arbitrary	0-10 km/h	traction limit
		100 km/h	$P_{ICE,max}$ + 20 kW boost power
		180 km/h	maximum speed
	Charging	0-10 km/h	traction limit
		100 km/h	$P_{ICE,max}$ - 3 kW charge power
		180 km/h	maximum speed
	Electric	0-20 km/h	acceleration 1 m/s²
		70 km/h	maximum speed
		135 km/h	recuperation up to 135 km/h
Power split	Arbitrary	0-10 km/h	traction limit
		100 km/h	$P_{ICE,max}$ + 20 kW boost power
		180 km/h	maximum speed
	Charging	0-10 km/h	traction limit
		100 km/h	$P_{ICE,max}$ - 3 kW charge power
		180 km/h	maximum speed
	Electric	0-20 km/h	acceleration 1.75 m/s²
		70 km/h	maximum speed
		135 km/h	recuperation up to 135 km/h

https://doi.org/10.51202/9783181023549 - Generiert durch IP 216.73.216.36, am 19.01.2026, 02:19:31. © Urheberrechtlich geschützter Inhalt. Ohne gesonderte Erlaubnis ist jede urheberrechtliche Nutzung untersagt, insbesondere die Nutzung des Inhalts im Zusammenhang mit, für oder in KI-Systemen, KI-Modellen oder Generativen Sprachmodellen.

To identify the optimal powertrain concept, a full factorial parameter variation is carried out. The basic parameters such as the power of the EM and the gear ratios are varied. Due to the limitation of the total electric power, the power of the P0-EM, as well as P2-EM, is set to 15 kW and the power of the P4-EM with 20 kW for both, the P0P4 and P2P4 hybrid configurations, confirms the requirements. The gear ratio of the reduction gear will be varied from 5 to 12 to identify the variants which can meet the requirements in electric operation state. The electric power of the EM installed in the PS-DHT is set to 50 kW for EM1 and 75 kW for EM2. The gear ratios of the planetary gear, reduction gear and final drive are also varied. The driving performance simulation allows to exclude powertrain variants which do not meet the driving performance requirements to lower the computational effort.

Driving cycles

For the efficiency evaluation of the different powertrains, two driving cycles are considered: The Worldwide Harmonized Light Duty Vehicle Test Cycle (WLTC), and a driving cycle conform with RDE requirements, shown in Figure 4. This cycle was generated using a methodology developed by [6]. It allows to generate RDE-compliant cycles which are representative for customer operation. In addition, the methodology allows to tailor the cycle so that the driving style can be described as very sporty within the RDE requirements. In comparison to the WLTC, the wheel power is higher. The sporty customer cycle of IAE has a duration of approx. 5750 s and covers a distance of approx. 95.8 km. The maximum speed is about 143 km/h.

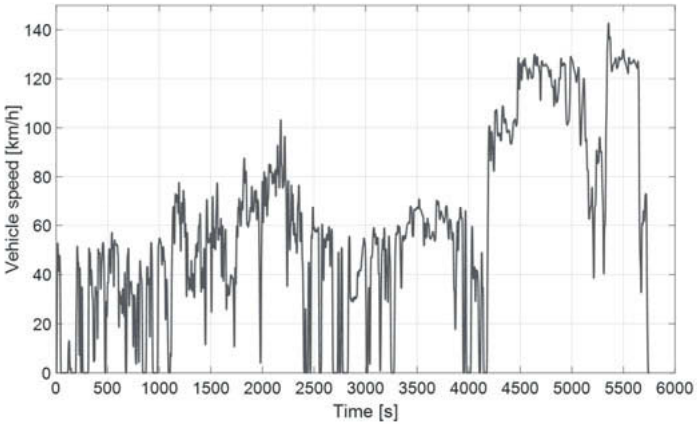


Fig. 4: Sporty real driving emissions (RDE) cycle generated by IAE

https://doi.org/10.51202/9783181023549 - Generiert durch IP 216.73.216.36, am 19.01.2026, 02:19:31. © Urheberrechtlich geschützter Inhalt. Ohne gesonderte Erlaubnis ist jede urheberrechtliche Nutzung untersagt, insbesondere die Nutzung des Inhalts im Zusammenhang mit, für oder in KI-Systemen, KI-Modellen oder Generativen Sprachmodellen.

Comparison and evaluation of drive train topologies

In this paper, the evaluation of the drive concepts focuses on driving performance and efficiency. To evaluate the efficiency, the SOC neutral CO_2 emissions in WLTC and RDE cycle are calculated. The acceleration time from 0 km/h to 100 km/h in hybrid operation is calculated and used to evaluate the driving performance.

Figure 5 shows the SOC neutral CO_2 emissions in WLTC and the acceleration time from 0 km/h to 100 km/h of all variants. With 124.4 g/km, the ICV shows the highest CO_2 emissions of all variants. Compared to the ICV the CO_2 emissions of the P0 are about 113.2 g/km and reduced by 9 %. The main reasons for this are the recuperation and load point shift of the ICE. In addition, the average engine efficiency is improved from 34.2 % for the ICV to 35.0 % for the P0 HEV. As a consequence of the ICE drag torque, the electric drive mode in the P0 architecture is not possible. Compared to the ICV, the P0-EM can be used while boosting so that the acceleration time in hybrid operation decreases from approx. 9.2 s to 8.2 s.

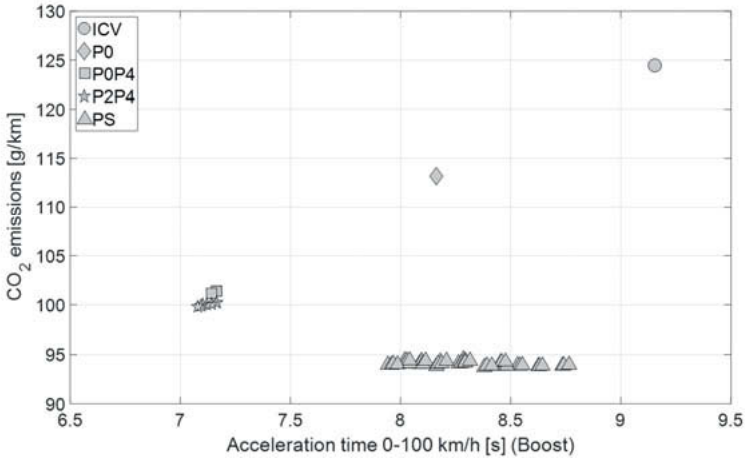


Fig. 5: CO_2 emissions in WLTC and acceleration time in hybrid operation

Due to the limited total power of the EM and the given power of the P0 EM, only two variants of the P0P4 topology comply with the driving performance requirements. The CO_2 emissions are about 101.2 g/km and 10 % lower compared to the P0 architecture. The lower emissions occur since the vehicle can be fully electrically driven by the P4-EM. More energy can be recuperated by more electric maximum power. Furthermore, the recuperation portion of a share

https://doi.org/10.51202/9783181023549 - Generiert durch IP 216.73.216.36, am 19.01.2026, 02:19:31. © Urheberrechtlich geschützter Inhalt. Ohne gesonderte Erlaubnis ist jede urheberrechtliche Nutzung untersagt, insbesondere die Nutzung des Inhalts im Zusammenhang mit, für oder in KI-Systemen, KI-Modellen oder Generativen Sprachmodellen.

of the braking energy with P4-EM is more efficient, because only the differential and the reduction stage lead to lower transmission losses. Depending on the driving situation, the braking energy can be recuperated by one or both of the two EMs. Compared to the P0 HEV, the average engine efficiency increases to approx. 35.9 %. The electrical rear axle allows high torques during acceleration and leads to a better driving performance compared to the P0 HEV and the ICV.

The evaluation provided six valid variants for the P2P4 architecture. The P2P4 has a similar CO_2 impact as the P0P4. At the same time, the average engine efficiency is only slightly increased to 36.2%. The main reason is that the total power of the EMs is the same. This leads to the fact that the energy generated via recuperation as well as the energy used for electric driving do not differ significantly. However, the results show a small difference regarding the CO_2 impact since the separating clutch of the P2P4 topology allows to disconnect the ICE during electric driving and recuperation. In addition, electric driving is more efficient in case of a P2P4 hybrid because the P2-EM can use all gears of the transmission. Thus, electric driving is possible more often. Since the total electric power of the P0P4 and P2P4 is the same, the acceleration time in hybrid mode only differs slightly.

The power split is represented by more variants and achieves the best efficiency in comparison to other topologies. Due to the characteristics of the power split architecture, the 2.0 L ICE with Atkinson cycle can operate at a higher mean efficiency of approx. 40.2%. The EM2 has significantly higher output power which leads to a higher recuperation potential and allows electric driving at higher wheel power. The driving performance depends on the PGS- and reduction gear ratio. Since many combinations of these gear ratios allow to fulfill the requirements, the acceleration time in hybrid mode ranges between 7.8 s and 8.8 s.

Figure 6 compares the acceleration time from 0 km/h to 100 km/h in hybrid operation for the variants with the highest performance. The powers of the EMs are also presented. The acceleration time from 0 km/h to 100 km/h of the ICV is about 9.2 s. The acceleration time for P0 HEV is about 1 s shorter than the ICV because of the boost power from the 15 kW P0-EM. The P0P4 and the P2P4 have the same total electric power. The acceleration time of P2P4 is about 0.1 s shorter. The reason for this is that the gear ratio at the rear axle is higher. When boosting with maximal power, the front axle reaches the traction limit. Thus, the acceleration time depends on the EM torque as well as the reduction gear ratio. The 7-speed DCT on front axle allows the P2-EM to operate at 135 km/h which is defined as a performance requirement for electric operation. Thus, the gear ratio of the reduction gear at the rear axle can be higher to provide a higher wheel torque. The P0P4 vehicle can only be electrically driven by the P4-EM. To reach the same speed requirement in electric operation the gear ratio of the reduction gear

https://doi.org/10.51202/9783181023549 - Generiert durch IP 216.73.216.36, am 19.01.2026, 02:19:31. © Urheberrechtlich geschützter Inhalt. Ohne gesonderte Erlaubnis ist jede urheberrechtliche Nutzung untersagt, insbesondere die Nutzung des Inhalts im Zusammenhang mit, für oder in KI-Systemen, KI-Modellen oder Generativen Sprachmodellen.

must be lower. The power split has more powerful drive machines, but it achieves a lower acceleration ability than P0P4 and P2P4 because the power split is integrated into a vehicle with front-wheel drive. However, the acceleration time is shorter than the P0.

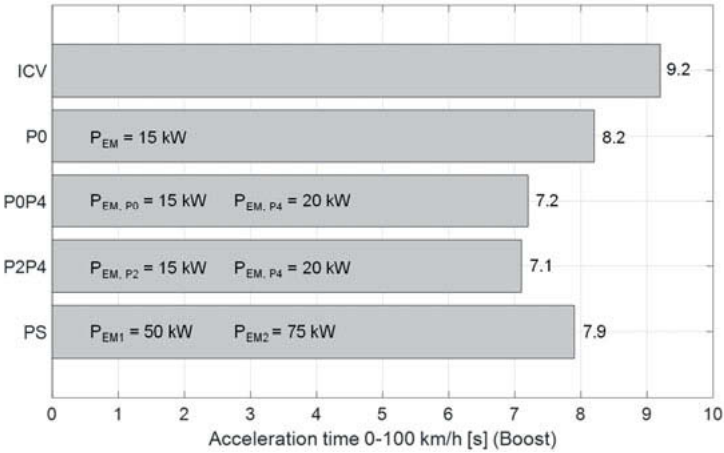


Fig. 6: Comparison of hybrid acceleration time from 0 km/h to 100 km/h for variants with the best performance

The CO_2 emissions in WLTC and RDE cycle are compared in Figure 7. Generally, the CO_2 emissions in the RDE cycle are higher than in the WLTC. The main reason is that the theoretical recuperation potential in WLTC is higher than in RDE. In addition, the difference of the CO_2 emissions between RDE cycle and WLTC for each topology is not the same. The CO_2 emissions of the ICV in RDE cycle are about 6 % higher than in WLTC. In contrast, the CO_2 emissions of the P0 HEV in RDE cycle are about 8 % higher than in WLTC. Compared to the differences of the ICV and P0 MHEV, the difference of CO_2 emissions between WLTC and RDE in case of P0P4 HEV and P2P4 HEV are about 10 % higher. The main reason for this is that the recuperation potential strongly influences the CO_2 emissions. The recuperation potential of the P0 HEV is significantly lower compared to systems with higher complexity such as P2P4 or PS-DHT. Thus, the difference between CO_2 emissions in WLTC and the RDE cycle are smaller in case of a P0 HEV. In addition, the ICV can only recuperate a comparably small amount of braking energy via its generator. This leads to lower differences between RDE and WLTC CO_2 emissions compared to other topologies.

https://doi.org/10.51202/9783181023549 - Generiert durch IP 216.73.216.36, am 19.01.2026, 02:19:31. © Urheberrechtlich geschützter Inhalt. Ohne gesonderte Erlaubnis ist jede urheberrechtliche Nutzung untersagt, insbesondere die Nutzung des Inhalts im Zusammenhang mit, für oder in KI-Systemen, KI-Modellen oder Generativen Sprachmodellen.

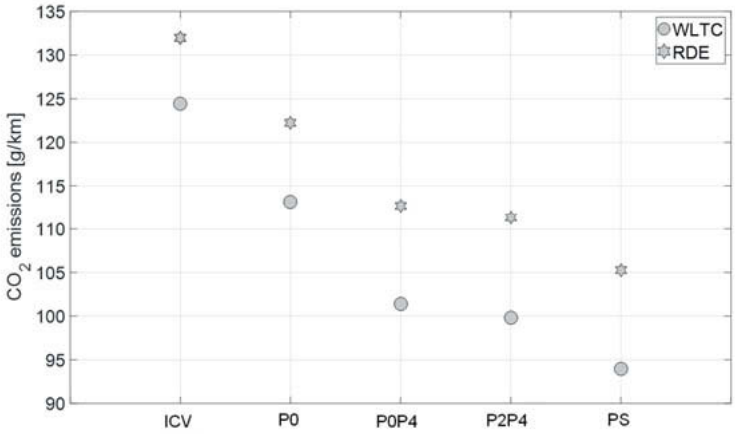


Fig. 7: CO_2 emissions in WLTC and RDE for variants with the best efficiency

Figure 8 shows operating mode specific energy shares at EM level of each topology for the variants with the highest efficiency in WLTC and RDE cycle. The negative energy represents the electric energy which is generated by the EM. The positive energy is used to drive electrically and to increase the load point of the ICE. The difference between the negative and positive energy share results from the auxiliaries' energy consumption.

The P0 can recuperate braking energy of about 2.2 kWh/100km. The P0-EM can improve the ICE efficiency by load point increase. It can be seen that electric drive is not possible. Instead, the energy provided by recuperation is used to decrease the load point of the ICE since the simulation is required to be SOC neutral. The P0P4 can achieve more recuperation energy. In contrast to the P0, the P0P4 spends most of the electrical energy for electric driving since this leads to lower CO_2 emissions than load point decrease. The P2P4 can recuperate a higher amount of braking energy in WLTC since the ICE can be disconnected from the drive train. In addition, the operating point of the P2-EM can be changed by a gear shift. As a result, the P2P4 HEV is able to store a higher amount of energy. Thus, more energy is used for electric driving and load point decrease compared with the P0P4 HEV. The power split concept reaches a similar amount of recuperated energy since cycle and vehicle parameters mainly influence the recuperation potential. To efficiently modify the gear ratio between ICE and wheel, the power split HEV often needs to charge the battery. As a consequence, the energy share

https://doi.org/10.51202/9783181023549 - Generiert durch IP 216.73.216.36, am 19.01.2026, 02:19:31. © Urheberrechtlich geschützter Inhalt. Ohne gesonderte Erlaubnis ist jede urheberrechtliche Nutzung untersagt, insbesondere die Nutzung des Inhalts im Zusammenhang mit, für oder in KI-Systemen, KI-Modellen oder Generativen Sprachmodellen.

of load point increase in WLTC is higher compared to other topologies. As a result of the increased energy due to recuperation and load point increase, the energy share of electric driving is higher.

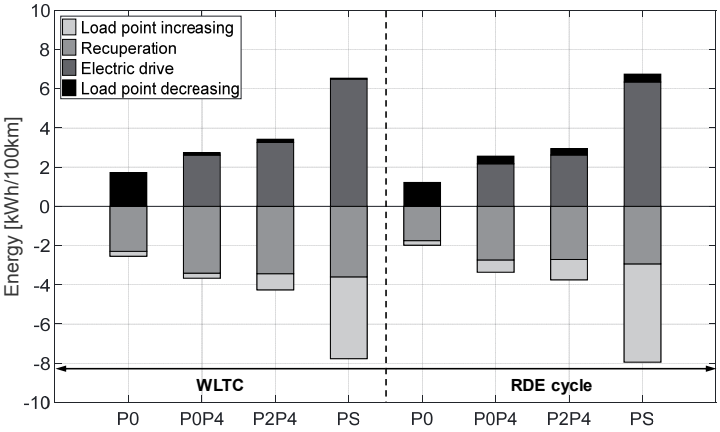


Fig. 8: Energy on EM level for different hybrid functions for variants with the best efficiency in WLTC and RDE

The operating mode specific energy shares in the RDE cycle are shown in Figure 8. Due to the cycle characteristics, the recuperated energy of all topologies is lower than in WLTC. In addition, the results show a higher energy share of load point decrease in RDE compared to WLTC. The reason is that either boosting is required or load point decrease is efficient in case the ICE provides a comparably high power. The difference between the total positive and negative energy is higher compared to the WLTC since the power consumption of the auxiliaries is higher.

The C-rate describes the ratio between the charge or discharge current of a battery and its capacity and is usually given in 1/h. It is an important parameter to describe the battery usage characteristics and to compare different batteries. The frequency distribution of the C-rate for the variants with best efficiency in WLTC is shown in Figure 10. The x-axis shows the C-rate in 1/h and the logarithmic y-axis shows the frequency distribution of the C-rate. Due to different voltage levels of 48V for the MHEV and 200 V for the power split, the C-Rate differs significantly.

https://doi.org/10.51202/9783181023549 - Generiert durch IP 216.73.216.36, am 19.01.2026, 02:19:31. © Urheberrechtlich geschützter Inhalt. Ohne gesonderte Erlaubnis ist jede urheberrechtliche Nutzung untersagt, insbesondere die Nutzung des Inhalts im Zusammenhang mit, für oder in KI-Systemen, KI-Modellen oder Generativen Sprachmodellen.

The C-rate of P0 HEV ranges between -8.5 1/h and 10 1/h. The comparably high frequencies of small positive C-rates result from the power demand of auxiliaries during standstill. Compared to other topologies the C-rate is lower in case the battery is discharged (C-rate>0) since electric driving is not possible. When the battery is charged during recuperation and load point increase, the C-rate is higher.

The C-rate of the P0P4 HEV is in the range of -20 1/h to 11 1/h. During battery discharge, higher C-rates occur compared to the P0 HEV since electric driving is used more often. In case the battery is charged, the C-rate is slightly higher compared to the P0 HEV since more electric power is available for recuperation. Although C-rates of up to -20 1/h occur, it can be concluded that the battery stress is not significantly higher compared to P0 HEV since the y-axis is scaled logarithmically and only few situations with high C-rates occur.

In WLTC, C-rates in the range of -18 1/h and 13 1/h occur in case of a P2P4 HEV. Compared to the P0P4 topology similar requirements regarding the battery usage can be concluded.

Compared to the parallel MHEV topologies, the battery of the PS HEV is operated at significantly lower C-rates since the voltage level is distinctly higher.

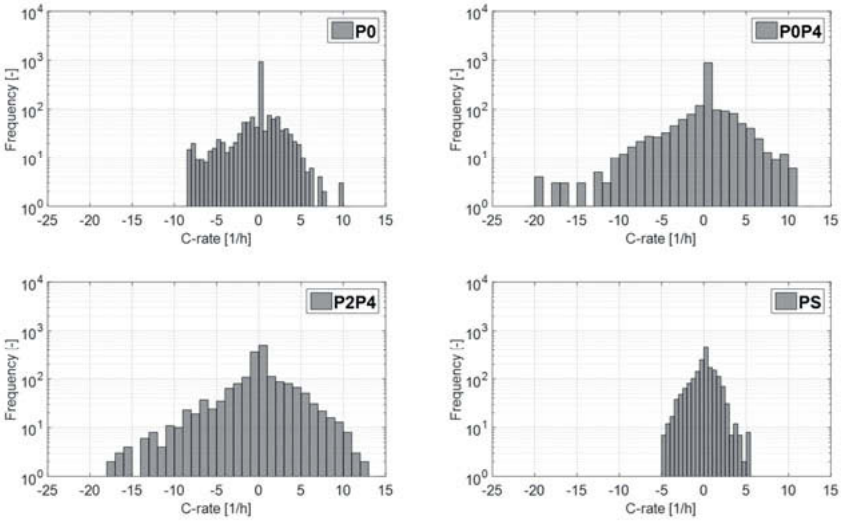


Fig. 10: Frequency distribution of the C-rate for variants with the best efficiency in WLTC

https://doi.org/10.51202/9783181023549 - Generiert durch IP 216.73.216.36, am 19.01.2026, 02:19:31. © Urheberrechtlich geschützter Inhalt. Ohne gesonderte Erlaubnis ist jede urheberrechtliche Nutzung untersagt, insbesondere die Nutzung des Inhalts im Zusammenhang mit, für oder in KI-Systemen, KI-Modellen oder Generativen Sprachmodellen.

Summary and Outlook

In this paper, several drive train topologies suitable for next-generation 48V HEV were investigated and compared regarding efficiency and driving performance. A P0P2 and a P0P4 topology were compared to an ICV, a present 48V MHEV solution (P0) and a PS-DHT. A small SUV as a base vehicle was selected since the small SUV segment shows a growing market share.

To consider realistic variants of the topologies, driving performance requirements were defined for different drive train states taking all possible interactions of the ICE and the battery into account. The requirements are identical in case of an MHEV to ensure a fair concept comparison. Since the PS-DHT is used as an efficiency benchmark and is not the main focus for optimization, differing requirements were defined.

To identify the best drive concepts, important drive train parameters were varied. For MHEV, the reduction gear ratio of the EMs on the rear axle was varied. In contrast, the power of the EMs, the gear ratio of the planetary gear set and the reduction gear ratio of the EM connected to the final drive were varied for the power split hybrid.

To compare the topologies regarding driving performance and efficiency, the SOC neutral CO_2 emissions in WLTC and an RDE cycle as well as the acceleration time form 0 km/h to 100 km/h in hybrid operation were calculated.

The results show that 48V HEV of the next generation offer a high potential regarding efficiency and driving performance compared to a typical 48V solution available on the market. In WLTC, the P0P4 and P2P4 topology provide a CO_2 emission reduction of approx. 11.7 % compared to the P0 topology. At the same time, the CO_2 emissions are slightly higher (approx. 6 %) compared to a high-voltage power split hybrid.

Additionally, 48V hybridization of the next generation provides more attractive driving performance compared to a conventional vehicle and a present P0 solution. The integration of two Ems into the drive train realizes temporary electric all-wheel-drive which leads to reduces acceleration times in hybrid operation of approx. 2 s compared to a conventional vehicle.

Taking into account the efficiency and performance improvements of the P0P4 HEV and P2P4 HEV as well as the costs, it can be concluded that next generation 48V topologies provide an attractive solution for future drive train hybridization compared to a power split hybrid.

The further development of 48V drive train concepts still requires additional investigations. For example, the optimal distribution of the electric power between the front and rear axle should be investigated. In addition, different battery capacities can be taken into account when identifying optimal drive train topologies.

https://doi.org/10.51202/9783181023549 - Generiert durch IP 216.73.216.36, am 19.01.2026, 02:19:31. © Urheberrechtlich geschützter Inhalt. Ohne gesonderte Erlaubnis ist jede urheberrechtliche Nutzung untersagt, insbesondere die Nutzung des Inhalts im Zusammenhang mit, für oder in KI-Systemen, KI-Modellen oder Generativen Sprachmodellen.

References

[1] Eichler, F., Bennewitz, K., Helbing, C., Philipp, K., Lück, P., Weiß, N., Felsch C.: Volkswagen Electrifies the New Golf. 38th Vienna Motor Symposium, 27st and 28, 2017, Hofburg Conference Centre, Vienna.

[2] Breitbach, H., Jausel, H., Garrard, T., Metz, D.: Elektrisch unterstützte Aufladung Status und Ausblick. MTZ - Motortechnische Zeitschrift, 2018, 79, 28-35.

[3] Sieg, C., Lange, A., Küçükay, F.: 48V Electrification of Dual-Clutch Transmissions. Hybrid and electric vehicles: 15th symposium, February 21st and 22nd, 2018, Stadthalle Braunschweig / ITS Mobility e.V. (ed.).

[4] Lange, A.: Optimierung Modularer Elektro- und Hybridantriebe. TU Braunschweig Dissertation, Braunschweig, 2018.

[5] Hengst, J., Seidel, T., Lange, A., Küçükay, F.: Evaluation of transmission losses of various Dedicated Hybrid Transmission (DHT) with a lossmap-based simulation model. Automotive and Engine Technology, 2019.

[6] Ringleb, A., Küçükay, F.: Representative driving cycles for Real Driving Emissions. Hybrid and electric vehicles: 14th symposium, February 21st and 22nd, 2017, Stadthalle Braunschweig / ITS Mobility e.V. (ed.).

https://doi.org/10.51202/9783181023549 - Generiert durch IP 216.73.216.36, am 19.01.2026, 02:19:31. © Urheberrechtlich geschützter Inhalt. Ohne gesonderte Erlaubnis ist jede urheberrechtliche Nutzung untersagt, insbesondere die Nutzung des Inhalts im Zusammenhang mit, für oder in KI-Systemen, KI-Modellen oder Generativen Sprachmodellen.

https://doi.org/10.51202/9783181023549 - Generiert durch IP 216.73.216.36, am 19.01.2026, 02:19:31. © Urheberrechtlich geschützter Inhalt. Ohne gesonderte Erlaubnis ist jede urheberrechtliche Nutzung untersagt, insbesondere die Nutzung des Inhalts im Zusammenhang mit, für oder in KI-Systemen, KI-Modellen oder Generativen Sprachmodellen.

Minimize Torsional Vibrations – Full Isolation if Necessary

Dr. **Ad Kooy**, **Roland Seebacher**,
Schaeffler Automotive Buehl GmbH & Co. KG, Bühl

Zusammenfassung

Dieser Beitrag stellt dar, wie Schaeffler auf die steigende Vielfalt an Antriebskonzepten und die daraus resultierenden Anforderungen an die Schwingungsdämpfung reagiert. Die Anforderungen sind vielfältig und umfassen Wechsel zwischen elektro- auf verbrennungsmotorischen Antrieb und die hieraus resultierenden Start-Stopp-Herausforderungen, reduzierte Bauräume, Fahren bei niedriger Motordrehzahl und erhöhte NVH-Anforderungen. Die Weiterentwicklung des Fliehkraftpendelprinzips und die Kombination verschiedener Dämpferprinzipien führen zu passgenauen Auslegungen. Darüber hinaus ermöglichen die in diesem Beitrag dargestellten Ansätze auch die weitere Absenkung der Drehzahl für den Fahrbetrieb, um Verbrauch und Emissionen einzusparen. Außerdem wurden Auslegungsmethoden von Fliehkraftpendeln beschrieben.

Bei der Suche nach neuen Dämpfungskonzepten spielen die zu Grunde liegenden Wirkprinzipien eine zentrale Rolle. Insbesondere das Prinzip der Antiresonanz ist dazu geeignet, auch für komplexe Bauraumvorgaben die passenden Dämpfungskonzepte zu entwickeln.

Abstract

This paper has shown some of the ways in which Schaeffler reacts to the growing variety of drive concepts and the resulting requirements for vibration damping. Requirements are very diverse and include changeovers from drives based on electric motors to those using internal combustion engines and the resulting start and stop challenges, reduced design spaces, driving at low engine speed and increased NVH requirements. The refinement of the centrifugal pendulum-type absorber principle and the combination of various damper principles lead to precise designs. In addition, the approaches presented in this paper allow another decrease in speed for driving, in order to reduce consumption and emissions. The design methods for centrifugal pendulum-type absorbers have also been described.

In the search for new damping concepts, the operating principles they are based on play an important role. In particular, the principle of anti-resonance is suitable for developing suitable damping concepts even for complex installation space requirements.

https://doi.org/10.51202/9783181023549 - Generiert durch IP 216.73.216.36, am 19.01.2026, 02:19:31. © Urheberrechtlich geschützter Inhalt. Ohne gesonderte Erlaubnis ist jede urheberrechtliche Nutzung untersagt, insbesondere die Nutzung des Inhalts im Zusammenhang mit, für oder in KI-Systemen, KI-Modellen oder Generativen Sprachmodellen.

1. Introduction

Schaeffler believes that classic internal combustion engines will continue to play an important role for a long time to come [1]. Predictions with a rather aggressive introduction of electrical vehicles (EV) show no great reduction of ICE`s until 2030, Fig. 1. After that, predictions are difficult, because of the strong influence of politics. The drive train however will change significantly because of the high percentage of hybrids. Numerous concepts are being developed to reduce fuel consumption. Combining the ICE-torque with the electrical motor (EM) torque enables to use a long drive ratio. Driving with a long ratio, reduces internal combustion engine losses due to lower speeds. If, however, the internal combustion engine is operated at just above the idle speed range, it is in a particularly economical range, but this also produces strong, low-frequency excitations with high vibration amplitudes. In addition, the ICE torque must be increased to prevent loss of performance. Other vibration-related challenges arise from downsizing and the increasing number of hybrid vehicles with various arrangements of the internal combustion engine, electric motor and transmission. The alternation of electric motor drives and internal combustion engine drives that is typical for hybrids and that is intended to go widely unnoticed by the driver, leads to additional tasks for the dampers in the start and stop phases of the internal combustion engine.

In order to package the electrical motors in the drive train, the space for the dampers is even more limited. On one hand, this leads to the need for very effective dampers, on the other hand the inertia of electrical motors can help to reduce torsional vibrations. Transitions between electrical and thermodynamic driving are required to go mainly unnoticed by the driver. This leads to growing expectations regarding comfort and driving, especially during the use of the ICE.

In order manage the ever-growing number of variants, transmission manufacturers rely on the increased use of CAE tools with the aim of including the requirements for vibration damping and noise behavior (noise vibration harshness, NVH) as early as possible in the development process and reduce the number of tests with real prototypes. This requires high development quality, something that Schaeffler ensures with actions such as the simulation of vehicle influences for tolerance evaluations and damper optimization [2,3]. Beyond that, it is important to develop effective and customized damping systems for the smaller and more complex design spaces. This paper aims to show some of the ways that Schaeffler looks for even better operational principles and keeps driving damper technology with innovative combinations.

https://doi.org/10.51202/9783181023549 - Generiert durch IP 216.73.216.36, am 19.01.2026, 02:19:31. © Urheberrechtlich geschützter Inhalt. Ohne gesonderte Erlaubnis ist jede urheberrechtliche Nutzung untersagt, insbesondere die Nutzung des Inhalts im Zusammenhang mit, für oder in KI-Systemen, KI-Modellen oder Generativen Sprachmodellen.

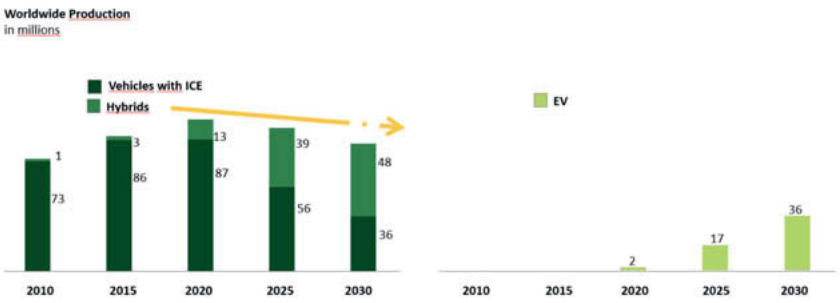


Fig. 1: Automotive – Market Growth Driven by New Technologies

2. Torsion Dampers for Hybrids

The arrangement of the electric motor also plays a significant role. In P0 and P1 arrangements, the additional torque of the electric motor must be transmitted by the damper; this is not the case in P2 to P4 arrangements [6]. In particular for P2 arrangements, the additional inertia of the electric motor helps to dampen the torsional vibrations, but can cause an additional important resonance, the input shaft resonance (IPS), Fig. 2. For a 4-cylinder application, with a typical transmission inertia, it is in an often-used engine speed range. One possibility to dampen this resonant frequency, is to reduce the excitation by the combination of an arc spring damper with a centrifugal pendulum absorber (CPA). Another option is to lower the frequency by an additional damper on the input shaft, Fig. 2.

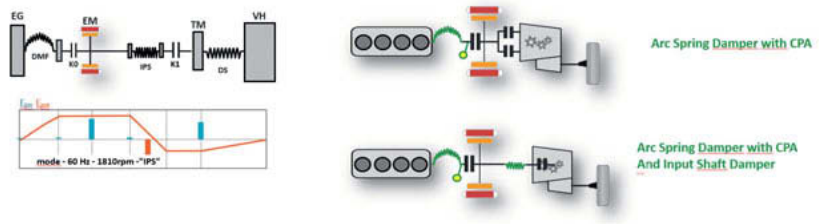


Fig. 2: Left: Input Shaft resonance (IPS), Right: possible solutions

Coil spring dampers can replace arc spring dampers only in cases of low ICE torque and/or fluctuations, saving costs. If a geared parallel arrangement for the EM instead of a coaxial arrangement is used, a preload by the EM is needed to prevent the gears from clattering.

https://doi.org/10.51202/9783181023549 - Generiert durch IP 216.73.216.36, am 19.01.2026, 02:19:31. © Urheberrechtlich geschützter Inhalt. Ohne gesonderte Erlaubnis ist jede urheberrechtliche Nutzung untersagt, insbesondere die Nutzung des Inhalts im Zusammenhang mit, für oder in KI-Systemen, KI-Modellen oder Generativen Sprachmodellen.

Due to the drag start, to re-start after sailing with the ICE turned off, there is another critical operating point in addition to regular starting. The restart should be unnoticed by the driver if possible. If a CPA is used, a couple-pendulum (also called GEN3-pendulum), with preloaded springs between the pendulums, can help prevent stopping noises, [4].

Dependent on the different drive train arrangements and drive train parameters, different types of dampers can be chosen, Fig. 3. In many cases they are combined with a CPA to reach the isolation targets.

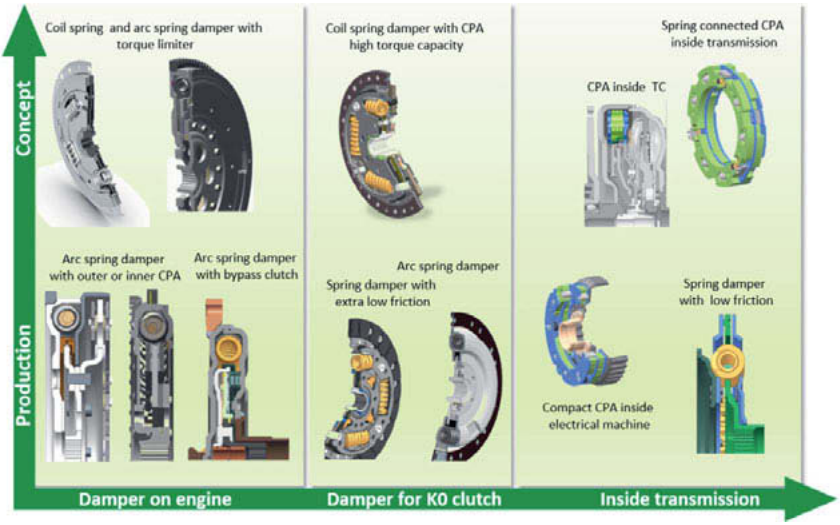


Fig. 3: Variety of dampers for different positions in the drive train

3. Refinement of the centrifugal pendulum-type absorber

Dual Mass Flywheels (DMF's) with Centrifugal pendulum-type absorbers (CPA) have been used since 2008 to isolate the torsional vibrations between the engine and the transmission and are now widely used. As shown in Fig. 3, very different products are being developed based on this principle. Around 20 million DMF's were already produced for transmission applications. Two-thirds of those are installed in the converter in automatic transmissions and around one-third in manual and double-clutch transmissions. For arrangements in the DMF, a distinction is made between internal DMF – in which pendulums are arranged in a space-saving fashion under the arc spring and external DMF where pendulums are placed next to

https://doi.org/10.51202/9783181023549 - Generiert durch IP 216.73.216.36, am 19.01.2026, 02:19:31. © Urheberrechtlich geschützter Inhalt. Ohne gesonderte Erlaubnis ist jede urheberrechtliche Nutzung untersagt, insbesondere die Nutzung des Inhalts im Zusammenhang mit, für oder in KI-Systemen, KI-Modellen oder Generativen Sprachmodellen.

the arc spring and achieve an even better isolation of the rotational irregularities due to the higher moment of inertia [4].

The great market success of the DMF can be attributed, amongst other things, to the fact that the physical principle inevitably results in a balance between excitation and pendulum vibration. In this process, the vibration amplitude keeps increasing until the exciting mass no longer vibrates. This means that the DMF can compensate different phase positions that can occur at higher speeds or when sailing. The natural frequency of the damper changes just as much via the centrifugal force increasing quadratically with speed, as the main excitation firing frequency of the internal combustion engine. The most important disturbance is the guide track accuracy of the rotating masses in conjunction with the flange, pendulum and roller geometry, that Schaeffler is able to guarantee with the highest precision due to its state-of-the-art manufacturing processes on an industrial scale.
Pendulum mass guide friction may constitute another disturbance. That is why very rigid rollers are mostly used here that are virtually friction free. Hardly any heat is lost because the DMF stores the engine's pulsating mechanical energy temporarily in an efficient manner. Finally, it releases the energy and dampens the powertrain.
Under tolerances, a slight offset of the pendulum masses may also occur, or the flange may be in a tilted position. Both may cause the pendulum to touch the flange. For this reason, ribs on the roller keep the components apart. In addition, sliding elements are used between the flange and the pendulum to minimize wear and friction [4].
This wide range of applications has led to the use of DMF in many powertrain positions, Fig. 3. It was initially developed to improve isolation in the DMF and in automatic transmission converters and, in a subsequent step, designed for the clutch disc. Meanwhile, some automatic transmission converters also use two DMF's at the same time.

4. Design of Centrifugal Pendulum-type Absorbers from idle speed on

The design of DMF in the range starting at idle speed has three objectives: Firstly, it is important to achieve good isolation even at low speeds. This requires as much mass as possible and a vibration angle that is as wide as possible. Secondly, it is important to prevent the pendulum from lifting off from the guide track at low speeds and wide vibration angels to prevent wear. Thirdly, the goal is to prevent as few damper impacts at the end of the guide track as possible at low speeds, in order to preserve the rubber stops that absorb part of the impact energy, to prevent inherent noise.

https://doi.org/10.51202/9783181023549 - Generiert durch IP 216.73.216.36, am 19.01.2026, 02:19:31. © Urheberrechtlich geschützter Inhalt. Ohne gesonderte Erlaubnis ist jede urheberrechtliche Nutzung untersagt, insbesondere die Nutzung des Inhalts im Zusammenhang mit, für oder in KI-Systemen, KI-Modellen oder Generativen Sprachmodellen.

The tuning order, which is determined by the path curvature, is an important tuning parameter for the optimization of isolation and oscillation angle of the pendulums. The oscillation angles of the pendulums are very large at low engine speed, but decrease disproportionately with increasing speed. If you now change the curvature of the pendulum at large angles, you automatically change the tuning order over the speed. By opening the curvature to large oscillation angles, the tuning order is lowered to low speeds. Conversely, we increase the tuning order towards low speeds by narrowing the curvature towards large vibration angles. With the help of so-called colour charts, the optimum curvature or pendulum arrangement can now be found for each pendulum version.

The colour charts in Fig. 4 show the results of many simulations. Shown is the isolation (colour charts left) and the oscillation angle (colour charts right) of different tuning orders over the engine speed. The upper colour charts show an example of a drive train with 4-cylinder engine and DMF. It is not surprising at first that we achieve the best result with a constant 2nd order over the speed. The good isolation can also be seen in the right diagram in comparison to a DMF without CPA. However, we also consider the oscillation angles, which increase strongly with decreasing speed and can also go to block. In order to prevent strength problems and to avoid annoying stop noises, it is advisable to shift the tuning order at lower speeds in the direction of higher order. And, as you can see in the left diagram, without serious losses in isolation.

https://doi.org/10.51202/9783181023549 - Generiert durch IP 216.73.216.36, am 19.01.2026, 02:19:31. © Urheberrechtlich geschützter Inhalt. Ohne gesonderte Erlaubnis ist jede urheberrechtliche Nutzung untersagt, insbesondere die Nutzung des Inhalts im Zusammenhang mit, für oder in KI-Systemen, KI-Modellen oder Generativen Sprachmodellen.

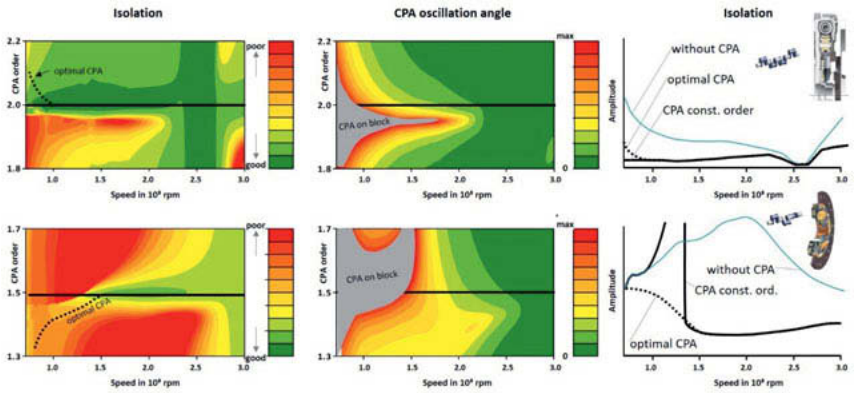


Fig. 4: Basic simulation for optimization of the guide track curvature of the pendulum using the example of a 4-cylinder engine with DMF (top) and a 3-cylinder engine with torsion-damped clutch disc on the gearbox input shaft (bottom)

The lower colour charts in Fig. 4 show an example of a conventional system, i.e. a system without DMF, with CPA on the torsion-damped clutch disc and 3-cylinder engine. And as you can see we have a completely different result here. With a constant 1.5th order you would drive straight into the red range at about 1400 rpm. This can also be clearly seen in the amplitude curve on the right. In contrast to the DMF, a shift in the direction of smaller orders is possible here. And as you can see in the right diagram, compared to a torsion damped clutch disc without CPA, this is a really impressive improvement. The reduction of the tuning order also fits the direction of the vibration angle.

5. Design in the start-and-stop range below idle speed

Speeds reduce quickly when the engine is turned off. Starting at a certain point, gravity dominates centrifugal force, and the pendulums lose contact with the rollers. This may lead to noticeable, undesirable noise, particularly for external DMF's whose pendulum masses are positioned far outside radially and which are not encapsulated as they would be in the internal DMF. Compared to this, the engine start is characterized by relatively strong excitations, so that contact at the end of the guide track dominates here.

https://doi.org/10.51202/9783181023549 - Generiert durch IP 216.73.216.36, am 19.01.2026, 02:19:31. © Urheberrechtlich geschützter Inhalt. Ohne gesonderte Erlaubnis ist jede urheberrechtliche Nutzung untersagt, insbesondere die Nutzung des Inhalts im Zusammenhang mit, für oder in KI-Systemen, KI-Modellen oder Generativen Sprachmodellen.

It is possible to calculate the impact energy of the vibrating components at the start, but this is more difficult when the components moving in relation to each other rebound because this leads to rotary motion that are dependent on the impact point and guide track tolerances.
For internal DMF's, with pendulums integrated into the flange, the noise described when turning off the engine can generally be reduced to a reasonable level. This is more difficult for external pendulums. One solution is the so-called couple-pendulum in which the pendulums support each other in a circumferential direction through springs [4,5].

Here the spring preload is selected in such a way that the pendulum remains in the guide track even if the engine is at a complete standstill, thus not losing contact between the pendulum, the roller and the flange. The effect of the spring forces overlapping with the centrifugal forces is largely compensated by correcting the order of the track. This type of spring arrangement is particularly helpful for first order pendulums, such as those needed for cylinder deactivation from four to two active cylinders. This is because gravity also generates a first order excitation in a rotating pendulum, which increases the excitation from cylinder deactivation.

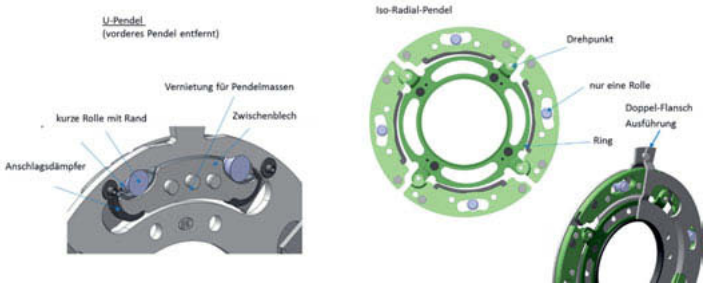


Fig. 5: Design of an DMF with U pendulum (left) and an Iso-radial pendulum (right)

Another potential solution is an DMF design principle with a U pendulum, Fig. 5 left. Here the pendulum mass is supported by the rollers right below the flange via a hardened intermediate piece with sheets installed on the side and located in a flange cavity. This way, the rollers can be designed much shorter and lighter which significantly reduces noise developing when stopping. Noise in the DMF is generated by the pendulum hitting the flange, which can be largely compensated by appropriate rubber dampers, as well as by the rollers hitting the pendulum and the flange, which is more difficult to manage. The sheets and the connecting

https://doi.org/10.51202/9783181023549 - Generiert durch IP 216.73.216.36, am 19.01.2026, 02:19:31. © Urheberrechtlich geschützter Inhalt. Ohne gesonderte Erlaubnis ist jede urheberrechtliche Nutzung untersagt, insbesondere die Nutzung des Inhalts im Zusammenhang mit, für oder in KI-Systemen, KI-Modellen oder Generativen Sprachmodellen.

piece together form a U-shaped cross section. This arrangement also allows slightly higher pendulum masses for improved isolation.

The new so-called Iso-radial pendulum solution takes an entirely different approach, Fig. 5 right. In this approach, the individual pendulums are connected at one point by a ring not located in the torque flow, which means that the pendulum masses are now synchronized. One of the usual two spherical rollers is eliminated, causing the pendulum to carry out a swivelling motion rather than a purely radial motion. This design eliminates the first order excitation from gravity on the individual pendulum masses. However, this principle does not help against contact loss at low speeds while stopping; here too, noise has to be controlled by stop elements. One advantage though is the fact that coupling via springs can be eliminated. This way, improved isolation can be achieved, particularly at low speeds.

6. New approaches to vibration damping

6.1 Analyses at the operating principle level

In Schaeffler's search for new damping concepts, one approach consists of using simple models to analyse different operating principles at the theoretical level. These models focus on operational parameters and are compared on a physical basis while maintaining the same inertia and spring energies. Limiting factors such as design space, costs and feasibility are not included until the second step. If an operating principle proves to be promising, the function of the new concept is analysed with regards to expanded operating situations such as an engine start. In a simulated vehicle model, this is carried out with all relevant non-linearities.

Generally, there are three types of vibration damper systems:

- Active systems: Energy is supplied to and extracted from the system externally. This can be carried out, for instance, by an electric motor in the powertrain to produce a counter-excitation. Another possibility are semi-active systems in which a parameter - such as a spring rate - is simulated specifically.
- Passive systems: Energy is stored temporarily, alternating between kinetic and potential energy, such as in a classic spring-mass damper such as the DMF or the DMF which temporarily stores potential energy in the centrifugal force field.
- Slipping systems: Energy is removed from the system. This can be achieved hydraulically, such as in a torque converter, or through friction, such as in a clutch [7].

Good results can also be achieved with an efficient combination of all these systems.

https://doi.org/10.51202/9783181023549 - Generiert durch IP 216.73.216.36, am 19.01.2026, 02:19:31. © Urheberrechtlich geschützter Inhalt. Ohne gesonderte Erlaubnis ist jede urheberrechtliche Nutzung untersagt, insbesondere die Nutzung des Inhalts im Zusammenhang mit, für oder in KI-Systemen, KI-Modellen oder Generativen Sprachmodellen.

The section below deals exclusively with passive systems. As shown in Fig. 6, basic elements for kinetic energy, potential energy and ratio can be combined arbitrarily and thus describe a nearly unlimited number of operating principles [8].

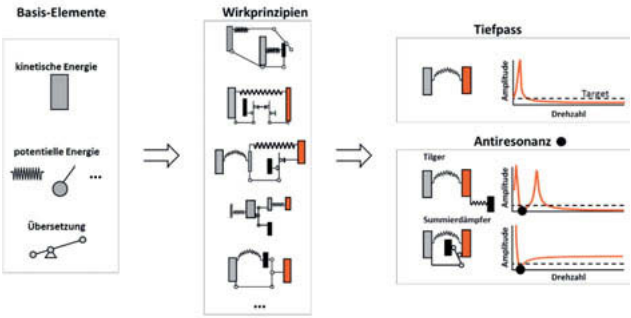


Fig. 6: Various operating principles for damping vibrations

The analysis of these operating principles shows two basic characteristics of all systems capable of vibrations: Each degree of freedom contains a resonance and an anti-resonance. Essentially, the goal is to manage the resonance while also using the anti-resonance effectively.

The anti-resonance principle is particularly promising when it comes to isolation at low speeds. This is because the vibration movement for a particular frequency is erased entirely. The torque fluctuations add up on a rotating mass so that the sum of all torques equals zero. Fig. 7 shows the anti-resonance principle can be achieved by a simple damper. The rotating mass is set in motion on one side by torques acting on them in a certain frequency. A damper, in turn, is supported on the vibrating mass by a spring and causes a torque that is phase shifted by 180°. The torque fluctuation of the damper grows with increasing frequency until it is equal to that of the mass that is acting on it and erases its motion entirely. Theoretically, designing the frequency of the anti-resonance to an arbitrary frequency. However, this creates an additional natural frequency that can manifest itself in a disturbing resonance magnification. It must be remembered that damping in the system has a severe effect on anti-resonance.

https://doi.org/10.51202/9783181023549 - Generiert durch IP 216.73.216.36, am 19.01.2026, 02:19:31. © Urheberrechtlich geschützter Inhalt. Ohne gesonderte Erlaubnis ist jede urheberrechtliche Nutzung untersagt, insbesondere die Nutzung des Inhalts im Zusammenhang mit, für oder in KI-Systemen, KI-Modellen oder Generativen Sprachmodellen.

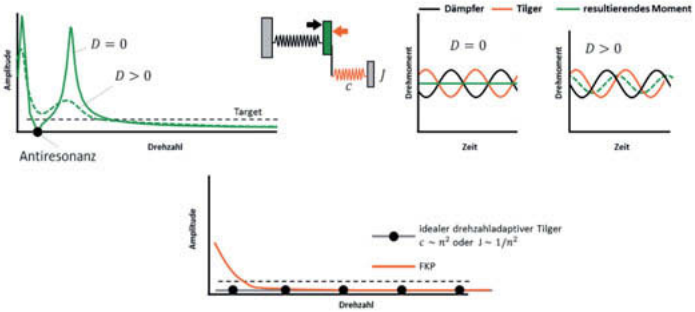


Fig. 7: Implementation of the anti-resonance principle using the example of a damper

Anti-resonance can also be achieved by means of a so-called summation damper or power splitting. Here too, torque amplitudes are added in such a way as to ensure that they completely erase each other with a frequency. These systems have a ratio as an additional parameter. The advantage of this is that no additional resonance is generated because there is no additional degree of freedom from an additional spring.

It is true for all anti-resonance systems that the amplitude of the counter excitation should be exactly inverse. It is possible to select the anti-resonance freely by carefully selecting the parameters. However, if the parameters remain constant, the anti-resonance also remains on a fixed frequency. The excitation frequency though changes in the vehicle in proportion to the engine speed. The problem can be solved by changing one of the relevant parameters in proportion to the excitation frequency. The DMF is one example. It uses the centrifugal force as an energy accumulator and thus, in a certain way, has a spring rate depending on the engine speed.

Limiting factors here include the limitation of the vibration angle by the design space and the non-linear curve of the tangential return force that decreases as the pendulum angle increases. This causes the DMF to lose potential with decreasing speed.

6.2 Application of operating principles for dampers on intermediate flange

However, design spaces are not always ideal in terms of offering sufficient DMF mass. That is why analysing the interaction of resonance and anti-resonance is well worth the effort. Operating principles can be helpful here too: If the damper is not arranged right on the secondary mass to be damped, but rather symmetrically between the primary and secondary mass,

https://doi.org/10.51202/9783181023549 - Generiert durch IP 216.73.216.36, am 19.01.2026, 02:19:31. © Urheberrechtlich geschützter Inhalt. Ohne gesonderte Erlaubnis ist jede urheberrechtliche Nutzung untersagt, insbesondere die Nutzung des Inhalts im Zusammenhang mit, für oder in KI-Systemen, KI-Modellen oder Generativen Sprachmodellen.

anti-resonance may result - without the interfering resonance in the higher speed range, Fig. 8.

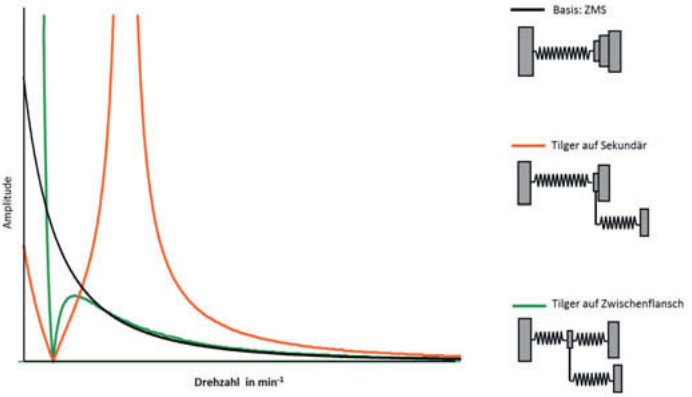


Fig. 8: Operating principle of the damper on the intermediate flange: Achievement of an anti-resonance without interfering resonance in a higher speed range

6.3 Implementation: Damper on intermediate flange

The symmetrical arrangement can be achieved by placing the damper between the two masses on a so-called intermediate flange. This is a potential option in combination with a DMF, if a DMF that is too heavy leads to strength problems, where possible limitation stops cause noise or if the available design space leaves too little clearance for radial deflection.

Fig. 9 shows an example with an awkward design space. The available design space does not have enough room for the radial expansion of the DMF. That is why the damper is placed on an intermediate flange. In combination with the DMF already in place, engine speeds can be decreased by around 200 rpm without any additional mass, which makes fuel consumption savings of approx. 4 % possible, Fig. 9.

https://doi.org/10.51202/9783181023549 - Generiert durch IP 216.73.216.36, am 19.01.2026, 02:19:31. © Urheberrechtlich geschützter Inhalt. Ohne gesonderte Erlaubnis ist jede urheberrechtliche Nutzung untersagt, insbesondere die Nutzung des Inhalts im Zusammenhang mit, für oder in KI-Systemen, KI-Modellen oder Generativen Sprachmodellen.

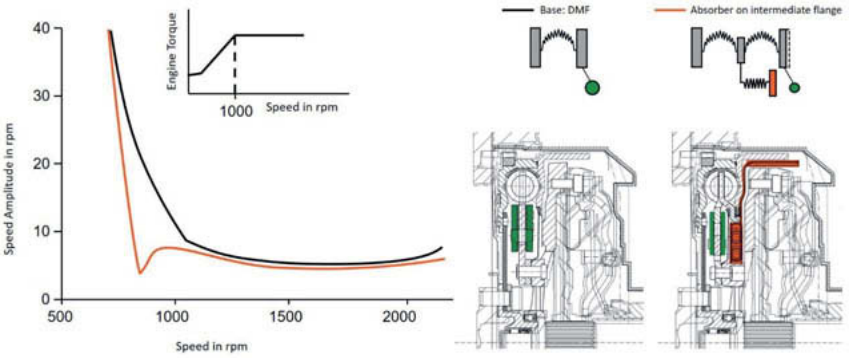


Fig. 9: Placing a damper on an intermediate flange to utilize anti-resonance

7. Rocker Damper

The physics behind this damper principle, is the idea to use the energy coil springs can store more efficiently. The maximum energy is mainly given by the available space and the selected spring material, leading to a minimum designable spring rate for a given needed torque capacity.

For a partial load, it would make sense to use a higher spring rate and use the so saved spring energy at full load for a lower spring rate. The result is a better isolation at full load than possible with a constant spring rate, Fig. 10. However, to design degressive spring rates out of coil springs is not easy. Coil springs, as a way to store spring energy, are very effective, technically and cost wise, but have a linear behaviour. To get a degressive characteristic out of them, the ratio converting the spring force to torque has to change over travel. Inspired by the rollers in a DMF, the combination of changing slopes in a rocker arm and its flange counterpart with intermediate rollers, give a fully flexible torque characteristic. Very low rates for idle torque, high rates for partial load and low rates for full torque can be realized, as long as the total spring energy is not exceeded.

The springs can be designed to max energy, instead to max torque, improving further the damper performance. Helpful is also the purely parallel spring actuation, leading to a more even stress distribution within one coil and higher spring energy. Transition areas between damper rates can be designed with fluent rate changes. The improved isolation for full torque compared to a standard design is also shown in Fig. 10.

https://doi.org/10.51202/9783181023549 - Generiert durch IP 216.73.216.36, am 19.01.2026, 02:19:31. © Urheberrechtlich geschützter Inhalt. Ohne gesonderte Erlaubnis ist jede urheberrechtliche Nutzung untersagt, insbesondere die Nutzung des Inhalts im Zusammenhang mit, für oder in KI-Systemen, KI-Modellen oder Generativen Sprachmodellen.

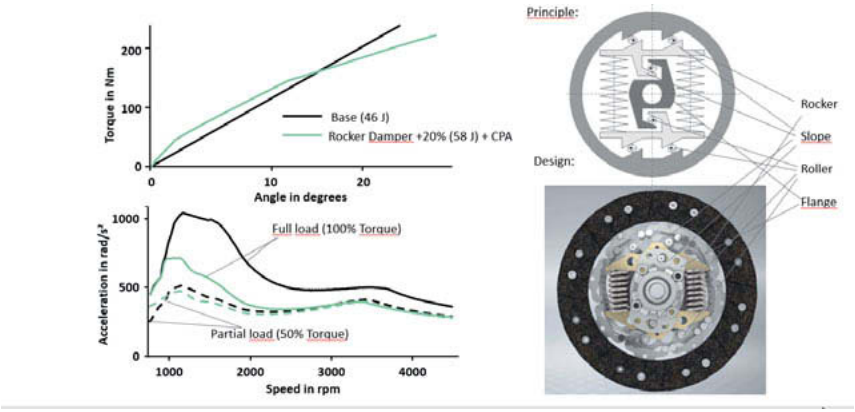


Fig. 10: Pendulum rocker damper, isolation in combination with a CPA

8. Reversed Radial Damper

The hybridization of drive trains, such as a P2 hybrid, means that the additional electric motor results in the installation space for torsion dampers becoming increasingly limited.
An interesting approach for a particularly slim damper is a so-called “reversed radial damper” (RRD), Fig. 11.

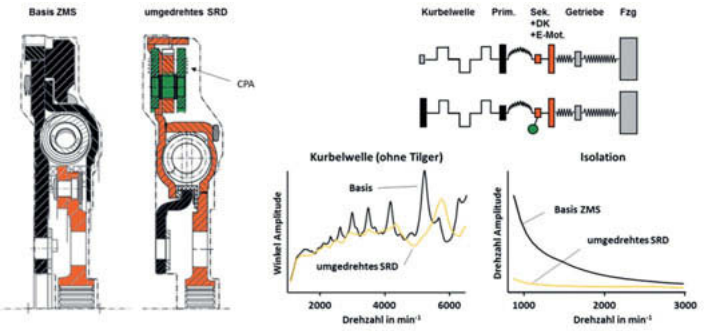


Fig. 11: Reversed radial damper (RRD) with DMF and flywheel on front end of the crankshaft

https://doi.org/10.51202/9783181023549 - Generiert durch IP 216.73.216.36, am 19.01.2026, 02:19:31. © Urheberrechtlich geschützter Inhalt. Ohne gesonderte Erlaubnis ist jede urheberrechtliche Nutzung untersagt, insbesondere die Nutzung des Inhalts im Zusammenhang mit, für oder in KI-Systemen, KI-Modellen oder Generativen Sprachmodellen.

With this concept, the primary mass is pushed to the front end of the crankshaft. The damper itself is reversed, i.e. the flange that actuates the arc spring is screwed directly to the crankshaft. The torque is tapped at the secondary side of the arc spring channel. This results in additional installation space, e.g. for an CPA, as shown in Fig. 11. The improvement in isolation is astonishing, as can be seen in Fig. 11. In addition, additional axial installation space is gained.

A further advantage is that an additional crankshaft absorber can possibly be dispensed with. The crankshaft end with the small inertia now sits at the damper. And this is precisely where the high-frequency crankshaft vibrations are observed. The friction of the arc spring helps to dampen the crankshaft vibrations. And as can be seen in the left diagram in Fig. 11, a considerable improvement is achieved compared to a crankshaft without absorber.

https://doi.org/10.51202/9783181023549 - Generiert durch IP 216.73.216.36, am 19.01.2026, 02:19:31. © Urheberrechtlich geschützter Inhalt. Ohne gesonderte Erlaubnis ist jede urheberrechtliche Nutzung untersagt, insbesondere die Nutzung des Inhalts im Zusammenhang mit, für oder in KI-Systemen, KI-Modellen oder Generativen Sprachmodellen.

9. Literature

[1] Kooy, A., Seebacher, R.: Best-in Class Dampers for Every Driveline Concept. 11th Schaeffler Symposium, Baden-Baden 2018

[2] Faust, H.: The Transmission – Now and in Future the Most Efficient Connection Between the Powertrain and the Road. 11. Schaeffler Symposium, Baden-Baden, 2018

[3] Heinrich, D.; Wittmann, C.; Walther, V.: Innovative CAE – Optimal Layout of Transmission Components. 11. Schaeffler Symposium, Baden-Baden, 2018

[4] Kooy, A.: Isolation is the Key – The Evolution of the Centrifugal Pendulum-type Absorber not only for DMF. 10. Schaeffler Symposium, Baden-Baden, 2014

[5] Heck, T.: Efficient Solutions for Automatic Transmissions – Torque Converters and Clutch Packs. 11. Schaeffler Symposium, Baden-Baden, 2018

[6] Reitz, D.: P2 HV Drives – The Most Efficient Hybridization for all Transmissions. 11. Schaeffler Symposium, Baden-Baden, 2018

[7] Küpper, K.: Think Systems – Software by LuK. 7. Schaeffler Symposium, Baden-Baden, 2002

[8] Reik, W.: Less is more! Using Unconventional Means to Design New Products. 9. Schaeffler Symposium, Baden-Baden, 2010

https://doi.org/10.51202/9783181023549 - Generiert durch IP 216.73.216.36, am 19.01.2026, 02:19:31. © Urheberrechtlich geschützter Inhalt. Ohne gesonderte Erlaubnis ist jede urheberrechtliche Nutzung untersagt, insbesondere die Nutzung des Inhalts im Zusammenhang mit, für oder in KI-Systemen, KI-Modellen oder Generativen Sprachmodellen.

Effective acoustic development of electrified powertrains

Combination of simulation and evaluation methods

Christian Möser, **Tobias Märkle**, **Kurt Hornung**, AUDI AG, Ingolstadt

Abstract

This paper describes an effective method of developing the acoustic characteristics of a powertrain at an early stage of the development process based on the example of the new Audi S tronic hybrid gearbox. The paper considers new challenges for the acoustic characteristics of the gearbox resulting from high-voltage electrification.

Powertrain Acoustics Development, as part of Audi's Overall Vehicle Development division, combines simulation and testing of the powertrain and vehicle, and is supported by powertrain development experts.

The simulation method described as a new tool of the acoustic engineer extends from the CAD data to evaluation and analysis of characteristic acoustic variables in different computation disciplines. It combines established tools and simulation aids based on standardisation and automation in pre- and post-processing, and is based on intelligent linkage of functions from ANSA, ArtemiS Suite and Python, through to machine learning. It creates system understanding, and helps in developing efficient powertrain acoustics within the overall vehicle.

Based on an example, a model validation with test rig measurements and more detailed analytical facilities are demonstrated. The results produced provide comprehensive means of understanding the behaviour of the system under analysis in a visually striking way, and give engineers the necessary knowledge to derive design measures from them. The time required for modelling, computing and result processing is much reduced by automation, meaning more time is available for detailed analysis of the results.

Zusammenfassung

Die vorliegende Arbeit beschreibt am Beispiel des neuen Audi S tronic Hybridgetriebes einen effektiven Weg, das akustische Verhalten eines Antriebs in einer frühen Entwicklungsphase zu entwickeln. Dabei wird auf neue Herausforderungen für die akustischen Eigenschaften des Getriebes durch die Hochvolt-Elektrifizierung eingegangen.

https://doi.org/10.51202/9783181023549 - Generiert durch IP 216.73.216.36, am 19.01.2026, 02:19:31. © Urheberrechtlich geschützter Inhalt. Ohne gesonderte Erlaubnis ist jede urheberrechtliche Nutzung untersagt, insbesondere die Nutzung des Inhalts im Zusammenhang mit, für oder in KI-Systemen, KI-Modellen oder Generativen Sprachmodellen.

Die Antriebsakustikentwicklung, als Teil der Gesamtfahrzeugentwicklung bei Audi, vereint Simulation und Versuch an Antrieb und Fahrzeug und wird durch Experten der Antriebsentwicklung unterstützt.

Die beschriebene Simulations-Vorgehensweise als ein neues Werkzeug des Akustikingenieurs führt von den CAD-Daten bis hin zur Auswertung und Analyse akustischer Kenngrößen in unterschiedlichen Berechnungsdisziplinen. Sie verbindet etablierte Werkzeuge und Simulationstools durch Standardisierung und Automatisierung in Pre- und Postprocessing und basiert auf einer intelligenten Verknüpfung von Funktionalitäten aus ANSA, ArtemiS Suite und Python bis hin zum maschinellen Lernen. Sie schafft Systemverständnis und hilft bei einer effizienten Akustikentwicklung eines Antriebs im Gesamtfahrzeug.

Anhand eines Beispiels werden eine Modellvalidierung mit Prüfstandsmessungen und tiefergehende Analysemöglichkeiten gezeigt. Die erzeugten Ergebnisse bieten umfassende Möglichkeiten das Verhalten des untersuchten Systems auf anschauliche Weise zu verstehen und geben dem Ingenieur das nötige Wissen um konstruktive Maßnahmen abzuleiten. Die einzusetzende Zeit für Modellierung, Rechnung und Ergebnisaufbereitung wird durch die eingesetzte Automatisierung stark reduziert und kann damit vermehrt für eine vertiefende Analyse der Ergebnisse genutzt werden.

Introduction and motivation

The increasing electrification of conventional powertrains in passenger cars and the development of all battery-electric powered vehicles pose new challenges to acoustic development. As opposed to the combustion engine, which produces a broad band of background noise largely masking tonal noise, that background is missing in an electric powered vehicle. At high driving speeds, rolling and wind noise remain to provide adequate masking. But at low speeds the tonal noise from the electric motor and gearbox predominates. This can in part be utilised for sound design purposes, as the typical “e” noise can elicit high levels of identification with the electric drive system and the vehicle, and represents a certain novelty. Even just gearing noise from the gearbox is readily perceived as electric motor noise. Normally, however, the tonal noise tends to be unwanted and – at least above a certain level – is perceived as disturbing.

Moreover, one of the aims of electric driving is to maximise energy recuperation in deceleration phases. The resultant coasting torque in the powertrain also poses a new acoustic challenge. Because now the thrust flanks of the gearing must be designed to attain low-noise transmission of higher moments.

https://doi.org/10.51202/9783181023549 - Generiert durch IP 216.73.216.36, am 19.01.2026, 02:19:31. © Urheberrechtlich geschützter Inhalt. Ohne gesonderte Erlaubnis ist jede urheberrechtliche Nutzung untersagt, insbesondere die Nutzung des Inhalts im Zusammenhang mit, für oder in KI-Systemen, KI-Modellen oder Generativen Sprachmodellen.

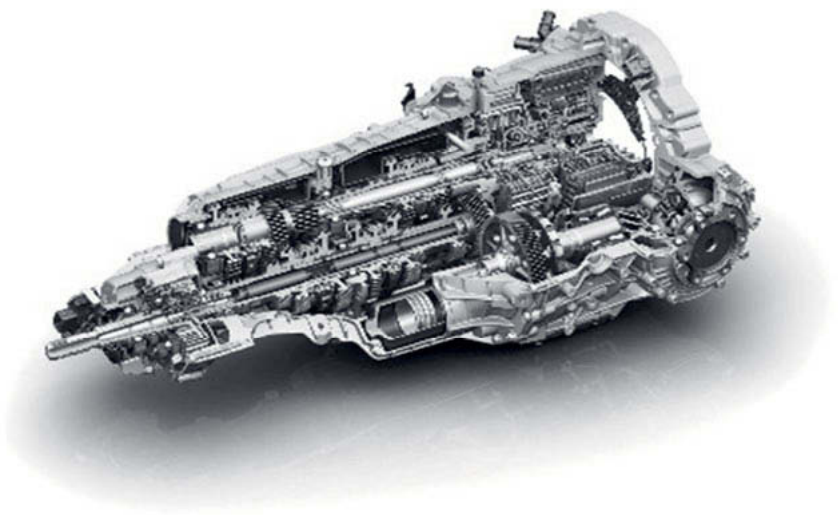


Fig. 1: Audi S tronic hybrid gearbox

Additionally, all-electric powered vehicles normally only have single-gear transmissions. They cover their entire speed range by means of a fixed transmission ratio between the wheel and the electric motor. The motor speed range available in this process is normally at least double that of standard combustion engines. In this context this means that, as well as developing a low-excitation powertrain, the final vehicle must also be non-sensitive to broad-band powertrain noise across the complete engine speed range.

For the aforementioned reasons, intensive study of the excitation and structure properties of electrified powertrains is necessary in order to achieve robust vehicle powertrain acoustics in line with the set goals. This can be done in a wide variety of different ways. The trend towards digitalisation also has to be observed in this respect however.

The following presents a powertrain noise simulation method, supported by analytics and measurement, which Audi has been continuously developing in recent years and is now in widespread use. By way of example, figure 1 shows the new Audi S tronic dual-clutch gearbox featuring a high-voltage electric motor, which Audi uses for plug-in hybrid models based on the modular longitudinal platform. The gearbox is detailed in [1]; the new electric motor is presented in [2].

https://doi.org/10.51202/9783181023549 - Generiert durch IP 216.73.216.36, am 19.01.2026, 02:19:31. © Urheberrechtlich geschützter Inhalt. Ohne gesonderte Erlaubnis ist jede urheberrechtliche Nutzung untersagt, insbesondere die Nutzung des Inhalts im Zusammenhang mit, für oder in KI-Systemen, KI-Modellen oder Generativen Sprachmodellen.

Organisation of acoustic development at Audi

At Audi, Acoustic Development is a main department within the Overall Vehicle Development division. In addition to the acoustic engineers responsible for the various model series, it includes experts in the development of body, chassis and powertrain component properties, as well as a directly assigned comprehensively equipped workshop and test rig unit. Thus work is carried out on the acoustic properties of Audi vehicles explicitly across multiple locations.

The Powertrain Acoustics group comprises a well-balanced team of test and simulation engineers. The proximity of the test and simulation engineers enables them to work closely together. Close and continual exchange of experience is possible at all times. This may relate to effects arising from drive tests, for example, or phenomena occurring on the test rig or in simulations which can be quickly clarified and understood based on mutual consultation and agreement. Cross-model coordination of simulation properties can be quickly organised through direct consultation among the engineers involved, and the relevance of an occurring phenomenon to the vehicle as a whole can be clarified directly.

Acoustic Development is supported by experts from the various product development departments. In relation to transmission, that means primarily the gearing developers in the Powertrain Development department.

All in all, a profound understanding of the drive system is attained on the basis of simulation and test results, subjective acoustic assessment, and the experience and skill of the engineers involved. This enables thorough, consistent and efficient acoustic development from the concept design of a powertrain through to production maturity. In this, the focus is consciously placed on the early phase of the development process.

Simulation workflow as an integral development tool [3]

Ever shorter development cycles also demand new, efficient methods in the field of acoustic development. Prompt feedback on the acoustic effects of design changes to individual components in the overall system is becoming ever more important, and accordingly more in demand, also with regard to powertrain electrification.

The structured approach to simulation presented in this paper through the example of the Audi S tronic hybrid gearbox is largely based on automated processes. It means the lead times to deliver an acoustic assessment based on simulation in response to new designs or design changes can be reduced to a fraction of what they used to be. As well as enabling the aforementioned prompt feedback itself, this also makes it possible to conduct extensive variant testing within a short space of time.

https://doi.org/10.51202/9783181023549 - Generiert durch IP 216.73.216.36, am 19.01.2026, 02:19:31. © Urheberrechtlich geschützter Inhalt. Ohne gesonderte Erlaubnis ist jede urheberrechtliche Nutzung untersagt, insbesondere die Nutzung des Inhalts im Zusammenhang mit, für oder in KI-Systemen, KI-Modellen oder Generativen Sprachmodellen.

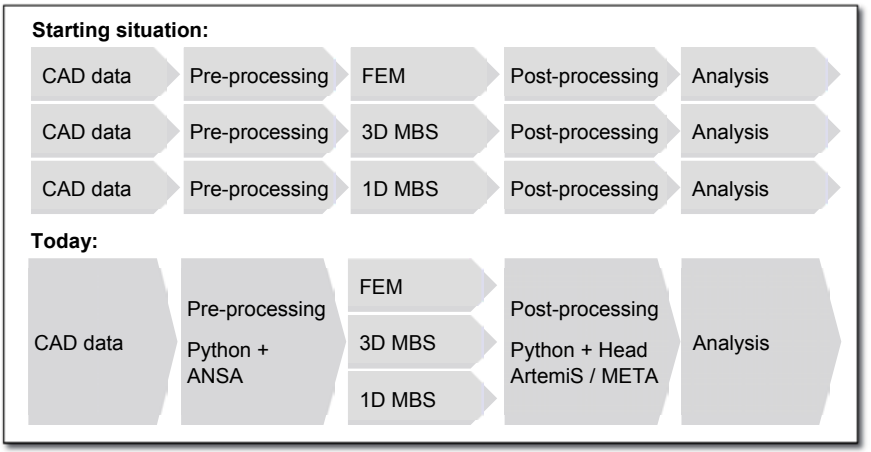


Fig. 2: Simulation process diagram

The method is applied in Audi's powertrain acoustics simulation for combustion engines, conventional and electrified automatic transmissions, and all-electric powertrains.

The underlying idea is based on a through-going process sequence (figure 2) covering the processing of geometric data in the form of CAD data, such as from PTC Creo Elements or CATIA, in relation to different computational models to realise a range of tasks and findings. It is followed by standardised and automated post-processing, including issue of a standard report document.

The method can in principle be described as the interaction between various functions controlled by Python scripts. A highlight feature of pre-processing is automatic recognition of components based on machine-learning parameters. Otherwise, ANSA functions are mainly activated. In post-processing the functions are Head ArtemiS Suite (time domain data) and META. The solvers deployed in-between are initiated manually by control files which are in part automatically generated. Audi mainly employs the following disciplines in its powertrain acoustics simulation:

- FEM with MSC Nastran: Modal and stiffness analyses, frequency response analyses
- 3D MBS with AVL EXCITE: Operationally excited time domain calculations
- 1D MBS with SimulationX: Torsional vibration analyses

https://doi.org/10.51202/9783181023549 - Generiert durch IP 216.73.216.36, am 19.01.2026, 02:19:31. © Urheberrechtlich geschützter Inhalt. Ohne gesonderte Erlaubnis ist jede urheberrechtliche Nutzung untersagt, insbesondere die Nutzung des Inhalts im Zusammenhang mit, für oder in KI-Systemen, KI-Modellen oder Generativen Sprachmodellen.

Standardised pre-processing

Normally, CAD data of a complete assembly is made available for acoustic assessment of the component under analysis. Single parts, such as a gear wheel or a housing panel, are placed in the complete assembly by way of the positioning functions.

Models and submodels for the applied computation disciplines are generated from just one CAD data set. So all statements made are automatically founded on a unified model data basis. When the underlying CAD data for one model is updated, the other models are automatically updated along with it.

The first step is normally (manual) filtering of the complete assembly. Components not relevant to the calculation (e.g. small screws, hoses or cables) are hidden in the complete assembly or removed.

Then automatic 3D meshing with finite elements takes place. This is done on the basis of specified meshing and quality criteria by way of the ANSA Batchmesh functions – activated by a Python script. If the algorithm severely infringes against the criteria for one component, or if automatic mesh generation is not possible, the algorithm prompts manual intervention. Thus, depending on the complexity of the component under analysis, different numbers of functions come together in which the user must intervene in the mesh generation and, for example, repair the CAD geometry, “heal” individual elements, or perform similar operations. Then the algorithm continues, building the model consistently with all other parts and running through the quality tests and documentation again.

A key element is the subsequent automatic recognition of the components from the complete assembly based on characteristic parameters. To that end, the components being used are first initialised in a so-called network file by means of a unique name. The first time the associated algorithm is called, it is then necessary to assign the components in the complete assembly correctly to the pre-defined names. This is aided by the overview shown in Fig. 4. In addition to the graphical depiction and highlighting of the component being sought, the CAD file name of the component is also displayed. The link is made by selecting the corresponding name from the dropdown list.

When assigning, characteristic parameters are automatically collected as training data and stored in a database. In subsequent runs, the components are then recognised on the basis of those parameters and automatically assigned to the names. No new manual assignment is required. Thanks to the Python machine learning functions, this also works for components that have been developed further with new features and so no longer exactly correspond to the initial design status. The database is populated with new entries on each recognition run, so the pool of training data is continually expanded. This recognition function works virtually

https://doi.org/10.51202/9783181023549 - Generiert durch IP 216.73.216.36, am 19.01.2026, 02:19:31. © Urheberrechtlich geschützter Inhalt. Ohne gesonderte Erlaubnis ist jede urheberrechtliche Nutzung untersagt, insbesondere die Nutzung des Inhalts im Zusammenhang mit, für oder in KI-Systemen, KI-Modellen oder Generativen Sprachmodellen.

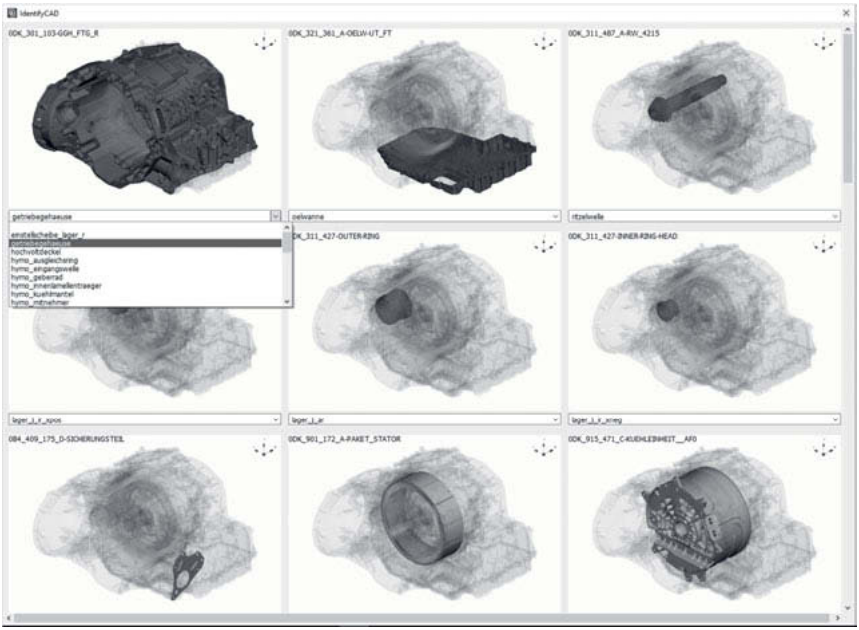


Fig. 4: Overview of component assignment

100% in practical application. The window from the initial run is always displayed in the process for monitoring and correction purposes. Conventional recognition features of single components, such as file names or part numbers, are no longer relevant.

Also, the components in the network file are not only assigned a name but also interlinked with each other. This describes which component connections are made by bolting, for example, within the complete assembly. Distances between the components are automatically calculated in order to identify the potential mating surfaces. A function to do this is activated in ANSA. A manual interim step can be inserted to exclude specific areas from the identification process. This is relevant where components are very close together but not connected.

In a further step, linking nodes with fixed node numbers are also defined. This makes it possible to always automatically assign a roller bearing ring, for example, or other submodel interfaces the same node number for use in the subsequent calculations.

Additionally, rotating assemblies such as transmission shafts can be automatically numerically “balanced”. Imbalance typically occurs in FE models even in the case of components based

https://doi.org/10.51202/9783181023549 - Generiert durch IP 216.73.216.36, am 19.01.2026, 02:19:31. © Urheberrechtlich geschützter Inhalt. Ohne gesonderte Erlaubnis ist jede urheberrechtliche Nutzung untersagt, insbesondere die Nutzung des Inhalts im Zusammenhang mit, für oder in KI-Systemen, KI-Modellen oder Generativen Sprachmodellen.

on a rotationally symmetrical design. It can be traced back to commonly encountered inaccuracies in the meshing of geometry with finite elements.

For special evaluation requirements, the generation of a structurally irrelevant surface mesh can also be requested. This consists of linear shell elements which co-use the corner nodes of the volume elements on the surface of the structure and are themselves of only minimal thickness. This is necessary, for example, for ERP (Equivalent Radiated Power) levels in FE calculations.

As a second application, the surface network can be used to save on memory space during calculation and evaluation. In combination with a likewise automatically generated set of nodes required for the surface mesh, the results can be reduced to this scope in subsequent post-processing. This makes high-performance representation and analysis of the results possible even in the case of large models.

Ultimately, structured and standardised computational models are created with a high degree of automation and can be used directly for downstream calculations. Automation greatly reduces susceptibility to error. In particular when repeating applications with new design versions, users can save significant amounts of time on modelling, and much more variant testing

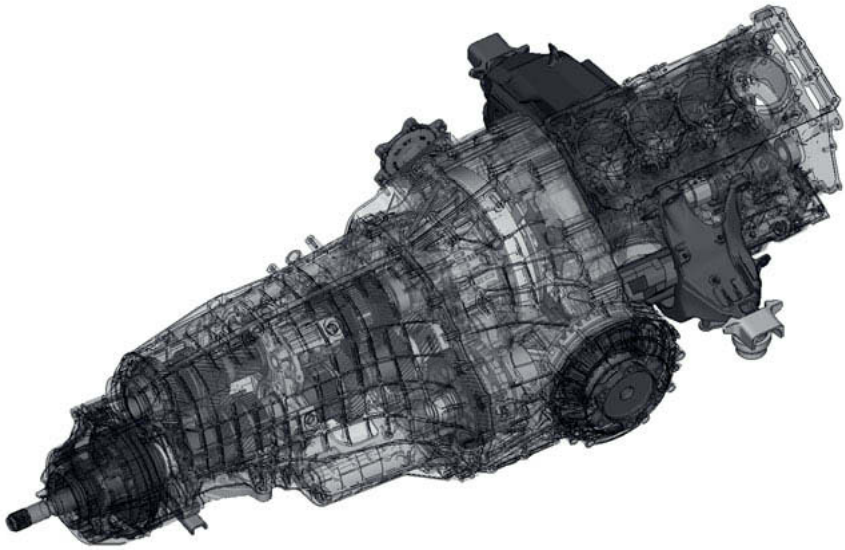


Fig. 5: FEM model of an Audi S tronic gearbox for 3D MBS calculation with a combustion engine

https://doi.org/10.51202/9783181023549 - Generiert durch IP 216.73.216.36, am 19.01.2026, 02:19:31. © Urheberrechtlich geschützter Inhalt. Ohne gesonderte Erlaubnis ist jede urheberrechtliche Nutzung untersagt, insbesondere die Nutzung des Inhalts im Zusammenhang mit, für oder in KI-Systemen, KI-Modellen oder Generativen Sprachmodellen.

is possible. Users do nevertheless still need expertise, in ANSA for example, to handle cases which the algorithm cannot cover.

Simulation of gearing excitation on the Audi S tronic dual-clutch transmission

The calculation is focused on excitation from the gearing as the primary source of noise in the operation of a gearbox. The underlying FE modules consolidated for the 3D MBS calculation are shown in assembled form in Fig. 5.

In addition to the FE modules, which in 3D MBS represent the flexible structures, depiction of the interfaces between them is another key aspect of the modelling. This is done in the 3D MBS software AVL EXCITE Power Unit used here. The complete model of the Audi S tronic gearbox is shown in Fig. 6. Here the linkage of the individual flexible structures (dark elements) with the (circular) interface elements is clearly seen. The grey rectangle represents the flexibly depicted housing. The key interfaces are roller bearings and gear meshing. There are modules to be inserted for each.

https://doi.org/10.51202/9783181023549 - Generiert durch IP 216.73.216.36, am 19.01.2026, 02:19:31. © Urheberrechtlich geschützter Inhalt. Ohne gesonderte Erlaubnis ist jede urheberrechtliche Nutzung untersagt, insbesondere die Nutzung des Inhalts im Zusammenhang mit, für oder in KI-Systemen, KI-Modellen oder Generativen Sprachmodellen.

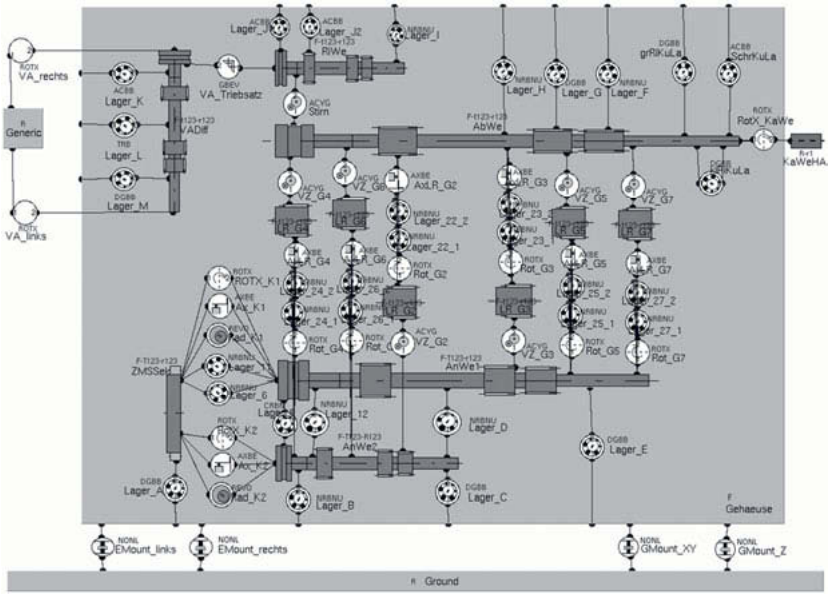


Fig. 6: Audi S tronic model in AVL EXCITE Power Unit

Depictions of roller bearings are fundamentally based on directional, in part fully coupled, force/path relationships. The underlying rigidities are determined internally based on entered geometric parameters.

The gear meshing can be depicted at various detailing levels. The easiest way is to only include the transmission ratio in the direction of rotation. However, this method is not used for acoustic testing on the gearing in question as it incorporates neither displacement forces or torque nor the tooth meshing rigidity. In order to account for excitation forces arising from the fluctuations in rigidity in the various directions in the gear meshing, a greater level of detailing (Advanced Cylindrical Gear Mesh) is required. This takes into account the macro-geometry of the gearing as well as the micro-corrections. The body of the wheel can be depicted entirely flexibly. Tooth bending and the actual tooth contact are calculated analytically.

With the 3D MBS model, speed build-ups can be calculated similarly to on a test rig. A fixed speed ramp is specified on the drive shaft output for the purpose. The load is placed on the gearbox input with a constant torque. At the output to the propeller shaft, part of the torque is diverted to the rear axle. This enables all acoustically relevant operating states to be covered.

https://doi.org/10.51202/9783181023549 - Generiert durch IP 216.73.216.36, am 19.01.2026, 02:19:31. © Urheberrechtlich geschützter Inhalt. Ohne gesonderte Erlaubnis ist jede urheberrechtliche Nutzung untersagt, insbesondere die Nutzung des Inhalts im Zusammenhang mit, für oder in KI-Systemen, KI-Modellen oder Generativen Sprachmodellen.

The gear and corresponding gearbox used are selected by opening and closing clutches and synchros. The gear selection can be conveniently specified by comprehensive parameter setting in the background of the model.

Post-processing from 3D MBS calculations

Following on from the actual calculation, extensive evaluation and analysis is possible with the model. In relation to the gearing acoustics, quasi-static and dynamic variables are primarily analysed. These include, to estimate the excitation level, the quasi-static and dynamic transmission error of a gear mesh and, to investigate the resultant effects, the structure-borne noise response at various measurement positions on the gearbox. The latter can be compared directly with measurement results from testing. Additionally, a wide range of other variables can be evaluated in order to identify transmission phenomena, such as bearing forces, acoustic power flows or energy stored in the system.

To provide convenient and partially automated evaluation right from the beginning, following an AVL EXCITE calculation the time data results are converted into an open exchange format, the ASAM ODS format atfx. This makes it possible to evaluate them in any suitable software program. In this case, the Head ArtemiS Suite familiar from testing is used. Just like after a measurement, it is possible in this way to realise any signal processing of the time data from the simulation to colormaps, order cuts or the like, up to signal tapping. Results from testing and simulation can thus be compared easily and with no differences in processing (frequency resolution, windowing, order width, etc.).

To gain an overview of the simulation results obtained, the simulation workflow presented provides the facility to generate a standard report. This is based on specification of characteristic nodes and coupling elements of the model in a control file, and is generated fully automatically by means of a Python script. The Head ArtemiS Suite is run in the background to generate charts and numerical values relating to the above variables from the atfx files with the simulation time data. These are then compiled and saved in user-friendly form in a pdf document.

Reverse calculation of the results back to the FE structure is also possible. Operating deflection shapes resolved by frequency or order for any simulation time points can be visualised, or the stored kinetic or potential energy can be depicted in spatially resolved form. Relevant results are written in appropriate form to open Nastran result file formats *.op2 and *.pch and are normally presented in the META post-processor from BETA CAE Systems. The recovery is based on evaluation of the modal participation factors calculated by AVL EXCITE. The operating deflection shape can be compiled by multiplication by the eigenvectors of the components stored in the preceding NASTRAN condensation process.

https://doi.org/10.51202/9783181023549 - Generiert durch IP 216.73.216.36, am 19.01.2026, 02:19:31. © Urheberrechtlich geschützter Inhalt. Ohne gesonderte Erlaubnis ist jede urheberrechtliche Nutzung untersagt, insbesondere die Nutzung des Inhalts im Zusammenhang mit, für oder in KI-Systemen, KI-Modellen oder Generativen Sprachmodellen.

Validation of simulation results by test rig measurement

The simulation results are validated on the basis of test rig measurements on a vehicle or powertrain. A typical powertrain design is shown in Fig. 7. The gearbox here is placed on a four-wheel drive test rig with four braking electric motors. As in the vehicle, it is driven by a combustion engine, or in the case of a hybrid transmission additionally by the built-in electric motor.

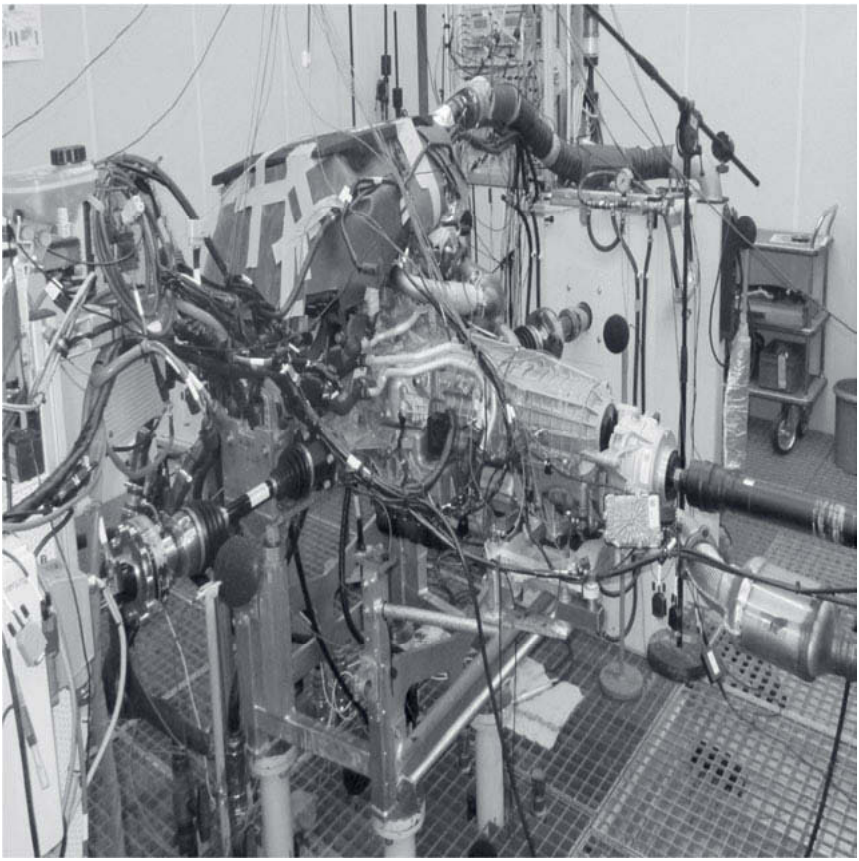


Fig. 7: Test rig construction for an Audi S tronic gearbox with a combustion engine

https://doi.org/10.51202/9783181023549 - Generiert durch IP 216.73.216.36, am 19.01.2026, 02:19:31. © Urheberrechtlich geschützter Inhalt. Ohne gesonderte Erlaubnis ist jede urheberrechtliche Nutzung untersagt, insbesondere die Nutzung des Inhalts im Zusammenhang mit, für oder in KI-Systemen, KI-Modellen oder Generativen Sprachmodellen.

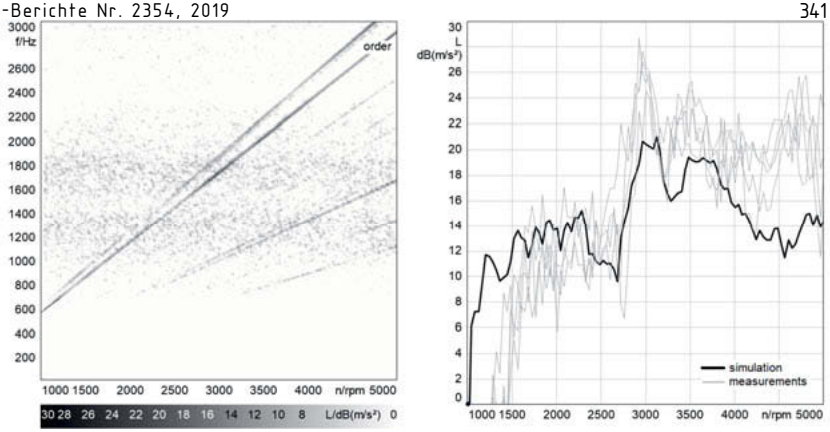


Fig. 8: Cross-checking measurement and calculation based on a speed build-up

The test rig room is clad with acoustic elements on all walls, so that the air-borne noise can be measured in parallel with the structure-borne.

The measurement and calculation can then be easily cross-checked using the aforementioned methods. Fig. 8 shows a speed build-up with a fixed ramp and a constant drive torque. The condition can be realised on a vehicle or powertrain test rig, and also simulated. The Campbell diagram on the left shows a simulation result at a measuring point at the interface from the gearbox to the subframe mounting in the vehicle. The order cut of the related gearing can be seen on the right. Shaded in grey are measurement results from various vehicles, each with the same gearbox configuration. It can be seen that the measurements open up a scatter band into which the simulation result fits. The characteristic trend, e.g. with a drop in level at around 2500 rpm and an excessive increase at 3000 rpm, is well depicted. The simulation shows rather too high levels in the lower speed range, and rather too low levels in the upper range. This is linked, among other factors, to the combustion engine, which causes the base level to rise towards higher speeds and has a corresponding effect on the order calculation.

More detailed analysis of the simulation results

In addition to the actual evaluation and analysis of structure-borne noise response at individual measuring points, other analytical tools are presented here. To that end, the excessive increase in structure-borne noise response at 3000 rpm from the previous section is investigated in more detail.

First the inducing gear mesh is analysed on the basis of its rotational path error. This is illustrated quasi-statically and dynamically in Fig. 9. The quasi-static rotational path error of the respective meshing order can be compared directly with the results from static models of the

https://doi.org/10.51202/9783181023549 - Generiert durch IP 216.73.216.36, am 19.01.2026, 02:19:31. © Urheberrechtlich geschützter Inhalt. Ohne gesonderte Erlaubnis ist jede urheberrechtliche Nutzung untersagt, insbesondere die Nutzung des Inhalts im Zusammenhang mit, für oder in KI-Systemen, KI-Modellen oder Generativen Sprachmodellen.

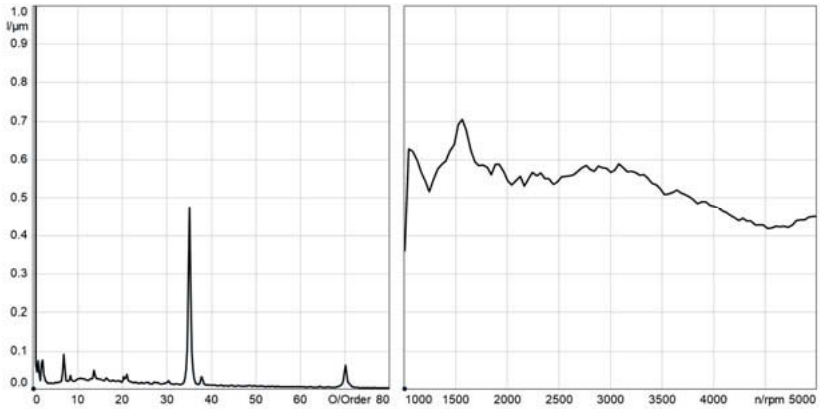


Fig. 9: Transmission error of the gearing quasi-statically (left) and for speed build-up (right) in the mesh order

gearing configuration. This incorporates the deformation of the wheel set and housing caused (quasi-)statically by the applied moment.

Dynamic analysis clearly shows effects from the speed build-up. These include, for example, resonance from the rotating shaft system and housing vibrations feeding back to the gear meshing. In this case, resonance can be said to exist at 1500 rpm for example. In the now interesting range around 3000 rpm, the dynamic rotational path error exhibits no resonant excessive increase. It can thus be assumed that there is resonance on the transfer path to the measuring point which results in an excessive increase in acceleration response but has no retrograde effect on the gear meshing.

One way to investigate the transmitting system is to analyse the transmitted acoustic power within the gearbox. The power is calculated in the standard report script. Taking account of phasing in the frequency range, it multiplies the applied forces and torque by the associated velocities at defined interface nodes of the model. Normally the roller bearings are defined as interfaces for the purpose. From this, the energy inflow and outflow of a component can be read, and conclusions can be drawn as to the possible transfer path of the structure-borne noise.

Figure 9 shows the power flows of the two drive shafts in the load case under analysis. Positive values signify power inflow, and negative values signify power outflow. There is in fact a noticeable irregularity here at around 3000 rpm. Energy is discharged from the loaded second drive shaft via the roller bearing designated “bearing 12” and absorbed by the first drive shaft. In bearing D this power flow is reversed. Here power is transmitted from the first drive shaft to

https://doi.org/10.51202/9783181023549 - Generiert durch IP 216.73.216.36, am 19.01.2026, 02:19:31. © Urheberrechtlich geschützter Inhalt. Ohne gesonderte Erlaubnis ist jede urheberrechtliche Nutzung untersagt, insbesondere die Nutzung des Inhalts im Zusammenhang mit, für oder in KI-Systemen, KI-Modellen oder Generativen Sprachmodellen.

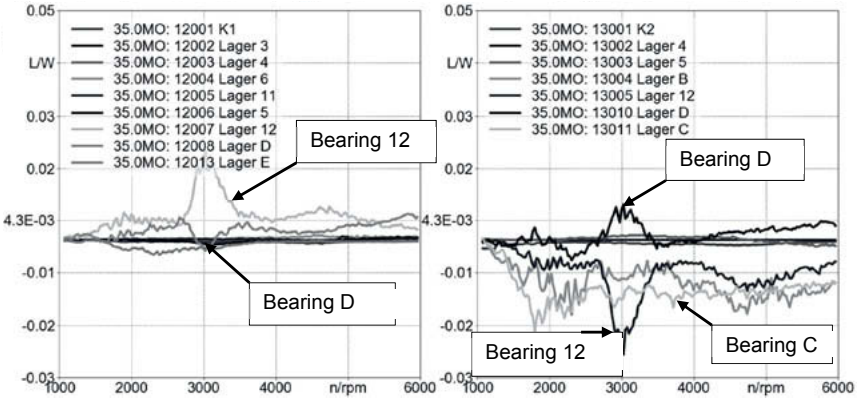


Fig. 9: Power flow analysis of first (left) and second (right) drive shaft

the second. In the identical axial position the second drive shaft is supported in the housing by bearing C. At this bearing a significant power outflow occurs across a wide speed range.

The energies in the system also give an indication of the prevailing behaviour. The standard report presents the kinetic energy in the rigid body movement and the energy converted by flexible deformation for each model component over the speed. The energy content of the flexible deformation is additionally subdivided into kinetic and potential components. This indicates whether the component in question is acting as mass or rigidity on the operating deflection shape. Fig. 10 presents the evaluation for the first and second drive shafts. There is indeed an increase in energies on the first drive shaft at 3000 rpm. Both the kinetic and potential

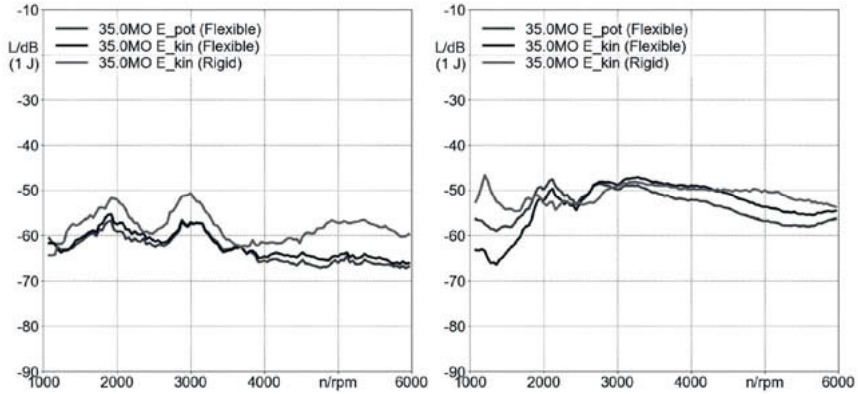


Fig. 10: Energy capacity of drive shaft 1 (left), drive shaft 2 (right)

https://doi.org/10.51202/9783181023549 - Generiert durch IP 216.73.216.36, am 19.01.2026, 02:19:31. © Urheberrechtlich geschützter Inhalt. Ohne gesonderte Erlaubnis ist jede urheberrechtliche Nutzung untersagt, insbesondere die Nutzung des Inhalts im Zusammenhang mit, für oder in KI-Systemen, KI-Modellen oder Generativen Sprachmodellen.

energy of the flexible component movement rise. This indicates an induced eigenform locally in the first drive shaft.

Fig. 11 presents the evaluation of the potential energies in the surrounding bearing points. All bearing points exhibit a resonant response in the analysed 3000 rpm range, and so participate in the operating deflection shape as spring force.

Ultimately, the preceding evaluations of acceleration, gearing, power and energy indicate the operating points (speeds) and frequencies, or orders, at which reverse calculation of the operating deflection shape is worthwhile. For this case, the operating deflection shape of the operating point under analysis, filtered by the relevant order, is shown in Fig. 12. Here the deflection shape in which the energy is stored is clearly seen. On bearing C, a high radial oscillation amplitude is discernible at the end of the shaft. This provides a plausible explanation for the potential energy in bearing C and in the second drive shaft. This may, firstly, be an indication that the bearing is modelled too softly or, secondly, also in fact indicate a yielding bearing point. Bearing 12 is located in the front area between the second and first drive shaft. It is interesting that here power is transmitted even though the first drive shaft is not participating in the actual torsional load flow. The energy analysis of the first drive shaft and of the operating deflection shape indicates that a bending eigenform of the thin front piece is being excited in the first drive shaft.

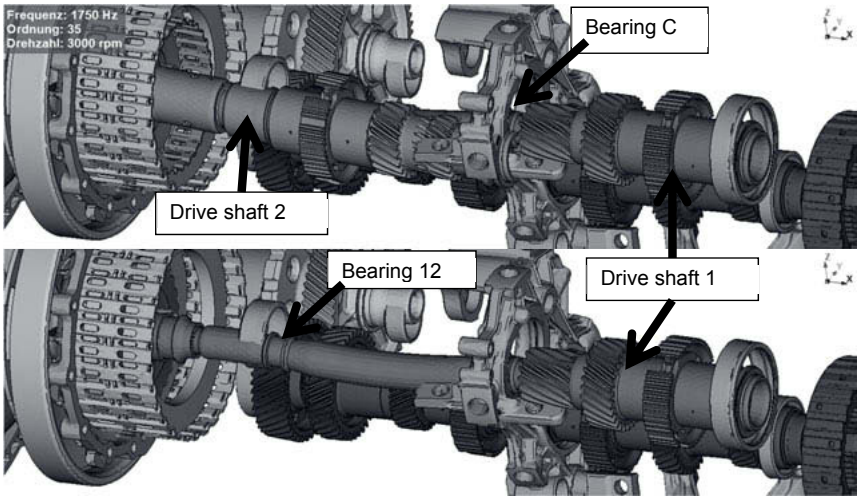


Fig. 12: Operating deflection shape of wheel set with second drive shaft (top) and without (bottom)

https://doi.org/10.51202/9783181023549 - Generiert durch IP 216.73.216.36, am 19.01.2026, 02:19:31. © Urheberrechtlich geschützter Inhalt. Ohne gesonderte Erlaubnis ist jede urheberrechtliche Nutzung untersagt, insbesondere die Nutzung des Inhalts im Zusammenhang mit, für oder in KI-Systemen, KI-Modellen oder Generativen Sprachmodellen.

As a result of the additional power flow from the first to the second drive shaft in bearing D and then through bearing C into the housing (see figure 9), an overall increase in housing excitation from the gear meshing due to the resonance of drive shaft 1 must be assumed. This provides a valuable guide for mitigating the excessive increase in acceleration response at this operating point detected in measurement and simulation as necessary.

Investigation of acoustic measures on the Audi S tronic hybrid gearbox

The new Audi S tronic hybrid gearbox is based on the dual-clutch transmission developed for conventional applications. As part of a kit, the wheel set is used in all derivatives of the gearbox [1].

Nevertheless, high-voltage electrification imposes new demands (see first chapter) on the adopted components. In addition to all-electric mode, the high recuperation capacity of the new electric motor is primarily cited. Owing to the resultant high loading on the gearing in thrust direction, a redesign of the micro-geometry on the thrust flanks has been incorporated into the development for acoustic reasons.

The gearing development department uses common computation tools such as KISSsoft and the FVA tools for gearing configuration and optimisation. Based on the example of the Audi S tronic hybrid gearbox, the primary assessment variable for acoustic optimisation is the peak-to-peak transmission error (PPTE). Other criteria are the contact pattern position and press distribution in the tooth contact. For the continuously meshed constant transmission ratio, the gearing development department proposes a flank line correction with simultaneous opposite interleaving. According to the calculation, these two modifications produce the lowest acoustic excitation for this gearing. In a first step, the flank angle correction will be implemented.

This gearing modification will also be dynamically assessed in a 3D MBS calculation using AVL EXCITE. The result of the simulation is shown in Fig. 13. A clear reduction in acceleration level of the order in question is seen. The efficacy can be checked and confirmed on the vehicle.

https://doi.org/10.51202/9783181023549 - Generiert durch IP 216.73.216.36, am 19.01.2026, 02:19:31. © Urheberrechtlich geschützter Inhalt. Ohne gesonderte Erlaubnis ist jede urheberrechtliche Nutzung untersagt, insbesondere die Nutzung des Inhalts im Zusammenhang mit, für oder in KI-Systemen, KI-Modellen oder Generativen Sprachmodellen.

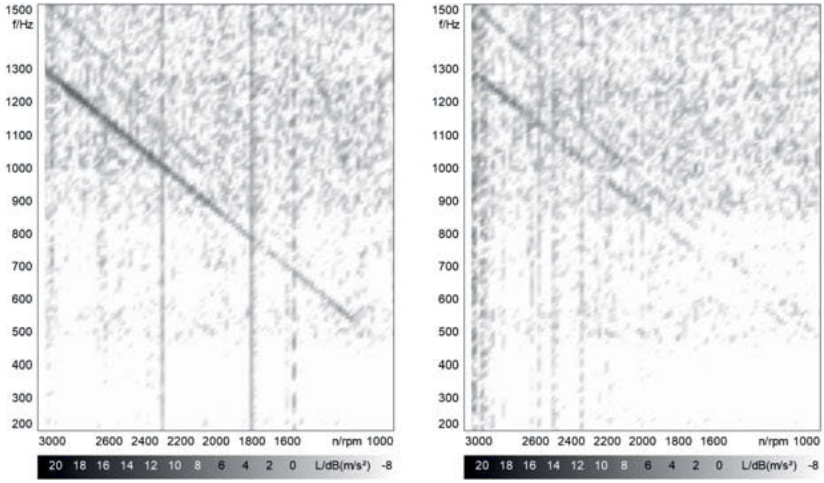


Fig. 13: Colormap from simulation of a speed run-down without (left) and with (right) new micro-correction

Summary and outlook

This paper describes an effective method of developing the acoustic characteristics of a powertrain using simulation, based on the example of the new Audi S tronic hybrid gearbox. The paper considers the new challenges for the acoustic characteristics of the gearbox resulting from high-voltage electrification.

The simulation method described extends from the CAD data to evaluation and analysis of characteristic acoustic variables in different computation disciplines. It combines established tools and simulation aids based on standardisation and automation in pre- and post-processing, and is based on intelligent linkage of functions from ANSA, ArtemiS Suite and Python. It also employs state-of-the-art methods such as machine learning.

The results produced are compiled and presented in standard reports. These also present a cross-check against test rig measurements. The reports provide comprehensive means of understanding the behaviour of the system under analysis in a visually striking way, and give acoustic engineers the necessary insight to derive and propose design measures from them. The time required for modelling, computing and result processing is much reduced by automation, meaning more time is available for detailed analysis of the results.

https://doi.org/10.51202/9783181023549 - Generiert durch IP 216.73.216.36, am 19.01.2026, 02:19:31. © Urheberrechtlich geschützter Inhalt. Ohne gesonderte Erlaubnis ist jede urheberrechtliche Nutzung untersagt, insbesondere die Nutzung des Inhalts im Zusammenhang mit, für oder in KI-Systemen, KI-Modellen oder Generativen Sprachmodellen.

The method thus makes a contribution to the ongoing widespread digital transformation of products and processes in the automotive industry, demonstrated by a concrete use case in acoustic development at Audi AG.

It is conceivable that an upgraded algorithm will be used in future, which will also by capable of handling analysis and result evaluation tasks. Starting from simple filter functions, learning techniques might identify irregularities in operating points, for example, and provide indication for design improvements.

Nevertheless, the experience and skill of the engineers involved will remain highly important. Because simulation still represents an ever more intelligent tool for analysis of the acoustic properties of a drive system. However, investigating the effects and assessing relevance to the overall vehicle will remain the responsibility of the acoustic engineer.

References

[1] Schmidt, A., Fleischmann, H.-P.: Enhancement of a Dual Clutch Transmission Kit – AUDI S tronic, AUDI AG Ingolstadt, Dritev 2018

[2] van der Meer, J., Hangen, G., Uhlig, J.: The new plug-in hybrid module as an addition to the AUDI S tronic gearbox family, Volkswagen AG Kassel, AUDI AG Ingolstadt, Dritev 2018

[3] Schwing, J., Märkle, T., Eichinger, B.: Wirksame Verknüpfung von Simulationsmethoden, Analysewerkzeuge und Auswerteverfahren in der Antriebsakustik [Effective interlinking of simulation methods, analytical tools and evaluation techniques in powertrain acoustics], AUDI AG Ingolstadt, Vehicle Acoustics conference, Haus der Technik Essen 2018

[4] Märkle, T., Eichinger, B., Schwing, J.: Calculation of the Structure Borne Noise of Vehicle Powertrains, their Validation and Re-calculation to the individual Source Contributions Part 1: Analysis of Structure Borne Noise and Noise Transfer Path in modern Powertrains with MBD Simulation, AUDI AG Ingolstadt, Aachen Acoustics Colloquium 2017

https://doi.org/10.51202/9783181023549 - Generiert durch IP 216.73.216.36, am 19.01.2026, 02:19:31. © Urheberrechtlich geschützter Inhalt. Ohne gesonderte Erlaubnis ist jede urheberrechtliche Nutzung untersagt, insbesondere die Nutzung des Inhalts im Zusammenhang mit, für oder in KI-Systemen, KI-Modellen oder Generativen Sprachmodellen.

https://doi.org/10.51202/9783181023549 - Generiert durch IP 216.73.216.36, am 19.01.2026, 02:19:31. © Urheberrechtlich geschützter Inhalt. Ohne gesonderte Erlaubnis ist jede urheberrechtliche Nutzung untersagt, insbesondere die Nutzung des Inhalts im Zusammenhang mit, für oder in KI-Systemen, KI-Modellen oder Generativen Sprachmodellen.

NVH-Challenges and solution approaches in electric drive development from the supplier‘s view

NVH-Herausforderung und Lösungsansätze in der Entwicklung elektrischer Antriebe aus Zulieferersicht

Christian Dassler, **Matthias Kurch**, **Mark Nichols**,
Schaeffler Technologies AG & Co. KG, Herzogenaurach

Zusammenfassung

Die Automobilindustrie erlebt aktuell einen richtungsweisenden Umbruch. Die Zukunft des Automobils wird von der Effizienzsteigerung und der fortschreitenden Elektrifizierung des Antriebsstrangs sowie von sich verändernden Mobilitätsanforderungen und der Digitalisierung geprägt sein. Schaeffler adressiert diese Herausforderungen mit seiner Strategie „Mobilität für morgen“. Dort stehen im Fokusfeld „umweltfreundliche Antriebe“, Produkte und Produktentwicklungen, wie unter anderem elektrische Achsen und Hybrid-Module. Die Entwicklung solcher elektrischen Antriebssysteme stellt Zulieferer vor vielfältige Herausforderungen. Eine Kernaufgabe im Produktentwicklungsprozess ist die Beherrschung der Akustikanforderungen des Kunden. Dabei müssen die Geräusche der E-Maschine, des Inverters und des Getriebes sowie deren subjektive Wahrnehmung fokussiert und als Gesamtsystem betrachtet werden. Aufgrund der fehlenden Maskierung durch die Geräuschkulisse des Verbrennungsmotors kann die NVH-Charakteristik dieser Quellen deutlich in das Zentrum der Wahrnehmung rücken. Zulieferer verantworten normalerweise allerdings nicht den gesamten Übertragungspfad von den genannten Anregern über deren Ankopplung in die umgebende Fahrzeugstruktur hinein in den Fahrzeuginnenraum, sondern den Antrieb und seine nahe Umgebung. Somit muss ein anregungsoptimales Antriebssystem entwickelt werden, wobei der Zulieferer die NVH-Optimierung der Zahneingriffe, Magnetkräfte, Frequenzen der Leistungselektronik, Gehäuseeigenschaften und deren Ankopplung oft ohne detaillierte Kenntnisse des finalen Fahrzeuges und den daraus folgenden Wechselwirkungen durchführen muss.

Die daraus resultierenden, spezifischen Herausforderungen können mit zeitgemäßen numerischen und experimentellen Analysemethoden beherrschet werden. Schaeffler verfügt über die Kompetenz diese Akustikanalysen für elektrische Achsen und Hybrid-Module durchzuführen und stellt somit eine erfolgreiche Entwicklung sicher. Der Beitrag stellt anhand aktueller,

https://doi.org/10.51202/9783181023549 - Generiert durch IP 216.73.216.36, am 19.01.2026, 02:19:31. © Urheberrechtlich geschützter Inhalt. Ohne gesonderte Erlaubnis ist jede urheberrechtliche Nutzung untersagt, insbesondere die Nutzung des Inhalts im Zusammenhang mit, für oder in KI-Systemen, KI-Modellen oder Generativen Sprachmodellen.

elektrischer Antriebssysteme Lösungsansätze für die NVH-Herausforderung dar und zeigt welche Kompetenzen Schaeffler einsetzt, um zukünftige Herausforderungen der Elektromobilität zu meistern.

Abstract

The automotive industry is currently going through a paradigm shift. Increased efficiency combined with the electrification of the powertrain, as well as digitalization and a change in mobility concepts are the key drivers for the automobile of tomorrow. The challenges arising from these developments are being addressed in the Schaeffler strategy “Mobility for tomorrow”. One of its major focus fields is “Eco-friendly drives”, which covers the development of corresponding products such as electric axles and hybrid modules. For the development of such electric drive systems, suppliers face various challenges, of which some are new, and in many cases different solutions are needed compared to conventional powertrain demands. One increasingly crucial task in the product development process is fulfilling the NVH requirements of the customer. Up to a certain degree however, the content of this task has changed. The noise of the electric motor, the inverter, the transmission and their psychoacoustic impact are key issues that must be addressed with respect to the whole system. This is especially true if an internal combustion engine no longer masks other sources of noise anymore. A supplier is usually not responsible for the entire transfer path from the excitation of the electric motor, inverter and transmission through their connection into the vehicle structure all the way to the passenger cabin, but for the electric powertrain and the interfaces to its surroundings.

Therefore, the aim is to develop a drive system that ensures an optimum in terms of excitation, whereas the supplier must provide and develop tooth contact forces, magnetic forces, frequencies of the power electronics, housing properties and interfaces to the vehicle frame mostly without detailed knowledge about the final vehicle and the corresponding interactions. The resulting challenges can be adequately tackled via numerical and experimental methods and tools ranging from standard to advanced. Schaeffler has grown for many years with such tools and built up the required competence and expertise to conduct acoustic analyses for electric axles and hybrid modules, in order to ensure a successful development. This paper introduces necessary considerations regarding NVH of electric drive system solutions and underlines the competences of Schaeffler to master the challenges of electrified mobility.

https://doi.org/10.51202/9783181023549 - Generiert durch IP 216.73.216.36, am 19.01.2026, 02:19:31. © Urheberrechtlich geschützter Inhalt. Ohne gesonderte Erlaubnis ist jede urheberrechtliche Nutzung untersagt, insbesondere die Nutzung des Inhalts im Zusammenhang mit, für oder in KI-Systemen, KI-Modellen oder Generativen Sprachmodellen.

Introduction

From the initial triumph of the automobile conquering individual mobility, its emissions have always been of interest. Not only regarding exhaust gases, but also the NVH behavior from the vantage point of the driver, passengers, and the surroundings. For around 140 years now, people have been conditioned for each of these perspectives. Thus, we have certain expectations based on our experience with NVH behavior, for example if we compare a mini van to a sportscar. This underlines the fact that the NVH characteristics are a key point of the driving experience. Thus, its development nowadays aims to achieve an experience that is desired for a particular vehicle, even via synthesized approaches. Due to the aforementioned paradigm shift, there are two major impacts on the acoustic requirements.

First, masking effects from an internal combustion engine are reduced or eliminated. This also means, that noise patterns we have been conditioned to expect are not available anymore. A popular approach is to inject synthesized sound which do not arise from the powertrain, but instead usually via discreetly placed speakers in the vehicle. Another approach is to utilize the powertrain itself for this task. However, this is currently not a common approach in the automotive industry. Furthermore, new expectations for acoustic feedback might develop over the next years and decades.

The second paradigm shift is the lowering of emissions, partially to a level of no emissions whatsoever, which also includes radiated noise. By implementing new technologies and vehicle platforms to fulfil the paradigm shift, our customers strictly confirm this trend towards zero emissions. In contrast, regulatory developments demand a certain external drive noise.

In addition to these issues requiring a solution, electric powertrains are subject to operating conditions that significantly differ from those of conventional powertrains, for example higher rotational speeds or high torque at low rotational speeds. This paper gives insight into how to tackle these challenges for an electric axle drive with its subsystems transmission, electric motor and power electronics. Furthermore, it provides an outlook about the potential of sound engineering for electric axle drives or similar electric drive systems and how a supplier can support his customer to achieve the desired experience for the end customer.

To actively shape the mobility for tomorrow and fulfil its ambitious demands, Schaeffler promotes the electrification of automobiles with products as electric axles or hybrid modules. For electric axles for example, modular concepts are available for both front- rear- and all-wheel drive electric axles with offset and coaxial alignment, thus flexibility is offered tailored to customer needs. All layouts are already available in mass production, former one even as a 2-speed variant. A superb NVH-behavior is an attribute that can be found from each variant.

https://doi.org/10.51202/9783181023549 - Generiert durch IP 216.73.216.36, am 19.01.2026, 02:19:31. © Urheberrechtlich geschützter Inhalt. Ohne gesonderte Erlaubnis ist jede urheberrechtliche Nutzung untersagt, insbesondere die Nutzung des Inhalts im Zusammenhang mit, für oder in KI-Systemen, KI-Modellen oder Generativen Sprachmodellen.

These experiences were essential to improve NVH competences with regard to electrified mobility solutions and provide the foundation of this work.

Electric Motor – Excitations and solution approaches

Every electric motor has by design an “acoustic fingerprint”, which is characterized by a number of factors, foremost the type of motor (e.g. synchronous motor or induction motor) and by its design topology. An overview of major parameters influencing the acoustic fingerprint is given in Fig. 1.

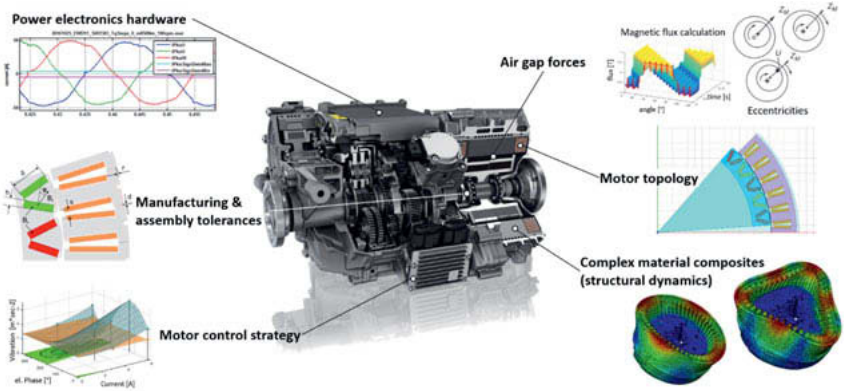


Fig. 1: Parameters influencing the “acoustic fingerprint” of an electric motor

For a number of these influencing parameters, analytical approaches can be used in very early design phases for a rough assessment of noise character. In later phases of the development, numerical simulation models are state-of-the-art.

Using only input data from the motor topology, i.e. motor type, pole pairs, phase numbers, slot number, and winding scheme, the primary motor orders can be derived and are known for layout of other components in the powertrain.

Once a more detailed geometric design is available, more precise calculations of the resulting spatial and temporal force distribution can be performed. Forces acting in radial, tangential and axial are quantified. Radial forces mainly induce forced mechanical vibrations distributed over the circumference in the stator and housing of the electric drive. Tangential forces on the other

https://doi.org/10.51202/9783181023549 - Generiert durch IP 216.73.216.36, am 19.01.2026, 02:19:31. © Urheberrechtlich geschützter Inhalt. Ohne gesonderte Erlaubnis ist jede urheberrechtliche Nutzung untersagt, insbesondere die Nutzung des Inhalts im Zusammenhang mit, für oder in KI-Systemen, KI-Modellen oder Generativen Sprachmodellen.

hand result in motor torque oscillations. Special consideration of axial forces should be taken if either the rotor or stator is skewed in line-shape.

In many motor designs, radially-acting forces on the motor housing represent the most critical source of noise. A typical approach is therefore to calculate the forced mechanical vibrations first in radial direction, which act both with a spatial and temporal periodicity, and compare this to the expected resonance modes and frequencies from the housing, as representatively shown in Fig. 2.

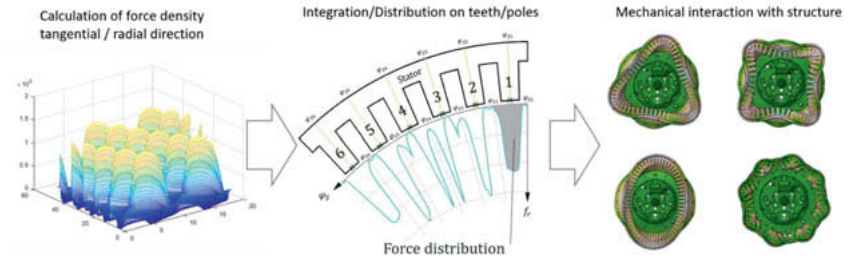


Fig. 2: Force shape calculation and interaction with mechanical structure

Once the acting forces of an electric motor design have been identified, they can be applied to a finite-element mechanical model of the motor structure (rotor, stator and housing).

There, the appropriate material modeling presents a typical challenge, as for the material properties of stator slot resin. Stator plates for instance are often stamped, stacked and laminated sheet metal. An experimental modal analysis of a stator plate stack is a feasible approach to

https://doi.org/10.51202/9783181023549 - Generiert durch IP 216.73.216.36, am 19.01.2026, 02:19:31. © Urheberrechtlich geschützter Inhalt. Ohne gesonderte Erlaubnis ist jede urheberrechtliche Nutzung untersagt, insbesondere die Nutzung des Inhalts im Zusammenhang mit, für oder in KI-Systemen, KI-Modellen oder Generativen Sprachmodellen.

determine material properties for an electric motor. Experimentally-determined values for stiffness and damping are fed back into finite element models by means of model updating methods and toolchains, indicated in Fig. 3.

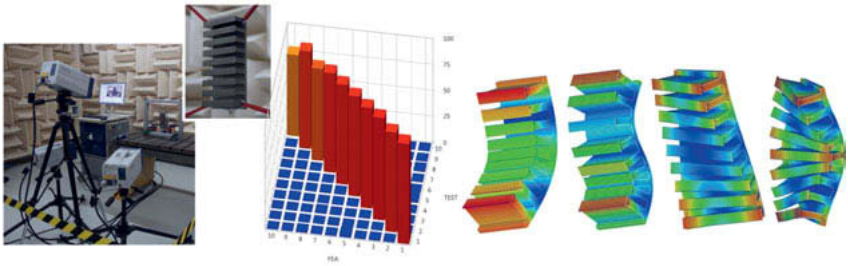


Fig. 3: Experimental modal analysis of a laminated stator plate stack and update of simulation model

As mentioned before, forces acting in tangential direction often do not have a direct impact on electric motor noise. The resulting rotational oscillations can influence the gear mesh noise of a connected transmission.
Using the calculated force data, potentially critical operating points of the electric motor itself, as well as components of the drivetrain can be assessed, and design changes made in a very early phase of development. A representative overview of the most important aspects of this process is given in Fig. 4.

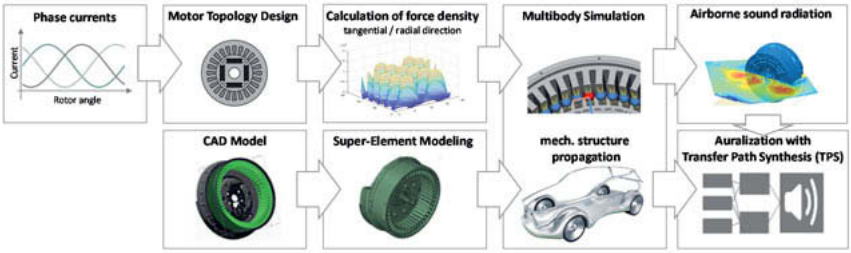


Fig. 4: Overview of electric motor NVH layout process

Cross-correlations between current displacement and rotor eccentricity should also be considered in the design-phase, as they could enhance resonance effects in the motor in certain operating ranges. If a certain motor design is set due to constrictions other than the noise and

https://doi.org/10.51202/9783181023549 - Generiert durch IP 216.73.216.36, am 19.01.2026, 02:19:31. © Urheberrechtlich geschützter Inhalt. Ohne gesonderte Erlaubnis ist jede urheberrechtliche Nutzung untersagt, insbesondere die Nutzung des Inhalts im Zusammenhang mit, für oder in KI-Systemen, KI-Modellen oder Generativen Sprachmodellen.

vibration behavior, active vibration control approaches can be used to compensate motor noise in certain operating points or within certain operating ranges. These approaches are generally integrated into the motor control strategy and introduce higher harmonics into the phase currents to shape the forces in the magnetic field to compensate vibrations. [1]

Another aspect of the NVH behavior of the electrified powertrain is the contribution of the power electronics. Noise originating from power electronics typically consists of the switching frequency of the inverter and speed-dependent sidebands resulting from the pulse-width modulation (PWM) frequency. A typical occurrence of power electronics noise is shown in Fig. 5.

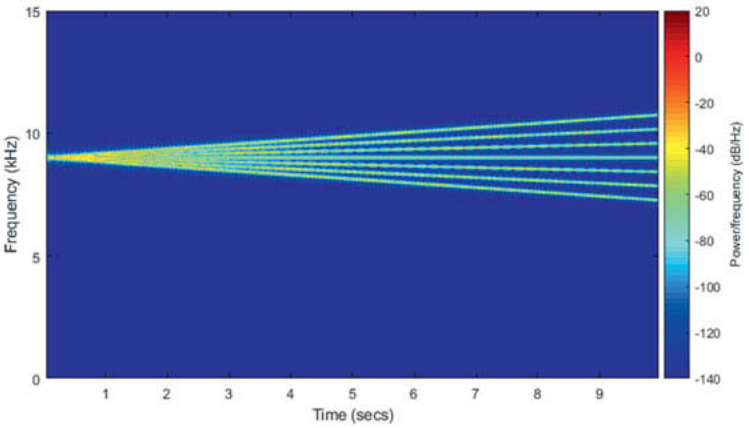


Fig. 5: Typical occurrence of power electronics noise

The frequency range of noise caused by power electronics is dependent on the maximum motor speed and is often significantly above 5 kHz and therefore mainly relevant as an audible noise. The specific switching frequency has influence on noise radiation and motor efficiency. Therefore, interdependencies in the design require the close cooperation between NVH engineers and software designers.

This is in particular a challenge for single-speed transmissions, where a high rotational speed range is utilized, thus high switching frequencies in the power electronics are necessary. In the complex decision process about the powertrain topology this must be considered.

There are several approaches [2] to modeling such a sound generated by power electronics with a varying degree of accuracy. Once a model is available that describes the vibrational

https://doi.org/10.51202/9783181023549 - Generiert durch IP 216.73.216.36, am 19.01.2026, 02:19:31. © Urheberrechtlich geschützter Inhalt. Ohne gesonderte Erlaubnis ist jede urheberrechtliche Nutzung untersagt, insbesondere die Nutzung des Inhalts im Zusammenhang mit, für oder in KI-Systemen, KI-Modellen oder Generativen Sprachmodellen.

characteristics of the power electronics noise in a mechanical structure, airborne sound simulation is often performed using either a finite element method (FEM) or a boundary element method (BEM) approach.

Transmissions – Excitations and solution approaches

Electric motors are capable of providing the required output torques for automobiles in the typical wheel speed range if dimensioned correspondingly. Due to cost and efficiency optimization, they are often designed for a higher speed range than is usually the case with internal combustion engines (ICE). Thus, transmissions with a fixed ratio which must cover a wide speed range are used for on-demand speed and torque conversion to the wheels. Furthermore, they are loaded heavily when energy recovery – recuperation is utilized. The relationship between torque (T) and rotational speed (ω) becomes clear if they are plotted as shown in Fig. 6 in the 4-quadrant (4Q) representation where ICE [3] and electric drive concepts are compared which are colored in red and green respectively. The diagram shows the possible speed and torque ranges for an electric motor with fixed gear ratio and an ICE transmission with five forward and one reverse gear. Noise is excited in the electric motor transmissions (EMT´s) due

https://doi.org/10.51202/9783181023549 - Generiert durch IP 216.73.216.36, am 19.01.2026, 02:19:31. © Urheberrechtlich geschützter Inhalt. Ohne gesonderte Erlaubnis ist jede urheberrechtliche Nutzung untersagt, insbesondere die Nutzung des Inhalts im Zusammenhang mit, für oder in KI-Systemen, KI-Modellen oder Generativen Sprachmodellen.

to speed and load-dependent oscillating forces. These excitations can be amplified by speed independent system resonances and non-linear effects or be shifted to other frequency ranges.

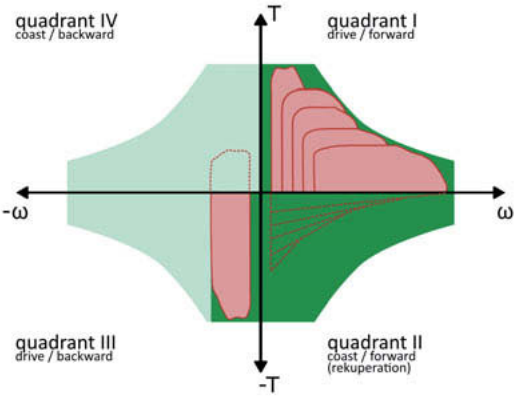


Fig. 6: 4-quadrant representation of ICE and electric drive

A significant source of excitation in an EMT is the gear meshing resulting in a variable engagement stiffness. The resulting dynamic periodic forces have a tonal character. The gear excitation does not correspond to a pure sinusoidal shape, so that in the frequency spectrum more harmonics are visible. For the holistic understanding of the excitation within the transmission, all gear meshes of the input, intermediate and load stages must be analyzed.

From the above points, the acoustic conditions of EMT´s differ significantly from those of internal combustion engines. This leads to several new acoustic challenges. The higher input speeds generate higher excitation frequencies due to compact and light electric machines. Recuperation causes high loads during coasting and thus increased excitation of the loaded gear mesh. Furthermore, for EMT´s the speed range between 0 rpm and idle speed is a utilized operating range and must be analyzed additionally. In terms of phenomena like rattling, EMT´s are relatively uncritical, since comparatively little rotational non-uniform irregularity is introduced through the electric motor, especially in the lower speed range. In addition, EMT´s often only have a fixed ratio, so there are no inactive gears - loose wheels - as in classic manual transmissions. Thus, for impulses, which are caused by load changes, it is possible to use the

https://doi.org/10.51202/9783181023549 - Generiert durch IP 216.73.216.36, am 19.01.2026, 02:19:31. © Urheberrechtlich geschützter Inhalt. Ohne gesonderte Erlaubnis ist jede urheberrechtliche Nutzung untersagt, insbesondere die Nutzung des Inhalts im Zusammenhang mit, für oder in KI-Systemen, KI-Modellen oder Generativen Sprachmodellen.

superior response dynamics of drive torque in electric motors in order to avoid or dampen load changes using to active control technologies.

For the acoustic design of an EMT an analytical order analysis at a very early stage of development is recommended. In this case, one considers the nominal orders of all installed components, all gear meshes as well as the individual gear stages and rolling bearing arrangements. To prevent potential problems already here, it is advisable to avoid overlapping of nominal orders and harmonics. As this is very likely to lead to amplitude modulation, resulting in sidebands and ultimately to increased perceptibility in the vehicle.

Due to the complexity of the application, an integrated simulation approach is essential for the development of EMT´s and the management of acoustic risks. This environment uses different software packages for static and dynamic analysis.

After the design of the micro- and macrogeometry of the gearing with calculation programs such as Bearinx [4] or MASTA [5], the oscillation excitation behavior of individual meshing operations is determined based on the transmission error. Load-related deformations in the tooth contact are included in the contact analysis. By calculating the transmission error while considering the deformation state of the entire transmission system, the time-varying stiffness behavior of individual gear meshes, as for example in a planetary gear set can be determined. The goal in the early project phase is to determine and minimize the excitation level by means of static calculations using application-specific limit values for the transmission error.

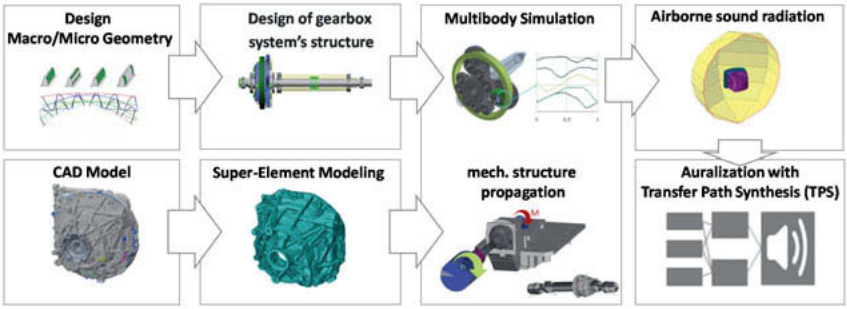


Fig. 7: Overview of Transmission NVH layout process

For the acoustic optimization and the overall understanding of the system, the speed-dependent dynamic excitation mechanisms must be analyzed. For this task, transient multi-body simulation (MBS) is an established method. The most important aspects of the simulation process are depicted in Fig. 7. Here, shafts and connecting elements of the transmission are modeled

https://doi.org/10.51202/9783181023549 - Generiert durch IP 216.73.216.36, am 19.01.2026, 02:19:31. © Urheberrechtlich geschützter Inhalt. Ohne gesonderte Erlaubnis ist jede urheberrechtliche Nutzung untersagt, insbesondere die Nutzung des Inhalts im Zusammenhang mit, für oder in KI-Systemen, KI-Modellen oder Generativen Sprachmodellen.

as a system of several rigid bodies. The model also includes rolling bearing models as load-dependent stiffness matrices or alternatively as a non-linear stiffness function. Elastic components such as housing and planetary carrier are described by super elements. For this purpose, finite element models of the components are imported and retained nodes are defined at the bearing points, bolted joints and evaluation points. Subsequently, a reduced model is constructed by means of the Craig-Bampton reduction [6]. To do that properly, it must be decided which maximum frequency the model should consider. This is determined from the rotational speed range of the transmission and its highest order.

With such an MBS model, during the development phase it can be analyzed how parameter adjustments of the macro-geometry influence the structure-borne sound excitation. Fig. 8 shows the simulation result of an example where the overlap ratio ε_β was optimized. The optimized design has in contrast to the reference an integer overlap ratio resulting in an improvement of 10 dB in a particular frequency range of this EMT.

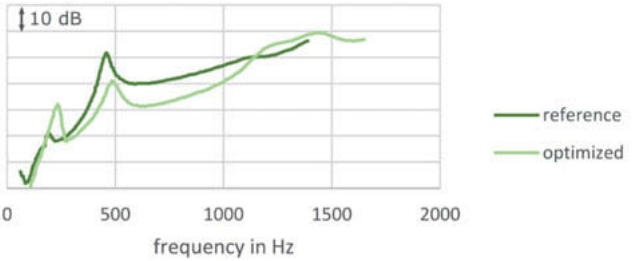


Fig. 8: MBS results of optimization ε_β

Due to the positive simulation results, the optimized variant found with numerical tools was implemented and analyzed on a test bench, as well as the reference variant before. Fig. 9 shows the results and confirms the improvement predicted by the MBS model. Such MBS are established in the NVH design process to target the customers' requirements. However, to

https://doi.org/10.51202/9783181023549 - Generiert durch IP 216.73.216.36, am 19.01.2026, 02:19:31. © Urheberrechtlich geschützter Inhalt. Ohne gesonderte Erlaubnis ist jede urheberrechtliche Nutzung untersagt, insbesondere die Nutzung des Inhalts im Zusammenhang mit, für oder in KI-Systemen, KI-Modellen oder Generativen Sprachmodellen.

successfully conduct such a simulation, in-depth understanding about the simulated systems is crucial.

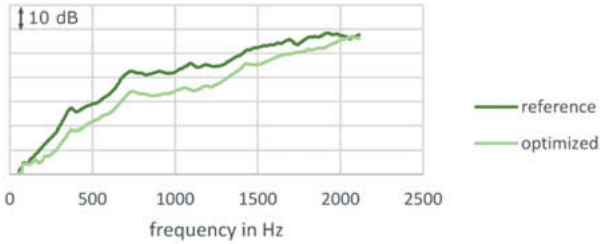


Fig. 9: Test results of optimization ε_β

Challenges and solutions of the system´s NVH behavior

In order to predict and optimize the vibroacoustic behavior of each sub-system in the powertrain, a complete system MBS approach is essential. MBS-models as described in the previous sections of individual powertrain components are integrated into an overall MBS model. The model is a significant step towards a digital representation of the whole electric axle and its

https://doi.org/10.51202/9783181023549 - Generiert durch IP 216.73.216.36, am 19.01.2026, 02:19:31. © Urheberrechtlich geschützter Inhalt. Ohne gesonderte Erlaubnis ist jede urheberrechtliche Nutzung untersagt, insbesondere die Nutzung des Inhalts im Zusammenhang mit, für oder in KI-Systemen, KI-Modellen oder Generativen Sprachmodellen.

final vehicle environment. The work flow is depicted in Fig. 10. This model is used to address challenges of the complete system´s NVH behavior and to analyze potential solutions.

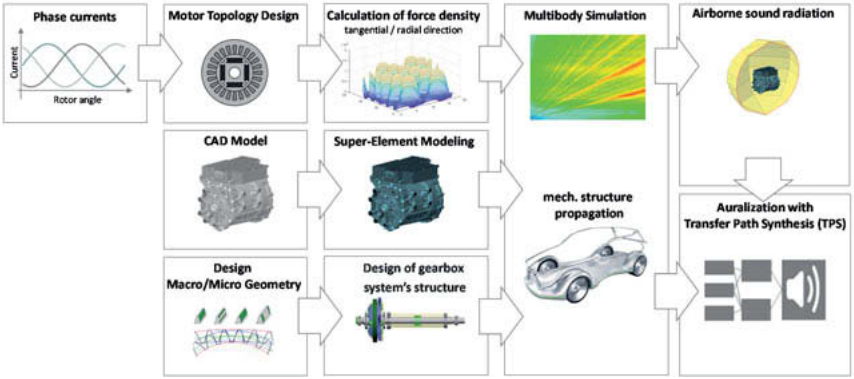


Fig. 10: Overview of electric axle system NVH layout process

With the MBS model described, development-related questions can be answered. For example, the speed-dependent acoustic excitation behavior of two designed macrogeometries can be evaluated and a decision recommendation can be made.

Usually, the natural frequencies of the complete electric axle with the connected electric powertrain mounts differs significant from those of the sub-systems. Thus, a run-up analysis of excitation forces from transmission and electric motor is executed to see if resonances are observable and have a significant contribution to the noise level. The application of damping elements is due to installation space specifications and cost requirements not recommended inside the electric axle system. The mistuning of resonances is also no expedient solution, because of the wide frequency range passed through. The analysis and optimization of the phase relations

https://doi.org/10.51202/9783181023549 - Generiert durch IP 216.73.216.36, am 19.01.2026, 02:19:31. © Urheberrechtlich geschützter Inhalt. Ohne gesonderte Erlaubnis ist jede urheberrechtliche Nutzung untersagt, insbesondere die Nutzung des Inhalts im Zusammenhang mit, für oder in KI-Systemen, KI-Modellen oder Generativen Sprachmodellen.

of the dynamic excitation forces for their mutual cancellation in the transmission might solve the issues and is also performed by MBS.
Furthermore, the MBS enables the analysis of the transfer paths in the electric axle system and forms the basis for determining the excitation quantities for the sound emission calculation.

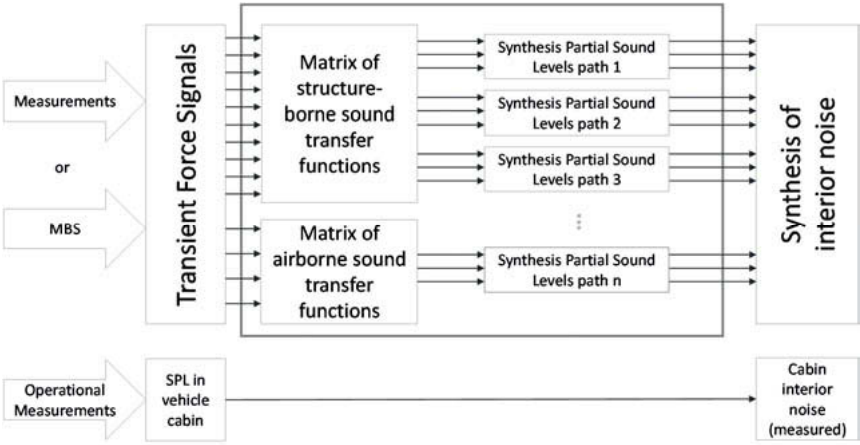


Fig. 11: Principal approach of a Transfer Path Synthesis (TPS)

At the same time, the MBS can also provide transient forces at interface points of the substructure carrying the powertrain and allows for the synthesis of global powertrain noise in a vehicle environment. The steps of this approach are shown in Fig. 11. R&D activities concerning powertrain soundscape design in the target vehicle can be addressed here.

Beside the previously shown challenges and solution approaches, an extensive system understanding that involves the effect of mass production is essential. Systematic research of the influence of manufacturing and assembly tolerances as variables in simulation models allows

https://doi.org/10.51202/9783181023549 - Generiert durch IP 216.73.216.36, am 19.01.2026, 02:19:31. © Urheberrechtlich geschützter Inhalt. Ohne gesonderte Erlaubnis ist jede urheberrechtliche Nutzung untersagt, insbesondere die Nutzung des Inhalts im Zusammenhang mit, für oder in KI-Systemen, KI-Modellen oder Generativen Sprachmodellen.

for the identification and focusing on dimensions critical for the NVH performance of a powertrain. Often, the tolerances of dimensions cannot be observed individually, but must be seen in the context of a tolerance chain influencing noise as shown in Fig. 12.

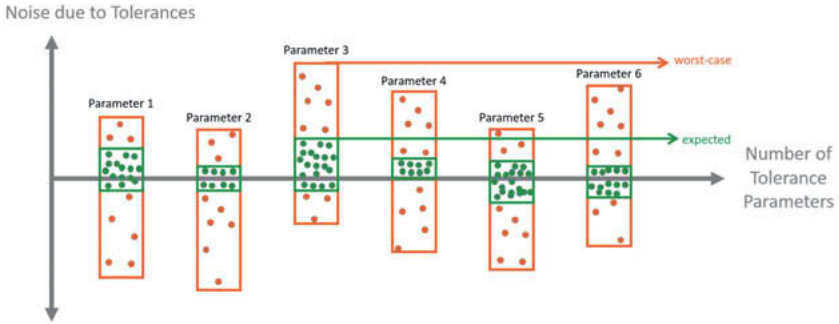


Fig. 12: Tolerance chain influencing noise

Here, the noise influence possible tolerance limits (in orange) as well as statistically probably tolerance limits (in green) are shown in a simplified manner. Performing this kind of assessment of a mass-produced system is particularly useful for identifying tolerances in the manufacturing process which should receive prioritized review. The tolerance parameter with the technical potential to cause the largest noise issue is often not the statistically most probable.

Conclusion

From the perspective of a supplier, it is vital to provide reliable methods and tools and apply them to achieve ambitious NVH targets. For this reason, it is crucial to fundamentally understand the subsystems electric motor, power electronics and transmission, as well as their impact on the NVH behavior, in particular, in mass production. Furthermore, it is helpful to understand the environment of the system, in this case an electric axle. However, in most cases, if we talk about new platforms for E-Mobility or electrified platforms, it is rarely possible to test the NVH behavior in-vehicle early on – often because the vehicle is being developed in parallel and is not available. We therefore update our knowledge and understanding continuously by means of prototype cars and validate our testing and simulation toolboxes in order to offer

https://doi.org/10.51202/9783181023549 - Generiert durch IP 216.73.216.36, am 19.01.2026, 02:19:31. © Urheberrechtlich geschützter Inhalt. Ohne gesonderte Erlaubnis ist jede urheberrechtliche Nutzung untersagt, insbesondere die Nutzung des Inhalts im Zusammenhang mit, für oder in KI-Systemen, KI-Modellen oder Generativen Sprachmodellen.

products with excellent NVH characteristics. Thus, we are not simply a supplier, but a partner that supports his customers to find solutions for a superb NVH behavior of the vehicle.

Outlook

When looking at vehicles today, the brand identity and the level of perceived quality is not defined merely by the optical design, performance data or materials used in manufacturing, but also by the sound of the powertrain. In this context, electrified powertrains initially lack the subtle, low- to mid-frequency ambient sound compared to high-powered internal combustion engine-based powertrains traditionally associated with upper- and premium-class vehicles.

Aside from the lack of emotions invoked by a powerful sounding engine, information regarding the vehicle state is also not delivered. Vibroacoustic feedback that indicates a change of load and speed often does not reach the driver. Despite exceptional performance characteristics, electrified vehicles tend to come up short on delivering the expected acoustic feedback from decades of conditioning by conventional vehicles.

Another factor must be considered as well. Due to the lack of masking effects previously supplied by internal combustion engines, exceptional care must be taken when shaping the soundscape inside the vehicle cabin. A supplier has only a limited range of options to influence masking, so comprehensive knowledge of the system with which the powertrain interacts is essential. Using state-of-the-art methods such as direct-force-based transfer path analyses and transfer path syntheses, Schaeffler can address this challenge as well.

In summary, powertrain NVH development from a supplier does no longer merely cover traditional tasks of achieving and surpassing defined target noise and vibration targets, but also incorporates legal requirements and emotionally relevant perception targets as new fields of work. This requires an even more intense partnership between the supplier and his customer

https://doi.org/10.51202/9783181023549 - Generiert durch IP 216.73.216.36, am 19.01.2026, 02:19:31. © Urheberrechtlich geschützter Inhalt. Ohne gesonderte Erlaubnis ist jede urheberrechtliche Nutzung untersagt, insbesondere die Nutzung des Inhalts im Zusammenhang mit, für oder in KI-Systemen, KI-Modellen oder Generativen Sprachmodellen.

in order to master the requirements of the future and set new benchmarks for the mobility for tomorrow.

References

[1] Harries, M; Hensgens, M.; De Doncker, R.W.: Noise Reduction Via Harmonic Current Injection for Concentrated-Winding Permanent Magnet Synchronous Machines

[2] Herrnberger, M.: Akustische Anregungsquellen in hochintegrierten Leistungselektroniken mobiler Antriebe, Tagungsband DAGA 2019, 2019

[3] Mitschke, M., Wallentowitz, H.: Dynamik der Kraftfahrzeuge. Springer Fachmedien, Wiesbaden, 2014

[4] Official product website Schaeffler Bearinx (2019)

[5] Official product website SMT Masta (2019)

[6] Craig, R.; Bampton, M: Coupling of Substructures for Dynamic Analysis, AIAA Journal, Vol. 12., 1313-1319 (1968)

https://doi.org/10.51202/9783181023549 - Generiert durch IP 216.73.216.36, am 19.01.2026, 02:19:31. © Urheberrechtlich geschützter Inhalt. Ohne gesonderte Erlaubnis ist jede urheberrechtliche Nutzung untersagt, insbesondere die Nutzung des Inhalts im Zusammenhang mit, für oder in KI-Systemen, KI-Modellen oder Generativen Sprachmodellen.

https://doi.org/10.51202/9783181023549 - Generiert durch IP 216.73.216.36, am 19.01.2026, 02:19:31. © Urheberrechtlich geschützter Inhalt. Ohne gesonderte Erlaubnis ist jede urheberrechtliche Nutzung untersagt, insbesondere die Nutzung des Inhalts im Zusammenhang mit, für oder in KI-Systemen, KI-Modellen oder Generativen Sprachmodellen.

Transmission system footprint related to fatigue, efficiency and NVH

Leistungsabdruck eines Getriebesystems bezüglich Lebensdauer, Effizienz und Geräuschverhalten

Dr. **Artur Grunwald**, GKN Driveline International GmbH,
ePowertrain Technology Centre Lohmar

Zusammenfassung

GKN entwickelt und fertigt seit über 15 Jahren elektrische Antriebsysteme für Fahrzeuge. Mehr als 750.000 Hybrid- und Elektrofahrzeuge mit Antriebssystemen von der GKN fahren bereits auf Straßen in Europa, Asien und Amerika. Der Automobilmarkt befindet sich im Wandel und die Umsetzung der Elektrifizierung von Fahrzeugflotten im größeren Umfang ist bereits gestartet. Hohe Anforderungen an die Zuverlässigkeit, die Effizienz und das Geräuschverhalten sind nicht neu, jedoch verschieben sich die Schwerpunkte der Entwicklung aufgrund wesentlich höherer Drehzahlen, höchster Effizienzanforderungen und fehlender Geräuschmaskierung für Antriebssysteme in Hybrid- und reinen Elektrofahrzeugen.

GKN unterstützt die Elektrifizierung des Antriebsstrangs seit vielen Jahren und setzt die anspruchsvollen Kundenanforderungen mit Engineering- und Fertigungsexpertise in Produkte um. Verschiedene Antriebssysteme mit permanent erregten Maschinen (PSM), asynchronen Maschinen (ASM) kombiniert mit Offset-, Layshaft- und Planetengetriebesystemen gehören zum Produktangebot der GKN. Spezielle Anforderungen von elektrifizierten Antriebssträngen, wie sehr hohe Drehzahlen, höchste Effizienz und gutes Geräuschverhalten sowie verkürzte Entwicklungszeiten erfordern eine solide Datenbasis mit entsprechenden Erfahrungen. Ausgehend von der ersten Skizze werden unter anderem lebensdauer-, effizienz- und geräuschrelevante Merkmale innerhalb einer Datenbank erfasst, visualisiert und als weitere Grundlage für die Dimensionierung verwendet. Dieser Leistungsabdruck des Antriebssystems visualisiert die relevanten Basismerkmale und erlaubt eine belastbare Abschätzung der notwendigen Validierung. Ein besonderes Augenmerk wird auf die geräuschspezifischen Merkmale gelegt, sowohl auf der Komponentenebene als auch im System. Anforderung der Fertigung mit entsprechender Robustheit und Kostenvorgaben sind wichtige Bestandteile des etablierten Prozesses. Die Methodik bietet Raum für Innovationen inklusive technologischer Sprünge mit entsprechender Risikobewertung. Elektrische, elektro-magnetische, me-

https://doi.org/10.51202/9783181023549 - Generiert durch IP 216.73.216.36, am 19.01.2026, 02:19:31. © Urheberrechtlich geschützter Inhalt. Ohne gesonderte Erlaubnis ist jede urheberrechtliche Nutzung untersagt, insbesondere die Nutzung des Inhalts im Zusammenhang mit, für oder in KI-Systemen, KI-Modellen oder Generativen Sprachmodellen.

chanische und thermische Merkmale beeinflussen sich gegenseitig und ermöglichen auf der Systemebene eine effektive Kombination. Für die Entwicklung der Komponenten, Teilsysteme und Komplettsysteme werden verschiedene parametrisierbare Softwarelösungen verwendet. GKN-Team untersucht typischerweise eine große Anzahl möglicher Konzepte auf System- und Komponentenebene zur Festlegung der finalen Struktur des Antriebsmoduls.

Die multifaktoriellen Parameteranalysen auf der Komponentenebene und Baugruppenebene, kombiniert mit systematischer Konzeptanalyse von Systemen, erlauben eine Bewertungen anhand des Leistungsabdruckes des Getriebesystems hinsichtlich Lebensdauer, Wirkungsgrad und Geräuschverhalten. Diese Methodik wird mit einigen Beispielen vorgestellt und Erfahrungen bei der Elektrifizierung des Antriebsstrangs hervorgehoben. Ins besonderem für global operierende Teams mit interdisziplinären Aufgabengebieten bietet diese Methodik eine effektive Fokussierung der generischen Aktivitäten und Validierung der bereits laufenden elektrifizierten Antriebssysteme in kürzester Zeit.

Abstract

GKN has been developing and manufacturing electric transmission systems for automotive since more than 15 years. More than 750.000 hybrid and e-drive vehicles with transmissions from GKN are on roads in Europe, Asia and America. The automotive market is in motion and the “state of the art” for the drivetrain is changing. The electrification of the drivetrain is moving on and former niche applications are on the way to be produced with higher quantities. High requirements for reliability, efficiency and NVH aren’t really new but there is a new focus of development for higher speed, higher efficiency and sensitivity to NVH due to missing masking noise in hybrid and e-drive vehicles.

GKN has supported drivetrain electrification since many years and applies the new high sophisticated requirements from OEM’s to GKN products with engineering and manufacturing expertise. Various transmission systems with permanent magnet synchronous machine (PSM) and asynchronous machine (ASM) combined with offset-, layshaft- and epicyclic-layout are on portfolio from GKN. Reliable databases and appropriate experience are required to cope with special needs from electrified transmission systems like very high rotational speed, high efficiency and good NVH combined with shortest development time. GKN team is compiling an internal database with features relevant for fatigue, efficiency and NVH. Intuitive visualization is essential for engineering rating of risk with required validation effort. Manufacturability with required robustness for sensitive features and cost target are important requirements from established process. Achieved results with visualized thresholders

https://doi.org/10.51202/9783181023549 - Generiert durch IP 216.73.216.36, am 19.01.2026, 02:19:31. © Urheberrechtlich geschützter Inhalt. Ohne gesonderte Erlaubnis ist jede urheberrechtliche Nutzung untersagt, insbesondere die Nutzung des Inhalts im Zusammenhang mit, für oder in KI-Systemen, KI-Modellen oder Generativen Sprachmodellen.

are used to fine tune the transmission dimensioning. Applied method enables innovation including technological steps with required verification and validation. Electrical, electromagnetical, mechanical parameters are influencing each other and can be combined in the most effective way on system level. Various software solutions with parametrization capabilities are used to develop components, sub-systems and full transmission systems including software, inverter, e-machine and gearbox. GKN typically assessed a large number of potential concepts on system, sub-system and component level before the final structure selection for particular application.

The multifactorial parameter analysis on component and sub-assembly level, combined with systematic analysis of concept on system level, enables rating of the performance footprint including improvements for fatigue, efficiency and last but not least NVH performance. This methodology will be demonstrated by means of a transmission and experiences in electrification of drivetrain will be highlighted. Applied method offers especially for global operating teams with interdisciplinary work nature an effective focus set of generic work and validation of ongoing electrification for real applications in shortest possible time.

GKN Driveline introduction

GKN Driveline is one of the world's leading automotive systems suppliers. Our vision is to be the number one supplier of driveline systems and solutions by operating our business to the highest standards of quality, integrity and performance. GKN Driveline operates with around 31,700 employees in 23 countries with 58 manufacturing facilities. AWD & e-drive systems contribute around 1/3 to the total sales value. GKN Driveline is recognized at many OEM’s as preferred partner with valuable technology with excellent engineering. GKN Driveline has a long history of delivering hybrid and electric automotive systems. More than 15 e-drive & hybrid series applications since 2002 with about 750.000 transmissions from GKN Driveline are on our roads today. GKN Driveline has a global foot print for R&D and manufacturing. Engineering teams are operating from concept to serial production with global expert network across the globe for knowhow transfer and product launch. Engineering teams from Germany, Italy, USA, Sweden, Japan and China are collaborating within application programs balancing durability, NVH and efficiency requirements for competitive costs in shortest possible time.

https://doi.org/10.51202/9783181023549 - Generiert durch IP 216.73.216.36, am 19.01.2026, 02:19:31. © Urheberrechtlich geschützter Inhalt. Ohne gesonderte Erlaubnis ist jede urheberrechtliche Nutzung untersagt, insbesondere die Nutzung des Inhalts im Zusammenhang mit, für oder in KI-Systemen, KI-Modellen oder Generativen Sprachmodellen.



Fig. 1: More than 15 GKN e-Powertrain applications since 2002

OEM requirements and layout definition

Requirements engineering become very important especially when the development time is shortened. Alignment with the OEM is essential in order to set up requirements for safety, interface, weight, efficiency, NVH and a clear breakdown from vehicle level to the driveline system with software, inverter, e-machine and gearbox. From sketch onwards clear communication and multi-disciplinary teams are required in order to drive programs successfully to mass production. Multiple transmission systems are available to accommodate relevant packaging requirements. GKN has developed building blocks including structures with and without disconnect functionality for electric and hybrid applications. GKN Driveline as system supplier is currently developing several e-drive & hybrid applications with different gear trains and integration level.

Most transmissions in e-drive are operating at very high speed. Selected mechanical structure of the gear train with or without disconnect needs to be aligned with appropriate e-motor technology in combination with inverter functionality. Various e-motor types could be used in the coaxial and offset transmission arrangement. Potential e-motor types are typically rated in terms of power density, inverter requirements, manufacturing costs, NVH and systemic losses in typical operational conditions. Fig. 2 shows two types of e-motor for driveline electrification with exemplary rating of main performance. The rating of listed performance features has an application specific nature and is based on GKN e-drive & hybrid experiences.

https://doi.org/10.51202/9783181023549 - Generiert durch IP 216.73.216.36, am 19.01.2026, 02:19:31. © Urheberrechtlich geschützter Inhalt. Ohne gesonderte Erlaubnis ist jede urheberrechtliche Nutzung untersagt, insbesondere die Nutzung des Inhalts im Zusammenhang mit, für oder in KI-Systemen, KI-Modellen oder Generativen Sprachmodellen.

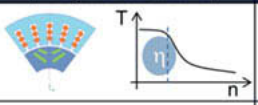
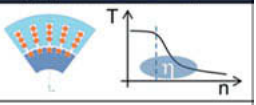
Transmission e-motor type for hybrid application Shown rating is based on GKN e-drive & hybrid experience. These features do have application **specific nature**.	**PSM** (PM-Synchronous Machine) 	**ASM** (Asynchronous Machine) 
Packaging and power density	+++	+
Efficiency performance **including** system losses across driving cycle	+++ / ++ (T↑ & n↓ / T↓ & n↑)	++ / ++ (T↑ & n↓ / T↓ & n↑)
Manufacturing, robustness & costs	++	+++
Failsafe without inverter (Back-EMF)	-	+++
NVH performance	+++	++

Fig. 2: Rating for typical types of e-machine e-drives & hybrids for one e-drive application

Low passive drag losses (e-machine & gearbox) at high speed, robust structure and competitive system costs may dominate the decision process. Various potential options for the structure of transmission system are evaluated in early program phase with OEM during the RFI-phase. Typical transmission structures are based on offset design, layshaft design or epicyclic design. Definition of the transmission structures is typically conducted on concept level considering various bearing arrangements, ratio split, packaging specification and integration level. Each structure has an impact related to possible packaging, weight, NVH, efficiency, durability, simplicity & costs. Finally, good balance for desired performance features is essential for a product with high quality with expected system robustness.

Especially packaging restriction and high power density with optimization flexibility are driving the final structure decision in the particular application. Various bearings and gears arrangements are analysed with synthesis approach with alignment to GKN internal experiences and external data from the market. Commercially available software tools and GKN-internal know-how is applied to support OEM for structure selection. Consistency in applying methods for solutions finding and good visualization from concept onwards with a clear link to experiences is essential for an effective development process. Fig. 3 shows examples of typical gear train structures in e-drive & hybrid applications.

https://doi.org/10.51202/9783181023549 - Generiert durch IP 216.73.216.36, am 19.01.2026, 02:19:31. © Urheberrechtlich geschützter Inhalt. Ohne gesonderte Erlaubnis ist jede urheberrechtliche Nutzung untersagt, insbesondere die Nutzung des Inhalts im Zusammenhang mit, für oder in KI-Systemen, KI-Modellen oder Generativen Sprachmodellen.

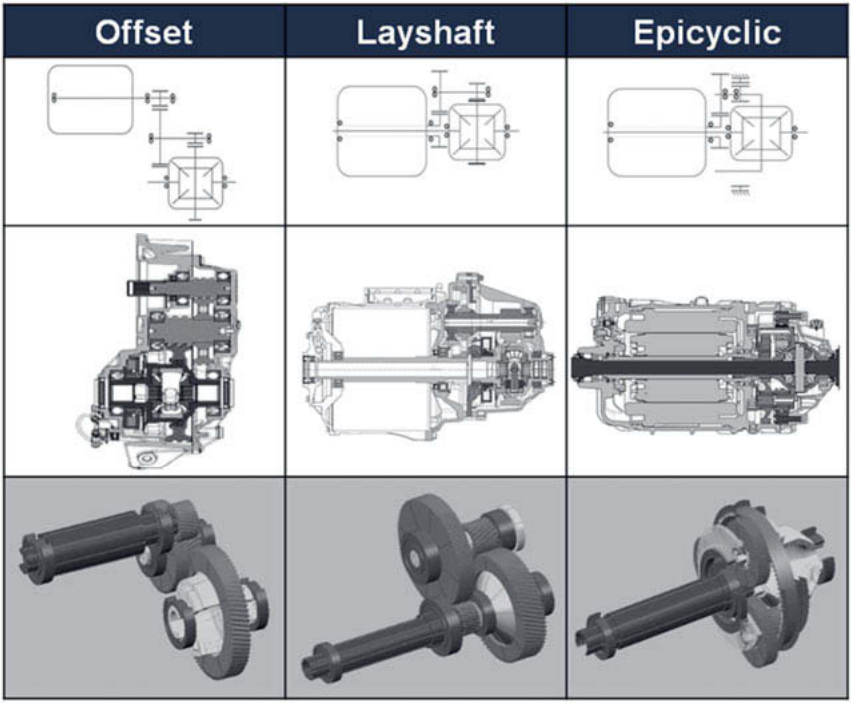


Fig. 3: Typical types of integration and mechanical structure in e-drives & hybrids

The outcome from above mentioned structure finding is typically a favourite structure on macro level with an overview of expected basic performance related to the specification. The most promising transmission structure with minimal complexity and best match with requirements will be prepared for further analysis in regards to efficiency, NVH and durability. GKN internal data from existing serial production transmissions is used to align the expected performance from selective structure with existing footprint for comparison. Performance data from GKN internal and competitive e-drive applications are collected within a benchmarking data cloud. This data cloud contains e-motor data, geometrical values from gear train, transmission bearings and shafts as well fatigue performance, efficiency and NVH-related performance. Visualization within a cloud of experienced performance out of mass production transmissions helps to derive appropriate effort of verification and validation. Fig. 4 shows generic example of typical visualization of performance features.

https://doi.org/10.51202/9783181023549 - Generiert durch IP 216.73.216.36, am 19.01.2026, 02:19:31. © Urheberrechtlich geschützter Inhalt. Ohne gesonderte Erlaubnis ist jede urheberrechtliche Nutzung untersagt, insbesondere die Nutzung des Inhalts im Zusammenhang mit, für oder in KI-Systemen, KI-Modellen oder Generativen Sprachmodellen.

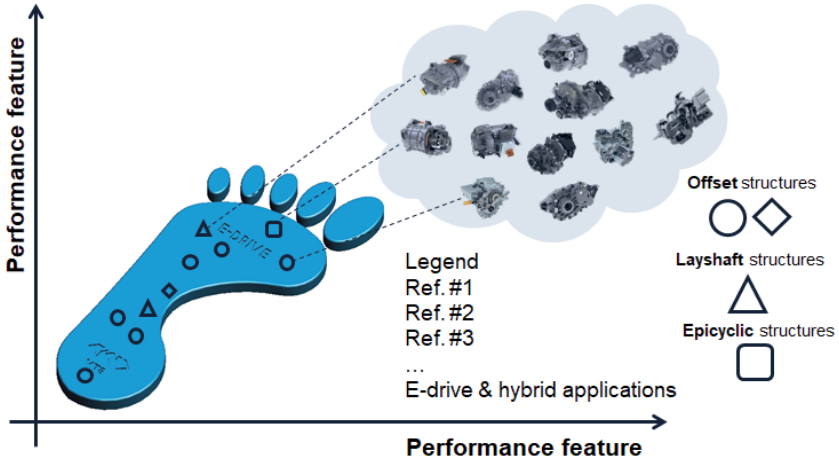


Fig. 4: Benchmarking of relevant performance features as a footprint

Standardized performance template with synchronized boundary conditions for feature evaluation is used across the global virtual transmission engineering team. Performance data of particular transmission system within the cloud of data based on experiences, allows the confirmation for state-of-the-art or an innovation zone. This type of performance overview helps to focus the engineering work from first sketch onwards step-by-step to the design freeze, followed by verification and validation of the transmission system.

Balancing the basic features from sketch onwards

Typically OEM is deeply involved into the layout finding concept, since the concept decision is primary driven by packaging and level of desired integration of e-machine and the gear train. Compatibility with available packaging, modularity and last but not least application related durability, efficiency and NVH features are used for the final concept decision. Most rated performance features do have an application specific nature. Experiences with the variety of different structures and different level of integration are essential for systematic and effective layout selection process. Figure 5 depicts one example of a comparison of three different layout structures for one exemplary e-drive application.

https://doi.org/10.51202/9783181023549 - Generiert durch IP 216.73.216.36, am 19.01.2026, 02:19:31. © Urheberrechtlich geschützter Inhalt. Ohne gesonderte Erlaubnis ist jede urheberrechtliche Nutzung untersagt, insbesondere die Nutzung des Inhalts im Zusammenhang mit, für oder in KI-Systemen, KI-Modellen oder Generativen Sprachmodellen.

Transmission e-motor type for hybrid application Shown rating is based on GKN e-drive & hybrid experience. These features do have application specific nature.	Offset (three independent shafts)	Layshaft (two shafts on one centre of distance)	Epicyclic (power split torque flow)
			
Flexibility and simplicity	+++	++	+
Integration capabilities	+	++	+++
Durability capabilities	++	+	+++
Efficiency / drag torque	+++ / +++	+++ / ++	+++ / +
NVH	++	++	+++

Fig. 5: Example of concept comparison for one e-drive application

During the selection process, each of above shown rating may become the “decision maker”. Finally, further important features like weight, development time and costs need to be taken into account for the particular application decision. Having chosen the favourite layout and structure, further deeper definition of the system is required in order to conduct parametric transmission optimization. More detailed models are used for further analysis including optimization of stress and fatigue of gears, bearings and housings using specified load cycles. Special transmission software and conventional commercial CAE tools are used for development and optimization. Transmission definition method is aligned with best practise failure mode driven analysis. Relevant failure modes such as shaft bending, gears contact and bending, housing fatigue, differential sub-system and bearing performance have been taken into account for dimensioning of the components.

Variation of geometries, followed by optimization, is collected for each application for final selection into a benchmarking data base. The relevant geometry and performance features are stored in a database. This data cloud is growing and enabling the GKN Driveline team to form a transmission system “right first time” with a very high confidence level. Alignment of the achieved transmission performance with GKN internal & external benchmark data is essential in order to derive appropriate validation. Gear macro geometry optimization is typically assessed by systematic modifying of module, pressure angle, helix angle, profile shift and centre of distance. Often the ideal solution for one of performances can result in unexpected deterioration of others. An example of results from multi-parametrical search of macro geometry is shown in Fig. 6.

https://doi.org/10.51202/9783181023549 - Generiert durch IP 216.73.216.36, am 19.01.2026, 02:19:31. © Urheberrechtlich geschützter Inhalt. Ohne gesonderte Erlaubnis ist jede urheberrechtliche Nutzung untersagt, insbesondere die Nutzung des Inhalts im Zusammenhang mit, für oder in KI-Systemen, KI-Modellen oder Generativen Sprachmodellen.

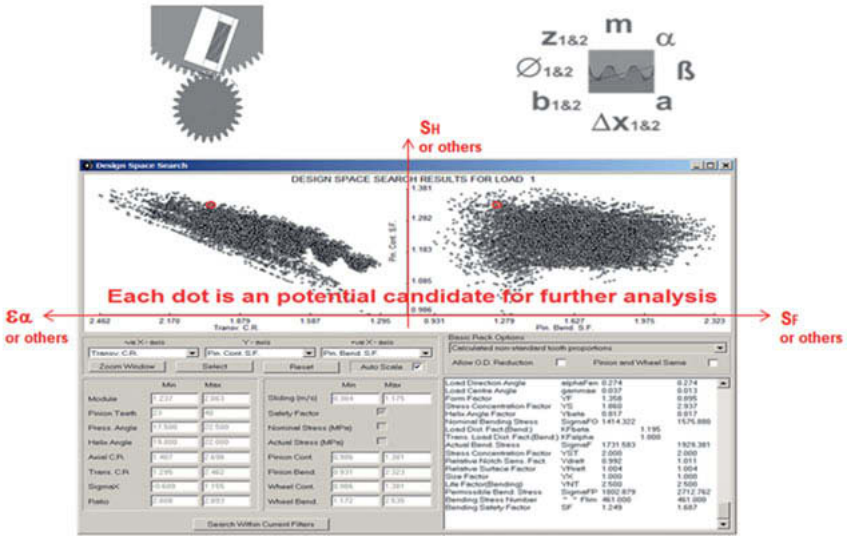


Fig. 6: Example of multi-parametrical search result for macro geometry

Consistency in applied methodology and intuitive visualization of results is very useful to select the best possible balance. The micro parametric search includes profile and helix angle incl. bias, profile and lead crowning, tip relief and others. The result is a cloud of candidates. Due to the systematically tuning of relevant gear geometries, consistent design improvement can be achieved for good balance of durability, efficiency and NVH. Chosen candidate should have sufficient margin for further tuning of relevant parameters for durability, efficiency and last but not least for NVH. High contact transverse contact ratios are typically good for NVH but may lead to higher sliding losses and destroy fatigue performance. Very tight packaging with low weight specification leads to limitation of the gear face width and installed bearing layout may limit the excessive enlarging of the helix angle for high helical contact ratio. Systematically search for best possible balance is essential for robust gear set option. Figure 7 shows typical optimization approach of transverse contact ratio versus helical overlap ratio.

https://doi.org/10.51202/9783181023549 - Generiert durch IP 216.73.216.36, am 19.01.2026, 02:19:31. © Urheberrechtlich geschützter Inhalt. Ohne gesonderte Erlaubnis ist jede urheberrechtliche Nutzung untersagt, insbesondere die Nutzung des Inhalts im Zusammenhang mit, für oder in KI-Systemen, KI-Modellen oder Generativen Sprachmodellen.

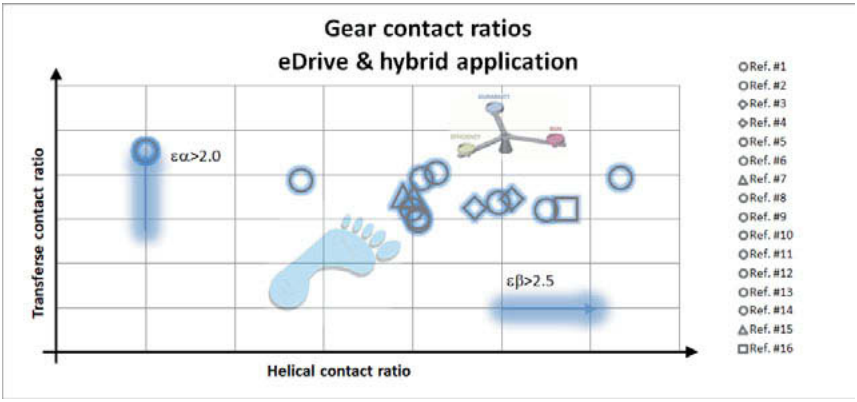


Fig. 7: Example of geometrical gear contact e-drive & hybrid applications

Based on chosen set of candidates further analysis is followed before the design freeze. High contact ratio gears with optimized sliding velocities are required for good NVH-performance. Good balanced contact ratio along the profile and across the lead is an enabler for further micro geometry optimization. An example of results from multi-parametrical search of micro geometry is shown in Fig. 8.

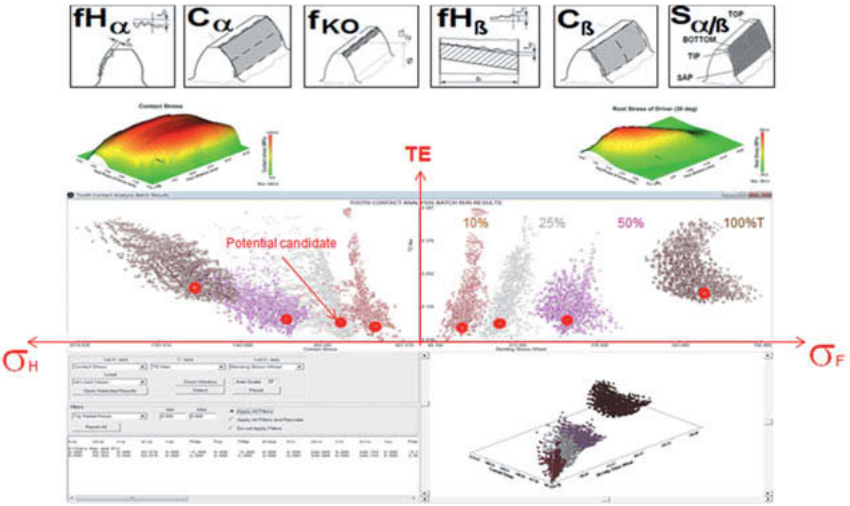


Fig. 8: Example of multi-parametrical search result for micro geometry

https://doi.org/10.51202/9783181023549 - Generiert durch IP 216.73.216.36, am 19.01.2026, 02:19:31. © Urheberrechtlich geschützter Inhalt. Ohne gesonderte Erlaubnis ist jede urheberrechtliche Nutzung untersagt, insbesondere die Nutzung des Inhalts im Zusammenhang mit, für oder in KI-Systemen, KI-Modellen oder Generativen Sprachmodellen.

Each candidate can be used for further evaluation including sensitivity improvements of the running gears. Results of micro geometry search are typically used for further analysis and specification of applicable tolerances to the main trade-off for contact stress and transmission error. The applied multifactorial sensitivity study, especially at component level, enables further rating improvements and optimization of product robustness especially in terms of durability and excitation level as transmission error.

Durability foot print

Balancing of durability versus efficiency & NVH is mandatory for the transmission engineering from sketch to the final product. Knowledge of expected load profile is essential for dimensioning of the gear train including gears, shafts, bearings, oil, housing and other components. Due to high loads in both directions (drive & coast) alternating material performance has to be considered for sizing of transmission system. Nearly the same torque level in drive and coast is present in e-drive & hybrid applications. Figure 9 shows an example of drive & coast torque requirements from some e-drive and hybrid applications.

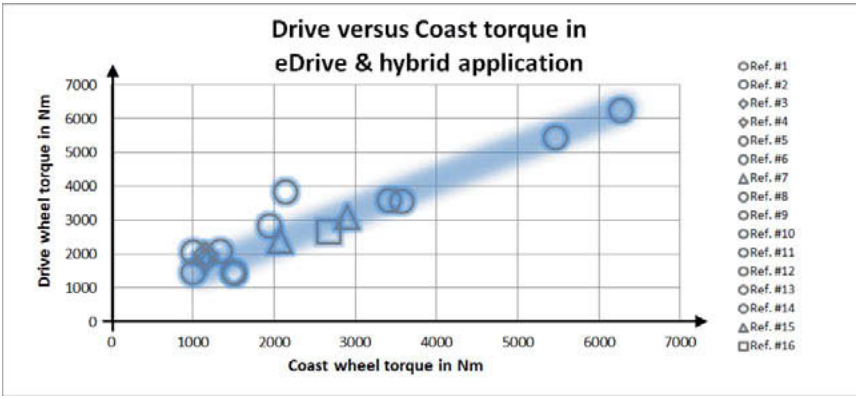


Fig. 9: Example of torque requirements in drive & coast condition

Typical ratios in today's e-drive & hybrid application are in the range of 8 to 12. The most applications are operating at very high speed. Maximal e-Motor speed in these applications is up to 18000rpm. In advanced pilot transmission projects is the input speed already above 25000rpm and higher transmission ratios are applied. Some typical speed versus torque specifications from today's applications are visualized in Figure 10.

https://doi.org/10.51202/9783181023549 - Generiert durch IP 216.73.216.36, am 19.01.2026, 02:19:31. © Urheberrechtlich geschützter Inhalt. Ohne gesonderte Erlaubnis ist jede urheberrechtliche Nutzung untersagt, insbesondere die Nutzung des Inhalts im Zusammenhang mit, für oder in KI-Systemen, KI-Modellen oder Generativen Sprachmodellen.

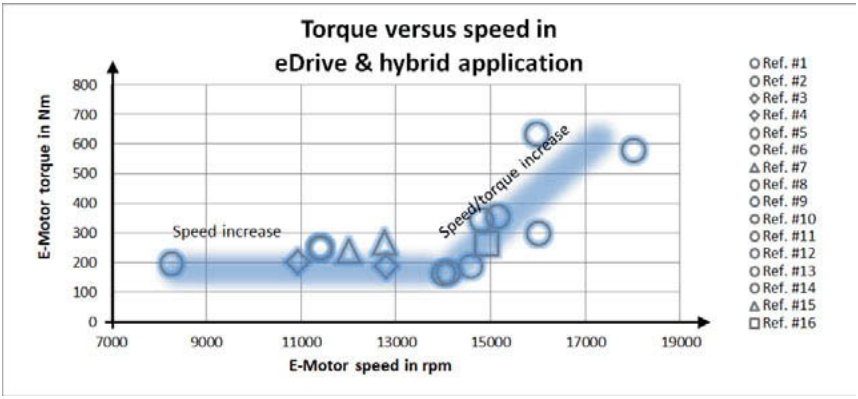


Fig. 10: Example of torque versus speed in e-drive & hybrid applications

Very high speed and high efficiency requirements with necessity of high contact ratios lead to down-sizing of gear components. Gear modules below 1,5mm are becoming state-of-the art in automotive transmissions. Figure 11 depicts the relation of torque versus gear module e-drive & hybrid applications.

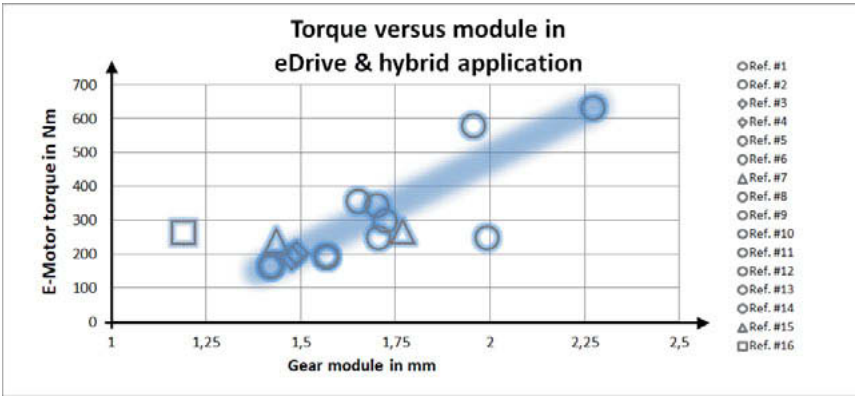


Fig. 11: Example of torque versus gear module in e-drive & hybrid applications

Especially in epicyclic applications the centre of distance and the outer diameter of the gear train can be reduced significantly. One example for such an epicyclic application with stepped planets was published during the 10th E-Motive conference in 2018 [1].

https://doi.org/10.51202/9783181023549 - Generiert durch IP 216.73.216.36, am 19.01.2026, 02:19:31. © Urheberrechtlich geschützter Inhalt. Ohne gesonderte Erlaubnis ist jede urheberrechtliche Nutzung untersagt, insbesondere die Nutzung des Inhalts im Zusammenhang mit, für oder in KI-Systemen, KI-Modellen oder Generativen Sprachmodellen.

Interdisciplinary teams are working simultaneously from sketch onwards to setup tooth count in gear train, number of magnets in e-machine and other rotation components with the task to reduce and separate excitation orders. Conflicting targets are typically visualized and balanced in in early program phase. High level of analysis is followed by high level manufacturing utilizing supplier expertise from first functional prototype. GKN Driveline engineers create gear concepts, analyse, optimize and manufacture helical gears in-house. Gear design and manufacturing tool development are aligned within the virtual transmission engineering (VTE) and manufacturing engineering (ME). Helical gear hobbing, heat treatment and gear finishing are balanced for best possible robustness. Helical gears analysis, specification on drawings and inspection in production are formed with highest possible commonalities in order to avoid possible misinterpretation of specified gear data. Typically gears quality 5 and better is required to cope with high NVH requirements with good fatigue performance. Figure 12 shows some capabilities which are used for manufacturing of high quality gears within GKN Driveline.

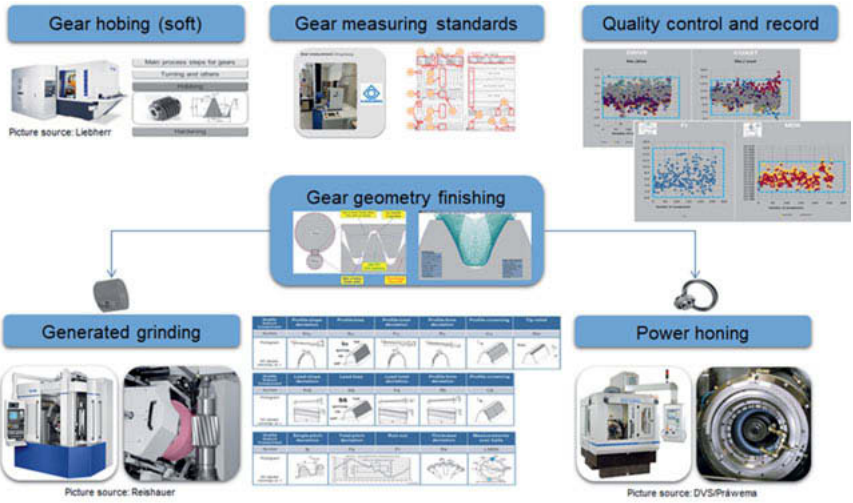


Fig. 12: Manufacturing and inspection capabilities

Efficiency foot print

Transmissions in e-drive & hybrids are required to operate at very high speed, remaining lightweight with low power loss performance in drive & coast modes. Efficiency analysis is conducted typically on system level with constant and variable conditions.

https://doi.org/10.51202/9783181023549 - Generiert durch IP 216.73.216.36, am 19.01.2026, 02:19:31. © Urheberrechtlich geschützter Inhalt. Ohne gesonderte Erlaubnis ist jede urheberrechtliche Nutzung untersagt, insbesondere die Nutzung des Inhalts im Zusammenhang mit, für oder in KI-Systemen, KI-Modellen oder Generativen Sprachmodellen.

Worldwide Harmonized Light Vehicles Test Cycle (WLTC) is used for instationary condition and maximal speed & torque performance is applied for full efficiency evaluation. Both conditions, constant and variable, are analysed virtually and experimentally. Figure 13 depicts a typical speed/torque profiles from e-Drive & hybrid applications during constant conditions for efficiency evaluation and variable WLTC.

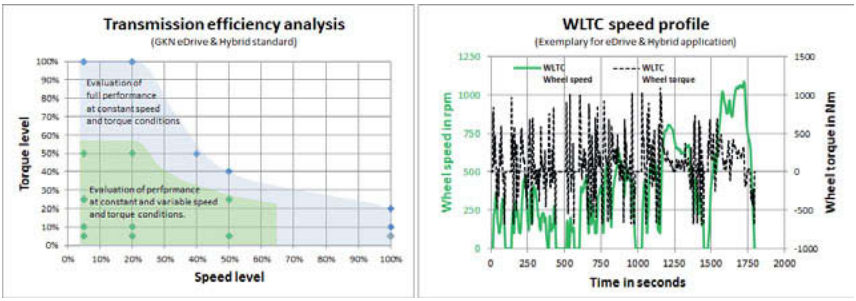
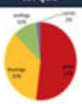
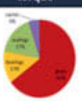


Fig. 13: Speed and torque profile from constant condition for efficiency evaluation and WLTC

Evaluation of losses across the whole transmission system is important in order to select the right technology and focus optimization effort for loss reduction. Transmission efficiency analysis includes losses through core hysteresis, active cooling, gear mesh sliding, churning, ventilation, bearings and losses in sealing devices. Component contribution at various operational conditions is evaluated in the very early program phase. Know-how in system and component level is important, in order not to underestimate e.g. rotor ventilation losses with over 1kW in some applications or sealing losses with over 45m/s sliding velocity on the e-motor shaft. Below Figure 14 shows exemplary efficiency at three different driving conditions with particular component contribution from one epicyclic transmission system.

Exemplary driving condition	Low speed & high torque	Moderate speed & torque	High speed & low torque
Component contribution to the total losses (here mechanical gearbox only as example)			
Input power	26.5kW	57.6kW	11.5kW
Input speed	1000rpm	5000rpm	10000rpm
Input torque	253Nm	110Nm	11Nm
Efficiency	> 97.2%	> 97.0%	> 80.7%

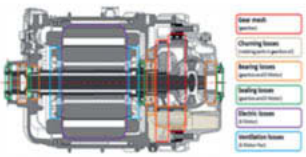


Fig. 14: Efficiency example of e-drive & hybrid application

https://doi.org/10.51202/9783181023549 - Generiert durch IP 216.73.216.36, am 19.01.2026, 02:19:31. © Urheberrechtlich geschützter Inhalt. Ohne gesonderte Erlaubnis ist jede urheberrechtliche Nutzung untersagt, insbesondere die Nutzung des Inhalts im Zusammenhang mit, für oder in KI-Systemen, KI-Modellen oder Generativen Sprachmodellen.

Furthermore, above data of power losses is used as input for a thermal analysis of the transmission structure. Due to very high speed conditions the thermal management is very demanding. Typically, the gearbox lubrication and cooling is achieved without an additional oil pump by using splash lubrication in combination with clever oil guidance and reservoir. Various software tools for loss calculation combined with Matlab scrips and aligned with smoothed particle hydrodynamics (SPH) analysis of oil flow, are used for thermal performance analysis. The task is to minimize splash losses and enable sufficient lubrication with heat transfer through the transmission system. Low viscosity oil with high thermal resistance is typically selected considering thermal degradation, oxidation and additive stability [2]. Critical components, e.g. e-motor bearings, sealing devices and lubricant are specified based on verified temperatures prediction.

NVH foot print

Good NVH balance starts with identification of order tracks and separation of mesh orders on system level considering inverter switching frequencies, e-motor orders from radial forces and torque ripple and last but not least the gear mesh orders. The high speed with low friction requires several specific optimization loops to achieve the demanding acoustic vehicle targets. Lack of background noise is highlighting any acoustic phenomena to a sensitive feature. Close collaboration between vehicle engineering and transmission engineering is very important in order to achieve representative NVH-control at End-Of-Line check (EOL) on system level. Figure 15 shows an overview of major engineering work for NVH verification of stricture-borne-noise (SBN) followed by air-borne-noise (ABN).

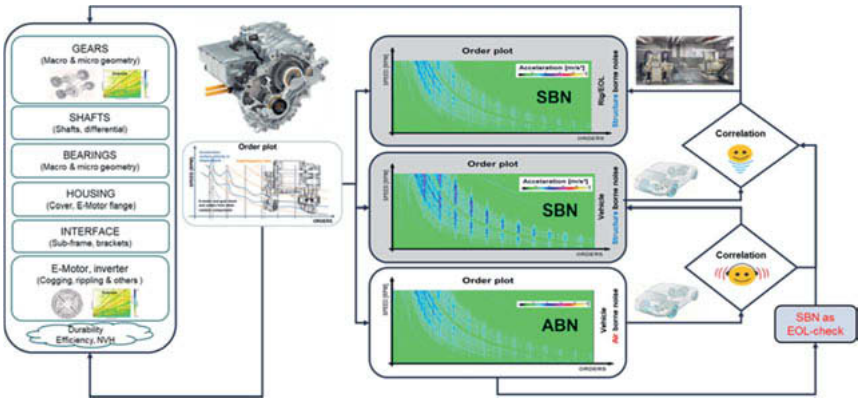


Fig. 15: NVH engineering with basic verification

https://doi.org/10.51202/9783181023549 - Generiert durch IP 216.73.216.36, am 19.01.2026, 02:19:31. © Urheberrechtlich geschützter Inhalt. Ohne gesonderte Erlaubnis ist jede urheberrechtliche Nutzung untersagt, insbesondere die Nutzung des Inhalts im Zusammenhang mit, für oder in KI-Systemen, KI-Modellen oder Generativen Sprachmodellen.

Based on results from shown way of working in Figure 15 a EOL-test procedure can be defined. Significant orders, in the most cases e-motor and main gear mesh orders are captured as an NVH-pattern for each transmission system as 100% EOL-check. Figure 16 shows an example of one order track and an EOL-trace for performance check.

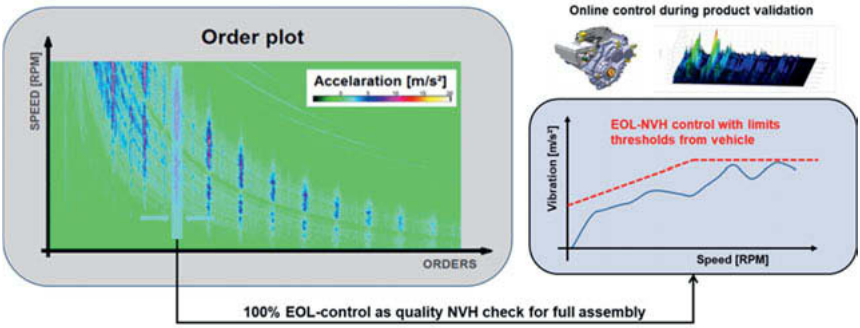


Fig. 16: Development of EOL-NVH control

For evaluation and optimization of the structure borne noise RomaxDesigner or Masta software and other conventional commercial software packages are used. NVH analysis with identification of eigenmodes, modal shape analysis, extended with summary of contribution from components is used for optimization. System response from excitation through various sources, e.g. e-machine ripple or gear mesh, is analysed on different transmission locations. Typically, several representative sensors are placed near to the bearings or annulus gear and on interface-brackets to the vehicle subframe. The response on these locations is analysed in terms of acceleration, velocity or vibrational amplitude. Results of energy contribution from components help to focus modifications for improvement and fine tuning of the structure borne noise characteristic. This approach enables systematically tuning of the system with modifications with highest impact for structure-borne-noise (SBN) and for air-borne-noise (ABN) respectively. Achieved virtual performance followed by experimental verification is the best practice for the development of acceptance criteria for the end-of-line (EOL) check. This approach enables a reliable alignment of structure borne measurements during the EOL with the expected NVH-performance in vehicle. Mesh tracking with particular orders and vibration level control at EOL (100% check) is the very last proof of system integrity related to NVH. Other test features, e.g. drag torque performance, can be measured on EOL-tester simultaneously to NVH.

https://doi.org/10.51202/9783181023549 - Generiert durch IP 216.73.216.36, am 19.01.2026, 02:19:31. © Urheberrechtlich geschützter Inhalt. Ohne gesonderte Erlaubnis ist jede urheberrechtliche Nutzung untersagt, insbesondere die Nutzung des Inhalts im Zusammenhang mit, für oder in KI-Systemen, KI-Modellen oder Generativen Sprachmodellen.

Summary and conclusions

Due to strategic early involvement since more than 15 years, GKN Driveline has a long history with specific experience in development and production of electrified transmission systems. This paper outlines a footprint of expertise and experience of GKN Driveline in terms of fatigue, efficiency and NVH in e-drive & hybrid applications. Success-run method combined with dedicated tests for subsystems and components are used for statistical probability evaluation of durability commitments. System efficiency evaluation is combined with experimental verification of thermal behaviour. Last but not least, transmission NVH-verification is conducted as 100% EOL-check.



Fig. 17: Footprint for durability, efficiency and NVH for e-drive & hybrid applications

A system approach shows the most effective way for best possible balance for durability, NVH and efficiency. Manufacturing process validation for several new e-drive and hybrids application is on-going in Europe & China. Standardization of existing products including commodity task of main sub-systems will enhance engineering flexibility and will reduce transmission system costs. We will continue our collaborative way of working within our global engineering community and our suppliers developing products beyond the conventional standards. Consistent engineering and manufacturing experience with automotive transmissions is enabling us to develop best in class components, sub-systems and full driveline systems, especially for electrical and hybrid vehicles.

https://doi.org/10.51202/9783181023549 - Generiert durch IP 216.73.216.36, am 19.01.2026, 02:19:31. © Urheberrechtlich geschützter Inhalt. Ohne gesonderte Erlaubnis ist jede urheberrechtliche Nutzung untersagt, insbesondere die Nutzung des Inhalts im Zusammenhang mit, für oder in KI-Systemen, KI-Modellen oder Generativen Sprachmodellen.

[1] From sketch to production, 10th E-Motive 2018, International conference on electric vehicle drives and e-mobility in Stuttgart, GKN Driveline, Dr. A. Grunwald

[2] Semi-Integrated ASM-Planetary Coaxial Electric Drive Module, 28th Aachener Colloquium 2018, Fahrzeug- und Motorentechnik, GKN Driveline, A. Schmeink

https://doi.org/10.51202/9783181023549 - Generiert durch IP 216.73.216.36, am 19.01.2026, 02:19:31. © Urheberrechtlich geschützter Inhalt. Ohne gesonderte Erlaubnis ist jede urheberrechtliche Nutzung untersagt, insbesondere die Nutzung des Inhalts im Zusammenhang mit, für oder in KI-Systemen, KI-Modellen oder Generativen Sprachmodellen.

Development of a New Next-generation CVT for Small Cars

Shuji Kurokawa, **Mikiko Kunihisa**, JATCO Ltd, Atsugi, Japan;
Yoshihiro Oyama, Nissan Motor Co., Ltd, Atsugi, Japan

Abstract

There are strong customer demands for minivehicles in Japan because of their excellent environmental performance and economy, while being based on unique specifications. In response to such demands, a new CVT was developed and put into production specifically for 100-Nm-class minivehicles. This paper describes this new next-generation CVT that is smaller, lighter and more economical as a result of utilizing key technologies accumulated through previous CVT development activities and further evolving the technologies for matching with the engine. This new CVT contributes to the improvement of class-leading vehicle fuel economy, quietness and driveability.

1. Introduction

Representing a key product category in Japan, mini-vehicles are required to provide high levels of environmental performance and economy while being based on unique specifications. A continuously variable transmission (CVT) newly developed by JATCO specifically for mini-vehicles has been adopted on a new mini-vehicle model developed by Nissan Motor Company. This paper outlines the new CVT and describes the technologies it incorporates.

2. Mini-vehicle market in Japan

2.1 Mini-vehicle specifications

Mini-vehicles are based on specifications original to Japan that were enforced in 1949 (Fig. 1).

https://doi.org/10.51202/9783181023549 - Generiert durch IP 216.73.216.36, am 19.01.2026, 02:19:31. © Urheberrechtlich geschützter Inhalt. Ohne gesonderte Erlaubnis ist jede urheberrechtliche Nutzung untersagt, insbesondere die Nutzung des Inhalts im Zusammenhang mit, für oder in KI-Systemen, KI-Modellen oder Generativen Sprachmodellen.

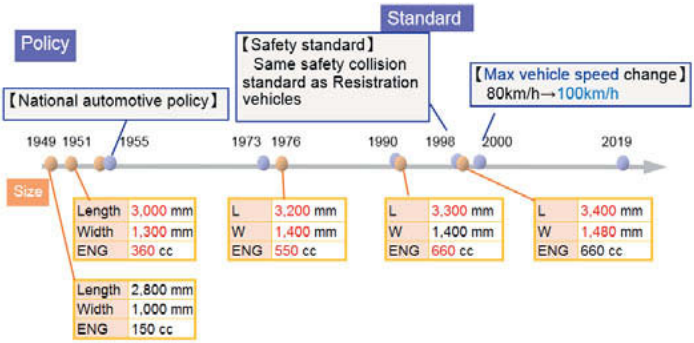


Fig. 1: Changes in mini-vehicle specifications

With a vehicle size suitable to Japan's road conditions, they play a vital role as a means of transportation in everyday life in areas where public transportation infrastructure is scarce. Compared with compact car specifications worldwide, mini-vehicle specifications are special in that they limit engine displacement to 660 cc and also the vehicle size to very small dimensions (Fig. 2).

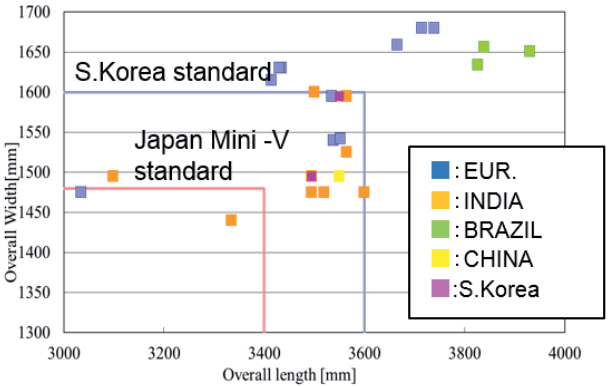


Fig. 2: Comparison with global compact car standards

In order to enhance interior comfort and safety within these small vehicle specifications, it is necessary to make the engine compartment smaller and to lower the mounting position of the powertrain. In this vehicle category, economy is especially emphasized.

https://doi.org/10.51202/9783181023549 - Generiert durch IP 216.73.216.36, am 19.01.2026, 02:19:31. © Urheberrechtlich geschützter Inhalt. Ohne gesonderte Erlaubnis ist jede urheberrechtliche Nutzung untersagt, insbesondere die Nutzung des Inhalts im Zusammenhang mit, für oder in KI-Systemen, KI-Modellen oder Generativen Sprachmodellen.

2.2 Market size

As shown in Fig. 3, mini-vehicles consistently account for approximately 35-40% of new car sales in Japan, making them key products that help to support the Japanese automotive industry. Mini-vehicles are not expected to undergo rapid electrification. It is projected that fuel economy will continue to be improved by further enhancing the overall efficiency of the powertrain built around an internal combustion engine (Fig. 4).

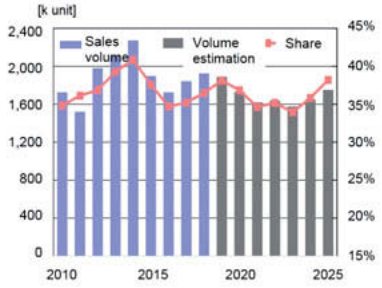


Fig. 3: Mini-vehicle market trends

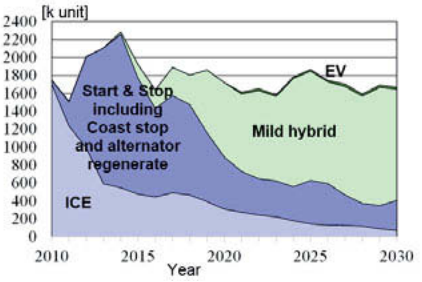


Fig. 4: Trends in mini-vehicle powertrain technologies

3. Development concept of CVT designed for mini-vehicles

In line with the future forecast for mini-vehicles, the new CVT was planned to be smaller and lighter than the CVT (JF015E) that JATCO currently supplies for use on small cars and mini-vehicles. That would enable the new CVT to fit in the engine compartment layout so as to ensure interior comfort and safety.

Based on the CVT technologies[1-3] accumulated to date, the new CVT designed specifically for mini-vehicles provides fuel economy and power performance matching the vehicle specifications and is also compatible with micro-hybridization.

3.1 Ratio coverage and through low ratio determined by vehicle specifications

Previously, efforts to secure launch performance in reverse gear had the effect of lowering the through low gear ratio in forward gears more than necessary owing to the relationship with the gear ratios of the planetary gear set in the forward/reverse switchover mechanism. That made it difficult to ensure compatibility with the desired fuel economy.

https://doi.org/10.51202/9783181023549 - Generiert durch IP 216.73.216.36, am 19.01.2026, 02:19:31. © Urheberrechtlich geschützter Inhalt. Ohne gesonderte Erlaubnis ist jede urheberrechtliche Nutzung untersagt, insbesondere die Nutzung des Inhalts im Zusammenhang mit, für oder in KI-Systemen, KI-Modellen oder Generativen Sprachmodellen.

Therefore, the planetary gear set of the forward/reverse changeover mechanism was optimized so that the forward/reverse gear ratios of the new CVT would be nearly the same. Together with the optimized ratio coverage explained below, the aim was to obtain both the desired launch performance and fuel economy.

Figure 5 shows the rate of improvement in fuel economy under Japan's JC08 emissions test mode as a function of the ratio coverage. Expanding the ratio coverage of the variator from 4.0 to 6.0 has a proportional effect on improving fuel economy. However, above 6.0 the effect of expanding the ratio coverage diminishes. Therefore, the ratio coverage of the new CVT was set at 6.0.

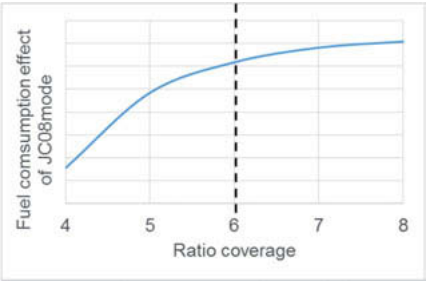


Fig. 5: Fuel economy improvement as a function of ratio coverage
Effect on fuel economy under JC08 mode

3.2 Package restrictions

Within an overall vehicle length limitation of 3400 mm, it is essential to shorten the longitudinal length of the engine compartment in order to secure larger interior space. That requires a reduction in the longitudinal length of the transmission in order to optimize the arrangement of each shaft and the operating system layout.

3.3 Selection of skeleton and specifications

The specifications were determined based on the foregoing requirements for the new CVT, and the constituent elements and their combinations were subjected to a decision analysis. As a result, the same skeleton as that of the company's midsize CVT was selected. In addition, the arrangement of each shaft was optimized and the length of the new CVT in the vehicle's longitudinal direction from the engine center was shortened by approximately 7 mm from the current JF015E. Table 1 compares the basic specifications of the JF015E and the new CVT, and Fig. 6 is a main cross-sectional view of the new unit.

https://doi.org/10.51202/9783181023549 - Generiert durch IP 216.73.216.36, am 19.01.2026, 02:19:31. © Urheberrechtlich geschützter Inhalt. Ohne gesonderte Erlaubnis ist jede urheberrechtliche Nutzung untersagt, insbesondere die Nutzung des Inhalts im Zusammenhang mit, für oder in KI-Systemen, KI-Modellen oder Generativen Sprachmodellen.

Table 1: Specifications

Item			JF015E (Current small CVT)	New CVT
Torque capacity			98 Nm	100 Nm
Control system			Electronic	←
Torque converter size			185 mm dia.	←
Gear ratio	Ratio coverage		7.3	6.0
	Pully ratio		2.200 - 0.550	2.411 - 0.404
	Final gear ratio		3.757	6.54 - 7.756
	Planetary gear ratios	1st	1.821	1.000
		2nd	1.000	
		Rev	1.714	0.952
Through low ratio			15.04	15.770
Weight (wet)			65.0	60.8
Overall length (mm)			346	356
Distance between Pulley shafts			147 mm	←

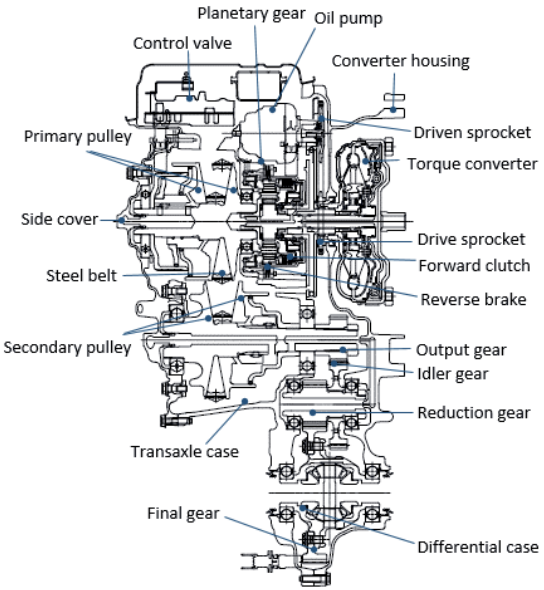


Fig. 6 Main cross-sectional view of new CVT

https://doi.org/10.51202/9783181023549 - Generiert durch IP 216.73.216.36, am 19.01.2026, 02:19:31. © Urheberrechtlich geschützter Inhalt. Ohne gesonderte Erlaubnis ist jede urheberrechtliche Nutzung untersagt, insbesondere die Nutzung des Inhalts im Zusammenhang mit, für oder in KI-Systemen, KI-Modellen oder Generativen Sprachmodellen.

4. Key technologies

4.1 Forward/reverse changeover mechanism

A double-pinion planetary gear set with a four-pinion specification was adopted to cancel excitation forces in the rotational, axial, radial and tilt directions in order to reduce reverse gear noise and also to make the forward/reverse gear ratios as close to 1.000 as possible so as to ensure fuel economy and power performance as mentioned above. In order to reduce the diameter of the clutch system of the forward/reverse switchover mechanism, the sun gear was integrated with the input shaft and its outer diameter was reduced and the reverse brake was attached to the outer diameter of the drum (Figs. 7 & 8).

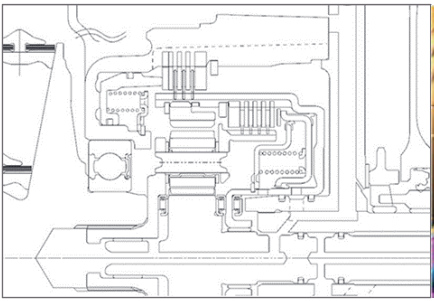


Fig. 7: Cross-sectional view of forward-reverse changeover mechanism

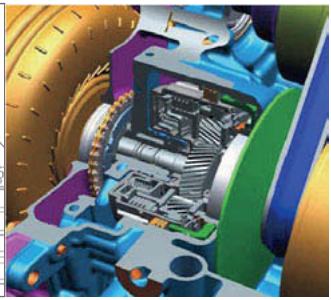


Fig. 8: 3D view of forward-reverse changeover mechanism

4.2 Variator configuration

The center distance between the pulley shafts was set at 147 mm, the same as that of the JF015E, so as to facilitate mixed production of both units on the same line. The shaft diameter of the fixed pulley half was reduced and the pulley outer diameter was also increased in order to expand the ratio coverage from 4.0 to 6.0. The primary pulley has a tandem structure to secure the desired pressure-receiving area while reducing inertia. To ensure the strength of the smaller shaft of the fixed pulley half, the method of supporting the roller bearing of the sliding pulley half was revised. The function of securing the roller bearing by means of a snap ring was transferred to the sliding pulley half.

The parking gear was installed on the secondary fixed pulley half because of the narrow layout toward the vehicle front and also to reduce the operating force. The tooth bottom was discontinued to reduce the weight. In addition, a Tosca simulation was conducted to optimize

https://doi.org/10.51202/9783181023549 - Generiert durch IP 216.73.216.36, am 19.01.2026, 02:19:31. © Urheberrechtlich geschützter Inhalt. Ohne gesonderte Erlaubnis ist jede urheberrechtliche Nutzung untersagt, insbesondere die Nutzung des Inhalts im Zusammenhang mit, für oder in KI-Systemen, KI-Modellen oder Generativen Sprachmodellen.

the pulley geometry while maintaining stiffness. That achieved a further weight reduction in addition to improving control followability.

Moreover, transmission efficiency of the new CVT was improved by adopting JATCO's latest low-friction belt.

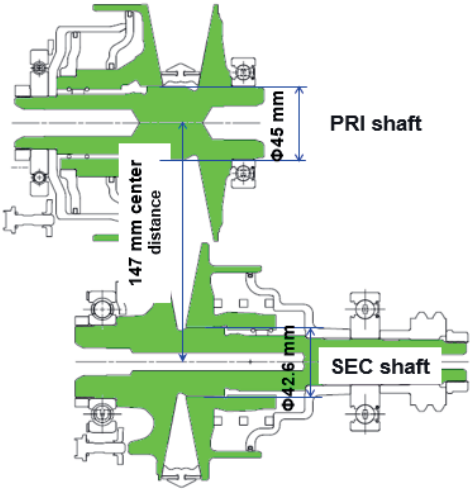


Fig. 9: Cross-sectional view of variator structure

4-3 Efforts to reduce mechanical losses

Low-friction ball bearings were adopted to support the variator pulleys and gear shafts, the pressure-receiving areas of the pulley system were optimized, and a high-efficiency belt was adopted. In addition, to reduce fluid churning resistance, the baffle plate was optimally located, the strainer suction port was optimized, and the fluid level was optimally designed.

4.4 Hydraulic system parts

The vane pump with a flow control valve that is used for the JF015E unit was adopted for the new CVT from the standpoints of fuel economy and performance. The discharge flow rate was optimized by means of the sprocket ratio.

Positioned below the unit, the control valve is of the single-stage pressure regulator type that was selected on the basis on a comprehensive judgment of fuel economy, performance and layout requirements. With this type, the secondary pulley is controlled by the line pressure. The in-fluid position of the 3-way solenoid valve (Fig. 10) and the uniform cross-sectional area

https://doi.org/10.51202/9783181023549 - Generiert durch IP 216.73.216.36, am 19.01.2026, 02:19:31. © Urheberrechtlich geschützter Inhalt. Ohne gesonderte Erlaubnis ist jede urheberrechtliche Nutzung untersagt, insbesondere die Nutzung des Inhalts im Zusammenhang mit, für oder in KI-Systemen, KI-Modellen oder Generativen Sprachmodellen.

of the flow passage inside the control valve provide both excellent pressure response and stability, thereby improving pressure controllability.

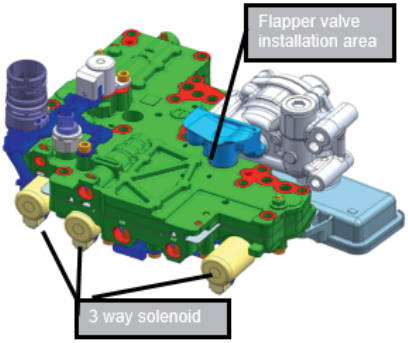


Fig. 10: Layout of hydraulic system components

4-5 Stop-start coasting system without an electric oil pump

For the new CVT, a D-ring is used as the sealing ring between the primary sliding pulley half and the cylinder, a low-leakage type of sealing ring is used between the secondary sliding pulley half and the cylinder, and a flapper valve is positioned in the hydraulic circuit between the control valve and the case (Fig. 10). These measures reduce fluid dripping inside the pressure chambers, making it possible to achieve a stop-start system including stop-start coasting.

4.6 Shift control

A two degree-of-freedom control system was adopted for gear ratio control, consisting of a feedback compensator and a feedforward compensator in order both to ensure ratio stability and improve responsiveness (Fig. 11). The feedback compensator functions to converge gear ratio deviations originating in external disturbances, in addition to improving ratio stability against torque disturbances. Convergence of gear ratio deviations is mainly accomplished with a proportional-integral-differential (PID) compensator and gear ratio stability against torque disturbances is primarily accomplished with a phase-advance compensator.

The feedforward compensator is configured with a transfer function consisting of the inverse system and target of the controlled object of the gear ratio control system. That was done to improve gear ratio responsiveness without sacrificing the stability and convergence obtained with the feedback compensator.

https://doi.org/10.51202/9783181023549 - Generiert durch IP 216.73.216.36, am 19.01.2026, 02:19:31. © Urheberrechtlich geschützter Inhalt. Ohne gesonderte Erlaubnis ist jede urheberrechtliche Nutzung untersagt, insbesondere die Nutzung des Inhalts im Zusammenhang mit, für oder in KI-Systemen, KI-Modellen oder Generativen Sprachmodellen.

As a result, this contributes to the attainment of the gear ratios needed by various performance parameters, including power performance, fuel economy and others.

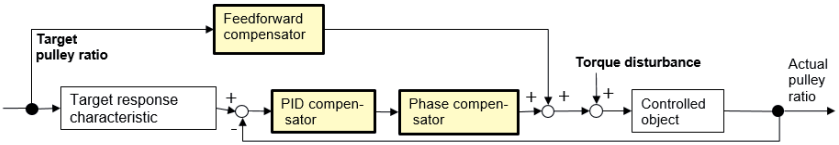


Fig. 11: Shift control model

5. Key development points for in-vehicle characteristics and levels obtained

5.1 Technologies for improving quietness

In order to secure interior quietness, it is necessary to reduce gear noise and belt noise that originate in the excitation forces of the CVT. In addition, it is also necessary to enhance the coupling rigidity between the engine and the CVT in order to reduce mount vibration caused by power plant resonance.

The following three technical measures shown in Fig. 12 were adopted for the newly developed CVT.

(1) Reduction of changes in cross-sectional rigidity between the engine and CVT

(2) Optimization of the bolt locations for connecting the engine and CVT

(3) Addition of rigidity elements between the engine cylinder head and transmission case

The adoption of these structural measures improved the natural bending frequency of the new powerplant by 1.5 times over that of the existing powerplant, thereby substantially reducing the vibration level of the mounts as shown in Fig. 13.

https://doi.org/10.51202/9783181023549 - Generiert durch IP 216.73.216.36, am 19.01.2026, 02:19:31. © Urheberrechtlich geschützter Inhalt. Ohne gesonderte Erlaubnis ist jede urheberrechtliche Nutzung untersagt, insbesondere die Nutzung des Inhalts im Zusammenhang mit, für oder in KI-Systemen, KI-Modellen oder Generativen Sprachmodellen.

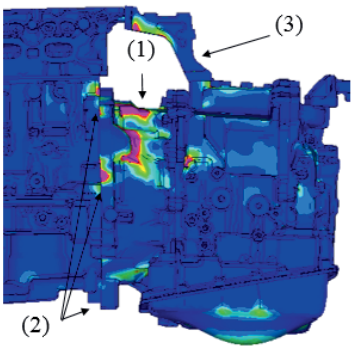


Fig. 12: Measures for improving natural bending frequency of powerplant

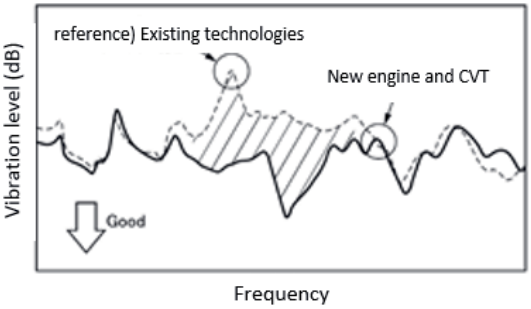


Fig. 13: Effect of improving natural vibration frequency of powerplant

5.2 Technologies for improving driveability

Driveability for mini-vehicles was established by incorporating the shift design technologies accumulated for small and midsize cars, while taking into account the mini-vehicle specification that restricts power performance. As shown in Fig. 14, the shift lines have been designed so that the seamless shifting inherent to the CVT suppresses the rise in engine speed in situations where the accelerator pedal is not depressed much such as during in-city driving. As the vehicle speed increases, the shift lines provide smooth, quiet driving performance with excellent fuel economy. On the other hand, the adoption of Dynamic Step (D-Step) shift control[(2)] provides shift performance like that of a stepped automatic transmission in which the engine speed and the vehicle speed rise together. This shift performance is provided in situations where the

https://doi.org/10.51202/9783181023549 - Generiert durch IP 216.73.216.36, am 19.01.2026, 02:19:31. © Urheberrechtlich geschützter Inhalt. Ohne gesonderte Erlaubnis ist jede urheberrechtliche Nutzung untersagt, insbesondere die Nutzung des Inhalts im Zusammenhang mit, für oder in KI-Systemen, KI-Modellen oder Generativen Sprachmodellen.

driver depresses the accelerator pedal deeply to obtain strong acceleration for merging with traffic or after passing through an electronic toll collection (ETC) gate on an expressway. As a result, this produces an exhilarating driving feeling characterized by a pleasant, rhythmical change in the engine sound as the vehicle accelerates, as shown in Fig. 15. In addition, the engine speed characteristic contributes to reducing interior noise without remaining at a constant level at high vehicle speeds.

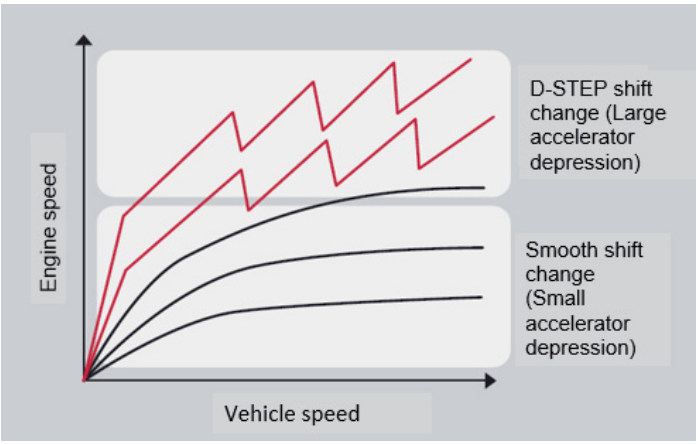


Fig. 14: D-Step shift schedule

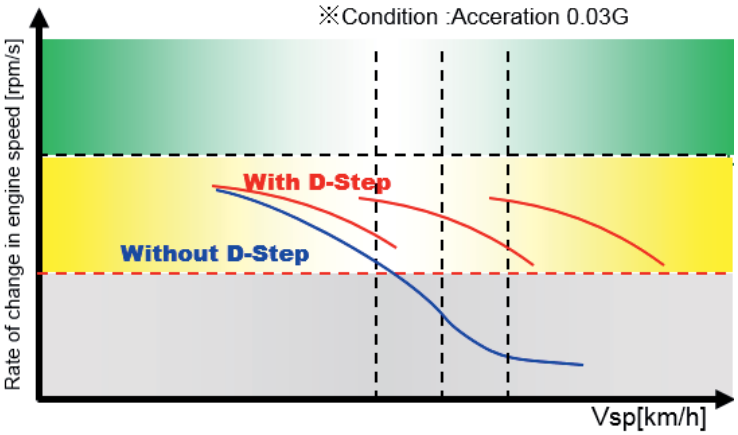


Fig. 15: D-Step effect

https://doi.org/10.51202/9783181023549 - Generiert durch IP 216.73.216.36, am 19.01.2026, 02:19:31. © Urheberrechtlich geschützter Inhalt. Ohne gesonderte Erlaubnis ist jede urheberrechtliche Nutzung untersagt, insbesondere die Nutzung des Inhalts im Zusammenhang mit, für oder in KI-Systemen, KI-Modellen oder Generativen Sprachmodellen.

5.3 Technologies for improving vehicle fuel economy

Contribution to fuel economy

As part of the efforts made to improve vehicle fuel economy, hardware measures were adopted to reduce mechanical losses under steady-state conditions as mentioned in section 4.3. Control improvements were also implemented for transient operation to improve the ability to trace the target gear ratio, thereby enabling the engine to better follow its operating line of excellent efficiency.

The reduction of mechanical losses has resulted in a noticeable improvement especially in the low-speed range compared with the company's JF015E unit that is currently being used on many mini-vehicles. Specifically, friction is reduced by approximately 8% overall during vehicle operation under Japan's JC08 test mode.

In addition to the reduction of mechanical losses, collaborative control with the engine or a hybrid system contributes approximately 6% of the 15.5% improvement obtained in vehicle fuel economy compared with the previous model for operation under the JCO8 test mode.

6. Conclusion

This paper has described a new CVT that has been developed specifically for mini-vehicles by thoroughly analyzing their functionality and performance requirements; it achieves strong competitiveness through the refinement of existing technologies. This new CVT contributes to further vehicle weight reduction and fuel economy improvement compared with the existing CVT model. This new unit will also be applicable to the global A-segment as a result of making minor modifications, which will further expand the customer base for CVTs.

References

(1) Haruhisa Nakano, Yoshikuni Kato, Naotoshi Okumara and Yuki Umeda, Development of a New-generation Eco-friendly CVT with Wide Ratio Coverage for Small Vehicles, JSAE Symposium text, No. 06-15, pp. 34-37 (Nov. 2015) (in Japanese).

(2) Kazumi Saito and Tatsuo Nakano, Development of a CVT for Application to Diesel Engine Vehicles, JSAE Symposium text, No. 03-14, pp. 49-53 (Nov. 2014) (in Japanese).

(3) Jun Shiomi, Yoshikuni Kato, Yoshiro Nakamoto, Tsutomu Saito and Hirofumi Okahara, Next-generation Eco-friendly CVT for 2.0-3.5L-class FWD Vehicles, Proceedings of JSAE, pp. 5-8, (May 2012) (in Japanese).

https://doi.org/10.51202/9783181023549 - Generiert durch IP 216.73.216.36, am 19.01.2026, 02:19:31. © Urheberrechtlich geschützter Inhalt. Ohne gesonderte Erlaubnis ist jede urheberrechtliche Nutzung untersagt, insbesondere die Nutzung des Inhalts im Zusammenhang mit, für oder in KI-Systemen, KI-Modellen oder Generativen Sprachmodellen.

New next generation eight-speed automatic transmission for FWD vehicles

Senior Research engineer, **Cheoljin Kim**,
HYUNDAI TRANSYS, Hwaseong, Korea

Abstract

Automatic transmission has been developing in multi-stages and recently electrification is processing rapidly to reduce fuel consumption. According to the multi-stages and electrification, the number of automatic transmission parts increase and transmission overall length also increase , which makes the environment of installing transmission worse after all.

The newly developed 8 speed automatic transmission for FWD vehicles was substantially shortened the whole length of transmission based on the current 8 speed automatic transmission through changing and optimizing its structure. In addition, in spite of reduction of transmission length, we improved vehicle power performance and fuel efficiency through expansion of gear span, efficiency improvement technology and weight reduction.

Introduction

Automatic transmission has been continuously developing to increase driving performance and reduce fuel consumption, recently a FWD10 speed automatic transmission has been mass produced. In order to respond to stringent environmental regulations, vehicle electrification is rapidly progressing. To achieve multi-stages of transmission, the number of components get increased and the electrification would worsen vehicle mountability in need of such as motor and engine clutches etc. to be installed inside the transmission.

The increasing number of vehicles equipped with turbochargers in compact cars also deteriorates the ability to mount the transmission, which makes it necessary to miniaturize the transmission.

The 8-speed automatic transmission (A8F42S) for the front-wheel-drive vehicle, which was recently developed, substantially reduced the overall length based on the current 8-speed automatic transmission (A8F42) through relocation and optimization of the structure. Nevertheless, vehicle power performance and fuel economy has greatly improved through the expansion of gear span, improvement of transmission efficiency and weight reduction.

The clutch, hydraulic system, torque converter and oil pump were newly designed to reduce the overall length of the transmission and planetary gears has been optimized with changing

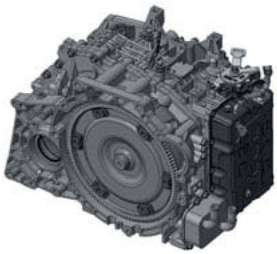
https://doi.org/10.51202/9783181023549 - Generiert durch IP 216.73.216.36, am 19.01.2026, 02:19:31. © Urheberrechtlich geschützter Inhalt. Ohne gesonderte Erlaubnis ist jede urheberrechtliche Nutzung untersagt, insbesondere die Nutzung des Inhalts im Zusammenhang mit, für oder in KI-Systemen, KI-Modellen oder Generativen Sprachmodellen.

current structure. To increase the transmission efficiency, the clutch drag and oil pump loss was minimized and low friction bearings were applied. By optimizing and relocation of the powertrain structure, fewer components and shorter overall length have reduced weight. It has been designed to be able to electrify with minimum change of vehicle layout since the initial stage of design.

In this paper, the methods regarding relocation of existing structure of transmission, reduction of overall length through optimization, efficiency improvement, weight reduction and electrification would be described.

<Specification Comparison>

	A8F42 (Existing Model)	A8F42S (New Model)
Torque Capacity [kgf.m]	47(DSL), 42(GSL)	47(DSL) 42(GSL)
Overall Length [mm]	408	372
Gear Span [1st/Top]	7.4~8.0	7.4~8.2
Weight [Dry, kg]	98	92



MINIMIZING, WEIGHT REDUCTION AND EFFICIENCY IMPROVEMENT

Figure 1 below shows that the 8-speed automatic transmission for front-wheel (A8F42), which is currently in production, has three sets of planetary gears, four sets of clutches and two sets of brakes. Which made vehicle mountability worse than 6-speed automatic transmission because the size of the transmission was inevitably increased due to the addition of one set of actuating elements. Furthermore, adding a motor and engine clutches, etc for electrification makes mounting regarding package would be very strained.

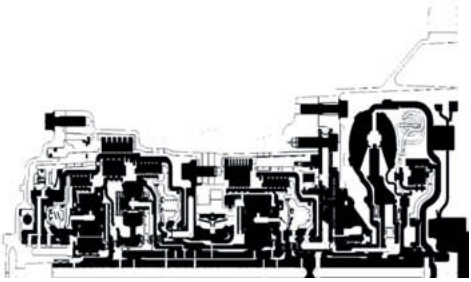


Fig. 1: Cross section of current 8 speed for FWD vehicle.

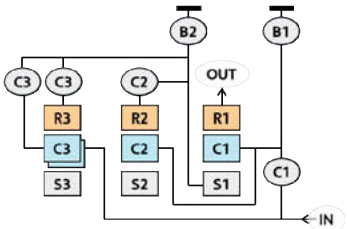


Fig. 2: Gear train schematic.

https://doi.org/10.51202/9783181023549 - Generiert durch IP 216.73.216.36, am 19.01.2026, 02:19:31. © Urheberrechtlich geschützter Inhalt. Ohne gesonderte Erlaubnis ist jede urheberrechtliche Nutzung untersagt, insbesondere die Nutzung des Inhalts im Zusammenhang mit, für oder in KI-Systemen, KI-Modellen oder Generativen Sprachmodellen.

The newly developed A8F42S has been reduced in size by about 9% compared to the current mass production A8F42, it was designed to be smaller despite the fact that it has one more operating set than 6-speed automatic transmission.

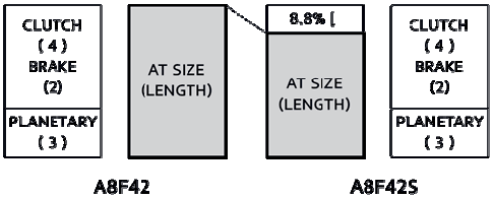


Fig. 3: Component number & AT size comparison

The following is a description of how we were able to reduce the overall length and weight of the transmission.

1. Integration of Front annulus gear and Transfer drive gear

It is not easy to reduce the overall length of the transmission which has the same power flow as the mass-produced 8-speed transmission. To solve this problem, it is necessary to eliminate existing components or to integrate functions between the parts to make them a single element. Although the annulus gear and the transfer drive gear in the front planetary gear were originally separate components, the newly designed A8F42S integrates both the annulus gear and the transfer drive gear. In other words, external teeth of transfer gear was formed outside of the annulus gear (internal gear) to carry out two functions as one part, thereby reduced the overall length up to 23.1 mm.

https://doi.org/10.51202/9783181023549 - Generiert durch IP 216.73.216.36, am 19.01.2026, 02:19:31. © Urheberrechtlich geschützter Inhalt. Ohne gesonderte Erlaubnis ist jede urheberrechtliche Nutzung untersagt, insbesondere die Nutzung des Inhalts im Zusammenhang mit, für oder in KI-Systemen, KI-Modellen oder Generativen Sprachmodellen.

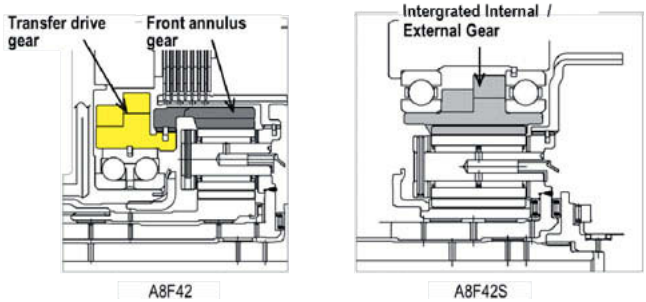


Fig. 4

2. Structure change of Center Support & C2 Clutch

The automatic transmission implements the speed change stages with plural planetary gears, clutches, brakes and each of the clutches and brakes is operated by hydraulic pressure.

The center support of A8F42 in the mass-production supports the transfer gear through the double ball angular bearing and supplies the hydraulic pressure to the C2 clutch [Fig 5].

This structure eventually leads to an increase in transmission length.

The A8F42S integrated the front annulus gear and the transfer drive gear with the current power flow intact, at the same time, changed the support structure and position of C2 clutch, the operating oil pressure path was changed to be able to flow through the shaft from the rear end of the transmission. This reduced the transmission length by 6.6mm. [fig.5]

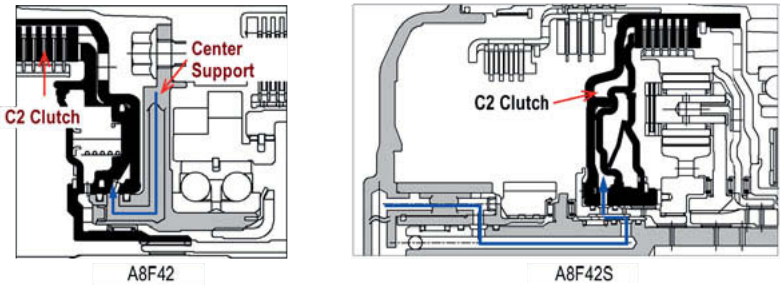


Fig. 5

https://doi.org/10.51202/9783181023549 - Generiert durch IP 216.73.216.36, am 19.01.2026, 02:19:31. © Urheberrechtlich geschützter Inhalt. Ohne gesonderte Erlaubnis ist jede urheberrechtliche Nutzung untersagt, insbesondere die Nutzung des Inhalts im Zusammenhang mit, für oder in KI-Systemen, KI-Modellen oder Generativen Sprachmodellen.

3. C3 & C4 Clutch Pack support structure

Finally, the support structure for the clutch pack was changed to reduce the size of the transmission.

Previously, the C3 and C4 clutch packs were supported at both ends using ball bearings and needle roller bearings. Now in order to reduce the overall length, clutch pack is singularly supported by locating bearings between the operating pressure oil lines of the clutches. [Figure 6]

In this way, the overall length of the transmission was reduced up to 6mm, and the gravity center of the clutch pack is designed to be located in the support part of single-type bearing so that there is no problem in performance and durability.

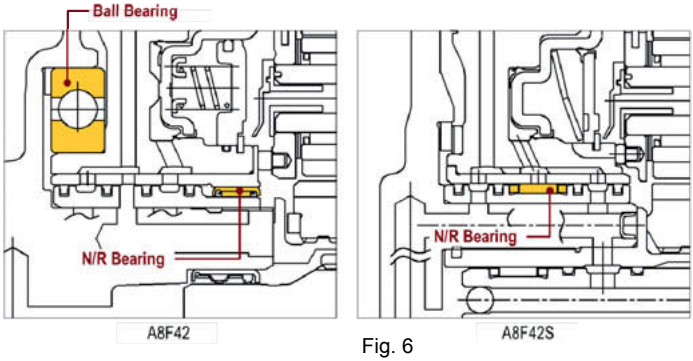


Fig. 6

4. Weight Reduction

Main methods to reduce the overall length have been described above. These not only reduced the overall length but also made it more lightweight.

The A8F42, which is now under mass-production, applied the support center made of cast iron, which was designed to withstand high loads, to provide a working fluid supply to the clutch and to equip a seal for operating hydraulic pressure.

On the other hand, the shape of the center support in the A8F42S was optimized to withstand the high loads of the bearings while using aluminum material, weight was reduced by eliminating the flow path for clutch operation and integrating the annulus gear and transfer drive gear. (approx. 0.6kg)

In addition, the overall length was reduced and also the total weight of the transmission was reduced by more than 3kg by reducing numbers of parts.

https://doi.org/10.51202/9783181023549 - Generiert durch IP 216.73.216.36, am 19.01.2026, 02:19:31. © Urheberrechtlich geschützter Inhalt. Ohne gesonderte Erlaubnis ist jede urheberrechtliche Nutzung untersagt, insbesondere die Nutzung des Inhalts im Zusammenhang mit, für oder in KI-Systemen, KI-Modellen oder Generativen Sprachmodellen.

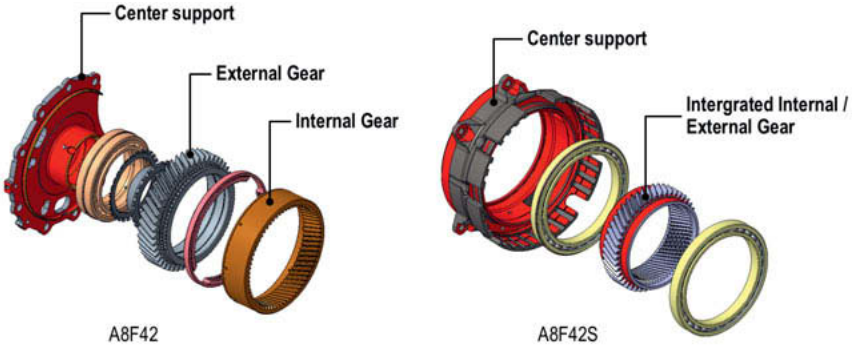


Fig. 7

EFFICIENCY IMPROVEMENT

Needless to say, the automatic transmission efficiency is more important than ever in accordance with the recent fuel efficiency regulations.

The 8-speed front-wheel 8-speed automatic transmission (A8F42), which is currently in production, boasts the world's highest level of transmission efficiency. However, the improved transmission (A8F42S) has significantly improved transmission efficiency while dramatically reducing transmission overall length.

1. Oil Pump

Oil pumps are one of the biggest losses in automatic transmissions using hydraulic control and We could improve transmission efficiency through optimization of capacity and minimized drive losses.

The oil pump of A8F42S is located on the same axis as the input shaft, which makes it difficult to reduce the diameter of the pump rotor, however, by optimizing the shape of peripheral components, the rotor diameter is reduced about 3% to improve overall transmission efficiency by 0.2%.

https://doi.org/10.51202/9783181023549 - Generiert durch IP 216.73.216.36, am 19.01.2026, 02:19:31. © Urheberrechtlich geschützter Inhalt. Ohne gesonderte Erlaubnis ist jede urheberrechtliche Nutzung untersagt, insbesondere die Nutzung des Inhalts im Zusammenhang mit, für oder in KI-Systemen, KI-Modellen oder Generativen Sprachmodellen.

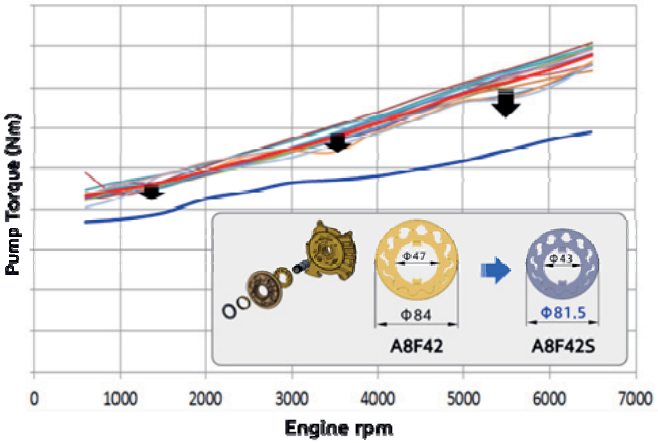


Fig. 8

2. Taper Bearing

The output axis and the differential drive gear axis of the automatic transmission are subjected to a high load from an axis that transmits the rotational force to the vehicle drive axis after deceleration in the transmission.

In order to withstand such a high load, they are mainly supported at both ends of a tapered roller bearing, which is robust against a high load but also has considerable bearing drag losses.

Many bearing specialists are doing a lot of research to reduce the friction loss, from the efforts, special coating was applied to the bearing roller to reduce the friction loss drastically.

Bearing for special coating has not been newly developed and coating method is same to existing way so that it can be applied without any design change.

https://doi.org/10.51202/9783181023549 - Generiert durch IP 216.73.216.36, am 19.01.2026, 02:19:31. © Urheberrechtlich geschützter Inhalt. Ohne gesonderte Erlaubnis ist jede urheberrechtliche Nutzung untersagt, insbesondere die Nutzung des Inhalts im Zusammenhang mit, für oder in KI-Systemen, KI-Modellen oder Generativen Sprachmodellen.

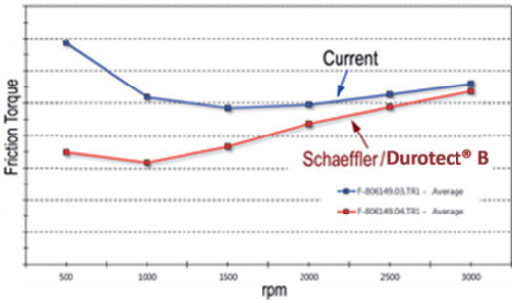


Fig. 9

3. Removing bearings by change of clutch pack support structure

Ball bearings were removed, weight, cost and efficiency was improved by changing the support structure of the clutch pack (removing ball bearings), which was previously described as a method to reduce the overall length.[Fig. 6]

4. Oil Guide

The differential assembly and differential drive gears of the transmission are constantly rotating elements and result in large friction losses, being exposed to the transmission oil during rotation. In order to reduce losses, the oil guide covers the periphery of the differential assembly and the churning loss varies depending on the shape of guide-oil. The shape of this cover of A8F42S was optimized through CFD analysis and the transmission efficiency has improved.

https://doi.org/10.51202/9783181023549 - Generiert durch IP 216.73.216.36, am 19.01.2026, 02:19:31. © Urheberrechtlich geschützter Inhalt. Ohne gesonderte Erlaubnis ist jede urheberrechtliche Nutzung untersagt, insbesondere die Nutzung des Inhalts im Zusammenhang mit, für oder in KI-Systemen, KI-Modellen oder Generativen Sprachmodellen.

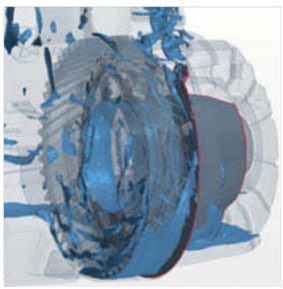


Fig. 10

As shown in Fig. 10, there is a large difference in the fluid shape from ATF churning depending on before and after the improvement of the oil guide shape.

OPTIONAL DEVICES

The A8F42S is available for various requirements of carmakers by applying various options.

1. ISG

ISG (Idle Stop & Go) is an inverter-integrated type that supports vehicle sailing and creep operation and is mounted inside the transmission

2. SBW

The A8F42S has SBC (Shift By Cable) as its basic configuration, and SBW (Shift By Wire) which is electric or hydraulic type can be applied as an option.

3. ATF Cooler (Warmer)

ATF cooler is equipped to side part of converter housing of transmission. At low temperature when starting the engine, the ATF temperature of the automatic transmission is increased by using cooling fluid from engine, which can contribute to the improvement of fuel economy by reducing the friction loss due to viscosity reduction.

4. Torque Converter CPA applied

The torsional vibration generated and transmitted from the engine is damped more effectively by CPA than the normal spring damper, thereby increase the lock-up direct coupling area and contribute to the improvement of vehicle fuel economy.

https://doi.org/10.51202/9783181023549 - Generiert durch IP 216.73.216.36, am 19.01.2026, 02:19:31. © Urheberrechtlich geschützter Inhalt. Ohne gesonderte Erlaubnis ist jede urheberrechtliche Nutzung untersagt, insbesondere die Nutzung des Inhalts im Zusammenhang mit, für oder in KI-Systemen, KI-Modellen oder Generativen Sprachmodellen.

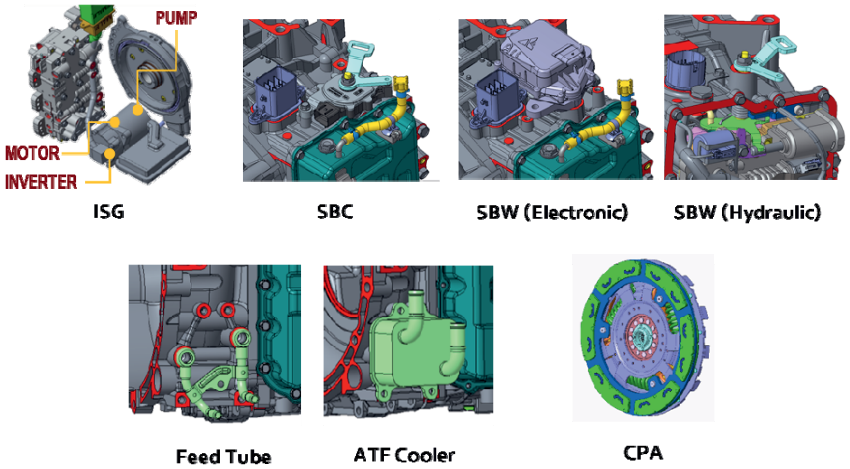


Fig. 11

ELECTRIFICATION

The newly developed A8F42S was considered to be electrified from the beginning of the design. Electrification is inevitable in order to respond to enhanced fuel efficiency regulations. However, the addition of elements such as engine clutch, motor, and torsional damper according to electrification increases the overall length, which inevitably deteriorates vehicle mountability.

As mentioned earlier, the A8F42S dramatically reduced the overall length of the current 8-speed gearbox, allowing the vehicle to be equipped with an electric transmission without substantial changing the layout of the current production vehicle. [fig. 12]

https://doi.org/10.51202/9783181023549 - Generiert durch IP 216.73.216.36, am 19.01.2026, 02:19:31. © Urheberrechtlich geschützter Inhalt. Ohne gesonderte Erlaubnis ist jede urheberrechtliche Nutzung untersagt, insbesondere die Nutzung des Inhalts im Zusammenhang mit, für oder in KI-Systemen, KI-Modellen oder Generativen Sprachmodellen.

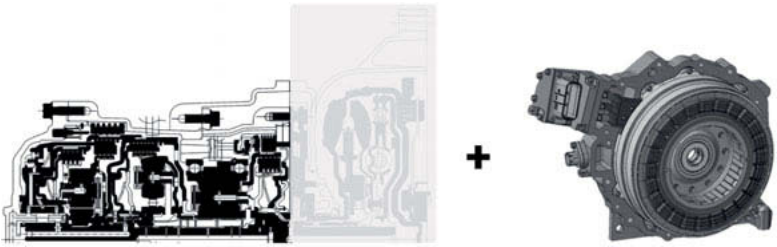


fig. 12

1. Modular Design

The A8F42S has been developed for electrification as an option since the initial stage.

This is to maximize the effect of minimizing the investment through commonation of the production line and the common use of parts. In order to electrify the existing transmission, the changes of internal parts of conventional transmission have been minimized.

A8F42H removed the torque converter from the A8F42S, added a motor, engine clutch, and torsional damper, changed the input shaft and oil pump shape for improvements of hydraulic pressure and lubrication.

The valve body is also configured in the same layout and designed to cope with electrification by adding only one solenoid valve for engine clutch control.

In addition to the above-mentioned parts, the A8F42S is fully compatible with the production line. Available TMED (Transmission Mounted Electric Device) system enables full hybrid function that can run on electricity.

https://doi.org/10.51202/9783181023549 - Generiert durch IP 216.73.216.36, am 19.01.2026, 02:19:31. © Urheberrechtlich geschützter Inhalt. Ohne gesonderte Erlaubnis ist jede urheberrechtliche Nutzung untersagt, insbesondere die Nutzung des Inhalts im Zusammenhang mit, für oder in KI-Systemen, KI-Modellen oder Generativen Sprachmodellen.

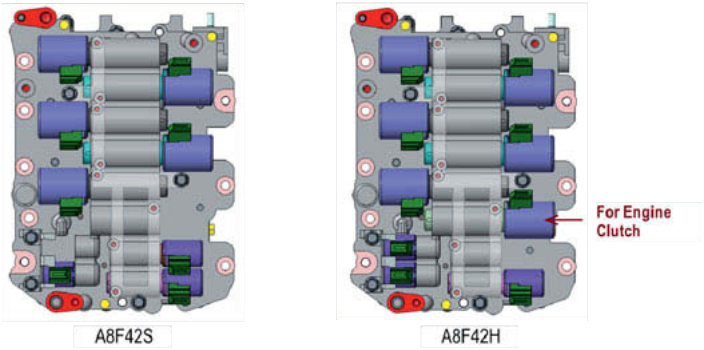


Fig. 13

2. Adaptability

As described earlier, if the transmission is electrified, the overall length is inevitably increased due to the addition of the components. This causes deterioration in vehicle package

The A8F42H(FHEV) is based on the A8F42S, which significantly reduces the length of the existing mass-produced 8-speed automatic transmission. Even with a 50-kW class motor, the transmission is only 44mm longer, allowing it to be mounted without major changes to the existing vehicle layout.

Table 1.

	Efficiency	Length	Weight
A8F42	-	-	-
A8F42S (Compare to A8F42)	**+1.4%**	**-35.7**	**-3.0kg**
A8F42H(Compare to A8F42S)	-	**+44mm**	-

https://doi.org/10.51202/9783181023549 - Generiert durch IP 216.73.216.36, am 19.01.2026, 02:19:31. © Urheberrechtlich geschützter Inhalt. Ohne gesonderte Erlaubnis ist jede urheberrechtliche Nutzung untersagt, insbesondere die Nutzung des Inhalts im Zusammenhang mit, für oder in KI-Systemen, KI-Modellen oder Generativen Sprachmodellen.

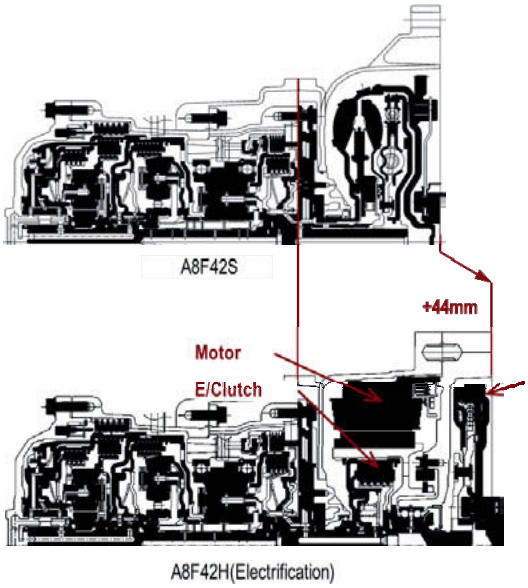


Fig. 14

CONCLUSION

In order to reduce the overall length, the front annulus gear and the transfer drive gear were integrated, and the structure of the center support and the operating hydraulic path of the C2 clutch were changed.

The existing ball bearings are eliminated by changing the structure of supporting the C3 & C4 clutch pack by a single needle roller bearing.

As a result, 35.7mm of the overall length was shortened compared to conventional front-speed 8-speed transmissions.

In terms of weight, reduced about 3kg by optimizing the structure through material change from steel to aluminum, shortening the overall length,

The transmission efficiency improved 1.4% compared to the conventional one by applying various efficiency improvement technologies such as reducing rotor diameter by 3% compared with the previous one, reducing friction losses by applying special coating on tapered

https://doi.org/10.51202/9783181023549 - Generiert durch IP 216.73.216.36, am 19.01.2026, 02:19:31. © Urheberrechtlich geschützter Inhalt. Ohne gesonderte Erlaubnis ist jede urheberrechtliche Nutzung untersagt, insbesondere die Nutzung des Inhalts im Zusammenhang mit, für oder in KI-Systemen, KI-Modellen oder Generativen Sprachmodellen.

roller bearing of output & differential axis, eliminating the existing ball bearings of C3 & C4 clutch pack and improving the oil churning loss through optimization of the shape of the oil guide etc.

The A8F42S has various options available. It is possible to use the ISG integrated with the inverter and extended function to support the sailing and creep operation of the vehicle, the electric or hydraulic type SBW, the ATF cooler(warmer), and the CPA applied torque converter.

The modular design was designed to minimize the change of conventional transmission and electrification, and it substantially improved the package adaptability to hybrid vehicles.

The newly developed A8F42S has been introduced above. The A8F42S not only improves on-board performance by reducing the overall length of the transmission with the use of the power flow of the mass-produced transmission, but also improves the transmission efficiency, weight, and expandability for electrification through modularization. It is considered as the world's best automatic transmission in every aspect.

REFERENCE

[1] Michikoshi, Y., Kusamoto, D., Ota, H., Ikemura, M. Et al., ‘‘Toyota New TNGA High-Efficiency Eight-Speed Automatic Transmission Direct Shift-8AT for FWD Vehicles,‘‘ SAE Technical Paper 2017-01-1093, doi:10.4271/2017-01-1093.

[2] Gaertner, L. and Ebenhoch, M., 2013, ‘‘The ZF Automatic Transmission 9HP48 transmission System Design and Mechanical Parts‘‘, SAE International, 2013-01-1276.

[3] Hyun Ku Lee, Sa Man Hong, Moo Suk Kim, Jin Wook Hur and Dong Kyu Yoo, ‘’A Research for the Noise Development of the FF 8th Speed Automatic Transmission’’ Trans. Korean Soc. Noise Vib. Eng., 26(5) : 559~566, 2016

https://doi.org/10.51202/9783181023549 - Generiert durch IP 216.73.216.36, am 19.01.2026, 02:19:31. © Urheberrechtlich geschützter Inhalt. Ohne gesonderte Erlaubnis ist jede urheberrechtliche Nutzung untersagt, insbesondere die Nutzung des Inhalts im Zusammenhang mit, für oder in KI-Systemen, KI-Modellen oder Generativen Sprachmodellen.

Efficient 6-Speed Manual Transmission for Modern Downspeeding Solutions

Dipl.-Ing. **Helmut Göbbels**, Dipl.-Ing. **Sebastian Scholz**,
Dipl.-Ing. **Steffen Volkmer**, Volkswagen AG, Wolfsburg



Abstract

Modern internal combustion engines are subject to strict legal regulations concerning fuel consumption and pollutant emissions. For this reason, they are currently characterized primarily by low displacement. This downsizing results in power deficits, which in turn are compensated for by using turbochargers. The latter improve powertrain performance and make high torques possible even at low engine speeds. Air and rolling resistance further put a powertrain's performance to the test, this particularly applies to heavy vehicles such as SUVs. When it comes to modern manual transmissions, this requires not only a ratio spread and a launch ratio that

https://doi.org/10.51202/9783181023549 - Generiert durch IP 216.73.216.36, am 19.01.2026, 02:19:31. © Urheberrechtlich geschützter Inhalt. Ohne gesonderte Erlaubnis ist jede urheberrechtliche Nutzung untersagt, insbesondere die Nutzung des Inhalts im Zusammenhang mit, für oder in KI-Systemen, KI-Modellen oder Generativen Sprachmodellen.

are as large as possible, but also that the engine power needs to be transmitted to the wheels with the highest possible efficiency.

The MQ281-6F (six-speed, front-wheel drive) was developed as a 2.5-shaft solution for a one-box design. In addition to the maximum possible ratio spread of 7.89, the MQ281 is characterized by high efficiency, even at low loads, as a result of its intelligent transmission fluid management capabilities. Depending on the engine and vehicle combination, the fuel consumption advantage in comparison to its predecessors can be up to 5 g of CO_2/km (including downspeeding). With a maximum torque capacity of 340 Nm, it meets the requirements for all vehicle classes in the high-volume segment – from the Polo, to the Tiguan, to the Caddy. When developing the MQ281, virtual development methods that assisted with the design of various efficiency measures were used. With a shifting travel of only 50 mm, the MQ281 guarantees maximum shifting comfort. All forward gears, as well as the final drive, are hard-machined, and this, together with the use of dual-mass flywheels, ensures a noise, vibration, and harshness (NVH) behavior in line with today's expectations.

1. Introduction

As a result of their high installation rates worldwide, manual transmissions take up a significant share of the transmission market. Among other things, this is due to their positive characteristics, including efficiency, ruggedness, and a good price-performance ratio. As the world's largest manufacturer of manual transmissions with an annual volume of 3 million units (in 2018), the Volkswagen Group currently has five transmission families. These manual transmissions are used for the various transverse platforms of the Volkswagen Group. The MQ family covers a torque range of 95 Nm to 465 Nm (Fig. 2:) and is used across all vehicle classes in the high-volume segment – from the up! to the Sharan (Fig. 1:).

https://doi.org/10.51202/9783181023549 - Generiert durch IP 216.73.216.36, am 19.01.2026, 02:19:31. © Urheberrechtlich geschützter Inhalt. Ohne gesonderte Erlaubnis ist jede urheberrechtliche Nutzung untersagt, insbesondere die Nutzung des Inhalts im Zusammenhang mit, für oder in KI-Systemen, KI-Modellen oder Generativen Sprachmodellen.



Fig. 1: Overview of manual transmissions at Volkswagen

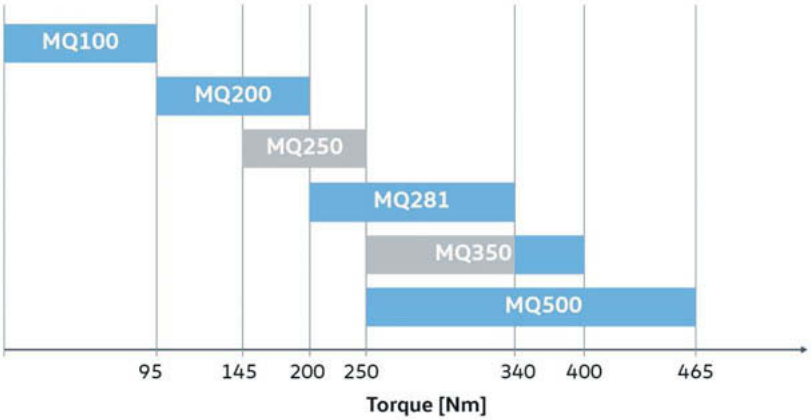
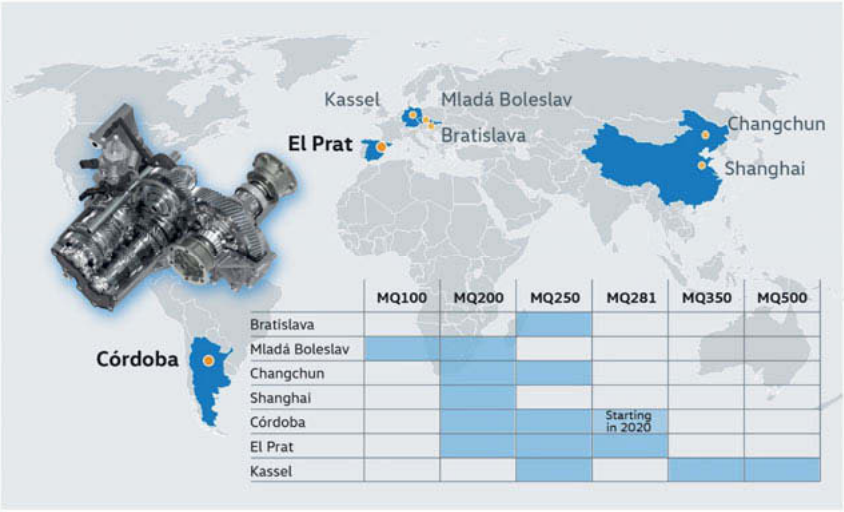


Fig. 2: Torque ranges for the MQ transmission family at Volkswagen

https://doi.org/10.51202/9783181023549 - Generiert durch IP 216.73.216.36, am 19.01.2026, 02:19:31. © Urheberrechtlich geschützter Inhalt. Ohne gesonderte Erlaubnis ist jede urheberrechtliche Nutzung untersagt, insbesondere die Nutzung des Inhalts im Zusammenhang mit, für oder in KI-Systemen, KI-Modellen oder Generativen Sprachmodellen.

The MQ transmission family at Volkswagen starts with the MQ100, which is manufactured in Mladá Boleslav (Czech Republic). With a torque range of up to 95 Nm and 5 speeds, it is used for the Small vehicle class. The MQ200 covers a torque range of up to 200 Nm. Depending on the specific application, it has 5 or 6 speeds, and it is used across vehicle classes – from the up! to the Touran. It is produced in Changchun (China), Shanghai (China), Mladá Boleslav (Czech Republic), Córdoba (Argentina), and El Prat (Barcelona). The basic design for the MQ250 had its debut in 1988, and has been continuously developed further since. It is based on a 2-shaft design, and is used as one variant with 5 speeds and another variant with 6 speeds. Maximum torque capacity is 250 Nm. Its characteristics make it possible to use it in all vehicle classes in the high-volume segment. It is produced in Changchun (China), Córdoba (Argentina), Bratislava (Slovakia), and Kassel, where the 3-shaft MQ350 is also manufactured. The MQ350 is designed for torques of up to 400 Nm and is especially suitable for use in heavy vehicles such as the Tiguan and for combining it with the 4MOTION all-wheel drive in sport sedans such as the Golf R. In addition, its specific characteristics support downspeeding, i.e., driving at a low speed in high gears while having low fuel consumption at the same time. The last model in the family is the MQ500, which is built in Kassel and is used for the engines with the highest torques – up to 465 Nm. It has 6 speeds and is used in the Midsize SUV and Van vehicle classes.



	MQ100	MQ200	MQ250	MQ281	MQ350	MQ500
Bratislava						
Mladá Boleslav						
Changchun						
Shanghai						
Córdoba				Starting in 2020		
El Prat						
Kassel						

Fig. 3: Production locations for MQ transmissions in the Volkswagen Group

https://doi.org/10.51202/9783181023549 - Generiert durch IP 216.73.216.36, am 19.01.2026, 02:19:31. © Urheberrechtlich geschützter Inhalt. Ohne gesonderte Erlaubnis ist jede urheberrechtliche Nutzung untersagt, insbesondere die Nutzung des Inhalts im Zusammenhang mit, für oder in KI-Systemen, KI-Modellen oder Generativen Sprachmodellen.

Both the Paris Agreement and European CO_2 regulations have made the requirements concerning internal combustion engine fuel consumption and emissions even more demanding. This, in combination with the trend toward heavy SUVs, downsizing, and new technologies, means that the MQ250 will no longer adequately meet future requirements for manual transmissions. Accordingly, Volkswagen is adding a highly efficient, high-torque manual transmission – the MQ281 – to its transmission family, so that it will be possible to reliably meet these stringent requirements. With a torque range of 200 to 340 Nm, the MQ281 is replacing the MQ250, and is also partially replacing the MQ350 within the torque range of 250 Nm to 340 Nm.

2. Development goals for the MQ281

The goal when developing the MQ281 was to create an efficient manual transmission which would carry forward the characteristics typical of Volkswagen. Another goal was to adhere to a modular assembly matrix strategy so that it would be possible to use it for a wide range of vehicle classes and powertrain combinations. Accordingly, the development focused on a large ratio spread, best-of-class shifting comfort, and high cost efficiency. Its torque range makes the MQ281 suitable for combining it both with gasoline and TDI engines. One particular challenge was to come up with a transmission design that, in terms of launch ratio, would be able to meet the requirements of both smaller engines with low displacement and engines in heavy vehicles with large wheels. In order to improve efficiency, targeted measures were used in order to optimize friction at bearings and seals. In addition, the performance specification required an increase in comfort to be achieved with NVH characteristics in line with today's expectations.

3. Design implementation

Both the conceptual phase and design phase for the MQ281-6F focused on the following aspects:

- Transmission case design
- Increasing efficiency with lower-friction main bearing points and a new seal design
- New lubrication strategy
- Synchronizer design
- Large ratio spread for:
  - Good starting performance
  - Low engine speeds at higher vehicle speeds

https://doi.org/10.51202/9783181023549 - Generiert durch IP 216.73.216.36, am 19.01.2026, 02:19:31. © Urheberrechtlich geschützter Inhalt. Ohne gesonderte Erlaubnis ist jede urheberrechtliche Nutzung untersagt, insbesondere die Nutzung des Inhalts im Zusammenhang mit, für oder in KI-Systemen, KI-Modellen oder Generativen Sprachmodellen.

- Modular assembly matrix system for the wheel sets for use with the various vehicle classes
- Improving cost efficiency by reducing the number of components

The following sections go over the important development steps and the results from the design implementation.

3.1 Configuration and design

The MQ281 has a 2.5-shaft design with a center distance of 80 mm between the transmission input shaft and output shaft. The center distance between the transmission input shaft and output shaft of the differential gear unit is 189.15 mm. Designing the center distances within the packaging space boundaries of the modular assembly matrix system posed high challenges for the development.

The gears are arranged as follows on the transmission shafts (Fig. 4:):

- Output shaft: Output shaft gears for 1st and 2nd gear
- Transmission input shaft: Output shaft gears for gears 3 to 6

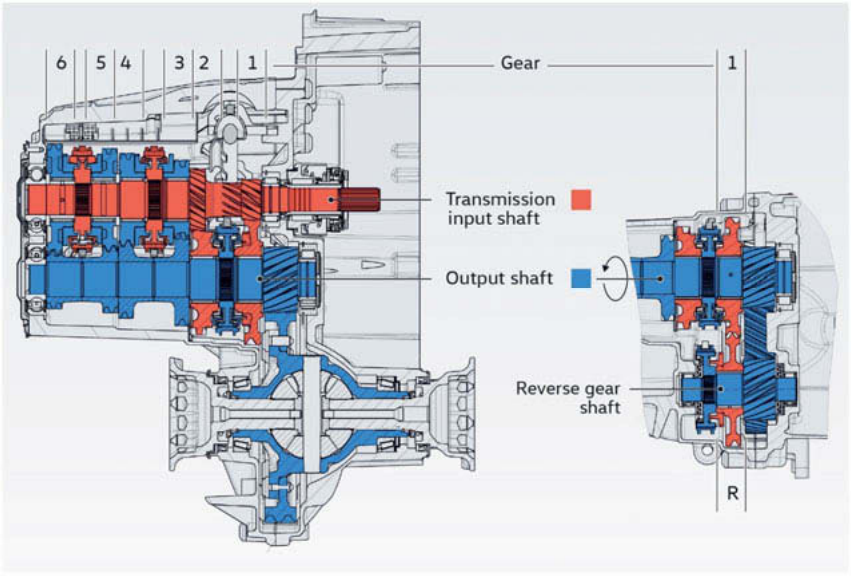


Fig. 4: MQ281: Transmission cross section and main components

https://doi.org/10.51202/9783181023549 - Generiert durch IP 216.73.216.36, am 19.01.2026, 02:19:31. © Urheberrechtlich geschützter Inhalt. Ohne gesonderte Erlaubnis ist jede urheberrechtliche Nutzung untersagt, insbesondere die Nutzung des Inhalts im Zusammenhang mit, für oder in KI-Systemen, KI-Modellen oder Generativen Sprachmodellen.

The modular strategy followed by Volkswagen was consistently adhered to when designing the gear ratios so as to ensure that it would be possible to use the MQ281 as widely as possible. Together with five wheel set combinations with different ratio spreads between 5.75 and 7.36, six available final drive ratios result, for a total of 30 possible transmission variants. The variant with the best starting performance has a launch ratio of 17.11.
As a result of packaging space optimization, the clutch housing of the MQ281 can accommodate a clutch with a max. diameter of 240 mm. This clutch meets the requirements for the various vehicle classes and powertrain combinations.

3.2 Efficiency optimization

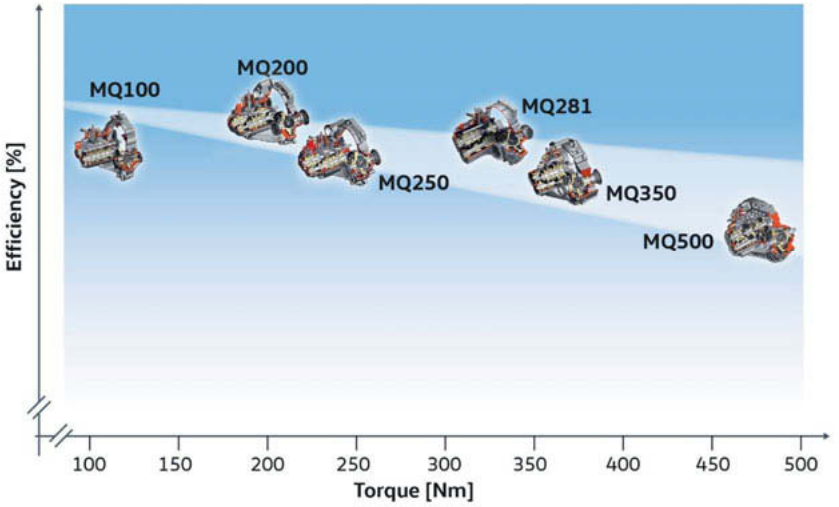


Fig. 5: Average mechanical efficiencies of Volkswagen MQ manual transmissions (NEDC)

When designing the MQ281, optimizing efficiency was a central development goal (Fig. 5:). In order to achieve this, special transmission fluid routing measures for reducing drag loss, a new bearing solution, and friction-optimized bearing seals are used. These changes enable the MQ281 to nearly reach the same efficiency as the MQ200 despite is larger dimensions and having a max. torque capacity of 340 Nm.

https://doi.org/10.51202/9783181023549 - Generiert durch IP 216.73.216.36, am 19.01.2026, 02:19:31. © Urheberrechtlich geschützter Inhalt. Ohne gesonderte Erlaubnis ist jede urheberrechtliche Nutzung untersagt, insbesondere die Nutzung des Inhalts im Zusammenhang mit, für oder in KI-Systemen, KI-Modellen oder Generativen Sprachmodellen.

3.3 Friction-optimized bearings and seals

Special attention was paid to a transmission output shaft bearing design that would be optimal in terms of friction. Instead of a pre-loaded taper roller bearing, a preload-free fixed-floating bearing arrangement was used. On the engine side, a cylindrical roller bearing with an inner ring is used. On the transmission side facing away from the engine, a deep-groove ball bearing with low-contact seals is used. This measure contributes significantly to reducing friction losses and to improving efficiency.

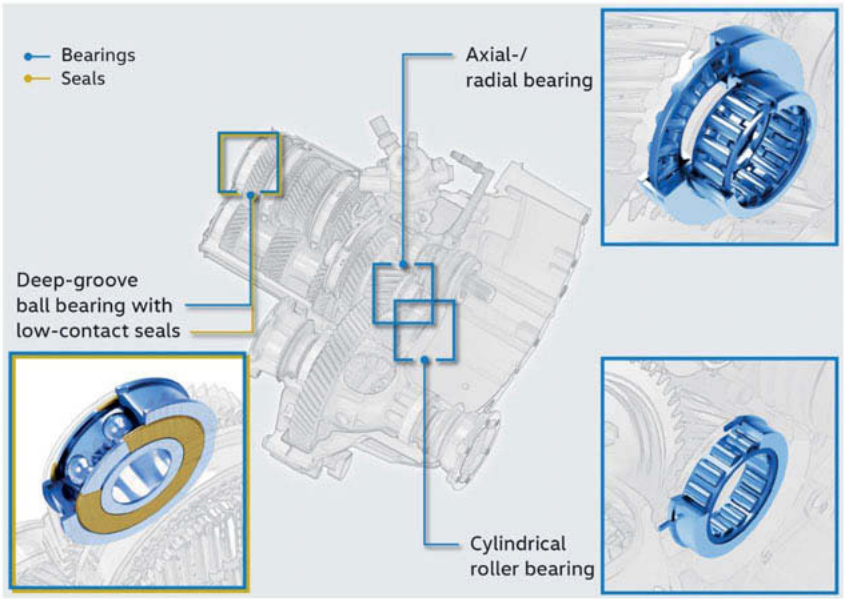


Fig. 6: Measures for reducing friction in the MQ281

In order to prevent axial displacement, clamping screws are used both at the transmission input shaft and at output shaft as per the modular assembly matrix approach. Axial/radial bearings without preload are used on both sides on the short shaft for the reverse gear, which significantly reduces friction within the transmission.

3.4 Transmission fluid simulation

In order to ensure the uniform and optimum lubrication of all relevant components under all operating conditions, the transmission fluid simulation for the MQ281 was conducted with the moving reference frame (MRF) method using a computational fluid dynamics (CFD) model

https://doi.org/10.51202/9783181023549 - Generiert durch IP 216.73.216.36, am 19.01.2026, 02:19:31. © Urheberrechtlich geschützter Inhalt. Ohne gesonderte Erlaubnis ist jede urheberrechtliche Nutzung untersagt, insbesondere die Nutzung des Inhalts im Zusammenhang mit, für oder in KI-Systemen, KI-Modellen oder Generativen Sprachmodellen.

(Fig. 7:). The delivery action as well as the turbulence generated by rotors such as gears were simulated with this method. The MRF simulation was used to lubricate:

- The shaft bearings
- The gears
- The needle roller bearings
- The transmission shafts
- The output shaft gear for the 6th gear
- The inner transmission lubrication

The simulation focused particularly on operating ranges with a low engine speed, which pose particularly demanding requirements regarding transmission fluid delivery. These ranges were examined based on various driving situations in order to improve the efficiency with targeted transmission fluid routing measures. Within this context, particular attention was paid to, among other things, the optimal lubrication of the 6th gear (Fig. 7:), which is a particular challenge during cornering in the case of transversely installed transmissions.



Fig. 7: Virtual transmission fluid distribution simulation using the moving reference frame method (Merkle & Partner)

In order to ensure transmission fluid delivery in this area, the guide tube for the reverse gear's shift fork was made longer. The transmission fluid that swirls up is routed with a transmission

https://doi.org/10.51202/9783181023549 - Generiert durch IP 216.73.216.36, am 19.01.2026, 02:19:31. © Urheberrechtlich geschützter Inhalt. Ohne gesonderte Erlaubnis ist jede urheberrechtliche Nutzung untersagt, insbesondere die Nutzung des Inhalts im Zusammenhang mit, für oder in KI-Systemen, KI-Modellen oder Generativen Sprachmodellen.

fluid guide into the tube and then directed through all the way to the 6th gear (Fig. 8:). For the inner lubrication of all output shaft gears, both the transmission input shaft and output shaft are hollowed-out. A gallery collects the swirled-up transmission fluid and directs it to the transmission input shaft. In addition, the gallery ensures that the transmission fluid is delivered to the deep-groove ball bearing on the side facing away from the engine (Fig. 8). A transmission fluid catch pan and a transmission fluid baffle ensure optimum lubrication of the fixed gears. With these transmission fluid routing measures, it was possible to reduce the lifetime transmission fluid volume to 1.5 l.

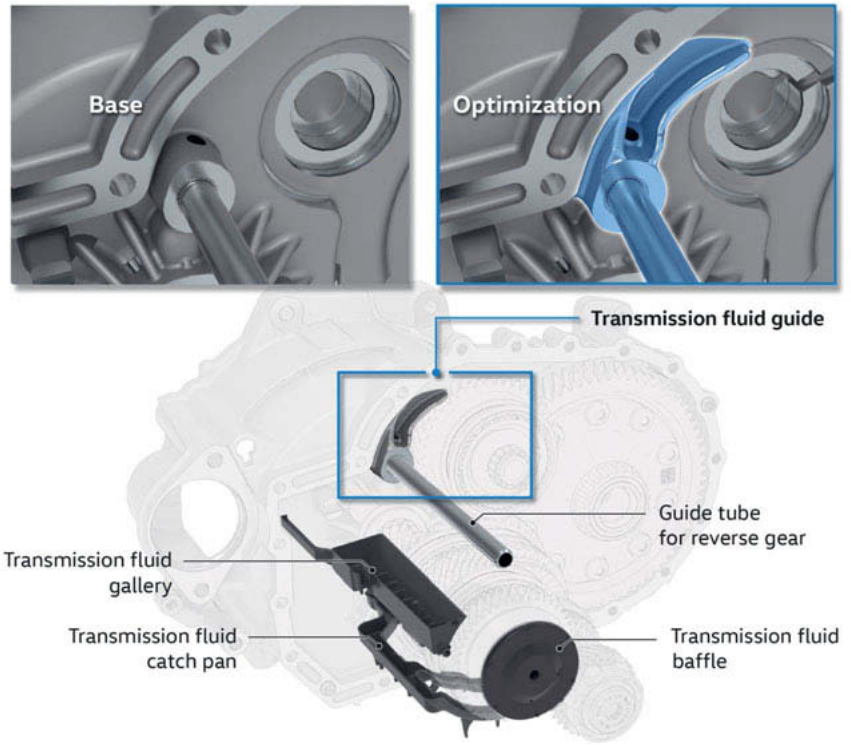


Fig. 8: Specific lubrication measures on the MQ281

3.5 Synchronizer

Two different cone systems are used for the synchronizer blocking rings for the transmission shaft and the transmission input gear on the MQ281 (Fig. 9:). In order to achieve consistently

https://doi.org/10.51202/9783181023549 - Generiert durch IP 216.73.216.36, am 19.01.2026, 02:19:31. © Urheberrechtlich geschützter Inhalt. Ohne gesonderte Erlaubnis ist jede urheberrechtliche Nutzung untersagt, insbesondere die Nutzung des Inhalts im Zusammenhang mit, für oder in KI-Systemen, KI-Modellen oder Generativen Sprachmodellen.

smooth synchronization, gears 1 and 2 use multi-cone systems that rest on output shaft, while gears 3 to 6 use single-cone systems located on the transmission input shaft. This synchronizer configuration made it possible to forgo the use of a multi-cone system on the 3rd gear. Accordingly, four identical rings could be used for gear positions 3 to 6. In combination with the inserted gear shoulders, this reduces the assembly complexity at the plant building the transmission. For the reverse gear, a single-cone system with a lead-free brass thread is used.



Fig. 9: Single-cone and multi-cone synchronizers (Oerlikon Friction Systems)

Both synchronizer systems use the proven combination of steel and carbon. The carbon coating as a friction partner to steel results in an appreciable improvement in performance and ruggedness. Accordingly, this type of friction material is used in virtually all Volkswagen manual transmissions and is being continuously developed further.
The output shaft gears for gears 1 and 2 have a monoblock design, which not only makes the components highly sturdy, but also comes with significant cost advantages when it comes to gear production. Another advantage when it comes to production is the fact that the multi-cone system can be coupled with the output shaft gear without the need for machining.

3.6 Case and housing structures

In order to take advantage of all optimization potentials, special focus was on the housing development. The case and housing structures for the MQ281 were designed with the help of finite element analysis using the "OptiStruct" topology optimization structural analysis solver. In addition to the transmission case and clutch housing, the focus was also on the pendulum

https://doi.org/10.51202/9783181023549 - Generiert durch IP 216.73.216.36, am 19.01.2026, 02:19:31. © Urheberrechtlich geschützter Inhalt. Ohne gesonderte Erlaubnis ist jede urheberrechtliche Nutzung untersagt, insbesondere die Nutzung des Inhalts im Zusammenhang mit, für oder in KI-Systemen, KI-Modellen oder Generativen Sprachmodellen.

support. The goal was to distribute a defined material volume within the defined packaging space in a manner optimal for loading so as to achieve the maximum possible local component stiffness with minimum material use. Various design proposals were simulated in multiple optimization steps, and the results were used to derive optimal case and housing part ribbing that would be suitable for production (Fig. 10:).

The following example (Fig. 10:) shows the optimization of the differential area on the clutch housing with a comparison between the concept model phase and implementation in production: On the left is the starting situation with star-shaped ribbing. On the right is the design after being optimized with OptiStruct and the resulting reduced ribbing and modified material distribution.

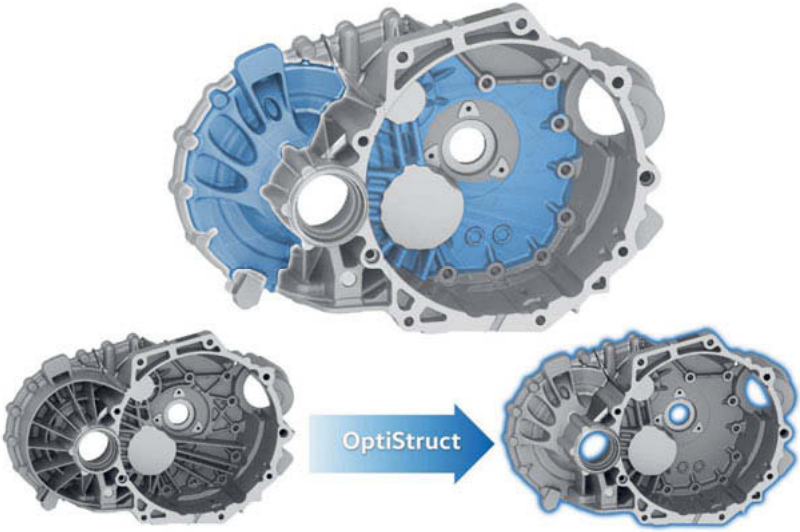


Fig. 10: Optimizing the ribbing on the clutch housing (OptiStruct)

3.7 Acoustics

When designing the acoustics for the MQ281, the virtual "acoustic fingerprint" development method was used. This method was used to simulate the sound radiation behavior at the transmission's connection points under consideration of an optimal gear engagement behavior (Fig. 11:). The results from the numerical simulations made it possible to identify critical total levels at the defined contact points and optimize the underlying structural weaknesses on the case in terms of transmission. As a result of this and of using a dual-mass flywheel with a

https://doi.org/10.51202/9783181023549 - Generiert durch IP 216.73.216.36, am 19.01.2026, 02:19:31. © Urheberrechtlich geschützter Inhalt. Ohne gesonderte Erlaubnis ist jede urheberrechtliche Nutzung untersagt, insbesondere die Nutzung des Inhalts im Zusammenhang mit, für oder in KI-Systemen, KI-Modellen oder Generativen Sprachmodellen.

compression stress-strain characteristic designed as per the engine application, the MQ281 already had NVH characteristics conforming to today's expectations during the design phase. In addition, the subsequent hard machining process for the wheel pairs not only ensures higher quality and ruggedness, but also further improvement in terms of acoustic behavior.

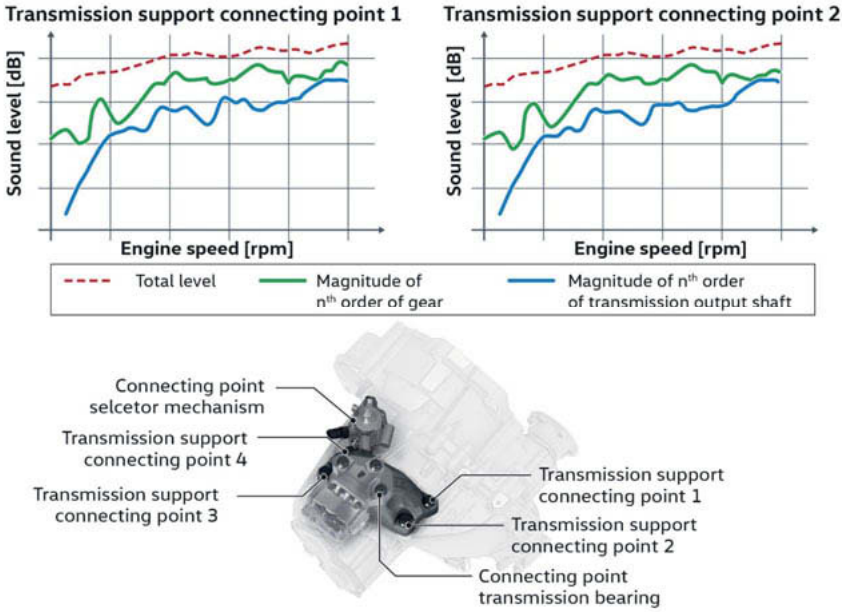


Fig. 11: Virtual acoustic optimization for the MQ281

4. Preparation for expansions

The transmission design for the MQ281 adheres to a sustainable approach that will make it possible to respond to future changes in market and customer requirements in a flexible manner. This approach will make it possible to use the MQ281 in an expanded range of use. In addition to the possible increase of the max. ratio spread to 7.89, even four-wheel drive applications and electrified drive configurations can be implemented. Furthermore, the hole distances on the case have already been selected in such a way that, in the future, it will also be possible to use magnesium as the material without requiring design changes.

As per the modular assembly matrix strategy, the center distance between the transmission input shaft and the differential was selected in such a way that it would be possible to use, for

https://doi.org/10.51202/9783181023549 - Generiert durch IP 216.73.216.36, am 19.01.2026, 02:19:31. © Urheberrechtlich geschützter Inhalt. Ohne gesonderte Erlaubnis ist jede urheberrechtliche Nutzung untersagt, insbesondere die Nutzung des Inhalts im Zusammenhang mit, für oder in KI-Systemen, KI-Modellen oder Generativen Sprachmodellen.

four-wheel drive variants as well, the existing power takeoff units from the Volkswagen modular assembly matrix system.

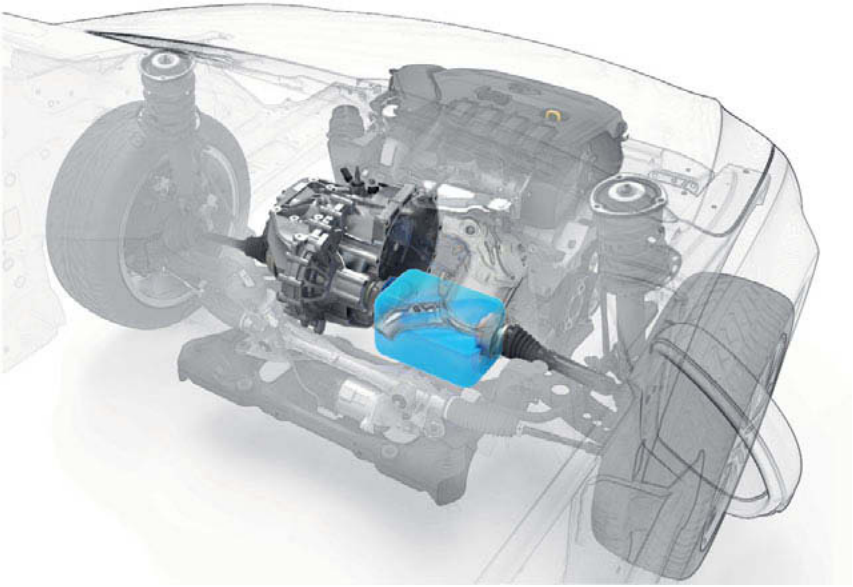


Fig. 12: Packaging space for expansions

The power takeoff unit packaging space is available for integrating an electric motor. This means that electrification can be implemented by using the four-wheel-drive-specific transmission design without having to make any further modifications to the case structure. The system, in the so-called P3 structure, being contemplated within this context would have better performance than a mild hybrid application by significantly increasing the potential regenerative braking power. In addition, this hybrid module will make it possible to implement features that were previously reserved for semi-automatic transmissions. In combination with an automatically operated clutch, for example, comfort features such as automated parking and brief, emission-free driving can be implemented.

https://doi.org/10.51202/9783181023549 - Generiert durch IP 216.73.216.36, am 19.01.2026, 02:19:31. © Urheberrechtlich geschützter Inhalt. Ohne gesonderte Erlaubnis ist jede urheberrechtliche Nutzung untersagt, insbesondere die Nutzung des Inhalts im Zusammenhang mit, für oder in KI-Systemen, KI-Modellen oder Generativen Sprachmodellen.

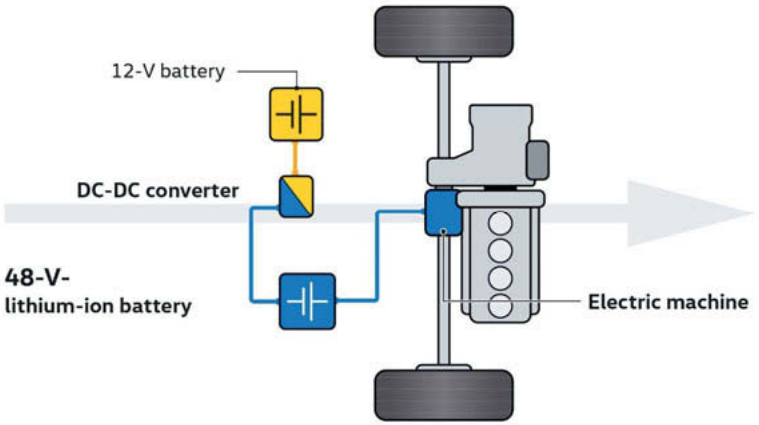


Fig. 13: Concept: mild hybrid plus drive in P3 structure

5. Summary and outlook

With its modern 2.5-shaft design and a torque range of 200 to 340 Nm, the new MQ281 replaces the MQ250 and, in certain cases, the MQ350 as well. At the same time, it represents the addition of a future-proof manual transmission to the MQ transmission range of the Volkswagen Group. To this end, it meets the packaging space requirements for various installation situations for Volkswagen Group vehicles.

The low drag torques, the large ratio spread, and the consistent use of virtual development methods made it possible to achieve the defined development goals.

The fact that it can be used in numerous Volkswagen Group platforms and vehicles means that the MQ281 can realize its full potential concerning CO_2 reduction. Depending on the relevant engine-transmission combination, a reduction of up to 5 g of CO_2/km can be achieved, which means that the MQ281 can make a considerable contribution to reducing whole-fleet fuel consumption.

With the option for a mild hybrid plus application, as well as its compatibility with four-wheel drive applications, the MQ281 is ready for the future and simultaneously meets all requirements concerning economic feasibility, comfort, and sportiness.

https://doi.org/10.51202/9783181023549 - Generiert durch IP 216.73.216.36, am 19.01.2026, 02:19:31. © Urheberrechtlich geschützter Inhalt. Ohne gesonderte Erlaubnis ist jede urheberrechtliche Nutzung untersagt, insbesondere die Nutzung des Inhalts im Zusammenhang mit, für oder in KI-Systemen, KI-Modellen oder Generativen Sprachmodellen.

https://doi.org/10.51202/9783181023549 - Generiert durch IP 216.73.216.36, am 19.01.2026, 02:19:31. © Urheberrechtlich geschützter Inhalt. Ohne gesonderte Erlaubnis ist jede urheberrechtliche Nutzung untersagt, insbesondere die Nutzung des Inhalts im Zusammenhang mit, für oder in KI-Systemen, KI-Modellen oder Generativen Sprachmodellen.

Efficiency improvements in transmissions using new latching technologies in clutch & hydraulic actuation systems

Dipl.-Ing. **Alexander Moser**, Dr.-Ing. **Friedrich Brezger**,
BorgWarner Drivetrain Engineering GmbH, Ketsch

Kurzfassung

Effizienzsteigerungen im Antriebsstrang werden durch Systemoptimierung wie auch Optimierungen an einzelnen Komponenten weitergetrieben. Mit fortgeschrittener Entwicklung stehen die zu erreichenden Potenziale und deren notwendigen Aufwände meist in ungünstigerem Verhältnis. In diesem Paper werden neue Entwicklungen an Kupplungs- und Bremssystemen in PKW-Getrieben skizziert, Ihre Aufwände diskutiert und ihre Potenziale aufgezeigt. Beispielsweise erfordern die verschiedenen Anforderungen an die Kupplungen und Bremsen bestimmte Umsetzungen, die nach Ihrer Optimierung eine Mindest-Leistungsaufnahme erfordern. Die wichtigsten Anforderungen sind die gute Regelbarkeit und Fail-Safe-Funktion. Die Regelbarkeit wird unter anderem durch die Nutzung weiter Kraftbereiche und damit hydraulischen Drücken bei nasslaufenden Systemen erreicht, die typischerweise Druckbereiche von 9 bis zu 20 bar nutzen. Je nach Triebstranglayout muss die Fail-Safe-Funktion in der Kupplung realisiert werden, was üblicherweise durch ein aufrecht Halten des Druckniveaus in der geschalteten Betriebssituation realisiert wird.

Durch neue hydraulische Architekturen und Betriebsstrategien, sowie durch die Integration neuer Funktionen in die hydraulischen Pfade können weiterhin diesen Anforderungen Rechnung getragen und gleichzeitig weitere Energieeinsparpotentiale gehoben werden. BorgWarner arbeitetet an Systemen und Komponenten, um die restlichen Potenziale bei gleichzeitig gewohnter oder erweiterter Funktionsumfänge zu heben. Verschiedene Systeme, wie elektrifizierte Pumpen, Druckspeicher, optimierte Kupplungsaktorik und arretierbare Systeme werden vorgestellt und Ihre Potenziale anhand von Referenzzyklen aufgezeigt. Für ausgewählte Konzepte werden die Umsetzung und der Machbarkeitsnachweis erster Prototypen vorgestellt und die Messergebnisse diskutiert. Zusammenfassend wird ein Ausblick gegeben, welche Effizienzverbesserungen in modernen Triebsträngen erreicht werden können.

https://doi.org/10.51202/9783181023549 - Generiert durch IP 216.73.216.36, am 19.01.2026, 02:19:31. © Urheberrechtlich geschützter Inhalt. Ohne gesonderte Erlaubnis ist jede urheberrechtliche Nutzung untersagt, insbesondere die Nutzung des Inhalts im Zusammenhang mit, für oder in KI-Systemen, KI-Modellen oder Generativen Sprachmodellen.

Abstract

Efficiency improvements in drive trains are continued by system optimization and single component optimization. The ratio between achievable potentials and their necessary efforts often gets worse with further development. In this paper new developments of clutch and brake systems in passenger car drivetrains are outlined and their efforts discussed as well as their potentials illustrated. As an example different demands on clutch and brake systems need specific implementations which still bear a minimum of necessary power demand after optimization. The most important demands are controllability and fail-safe-functionalities. The simple controllability is achieved amongst other things by using wide force ranges and therefore wide pressure ranges in lubricated systems which are typical at 9 to 20 bar. Depending on drive train layouts a fail-safe-functionality must be implemented in clutches, which is usually achieved by maintaining the pressure level in clutch actuator in the engaged operating situation.

By introduction of new hydraulic architectures and operating strategies as well as by integration of new functionalities in hydraulic paths this demands can be fulfilled and efficiency potentials can be raised at the same time. BorgWarner is developing systems and components in order to raise these potentials and maintaining or even adding further functions. Different systems like electrified pumps, hydraulic accumulators, optimized clutch actuation and latching devices are introduced and their potentials are shown with help of simulation in reference cycle. For selected concepts the implementation and their feasibility study with first prototypes are presented and measurement results are discussed. As a summary an outlook is given showing the possible efficiency improvements in modern drive trains.

Introduction

The current situation of the automotive industries demands research for more efficient alternatives and at the same time, it is an enabler for this efforts since there are defined fines on exceeding CO_2 limits, too. The possible solutions for more efficient drivetrains are growing bigger at the same time. In addition to the various approaches of transmission types such as Dual Clutch Transmissions (DCT), Continuously Variable Transmissions (CVT), Automatic Transmissions (AT) and Automated Manual Transmissions (AMT), the number of individual technical solutions providing functions in series production safely rises. By taking the electrification into account the solution space grows even bigger. For future vehicles it will be important to recognize the potentials of different systems very early. The technologies must be devel-

https://doi.org/10.51202/9783181023549 - Generiert durch IP 216.73.216.36, am 19.01.2026, 02:19:31. © Urheberrechtlich geschützter Inhalt. Ohne gesonderte Erlaubnis ist jede urheberrechtliche Nutzung untersagt, insbesondere die Nutzung des Inhalts im Zusammenhang mit, für oder in KI-Systemen, KI-Modellen oder Generativen Sprachmodellen.

oped sustainably to be able to reuse the enormous development efforts for a plurality of products. Especially when looking at future use of Electric Vehicles (EV) these electric drive trains are pointing to a need of multispeed transmissions. The design of DCTs may have a special meaning since they are interesting for not only Hybrid but also Electric Vehicles since they shift smoothly and efficient. They can interact with the dynamics of electric motors easily. BorgWarner develops components in order to raise energy efficiency by using the systemic potentials. In the following chapters the new components are introduced and they are examined in interaction with the driver, vehicle and environment.

Dual Clutch Transmissions and improvements in hydraulic architecture

Overview

As shown in numerous publications a dual clutch transmission consists of two transmissions responsible for either all even or odd gears. With overlap shifts the power flow changes from one to the other part of transmission. In both Hybrid or conventional vehicle, the DCT utilizes a hydraulic pump for actuation of the clutch and shift forks, which converts mechanical power into hydraulic one. Conventional vehicles and also different EV drive trains with multispeed transmissions are using this technique. The pump generates the so-called system pressure, which is usually controlled on different pressure levels depending on the operating condition of the vehicle. Therefore, an arrangement of valves and solenoids is necessary to adapt the pressure level to the awaited demands at different hydraulic power consumers. Usually, the clutches are implemented as “normally open”, which means, that they are only engaging with applied pressure. If the pressure in the clutch actuator drops, they disengage. This implementation is a consequence of a Fail-Safe-Strategy of the whole drive train. Depending on the remaining architecture the clutch could also be implemented as “normally closed” that means, it is a pressure necessary to disengage the device, otherwise it has full torque capacity. In a hybridized DCT there can be a third clutch implemented to disengage the drive train from the combustion engine. Fig. 1 shows a “triple clutch” arrangement with electric engine for a P2 hybrid.

https://doi.org/10.51202/9783181023549 - Generiert durch IP 216.73.216.36, am 19.01.2026, 02:19:31. © Urheberrechtlich geschützter Inhalt. Ohne gesonderte Erlaubnis ist jede urheberrechtliche Nutzung untersagt, insbesondere die Nutzung des Inhalts im Zusammenhang mit, für oder in KI-Systemen, KI-Modellen oder Generativen Sprachmodellen.



Fig. 1: P2-hybrid module, containing power electronics, dual clutch + disconnect clutch [Cha17]

Further consumers of hydraulic power are for example the actuators for gear shifts itself. The lubrication of gears and bearings as well as cooling for clutch disks demands a noticeably volume flow, which is typically part of the hydraulic system. Here, bigger volume flows with a small maximal pressure (e.g. ~3 bar – 5 bar) are necessary. In order to actuate a clutch, a piston is either located at the rotating shaft or it is situated stationary in the transmission housing applying force and travel with a so-called engage bearing. The system pressure is controlled by a combination of a pilot solenoid and downstream valve. These ensure an pressure level adapted to the torque demands by the operating condition of the vehicle. By lowering pressure and limiting flow the hydraulic circuit already improves efficiency. In a hybrid, the transmission fluid pump could be either permanent driven by the input shaft of the transmission, or the pump is driven by a small electric motor which allows the pump speed to operate independently from the transmission speed.

DCT Hydraulic Architectures Improving Efficiency

In hydraulic systems, there are several hydraulic and mechanic power losses and some approaches to reduce them. BorgWarner investigated several approaches and shows improvements by new system architectures as well as including new components, too. [Guo15]

https://doi.org/10.51202/9783181023549 - Generiert durch IP 216.73.216.36, am 19.01.2026, 02:19:31. © Urheberrechtlich geschützter Inhalt. Ohne gesonderte Erlaubnis ist jede urheberrechtliche Nutzung untersagt, insbesondere die Nutzung des Inhalts im Zusammenhang mit, für oder in KI-Systemen, KI-Modellen oder Generativen Sprachmodellen.

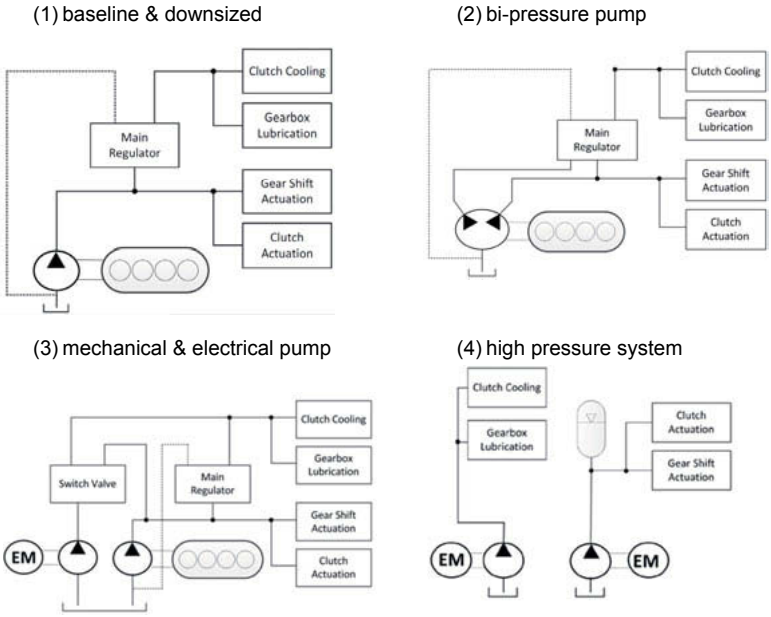


Fig. 2: Alternative actuation architectures for DCTs: (1) conventional baseline as well as downsized pump; (2) Bi-Pressure pump; (3) one electrical and one mechanical pump; (4) high pressure system with two independent, electrically driven pumps [Guo15]

A summary of results of alternative actuation systems in a DCT is given: (1) the baseline 16.5 cc/rev , as well as a downsized pump 12.6 cc/rev; (2) Bi-Pressure pump architecture 12.6 cc/rev; (3) one electrical pump 1.7 cc/rev and one mechanical pump 7.1 cc/rev; (4) Two pump system whereas one pump is a high pressure system charging an accumulator, which provides the pressure for actuating clutches and gear shifts as shown in Fig. 2. All these proposals are simulated at reference vehicle parameters in WLTC and show good effects on energy savings compared with the baseline.

The fourth example in Fig. 2 was also built up in a Demo-Car and improvements shown [Mos11]. Therefore, a whole independent system was integrated like shown in Fig. 3.

https://doi.org/10.51202/9783181023549 - Generiert durch IP 216.73.216.36, am 19.01.2026, 02:19:31. © Urheberrechtlich geschützter Inhalt. Ohne gesonderte Erlaubnis ist jede urheberrechtliche Nutzung untersagt, insbesondere die Nutzung des Inhalts im Zusammenhang mit, für oder in KI-Systemen, KI-Modellen oder Generativen Sprachmodellen.

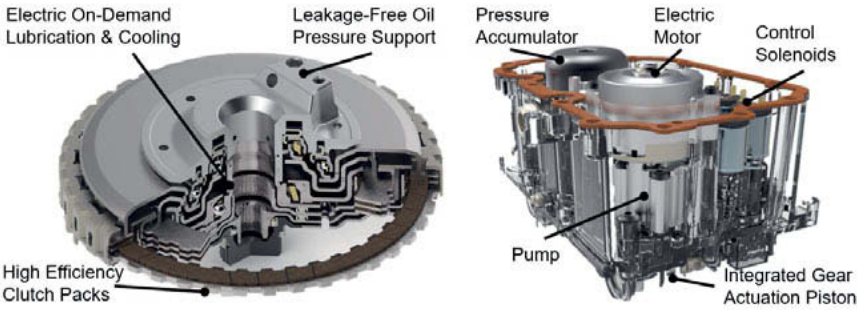


Fig. 3: High pressure actuated dual clutch with engage bearings; right: hydraulic system containing pump, electric motor, solenoids and accumulator [Mos11]

As shown in the high pressure application, there are engage bearings used, because here the hydraulic actuator can be implemented as practically sealed. This technique is also common in usual pressure levels. Here, the leakage losses of an oil feed are avoided totally, but the friction losses are present, too. The friction losses are not only geometry and lubrication dependent but also force and speed dependent. The friction torque of one engage bearing in a proper designed gearbox at “normal” operating conditions can be estimated as 0.1 – 0.5 Nm. But there is a further bearing inside the clutch closing the axial force flow and this is therefore higher loaded compared to the existing one included in a clutch system with oil feed, see Fig. 3.

The oil feeds of clutches are designed with so-called rectangular seals. There are many investigations about their leakage and friction behavior, as for instance FVA 678 [Pol15]. The friction torques are dependent of diameter, relative speeds, differential pressures (left and right side), material, geometric design, surfaces and further influences. Typical friction torques at oil feeds in passenger cars are around 0.4 – 2.3 Nm and leakage around 0.03 – 0.25 l/min for one pressure channel (2x rectangular seals).

Introduction of New Components in Clutch Systems

Changing hydraulic architecture shows already good improvements. For even further systemic improvement also the components can be advanced in that manner, that still the transmission control unit strategies are working the same way by keeping pressure levels and actuation characteristics. Only slightly changes in architecture are necessary. The following chapters are describing the “Mechanical Latching Clutch”, the “Latching Hub” applicable for Clutch systems

https://doi.org/10.51202/9783181023549 - Generiert durch IP 216.73.216.36, am 19.01.2026, 02:19:31. © Urheberrechtlich geschützter Inhalt. Ohne gesonderte Erlaubnis ist jede urheberrechtliche Nutzung untersagt, insbesondere die Nutzung des Inhalts im Zusammenhang mit, für oder in KI-Systemen, KI-Modellen oder Generativen Sprachmodellen.

in arbitrary gearboxes actuated through an oil hub and the “Latching Valve” applicable for clutches using an engage bearing or brakes.

Mechanical Latching Clutch

The latching mechanism which was already introduced in [Bre17] uses a principle which involves force-displacement characteristics of Belleville springs. Using an asymmetric snap ring and ramp in the clutch housing, a kind of detent mechanism is established. After reaching the engaged condition of the multidisc clutch, the latching mechanism is activated by slightly increasing the pressure further and the slotted ring is pushed into a detent groove. At this point the pressure required to hold the clutch at full torque carrying capacity can be reduced as the detent contributes to the clamping load. Pressure is only required to keep the snap ring in the detent groove. Force magnification depends on the angles formed by the components involved. To avoid high oil pressures, the near constant force portion of the spring’s characteristic curve is used, as shown in the ‘engaged’ cross-section of the diagram in Fig. 4.

CVTs are also a prime candidate for BorgWarner’s development work. Although the high pressure circuit for the chain transmission is not changed, the savings for a typical mid-sized car of 53.9 W hydraulic power and 26.9 W mechanical power can be achieved if the FWD clutch and the torque converter lockup clutch are latched. [Bre17] Doing so, reduces pressure to 3 bar which is, in any case, necessary for lubrication. This equates to about 1.75 gCO_2/km in a representative customer cycle. The solution also provides for failsafe applications since the latching clutch disengages completely when pressure is further lowered. The test bench results with prototypes verify simulations and dimensioning calculations as well as endurance runs of 500’000 shifts.

https://doi.org/10.51202/9783181023549 - Generiert durch IP 216.73.216.36, am 19.01.2026, 02:19:31. © Urheberrechtlich geschützter Inhalt. Ohne gesonderte Erlaubnis ist jede urheberrechtliche Nutzung untersagt, insbesondere die Nutzung des Inhalts im Zusammenhang mit, für oder in KI-Systemen, KI-Modellen oder Generativen Sprachmodellen.

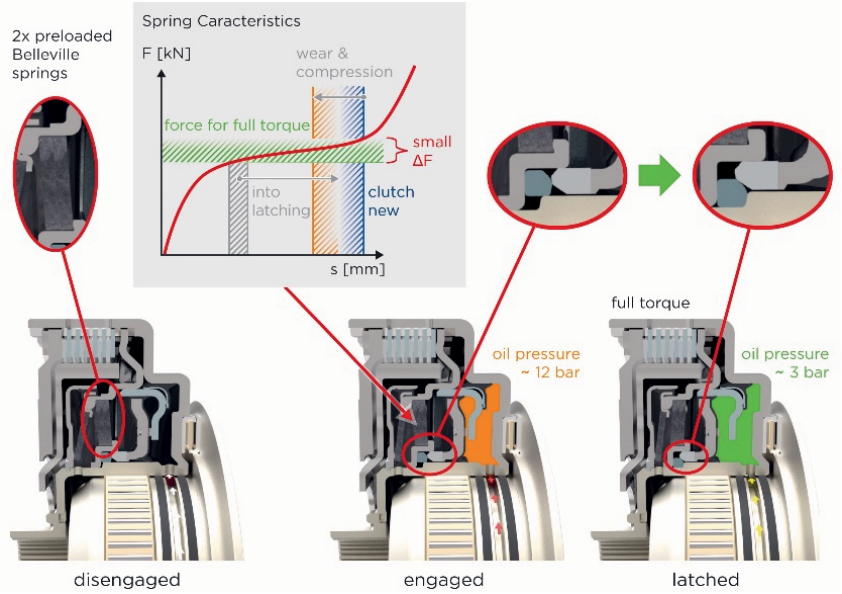


Fig. 4: CAD Cross section of Mechanical Latching Clutch with 3 operating conditions: disengaged, engaged & controllable torque capacity, latched and hold with low pressure [Bre17]

Latching Hub

Description and Function

As shown in the state of art power reduction potentials are raised by reduction of system pressure which results in primary and secondary effects. Primary effect is less conversion of mechanical power into hydraulic power. Secondary effects are evoked by less losses at oil feeds by reduction of friction and leakage. This leakages occurs not only at oil feed but also at all involved valves and solenoids, since there is less pressure difference to environment. BorgWarner therefore developed the so-called Latching Hub, which could be implemented design space neutral (depending on reference clutch). This Latching Hub is also capable of Fail-Safe-Feature like it is described now, see also Fig. 5:

https://doi.org/10.51202/9783181023549 - Generiert durch IP 216.73.216.36, am 19.01.2026, 02:19:31. © Urheberrechtlich geschützter Inhalt. Ohne gesonderte Erlaubnis ist jede urheberrechtliche Nutzung untersagt, insbesondere die Nutzung des Inhalts im Zusammenhang mit, für oder in KI-Systemen, KI-Modellen oder Generativen Sprachmodellen.

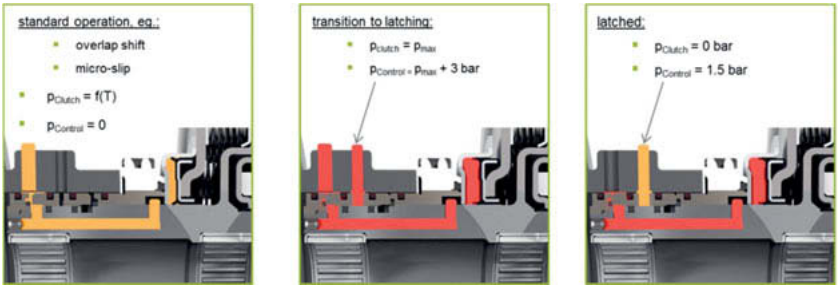


Fig. 5: Latching Hub in its 3 operating states: left: deactivated; middle: transition to latching; right: latched

An additional oil channel is duct to the rotatory feedthrough, this channel is used to operate the so-called Control Pressure. If the control unit detects no further change in gear during driving, the clutch can be actuated shortly with its maximum pressure. The clutch gains its maximum torque capacity regardless whether needed or not. Almost simultaneously the Control Pressure is increased up to that maximum pressure and little further. Inside the oil feed, there are axial moveable rings. By having the Control Pressure at a higher level than the clutch pressure input the axial moveable ring is moved and covering the pressure input in the rotating shaft. Therefore an O-Seal is squeezed axially, ensuring total sealing of the rotating input. After that, the system applied clutch pressure is reduced to zero, the Control Pressure is reduced to 1.5 bar afterwards and the clutch and rotating shaft is still pressurized with maximum pressure. The clutch is latched and the losses of oil feed are drastically reduced to the level corresponding to 1.5 bar. In order to return to a controllable state, the clutch input pressure is just raised and Control Pressure is set to zero. Doing so, a no noticeable return to a torque controlled operating condition is made. Here, a slip controlled state or the next gear shift can be initiated. In an unlikely failure of the system the control pressure drops to zero. Because of the latched pressure within the shaft, the axial moveable ring uncovers the input and the oil pressure is released; the clutch disengages.

This system is presented at the example of dual clutch systems, but of course, also automatic transmissions can benefit from this function in its clutches and brakes as well as torque converter lock-up clutch. There are big advantages of this systems regarding the power savings and therefore a significant CO2 reduction. Looking closely at sportive vehicles, one can imaging to even raise the top speed slightly, too. There are primary and secondary effects when latching clutches is enabled. By reducing whole system pressure the pump does require less

https://doi.org/10.51202/9783181023549 - Generiert durch IP 216.73.216.36, am 19.01.2026, 02:19:31. © Urheberrechtlich geschützter Inhalt. Ohne gesonderte Erlaubnis ist jede urheberrechtliche Nutzung untersagt, insbesondere die Nutzung des Inhalts im Zusammenhang mit, für oder in KI-Systemen, KI-Modellen oder Generativen Sprachmodellen.

torque. At the same time all volume flows are reduced, since leakage losses are also decreasing since they are proportional to pressure level. Every valve and solenoid involved reduce their loss. A very big advantage occurs at the pressure reduction valve, which is responsible for lubrication and cooling. It does not need to reduce pressure in that dimension like before. At the rotatory feedthrough the leakage and friction sinks drastically. Less friction means direct mechanic energy saving in drive train. One example is given in Fig. 6 at typical dual clutch transmission using direct acting valves already:

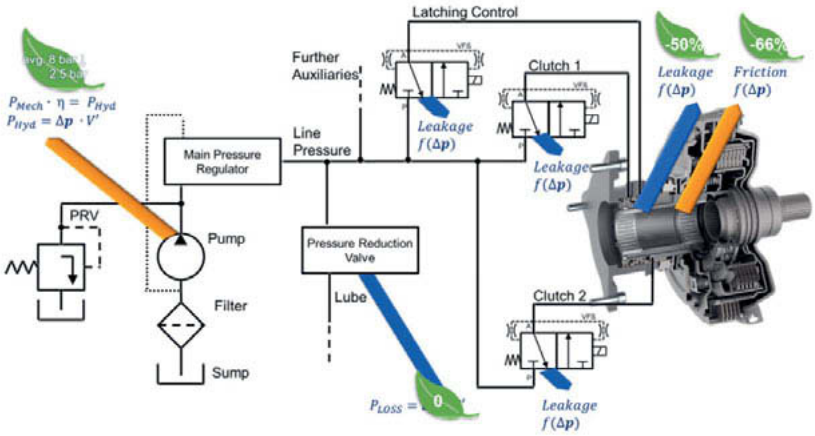


Fig. 6: Scheme of hydraulic architecture using Latching Hub and marked spots of savings (blue = leakage, orange = mechanical)

Depending on the reference cycle (NEDC; WLTC;) and hydraulic architecture as well as utilized components and therefore geometries, there can be savings between 136 W – 200 W compared to a conventional drive train layout.

Test Bench Measurement Results

In order to proof function in several operating conditions an example measurement of the first prototype is shown in Fig. 7. For observing the clutch torque capacity its input shaft and output shaft of clutch 1 is forced in different speeds. Here, a relative speed of 20 rpm is set at a total speed of 1000 rpm. There are four different areas visible: first, the clutch pressure can be arbitrary controlled. The transmitted torque (orange) follows proportional to the applied pressure(dark blue). This would be the case at low engine speeds of the vehicle in order to damp

https://doi.org/10.51202/9783181023549 - Generiert durch IP 216.73.216.36, am 19.01.2026, 02:19:31. © Urheberrechtlich geschützter Inhalt. Ohne gesonderte Erlaubnis ist jede urheberrechtliche Nutzung untersagt, insbesondere die Nutzung des Inhalts im Zusammenhang mit, für oder in KI-Systemen, KI-Modellen oder Generativen Sprachmodellen.

torque oscillations of combustion engine or during an overlap shift. Afterwards the pressure level is kept stationary in this example to observe the transmitted of torque level better. In second phase, the clutch pressure is raised to maximum and the Control Pressure to max +3 bar (light blue). The input pressure drops to zero afterwards and then Control Pressure is lowered to 2.5 bar. In third phase, this condition is kept over three minutes to watch curve. No significant drop is observed. That means the pressure within the clutch is kept and the whole rotating device is sealed properly. In last phase 4 the Fail-Safe-functionality is tested. Here, the control pressure is dropped to zero, simulating a system failure. The clutch disengages immediately as seen by torque drop.

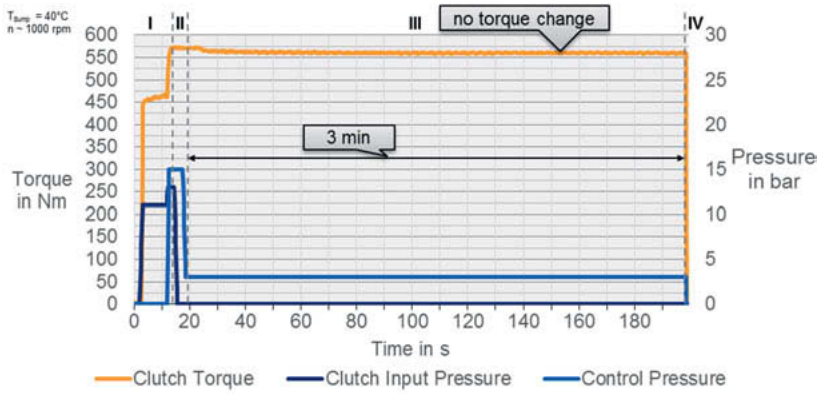


Fig. 7: Example measurement of the Latching Hub tested with BorgWarner Dual Clutch System

In regular operation condition, one would raise input pressure and drop control pressure in order to transit into a controlled mode, where pressure is proportional to transmitted torque again. In conclusion, the functional tests were all successful, now durability testing have to follow.

Latching Valve

Description and Function

As described in state of art, there are clutches actuated through engage bearings. Also here efficiency improvements are desired. For that application BorgWarner developed the so-called Latching Valve and it is firstly designed for dual clutches or dual brakes. Instead of utilizing an additional oil duct like the Latching Hub, the pressure of the opposite clutch or brake is used.

https://doi.org/10.51202/9783181023549 - Generiert durch IP 216.73.216.36, am 19.01.2026, 02:19:31. © Urheberrechtlich geschützter Inhalt. Ohne gesonderte Erlaubnis ist jede urheberrechtliche Nutzung untersagt, insbesondere die Nutzung des Inhalts im Zusammenhang mit, für oder in KI-Systemen, KI-Modellen oder Generativen Sprachmodellen.

Using new valves based on known working principles absolutely tight valve seats can be introduced. This mechanism allows dropping the pressure to zero after reaching an target latching pressure, which means a “locking” of hydraulic pressure. In the presented prototype no failsafe mechanisms are in place to disengage clutch or brake during a system failure. In order to open a latched valve again not only line pressure has to be re-raised but also a second control pressure is required. Ideally the control pressure for re-opening equals the kisspoint pressure of the second clutch or brake. Doing so, the pressure in the first latched clutch can be reduced as the pressure in the second clutch or brake is increased. The hydraulic circuit diagram according to [Pat15] is shown in Fig. 8, left. The cross sections of valves interacting is shown right.

Depending on the application, these hydraulic valves can be accommodated in the housing (provided at brakes or clutches with engage bearings). A positioning in front of a rotatory feedthrough is not possible, because these have leakage for function and production reasons. Excluding the variant with release bearings, all losses during steady state operation of the engaged clutch are eliminated by this concept. For the excluded variant with release bearings only the mechanical friction losses are still in place. Especially in future electric vehicle transmissions these arrangement of valves is highly effective. Since one can imagine, that one electrical pump is mainly supporting lubrication and only driven in overload mode, when shift intention is detected.

https://doi.org/10.51202/9783181023549 - Generiert durch IP 216.73.216.36, am 19.01.2026, 02:19:31. © Urheberrechtlich geschützter Inhalt. Ohne gesonderte Erlaubnis ist jede urheberrechtliche Nutzung untersagt, insbesondere die Nutzung des Inhalts im Zusammenhang mit, für oder in KI-Systemen, KI-Modellen oder Generativen Sprachmodellen.

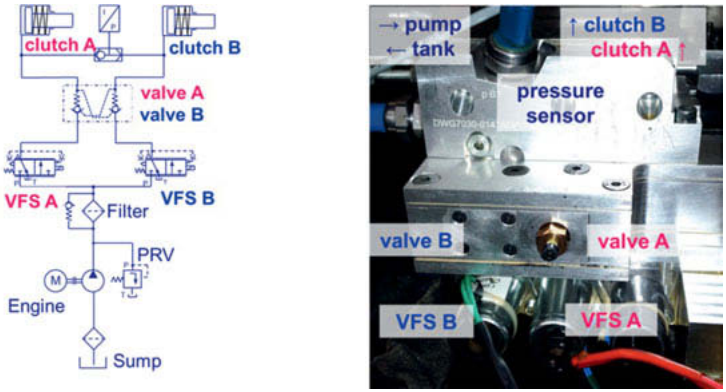


Fig. 8: Left: exemplary hydraulic architecture for a dual brake system using the Latching Valve [Pat15]; right: picture of testbed implementation

Test Bench Measurement Results

Like in the Latching Hub device before, the latched pressure is also dependent on the system which is installed. In order to have a very realistic setup, a dual brake of an EV transmission was used. In that transmission, the spring stiffness is very high and the compression of the friction plates is kept normal. Even in that ambitious application, the results look very promising as shown in Fig. 9.

Only 1.8 bar pressure difference between start of latching and end of latching is measured. Establishing a conservative estimation, presuming that the loss is only an effect of oil leakage and neglecting compression and setting of friction material, in this specific brake the loss would correspond to 0.005 ml/min.

https://doi.org/10.51202/9783181023549 - Generiert durch IP 216.73.216.36, am 19.01.2026, 02:19:31. © Urheberrechtlich geschützter Inhalt. Ohne gesonderte Erlaubnis ist jede urheberrechtliche Nutzung untersagt, insbesondere die Nutzung des Inhalts im Zusammenhang mit, für oder in KI-Systemen, KI-Modellen oder Generativen Sprachmodellen.

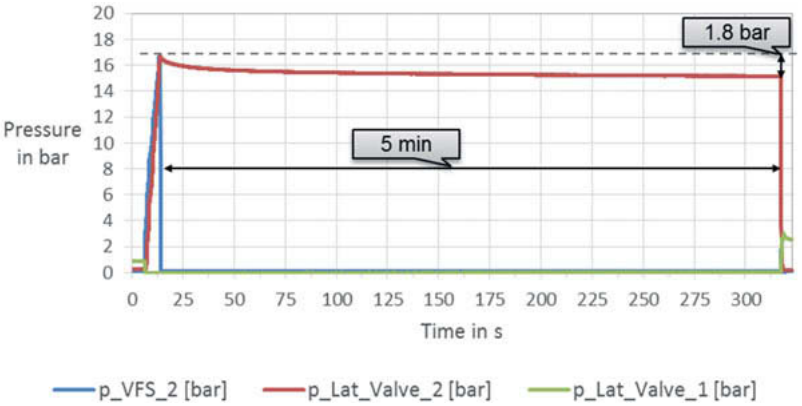


Fig. 9: Measurement results of first prototypes Latching Valves with a stiff double brake for EV transmissions

Efficiency Improvements per Application DCT, AT, EV

Baseline DCT Power Savings with Latching Hub

Simulating the 7speed DCT transmission of a car in D-segment in WLTC with 350 Nm engine, the benefits of latching can be calculated. The model without latching is verified by various testing. The simulation model is adapted to latching by reducing the pressure demand after a shift immediately and raising the pressure before next shift again. Therefore the line pressure is reduced in latching mode to 2 bar, which is used for lubrication purpose. Here the typical slip operation of clutches underneath 2.000 rpm of combustion engine is neglected. In order to do that in an actual car, new damping- / isolation devices like the BorgWarner Variable Spring Absorber (VSA) becomes necessary. Taking a standard gear pump (16cc/rev) and standard oil feeds into account, the average power advantage using latching in the whole WLTC class 3 is 115 W which equals roughly 2.01 gCO_2/km. Using the downsized pump (12cc/rev) as proposed in [Guo15] there are savings of 100 W possible.

Two Pumps & Bi-Pressure Pump DCT with Latching Hub

Looking closely at the two proposed hydraulic architecture improvements in [Guo15], using two different pressure circuits as shown in Fig. 2, picture 2 & 3 utilizing a two port pump (bi-pressure) or two pumps, one can calculate following power demands for a vehicle in D-segment in WLTC: The bi-pressure pump system has a power demand of 233 W and could be

https://doi.org/10.51202/9783181023549 - Generiert durch IP 216.73.216.36, am 19.01.2026, 02:19:31. © Urheberrechtlich geschützter Inhalt. Ohne gesonderte Erlaubnis ist jede urheberrechtliche Nutzung untersagt, insbesondere die Nutzung des Inhalts im Zusammenhang mit, für oder in KI-Systemen, KI-Modellen oder Generativen Sprachmodellen.

decreased by 82 W. The two pump system using one mechanical and one electrical pump has a power demand of 207 W and can be decreased by 78 W.

DCTs with Pressure Accumulator Savings Utilizing Latching Valve

Using the introduced mid or high pressure architecture with two separate pumps, the Latching Valve can additional improve the efficiency slightly. It helps decreasing the leakage of the flow solenoid in the accumulator. In [Guo15] it has been shown that a vehicle of D-segment demands a mechanical power off 127 W when introducing an accumulator and an electrical pump. By utilizing the latching valve it can be reduced by 70 W. If the very efficient high pressure system is used, it has been shown, that there is an average power demand of only 90 W. Latching can improve only a little, since the accumulator and the stationary piston are already pretty dense. With Latching valve , the power demand is reduced only by 10 W.

Electric Vehicle with 2-Speed Transmission Utilizing Latching Mechanism

Since there is no clear trend of EV transmission architectures yet, the following generic example is introduced. Assuming the two gears are used in same frequency and engaged with clutches. That means, one clutch is engaged 50% of time using an average normal force of 6.5 kN (corresponding to 7 bar pressure) at an average speed of 1700 rpm. In the other amount of time the clutch is disengaged and its average input speed is 2400 rpm.

Engaging the clutch with engage bearings, one can make a rough, linearized approach. Because of the preload of engage bearings there is also a noticeable loss during disengaged operating condition. In sum, the average mechanical losses are around 50 W. In addition, the pump needs to maintain the average of 7 bar during engaged mode. This power consumption can be reduced to almost zero when using Latching Valve, keeping the clutch piston sealed at highest torque capacity.

Using a rotatory oil feed instead the same operating condition distribution applies. Here, the mechanical power loss at the oil feed can be calculated to an average of 71 W. As well as in the example above, the pump power demands are on top. But now, introducing the Latching Hub, the mechanical loss drops to 34.5 W. Additionally, the pump needs to maintain at least 1.5 bar to keep the latching hub in sealed condition in difference to the before mentioned Latching Valve with engage bearings.

In general, there is no conclusion possible, which approach may be better; a close look at the installed pump and hydraulic architecture is necessary, because there will always be a low pressure level necessary for gear lubrication. However, energy improvements with latching devices are possible in noticeable manner.

https://doi.org/10.51202/9783181023549 - Generiert durch IP 216.73.216.36, am 19.01.2026, 02:19:31. © Urheberrechtlich geschützter Inhalt. Ohne gesonderte Erlaubnis ist jede urheberrechtliche Nutzung untersagt, insbesondere die Nutzung des Inhalts im Zusammenhang mit, für oder in KI-Systemen, KI-Modellen oder Generativen Sprachmodellen.

Conventional Automotive Using Latching Valve & Latching Hub

In modern ATs there are various clutches and brakes to provide different ratios with a smart nesting of planetary gear sets. The clutches enable a convenient uninterrupted shifting during acceleration. In conventional vehicles there is a trend to even higher number of gears. One example is the presented 9HP gearbox by ZF [Fis12]. It includes 4 multi-disk clutch systems where two of them are designed as brakes. Furthermore, in this special example two dog clutches are integrated. This type of transmission needs a hydraulic system for shifting and usually also for keeping selected gears engaged (except dog clutches). Currently many common automatic transmissions have 8 gears and 5 clutches designed as lubricated multi-disc clutches. These clutches utilize mainly rotatory feedthroughs for actuation. In a typical 8-speed automatic gearbox with 5 shift elements there are 3 clutches and 2 brakes; all are designed as lubricated multidisc clutches. Driving the WLTC one can determine that all clutches are actuated round about 60% of the time. The average pressures reach from 3.5 to 6.5 bar, since the demanded torques are relatively low compared to possible torques of a D/F-segment vehicle. Even in this case are significant savings possible when there is a device reducing demanded pressure to 1 or 3 bar. Following table 1 shows results in WLTC class 3 cycle compared to a baseline without additional pressure reduction devices. It is also analyzed the case when only one of the 3 clutches can be operated with reduced pressure.

Table 1: Power saving potentials of a vehicle with 8 speed gearbox in WLTC when clutches can be latched at different pressure levels or only a single clutch is latched at 1 bar [Bre17]

WLTC class 3, D/F class		all clutches latched		1 clutch latched @1bar		
		1 bar	3 bar	C	D	E
equivalent CO_2	gCO_2/km	4.5	3.5	1.1	1.5	1.8
mech. power	W	256.8	199.4	64.1	84.2	105.4

P2-Hybrids Using Multidisk Disconnect Clutch

The disconnect clutch is kept engaged during Combustion Engine (CE) supported drive. This is also certification relevant, since the cycles are driven with loaded and unloaded battery levels. A typical automatic transmission with a P2 Hybrid Module in front is shown in Fig. 10. The disconnect clutch is nested inside the electrical motor. In order to gain additional savings in EV

https://doi.org/10.51202/9783181023549 - Generiert durch IP 216.73.216.36, am 19.01.2026, 02:19:31. © Urheberrechtlich geschützter Inhalt. Ohne gesonderte Erlaubnis ist jede urheberrechtliche Nutzung untersagt, insbesondere die Nutzung des Inhalts im Zusammenhang mit, für oder in KI-Systemen, KI-Modellen oder Generativen Sprachmodellen.

driving mode, a clutch with less disks for less drag torque should be chosen, but at the same time the applied forces in engaged mode raise since the clutch pack needs to transmit high torques from the combustion engine. Here, the latching mechanism helps saving energy.

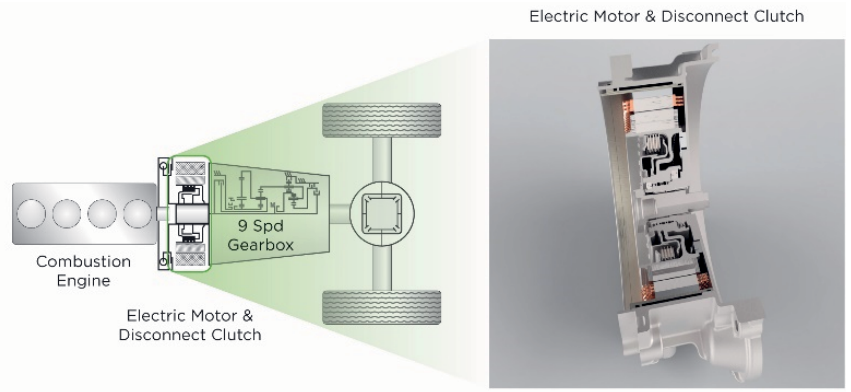


Fig. 10: Left: Scheme of a P2-Hybrid with a 9-speed automatic transmission; right: a P2-Module concept with disconnect clutch inside the electric motor [Bre17]

Simulating such a disconnect clutch with and without latching functionality in WLTC of a car in D/F-segment with a direct connected gear pump for whole system shows Fig. 11. Here the pressure of disconnect clutch is not adapted to torque, it keeps maximum torque capacity. I can be shown that the average power demand of this functionality drops from 110 W to 36 W.

https://doi.org/10.51202/9783181023549 - Generiert durch IP 216.73.216.36, am 19.01.2026, 02:19:31. © Urheberrechtlich geschützter Inhalt. Ohne gesonderte Erlaubnis ist jede urheberrechtliche Nutzung untersagt, insbesondere die Nutzung des Inhalts im Zusammenhang mit, für oder in KI-Systemen, KI-Modellen oder Generativen Sprachmodellen.

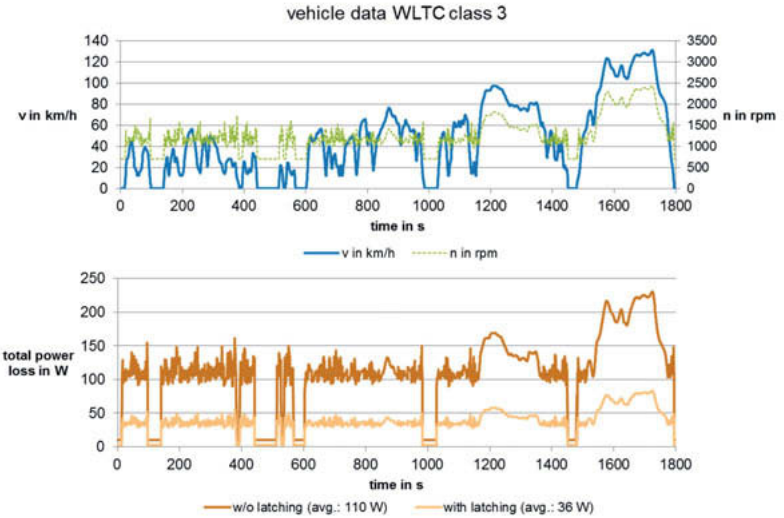


Fig. 11: Vehicle speed and engine speed in WLTC3 of hybrid with 9speed gearbox; bottom: summed hydraulic & mechanical power losses when pressure adapted to torque (w/o latching) and when engaged with only 1.5 bar (with latching) [Bre17]

Summary and Outlook

First, four different approaches in hydraulic architecture were introduced, improving the energy efficiency in DCTs. The results of different improvements of DCTs as well as of typical AT and CVT FWD clutch can be seen in comparison in Table 2. Afterwards the BorgWarner Latching mechanisms, namely: Mechanical Latching Clutch, Latching Hub and Latching Valve were introduced and their usage in drivetrain application was explained. The prototype tests were successfully demonstrating the functioning. This improvements were added to verified simulation model to see their effect in total vehicle applications, the results are also shown in Table 2. Since the Latching mechanisms are suitable for different transmission and drive train topologies a further evaluation of their power consumption improvements are shown. Since there are alternatives in improving the baseline for each application a good effort-saving-ratio can be calculated.

https://doi.org/10.51202/9783181023549 - Generiert durch IP 216.73.216.36, am 19.01.2026, 02:19:31. © Urheberrechtlich geschützter Inhalt. Ohne gesonderte Erlaubnis ist jede urheberrechtliche Nutzung untersagt, insbesondere die Nutzung des Inhalts im Zusammenhang mit, für oder in KI-Systemen, KI-Modellen oder Generativen Sprachmodellen.

Table 2: Power improvements in Watt in respect to the different drive trains of a D-segment vehicle in WLT

Power [W] WLTC	DCT conv.	DCT opt	DCT bi-pres.	DCT mech. + e.pump	DCT on-demand	AT (8spd)	CVT	Hybrid C0
Latching improvement	Δ 115	Δ 100	Δ 82	Δ 78	Δ 10-70	Δ 257	Δ 100	Δ 74
gCO2/100km reduction	2.02	1.75	1.44	1.37	0.18 - 1.23	4.5	1.75	1.29

Literature

[Aoy14] Aoyama, T., Takahara, H., Kuwabara, S., Miyata, H. et al., „Development of New Generation Continuously Variable Transmission" SAE Technical Paper 2014-01-1728. 2014

[Aud09] Audi of America, LLC: “Service Training; Audi new Technology 2009-2010” © 2009 Audi of America, LLC

[Bre17] Brezger, F.; Moser, A.: “Latching clutches in different drivetrains improve efficiency” in 6th International Congress and Expo CTI Symposium, China, company BorgWarner in Shanghai. 2017

[Cha17] Chamberlin, B.; Gold, E.: „HEV P2 Module Concepts for Different Transmission Architectures Clutch and E-motor Options” in 6th International Congress and Expo CTI Symposium China, company BorgWarner in Shanghai. 2017

[Eng04] Englisch, A.; Faust, H.; Homm, M.; Teubert, A.; Vornehm, M.: „High Performance CVT Components“. International Continuously Variable Transmission Conference. 2004

[Fis12] Fischer, Manfred; Greiner, Jürgen; Ebenhoch, Michael; Scherer, Heribert; Girres, Gaston: „Prepared for the future – the new nine speed automatic transmission for transverse installation”. Presented at the CTI Annual Congress on 05, 22, 2012

[Guo15] Guo, C.; Semenov, D.; Moser, A.; Spangler, C.: Comparison of DCT Actuation Systems – an evaluation of system efficiency and cost” in 4th International Congress and Expo CTI Symposium China, von Firma BorgWarner in Shanghai. 2015

https://doi.org/10.51202/9783181023549 - Generiert durch IP 216.73.216.36, am 19.01.2026, 02:19:31. © Urheberrechtlich geschützter Inhalt. Ohne gesonderte Erlaubnis ist jede urheberrechtliche Nutzung untersagt, insbesondere die Nutzung des Inhalts im Zusammenhang mit, für oder in KI-Systemen, KI-Modellen oder Generativen Sprachmodellen.

[Luy13] Lu, Y.; Liu, M.; Liu, Y.: „Modeling and Simulation of a New Type Hydraulic System on CVT". SAE-China and Fisita (eds.) Proceedings of the FISITA 2012 World Automotive Congress. DOI 10.1007/978-3-642-33744-4_31. © Springer-Verlag Berlin Heidelberg 2013.

[Mos11] Moser, A.; Saxena, V.; Schaefer, M.; Ritschel, M.: „ Insight on Wet Clutch Efficiency" In 10th International Congress and Expo CTI Symposium Germany, von Firma BorgWarner in Berlin. 2011

[Pat15] Offenlegungsschrift Deutsches Patent- und Markenamt: DE 10 2013 012 538 A1 2015.01.29

[Pol15] Poll, G.; Schüller, M: „Optimierung und Reibungsreduktion von Drehdurchführungen" in FVA 678 I Forschungsreport 2015, Abschlussbericht. 2015

[Spa14] Spangler, C.; Waterstredt, J.: „Accumulator Technology for Automatic Transmission Stop-Start Readiness". In 13th International Congress and Expo CTI Symposium Germany, von Firma BorgWarner in Berlin. 2014

https://doi.org/10.51202/9783181023549 - Generiert durch IP 216.73.216.36, am 19.01.2026, 02:19:31. © Urheberrechtlich geschützter Inhalt. Ohne gesonderte Erlaubnis ist jede urheberrechtliche Nutzung untersagt, insbesondere die Nutzung des Inhalts im Zusammenhang mit, für oder in KI-Systemen, KI-Modellen oder Generativen Sprachmodellen.

Flexible Oil Management for Dual-clutch Transmissions

Dipl.-Ing. **M. Bahne**, Dr.-Ing. **A. Wiesebrock**,
Magna Powertrain Transmission Systems, Untergruppenbach

Zusammenfassung

Über die Fahrzeuglebensdauer hinweg betrachtet sind variable Wartungsintervalle ein Schlüssel, weniger Kosten, Gewicht zu generieren und Ressourcen zu schonen. Das flexible Schmierölmanagement von Magna Powertrain und BMW ist für automatisch geschaltete Getriebe konzipiert. Es berücksichtigt das wirkliche Fahrerverhalten und ermöglicht geringere Ölfüllmengen sowie längere Ölwechselintervalle.

Abstract

Over the lifetime of a vehicle, variable service intervals are one key to decrease costs, lighten weight, and save resources. The flexible lubrication oil management by Magna Powertrain and BMW is created for automatically shifted transmissions. It is based on real driver's behavior and enables smaller oil fill volumes as well as extended oil change intervals.

Why flexible oil change intervals?

Usual fixed-service intervals for automatically shifted transmissions are intended for loads [1] that most drivers hardly ever come close to. This approach ensures safety margins for use cases like regular trailer operation, high heat, humidity, demanding topography, and very sporty drivers. The drawback is that the transmission oil fill volume is over-dimensioned for average drivers, thus increasing weight, CO2 emissions and service costs. On-demand oil management [2] offers advantages, especially for automatic transmissions that use wet clutches. Manual transmissions for passenger cars, usually with dry clutches, need just approximately 1.5 l oil for wheel set lubrication as life-time operation. In automatic transmissions, life-time oil filling would increase weight and consequently fuel consumption. Another reason why flexible oil intervals become more relevant is that engine torques have risen about 35 % through the last 15 years. This effectively means many car drivers are pushing the load limits of their powertrains to an even less extent. A prerequisite for a flexible oil management is to know the lubrication oil condition as precisely as possible. Such a management, developed by Magna Powertrain and BMW for dual-clutch transmissions, is based on an advanced load

https://doi.org/10.51202/9783181023549 - Generiert durch IP 216.73.216.36, am 19.01.2026, 02:19:31. © Urheberrechtlich geschützter Inhalt. Ohne gesonderte Erlaubnis ist jede urheberrechtliche Nutzung untersagt, insbesondere die Nutzung des Inhalts im Zusammenhang mit, für oder in KI-Systemen, KI-Modellen oder Generativen Sprachmodellen.

monitoring and damage prediction models. They enable reduced oil fill volume and extended change intervals for most car drivers.

Extended oil change intervals

FIGURE 1 illustrates typical oil change intervals as well as the advantages of the flexible oil management. The consideration includes the typical intervals of transmissions types like Torque-converter Automatic Transmissions (ATs), Continuous Variable Transmissions (CVTs) and Dual-clutch Transmissions (DCTs) for a Front Wheel Drive (FWD). The shaded upper part of the AT column in FIGURE 1 (left) represents transmissions with a claimed lifetime filling for normal drivers, being assumed for 240.000 km in this illustration. At higher loads (“hard” drivers), however, ATs require an earlier oil change. Regarding the range up to the next oil change in relation to the oil fill volume,

the AT performs best, and the CVT and DCT are second on a similar level. The AT´s advantage is primarily based on the hydrodynamic torque converter that does not have to handle frictional power. However, thanks to the flexible oil management and a specifically optimized oil, the 7DCT300 by Magna Powertrain is on par with the best ATs. FIGURE 1 (right) shows the required oil fill volume of these three types. The 7DCT300 needs significantly less oil fill volume compared to the best ATs. The flexible oil management has been in series use since 2017. Typical oil change intervals are between 60,000 and 125,000 km. BMW succeeded in extending oil change intervals by approximately 50 %, while reducing the oil fill volume by 35 % compared to mean values of DCTs. A large majority of car owners profit from the flexible oil management. Just a small minority of “hard” drivers must accept shorter change intervals like usual DCTs.

https://doi.org/10.51202/9783181023549 - Generiert durch IP 216.73.216.36, am 19.01.2026, 02:19:31. © Urheberrechtlich geschützter Inhalt. Ohne gesonderte Erlaubnis ist jede urheberrechtliche Nutzung untersagt, insbesondere die Nutzung des Inhalts im Zusammenhang mit, für oder in KI-Systemen, KI-Modellen oder Generativen Sprachmodellen.

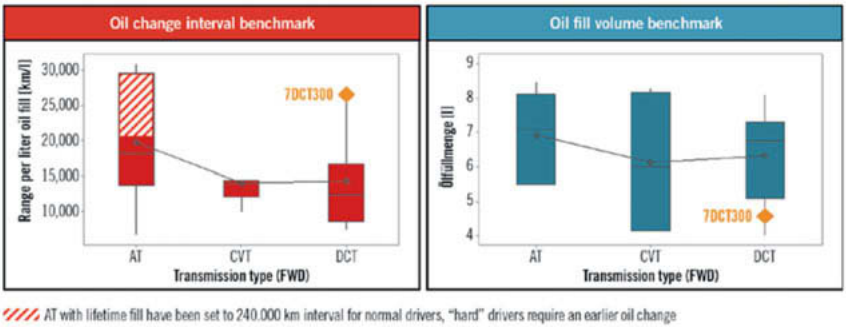


Fig. 1: Oil change intervals and oil fill volumes of the 7DCT300 compared to common ATs, CVTs and DCTs (© Magna)

Findings from real-life operation

The potential of the flexible oil management becomes obvious when looking at real driving data. Driving profiles from more than 2000 owners of a BMW C-segment passenger car show a wide range of different loads, FIGURE 2. Here, the transmission input power varies significantly under different boundary conditions like city or constant driving, raising slopes, sporty driving, etc. The average transmission input power was just 12.5 kW (including coasting phases). Within one year, the average of drivers reached just 10,000 km (6214 mi), with a minority reaching smaller or larger mileages. The average speed was just 37 km/h (23 mph). Only a few drivers regularly drove at very high speeds and accompanying high loads. Loads within the torque path and clutch system can vary by a factor of 10, depending on individual driving style and conditions. The field data shows that fixed service intervals inadequately represent the behavior of most drivers. This explains the huge potential for smaller oil fill volumes and extended change intervals.

https://doi.org/10.51202/9783181023549 - Generiert durch IP 216.73.216.36, am 19.01.2026, 02:19:31. © Urheberrechtlich geschützter Inhalt. Ohne gesonderte Erlaubnis ist jede urheberrechtliche Nutzung untersagt, insbesondere die Nutzung des Inhalts im Zusammenhang mit, für oder in KI-Systemen, KI-Modellen oder Generativen Sprachmodellen.

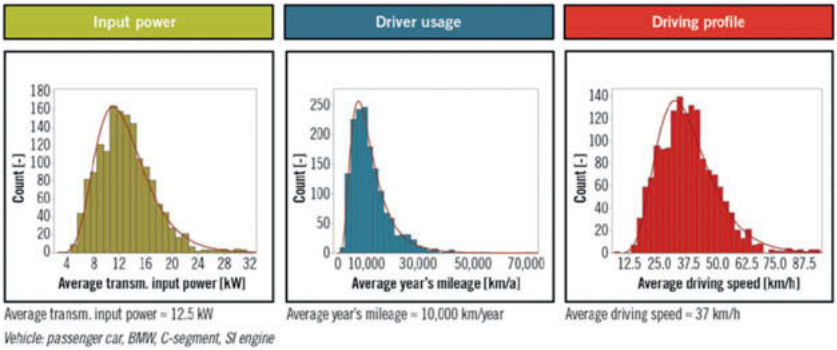


Fig. 2: Driving profiles from more than 2000 owners of a BMW C-segment passenger car (© Magna)

Operation principle of the monitoring software

A modular built-up software model within the Transmission Control Unit (TCU) records the transmission loads, and processes and interfaces the data usage, FIGURE 3. The data acquired from the transmission are transferred in the module model input (green) to the damage model (orange) of the load monitoring via a CAN interface. Here, they are matched with a prediction and reaction model. The boundary conditions control when both models are activated each. The next diagnostics module (blue) is responsible for checking the results for integrity and plausibility, and for carrying out a so-called de-bouncing. This function dampens the recording of load peaks – primarily in early lifetime – to prevent premature data interpretation. This can be compared to the average fuel consumption displayed shortly after fueling, which obviously cannot be precise. However, over longer use, the software learns to classify the transmission load data correctly, making debouncing unnecessary. After all, the driver interface (red) is needed to provide the data for external use on several channels. This can be the warning light, the service diagnosis interface (OBD) or an over-the-air interface (OTA) for real-time data transfer in communication processes between customer, garage and OEM.

https://doi.org/10.51202/9783181023549 - Generiert durch IP 216.73.216.36, am 19.01.2026, 02:19:31. © Urheberrechtlich geschützter Inhalt. Ohne gesonderte Erlaubnis ist jede urheberrechtliche Nutzung untersagt, insbesondere die Nutzung des Inhalts im Zusammenhang mit, für oder in KI-Systemen, KI-Modellen oder Generativen Sprachmodellen.

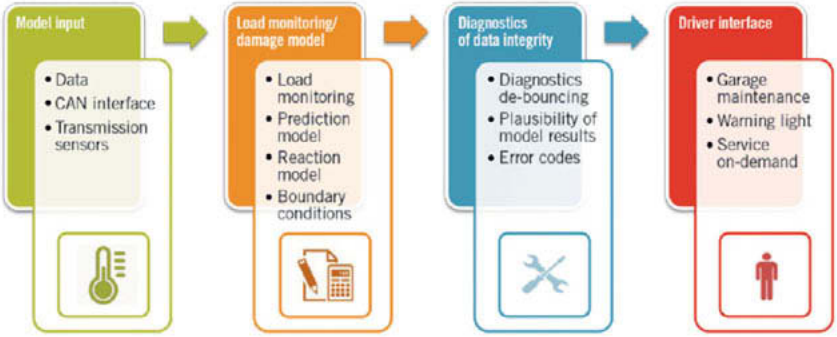


Fig. 3: Modular software model in the transmission control unit (© Magna)

Interaction of prediction model and reaction model

The prediction and the reaction model in the damage model of the TCU can complement each other usefully, FIGURE 4. The prediction model's operating principle is to match consolidated knowledge regarding load and damage with the data being delivered via CAN. These are for example temperature, engine torque and engine speed, as well as transmission internal and component-specific data. Today´s prediction model accuracy is quite precise, because there is comprehensive experience from development, calculation and real driving. However, prediction models have no insight into the real condition of components or lubricants; the prediction is made solely by matching knowledge and vehicle data that can be used indirectly. For example, it is known which load and consequently damage engine torque will probably cause. This can be cumulated in the model level. The reaction model in contrast relies on measured changes or degradation of a component using dedicated sensors. Therefore, it can take component tolerances into account or detect unusual wear. This is why this model delivers measurement data from the beginning, whereas the prediction model, as described earlier, starts to evaluate lifetime prediction after a calibration phase. Accuracy will increase with lifetime. Lifetime prediction become even better by combining both models, and thus allowing smaller safety factors to be defined in the model. The principal correlation between loads and cumulated damage is exemplarily shown in FIGURE 5. The solid blue line within the Stress-number (S-N) diagram represents the maximal load which can be cumulated before damage occurs. The solid green line stands for the load spectrum when operating an exemplary vehicle; it lies well below the maximum load. The dotted green line represents a higher mileage and shows how load converges to maximum load over time based on load monitoring. Before it meets the blue line, maintenance should be carried out. The more exact and filigree the damage models

https://doi.org/10.51202/9783181023549 - Generiert durch IP 216.73.216.36, am 19.01.2026, 02:19:31. © Urheberrechtlich geschützter Inhalt. Ohne gesonderte Erlaubnis ist jede urheberrechtliche Nutzung untersagt, insbesondere die Nutzung des Inhalts im Zusammenhang mit, für oder in KI-Systemen, KI-Modellen oder Generativen Sprachmodellen.

are, the more precisely the right timing for oil change can be predicted. The red line stands for too roughly classified loads and thus less precise prediction.

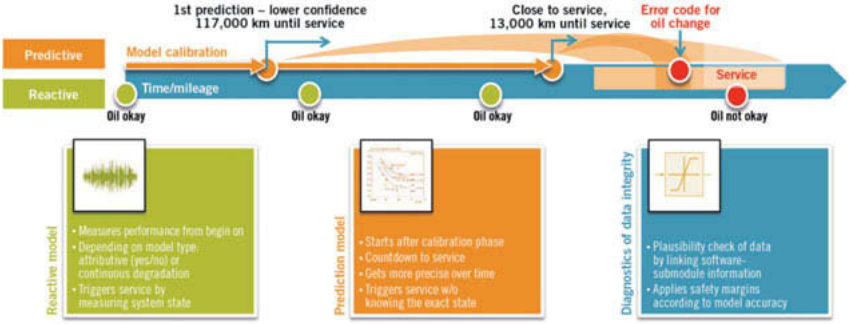


Fig. 4: Interaction of the prediction model and the reaction model (© Magna)

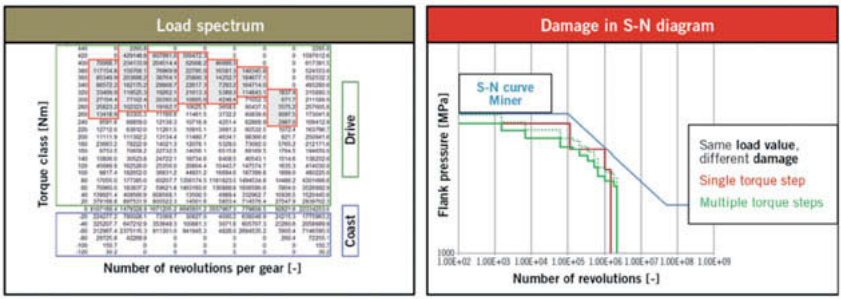


Fig. 5: The quality of the prediction increases with the accuracy of the damage model (© Magna)

Benefit for future applications

Weight optimization for CO2 reduction is a continuous challenge [3]. As a part of a “design-to-target”, Magna Powertrain consequently and regularly makes damage calculations of its products. Regarding transmissions, this applies for gear wheel sets, clutches and oil, etc. The more extensive the knowledge of customer use load spectra is, the more precise the prediction models can be designed. In the next DCT generation, the torque to weight ratio will be another 25 % better through improvements in all these areas. The flexible oil management is a major contributor to that. Beyond that, the oil management is a valuable element to reduce weight of

https://doi.org/10.51202/9783181023549 - Generiert durch IP 216.73.216.36, am 19.01.2026, 02:19:31. © Urheberrechtlich geschützter Inhalt. Ohne gesonderte Erlaubnis ist jede urheberrechtliche Nutzung untersagt, insbesondere die Nutzung des Inhalts im Zusammenhang mit, für oder in KI-Systemen, KI-Modellen oder Generativen Sprachmodellen.

module-based and hybrid drivetrains [4]. One reason why Magna Powertrain favors the P2.5 architecture is that the small high-speed e-machine causes comparatively little weight and no installation length. In combination with flexible oil management, the new hybrid transmission 7HDT400 (48 V) offers a maximum-torque-to-weight ratio close to an AT without hybridization, FIGURE 6. When increasing electrification further, the advantage becomes even more obvious: Within one vehicle platform, the whole range from 48-V to high voltage hybrid drives can be implemented without having to modify the installation position or the front axle design due to significantly more weight.

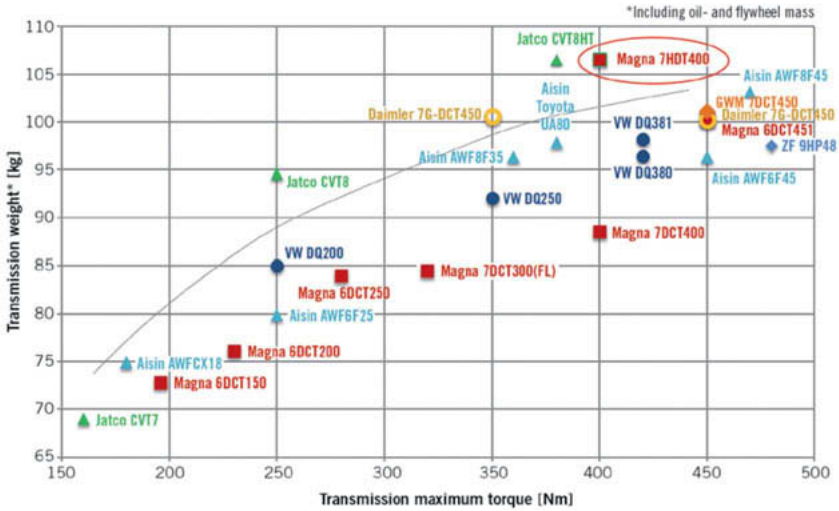


Fig. 6: The maximum-torque-to-weight ratio of the 48-V hybrid transmission 7HDT400 is close to an AT without hybridization (© Magna)

Potentials through communication

Much of the benefits of the flexible oil management can be opened with present technical means. When oil change is due, the car driver can be informed by a classic display. Furthermore, technical methods are available that practically rely on real-time communication. BMW has been offering tele services for many years, which enable transferring maintenance data between driver or vehicle and the OEM. As described before, the monitoring software offers interfaces that can be used for any OTA service models. While GSM is functionally restricted

https://doi.org/10.51202/9783181023549 - Generiert durch IP 216.73.216.36, am 19.01.2026, 02:19:31. © Urheberrechtlich geschützter Inhalt. Ohne gesonderte Erlaubnis ist jede urheberrechtliche Nutzung untersagt, insbesondere die Nutzung des Inhalts im Zusammenhang mit, für oder in KI-Systemen, KI-Modellen oder Generativen Sprachmodellen.

in terms of data size and speed, newer protocols like 4G or 5G in future allow further improvements to communication quantity and quality. One additional benefit is to gain more and more precise data from the field, thus being able to further improve prediction accuracy. An increasing number of users will improve quality as additional benefit. Another attractive option is offering new service models to the car owners that include their familiar communications end devices. For example, instead of the simple message that a service is due, the OEM could provide car drivers with comprehensive feedback, how service costs could be reduced. Besides, service packages priced specifically to customers can be offered which reflect individual needs.

Summary

Flexible oil management based on a prediction and reaction damage model allow BMW and Magna Powertrain for reducing fill volumes for a transmission up to 35 % as well as stretching change intervals by approximately 50 %. The reduced weight contributes to less CO2 emission, and longer intervals save average service costs for car owners. The benefit of flexible oil management grows with future communication solutions. This will allow for further optimization of the models, improve communication between the OEM and end customer, and make possible personal service offerings to car drivers. The next load monitoring software generation will contain new subsystems to use take advantage of these opportunities to full effect. The more detailed prediction and reaction model will allow for even longer oil change intervals, and one is prepared with flexible software interfaces for future OTA communication concepts.

[1] Krieger, H.: Alterung von Schmierstoffen im Zahnradprüfstand und in Praxisgetrieben. Munich, Technical University, Dissertation, 2004

[2] Bahne, M.; Wiesebrock, A.: Flexible Oil Change Management for Dual Clutch Transmissions. 17th CTI Symposium, Berlin, December 03-06, 2018

[3] Bahne, M.; Frey, U.: Transmission Technology Contribution to CO2 Roadmap – a Benchmark. 39th International Vienna Motor Symposium, April 26 and 27, 2018

[4] Gindele, J.: A Comprehensive System Approach for Future Powertrain Application. 12th CTI Symposium USA , Novi, May 14 to 17, 2018

https://doi.org/10.51202/9783181023549 - Generiert durch IP 216.73.216.36, am 19.01.2026, 02:19:31. © Urheberrechtlich geschützter Inhalt. Ohne gesonderte Erlaubnis ist jede urheberrechtliche Nutzung untersagt, insbesondere die Nutzung des Inhalts im Zusammenhang mit, für oder in KI-Systemen, KI-Modellen oder Generativen Sprachmodellen.

Single vs. Multi-Cone Synchronizers with Carbon Friction Lining – A Comparison of Load Limits and Deterioration Behavior

Einfach- vs. Mehrfachkonus-Synchronisierungen mit Carbon-Reibbelag – Ein Vergleich von Belastungsgrenzen und Schädigungsverhalten

M.Sc. **Ulrich Stockinger**, Dr.-Ing. **Hermann Pflaum**,
Prof. Dr.-Ing **Karsten Stahl,**
FZG – Gear Research Centre (FZG), Technical University of Munich

Zusammenfassung

Synchronisierungen werden in sehr großen Stückzahlen in PKW- und NKW-Getrieben eingesetzt. Um Kosten zu optimieren und die Effizienz von Getrieben zu steigern, ist es entscheidend die relativen Belastungsgrenzen von Einfach- im Vergleich zu Mehrfachkonus-Synchronisierungen mit Carbon-Reibbelag sowie die zugeordneten Schädigungsmechanismen zu kennen. Belastungsgrenzen von Einfach- und Mehrfachkonus-Synchronisierungen wurden experimentell auf dem Prüfstand SSP-180 ermittelt und vergleichend bewertet. In Einstufen-Dauerschaltversuchen wurden unterschiedliche Lastniveaus betrachtet und die Einflüsse von Gleitgeschwindigkeit, Reibarbeit und Reibleistung auf die Schädigung bestimmt. Die Ausfallursachen der verschiedenen Synchronisierungen werden beschrieben und der neue Kennwert $\mu_{min,grad}$ eingeführt, um das Schädigungsverhalten von Einfach- und Mehrfachkonus-Synchronisierungen quantitativ zu vergleichen. Entgegen den Erwartungen zeigt die untersuchte PKW-Einfachkonus-Synchronisierung bei gleichen spezifischen Beanspruchungen eine stärkere Schädigung des Reibsystems in den Dauerschaltversuchen als die Mehrfachkonus-Synchronisierungen. Thermo-mechanische Simulationen in Kombination mit Prüfstandversuchen zeigen, dass die Maximaltemperatur während einer Schaltung einen signifikanten Einfluss auf das Schädigungsverhalten und damit auf die Lebensdauer von Synchronisierungen mit Carbon-Reibbelag hat.

https://doi.org/10.51202/9783181023549 - Generiert durch IP 216.73.216.36, am 19.01.2026, 02:19:31. © Urheberrechtlich geschützter Inhalt. Ohne gesonderte Erlaubnis ist jede urheberrechtliche Nutzung untersagt, insbesondere die Nutzung des Inhalts im Zusammenhang mit, für oder in KI-Systemen, KI-Modellen oder Generativen Sprachmodellen.

Abstract

Synchronizers are widely used in gear boxes of car and truck transmissions. Optimizing costs and improving the efficiency of gear boxes require knowledge about the relative load limits of single and multi-cone synchronizers with carbon friction linings and their corresponding deterioration mechanisms. Load limits for single and multi-cone synchronizers with carbon friction lining used in cars were determined experimentally using the component test rig SSP-180 and compared against each other. Different load stages were run in life cycle tests and the influences of sliding velocity, friction work and frictional power were investigated. The synchronizers' failure mode is described and the novel specific value $\mu_{min,grad}$ is introduced that is able to quantify the deterioration of different synchronizer systems. During life cycle tests at the same specific load level, the single cone synchronizers, contrary to expectations, displayed greater damage compared to the multi-cone synchronizers. Calculations of the friction surface temperature in thermo-mechanical simulations, in combination with experiments on the test rig, show that the maximum temperature during the engagement has a significant influence on deterioration and endurance life of synchronizers with carbon friction lining.

1 Introduction

Synchronizers are widely used in gear boxes of car and truck transmissions. These machine elements synchronize the rotational speed of the output shaft and the gear wheel to be engaged to ensure smooth gear changing. For the synchronization process, a cone clutch with up to three friction surfaces is used to accelerate or decelerate input shaft and gear wheel, which have different rotational speeds. After synchronization, torque is transferred by a positive dog clutch. The synchronization process is described in detail by [1, 2]. Multi-cone synchronizers are especially used in lower gears as their torque capacity is significantly higher than that of single cone synchronizers. Higher friction torque results in faster shifting times, but the greater complexity of multi-cone synchronizers makes them more expensive and can raise the drag torque [3]. Fig. 1 shows a typical double cone synchronizer and its components. The blocker and the inner ring are coupled together by lugs on the inner ring and pockets on the blocker ring. Additionally the intermediate ring is coupled with the gear wheel by lugs and the corresponding pockets on the gear wheel. Torque generated between the axial plane surfaces of the inner ring and the gear wheel is much smaller than that between the friction surfaces. It contributes approximately 5 % to the overall torque of the whole synchronizer [4]. A triple cone synchronizer has an additional conical friction surface on the inner ring which is in contact with a cone on the gear wheel. Research on multi-cone synchronizers is reported by [4 bis 9]. Erdmann [4] investigates the efficiency of a synchronizer, defined as the quotient of measured to

https://doi.org/10.51202/9783181023549 - Generiert durch IP 216.73.216.36, am 19.01.2026, 02:19:31. © Urheberrechtlich geschützter Inhalt. Ohne gesonderte Erlaubnis ist jede urheberrechtliche Nutzung untersagt, insbesondere die Nutzung des Inhalts im Zusammenhang mit, für oder in KI-Systemen, KI-Modellen oder Generativen Sprachmodellen.

calculated friction torque. Experiments in [4] measure the lowest efficiency for an increasing shifting force and the highest efficiency for a decreasing shifting force during the engagement. Other parameters, like surface pressure, sliding velocity, and temperature influence the efficiency to a lesser degree. Sykes [5] describes the development process of new brass triple cone synchronizers and associated problems during testing and their respective solutions. Abdel Halim et al. [6] demonstrates the advantages of multi-cone synchronizers compared to single cone synchronizers, like greater torque capacity theoretically, and on the test rig.

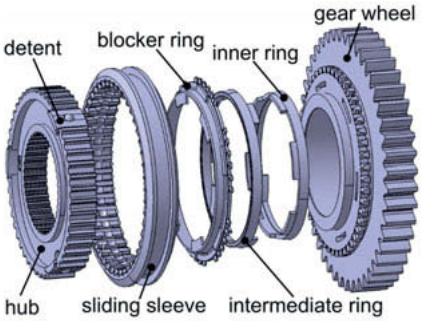


Fig. 1: Double Cone Synchronizer

For a safe synchronization process, the friction torque has to exceed the blocking release torque (index torque) when the rotational speeds are different [1]. The friction torque T_F, the torque that acts on the friction surfaces and synchronizes the rotational speed, is calculated by [2]:

$$T_F = n \cdot F_{ax} \cdot \frac{d_m \cdot \mu}{2 \cdot \sin \alpha} \tag{1}$$

F_{ax} is the axial force on the blocker ring, μ the coefficient of friction (CoF) between the cones, d_m is the mean cone diameter, n the amount of friction surfaces, and α is the cone angle (angle between cone and cone axis). The equation assumes that for multi-cone synchronizers, μ is the same on each friction surface and d_m is the mean value of each friction surface's mean cone diameter. The blocking release torque T_Z is [2]:

$$T_Z = F_{ax} \cdot \frac{d_D}{2} \cdot \frac{1 - \mu_D \cdot \tan\frac{\beta}{2}}{\mu_D + \tan\frac{\beta}{2}} \tag{2}$$

d_D is the pitch diameter (interface between blocker teeth and sliding sleeve), μ_D is the coefficient of friction of the chamfers, and β the chamfer angle (angle between both tooth flanks).

https://doi.org/10.51202/9783181023549 - Generiert durch IP 216.73.216.36, am 19.01.2026, 02:19:31. © Urheberrechtlich geschützter Inhalt. Ohne gesonderte Erlaubnis ist jede urheberrechtliche Nutzung untersagt, insbesondere die Nutzung des Inhalts im Zusammenhang mit, für oder in KI-Systemen, KI-Modellen oder Generativen Sprachmodellen.

To block the gear engagement during synchronization successfully, $T_F > T_Z$, and relation (3) has to be satisfied. If the static CoF between the cones exceeds tanα, self-locking can occur [2].

$$\mu > \frac{d_D}{n \cdot d_m} \cdot \sin\alpha \cdot \frac{1 - \mu_D \cdot \tan\frac{\beta}{2}}{\mu_D + \tan\frac{\beta}{2}} \tag{3}$$

Different failure modes of synchronizers cause clashing. A clash happens when the sliding sleeve tries to mesh with the clutch teeth of the gear wheel, while there is still a significant rotational speed difference between these parts. Typical failure modes are described by [1, 2, 10 bis 14] and are summarized as follows:

- The coefficient of friction on the friction surfaces is too low during synchronization.
- Wear on the friction surfaces reduces the axial gap between blocker ring and gear wheel to zero. Torque is not transferred through cones but the plane face.
- Components of synchro unit break (e.g. blocker ring).
- Chamfer angle of blocking ring changes due to wear.
- Desynchronization after free flight phase because of high drag losses.
- Inadequate pre-synchronization

In applications with high loads, Carbon is used as friction lining because it can stand higher surface pressure, friction work and power compared to other friction linings. Due to the low thermal conductivity of carbon friction linings, multi-cone synchronizers, which have small thermal mass and worse cooling compared to single cone systems, exhibit high surface temperatures during the engagement which damage both friction lining and lubricant.

Acuner et al. [11] investigate failure modes of single cone synchronizers with carbon friction linings and define a lubricant related and a friction lining related failure mode. Due to high surface temperatures, crack products from the lubricant block the friction lining's pores and significantly reduce the core roughness depth sRk. The reduction of sRk correlates well with the reduction of μ_{min} (minimum CoF in the range of 5…90 % v_{gmax} during an engagement). This reduces the CoF at the beginning of the synchronization process. Relation (3) is not satisfied, which results in early clash of the synchronizer. Osanai et al. [15] and Maeda et al. [16] describe the same effect for paper friction linings. A second failure mode is the deterioration of friction linings' matrix. Exceeding a specific temperature level causes this type of deterioration. It results both in lower mechanical strength and reduced adhesion of the carbon particles for particle based friction linings. Acuner et al. [11] observe breaking fibers for woven friction linings in SEM investigations.

https://doi.org/10.51202/9783181023549 - Generiert durch IP 216.73.216.36, am 19.01.2026, 02:19:31. © Urheberrechtlich geschützter Inhalt. Ohne gesonderte Erlaubnis ist jede urheberrechtliche Nutzung untersagt, insbesondere die Nutzung des Inhalts im Zusammenhang mit, für oder in KI-Systemen, KI-Modellen oder Generativen Sprachmodellen.

Häggström [17] describes that over 200 °C focal temperature, hot spots occur for the CFRP carbon friction lining. Degradation of performance and significant wear start around 230…250 °C. The tests were stopped after 10.000 cycles and did not lead to failure of the synchronizers.

Several publications describe thermo-mechanical simulations of synchronizers [4, 12, 14, 18 bis 24]. Erdmann [4], based on preliminary work from Spreckels [20] and Neudörfer [19], who set up the model and determined material parameters for different friction linings, conducts 2D and 3D thermo-mechanical simulations on multi-cone synchronizers. The pressure distribution on the friction surface was inhomogeneous both in axial and circumferential direction due to the inhomogeneous cross section of the blocker ring. Häggström et al. [24] describes his approach to simulate the thermal behavior of a single cone synchronizer and studies influencing parameters on the maximum surface temperature. Straightness and initial angle difference influence the maximum friction surface temperature more than the bulk design of the synchronizer. Häggström et al. [23] extend their work and introduce a methodology to validate their simulations. Furthermore Häggström et al. [17, 25] investigate influences of manufacturing tolerances, like relative cone angles or out-of-roundness for Carbon and Molybdenum (Mo) friction linings. An out of roundness leads to higher maximum surface temperatures. The maximum surface temperature can be optimized by a suitable cone angle. Acuner et al. [18] and Neudörfer [19] confirm this in their research.

However, a lot of research on synchronizers has been conducted, the performance of single and multi-cone synchronizers with Carbon friction lining has not been investigated in detail. This study aims to determine load limits and introduces an evaluation method to compare the performance of different synchronizer systems. Further results are presented in [26].

2 Method

Load limits for single and multi-cone synchronizers with carbon friction lining are determined experimentally using the component test rig SSP-180. Therefore, the chosen hypothetical test conditions and loads are significantly higher than the typically specified lifetime transmission conditions in order to artificially generate overload and misuse to generate failures.

2.1 Test rig, synchronizers and lubricant

The endurance tests were performed on the ZF/FZG synchronizer standard test rig SSP-180. Fig. 2 shows the concept of the test rig. For each test, two sets of synchronizers (1-2) and (4-5) are mounted to the test rig on each side (A/B) of the sliding sleeve (3). The gear wheel (1) on the A-side (left) is stationary. Gear wheel (5) and inertia (7) are fixed to shaft (6) and rotate

https://doi.org/10.51202/9783181023549 - Generiert durch IP 216.73.216.36, am 19.01.2026, 02:19:31. © Urheberrechtlich geschützter Inhalt. Ohne gesonderte Erlaubnis ist jede urheberrechtliche Nutzung untersagt, insbesondere die Nutzung des Inhalts im Zusammenhang mit, für oder in KI-Systemen, KI-Modellen oder Generativen Sprachmodellen.

with constant rotational speed. Inertia (9), which is fixed to shaft (8) together with hub (10), is changed according to the required friction work of the test. The synchronizers' friction behavior is measured on the A-side of the test rig. During one cycle, the sliding sleeve moves from the A- to the B-side and back and engages the two synchronizers consecutively. Moving the sliding sleeve to the A-side breaks shaft (8) and inertia (9) down to standstill. Engaging synchronizer (4) accelerates (8-9) up to n_0.

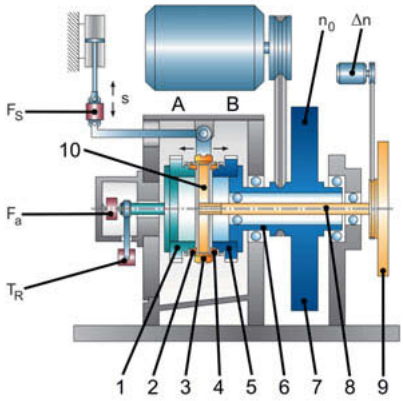


Fig. 2: Test rig SSP-180 according to [12]

The tests were run with single (EK73), double (DK73) and triple (TK73) cone synchronizers with a dual layer carbon friction lining from the same modular system, shown in Fig. 3.
Table 1 summarizes their geometrical parameters. The performance tests were conducted with a manual transmission fluid MTF-Car from series production (kinematic viscosity 27.6 mm²/s at 40 °C, 6.1 mm²/s at 100 °C) typically used in cars.



Fig. 3: Synchronizers

https://doi.org/10.51202/9783181023549 - Generiert durch IP 216.73.216.36, am 19.01.2026, 02:19:31. © Urheberrechtlich geschützter Inhalt. Ohne gesonderte Erlaubnis ist jede urheberrechtliche Nutzung untersagt, insbesondere die Nutzung des Inhalts im Zusammenhang mit, für oder in KI-Systemen, KI-Modellen oder Generativen Sprachmodellen.

Table 1: Geometry parameters of tested synchronizers

	Friction surface	EK73	DK73	TK73
Average diameter / mm	**Outside**	72.3	73.0	73.0
	Middle		66.9	66.9
	Inside			61.7
Width of friction surface / mm	**Outside**	8.0	6.5	6.5
	Middle		7.1	7.1
	Inside			6.6
Cone angle / °		7.5	7.5	7.5

Each test starts with 50 running-in cycles on 50 % of the load stages' axial force and rotational speed. Afterwards, a single step life cycle test is performed until the synchronizer fails because of clashing. The test rigs' vibration monitor detects clashes and ends the test. Similar specific load parameters are used, to compare the friction performance of different synchronizer systems. Table 2 summarizes the tested load stages for the three types of synchronizers. The axial force between the three different synchronizer systems varies corresponding to the different friction areas. Both contact pressure and sliding velocity give the mean values over all friction surfaces. The oil flow through a perforated plate cools the synchronizer from the top. If not mentioned differently, the oil temperature was kept at ϑ_{oil} = 80 °C and the oil flow at V_{oil} = 5 l/min. The cycle time was adapted that the specific mean power per cycle is about 60 mW/mm².

Table 2: Load stages for different synchronizer systems (EK73, DK73, TK73)

Load stage	Mean. contact pressure p / N/mm²	Mean. sliding velocity $v_{g,max}$ / m/s	Spec. friction work q / J/mm²
LS1	4.0	4.5	0.7
LS2	4.0	6.5	0.7
LS3	4.0	8.0	0.7
LS4	4.0	4.5	0.9
LS5	4.0	6.5	0.9
LS6	4.0	8.0	0.9
LS7	4.0	4.5	1.1
LS8	4.0	6.5	1.1
LS9	4.0	8.0	1.1

2.2 Failure mode and evaluation of tests

All synchronizers failed because the values of CoF at the beginning of the engagement were too low. As an example, Fig. 4 shows the development of the friction characteristic during one test on LS9 for the triple cone synchronizer. Over the endurance life, the CoF almost does not

https://doi.org/10.51202/9783181023549 - Generiert durch IP 216.73.216.36, am 19.01.2026, 02:19:31. © Urheberrechtlich geschützter Inhalt. Ohne gesonderte Erlaubnis ist jede urheberrechtliche Nutzung untersagt, insbesondere die Nutzung des Inhalts im Zusammenhang mit, für oder in KI-Systemen, KI-Modellen oder Generativen Sprachmodellen.

change at low sliding velocities, but significantly decreases at high sliding velocities. The axial wear of all synchronizers was less than 0.4 mm and thus not the reason for the failure of the synchronizers.

The minimum CoF μ_{lock} at which the synchronizers still satisfy $T_F > T_Z$, highly differs between single and multi-cone synchronizers (equation (3)). Although, the blocker ring's chamfer angle β differs between the investigated double/triple and the single cone synchronizers, μ of the two multi-cone synchronizers can decrease further until the synchronizer fails, than for the single cone synchronizer. μ_{lock} is estimated by equation (3) for the single cone $\mu_{lock} = 0.083$, the double cone $\mu_{lock} = 0.069$ and the triple cone synchronizer $\mu_{lock} = 0.049$. μ_D is assumed constant in this calculation.

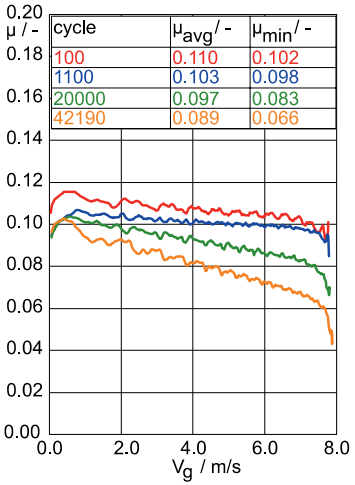


Fig. 4: Change of friction characteristic during endurance life; TK73, LS9, V150, MTF-Car

The friction behavior is evaluated using the following specific values:

- μ_{avg} : average CoF over the interval 60-0% $v_{g,max}$
- μ_{min} / $\mu_{min,97}$: minimum CoF in the interval 5-90 % $v_{g,max}$ / 5-97 % $v_{g,max}$
- N: cycles till failure of the synchronizer
- $\mu_{min,Grad}$ / $\mu_{min,Grad97}$: neg. gradient of μ_{min} / $\mu_{min,97}$ in the interval 33-100 % N

As the blocking safety between single, and multi-cone synchronizers differ, the cycles N until failure of different systems cannot be compared. This is why the specific value $\mu_{min,Grad}$, which

https://doi.org/10.51202/9783181023549 - Generiert durch IP 216.73.216.36, am 19.01.2026, 02:19:31. © Urheberrechtlich geschützter Inhalt. Ohne gesonderte Erlaubnis ist jede urheberrechtliche Nutzung untersagt, insbesondere die Nutzung des Inhalts im Zusammenhang mit, für oder in KI-Systemen, KI-Modellen oder Generativen Sprachmodellen.

describes the negative slope of the minimum CoF's regression line in the trend plot, was developed to describe and compare the deterioration behavior of different synchronizer systems. This specific value describes the change of μ_{min} during the endurance life and is similar to the specific values suggested by [12]. As $\mu_{min,grad}$ just covers the minimum CoF in a range of 5-90 % $v_{g,max}$ and the minimum CoF occurs at higher sliding speeds than 90 % $v_{g,max}$, the range of $\mu_{min,97}$ was extended to 5-97 % $v_{g,max}$. The specific values $\mu_{min,grad}$ and $\mu_{min,Grad,97}$ are small, as they describe the hypothetical decrease of μ_{min}/ $\mu_{min,97}$, if the test would run up to 100.000 cycles. For all figures, $\mu_{min,grad}$ and $\mu_{min,Grad,97}$ are multiplied by 100.000.

2.3 Thermo-mechanical simulation

The maximum surface temperature during clutch engagement is investigated in thermo-mechanical simulations. Consecutive static mechanical and transient thermal simulations were performed. Only the main synchronization phase is simulated, the pre-synchronization is neglected. The engagement is divided into several steps. Firstly, the deformation under static load is calculated. Both pressure distribution and displacement are input data for the heat flux calculation on the friction surface. The resulting temperature field of the thermal simulation is then again input parameter for the static mechanical simulation. The simulation ends, when the kinetic energy of the inertia is completely transferred into heat. The simulations aim to evaluate pressure and temperature distribution on the friction surface. Acuner [12] and Mileti [22] developed the simulation code based on the concept of [19] and [4]. In this paper, it was adapted to the requirements of the investigated multi-cone synchronizers. Mileti [22] et al. give a detailed description of the simulation process.

All simulations are 2D, performed with Ansys APDL, and post processed with Matlab. At the beginning, the axial force is raised from zero to the predetermined value within 0.1 s. For the comparison of different synchronizer systems, their friction surfaces were meshed with the same element type and size. In every load stage, only one cycles is simulated with adiabatic boundary conditions. The CoF throughout the whole engagement process is set constant to 0.1. Table 3 summarizes the material parameters used in the simulation. Due to these restrictions and the fact that the contact surfaces are assumed to be smooth in the simulation, the evaluated maximum temperatures represent reference temperatures.

https://doi.org/10.51202/9783181023549 - Generiert durch IP 216.73.216.36, am 19.01.2026, 02:19:31. © Urheberrechtlich geschützter Inhalt. Ohne gesonderte Erlaubnis ist jede urheberrechtliche Nutzung untersagt, insbesondere die Nutzung des Inhalts im Zusammenhang mit, für oder in KI-Systemen, KI-Modellen oder Generativen Sprachmodellen.

Table 3: Material parameters for the thermo-mechanical simulation [19]

Parameter	Steel	Carbon
E /N/mm²	210.000	800
v / -	0,30	0,25
α_L / 10^{-6} 1/K	13	70
λ / W/mK	43,5	0,5
ρ / kg/m³	7850	1100
c_p / kJ/(kgK)	540 [27]	1500

3 Results and discussion

The load parameters' influence on the deterioration behavior depends on the type of synchronizer (single, double or triple cone). Fig. 5 summarizes the results of 24 tests. Tests with the same friction work exhibit greater damage (higher $\mu_{min,grad97}$) when the sliding velocity and, respectively, the friction power is increased. An increased sliding velocity increases the peak friction power at the beginning of the engagement and, therefore, higher surface temperatures occur. Comparing load stages with the same friction power/sliding velocity, $\mu_{min,grad97}$ is shown to increase with friction work. Stockinger et al. [26] present further influencing parameters on the deterioration behavior. During life cycle tests at the same specific load level, the single cone synchronizers, contrary to expectations, displayed greater damage compared to the multi-cone synchronizers. The deterioration is similar for double and triple cone synchronizers, except for two tests at q = 0.9 J/mm² and $v_{g,max}$ = 6.5 m/s.

https://doi.org/10.51202/9783181023549 - Generiert durch IP 216.73.216.36, am 19.01.2026, 02:19:31. © Urheberrechtlich geschützter Inhalt. Ohne gesonderte Erlaubnis ist jede urheberrechtliche Nutzung untersagt, insbesondere die Nutzung des Inhalts im Zusammenhang mit, für oder in KI-Systemen, KI-Modellen oder Generativen Sprachmodellen.

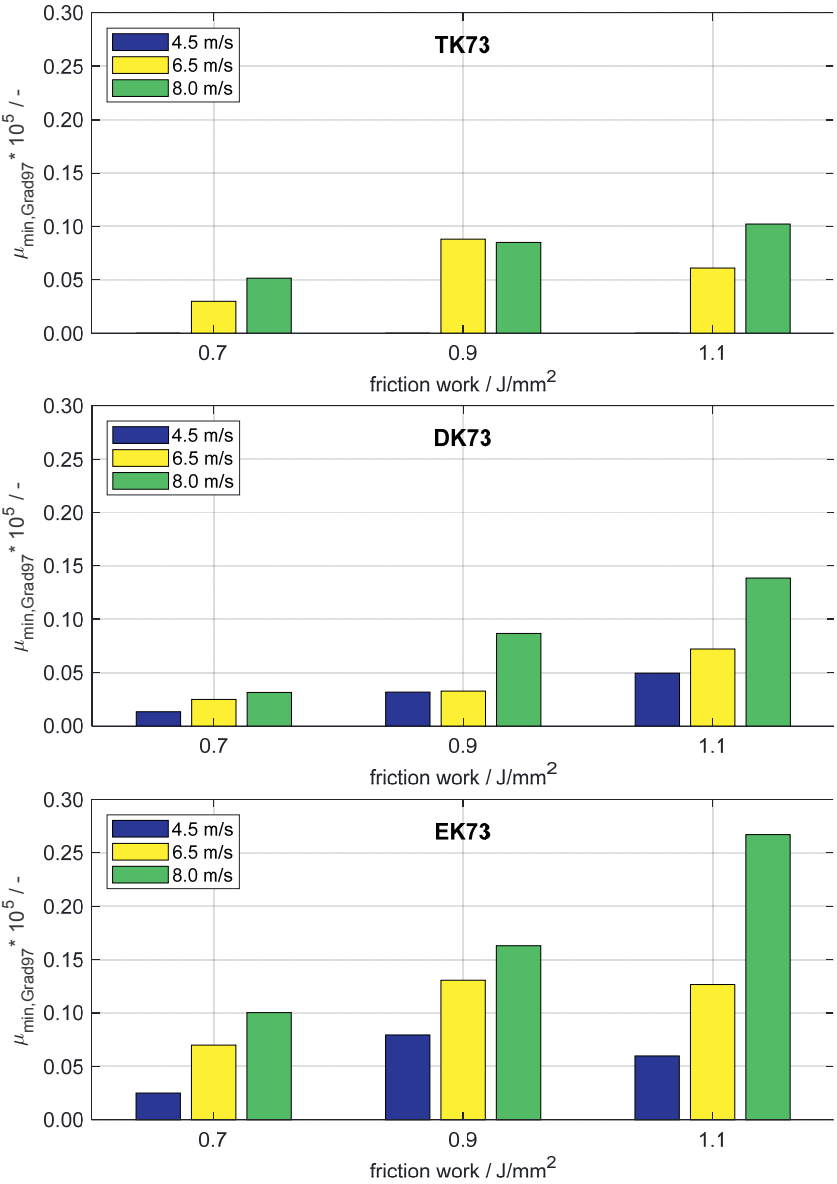


Fig. 5: Influence of load parameters on $\mu_{min,Grad97}$ for single and multi-cone synchronizers, MTF-Car; ϑ_{oil} = 80 °C

https://doi.org/10.51202/9783181023549 - Generiert durch IP 216.73.216.36, am 19.01.2026, 02:19:31. © Urheberrechtlich geschützter Inhalt. Ohne gesonderte Erlaubnis ist jede urheberrechtliche Nutzung untersagt, insbesondere die Nutzung des Inhalts im Zusammenhang mit, für oder in KI-Systemen, KI-Modellen oder Generativen Sprachmodellen.

Fig. 6 combines results from rig testing (deterioration of synchronizers, rated with $\mu_{min,grad97}$) with the maximum friction surface temperature increase observed in the 2D thermo-mechanical simulations. The maximum friction surface temperature increase was calculated via simulations, for each test shown in Fig. 5. Higher maximum temperature increases lead to greater deterioration of the synchronizer system. FEM simulations show that, the blocker ring of the single cone synchronizer deforms more than that of the double cone synchronizer, causing a more unsteady pressure distribution on the friction surface. This results in higher local surface temperatures on the friction surface of the single cone synchronizer and, therefore, a greater deterioration of friction lining and lubricant. Roughness measurements of the surfaces confirmed an unsteady, smoothened friction surface. Erdmann [4] confirms a non-uniform pressure distribution for synchronizer rings in the axial and circumferential direction due to deformation of the non-axisymmetric synchronizer rings under axial load.

Increasing maximum surface temperature results in greater deterioration of the synchronizer system. These findings correlate well with Häggström et al. [14] who describe the focal temperature increase as a suitable parameter to predict failure of Mo synchronizers.

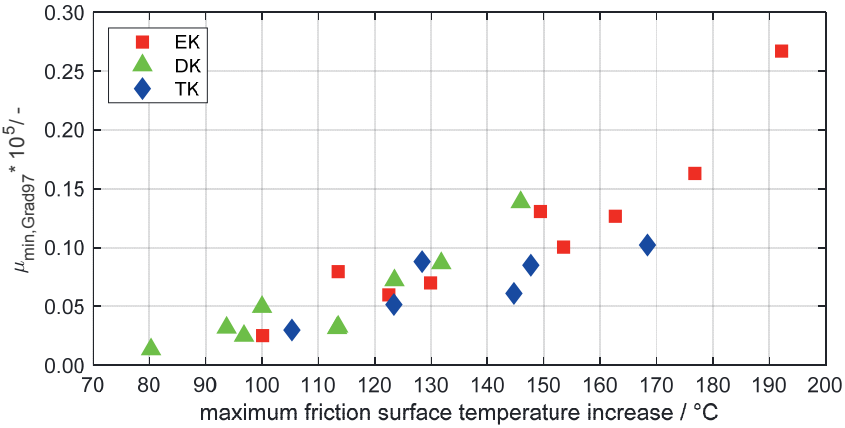


Fig. 6: Influence of maximum friction surface temperature increase on $\mu_{min,Grad97}$, EK73/DK73: LS1-9; TK73: LS2/3/5/6/8/9, MTF-Car; ϑ_{oil} = 80 °C

https://doi.org/10.51202/9783181023549 - Generiert durch IP 216.73.216.36, am 19.01.2026, 02:19:31. © Urheberrechtlich geschützter Inhalt. Ohne gesonderte Erlaubnis ist jede urheberrechtliche Nutzung untersagt, insbesondere die Nutzung des Inhalts im Zusammenhang mit, für oder in KI-Systemen, KI-Modellen oder Generativen Sprachmodellen.

4 Conclusion

Load limits for single and multi-cone synchronizers with carbon friction lining used in cars were determined experimentally using the component test rig SSP-180. The specific value $\mu_{min,Grad97}$ proved suitable to compare deterioration behavior of different synchronizer systems as well as the influence of load parameters on the deterioration behavior. All synchronizers failed because the values of coefficient of friction at the beginning of the clutch engagement were too low. During life cycle tests at the same specific load level, single cone synchronizers, displayed greater damage compared to multi-cone synchronizers. The bigger deformation of the single cone's blocker ring, compared to that of the multi cone synchronizers, caused a more unsteady pressure distribution on the friction surface, which resulted in higher local temperatures of the single cone synchronizer and, therefore, a greater deterioration of friction lining and lubricant. Thermo-mechanical simulations, in combination with experiments on the test rig, show that the maximum temperature during the engagement has a significant influence on the endurance life of synchronizers with carbon friction lining.

5 Acknowledgments

The results presented were achieved in research projects sponsored by Forschungsvereinigung Antriebstechnik e.V. (FVA, http://www.fva-net.de). The authors wish to thank FVA and the companies and their staffs who supported the projects.

6 Literaturangaben

[1] Socin, R. J. u. Walters, L. K.: Manual Transmission Synchronizers. SAE Technical Paper Series. SAE Technical Paper Series. SAE International400 Commonwealth Drive, Warrendale, PA, United States 1968

[2] Naunheimer, H., Bertsche, B., Lechner, G. u. Ryborz, J.: Fahrzeuggetriebe. Grundlagen, Auswahl, Auslegung und Konstruktion. Berlin, Heidelberg: Springer-Verlag 2007

[3] Pingale, A.: Development of Compact Synchronizer Technology for Manual and Automated Transmissions. SAE Technical Paper Series. SAE Technical Paper Series. SAE International400 Commonwealth Drive, Warrendale, PA, United States 2014

[4] Erdmann, K.: Einflussfaktoren auf die Leistungsfähigkeit von Mehrfachsynchronisierungen, Leibniz Universität Hannover Dissertation. Hannover 2008

[5] Sykes, L. M.: The Jaguar XJ220 Triple-Cone Synchronizer A Case Study. SAE Technical Paper Series. SAE Technical Paper Series. SAE International400 Commonwealth Drive, Warrendale, PA, United States 1994

https://doi.org/10.51202/9783181023549 - Generiert durch IP 216.73.216.36, am 19.01.2026, 02:19:31. © Urheberrechtlich geschützter Inhalt. Ohne gesonderte Erlaubnis ist jede urheberrechtliche Nutzung untersagt, insbesondere die Nutzung des Inhalts im Zusammenhang mit, für oder in KI-Systemen, KI-Modellen oder Generativen Sprachmodellen.

[6] Abdel-Halim, N. A., Barton, D. C., Crolla, D. A. u. Selim, A. M.: Performance of multi-cone synchronizers for manual transmissions. Proceedings of the Institution of Mechanical Engineers, Part D: Journal of Automobile Engineering 214 (2000) 1, S. 55–65

[7] Okazaki, Y. u. Komatsuzaki, K.: Double Cone Synchronizer with Paper Lining for Medium Duty Trucks. SAE Technical Paper Series. SAE Technical Paper Series. SAE International400 Commonwealth Drive, Warrendale, PA, United States 1990

[8] Bamane, S. u. Sonawane, P.: Multi Cone Synchronizer System: A Review. International Journal for Scientific Research & Development (2016) 4, S. 616–621

[9] D'Orazio, A., Caudano, M., UBERTI, M. u. URBINATI, M.: GUDA-4 Multi Cone Synchronizer Dynamic Modeling and Experimental Bench Test Rig to Improve Manual Transmission Shiftability (Gear Unit Design and Applications). The Proceedings of the JSME international conference on motion and power transmissions II.01.202 (2001) 0, S. 649–656

[10] Rank, R.: Untersuchungen zur Lebensdauerprüfung von Synchronisierungen, TU München Dissertation 1995

[11] Acuner, R., Pflaum, H. u. Stahl, K.: Tribologische Schädigungsmechanismen von Synchronisierungen mit Carbon-Reibwerkstoffen. GETLUB - Tribologie- und Schmierstoffkongress. 2016, S. 239–251

[12] Acuner, R.: Synchronisierungen mit Carbon-Reibwerkstoffen unter hohen und extremen Beanspruchungen, TU München Dissertation 2016

[13] Wanli, X., Wei, Z., Bin, S. u. Ximeng, X.: Investigation of manual transmission synchronizer failure mechanism induced by interface material/lubricant combinations. Wear 328-329 (2015), S. 475–479

[14] Häggström, D., Sellgren, U. u. Björklund, S.: Evaluation of synchronizer loading parameters and their ability to predict failure. Proceedings of the Institution of Mechanical Engineers, Part J: Journal of Engineering Tribology 232 (2018) 9, S. 1093–1104

[15] Osanai, H., Ikeda, K. u. Kato, K.: Relations Between Temperature in Friction Surface and Degradation of Friction Materials During Engaging of Wet Friction Paper. SAE Technical Paper Series. SAE Technical Paper Series. SAE International400 Commonwealth Drive, Warrendale, PA, United States 1990

[16] Maeda, M. u. Murakami, Y.: Testing Method and Effect of ATF Performance on Degradation of Wet Friction Materials. SAE Technical Paper Series. SAE Technical Paper Series. SAE International400 Commonwealth Drive, Warrendale, PA, United States 2003

[17] Häggström, D.: Towards model-based development of heavy truck synchronizers, KTH Royal Institute of Technology Dissertation. Stockholm 2018

https://doi.org/10.51202/9783181023549 - Generiert durch IP 216.73.216.36, am 19.01.2026, 02:19:31. © Urheberrechtlich geschützter Inhalt. Ohne gesonderte Erlaubnis ist jede urheberrechtliche Nutzung untersagt, insbesondere die Nutzung des Inhalts im Zusammenhang mit, für oder in KI-Systemen, KI-Modellen oder Generativen Sprachmodellen.

[18] Acuner, R., Voelkel, K., Pflaum, H. u. Stahl, K.: Influence of Cone-Angle-Difference on Performance of Synchonizers with Carbon Friction Linings. Getriebe in Fahrzeugen 2014 - VDI-Berichte 2218. 2014, S. 595–610

[19] Neudörfer, S.: Thermomechanische Einflüsse auf die Tribologie von Synchronisierungen, Leibniz Universität Hannover Dissertation. Hannover 2008

[20] Poll, G. u. Spreckels, M.: Influence of temperature distribution on the tribological performance of automotive synchronisers. In: Tribological Research and Design for Engineering Systems, Proceedings of the 29th Leeds-Lyon Symposium on Tribology. Tribology Series. Elsevier 2003, S. 613–621

[21] Spreckels, M.: Einfluss der Temperaturverteilung auf das tribologische Verhalten von Synchronisierungen, Leibniz Universität Hannover Dissertation. Hannover 2001

[22] Mileti, M., Pflaum, H. u. Stahl, K.: TorqueLINE Cone Clutch: Thermo-Mechanical Stability of Cone Clutches for ATs. In: Dritev. International VDI Congress Dritev - Drivetrain for Vehicles, EDrive, Transmissions in Mobile Machines: June 27 and 28, 2018, Bonn. VDI-Berichte, Bd. 2328. Düsseldorf: VDI Verlag GmbH 2018

[23] Häggström, D., Sellgren, U., Stenström, W. u. Björklund, S.: A Verified and Validated Model for Simulation-Driven Design of Heavy Duty Truck Synchronizers. Volume 10: ASME 2015 Power Transmission and Gearing Conference; 23rd Reliability, Stress Analysis, and Failure Prevention Conference. ASME Sunday 2015, V010T11A045

[24] Häggström, D., Stenström, W., Sellgren, U. u. Björklund, S.: Parameter study of the thermomechanical performance of heavy duty synchronizers. Getriebe in Fahrzeugen 2015 - VDI-Berichte2256. 2015, S. 597–620

[25] Häggström, D., Sellgren, U. u. Björklund, S.: The effect of manufacturing tolerances on the thermomechanical load of gearbox synchronizers. Procedia CIRP 72 (2018), S. 1202–1207

[26] Stockinger, U., Pflaum, H. u. Stahl, K.: Single vs. Multi-Cone Synchronizers with Carbon Friction Lining – A Comparison of Load Limits and Deterioration Behavior. Forschung im Ingenieurwesen (2019)

[27] Richter, F.: Physikalische Eigenschaften von Stählen und ihre Temperaturabhängigkeit. Polynome und graphische Darstellungen; Mitteilung aus dem Forschungsinstitut der Mannesmann AG. Stahleisen-Sonderberichte, Bd. 10. Düsseldorf: Verl. Stahleisen 1983

https://doi.org/10.51202/9783181023549 - Generiert durch IP 216.73.216.36, am 19.01.2026, 02:19:31. © Urheberrechtlich geschützter Inhalt. Ohne gesonderte Erlaubnis ist jede urheberrechtliche Nutzung untersagt, insbesondere die Nutzung des Inhalts im Zusammenhang mit, für oder in KI-Systemen, KI-Modellen oder Generativen Sprachmodellen.

https://doi.org/10.51202/9783181023549 - Generiert durch IP 216.73.216.36, am 19.01.2026, 02:19:31. © Urheberrechtlich geschützter Inhalt. Ohne gesonderte Erlaubnis ist jede urheberrechtliche Nutzung untersagt, insbesondere die Nutzung des Inhalts im Zusammenhang mit, für oder in KI-Systemen, KI-Modellen oder Generativen Sprachmodellen.

Triple wet clutch module and actuation system, shift cylinders and park lock for modern Hybrid Transmissions

Architecture and technical description of a triple wet clutch unit and the related active and passive clutch and shift actuation system

Dipl.-Ing. **Olivier Simon**, Valeo Transmissions, Amiens, France;
Dipl.-Ing. (FH) **Wilhelm Heubner**, Valeo Actuation Systems, Ebern

Abstract

Bei P2-Hybridarchitekturen haben integrierte Lösungen von Triple Wet Clutches mit effizienten Aktuierungssystemen bei mehreren OEM-Projekten einen hohen Stellenwert. Insbesondere bei DHT- oder Hybrid-FWD-Architekturen, bei denen es um die Abmessungen in axialer Richtung geht, bietet die Integration der Trennkupplung zwischen ICE und Getriebe (C0) in ein Triple Wet Clutch Modul (TWC) eine intelligente Designlösung.
Das Papier beschreibt verschiedene Architekturen von TWC mit Zentraleinrückern (CSC) und integrierten Betätigungskolben mit Schwerpunkt auf P2-Offline-Hybridarchitekturen und den damit verbundenen Vor- und Nachteilen.
Der Beitrag beschreibt auch ein innovatives Betätigungssystem des TWC Moduls, das auch weitere Getriebefunktionen wie Parksperre und Schaltzylinder betätigt. Das Betätigungssystem ist eine Innovation von Valeo, die auf die Bedürfnisse der DHTs zugeschnitten wurde. Es kann drei Kupplungen betätigen und die Schaltung der Gänge und Ansteuerung des Parksperrzylinders durchführen.
Moderne DCTs und DHTs verwenden so genannte "On-Demand"-Aktuierungsysteme, um die ständigen Verluste der zentralen Powerpacks zu vermeiden, die durch ihr konstant hohes Druckniveau und den Leckagen in den Steuerventilen entstehen.
Die hydraulische Betätigung der Kupplungen und Zylinder bringt eine hohe Leistungsdichte und damit Vorteile im gesamten Aufbau des Getriebes. Der Schwerpunkt der Entwicklungsarbeit liegt auf niedrigem Stromverbrauch, geringem Gewicht, kleinen Einbauräumen, die frei positioniert werden können, und attraktiven Preisen. Ein geschlossener Ölkreislauf mit eigenem Ölbehälter ermöglicht eine lebenslange Befüllung und freie Wahl des Schmieröls.

https://doi.org/10.51202/9783181023549 - Generiert durch IP 216.73.216.36, am 19.01.2026, 02:19:31. © Urheberrechtlich geschützter Inhalt. Ohne gesonderte Erlaubnis ist jede urheberrechtliche Nutzung untersagt, insbesondere die Nutzung des Inhalts im Zusammenhang mit, für oder in KI-Systemen, KI-Modellen oder Generativen Sprachmodellen.

In case of P2 hybrid architectures, integrated solutions of Triple Wet Clutches with efficient actuation systems are having a big attention on several OEM projects. Efficient ways for hybridization can be achieved either using existing dual clutches gearboxes, either using dedicated hybrid transmissions (DHT). In those cases the packaging constraints in axial direction are at stake, particularly on FWD applications. The integration of the disconnecting clutch between ICE and gearbox (C0) inside a the Triple Wet Clutch (TWC) is providing smart design solution. The paper will describe different architectures of TWC with Clutch Slave Cylinders (CSC) and piston type actuation technologies focusing on P2 Off-line hybrid architectures, and their associated advantages and drawbacks.
The paper will also describe an innovative actuation system of the TWC, managing also some gearbox functions as park lock and gear shift cylinders. The actuation system is a Valeo innovation which considers the needs of DHTs. It can actuate three clutches and operate the shifting of the gears and park lock cylinders. Modern DCTs and DHTs use so called "on-demand" actuation systems to avoid the constant losses of central power packs, which are generated by their constant high pressure level and leakages in the spool valves. The hydraulically actuation of the clutches and shifters brings a high power density and therefore advantages in the gearbox packaging. The focus of the development work is on low power consumption, low weight, small packaging free in positioning, and attractive pricing. A closed oil circle with an own oil reservoir allows lifetime filling and free choice of the lubrication oil.

Introduction: several clutches arrangement solutions

In case of P2 off-line gearbox hybridization, OEM can chose different architecture options. The first option is a “P2 off-line module” [1]. The P2 off-line module (Fig.1) is a very interesting solution for FWD cars with several transmission types to be hybridized (DCT, AMT or AT gearboxes), it includes the C0 clutch and the damper, and is connected with a chain to a 48V E-motor. The P2 off-line module as being is versatile solution, allows for example to use existing standard Double Wet Clutches, in case of hybridization of a DCT, either using a CSC actuation or a rotary feeding piston actuation technology (Fig. 2 & Fig.3).

https://doi.org/10.51202/9783181023549 - Generiert durch IP 216.73.216.36, am 19.01.2026, 02:19:31. © Urheberrechtlich geschützter Inhalt. Ohne gesonderte Erlaubnis ist jede urheberrechtliche Nutzung untersagt, insbesondere die Nutzung des Inhalts im Zusammenhang mit, für oder in KI-Systemen, KI-Modellen oder Generativen Sprachmodellen.

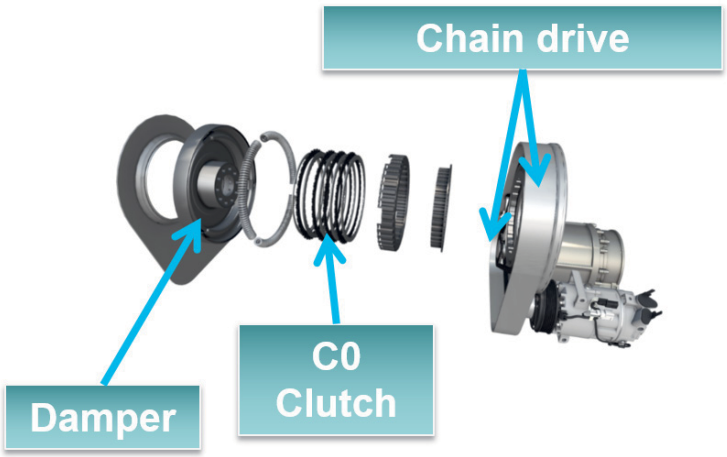


Fig. 1: P2 off-line module



Fig. 2: DWC with dCSC actuation



Fig. 3: DWC with piston actuation

The second option is the Triple Wet Clutch Module. In case there is only one transmission to be hybridized, the TWC will probably present the advantage of good packaging optimization and function integration. The packaging optimization will be achieved with a smart arrangement of the three clutches in the given packaging, and the function integration will be done thanks to the combination of different actuation components in the same actuation module, as we will see below. However this solution will remain specific to a given packaging, therefore somewhere more difficult to standardize to other applications.

https://doi.org/10.51202/9783181023549 - Generiert durch IP 216.73.216.36, am 19.01.2026, 02:19:31. © Urheberrechtlich geschützter Inhalt. Ohne gesonderte Erlaubnis ist jede urheberrechtliche Nutzung untersagt, insbesondere die Nutzung des Inhalts im Zusammenhang mit, für oder in KI-Systemen, KI-Modellen oder Generativen Sprachmodellen.

Triple Wet Clutches off line unit - CSC Actuation

The TWC with CSC actuation presents the advantage of having an optimized CO_2 efficiency, thanks to CSC actuation and removal the internal seals inside the clutches, usually used with rotary feeding and piston actuated clutches.
CO_2 efficiency simulations have been presented in previous papers from Valeo [2]. TWC with actuation of the three clutches by CSC is probably the most optimized architecture of wet clutches relative to CO_2 efficiency, and presents an efficiency gap compared to less optimized architectures which can reach 2%, which is very significant.
The Fig.4 represents an example of TWC with CSC, having a connection to an off-line 48 V or high voltage E-motor realized by a gear set. The C0 clutch is actuated from the left by a CSC, and the C1 & C2 clutches from the right by a double CSC. The TWC is supported by two support bearings.

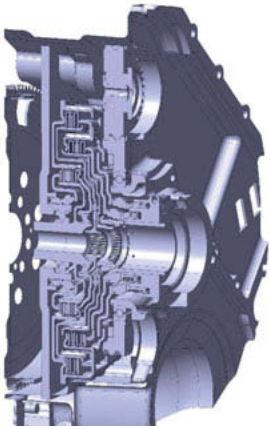


Fig. 4: Triple Wet Clutch Module with CSC passive actuation

The gear connected to the clutch is supported by a bearing directly linked to the gearbox. This allows to control very precisely the distance tolerance between the rotation axis of gear connected to the clutch and the rotation axis of the gear connected to the E-motor, in order to obtain good NVH performance. The misalignment between the triple clutch unit and the gear is managed by an innovative misalignment compensation device, capable to transmit torque and compensate the off axis. The design of the TWC represented on Fig.4 is optimized to cope

https://doi.org/10.51202/9783181023549 - Generiert durch IP 216.73.216.36, am 19.01.2026, 02:19:31. © Urheberrechtlich geschützter Inhalt. Ohne gesonderte Erlaubnis ist jede urheberrechtliche Nutzung untersagt, insbesondere die Nutzung des Inhalts im Zusammenhang mit, für oder in KI-Systemen, KI-Modellen oder Generativen Sprachmodellen.

with very tight axial packaging, typical for DHT with FWD vehicle applications, with the three clutches nested on the same vertical axis.

Triple Wet Clutch off line module – Rotary feeding and piston Actuation

Other architectures are possible with rotary feeding and piston actuation, depending on customer choices relative to actuation type. The triple clutch module is still connected to a 48V or high voltage E-motor with a gear set. The appropriate support of the TWC is still ensured with two support bearings as shown on Fig.5. There is a similar misalignment device as described in previous paragraph, between the triple clutch unit and the gear.
Depending on packaging possibilities, a possible smart arrangement is to actuate the C0 clutch by a CSC, allowing better CO_2 performances compared with C0 piston actuation.
In this configuration, actuation maximum pressure of C1 and C2 would be around 18 bars, as the actuation pressure of C0 with CSC would de around 40 bars. This difference of actuation pressure range can be easily managed with the Valeo actuation system described below with two pumps, the first one managing the C1 & C2, and the second one managing the C0, shift actuators and park lock.

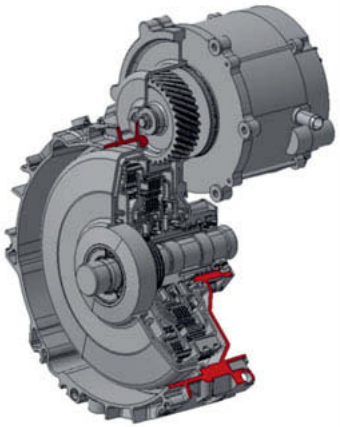


Fig. 5: Triple Wet Clutches unit with rotary feeding and C1 & C2 piston actuation

https://doi.org/10.51202/9783181023549 - Generiert durch IP 216.73.216.36, am 19.01.2026, 02:19:31. © Urheberrechtlich geschützter Inhalt. Ohne gesonderte Erlaubnis ist jede urheberrechtliche Nutzung untersagt, insbesondere die Nutzung des Inhalts im Zusammenhang mit, für oder in KI-Systemen, KI-Modellen oder Generativen Sprachmodellen.

Actuation system

New hybrid transmissions and DHTs have a big focus on efficiency. Conventional power packs generate losses by constant high line pressures, leakages in valves, rotating seals for piston type wet clutch actuation, and actuators, and in case of mechanical driven pumps by far too high oil flow at higher engine speed. Even power packs with electrically driven pumps and accumulators cannot be considered as “on-demand-actuation systems”, as they still work with high line pressures and leaky valves.
The Valeo powertrain actuation system works with real on-demand-actuation, the pressure for the actuation of the clutches is only created when it is needed, in the level which is actually needed, and can be kept without leakages and the need of running pumps for a longer period. The same philosophy is used at the actuation cylinders. Additionally, it is very important for an efficient system to separate high pressure supply for actuation from low pressure for lubrication and clutch cooling.

The clutch actuation is done by an electrically driven dual flow pump with two inlets and two outlets, see Fig. 6. The roller vane pump which is used here can provide the two independent flows with only one set of pump stator and rotor, is robust against contaminations and cost-effective. The flow in both outlets is proportional to the pump speed and is guided over check valves to the CSCs. The pressure on both outlets can be regulated independently by two proportional valves.

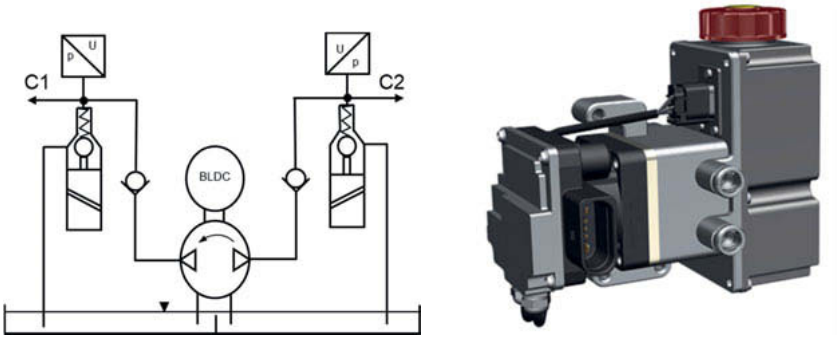


Fig. 6: Hydraulic Double Clutch Actuator

https://doi.org/10.51202/9783181023549 - Generiert durch IP 216.73.216.36, am 19.01.2026, 02:19:31. © Urheberrechtlich geschützter Inhalt. Ohne gesonderte Erlaubnis ist jede urheberrechtliche Nutzung untersagt, insbesondere die Nutzung des Inhalts im Zusammenhang mit, für oder in KI-Systemen, KI-Modellen oder Generativen Sprachmodellen.

The proportional valves are designed in ball seat technology, which is unusual in gearbox hydraulics. The reasons for this design are robustness against contamination, cost-effective components and leak-tightness in closed position. This enables, in combination with CSC-type actuation of the wet clutches, that the pressure can be kept on the desired level only by actuating the proportional valve with relatively low electrical current consumption, and the motor-pump can be stopped.
The BLDC motor and the proportional valves are driven by an integrated electronic control unit (ECU), which is regulating the pressure in closed loop with the help of integrated pressure sensors. The ECU is connected to the transmission control unit (TCU) via CAN interface, receives commands for pressures on both channels and operation modes, and sends actual data and diagnostic values. It starts and stops the motor, and decides the motor speed according to the operation modes.
The actuator has its own reservoir, which is divided below a certain level into two chambers in order to maintain the function in one circle even when the other circle would be leaky. In this case the DCT would be operated similar to an AMT (automated manual transmission). The closed oil circle allows, together with the robust valves and pump, to omit a suction filter, which improves the function at low temperature. Filtering is done on pressure side and on the connectors, to avoid contamination from outside.

The shifting and the park lock actuation are made by a second electrically driven pump in combination with cylinders with integrated locking magnets. The single flow pump has two ports, which change the function from inlet to outlet or vice versa when the sense of rotation is changed.
All actuation cylinders can be connected in parallel without any valve in between. The pistons have as many grooves as desired positions, in case of a shift cylinder normally three, e.g. for gear 1, neutral and gear 3; in case of the park lock cylinder there are two grooves for engaged and disengaged position. The pawl magnets are moving the locking pins, which are spring loaded in the locked position. The geometry of groove and pin is chosen in a way that the locked piston does not move even under maximum pressure. The cylinders have integrated position sensors.

https://doi.org/10.51202/9783181023549 - Generiert durch IP 216.73.216.36, am 19.01.2026, 02:19:31. © Urheberrechtlich geschützter Inhalt. Ohne gesonderte Erlaubnis ist jede urheberrechtliche Nutzung untersagt, insbesondere die Nutzung des Inhalts im Zusammenhang mit, für oder in KI-Systemen, KI-Modellen oder Generativen Sprachmodellen.

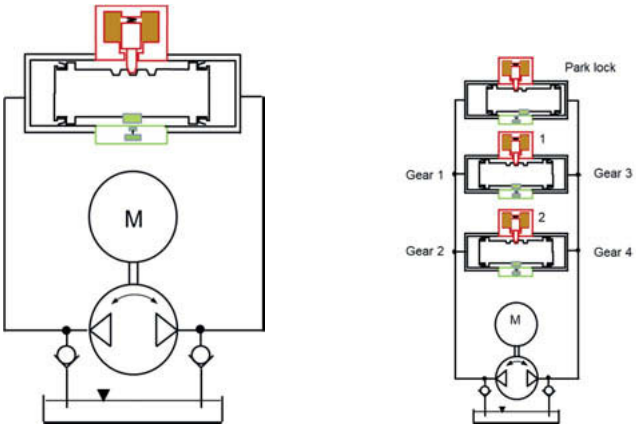


Fig. 7: Schematic shifting system

The reversible pump moves the released piston by pumping the oil from the one side to the other side of the double-acting cylinder; the synchronizing is done by controlling the torque of the pump motor in closed loop with the signals from the position sensor. The pressure acts on one side of each of the cylinders, but only the released one is moving.

Both ports of the pump have a connection to the reservoir via a check-valve. This enables that volume losses caused for example by bleeding orifices can be compensated on the actual inlet port.

The motor is also driven by an integrated ECU, which is regulating the motor speed and limits dynamically the motor torque according to the commands of the TCU. The ECU is connected to the transmission control unit (TCU) via CAN interface, receives commands for sense of rotation, motor speed and torque limit, and sends actual data and diagnostic values. The pawl magnets and position sensors are directly wired to the TCU, in order to divide the tasks and to gain a higher safety level.

The actuation of the engine clutch (C0) is also made by the shift pump. When all pistons are locked in neutral or shifted position, a valve to the clutch actuation branch can be opened and the clutch can be pressurized in the same way as the other clutches.

https://doi.org/10.51202/9783181023549 - Generiert durch IP 216.73.216.36, am 19.01.2026, 02:19:31. © Urheberrechtlich geschützter Inhalt. Ohne gesonderte Erlaubnis ist jede urheberrechtliche Nutzung untersagt, insbesondere die Nutzung des Inhalts im Zusammenhang mit, für oder in KI-Systemen, KI-Modellen oder Generativen Sprachmodellen.

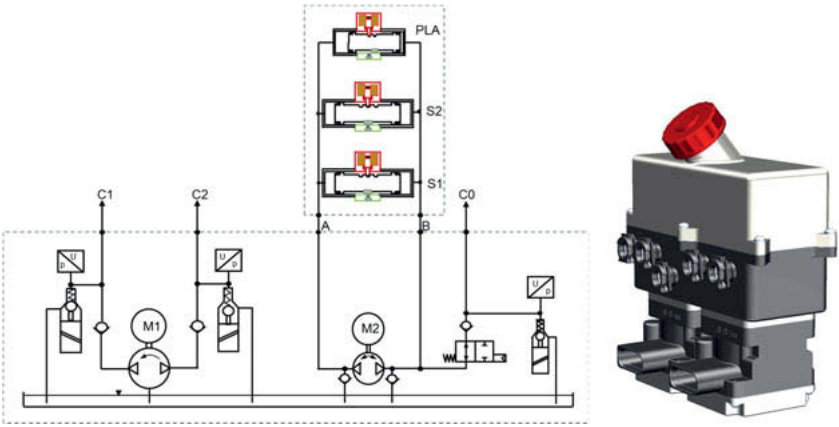


Fig. 8: Schematic triple clutch and shift actuator

When hydraulically shifting will not be used in the transmission, the third clutch can be operated by a modified version of the dual flow pump. The motor will be made reversible, and the 4 ports of the dual flow pump change their function from inlet to outlet or vice-versa with the sense of rotation. For example C1 and C2 are pressurized in clockwise rotation, and the C0 clutch in anti-clockwise sense of rotation. The circles are separated by check-valves.

Active lubrication and dedicated cooling of the clutch pack by a separate low-pressure optimized motor pump reduces losses in the transmission by reduced friction in the gears and bearings and reduced drag losses in the open clutches. An additional gain can be achieved with dry sump lubrication. This low pressure systems have to be adapted to the transmission, there a lot of different solutions.

The chosen example shows a schematic with a heat exchanger, a lubrication and a cooling circle. When the pump is running anticlockwise, it supplies oil for lubrication. Due to the higher pressure drop in the heat exchanger, caused by the higher viscosity, the cold oil will partly bypass the heat exchanger through the preloaded check valve. This helps for a faster warm-up and will reduce losses in the gear meshes and lubrication. Warm oil will only pass the heat exchanger, because the pressure drop in the heat exchanger will be reduced. When the pump is running clockwise, it supplies oil to lubrication and cooling, divided up by the orifices and the flow resistance of the following circle.

https://doi.org/10.51202/9783181023549 - Generiert durch IP 216.73.216.36, am 19.01.2026, 02:19:31. © Urheberrechtlich geschützter Inhalt. Ohne gesonderte Erlaubnis ist jede urheberrechtliche Nutzung untersagt, insbesondere die Nutzung des Inhalts im Zusammenhang mit, für oder in KI-Systemen, KI-Modellen oder Generativen Sprachmodellen.

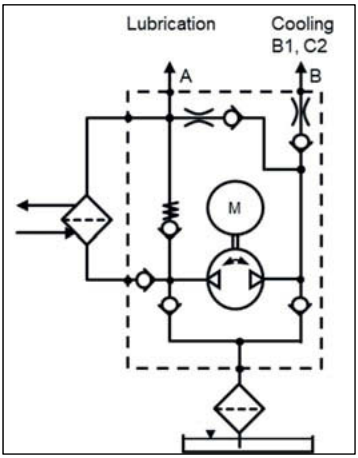


Fig. 9: Lubrication and cooling pump with heat exchanger

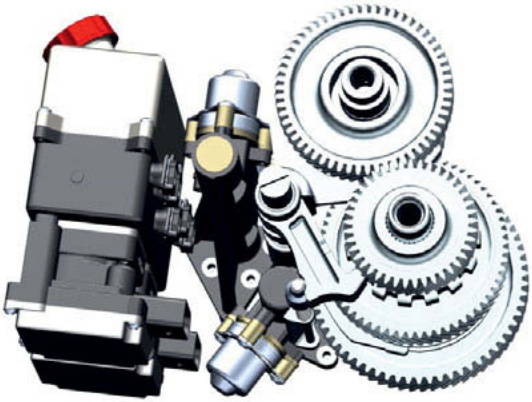


Fig. 10: Actuation system integration on a DHT gearbox

https://doi.org/10.51202/9783181023549 - Generiert durch IP 216.73.216.36, am 19.01.2026, 02:19:31. © Urheberrechtlich geschützter Inhalt. Ohne gesonderte Erlaubnis ist jede urheberrechtliche Nutzung untersagt, insbesondere die Nutzung des Inhalts im Zusammenhang mit, für oder in KI-Systemen, KI-Modellen oder Generativen Sprachmodellen.

Conclusion

The triple wet module is an attractive solution for Hybrid Transmissions. In case of P2 off-line for DHT or Hybrid FWD transmissions, where the axial packaging is at stake, an innovative arrangement of three clutches nested on same vertical axis has been proposed. In order to obtain a good NVH performance on the gear set connection between E-motor and clutches, a robust design of the gear set associated with a new misalignment compensation system has been described.

The actuation system plays an important role in the efficiency of the gearbox. Real "on-demand-actuation" avoids losses due to constantly high pressures and leakages, and reduces the stress on the components. Lubrication and oil cooling with separate oil pump systems can also contribute to an efficient system.

References in this document

[1] P2 Off Line module compared with other architectures, CTI Symposium Automotive Transmissions, Valeo Powertrain systems, Berlin, December 2018

[2] Dual Wet Clutches for Hybrid power trains, challenges for packaging and fuel efficiency optimization, CTI Symposium Automotive Transmissions, Valeo Powertrain systems, Berlin, December 2017

https://doi.org/10.51202/9783181023549 - Generiert durch IP 216.73.216.36, am 19.01.2026, 02:19:31. © Urheberrechtlich geschützter Inhalt. Ohne gesonderte Erlaubnis ist jede urheberrechtliche Nutzung untersagt, insbesondere die Nutzung des Inhalts im Zusammenhang mit, für oder in KI-Systemen, KI-Modellen oder Generativen Sprachmodellen.

https://doi.org/10.51202/9783181023549 - Generiert durch IP 216.73.216.36, am 19.01.2026, 02:19:31. © Urheberrechtlich geschützter Inhalt. Ohne gesonderte Erlaubnis ist jede urheberrechtliche Nutzung untersagt, insbesondere die Nutzung des Inhalts im Zusammenhang mit, für oder in KI-Systemen, KI-Modellen oder Generativen Sprachmodellen.

New All-Wheel Drive Systems in Mercedes-Benz SUVs

Sven Stöhr, **Ralf Koesling**, **Volker Marx**,
Daimler AG, Stuttgart

Zusammenfassung

Mit der Markteinführung der M-Klasse hat Mercedes-Benz 1997 das Segment der Premium-SUVs begründet. Seit Herbst 2015 heißt die Modellfamilie GLE, was ihre Stellung als Luxus-SUV der zur E-Klasse gehörenden Modellfamilie verdeutlicht.

Erstmals wird bei Fahrzeugen mit Sechs- und Achtzylindermotoren sowie bei Plug-in-Hybriden ein vollvariabler Allradantrieb (Torque-on-Demand) angeboten, der die Momentenverteilung zwischen der Vorder- und Hinterachse entsprechend dem ausgewählten Fahrprogramm regelt. Mit dem optionalen Offroadpaket steht als Weltneuheit ein vollvariabler Allradantrieb mit Low- und High-Range-Modus zur Verfügung, sodass der GLE auf Wunsch so geländetauglich wie noch nie ist.

Abstract

Mercedes-Benz established the premium SUV segment with the launch of the M-Class in 1997. Since 2015, the model family has been called GLE to underline its position as the luxury SUV of the model family belonging to the E-Class.

For the first time, vehicles with four- and six cylinder engines are available with fully variable all-wheel drive (Torque-on-Demand) that regulates the torque distribution between the front and rear axles according to the selected drive program.

The optional Off-Road package offers the world's first fully variable all-wheel drive with high and low range modes, turning the GLE into an all-terrain vehicle as never before.

https://doi.org/10.51202/9783181023549 - Generiert durch IP 216.73.216.36, am 19.01.2026, 02:19:31. © Urheberrechtlich geschützter Inhalt. Ohne gesonderte Erlaubnis ist jede urheberrechtliche Nutzung untersagt, insbesondere die Nutzung des Inhalts im Zusammenhang mit, für oder in KI-Systemen, KI-Modellen oder Generativen Sprachmodellen.

All-Wheel Drive System Development at Mercedes-Benz SUVs of the last 40 years

Production of the G-Class W460 began in Graz in 1979. The "G" stood (in German) for "all-terrain vehicle", illustrating the new Mercedes-Benz all-terrain vehicle's suitability for off-road use. The all-wheel history of the G-Class started out with a manually selectable front axle and an integrated off-road differential gear set.



Fig. 1: All Wheel Drive System History

Unveiled in 1989, the 463 model series turned the G-Class into a more high-grade vehicle, developing it more in the direction of a passenger car. In comparison with the 460 model series, it came with permanent all-wheel drive with a manually selectable off-road gear.

In 1991, Graz made the switch from the 460 model series to the 461 model series, which was aimed at customers who, in contrast to the 463 model series, attached greater importance to technology than to comfort.

In the early 1990s, the company identified the potential for a new, more comfortable segment of off-road automobiles. This led to the development of the M-Class of the 163 model series, which made its debut in 1997, focusing on the combination of off-road capability and comfort. A decision was made in favor of permanent all-wheel drive with an open differential. However, the differential locks were replaced by a further-developed variant of the electronic traction system, which reduced the differential rotational speeds on slippery surfaces by intervening in the braking system.

In 2005, the M-Class (W164) replaced the previous W163 model series and was equipped with a new transfer case with 50:50 torque distribution. This was also used in the related R-Class

https://doi.org/10.51202/9783181023549 - Generiert durch IP 216.73.216.36, am 19.01.2026, 02:19:31. © Urheberrechtlich geschützter Inhalt. Ohne gesonderte Erlaubnis ist jede urheberrechtliche Nutzung untersagt, insbesondere die Nutzung des Inhalts im Zusammenhang mit, für oder in KI-Systemen, KI-Modellen oder Generativen Sprachmodellen.

(251 model series) and GL-Class (X164). An Off-Road package was optionally available for the W164. It included among other things a middle- and rear-differential lock and a low range mode, which made it possible for an off-road gear to be engaged even while driving (shift-on-the-move).

Starting in 2011, the successors W166 and X166 of the M- and GL-Class were launched on the market. They started out with the familiar transfer cases from the 164 model series. For the facelift in 2015, the ML- and GL-Class were renamed GLE- and GLS-Class to emphasize their relationship with the G-Class. The GLE Coupé extended the platform portfolio with the C292 to include a new segment of SUV coupés. The use of the new nine-speed automatic transmission (NAG3) made it necessary for the transfer cases to be strengthened.

Requirements on the new All-Wheel Drive System

The development of the new transfer case portfolio for the new derivatives of the GLE-Class focused on improving the driving dynamics without tolerating any compromises in terms of traction and driving safety. The key criteria were the on-road capabilities of longitudinal agility, lateral agility and backlash effect as well as the off-road capabilities of rock climbing, driving on sand and slippery surfaces as well as general driving safety. Compared with the previous model series, all the criteria were significantly improved, with the development goals being achieved on every front.



Fig. 2: Requirements on the New All-Wheel Drive System

https://doi.org/10.51202/9783181023549 - Generiert durch IP 216.73.216.36, am 19.01.2026, 02:19:31. © Urheberrechtlich geschützter Inhalt. Ohne gesonderte Erlaubnis ist jede urheberrechtliche Nutzung untersagt, insbesondere die Nutzung des Inhalts im Zusammenhang mit, für oder in KI-Systemen, KI-Modellen oder Generativen Sprachmodellen.

Particularly with regard to the criteria of longitudinal agility and backlash effect, the selective pre-supply of torque to the front axle differential resulted in a significantly improved utilization of the transient behavior of all the new engines through a reduction of the backlash effect damping.

Technically, the enhanced driving dynamics is realized by selective under- or oversteer by an electronically controlled longitudinal transfer case with variable distribution from 0 to 100% (Torque on Demand) of the drive torque.

Further objectives with regard to the vehicle integration of the transfer cases were:

- efficient operation of the transfer cases with low drag torque.
- the isolation of the transmission oil from the environment to prevent harmful effects through dirt or water ingress and to be able to rule out any oil leakage from the transmission under all driving conditions.
- the optimum of transfer and distribution of the engine torque to the road in a wide range of (special) driving maneuvers as well as damage-free endurance of the resulting peak torques, including with maximum payload, trailer load and on a wide variety of road surfaces.
- guaranteeing of the functions in spite of mechanical vehicle influences such as vibrations and off-road forces, stone chips and dirt accumulation when driving on poor roads.
- damage-free operation at high and low ambient/component temperatures, while driving and during heating.
- Low operation noise of the transfer cases with regard to NVH, including in the rpm window of the natural resonances.
- compliance with the requirements on the E/E and EMC environment.
- compliance with the high Mercedes-Benz corrosion standards.
- compliance with the requirements of the assembly process.

The Mercedes-Benz SUV- All-Wheel Drivetrain

In the conventional Mercedes-Benz powertrains of the 167 and new 463 model series, the transfer case is next to the automatic transmission. The output torque from the automatic transmission is optionally increased in the transfer case in low range mode and transferred to the front and rear prop shafts. They connect the transfer case to the front and rear axle differentials, where the torque is again split between the left and right side-shafts. Fig. *3* presents these components of the drivetrain.

https://doi.org/10.51202/9783181023549 - Generiert durch IP 216.73.216.36, am 19.01.2026, 02:19:31. © Urheberrechtlich geschützter Inhalt. Ohne gesonderte Erlaubnis ist jede urheberrechtliche Nutzung untersagt, insbesondere die Nutzung des Inhalts im Zusammenhang mit, für oder in KI-Systemen, KI-Modellen oder Generativen Sprachmodellen.

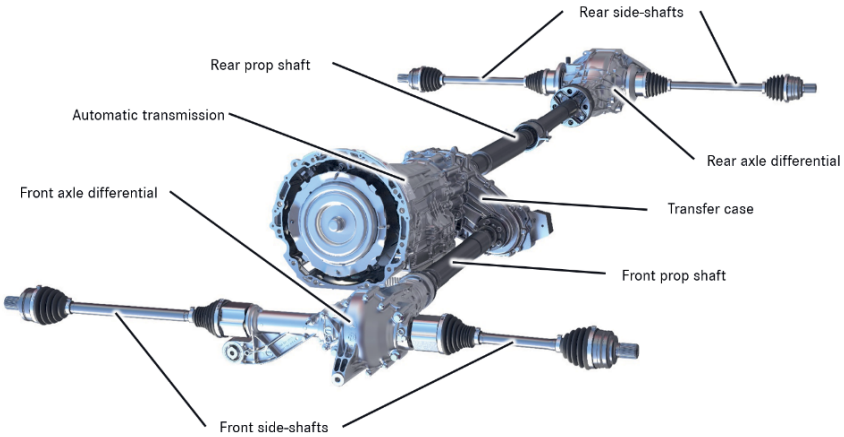


Fig. 3: Drivetrain of the new GLE-Class

Modular Architecture of All-Wheel Drive Powertrain

During the development of the new Mercedes-Benz powertrains, great importance was attached to the establishment of a consistent platform strategy. The individual engines and powertrain components can be combined in countless variants for use in different vehicles.



Fig. 4: Modular Powertrain Platform

https://doi.org/10.51202/9783181023549 - Generiert durch IP 216.73.216.36, am 19.01.2026, 02:19:31. © Urheberrechtlich geschützter Inhalt. Ohne gesonderte Erlaubnis ist jede urheberrechtliche Nutzung untersagt, insbesondere die Nutzung des Inhalts im Zusammenhang mit, für oder in KI-Systemen, KI-Modellen oder Generativen Sprachmodellen.

The modular construction kit of the new GLE- and G-Class with the engine variants used in all derivatives of the two model series, the transmission heads, nine-speed automatic transmission variants and the new transfer cases and the 4x2 adapter housing.

Engine Portfolio of the new GLE- and G-Class

In comparison with the respective previous model series, the new GLE- and G-Class are powered by almost totally new engines. In the 6-cylinder gasoline engine segment, the M256 inline engine, which belongs to the new Mercedes-Benz powertrain architecture family, replaces the previous V6 petrol engine M276. In the 6-cylinder diesel engine segment, the OM642 is replaced by the OM656. Here too, there is a change of concept from a V-type engine to an inline engine. Further introductions of new engine variants are planned in early next future.

In every engine, various technology modules ensure a high specific power output, low specific consumption and emissions, through both in-engine measures and further-improved exhaust aftertreatment systems.

For exhaust aftertreatment, all the diesel engines are equipped with a passive SCR catalyst, while, depending on the market, the gasoline engines feature a passive gasoline particulate filter.

9G-TRONIC Automatic Transmission

While the W166 is available with an automatic transmission with either nine or seven speeds, the 167 model series comes exclusively with a nine-speed automatic transmission. With nine forward speeds, this automatic transmission makes for exceptional dynamics, efficiency and comfort, such as fast and smooth gearshifts. At the same time, the automatic transmission helps to further reduce the fuel consumption and emissions.

The conceptually defined ratio spread, for example, creates the basis for generally lower engine speeds, this resulting in further improvements in ride comfort and noise level.

The 9G-TRONIC in its different+ variants is not only suitable for conventional powertrains, but also for electrified powertrains, e.g. in combination with an integrated starter-alternator (ISA) or a plug-in hybrid powertrain.

https://doi.org/10.51202/9783181023549 - Generiert durch IP 216.73.216.36, am 19.01.2026, 02:19:31. © Urheberrechtlich geschützter Inhalt. Ohne gesonderte Erlaubnis ist jede urheberrechtliche Nutzung untersagt, insbesondere die Nutzung des Inhalts im Zusammenhang mit, für oder in KI-Systemen, KI-Modellen oder Generativen Sprachmodellen.

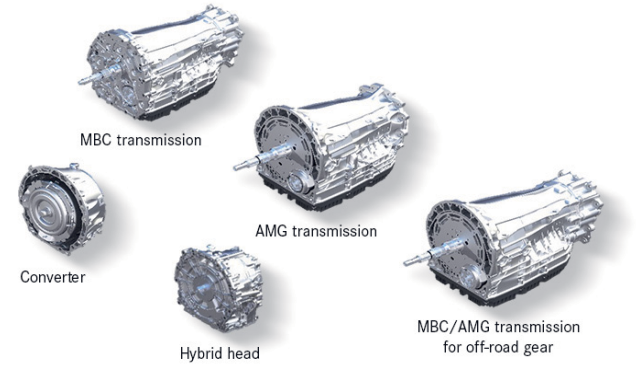


Fig. 5: Automated Transmission Overview

New 4MATIC Transfer Case Variants of GLE-Class

The modular transfer case kit of the 167 model series consists of three transfer case variants, which transfer some of the torque from the input of the longitudinal transfer case by a chain to the front axle and which are described in greater detail below.

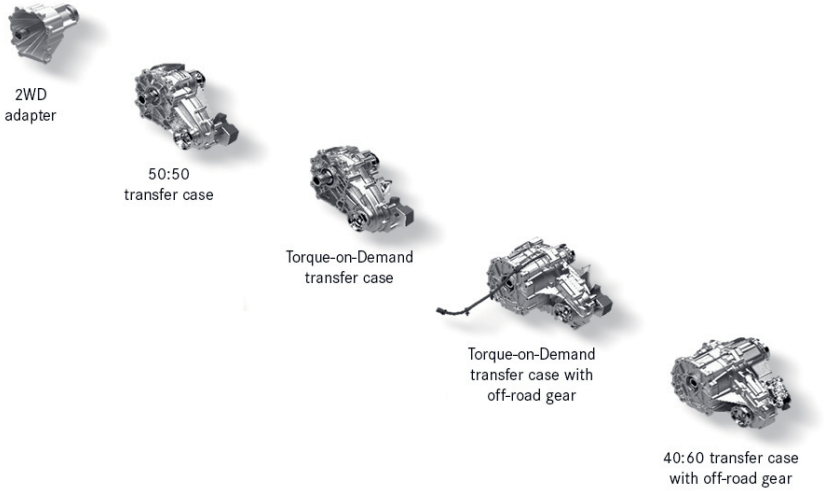


Fig. 6: Overview of the new Transfer Case Variants

https://doi.org/10.51202/9783181023549 - Generiert durch IP 216.73.216.36, am 19.01.2026, 02:19:31. © Urheberrechtlich geschützter Inhalt. Ohne gesonderte Erlaubnis ist jede urheberrechtliche Nutzung untersagt, insbesondere die Nutzung des Inhalts im Zusammenhang mit, für oder in KI-Systemen, KI-Modellen oder Generativen Sprachmodellen.

The new transfer case variants include single- and double speed transfer cases. Single speed cases are connected via adapter housing to the automatic transmission. Transfer cases with off-road gear by high/low differential planetary gear set are screwed directly to the nine speed automatic transmission.

Torque Distribution 50:50 Transfer Case

In combination with the conventional 4-cylinder engines, the entry-level variant is a transfer case that is flanged onto the 9G-TRONIC and which distributes the drive torque to the front and rear axles in a fixed ratio of 50:50 percent. This variant has no lock.



Fig. 7: 50:50 Transfer Case

- Torque distribution: 50% / 50% by means of open differential
- Weight: 20.9 kg
- Lubrication concept: passive lubrication, oil supplied to the components around the main shaft via the chain with oil capacity: 600 ml
- Maximum input torque: 2,800 Nm
- Maximum input shaft speed: 7,000 rpm

https://doi.org/10.51202/9783181023549 - Generiert durch IP 216.73.216.36, am 19.01.2026, 02:19:31. © Urheberrechtlich geschützter Inhalt. Ohne gesonderte Erlaubnis ist jede urheberrechtliche Nutzung untersagt, insbesondere die Nutzung des Inhalts im Zusammenhang mit, für oder in KI-Systemen, KI-Modellen oder Generativen Sprachmodellen.

Torque-on-Demand Transfer Case – Single Speed

The new Mercedes-Benz Torque-on-Demand transfer case is used in combination with all engine combinations. It contains an electromechanically controlled multi-plate clutch, which, in comparison with the 50:50 transfer case, allows a variable distribution of the drive torque between the axles from 0% to 100%. As the default, the drive torque is transferred directly to the rear axle by a continuous output shaft. When required, the electric servomotor increases the pressure on the multi-plate clutch via a ball ramp, thereby transferring the drive torque to the front axle as well.

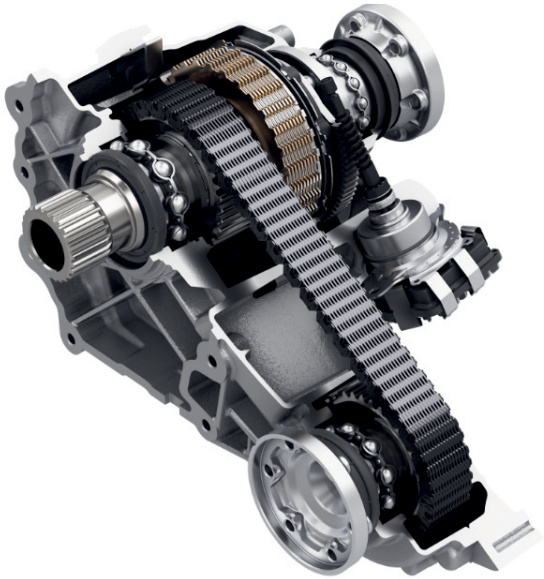


Fig. 8: Torque-on-Demand transfer case – single speed

- Torque distribution: variable
- Clutch torque: 1600 Nm nominal value
- Weight: 23.7 kg
- Lubrication concept: passive lubrication, oil supplied to the components around the main shaft via the chain with oil capacity: 750 ml
- Maximum input torque: 2,800 Nm
- Maximum input shaft speed: 7,000 rpm

https://doi.org/10.51202/9783181023549 - Generiert durch IP 216.73.216.36, am 19.01.2026, 02:19:31. © Urheberrechtlich geschützter Inhalt. Ohne gesonderte Erlaubnis ist jede urheberrechtliche Nutzung untersagt, insbesondere die Nutzung des Inhalts im Zusammenhang mit, für oder in KI-Systemen, KI-Modellen oder Generativen Sprachmodellen.

Torque-on-Demand Transfer Case – Double Speed

A new Torque-on-Demand transfer case with off-road differential gear set is optionally available for the 6- cylinder engines as part of the Off-Road Package. In addition to the electromechanically controlled multi-plate clutch, this transfer case also contains a low range stage for off-road use.

The off-road differential gear set significantly increases the torque at the drive wheels, making it possible, for example, to drive in highly challenging terrain, to pull away on extreme grades and, conversely, drive downhill with a significantly increased braking effect from the engine.

As the default, the drive torque is transferred to the rear axle and, when required, also to the front axle via a multi-plate clutch controlled similarly to the Torque-on-Demand transfer case variant without off-road reduction gear.

Reduction is by means of a differential planetary gear set in which a shift fork, also electromechanically controlled, can be used to switch between low and high range mode.

Due to the absence of synchronization, shifting to low range mode can be done only with the vehicle stationary.

Shifting out of the off-road gear (leaving the low range mode) is synchronized and allowable up to a maximum vehicle speed of 50 km/h.

The transfer case additionally includes a static lock mode in which the multi-plate clutch is locked by a specific hold device unit, even in the currentless state. This means that the parking lock acts not only on the rear axle, but also on the front axle, enabling the vehicle to be parked also off-road and on slippery surfaces.

https://doi.org/10.51202/9783181023549 - Generiert durch IP 216.73.216.36, am 19.01.2026, 02:19:31. © Urheberrechtlich geschützter Inhalt. Ohne gesonderte Erlaubnis ist jede urheberrechtliche Nutzung untersagt, insbesondere die Nutzung des Inhalts im Zusammenhang mit, für oder in KI-Systemen, KI-Modellen oder Generativen Sprachmodellen.

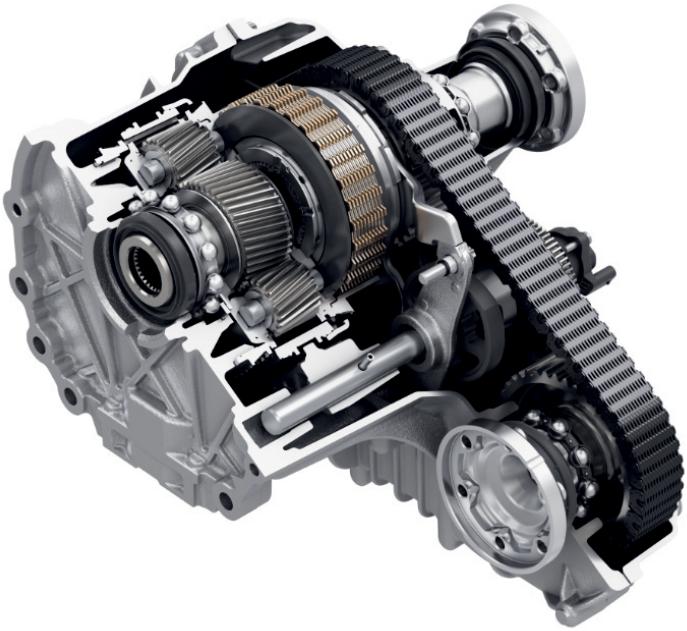


Fig. 9: Torque-on-Demand Transfer Case with Low Gear Differential – Double Speed

- Torque distribution: variable
- Clutch torque: 2800 Nm nominal value
- Low range gear ratio: i = 2.93 by planetary gear set with 4 planets
- Synchronization: low-high shifting, synchronized
- Weight: 41.4 kg
- Lubrication concept: active lubrication by oil pump as well as passive lubrication of the components around the main shaft via the chain, Oil capacity: 1,500 ml
- Maximum input torque: 2,800 Nm
- Maximum input shaft speed: 7,000 rpm

The Torque-on-Demand transfer case with off-road gear is used in the GLE model series together with a vent pipe that leads from the transfer case vent nozzle via the transmission clamping tab to the traction head. This makes it possible to meet the required fording depth of the vehicle.

https://doi.org/10.51202/9783181023549 - Generiert durch IP 216.73.216.36, am 19.01.2026, 02:19:31. © Urheberrechtlich geschützter Inhalt. Ohne gesonderte Erlaubnis ist jede urheberrechtliche Nutzung untersagt, insbesondere die Nutzung des Inhalts im Zusammenhang mit, für oder in KI-Systemen, KI-Modellen oder Generativen Sprachmodellen.

Torque Flow at different Operating Positions

The following illustrations show the Torque-on-Demand longitudinal transfer case with off-road gear in the various operating positions.

The torque-transferring components are shown on the left-hand side of each illustration, while the combination of control unit, electric motor, worm shaft, actuator shaft, ball ramp and shift fork in the corresponding operating position is shown on the right-hand side.

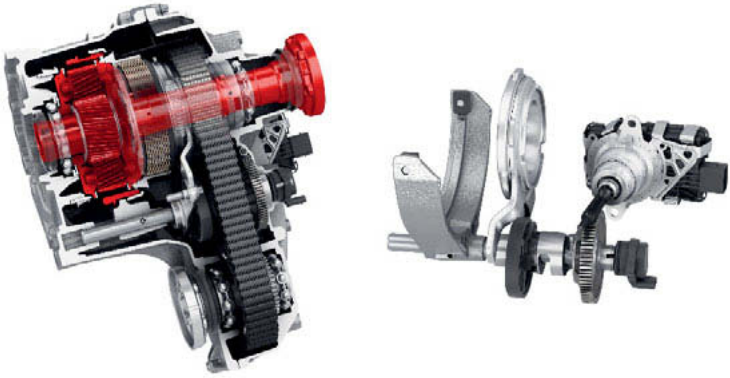


Fig. 10: Torque-on-Demand transfer case with low gear differential in high range mode and with 100% drive torque at the rear axle

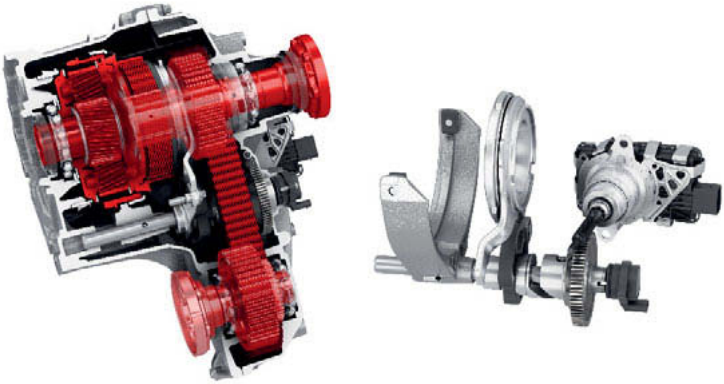


Fig. 11: Torque-on-Demand transfer case with low gear differential in high range mode and with the drive torque distributed to the front and rear axles

https://doi.org/10.51202/9783181023549 - Generiert durch IP 216.73.216.36, am 19.01.2026, 02:19:31. © Urheberrechtlich geschützter Inhalt. Ohne gesonderte Erlaubnis ist jede urheberrechtliche Nutzung untersagt, insbesondere die Nutzung des Inhalts im Zusammenhang mit, für oder in KI-Systemen, KI-Modellen oder Generativen Sprachmodellen.

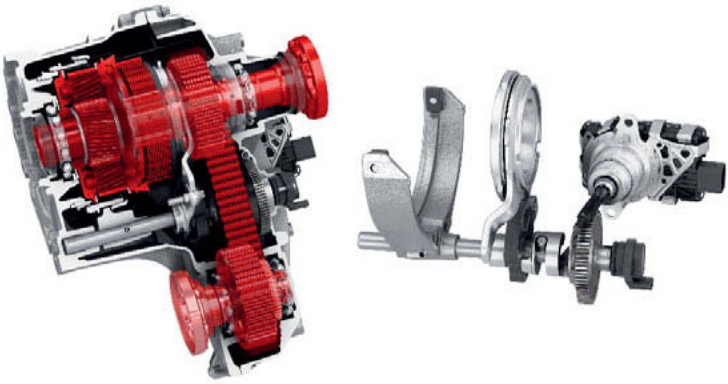


Fig. 12: Torque-on-Demand transfer case with low gear differential in low range mode and with the drive torque distributed to the front and rear axles

Torque Transfer Operation Strategy

Compared with the previous model the new GLE has further-enhanced agility and driving safety, especially when cornering, by means of selective yaw moment control (over- or understeer).

The control unit of the Torque-on-Demand transfer case computes the optimal torque distribution between the front and rear axles by continuously analyzing the driving dynamics and adjusts the distribution using the actuators on the multi-plate clutch.

The on-road operation strategy additionally takes account of the following drive-program-specific settings:

- Pulling away in on-road operation up to approx. 10 km/h with the multi-plate clutch closed to the maximum possible extent for an optimum of traction.
- The clutch torque is controlled depending on, among other things, the steering angle and the driving speed.
- The "Comfort" drive program is configured for all on-road road surfaces (dry asphalt, wet asphalt and snow-covered roads). This provides stable neutral handling.
- The "Sport" drive program gives priority to the driving dynamics with a rear-wheel drive bias. This allows a slight tendency to oversteer.

The Torque-on-Demand system also makes for improved performance in off-road operation, as control of the multi-plate clutch is fully variable.

https://doi.org/10.51202/9783181023549 - Generiert durch IP 216.73.216.36, am 19.01.2026, 02:19:31. © Urheberrechtlich geschützter Inhalt. Ohne gesonderte Erlaubnis ist jede urheberrechtliche Nutzung untersagt, insbesondere die Nutzung des Inhalts im Zusammenhang mit, für oder in KI-Systemen, KI-Modellen oder Generativen Sprachmodellen.

On the one hand, this delivers maximum traction as with a 100% longitudinal lock, whereas, at large steering angles, the clutch is opened to the necessary extent as required, making it possible to achieve an ideal turning circle also in off-road operation.
In addition, the Torque-on-Demand strategy reacts to the individual drive programs also in off-road operation:

- In the Off-Road drive program, the all-wheel drive performance is significantly enhanced with regard to traction, especially on sand, while the driving dynamics has no priority in this program.
- In the Off-Road+ drive program, the all-wheel drive performance is significantly enhanced with regard to traction, especially on rock, gravel and grass, while the driving dynamics has no priority in this program.
- Selecting the off-road gear (low range mode) increases the drive torque to allow very slow, sensitive driving in extreme off-road terrain as well as on high up- or downgrades.

Various sensor signals are used to analyze the current operating situation of the vehicle and to calculate an appropriate distribution of the drive torque. These sensor signals include:

- Gas pedal position
- Brake pedal position
- Steering wheel angle
- Engine speed
- Engine torque
- Vehicle speed
- Longitudinal acceleration
- Lateral acceleration
- Calculated temperature of the transfer case oil

The integration of transfer case control into the FlexRay™ data bus system makes it possible for the signals from the various sensors, which reproduce the current operating situation of the vehicle, to be managed with regard to both data volume and data transfer speed and for them to be used as control variables.

https://doi.org/10.51202/9783181023549 - Generiert durch IP 216.73.216.36, am 19.01.2026, 02:19:31. © Urheberrechtlich geschützter Inhalt. Ohne gesonderte Erlaubnis ist jede urheberrechtliche Nutzung untersagt, insbesondere die Nutzung des Inhalts im Zusammenhang mit, für oder in KI-Systemen, KI-Modellen oder Generativen Sprachmodellen.

The G-Class Transfer Case – Drivetrain

As already its predecessor, the new G-Class will continue to set the standards in its luxury off-road vehicles, particularly on off-road capability, robustness, quality and safety, and luxury comfort. The overall target of development was to make the new G-Class even more powerful in off-road performance, due to its standard ladder-type frame, the three 100-percent differential locks and the LOW RANGE offroad ratio.

Large ground clearance and long tension travel still form the basis for the further improved off-road properties of the G-Class:

- Climbing ability up to 100% with corresponding surface
- Ground clearance between the axles 241 millimeters plus 6mm maximum fording depth of now 70 centimeters in water and mud passages
- Handling stability at inclined positions of 35 °
- Angle of approach/departure: 30 °, front: 31 °
- Ramp angle: 26 °
- Tension travels: Front axle travel of 85/100 millimeters and rear axle travel of 82/142 millimeters (compression/rebound)

Torque Distribution 40:60 Transfer Case – Double Speed

The new 40:60 transfer case with off-road gear is flanged directly to the 9G TRONIC nine-speed automatic transmission, i.e. without adapter for the shaft interface and without intermediate housing.

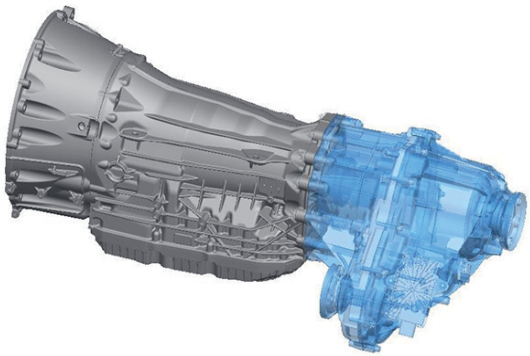


Fig. 13: The new 40:60 transfer case with 9G TRONIC

https://doi.org/10.51202/9783181023549 - Generiert durch IP 216.73.216.36, am 19.01.2026, 02:19:31. © Urheberrechtlich geschützter Inhalt. Ohne gesonderte Erlaubnis ist jede urheberrechtliche Nutzung untersagt, insbesondere die Nutzung des Inhalts im Zusammenhang mit, für oder in KI-Systemen, KI-Modellen oder Generativen Sprachmodellen.

With housing and main shaft adaptation, the same transfer case is used in the 470 model series (Mercedes-Benz X-Class), albeit in this case with the 7G TRONIC automatic transmission and an intermediate housing.

As a significant difference from the 50/50 torque distribution of the previous transfer case in the 463 model series, the new transfer case is so configured that, with sufficient traction, the drive torque is distributed 40% to the front axle and 60% to the rear axle, which is advantageous in the majority of driving conditions. The gear ratio can be changed from 1.00 (HIGH RANGE) to 2.93 (LOW RANGE) for off-road driving. These shifts are possible from HIGH RANGE to LOW RANGE up to 40 km/h and from LOW RANGE to HIGH RANGE up to 70 km/h.

Similarly to the off-road transfer case of the GLE-Class, the transfer case of the G-Class also includes a static lock mode in which the multi-plate clutch is locked by a specific hold device unit, even in the currentless state.
This means that the parking lock acts not only on the rear axle, but also on the front axle, enabling the vehicle to be parked also off-road and on slippery surfaces.

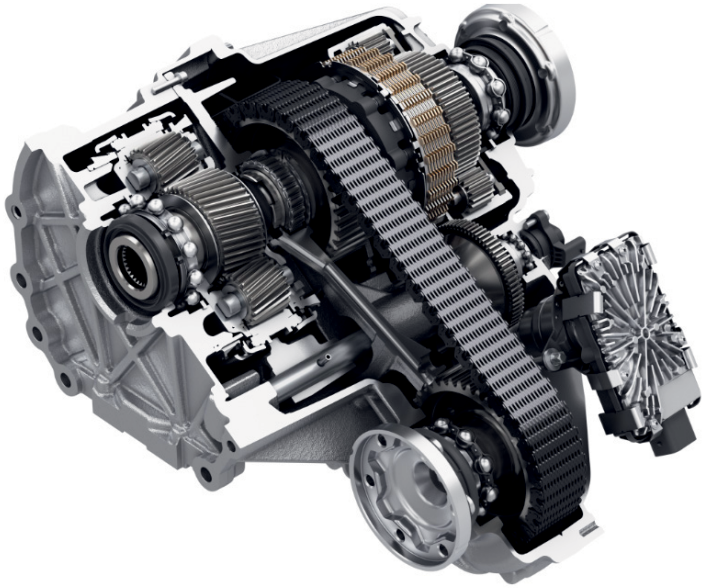


Fig. 14: Transfer Case with differential planetary gear set and longitudinal clutch lock

https://doi.org/10.51202/9783181023549 - Generiert durch IP 216.73.216.36, am 19.01.2026, 02:19:31. © Urheberrechtlich geschützter Inhalt. Ohne gesonderte Erlaubnis ist jede urheberrechtliche Nutzung untersagt, insbesondere die Nutzung des Inhalts im Zusammenhang mit, für oder in KI-Systemen, KI-Modellen oder Generativen Sprachmodellen.

- Torque distribution: 40% / 60% by planetary gear set
- Clutch torque: 1600 Nm nominal value (longitudinal lock)
- Low range gear ratio: i = 2.93 by planetary gear set with 4 planets
- Synchronization: low-high and high-low shifting synchronized
- Weight: 50.8 kg
- Lubrication concept: active lubrication by oil pump as well as passive lubrication of the components around the main shaft via the chain
- Maximum input torque: 2,800 Nm
- Maximum input shaft speed: 7,000 rpm
- Oil capacity: 1,500 ml

In the G- Class, a 40:60 torque distribution transfer case is vented together with the 9G TRONIC through vent pipes with openings above the fording line in the area of the dome strut.

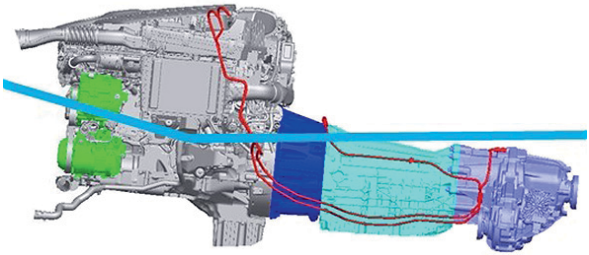


Fig. 15: Vent lines (red), engine, transmission and transfer case during fording

https://doi.org/10.51202/9783181023549 - Generiert durch IP 216.73.216.36, am 19.01.2026, 02:19:31. © Urheberrechtlich geschützter Inhalt. Ohne gesonderte Erlaubnis ist jede urheberrechtliche Nutzung untersagt, insbesondere die Nutzung des Inhalts im Zusammenhang mit, für oder in KI-Systemen, KI-Modellen oder Generativen Sprachmodellen.

Conclusion

The initially mentioned primary goals of improved comfort and enhanced on- and off-road performance for the new all-wheel drive generation of the GLE-Class were achieved through the use of a Torque-on- Demand system. In detail, this was enabled by a reduced powertrain backlash with consequently lower susceptibility to the back lash effect. This made it possible to reduce back lash effect damping of the powertrain while allowing more agile driving characteristics (pulling away and flexibility). The potential of the integrated starter generator can be exploited to the full only with the multi-plate clutch in the transfer cases, since the rapid torque build-up of the electric motor does not need to be damped (pulling away and flexibility hesitation). All in all, this makes for sportier driving characteristics.

Safety is also improved, as the vehicle's handling is more stable thanks to intelligent activation of the all-wheel drive, with optimized interaction between the Torque-on-Demand system, the ESP and the braking system.

The platform of transfer cases for the SUVs is rounded off by another new transfer case with off-road gear for the G- and X-Class that, thanks to a 40:60 distribution, continues to deliver the characteristics specific to the G-Class. Due to the cooperation project in the development of the new SUV transfer case portfolio, a common parts strategy has made it possible to gather a great deal of experience while at the same time harnessing synergies and constantly increasing the maturity level across all projects.

References

[1] Maisch, M.; Homm, M.; Keller, U.: The High Efficient 9GH- Tronic Plug-In Hybrid *T*ransmission by Mercedes Benz, 14th International CTI Symposium, Berlin 2015.

https://doi.org/10.51202/9783181023549 - Generiert durch IP 216.73.216.36, am 19.01.2026, 02:19:31. © Urheberrechtlich geschützter Inhalt. Ohne gesonderte Erlaubnis ist jede urheberrechtliche Nutzung untersagt, insbesondere die Nutzung des Inhalts im Zusammenhang mit, für oder in KI-Systemen, KI-Modellen oder Generativen Sprachmodellen.

Development of New Hybrid AWD System for the SUV Segment

Koichi Hasegawa, **Daichi Kosaka**, **Satoshi Shimizu**,
Kana Kawabata, **Hiroyuki Tsukashima**,
Toyota Motor Corporation, Aichi, Japan

1: Abstract

This paper analyzes the driving conditions that require all-wheel drive (AWD) capabilities, and introduces a method for identifying the target dynamic performance attributes of a sports utility vehicle (SUV) equipped with an AWD system. This paper also describes how these performance targets were achieved using a front-wheel drive-based hybrid AWD system in which the non-driven rear wheels are powered via a motor.

- Traction Performance

To ensure standing start and acceleration performance on snowy or otherwise slippery road surfaces, driving force must be generated at the non-driven rear wheels to compensate for driving force loss that occurs when the main front driven wheels slip. To accomplish this objective, a new rear transaxle with a built-in drive motor was developed, which enables the generation of greater driving force than a conventional transaxle in a more compact package.

In addition, to facilitate driving over uneven and other rough road surfaces, the new “Trail mode” was developed based on coordination between powertrain, brake, and AWD controls under a concept called AWD Integrated Management (AIM).

- Handling Performance

Handling on snowy roads was ensured by the development of a new control capable of independently distributing greater driving force to the non-driven rear wheels than the front wheels when these conditions are detected.

2: Introduction

Fuel-efficient hybrid and electrified vehicles are growing in popularity and availability in response to the growing need to reduce automotive CO_2 emissions and fuel consumption as part of measures to address global warming. Toyota Motor Corporation launched an electrical all-wheel drive (AWD) system for hybrid vehicles in 2001. Although steadily updated since then, this electrical AWD system has been completely

https://doi.org/10.51202/9783181023549 - Generiert durch IP 216.73.216.36, am 19.01.2026, 02:19:31. © Urheberrechtlich geschützter Inhalt. Ohne gesonderte Erlaubnis ist jede urheberrechtliche Nutzung untersagt, insbesondere die Nutzung des Inhalts im Zusammenhang mit, für oder in KI-Systemen, KI-Modellen oder Generativen Sprachmodellen.

redesigned for installation in the latest RAV4 in accordance with the launch of the fourth generation hybrid system for sports utility vehicles (SUVs), which features major changes from the third generation.

The development of this new electrical AWD system aimed to achieve four-wheel drive (4WD) performance that combines the power of an SUV with a careful focus on.

This paper describes the performance requirements of an AWD system for SUVs and how these requirements were achieved.

3: AWD Performance

Before identifying the required dynamic performance attributes of an SUV, this development analyzed the overall SUV category.

As a result, the development target was narrowed down from SUVs with full-time 4WD cross-country capabilities to SUVs based on front-wheel drive (FWD) passenger vehicle platforms (Figure 1). It was assumed that this SUV would be driven in daily and camping usage scenarios (i.e., not for work use).

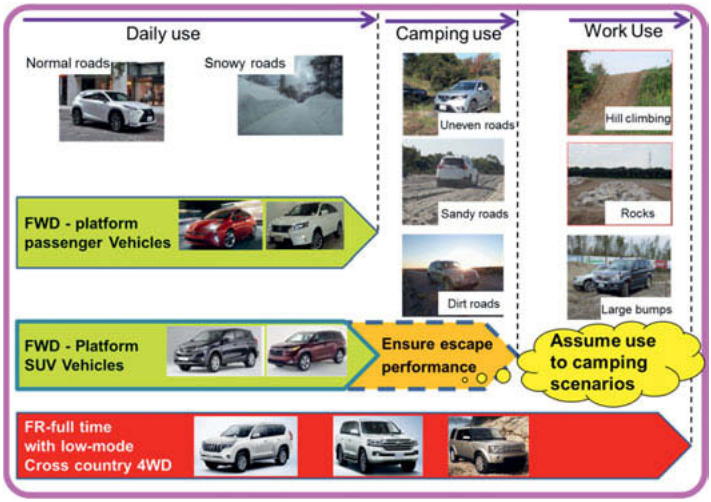


Fig. 1: Assumed driving scenarios according to AWD vehicle categories.

The key driving scenarios and required performance attributes of a passenger vehicle-based SUV were defined as follows.

https://doi.org/10.51202/9783181023549 - Generiert durch IP 216.73.216.36, am 19.01.2026, 02:19:31. © Urheberrechtlich geschützter Inhalt. Ohne gesonderte Erlaubnis ist jede urheberrechtliche Nutzung untersagt, insbesondere die Nutzung des Inhalts im Zusammenhang mit, für oder in KI-Systemen, KI-Modellen oder Generativen Sprachmodellen.

a) Hill climbing performance on snowy roads
b) Standing start and acceleration performance on snowy urban roads
c) Handling performance on winding snowy roads
d) Driving performance over rough roads in various camping-based driving scenarios

The vehicle performance targets for a), c), and d) above are closely linked with the design requirements of the newly developed rear transaxle and rear motor output. The following sections describe these items in more detail.

- Hill climbing performance on snowy roads

Users expect SUVs to have greater performance than passenger vehicles built on the same platform, and are likely to use these SUVs in harsher scenarios. For this reason, this development set a tougher hill climbing gradient target than for a passenger vehicle. In addition, anticipating rougher accelerator operation and greater front wheel slip, a passenger vehicle-based SUV must be capable of compensating for front-wheel driving force loss at the rear wheels. Sufficient acceleration to enable stable standing start performance on hills was also set as a performance target.

- Handling performance on winding snowy roads

In the initial development phase, the performance of SUVs in similar categories was compared on an artificial low traction road. To achieve class-top handling performance, the development aimed to enhance the capability of the SUV to trace an intended driving line through corners while ensuring rear stability.

- Driving performance over rough roads in various camping – base driving scenarios

Common types of rough roads include sandy, uneven, and rocky surfaces. This development aimed to enable the vehicle to safely negotiate these types of roads.
The development focused on achieving driving performance on the following two typical road surfaces.

1: High-resistance sandy roads requiring large AWD driving force
2: Uneven roads on which one set of wheels is pushed out of contact with the road surface, requiring traction by the other set of wheels

Figure 2 shows the relationship between these target performance attributes and the output characteristics of the motor built into the rear transaxle.

https://doi.org/10.51202/9783181023549 - Generiert durch IP 216.73.216.36, am 19.01.2026, 02:19:31. © Urheberrechtlich geschützter Inhalt. Ohne gesonderte Erlaubnis ist jede urheberrechtliche Nutzung untersagt, insbesondere die Nutzung des Inhalts im Zusammenhang mit, für oder in KI-Systemen, KI-Modellen oder Generativen Sprachmodellen.

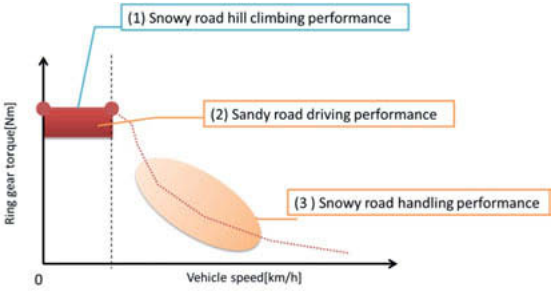


Fig. 2: Relationship between rear transaxle performance and target vehicle performance.

4: Vehicle System

This section describes the system adopted to realize the identified performance targets.

a) Overall Vehicle System

Figure 3 shows the overall vehicle system configuration. The main front driven wheels are integrated with a hybrid system, which is driven by an engine and motor. The driving torque generated by this engine and motor is distributed by a power split device.

The rear non-driven wheels can be powered by the motor built into the rear transaxle.The front and rear motors are driven through front and rear inverters after the boost converter steps up the voltage supplied by the high-voltage battery. The overall vehicle system does not include an intervening propeller shaft that mechanically links the front and rear wheels. This means that the front and rear wheels can be driven independently.

https://doi.org/10.51202/9783181023549 - Generiert durch IP 216.73.216.36, am 19.01.2026, 02:19:31. © Urheberrechtlich geschützter Inhalt. Ohne gesonderte Erlaubnis ist jede urheberrechtliche Nutzung untersagt, insbesondere die Nutzung des Inhalts im Zusammenhang mit, für oder in KI-Systemen, KI-Modellen oder Generativen Sprachmodellen.

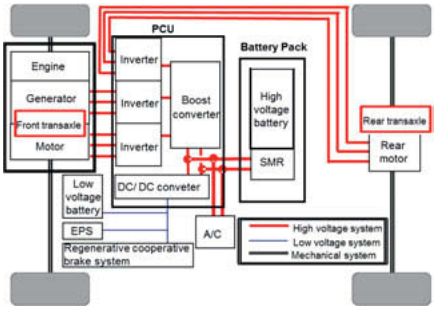


Fig. 3: Vehicle system configuration.

b) Newly developed transaxle

Figure 4 shows the basic configuration of the newly developed Q610 rear transaxle. The basic structure consists of three axes configured with two sets of reduction gears. The transaxle uses automatic transmission fluid (ATF) for lubrication, which is also used for motor cooling.To accomplish the performance targets described above, sufficient driving torque must be generated at the non-driven rear wheels at low speeds from a standing start. However, from the standpoint of mountability, the size of the transaxle could not be increased. This apparent contradiction was resolved by adopting a compact high-speed motor and a counter gear with a higher reduction ratio. These measures increased the maximum axial torque of the ring gear by 1.3 times from 950 to 1,300 Nm, while only slightly increasing the maximum axial rotational speed of the ring gear from 1,530 to 1,570 rpm.

Table 1 compares the specifications of the Q610 rear transaxle with the previous Q211 model.

https://doi.org/10.51202/9783181023549 - Generiert durch IP 216.73.216.36, am 19.01.2026, 02:19:31. © Urheberrechtlich geschützter Inhalt. Ohne gesonderte Erlaubnis ist jede urheberrechtliche Nutzung untersagt, insbesondere die Nutzung des Inhalts im Zusammenhang mit, für oder in KI-Systemen, KI-Modellen oder Generativen Sprachmodellen.

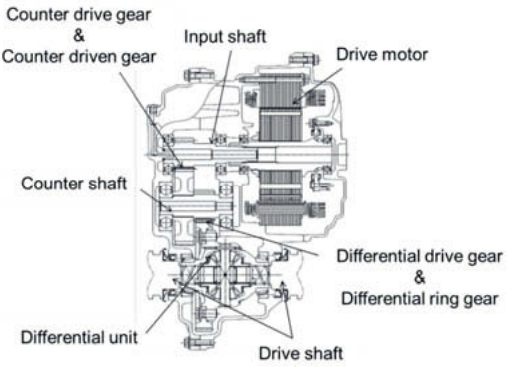


Fig. 4: Cross-section of new rear transaxle (Q610).

Table 1: Rear transaxle specification chart

Rear trans axle		Q610 (New generation)	Q211 (Previous generation)
Motor	Type	Synchronous AC motor	
	Max. power	40 kw	50 kw
	Max. torque	121 Nm	139 Nm
	Max. speed	17000 rpm	10500 rpm
Counter grear ratio		2.733	1.739
Differential gear ratio		3.944	
Max. ring gear torque		1300 Nm	950 Nm

5: AWD Control

The development aims for the new AWD control were as follows.

1: To enable stable and high driving performance on snowy and other low traction roads, by accurately and rapidly detecting road surfaces and vehicle states requiring AWD system control.

2: To restrict energy loss caused by reduced output due to motor heat generation and gear engagement loss, by stopping motor drive when AWD control is not required.

https://doi.org/10.51202/9783181023549 - Generiert durch IP 216.73.216.36, am 19.01.2026, 02:19:31. © Urheberrechtlich geschützter Inhalt. Ohne gesonderte Erlaubnis ist jede urheberrechtliche Nutzung untersagt, insbesondere die Nutzung des Inhalts im Zusammenhang mit, für oder in KI-Systemen, KI-Modellen oder Generativen Sprachmodellen.

To achieve these aims, the AWD control system configuration is as follows.

1: Feedforward control that acts in accordance with the front/rear dynamic load distribution

2: Slip feedback control that acts in accordance with the difference in slip ratios at the front and rear wheels

3: Yaw rate feedback control that acts in accordance with the yaw rate deviation

Figure 5 shows the overall flow of the AWD control.

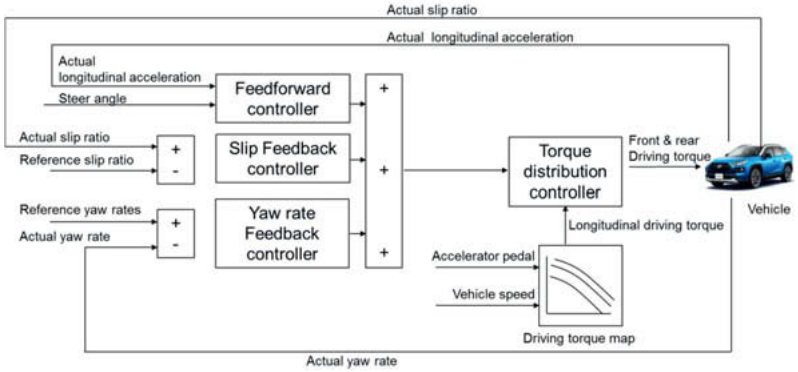


Fig. 5: Block diagram of AWD system.

The following sections describe an outline of the control carried out by the system in each driving scenario.

5-1: Standing Start Control

To ensure standing start performance on a steep slope, it is important to overcome the resistance of the slope and generate sufficient driving force to accelerate the vehicle. Since the main front driven wheels are susceptible to slip particularly on snowy roads, the rear non-driven wheels must compensate for the driving force lost when the front wheels slip and help to ensure sufficient driving force to accelerate the vehicle. This control achieves the required traction performance even on steep and slippery snowy roads using a basic feedforward control that applies a driving force distribution ratio in advance based on the load distribution at the front and rear wheels (Eq. 1). Furthermore, this is a two degree of freedom controller that

https://doi.org/10.51202/9783181023549 - Generiert durch IP 216.73.216.36, am 19.01.2026, 02:19:31. © Urheberrechtlich geschützter Inhalt. Ohne gesonderte Erlaubnis ist jede urheberrechtliche Nutzung untersagt, insbesondere die Nutzung des Inhalts im Zusammenhang mit, für oder in KI-Systemen, KI-Modellen oder Generativen Sprachmodellen.

also incorporates feedback control in accordance with slip generated when the vehicle moves off (Eq. 2).

$$ksff = \frac{W_{r0} + \frac{H}{L} GxM}{Mg} s \text{ - (1)} \quad ksfb = Kp_{\text{slip}} \times eslip + Kd_{slip} \frac{d\ eslip}{dt} + Ki_{slip} \int eslip\ dt \text{ - (2)}$$

$$\text{e}slip = slipact - slipref \text{ - (3)}$$

In addition, since this AWD system has no propeller shaft and is capable of independent front/rear driving force distribution, the feedback control can use this capability to distribute greater driving force to the rear wheels.

5-2: Cornering Control

When cornering on a snowy road, vehicles are susceptible to understeer when the grip limit of the front tires is exceeded. Consequently, the cornering control activates when the system judges that the vehicle is cornering. This consists of three separate control elements: a feedforward control that applies a fixed driving force distribution ratio to the front and rear wheels, a slip feedback control that acts in accordance with front/rear wheel slip (Eq. 4), and yaw rate feedback control that calculates the control amount based on the deviation between the reference and actual yaw rates (Eq. 5). As described in Eq. 7, these controls are integrated to calculate a total control amount, which permits up to 80% of the driving force to be distributed to the rear wheels.

$$kyawslipfb = Kp_{slip} \times eslip + Kd_{slip} \frac{d\ eslip}{dt} + Ki_{slip} \int eslip\ dt \text{ - (4)}$$

$$kyawfb = Kp_{yaw} \times eyaw + Kd_{yaw} \frac{d\ eyaw}{dt} + Ki_{yaw} \int eyaw\ dt \text{ - (5)}$$

$$\text{e}yaw = sgn(\delta) \times (yawref - yawact) \text{ - (6)}$$

5-3: Rough Road Control

Figure 6 shows an image of a vehicle moving off on an uneven road as a typical example of a rough road driving scenario.On this type of road, the wheels on one side may be pushed up in the air. In this case, due to the characteristics of the differential, driving force cannot be transferred to the wheel contacting the ground if one wheel is not in contact with the ground, even if driving torque is applied. As a

https://doi.org/10.51202/9783181023549 - Generiert durch IP 216.73.216.36, am 19.01.2026, 02:19:31. © Urheberrechtlich geschützter Inhalt. Ohne gesonderte Erlaubnis ist jede urheberrechtliche Nutzung untersagt, insbesondere die Nutzung des Inhalts im Zusammenhang mit, für oder in KI-Systemen, KI-Modellen oder Generativen Sprachmodellen.

result, sufficient driving force cannot be ensured in these conditions. To resolve this issue, the new Trail Mode was developed based on coordination between powertrain, brake, and AWD controls under a concept called AWD Integrated Management (AIM).【Figure 7】 shows an outline of AIM.



Fig. 6: Moving off on uneven road.

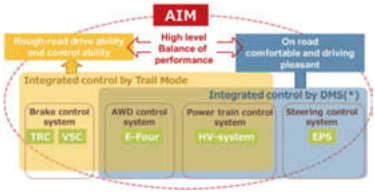


Fig. 7: Conceptual diagram of AIM.

The following integrated control is activated when the user selects Trail Mode.

- The amount of driving force generated when the accelerator is depressed is restricted to allow the driver to read the road surface more easily.
- The amount of driving force distributed to the rear wheels of the AWD system is maximized to ensure the greatest possible application of driving force.
- Brake limited slip differential (LSD) control is applied to vehicle wheels that slip to prevent driving force loss in these conditions.

This integrated control facilitates standing start performance on uneven road surfaces. Table 2 compares the characteristics of each vehicle driving mode.

Table 2: Specifications of each driving mode

		Throttle control shift schedule	Driving force distribution	Steering assist	Brake control
	SPORT	SPORT	Same as normal	SPORT	Same as normal
	ECO	ECO	Same as normal	Same as normal	Same as normal
	NORMAL	Same as normal	Same as normal	Same as normal	Same as normal
	TRAIL	TRAIL *Only throttle control	TRAIL	Same as normal	TRAIL

https://doi.org/10.51202/9783181023549 - Generiert durch IP 216.73.216.36, am 19.01.2026, 02:19:31. © Urheberrechtlich geschützter Inhalt. Ohne gesonderte Erlaubnis ist jede urheberrechtliche Nutzung untersagt, insbesondere die Nutzung des Inhalts im Zusammenhang mit, für oder in KI-Systemen, KI-Modellen oder Generativen Sprachmodellen.

6: Performance Verification

The following sections describe the results of the performance verifications carried out for each control.

6-1: Standing Start Performance on Steep Snowy Road

The following results were achieved for standing start performance on a steep snowy road.

A standing start test was carried out on a road with a gradient of 20% and covered in compacted snow.

The test involved braking the vehicle to a stop and then moving off by depressing the accelerator pedal.

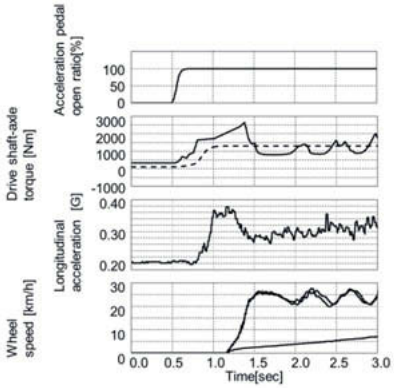


Fig. 8: Snow hill climb result.

Figure 8 shows the results.

The test verified that the vehicle moved off powerfully with little difference in slip between the front and rear wheels.

6-2: Cornering Performance on Snowy Road

The following results were achieved in an acceleration and cornering test on a low traction road. The test driver approached the corner on a straight road at a constant speed of 40 km/h, and entered the corner (radius: 150R) at the same constant speed. The driver then began to turn the steering wheel, and depressed the accelerator at the point that a steady-state turn was achieved.

https://doi.org/10.51202/9783181023549 - Generiert durch IP 216.73.216.36, am 19.01.2026, 02:19:31. © Urheberrechtlich geschützter Inhalt. Ohne gesonderte Erlaubnis ist jede urheberrechtliche Nutzung untersagt, insbesondere die Nutzung des Inhalts im Zusammenhang mit, für oder in KI-Systemen, KI-Modellen oder Generativen Sprachmodellen.

The longitudinal acceleration in the test was set to approximately 0.10 G. Figure X shows an image of the vehicle course in this test.

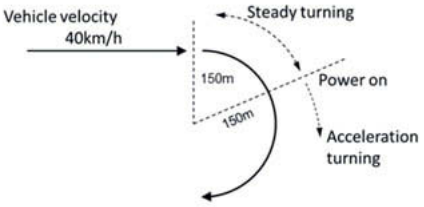


Fig. 9: Course of power-on transient maneuver.

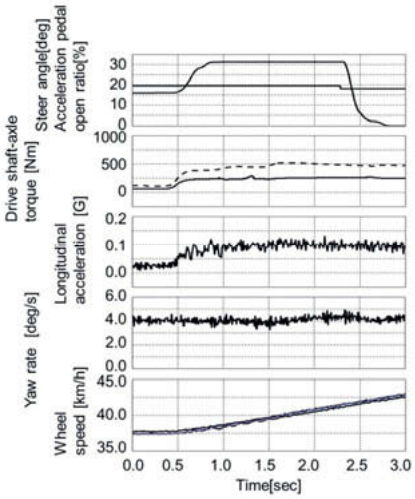


Fig.10: Power-on transient maneuver.

Figure 10 shows the results.
From figure 10, it can be seen that the rear wheel drive shaft axial torque exceeds the drive shaft axial torque of the front wheels from the time of acceleration. Since the slip of the tire is suppressed, the under steer of the vehicle due to the acceleration slip is suppressed.

https://doi.org/10.51202/9783181023549 - Generiert durch IP 216.73.216.36, am 19.01.2026, 02:19:31. © Urheberrechtlich geschützter Inhalt. Ohne gesonderte Erlaubnis ist jede urheberrechtliche Nutzung untersagt, insbesondere die Nutzung des Inhalts im Zusammenhang mit, für oder in KI-Systemen, KI-Modellen oder Generativen Sprachmodellen.

6-3: Rough Road Standing Start Performance

Figure 11 and figure 12 shows the results of a standing start test on an uneven road as a typical example of rough road standing start performance.

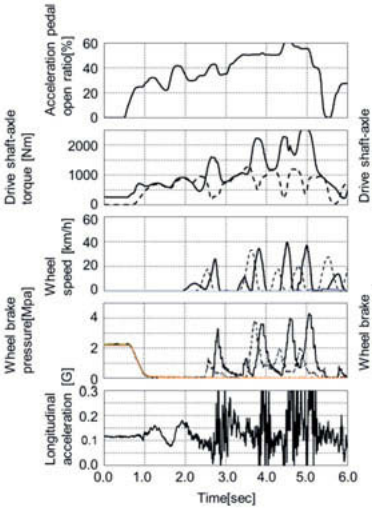


Fig. 11: Starting on uneven road. (Without "Trail mode")

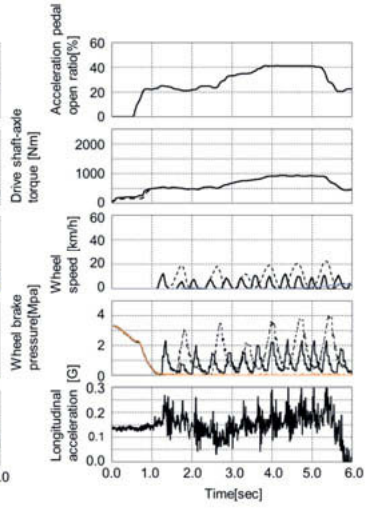


Fig. 12: Starting on uneven road. (With "Trail mode")

By comparing Figure 11 and 12 in the "TRAIL MODE", the slip of the wheel is suppressed by operating the brake control frequently. As a result, it can be understood that the longitudinal acceleration of the vehicle body is maintained.

7: Conclusions

This development defined the assumed driving scenarios of a passenger vehicle-based SUV and identified the vehicle performance attributes required by these scenarios. The following results were obtained.

- A new rear transaxle was developed to ensure equivalent standing start performance on steep snowy roads to a conventional passenger vehicle.
- Taking advantage of the characteristics of an AWD system without a propeller shaft, an independent driving force control was developed that simultaneously achieves greater cornering traceability and stability than the previous model.

https://doi.org/10.51202/9783181023549 - Generiert durch IP 216.73.216.36, am 19.01.2026, 02:19:31. © Urheberrechtlich geschützter Inhalt. Ohne gesonderte Erlaubnis ist jede urheberrechtliche Nutzung untersagt, insbesondere die Nutzung des Inhalts im Zusammenhang mit, für oder in KI-Systemen, KI-Modellen oder Generativen Sprachmodellen.

- A new driving mode (called Trail Mode) was developed that integrates powertrain, brake, and AWD controls under the AIM concept. This mode facilitates standing start performance on uneven rough roads.

8: NOTATION

g :Gravitational acceleration
M : Vehicle mass
L : Wheelbase
H : Distance from ground to center of gravity
Wro : Static rear wheel loading
δ : Front steer angle
ksff : Feedforward rear driving force distribution ratio according to wheel loading
ksfb : Feedback rear driving force distribution ratio according to slip error
ksff : Feedforward rear driving force distribution ratio according to steer angle and vehicle speed
kyawslipfb: Feedback rear driving force distribution ratio according to slip error (yaw rate control)
kyawfb : Feedback rear driving force distribution ratio according to yaw rate error
eslip : Slip error
eyaw : Yaw rate error
yawref : Reference Yaw rata
yawact : Actual Yaw rate
slipref : Reference slip ratio between front and rear wheel
slipact : Actual slip ratio between front and rear wheel
Kpslip : Slip feedback proportional gain
Kdslip : Slip feedback differential gain
Kislip : Slip feedback integral gain
Kpyaw : Yaw rate feedback proportional gain
Kdyaw : Yaw rate feedback differential gain
Kiyaw : Yaw rate feedback integral gain
V : Vehicle speed
G_x : Vehicle longitudinal acceleration
G_x : Vehicle lateral acceleration

https://doi.org/10.51202/9783181023549 - Generiert durch IP 216.73.216.36, am 19.01.2026, 02:19:31. © Urheberrechtlich geschützter Inhalt. Ohne gesonderte Erlaubnis ist jede urheberrechtliche Nutzung untersagt, insbesondere die Nutzung des Inhalts im Zusammenhang mit, für oder in KI-Systemen, KI-Modellen oder Generativen Sprachmodellen.

γ : Vehicle actual Yaw rate
R0 : Steady turning radius
R1 : Acceleration turning radius

9: Reference

1) Suzuki, K.: “Development of New Electronic Controlled 4WD System for Passenger Cars,” JSAE Latest Drivetrain Technologies Symposium, No. 9806, 1998
2) Kondo, K.: “Development of Electrical 4WD System for Hybrid Vehicles” (in Japanese), Proceedings of the Society of Automotive Engineers of Japan, No. 101-01, pp. 13-16, 2001
3) Nakamura, K.: “Development of Motor Assisted 4WD System Applied for Small FF vehicle,” Proceedings of the Society of Automotive Engineers of Japan, No. 83-02, pp. 1-4, 2002
4) Handa, K.: “Development of Mitsubishi Outlander PHEV” (in Japanese), Automotive World Specialist Technical Seminar, 2014
5) Suzuki, K.: “A Study of Wheel Slip Control Using Simple Control Method for 1 Motor EV” (in Japanese), Proceedings of the Society of Automotive Engineers of Japan, No. 28-14, pp. 1-4., 2014

https://doi.org/10.51202/9783181023549 - Generiert durch IP 216.73.216.36, am 19.01.2026, 02:19:31. © Urheberrechtlich geschützter Inhalt. Ohne gesonderte Erlaubnis ist jede urheberrechtliche Nutzung untersagt, insbesondere die Nutzung des Inhalts im Zusammenhang mit, für oder in KI-Systemen, KI-Modellen oder Generativen Sprachmodellen.

Volkswagen's electric drivetrains of the new modular e-drive kit (MEB)

Dipl.-Ing. **Peter Lück**, Dr. rer. nat. **Karsten Bennewitz**,
Dr.-Ing. **Jonas Tousen**, Volkswagen AG, Wolfsburg



Zusammenfassung

Dieser Vortrag gibt erste Einblicke in den Modularen Elektrifizierungs-Baukasten (MEB) von Volkswagen. Den MEB-Baukasten bezeichnet Volkswagen auch als wirtschaftliches und technologisches Rückgrat der anstehenden Elektrooffensive. Bis Ende 2022 wird weltweit die Produktion von 27 MEB-Fahrzeugen für Konzernmarken starten. Bis 2028 kommen fast 70 neue E-Modelle auf den Markt [1], [2]. Damit bildet der MEB die Grundlage für die Industrialisierung der Elektromobilität im Volkswagen Konzern. Die Botschaft lautet: Die Elektrifizierung der Mobilität für eine breite Bevölkerungsschicht wird von Volkswagen offensiv und energisch vorangetrieben. Der Volkswagen Konzern soll bis 2050 in allen Bereichen vollkommen CO2-neutral werden.

https://doi.org/10.51202/9783181023549 - Generiert durch IP 216.73.216.36, am 19.01.2026, 02:19:31. © Urheberrechtlich geschützter Inhalt. Ohne gesonderte Erlaubnis ist jede urheberrechtliche Nutzung untersagt, insbesondere die Nutzung des Inhalts im Zusammenhang mit, für oder in KI-Systemen, KI-Modellen oder Generativen Sprachmodellen.

Die MEB-Plattform stellt den von Volkswagen eigens für E-Autos konzipierten fahrbaren Unterbau dar. Das Chassis mit unterschiedlichen Radständen verfügt über eine im Fahrzeugboden verbaute flache Hochvoltbatterie, über den E-Antrieb mit Pulswechselrichter und Ein-Ganggetriebe, die Hochvoltverkabelung und das Ladegerät. Grundsätzlich können zwei E-Antriebe verbaut werden, an der Hinterachse eine permanenterregte Synchronmaschine (PSM) mit einer Leistung von 150 kW und optional zusätzlich an der Vorderachse eine Asynchronmaschine (ASM) mit einer Leistung von 75 kW.

Abstract

This paper is providing first insights into Volkswagen's new modular e-drive kit (MEB). Volkswagen also points to the modular electrification kit (MEB) as the commercial and technological backbone of the upcoming electric offensive. By the end of 2022, production of 27 MEB vehicles for Group brands will start worldwide. The Group is planning to launch almost 70 new electric models in the next ten years [1], [2]. The MEB is thus the basis for the industrialization of electric mobility within the Volkswagen Group. The message is: Volkswagen is putting enormous energy and commitment into the electrification of mobility for a broad sector of the car customers. The Volkswagen Group has set milestones in all areas to be achieved in the coming years on the road to complete decarbonization by 2050.

The MEB platform is a vehicle structure specifically developed by Volkswagen for electric vehicles. The chassis with various wheelbases is equipped with a flat high-voltage battery built into the floor, the electric drive with power inverter and single-speed transmission, the high-voltage wiring and the charging device. Basically, two e-drives can be installed: a permanent-magnet synchronous machine (PSM) with an output of 150 kW at the rear axle, and optional in addition an asynchronous machine (ASM) with 75 kW at the front axle.

https://doi.org/10.51202/9783181023549 - Generiert durch IP 216.73.216.36, am 19.01.2026, 02:19:31. © Urheberrechtlich geschützter Inhalt. Ohne gesonderte Erlaubnis ist jede urheberrechtliche Nutzung untersagt, insbesondere die Nutzung des Inhalts im Zusammenhang mit, für oder in KI-Systemen, KI-Modellen oder Generativen Sprachmodellen.

1. Introduction

Volkswagen is committed to the systematic advancement of electric mobility. The progressive ID. family, an all-new generation of electric vehicles, will come to market as of 2020. There will be zero-emissions vehicles of different classes with ranges on the level of today's petrol cars. The ID. CROZZ, ID. VIZZION and ID. BUZZ have already been unveiled to the public. The first ID. model to be launched to the market in 2020 will be the ID. – an affordable, four-door, fully connected compact car (fig. 1). The Volkswagen Group plans to launch 27 MEB vehicles worldwide by 2022. Among these will be electric models from the Audi, Seat, Skoda, Volkswagen and Volkswagen Commercial Vehicles brands.



Fig. 1: The ID. family

The ID. will mark the debut of the world's first model based on the modular electrification kit (MEB), a technology platform developed specifically for all-electric vehicles (fig. 2). The components of the electric drive system and the package are carefully and systematically intermeshed.

The high-voltage battery, a high-performance lithium-ion system, is located into the vehicle floor between the axles. This saves space for a generously proportioned interior, while ensuring an optimum weight distribution of almost 50:50 percent front-to-rear and a low centre-of-gravity. It is scalable, adaptable for different cell types and equipped with integrated liquid cooling. It is thus relatively easy to integrate into the various power outputs of the ID. models. Depending upon battery size and the ID. model, ranges of approx. 330 km to more than 550 km can be achieved (according to WLTP).

https://doi.org/10.51202/9783181023549 - Generiert durch IP 216.73.216.36, am 19.01.2026, 02:19:31. © Urheberrechtlich geschützter Inhalt. Ohne gesonderte Erlaubnis ist jede urheberrechtliche Nutzung untersagt, insbesondere die Nutzung des Inhalts im Zusammenhang mit, für oder in KI-Systemen, KI-Modellen oder Generativen Sprachmodellen.

The ID. vehicle models will be equipped with a type 2 charging connector and an 11 kW AC charger as standard. This enables charging via an AC connection - either with 2.3 kW via a standard domestic socket, at a wallbox or AC charging station with up to 11 kW charging power. Significantly shorter charging times are possible with the optional CCS (combined charging system) charging port. It enables DC charging of the HV battery with up to 125 kW, 80 percent of its energy content can be recharged within 30 minutes.

Basically two electric drives can be installed in the platform, so that driving of one or both axles can be realized by the scalable components of the MEB.

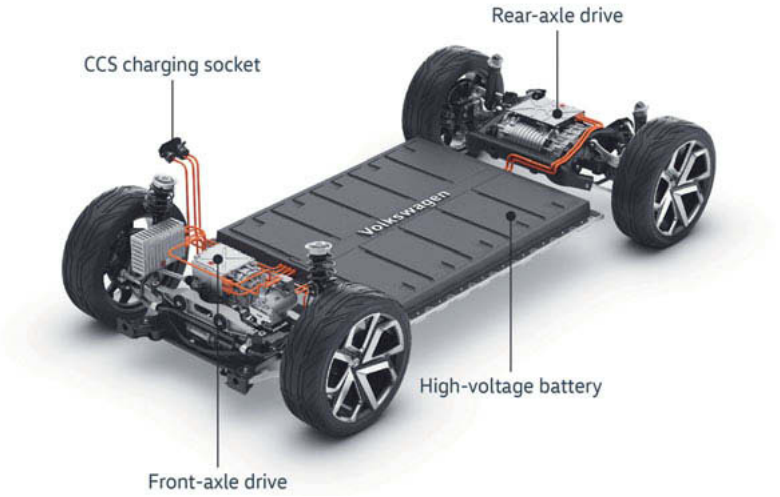


Fig. 2: MEB platform

The zero-emission drive of the ID. consists primarily of the electric machine incorporated into the rear axle, including power inverter and single-speed transmission, a space-saving high-voltage battery installed in the vehicle floor and the auxiliary components located at the front end of the vehicle. The compact e-drive comprises the electric machine, power inverter and single-speed transmission.

Offering a driving range on the level of today's petrol-driven vehicles and available for the same price as a diesel car, the ID. also has the potential to facilitate the breakthrough of environmentally friendly electric mobility and start a new era of electric drive systems.

https://doi.org/10.51202/9783181023549 - Generiert durch IP 216.73.216.36, am 19.01.2026, 02:19:31. © Urheberrechtlich geschützter Inhalt. Ohne gesonderte Erlaubnis ist jede urheberrechtliche Nutzung untersagt, insbesondere die Nutzung des Inhalts im Zusammenhang mit, für oder in KI-Systemen, KI-Modellen oder Generativen Sprachmodellen.

2. The Electric Drivetrains for the MEB

Two newly developed electric axle drives are available for the MEB. The main drive is a permanent-magnet synchronous machine (PSM, fig. 3) at the rear axle. It is combined with a power inverter (PI) and a single-speed transmission in an axle-parallel configuration. It generates a power output of 150 kW, a torque of 310 Nm and a maximum rotational speed of 16,000 rpm. The PSM is a system component with a high power density and high efficiency that supplies consistent power output across a wide speed range.

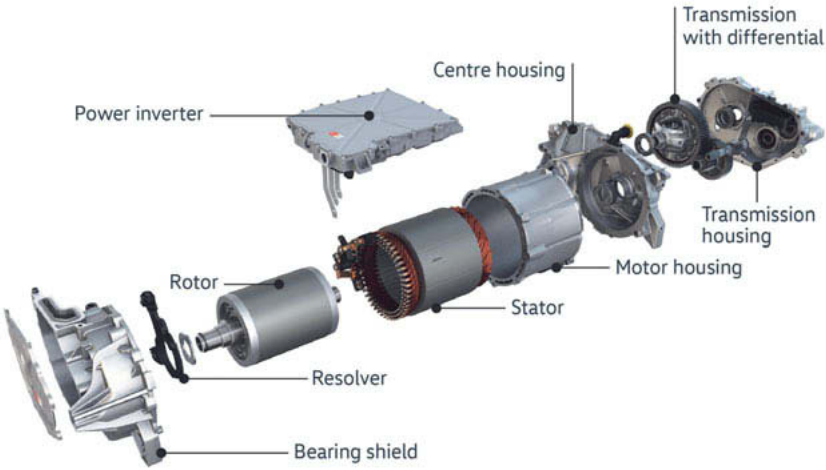


Fig. 3: MEB rear-axle drive

Depending on the vehicle concept, the front axle of an MEB vehicle can also be driven. Here, an asynchronous machine (ASM) with power inverter and single-speed transmission in a coaxial configuration serves as an additional drive for boost and all-wheel-drive functions. It has a power output of 75 kW, a torque of 151 Nm and a maximum rotational speed of 14,000 rpm. An ASM is notable for its power capacity to run on overload for short periods and at low drag losses. Therefore, it fits perfect for providing a temporary power boost.

The configuration, the technical characteristics and the performance data will be described below in particular using the example of the PSM.

https://doi.org/10.51202/9783181023549 - Generiert durch IP 216.73.216.36, am 19.01.2026, 02:19:31. © Urheberrechtlich geschützter Inhalt. Ohne gesonderte Erlaubnis ist jede urheberrechtliche Nutzung untersagt, insbesondere die Nutzung des Inhalts im Zusammenhang mit, für oder in KI-Systemen, KI-Modellen oder Generativen Sprachmodellen.

2.1. The Power Inverter (PI)

The three-phase alternating current for the electric machine is generated by a liquid-cooled power inverter (PI) mounted directly on the electric machine. Fig. 4 shows the power inverter.

Inside the power inverter, three IGBT power modules of the latest generation are connected to form a classic B6 power inverter. Inside the module carrier, the power modules are cooled and framed so that the driver board can be plugged directly onto the power module's contact pins. The controller board is installed above the module carrier and driver board in a space-saving package.

Additional significant components inside the PI are the filter unit for the DC input, the DC link capacitor, the busbars for the machine's AC contacts and the liquid cooling unit.

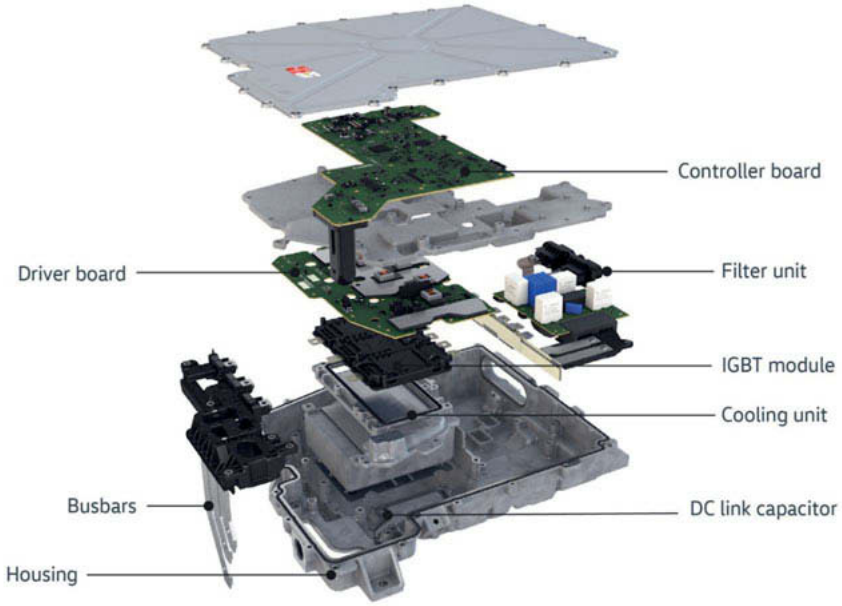


Fig. 4: Power inverter (PI)

The modular design of the PI is configured for high volume industrialization. From the power module via the module carrier to the power and controller modules, a modular system is cre-

https://doi.org/10.51202/9783181023549 - Generiert durch IP 216.73.216.36, am 19.01.2026, 02:19:31. © Urheberrechtlich geschützter Inhalt. Ohne gesonderte Erlaubnis ist jede urheberrechtliche Nutzung untersagt, insbesondere die Nutzung des Inhalts im Zusammenhang mit, für oder in KI-Systemen, KI-Modellen oder Generativen Sprachmodellen.

ated that provides a basis on which further e-drive projects can be realized with minor modifications. Moreover, the fully automated production of the power inverter ensures structural and functional quality even in mass production.

Importing and processing the sensor data for regulating the current values for the electric machine is a highly dynamic process. The result is optimum power utilization, especially at dynamic operating points. Some vehicle functions, such as vibration damping and slip-control functions, were integrated directly into the power inverter. Thus, interventions can be implemented without delay of bus communication. The advantages of this design are more direct adaptation options in the development process as well as optimal adoptions to the specific vehicle driving behaviour.

In the MEB platform, the DC/DC converter for supplying the vehicle's 12 V electrical system is not integrated into the PI, but designed as a separate, liquid-cooled component. The converter can be variably installed into the vehicle and is available in two power classes with 1.8 kW and 3.0 kW, respectively.

2.2. PSM Rear-Axle Drive

The electric drive for the rear axle is designed as a permanent-magnet, three-phase synchronous machine (PSM) with four permanent-magnet pole pairs and a maximum rotational speed of 16,000 rpm. It consists of the main modules power inverter, four-part housing concept (bearing shield, motor housing, centre housing and transmission housing, see fig. 4), stator, rotor, resolver with temperature sensor and the single-speed transmission. The e-drive is manufactured at the Volkswagen plant in Kassel. Rotor and stator are supplied by the Volkswagen plant Salzgitter.

The stator contains the windings with the busbars for the three-phase connection. The rotor is designed as a non-salient pole internal rotor and equipped with permanent magnets made from a neodymium alloy. Stator and rotor are mounted inside a cast housing that also incorporates the liquid cooling. The rotor bearings on the output side (A-side) and on the opposite side (B-side) are inside bearing shields which are screwed together axially over the entire length of the machine housing.

Located on the bearing shield on the B-side are the bushing and contact bridges for the three-phase connection, the resolver for detecting the rotor position, the sensor for determining the

https://doi.org/10.51202/9783181023549 - Generiert durch IP 216.73.216.36, am 19.01.2026, 02:19:31. © Urheberrechtlich geschützter Inhalt. Ohne gesonderte Erlaubnis ist jede urheberrechtliche Nutzung untersagt, insbesondere die Nutzung des Inhalts im Zusammenhang mit, für oder in KI-Systemen, KI-Modellen oder Generativen Sprachmodellen.

winding temperature and the signal plug. The B-side bearing shield is closed by a bearing-shield cover. The signals from the resolver and the temperature sensor are transmitted to the power inverter by cable via a plug.

The single-speed transmission reduces the rotational speed of the electric machine for driving the wheels. The transmission and the differential use the e-machine's A-side bearing shield as part of their housing and are therefore integrated into the drive to save weight (see fig. 4).

2.2.1. Structure of the Stator

The stator consists largely of the lamination stack and the three-phase shaped-wire winding (fig. 5). The lamination stack is made up of separate coated sheet-metal laminations with an outside diameter of 220 mm. The sheet-metal used for the production of the laminations has a high magnetic conductivity, a thickness of 0.27 mm and is coated on both sides with a layer of electrical insulation. The total lamination stack consists of four sub-stacks which are offset by 90 degrees each during assembly. This minimises the influence that the direction of the metal's grain has on the homogeneity of the rotating magnetic field.

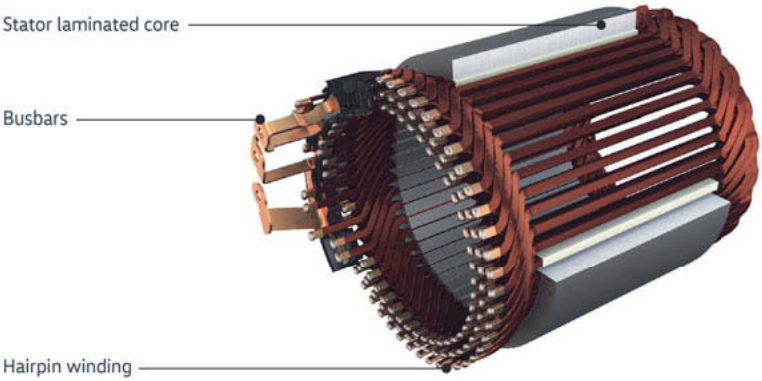


Fig. 5: PSM stator

https://doi.org/10.51202/9783181023549 - Generiert durch IP 216.73.216.36, am 19.01.2026, 02:19:31. © Urheberrechtlich geschützter Inhalt. Ohne gesonderte Erlaubnis ist jede urheberrechtliche Nutzung untersagt, insbesondere die Nutzung des Inhalts im Zusammenhang mit, für oder in KI-Systemen, KI-Modellen oder Generativen Sprachmodellen.

Fixing the coils into the stator grooves, welding one side of the coils to the three phases (fig. 5) and connecting the contact bridge takes place automatically in a dedicated production facility. The end windings of this stator structure contains a contact device for the temperature sensor. The stator is also dip-impregnated with resin for additional insulation, improved thermal connection and reinforcement of the windings. The finished stator undergoes automated test procedures and is also automatically joined to the motor housing by a shrink-fit process.

2.2.2. Structure of the Rotor

The rotor consists of the rotor shaft, the lamination stack with embedded permanent magnets arranged in a v-shape, the balancing discs and the resolver for detecting the rotor position and speed. The rotor lamination stack is constructed of four different layered sub-segments. The end faces of the rotor are closed with balancing discs and connected together by four tensioning screws that pass through the lamination stack (fig. 6). The rotor lamination stack with the embedded magnets is pre-assembled by an automated process and is joined to the rotor shaft by a shrink-fit process.

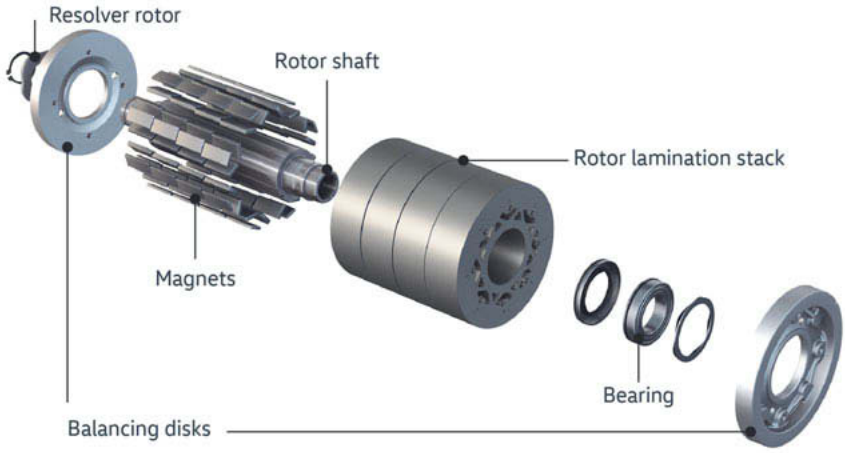


Fig. 6: Exploded view of the rotor

The magnet pockets are arranged differently from segment to segment. The angular position of each differs by a few degrees. The permanent magnets (three per pole and segment, 24 per segment) are positioned according to the layering of the individual segments and have the same length. They are secured using an expending magnetic coating. When the total rotor

https://doi.org/10.51202/9783181023549 - Generiert durch IP 216.73.216.36, am 19.01.2026, 02:19:31. © Urheberrechtlich geschützter Inhalt. Ohne gesonderte Erlaubnis ist jede urheberrechtliche Nutzung untersagt, insbesondere die Nutzung des Inhalts im Zusammenhang mit, für oder in KI-Systemen, KI-Modellen oder Generativen Sprachmodellen.

package is assembled from the four segments, this results in a helical arrangement of the magnets along the longitudinal axis, this leads in particular to the acoustic optimization of the electric machine. The rotor sheet metal is made from the same material as the stator sheet and incorporate cams for die-cutting the stack.

The rotor shaft is designed as a hollow shaft, made from two parts welded together. It is connected to the transmission's input shaft via longitudinal internal splines. The shafts are arranged in a triple-bearing (in the bearing shield, centre housing and transmission housing, see fig. 4) and fitted with friction-optimised grooved ball bearings. This minimizes mechanical losses.

The rotor has to be heated up for the shrink-fit process of rotor and drive shaft. This also causes thermal activation and curing of the expanding magnetic coating, which fixes the permanent magnets in the pockets.

2.2.3. Resolver with Temperature Sensor

The control of the PSM by the power inverter requires the detection of the rotor position, in order to direct current flow correctly into the stator's three-phase windings. This task is done by the resolver. It consists of a rotor on the rotor shaft and a stator fixed to the B-side bearing shield (fig. 7).

A dedicated fixing point is formed into one of the hairpins on the stator windings, where a temperature sensor for determining the temperature of the stator windings is mounted.

The signals from the resolver and temperature sensors are transmitted to the PI via a signal plug and cable and subsequently evaluated.

The power inverter is bolted to the motor housing. The three busbars to connect the stator's phase windings are an integral part of the PI and are fastened to the stator's contact bridge after it has been fixed to the motor housing.

Both the A- and the B-side end shields contain special crash elements that block the drive with the body frame in the event of a rear-end crash, thus preventing penetration into the HV battery.

https://doi.org/10.51202/9783181023549 - Generiert durch IP 216.73.216.36, am 19.01.2026, 02:19:31. © Urheberrechtlich geschützter Inhalt. Ohne gesonderte Erlaubnis ist jede urheberrechtliche Nutzung untersagt, insbesondere die Nutzung des Inhalts im Zusammenhang mit, für oder in KI-Systemen, KI-Modellen oder Generativen Sprachmodellen.

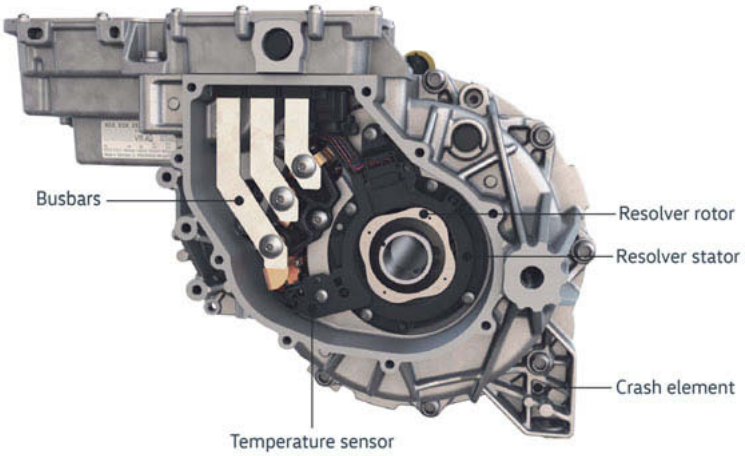


Fig. 7: Components on the PSM's B-side bearing shield

2.2.4. Cooling and Heating of the E-Axle Drive

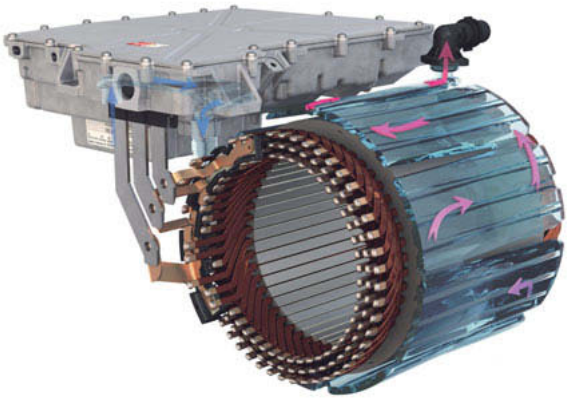


Fig. 8: Coolant flow through the PI and stator

The e-axle drive is liquid cooled. The coolant flow into the e-drive runs first through the power inverter, because the semiconductors specify the maximum permissible coolant temperature. Having flowed through the PI, the coolant is then guided via a sealing pipe plug element into

https://doi.org/10.51202/9783181023549 - Generiert durch IP 216.73.216.36, am 19.01.2026, 02:19:31. © Urheberrechtlich geschützter Inhalt. Ohne gesonderte Erlaubnis ist jede urheberrechtliche Nutzung untersagt, insbesondere die Nutzung des Inhalts im Zusammenhang mit, für oder in KI-Systemen, KI-Modellen oder Generativen Sprachmodellen.

the cooling jacket of the motor housing. The heat, which is generated mainly by ohmic losses in the stator copper windings, travels through the insulation system and the lamination stack to the cooling jacket in the motor housing. The cooling medium is fed through circumferential cooling channels optimised for pressure loss between the stator mount and the outer housing and, at the end of the cooling jacket, guided through a coolant connecting hose into the outer cooling circuit of the vehicle (fig. 8).

2.2.5. Technical Data of MEB E-Drives

The compact MEB axle drives for the ID. vehicle family provide a remarkable drive performance. The axle-parallel MEB rear-axle drive, a permanent-magnet synchronous machine with integrated PI and single-speed transmission, delivers a peak power of 150 kW and a maximum torque of 310 Nm. This electric machine is operated up to a maximum speed of 16,000 rpm (fig. 9, fig. 10).

		MEB rear-axle drive	MEB front-axle drive
			
Machine type		PSM	ASM
Design voltage	[V]	320	320
Power (peak, 30 sec)	[kW]	150	75
Max. torque	[Nm]	310	151
Max. speed	[rpm]	16,000	14,000
Weight *	[kg]	90	60

***** Sum of PI, machine and single-speed transmission

Fig. 9: Technical data of MEB rear- and front-axle drive

The excellent performance of the front-axle machine is also shown by the full-load diagram of torque and power versus rotational speed (fig. 10). The max. torque of 310 Nm is already available at zero rpm, the max. power will be available between 5,000 and 8,000 rpm and the machine operates up to a max. speed of 16,000 rpm.

https://doi.org/10.51202/9783181023549 - Generiert durch IP 216.73.216.36, am 19.01.2026, 02:19:31. © Urheberrechtlich geschützter Inhalt. Ohne gesonderte Erlaubnis ist jede urheberrechtliche Nutzung untersagt, insbesondere die Nutzung des Inhalts im Zusammenhang mit, für oder in KI-Systemen, KI-Modellen oder Generativen Sprachmodellen.

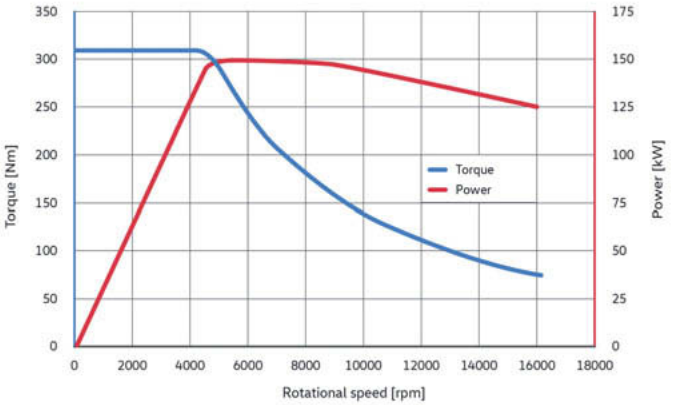


Fig. 10: PSM torque and power vs. rotational speed, full-load diagram

The design of the e-drives is based on a detailed evaluation of the energy throughput in the e-machine characteristics map for various driving cycles. When designing the magnetic circuit, particular attention was paid to the operating points in city driving cycles to ensure that the e-drives run especially efficiently under those circumstances. The efficiencies are well above 90 percent in a wide customer-relevant map range (see fig. 11).

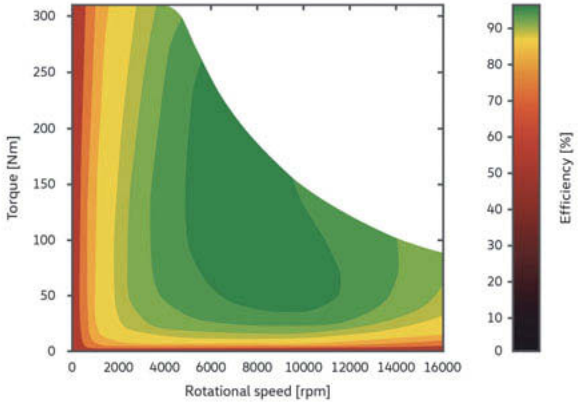


Fig. 11: PSM efficiency map

https://doi.org/10.51202/9783181023549 - Generiert durch IP 216.73.216.36, am 19.01.2026, 02:19:31. © Urheberrechtlich geschützter Inhalt. Ohne gesonderte Erlaubnis ist jede urheberrechtliche Nutzung untersagt, insbesondere die Nutzung des Inhalts im Zusammenhang mit, für oder in KI-Systemen, KI-Modellen oder Generativen Sprachmodellen.

As an additional drive for four-wheel drive and boost functions, the coaxial MEB front-axle drive, an asynchronous machine with integrated PI and single-speed transmission, is available. It delivers a peak power of 75 kW and a maximum torque of 151 Nm. This electric machine is operated up to a maximum speed of 14,000 rpm.

2.2.6. The MEB Rear-Axle Drive compared with the e-Golf Drive

The comparison between the technical data of the new MEB rear-axle drive and the e-drive in the current e-Golf [3], [4], [5] illustrates the development progress achieved (fig. 12).

Peak power could be increased by 50 percent to 150 kW and torque by seven percent to 310 Nm. Despite the increases in power and torque, the weight of the MEB rear-axle drive was reduced by 18 percent to 90 kg. This results in a specific power-to-weight ratio for the MEB rear-axle drive of 1,667 W/kg, which represents a significant increase of 82 percent relative to the e-drive in the e-Golf.

		MEB rear-axle drive	e-Golf drive
			
Machine type		PSM	PSM
Design voltage	[V]	320	320
Power (peak, 30 sec)	[kW]	150	100
Max. torque	[Nm]	310	290
Max. speed	[rpm]	16,000	12,000
Weight *	[kg]	90	109
Ratio single-speed transmission		11.5:1	9.02:1

***** Sum of PI, machine and single-speed transmission

Fig. 12: Comparison of MEB rear-axle and e-Golf drive

2.3. Single-Speed Transmission

The single-speed transmission steps down the rotational speed of the electric machine (maximum 16,000 rpm) for driving the wheels. The overall ratio is achieved by a two-stage spur-gear set via an intermediate shaft (fig. 13).

https://doi.org/10.51202/9783181023549 - Generiert durch IP 216.73.216.36, am 19.01.2026, 02:19:31. © Urheberrechtlich geschützter Inhalt. Ohne gesonderte Erlaubnis ist jede urheberrechtliche Nutzung untersagt, insbesondere die Nutzung des Inhalts im Zusammenhang mit, für oder in KI-Systemen, KI-Modellen oder Generativen Sprachmodellen.

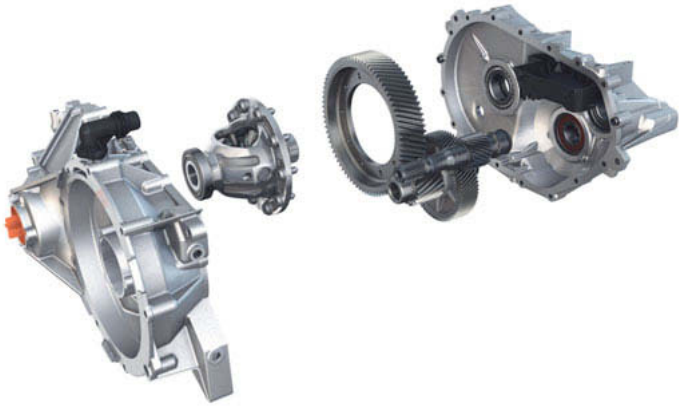


Fig. 13: Single-speed transmission of the MEB rear-axle drive

The acoustic characteristics of the gearing and housing have been optimised. The electric machine and transmission share the same shaft bearing, which contributes to the reduction of friction. Oil supply to the transmission components is provided by a lifetime oil filling. The oil is guided specifically to the lubrication points and kept clear of splash areas. Furthermore, the driveshaft bearing has been changed from a pretension tapered roller bearing to a lower-loss fixed/floating bearing.

The overall transmission ratio can be adapted to the type of vehicle. An overall ratio of 11.5:1 is planned for its first use in the ID., enable a top speed of 160 km/h.

A transmission parking lock is intentionally avoided at the MEB. Instead, the drive axle is locked when at a standstill by an electronically activated parking brake.

3. Summary

The powertrain systems in the Volkswagen MEB are part of a modular construction kit, whose components enable the configuration of various different electrified powertrain systems for electric vehicles.

The axle-parallel rear-axle drive in the MEB consists of a highly efficient, permanent-magnet synchronous machine, a friction-optimised single-speed transmission and a highly compact power inverter fastened to the electric machine. In combination with the high-voltage lithium-ion battery, the e-drive in the Volkswagen ID. delivers a maximum torque of 310 Nm and a maximum power of 150 kW. For all-wheel-drive applications, there is an additional coaxial e-

https://doi.org/10.51202/9783181023549 - Generiert durch IP 216.73.216.36, am 19.01.2026, 02:19:31. © Urheberrechtlich geschützter Inhalt. Ohne gesonderte Erlaubnis ist jede urheberrechtliche Nutzung untersagt, insbesondere die Nutzung des Inhalts im Zusammenhang mit, für oder in KI-Systemen, KI-Modellen oder Generativen Sprachmodellen.

drive available for the front axle. It consists of an innovative asynchronous machine likewise paired with a friction-optimised single-speed transmission and attached power inverter.

The MEB for electrified powertrains represents the systematic continuation of Volkswagen's modularization approach for new vehicles. Thanks to systematic development for high volumes, development and component costs can be significantly reduced. This is an essential prerequisite for the reduction of vehicle costs and thus increasing the market penetration of electric vehicles.

Offering a driving range on the level of today's petrol-driven vehicles and available for the same price as a diesel car, the ID. also has the potential to facilitate the breakthrough of environmentally friendly electric mobility and start a new era of electric drive systems.

Literature

[1] Volkswagen Newsroom, Volkswagen Group News, 11.09.2018
The Volkswagen Group launches the most comprehensive electrification initiative in the automotive industry with "Roadmap E"

[2] Volkswagen Newsroom, Speeches Annual Media Conference 2019, 12.03.2019
https://www.volkswagen-newsroom.com/en/press-releases/volkswagen-plans-22-million-electric-vehicles-in-ten-years-4750

[3] F. Eichler, K. Bennewitz, C. Helbing, P. Lück, et.al.
Volkswagen Electrifies the New Golf
38th Vienna Motor Symposium, Vienna, 2017

[4] P. Lück, G. Kruse, J. Tousen, et.al.
The electric powertrain matrix from Volkswagen
MTZ - Motortechnische Zeitschrift, Issue 2/2014, 2014

https://doi.org/10.51202/9783181023549 - Generiert durch IP 216.73.216.36, am 19.01.2026, 02:19:31. © Urheberrechtlich geschützter Inhalt. Ohne gesonderte Erlaubnis ist jede urheberrechtliche Nutzung untersagt, insbesondere die Nutzung des Inhalts im Zusammenhang mit, für oder in KI-Systemen, KI-Modellen oder Generativen Sprachmodellen.

Volvo Cars modular Electric Axle Drive

M.Sc. **Mathias Jörgensson**, B.Sc. **Christian Wolrath**,
B.Sc. **Johan Hallnéus**,
Volvo Car Group, Göteborg, Sweden

Abstract

Volvo Cars will launch a broad range of full electric vehicles between 2019 and 2022 under the brands Polestar and Volvo. These machines will be further fitted with a range of hybrid and hybrid plug-in options for all models, making it one of the world's broadest electrified car offerings in the market.

A scalable modular system was developed taken into consideration different performance and installation requirements but also the ability to add future functions .This paper shows evaluation of different concepts and the design of an by

Volvo Cars fully in-house designed, verified and manufactured e-axle transmission. Manufactured in engine plants alongside with awarded Volvo Engine Architecture powertrains.

The architecture is scalable for a full range of power positions in future. Modularity considering not only design & installation but also assembly process, sourcing, procurement, development tools, CAE methods and models.

Volvo Cars electrification strategy

Volvo Cars will introduce a portfolio of electrified cars across its model range, embracing fully electric cars, plug in hybrid cars and mild hybrid cars. It will launch several fully electric cars starting in 2019, both Volvo models and high performance electrified cars from Polestar, Volvo Cars' performance car arm. These cars will be supplemented by a range of plug in hybrid and mild hybrid 48 volt options on all models, representing one of the broadest electrified car offerings of any car maker. This means that there will in future be no Volvo cars without an electric motor, as pure ICE cars are gradually phased out and replaced by ICE cars that are enhanced with electrified options. Volvo Cars has stated that it plans to have sold a total of 1 million electrified cars by 2025.The statement underlines Volvo Cars' commitment to minimizing its environmental impact and making the cities of the future cleaner. Volvo Cars is focused on reducing the carbon emissions of both its products as well as its operations. It aims to have climate neutral manufacturing operations by 2025.The decision also follows the announcement

https://doi.org/10.51202/9783181023549 - Generiert durch IP 216.73.216.36, am 19.01.2026, 02:19:31. © Urheberrechtlich geschützter Inhalt. Ohne gesonderte Erlaubnis ist jede urheberrechtliche Nutzung untersagt, insbesondere die Nutzung des Inhalts im Zusammenhang mit, für oder in KI-Systemen, KI-Modellen oder Generativen Sprachmodellen.

that Volvo Cars will turn Polestar into a new separately-branded electrified global high performance car company. In the electric drive system, electric axles play an important role. They are suitable for use in pure electric drives and plug-in hybrids both for front and rear installations. This paper shows the design of Volvo Cars Modular Electric Propulsion transmission for electric axles with fully in-house design and verification. Manufactured in engine plant alongside with Volvo Engine Architecture manufacturing, the Modular Electric Propulsion architecture is scalable for full range of power positions in the future.

History

All change takes time. If we look back in the history it is obvious that the major changes are done with slow pace. The 1950's and 1960's were expansive years for Volvo Cars. Production volumes increased year by year and when it suddenly became clear that the availability of fuel and the effect on fuel prices could be a limiting factor for future mobility it triggered new ideas around efficient transportation. In 1976 Volvo Cars presented 2 different electrically driven concept vehicles for efficient city transport - Volvo Electric Car.



Fig. 1: Electric Car prototype 1976.

Two different prototypes were built with the typical character of city cars. Built with variations in driveline technology and seating capacity. One car was aimed for city personal transport and the other car was designed as a mail delivery vehicle.

https://doi.org/10.51202/9783181023549 - Generiert durch IP 216.73.216.36, am 19.01.2026, 02:19:31. © Urheberrechtlich geschützter Inhalt. Ohne gesonderte Erlaubnis ist jede urheberrechtliche Nutzung untersagt, insbesondere die Nutzung des Inhalts im Zusammenhang mit, für oder in KI-Systemen, KI-Modellen oder Generativen Sprachmodellen.

Table 1:

Technical data Volvo Electric Car 1976	
Vehicle Length	2.68
Weight	1200 kg
Top speed	Top speed 70 km/h
Electric drive power	Electric drive power 9,5 kW
Electric drive version 1	Series wound 72 VDC
Electric drive version 2	Shunt motor with CVT 60 VDC

Since 1976 there have been various BEV, PHEV & mild hybrid programs started within Volvo Car, however it did take time until a Volvo EV car did reach Volvo customers. The 1st generation e-axle was introduced with C30 2011, followed by the V60 D6 PHEV which went into production 2012.The 3rd generation e-axle was introduced in XC90 T8 PHEV 2014, later introduced also in the S/V90 and XC60. Last year it was also introduced in the new S/V60. All these PHEVs with our 3rd generation e-axel are still in production and are outselling the forecasted volumes.

The e-axle described in this presentation is the 4th generation of e-axle in a Volvo Car BEV and PHEV.

https://doi.org/10.51202/9783181023549 - Generiert durch IP 216.73.216.36, am 19.01.2026, 02:19:31. © Urheberrechtlich geschützter Inhalt. Ohne gesonderte Erlaubnis ist jede urheberrechtliche Nutzung untersagt, insbesondere die Nutzung des Inhalts im Zusammenhang mit, für oder in KI-Systemen, KI-Modellen oder Generativen Sprachmodellen.

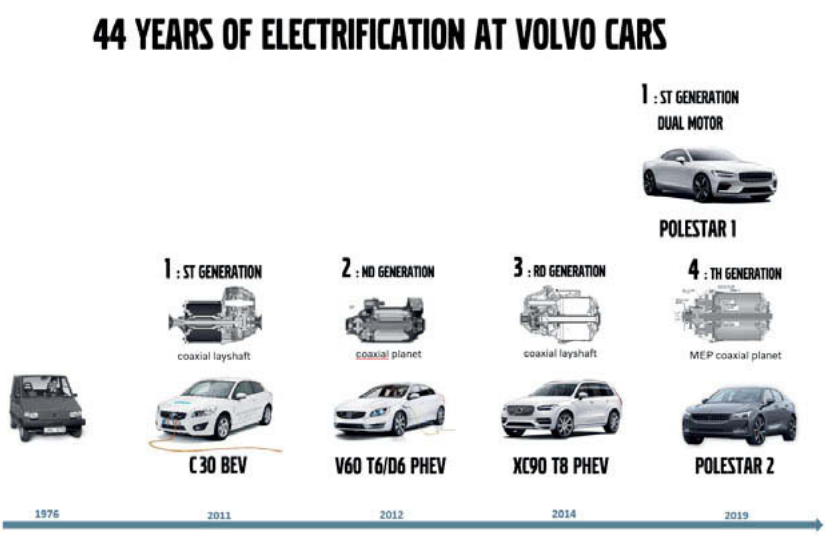


Fig. 2: Volvo car electrification & e-axle from 1976 to 2020.

Polestar 1

The Polestar 1 is forming a halo for the future electric brand. The performance vehicle is a two-door, 2+2 seat grand tourer coupé with an ‘electric performance hybrid’ drivetrain. An electric car supported by an internal combustion engine, it has a range of 150 km (94 m), pure electric power alone – Its output of 600 hp and 1000 Nm of torque places the car firmly in the performance car segment.

https://doi.org/10.51202/9783181023549 - Generiert durch IP 216.73.216.36, am 19.01.2026, 02:19:31. © Urheberrechtlich geschützter Inhalt. Ohne gesonderte Erlaubnis ist jede urheberrechtliche Nutzung untersagt, insbesondere die Nutzung des Inhalts im Zusammenhang mit, für oder in KI-Systemen, KI-Modellen oder Generativen Sprachmodellen.



Fig. 3: Polestar 1

The polestar 1 uses the 1st generation of dual machine e-axel developed by VCC. In principle its one electric machine per rear wheel connected via a one stage 3 pcs planetary gear set. This arrangement enables speed and torque control for each wheel independently and thereby it can be utilized for different condition on each wheel. It supports the driver with precise acceleration on each wheel to keep the maximum road grip and maintain speed while cornering regardless of the friction or surface.

The solution also enables the possibility to vector the torque and speed between the wheels this can be used to make the vehicle more agile but also enhance stability and safe feel.

https://doi.org/10.51202/9783181023549 - Generiert durch IP 216.73.216.36, am 19.01.2026, 02:19:31. © Urheberrechtlich geschützter Inhalt. Ohne gesonderte Erlaubnis ist jede urheberrechtliche Nutzung untersagt, insbesondere die Nutzung des Inhalts im Zusammenhang mit, für oder in KI-Systemen, KI-Modellen oder Generativen Sprachmodellen.

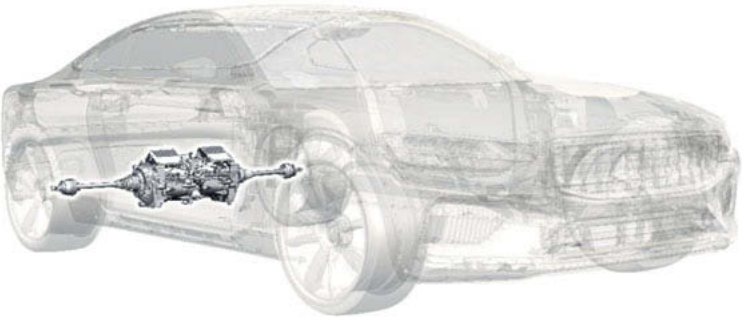


Fig. 4: Polestar 1 e-axle.

Polestar 2



Fig. 5: Polestar 2.

https://doi.org/10.51202/9783181023549 - Generiert durch IP 216.73.216.36, am 19.01.2026, 02:19:31. © Urheberrechtlich geschützter Inhalt. Ohne gesonderte Erlaubnis ist jede urheberrechtliche Nutzung untersagt, insbesondere die Nutzung des Inhalts im Zusammenhang mit, für oder in KI-Systemen, KI-Modellen oder Generativen Sprachmodellen.

Polestar 2 is a premium five-door fastback with two electric machines and a 78 kWh battery capacity that will enable a targeted range of 500 km, based on Volvo Car Group's adaptable Compact Modular Architecture platform (CMA).
For Polestar, performance underlies the entire driving experience. The all-wheel drive electric powertrain in Polestar 2 produces 300 kW (408 hp) and 660 Nm (487 lb-ft). This translates to a 0-100 km/h acceleration time of less than 5 seconds.

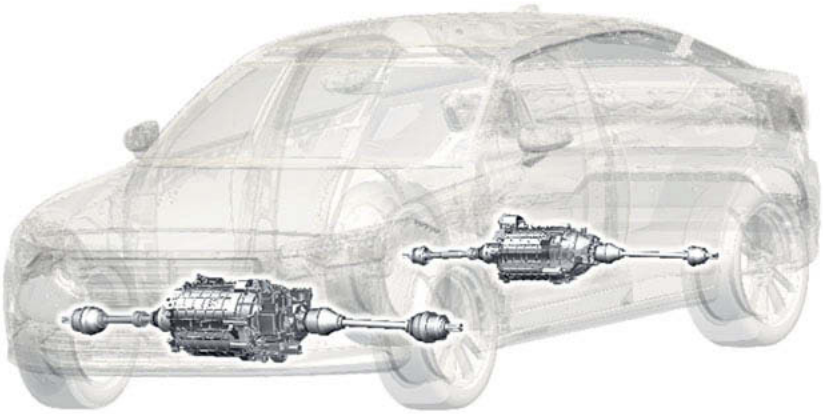


Fig. 6 : Polestar 2 e-axles.

The full electric AWD drivetrain features one machine on the front axle and one on the rear. Each e-machine transmitting the power to the road by a transmission from the 4th generation coaxial e-axle containing a compact compound planetary gear set.
State-of-the-art electric drivetrain promises ranges for everyday practicality, and at the same time potential for quick acceleration due to instant torque. In a very compact space, torque conversion must be assured while maintaining good efficiency and acoustics.

https://doi.org/10.51202/9783181023549 - Generiert durch IP 216.73.216.36, am 19.01.2026, 02:19:31. © Urheberrechtlich geschützter Inhalt. Ohne gesonderte Erlaubnis ist jede urheberrechtliche Nutzung untersagt, insbesondere die Nutzung des Inhalts im Zusammenhang mit, für oder in KI-Systemen, KI-Modellen oder Generativen Sprachmodellen.

Electric axle concept

Electric axles play an important role in the electric drive system. Suitable for use in pure electric drives and hybrids both for front and rear installations. This paper shows the design of an electric axle with high performance density that fulfils the stringent requirement on NVH, strength, efficiency, scalability, weight and cost. Simplicity have also been a key word in the design work.

A modular system for the e-axle allows to vary the output power as well as to have an optional range of gear ratios in order to expand the useable vehicle speed range, it allows installation in both Volvo Car CMA & SPA platform on front and rear axle.

At current state-of-the-art axle drives the e-motor is positioned either with an offset parallel to the wheel axle and driveshaft or with the e-motor coaxial to the wheel axle and driveshaft.

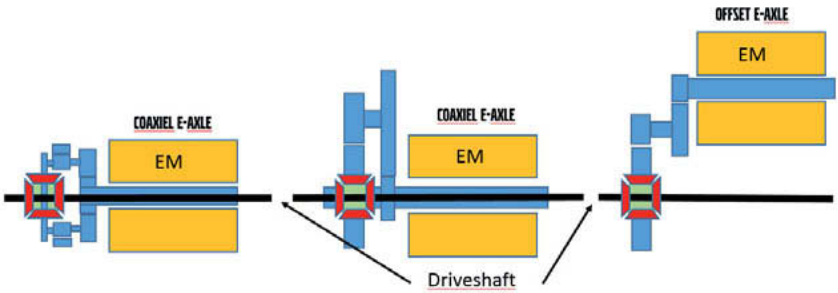


Fig. 7: Coaxial & offset position of EM.

The power is transferred via a layshaft transmission with helical gear in 2 gear step or a planet gear transmission in 1 or 2 step into the differential.

For the in house developed e-axle the Volvo team decided for a design of all components and the system in coaxial position towards the wheel axle in combination with a planet gear transmission. This results in compact dimensions and low weight, but considering the planetary gear set also to have a high torque density and low inertia. Installation in large platform SPA and small platform CMA was possible with minor modifications.

The rotor axle of the e- machine is designed as hollow shaft, which's force is transmitted via a compound planet gear set and a spur gear differential. The first gear step is adapted to vary gear ratio 6 -11, second step have a fixed gear ratio.

https://doi.org/10.51202/9783181023549 - Generiert durch IP 216.73.216.36, am 19.01.2026, 02:19:31. © Urheberrechtlich geschützter Inhalt. Ohne gesonderte Erlaubnis ist jede urheberrechtliche Nutzung untersagt, insbesondere die Nutzung des Inhalts im Zusammenhang mit, für oder in KI-Systemen, KI-Modellen oder Generativen Sprachmodellen.

The base layout is common for EFAD (Electric front axle drive) and ERAD (Electric rear axle drive).
The transmission has an integrated planet carrier and spur gear differential as standard with option to be modified for features as disconnect functions within the system layout.



Fig. 8: Coaxial transmission Polestar 1



Fig. 9: Coaxial transmission Polestar 2

Modularity & features
Modularity is another key word the engineers have strived for. With a modular system the e-axle allows to vary the output power as well as to have an optional range of gear ratios in order to expand the useable vehicle speed range.
It allows installation in all Volvo Cars future vehicles front and rear axle. With a modular strategy also comes flexibility within manufacturing process, development and supplier synergies. The major subsystem, gears and differential internal parts are common for all variants.

https://doi.org/10.51202/9783181023549 - Generiert durch IP 216.73.216.36, am 19.01.2026, 02:19:31. © Urheberrechtlich geschützter Inhalt. Ohne gesonderte Erlaubnis ist jede urheberrechtliche Nutzung untersagt, insbesondere die Nutzung des Inhalts im Zusammenhang mit, für oder in KI-Systemen, KI-Modellen oder Generativen Sprachmodellen.

For the housings it is important to keep reference point and clamping hard points common for synergies in manufacturing process, also the interface to electric machine in A-shield (the housing between transmission and EM) is common.

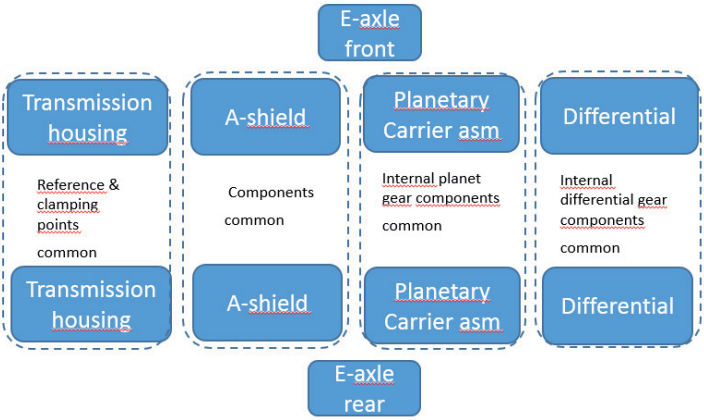


Fig. 10 BOM structure and commonality

The ERAD and EFAD have a common installation in all vehicles but unique between SPA and CMA platform, there is also a unique mount system for ERAD vs EFAD.
With modularity it is possible to find synergies in engineering, sourcing, procurement, test and CAE.

Reference

[1] Experience from 40 years with Volvo Cars Electrification Robert Eriksson, Volvo Car Group.

https://doi.org/10.51202/9783181023549 - Generiert durch IP 216.73.216.36, am 19.01.2026, 02:19:31. © Urheberrechtlich geschützter Inhalt. Ohne gesonderte Erlaubnis ist jede urheberrechtliche Nutzung untersagt, insbesondere die Nutzung des Inhalts im Zusammenhang mit, für oder in KI-Systemen, KI-Modellen oder Generativen Sprachmodellen.

Innovative transmission concept for hyper-high-speed electromechanical powertrains

Daniel Schweigert, **Marco Mileti**, **Bernd Morhard**, **Martin Sedlmair**, **Max Fromberger**, **Michael Otto**, **Thomas Lohner**, **Karsten Stahl**,
Gear Research Center (FZG), Technical University of Munich

Abstract

More and more high-rev transmission concepts are being used in BEVs to enhance the power density of the electric machines and the transmission system as a whole. The decreased gear input torques deriving from the high speeds mean that the entire drivetrain's weight and space can be accordingly reduced. However, these advantages are offset by new challenges with respect to load capacity, efficiency and NVH behaviour. All these aspects are being investigated in the joint project "Speed4E" under the leadership of the Gear Research Centre (FZG) of the Technical University of Munich (TUM). The main goals of Speed4E are the development of an innovative driveline concept for electric vehicles with input speeds up to 50,000 rpm, extensive investigations on test benches and the first integration of a hyper-high-speed electromechanical powertrain in a demonstrator vehicle.

The system is built of two electric motors and two parallel power paths to provide the opportunity of power splitting and therefore efficiency and NVH-optimization. Hence, two sub-transmissions are necessary to merge the power of the sub-drivelines onto the differential. One sub-transmission is designed as a shiftable two-speed gearbox, in order to guarantee high torque at low speeds and a high efficiency at cruise speed. On the other hand, the second subsystem is designed as a planetary gearbox characterized by a high transmission ratio, to reach high power density. Especially for the fixed-speed sub-transmission, different gear designs (i.e. Reference, Low-Loss and NVH-Optimized) were developed to investigate the impact of different parameters on the efficiency and NVH behaviour in high-speed electromechanic powertrains. A special focus will be set during the project on obtaining a high level of integration and modularity, to guarantee a high degree of practical relevance.

After a presentation of the main project goals and the consortium partners, the paper describes the design of the electromechanical powertrain. In addition, first simulative results of the efficiency and NVH-behaviour will be presented and extensively discussed.

https://doi.org/10.51202/9783181023549 - Generiert durch IP 216.73.216.36, am 19.01.2026, 02:19:31. © Urheberrechtlich geschützter Inhalt. Ohne gesonderte Erlaubnis ist jede urheberrechtliche Nutzung untersagt, insbesondere die Nutzung des Inhalts im Zusammenhang mit, für oder in KI-Systemen, KI-Modellen oder Generativen Sprachmodellen.

Speed4E is funded by the Federal Ministry of Economic Affairs and Energy (BMWi), supervised by the German Aerospace Agency and supported by the Forschungsvereinigung Antriebstechnik e.V. (FVA).

1. Introduction and motivation

The need to dramatically reduce the local emissions of passenger and light-duty commercial vehicles is nowadays mainly being dealt with by electrifying classic drivelines. Although many new high-efficient concepts are being presented by traditional and new manufacturers, one of the most compelling problems to solve is still the maximum reach obtainable with electric vehicles. Due to the low energy density of batteries w.r.t. traditional fossil fuels, efficiency optimization has become one of the main challenges to face in the next generation of battery electric vehicles. Furthermore, as batteries are the one of the main cost-drivers in the drivetrain, a cost-effective drivetrain, providing lightweight and high efficiency, would allow the installation of more batteries and thus higher ranges for the vehicle itself.

Increasing the driving speed of the electric motors is one way to achieve this goal that has proven highly effective over recent years. Indeed, many companies and research institutes have started dealing with high-speed. The increase in power density of the electric motors permits an effective use of the available space and reduces costs e.g. of the active materials of rotors and stators. Beside this, however, when developing a high-efficient electrified powertrain, one of the most important and at the same time challenging tasks is to obtain an intelligent integration of all components. This way, the synergies between electrical and mechanical components can be exploited at their best. So, the optimization regarding all subcomponents has not just to be carried out at local level, but also and mainly at system and vehicle level. The project Speed2E, where maximum driving speeds of up to 30,000 rpm were reached, could successfully demonstrate the advantages of such a design. Hence, in order to develop and further improve a drivetrain with the mentioned characteristics of high-efficiency, lightweight and cost-effectiveness, the project Speed4E was started. One of the main goals is the ulterior increase of driving speed.

Nonetheless, in order to achieve those ambitious goals, numerous challenges have to be faced and technological leaps addressed. In fact, even though a high revving motor has many advantages, it indeed requires a more complex gearbox with higher transmission ratios. Further, a special focus has to be set onto the dynamic behaviour of all components, as the excitation frequencies grow considerably. Indeed, discomforts such as noise and vibrations would not be accepted by the driver.

https://doi.org/10.51202/9783181023549 - Generiert durch IP 216.73.216.36, am 19.01.2026, 02:19:31. © Urheberrechtlich geschützter Inhalt. Ohne gesonderte Erlaubnis ist jede urheberrechtliche Nutzung untersagt, insbesondere die Nutzung des Inhalts im Zusammenhang mit, für oder in KI-Systemen, KI-Modellen oder Generativen Sprachmodellen.

Additionally, it is not yet clear to which point the increase of the driving speed of the electric motors still generates a sensible increase in power density and efficiency of the whole driveline. The individuation of such a point is amongst others also an overarching objective of Speed4E.

2. Speed4E

Speed4E is a publicly funded research project, and the result of a strong collaboration between industry and research institutions. The main goal of Speed4E is the development of a hyper-high-speed drivetrain for electric vehicles. Said drivetrain is intended to be highly efficient and at the same time cost effective. To realize this objective, the maximum driving speed of the electric motors was set to 50,000 rpm. The designed drivetrain is to be manufactured and tested during the project on several purpose-built test-rigs. Additionally, two drivelines are to be integrated in existing electric vehicles, resulting in a first-time testing of a high-speed drivetrain. The numerous and innovative components, systems and functionalities developed for the Speed4E drivetrain can be subdivided in three categories: component, system and vehicle level. [Mil18]

At component level, highly-efficient power electronic modules were developed to satisfy the high-frequent current demand of the electric motors. Purpose-built, efficient SiC half-bridges are being employed to minimize losses. Also the topology of the modules perfectly adapts to the idea of high-integration being followed within the project. The development of the power electronics is carried out by the University of Hanover (IAL-LE) and the company Lenze. Following the power flux, the electric motors are being described. As the powertrain is defined by a double-electric architecture, both an induction and a synchronous motor were designed by the University of Hanover (IAL-AS) and the company ATE. In order to guarantee maximum modularity to the system, the topology of both motors is equal, making different configurations and power classes possible. The maximum power of both motors is of about 230 kW but can be increased to up to 540 kW in an all road configuration. The choice of different electric motors was mainly driven by the opportunities made available with a combination of the low drag losses of an induction motor and the high efficiency of the synchronous machine. Finally, an innovative gearbox was designed for hyper-high input speeds in a strong collaboration between the Technical University of Munich (FZG), the University of Hanover (IMKT) and the companies Magna and Schaeffler. It basically consists of two independent sub-transmissions that merge the power on the final-drive stage. Providing a total of three speeds it enables the creation of optimized operational strategies to further improve the overall efficiency. The shiftable sub-transmission (ST) is actuated by an innovative linear actuator for comfortable and rapid shifting of the dog clutch designed by the Technical University of Darmstadt (IMS). Newly

https://doi.org/10.51202/9783181023549 - Generiert durch IP 216.73.216.36, am 19.01.2026, 02:19:31. © Urheberrechtlich geschützter Inhalt. Ohne gesonderte Erlaubnis ist jede urheberrechtliche Nutzung untersagt, insbesondere die Nutzung des Inhalts im Zusammenhang mit, für oder in KI-Systemen, KI-Modellen oder Generativen Sprachmodellen.

developed bearing and sealing concepts for the gearbox are being created in collaboration with Freudenberg Sealing Technologies.

At system level, the realization of a modular, highly-integrated driveline was followed for all components. The most ambitious goal at system level is, however, the creation of a highly integrated and holistic thermal management coupled with innovative lubrication concepts. Indeed, by creating one circuit for cooling and lubrication the warmth generated by the losses of power electronics and electric motors can be directly transported by the lubricant itself. Through an intelligent control of the valves, the overall losses of the drivetrain can be further reduced. The development of a suitable fluid, which serves both as cooling and lubricating medium is carried out by Fuchs Lubricants. All components are simulated singularly and as a whole by the research institutions and the company AVL.

At vehicle level, the mechanical, electrical and electronic integration of the drivetrain is coordinated by AVL, the BEV being a BMW i3. The Partner BMW also performs the vehicle testing. A schematic division of the tasks between project partners can be appreciated in Fig. 1.

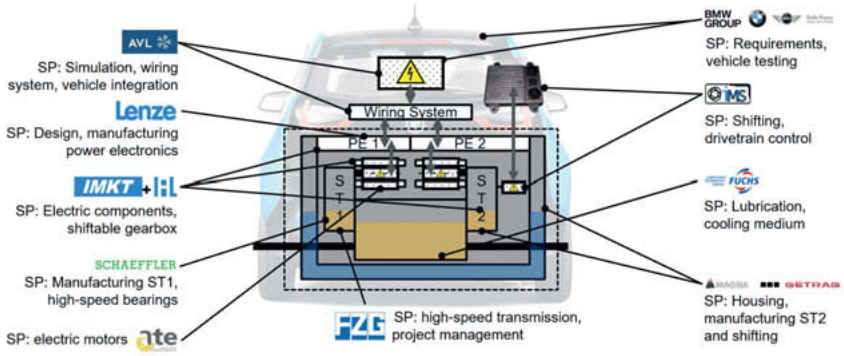


Fig. 1: Schematic overview of the tasks and the project partners of Speed4E [Sch18]

https://doi.org/10.51202/9783181023549 - Generiert durch IP 216.73.216.36, am 19.01.2026, 02:19:31. © Urheberrechtlich geschützter Inhalt. Ohne gesonderte Erlaubnis ist jede urheberrechtliche Nutzung untersagt, insbesondere die Nutzung des Inhalts im Zusammenhang mit, für oder in KI-Systemen, KI-Modellen oder Generativen Sprachmodellen.

3. Gearbox Design

The gearbox is divided into two sub-transmissions (ST) ST1 and ST2, which are connected to two electric machines EM1 and EM2, respectively (Fig. 3). ST1 has a planetary gear set with a following spur gear stage, a fixed gear ratio of 26.4 and is driven by an asynchronous inductive machine with a nominal power of about 60 kW. ST2 is designed as a three stage helical gear set with two speeds and is connected to the permanent magnet synchronous machine EM2 with a nominal power of 75 kW. In the first speed, the gear ratio of 36 provides high starting torque at low vehicle speeds. The second speed, with a gear ratio of 20.4, represents an overdrive to minimize the energy consumption of the powertrain at high vehicle speeds. Fig. 4 illustrates the gearbox with the electric machines, the two sub-transmissions and the innovative shifting by a voice coil actuator.

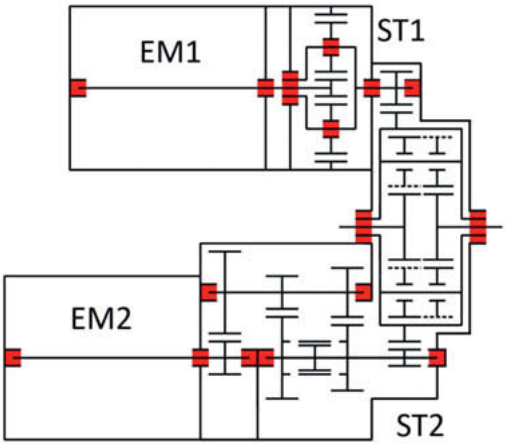


Fig. 3: Schematic representation of the gearbox design [Mil18]



Fig. 2: Visualization of the Speed4E powertrain with the power electronics and closed housing

The two power paths of the system are added together at the final drive, which features an innovative planetary differential [Hei05] that has been provided by the project partner Schaeffler. Hereby, the power split transmission architecture enables intelligent operating strategies by distributing the required drive power to the two electric machines. Those operating

https://doi.org/10.51202/9783181023549 - Generiert durch IP 216.73.216.36, am 19.01.2026, 02:19:31. © Urheberrechtlich geschützter Inhalt. Ohne gesonderte Erlaubnis ist jede urheberrechtliche Nutzung untersagt, insbesondere die Nutzung des Inhalts im Zusammenhang mit, für oder in KI-Systemen, KI-Modellen oder Generativen Sprachmodellen.

strategies can be implemented to either increase the powertrain efficiency [Idl16] or to reduce the noise emissions by avoiding unfavourable load ratios or input speeds. [Gwi14, Gwi17]

Fig. 2 shows the developed drivetrain with the power electronics, mounted directly on the machines and the closed housing, made of an aluminium cast alloy. The structure is designed to offer a high stiffness and low weight at the same time. As the project follows a highly integrated design approach, the cooling circuit for the gear, the electric machines and the power electronics is mainly integrated into the housing.

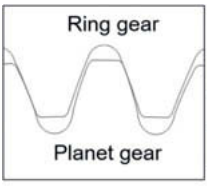


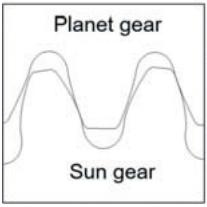
Fig. 4: Speed4E - Gearbox with the electric machines, the two sub-transmissions and the shifting [Mil19]

The powertrain will be extensively tested at two test rigs at IMKT in Hannover and at FZG in Munich and in two test vehicles. The testing at IMKT will be focused on ST2 and in particular the bearing, sealing and shifting concept. The scope of the testing at the FZG test-rig covers the investigation of the efficiency and NVH behaviour.

Gearing designs of Sub-Transmission 1

In order to investigate the impact of different gear parameters on the efficiency and noise-behaviour of the planetary gear set in ST1, three different gearing designs were developed. The reference gear set represents a balanced design between good efficiency and NVH behaviour. In addition, a Low-Loss gearing and a NVH-Optimized de-





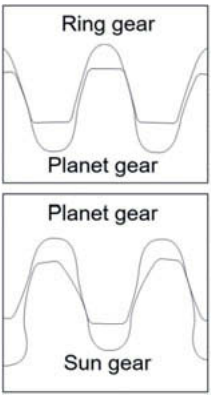
	Sun gear	Planet gear	Ring gear
z	24	63	-149
α_n	20°		
b	17.75 mm		
a	48.50 mm		
β	11.50°		
m_n	1.10 mm		
ϵ_α	1.438	1.494	
ϵ_β	1.082		
H_V	0.113	0.030	

Fig. 5: **Reference Design** of the planetary gear set with meshing geometries and main specifications

https://doi.org/10.51202/9783181023549 - Generiert durch IP 216.73.216.36, am 19.01.2026, 02:19:31. © Urheberrechtlich geschützter Inhalt. Ohne gesonderte Erlaubnis ist jede urheberrechtliche Nutzung untersagt, insbesondere die Nutzung des Inhalts im Zusammenhang mit, für oder in KI-Systemen, KI-Modellen oder Generativen Sprachmodellen.

sign were designed and will be investigated on the test rig. The configuration shows a rotating sun gear and planet carrier, whereas the ring gear is mounted in the housing. The planetary gear set is driven by sun gear and contains three planet gears in total. The gearing ratio of the planetary stage is about 7. All gearing designs show the same centre distance (a) and tooth width (b) to ensure an easy integration into the transmission housing.

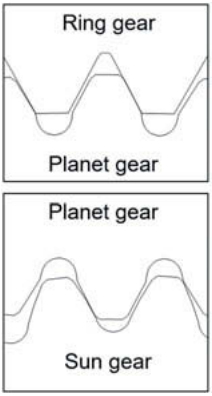
Fig. 5 shows the meshing geometries and main specifications of the reference gearing design. It represents a state of the art design with a high total overlap ratio ($\varepsilon_\alpha + \varepsilon_\beta$) and a low gear tooth loss factor H_V. Fig. 6 shows the NVH-Optimized gear set and its main specification. In comparison to the Reference Design, both the overlap and the contact ratio are increased, to achieve a better vibration behaviour of the meshing. On the other hand, the increased contact ratio affects efficiency due to larger sliding velocities, which is why the NVH-Optimized variant shows a higher tooth loss factor. Furthermore, the larger helix angle (β) also results in larger axial forces in the meshings on the planet and hence also in an increased tilting moment which could lead to an unequal load distribution.



	Sun gear	Planet gear	Ring gear
z	25	62	-149
α_n	17.5°		
b	17.75 mm		
a	48.50 mm		
β	21.75°		
m_n	1.05 mm		
ϵ_α	1.620	1.672	
ϵ_β	2.106		
H_V	0.151	0.027	

Fig. 6: **NVH-Optimized** gearing design of the planetary gear set with meshing geometries and main specifications

Finally, the Low-Loss gear design is represented in Fig. 7. The aim of the Low-Loss variant is to reduce load-dependent gear losses by concentrating the gear mesh around the pitch point in order to reduce sliding velocities along the path of contact [Hin14, Wim06].



	Sun gear	Planet gear	Ring gear
z	33	82	-198
α_n	25°		
b	17.75 mm		
a	48.50 mm		
β	16.80°		
m_n	0.81 mm		
ϵ_α	0.857	0.843	
ϵ_β	2.119		
H_V	0.060	0.016	

Fig. 7: **Low-Loss** gearing design of the planetary gear set with meshing geometries and main specifications

https://doi.org/10.51202/9783181023549 - Generiert durch IP 216.73.216.36, am 19.01.2026, 02:19:31. © Urheberrechtlich geschützter Inhalt. Ohne gesonderte Erlaubnis ist jede urheberrechtliche Nutzung untersagt, insbesondere die Nutzung des Inhalts im Zusammenhang mit, für oder in KI-Systemen, KI-Modellen oder Generativen Sprachmodellen.

This is mainly achieved by reducing the module (m_n) of the planetary gear set to 0.81 mm. Also the pressure angle was raised to 25°. The reduced transverse contact ratio (ε_α) is smaller than 1, and thus typical for a Low-Loss design. To comply with the required safety factors and to receive an integer total overlap ratio ($\varepsilon_\alpha + \varepsilon_\beta$) the helix angle ($\beta$) was adjusted to 16.8°. The Low-Loss design results in very small gear loss factors (H_V) of 0.06 in the sun-planet contact and of 0.016 in the contact of the planets with the internal ring gear.

4. Results

For investigations on the Noise-Vibration-Harshness and the Efficiency of the planetary gear set three different gearing designs were newly developed. The Reference Design has well-adjusted geometric parameters which should lead to moderate load-dependent gear losses and to a good NVH behaviour. Both the NVH-Optimized design and the Low-Loss design should allow detailed investigations of the highly improved noise behaviour and the reduced load-dependent gear losses respectively, e.g. an improved overall efficiency on the test rig. In order to predict the behaviour of the three gear designs, simulations on the efficiency and the NVH were performed.

Efficiency Simulation

Below the results of the efficiency simulations of the three gear designs are presented. The efficiency simulations were calculated with the FVA-software WTplus [Kur16]. WTplus is able to calculate the power losses occurring in gear boxes which allows to predict the steady-state temperature, transient operating conditions, and the temperature distribution to mention only a few features. The application for this paper has its focus on the loss behaviour of the gearings, bearings, and the sealing considering ST1. The efficiency performance maps shown on Fig. 8-Fig. 10 were calculated with discrete operating points under injection lubrication conditions and the bearing preload of ST1. The only differences are the three gear designs of the planetary gear set which were introduced before. For all three designs the general efficiency behaviour is similar. Given a rotational speed, lowering the input torque

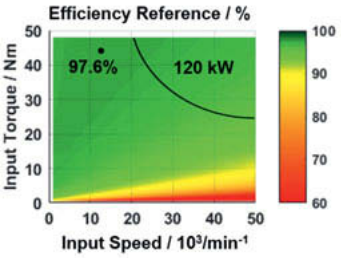


Fig. 8: Efficiency performance map of the reference gear design

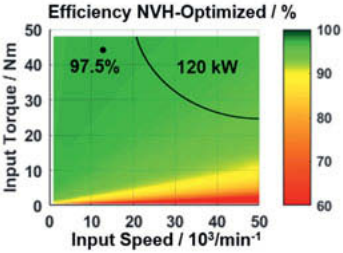


Fig. 9: Efficiency performance map of the NVH-optimized gear design

https://doi.org/10.51202/9783181023549 - Generiert durch IP 216.73.216.36, am 19.01.2026, 02:19:31. © Urheberrechtlich geschützter Inhalt. Ohne gesonderte Erlaubnis ist jede urheberrechtliche Nutzung untersagt, insbesondere die Nutzung des Inhalts im Zusammenhang mit, für oder in KI-Systemen, KI-Modellen oder Generativen Sprachmodellen.

results in a lower efficiency. Given an input torque, with increasing rotational speeds increasing no-load losses lead to decreasing efficiency. The plateau with the best efficiency factors of the three gear designs is located in an area beneath 25,000 rpm and above an input torque of 15 Nm. The highest simulated efficiencies are to be found at an Input Torque of 45 Nm and revolution speeds of 12,500 min^{-1} of the input shaft. With a maximum efficiency of 97.8 %, the Low-Loss design shows the best results to be seen in Fig. 10. The Reference Design in Fig. 8 also has a high efficiency with a maximum of about 97.6 %. The NVH-Optimized design has a slightly lower maximum efficiency of about 97.5 % (Fig. 9). For the examination of the different constituent parts of the gear box losses, the load-dependent gear loss torque (T_{LGP}), the no-load gear loss torque (T_{LG0}), the load-dependent bearing loss torque (T_{LBP}), the no-load bearing loss torque (T_{LB0}) and the sealing loss torque (T_{LS}) are shown in Fig. 12. Relating to the gear loss factor (H_V) according to Ohlendorf [Ohl58], the Low-Loss design shows the lowest load-dependent gear loss torque (T_{LGP}). The higher H_V-value of the Reference Design results in a higher value of T_{LGP}. The highest value of T_{LGP} has the NVH-Optimized gear design. The dominating no-load gear loss torque (T_{LG0}) is due to the high speed of the input shaft of 30,000 min^{-1} and related to the oil squeeze losses of the planetary gear set calculated according to Kettler [Ket02]. Due to the higher pitch line velocity at the sun gear, the value of T_{LG0} is slightly higher for the Low-Loss design than for the Reference Design. Nonetheless, the Low-Loss design reduces the loss torque by approximately 0.1 Nm (Fig. 12), which corresponds to a power loss saving of about 300 W at 30,000 rpm and an input torque of 30 Nm.

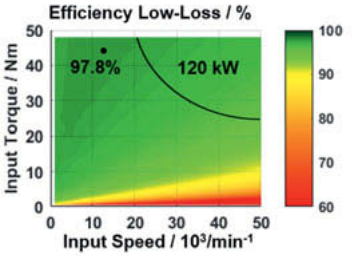


Fig. 10: Efficiency performance map of the Low-Loss gear design

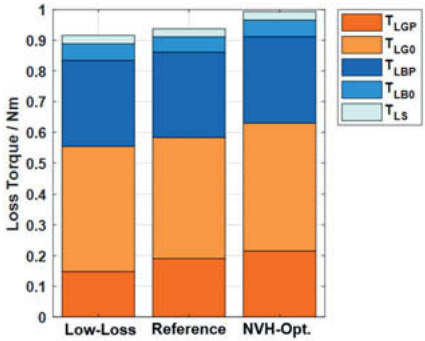


Fig. 11: Loss Torque of the different gearing designs referred to the input shaft at an input torque of 30 Nm and 30,000 rpm

https://doi.org/10.51202/9783181023549 - Generiert durch IP 216.73.216.36, am 19.01.2026, 02:19:31. © Urheberrechtlich geschützter Inhalt. Ohne gesonderte Erlaubnis ist jede urheberrechtliche Nutzung untersagt, insbesondere die Nutzung des Inhalts im Zusammenhang mit, für oder in KI-Systemen, KI-Modellen oder Generativen Sprachmodellen.

NVH Simulation

In comparison to conventional vehicles, the design of transmissions integrated into fully electric cars faces new acoustical challenges due to the missing masking sound of the combustion engine. The continuing trend towards higher drive speeds is intensifying the problem, as, for example, subcritical operation over the entire engine speed range becomes more and more difficult to implement. [Gwi16]

To understand the effects of different parameters on the vibration behaviour in high speed transmissions driven by electric machines, the gearing designs being introduced will be extensively investigated on the test rig and in the simulation software DZP. [Gri11]

This software is, among other things, able to analyse the vibration behaviour by calculating quasi-static and dynamic parameters for specific operating points or over the whole range of operation. The diagrams in Fig. 12 show the characteristics of the static transmission error (STE) of the three gearing designs for 10 different load steps and the first three orders relative to the pinion speed. In addition, Fig. 13 illustrates the characteristics of the tooth force level (TFL) and the dynamic factor K_V over the entire rev range with the nominal input torque of 30 Nm. The STE is an indicator for the vibration behaviour of a gearing at low speeds, whereas the tooth force level displays the excitation at high input speeds. These parameters are calculated quasi static (STE: $n = 0$, TFL: $n \rightarrow \infty$) and therefore are very suitable to analyse and optimize the dynamic behaviour of gearing designs in early design phases.

Due to the very wide rev range, a compromise between a good excitation characteristic at low and high speeds should be found in the modification design process. As the STE is an indicator for the vibration behaviour of a gearing at low speeds, the gear modifications were intended to minimize the STE at high input torque, which occur mostly at low vehicle speeds. Therefore, the Reference and NVH-Optimized variant show the lowest STE values at medium to high input torque. As a result of the tooth geometry, which is in the case of the Low-Loss gearing

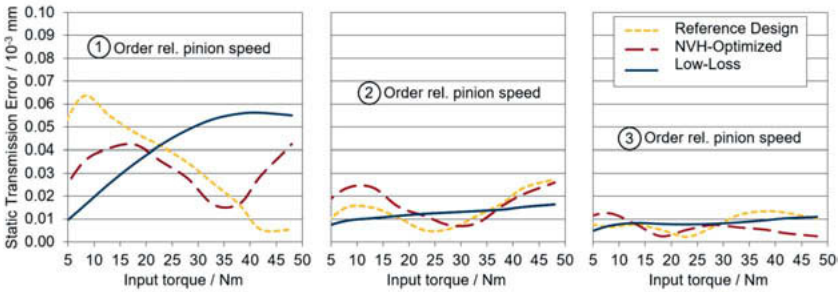


Fig. 12: Static transmission error of the meshing sun gear/planet gear for different input torque and the first three pinion orders

https://doi.org/10.51202/9783181023549 - Generiert durch IP 216.73.216.36, am 19.01.2026, 02:19:31. © Urheberrechtlich geschützter Inhalt. Ohne gesonderte Erlaubnis ist jede urheberrechtliche Nutzung untersagt, insbesondere die Nutzung des Inhalts im Zusammenhang mit, für oder in KI-Systemen, KI-Modellen oder Generativen Sprachmodellen.

characterized by a low tooth size with low lever arms of the resulting meshing forces, this gear design in comparison to the Reference and NVH-Optimized design shows very high mesh stiffness. That's why the modification values for the Low-Loss gearing are very low and show only slight impacts at high input torque.

The left diagram in Fig. 13 illustrates the characteristics of the tooth force level of the three gearing designs, which indicates the dynamic behaviour of the meshes at high input speeds. As the available input toque of the electric machines decreases with increasing speeds, the tooth modifications were designed to reach low tooth force levels at low to medium input torque. Hence, the Reference and NVH-Optimized gearing designs show the lowest tooth force levels at low to medium input torques. Again, the high meshing stiffness of the Low-Loss gearing affects the dynamic behaviour, as the gear stiffness fluctuation during the meshing is also more pronounced in comparison to the other two gearing designs.

Finally, the parameter K_V is an indicator for the dynamic tooth forces relative to the static forces of the meshing. The characteristics of K_V shows resonance oscillations at the peaks, occurring when the excitation frequency hits the natural frequency of the gearings. As expected, the NVH-Optimized variant shows reasonable vibration behaviour over the entire operating area with a slight peak ($K_V = 1.05$) at the 1^{st} harmonic of the mesh frequency at around $26500\ min^{-1}$.

The Reference Design shows larger amplitudes of up to $K_V = 1.17$, which occur at a pre-resonance at around $16500\ min^{-1}$. The amplitudes at the main resonance ($32500\ min^{-1}$) could be effectively lowered by tooth flank modifications.

As expected, the Low-Loss gearing design shows the highest amplitudes of the three variants. The 1^{st} harmonic of the mesh frequency appears with an amplitude of around $K_V = 1.44$ with additional pre-resonances. Those dynamic forces are expected to lead into significant noise excitations in case of the Low-Loss variant.

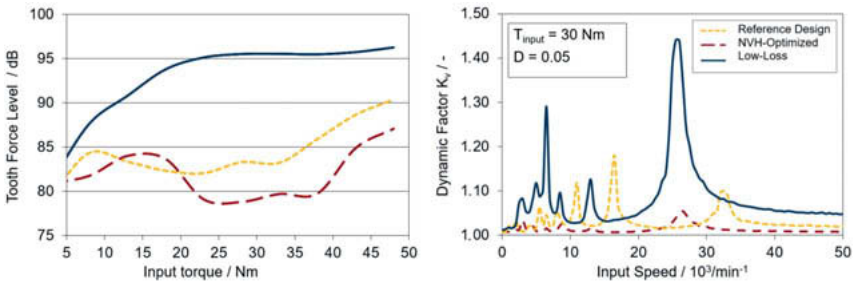


Fig. 13: Characteristics of the tooth force level and dynamic factor for nominal input torque of 30 Nm

https://doi.org/10.51202/9783181023549 - Generiert durch IP 216.73.216.36, am 19.01.2026, 02:19:31. © Urheberrechtlich geschützter Inhalt. Ohne gesonderte Erlaubnis ist jede urheberrechtliche Nutzung untersagt, insbesondere die Nutzung des Inhalts im Zusammenhang mit, für oder in KI-Systemen, KI-Modellen oder Generativen Sprachmodellen.

Conclusions from the simulation results

The simulations of efficiency reveal results as expected. With gear loss factors H_v of 0.06 and 0.016, the Low-Loss gear design shows the lowest load-dependent gear losses and results in the best overall efficiency. The better dynamic behavior of the NVH-Optimized gearing design causes a higher tooth loss factor and the lowest overall efficiency. The reference gearing design with its balanced properties lies in terms of efficiency in between the Low-Loss design and the NVH-Optimized design. As expected, the results of the NVH-simulations indicate the best vibration behavior for the NVH-Optimized design, whereas the Low-Loss design shows significant disadvantages in the resonance behavior and the characteristics of the tooth force level. Again, the well balanced Reference Design is positioned between the two other designs.

5. Summary and Outlook

Speed4E is a joint project between industrial partners and universities. Its main goal is to develop a hyper-high-speed drivetrain for electric vehicles. The developed 3-speed drivetrain improves efficiency and cost effectiveness of the BEV thanks to a highly integrated design, an intelligent control strategy - capable of determining the optimal power split ratio and transmission speed – and a holistic thermal management approach.

To investigate the impact of various gearing parameters, three different gearing designs for the planetary gearbox in sub-transmission 1 were developed. In particular, the efficiency and vibration behavior of the gearing designs will be examined in detail during the project.

So far, the calculations carried out show the expected tendencies. The efficiency simulations indicate a considerable reduction of the load-dependent gearing losses through the Low-Loss design. The dominating no-load gear losses at high revolutions need to be taken into account in further investigations. Analogously, the NVH-Optimized variant shows the best excitation behavior, especially at high speeds or in the range of the resonance frequencies. In the future, measurement on the Speed4E test rig will be used to validate the simulative predicted efficiency and NVH-behavior at revolutions up to 50,000 min^{-1}.

6. Acknowledgements

Speed4E is a project funded by the German Federal Ministry for Economic Affairs and Energy (BMWi) and supervised by the German Aerospace Center (DLR). Special thanks go to the Forschungsvereinigung Antriebstechnik e.V. (FVA) for accompanying the project. Finally, many thanks go to all project partners both from industry and universities for all the excellent collaboration and support.

https://doi.org/10.51202/9783181023549 - Generiert durch IP 216.73.216.36, am 19.01.2026, 02:19:31. © Urheberrechtlich geschützter Inhalt. Ohne gesonderte Erlaubnis ist jede urheberrechtliche Nutzung untersagt, insbesondere die Nutzung des Inhalts im Zusammenhang mit, für oder in KI-Systemen, KI-Modellen oder Generativen Sprachmodellen.

References

[Gri11] Griggel, T.; Heider, M.; Bihr J.: DZP, Version 5.0 und DZPopt, Version 2.0 (2011).

[Gwi14] Gwinner, P.; Otto, M.; Stahl, K.: Design of Low Excitation Gearings for Electric Vehicles. CTI - Car Training Institute (Hg.) 2014 – 13th international CTI Symposium (2014).

[Gwi16] Gwinner, P.; Otto, M.; Stahl, K.: Acoustical Behavior of High-Speed-Gearings for Electrified Automotive Powertrains. FISITA 2016 World Automotive Congress, Busan (2016).

[Gwi17] Gwinner, P.; Stahl, K.; Rupp, S.; Strube, A.: Innovatives Hochdrehzahl-Antriebsstrangkonzept für hocheffiziente elektrische Fahrzeuge. ATZ - Automobiltechnische Zeitschrift 119. Heft: 3, S. 72–75 (2017).

[Hei05] Heizenröther, M.: Das Stirnraddifferential mit Innenverzahnung im Vergleich zum Kegelraddifferential inklusive einer Sperrwertanalyse, Dissertation, Technische Universität München (2005).

[Hin14] Hinterstoißer, M.: Zur Optimierung des Wirkungsgrades von Stirnradgetrieben, Dissertationen, TU München (2014).

[Idl16] Idler, S.; Gwinner, P.; Stahl, K.; König, R.; Rinderknecht, S.: Innovative Super-High Multiple Speed Concept for the Electrified Automotive Powertrain. CoFAT - Conference on Future Automotive Technology, Fürstenfeld (2016).

[Ket02] Kettler; Jörg: FVA-Nr. 313 - Heft 639 Planetengetriebe-Sumpftemperatur - Abschlussbericht (2002).

[Kur16] Kurth, F.; Geiger, J.; Sedlmair, M.: Forschungsvorhaben Nr. 69 VI- FVA-EDV Programm WTplus. Forschungsvereinigung Antriebstechnik e.V., Frankfurt /Main (2016).

[Mil19] Mileti, M.; Schweigert, D.; Pflaum, H.; Stahl, K.: Speed4E: Hyper-High-Speed Driveline and Gearbox for BEVs. CTI Symposium USA, Novi (2019).

[Mil18] Mileti, M.; Strobl, P.; Pflaum, H.; Stahl, K.: Design of a hyper-high-speed Powertrain for EV to achieve maximum ranges. CTI Symposium Germany, Berlin (2018).

[Ohl58] Ohlendorf, H.: Verlustleistung und Erwärmung von Stirnrädern, Dissertation, Technische Hochschule München (1958).

[Sch18] Schweigert, D.; Gwinner, P.; Otto, M.; Stahl, K.: Noise and Efficiency Characteristics of High-Rev Transmissions in Electric Vehicles. E- Motive Expert Forum Electric Vehicle Drives Topic, Stuttgart (2018).

https://doi.org/10.51202/9783181023549 - Generiert durch IP 216.73.216.36, am 19.01.2026, 02:19:31. © Urheberrechtlich geschützter Inhalt. Ohne gesonderte Erlaubnis ist jede urheberrechtliche Nutzung untersagt, insbesondere die Nutzung des Inhalts im Zusammenhang mit, für oder in KI-Systemen, KI-Modellen oder Generativen Sprachmodellen.

[Wim06] Wimmer, A. J.: Lastverluste von Stirnradverzahnungen - Konstruktive Einflüsse, Wirkungsgradmaximierung, Trobologie, Dissertation, Technische Universität München (2006).

https://doi.org/10.51202/9783181023549 - Generiert durch IP 216.73.216.36, am 19.01.2026, 02:19:31. © Urheberrechtlich geschützter Inhalt. Ohne gesonderte Erlaubnis ist jede urheberrechtliche Nutzung untersagt, insbesondere die Nutzung des Inhalts im Zusammenhang mit, für oder in KI-Systemen, KI-Modellen oder Generativen Sprachmodellen.

GKN's ActiveConnect AWD system as an energy-efficient solution for electrified vehicles

Christoph Schmahl, **Michael Höck**, **Dirk Ressin**, **Mathias Kesseler**,
GKN ePowertrain, Lohmar

Zusammenfassung

Sowohl bei P1- bis P3-Hybridfahrzeugen mit Quermotor als auch bei batterieelektrischen Fahrzeugen erfolgt die Verallradung bisher in der Regel durch eine Elektrifizierung beider Achsen. Die dezentralisierte Erzeugung der Antriebsleistung durch ein solches „Dualmotor-Konzept" wirkt sich jedoch negativ auf die Fahrzeugeffizienz aus und ist darüber hinaus vergleichsweise kostenintensiv.

Als vielversprechende Alternative für elektrifizierte Fahrzeuge bietet sich das intelligente Allradantriebssystem mit „ActiveConnect" von GKN an, welches die Vorder- und Hinterachse mechanisch verbindet. Die implementierte ActiveConnect-Technologie ermöglicht durch bedarfsgerechtes Zuschalten des Allradsystems eine Reduzierung der Schleppmomente des Antriebstranges. Im Gegensatz zu den, bei elektrifizierten Fahrzeugen bisher üblichen, Dualmotor-Konzepten ermöglicht die mechanische Antriebsstrangarchitektur die gesamte Antriebsleistung durch eine einzige Antriebseinheit zur Verfügung zu stellen. In Kombination mit der ActiveConnect-Funktion ergibt sich hieraus eine Reihe erheblicher Vorteile hinsichtlich Fahrzeugeffizienz, Kosten, Fahrzeugmobilität und Fahrperformance sowie ein geringer Entwicklungs- und Integrationsaufwand bei Hybridfahrzeugen in Form von P1- bis P3.

Abstract

For P1 to P3 hybrid vehicles with east/west engine configurations as well as for battery electric vehicles, AWD is generally realized by electrification of both axles. However, the decentralised generation of drive power by such a "dual motor concept" has a negative effect on vehicle efficiency and is also comparatively cost-intensive.

A promising alternative for electrified vehicles is the intelligent all-wheel drive system with "ActiveConnect" from GKN, which mechanically connects the front and rear axles. The ActiveConnect technology enables the drag torque of the drivetrain to be reduced by engaging the all-wheel system only when required. In contrast to the common dual-motor concepts in electrified vehicles, the mechanical drivetrain architecture enables the entire drive power to be provided

https://doi.org/10.51202/9783181023549 - Generiert durch IP 216.73.216.36, am 19.01.2026, 02:19:31. © Urheberrechtlich geschützter Inhalt. Ohne gesonderte Erlaubnis ist jede urheberrechtliche Nutzung untersagt, insbesondere die Nutzung des Inhalts im Zusammenhang mit, für oder in KI-Systemen, KI-Modellen oder Generativen Sprachmodellen.

by a single drive unit. In combination with the ActiveConnect function, this results in a number of significant advantages in terms of vehicle efficiency, costs, vehicle mobility and performance as well as low development and integration effort for hybrid vehicles in the form of P1 to P3.

Introduction

All-wheel drive (AWD) vehicles are enjoying increasing popularity [1]. The reason for the rising number of sales are, amongst other things, the benefits regarding safety aspects and a higher degree of mobility and driving dynamics, which AWD vehicles offer relative to comparable front and rear-wheel drive vehicles.

As a consequence, more and more electrified vehicles are also being equipped with AWD systems [1]. For hybrid electric vehicles (HEV) with engines in east-west configuration as well as for battery electric vehicles (BEV), the AWD is generally realized by electrification of the secondary axle. However, the decentralized generation of drive power by motors on both axles is comparatively cost-intensive and has a negative impact on vehicle efficiency.

A promising alternative is GKN's mechanical AWD system with ActiveConnect. The mechanical drivetrain architecture allows use of a single source of propulsion power. In combination with the ActiveConnect function, which enables a decoupling of rotating AWD components when not required for traction purpose, the vehicle's efficiency is improved, costs are reduced and mobility and driving dynamics are considerably increased.

The following article illustrates the above-mentioned advantages of a mechanical AWD solution over an electrified secondary axle using the example of battery electric vehicles. Based on specific application scenarios, an analysis is carried out to determine the suitability of the mechanical system for both electric and hybridized vehicles.

GKN's ActiveConnect AWD technology

An analysis of the active use of a mechanical hang-on AWD system clearly shows that even on roads with low friction values (e.g. on snow), the operating period of an AWD system is only 25 % (see fig. 1 a). When driving on the motorway with a high friction value, the operating period of the AWD system can even fall below 1 %.

Based on these investigations, the ActiveConnect AWD technology was developed. The ActiveConnect system is shown in fig. 1 b). In contrast to a conventional all-wheel drivetrain, the ActiveConnect system offers the possibility of disconnecting the Power Take-off Unit (PTU) and the Rear Drive Unit (RDU) from the front and rear axle by optimally arranged clutches, which leads to a significant reduction in the drag torque of the driveline. A comparison of drag torques when the AWD system is active and disconnected is shown in fig. 1 c).

https://doi.org/10.51202/9783181023549 - Generiert durch IP 216.73.216.36, am 19.01.2026, 02:19:31. © Urheberrechtlich geschützter Inhalt. Ohne gesonderte Erlaubnis ist jede urheberrechtliche Nutzung untersagt, insbesondere die Nutzung des Inhalts im Zusammenhang mit, für oder in KI-Systemen, KI-Modellen oder Generativen Sprachmodellen.

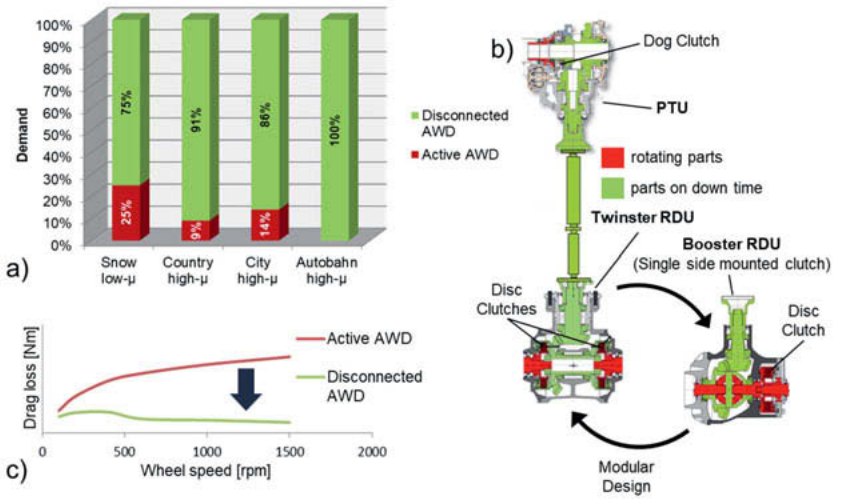


Fig. 1: Increased efficiency due to the modular GKN ActiveConnect system

Modularity was the key design task for the ActiveConnect system, as shown in fig. 1 b). The rear axle can be designed as a Booster RDU with a single side mounted clutch, which offers the performance benefits of a conventional AWD system. An optional Twinster RDU is available to further improve mobility and driving dynamics. The Twinster RDU enables active torque vectoring as well a cross-axle locking functionality by two separately controlled disc clutches. However, both RDU options offer the same high potential for energy savings. For more information, see [2] for a detailed comparison of the Booster and Twinster RDU.

The ActiveConnect technology was first brought into series production by GKN in 2014 and has already enabled significant fuel savings to be made in conventional vehicles with combustion engines. However, this AWD approach can also be applied to electrified vehicles. The use of a mechanical Disconnect-AWD system offers a whole range of benefits in terms of cost, energy efficiency, driving dynamics and integration effort relative to an electrified secondary axle. In the following sections, these advantages will be illustrated using exemplary BEVs.

Transfer of the mechanical ActiveConnect system to battery electric vehicles

Power, volume and efficiency of electrical machines develop according to certain laws - the so-called “growth laws”. One source frequently referred to in this context is [3]. Derived on the basis of the transformer, an increase in all the linear dimensions of an electric machine by

https://doi.org/10.51202/9783181023549 - Generiert durch IP 216.73.216.36, am 19.01.2026, 02:19:31. © Urheberrechtlich geschützter Inhalt. Ohne gesonderte Erlaubnis ist jede urheberrechtliche Nutzung untersagt, insbesondere die Nutzung des Inhalts im Zusammenhang mit, für oder in KI-Systemen, KI-Modellen oder Generativen Sprachmodellen.

factor k causes an increase in power by factor k^4, while power loss and volume only increase by the factor k^3. The exact growth proportions may vary, depending on the literature [4, 5]. However, it is apparent from all sources that the power of electrical machines increases more quickly than its volume and power loss. With increasing power, therefore, electric machines become more efficient, as illustrated in [6] with efficiency measurements on induction motors, and more cost-effective due to lower material costs per power. In addition, the assembly costs are almost scale-invariant and thus contributing to lower overall production costs in relation to the motor power.

For the following energy efficiency and cost analysis, three exemplary battery electric AWD vehicle architectures are considered (see fig. 2).

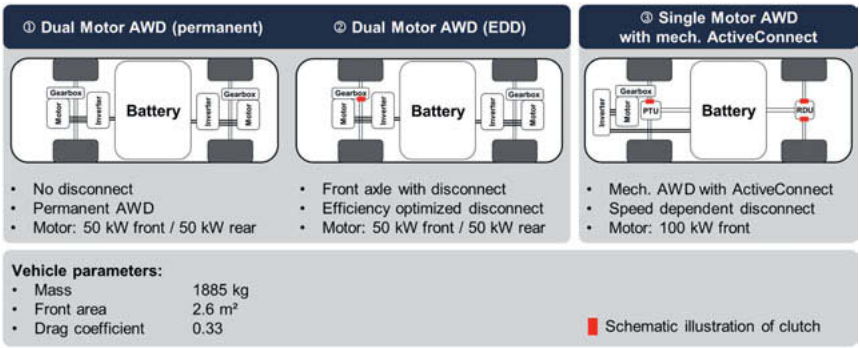


Fig. 2: Exemplary vehicle concepts, which were considered in the following study

The first vehicle is equipped with a dual motor system, which consists of two permanently driven motors ①. The second vehicle is additionally equipped with an Electronic Disconnect Differential (EDD) to disconnect the electric motor from the front axle ②. According to growth laws, the electrification of both axles and the corresponding distribution of drive power between two motors with comparatively low power have a negative effect on efficiency and costs. In addition, two inverters and two gearboxes are required for the power transfer.

A BEV with an ActiveConnect AWD system is compared with both introduced vehicle concepts ③. The disconnection of the AWD system limits power transmission to a single inverter, motor and gearbox. In addition to the reduced number of active drivetrain components, the drive power is provided by a single, powerful motor, which makes optimum use of the growth laws.

https://doi.org/10.51202/9783181023549 - Generiert durch IP 216.73.216.36, am 19.01.2026, 02:19:31. © Urheberrechtlich geschützter Inhalt. Ohne gesonderte Erlaubnis ist jede urheberrechtliche Nutzung untersagt, insbesondere die Nutzung des Inhalts im Zusammenhang mit, für oder in KI-Systemen, KI-Modellen oder Generativen Sprachmodellen.

For the dual motor concepts, the drive power is generated by two 50 kW motors. The EDD system is controlled by an online optimization strategy, which connects the front machine only in driving conditions where an efficiency advantage is achieved. The vehicle with the Active-Connect AWD system is equipped with a single 100 kW motor. In total, all three vehicle concepts have an equal drive power.

The control concept of the ActiveConnect function considers several parameters, but for use in a legislative driving cycle without cornering and without high accelerations, the vehicle speed remains as the dominant factor. Therefore, a simplified control strategy related to the vehicle speed was used. It is assumed that the vehicle uses the AWD system at low speeds to optimize traction and that the AWD function is deactivated for efficiency reasons above a defined threshold.

As can be seen in [6], the efficiency of the motors is subject to a certain variation due to different design parameters. In order to consider the impact of this variation, the simulation was based on multiple permanent magnet motors (PMSM), resulting in a possible range of energy consumption. Fig. 3 shows the energy consumption based on the WLTC (Worldwide harmonized Light Duty Test Cycle) for both vehicles with dual motor AWD and the vehicle with a single motor and the mechanical ActiveConnect AWD with regard to the disconnection threshold.

With low disconnection thresholds, mean energy savings of 9 % are obtained for the vehicle concept with the ActiveConnect AWD compared to the dual-motor system with permanent AWD. As the threshold speed increases, the efficiency advantage is reduced due to the drag torques of the mechanical drivetrain. In practice, however, disconnection thresholds have been established below 40 km/h. Compared with the vehicle with the dual motor concept and EDD system, a mean energy consumption benefit of 6 % can be obtained. The consumption-optimized interaction of the front and rear motor cannot compensate the efficiency advantage of the more efficient high-powered motor of the vehicle with the ActiveConnect system.

https://doi.org/10.51202/9783181023549 - Generiert durch IP 216.73.216.36, am 19.01.2026, 02:19:31. © Urheberrechtlich geschützter Inhalt. Ohne gesonderte Erlaubnis ist jede urheberrechtliche Nutzung untersagt, insbesondere die Nutzung des Inhalts im Zusammenhang mit, für oder in KI-Systemen, KI-Modellen oder Generativen Sprachmodellen.

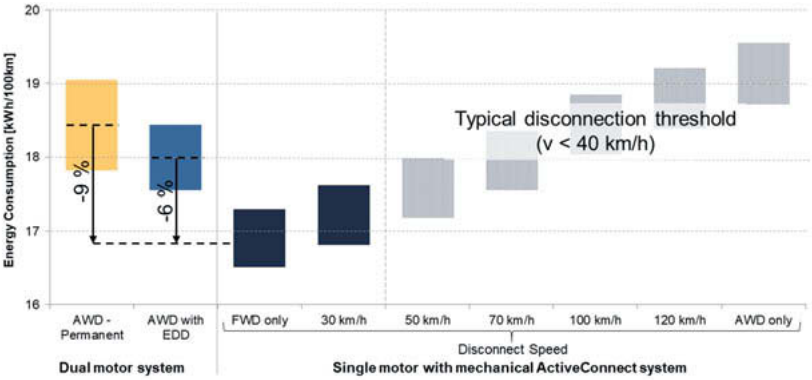


Fig. 3: Possible range of energy consumption for the three AWD concepts in the WLTC based on different PMSM and with regards to the disconnection threshold of the mechanical AWD system

By using a single motor, a cost benefit is achieved which is determined by the growth laws of electric machines and the reduced number of complex drivetrain components. Table 1 provides a cost estimate based on current market prices for the introduced AWD concepts, in which only the component costs of the electric motors, inverters, gears and the ActiveConnect AWD system are evaluated. The costs associated with wiring, cooling and a potential modification of the battery are not taken into account as these are very specific and difficult to assess for each application.

Table 1: Cost savings due to a mechanical ActiveConnect system relative to a dual motor system. Estimate on component basis

Dual Motor Concept (Reference)	**Cost reduction potential: Single Motor Concept with ActiveConnect-AWD**	
	Twinster RDU	**Booster RDU** (Single side mounted clutch)
Permanent AWD	4 %	9 %
AWD with EDD	8 %	13 %

The generation of the drive power by a single powerful machine and the subsequent distribution by a mechanical AWD system enables the full system torque to be applied to one axle. This offers a range of mobility advantages as illustrated in fig. 4.

https://doi.org/10.51202/9783181023549 - Generiert durch IP 216.73.216.36, am 19.01.2026, 02:19:31. © Urheberrechtlich geschützter Inhalt. Ohne gesonderte Erlaubnis ist jede urheberrechtliche Nutzung untersagt, insbesondere die Nutzung des Inhalts im Zusammenhang mit, für oder in KI-Systemen, KI-Modellen oder Generativen Sprachmodellen.

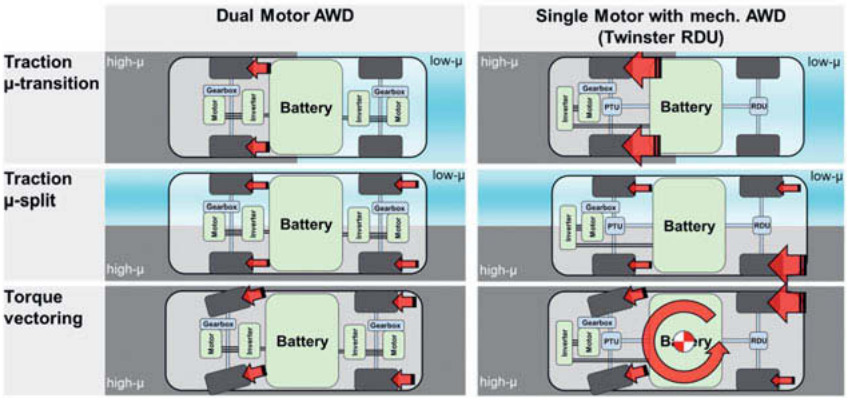


Fig. 4: Improved mobility through subsequent distribution of drive power by a mechanical AWD system, illustrated for common driving manoeuvres

With equivalent system power, this results a mobility disadvantage in terms of off-road capabilities and traction for dual-motor vehicles. If the ActiveConnect system is enhanced with a Twinster RDU, it is possible to improve driving dynamics considerably by means of torque vectoring and a cross-axle locking functionality.

Application scenarios for electrified vehicles

Based on findings from the previous section, the suitability of the mechanical Active-Connect system will be discussed for particular vehicle concepts. Fig. 5 gives an overview of possible vehicle concepts for which a mechanical AWD system is suitable.

The ActiveConnect system can be used as a hang-on solution to provide optional AWD for primarily front-wheel drive vehicles with east-west engine configuration. For AWD vehicles in HEV configuration with DHT (Dedicated Hybrid Transmission) or BEV vehicles, cost-effective and compact integration of the PTU directly into the gearbox is an option.

Fig. 5 shows a schematic representation of the battery. At first glance this appears to be in direct conflict with the propshaft. However, with a flat battery design the propshaft could be placed above the battery. If this is not possible, the modular battery design offers the option of designing a recess in the bottom part of the battery. This type of "bridge solution" is already being used today in series production of vehicles with standard drivelines.

https://doi.org/10.51202/9783181023549 - Generiert durch IP 216.73.216.36, am 19.01.2026, 02:19:31. © Urheberrechtlich geschützter Inhalt. Ohne gesonderte Erlaubnis ist jede urheberrechtliche Nutzung untersagt, insbesondere die Nutzung des Inhalts im Zusammenhang mit, für oder in KI-Systemen, KI-Modellen oder Generativen Sprachmodellen.

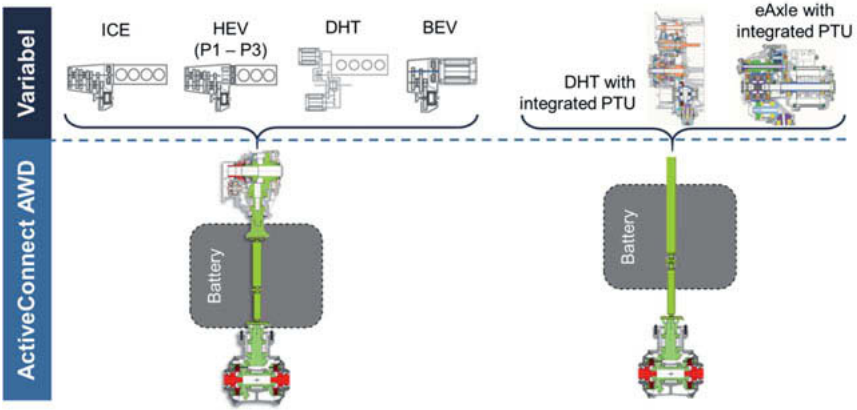


Fig. 5: GKN ActiveConnect-AWD for various different vehicle concepts

For BEVs, a mechanical ActiveConnect system is suitable for vehicles in the medium and low-price segment or in the commercial vehicle sector, as the cost savings are particularly relevant here. In lower price segments, the batteries tend to be smaller, which simplifies the integration of a propshaft. The negative effects of the propshaft on the interior design are also considered less critical. The trend for vehicles in the lower price segment is to have lower drive power. According to the growth laws, the efficiency of electric machines is approaching a maximum value in the range of high power. In order to make optimum use of the efficiency advantage of a single machine, it is recommended to apply the ActiveConnect system to electrified vehicles with low drive power.

The development of multi-speed transmissions for BEVs is currently being considered for certain applications [6]. This poses a challenge for dual motor systems. Either both axles have to be equipped with a multi-speed transmission, which leads to high costs, or a compromise has to be found for the secondary axle at the expense of driving dynamics and efficiency. A mechanical AWD system, on the other hand, only requires a single multi-speed transmission without a compromise for the secondary axle. For multi-speed transmissions a mechanical system should be considered in future concept developments.

Many of the findings from the field of BEVs can also be transferred to HEVs. In the following, the suitability of a mechanical ActiveConnect system for HEVs will be analysed using three scenarios as examples.

https://doi.org/10.51202/9783181023549 - Generiert durch IP 216.73.216.36, am 19.01.2026, 02:19:31. © Urheberrechtlich geschützter Inhalt. Ohne gesonderte Erlaubnis ist jede urheberrechtliche Nutzung untersagt, insbesondere die Nutzung des Inhalts im Zusammenhang mit, für oder in KI-Systemen, KI-Modellen oder Generativen Sprachmodellen.

Scenario 1: OEM with low AWD market share (AWD < 20 %)

OEMs with a high percentage of vehicles with front-wheel drive focus primarily on a hybridisation of the front axle in order to achieve a high reduction in fleet consumption. Hybridisation takes place in the form of P1 to P3 configurations or through DHT concepts, in accordance with fig. 5.

The implementation of AWD again raises the question of the use of an electrical secondary axle or a mechanical ActiveConnect system. The same considerations apply as previously for BEVs. The mechanical approach is beneficial in terms of cost, efficiency, mobility and driving performance, whereas a dual-motor system simplifies the battery design and the design of the passenger cabin.

Scenario 2: OEM with high AWD market share (AWD > 80 %)

Due to the high market share of AWD vehicles, the hybridization can be realized with an electrified secondary axle (P4 axle) to successfully affect the fleet consumption.

Scenario 3: OEM with average AWD market share (e.g. AWD ≈ 40 %)

A suitable solution is more complicated here. The OEM can decide in favor of a P4 concept to implement AWD if the reduction in fleet consumption is sufficient. However, if these savings are too low, additional hybrid systems are required for the front-wheel-drive vehicles, which would lead to an increase in development expenditure. Instead of using a P4 axle, hybridization of the front axle can be considered with the option of a mechanical hang-on AWD system. This allows both, the front-drive and AWD vehicles, to be hybridized and the fleet consumption to be influenced more effectively.

Table 2 shows a transparent comparison of a mechanical solution and a P4 axle. The advantages and disadvantages should be considered when selecting the concept.

https://doi.org/10.51202/9783181023549 - Generiert durch IP 216.73.216.36, am 19.01.2026, 02:19:31. © Urheberrechtlich geschützter Inhalt. Ohne gesonderte Erlaubnis ist jede urheberrechtliche Nutzung untersagt, insbesondere die Nutzung des Inhalts im Zusammenhang mit, für oder in KI-Systemen, KI-Modellen oder Generativen Sprachmodellen.

Table 2: Comparison of hybridization using a P4 axle or a P1 - P3/DHT solution with a mechanical AWD system.

Requirement	P4 Axle	P0 – P3/DHT with mechanical ActiveConnect-AWD
AWD up to v_{max}	Generally limited to low speed	Yes
Full electric AWD driving	No	Yes
Max. torque per axle / Off-road traction capability	Limited by axle torque	Full system torque available on both axles
Recuperation	Only P4-Axle	Both axles
Integration effort	High	Medium
Fleet consumption	Impact only on AWD vehicles	Hybridization also covers front-wheel drive
Impact on passenger compartment design	No	Yes

Summary

This article discusses the application of mechanical AWD systems in electrified vehicles as an alternative to an electrified secondary axle.

An analysis of vehicle efficiency and system costs was carried out using the example of battery electric vehicles equipped with dual motor systems and mechanical AWD systems. The ActiveConnect function enables the mechanical AWD system to be disconnected when not in use for traction purposes, reducing the number of components involved in energy transfer. The mechanical distribution of torque to both axles enables the generation the drive power with a single motor. Based on the so-called “growth laws” for electric machines, additional efficiency and cost benefits occur as a result. Simulations show that, in comparison with comparable dual motor concepts, possible energy savings of around 9 % and cost savings of up to 13 % can be expected.

The axle torque of a dual motor AWD is limited to the torque of the respective motor. A mechanical AWD system, on the other hand, enables to transfer the full system torque to each axle. This provides substantial mobility benefits, particularly on poor road surfaces and off-road. The modular ActiveConnect system also offers the option of a cross-axle locking and torque-vectoring functionality, which significantly increases driving dynamics, particularly for heavy vehicles.

The suitability of a mechanical AWD system is strongly dependent on the respective application scenario. For battery electric vehicles, application is recommended in the lower price segment or for electric commercial vehicles with low to medium drive power. For hybrid vehicles,

https://doi.org/10.51202/9783181023549 - Generiert durch IP 216.73.216.36, am 19.01.2026, 02:19:31. © Urheberrechtlich geschützter Inhalt. Ohne gesonderte Erlaubnis ist jede urheberrechtliche Nutzung untersagt, insbesondere die Nutzung des Inhalts im Zusammenhang mit, für oder in KI-Systemen, KI-Modellen oder Generativen Sprachmodellen.

there are significant advantages in a mechanical AWD solution for OEMs with high to medium quantities of front-wheel drive vehicles.
The underlying investigation shows that for electrified vehicles, a mechanical AWD system is an attractive alternative to an electrified secondary axle, which should be taken into account when designing new vehicles.

References

[1] GKN Internal Analysis, 2018
[2] Höck, M.: “Efficient Driveline Differentiation by a Modular Axle Concept”. ATZ worldwide, Issue 9/2015
[3] Spring, E.: Elektrische Maschinen: “Eine Einführung”. Springer Berlin Heidelberg, 2009
[4] Reichert, K.: “Elektrische Antriebe energie-optimal auslegen und betrieben” RAVEL Impulse Programme. Federal Office for Business Activities, 1993
[5] Basler, A.: “Eine modulare Funktionsarchitektur zur Umsetzung einer gesamtheitlichen Betriebsstrategie für Elektrofahrzeuge”. KIT Scientific Publishing, 2015
[6] Pyrhönen, J.: “Design of Rotating Electrical Machines”. Wiley, 2008
[7] Güth, D. et al.: „Seamless-Shift Two-Speed eAxle with Torque Vectoring”. Dritev – Drivetrain for Vehicles. VDI-Berichte 2328, 2018

https://doi.org/10.51202/9783181023549 - Generiert durch IP 216.73.216.36, am 19.01.2026, 02:19:31. © Urheberrechtlich geschützter Inhalt. Ohne gesonderte Erlaubnis ist jede urheberrechtliche Nutzung untersagt, insbesondere die Nutzung des Inhalts im Zusammenhang mit, für oder in KI-Systemen, KI-Modellen oder Generativen Sprachmodellen.

https://doi.org/10.51202/9783181023549 - Generiert durch IP 216.73.216.36, am 19.01.2026, 02:19:31. © Urheberrechtlich geschützter Inhalt. Ohne gesonderte Erlaubnis ist jede urheberrechtliche Nutzung untersagt, insbesondere die Nutzung des Inhalts im Zusammenhang mit, für oder in KI-Systemen, KI-Modellen oder Generativen Sprachmodellen.

Schaeffler eAxle family – future solutions for the electric drivetrain

Dipl.-Wirtsch.-Ing. **Andreas Kinigadner**,
Dipl.-Ing. (FH) **Thorsten Biermann**,
Schaeffler Technologies AG & Co. KG, Herzogenaurach

Zusammenfassung

Mittlerweile ist zu erwarten, dass elektrifizierte Fahrzeuge im Lauf des nächsten Jahrzehnts hohe Stückzahlen erreichen und damit zum Mittel der Wahl wird, was die Reduzierung des CO2-Ausstoßes betrifft. Zudem ist zu erwarten, dass der mechatronische Integrationsgrad deutlich steigt. Die Entwicklung elektrischer Achssysteme geht weit über den Elektromotor und das Getriebe hinaus. Ein Optimum an Effizienz, Reichweite und Systemkosten ist nur durch das Zusammenspiel von Motor, Leitungselektronik, Sensorik, mechanischer Integration sowie der Ansteuerstrategie zu erreichen und verlangt daher einen systemorientierten Ansatz. Gemeinsam ist allen zukünftigen Aggregate-Konzepten, dass sie einen hohen Integrationsgrad von Mechanik und Elektrik/Elektronik aufweisen, dabei werden sehr unterschiedliche Topologien für den Antriebsstrang realisiert.

Um einerseits eine große Vielzahl an Fahrzeugen und Antriebskonzepten unterstützen zu können, andererseits aber den Entwicklungsaufwand zu begrenzen, ist ein modularer Technologieansatz für elektrische Achssysteme zielführend. Entstanden ist eine Familie elektrischer Antriebsachsen, die eine optimale Lösung für die unterschiedlichsten Kundenanwendungen und Plattformen bietet. So eignet sich der Antriebsbaukasten nicht nur für den Einsatz in rein elektrisch angetriebenen Fahrzeugen, sondern auch für Hybrid-Anwendungen. Um das Leistungsspektrum von Voll- und Plug-In-Hybridfahrzeugen abzudecken, stehen schaltbare zweigängige sowie eingängig abkoppelbare Lösungen zur Verfügung. Für rein elektrisch angetriebene Fahrzeuge bietet der Baukasten sowohl eingängige als auch mehrgängige lastschaltfähige Achsen, die durch eine intelligente Wahl der Übersetzung und der Gestaltung des Antriebssystems eine optimale Leistungsdichte bezogen auf das geforderte Anfahrmoment und die Endgeschwindigkeit bereitstellen. Durch die wahlweise Gestaltung des Antriebsstranges in koaxialer oder auch achsparalleler Anordnung ist es ferner möglich, unterschiedlichste Plattformen vom reinen Sportwagen mit hohen Ansprüchen an die Leistungsdichte als auch SUVs zu bedienen. Zusätzlich ist es möglich, jede Antriebsachse unabhängig von der Anordnung des Antriebstranges oder der Leistungsklasse mit zusätzlichen

https://doi.org/10.51202/9783181023549 - Generiert durch IP 216.73.216.36, am 19.01.2026, 02:19:31. © Urheberrechtlich geschützter Inhalt. Ohne gesonderte Erlaubnis ist jede urheberrechtliche Nutzung untersagt, insbesondere die Nutzung des Inhalts im Zusammenhang mit, für oder in KI-Systemen, KI-Modellen oder Generativen Sprachmodellen.

Funktionsmodulen auszustatten. Die Mehrfachverwendung der mechanischen und elektrischen Subsysteme in unterschiedlichen Antriebssträngen hilft, sowohl die Entwicklungszeiten als auch die damit verbundenen Kosten deutlich zu reduzieren. Dies liegt im Interesse von Zulieferer als auch des OEMs, übergreifende Standards und auch Lösungen zu generieren, die über die einzelnen Plattformen hinaus Synergien aufweisen.

Abstract

Electrified cars are expected to reach high quantities during the current decade and become the solution of choice for reducing CO_2 emissions. It is also expected that the level of integration for mechatronic systems will also increase. The development of electric axle systems goes beyond the electric machine and the transmission. Reaching an optimum in terms of efficiency, range and system costs can only be achieved through the interaction of the electric machine, power electronics, sensor technology, mechanical integration, and system control strategy and thus requires a system-oriented approach. Future system concepts have a high degree of mechanical, electrical, and electronic integration in common, enabling a large number of powertrain configurations to be produced. In order to support a large number of vehicles and drive concepts on the one hand and yet minimize the development outlay on the other, Schaeffler has developed a modular technology approach for electric axle systems. The result is a family of electric axles that offers an optimum solution for different customer applications and platforms. A modular system approach is not only suitable for purely electric vehicles, but also for hybrid applications. The portfolio includes shiftable two-speed transmissions as well as single-speed solutions with decoupling functionality to cover the performance range of full and plug-in hybrid vehicles. For battery electric vehicles, the modular system offers both single-speed and multi-speed applications without torque interruption during shifting. By choosing the right gear ratios in combination with intelligent design of the electric drive system, an optimum power density can be achieved regarding the requirements for launch torque and vehicle top speed. The flexibility in system configurations with coaxial or parallel axis transmission design allows a range of vehicle applications from sports cars with high power density requirements to SUVs. In addition, each axle configuration can be equipped with a torque vectoring module, irrespective of the powertrain arrangement or performance class. The multiple use of the mechanical and electrical subsystems in different powertrains helps to reduce both the development time and the associated costs. It is in the interest of the supplier and the OEM to generate comprehensive standards and solutions, which lead to synergies across the individual platform.

https://doi.org/10.51202/9783181023549 - Generiert durch IP 216.73.216.36, am 19.01.2026, 02:19:31. © Urheberrechtlich geschützter Inhalt. Ohne gesonderte Erlaubnis ist jede urheberrechtliche Nutzung untersagt, insbesondere die Nutzung des Inhalts im Zusammenhang mit, für oder in KI-Systemen, KI-Modellen oder Generativen Sprachmodellen.

Introduction

The electrification of vehicles is mainly necessitated by CO_2 legislation. Electric axles can be enablers in achieving emission targets and new e-axle concepts have been derived and developed up to volume production during the last few years. With the limited resources for development and a varied range of customer preferences, a smart, flexible and multifunctional electric axle portfolio would seem to be desirable. The percentage of purely electric vehicles is expected to increase and interest and demand will drive the development of efficient, functional and affordable solutions. An ideal situation with regard to driving performance and consumption can only be achieved if the transmission functionality, electric motor, and power electronics specifications are all perfectly matched. [1] At the same time, the requirements for the package, weight, and comfort have to be considered. Therefore, the joint development of the disciplines electric motor, power electronics, and transmission has to be seen as a base discipline, which can be expanded by adding actuators e.g. for parking lock or gearshift functionalities. This is a challenge for a supplier who must comply with the development goals with regard to function, cost, and time despite the high level of complexity and associated outlay.

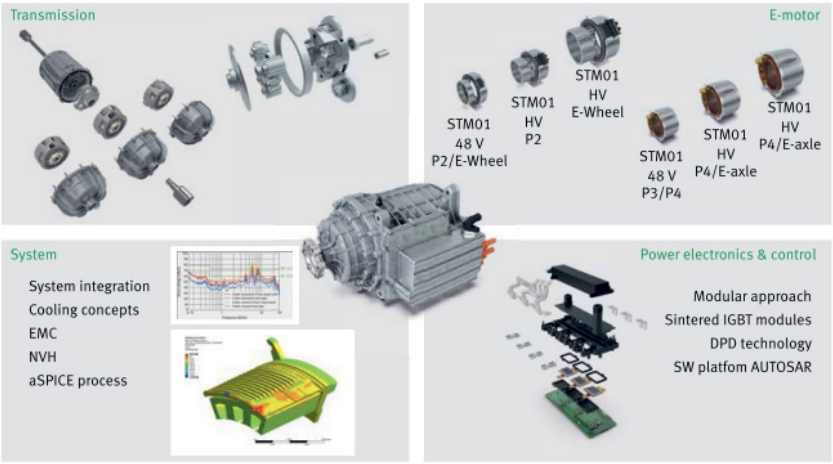


Fig. 1: Development parameters for an electric axle drive

In addition to the scope of the electric axle, this system expertise needs to be available in the interfaces to the internal combustion engine or fuel cell in case of hybridization and in the superordinate interfaces to the vehicle control units. The interactions of the mechanical, elec-

https://doi.org/10.51202/9783181023549 - Generiert durch IP 216.73.216.36, am 19.01.2026, 02:19:31. © Urheberrechtlich geschützter Inhalt. Ohne gesonderte Erlaubnis ist jede urheberrechtliche Nutzung untersagt, insbesondere die Nutzung des Inhalts im Zusammenhang mit, für oder in KI-Systemen, KI-Modellen oder Generativen Sprachmodellen.

trical, information-technology-related, and thermally interconnected subsystems are therefore taken into consideration. The prerequisite for this analysis is expertise in incorporating and continuously optimizing simulation tools and test results from test rigs or vehicle tests along the entire development chain, see Fig. 1.

Parameters of a modular product approach

A modular technology approach is desirable to cover a large number of vehicles with electrified powertrains. An ideal situation with regard to driving performance and consumption can only be achieved if the gear ratios, electric motor, and power electronics are all perfectly matched. [2] At the same time, the requirements for installation space, weight, and comfort need to be met. Therefore, different system layers (see Fig. 2) not only containing mechanical and electrical components or subsystems but also software, are needed for the proper function of the powertrain.

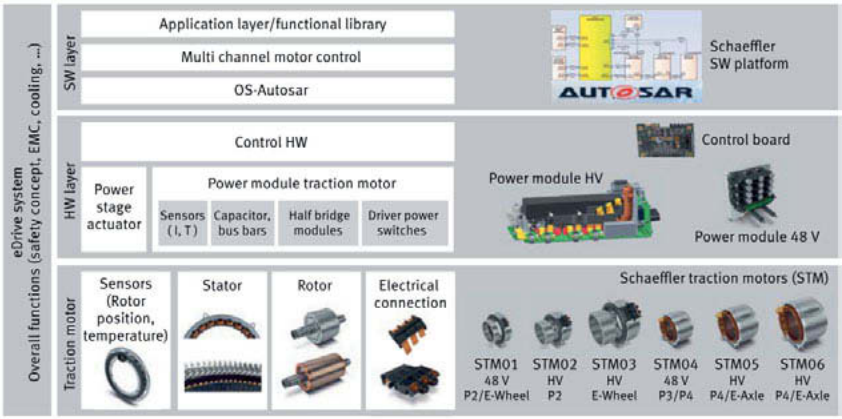


Fig. 2: Modular technology platform for electric drive systems

The mechanical components comprise the different transmission designs including an electric machine which can be implemented with a scalable output. Both permanently-excited and asynchronous machines can be implemented depending on the power density and further requirements. The hardware includes all the key components of the power electronics, such as switches, sensors, and capacitors. In order to ensure the thermal robustness of the power electronics, heat sinks and coolant integration have to be taken into consideration in the design. In addition, the hardware includes a control board which operates the functions of the electric machine, power electronics, and specific functions at vehicle level. The software

https://doi.org/10.51202/9783181023549 - Generiert durch IP 216.73.216.36, am 19.01.2026, 02:19:31. © Urheberrechtlich geschützter Inhalt. Ohne gesonderte Erlaubnis ist jede urheberrechtliche Nutzung untersagt, insbesondere die Nutzung des Inhalts im Zusammenhang mit, für oder in KI-Systemen, KI-Modellen oder Generativen Sprachmodellen.

has also been developed according to a function-oriented approach and includes a functional library which also defines hardware requirements.

Electric machine

For electric axle applications with full driving capabilities, we will take a look at high-voltage electric machines here. In addition to the different types of asynchronous and permanently-excited machines, a high range of power outputs must be implemented due to the different vehicle requirements.

Continuous model building and simulation are necessary to dimension the most suitable electric machine in all development stages. [2] The application defines the electric machine design through parameters such as minimum voltage, maximum current, installation space, and cooling capabilities. In addition to the main function of producing the defined speed-torque behavior, the cooling capacity and copper filling ratio also have to be taken into consideration in order to ensure long-lasting continuous performance. For reasons of cost and weight, the reduction of material by means of a clever design is an additional option, as long as this is possible without impairing the function. For the best NVH behavior on a system level, we must also take a look at the occurring forces as well as cogging and ripple torques. For reasons of efficiency, reduced harmonics, which induce eddy-current-driving voltages and thereby result in losses due to heating of the stator and rotor, are relevant. These partially conflicting effects must be considered and balanced in order to optimally meet all the requirements. The electric machine design must be oriented towards the requirements of the application and the expected load cycle.

Distributed winding has proven to be advantageous for a high torque density along with low harmonics and good heat flow from the current-carrying winding into the stator's laminated core. Hairpin or I pin technology is suitable for the production of such windings. Further improvements of hairpin design mainly focus on reducing the height of the winding heads and increasing the efficiency. Distributed wave winding is a beneficial alternative to hairpin technology. Wave winding is produced in a kind of braiding process and then inserted into the stator slots. Compared to a hairpin winding it is easier to implement designs with high number of slots and conductors because the welding process is eliminated. This helps to reduce eddy current losses, increase the cooling surface area of the slots and most of all reduce the height of the winding heads. This type of electric machine achieves an efficiency of 94 % in WLTP operation. [2] A stator design with a distributed winding is very flexible and can be used for permanently-excited synchronous motors, asynchronous motors, or even separately

https://doi.org/10.51202/9783181023549 - Generiert durch IP 216.73.216.36, am 19.01.2026, 02:19:31. © Urheberrechtlich geschützter Inhalt. Ohne gesonderte Erlaubnis ist jede urheberrechtliche Nutzung untersagt, insbesondere die Nutzung des Inhalts im Zusammenhang mit, für oder in KI-Systemen, KI-Modellen oder Generativen Sprachmodellen.

excited synchronous motors. The electric machine suitable for electric axle applications have a ratio of stator diameter to active length that is below 1.8, see Fig. 3.



Technology cluster	
Ratio diameter / active length	<1.8
Platform power range	60 kW – 300 kW
Motor technology	w/ or w/o magnet depends on customer requirements
PE 48 V	modules for integration (control, driver stage, power stage 48 V, sensors, software)
PE High-Voltage	modules for integration (control, driver stage, power stage 400 V – 800 V, sensors, software)

Fig. 3: Modularity of the electric machine

Power electronics (PE)

As in the case of the electric machine, specific requirements also influence the functional design of power electronics. The most relevant parameters are robustness (temperature and vibration), power density and flexible design due to package limitations, loss optimization, torque accuracy, functional safety, and the utilization of various voltage levels regarding specific battery configurations. [2] The PE contain a control module and a power module.

As the name suggests, the control board contains the actual intelligence of the PE and an optional actuator power stage here. It is ideally suited for use in an electric axle application, even in combination with e.g. a parking lock or gearshift unit. A wide range of applications require a power module that must be designed with scalable semiconductors. More than 3 phases can be realized by using IGBT (Insulated-Gate Bipolar Transistors) half-bridge modules, which are silicon semiconductors. In addition, the capacitor and bus bars are current carrying parts. Identical cooling interfaces and contacting are always used for the purposes of standardization. Since robustness requirements are high, soldering connections and aluminium bond wires are avoided in critical areas of the board. Sinter technology increases the

https://doi.org/10.51202/9783181023549 - Generiert durch IP 216.73.216.36, am 19.01.2026, 02:19:31. © Urheberrechtlich geschützter Inhalt. Ohne gesonderte Erlaubnis ist jede urheberrechtliche Nutzung untersagt, insbesondere die Nutzung des Inhalts im Zusammenhang mit, für oder in KI-Systemen, KI-Modellen oder Generativen Sprachmodellen.

cycle stability of the IGBT module by several times compared to conventional technology. The modularity of the power modules can be seen in Fig. 4.

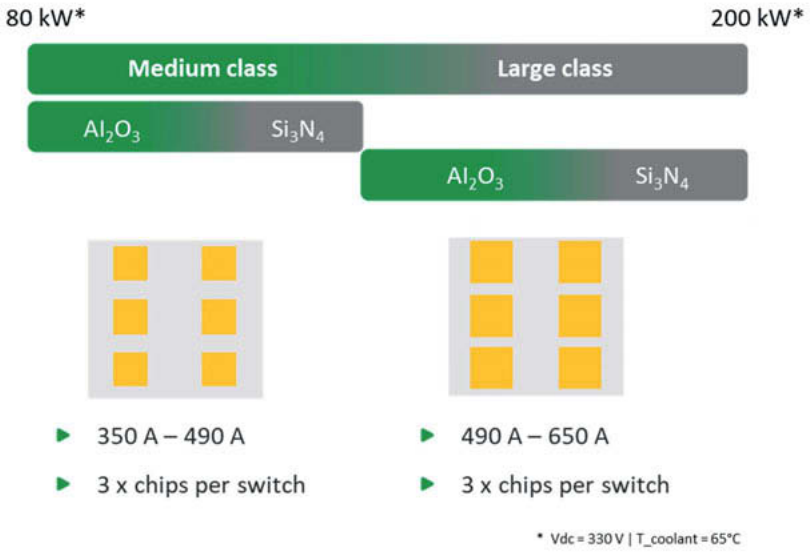


Fig. 4: Modularity of the power electronics

The carrier frame is the physical connector between the power and control module as well as the functional conductor of the coolant for the current carrying components and the heat sink. Thermal robustness is achieved by CFD simulations and by taking the relevant heat flows into consideration.

Thanks to the flexibility of the installation space and the modular approach, it is easy to respond to different requirements. It has been demonstrated that the basic concept selected for the power electronics has the necessary flexibility to meet different electric axles requirements. In addition to the hardware scope, the software is an important area which is represented by a functional software library with all the relevant software modules. The library contains functions such as signal analysis, motor and current control, monitoring functions for safety issues, e.g. for power derating caused by thermal effects, and superordinate control for functional integration into the powertrain. In addition, all the required hardware circuits and their definition are included. The software layout can be specifically adjusted to match

https://doi.org/10.51202/9783181023549 - Generiert durch IP 216.73.216.36, am 19.01.2026, 02:19:31. © Urheberrechtlich geschützter Inhalt. Ohne gesonderte Erlaubnis ist jede urheberrechtliche Nutzung untersagt, insbesondere die Nutzung des Inhalts im Zusammenhang mit, für oder in KI-Systemen, KI-Modellen oder Generativen Sprachmodellen.

special customer requirements and the architecture follows AUTOSAR paradigms to allow a high level of reutilization.

Transmission

Over the last few years, different single and two-speed transmissions have entered the market in BEV and HEV applications. Basically, these transmissions enable a target axle torque to be achieved which satisfies the customer during all relevant driving manoeuvres. In addition, a specific focus must be placed on the weight, package, robustness, and NVH in order to meet customer expectations. [3] Two package options are relevant when designing the transmission for single-speed layouts. Parallel and coaxial designs are distinguished according to the use of the differential. Parallel designs are realized by equipping the differential with a final drive gear. Alternatively, the Schaeffler lightweight differential allows compact coaxial designs where no final drive gearing exists and the differential drives the housing directly. During upstream powerflow, gear wheels or planetary gear sets mesh with the differential in the case of parallel designs or are directly connected with the differential in coaxial designs. Designing the transmission to be short in an axial direction provides the option of installing more electric power or enables the transmission to be fitted in an even wider range of vehicle packages. Therefore, the coaxial design uses the lightweight or spur gear differential due to its approximately 30 % shorter design length compared to a bevel gear differential with the same torque capacity. [4] In this way, the side shafts are provided with as much space as possible and their maximum angle of deflection is not exceeded. This design of the spur gear differential thus allows simultaneous use of the differential housing as the planet gear carrier for the transmission ratio gearing. The gearing of the differential is thus located in a housing with a planetary gear unit. The use of a so-called stepped planetary gear set offers another solution. In a stepped planetary gear unit, the planet is provided with an increment and has two levels of gearing, see Fig. 5.

The use of a stepped planetary gear set allows ratios of more than 10 which would otherwise only be possible with two linked planetary gear units. The torque at the differential cage in this design is increased by the factor (i0 - 1) as a function of the stationary gear ratio of the epicyclic gearing i0. A second glance however reveals a further benefit which is not feasible with an unstepped planetary gear set. While the gearing for the differential is arranged axially adjacent to the planetary gear stage on conventional planetary gear units, using the stepped planetary gear set allows the spur gear on the differential to be shifted into the space occupied by the planetary gear set. This produces a highly integrated and extremely short transmission concept. The sun gear only partially protrudes into the planetary gear set space and

https://doi.org/10.51202/9783181023549 - Generiert durch IP 216.73.216.36, am 19.01.2026, 02:19:31. © Urheberrechtlich geschützter Inhalt. Ohne gesonderte Erlaubnis ist jede urheberrechtliche Nutzung untersagt, insbesondere die Nutzung des Inhalts im Zusammenhang mit, für oder in KI-Systemen, KI-Modellen oder Generativen Sprachmodellen.

only meshes with the large planet gear. With this design, an overlapping configuration can be realized which produces 4,000 Nm of axle torque from 150 mm of axial length.

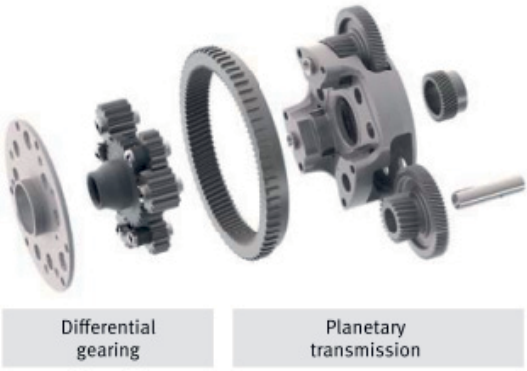


Fig. 5: Stepped planetary gear set for electric axle applications

Fig. 6 shows the modular transmission approach for coaxial designs where overall ratios between 11 and up to 19 can be achieved by using only the stepped planetary gear set for the longer ratios. Transmission modifications consisting of an additional upstream planetary

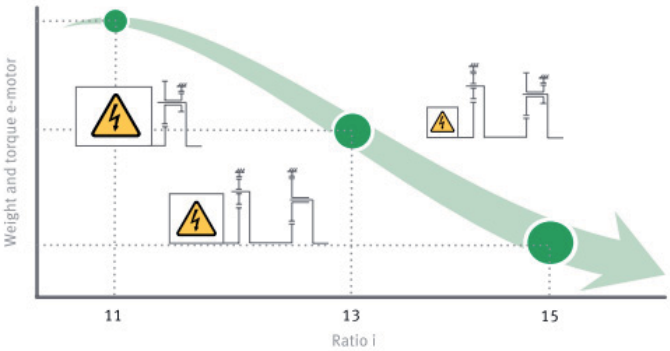


Fig. 6: Coaxial concepts for scalable ratios

set with a single or stepped planetary set are required for higher ratios. The modularity can be determined by comparing the short and long gear ratio application with the required ad-

https://doi.org/10.51202/9783181023549 - Generiert durch IP 216.73.216.36, am 19.01.2026, 02:19:31. © Urheberrechtlich geschützter Inhalt. Ohne gesonderte Erlaubnis ist jede urheberrechtliche Nutzung untersagt, insbesondere die Nutzung des Inhalts im Zusammenhang mit, für oder in KI-Systemen, KI-Modellen oder Generativen Sprachmodellen.

justments. Since the same differential gearing is used for all the gear sets, the only differences are to be found in the running gearing in the second planetary gear stage, while the ring gears and the differential housing have an identical design.

The coaxial transmission kit generates synergies for offset designs where the same planetary gear sets are used but with additional final drive gearing. Thereby even higher gear ratios can be achieved as shown in Fig. 7. Some of the components, which have been developed for the coaxial application, can also be used in the parallel axis drives with only marginal changes to the design. An advantage of reusing the components is the existing depth of testing.

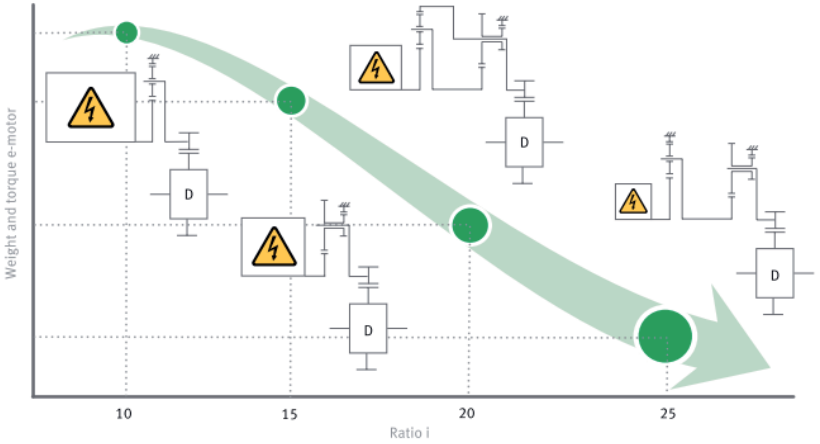


Fig. 7: Parallel axis concepts for scalable ratios

A current design for a single-speed application can be seen in Fig. 8. With a peak power of 147 kW and a peak torque of 268 Nm, this application has a transmission ratio of 15.14 and an axial length of 515 mm. A parking lock can be integrated and will be operated using an electro-mechanical actuation system. The electric machine is designed for active rotor cooling which enables the high power density of the complete system.

The modular product approach provides the option of functional enlargements for decoupling, multi-speeds, and torque vectoring. Decoupling and non-power shift 2-speed systems are capable in HEVs and PHEVs, where at a certain speed either the electric machine is disengaged from the wheel or the transmission shifts to a longer gear ratio for high speed driving. An example of an offset 2-speed electric axle can be seen in Fig. 9.

https://doi.org/10.51202/9783181023549 - Generiert durch IP 216.73.216.36, am 19.01.2026, 02:19:31. © Urheberrechtlich geschützter Inhalt. Ohne gesonderte Erlaubnis ist jede urheberrechtliche Nutzung untersagt, insbesondere die Nutzung des Inhalts im Zusammenhang mit, für oder in KI-Systemen, KI-Modellen oder Generativen Sprachmodellen.



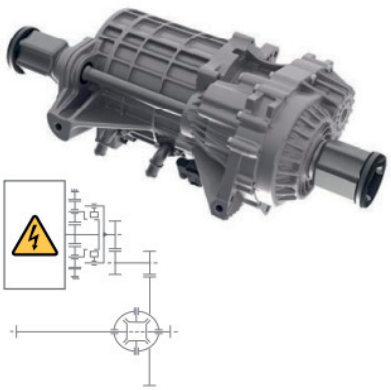
Fig. 8: Schaeffer coaxial design of the electric axle drive system

The first speed ratio covers speeds up to 120 km/h while the second gear is intended exclusively for longer distance travel at higher speeds. The combination of planet and spur gear drives produces a very compact design. The wheel distance of the rotor shaft from the differential output shaft is only 127.5 mm. The transmission has a ratio of 15 in first gear and 5 in second. The design of the shifting module, including the actuator, is therefore identical to the solution already described for the coaxial powertrain. In addition, a neutral position allows a decoupling function where this solution could also be adapted by omitting the second speed synchronizer unit.

A separate option that can be combined with parallel and coaxial designs is torque vectoring which accelerates or brakes at least one of the two wheels. This option is achieved in the Schaeffler axle drives by using an electromechanically-driven, three-stage planetary gear drive, the so-called superimposing transmission. By using this transmission and an additional traction motor, a specific “dynamic bracing moment” can be produced between the output shafts. The wheel, which is then accelerated by the normal adjustment range of the mechanical differential, transmits a greater torque and produces the correspondingly greater tractive force. This tractive force thus ensures there is a corresponding yawing moment around the vehicle’s vertical axle. The superimposing transmission allows the servomotor to have a ratio of around 40 to the wheel. If a torque of approximately 30 Nm is produced at the torque vec-

https://doi.org/10.51202/9783181023549 - Generiert durch IP 216.73.216.36, am 19.01.2026, 02:19:31. © Urheberrechtlich geschützter Inhalt. Ohne gesonderte Erlaubnis ist jede urheberrechtliche Nutzung untersagt, insbesondere die Nutzung des Inhalts im Zusammenhang mit, für oder in KI-Systemen, KI-Modellen oder Generativen Sprachmodellen.

toring motor by this gear ratio, this produces a differential moment of 1,200 Nm between the wheels. This order of magnitude is required to ensure the system functions adequately across almost the whole speed range. In this type of system, significantly less electrical system power is required for lateral torque distribution than with drive concepts which have one electric drive per wheel. A maximum output of 6 to 7 kW is therefore sufficient for the servomotor to be used in the vehicle. [5]



Technical data

System weight in kg	74
Power in kW max./continuous	100/60
Output torque in Nm max./continuous	3,000/1,650
Input speed in rpm	18,200
Offset/System length in mm	Ø 127.5 x 485
Ratio	15/5

Customer benefits

- P4 with full e-drive option
- WLTC driving cycle without combustion engine possible
- Electric AWD option w/o mechanical cardan shaft, less mech. losses
- 1st gear for high torque and max. acceleration
- Boost and recuperation at high speed due to 2nd gear
- Optional with 48 V technology

Fig. 9: Offset design of a two-speed electric axle drive

The latest ideas offer even more functionality by using coaxial or parallel base transmissions in regard to higher launch performance and high speed efficiency. While gearshifts are not becoming a comfort issue, the stepped planetary set can be adapted so that a second input is connected to an additional sun gear. Both inputs are connected to clutch packs. This layout allows gear steps between 1.5 and 2. Due to comfort issues and the experience with conventional powertrains with automatic transmissions, the highest gear steps are normally 1-2 and reach values of up to 2. Analysis of this shift showed that acceptance is at a level from 6 to 8 on an ATZ evaluation scale. Medium loads result in a better rating and high loads

https://doi.org/10.51202/9783181023549 - Generiert durch IP 216.73.216.36, am 19.01.2026, 02:19:31. © Urheberrechtlich geschützter Inhalt. Ohne gesonderte Erlaubnis ist jede urheberrechtliche Nutzung untersagt, insbesondere die Nutzung des Inhalts im Zusammenhang mit, für oder in KI-Systemen, KI-Modellen oder Generativen Sprachmodellen.

a worse rating during gear shifts which can be considered and cleverly implemented in the shifting strategy.

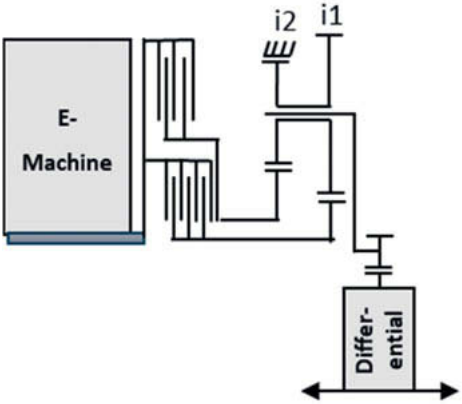


Fig. 10: Stick diagram of a power shift electric axle drive

Fig. 10 shows the stick diagram of a two-speed electric axle in an offset design with power shift capability. The parking lock should be considered in BEV applications. There are alternative methods of actuation and the illustrated concept can be e.g. actuated by a power pack including valves for clutch actuation, parking lock, clutch pack cooling as well as optional rotor cooling and gear set lubrication. Electric machine speed reaches up to 12,000 rpm and 270 Nm torque at the transmission inputs. This application illustrates an alternative for expanded use of a specific electric drive system at a certain power level. This enables higher launch torque and reduced rotational speed of the electric machine at top speeds to be realized in comparison to single-speed solutions. In addition, the option to perform gearshifts during driving provides the potential for more efficient operating points, resulting in an extended driving range.

System Development

The increased complexity of developing powertrain systems requires methods which enable efficient development especially in regard to cost and time. [6] The boundary conditions of the powertrain and the relevant vehicle requirements must be taken into consideration. From an upper level, the powertrain perspective, development is carried out for all the requirements regarding the electric machine, power electronics and transmission including optional

https://doi.org/10.51202/9783181023549 - Generiert durch IP 216.73.216.36, am 19.01.2026, 02:19:31. © Urheberrechtlich geschützter Inhalt. Ohne gesonderte Erlaubnis ist jede urheberrechtliche Nutzung untersagt, insbesondere die Nutzung des Inhalts im Zusammenhang mit, für oder in KI-Systemen, KI-Modellen oder Generativen Sprachmodellen.

actuators as well as their relevant interactions. Activities on the system and subsystem level are carried out simultaneously so that integration and verification are also overlapping activities between the system levels, e.g. the software of power electronics, torque accuracy of the electric machine or the mechanical systems in the transmission are calibrated and tested while the electric axle system is prepared for verification. The objective is to reach a maturity level that leads to a high-quality system. As a result of continuous optimization of the previously described subsystems (electric machine, power electronics, transmission) in combination with system development, the latest electric axle technology has enabled the torque and power output to be increased while cutting weight and size.

Conclusion and summary

Drive units for both hybrid and purely electric vehicles are explained from the perspective of a transmission which provides a wide range of applications. A single-speed transmission is a base application that can be produced in various modular designs. Shiftable applications for HEV and PHEV purposes can also be derived from the modular transmission kit. Even a power shift capability can be seen as beneficial, with electric machine downspeeding at top speed and increased axle torque for a better launch performance. Power electronics with a smart and functional design of the carrier frame, for example in combination with half-bridge modules, enable a power scale from 60 kW up to 300 kW. The electric machine technology for this modular kit includes permanently-excited or asynchronous machines. Wave winding technology is seen as beneficial by scaling power and optimizing losses so that an efficiency of 94 % can be achieved. System development is a key element of electric axle drive development in order to fulfil high standards over all the required disciplines.

https://doi.org/10.51202/9783181023549 - Generiert durch IP 216.73.216.36, am 19.01.2026, 02:19:31. © Urheberrechtlich geschützter Inhalt. Ohne gesonderte Erlaubnis ist jede urheberrechtliche Nutzung untersagt, insbesondere die Nutzung des Inhalts im Zusammenhang mit, für oder in KI-Systemen, KI-Modellen oder Generativen Sprachmodellen.

[1] Englisch, A.; Pfund, Th.: Schaeffler E-Mobility – With Creativity and System Competence in the Field of Endless Opportunities. 11. Schaeffler Kolloquium, Baden-Baden, 2018

[2] Pfund, T.: The Schaeffler eDrive Plattform – Modular and Highly Integrated. 11. Schaeffler Kolloquium, Baden-Baden, 2018

[3] Daniel, B.: eAxle Family in Coaxial and Offset Arrangements. 16th International CTI Symposium Automotive Transmissions, Berlin, 2017

[4] Biermann, T.: Light, compact and efficient: Schaeffler Differential systems set the pace. 10. Schaeffler Kolloquium, Baden-Baden, 2014

[5] Biermann, T.: The Innovative Schaeffler Modular E-Axle. 11. Schaeffler Kolloquium, Baden-Baden, 2018

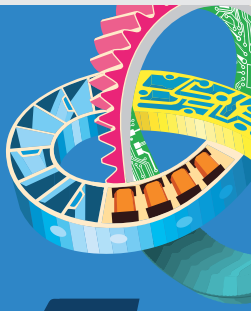
[6] INCOSE: Systems Engineering Handbook. 4. Edition, San Diego, 2015

https://doi.org/10.51202/9783181023549 - Generiert durch IP 216.73.216.36, am 19.01.2026, 02:19:31. © Urheberrechtlich geschützter Inhalt. Ohne gesonderte Erlaubnis ist jede urheberrechtliche Nutzung untersagt, insbesondere die Nutzung des Inhalts im Zusammenhang mit, für oder in KI-Systemen, KI-Modellen oder Generativen Sprachmodellen.

https://doi.org/10.51202/9783181023549 - Generiert durch IP 216.73.216.36, am 19.01.2026, 02:19:31. © Urheberrechtlich geschützter Inhalt. Ohne gesonderte Erlaubnis ist jede urheberrechtliche Nutzung untersagt, insbesondere die Nutzung des Inhalts im Zusammenhang mit, für oder in KI-Systemen, KI-Modellen oder Generativen Sprachmodellen.

https://doi.org/10.51202/9783161023549 - Generiert durch IP 216.73.216.36, am 19.01.2026, 02:19:31. © Urheberrechtlich geschützter Inhalt. Ohne gesonderte Erlaubnis ist jede urheberrechtliche Nutzung untersagt, insbesondere die Nutzung des Inhalts im Zusammenhang mit, für oder in KI-Systemen, KI-Modellen oder Generativen Sprachmodellen.

VDI Wissensforum



Dritev

19th International VDI Congress

Dritev – Drivetrain for Vehicles

ISBN 978-3-18-092354-3

https://doi.org/10.51202/9783181023549 - Generiert durch IP 216.73.216.36, am 19.01.2026, 02:19:31. © Urheberrechtlich geschützter Inhalt. Ohne gesonderte Erlaubnis ist jede urheberrechtliche Nutzung untersagt, insbesondere die Nutzung des Inhalts im Zusammenhang mit, für oder in KI-Systemen, KI-Modellen oder Generativen Sprachmodellen.

VDI Wissensforum

VDI-Berichte 2354



EDritev

International Conference
EDrive

July 10 and 11, 2019, Bonn

Main topics:

- Current OEM concepts for the electrified drive system
- Application of power semiconductors in e-engines, converters and onboard charging units
- What's the impact from AUTOSAR and ASIL?
- Design and test methods of electrified powertrains
- Intelligent topology optimisation to improve system behaviour and power distribution
- Innovative transmission and four-wheel-drive concepts for the electrified drive system
- Development potentials for e-engines

https://doi.org/10.51202/9783181023549 - Generiert durch IP 216.73.216.36, am 19.01.2026, 02:19:31. © Urheberrechtlich geschützter Inhalt. Ohne gesonderte Erlaubnis ist jede urheberrechtliche Nutzung untersagt, insbesondere die Nutzung des Inhalts im Zusammenhang mit, für oder in KI-Systemen, KI-Modellen oder Generativen Sprachmodellen.

https://doi.org/10.51202/9783161023549 - Generiert durch IP 216.73.216.36, am 19.01.2026, 02:19:31. © Urheberrechtlich geschützter Inhalt. Ohne gesonderte Erlaubnis ist jede urheberrechtliche Nutzung untersagt, insbesondere die Nutzung des Inhalts im Zusammenhang mit, für oder in KI-Systemen, KI-Modellen oder Generativen Sprachmodellen.

VDI-BERICHTE
Herausgeber:
VDI Wissensforum GmbH

https://doi.org/10.51202/9783181023549 - Generiert durch IP 216.73.216.36, am 19.01.2026, 02:19:31. © Urheberrechtlich geschützter Inhalt. Ohne gesonderte Erlaubnis ist jede urheberrechtliche Nutzung untersagt, insbesondere die Nutzung des Inhalts im Zusammenhang mit, für oder in KI-Systemen, KI-Modellen oder Generativen Sprachmodellen.

Bibliographische Information der Deutschen Nationalbibliothek
Die Deutsche Nationalbibliothek verzeichnet diese Publikation in der Deutschen Nationalbibliographie; detaillierte bibliographische Daten sind im Internet unter www.dnb.de abrufbar.

Bibliographic information published by the Deutsche Nationalbibliothek (German National Library)
The Deutsche Nationalbibliothek lists this publication in the Deutsche Nationalbibliographie (German National Bibliography); detailed bibliographic data is available via Internet at www.dnb.de.

© VDI Verlag GmbH · Düsseldorf 2019
Alle Rechte vorbehalten, auch das des Nachdruckes, der Wiedergabe (Photokopie, Mikrokopie), der Speicherung in Datenverarbeitungsanlagen und der Übersetzung, auszugsweise oder vollständig.

Der VDI-Bericht, der die Vorträge der Tagung enthält, erscheint als nichtredigierter Manuskriptdruck.
Die einzelnen Beiträge geben die auf persönlichen Erkenntnissen beruhenden Ansichten und Erfahrungen der jeweiligen Vortragenden bzw. Autoren wieder. Printed in Germany.

ISSN 0083-5560
ISBN 978-3-18-092354-3

https://doi.org/10.51202/9783181023549 - Generiert durch IP 216.73.216.36, am 19.01.2026, 02:19:31. © Urheberrechtlich geschützter Inhalt. Ohne gesonderte Erlaubnis ist jede urheberrechtliche Nutzung untersagt, insbesondere die Nutzung des Inhalts im Zusammenhang mit, für oder in KI-Systemen, KI-Modellen oder Generativen Sprachmodellen.

Content

Power Electronic

Wide-Band-Gap (WBG) power semiconductor switches for automotive HV battery chargers – Opportunities & challenges 1
M. Elshaer, C. Chen, Ford Motor Company, Dearborn, Michigan, U.S.A.

System impacts to the electrical drive by using SIC-power semiconductors. 15
H. Schäfer, hofer eds GmbH, Würzburg

Challenges of sensorless high-speed drives with PM motors 29
M. Stulrajter, M. Pacha, NXP Semiconductors, Roznov pod Radhostem, Czech Republic

48V to 12V Converters for xEV Applications – Managing the headaches of dual voltage automotive architectures 45
J. Grabowski, ON Semiconductor, Ann Arbor, Mi. USA;
A. Colognese, ON Semiconductor Germany GmbH, Munich

Optimization Electric Motor

New concepts for electrical drive trains for high power density. 55
B. Müller, C. Angrick, M. Fritz, Schaeffler Automotive GmbH, Bühl

Overview of stator technologies motors for electro mobility in passcars – The right technology for each application 67
A. Gehring, M. Beringer, M. Özdemir, ZF Friedrichshafen AG, Schweinfurt

Nidec next generation electric traction motor 77
M. Özbek, J. Trommer, Nidec Motors & Actuators Germany GmbH, Bietigheim-Bissingen;
K. Akiyama, Y. Yamada, Nidec Corporation, Kyoto, Japan

https://doi.org/10.51202/9783161023549 - Generiert durch IP 216.73.216.36, am 19.01.2026, 02:19:31. © Urheberrechtlich geschützter Inhalt. Ohne gesonderte Erlaubnis ist jede urheberrechtliche Nutzung untersagt, insbesondere die Nutzung des Inhalts im Zusammenhang mit, für oder in KI-Systemen, KI-Modellen oder Generativen Sprachmodellen.

Development Methods for Electrified Powertrains

Enhanced application of high-performance-computing in the design process of high-power-density traction motors 85
D. P. Morisco, Robert Bosch GmbH, Schwieberdingen;
I. Liviu Iepure, Robert Bosch GmbH, Renningen

Great Wall Motors' 2nd generation of Pi4 platform – A high performance PHEV for premium SUV in China 99
Y. Le Neindre, Great Wall Motors Co, Baoding, China

Optimisation of electric motor acoustics of a hybrid dual clutch gearbox using virtual methods 111
M. Kruse, H. Decker, Sebastian Eulert, Volkswagen AG Group Components, Kassel

Human/machine readable language representation method in HEV drivetrain testing 125
A. Alkan, CPT Zwei GmbH, Berlin

Automotive System Requirements for Electrical Drives

Impact of hybridization on functional safety for low voltage eMotors – Impact of electrical and hybrid architectures (P2... P4) on the ASIL of electrical machines (eMotors) 141
M. Maillard, L. Laurenty, S. Chretien, VALEO Powertrain Systems, Créteil, France

AUTOSAR Adaptive Platform – The standardized software framework for safe and intelligent e-mobility 151
M. Niklas, Continental Corporation, Regensburg;
G. Reichart, AUTOSAR Partnership, Munich

A modular Concept for EMI shielding of thermoplastic housings for E-Cars – An innovative approach to support weight saving and function integration 161
V. Schroiff, Freudenberg Sealing Technologies GmbH & Co. KG, Weinheim

https://doi.org/10.51202/9783161023549 - Generiert durch IP 216.73.216.36, am 19.01.2026, 02:19:31. © Urheberrechtlich geschützter Inhalt. Ohne gesonderte Erlaubnis ist jede urheberrechtliche Nutzung untersagt, insbesondere die Nutzung des Inhalts im Zusammenhang mit, für oder in KI-Systemen, KI-Modellen oder Generativen Sprachmodellen.

Many thanks to the Gold-Sponsors of the Congress:



www.iot.bosch.com



www.castrol.com/de



www.gkndriveline.com



www.magna.com



www.daimler.de



www.zf.com

https://doi.org/10.51202/9783161023549 - Generiert durch IP 216.73.216.36, am 19.01.2026, 02:19:31. © Urheberrechtlich geschützter Inhalt. Ohne gesonderte Erlaubnis ist jede urheberrechtliche Nutzung untersagt, insbesondere die Nutzung des Inhalts im Zusammenhang mit, für oder in KI-Systemen, KI-Modellen oder Generativen Sprachmodellen.

https://doi.org/10.51202/9783161023549 - Generiert durch IP 216.73.216.36, am 19.01.2026, 02:19:31. © Urheberrechtlich geschützter Inhalt. Ohne gesonderte Erlaubnis ist jede urheberrechtliche Nutzung untersagt, insbesondere die Nutzung des Inhalts im Zusammenhang mit, für oder in KI-Systemen, KI-Modellen oder Generativen Sprachmodellen.

Wide-Band-Gap (WBG) Power Semiconductor Switches for Automotive HV Battery Chargers – Opportunities & challenges

Mohamed Elshaer, **Chingchi Chen**,
Ford Motor Company, Dearborn, Michigan, U.S.A.

Abstract

This paper discusses the opportunities and challenges of using wide-bandgap (WBG) devices in the electric vehicle's onboard charger. Constraints limiting the adoption of such technology are investigated. Switching frequency impact on semiconductor devices' losses and magnetic components' design is analyzed. While the theoretical advantages of WBG-based power converters have been extensively researched, this paper aims to address the attributes making this technology practical for automakers. A comparison between silicon superjunction (Si-SJ)-based design and silicon carbide (SiC)-based design is presented. Furthermore, a breakdown of system efficiency and component losses are provided to illustrate the key areas which need improvement. Several systems are designed and optimized to quantify the benefits of increasing the system frequency.

I. Introduction

The Power metal oxide semiconductor field effect transistor (MOSFET) has been a key component in high voltage and high frequency switching power supplies [1]. The well-known silicon limit derived by Baliga [2] shows the quadratic dependence of the specific on-state resistance on the breakdown voltage, eq. 1. This equation was derived using the one-dimensional Poisson theory and was known to be the limit of silicon. With the introduction of the Superjunction concept in the late 90s, it was clear that improvements beyond the so-called Si-limit are achieved by introducing two or three-dimensional structures [3]. Infineon and STMicroelectronics were the first to commercialize this technology through the CoolMOS and MDmech concepts [3, 4]. By swapping the drift region with an alternatively stacked heavily doped N and P regions, the specific on-state resistance became linear with respect to the breakdown voltage, eq.2 [5]. While Superjunction technology allows for lower on-state resistance by increasing the doping levels, the cell pitch must be proportionally reduced to stay within the limits of the critical

https://doi.org/10.51202/9783181023549 - Generiert durch IP 216.73.216.36, am 19.01.2026, 02:19:31. © Urheberrechtlich geschützter Inhalt. Ohne gesonderte Erlaubnis ist jede urheberrechtliche Nutzung untersagt, insbesondere die Nutzung des Inhalts im Zusammenhang mit, für oder in KI-Systemen, KI-Modellen oder Generativen Sprachmodellen.

electric field [6]. The minimum cell pitch was derived to be 0.18 µm and 0.05 µm for Si and SiC, respectively [5].

$$R_{sp.conv} = \frac{4V_B^2}{\mu_n \varepsilon_s E_c^3} \quad (1)$$

$$R_{sp,SJ} = \frac{4V_B}{\mu_n \varepsilon_s E_C^2} d \quad (2)$$

Overcoming the Silicon limit can also be achieved by replacing Silicon with wide-bandgap (WBG) semiconductors [16]. Table 1 summarizes the superior material properties of SiC semiconductors as compared to Si [9]. It can be illustrated by using eq. 1 that even when using the conventional planar MOSFET technology, the on-state specific resistance can be reduced by many orders of magnitudes when replacing Silicon with SiC semiconductors. Under the theoretical limit, the minimum power loss in conventional MOSFET and SJ MOSFET are derived in [9]. This quantitative analysis showed that SiC devices have high heat density due to their smaller die area to handle the same current. Hence, new heat extraction methods will relieve the constraints of smaller die sizes, therefore help accelerate the adoption of WBG devices [8].

Table 1: Material Parameters [9].

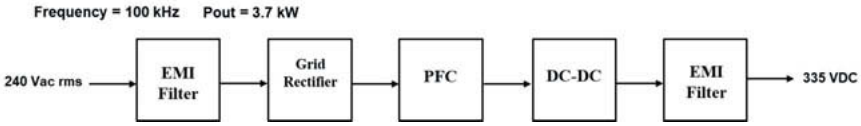
Material	E_g *(eV)*	n_i *(cm^{-3})*	ε_r	μ_n *(cm^2/V-s)*	E_c *(MV/cm)*	v_{sat} *(10^7 cm/s)*
Si	1	1.5×10^{10}	11.8	1350	0.25	1
4H-SiC	3.39	8.2×10^{-9}	10	720	2	2

II. Onboard Charger Architecture

The onboard charger discussed in this paper consists mainly of two power conversions stages coupled by an energy storage capacitor in between. The first stage is a non-isolated power factor correction (PFC) circuit interfaced directly to the AC grid. This circuit is used to regulate the grid current and improve its power quality. The second state is made of an isolated DC-DC converter that is used to regulate the HV battery power and isolate the AC grid from the vehicle's HV bus. Additionally, EMI filters are used at both the grid and HV-battery sides to attenuate differential-mode (DM) and common-mode (CM) currents generated by the switching de-

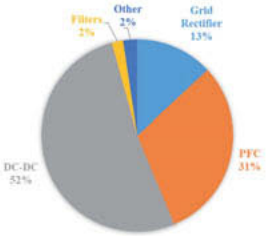
https://doi.org/10.51202/9783181023549 - Generiert durch IP 216.73.216.36, am 19.01.2026, 02:19:31. © Urheberrechtlich geschützter Inhalt. Ohne gesonderte Erlaubnis ist jede urheberrechtliche Nutzung untersagt, insbesondere die Nutzung des Inhalts im Zusammenhang mit, für oder in KI-Systemen, KI-Modellen oder Generativen Sprachmodellen.

vices. Fig. 1 (a) shows the system architecture block diagram, where each block will be discussed in detail in later sections. Furthermore, based on the calculated results from those sections, the loss breakdown of the state-of-the-art 3.7 kW charger is given in fig. 1 (b), where the DC-DC stage consumes the highest loss followed by the PFC circuit then the grid side rectifier.



(a)

Circuit	Power (W)
Grid Rectifier	27.5
PFC	64.3
DC-DC	109.31
Filters	4
Other	5



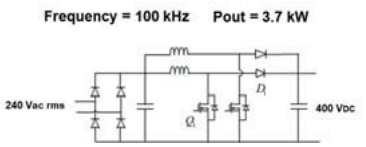
(b)

Fig. 1: Onboard Charger (a) System architecture block diagram (b) Power loss breakdown.

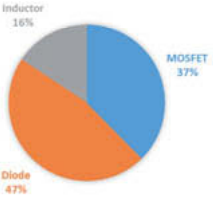
A. PFC Circuit

The PFC-boost converter topology is widely used in vehicle charger applications due to its simplicity and low cost. Fig. 2 (a) shows its topology which consists of a full-bridge diode rectifier followed by two interleaved non-isolated boost converters. Over the past few years SiC Schottky diodes gained popularity in commercial products due to their low reverse recovery chargers when compared to Si-diodes. It was determined that the best efficiency is achieved when switching Si-SJ MOSFET against SiC diode [17]. Hence, this will be the baseline design in this paper. Table 2 shows the parameters of the semiconductor devices in fig. 2(a). The loss breakdown of the PFC circuit is shown in fig. 2 (b) for a 400 V output DC bus. While a significant reduction in semiconductor loss is achieved when using SiC diode, still semiconductor devices consume the majority of the losses while the inductor consumes only 16%.

https://doi.org/10.51202/9783181023549 - Generiert durch IP 216.73.216.36, am 19.01.2026, 02:19:31. © Urheberrechtlich geschützter Inhalt. Ohne gesonderte Erlaubnis ist jede urheberrechtliche Nutzung untersagt, insbesondere die Nutzung des Inhalts im Zusammenhang mit, für oder in KI-Systemen, KI-Modellen oder Generativen Sprachmodellen.



Circuit	Power (W)
MOSFET	24.2
Diode	30
Inductor	10.1



(a) (b)

Fig. 2: PFC power conversion stage (a) Circuit schematic (b) Loss breakdown.

Table 2: Si MOSFET and SiC diode used in Fig. 2(a)

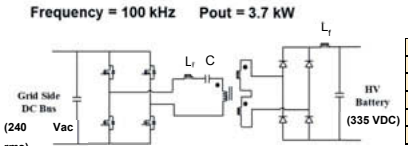
Device types	V_{DSS} (V)	$R_{DS(ON)}$ (mΩ)	Chip Area (mm^2)	R_{sp} (mΩ cm^2)	$R_{\Theta jc}$ (□C/W)
Si SJ MOSFET	600	80	33.03	23.8	0.5
SiC diode	650	-	3.17	-	2

B. Isolated DC-DC circuit

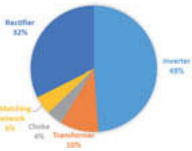
Galvanic isolation is a key design constraint for the DC-DC power stage. High-frequency transformers are typically employed to realize the isolation requirement. Hence, an inverter is needed on the primary side, and a rectifier is needed on the secondary side. For a 400 V DC bus on the primary side, the Si-SJ MOSFET has been a popular device in commercial products due to its superior switching performance, high reliability, and relatively low cost.

In order to take advantage of the Si-SJ MOSFET fast switching capability, soft-switching resonant/ quasi-resonant circuits are used. These family of topologies can achieve zero voltage switching (ZVS) turn-on thus allowing the body-diode of the complimentary MOSFET to turn-off before tuning-on the MOSFET channel. By using these topologies, the working frequency can be increased leading to an increased DC-DC power density. There is a large variety of matching network topologies that can be used to realize soft-switching and adjust the converter's voltage gain [14, 15, 18]. Fig. 3 shows the topology of a typical quasi-resonant DC-DC converter. The loss breakdown for this circuit is given in fig. 3 (b). The majority of power losses are consumed in the semiconductor devices.

https://doi.org/10.51202/9783181023549 - Generiert durch IP 216.73.216.36, am 19.01.2026, 02:19:31. © Urheberrechtlich geschützter Inhalt. Ohne gesonderte Erlaubnis ist jede urheberrechtliche Nutzung untersagt, insbesondere die Nutzung des Inhalts im Zusammenhang mit, für oder in KI-Systemen, KI-Modellen oder Generativen Sprachmodellen.



Circuit	Power (W)
Inverter	53.4
Transformer	10.76
Choke	4.5
LC Matching Network	5.2
Rectifier	35.45



(a) (b)

Fig. 3: Isolated DC-DC converter (a) Circuit schematic (b) Loss breakdown.

III. Comparison between Si-SJ and SiC MOSFETs

In order to quantify the advantage of SiC MOSFETs over Si-SJ MOSFET, two MOSFETs with similar current ratings are selected for this study, as summarized in table 3. The Chip area of the SiC MOSFET is more than 4X smaller than that of the Si SJ MOSFET. While the specific on-state resistance of the SiC MOSFET is 7X smaller than that of the Si SJ MOSFET, the maximum allowed power dissipation in it is smaller due to its smaller die size

Table 3: MOSFET Parameters Comparison (at room temperature).

Device types	V_{DSS} (V)	$R_{DS(ON)}$ (mΩ)	Chip Area (mm^2)	R_{sp} (mΩ cm^2)	$R_{\Theta jc}$ (□C/W)
SiC MOSFET	650	78	7.54	3.4	0.91
Si SJ MOSFET	600	80	33.03	23.8	0.5

The theoretical limits of the specific on-state resistance for both the conventional and Super-junction MOSFETs are plotted in fig. 4. In order to gain a perspective on where the technology stands as compared to the theoretical limits, the MOSFETs used in this study are overlaid in the same plot. It is shown that all of the considered MOSFETs are below the conventional Silicon limit. While the SiC MOSFET has lower specific on-state resistance than that of Si-SJ MOSFET, it is still much higher than the theoretical limits of both SJ-Si and conventional SiC MOSFETs. Hence, it is expected that both technologies to continue improving [7, 10].

https://doi.org/10.51202/9783181023549 - Generiert durch IP 216.73.216.36, am 19.01.2026, 02:19:31. © Urheberrechtlich geschützter Inhalt. Ohne gesonderte Erlaubnis ist jede urheberrechtliche Nutzung untersagt, insbesondere die Nutzung des Inhalts im Zusammenhang mit, für oder in KI-Systemen, KI-Modellen oder Generativen Sprachmodellen.

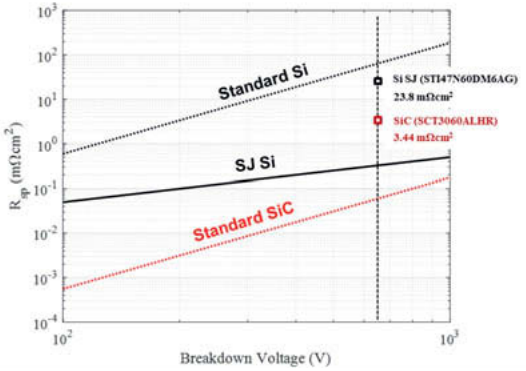


Fig. 4: Theoretical limits of the specific on-state resistance [5].

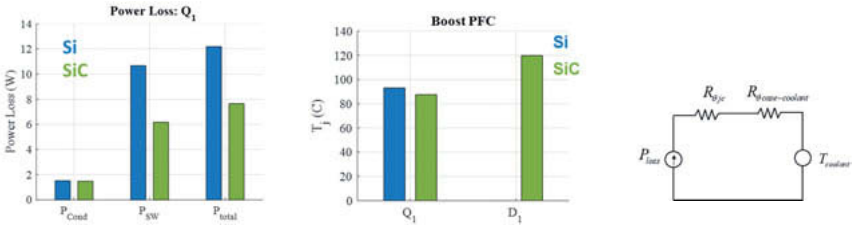
Lower specific on-state resistance allows in some cases moving to a smaller package (e.g. swapping TO-247 with TO-220). The TO-220 package has about half of the TO-247 source inductance thus improving the switching behavior and lowering the losses [10]. A SiC-based 12.5 kW 500 kHz resonant DC-DC converter with integrated PCB winding transformer was introduced in [15]. The switching characteristics of three different SiC MOSFETs were evaluated. Experimental results showed that the three-lead TO247 package had very poor switching characteristics and high turn-off losses. Additionally, the four-lead TO247 (with Kelvin Connection) had superior switching transient and lower turn-off losses. New packages with lower parasitic inductances are needed to support high-frequency devices.

A. PFC circuit switching devices losses

It has been shown that the best efficiency is achieved when switching the Si-SJ MOSFET against SiC diode, due to the SiC diode's low reverse recovery charge [17]. However, the advantages of switching a conventional SiC MOSFET against a SiC diode needs further investigation. Hence, the SJ MOSFET is swapped with the SiC MOSFET from table 2. Fig. 5 shows a power loss comparison between Si-SJ and SiC designs, based on the parameters from their datasheets. Both designs are operated at 100 kHz and supply a 3.7 kW load. The power loss breakdown shown in fig. 5 (a) indicates that the conduction loss of both MOSFETs is approximately equal due to their similar on-state resistances. Furthermore, the switching losses of the SiC MOSFET is 43 % lower than that of the Si-SJ MOSFET, due to smaller package stray inductance and device stray capacitance. Further, their junction temperatures are estimated based on the thermal equivalent circuit in fig. 5(c), assuming the device case-

https://doi.org/10.51202/9783181023549 - Generiert durch IP 216.73.216.36, am 19.01.2026, 02:19:31. © Urheberrechtlich geschützter Inhalt. Ohne gesonderte Erlaubnis ist jede urheberrechtliche Nutzung untersagt, insbesondere die Nutzung des Inhalts im Zusammenhang mit, für oder in KI-Systemen, KI-Modellen oder Generativen Sprachmodellen.

to-coolant thermal resitance is 1.5 °C/W. While the net power loss in the SiC MOSFET is lower, reduction in its junction temperature is not pronounced, as shown in fig. 5(b). Because of the SiC MOSFET's small die area, the junction-to-case thermal resistance is higher.



(a) (b) (c)

Fig. 5: Comparison between Si-SJ and SiC-based designs. (a) MOSFET power loss (b) Junction temperature (c) Thermal equivalent circuit model ($R_{\Theta\ case\text{-}coolant}$ = 1.5 °C/W).

Increasing the switching frequency could help reduce the inductor size and cost. In order to quantify the cost-benefit of increasing the frequency, four SiC MOSFETs with different die areas are compared in this study. Fig. 6 shows the junction temperature as a function of die area for both 100 kHz and 200 Hz designs. It can be shown that operation at 200 kHz results in a junction temperature that exceeds 150 °C when using the SiC MOSFET with a chip area of 7.54 mm^2. Increasing the frequency to 200 kHz while maintaining a tolerable junction temperature would require doubling the die area – leading to an unfavorable cost increase to the overall system.

https://doi.org/10.51202/9783181023549 - Generiert durch IP 216.73.216.36, am 19.01.2026, 02:19:31. © Urheberrechtlich geschützter Inhalt. Ohne gesonderte Erlaubnis ist jede urheberrechtliche Nutzung untersagt, insbesondere die Nutzung des Inhalts im Zusammenhang mit, für oder in KI-Systemen, KI-Modellen oder Generativen Sprachmodellen.

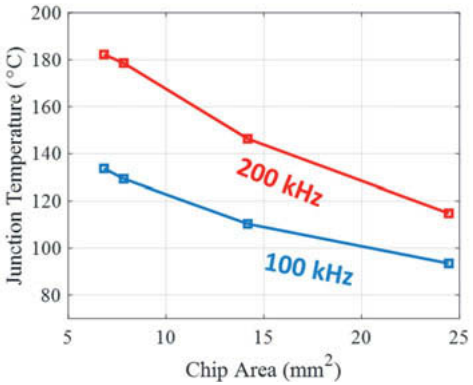
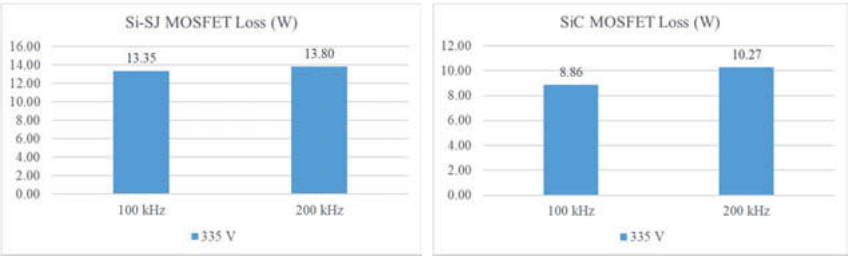


Fig. 6: Junction temperature comparison as a function of chip area.

B. Isolated DC-DC converter MOSFET losses

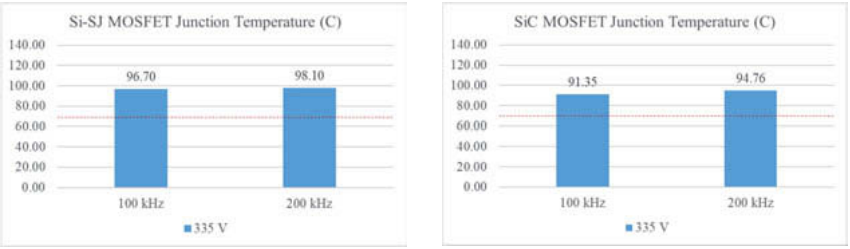
The DC-DC inverter is designed to guarantee ZVS turn-on at high output loads. Soft-switching losses of both the Si-SJ and SiC MOSFETs are comparable. Hence, for this analysis, it is assumed that the conduction losses are dominant and soft-switching losses are neglected. Two designs are optimized to operate at 100 kHz and 200 kHz. The MOSFET dv/dt and dead-time are fixed for these two designs. The MOSFETs power losses at the rated load are presented in fig. 7. The loss in the Si-SJ MOSFET is higher due to its increased on-state resistance at high junction temperature at full load. Fig. 8 shows the junction temperature of both the Si-SJ and SiC designs. It is assumed that the coolant temperature is 70 °C. Due to the SiC MOSFET's higher thermal resistance and body diode forward voltage, its junction temperature is comparable to the Si-SJ MOSFET.

https://doi.org/10.51202/9783181023549 - Generiert durch IP 216.73.216.36, am 19.01.2026, 02:19:31. © Urheberrechtlich geschützter Inhalt. Ohne gesonderte Erlaubnis ist jede urheberrechtliche Nutzung untersagt, insbesondere die Nutzung des Inhalts im Zusammenhang mit, für oder in KI-Systemen, KI-Modellen oder Generativen Sprachmodellen.



(a) (b)

Fig. 7: Inverter MOSFET total loss at different PWM switching frequency. (a) Si-SJ MOSFET (b) SiC MOSFET.



(a) (b)

Fig. 8: Inverter MOSFET Junction temperature rise at different battery voltage levels. (a) Si-SJ MOSFET (b) SiC MOSFET.

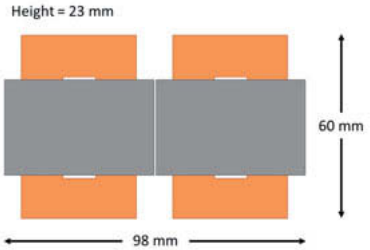
IV. Design considerations for magnetic components

A. PFC Inductor

Operation at a higher frequency can help reduce the inductor size which is manifested in smaller copper winding and ferrite core sizes. In order to improve the power factor at light load and limit the EMI filter size, the inductance value is chosen to limit the inductor's peak-to-peak current ripple. Inductor current ripple is typically chosen to be below 30% of the peak input current. Based on this assumption, the design of two 120 µH inductors is shown in fig. 10. These inductors are used as part of the 3.7 kW interleaved PFC boost circuit. The operating

https://doi.org/10.51202/9783181023549 - Generiert durch IP 216.73.216.36, am 19.01.2026, 02:19:31. © Urheberrechtlich geschützter Inhalt. Ohne gesonderte Erlaubnis ist jede urheberrechtliche Nutzung untersagt, insbesondere die Nutzung des Inhalts im Zusammenhang mit, für oder in KI-Systemen, KI-Modellen oder Generativen Sprachmodellen.

frequency is 100 kHz. N49 is selected for the core material. The inductor coil has 16 turns constructed in an 8 layer 2 oz printed circuit board (PCB).
Increasing the frequency can help reduce either the ferrite core or copper sizes or both. In this study, two inductor designs are optimized to operate at 100 kHz, and 200 kHz with a peak flux density of 300 mT. The inductance values are calculated to be 120 µH and 60 µH for the 100 kHz and 200 kHz designs, respectively.

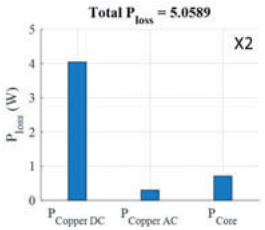


PCB Dimensions	98 mm X 60 mm
Effective Core Volume	60 mL
Structure Volume	135.24 mL

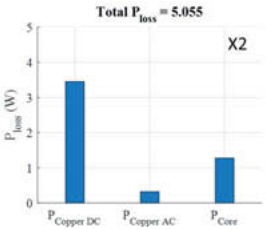
Fig. 10: PFC inductor dimensions for the baseline design.

The DC copper losses are expected to be dominant because the AC-current component and its associated harmonics are much smaller than the DC component. The loss breakdown for these two inductor designs is calculated and presented in fig. 11. They have approximately equal net losses. While the copper loss decreases with increase of frequency due to the fact that fewer winding turns are needed, the core loss increases with frequency. It was assumed that these two inductors have the same peak flux densities; thus their cores' cross-sectional area are sized according to the operation frequency and material saturation requirements — operation at higher frequency results in a reduced mean-length-per-turn winding due to smaller core size. Hence the copper loss is expected to reduce. On the other hand, the core loss increases with frequency due to the ferrite material's non-linear power loss density. The effective core volume is 60 mL and 30 mL for the 100 kHz and 200 kHz designs, respectively. Although the volume of the core is decreasing with frequency, the net core loss is approximately equal.

https://doi.org/10.51202/9783181023549 - Generiert durch IP 216.73.216.36, am 19.01.2026, 02:19:31. © Urheberrechtlich geschützter Inhalt. Ohne gesonderte Erlaubnis ist jede urheberrechtliche Nutzung untersagt, insbesondere die Nutzung des Inhalts im Zusammenhang mit, für oder in KI-Systemen, KI-Modellen oder Generativen Sprachmodellen.



(a)

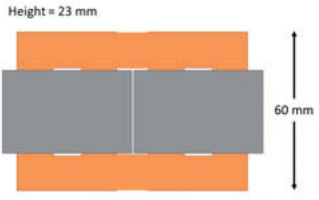


(b)

Fig. 11: PFC inductor loss breakdown: (a) 100 kHz design (b) 200 kHz design.

B. DC-DC main transformer

The power transformer in the DC-DC converter has a tangible impact on the charger cost. Power and switching frequency are key factors for determining the copper winding and ferrite core sizes. Increasing the frequency help reduce the volt-second across the transformer windings thus reducing the number of turns required for maintaining a peak flux density. Additionally, operation at higher frequency reduces the flux density inside the core which translates into lower ferrite losses. This paper investigates the benefits of increasing the frequency as it pertains to copper winding size.



PCB Dimensions	98 mm X 60 mm
Effective Core Volume	60 mL
Structure Volume	135.24 mL

(a)



(b)

Fig. 12: DC-DC converter main power transformer (a) baseline design and its dimentions (b) Transformer loss breakdown (P_o = 3.7 kW, V_{in} = 400 V and V_o = 335 V).

https://doi.org/10.51202/9783181023549 - Generiert durch IP 216.73.216.36, am 19.01.2026, 02:19:31. © Urheberrechtlich geschützter Inhalt. Ohne gesonderte Erlaubnis ist jede urheberrechtliche Nutzung untersagt, insbesondere die Nutzung des Inhalts im Zusammenhang mit, für oder in KI-Systemen, KI-Modellen oder Generativen Sprachmodellen.

Matrix transformers became a key enabler for PCB-based windings transformers [11,12]. It offers the flexibility of connecting windings in either a series or parallel configurations; thus current can be split between secondary windings. Due to lowers leakage flux from the secondary coils, the AC winding resistance can be further reduced. Fig. 12 (a) shows the baseline design of a 100 kHz 3.7 kW transformer. This transformer structure enables coupling between the primary coil and each of the secondary coils while decoupling the secondary coils' flux path. Coupling between the primary coil and each of the secondary coils is controlled by adjusting the cores' cross-sectional area.

In order to quantify the impact on copper size as a function of frequency, two transformer designs are optimized to operate at 100 kHz and 200 kHz. The winding of the 100 kHz design, which is referred to as the baseline design, is constructed by 4 PCB boards. Each board consists of a standard six-layer PCB: the two outer layers are made with 2 oz copper, and the 4 inner layers are made with 1 oz copper. The primary and secondary windings are interleaved to lower the windings AC losses: outer layers carry the primary winding current, and inner layers carry the secondary winding current. Operation at 200 kHz can help reduce copper size by 25 %. Instead of using four PCB boards, as in the case of the baseline design, three PCB boards are used to construct the transformer windings, which translates to a 25 % reduction in winding cost. Fig. 12 (b) summarizes the transformer loss breakdown for these two designs.

V. Conclusions

The feasibility of using SiC MOSFETs in the electric vehicle onboard charger has been investigated. Results suggest that while the SiC material has superior properties over silicon. However, SiC provides limited benefits on loss and size reduction following common design practices as well as practical constraints. In the meantime, matured silicon manufacturing infrastructure and continuous improvement in superjunction technology makes 650 V Si superjunction MOSFETs very competitive in the foreseeable future. Wide-band-gap technologies should be further improved in performance and reliability with sufficient margins to compete against Si counterparts, without substantial cost premiums.

https://doi.org/10.51202/9783181023549 - Generiert durch IP 216.73.216.36, am 19.01.2026, 02:19:31. © Urheberrechtlich geschützter Inhalt. Ohne gesonderte Erlaubnis ist jede urheberrechtliche Nutzung untersagt, insbesondere die Nutzung des Inhalts im Zusammenhang mit, für oder in KI-Systemen, KI-Modellen oder Generativen Sprachmodellen.

References

[1] A. S. Abdelrahman, Z. Erdem, Y. Attia and M. Z. Youssef, "Wide Bandgap Devices in Electric Vehicle Converters: A Performance Survey," in *Canadian Journal of Electrical and Computer Engineering*, vol. 41, no. 1, pp. 45-54, winter 2018.

[2] B. J. Baliga, "Power semiconductor device Fig. of merit for high-frequency applications", *IEEE Electron Device Lett.*, vol. 10, pp. 455, Oct. 1989.

[3] G. Deboy, M. März, J.-P. Stengl, H. Strack, J. Tihanyi, and H. Weber, “A new generation of high voltage MOSFETs breaks the limit line of silicon,” in IEDM Tech. Dig., 1998, pp. 683–685.

[4] M. Saggio, D. Fagone, and S. Musumeci, “MDmesh: Innovative technology for high voltage power MOSFETs,” in Proc. 12th Int. Symp. Power Semiconductor Device ICs, 2000, pp. 65–68.

[5] H. Kang and F. Udrea, "True Material Limit of Power Devices—Applied to 2-D Superjunction MOSFET," in *IEEE Transactions on Electron Devices*, vol. 65, no. 4, pp. 1432-1439, April 2018.

[6] Tatsuhiko Fujihira. “Theory of Semiconductor Superjunction Devices,” in Japan Society of Applied Physics, vol. 36, no. 2, pp. 6254—6262, 1997

[7] J. Sakakibara, Y. Noda, T. Shibata, S. Nogami, T. Yamaoka, and H. Yamaguchi, “600V-class Super Junction MOSFET with High Aspect Ratio P/N Columns Structure,” 20th Int. Symp. Power Semicond. Devices ICs, pp. 299–302, 2008.

[8] F. Udrea, G. Deboy, and T. Fujihira, “Superjunction power devices, history, development and future prospects”, IEEE Transactions on Electron Devices, vol. 64, no. 3, pp. 720-734, Mar. 2017.

[9] A. Nakajima, M. Shimizu and H. Ohashi, "Power Loss Limit in Unipolar Switching Devices: Comparison Between Si Superjunction Devices and Wide-Bandgap Devices," in *IEEE Transactions on Electron Devices*, vol. 56, no. 11, pp. 2652-2656, Nov. 2009.

[10] Infineon Technologies, “CoolMOSTM C7 : Mastering the Art of Quickness,” Apr. 2013.

https://doi.org/10.51202/9783181023549 - Generiert durch IP 216.73.216.36, am 19.01.2026, 02:19:31. © Urheberrechtlich geschützter Inhalt. Ohne gesonderte Erlaubnis ist jede urheberrechtliche Nutzung untersagt, insbesondere die Nutzung des Inhalts im Zusammenhang mit, für oder in KI-Systemen, KI-Modellen oder Generativen Sprachmodellen.

[11] Chao Fei, Fred C. Lee, Qiang Li, "High-Efficiency High-Power-Density LLC Converter With an Integrated Planar Matrix Transformer for High-Output Current Applications", *Industrial Electronics IEEE Transactions on,* vol. 64, no. 11, pp. 9072-9082, 2017.

[12] D. Huang, S. Ji and F. C. Lee, "LLC Resonant Converter With Matrix Transformer," in *IEEE Transactions on Power Electronics,* vol. 29, no. 8, pp. 4339-4347, Aug. 2014.

[13] S. Harada *et al*., "First Demonstration of Dynamic Characteristics for SiC Superjunction MOSFET Realized using Multi-epitaxial Growth Method," *2018 IEEE International Electron Devices Meeting (IEDM)*, San Francisco, CA, 2018, pp. 8.2.1-8.2.4.

[14] B. Li, Q. Li and F. C. Lee, "A WBG based three phase 12.5 kW 500 kHz CLLC resonant converter with integrated PCB winding transformer," *2018 IEEE Applied Power Electronics Conference and Exposition (APEC)*, San Antonio, TX, 2018, pp. 469-475.

[15] B. Li, Q. Li and F. C. Lee, "A WBG based three phase 12.5 kW 500 kHz CLLC resonant converter with integrated PCB winding transformer," *2018 IEEE Applied Power Electronics Conference and Exposition (APEC)*, San Antonio, TX, 2018, pp. 469-475.

[16] D. Garrido-Diez and I. Baraia, "Review of wide bandgap materials and their impact in new power devices," *2017 IEEE International Workshop of Electronics, Control, Measurement, Signals and their Application to Mechatronics (ECMSM)*, Donostia-San Sebastian, 2017, pp. 1-6.

[17] F. Chimento, S. Musumeci, A. Raciti, M. Melito and G. Sorrentino, "Super-Junction MOSFET and SiC Diode Application for the Efficiency Improvement in a Boost PFC Converter," *IECON 2006 - 32nd Annual Conference on IEEE Industrial Electronics*, Paris, 2006, pp. 2067-2072.

[18] B. Li, Q. Li and F. C. Lee, "A novel PCB winding transformer with controllable leakage integration for a 6.6kW 500kHz high efficiency high density bi-directional on-board charger," *2017 IEEE Applied Power Electronics Conference and Exposition (APEC)*, Tampa, FL, 2017, pp. 2917-2924.

https://doi.org/10.51202/9783181023549 - Generiert durch IP 216.73.216.36, am 19.01.2026, 02:19:31. © Urheberrechtlich geschützter Inhalt. Ohne gesonderte Erlaubnis ist jede urheberrechtliche Nutzung untersagt, insbesondere die Nutzung des Inhalts im Zusammenhang mit, für oder in KI-Systemen, KI-Modellen oder Generativen Sprachmodellen.

System impacts to the electrical drive by using SIC-power semiconductors

Dr. **Heinz Schäfer**, hofer eds GmbH, Würzburg

Zusammenfassung

Derzeit kommen für Leistungshalbleiter im Traktionsbereich hauptsächlich IGBTs zum Einsatz. Für zukünftige Applikationen, die eine höhere Schaltfrequenz als 10 kHz erfordern, steigen jedoch die sogenannten Schaltverluste stark an, was sich nachteilig auf den Wirkungsgrad des Antriebs auswirkt.

Mit SIC-Leistungshalbleiter kann dieser Nachteil bei hohen Schaltfrequenzen jedoch reduziert werden.

Beim Einsatz von SIC-Leistungshalbleiter müssen besonders die Einflüsse auf die elektrische Maschine, wie Wicklungsisolation (Alterung) und Lager (Lagerströme), beachtet werden.

Beachtung finden aber auch die Einflüsse auf die EMV und NVH des elektrischen Antriebes.

Ferner soll natürlich auch der Einfluss auf den Wirkungsgrad des elektrischen Antriebes in unterschiedlichen Lastpunkten untersucht werden.

Abstract

In existing traction drive applications, mainly IGBT's will be used for the power semiconductors. For future applications with a demand on higher switching frequencies greater than 10 kHz, the so-called switching losses are also increased. This will have a negative impact to the efficiency of the electrical drive.

By using SIC-power semiconductors, these switching losses can be reduced.

On the other hand, by using SIC-power semiconductors, the impacts to the electrical machine, e.g. winding isolation (aging) and bearing (bearing currents) has to be considered.

Impact regarding EMC and NVH of the electrical drive will be also evaluated.

Further, the impact on the efficiency of the electrical drive in different working points should be investigated.

https://doi.org/10.51202/9783181023549 - Generiert durch IP 216.73.216.36, am 19.01.2026, 02:19:31. © Urheberrechtlich geschützter Inhalt. Ohne gesonderte Erlaubnis ist jede urheberrechtliche Nutzung untersagt, insbesondere die Nutzung des Inhalts im Zusammenhang mit, für oder in KI-Systemen, KI-Modellen oder Generativen Sprachmodellen.

1. Typical electrical drive train

In figure 1, a typical electrical drive train is depicted. Not considered in this figure is the battery charger and the mechanical transmission.

Normally the energy storage will be a Li-Ion-battery with a nominal voltage of approx. 300 V to 800 V. A typical inverter will be a three phase inverter based on IGBT-power switches with a switching frequency of approx. 10 kHz. The electrical machine for an axle drive can be a PSM, FSM or IM, tailored to the application.

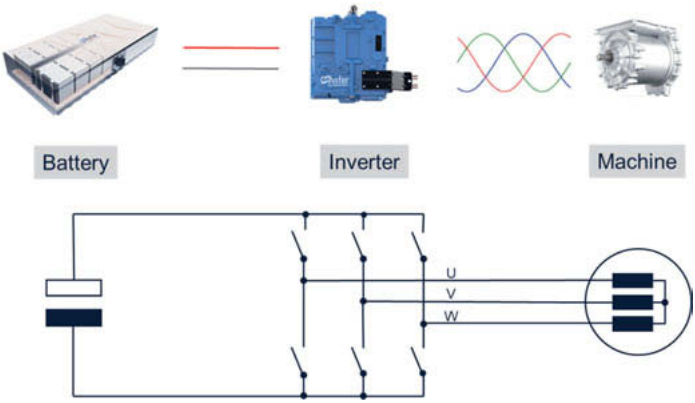


Fig. 1: Typical electrical drive

2. Motivation for using power-switches based on SIC-semiconductors

The power for a typical electrical traction drive is in a range of 80 to 300 kW. The typical losses within the electrical drive is in a range of 3% to 7% related to the total losses of the electrical car.

Compared to the existing SI-technology (IGBT), the SIC-Technology can provide many advantages like, higher reverse voltages, higher switching frequencies, lower switching – and conducting losses. Together with a higher thermal conductivity, we can achieve a very compact and efficient power electronic for drive train applications.

The improvement of power, power density and efficiency in relation with a simultaneous reduction of the total assembly space, weight and costs are big advantages for future electrical cars.

https://doi.org/10.51202/9783181023549 - Generiert durch IP 216.73.216.36, am 19.01.2026, 02:19:31. © Urheberrechtlich geschützter Inhalt. Ohne gesonderte Erlaubnis ist jede urheberrechtliche Nutzung untersagt, insbesondere die Nutzung des Inhalts im Zusammenhang mit, für oder in KI-Systemen, KI-Modellen oder Generativen Sprachmodellen.

3. SIC-semiconductors for compact and efficient electrical drives

3.1 Advantages of SIC-semiconductors

The semiconductor material of SIC has a big band gap compared to the other materials. These offers many advantages.

In figure 2 the material properties of two different semiconductors are depicted.

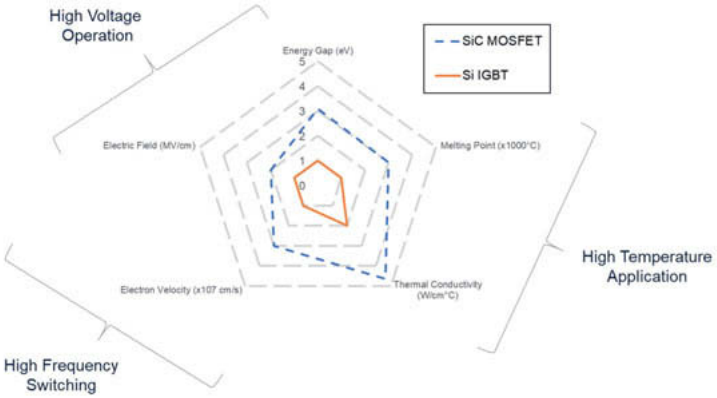


Fig. 2: Comparison of power semiconductors

As well as silicon carbide as gallium nitride to have better electrical properties as silicon and enable higher switching frequencies and lower one state resistance especially within partly load. Further SIC has excellent thermal properties whereby very high operation temperature are possible and the demand for cooling can be reduced.

If we compare two power devices (1200 V / 300 A) based on silicon or silicon carbide directly, it can be depicted in figure 3, that especially the switching losses within the SIC-module is much lower. But the voltage drop related to the nominal current is higher. Besides the lower switching losses the high board thermal capacity of the SIC-components is also a further advantages. Especially, with an inverter with high efficiency, the demand for cooling can be reduced significantly and therefore also the installation space, the weight and system costs.

https://doi.org/10.51202/9783181023549 - Generiert durch IP 216.73.216.36, am 19.01.2026, 02:19:31. © Urheberrechtlich geschützter Inhalt. Ohne gesonderte Erlaubnis ist jede urheberrechtliche Nutzung untersagt, insbesondere die Nutzung des Inhalts im Zusammenhang mit, für oder in KI-Systemen, KI-Modellen oder Generativen Sprachmodellen.

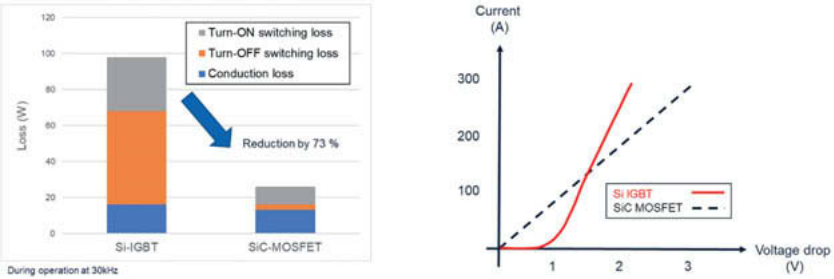


Fig. 3: Comparison of power losses

And in figure 4 there is shown a comparison for a given application realized with IGBT and SIC.

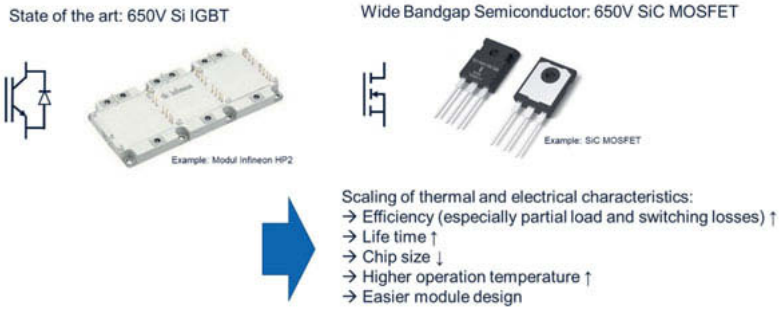


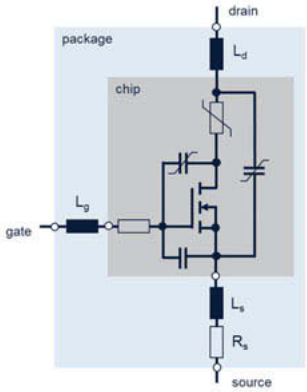
Fig. 4: Technical comparison

3.2 Disadvantages of SIC-semiconductors

The practical implementation of the “positive” technical properties to economical products and applications also some “negative” properties has to be considered:

- The manufacturing process of silicon carbide crystals is very expensive at this time
- SIC- wafer to this day contains 5 - 10 defects per cm^2 (micropipes). That means, an acceptable yield will only be possible for small chips.
- SIC-wafer are with 3” much lower as Si-Wafer with 6” to 8”
- Also the „parasitics“ will be more important compared to existing solutions (see figure 5 and 6)

https://doi.org/10.51202/9783181023549 - Generiert durch IP 216.73.216.36, am 19.01.2026, 02:19:31. © Urheberrechtlich geschützter Inhalt. Ohne gesonderte Erlaubnis ist jede urheberrechtliche Nutzung untersagt, insbesondere die Nutzung des Inhalts im Zusammenhang mit, für oder in KI-Systemen, KI-Modellen oder Generativen Sprachmodellen.



	Typical Package Inductance		
	Module	TO-247	TO-220
L_d [nH]	20…40**	4…7 (<1)*	3…5 (<1)*
L_g [nH]		12…14	7…12
L_s [nH]		9…16	6…12

* Via tab
** total inductance (Ld+Ls)

Fig. 5: Parasitics of a power semiconductor

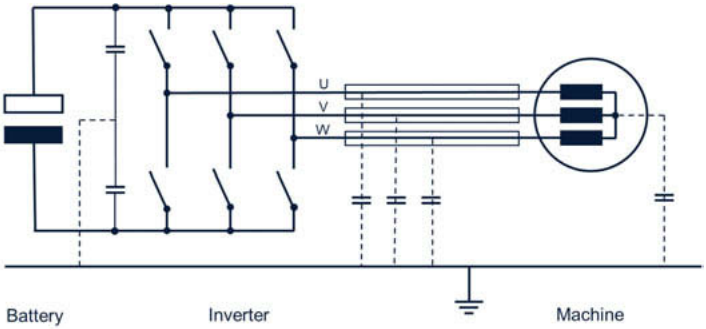


Fig. 6: Parasitics Capacities

Summary:
SIC-Chips have many advantages, but are more expensive as SI-Chips. Therefore, it is very important to consider the system costs in total.

4. Reduction of current ripple in an electrical machine

As very well known, the power density of an electrical machine can be increased by increasing the speed of the electrical machine. That means, it is possible to reduce the installation space by increasing the speed under remaining the peak power of the electrical machine. For such

https://doi.org/10.51202/9783181023549 - Generiert durch IP 216.73.216.36, am 19.01.2026, 02:19:31. © Urheberrechtlich geschützter Inhalt. Ohne gesonderte Erlaubnis ist jede urheberrechtliche Nutzung untersagt, insbesondere die Nutzung des Inhalts im Zusammenhang mit, für oder in KI-Systemen, KI-Modellen oder Generativen Sprachmodellen.

kind of applications, we have to adapt the number of pol pairs of the electrical machine and also the switching frequency of the inverter.

For typical existing applications a switching frequency of approx. 4 kHz to 10 kHz will be applied in order to achieve a max. fundamental frequency of approx. 1 kHz. Typical voltage /current-characteristics are depicted in figure 7. For a higher speed of the electrical machines it makes sense to increase the switching frequency.

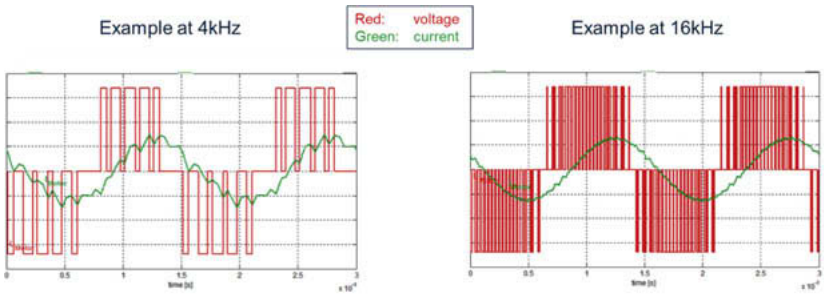


Fig. 7: Current Characteristic: Influence of switching frequency

Especially for high speed applications the inductance within high utilized electrical machines are comparable low. Because the inverter has a switching operation, the phase current in the electrical machine have many harmonics. These current harmonics produces additional ohmic losses within the electrical machine and will contribute to heat up the machine.

Usually the electrical parameters (resistance, inductivity and magnetic flux) are treated as constants. However, especially the inductivity may vary in a range up to 40%, depending on the actual rotor position and the stator currents. The reason for the high variation of the inductance will also described as saturation of the iron within the magnetic circuit (see figure 8).

The comparable low inductance within the saturation area leads also to higher amplitudes of the current harmonics.

https://doi.org/10.51202/9783181023549 - Generiert durch IP 216.73.216.36, am 19.01.2026, 02:19:31. © Urheberrechtlich geschützter Inhalt. Ohne gesonderte Erlaubnis ist jede urheberrechtliche Nutzung untersagt, insbesondere die Nutzung des Inhalts im Zusammenhang mit, für oder in KI-Systemen, KI-Modellen oder Generativen Sprachmodellen.

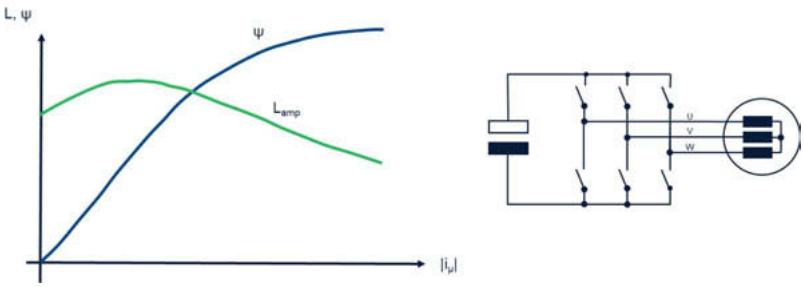


Fig. 8: Saturation within an electrical machine

5. Influences regarding the winding insulation (aging) of the electrical machine

The development of compact and efficient electrical machines is connected with the improvement of the properties of the insulation system, especially in relation to the electrical, thermal, chemical and mechanical stress.

For example, the wire insulation of the winding within the electrical machine, will be stressed with approx. 2 times of the DC-Link voltage.

The reason for this over voltage is the super position of the reflected voltage wave with the inverter output voltage.

A so called travelling wave will arise, if a rectangular voltage with a very high rising edge (in a range of ns), that means very high frequency.

This so called “reflected wave phenomena” will arise, if the wave impedance will change during the direction of a wave.

In the figure 9 the reflection and refraction of a voltage travelling wave is depicted.

https://doi.org/10.51202/9783181023549 - Generiert durch IP 216.73.216.36, am 19.01.2026, 02:19:31. © Urheberrechtlich geschützter Inhalt. Ohne gesonderte Erlaubnis ist jede urheberrechtliche Nutzung untersagt, insbesondere die Nutzung des Inhalts im Zusammenhang mit, für oder in KI-Systemen, KI-Modellen oder Generativen Sprachmodellen.

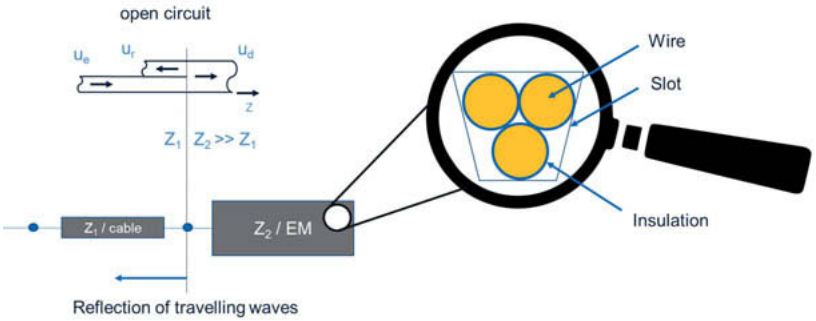


Fig. 9: Impact to winding insulation

The grade of reflection can be determined with the following equation:

$$r = \frac{Z_2 - Z_1}{Z_2 + Z_1}$$

r: $Reflection\ coefficient$
Z_1: $Wave\ impedance\ of\ the\ cable$
Z_2: $Wave\ impedance\ of\ the\ elctric\ machine$

The relation between rise time t_r, and the critical cable length l_{crit} is

$$l_{crit} \approx \frac{\vartheta_{cable*} \cdot t_r}{2}$$

$$l_{crit}\ (IGBT) \approx 3{,}75m$$

$$l_{crit}\ (SIC) \approx 0{,}75m$$

ϑ_{cable}: $wave\ speed\ within\ the\ cable\ (typical\ 150\ m/\mu s)$
t_r: $rise\ time\ (IGBT\ \approx 0{,}05\ \mu s)(SSIC \approx 0{,}01\ \mu s)$

This voltage overshoot at the terminal of the electrical machine can lead to a so called “partial discharge” within the winding of the electrical machine and can accelerate the aging of the insulation material.

6. Influences regarding EMI

The pulsating operation behaviour of the power electronics can lead to the following challenges:

https://doi.org/10.51202/9783181023549 - Generiert durch IP 216.73.216.36, am 19.01.2026, 02:19:31. © Urheberrechtlich geschützter Inhalt. Ohne gesonderte Erlaubnis ist jede urheberrechtliche Nutzung untersagt, insbesondere die Nutzung des Inhalts im Zusammenhang mit, für oder in KI-Systemen, KI-Modellen oder Generativen Sprachmodellen.

- Disturbance of sensor or radio receiver
- Non-admission of a car due to EMC-regulations and norm
- Bearing currents in the electrical machine and transmission

The following considerations are based on an electrical powertrain depicted in figure 10.
The power electronics linked the DC-site to the AC-site. The transformation from DC-voltage to the three phase system take place via pulse with modulation or space vector modulation for example. This is the reason for the conducted HF-disturbance signals, transmitted from the power electronics.

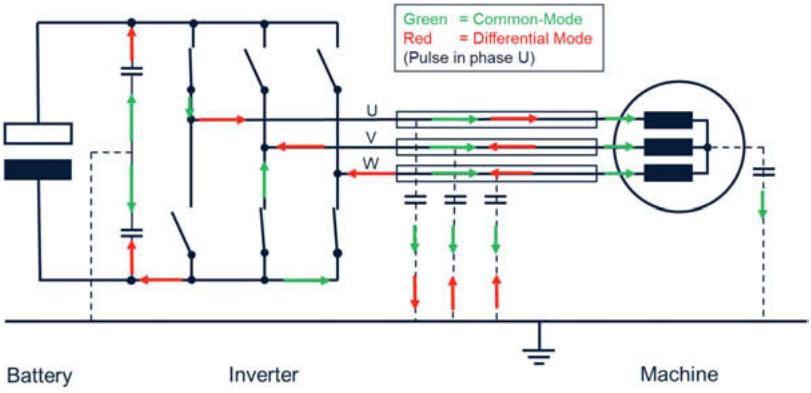


Fig. 10: CM/DM- Mode in a 3 Phase system

As mentioned before the reason for the common mode voltage is the super position of the three phases. The definition of the common mode voltage can be described as the average of the three phase voltages related to Ground (see figure 11)

$$u_{cm} = \frac{u_{u0} + u_{v0} + u_{w0}}{3}$$

u_{cm} contains only discrete values.

$$u_{cm} = \pm\frac{u_d}{2}, \pm\frac{u_d}{6}$$

https://doi.org/10.51202/9783181023549 - Generiert durch IP 216.73.216.36, am 19.01.2026, 02:19:31. © Urheberrechtlich geschützter Inhalt. Ohne gesonderte Erlaubnis ist jede urheberrechtliche Nutzung untersagt, insbesondere die Nutzung des Inhalts im Zusammenhang mit, für oder in KI-Systemen, KI-Modellen oder Generativen Sprachmodellen.

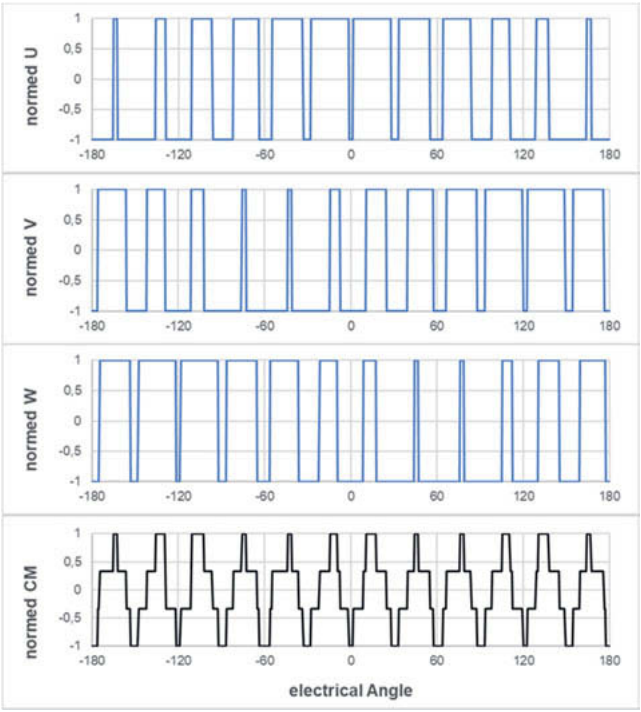


Fig. 11: Generation of CM voltage

The EMI behaviour of the power electronics can be characterized for a typical pulse. In figure 12 the related frequency spectrum is depicted.

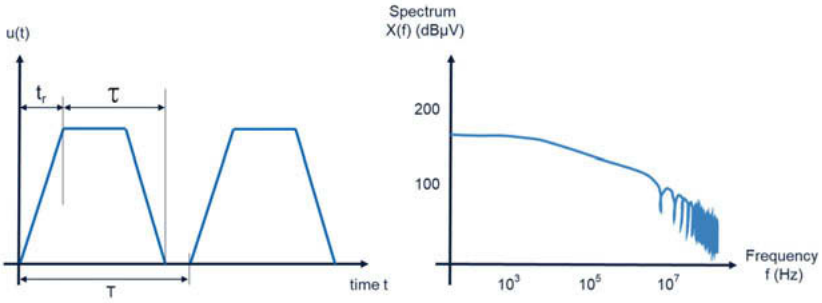


Fig. 12: Spectrum of a typical pulse

https://doi.org/10.51202/9783181023549 - Generiert durch IP 216.73.216.36, am 19.01.2026, 02:19:31. © Urheberrechtlich geschützter Inhalt. Ohne gesonderte Erlaubnis ist jede urheberrechtliche Nutzung untersagt, insbesondere die Nutzung des Inhalts im Zusammenhang mit, für oder in KI-Systemen, KI-Modellen oder Generativen Sprachmodellen.

The disturbance spectrum is given by the following equation:

$$X_{(f)} = 2U_d * \frac{\tau}{T} * \frac{\sin(\pi * f * \tau)}{\pi * f * \tau} * \frac{\sin(\pi * f * t_r)}{\pi * f * t_r}$$

U_d: $DC - link\ voltage$
τ : $Pulse\ time$
t_r : $Rise\ time$
T : $Switching\ time$
f : $Frequency$

The spectrum is initially constant until a frequency of 10 kHz. Over f = 10 kHz, the frequency will be decreased with 20 dB per decade. Over a frequency f > 1,6 MHz, the spectrum will be decreased to 40 dB.
The second cut off frequency is resulting from the term:

$$\frac{sin(\pi * f * t_r)}{\pi * f * t_r}$$

If we are increase the rise time t_r, that means to reduce the voltage stepless also the value of the spectrum will be reduced in the higher frequency range.

7. Technical reasons for special bearing currents in the EM

There are mainly two reasons for high frequency bearing currents within inverter supplied electrical machines. On the one hand leads the rectangular output voltage of the inverter to a common mode voltage, on the other the design of a three phase electrical machine built up a common mode circuit, mainly consisting of distributed capacities and supplied from the common mode voltage, see figure 13.

In this paper exemplary the capacitive current also described as a du/dt-current will be considered.

https://doi.org/10.51202/9783181023549 - Generiert durch IP 216.73.216.36, am 19.01.2026, 02:19:31. © Urheberrechtlich geschützter Inhalt. Ohne gesonderte Erlaubnis ist jede urheberrechtliche Nutzung untersagt, insbesondere die Nutzung des Inhalts im Zusammenhang mit, für oder in KI-Systemen, KI-Modellen oder Generativen Sprachmodellen.

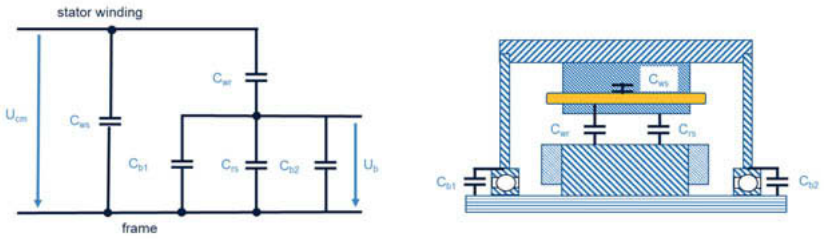


Fig. 13: HF-structure of an electrical machine

8. Reduction of the common mode voltage via special space vector modulation

As mentioned, the reason for appearing the capacitive injected interferences (voltages, currents) can be found in the existence of a common mode voltage U_{cm}.

Due to the fact, that the generation of the common mode voltage is given by pulsing in the power electronics it makes sense to change the used pulse pattern in order to reduce the common mode voltage on the one hand and reduce the number of switching ramps within the common mode voltage.

A new approach to utilize both possibilities without influencing the grad of modulation provides the method of “sequential pulse placement” (SPI). The SIP is based on the basic classical space vector modulation depicted in figure 14.

The modification of the pulse pattern consists in a replica of a reference voltage space vector based on two border vectors in combination with yours against vectors.

For example to build up a reference voltage space vector within sector 1.

A possible switching sequence could be $\underline{u}_1$, $\underline{u}_2$, $\underline{u}_5$ as described in the figure 14.

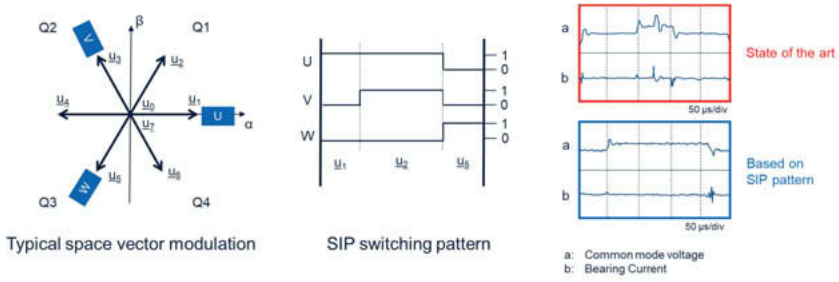


Fig. 14: Reduction of bearing currents: SIP-space vector modulation

https://doi.org/10.51202/9783181023549 - Generiert durch IP 216.73.216.36, am 19.01.2026, 02:19:31. © Urheberrechtlich geschützter Inhalt. Ohne gesonderte Erlaubnis ist jede urheberrechtliche Nutzung untersagt, insbesondere die Nutzung des Inhalts im Zusammenhang mit, für oder in KI-Systemen, KI-Modellen oder Generativen Sprachmodellen.

The advantages is to neglect the zero vectors as used in the classical space vector modulation, therefore the common mode voltage can be reduced if the SIP - method will be applied.
In the figure 14, the measurement results confirm the use of SIP in view of a reduced common mode voltage and bearing current.

9. Summary

Especially for high power electrical traction drives in relation with high utilized electrical machines, it is possible to achieve a very compact and efficient power electronics by using SIC.
Concerning cost issues, we have to consider the total costs of an electrical drive system and not only the costs for the power modules.
In this context by using SIC, it is very important to know also the impacts to an electrical drive regarding over voltages (aging of winding insulation), EMI-behaviour and bearing currents and also to know counter measures in order to reduce these “negative” impacts.

https://doi.org/10.51202/9783181023549 - Generiert durch IP 216.73.216.36, am 19.01.2026, 02:19:31. © Urheberrechtlich geschützter Inhalt. Ohne gesonderte Erlaubnis ist jede urheberrechtliche Nutzung untersagt, insbesondere die Nutzung des Inhalts im Zusammenhang mit, für oder in KI-Systemen, KI-Modellen oder Generativen Sprachmodellen.

https://doi.org/10.51202/9783181023549 - Generiert durch IP 216.73.216.36, am 19.01.2026, 02:19:31. © Urheberrechtlich geschützter Inhalt. Ohne gesonderte Erlaubnis ist jede urheberrechtliche Nutzung untersagt, insbesondere die Nutzung des Inhalts im Zusammenhang mit, für oder in KI-Systemen, KI-Modellen oder Generativen Sprachmodellen.

Challenges of sensorless high-speed drives with PM motors

Ing. **Marek Stulrajter**, Ph.D, Ing. **Matej Pacha**, Ph.D,
NXP Semiconductors, Roznov pod Radhostem, Czech Republic

Abstract

The paper deals with three-phase permanent magnet (PM) machines operated in the high-speed region and sensorless mode. The most common PM machines in the automotive area are permanent magnet synchronous motors (PMSM) and brushless DC motors (BLDC). A six-step commutation technique is used to control the BLDC motors, with disconnected motor phase for sensorless operation. Conventional field-oriented control (FOC) extended with a Back-EMF observer is used for PMSMs control without position sensor. The aim of the paper is to describe limitations of these basic sensorless control techniques focusing on challenges in high speed area, and to introduce tips and tricks how to extend the speed operating range.

1 Introduction

Nowadays, a wide variety of high-speed drives is becoming more and more popular within industrial motor control applications. Industries like automotive, aerospace, or medical with applications such as machine tools, gas compression, turbochargers, pumps and so on, profit from the high ratio factor between high-power density and given weight-volume. In other words, high-speed motors are designed to be gearless machines. Gearless feature is aligned with the cost and size reduction trend, and brings the performance, efficiency and reliability increase due to the gearbox absence. On the contrary, high-speed operation without gearbox makes the challenge for machine designers as well as the motor control designers.

From the electric machine design perspective, there are several motor types available today and being considered for high-speed applications. In general, induction machines, reluctance machines, or machines utilizing permanent magnets for excitation, are candidates combining different features that may be considered as a pros or cons depending on the application requirements.

Induction machines (ACIM), known as asynchronous, bring simple, cheap and robust construction without permanent magnets, low cost maintenance, and capability to operate in open loop control or in volt per hertz control. The list of disadvantages starts with higher magnetizing current and losses in the rotor bars which go against the high efficiency requirement in automotive. Further, the field-oriented control and sensorless control of ACIMs are indeed complex

https://doi.org/10.51202/9783181023549 - Generiert durch IP 216.73.216.36, am 19.01.2026, 02:19:31. © Urheberrechtlich geschützter Inhalt. Ohne gesonderte Erlaubnis ist jede urheberrechtliche Nutzung untersagt, insbesondere die Nutzung des Inhalts im Zusammenhang mit, für oder in KI-Systemen, KI-Modellen oder Generativen Sprachmodellen.

which may be an issue if assuming the CPU utilization in microprocessor control. Despite these facts, there are intentions to use ACIMs with solid rotors in the high-speed applications [2,3] also in sensorless mode with improved stator flux estimators, and speed observers [4,5]

The most known motors from the reluctance machine category are reluctance synchronous motor (RSM) and switched reluctance motor (SRM). RSM combines the features of ACIM and the reluctance torque which is achieved by introducing barriers into the rotor. This yields to the induction machine operated synchronously. RSMs are known by significant variation of parameters which makes the control more difficult, especially the sensorless techniques. SRMs are characterized by a simple rotor and stator construction, without any PMs or coils on the rotor. This makes these motors very robust and fault tolerant with relatively simple control even in sensorless mode [6]. These motors are used in high-speed applications in military, space, and domestic applications, aviation and automotive traction applications, i.e. hybrid-electric vehicles, and mining industry, energy storage, and recovery systems [7,8,9].

All above mentioned PM-less motor types have one common issue. Lower efficiency factor does not meet the requirements coming from battery applications like hybrid or battery electric vehicles. Due to this reason, the PM machines are naturally being investigated and considered as a solution for high-speed applications. In other words, if assuming up to base speed operation, negligible excitation (reactive) power leads to unity power factor operation and makes PM machines very attractive. There is a wide spectrum of PM motors. The paper focuses on three-phase machines, the brushed DC motors are not considered.

Three-phase permanent magnet synchronous motor (PMSM), also known as a sinusoidal Back-EMF motor, utilizes the magnetizing energy from the PMs located on the rotor that yields to low excitation losses. Thanks to rapid progress in power and microelectronics and advanced motor design methods, high efficient super highspeed PMSM drives are possible [10]. High-speed operation requires also higher sampling rate hence more frequent FOC calling. However, the FOC execution time versus available calculation time-window given by sampling frequency defines the limits for MCU controller. The shorter execution of the control algorithm the higher sampling frequency can be selected and higher speed level targeted.

Brushless direct current (BLDC) motor, known as a trapezoidal Back-EMF motor, also benefits from the PM on the rotor. However, trapezoidal induced voltage requires a trapezoidal control approach to achieve high performance and high efficiency. A six-step commutation control is primarily used for BLDC motors, which combines a huge advantage of simplicity, short execution time, and easy migration to a sensorless configuration. On the contrary, torque ripple coming from the commutation events which yields to noise, vibration and lower EMC, may be a limiting factor for some industrial applications. However, the fact that control algorithm is much

https://doi.org/10.51202/9783181023549 - Generiert durch IP 216.73.216.36, am 19.01.2026, 02:19:31. © Urheberrechtlich geschützter Inhalt. Ohne gesonderte Erlaubnis ist jede urheberrechtliche Nutzung untersagt, insbesondere die Nutzung des Inhalts im Zusammenhang mit, für oder in KI-Systemen, KI-Modellen oder Generativen Sprachmodellen.

simpler than FOC makes BLDC motors well suited for high-speed applications pumps, funs, [11].

To ensure the highest performance of the PM motors operated within entire speed range, the FOC as well as six-step control require the rotor position information. Assuming the PMSM applications, then the rotor position sensor coupling brings difficulties at high speeds thus the sensorless approach is a subject of the feasibility study. The BLDCs mainly use HALL sensors to determine the rotor sector position. Even if the HALL is contact-less, there is an intention to remove it and operate BLDCs in sensorless mode.

This article

2 Permanent Magnet Machines in Automotive

Omitting the stepper motors and brushed DC motors, the most popular PM motors in automotive area are PMSM and BLDC motors. Both motors are three-phase, with PM on the rotor, supplied by a voltage source inverter, running at synchronous speed and both needs the rotor position information. Despite these common features, these two motors are different.

The major difference between these two motors is in the shape of magnetic field distribution inside the motor air gap. This shape is given by the type of the PM magnetisation. Radial magnetisation leads to rectangular shape of magnetic field distribution, while parallel magnetisation produces a sinusoidal shape of the magnetic field distribution. [12]

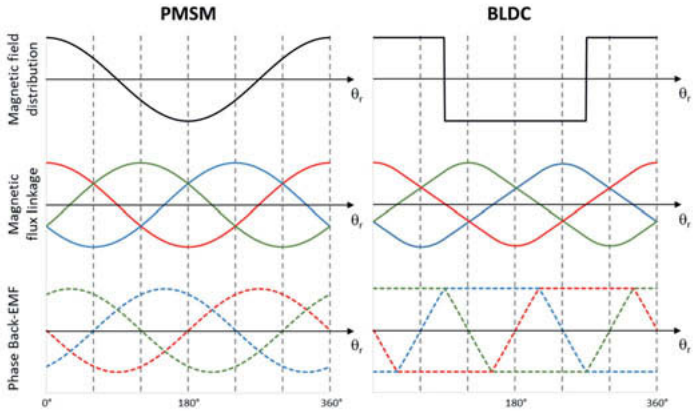


Fig. 1: Magnetic field distribution in PM motor

As shown in Fig. 1, the sinusoidal magnetic field distribution leads to the sinusoidal flux linkage. Forming a rotary field, the shape of induced voltages (Back-EMF) is sinusoidal and we refer to

https://doi.org/10.51202/9783181023549 - Generiert durch IP 216.73.216.36, am 19.01.2026, 02:19:31. © Urheberrechtlich geschützter Inhalt. Ohne gesonderte Erlaubnis ist jede urheberrechtliche Nutzung untersagt, insbesondere die Nutzung des Inhalts im Zusammenhang mit, für oder in KI-Systemen, KI-Modellen oder Generativen Sprachmodellen.

such motor as to sinewave machine or PMSM. The rectangular magnetic field distribution forms a triangle shape flux linkage, and trapezoidal shape of induced voltage. In this case, we refer to a trapezoidal machine or BLDC motor.

Fig. 1 shows an ideal case of both motors, in fact the real PMSM contains higher harmonic components in the Back-EMF, e.g. 5^{th}, 7^{th}, 9^{th} or 11^{th}. The smaller magnitude of these harmonic components, the higher quality PMSM motor. The Back-EMF shape of both motors depends on several factors like quality of magnets, magnetisation, saturation and so on. The more realistic phase Back-EMF waveform of BLDC motor is depicted in Fig. 2.

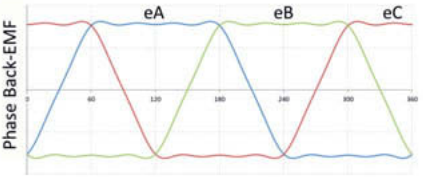


Fig. 2: Phase Back-EMF voltages of real BLDC motor

Having the PM motors identified, then the proper control technique can be proposed. The FOC is used to generate a sinusoidal phase current. Applying the FOC to PMSM motors the resulting toque will be smooth. In case of BLDC, there is a DC value seen in the Back-EMF waveform, however only in two phases at any time. It means, the same pattern of the supply voltage should be applied to achieve maximal torque. The most conventional control technique for BLDC motors is six-step commutation control where only two phases are excited at any time and the third one is disconnected at the same time.

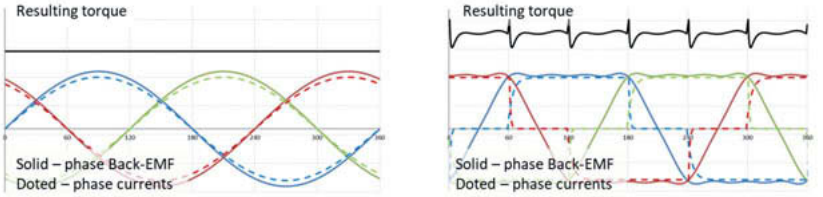


Fig. 3: Torque production PMSM with FOC (left) and BLDC with 6-step control (right)

As seen in Fig. 3, the combination of FOC and sinewave machine (PMSM) results to a smooth torque operation without any noise, vibration and electromagnetic emissions coming from the control itself. On the contrary, six-step commutation approach introduces a significant ripple into the torque. The main source of the torque ripple is commutation process, where a new

https://doi.org/10.51202/9783181023549 - Generiert durch IP 216.73.216.36, am 19.01.2026, 02:19:31. © Urheberrechtlich geschützter Inhalt. Ohne gesonderte Erlaubnis ist jede urheberrechtliche Nutzung untersagt, insbesondere die Nutzung des Inhalts im Zusammenhang mit, für oder in KI-Systemen, KI-Modellen oder Generativen Sprachmodellen.

voltage vector is applied, and a new set of phases is conducting current. Despite this drawback, the BLDC motors are very popular in pump or fan applications where torque ripple does not play a role, but the simplicity and robustness are appreciated.

3 Sensorless control of BLDC motor – six-step commutation control

In the brushed DC motor, the commutator and brushes reverse the current polarity in rotor winding such way that stator field created by PMs and rotor magnetic field are perpendicular. The BLDC motor is equivalent to an inverted brushed DC motor, where the magnet rotates while the conductor remains stationary. The current polarity control is performed electronically by power transistors based on the rotor flux position. This process is called commutation.

The position of the rotor can be obtained by a position sensor or a proper sensorless technique. BLDC motor does not require an absolute sensor, a simple sensor returning the information about the physical pole edge on the rotor. For that reason, a simple, reliable and contactless Hall effect sensor is used [13].

For space constrain applications or cost reductions reasons, a sensorless control of BLDC may be required. In six-step commutation control, the BLDC is operated in two-phase model were only two phases are energized at any time while the third phase is disconnected. Thanks to Faraday's law and electromagnetic induction, the electromotive force (EMF) is produced on disconnected phase by a moving magnetic (rotor) field. In other words, the motor phase behaves as a sensor during the time it is neither powered nor grounded. The voltage seen on the terminal of disconnected phase is known as back electromotive force (BEMF) and depends on the flux ψ of the permanent magnets and the speed ω and position θ of rotating magnetic field – the rotor.

$$BackEMF\ voltage = \frac{d\psi}{dt} = \frac{\partial\psi}{\partial\theta} \cdot \frac{\partial\theta}{dt} = \frac{\partial\psi}{\partial\theta} \cdot \omega$$

Measured back-EMF has the shape displayed in Fig. 2. This waveform is directly linked with the rotor position, and zero-crossing instances can be used to estimate the sector of the rotor position. Precise evaluation of the zero-cross event requires the back-EMF voltage to be sensed properly.

3.1 Back-EMF Voltage Sensing

Precise and synchronized measurement of the back-EMF voltage is key for sensorless operation of the BLDC motor. For back-EMF sensing, the PWM signal is applied on the high-side switches and back-EMF voltage has to be sampled during the PWM on-time, Fig. 4.

https://doi.org/10.51202/9783181023549 - Generiert durch IP 216.73.216.36, am 19.01.2026, 02:19:31. © Urheberrechtlich geschützter Inhalt. Ohne gesonderte Erlaubnis ist jede urheberrechtliche Nutzung untersagt, insbesondere die Nutzung des Inhalts im Zusammenhang mit, für oder in KI-Systemen, KI-Modellen oder Generativen Sprachmodellen.

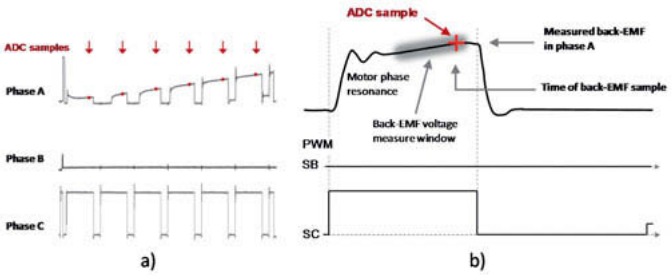


Fig. 4: Back-EMF voltage measurement

Once the back-EMF voltage measurement is successfully done a postprocessing is needed to evaluate the real BEMF zero-cross event and estimate the next commutation event [11].

3.2 Back-EMF Voltage Zero-cross Method

The method calculates the next commutation time T_{CMT} which is derived from the time of actual zero-cross event T_{ZC} and the time of previous zero-cross event T_{ZC-1}, Fig. 5.
Zero-crossing instants measurement is improved by applying an interpolation method in case the real zero-cross instant lies between two samples of measured back-EMF, and then the next commutation event appears at T_{CMT}, [11,14].

https://doi.org/10.51202/9783181023549 - Generiert durch IP 216.73.216.36, am 19.01.2026, 02:19:31. © Urheberrechtlich geschützter Inhalt. Ohne gesonderte Erlaubnis ist jede urheberrechtliche Nutzung untersagt, insbesondere die Nutzung des Inhalts im Zusammenhang mit, für oder in KI-Systemen, KI-Modellen oder Generativen Sprachmodellen.

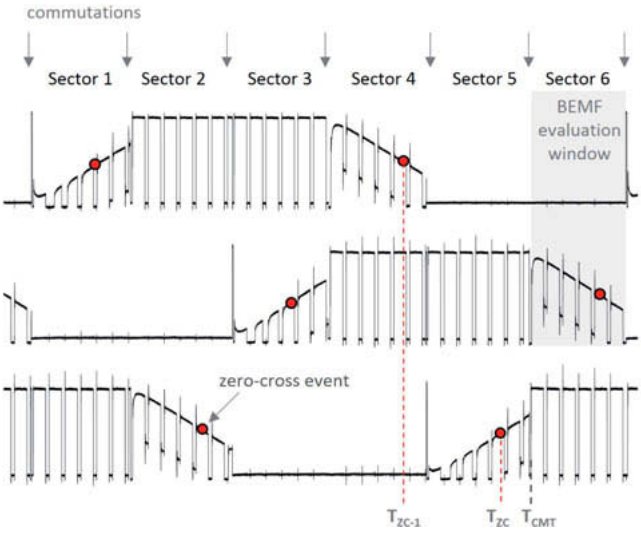


Fig. 5: Back-EMF zero-cross detection method principle

4 Sensorless control of PMSM – field-oriented control

High-performance motor control is characterized by smooth rotation over the entire speed range, full torque control at zero speed, and fast acceleration/deceleration. To achieve such control, field-oriented control is used for PM synchronous motors. The FOC concept is based on an efficient torque control requirement, which is essential for achieving a high control dynamic.

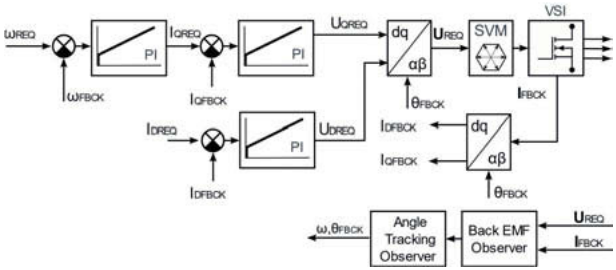


Fig. 6: Conventional FOC scheme in sensorless mode

https://doi.org/10.51202/9783181023549 - Generiert durch IP 216.73.216.36, am 19.01.2026, 02:19:31. © Urheberrechtlich geschützter Inhalt. Ohne gesonderte Erlaubnis ist jede urheberrechtliche Nutzung untersagt, insbesondere die Nutzung des Inhalts im Zusammenhang mit, für oder in KI-Systemen, KI-Modellen oder Generativen Sprachmodellen.

In case of PMSM and FOC (Fig. 6), the information about the rotor flux position must be as precise as possible. For that purpose, an absolute or relative mechanical sensor has to be used. The most common sensors are resolvers, encoders or GMR. These sensors are, however, expensive and space consuming. As an alternative solution, a sensorless control can be used. Nowadays, there are numerous sensorless techniques available. They are categorized based on the operating speed range, e.g. zero and very low speeds or mid and high-speeds. Anisotropy-based techniques utilizing high-frequency excitation signal are used for low speeds, while model-based techniques are used for mid and high-speeds [15]. This paper targets the high-speed applications with model-based observers to estimate Back-EMF and rotor position.

4.1 Back-EMF voltage observer

It is well known, that the rotor position information is included in the back-EMF voltage generated by the rotor movement. Because the back-EMF in PM synchronous motors rises proportionally with the rotor angular speed, above certain speed the generated back-EMF is in amplitude large enough to be sufficiently separated from the noise and therefore sensorless techniques based on calculation of the rotor position from the motor model can be utilized.

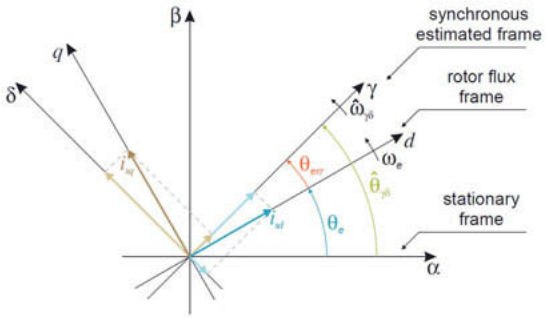


Fig. 7: Estimated and real reference frame

The proposed method is based on estimating the saliency based back-EMF of the motor model transformed into a quasi synchronously rotating quadrature frame and adjusting the position of the frame, such as to minimize the amplitude of EMF voltage in the γ-axis of the estimated frame (Fig. 7). To make the observer more robust, it is advantageous to form the observer in

https://doi.org/10.51202/9783181023549 - Generiert durch IP 216.73.216.36, am 19.01.2026, 02:19:31. © Urheberrechtlich geschützter Inhalt. Ohne gesonderte Erlaubnis ist jede urheberrechtliche Nutzung untersagt, insbesondere die Nutzung des Inhalts im Zusammenhang mit, für oder in KI-Systemen, KI-Modellen oder Generativen Sprachmodellen.

both γ and δ axes. Then the resulting back-EMF estimates can be divided, to extract the information about the displacement between the estimated and rotor flux reference frames while reducing the effect of the observer parameter variation [1,16].

4.2 Position tracking observer

Position displacement θ_{ERR} is obtained as an arctangent of ratio between γ and δ back-EMF estimates. The goal is to drive the position of the estimated $\gamma\delta$ frame to achieve the zero displacement θ_{ERR}=0. A simple phase locked loop mechanism with standard PI controller used as the loop compensator is adopted as shown in Fig. 8, [1].

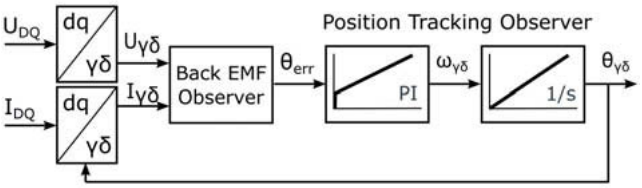


Fig. 8: Estimated and real reference frame

5 High-speed challenges in sensorless mode

Different motor requires different control technique and different control technique represents individual requirements for e.g. MCU configuration, control structure design, algorithm discretization or tuning processes. Many challenges are still posed like high-speed level exceeding the MCU capability, variable or dynamic speed operation, and requirement of stable control over a wide speed range [10].

5.1 BLDC and six-step commutation control - high speed limitations

The higher speed of the motor, the shorter commutation period and reduced number of PWM pulses in back-EMF signal is available. Reduced number of PWM pulses leads to reduced number of BEMF samples. Precision of both previously mentioned sensorless strategies depends on number of samples, the higher the better.

https://doi.org/10.51202/9783181023549 - Generiert durch IP 216.73.216.36, am 19.01.2026, 02:19:31. © Urheberrechtlich geschützter Inhalt. Ohne gesonderte Erlaubnis ist jede urheberrechtliche Nutzung untersagt, insbesondere die Nutzung des Inhalts im Zusammenhang mit, für oder in KI-Systemen, KI-Modellen oder Generativen Sprachmodellen.

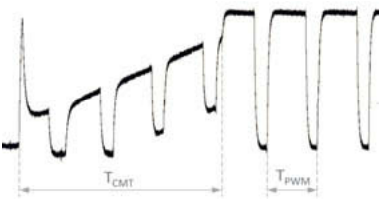


Fig. 9: Back-EMF shape during short commutation period

The ratio between the commutation period T_{CMT} and PWM period T_{PWM} indicates whether above mentioned sensorless techniques (Fig. 5) become limited. Commutation period for nominal angular speed ω_{el} can be calculated as follows:

$$T_{CMT} = \frac{1}{6 \times \frac{\omega_{el}}{2\pi}}$$

Three and more PWM pulses during the commutation period ensure enough high probability of a successful zero-cross detection and subsequently sensorless operation. Less than three PWM pulses will end up in fault mode. For that purpose, an oversampling approach has been proposed to overcome depicted limitation and extend the operation speed range [11].

5.2 PMSM and FOC - high speed operation considerations

Having the rotor spinning too fast, there is phenomenon that needs to be taken into the consideration. The rotor spins at a speed which moves the rotor from a position $\theta_{(1)}$ to position $\theta_{(2)}$ within one sampling period T_{samp}. This position offset θ_{OFF} may disturb the control because the acting voltages are calculated for rotor position at $\theta_{(1)}$, but rotor and rotor flux have changed their position in the meantime to $\theta_{(2)}$. Position offset θ_{OFF}, caused by the discrete control process , depends on the given sampling period and actual angular motor speed [17].

Having the position offset expressed, then it is possible to compensate it and suppress its negative impact to motor control performance. Fig. 10 shows an example of two approaches for a straight-forward delay compensation.

https://doi.org/10.51202/9783181023549 - Generiert durch IP 216.73.216.36, am 19.01.2026, 02:19:31. © Urheberrechtlich geschützter Inhalt. Ohne gesonderte Erlaubnis ist jede urheberrechtliche Nutzung untersagt, insbesondere die Nutzung des Inhalts im Zusammenhang mit, für oder in KI-Systemen, KI-Modellen oder Generativen Sprachmodellen.

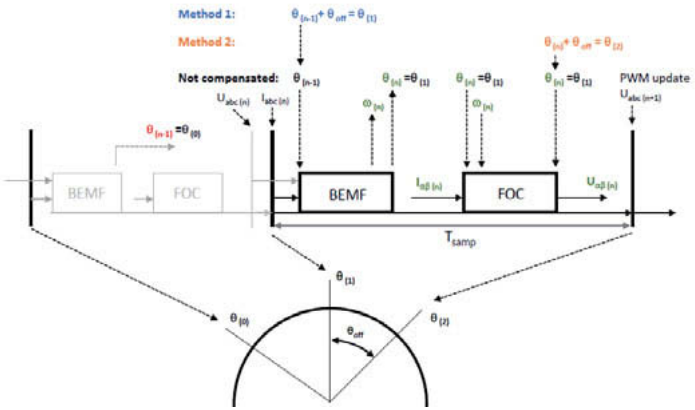


Fig. 10: Algorithm timing and rotor position at high speed operation

5.3 Computation power of the high-speed controller

Another key factor in the high-speed control is the MCU itself used for motor control. There is countless number of MCUs available on the market. Targeting the high-speed domain, it is suggested to pick the MCU with dedicated motor control feature set. The second important parameter is the performance of the MCU core which has an impact to execution time of the control algorithm.

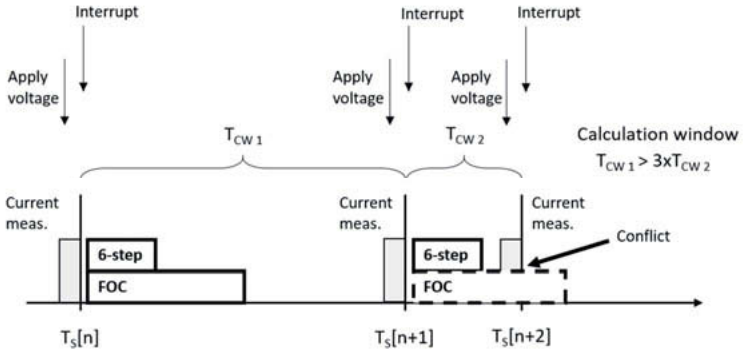


Fig. 11: Limitation by an execution time of the control algorithm

The motor control process is a real time interrupt driven procedure. The ADC end of conversion interrupt starts when all motor quantities are successfully processed and measured. Then the

https://doi.org/10.51202/9783181023549 - Generiert durch IP 216.73.216.36, am 19.01.2026, 02:19:31. © Urheberrechtlich geschützter Inhalt. Ohne gesonderte Erlaubnis ist jede urheberrechtliche Nutzung untersagt, insbesondere die Nutzung des Inhalts im Zusammenhang mit, für oder in KI-Systemen, KI-Modellen oder Generativen Sprachmodellen.

control algorithm calculates new set of voltage vector based on the reference and feedback signals. Different control techniques represent different complexity level that leads to different CPU load. As seen in Fig. 11, the FOC algorithm represents much complex task than six-step commutation control. In summary, the CPU utilization depends on the algorithm complexity and the computational power of the MCU.

The second parameter depicted in the Fig. 11 is the sampling time. The sampling frequency depends mainly on the electric motor and its parameters. Assuming high-speed drives, the motors are then characterized by a small electric time constant. In high-dynamic drives, a relatively small mechanical time constant characterizes the motor.

The most important criterion is then selection of the sampling frequency enough high for given high-speed motor and to be sure, that execution of the control algorithm does not exceed the calculation windows, as seen in Fig. 11.

6 High-Speed BLDC Sensorless Six-step Control

6.1 Back-EMF oversampling

The main goal is to get more samples of the back-EMF signal within one PWM pulse instead of one sample at the end of PWM pulse. Acquired data series is then used for back-EMF zero-cross estimation.

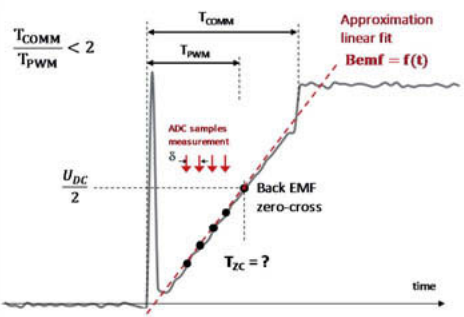


Fig. 12: Critical number of PWM pulses in back-EMF

Fig.6 shows a use-case when commutation period contains even less than two PWM pulses with 100% duty-cycle. In this case the first PWM pulse is oversampled to get a slope of investigated back-EMF. For this purpose, least-squares (LSQ) method has been adopted and implemented. LSQ method is a standard approach in linear regression analyses to approximate the oversampled (overdetermined) system. [11]

https://doi.org/10.51202/9783181023549 - Generiert durch IP 216.73.216.36, am 19.01.2026, 02:19:31. © Urheberrechtlich geschützter Inhalt. Ohne gesonderte Erlaubnis ist jede urheberrechtliche Nutzung untersagt, insbesondere die Nutzung des Inhalts im Zusammenhang mit, für oder in KI-Systemen, KI-Modellen oder Generativen Sprachmodellen.

6.2 Back-EMF reconstruction using LSQ method

Reconstructed envelop of oversampled back-EMF signal represents the time dependent function that can be used to calculate the zero-cross instant T_{ZC} even if the real zero-cross event appears outside the oversampled region. As seen in Fig. 12, the back-EMF signal has a linear shape and therefore linear approximation is implemented to find the best fit with the back-EMF envelope. Complete math description is available in [11].

The final Back-EMF zero-crossing formula:

$$\boldsymbol{T_{ZC}} = \frac{U_{DC}}{2a_1} - \frac{a_0}{a_1} + T_{1_0}$$

where a_0 and a_1 are coefficients for n-points approximation, U_{DC} is the DC-bus voltage and T_{1_0} is the time of the first sample of back-EMF voltage. Based on the number of samples, the matrix for a_0 and a_1 determination can be derived [11].

7 Experimental verification

Both types of PM motor have been verified experimentally. The BLDC motor was controlled by six-step commutation control with oversampling approach. Targeting application was high-speed pump. The PMSM motor was verified on turbocharger application controlled by sensorless FOC.

7.1 High-speed BLDC with back-EMF oversampling

Fig. 13 shows results at full speed, it means mechanical speed is 60 000rpm.

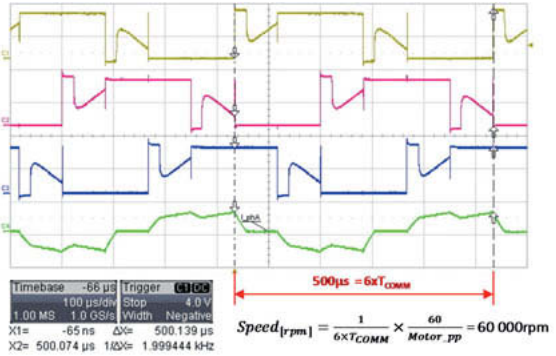


Fig. 13: Phase back-EMF signals and DC-link current at 60,000 rpm

[11] briefly introduces the conventional six-step commutation control of a BLDC motor in sensorless mode. It has been shown that standard sensorless approaches do have limitations if

https://doi.org/10.51202/9783181023549 - Generiert durch IP 216.73.216.36, am 19.01.2026, 02:19:31. © Urheberrechtlich geschützter Inhalt. Ohne gesonderte Erlaubnis ist jede urheberrechtliche Nutzung untersagt, insbesondere die Nutzung des Inhalts im Zusammenhang mit, für oder in KI-Systemen, KI-Modellen oder Generativen Sprachmodellen.

target the high-speed area. The lack of PWM pulses within a commutation interval significantly limits these methods.

A new approach using an oversampling and least square method offers a possibility to estimate the time of zero-crossing event. The oversampling approach brings an advantage of extending the motor operational range, however, it also increases a complexity of the control algorithm. This is important for a precise and synchronize timing of the application. It is highly recommended to use an MCU which directly supports multi-sampling synchronized with timer units and PWM unit.

7.2 High-speed PMSM with compensation

Based on the theoretical description, the PMSM motor was controlled by sensorless FOC with proposed compensations. Mechanical speed during the test was 10k rpm which is 80k rpm in electrical interpretation.

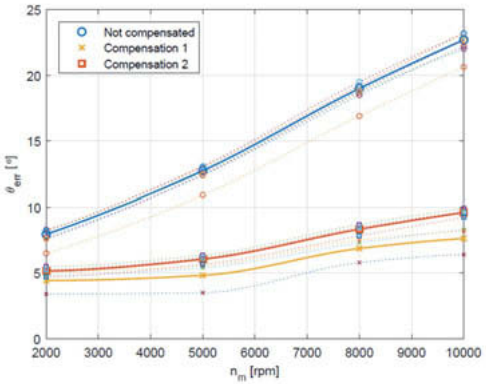


Fig. 15: Position steady-state error as function of speed with and without compensation

The position error means an offset between the reference frame position acquired by encoder and estimated reference frame, Fig. 7. Fig. 15 shows this position error as a function of the speed. All data points were measured in steady-state as the highest value of position error for given speed. With compensated delay the position error value drops significantly and improves the motor control performance.

To make the position error zero, the subject of further work is identification of all transportation delays in the control loop and their compensation.

https://doi.org/10.51202/9783181023549 - Generiert durch IP 216.73.216.36, am 19.01.2026, 02:19:31. © Urheberrechtlich geschützter Inhalt. Ohne gesonderte Erlaubnis ist jede urheberrechtliche Nutzung untersagt, insbesondere die Nutzung des Inhalts im Zusammenhang mit, für oder in KI-Systemen, KI-Modellen oder Generativen Sprachmodellen.

8 References

[1] Filka, R.: Sensorless Control of IPM Synchronous Motors for Entire Speed Range Including Start-Up, dissertations, University of Zilina, 2008

[2] Gieras, J. F., Saari , J.: Performance Calculation for a High-Speed Solid-Rotor Induction Motor, in IEEE Transactions on Industrial Electronics, 2012, vol. 59, iss. 6, pp. 2689 – 2700. ISSN 0278-0046.

[3] Pyrhonen, J., Nerg, J., Kurronen, P., Lauber, U.: High-Speed High-Output Solid-Rotor Induction-Motor Technology for Gas Compression, in IEEE Transactions on Industrial Electronics 2010

[4] Byoung-Gun Park, Dong-Jun Kim, Pil-Wan Han, Yon-Do Chun, Jae-Hak Choi: Sensorless control using improved stator flux estimator for high-speed induction motors, 2015 18th International Conference on Electrical Machines and Systems (ICEMS)

[5] Bo Wang, Yong Yu, Wei Sun, Dianguo Xu: High performance field-weakening control algorithm of sensorless induction motor using speed adaptive full-order observer, 2014 17th International Conference on Electrical Machines and Systems (ICEMS)

[6] 3-Phase Switched Reluctance (SR) Sensorless Motor Control Using a 56F80x, 56F8100 or 56F8300 Device, Application note, NXP Semiconductor, 2/2005, https://www.nxp.com/files-static/product/doc/AN1932.pdf

[7] Watkins, S. J., Winward, E.: Modelling and control of an ultra-high-speed switched reluctance machine, in 8th IET International Conference on Power Electronics, Machines and Drives (PEMD 2016)

[8] Besharati, M., Widmer, J., Atkinson, G., Pickert, V., Washington, J.: Super-high-speed switched reluctance motor for automotive traction, in 2015 IEEE Energy Conversion Congress and Exposition (ECCE), Pages: 5241 - 5248

[9] Yasa, Y., Sozer, Y., Garip, M.: High-speed switched reluctance machine: Natural frequency calculation and acoustic noise prediction. Turkish Journal of Electrical Engineering & Computer Sciences. 2018, pp. 999 - 1010.

[10] Zhao, L., Ham, Ch., Wu, S.-T., Zheng, L., Seigneur, H., Kalpathy, B. S., Kapat, J., Vaidya, J., Chow, L.: Development of A Super High-Speed Permanent Magnet Synchronous Motor (PMSM) Controller and Analysis of The Experimental Results. Journal of Systemics, Cybernetics and Informatics. 2005.

[11] Stulrajter, M., Makys, P., Rafajdus., P.: Sensorless control of high speed BLDC. 2017 IEEE International Symposium on Sensorless Control for Electrical Drives (SLED). Sept. 2017, pp. 225–230.

https://doi.org/10.51202/9783181023549 - Generiert durch IP 216.73.216.36, am 19.01.2026, 02:19:31. © Urheberrechtlich geschützter Inhalt. Ohne gesonderte Erlaubnis ist jede urheberrechtliche Nutzung untersagt, insbesondere die Nutzung des Inhalts im Zusammenhang mit, für oder in KI-Systemen, KI-Modellen oder Generativen Sprachmodellen.

[12] Sakunthala, S., Kiranmayi, R., Mandadi, P. N.: A study on industrial motor drives: Comparison and applications of PMSM and BLDC motor drives, 2017 International Conference on Energy, Communication, Data Analytics and Soft Computing (ICECDS), Chennai, 2017, pp. 537-540.

[13] 3-phase Sensorless BLDC Motor Control Kit with the S12 MagniV MC9S12ZVM, Application Note, NXP Semiconductor, 08/2013, https://www.nxp.com/docs/en/application-note/AN4704.pdf

[14] B.-G. Gu, J. S. Park, J-H. Choi, S-H. Rhyu, I-S. Jung: Optimal Lead Angle Calculation for Brashless DC Motor, The 2010 International Power Electronics Conference, June 2010, 1416-1420

[15] Filka, R., Balazovic, P., Dobrucky, B.: A Seamless Whole Speed Range Control of Interior PM Synchronous Machine without Position Transducer. 12th International Conference on Power Electronics and Motion Control Conference. EPE-PEMC 2006. pp. 1008 - 1014.

[16] 3-phase Sensorless PMSM Motor Control Kit with S32K144, Application Note, NXP Semiconductor, 08/2018, https://www.nxp.com/docs/en/application-note/AN12235.pdf

[17] Zossak, S., Musak, M., Stulrajter, M., Makys, P.: Challenges of Sensorless Controlled High-speed PMSM Drives. Applied to 2019 IEEE International Symposium on Sensorless Control for Electrical Drives (SLED). Sept. 2019

https://doi.org/10.51202/9783181023549 - Generiert durch IP 216.73.216.36, am 19.01.2026, 02:19:31. © Urheberrechtlich geschützter Inhalt. Ohne gesonderte Erlaubnis ist jede urheberrechtliche Nutzung untersagt, insbesondere die Nutzung des Inhalts im Zusammenhang mit, für oder in KI-Systemen, KI-Modellen oder Generativen Sprachmodellen.

48V to 12V Converters for xEV Applications

Managing the headaches of dual voltage automotive architectures

John Grabowski, ON Semiconductor, Ann Arbor, Mi. USA;
Andrea Colognese, ON Semiconductor Germany GmbH, Munich

Abstract

The modern 48V vehicle architecture is integrated into Mild Hybrid Electric Vehicles (MHEV). The primary advantage of the 48V architecture is improved fuel economy. Albeit, this advantage comes with both increased complexity and cost. The sub-system designs used to support a dual architecture vehicle require fundamentally new components such as the 48V to 12V bi-directional voltage converter. The methods for overcoming the design challenges are highlighted in this paper and includes sub-system design details for maximizing cost and efficiency. This topic is of interest to those wishing to understand the complexities of incorporating a superior converter design in a MHEV.

Introduction

With the recent popularization of Mild Hybrid Electric Vehicles (MHEV) many new vehicle architectures have been introduced generating new systems considerations that need to be addressed. One such consideration is the details involved in the management of the new multiple battery architecture. In order to produce the power required for the many hybrid features, a higher voltage battery system is required. The 48V battery provides the higher power required while still maintaining a safe-to-handle voltage level. In these dual-voltage architecture vehicles, there is typically only a single power generating source located on the 48V system side. The system diagram for a typical dual battery architecture is shown in Figure 1.

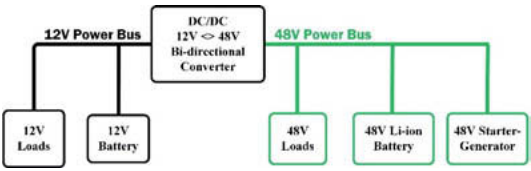


Fig. 1: MHEV Dual Voltage Architecture

This type of architecture generates new requirements for the charging of the 12V battery and for providing the power to the other 12V loads. A 48V to 12V converter is required to step down

https://doi.org/10.51202/9783181023549 - Generiert durch IP 216.73.216.36, am 19.01.2026, 02:19:31. © Urheberrechtlich geschützter Inhalt. Ohne gesonderte Erlaubnis ist jede urheberrechtliche Nutzung untersagt, insbesondere die Nutzung des Inhalts im Zusammenhang mit, für oder in KI-Systemen, KI-Modellen oder Generativen Sprachmodellen.

the 48V to the 12V energy used to charge the battery and operate the loads. Furthermore, this converter must accept the 48V energy produced by the vehicle's integrated starter/generator (ISG) and convert it to 12V.

The starting capability of the 48V battery is often insufficient for starting the vehicle at very low temperatures. This often is the case when LI-Ion battery systems are implemented with their selection criteria being based upon maximizing the battery's power density. When choosing a Li-Ion battery cell chemistry, there is a fundamental trade-off between power density and cold temperature performance. The requirement for providing additional cold temperature starting current dictates that the converter design is bi-directional. This bi-directional design permits the two batteries to share stored energy between one another, in either direction. This of course can only be done by the use of a bi-directional electronic converter. Hence, practically every MHEV will have the requirement of ~~a~~ bidirectional 48V to 12V conversion. Since this converter is a new addition to the base vehicle structure, it must be compact and lightweight. It will also conduct large amounts of current and therefore must be very efficient. Great lengths have been taken to achieve these two simultaneous requirements.

Converter Requirements

The 48V to 12V converter specifications are highly dependent on the vehicle type and options present. In general the 12V output power must meet a minimum value that supports the system with all 12V equipment switched on at the same time. This may not be a typical situation, but the converter must be capable of this power level. Table 1 shows the typical ~~and~~ range of design specifications required.

https://doi.org/10.51202/9783181023549 - Generiert durch IP 216.73.216.36, am 19.01.2026, 02:19:31. © Urheberrechtlich geschützter Inhalt. Ohne gesonderte Erlaubnis ist jede urheberrechtliche Nutzung untersagt, insbesondere die Nutzung des Inhalts im Zusammenhang mit, für oder in KI-Systemen, KI-Modellen oder Generativen Sprachmodellen.

Table 1: Typical Converter Specifications

	Minimum	Typical	Maximum
Power level (kW)		1.0, 2.5, 3.0, 3.5	
Input voltage range (V)	6.0		16.0
Output voltage range	31	48	54
Efficiency (%)	95		
Protection class		IP6K9K	
Phase number	4		8
Input protection	80V	B2B MOSFET's	100V
Output protection	40V	B2B MOSFET's	

Converter Topologies

The bidirectional converter required for the MHEV application can be configured using several different topologies. The most common is the interleaved, synchronous buck-boost, bidirectional voltage converter. This converter type is designed to have several identical phases, connected in parallel, functioning as a much larger converter. These "interleaved" phases work together and can be disabled when required. The diagram of a single phase of this converter is shown in Figure 2.

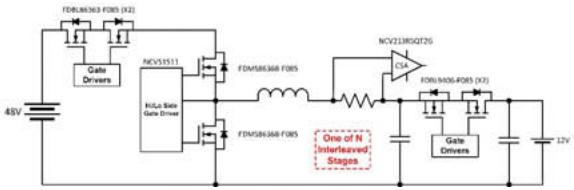


Fig. 2: Buck-Boost 48V-12V Bidirectional Converter – Single Phase

The main blocks that constitute this converter are the source-disconnect switch, buck-boost half-bridge, the current sensing stage, and the load-disconnect switch. The source-disconnect switch, permits disconnection of the converter from the 48V battery. The input buck-boost stage is the main converter circuit and is shown as a synchronous topology. The synchronous design is most common, due to the lower power losses. In previous designs the recirculating diode, which conducts during the recirculating current phase, was realized with a simple silicon

https://doi.org/10.51202/9783181023549 - Generiert durch IP 216.73.216.36, am 19.01.2026, 02:19:31. © Urheberrechtlich geschützter Inhalt. Ohne gesonderte Erlaubnis ist jede urheberrechtliche Nutzung untersagt, insbesondere die Nutzung des Inhalts im Zusammenhang mit, für oder in KI-Systemen, KI-Modellen oder Generativen Sprachmodellen.

diode. With higher efficiency being a major concern, this diode is replaced with an active semiconductor switch. The active switch acts in much the same way as did the diode, but when conducting current it has a much lower forward voltage resulting in a lower power loss.

The synchronous buck-boost converter stage is actually two switching circuits combined into a single stage. The power switches control the current flow in the main energy converting component, the inductor. The direction of this current dictates the direction of the power flow, and thus determines which battery will receive the current from the other. Depending on which battery is chosen as the source, this will determine the direction of the current flow. For instance, if the12V battery requires charge, then the switches, will be controlled in a manner which produces current flow as shown in the buck example of Figure 3. If the 48V battery requires charge, then the control will cause the switching to produce current flow as shown in the boost portion of Figure 3.

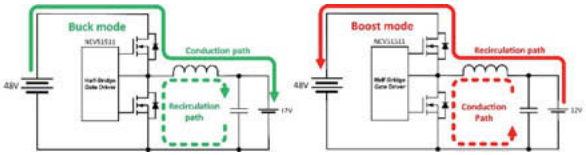


Fig. 3: Buck-Boost Conversion

The current sensing stage (in figure 2) is responsible for monitoring the inductor current. A popular current sensing method is to place a precision shunt resistor in the path of the inductor current. Based on principles of Ohm's law, the changes in the current flow results in a change in the voltage across the shunt. As shown in figure 2, the shunt is placed across the inputs of an amplifier. The amplifier measures the voltage across the shunt and introduces a gain for the ADC that follows in the signal conditioning path.

During normal operation the shunt voltage can vary from millivolts to in excess of 48 volts, with respect to ground. At the same time, the shunt's differential voltage could be very small, in the order of tens or hundreds of millivolts. This large difference in the desired versus the undesired voltage signals present a formidable problem for the amplifier. The inductor current is the primary controlled variable in the entire converter, making the amplifiers performance paramount for system accuracy, with impact on overall performance and efficiency.

https://doi.org/10.51202/9783181023549 - Generiert durch IP 216.73.216.36, am 19.01.2026, 02:19:31. © Urheberrechtlich geschützter Inhalt. Ohne gesonderte Erlaubnis ist jede urheberrechtliche Nutzung untersagt, insbesondere die Nutzung des Inhalts im Zusammenhang mit, für oder in KI-Systemen, KI-Modellen oder Generativen Sprachmodellen.

In a simplified way, this problem sets the performance criteria for the amplifier; It is required to amplify small differential signals and provide a high common mode rejection, while withstanding high transient voltages (up to 60V in some cases). In order to address the problem, three specifications need to be carefully selected:

• Common Mode voltage range (wider the better, in order to handle higher transient voltages)
• Input Offset Voltage (small the better, indicated higher accuracy)
• Common Mode Rejection Ratio (higher the better)

In conventional Operational Amplifiers the input terminal voltages are limited to the supply rails ±0.6 volts, thus limiting the common mode voltage range. In addition, the shunt size and precision could impact measurement accuracy. In the last couple decades, with the development of advanced fab processes and IC design architectures, dedicated current sense amplifiers provide a wide common mode voltage range (up to 40V or 80V) and high precision (as low as 10uV offset) to enable system designers to achieve highly accurate and fast current monitoring systems.

The single phase converter representation shown in Figure 2 is one phase of many required to create the fully functional 48V to 12V converter. The paralleling of several identical phases together will create a converter capable of higher power levels. This configuration is known as interleaving. Each phase operates independently and are combined to produce a converter with the capabilities of a much larger converter. There are several reasons for using interleaving rather than designing a single larger converter. First, the current levels in each phase are reduced to alleviate the stress on the power switches, conductors, and the main inductor. In addition, each phase can be used independently as necessary. In addition, the converter power level design can be made modular. The number of interleaved phases used is completely up to the designer. The interconnection scheme for each of the individual interleaved phases of a four phase converter is shown in Figure 4.

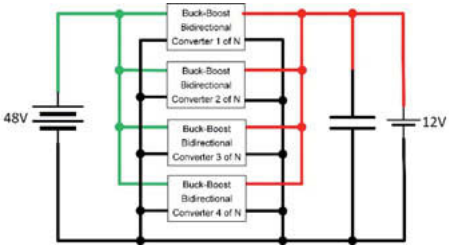


Fig. 4: 48V-12V Interleaved Bidirectional Converter Overview

https://doi.org/10.51202/9783181023549 - Generiert durch IP 216.73.216.36, am 19.01.2026, 02:19:31. © Urheberrechtlich geschützter Inhalt. Ohne gesonderte Erlaubnis ist jede urheberrechtliche Nutzung untersagt, insbesondere die Nutzung des Inhalts im Zusammenhang mit, für oder in KI-Systemen, KI-Modellen oder Generativen Sprachmodellen.

During typical vehicle operation, the 12V system has power requirements that fluctuate over time based on the vehicle operating profile. For some vehicle operating profiles, full power may be required, while at other times low power may be sufficient. In order to improve the overall efficiency of the converter, the interleaved converter can temporally add or remove phases from operation. This is done to more closely match the power demand with the number of phases in operation. When commanded, multiple phases are switched off by the use of the battery-disconnect switches. In addition, during periods of moderate power demand, while some phases are turned off, the converter control can substitute idle phases with phases that have been previously operating to evenly distribute the thermal load across all phases.

The load-disconnect switch stages are responsible for electrically connecting and disconnecting each phase from the 12V battery. It consists of back-to-back power MOSFET's, rated at the phase output current level. These switches may need to be operated continuously and therefore require gate drivers suitable of 100% on-time controllability. During some failure modes the MOSFET's can be opened to disconnect a failed stage from operation. The corresponding source-disconnect switch must also be disconnected to completely isolate the failed circuitry.

Converter Design

This circuitry required for each stage of this converter is as follows:

1. Source-disconnect power stage
    a. 80V/100 trench power MOSFET's
    b. High-side gate driver
2. Synchronous buck/boost power stage
    a. 80V/100V trench power MOSFET's
    b. High-side and Low-side gate driver
    c. Power inductor
3. Current sensing amplifier stage
    a. Current Sense Amplifier
4. Load-disconnect power stage
    a. 40V trench power MOSFET's
    b. High-side gate driver

The power semiconductor design for each of the source-disconnect stages can be achieved using discrete MOSFET's or an integrated MOSFET power module. 80V or 100V Trench

https://doi.org/10.51202/9783181023549 - Generiert durch IP 216.73.216.36, am 19.01.2026, 02:19:31. © Urheberrechtlich geschützter Inhalt. Ohne gesonderte Erlaubnis ist jede urheberrechtliche Nutzung untersagt, insbesondere die Nutzung des Inhalts im Zusammenhang mit, für oder in KI-Systemen, KI-Modellen oder Generativen Sprachmodellen.

MOSFET' devices are typically used for the source-disconnect stage. The primary purpose of this stage is to isolate the input of each of the interleaved stages from the other stages as well as the 48V battery. The back-to-back switch configuration is used to perform two distinct functions. First, when the pair of devices are turned on conduction is permitted in both directions. Second, when both switches are turned off, current is blocked in both directions. Each of these devices must be controlled by a gate driver device that has high-side drive capability, since these MOSFET's can be operated at 48V or higher potentials. Once in operation, these devices may need to remain in conduction for extended periods of time. This implies that the gate drivers must ~~also~~ be capable of 100% on-time using a charge-pump type design.

The buck-boost stages are the heart of the converter. Each one consists of two main MOSFET devices connected to a power inductor. These devices are typically 80V or 100V trench MOSFET devices. These MOSFET's must be controlled by high-side and low-side gate drivers. They may be independently packaged or co-packed into a dual driver IC. The main power inductor is designed to store the converters energy. Depending on the current direction, it will deliver the demanded energy to either of the two batteries based on the converter controller commands. The converter controller issues the commands to control the two main switches which determine the direction of ~~the~~ power flow in the converter. For this stage to operate properly, the current must be accurately monitored for the converter controller to properly adjust the main inductor current. The use of a Current Sense Amplifier is ideal for this task, as they are designed to have extremely low error.

The power semiconductor design for each of the load-disconnect stages can be achieved using discrete MOSFET's or an integrated MOSFET power module. 40V trench MOSFET devices are used for the load-disconnect stages. The primary purpose of this stage is to isolate the output of each of the interleaved stages from the others and from the 12V battery. The back-to-back switch configuration is used to perform the same isolation functions as in the source-disconnect stages. It permits conduction in both directions and also blocks conduction in both directions. These devices must also be controlled by a gate driver device that has high-side drive capability and is capable of 100% on-time operation.

Converter Operation

The bi-directional converter has several different modes of vehicle operation. During vehicle start the current for the ISG is drawn from the 48V battery. If the battery has insufficient charge~~,~~

https://doi.org/10.51202/9783181023549 - Generiert durch IP 216.73.216.36, am 19.01.2026, 02:19:31. © Urheberrechtlich geschützter Inhalt. Ohne gesonderte Erlaubnis ist jede urheberrechtliche Nutzung untersagt, insbesondere die Nutzung des Inhalts im Zusammenhang mit, für oder in KI-Systemen, KI-Modellen oder Generativen Sprachmodellen.

the converter will be commanded into the boost mode to provide additional starting current from the 12V battery. It is common for a Li-Ion battery to have poor performance at cold temperatures and during these times power from the 12V battery may be required to start the vehicle. In this event, the converter will be commanded to deliver current from the 12V battery to aid the 48V battery in starting the vehicle. Typically, additional engine start/stops will be postponed until all systems have reached normal operating temperature, then normal vehicle re-starts will commence.

During periods where the vehicle is warm and driving, but not requiring significant acceleration, the converter will operate in the typical buck mode. In this mode the converter will be commanded to deliver current from the 48V battery to the 12V battery. The converter will provide the necessary current to supply all of the 12V loads as well as provide any required charging of the 12V battery.

While the vehicle is operating in the normal driving mode and significant vehicle acceleration is requested, the converter will be switched into the boost mode where additional current will be delivered to the ISG motor to aid in accelerating the vehicle. Following the acceleration event, the system will return to the normal driving mode, with the converter in the buck mode. See Table 2. for the descriptions of the various vehicle and converter operating modes.

Table 2: Bidirectional Converter Operating Modes

Vehicle mode	Converter mode	Current direction
Cold starting	Boost mode	12V battery → 48V battery
Vehicle acceleration	Boost mode	12V battery → 48V battery
Vehicle driving	Buck mode	48V battery → 12V battery

Summary/Conclusions

With the widespread introduction of many new Mild Hybrid Electric Vehicles the global vehicle manufacturers are betting on these new topologies to have a positive impact on their overall fleet MPG. Each company is measured by a factor called the Corporate Average Fuel Economy (CAFÉ), used to gauge each auto company's progress at improving their vehicle's green footprint. A direct consequence of the MHEV proliferation is the increase of the 48V battery sub-systems, and as long as they retain 12V electrical components, a 48V to 12V converter will be required.

https://doi.org/10.51202/9783181023549 - Generiert durch IP 216.73.216.36, am 19.01.2026, 02:19:31. © Urheberrechtlich geschützter Inhalt. Ohne gesonderte Erlaubnis ist jede urheberrechtliche Nutzung untersagt, insbesondere die Nutzung des Inhalts im Zusammenhang mit, für oder in KI-Systemen, KI-Modellen oder Generativen Sprachmodellen.

Many different possible topologies for this converter could be envisioned. The interleaved synchronous buck-boost converter topology has become the most widespread due to its simplicity and high efficiency. Also, it is chosen for its ability to be designed in multiple interleaved phases, which support its high efficiency over a wide operating range. This is important because the 12V vehicle loads vary greatly over time and even though the converter needs to function at the maximum load point, it seldom stays there for long. When the loading is light, the converter will shed unnecessary interleaved phases, by use of the disconnect switches to reduce losses and maintain high efficiency.

Therefore, the cost of this converter will be considered a consequence of adding a 48V battery sub-system to any vehicle. Should future vehicle designs move additional system components to the 48V bus the capacity and cost of the converter will be reduced.

https://doi.org/10.51202/9783181023549 - Generiert durch IP 216.73.216.36, am 19.01.2026, 02:19:31. © Urheberrechtlich geschützter Inhalt. Ohne gesonderte Erlaubnis ist jede urheberrechtliche Nutzung untersagt, insbesondere die Nutzung des Inhalts im Zusammenhang mit, für oder in KI-Systemen, KI-Modellen oder Generativen Sprachmodellen.

https://doi.org/10.51202/9783181023549 - Generiert durch IP 216.73.216.36, am 19.01.2026, 02:19:31. © Urheberrechtlich geschützter Inhalt. Ohne gesonderte Erlaubnis ist jede urheberrechtliche Nutzung untersagt, insbesondere die Nutzung des Inhalts im Zusammenhang mit, für oder in KI-Systemen, KI-Modellen oder Generativen Sprachmodellen.

New concepts for electrical drive trains for high power density

Bruno Müller, **Carsten Angrick**, Dr. **Martin Fritz**,
Schaeffler Automotive GmbH, Bühl

Zusammenfassung

Die Elektrifizierung von Kraftfahrzeugantrieben erfordert modulare Lösungen, um die heterogenen Anforderungen bzgl. Anwendungsfällen, Bauraum und Leistungsskalierung unter Berücksichtigung des Zielkonflikts aus Variantenvielfalt und Kostendruck zu adressieren. Mit einem konsequenten Plattformansatz, der sämtliche Systemkomponenten des elektrischen Antriebs von E-Motor, Leistungselektronik, Sensoren bis zur Software umfasst, können anwendungsoptimale Lösungen hoher Leistungsdichte bei gleichzeitig hohem Grad an Re-use und Kosteneffizienz realisiert werden.

Abstract

The electrification of vehicle powertrains requires modular solutions to address the heterogenous requirements concerning different application areas, packaging space conditions and performance scaling while regarding the target conflict consisting of the number of variants and cost pressure. With a consistent platform approach comprising all system components of the electrified automotive powertrain ranging from e-motor, power electronics, sensors to software application-specific, high power density solutions with a high degree of re-use and cost efficiency can be realized.

Introduction

The development of electric drives goes way beyond the electric motor. Optimal efficiency, range, and system costs can only be achieved through the interaction of the motor, power electronics, sensors, mechanical integration, and control strategy, which is why a system-oriented approach is needed.

Schaeffler already proved back in 2011 that it possesses system expertise with the “Active e-drive” concept vehicle. The combustion engine in a Škoda Octavia was replaced with two electric axle drives, each with 105 kW of nominal power.

Even then, these motors were units that had been developed within the company. While the gear ratio of the motor and axle speed was fixed initially, a third generation rear axle drive with

https://doi.org/10.51202/9783181023549 - Generiert durch IP 216.73.216.36, am 19.01.2026, 02:19:31. © Urheberrechtlich geschützter Inhalt. Ohne gesonderte Erlaubnis ist jede urheberrechtliche Nutzung untersagt, insbesondere die Nutzung des Inhalts im Zusammenhang mit, für oder in KI-Systemen, KI-Modellen oder Generativen Sprachmodellen.

a two-speed transmission and nominal power reduced to 65 kW was employed in the same concept vehicle beginning in 2014. The drive now included new power electronics developed within the company. Both generations of the concept vehicle had torque vectoring in each wheel independently. While the power electronics (PEU) for the traction drive was still a separate system at this time, the PEU for torque vectoring was already installed on the axle.
Meanwhile, it is now foreseeable that electrified vehicle quantities will reach large proportions during the current decade and that the degree of mechatronic integration will increase considerably. At the same time, very different topologies are being implemented for the powertrain, which can be classified based on its installation position [1]. Four classes of aggregates are needed for the design implementation of these powertrains:

- Hybrid modules for integration in the powertrain of the combustion engine
- Dedicated hybrid transmissions for specifically realizing hybrid and electric driving modes
- Electric axle drives for dedicated hybrid powertrains and purely electric vehicles
- Wheel-hub drives for new mobility concepts



Fig. 1: Powertrain concepts with an integrated electric drive

Their complexity is increased by the fact that electric drives can be operated at various voltage levels, ranging from 48 V for initial hybridization to 400 V in purely battery-driven vehicles. More and more manufacturers are already launching projects with an 800 V on-board electric system in order to achieve short battery charging times at acceptable current levels. Accordingly, the power spectrum of electric drives is very broad – from 20 kW to more than 300 kW.
Something that all future aggregate concepts have in common is that they will integrate the mechanical and electrical/electronic systems to a large degree, Fig. 1. However, the requirements for electric motors are very different. For example, the axial installation space is limited

https://doi.org/10.51202/9783181023549 - Generiert durch IP 216.73.216.36, am 19.01.2026, 02:19:31. © Urheberrechtlich geschützter Inhalt. Ohne gesonderte Erlaubnis ist jede urheberrechtliche Nutzung untersagt, insbesondere die Nutzung des Inhalts im Zusammenhang mit, für oder in KI-Systemen, KI-Modellen oder Generativen Sprachmodellen.

both in hybrid modules as well as in wheel-hub motors. Moreover, the speed is directly coupled to the powertrain, meaning that power scaling mainly needs to happen via the torque of the e-machine. While electric axle drives have greater axial installation space available, the diameter is generally limited due to the installation position. The fact that e-axles always have at least one transmission stage leads to e-motors that generate their power from speed instead of torque, enabling smaller designs and material savings. The same applies for most dedicated hybrid transmissions. In contrast, power electronics are largely independent of the powertrain type; they are mainly defined by the voltage level, the amount of current needed for maximum output, and the installation space specified for the powertrain, the requirements on the cooling system and the control frequency of the electrical drive system.

The large number of requirements listed necessitates a modular approach for various installation spaces and power classes. This is even more true since – depending on the design – the drive's electric and electronic components make up to 70 to 80 percent of the total added value and are therefore key elements in the total cost.

Modular Approach - Developing a Technology Platform

In order to support a large number of vehicles and drive concepts on the one hand and yet minimize the development expenses on the other, Schaeffler has developed a modular technology approach for electric drives. Its three levels (Fig. 2) not only include electrical components, but also the hardware and software needed to control them.

The electric motors form the base of the platform. Due to the different requirements described at the beginning different kind of motors are the best solution for different kind of applications. For P2 applications maximizing the torque density in the shortest possible axial space is the most important feature. This is conventionally addressed by concentrated winding motors. Distributed windings with very short winding heads like wave-winding motors are also suited for these applications. For high-speed applications only stators with distributed windings are feasible; for the rotor however solutions without the use of magnets can be used depending on the scope of usage.

The middle level of Fig. 2 includes the power electronics with all key components, such as the power switches, capacitor, bus bars, driver stages, and sensors. Another part of the platform concept is a carrier frame that serves to channel the coolant and as a heat sink for all components of the power electronics. Also pertaining to the second level is the hardware for the drive control, the specifications of which not only depend on the electric motor and power electron-

https://doi.org/10.51202/9783181023549 - Generiert durch IP 216.73.216.36, am 19.01.2026, 02:19:31. © Urheberrechtlich geschützter Inhalt. Ohne gesonderte Erlaubnis ist jede urheberrechtliche Nutzung untersagt, insbesondere die Nutzung des Inhalts im Zusammenhang mit, für oder in KI-Systemen, KI-Modellen oder Generativen Sprachmodellen.

ics, but also on the functions carried out at the vehicle level, thereby requiring it to be implemented specific to the application. A key example of this is the communication network, which may be realized as a FlexRay, CAN, or CAN FD network.

For this reason, it cannot be separated from the third level where the software platform is located, which has likewise been developed according to a function-oriented approach. The software includes a functional library based on AUTOSAR, which also defines the requirements for the associated hardware.

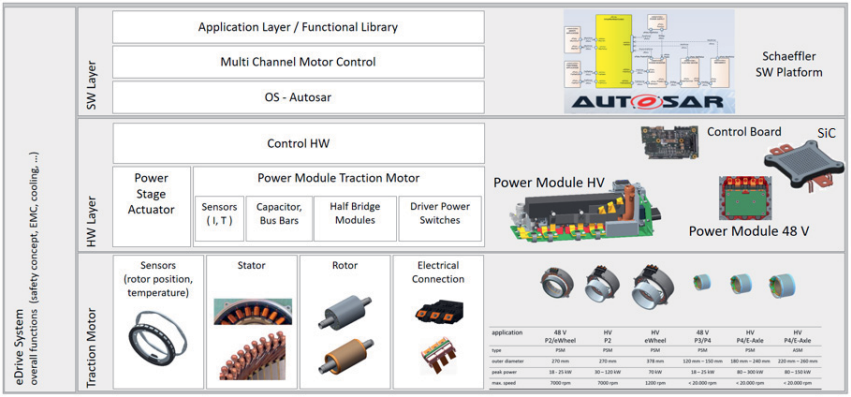


Fig. 2: Schaefflers platform approach

Platform Components

Electric Motors

When regarding highly-integrated powertrains such as hybrid modules, electric axles, or wheel-hub drives, it is difficult to identify the electric motor as an independently functioning unit. The complete motor function often cannot be tested until the powertrain has been assembled, since multifunctional modules are also determining factors for the functioning of other subsystems. Examples of this are bearing arrangements that also provide support for an integrated drive, or rotor carriers that are also plate carriers for a clutch.

In addition to the main function, that of representing defined speed-torque behavior, other demands need to be handled by this magnetic circuit as well:

- Ideal cooling-down capacity and a high copper filling ratio to ensure long-lasting continuous performance

https://doi.org/10.51202/9783181023549 - Generiert durch IP 216.73.216.36, am 19.01.2026, 02:19:31. © Urheberrechtlich geschützter Inhalt. Ohne gesonderte Erlaubnis ist jede urheberrechtliche Nutzung untersagt, insbesondere die Nutzung des Inhalts im Zusammenhang mit, für oder in KI-Systemen, KI-Modellen oder Generativen Sprachmodellen.

- Minimal use of materials in order to optimize costs
- Minimized harmonically occurring radial and tangential force effects in the stator for NVH optimization
- Minimized harmonics, which for their part likewise generate force effects, but also induce eddy-current-driving voltages and ultimately contribute towards losses and stator/rotor heating
- Minimal cogging and ripple torques
- Very flexible and scalable production technologies to simultaneously address different kind of (low-volume) applications

And the list goes on and on, as any detailed analysis of the individual phenomena will show. Thus there is an optimization problem, the solution for which must be oriented towards the requirements of the application and the expected load cycle.

Distributed winding has proven to be advantageous for a high torque density along with low harmonics and good heat flow from the current-carrying winding into the stator's laminated core. Hairpin or I-pin technology is suitable for the production of such windings. Further improvements of hairpin design mainly focus on reducing the height of the winding heads and increasing the efficiency. The requirements for this production technology are high, since there is a high number of weld points for each stator. Compared to coiled wires, the bars have a much larger cross-section, leading to eddy current and skin effect related losses during operation that greatly increase the more frequent changes in polarity become.

While the fact of larger coil ends compared to concentrated winding is considerably alleviated through hairpin technology, it nevertheless continues to persist. For this reason, there are still applications for electric machines where the advantages of distributed winding no longer outweigh the disadvantages, such as applications with extremely short axial installation spaces, e.g. 48 V hybrid modules, in which the active motor length is far less than 50 mm. At the same time, this is a good example of the strong influence of the available production technology.

The smaller the coil ends can be made, the further the application limit of distributed winding will shift in the direction of shorter axial lengths.

Schaeffler has investigated whether there are alternatives to hairpin winding that utilize the advantages, yet minimize the disadvantages. One good alternative is wave winding, in which the distributed winding is produced in a kind of braiding process and then joined in the stator slots. By allowing certain concessions with regard to the copper filling ratio, it is possible to work with smaller cross-sections. The potential number of slots is thereby increased and the effect of the eddy current losses reduced.

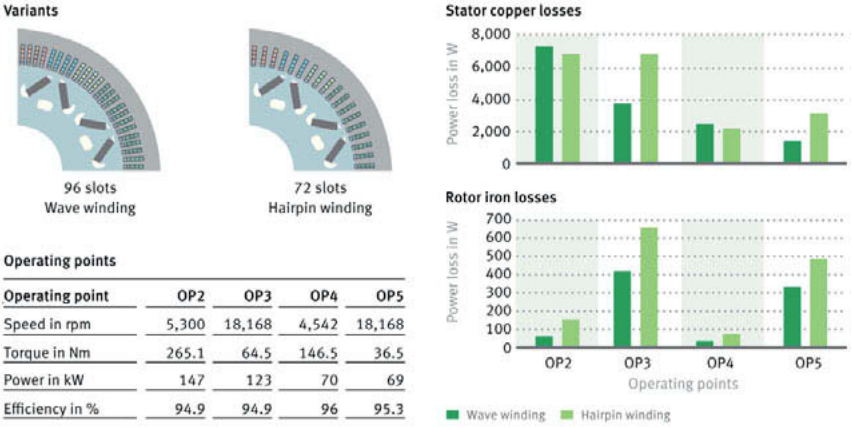
https://doi.org/10.51202/9783181023549 - Generiert durch IP 216.73.216.36, am 19.01.2026, 02:19:31. © Urheberrechtlich geschützter Inhalt. Ohne gesonderte Erlaubnis ist jede urheberrechtliche Nutzung untersagt, insbesondere die Nutzung des Inhalts im Zusammenhang mit, für oder in KI-Systemen, KI-Modellen oder Generativen Sprachmodellen.

The extent to which the advantages and disadvantages come into force depends on the specific application case. In order to quantify the differences, the comparison between the hairpin and wave winding was depicted using a specific example, namely their use in an electric axle of a purely electrical powertrain in the C segment. In coordination with the downstream gear stage, this resulted in the following specification values:

- P max = 147 kW
- M max = 265 Nm
- n max = 18,000/min.

The table in Fig. 3 shows the performance data of the e-machine with wave winding at selected, application-specific load points, with an outside stator diameter of 220 mm, 96 slots, and an active length of 110 mm.

A second motor with the same installation space requirements was designed using hairpin technology, whereby 72 slots were able to be implemented. Subsequently, the stator and rotor losses at the same operating points were compared with each other. This shows that the stator losses in hairpin winding are somewhat less in the lower speed range than in the motor with the wave winding. In contrast, hairpin winding scores much worse in the upper speed range due to the high frequency losses. Moreover, the rotor losses are less at all operating points compared when wave winding was used, an effect that is mainly due to the lower harmonics. In addition, the greater number of slots for wave winding results in a larger overall surface, which is useful for heat dissipation.



Operating points

Operating point	OP2	OP3	OP4	OP5
Speed in rpm	5,300	18,168	4,542	18,168
Torque in Nm	265.1	64.5	146.5	36.5
Power in kW	147	123	70	69
Efficiency in %	94.9	94.9	96	95.3

Fig. 3: Comparison of wave winding and hairpin designs

https://doi.org/10.51202/9783181023549 - Generiert durch IP 216.73.216.36, am 19.01.2026, 02:19:31. © Urheberrechtlich geschützter Inhalt. Ohne gesonderte Erlaubnis ist jede urheberrechtliche Nutzung untersagt, insbesondere die Nutzung des Inhalts im Zusammenhang mit, für oder in KI-Systemen, KI-Modellen oder Generativen Sprachmodellen.

Power Electronics

The specific requirements for power electronics in automotive applications result from their integration in electrified powertrain systems such as electric axles, hybrid modules and dedicated hybrid transmissions, their high quantities and broad range of performance.

- High level of robustness, since the variance of the user profiles increases at high quantities, on the other side environment-related requirements get tougher in highly-integrated powertrains concerning e.g. vibrations and ambient temperature
- High power density in limited installation spaces, resulting in special requirements regarding heat dissipation
- Flexibility of the design, as the installation spaces vary strongly in the different applications
- Optimal current forming to minimize harmonic losses and optimize efficiency
- High torque accuracy under all operating conditions
- Operational reliability in a wide range of operating voltages in order to respond to specific battery configurations
- Fulfilment of functional safety requirements

In the same as for electric motors, a detailed analysis would add to this list indefinitely. In addition, power electronics need to be adapted to the application-specific power requirements. To scale power electronics in various applications in the light of the specified requirements, Schaeffler has developed a modular concept, which is explained as follows on the basis of a sample implementation in an 85 kW class hybrid module, Fig. 4.

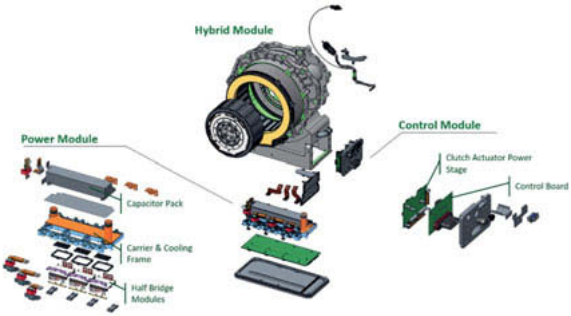


Fig. 4: Modular power electronics concept for the application example of a P2 hybrid module

https://doi.org/10.51202/9783181023549 - Generiert durch IP 216.73.216.36, am 19.01.2026, 02:19:31. © Urheberrechtlich geschützter Inhalt. Ohne gesonderte Erlaubnis ist jede urheberrechtliche Nutzung untersagt, insbesondere die Nutzung des Inhalts im Zusammenhang mit, für oder in KI-Systemen, KI-Modellen oder Generativen Sprachmodellen.

In the first step there must be strict separation between the control module and the power module. The control module consists of the control board, the actual intelligence of the power electronics, and an optional actuator power amplifier. As a rule, the control board can be used to depict two engine control channels. In the sample case, the second channel is provided for controlling the K0 actuator in the P2 hybrid module. As an alternative, it can also be used for a gearshift actuator in
a two-speed axle, a parking lock, or a second traction drive in a power split transmission. In the power module, it is first necessary to consider the scaling of the power semiconductors which make up a large portion of the value and entail a lot of the effort needed for the qualification. Schaeffler has decided to use half-bridge modules as the smallest unit, since they also enable the construction of multiphase drive systems (with more than three phases). In order to satisfy the range of requirements, two mechanical sizes and one basic population quantity (chip size and number of chips) were defined.
The interfaces to the outside for contacting and cooling are always the same. Moreover, for the sake of robustness, special importance was placed on avoiding soldering connections and aluminium bond wires in the mounting and connecting techniques used at critical points in the module. In the current design, the IGBTs (Insulated-Gate Bipolar Transistors) and parallel diodes are made using silicon semiconductors.
However, the use of wide-bandgap semiconductors is being considered as an alternative, as it is conceivable in the same module at activation frequencies of up to 20 kHz. Frequencies even higher than this require adaptations to be made to the basic design of the power electronics. Fig. 5 illustrates the basic scaling approach.
The consistent use of sinter technology increases the cycle stability of the IGBT modules by a factor of 10 in comparison with conventional aluminum bond wire technology. Other basic components involved in carrying current are the capacitor and the bus bars, which also lead to a loss of power due to the flow of current. The flexibility of the installation space is controlled by the central carrier frame (Fig. 4 and 6)
“Carrier and cooling frame”). This injection-molded part controls the flow of coolant, connects the current-carrying components to the heat sink, and arranges the basic components with respect to each other. CFD simulation is used to optimize this component in order to ensure symmetrical warming of the half bridges.
Moreover, the electrical connections are optimized with regard to parasitic inductances and capacities. In the specific example, a power density of more than 30 kW/l was able to be represented.

https://doi.org/10.51202/9783181023549 - Generiert durch IP 216.73.216.36, am 19.01.2026, 02:19:31. © Urheberrechtlich geschützter Inhalt. Ohne gesonderte Erlaubnis ist jede urheberrechtliche Nutzung untersagt, insbesondere die Nutzung des Inhalts im Zusammenhang mit, für oder in KI-Systemen, KI-Modellen oder Generativen Sprachmodellen.

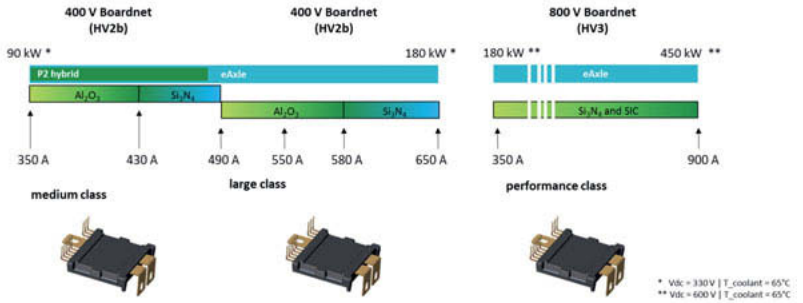


Fig. 5: Performance scaling of IGBT power switches

Thanks to the flexibility of the installation space and the modular approach, it is easy to react to deviating requirements. Fig. 6 shows an example of a design for use in an electric axle with a maximum output of 150 kW.

An EMC filter can be integrated on the DC side as an option and can be dimensioned in a way to omit shielding for the DC supply. This represents a good option for optimizing the system costs at the vehicle level. It was able to be demonstrated that the basic concept selected for the power electronics has the necessary flexibility to meet the different requirements of P2 and P4 high-voltage drives with regards to the installation space and electric output.

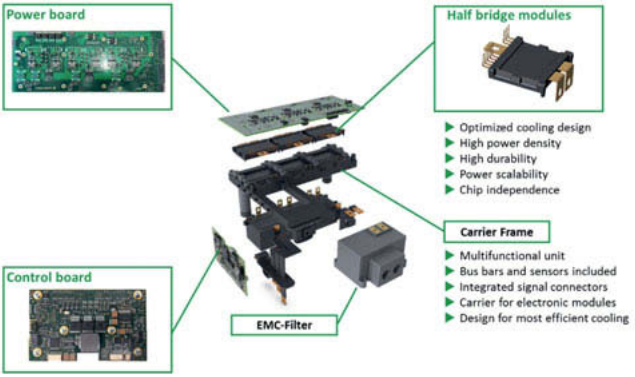


Fig. 6: Example of a modular power electronics for application in electric axles

https://doi.org/10.51202/9783181023549 - Generiert durch IP 216.73.216.36, am 19.01.2026, 02:19:31. © Urheberrechtlich geschützter Inhalt. Ohne gesonderte Erlaubnis ist jede urheberrechtliche Nutzung untersagt, insbesondere die Nutzung des Inhalts im Zusammenhang mit, für oder in KI-Systemen, KI-Modellen oder Generativen Sprachmodellen.

Software

The approach pursued by Schaeffler involves the development of an extensive function-oriented software library, which also includes the specifications for the required hardware. The following are key elements of the library:

- Analysis of sensor signals, such as for determining the rotor position, the phase currents, or temperatures at defined points
- Functions for motor control as a function of the motor type used (PSM, ASM)
- Functions for current control, such as a field-oriented control system that considers all relevant influencing variables (e.g. field weakening)
- Superordinate controllers for functional integration in the powertrain, which can also be integrated as customer modules upon special request
- Monitoring functions, such as for controlling power derating for thermal reasons and for providing functional safety

In addition to software modules, the library also contains any necessary hardware circuits, along with their definitions and preferred components. Special rules define the implementation in the final layout to guarantee optimum heat dissipation or electromagnetic compatibility.
This layout is prepared specifically to the application in order to react to special customer requirements. The various communication network options (CAN, FlexRay) have already been mentioned as examples.
With regards to the architecture, the software strictly follows the AUTOSAR paradigms in order to guarantee a high level of reutilization, Fig. 7.

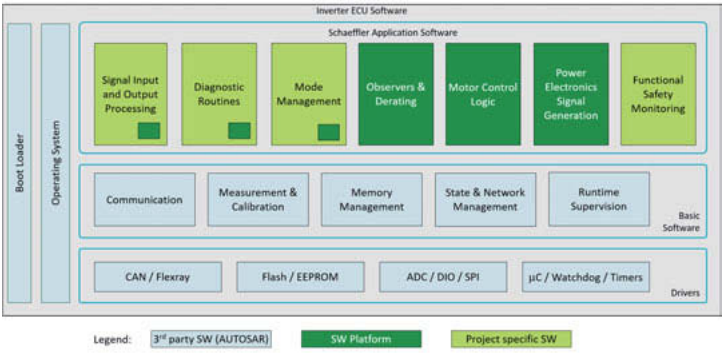


Fig. 7: High-level software architecture

https://doi.org/10.51202/9783181023549 - Generiert durch IP 216.73.216.36, am 19.01.2026, 02:19:31. © Urheberrechtlich geschützter Inhalt. Ohne gesonderte Erlaubnis ist jede urheberrechtliche Nutzung untersagt, insbesondere die Nutzung des Inhalts im Zusammenhang mit, für oder in KI-Systemen, KI-Modellen oder Generativen Sprachmodellen.

Summary and Outlook

Due to a growing variety of electrified powertrains in ever greater quantities, new solutions are needed for the electric drive. Schaeffler has found an answer to the balancing act between variety and standardization with its scalable technology platform for electric drives. This platform includes both the electric motor as well as the power electronics and the hardware/software for drive control. Based on different applications (P2 hybrid modules and P4 axle drives with high-voltage technology), it has been shown that a targeted approach is able to cover a very broad application spectrum.

The technologies used in the platform correspond to the very highest demands for efficiency, power density, and scalability. It has been developed in a modular fashion so that hardware and software from third-party providers can be seamlessly integrated.

Future generations of electric drives will be characterized by increasing integration of electrical, electronic, and mechanical elements. If the opportunities offered by the Schaeffler technology platform are consistently put to use, it will be possible to obtain considerable improvements at the system level. For example, the current development stage of the axle drive mentioned above at the beginning, with a 15 kg reduction in the overall weight, has doubled the maximum torque, which is now available for 60 seconds instead of only 10 while the nominal power has more than doubled, going from 60 to 145 kW.

https://doi.org/10.51202/9783181023549 - Generiert durch IP 216.73.216.36, am 19.01.2026, 02:19:31. © Urheberrechtlich geschützter Inhalt. Ohne gesonderte Erlaubnis ist jede urheberrechtliche Nutzung untersagt, insbesondere die Nutzung des Inhalts im Zusammenhang mit, für oder in KI-Systemen, KI-Modellen oder Generativen Sprachmodellen.

Literature

[1] Englisch, A.; Pfund, Th.: Schaeffler E-Mobility – With Creativity and System Competence in the Field of Endless Opportunities. 11. Schaeffler Kolloquium, Baden-Baden, 2018

[2] Reitz, D.: One Idea, Many Applications – Further Development of the Schaeffler Hybrid Module. 11. Schaeffler Kolloquium, Baden-Baden, 2018

https://doi.org/10.51202/9783181023549 - Generiert durch IP 216.73.216.36, am 19.01.2026, 02:19:31. © Urheberrechtlich geschützter Inhalt. Ohne gesonderte Erlaubnis ist jede urheberrechtliche Nutzung untersagt, insbesondere die Nutzung des Inhalts im Zusammenhang mit, für oder in KI-Systemen, KI-Modellen oder Generativen Sprachmodellen.

Overview of stator technologies motors for electro mobility in passcars

The right technology for each application

Alexander Gehring, Dr. **Matthias Beringer**, **Murat Özdemir**,
ZF Friedrichshafen AG, Schweinfurt

Zusammenfassung

Die Elektromobilität gewinnt immer stärker an Bedeutung. Allerdings besteht noch große Unsicherheit darüber, welche Antriebstechnologien und -konzepte mit welchem Produktionsvolumen, zum Einsatz kommen. Die Bandbreite reicht von kleinen Micro- Hybriden bis zu rein elektrischen Batteriefahrzeugen.

Für den Elektromotorsentwickelt ZF verschiedene Technologien, um für jede Anforderung die optimale Lösung anbieten zu können.

In diesem Artikel widmen wir uns den verschiedenen Technologien des Stators, da in den letzten Jahren hier einige Technologiesprünge in Design und Herstellbarkeit erzielt werden konnten. Desweitern stellt der Stator aus Kostengesichtspunkten eine der A-Komponenten eines elektrischen Antriebssystems dar.

Abstract

Electro mobility becomes more and more important. Nevertheless it is still unclear, which powertrain technology and concepts will be used and which volume distribution will come. The variety ranges from micro hybrids to full electric battery driven vehicles.

ZF develops different technologies for these electric propulsion systems to offer the optimal solution for each application.

This article focuses on the stator designs and technologies, since the last decade has brought some major technology milestone both in design and production technology. Further on the stator represents from the cost point of view one of the A- components of an electric traction drive system.

Introduction

In the past 20 years several approaches have been made to electrify the powertrain: From 42V in the beginning of the millennium over high voltage hybrid powertrain without the ability to

https://doi.org/10.51202/9783181023549 - Generiert durch IP 216.73.216.36, am 19.01.2026, 02:19:31. © Urheberrechtlich geschützter Inhalt. Ohne gesonderte Erlaubnis ist jede urheberrechtliche Nutzung untersagt, insbesondere die Nutzung des Inhalts im Zusammenhang mit, für oder in KI-Systemen, KI-Modellen oder Generativen Sprachmodellen.

charge from external (so called HEV) to plug in hybrids, pure electric battery and fuel cell electric vehicles.

In the last years several factors have been driving the development of electric motor technologies, amongst others higher efficiency, increased power density and reduction of costs.

Although the physical principle of an electric motor is over 100 years old and motors are being produced in millions per year, there was no major technology improvement for several decades.

The automotive industry with its extensive requirements like:

- Temperature
- Vibration/ Acoustics
- Power density
- Efficiency
- Packaging
- Reliability
- Safety

has accelerated the development in motor technologies.

Today there is no common and final electrification strategy in the pass car market, so there is still a wide variety of topologies and power demands.

In the field of parallel hybrid powertrains basically the permanent excited synchronous motors, called PSM is being used dominantly.

Whereas in the area of axle drive systems both for hybrid applications and pure electric vehicles still different motor technologies are being used:

- Permanent excited motor (PSM)
- Asynchronous motors (ASM)
- Separately excited synchronous motor (SESM)

Those technologies differ mainly in their rotor design and technology. But the stator has also a significant impact on design, robustness, efficiency and cost.

We have seen some impressive technology developments regarding design and especially regarding production costs. Therefore the focus on the following pages lays on the stator technologies

Figure 1 shows an overview about the major stator technologies: single tooth winding, insertion winding of round wires and rectangular wire winding such as hairpin for example.

https://doi.org/10.51202/9783181023549 - Generiert durch IP 216.73.216.36, am 19.01.2026, 02:19:31. © Urheberrechtlich geschützter Inhalt. Ohne gesonderte Erlaubnis ist jede urheberrechtliche Nutzung untersagt, insbesondere die Nutzung des Inhalts im Zusammenhang mit, für oder in KI-Systemen, KI-Modellen oder Generativen Sprachmodellen.

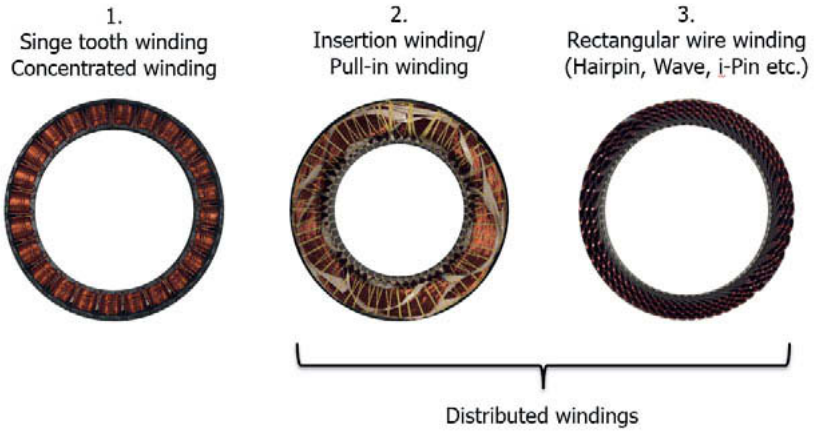


Fig. 1: Overview of stator winding technologies

Single tooth winding

The single tooth or concentrated winding technology is a very well know technology also in the automotive business. Figure 2 show a single tooth for an inner runner machine including electric lamination package, the insulating paper, the end caps and the round copper wire.



Fig. 2: Stator tooth with concentrated winding

The copper is wound around the electric sheet metal package by rotating the sheet metal package. The production method is very simple and requires relatively small amount of investment and can easily be multiplied. The usage of copper wires with a diameter > 1mm required

https://doi.org/10.51202/9783181023549 - Generiert durch IP 216.73.216.36, am 19.01.2026, 02:19:31. © Urheberrechtlich geschützter Inhalt. Ohne gesonderte Erlaubnis ist jede urheberrechtliche Nutzung untersagt, insbesondere die Nutzung des Inhalts im Zusammenhang mit, für oder in KI-Systemen, KI-Modellen oder Generativen Sprachmodellen.

some development efforts on the supplier side, but in the last 15 years such technologies became standard.

This technology provides a certain degree of freedom to the motor designer since the number of turns as well as the diameter of the copper wire can be chosen according to the technical requirements. The typical diameter in the field of parallel hybrids varies form 0.6 mm up to 1.8 mm. A change of wire diameter is easy to realise, only the moulding tooling of the end caps needs to be adapted besides some production fixtures.

Another advantage is the relatively small winding head. Typically the length of the head is only 12…20 mm, depending on the number and width of the stator slots. Although on one side of the stator so called connection rings are required to connect the single windings, the packaging space is still very short. Figure 3 shows a cross section of the connection side of such a stator including the winding, the connection rings and the insulation material.

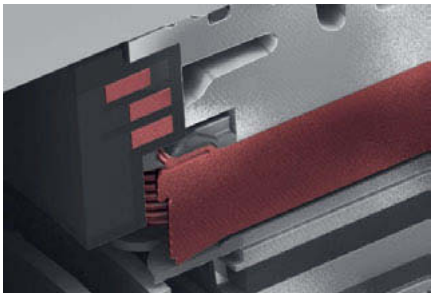


Fig. 3: Cross section of single tooth stator

The single tooth technology has its technical limits though. The increased power demands in parallel hybrid powertrains on the one hand and the special packaging space in axle drive units (small in diameter and long in active length) could not be realized in this design.

The usage of round wires has disadvantages in the head transfer from the centre wires of a winding to the surface. So the temperature distribution is very unequally and thus the continuous power is limited by the hottest wire in the centre of the winding. The cooling can be improved e.g. by using an oil spray cooling, where the oil of the transmission directly cools the stator winding. However also this method has its limits regarding the active length of the stator. ZF investigation has shown that single tooth technology can be used reasonable for motor with active lengths up to approx. 80mm.

https://doi.org/10.51202/9783181023549 - Generiert durch IP 216.73.216.36, am 19.01.2026, 02:19:31. © Urheberrechtlich geschützter Inhalt. Ohne gesonderte Erlaubnis ist jede urheberrechtliche Nutzung untersagt, insbesondere die Nutzung des Inhalts im Zusammenhang mit, für oder in KI-Systemen, KI-Modellen oder Generativen Sprachmodellen.

Above that length it is recommended to use rectangular winding, described in the chapter over the next.
Another disadvantage is an electrical design limitation based on the high number of necessary pole pairs and the high number of slots accordingly. The high number of pole pairs limits the rotational speed of the electric machine due to the increased high-frequency losses within the magnets and the lamination stack. The higher the number of slots the higher is the number of connection points and the number of sheet metal packages. Also a more complex design of connection rings has to be used which all in all leads to a commercially non-competitive design.
In total the single tooth stator is a technically and commercially attractive solution in the area of mild hybrids and plug-in hybrids with medium power demands.

Distributed winding

In contrast to the single tooth winding the distributed windings are assembled in the round stator sheet metal package. This means that a more complex insertion process is necessary in order to achieve the high automotive requirements regarding quality, costs and technical characteristics like efficiency and power density.
From an electromechanical point of view distributed windings provide some advantages regarding NVH and adaption to customer specific requirements for example by switching from parallel to star connection, utilizing parallel and serial paths and using different sizes of wire diameters in the same stator.
From a mechanical point of view it is distinguished between round and rectangular wires which will be explained in the next chapters.

Distributed winding with round wires

The basic principle design and production technology of distributed windings with round wires has been known for a long time. It is used in various industries since it can be easily produced and would not even require any thermal connection methods in the simplest applications: The ends of the round wires are crimped together and provide a power connection through a cable lug.
However in automotive applications the story is different: Efficiency, cooling and thus constant power and quality are very important.
Therefore stators with round wires are typically produced with the pull-in process which allows a higher copper filling factor than needle winding. The pull-in process and the following connecting and form pressing process requires detailed knowledge about fixture designs, since the copper wire with the insulation shield may not be damaged during the entire process.

https://doi.org/10.51202/9783181023549 - Generiert durch IP 216.73.216.36, am 19.01.2026, 02:19:31. © Urheberrechtlich geschützter Inhalt. Ohne gesonderte Erlaubnis ist jede urheberrechtliche Nutzung untersagt, insbesondere die Nutzung des Inhalts im Zusammenhang mit, für oder in KI-Systemen, KI-Modellen oder Generativen Sprachmodellen.

Figure 4 shows the winding head of such a stator

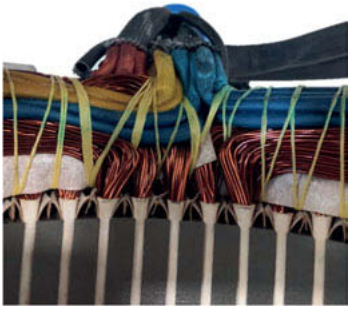


Fig. 4: Winding head and power connector of distributed stator with round wires

The picture gives an impression about the complexity of the assembly:

- Wire windings are prepared outside of the stator sheet metal package
- Windings are being pulled into the stator slots, that are already filled with insulation paper
- Connection points like star points, parallel and serial branches are assembled within the winding head
- Winding ends are being bend at the end of the stator to form a winding head and collect at the power connecting point
- Additional insulation paper needs to be assembled between the phases in the winding head, mostly by manual work
- The winding head needs to be pressed down to reduce packaging and to increase the density and thus the heat transfer out of the copper
- Power connection components are being assembled
- The stator assembly will be impregnated to improve mechanical stability, thermal behaviour and improve insulation of the copper

This design has been seen combined with ASM and PSM rotors both in plug in hybrids and electric axles.

Distributed winding with rectangular wires

In the beginning of the millennium first attempts were taken to work with rectangular copper wires in single tooth technologies. Especially the insulation was the biggest challenge at that

https://doi.org/10.51202/9783181023549 - Generiert durch IP 216.73.216.36, am 19.01.2026, 02:19:31. © Urheberrechtlich geschützter Inhalt. Ohne gesonderte Erlaubnis ist jede urheberrechtliche Nutzung untersagt, insbesondere die Nutzung des Inhalts im Zusammenhang mit, für oder in KI-Systemen, KI-Modellen oder Generativen Sprachmodellen.

time. High degree of mechanical loads during production and also in operation damaged the insulation with corresponding failures in the stator assembly.
The insulation materials and processes have improved significantly over the last years. Additional efforts have been taken regarding handling and automation of rectangular wires. These two major achievements are the basis for the big success of distributed windings with rectangular wires. Figure 5 shows the cross section of such a stator.

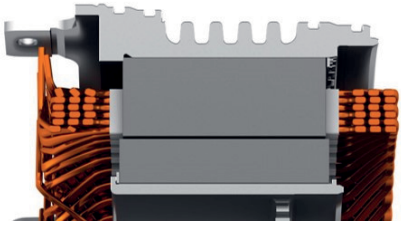


Fig. 5: Cross section of hairpin stator

There are different possibilities of producing such stators. After intense investigations and calculations ZF has decided to industrialize the hair-pin design.
It combines various advantages of different other technologies:

- It allows a very high degree of automation during production. So costs are reduced and repeatable quality is increased
- High copper filling factor improves efficiency
- Rectangular wires provide better cooling behaviour and thus provide increased continuous power and torque ratings

Some disadvantages of the design need to be considered, that mainly have impact on production costs:

- High amount of investment for production machinery and equipment
- High amount of contacting points of the hairpins and to the connection rings

High efforts have been taken in the past years and it was managed to compensate these disadvantages and reduce production costs:

- The production machinery was designed with high flexibility regarding diameter and length of the stator. So with only small adaptation in fixtures the same production equipment can be used for different motor sizes
- High degree of automation allows high usage rate with only little personnel costs

https://doi.org/10.51202/9783181023549 - Generiert durch IP 216.73.216.36, am 19.01.2026, 02:19:31. © Urheberrechtlich geschützter Inhalt. Ohne gesonderte Erlaubnis ist jede urheberrechtliche Nutzung untersagt, insbesondere die Nutzung des Inhalts im Zusammenhang mit, für oder in KI-Systemen, KI-Modellen oder Generativen Sprachmodellen.

- Simultaneous welding of multiple hairpins to the connection rings allows dramatically reduction of production time

Figure 6 shows the winding head of a hairpin stator.

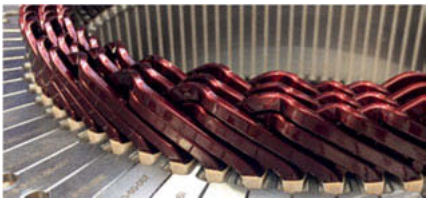


Fig. 6: Winding head of hairpin stator

Another promising winding technology based on rectangular wires is the so called wave winding. Within wave wound stators, the wires are bend outside of a stator towards a wave profile and then inserted radially into the stator. This technology eliminates several disadvantages within the hair-pin technology, like the high number of welding points, but also introduces additional challenges, e.g. restrictions within layout of the winding scheme.

Compared with distributed winding with round wires the copper filling factor can be increased from about 50% to 55…60%. Correspondingly the efficiency could be increased by 1…3% percentage points, which either leads to a reduction of battery costs on the vehicle side or increases the driving range of the vehicle.
By improved cooling behaviour the constant power could also be increased in the range of 5…10%. In plug in hybrids and battery driven vehicles the motor is basically always in operation, since it either drives the vehicle in motor mode or charges the battery in generator mode. So increasing the constant power is a major requirements with increasing electrification.

All in all the trend towards more complex and reliable rectangular wire technologies will come up within the next years which will all have their focus on higher performance and efficiency combined with robust production processes and lowest costs.

https://doi.org/10.51202/9783181023549 - Generiert durch IP 216.73.216.36, am 19.01.2026, 02:19:31. © Urheberrechtlich geschützter Inhalt. Ohne gesonderte Erlaubnis ist jede urheberrechtliche Nutzung untersagt, insbesondere die Nutzung des Inhalts im Zusammenhang mit, für oder in KI-Systemen, KI-Modellen oder Generativen Sprachmodellen.

Summary

The electrification in the pass car market has just begun and the distribution between mild hybrid, plug in hybrids and pure electric vehicles is not defined yet. Therefore it is necessary to further develop all necessary technologies to improve efficiency and reduce costs.

As described in this article the stator as one major part dramatically influencing efficiency and costs of the electric motor has already gone through various development steps in the last years. However there is further room of improvement in the years to come.

https://doi.org/10.51202/9783181023549 - Generiert durch IP 216.73.216.36, am 19.01.2026, 02:19:31. © Urheberrechtlich geschützter Inhalt. Ohne gesonderte Erlaubnis ist jede urheberrechtliche Nutzung untersagt, insbesondere die Nutzung des Inhalts im Zusammenhang mit, für oder in KI-Systemen, KI-Modellen oder Generativen Sprachmodellen.

https://doi.org/10.51202/9783181023549 - Generiert durch IP 216.73.216.36, am 19.01.2026, 02:19:31. © Urheberrechtlich geschützter Inhalt. Ohne gesonderte Erlaubnis ist jede urheberrechtliche Nutzung untersagt, insbesondere die Nutzung des Inhalts im Zusammenhang mit, für oder in KI-Systemen, KI-Modellen oder Generativen Sprachmodellen.

Nidec Next Generation Electric Traction Motor

Dr. **Markus Özbek**, **Jörg Trommer**,
Nidec Motors & Actuators Germany GmbH, Bietigheim-Bissingen;
Kazunari Akiyama, **Yosuke Yamada**,
Nidec Corporation, Kyoto, Japan

Zusammenfassung

Als weltweit führender Hersteller von Elektromotoren steigt Nidec nun in den Bereich der elektrischen Traktionsmotoren für Hybrid- und Elektrofahrzeuge ein. Der Elektromotor der nächsten Generation von Nidec zeigt eine hohe Leistungsdichte dank einer neuartigen automatisierten Fertigungstechnik, bei der runde Drahtschlitze radial in der Stator eingeführt werden. Dies führt zu einem hohen Füllfaktor des Kupfers im Stator sowie zu niedrigen Spulenenden im Vergleich zum axialen Einführen, das bei Elektromotoren mit verteilten runden Drahtwicklungen am häufigsten eingesetzt wird. Darüber hinaus führt die Konstruktion mit Permanentmagnetrotor zu einem hohen Wirkungsgrad und einer kompakten Bauweise. Der Traktionsmotor ist in Nidecs eigener Elektrischen Antriebsachse enthalten, die im Mai 2019 auf den Markt gebracht und in dieser Publikation vorgestellt wird.

Abstract

As a world leading electric motor manufacturer, Nidec is now entering the field of electric traction motors for hybrid and electric vehicles. Nidec's next generation electric traction motor shows a high power density thanks to a novel automated production technique by inserting round wire slits radially into the stator slots. This gives a high fill factor of the copper inside the slots as well as low coil ends compared to axial insertion which is the more commonly used technique on electric motors with distributed round wire windings. Furthermore, the permanent magnet rotor design results in a high efficiency and compact design. The motor is included in Nidec's own e-Axle that is introduced to the market in May 2019 and presented in this paper.

1. Introduction

Nidec was founded in Kyoto, Japan in 1973 and has since grown into a world-leading comprehensive electric motor manufacturer employing over 100,000 people throughout the world. In 1993, the company branched off into the automotive motor market which now constitutes its fastest growing business segment. Nidec's electric power steering motors, in particular, have

https://doi.org/10.51202/9783181023549 - Generiert durch IP 216.73.216.36, am 19.01.2026, 02:19:31. © Urheberrechtlich geschützter Inhalt. Ohne gesonderte Erlaubnis ist jede urheberrechtliche Nutzung untersagt, insbesondere die Nutzung des Inhalts im Zusammenhang mit, für oder in KI-Systemen, KI-Modellen oder Generativen Sprachmodellen.

captured the largest global market share and helped cement the company's position in the industry. As a world leading manufacturer of electric motors in a variety of fields, Nidec is now entering the mass market of traction motors for hybrid- and electric vehicles. The requirements on electric motors for vehicle traction applications are especially high due to the harsh environment in sense of temperature differences, vibrations, and external impacts (dirt, humidity, altitude, etc.) as well as the dynamic performance they need to provide in terms of acceleration and speed. There over, the high mass production rates in automotive requires it to be produced with highest quality to a cost effective level. Especially, decisions on type of coils, winding pattern, rotor type and cooling strategy are decisive for a successful market introduction to fulfil the customer needs. In this paper, Nidec's next generation electric traction motor entering the market in May 2019 will be presented. The performance, efficiency and size will be highlighted as well as its high slot fill factor together with low coil ends which are possible due to a new type of automated production technique. Finally, Nidec's new e-Axle which comprises the presented electric motor, an inverter and gear-set will be presented.

2. Nidec traction electric motor

The choice of electric motor technology is described in this chapter and highlights the permanent magnet rotor design and stator distributed winding technology. Furthermore, the novel production technique of the stator winding will be included and finally the efficiency of the motor will be shown.

Rotor

The design of the rotor is decisive for the efficiency and power density of the motor. Several types of rotors exist in automotive for different applications. Although, an optimal choice can be obtained for a specific working point of the motor, automotive applications require the motor to be efficient on a larger range of working points depending on specific use cases and applied driving cycle for the vehicle. Different types of rotors applied on motors include asynchronous motors, permanent magnet synchronous motors and externally excited rotors which are the most common in today's vehicle applications. To achieve a high power density for the application in Nidec's e-Axle, which is presented in Chapter3, a permanent magnet type of rotor is chosen. The design and alignment of the magnets with arc-shape, as depicted on Figure1, are done to fulfil a nearly sinus-shaped current wave form for minimizing torque ripple and harmonics as well as having a high efficiency over a large range of working points. For further optimization, air pockets (magnetic field barriers) are designed for optimizing the directed magnetic field to achieve requirements. The rotor shaft is hollow for applications that allow oil-

https://doi.org/10.51202/9783181023549 - Generiert durch IP 216.73.216.36, am 19.01.2026, 02:19:31. © Urheberrechtlich geschützter Inhalt. Ohne gesonderte Erlaubnis ist jede urheberrechtliche Nutzung untersagt, insbesondere die Nutzung des Inhalts im Zusammenhang mit, für oder in KI-Systemen, KI-Modellen oder Generativen Sprachmodellen.

cooling of the motor. The design uses the rotational forces to spray oil radially from the shaft directly onto the coil-ends of the electric motor, which gives better cooling and hence a higher continuous performance which is highlighted in Chapter3.



Fig. 1: Simplified rotor design depiction showing one pole with arc-shaped magnet.

Winding

Another important choice to be made on traction electric motors is the winding technology. Mainly, two types of winding pattern are currently used in automotive; concentrated winding and distributed winding and both technologies have their pros and cons. As for the concentrated winding, where the coils are inserted around a single stator tooth, it offers a very compact structure thanks to the copper being close to the stator core on the motor end, resulting in low coil ends. Drawbacks with concentrated winding are torque ripples and harmonics in the voltage supply line which may affect total vehicle NVH performance as well as efficiency. This applies especially for high speed electric motors. For Nidec's next generation traction motor, the choice fell on distributed winding to minimize harmonics distortion and to achieve a high efficiency as the application of traction motors tend to go towards high speed rather than high torque in certain powertrain architectures and hence also gives material reduction compared to high torque motors.

For the coil, mainly two types are applicable for automotive applications; squared wires (in form of hair-pins) and round slit wired coils. One of the main advantages of hair-pin is the high amount of copper inside a slot in relation to the total area of the slot, i.e. fill-factor. Hair-pin type is claimed to have a slot fill-factor of around 60% as shown in Figure2. It shall be noted that the slot shape is designed as a rectangular shape around the wires and not the other way around which limits the motor designer to choose an optimal design for the slot shape. More fairly, if the slot shape is designed trapezoidal (white dashed area in middle of Figure2), which would be a preferred design compared to rectangular slot shape, the slot fill factor would be around 55%. As Nidec utilizes a production method that results in a high fill-factor with round

https://doi.org/10.51202/9783181023549 - Generiert durch IP 216.73.216.36, am 19.01.2026, 02:19:31. © Urheberrechtlich geschützter Inhalt. Ohne gesonderte Erlaubnis ist jede urheberrechtliche Nutzung untersagt, insbesondere die Nutzung des Inhalts im Zusammenhang mit, für oder in KI-Systemen, KI-Modellen oder Generativen Sprachmodellen.

wires, which have the benefit of lower eddy currents than the thicker squared wires, both advantages of hair-pin and round wire can be utilized. Comparing to hair-pin the cassette insertion method with round wires of 52% as can be seen on the right in Figure2.



Fig. 2: Three generations of e-axles are presented from Nidec to enter world markets

Cassette insertion production

To achieve a high slot fill-factor in mass-production, Nidec has developed together with Nittoku Engineering a method called cassette insertion, which allows the copper wire to be inserted radially instead of axially. This allows a higher fill-factor compared to axial insertion due to that the insertion forces are lower, especially for longer stators. As a result, the copper wire can be packed denser. Moreover, the lower insertion force reduces the risks of damaging the insulation layer around the coils. The method is automated and includes a so called cassette which is pre-wounded with the coil wires for each phase and subsequently from the inside of the stator the coils are fed into the corresponding slot with a wedge. The stator with the cassette are depicted in Figure3.

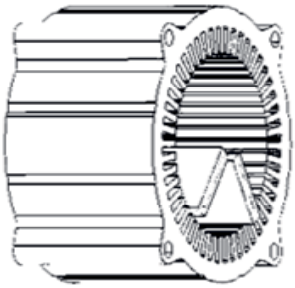


Fig. 3: Automated radial insertion of the coils gives high slot fill factor with low coil ends.

https://doi.org/10.51202/9783181023549 - Generiert durch IP 216.73.216.36, am 19.01.2026, 02:19:31. © Urheberrechtlich geschützter Inhalt. Ohne gesonderte Erlaubnis ist jede urheberrechtliche Nutzung untersagt, insbesondere die Nutzung des Inhalts im Zusammenhang mit, für oder in KI-Systemen, KI-Modellen oder Generativen Sprachmodellen.

Another benefit with radial insertion is the possibility to lap parts of the phase coils at the motor ends side by side as depicted in Figure 4. This gives compact and low coil-heads and allows insulation paper to be inserted between the phases which results in a tighter alignment by pressing down the coil-heads further. The insulation paper also reduces the inductance leakage between the coils in the coil-heads which increases the efficiency of the electric motor.

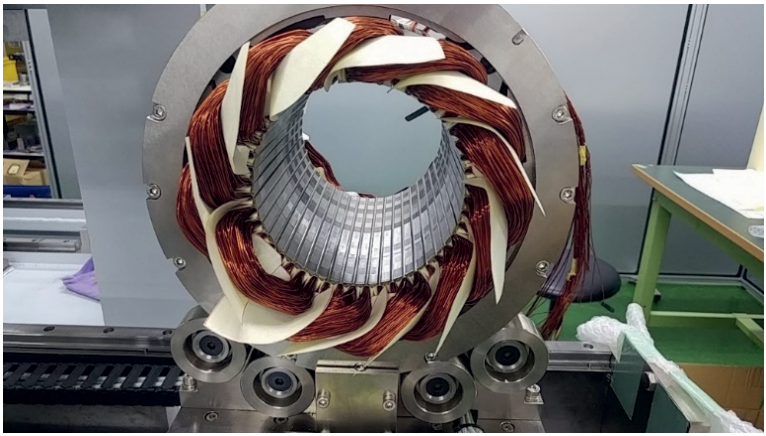


Fig. 4: Radial insertion allows the coil ends to be lapped side by side and tightly pressed due to possibility to insert insulation paper between the phases.

The choice of permanent magnets rotor with Nidec's design of the magnets and magnet barriers, together with the round wire in a distributed winding configuration, results in a high efficiency of the electric motor as shown in Figure 5. A maximum efficiency closely to 97% can be achieved and the efficiency can be maintained over a large working area of speed and torque.

Motor Torque [Nm]	1000	2000	3000	4000	5000	6000	7000	8000	9000	10000	11000	12000	13000	14000
300	81.21	89.07	92.11											
250	84.25	90.99	93.45	94.63										
200	87.21	92.68	94.65	95.43	95.07									
150	89.88	94.22	95.64	96.18	96.18	95.13	93.17							
100	92.46	95.60	96.49	96.65	96.93	96.41	95.20	93.98	93.00	91.96				
50		96.89	96.94	96.68	96.45	96.01	95.60	94.39	93.64	92.30	91.31	90.72	89.77	88.19
0														
-50		96.82	96.89	96.71	96.49	96.28	95.55	94.48	93.28	92.12	90.96	89.74	89.10	88.01
-100	91.72	95.40	96.37	96.70	96.73	96.33	95.65	94.87	93.90	93.26	92.17	91.09	90.11	
-150	88.57	93.83	95.47	96.11	96.37	95.69	94.89	93.59						
-200	85.13	92.08	94.35	95.30	95.43	94.62								
-250	81.06	90.08	93.02	94.29	94.07									
-300	76.18	87.52	91.26	93.02										

Motor Speed [rpm]

Fig. 5: Efficiency table of the Nidec electric motor shows peak efficiency close to 97%.

https://doi.org/10.51202/9783181023549 - Generiert durch IP 216.73.216.36, am 19.01.2026, 02:19:31. © Urheberrechtlich geschützter Inhalt. Ohne gesonderte Erlaubnis ist jede urheberrechtliche Nutzung untersagt, insbesondere die Nutzung des Inhalts im Zusammenhang mit, für oder in KI-Systemen, KI-Modellen oder Generativen Sprachmodellen.

3. Nidec e-Axle

First application for Nidec's traction motor is the in-house developed e-Axle, shown in Figure6, introduced in May 2019 to the mass market in the fully electric sedan Aion S from GAC [1]. With Nidec's vertical integration strategy, all components except the reduction gear are in-sourced and offer an optimally designed system.



Fig. 6: Three Nidec e-Axle which is in production from May 2019

By integrating the inverter, which was separately mounted in Nidec's first e-Axle design announced in September 2017, the system weighs in at 87kg while achieving a peak power output of 150kW and a maximum system torque output of 3,900Nm, as listed in Table1. The new fully integrated design obviates the need for wiring between components, resulting in a more compact system that increases design flexibility. The e-Axle covers a wide array of applications, ranging from compact cars to SUV platforms and is compatible with AWD vehicles with an optional clutch mechanism that can be disengaged when one wheel pair need to be powered. Production is scheduled to May 2019, starting in China and later expanding globally.

Table1: Specifications of the Nidec e-Axle

Power (peak, 30s)	150	kW
Power (continuous)	60	kW
Weight (no park-lock)	87	kg
Torque	3900	Nm
Gear ratio	1:11	-
Height	331	mm
Width	487	mm
Length	463	mm

https://doi.org/10.51202/9783181023549 - Generiert durch IP 216.73.216.36, am 19.01.2026, 02:19:31. © Urheberrechtlich geschützter Inhalt. Ohne gesonderte Erlaubnis ist jede urheberrechtliche Nutzung untersagt, insbesondere die Nutzung des Inhalts im Zusammenhang mit, für oder in KI-Systemen, KI-Modellen oder Generativen Sprachmodellen.

Cooling

The cooling concept of an electric drive system is essential for the vehicle performance as it decides the continuous power output and has a high impact on the system efficiency. Electric motors for vehicle application can either be air-cooled, water cooled or oil cooled. As water cooling is not suitable to be applied to direct active parts of the motor (such as core laminations or copper wire) due to conductivity of water as well as its corrosive nature, it is best applied to include a water-jacket around the stator. This reduces the thermal conductivity between the water and the electric motor but allows simple integration of the motor in the vehicle and its cooling water-circuit. Alternatively, oil-cooling can be chosen. Conventional ATF-oil can be directly applied to all parts of the motor with lower risks of corrosion and allows direct cooling. On Nidec's electric motor which is applied to Nidec's e-Axle system, both water and oil cooling are used. The oil-cooling part, acting on the motor, utilizes splash effects from the gear-set as well as an oil-pump drive flow. As for the rotor, Nidec has designed an innovative rotor shaft that allows oil being fed directly to the coil-ends when the rotor is turning. This is especially important in low speed and high torque area, where the splash effect from the gear-set may not be sufficient. As for the inverter, the water coolant system of the vehicle is used which allows for a quick and effective cooling of the power electronics. The same water channel leads to an oil-water heat-exchanger that further reduces the oil temperature of the e-Axle. The usage of a hybrid cooling concept of water and oil allows a higher amount of heat being dissipated from the system.

4. Conclusion and Summary

In this paper, the next generation electric traction motor from Nidec is presented and shows a high slot fill-factor, low coil-head length and high efficiency. The high slot-fill factor and low coil-heads could be realized by inserting the coil-windings radially with a new automated method called cassette insertion. The Nidec electric motor is applied for the first time on the in-house developed e-Axle which is introduced in May 2019. The e-Axle shows compact and light-weight features with a hybrid water and oil cooling circuit resulting in a high power density. Further development on the e-Axle includes a more compact inverter with SiC semiconductors and magnet less rotor technologies. With the presented electric motor and e-Axle, Nidec aims to be a leading supplier in this area and to strengthen the position as electric motor maker.

References:

[1] https://www.nidec.com/en-Global/product/news/2018/news1210-01/

https://doi.org/10.51202/9783181023549 - Generiert durch IP 216.73.216.36, am 19.01.2026, 02:19:31. © Urheberrechtlich geschützter Inhalt. Ohne gesonderte Erlaubnis ist jede urheberrechtliche Nutzung untersagt, insbesondere die Nutzung des Inhalts im Zusammenhang mit, für oder in KI-Systemen, KI-Modellen oder Generativen Sprachmodellen.

https://doi.org/10.51202/9783181023549 - Generiert durch IP 216.73.216.36, am 19.01.2026, 02:19:31. © Urheberrechtlich geschützter Inhalt. Ohne gesonderte Erlaubnis ist jede urheberrechtliche Nutzung untersagt, insbesondere die Nutzung des Inhalts im Zusammenhang mit, für oder in KI-Systemen, KI-Modellen oder Generativen Sprachmodellen.

Enhanced Application of High-Performance-Computing in the Design Process of High-Power-Density Traction Motors

M.Sc. **David Philipp Morisco**,
Robert Bosch GmbH, Schwieberdingen;
Dr. **Ioan Liviu Iepure**,
Robert Bosch GmbH, Renningen

Zusammenfassung

Während des Entwicklungsprozesses elektrischer Maschinen wird heutzutage ein erheblicher Aufwand betrieben, um Leistung und Ausnutzung möglichst präzise zu berechnen. Vor allem bei hoch performanten Traktionsantrieben ist die simulative Bewertung komplexer elektromagnetischer Einflüsse wesentlicher Bestandteil des Berechnungsprozesses. Dabei stehen besonders die durch dreidimensionale elektromagnetische Effekte auftretenden Zusatzverluste im Fokus, deren Berechnung mittels klassischer Ansätze zwar mit kurzen Rechenzeiten aber auch mit teilweise erheblicher Ungenauigkeit einhergeht. Wesentlich genauer, aber auch verbunden mit stark erhöhter Rechenzeit, ist die dreidimensionale finite Elemente Simulation (3D-FEM). Insbesondere wenn die Berechnung auf lokalen Rechnersystemen erfolgt, ist dabei oftmals ein akzeptabler Zeitaufwand nicht zu erreichen.
Mit der zunehmenden Verfügbarkeit von Großrechnersystemen (High Performance Computing - HPC) ist es möglich, die Berechnungszeit bei gleichbleibender Genauigkeit zu reduzieren, wenn eine entsprechend geeignete Solver-Architektur verwendet wird.
Im Rahmen des Vortrages werden zunächst die notwendigen Systemanforderungen sowie die Eigenheiten für die distributive elektromagnetische Berechnung dreidimensionaler Maschinenmodelle dargestellt. Anhand eines Beispiels aus dem Auslegungsprozess elektrischer Traktionsantriebe wird anschließend die Notwendigkeit einer genauen simulativen Bewertung ebenso veranschaulicht, wie auch die Stärke der Anwendung von HPC Systemen für elektromagnetische Simulationen.

Abstract

During the design process of electrical machines, nowadays an impressive effort is done to precisely calculate power and efficiency. Especially in the field of high-power-density traction motors the simulative evaluation of complex electromagnetically impacts is one key feature within the design process. Special focus is set on the additional losses caused by three dimensional electromagnetic effects, which can be calculated by using commonly applied

https://doi.org/10.51202/9783181023549 - Generiert durch IP 216.73.216.36, am 19.01.2026, 02:19:31. © Urheberrechtlich geschützter Inhalt. Ohne gesonderte Erlaubnis ist jede urheberrechtliche Nutzung untersagt, insbesondere die Nutzung des Inhalts im Zusammenhang mit, für oder in KI-Systemen, KI-Modellen oder Generativen Sprachmodellen.

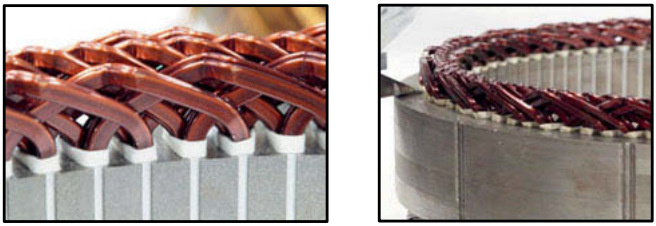
analytical state-of-the-art approaches. Although the calculation time is short, the result using classical approaches suffers of low accuracy due to necessary simplifying assumptions. A considerable higher accuracy offers the application of 3D finite element analysis (FEA). However, this is related to increased calculation time because of the applied complex 3D modelling. In particular, if local desktop systems are used, it is not possible to achieve acceptable calculation times.

With increasing availability of high-performance-computing (HPC) and the application of suitable solvers, the calculation time can be significantly reduced while ensuring a high accuracy for the calculated results.

In this paper the application of HPC systems combined with enhanced 3D FEA is presented regarding the design process of high-power-density traction motors. The necessary system requirements are presented as well as the system performance. Also the characteristics of the distributed solving on multicore systems is illustrated. An example from the field of traction motors is presented to emphasize the benefit and the need for enhanced FEA within the design process.

Introduction

In the context of global warming, electric vehicles are expected to help decrease the CO_2 emissions and mitigate the climate change. Thus, high efficiency traction motors are required. Improving the efficiency of such a machine is very challenging because of the severe constraint of high torque density and thus high current load. The acute interest for a high torque density encouraged the preferred application of bar-wound winding over stranded wire windings. Moreover, the bar-wound winding offers several advantages regarding the application of



(a) (b)

Fig. 1: Examples of bar-wound winding applied to traction motors.

traction motors such as an easier implementation of the automization process of the winding manufacturing or a better cooling link. Fig. 1 shows the bar-wound winding of the stator core. Accompanying with high current load, the bar-wound winding increases the susceptibility of

https://doi.org/10.51202/9783181023549 - Generiert durch IP 216.73.216.36, am 19.01.2026, 02:19:31. © Urheberrechtlich geschützter Inhalt. Ohne gesonderte Erlaubnis ist jede urheberrechtliche Nutzung untersagt, insbesondere die Nutzung des Inhalts im Zusammenhang mit, für oder in KI-Systemen, KI-Modellen oder Generativen Sprachmodellen.

the machine regarding 3D effects such as current displacement in the end-windings or additional iron core losses at the end region of the stator. Therefore, it is essential to estimate the losses as accurate as possible. With the application of bar-wound winding technology an accurate modelling of the windings becomes possible in the FEA as the conductors show large cross section areas compared to the stranded wire windings. Hence, it is possible to create high complex 3D models consisting of the whole geometry including the complex winding in detail.

Several publications cover the influence of three dimensional electromagnetical effects on the machine performance and in particular on the occurring losses. In [1] the influence of the end-winding leakage field on the additional stator core stray losses is assessed and estimated. It is shown that for high-power-density machine design the leakage field cause noteable additional losses within the end region of the stator core. Subsequently a solution is presented to achieve a reduction of the additional losses without compromising the torque density significantly and thus improving the efficiency. Since the leakage magnetic field from the end-winding also interfuses the conductors itself, additional losses due to current displacement can be expected. The publications [2] - [4] analyse the additional eddy currents within the conductors of the end-winding. It is shown that classical approaches show relatively large deviations compared to high complex 3D FEA, and thus offer no suitable solution for precise loss prediction. Since the calculation time for the complex models increases significantly if local desktop systems are used, the application of an HPC system is suggested.

High-Performance-Computing

Due to increasing complexity of the models, the solving time increases. Hence, the direct implementation of the 3D FEA models within the design evaluation process is not reasonable if standard desktop systems are used. Therefore an HPC system is the preferred environment for the calculation to reduce the calculation time significantly. The main system structure is depicted in Fig. 2. Key part and kernel of the system is the fourteen data rate (FDR) file system. Directly linked to the FDR are the visualization nodes (VN), the management nodes (MGMN), the calculation nodes (CN) and the filer. The main file system is attached to the FDR system via the network nodes.

For the execution of a calculation, the user logs on to a visualization node and starts the job, usually by using special submit scripts for automated job execution. Accordingly, the job is processed to the FDR system and distributed towards the CN parts of the system. While the solving is performed, the intermediate results are buffered to the filer. After finishing the

https://doi.org/10.51202/9783181023549 - Generiert durch IP 216.73.216.36, am 19.01.2026, 02:19:31. © Urheberrechtlich geschützter Inhalt. Ohne gesonderte Erlaubnis ist jede urheberrechtliche Nutzung untersagt, insbesondere die Nutzung des Inhalts im Zusammenhang mit, für oder in KI-Systemen, KI-Modellen oder Generativen Sprachmodellen.

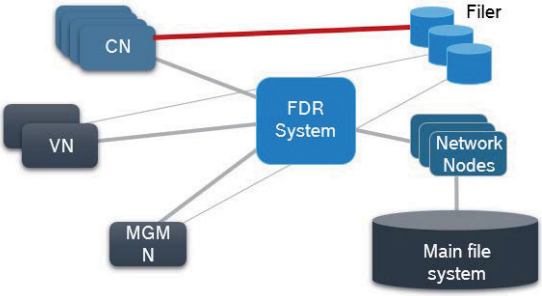


Fig. 2: Basic HPC system layout

calculation, the MGMN use the distributed results for creating the merged results of the calculation. Finally, the final results are passed by the network nodes to the main file system, whence they are available for a detailed evaluation. To manage the job submission and distribution effectively a parametrized IBM load sharing facility (LSF) job scheduler is used.

Parallelization of Single Calculations

The state-of-the-art application of HPC systems is the parallelized calculation of different designs using several cores from different CN and thus 1 calculation is executed on 1 core. Since the 3D models used in this paper are highly complex and contain a large number of elements, the single calculation is not sufficient; hence, the distributed solving must be extended to 1 calculation distributed to several cores. Therefore, it is necessary to perform a

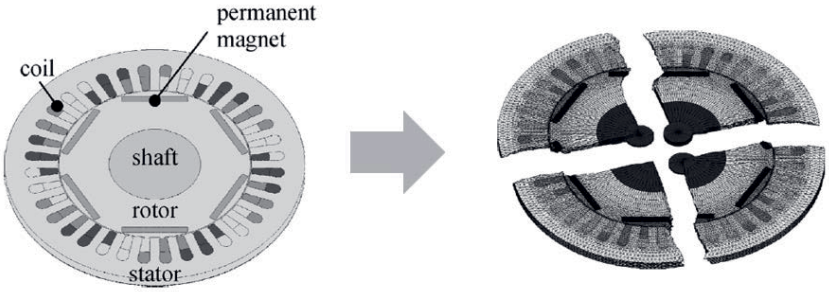


Fig. 3: Partitioning of the model for distributed solving

partitioning of the mesh into sub models as shown in Fig. 3. Afterwards, the sub models can be solved distributed onto the CN of the HPC system. In [6] - [8] the general method behind the mesh partitioning based on domain decomposition (DDM) approaches and the distributed solving from the electromagnetic point of view is shown. Fig. 4 depicts the automated workflow

https://doi.org/10.51202/9783181023549 - Generiert durch IP 216.73.216.36, am 19.01.2026, 02:19:31. © Urheberrechtlich geschützter Inhalt. Ohne gesonderte Erlaubnis ist jede urheberrechtliche Nutzung untersagt, insbesondere die Nutzung des Inhalts im Zusammenhang mit, für oder in KI-Systemen, KI-Modellen oder Generativen Sprachmodellen.

on the Bosch HPC for distributed solving of the large scaled models by using a Bosch in-house solution. First, the job is sent to the LSF system. Subsequently, the sub models are distributed to different CN onto the system. While the solving takes place, the whole process is monitored regarding the end or termination of a calculation. Once the calculation job is finished, the

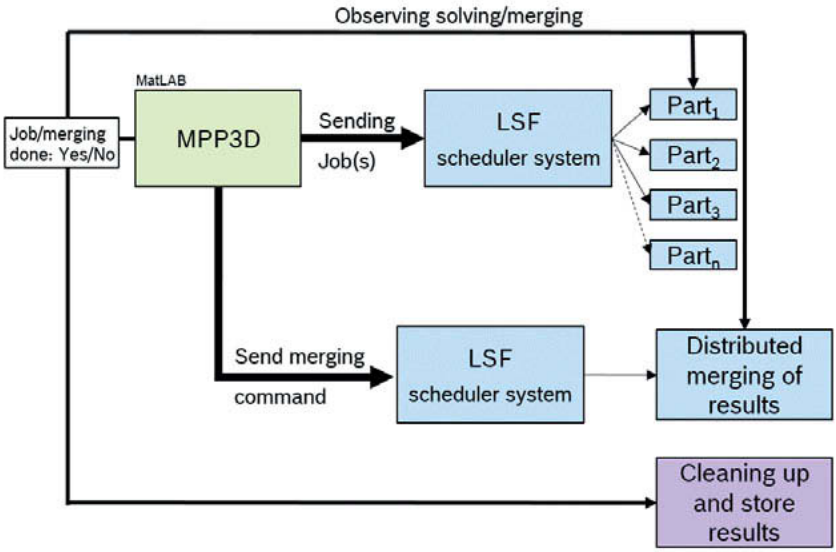


Fig. 4: Overview of workflow of Bosch in-house tool for distributed solving on HPC systems

merging of the distributed results is started. Therefore, the results from the sub-model calculations are collected and merged together using the MGMN.

System Performance

To evaluate the system performance, several test models A - D as depicted in Fig. 5, with increasing complexity and number of elements had been computed using the explained

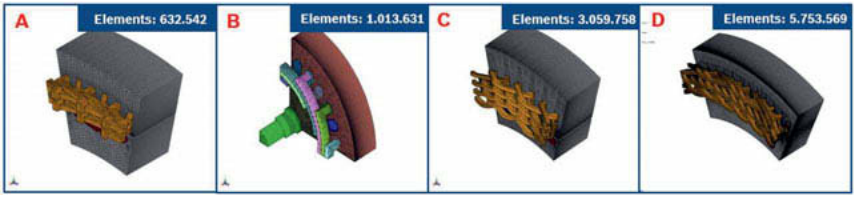


Fig. 5: Test models for system performance evaluation

https://doi.org/10.51202/9783181023549 - Generiert durch IP 216.73.216.36, am 19.01.2026, 02:19:31. © Urheberrechtlich geschützter Inhalt. Ohne gesonderte Erlaubnis ist jede urheberrechtliche Nutzung untersagt, insbesondere die Nutzung des Inhalts im Zusammenhang mit, für oder in KI-Systemen, KI-Modellen oder Generativen Sprachmodellen.

workflow. For the test, 1 electrical period has been calculated on a local desktop system using 1 core and additionally on the HPC system using 128 cores. For the electromagnetical calculation eddy currents within the winding, the iron and the magnets had been enabled. The resulting calculation time is presented in Tab. 1. It can be seen that for increasing complexity

	Elements	1 Core	128 Core
Model "2D"	9.051	3m	4m
Model A	623.542	2d 18h 24m	3h 49m
Model B	1.013.631	5d 07h 23m	5h 11m
Model C	3.059.758	22d 19h 15m	18h 36m
Model D	5.753.569	46d 11h 18m	1d 11h 28m

Tab. 1: Resulting calculation time

the calculation time increase as well, which was indeed expectable. However, it is interesting to find, that already for a model including ~ 1 million elements the calculation on a single core is not sufficient. The models C and D are of special interest, as they represent realistic designs of traction motors. Here a significant reduction of calculation time can be achieved by using 128 cores instead of 1 single core. Since many different jobs from several users are performed simultaneously on the HPC system a decreased speedup can appear. Fig. 6 shows the

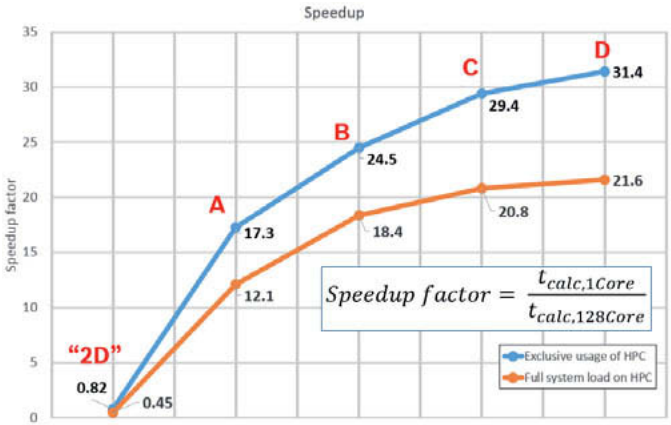


Fig. 6: Speedup factor for models A - D

evaluated speedup factor for the models A – D regarding the exclusive usage of the HPC

https://doi.org/10.51202/9783181023549 - Generiert durch IP 216.73.216.36, am 19.01.2026, 02:19:31. © Urheberrechtlich geschützter Inhalt. Ohne gesonderte Erlaubnis ist jede urheberrechtliche Nutzung untersagt, insbesondere die Nutzung des Inhalts im Zusammenhang mit, für oder in KI-Systemen, KI-Modellen oder Generativen Sprachmodellen.

system and the full load of the system. If using the system “exclusive” it is ensured that in the specific part of the HPC system, where the job is performed, at the same time no other job is running on unused cores. Therefore, the memory bus is exclusively used by the job related cores, and thus the maximum speedup is achieved. On the other hand the “full system load” scenario constitutes that the full HPC system is used, whereat the bus systems have to vectorise the traffic for different jobs which decreases the calculation speed.

As a consequence of this results, the distributed solving of highly complex 3D FEA models for electromagnetic calculations is performed in a specific part of the system, where an exclusive usage is ensured.

Application Example: Additional Stator Core Iron Losses

Theoretical Background

Opposed to a stranded wire winding, a bar-wound stator provides advantages such as automatic manufacturing process, easier cooling and better insulation. Additional to the above mentioned properties, it also provides higher slot filling and more compact end-windings. Hence, the bar-wound stator has a lower DC resistance. However, the skin and proximity effect

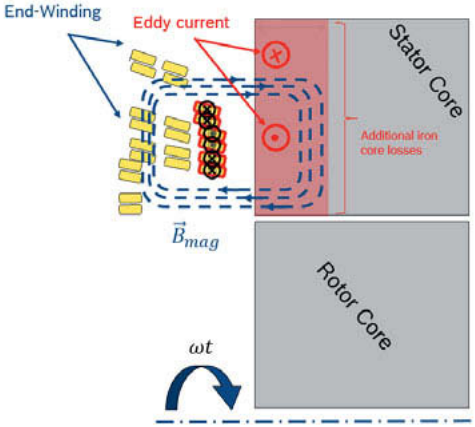


Fig. 7: Additional eddy currents in the stator core laminations due to the leakage magnetic field

increase the AC resistance of a bar-wound stator at high frequency operation and the tighter windings heads may also induce slightly higher iron losses in the stator core. These two potential sources of loss increment need to be carefully addressed for an accurate efficiency assessment. The winding-head proximity to the laminations together with the high electric loading and relatively high operating frequency may cause increased eddy currents on the

https://doi.org/10.51202/9783181023549 - Generiert durch IP 216.73.216.36, am 19.01.2026, 02:19:31. © Urheberrechtlich geschützter Inhalt. Ohne gesonderte Erlaubnis ist jede urheberrechtliche Nutzung untersagt, insbesondere die Nutzung des Inhalts im Zusammenhang mit, für oder in KI-Systemen, KI-Modellen oder Generativen Sprachmodellen.

axial sides of the stator core. The leakage magnetic flux from the winding-heads causes an axial magnetic flux component in the stator core. Hence eddy currents are induced in the in-plane laminations. Fig. 7 illustrates the physical background. Here the leakage magnetic flux arising from the current through the end-winding is shown as $\vec{B}_{mag}$, penetrating the end-region of the stator core and thus inducing eddy currents located close to the end.

Traction Motor Model

Fig. 8 depicts the traction motor model used for the calculation of the additional losses. To ensure a valid result for the complex leakage field, the meshing is chosen in an appropriate

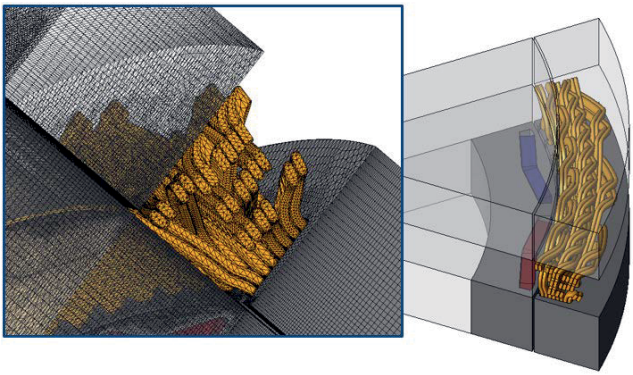


Fig. 8: Traction motor model

way close to the end-winding region. Within the stator core laminations an extruded mesh has been chosen to model the laminations equivalent by using different electrical resistivity in z-

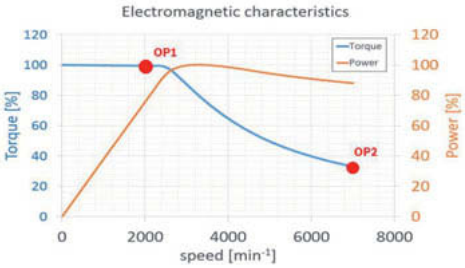


Fig. 9: Maximum torque/speed characteristics including evaluated operating points

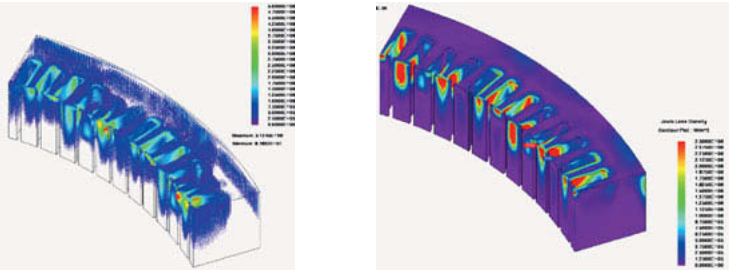
direction and xy-plane. The model consists of ~5.7 million elements and is evaluated at two operating points shown in Fig. 9. And Tab. 2. Both operating points are chosen on the maximum torque characteristics of the design. The first operating point is chosen at full

https://doi.org/10.51202/9783181023549 - Generiert durch IP 216.73.216.36, am 19.01.2026, 02:19:31. © Urheberrechtlich geschützter Inhalt. Ohne gesonderte Erlaubnis ist jede urheberrechtliche Nutzung untersagt, insbesondere die Nutzung des Inhalts im Zusammenhang mit, für oder in KI-Systemen, KI-Modellen oder Generativen Sprachmodellen.

	OP1	OP2
n	2000 min^{-1}	7000 min^{-1}
f_{el}	266.67 s^{-1}	933.33 s^{-1}
I_{rms}	300 A	208 A
φ	42 °el	78 °el

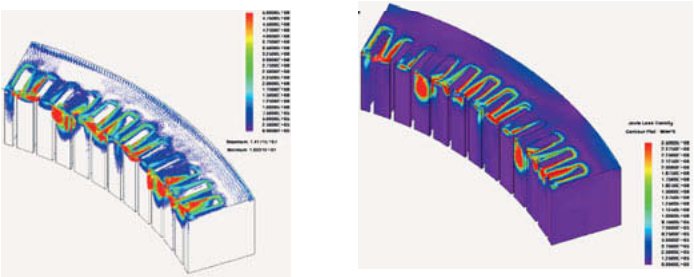
Tab. 2: Operating points

available current and base speed while the second is chosen at maximum speed and full nominal current. Both operating points lead to strong magnetic field magnitudes as the full nominal current is applied. Thus, a noticeable effect regarding additional eddy currents within the stator core end-region can be expected. In Fig. 10 the eddy currents a) and the resulting



a) b)

Fig. 10: Eddy currents a) and joule loss density b) at operating point OP1.



a) *b)*

Fig. 11: Eddy currents a) and joule loss density b) at operating point OP2.

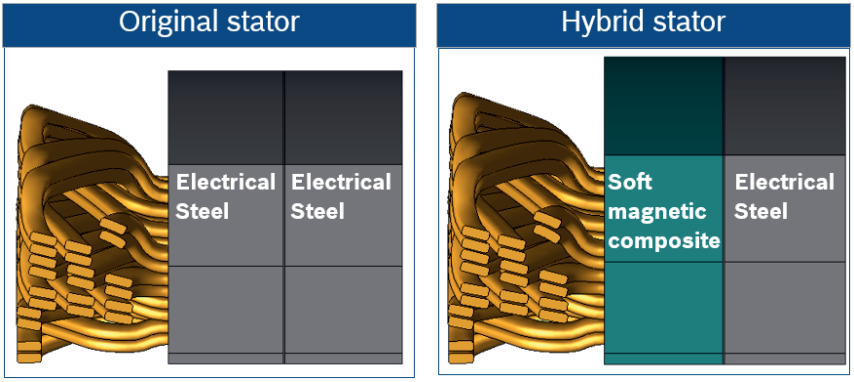
joule loss density b) is shown for operating point OP1 respectively for OP2 in Fig. 11 a) and

https://doi.org/10.51202/9783181023549 - Generiert durch IP 216.73.216.36, am 19.01.2026, 02:19:31. © Urheberrechtlich geschützter Inhalt. Ohne gesonderte Erlaubnis ist jede urheberrechtliche Nutzung untersagt, insbesondere die Nutzung des Inhalts im Zusammenhang mit, für oder in KI-Systemen, KI-Modellen oder Generativen Sprachmodellen.

b). In [1] the detailed evaluation algorithm for the additional eddy current and iron core losses is outlined.

Novel Hybrid Stator Core Design

As the combined application of HPC and enhanced 3D FEA enables now a sufficiently short evaluation time for large scaled models, a novel stator core design with reduced losses is introduced and evaluated. Therefore, within the stator core the laminations of the outer-region part is replaced by soft magnetic composite (SMC) material. Considering the lower electrical conductivity of SMC, placing the SMC segments on the sides, near the end-winding, promises a reduction of the induced in-plane eddy currents. Fig. 12 depicts the hybrid stator core design.



a) b)

Fig. 12: Initial stator core design a) and novel hybrid stator core design b).

It is well known that by replacing the stator laminations with an SMC material the efficiency can increase at high frequency operation, while it might decrease it at lower frequencies. Because of its lower magnetic permeability, a complete SMC stator can also lead to a slightly lower torque density. Thus, replacing only some stator sheets with an SMC material was adopted as a compromise solution. This should improve the efficiency without decreasing the torque density.

At the same time, the use of SMC on the stator core sides promises to reduce the eddy current losses caused by the winding head flux leakage. The elimination of this eddy currents loss component might compensate the typical SMC higher hysteresis losses at low frequencies.

Results

The two operating points defined in Fig. 9 are recalculated for the new stator. As a first concept

https://doi.org/10.51202/9783181023549 - Generiert durch IP 216.73.216.36, am 19.01.2026, 02:19:31. © Urheberrechtlich geschützter Inhalt. Ohne gesonderte Erlaubnis ist jede urheberrechtliche Nutzung untersagt, insbesondere die Nutzung des Inhalts im Zusammenhang mit, für oder in KI-Systemen, KI-Modellen oder Generativen Sprachmodellen.

proof calculation, only the material was substituted and the stator cross- section has not been yet optimized for the new material properties. Due to the lower magnetic permeability of the SMC material a slightly torque decrease can be noticed on Fig. 13 and Fig.14. The illustrated torque decrease amounts to 1.7% at OP1, respectively to 2.6% at OP2, which was found

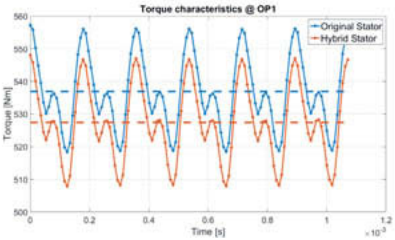


Fig. 13: Torque at operating point OP1

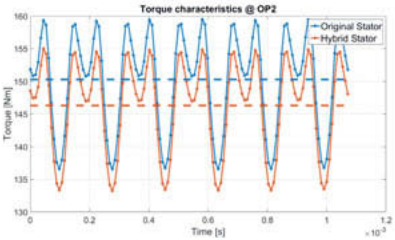


Fig. 14: Torque at operating point OP2

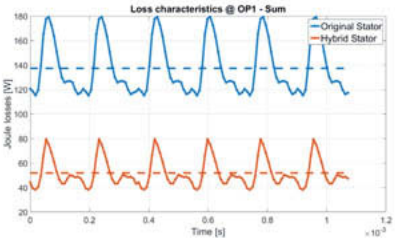


Fig. 15: Additional joule losses at OP1

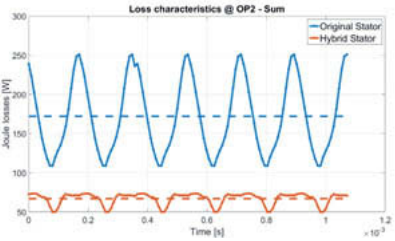


Fig. 16: Additional joule losses at OP2

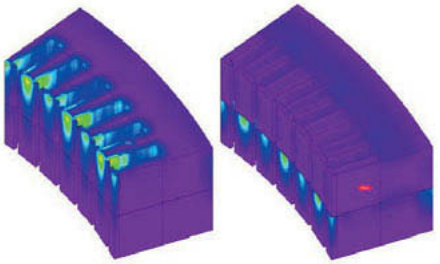


Fig. 17: Joule loss density at OP1

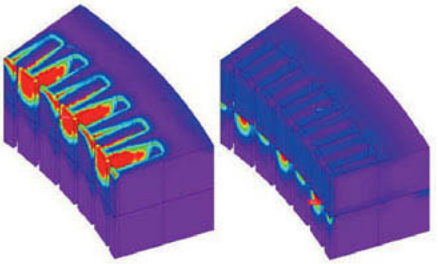


Fig. 18: Joule loss density at OP2

acceptable as a first result. Fig. 15 and Fig. 16 show the stator in-plane eddy current losses, computed during the FEA analysis. Fig. 17 illustrates the in-plane eddy currents loss density distribution on the stator core for OP1, while Fig. 18 shows the same for OP2. In both cases, the same behaviour can be observed. The loss density is considerably reduced in the stator outer part for the new stator core while the loss density slightly increases in the inner lamination

https://doi.org/10.51202/9783181023549 - Generiert durch IP 216.73.216.36, am 19.01.2026, 02:19:31. © Urheberrechtlich geschützter Inhalt. Ohne gesonderte Erlaubnis ist jede urheberrechtliche Nutzung untersagt, insbesondere die Nutzung des Inhalts im Zusammenhang mit, für oder in KI-Systemen, KI-Modellen oder Generativen Sprachmodellen.

part. This can be explained by a slower damping of the magnetic flux axial component due to the isotropic magnetic permeability of the outer SMC segment and due to the lack of eddy currents in the outer SMC segment. The overall efficiency was calculated using

$$\eta = \frac{M_i \cdot \omega}{M_i \cdot \omega + P_{total}}$$

where $M_i$is the resulting torque of the motor at the angular frequency ω and P_{total} are the total losses at the corresponding operating point. Tab. 3 summarizes the obtained reduced stator core losses at both operating points while Tab. 4 shows the same for the evaluated efficiencies.

$P_{vFe,Stator}$ [W]	OP1	OP2
Original stator	1087.1	4235.6
Hybrid stator	736.3	2810.9
Δ in %	**-32**	**-34**

Tab. 3: Resulting stator core losses

Efficiency [%]	OP1	OP2
Original stator	89.1	90.1
Hybrid stator	89.2	91.1
Δ in %	**+0.1**	**+1.0**

Tab. 4: Resulting efficiencies

The efficiency at high speed operations was improved by 1.0% without compromising the efficiency at base speed.

Summary

A comprehensive understanding and calculation of the electric power losses is required to accurately predict the performance of an electric machine. Separating the iron losses on components which can be directly calculated during the time stepping finite element computation helps to identify where potential improvements are possible.

It was shown that the winding head stray field may cause additional iron losses on the sides of the stator core. These additional losses amount to approximately 11% of the total iron losses at calculated maximum torque/base speed operating point. Thus, a possible place for

https://doi.org/10.51202/9783181023549 - Generiert durch IP 216.73.216.36, am 19.01.2026, 02:19:31. © Urheberrechtlich geschützter Inhalt. Ohne gesonderte Erlaubnis ist jede urheberrechtliche Nutzung untersagt, insbesondere die Nutzung des Inhalts im Zusammenhang mit, für oder in KI-Systemen, KI-Modellen oder Generativen Sprachmodellen.

improvement has been identified. This problematic nature is widely known in large turbo generators where all kind of screens are adopted to reduce these additional stray losses.
The proposed hybrid stator core manages to improve the efficiency at high frequency operation without compromising it at the base speed. Furthermore, an efficiency increase of 1.0% was obtain without compromising the torque/power density.
The new stator reduces the eddy currents loss caused by the winding head magnetic field leakage without adding any additional components like ferromagnetic screen.

Literature

[1] Morisco, D.P.; Iepure, I.L.; Möckel, A.: "*Enhanced 3D Finite Element Method Analysis of a Permanent Magnet Machine with Reduced Stator-Core Iron Losses*", IEEE International Electrical Machines & Drives Conference (IEMDC), Miami Fl., May, 2017

[2] Morisco, D.P.; Iepure, I.L.; Möckel, A.: "*AC-Losses in the End-Winding Structure of Bar-Wound Windings*", JMAG User Conference (Tokio), Dec., 2016

[3] Morisco, D.P.; Iepure, I.L.: "Stromverdrängung durch Stirnraumfelder im Wickelkopf von hochausgenutzten Traktionsantrieben", Kleinmaschinenkolloquium (Ilmenau), Mar., 2018

[4] Sano, H.; Asanuma, T.; Semba, K.; "*Loss calculation of bar-wound high-power-density PMSMs with massively parallel processing*", IEEE International Electrical Machines & Drives Conference (IEMDC), Miami Fl., May, 2017

[5] Morisco, D.P.; Iepure, I.L.; Möckel, A.: "Enhanced 3D Finite Element Method Analysis of Permanent Magnet Machines using HPC Systems and Massively Parallel Processing", Powersys Usergroup (Paris Fr.), Nov., 2017

[6] Nakano, T.; et.al; „*Parallel Computing of Magnetic Field for Rotating Machines on the Earth Simulator*", IEEE transactions on Magnetics, Vol. 46, No. 8, Aug., 2010

[7] Semba, K.; Tani, K.; Yamada, T.; "Parallel Performance of Multithread ICCG Solver Based on Algebraic Block Multicolor Ordering in Finite Element Electromagnetic Field Analyses", IEEE Transactions on Magnetics, Vol. 49, No. 5, May, 2013

[8] Semba, K.; Katagiri, H.; Asanuma, T.; "*Realistic and Very Fast Simulation of Electric Machines and Apparatus by using Massively Parallel Processing*", IEEE International Conference on Electrical Machines and Systems (ICEMS), Sydney, Aug., 2017

https://doi.org/10.51202/9783181023549 - Generiert durch IP 216.73.216.36, am 19.01.2026, 02:19:31. © Urheberrechtlich geschützter Inhalt. Ohne gesonderte Erlaubnis ist jede urheberrechtliche Nutzung untersagt, insbesondere die Nutzung des Inhalts im Zusammenhang mit, für oder in KI-Systemen, KI-Modellen oder Generativen Sprachmodellen.

https://doi.org/10.51202/9783181023549 - Generiert durch IP 216.73.216.36, am 19.01.2026, 02:19:31. © Urheberrechtlich geschützter Inhalt. Ohne gesonderte Erlaubnis ist jede urheberrechtliche Nutzung untersagt, insbesondere die Nutzung des Inhalts im Zusammenhang mit, für oder in KI-Systemen, KI-Modellen oder Generativen Sprachmodellen.

Great Wall Motors' 2nd Generation of Pi4 Platform

A high performance PHEV for Premium SUV in China

Yvan Le Neindre, Great Wall Motors Co, Baoding, China

Abstract

Great Wall Motors will be introducing in July 2019 its second generation of Pi4 Platform, a Dual Axle PHEV architecture based on a P0-P4 topology. Improvements made on components (engine, transmission, battery & braking system) as well as function features enabled to make significant improvements on longitudinal dynamics as well as fuel economy.

Introduction of Pi4 Architecture

Following the successful launch in China in March 2018 of its first generation of dual axle PHEV architecture, the Pi4 platform, applied on the WEY P8, Great Wall Motors Co, will release in July 2019 its second generation of Pi4 Platform.

GWM's Pi4 platform is a flexible platform architecture adopting a P0-P4 Topology.

The core of this architecture is a hybrid dual axle solution, which can completely decouple front and rear axle.

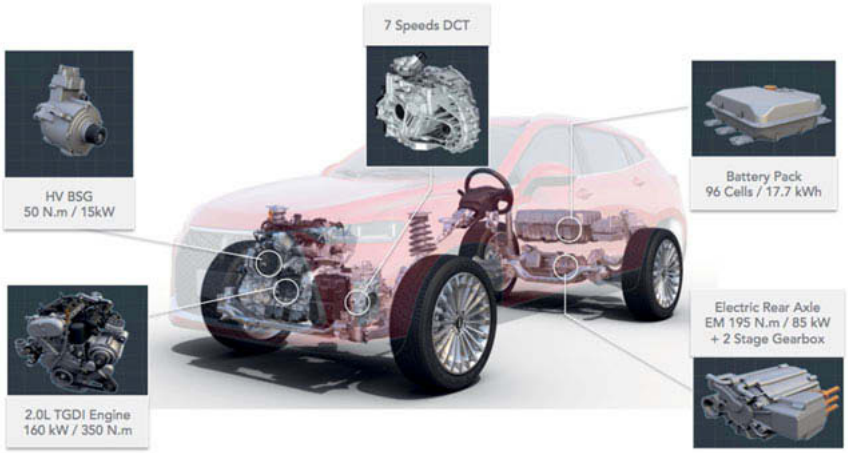


Fig. 01: The dual axle powertrain of Pi4 Platform

https://doi.org/10.51202/9783181023549 - Generiert durch IP 216.73.216.36, am 19.01.2026, 02:19:31. © Urheberrechtlich geschützter Inhalt. Ohne gesonderte Erlaubnis ist jede urheberrechtliche Nutzung untersagt, insbesondere die Nutzung des Inhalts im Zusammenhang mit, für oder in KI-Systemen, KI-Modellen oder Generativen Sprachmodellen.

The front axle is composed of

- 2.0L Gasoline Engine, which can develop a maximum power 160 kW and a maximum torque of 350 N.m.
- In-house developed 7 speed Dual Clutch Transmission (as opposed to the 6 speed DCT used in first Generation)
- High voltage Belt Starter Generator, connected to the engine Front End Accessory drive, which can perform engine start with a peak torque of 50 N.m and ensure boost & power derivation with a peak power of 15 kW.

The rear axle is composed of:

- Rear E-Motor that is designed to fulfill Pure Electric Driving and Regenerative Braking needs. The E Motor can reach a maximum peak torque of 195 N.m and a peak power of 85 kW.
- Rear Axle 2 speed Transmission used to operate the rear axle E-motor at its best operating points and maximize fuel savings and electric driving range.

A 96 cells Li Ion HV Battery powers the power train. The Battery Pack has a total energy of 17.7 kWh and can ensure an electric driving range of over 70 km on NEDC cycle (as opposed to the 14.2 kWh Battery Pack used in first Generation).

Benefits of Pi4 Platform compared to other Architectures

The Pi4 Platform compared to other architecture (ex P2 Hybrids) offers significant advantages. By offering low mechanical friction, higher regenerative power potential and more degree of freedom for optimal set point strategy, the GWM's Pi4 Platform offers a very high level of efficiency compared to benchmark competitors.

The Pi4 platform offer also significant advantages compared to other architectures regarding longitudinal dynamics. According to simulation results a similar vehicle equipped with P2 Architecture could offer approximately 8% of improvement for the time response for 0-100 km/h compare to conventional reference, whereas the Pi4 could offer over 30% improvements on longitudinal dynamics due to the ability to combine torque supply of front and rear axle and a lower effect of torque limitation on the front axle (gearbox limitations on 1st and second gear & tire adherence limits). With the benefit of the added power of the rear axle the Pi4 can for instance reach 0-100 km/h in 5.8s (when enabling Sport+ mode).

https://doi.org/10.51202/9783181023549 - Generiert durch IP 216.73.216.36, am 19.01.2026, 02:19:31. © Urheberrechtlich geschützter Inhalt. Ohne gesonderte Erlaubnis ist jede urheberrechtliche Nutzung untersagt, insbesondere die Nutzung des Inhalts im Zusammenhang mit, für oder in KI-Systemen, KI-Modellen oder Generativen Sprachmodellen.

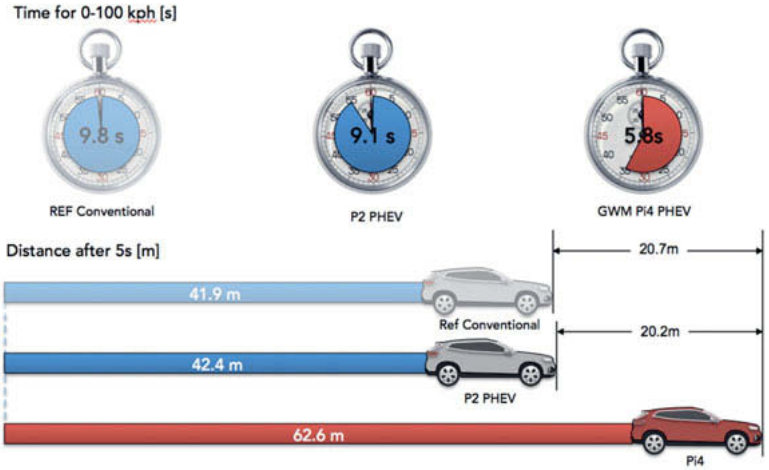


Fig. 02: Benefits of Pi4 Platform on Longitudinal Dynamics

In addition to improved longitudinal dynamics, the P0-P4 topology offer major improvements on grade ability and allow to reach performances comparable to mechanical 4WD in low adherence conditions.

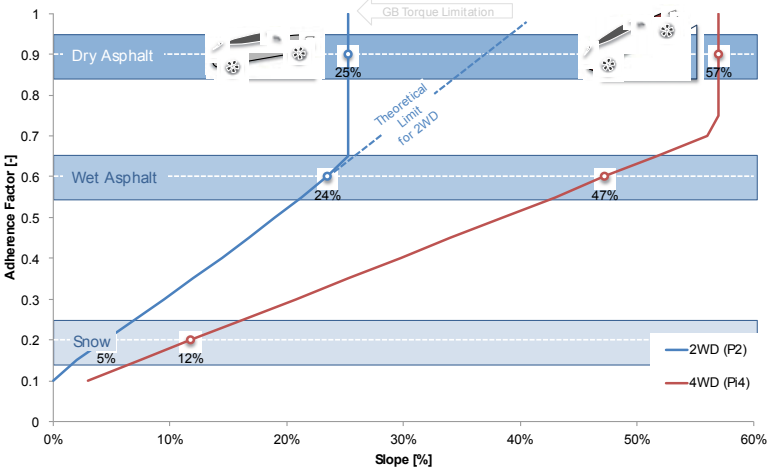


Fig. 03: Benefits of Pi4 Platform on Gradeability

https://doi.org/10.51202/9783181023549 - Generiert durch IP 216.73.216.36, am 19.01.2026, 02:19:31. © Urheberrechtlich geschützter Inhalt. Ohne gesonderte Erlaubnis ist jede urheberrechtliche Nutzung untersagt, insbesondere die Nutzung des Inhalts im Zusammenhang mit, für oder in KI-Systemen, KI-Modellen oder Generativen Sprachmodellen.

Based on simulations, a FWD vehicle can ensure a maximum grade ability that could range from 20 to 30% grade on dry asphalt depending on vehicle weight and gearbox limitations. Thanks to the electric rear axle, the Pi4 can ensure to reach up 55 to 60% grade on dry asphalt and offers performances consistent with market expectations for a SUV class vehicle.

Main Features of the Pi4 Platform

The driver can select 8 (5+3) different drive modes to adjust the system to the driving environment. Regardless of selected drive mode, the control system checks that the combination of drivability, driving experience, environmental impact and fuel economy is always optimal in relation to the driving conditions.

- AUTO Mode: is the standard operating mode of the Vehicle. This mode ensures the best use of the battery energy in charge depleting and charge sustaining mode while maximizing fuel economy for the Driver. The system determine based on the optimization strategies the optimal start conditions for the engine in order to minimize fuel consumption. Once started the system determine optimal torque distribution between E-Motor, Engine & BSG and select optimal gear set point on front and rear transmission.
- EV Mode: This option focuses on pure electric drive as well as low energy consumption, and helps the driver to maximize electric driving range on the HV battery.
- SPORT Mode: In this mode, electrical boosting power will be enhanced to support engine power and provide optimal longitudinal performance. The activation of this mode selects different tuning of the power train to improve longitudinal dynamic performances.
- AWD Mode: In this mode (AWD and 3 sub modes: Snow, Mud, Sand) the target is to ensure optimal 4WD motricity for the driver. This mode allows the driver to handle situations such as driving on low adherence road (snow, mud or sand) or assists the driver on climbing steep slopes. In AWD Mode, power is released from the powertrain through two paths: while engine power is supplied to the front axis for vehicle traction, a fraction of its power can be derived from the front BSG to the rear motor to ensure 4WD.
- SAVE Mode: the systems offer a Save Mode to enable the driver to store (or restore) energy in the battery that could be used latter when he requires it. The aim is for instance to let driver preserve some energy during depleting phase if he starts driving on highway but intends latter to drive in a urban area where EV driving is preferred.

https://doi.org/10.51202/9783181023549 - Generiert durch IP 216.73.216.36, am 19.01.2026, 02:19:31. © Urheberrechtlich geschützter Inhalt. Ohne gesonderte Erlaubnis ist jede urheberrechtliche Nutzung untersagt, insbesondere die Nutzung des Inhalts im Zusammenhang mit, für oder in KI-Systemen, KI-Modellen oder Generativen Sprachmodellen.

The hybrid system is constantly monitoring the driving conditions to ensure the optimal set point for the system (engine start, torque distribution, gear set point) and maximize the fuel savings for the customer.

The Plug-In charging feature enables customers to enjoy daily commuting in full electric mode with an unrivalled comfort and a very frugal cost of use. The 17.7 kWh battery allows driving over **70 km** in pure electric with a sufficient driving range to ensure most of the daily commuting in electric mode and ensure combined fuel consumption on NEDC as low as **1.6L/100 km**.
In charge sustaining phase, the system automatically adjust the settings and maximize the use of fuel and the kinetic energy of the vehicle to ensure the charge of the battery. In these conditions, the vehicle can reach a fuel consumption as low as **6.1 L/100 km** on NEDC cycle in Charge Sustaining phase.

Based on available market data, this fuel consumption performance rank the Pi4 power train among some of the best of its class regarding energy consumption and fuel economy without compromising performances and drivability.

Presentation of Pi4 Gen2: Transmission
The first generation of Pi4 Platform was equipped with a 6 speed DCT when it was launched on the Chinese market in March 2018. In its second generation of PHEV, Great Wall Motors choose to select its awarded in-house 7 speed DCT, the 7DCT450, to equip its Pi4 Platform.
Launched in 2017 for conventional power train this seven speed wet clutch gearbox is the demonstration of the expertise of Great Wall Motors' Transmission subsidiary, FECO, in automatic transmission [1]. Thanks to its world-class team of engineers and strong in house capability in design, testing, calibration, SW and NVH, the 7DCT450 is ensuring:

- High reliability and stability in use
- Strong torque performances
- High efficiency with the use of low viscosity oil & optimized mechanical design
- Excellent NVH performances by optimized gear design & shifting control

As a result the 7DCT450 received in 2017 the Transmission award and was ranked No.1 from the World Top 10 Transmission by China CarBingo Academy (CBA).

https://doi.org/10.51202/9783181023549 - Generiert durch IP 216.73.216.36, am 19.01.2026, 02:19:31. © Urheberrechtlich geschützter Inhalt. Ohne gesonderte Erlaubnis ist jede urheberrechtliche Nutzung untersagt, insbesondere die Nutzung des Inhalts im Zusammenhang mit, für oder in KI-Systemen, KI-Modellen oder Generativen Sprachmodellen.



Fig. 04: Great Wall Motors' 7DCT450

Applying this best in class transmission to its second generation of Pi4 Platform enabled GWM's engineers to offer simultaneously improvement in longitudinal dynamics and fuel economy thanks to its wider gear span compared to the 6DCT of the first generation.

In order to enable the integration of the 7DCT450 in the Pi4 Platform, GWM's engineer developed for this project an electric oil pump (EOP) to supply oil for lubrication, actuation (pre-engagement & engine start) & cooling of the transmission when the vehicle is driven in pure electric mode.

Specific SW updates of the TCU, such as Launch Control & Race Start, were also performed in order to improve longitudinal dynamics compared to the previous generation of the Pi4 Platform.

Battery Pack Improvements

Regarding the Battery Pack, GWM's engineers choose to upgrade the cells type with cell capacity rising from 37 Ah to 51 Ah. As a results the 96 cells battery pack reaches a total usable energy of 17.7 kWh, which enable the Pi4 Gen 2 to reach an electric driving range of over 70 km (as compared to the 50 km AER achieved for the 1st generation).

https://doi.org/10.51202/9783181023549 - Generiert durch IP 216.73.216.36, am 19.01.2026, 02:19:31. © Urheberrechtlich geschützter Inhalt. Ohne gesonderte Erlaubnis ist jede urheberrechtliche Nutzung untersagt, insbesondere die Nutzung des Inhalts im Zusammenhang mit, für oder in KI-Systemen, KI-Modellen oder Generativen Sprachmodellen.

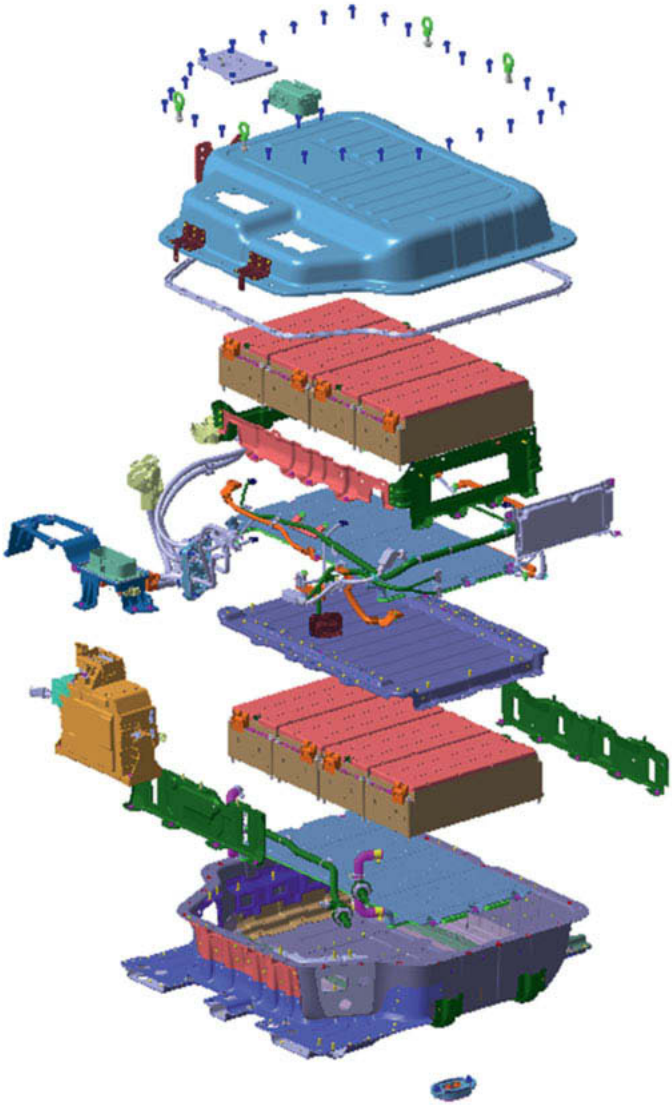


Fig. 05: Pi4 Gen 2 Battery Pack – 96 cells - 51 Ah

https://doi.org/10.51202/9783181023549 - Generiert durch IP 216.73.216.36, am 19.01.2026, 02:19:31. © Urheberrechtlich geschützter Inhalt. Ohne gesonderte Erlaubnis ist jede urheberrechtliche Nutzung untersagt, insbesondere die Nutzung des Inhalts im Zusammenhang mit, für oder in KI-Systemen, KI-Modellen oder Generativen Sprachmodellen.

To match with the upgrade of the battery pack usable energy, the maximum charging power of OBC have been raised to 6.6kW (compared to the 3.3 kW of Pi4 Gen1), which enables to achieve charging completion time within 3.5 hours (compared to 5.5 hours necessary at a 3.3 kW charging rate).

While this extended usable energy can offer significant improvement for pure electric (nearly 50% extension of electric driving range), the longer electric drive duration and the change of cell type lead to more stringent requirement for the battery pack cooling.

Relying on the strong in-house expertise of its battery pack business unit, SVOLT, Great Wall Motors developed specific cooling solution in order to achieve robust and repeatable performances in a very wide range of thermal environment.

Specific improvements made for cooling include especially:

- Optimization of the cooling plate with addition of holes to improve heat exchanges
- Optimization of module structure with improvement of heat transfer of the side plate to cooling plate

As a result the thermal performance index, as defined as the ratio of temperature difference between warmest cell and coolant divided by the heat generated in the cells, have been reduced from 3 to 2.5 K/W, achieving state of the art on the market for cooling performances.

Presentation of Pi4 Gen2: Regenerative Braking System

In order to optimize further vehicle efficiency and maximize the electric driving range for the customer, GWM selected for its second generation of Pi4 platform an upgraded version of the Cooperative Regenerative Braking System (CRBS) from Bosch.

The addition of iBooster in the system enable a higher level of regenerative braking in a wide range of deceleration levels compared to the version used on the 1st generation.

Extensive calibration work between Chassis and Powertrain system enabled to maximize the electric driving range with an increase of 2 km as compared to the achievable performances with previous braking system.

https://doi.org/10.51202/9783181023549 - Generiert durch IP 216.73.216.36, am 19.01.2026, 02:19:31. © Urheberrechtlich geschützter Inhalt. Ohne gesonderte Erlaubnis ist jede urheberrechtliche Nutzung untersagt, insbesondere die Nutzung des Inhalts im Zusammenhang mit, für oder in KI-Systemen, KI-Modellen oder Generativen Sprachmodellen.

Improvement of Longitudinal Dynamics

In order to further improve longitudinal dynamic compared to its first generation, significant improvements have been made on the SW and the calibration. These upgrades on performances were achieved mainly through:

- Launch Control: Integration of high performance launch control strategy in the TCU
- Integration of Sport +: Adjustments of specific settings for shifting maps, torque gradient and maximum torque (within limits of component durability & tire adherence limitations).

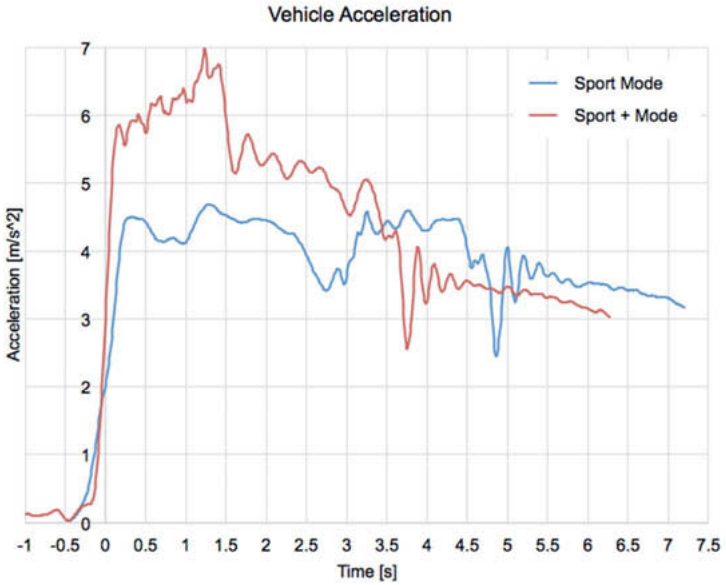


Fig. 06: Improvement of Pi4 Gen2 on Longitudinal Dynamics

This improvement enables to improve by nearly 50% torque response and offer steep acceleration profile in the launch phase.

With these strategies the acceleration time to reach 0-100 km/h can be achieved in 5.8s (compared to the 6.5s achieved in Pi4 Gen1) offering very high dynamic performances for a SUV of this category.

https://doi.org/10.51202/9783181023549 - Generiert durch IP 216.73.216.36, am 19.01.2026, 02:19:31. © Urheberrechtlich geschützter Inhalt. Ohne gesonderte Erlaubnis ist jede urheberrechtliche Nutzung untersagt, insbesondere die Nutzung des Inhalts im Zusammenhang mit, für oder in KI-Systemen, KI-Modellen oder Generativen Sprachmodellen.

Improvement of Efficiency

The previous generation of Pi4 Platform achieved a fuel consumption of 6.8L/100 km on NEDC cycle in charge sustaining phase. Its average vehicle efficiency of 28.7% were already higher than most of its competitor in the PHEV SUV segment equipped with P2 AT transmission.

By combining improvements on the components efficiency (improvement of the engine BSFC map, 7DCT efficiency, CRBS), the setpoint strategy (start / stop, gear setpoint & SOC management) as well as improvement on the vehicle enabled GWM's engineers to increase the vehicle efficiency to a top value of 30.5% and reduced the fuel consumption to 6.1 L/100 km on NEDC cycle in CS phase.

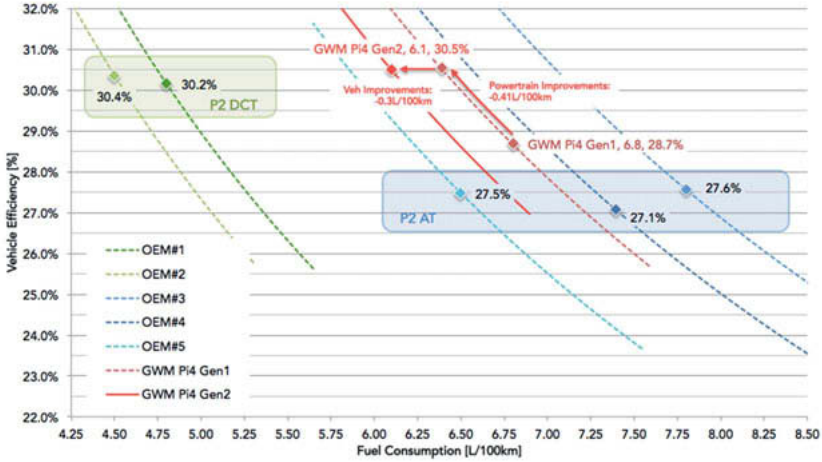


Fig. 07: Improvement of Pi4 Gen2 Efficiency

Improvement of Thermal Management

With an extremely wide range of climatic conditions, meeting the diverse needs of customer in China and ensuring robust and repeatable performances can be seen as a technical challenge. With the experience gained during its first generation and through repeated validation in extreme conditions, GWM offered for its second generation significant improvements on the vehicle and power train thermal management.

Some of the key improvements on thermal management include:

https://doi.org/10.51202/9783181023549 - Generiert durch IP 216.73.216.36, am 19.01.2026, 02:19:31. © Urheberrechtlich geschützter Inhalt. Ohne gesonderte Erlaubnis ist jede urheberrechtliche Nutzung untersagt, insbesondere die Nutzung des Inhalts im Zusammenhang mit, für oder in KI-Systemen, KI-Modellen oder Generativen Sprachmodellen.

- Improvement of Battery Cooling to offer robust performances in extreme warm environment
- Improvement of Battery Warm-up strategy to enable faster hybrid features in extreme cold conditions
- Add-on of High Voltage PTC (compared to Fuel Heater in previous generation) to enable more efficient and emission free heating for the cabin comfort in cold conditions

With these upgrades, the 2nd Generation of Pi4 Platform can offer robust and reliable performance for the power train without compromising driver's thermal comfort.

Technical Roadmap and future evolutions of Pi4 Platform

The second generation of Pi4 platform, through its evolutive and modular design approach, will offer to customer a great leap forward in performances in line with market expectation for Premium SUV.

Great Wall Motors Engineers are already working on the future evolution of this platform with the next generation of the in-house DCT, the XDCT, a high torque capacity, highly compact, light and efficient transmission [2].

The experience gained during the development of the first two generations of Pi4 platform, as well as the strong expertise in transmission design, will enable GWM to deliver in the future a range of powertrains both in P2 and P2 + P4 configuration to offer to its customers a wide range of solutions that combine optimal user benefits and respect to urban environment.

[1] Lipeng Zheng: First 7-Speed DCT developed and produced in China. 16th CTI Symposium Berlin. Dec 2017

[2] Gerhard Henning: FECO E-CHUANG Transmission and Hybrid Strategy Roadmap. 17th CTI Symposium Berlin. Dec 2018

https://doi.org/10.51202/9783181023549 - Generiert durch IP 216.73.216.36, am 19.01.2026, 02:19:31. © Urheberrechtlich geschützter Inhalt. Ohne gesonderte Erlaubnis ist jede urheberrechtliche Nutzung untersagt, insbesondere die Nutzung des Inhalts im Zusammenhang mit, für oder in KI-Systemen, KI-Modellen oder Generativen Sprachmodellen.

https://doi.org/10.51202/9783181023549 - Generiert durch IP 216.73.216.36, am 19.01.2026, 02:19:31. © Urheberrechtlich geschützter Inhalt. Ohne gesonderte Erlaubnis ist jede urheberrechtliche Nutzung untersagt, insbesondere die Nutzung des Inhalts im Zusammenhang mit, für oder in KI-Systemen, KI-Modellen oder Generativen Sprachmodellen.

Optimisation of electric motor acoustics of a hybrid dual clutch gearbox using virtual methods

Dipl.-Ing. **Marcus Kruse**, Dr. **Harald Decker**,
Dipl.-Ing., Dipl.-Wirtsch.-Ing. **Sebastian Eulert**,
Volkswagen AG Group Components, Kassel

Zusammenfassung

Das von der Audi AG und Volkswagen AG Komponente gemeinschaftlich entwickelte Doppelkupplungs-Getriebe DL382E-7A aus dem S tronic® - Baukasten wird seit 2018 in den Baureihen A6 und Q5 von Audi eingesetzt. Neben den Anforderungen an die Leistungsdichte sowie an den Wirkungsgrad der Elektromaschine wurden die akustischen Anforderungen und damit die Anforderungen für leises Fahren im Rahmen des Entwicklungsprozesses des elektrifizierten Getriebes hoch priorisiert [1]. Um den hohen akustischen Anforderungen gerecht zu werden, wurde mit Fokus auf den elektromagnetisch bedingten Geräuschursachen ein (virtueller) Baukasten im Rahmen der Entwicklung erfolgreich eingesetzt. Die darin enthaltenen Techniken ermöglichten es, das elektromagnetisch bedingte Geräuschverhalten des Antriebs zu simulieren und zielführende Optimierungsmaßnahmen zu identifizieren. Der Baukasten hält zunächst eine Technik zur Simulation der Anregung der Elektromaschine in Form von dynamischen Luftspaltkräfte bereit. Das Ergebnis der Simulation ist der akustische Fingerabdruck, der einer Visualisierung der Amplituden der Luftspaltkräfte über der Drehzahl und dem Drehmoment der elektrischen Maschine entspricht. Die Technik zur Simulation der Anregung ist geknüpft an die Parametervariation und –optimierung der Geometrie des Elektroblechschnitts. Damit konnte im Falle des DL382E-7A eine Minimierung der anregenden Luftspaltkräfte auf virtueller Basis erfolgreich durchgeführt werden. Der Effekt der geringeren Anregung des optimierten Blechschnitts auf den Körperschall wurde einerseits durch geeignete Körperschallsimulationen sowie andererseits durch entsprechende Versuchstechniken zur Ermittlung des Körper- und Luftschalls des Antriebs auf einem Akustikprüfstand bestätigt. Eine weitere Technik aus dem Baukasten zur Minimierung der anregenden Luftspaltkräfte ist die Anpassung der Ansteuerung der Elektromaschine. Dabei werden zusätzlich zu den drehmomentbildenden Grundoberschwingungen der Umrichterspannung gezielt Oberschwingungen der Spannung mit abgestimmter Frequenz, Amplitude und Phase durch eine Akustikfunktion im Umrichter

https://doi.org/10.51202/9783181023549 - Generiert durch IP 216.73.216.36, am 19.01.2026, 02:19:31. © Urheberrechtlich geschützter Inhalt. Ohne gesonderte Erlaubnis ist jede urheberrechtliche Nutzung untersagt, insbesondere die Nutzung des Inhalts im Zusammenhang mit, für oder in KI-Systemen, KI-Modellen oder Generativen Sprachmodellen.

eingestellt. In der Elektromaschine resultieren optimierte Stromoberschwingungen die letztlich den relevanten anregenden Luftspaltkräften entgegenwirken. Durch Anwendung der Technik konnten die akustischen Eigenschaften des DL382E-7A und damit letztlich die Fahrzeugakustik verbessert werden. Eine messtechnische Verifikation der Optimierungsmaßnahme erfolgte durch Messung der beruhigten Oberflächenschwingungen des Antriebsgehäuses mittels 3D-Laservibrometrie.

Abstract

The dual clutch gearbox DL382E-7A from the S tronic® modular assembly matrix, developed jointly by Audi AG and Volkswagen AG Group Components, has been used since 2018 in the A6 and Q5 model series from Audi. In addition to the demands on the power density as well as the efficiency of the electric motor, high priority has been placed on the acoustic demands and, as such, the requirement for quiet driving in the course of the development process of the electrified gearbox [1]. In order to do justice to the high acoustic demands, a (virtual) model has been employed with success in the course of development with a focus on the causes of electromagnetic-related noise. The methods contained therein make it possible to simulate the electromagnetic-related noise behaviour of the drive and to identify productive optimisation measures. The model primarily features a method for simulating the excitation of the electric motor in the form of dynamic air gap forces. The result of the simulation is the acoustic fingerprint, which represents a visualisation of the amplitudes of the air gap forces over the speed and the torque of the electric motor. The method of simulating the excitation is linked to the parameter variation and optimisation of the geometry of the electrical sheet section. In the case of the DL382E-7A, it was possible to successfully achieve a minimisation of the forces from air gap excitation on a virtual basis. The effect of less excitation of the optimised electrical sheet on structure-borne noise was confirmed, on one hand, through suitable structure-borne noise simulations and also, on the other, by relevant trial methods for determining the structure-borne and airborne noise of the drive unit on an acoustic test bed. Another method from the model for minimisation of the forces from air gap excitation is the adaptation of electric motor actuation. Here, in addition to the torque-forming basic harmonics of the inverter voltage, targeted harmonics of the voltage with a coordinated frequency, amplitude and phase were set in the inverter via an acoustic function. The result is optimised current harmonics in the electric motor that ultimately counteract the relevant forces from air gap excitation. By employing the method, it was possible to improve the acoustic properties of the DL382E-7A and as such the vehicle

https://doi.org/10.51202/9783181023549 - Generiert durch IP 216.73.216.36, am 19.01.2026, 02:19:31. © Urheberrechtlich geschützter Inhalt. Ohne gesonderte Erlaubnis ist jede urheberrechtliche Nutzung untersagt, insbesondere die Nutzung des Inhalts im Zusammenhang mit, für oder in KI-Systemen, KI-Modellen oder Generativen Sprachmodellen.

acoustics. Verfication of the optimisation measure using test instrument technology was carried out by measuring the calmed surface vibrations of the drive housing by means of 3D laser vibrometry.

1. The dual clutch gearbox DL382E-7A focusing on the hybrid module

The electrified dual clutch gearbox DL382E-7A from the S tronic® modular assembly matrix, developed jointly by Audi AG and Volkswagen AG Group Components Kassel, has been used since 2018 in the A6 and Q5 model series from Audi [1]. Electrification of the gearbox is achieved using a hybrid module. This comprises a cooling unit and an electric motor consisting of a stator and internal rotor and is housed between the dual-mass flywheel and the dual clutch in a hybrid-specific gearbox housing.

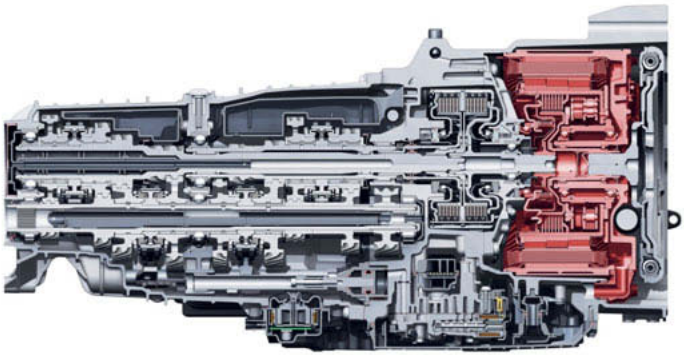


Fig. 1: Cross section of 7 SPEED S TRONIC® Hybrid



Fig. 2: Assembly overview (clutch with centrifugal pendulum / rotor / stator / cooling unit / sensors) [2]

https://doi.org/10.51202/9783181023549 - Generiert durch IP 216.73.216.36, am 19.01.2026, 02:19:31. © Urheberrechtlich geschützter Inhalt. Ohne gesonderte Erlaubnis ist jede urheberrechtliche Nutzung untersagt, insbesondere die Nutzung des Inhalts im Zusammenhang mit, für oder in KI-Systemen, KI-Modellen oder Generativen Sprachmodellen.

The outer plate carrier located in the rotor has a clutch inside for separating the combustion engine from the drive train. A centrifugal pendulum supplements the dual-mass flywheel. The stator is characterised by a high number of slots and also a distributed winding.



Fig. 3: Sheet section [2]

Significant demands on the gearbox were, among other things, integration in the existing modular assembly matrix with minimum expansion of the installation space. As before, the effectiveness of the overall module needed to be configured with optimised efficiency for optimal interplay with the gearbox. The performance should be utilised right up to the limits. Particular attention was placed on fulfilling the ambitious acoustic aims: The high demands on quiet driving had to be met.

2. Relevant causes of noise in the electric motor

Basically, the causes of noise in electric motors can be divided into three categories: electromagnetic, mechanical and ventilation-related causes [3].

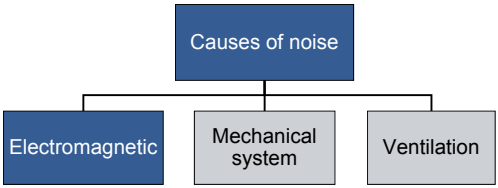


Fig. 4: Causes of noise in electric motors

https://doi.org/10.51202/9783181023549 - Generiert durch IP 216.73.216.36, am 19.01.2026, 02:19:31. © Urheberrechtlich geschützter Inhalt. Ohne gesonderte Erlaubnis ist jede urheberrechtliche Nutzung untersagt, insbesondere die Nutzung des Inhalts im Zusammenhang mit, für oder in KI-Systemen, KI-Modellen oder Generativen Sprachmodellen.

The cause of noise dominating in practice is electromagnetic and comes by way of interfacial forces from the Maxwell stress tensor, which are referred to hereafter as (dynamic) air gap forces. The dynamic air gap forces can excite vibrations in the stator and rotor of the electric motor.

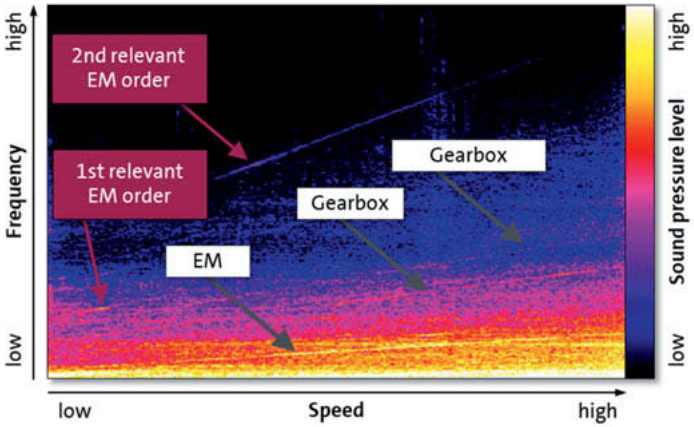


Fig. 5: Campbell graph of the sound pressure level in the vehicle interior with relevant electromagnetic-related abnormalities in the development process

This structure-borne noise is conducted through transfer paths in the drive to the surface of the drive and results in vibration of the components (usually the housing) located on the surface, which ultimately lead to the emission of airborne noise. Acoustic transfer paths (for structure-borne as well as airborne noise) in the vehicle (e.g. mounting points and body parts) direct the noise into the inside of the vehicle where ultimately the driver can detect structure-borne and airborne noise. In the case of DL382E-7A, electromagnetic-related acoustic abnormalities were encountered in the development process, which were perceived as disruptive. It was possible to allocate the source of the abnormalities unequivocally to the electric motor by means of an order analysis: The first abnormal mechanical order equated to the multiple of the number of poles of the electric motor, while the second abnormal order equated to the number of slots of the electric motor (slot harmonics).

https://doi.org/10.51202/9783181023549 - Generiert durch IP 216.73.216.36, am 19.01.2026, 02:19:31. © Urheberrechtlich geschützter Inhalt. Ohne gesonderte Erlaubnis ist jede urheberrechtliche Nutzung untersagt, insbesondere die Nutzung des Inhalts im Zusammenhang mit, für oder in KI-Systemen, KI-Modellen oder Generativen Sprachmodellen.

3. (Virtual) methods for optimisation of the acoustic properties

To facilitate the high acoustic aims of the electrified drive with the focus on the electric motor and the previously demonstrated acoustic abnormalities, a module with mainly virtual methods was employed. One major method is the simulation of dynamic air gap forces using the Finite Element Method. By using the “multi-slice” method, a discrete skewing of the rotor can be calculated based on two-dimensional models of the electric motor [4]. The forces are evaluated in radial and tangential direction in a central assessment line in the air gap of the motor.

To minimise excitation in the form of dynamic air gap forces, two methods were developed.

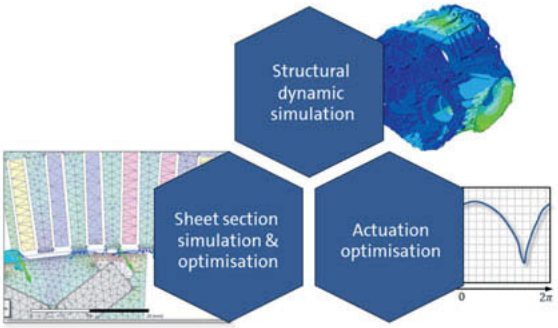


Fig. 6: Module with (virtual) methods for optimisation of the acoustic properties of electrified drives with the focus on the electric motor

One method involved optimising the process of parameter variation and optimisation, which preferentially varies geometrical parameters of the sheet section in order to reduce the dynamic air gap forces. In addition to sheet section optimisation, the module also makes allowance for another method to minimise the dynamic air gap forces and thereby the electromagnetic-related noise from the drive. In contrast to sheet section optimisation, the method does not require any adjustment to the actual hardware, i.e. the constructive conditions, rather an adaptation of electric motor actuation. Aside from actual regulation (aimed at adherence to the mean torque) depending on the order to be optimised, targeted voltage harmonics were set accordingly by means of acoustic functions in the inverter of the electric motor that exhibit a frequency, amplitude and phase targeted towards minimal excitation. Unlike in standard oper-

https://doi.org/10.51202/9783181023549 - Generiert durch IP 216.73.216.36, am 19.01.2026, 02:19:31. © Urheberrechtlich geschützter Inhalt. Ohne gesonderte Erlaubnis ist jede urheberrechtliche Nutzung untersagt, insbesondere die Nutzung des Inhalts im Zusammenhang mit, für oder in KI-Systemen, KI-Modellen oder Generativen Sprachmodellen.

ation, lightly modified phase currents flow in the electric motor that are distinguished by modified current harmonics with unaltered fundamental oscillation amplitude and phase. The ensuing upper harmonics act against the relevant air gap forces.

For both methods, it is generally not necessary for a qualitative reduction of the level to simulate the structure-borne noise level. In order to quantify the reduction of the structure-borne noise on the basis of simulated air gap forces, however, the structure-borne noise is simulated by means of the Finite Element Method. Here, the existing structural dynamic model is applied to the nodes (stator and rotor) close to the air gap with the previously simulated radial and tangential air gap forces (in consideration of the skewed position). The simulation procedure supplies the levels according to the order depending on the speed for a given torque.

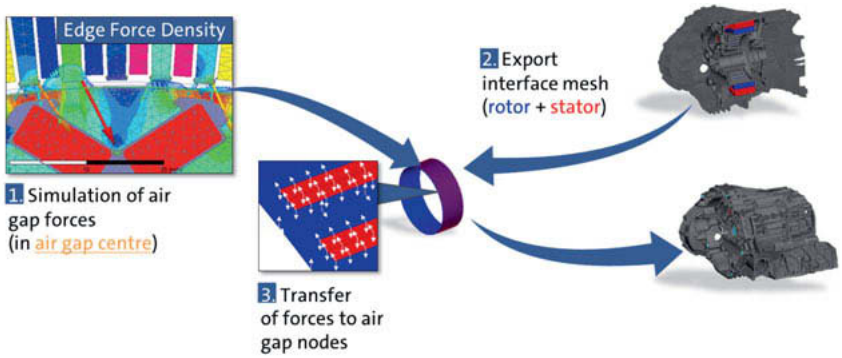


Fig. 7: Simulation of air gap forces and subsequent transfer to a structural dynamic model for the simulation of structure-borne levels

The output of the structure-borne noise can through pointwise, i.e. through evaluation in discrete nodes of the FE model, or alternatively through planar evaluation of the structure-borne noise. For planar evaluation, it is first necessary during pre-processing to sub-divide the areas of the drive near the surface (i.e. the housing) into sub-surfaces. In this way, a summation of the area-weighted surface normal velocity squared of the surface nodes is possible during post-processing according to sound level simulation or ERP simulation (ERP = Equivalent Radiated Power). This facilitates a localisation of structure-borne noise hotspots in the simulation in contrast to pointwise evaluations of the structure-borne noise level (virtual acceleration sensors).

https://doi.org/10.51202/9783181023549 - Generiert durch IP 216.73.216.36, am 19.01.2026, 02:19:31. © Urheberrechtlich geschützter Inhalt. Ohne gesonderte Erlaubnis ist jede urheberrechtliche Nutzung untersagt, insbesondere die Nutzung des Inhalts im Zusammenhang mit, für oder in KI-Systemen, KI-Modellen oder Generativen Sprachmodellen.

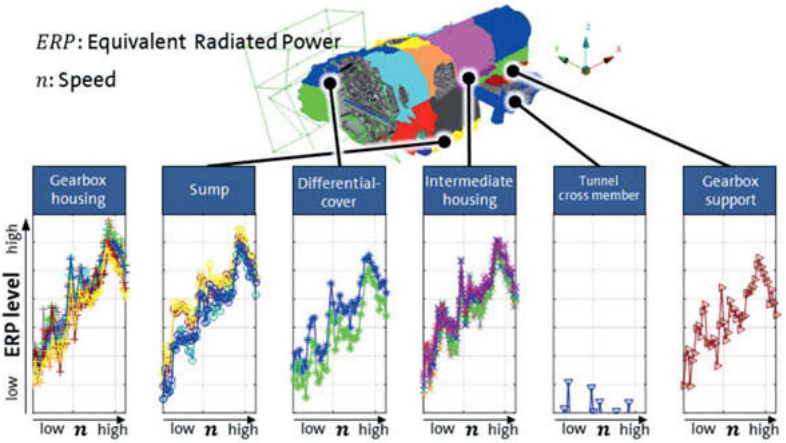


Fig. 8: Planar evaluation of simulated structure-borne noise in the form of equivalent radiated power (ERP) for simple localisation of hotspots (here: 2nd relevant EM order)

Other methods (out of an experimental toolbox) have the aim of validating the response of the drive previously virtualised using the methods. They further enable fine-tuning of the models, for example, through a comparison of the simulated and measured eigenmodes and subsequent model adjustments. An acoustic test bed set-up in the Kassel factory makes it possible to carry out measurements of structure-borne noise on and in the drive using acceleration sensors and measurements of airborne noise by means of microphones. To visualise the oscillations of the drive structures near the surface (e.g. the housing), a 3D laser vibrometer is used. A localisation of structure-borne hotspots and potentially acoustic-critical component areas is enabled in this way.

4. Optimisation of the electrical sheet section

In order to reduce the causes of electromagnetic-related noise from the DL382E-7A due to slot harmonics, the virtual method for optimisation of the electrical sheet section was used. The process is based on a parametric geometry model of the electrical sheet section. In the geometry model, the sheet section is represented in the form of radii, angles, dimensions and other entities whose respective geometrical characteristics can be varied via parameters. The associated preprocessor for the formation of geometry variants is actuated automatically via the FE preprocessor in order to generate a variety of geometries of the sheet section from stator and rotor, which are then automatically meshed and simulated in terms of the dynamic air gap

https://doi.org/10.51202/9783181023549 - Generiert durch IP 216.73.216.36, am 19.01.2026, 02:19:31. © Urheberrechtlich geschützter Inhalt. Ohne gesonderte Erlaubnis ist jede urheberrechtliche Nutzung untersagt, insbesondere die Nutzung des Inhalts im Zusammenhang mit, für oder in KI-Systemen, KI-Modellen oder Generativen Sprachmodellen.

forces. Other secondary variables (such as the mean torque) are likewise calculated in this regard for each of the variants considered.

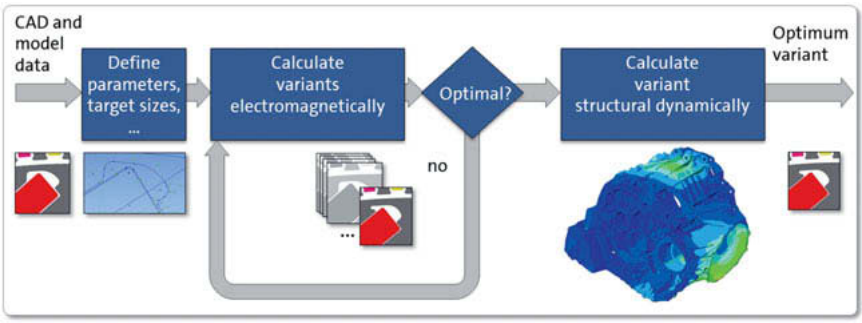


Fig. 9: Process of parameter variation and optimisation of the sheet section geometry

The maximum torque at nominal speed in the basic setting range of the electric motor was set as the operating point, which equates to one of the operating points complained about. With regard to the mechanical order of the air gap forces to be optimised, further consideration is ultimately only given to the geometry variants that exhibit reduced amplitudes of the radial forces in the relevant motor order compared with the initial state.

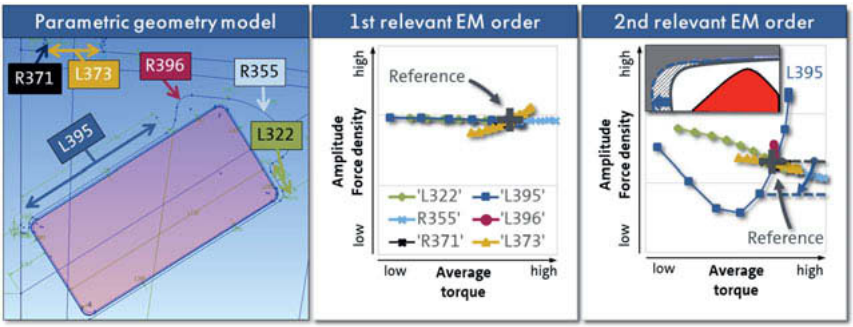


Fig. 10: Parametric geometry model of the sheet section and also results from parameter variation and optimisation

According to a sensitivity analysis, it was possible using the method to identify a significant geometry parameter (L395) in the rotor sheet section with respective optimum value. An adjustment of the parameter value resulted in an altered cavity in the rotor near the air gap compared with the initial state. Aside from a reduction of the target figure, the optimum geometry

https://doi.org/10.51202/9783181023549 - Generiert durch IP 216.73.216.36, am 19.01.2026, 02:19:31. © Urheberrechtlich geschützter Inhalt. Ohne gesonderte Erlaubnis ist jede urheberrechtliche Nutzung untersagt, insbesondere die Nutzung des Inhalts im Zusammenhang mit, für oder in KI-Systemen, KI-Modellen oder Generativen Sprachmodellen.

variant fulfils important secondary conditions of the optimisation task. On one hand, the mean torque and thereby the performance are only marginally impaired. Through minor manual adjustments to the cavity, it was possible to practically avoid a reduction in torque.

On the other hand, the amplitude of the first relevant electric motor order - which is likewise present in the Campbell graphs of the sound pressure level - are influenced by the geometry adjustments only slightly. An integral simulation of the radial air gap forces, i.e. across a variety of (motor) operating points, shows that the effect of the amplitude reduction is achieved globally, thereby confirming the optimisation result based primarily on the excitation.

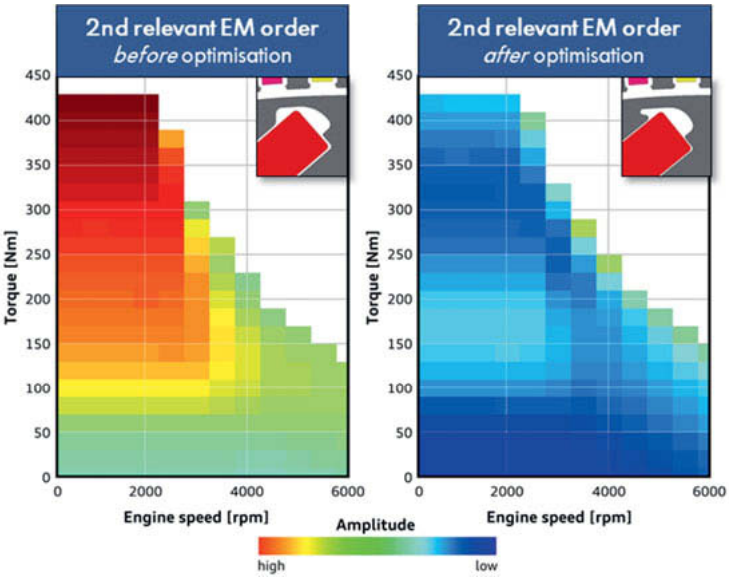


Fig. 11: Acoustic fingerprint of the simulated radial force density amplitudes in the slot harmonics before and after sheet section optimisation

Since no other adjustments to the design were carried out, a respective significant lowering of the level was expected in the structure-borne noise on the housing of the hybrid module. The structural dynamic model of the hybrid module described at the start was applied for this purpose to the air gap node of stator and rotor with the dynamic air gap forces.

https://doi.org/10.51202/9783181023549 - Generiert durch IP 216.73.216.36, am 19.01.2026, 02:19:31. © Urheberrechtlich geschützter Inhalt. Ohne gesonderte Erlaubnis ist jede urheberrechtliche Nutzung untersagt, insbesondere die Nutzung des Inhalts im Zusammenhang mit, für oder in KI-Systemen, KI-Modellen oder Generativen Sprachmodellen.

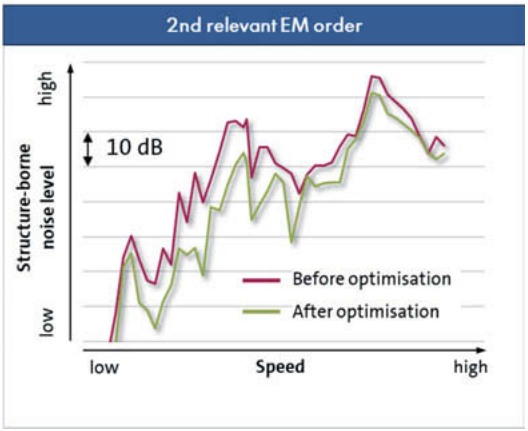


Fig. 12: Simulated structure-borne noise level on the housing of the hybrid module in slot harmonics before and after sheet section optimisation

The result of the simulation procedure, applied to the excitation of the original sheet section as well as that of the adapted plate section, is a noteworthy reduction in the order stages of the structure borne noise level of the slot harmonics. A speed curve at maximum torque was simulated here.

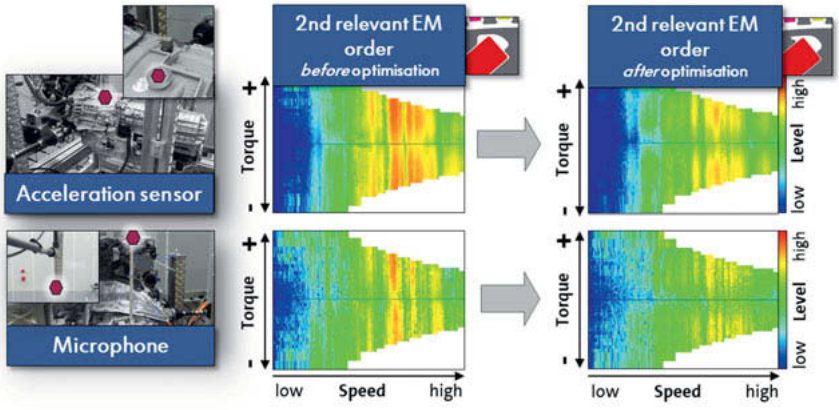


Fig. 13: Experimentally determined acoustic fingerprints from structure-borne and also airborne noise in the slot harmonics of the drive before and after sheet section optimisation

https://doi.org/10.51202/9783181023549 - Generiert durch IP 216.73.216.36, am 19.01.2026, 02:19:31. © Urheberrechtlich geschützter Inhalt. Ohne gesonderte Erlaubnis ist jede urheberrechtliche Nutzung untersagt, insbesondere die Nutzung des Inhalts im Zusammenhang mit, für oder in KI-Systemen, KI-Modellen oder Generativen Sprachmodellen.

A final verification of the optimisation result is based on test instrument-generated fingerprints from recorded acceleration levels on the housing of the hybrid module and also by means of microphone measurements near the power unit of the sound pressure levels. The acoustic fingerprint is based on numerous speed curves at various torque increments and on highly-automated data recording and evaluation of these series of measurements.

5. Optimisation of electric motor actuation

The Campbell chart of the sound pressure level in the vehicle interior shown at the start exposed an additional cause of noise - in addition to the peaking of slot harmonics levels - with mechanical order congruous to a multiple of the number of poles of the electric motor, which allows conclusions to be drawn about the excitation by the electric motor. Since sheet section optimisation in terms of this mechanical order was not productive, a method for adapting the actuation of the electric motor was employed. To reduce the amplitudes of the air gap forces of this order, it is necessary in the electric motor for currents to flow with modified harmonics contrary to standard operation. Furthermore, the current harmonics must exhibit an electric order number corresponding with the mechanical order of the forces. It was possible to facilitate this correlation using a virtual method entailing the analytical calculation of interdependencies from stator and rotor fields. Moreover, the amplitudes and phases of the harmonics must be optimally adapted to the air gap forces so that the (radial) forces are minimised.

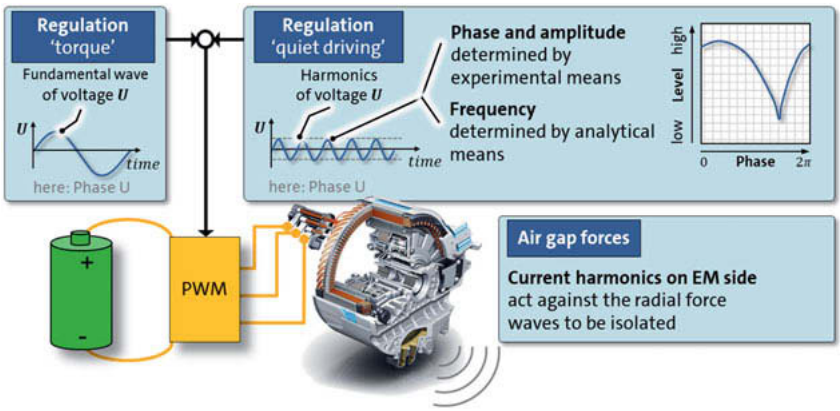


Fig. 14: Active principle of optimisation of electric motor actuation for quiet driving

https://doi.org/10.51202/9783181023549 - Generiert durch IP 216.73.216.36, am 19.01.2026, 02:19:31. © Urheberrechtlich geschützter Inhalt. Ohne gesonderte Erlaubnis ist jede urheberrechtliche Nutzung untersagt, insbesondere die Nutzung des Inhalts im Zusammenhang mit, für oder in KI-Systemen, KI-Modellen oder Generativen Sprachmodellen.

The optimum harmonics oscillations result from acoustic functions in the inverter, which apart from torque-forming voltage components of the inverter (basic oscillation) set voltage harmonics that ultimately generate the current harmonics mentioned and bring about a minimisation of the forces. The optimum phases and amplitudes of the voltage harmonics are speed and torque dependent and were determined through relevant test bed trials. Here, the specifications from phase and amplitude of the harmonics of the inverter voltage of the acoustic function were varied and, at the same time, airborne and structure-borne noise of the drive recorded. It was possible, in this way, to determine a characteristic for the acoustic function, which was successfully applied and tested in the vehicle.

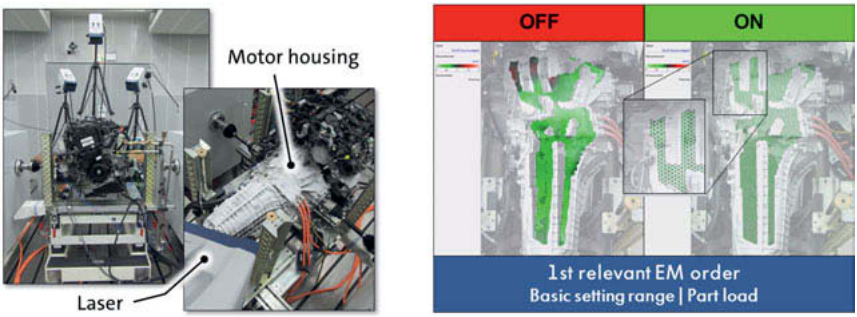


Fig. 15: Experimental verification of optimised actuation due to surface velocities of the hybrid module housing measured using 3D laser vibrometry

Verification of the optimisation measure was achieved as before through 3D laser vibrometry measurements, which reveal an almost completely settled oscillation pattern of the housing components with the function switched on. A further important contribution was thereby made towards fulfilment of the high acoustic demands on quiet driving with the DL382E-7A.

https://doi.org/10.51202/9783181023549 - Generiert durch IP 216.73.216.36, am 19.01.2026, 02:19:31. © Urheberrechtlich geschützter Inhalt. Ohne gesonderte Erlaubnis ist jede urheberrechtliche Nutzung untersagt, insbesondere die Nutzung des Inhalts im Zusammenhang mit, für oder in KI-Systemen, KI-Modellen oder Generativen Sprachmodellen.

6. Literature references

[1] Schmidt, A.: Enhancement of a Dual Clutch Transmission Kit – Audi S tronic, Dritev - Drivetrain for Vehicles 2018

[2] van der Meer, J.: The new plug-in hybrid module as an addition to the AUDI S tronic gearbox family, Dritev - Drivetrain for Vehicles 2018

[3] Gieras, J.: Noise of Polyphase Electric Motors. Boca Raton: Taylor & Francis Group, 2006

[4] Williamson, S.: Representation of Skew in Time-Stepped Two-Dimensional Finite-Element Models of Electrical Machines. IEEE Industry Society Annual Meeting, 1994

https://doi.org/10.51202/9783181023549 - Generiert durch IP 216.73.216.36, am 19.01.2026, 02:19:31. © Urheberrechtlich geschützter Inhalt. Ohne gesonderte Erlaubnis ist jede urheberrechtliche Nutzung untersagt, insbesondere die Nutzung des Inhalts im Zusammenhang mit, für oder in KI-Systemen, KI-Modellen oder Generativen Sprachmodellen.

Human/Machine Readable Language Representation Method in HEV Drivetrain Testing

Alkin Alkan, CPT Zwei GmbH, Berlin

Kurzfassung

Der Antriebsstrang für Hybrid- und Elektrofahrzeuge (HEV) spielt eine Schlüsselrolle bei der Erfüllung hoher Anforderungen an die Fahrzeugentwicklung, die durch hohe Anforderungen an Komfort und Fahrdynamik sowie strenge gesetzliche Vorschriften gestellt werden. HEV-Antriebsstränge führen zu einem hohen Aufwand für Entwicklung und Test. Das Testen spielt eine wichtige Rolle als Feedback-Mechanismus, der die Qualität und Zuverlässigkeit der entwickelten Hard- und Software gewährleistet. Testfälle werden aus Normen, Anforderungen und Designparametern abgeleitet. In einem Unternehmen mit mehreren Teams an mehreren Standorten, die an verschiedenen Projekten arbeiten, war die Standardisierung von Testspezifikationen von großer Bedeutung, um Verständlichkeit, Anpassungsfähigkeit und Wiederverwendbarkeit zu gewährleisten. Um dies zu erreichen, wurde eine menschenlesbare Sprache mit einem generischen Dateiformat für die Testspezifikation entwickelt, um die Testfälle unabhängig von Standort, Testumgebung oder Projekt zu spezifizieren.

Die maschinenlesbare Sprache wird unter Berücksichtigung von schlüsselwortgetriebenen Tests entwickelt. Die Idee hinter dem Keyword-Driven-Testing-Approach ist die Fähigkeit für Testingenieure, Testfälle zu entwerfen, die Keywords nach den Regeln der Sprache kombinieren, die Testschritte repräsentieren. Die KDT-Architektur ermöglicht es Testingenieuren, verschiedene Varianten von automatisierten Testfällen mit festen Schlüsselwörtern zu erstellen, ohne dass Programmierkenntnisse erforderlich sind. Die erstellten Testspezifikationen sind auch für andere Disziplinen leicht verständlich, was wiederum den interdisziplinären Testfallprüfungsprozess erleichtert. Darüber hinaus können die Testspezifikationen leicht ausgetauscht und zwischen Standorten und Projekten angepasst werden. KDT basiert auf drei wesentlichen Faktoren:

1. Eine vom Menschen/Maschine lesbare Sprache, bestehend aus Schlüsselwörtern und Phrasen, basierend auf der Prüfterminologie und den Anforderungen an HEV-Antriebsstränge.
2. Ein Parser (Compiler), der für die Überprüfung der Syntax (Sprachregeln), die Validierung der definierten Prüfschritt-Aggregate (Parameter, Signale usw.), das Ersetzen der generischen Prüfschritt-Aggregate durch ihre projektspezifischen Aggregate oder

https://doi.org/10.51202/9783181023549 - Generiert durch IP 216.73.216.36, am 19.01.2026, 02:19:31. © Urheberrechtlich geschützter Inhalt. Ohne gesonderte Erlaubnis ist jede urheberrechtliche Nutzung untersagt, insbesondere die Nutzung des Inhalts im Zusammenhang mit, für oder in KI-Systemen, KI-Modellen oder Generativen Sprachmodellen.

Werte und das Zuordnen von Prüfschritten zu ihrer entsprechenden Automatisierungsfunktion zuständig ist.

3. Eine abstrakte Schicht auf einem Automatisierungs-Kernframework - eine Reihe von generischen Funktionen, die für die Testausführung und -auswertung verantwortlich sind.

Die menschenlesbare Sprache in Kombination mit einer abstrakten Schicht, die auf einem Automatisierungskernframework implementiert ist, ist unabhängig von dem Automatisierungssystem, das für die Testumgebung an einem Standort implementiert ist, und erhöht somit die Zusammenarbeit und Synergie zwischen verschiedenen Teststandorten mit unterschiedlichen Testumgebungen – System-Dyno, Hardware in den Loop-Simulationsprüfständen, E-Maschinen-Emulatoren und Testfahrzeugen.

Dieser Vortrag beschäftigt sich hauptsächlich mit der menschen- und maschinenlesbaren Sprachdarstellung von Testfällen für HEV-Antriebsstränge. Die Kernpunkte sind:

- Definition der Sprache – der Wortschatz und die Syntaxregeln, die die Terminologie der HEV-Antriebsstrangprüfung erfüllen.
- Generische Testspezifikation – Zusätzliche Projektdateien und Aggregationsregeln eingeführt, um generische Testschrittdefinitionen zu gewährleisten, die problemlos zwischen verschiedenen Projekten wiederverwendet werden können.
- Parser – Konvertierung der generischen Testschritte in projekt/testumgebungs-spezifische und schließlich Zuordnung zu den entsprechenden abstrakten Automatisierungsfunktionen.
- Abstraktion der Automatisierungsfunktionen für die Testausführung und Ergebnisauswertung – ein Automatisierungs-Kernframework, das sich mit verschiedenen Automatisierungssystemen beschäftigt, die auf verschiedenen Testumgebungen an mehreren Standorten implementiert sind.

Abstract

The drivetrain for hybrid and electric vehicles (HEV) plays a key role in meeting high requirements on vehicle development which are placed by high standards for convenience and drive dynamics together with strict statutory regulations. HEV drivetrains result in high overhead for development and testing. Testing plays an important role as the feedback mechanism ensuring the quality and reliability of the hardware and software developed. Test cases are derived from norms, requirements and design parameters. In an organization with multiple teams in multiple locations working on various projects, standardization of test specifications has been of great importance to ensure comprehensibility, adaptability, and reusability. To accomplish that, a

https://doi.org/10.51202/9783181023549 - Generiert durch IP 216.73.216.36, am 19.01.2026, 02:19:31. © Urheberrechtlich geschützter Inhalt. Ohne gesonderte Erlaubnis ist jede urheberrechtliche Nutzung untersagt, insbesondere die Nutzung des Inhalts im Zusammenhang mit, für oder in KI-Systemen, KI-Modellen oder Generativen Sprachmodellen.

human/machine readable language using a generic test specification file format have been developed to specify the test cases independent of test location, test environment, or project. The human/machine readable language is developed by taking into consideration keyword-driven testing. The idea behind the keyword driven testing approach is the ability for test engineers to design test cases combining keywords according to the rules set by the language that represent test steps. KDT architecture allows test engineers to create different variations of automated test cases using fixed set of keywords, without requiring any coding skills. The created test specifications can also be understood easily by other disciplines, which in turn makes the interdisciplinary test case review process easier. Moreover, the test specifications can easily be exchanged and adapted between locations and projects. KDT is based on three major factors:

1. A human/machine readable language consisting of keywords and phrases based on the testing terminology and needs for HEV drivetrains.
2. A parser (compiler), which is responsible for checking syntax (language rules), validating the defined test step aggregates (parameters, signals etc.), replacing the generic test step aggregates with their project specific ones or values, and mapping test steps to their corresponding automation function.
3. An abstract layer on top of an automation core framework – a set of generic functions, which is responsible for the test execution and evaluation.

Human/Machine readable language combined with an abstract layer implemented on an automation core framework is independent of automation system implemented for the testing environment at a test location and therefore increases the cooperation and synergy between different test locations having various testing environments - system dyno, hardware in the loop simulation test benches, e-machine emulators, and test vehicles.

This presentation mainly deals with the human/machine readable language representation of test cases for HEV drivetrains. The key points are:

- Definition of the language – the vocabulary and syntax rules fulfilling HEV drivetrain testing terminology.
- Generic test specification – Additional project files and aggregation rules introduced to ensure generic test step definitions, which are easily reused between different projects.
- Parser – converting the generic test steps into project/test environment specific ones and finally mapping those to their corresponding abstract automation functions.

https://doi.org/10.51202/9783181023549 - Generiert durch IP 216.73.216.36, am 19.01.2026, 02:19:31. © Urheberrechtlich geschützter Inhalt. Ohne gesonderte Erlaubnis ist jede urheberrechtliche Nutzung untersagt, insbesondere die Nutzung des Inhalts im Zusammenhang mit, für oder in KI-Systemen, KI-Modellen oder Generativen Sprachmodellen.

- Abstraction of automation functions for test execution and result evaluation – an automation core framework dealing with various automation systems implemented on different test environment setups in multiple locations.

Introduction

The following products are being tested by HEV system test:

- High Voltage Drivetrain: Electric Drive includes the motor for hybrid and electric vehicles as well as the associated power electronics. Motor, power electronics and a reducer have been integrated in a compact and cost-effective axle drive system. It is scalable and can be used in a wide range of vehicles, from Plug-in hybrids to powerful electric vehicles. This electronic system supplies both the electric motor as well as the high voltage battery with electricity. [1]
-



Fig. 1: High Voltage Drivetrain [1]

- Power Electronics: includes an inverter and a DC/DC converter. The inverter converts the direct current of the battery into the three-phase alternating current that is required by the electric motor. During recuperation, the power electronics converts the alternating current generated by the electric motor into direct current, and thus charges the battery. The DC/DC supplies the 12 Volt boardnet of the hybrid and electric vehicles with power, which makes the 12 Volt alternator redundant. [2]
-



Fig. 2: Power Electronics [2]

https://doi.org/10.51202/9783181023549 - Generiert durch IP 216.73.216.36, am 19.01.2026, 02:19:31. © Urheberrechtlich geschützter Inhalt. Ohne gesonderte Erlaubnis ist jede urheberrechtliche Nutzung untersagt, insbesondere die Nutzung des Inhalts im Zusammenhang mit, für oder in KI-Systemen, KI-Modellen oder Generativen Sprachmodellen.

- 48 V Eco Drive: To electrify the drivetrain below the safety-relevant 60-volt-level is far less expensive compared to high voltage hybridization - and yet highly efficient. 13% fuel savings make it a must-have in future mobility. Vehicles with a supplementary 48V power supply offer an advanced start-stop function and additional drivetrain features like recuperation, sailing and electric boost. Other high-power consumers can be adapted to 48V, which will lead to a further increase in efficiency. [3]



Fig. 3: 48 V Eco Drive [3]

These products describe above have a high functional density and complex control units which leads to high risk of potential failure. The malfunctions can in return lead to potential risk for life and limb. HEV system test activities are based on the ISO26262 standard for functional safety of electrical and/or electronic systems in production automobiles, which implies three different system levels to be considered for testing:

- HW-SW Level: testing of system element consisting of HW- and SW-Parts after HW-SW integration
- (Sub-)System Level: testing of (sub-) system functionalities after system integration
- Vehicle Level: testing of system functionalities after vehicle integration

These system testing levels are derived from the system architectural design shown in the Figure 4 below:

https://doi.org/10.51202/9783181023549 - Generiert durch IP 216.73.216.36, am 19.01.2026, 02:19:31. © Urheberrechtlich geschützter Inhalt. Ohne gesonderte Erlaubnis ist jede urheberrechtliche Nutzung untersagt, insbesondere die Nutzung des Inhalts im Zusammenhang mit, für oder in KI-Systemen, KI-Modellen oder Generativen Sprachmodellen.

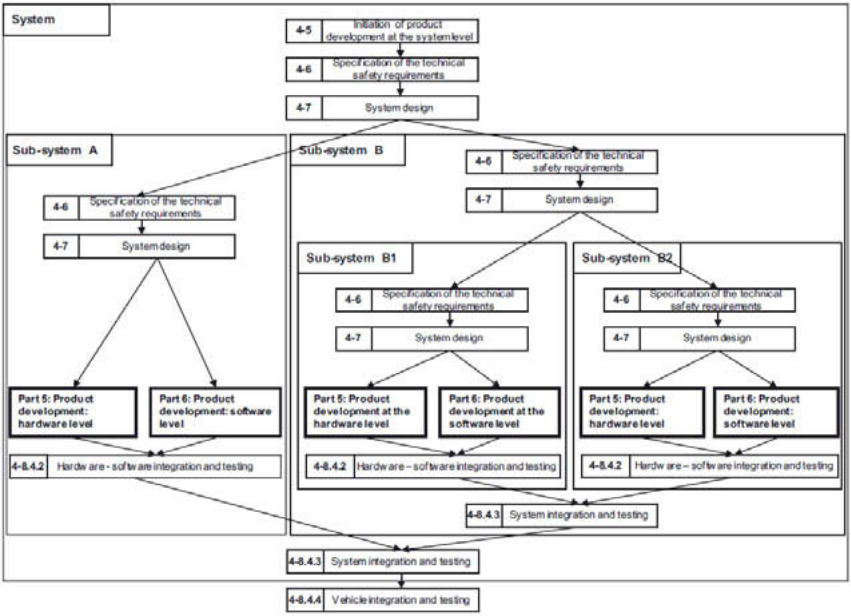


Fig. 4: System architectural design proposed by ISO26262

As shown in Figure 4 the system is composed to sub-systems which are composed of again sub-systems or HW/SW products. Each of the sub system shall be tested against system requirements after their respective integration tests (system or HW-SW). Finally, the whole system is tested on vehicle level after vehicle integration.

This standard has been realized and represented by the following architecture explained as follows:

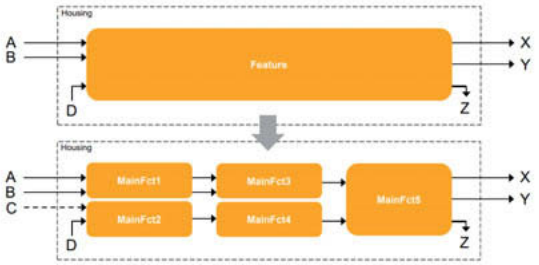


Fig. 5: Exploded view of a feature

https://doi.org/10.51202/9783181023549 - Generiert durch IP 216.73.216.36, am 19.01.2026, 02:19:31. © Urheberrechtlich geschützter Inhalt. Ohne gesonderte Erlaubnis ist jede urheberrechtliche Nutzung untersagt, insbesondere die Nutzung des Inhalts im Zusammenhang mit, für oder in KI-Systemen, KI-Modellen oder Generativen Sprachmodellen.

Figure 5 depicts an exploded view of a feature defined in the system architecture. The features are composed of several main functions which can interact with each other.

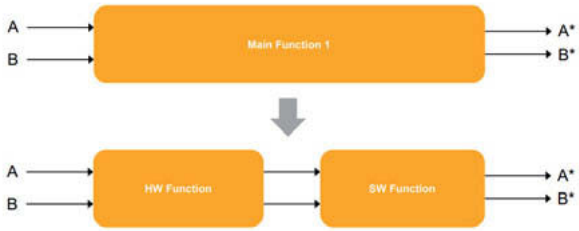


Fig. 6: Exploded view of a main function (mech include)

Figure 6 shows the exploded view of a single main function. The main functions are composed of HW and SW functions. Following this architecture, the following test types corresponding to their requirement types are derived:

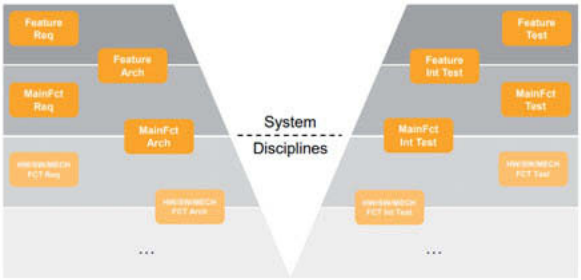


Fig. 7: V Cycle Diagram

Figure 7 depicts requirement and their respective test typed with respect to the V cycle diagram. Of course, system test activities only include the system level. The system test types are defined as follows:

- Feature Test: Functional behaviour of individual features, derived from feature requirements.
- Feature Integration Test: Interaction between main functions of a feature, derived from feature architecture.
- Main Function Test: Functional behaviour of individual main functions, derived from functional requirements.

https://doi.org/10.51202/9783181023549 - Generiert durch IP 216.73.216.36, am 19.01.2026, 02:19:31. © Urheberrechtlich geschützter Inhalt. Ohne gesonderte Erlaubnis ist jede urheberrechtliche Nutzung untersagt, insbesondere die Nutzung des Inhalts im Zusammenhang mit, für oder in KI-Systemen, KI-Modellen oder Generativen Sprachmodellen.

- Main Function Integration Test: Interaction between HW/SW/MECH functions of a main function, derived from main function architecture.

These tests are performed on different testing environments which can be grouped as follows:

- System Hardware in the Loop (HiL) Test Bench: The low voltage hardware components and control algorithm software are introduced to the simulated environment including the power-electronics and the e-motor models.
- System Power HiL (Emulator) Test Bench: On these test benches, complete inverter component is tested; only e-motor is simulated.
- System Dyno Test Bench: The drivetrains are introduced to various loads in form of speed or torque provided by a dyno under specific constraints (ambient temperature, coolant temperature, high-battery-voltage, low-battery-voltage) by other devices (high and low voltage supply, climate chamber, and heating-cooling-units)
- Testing Vehicle: The drivetrains are tested on a vehicle with special testing equipment.

The Need for a Generic Specification Language

As stated in the introduction part, the tests are derived from their respective system requirements. While doing, so the following fundamental testing process is followed:

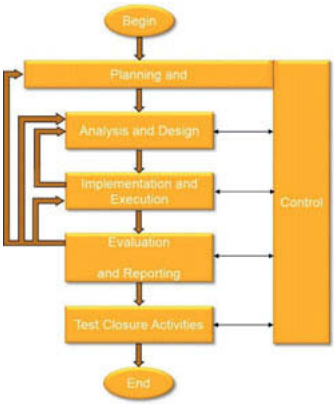


Fig. 8: Fundamental test activity process

In Figure 8 the steps through a test activity is shown. During the analysis and design step, the planned system requirements are analysed, and test cases are derived from them accordingly. At the end of this step test specifications, where all the test steps and test fit criteria are described, are obtained as a product. According to this specification, the test case shall be able

https://doi.org/10.51202/9783181023549 - Generiert durch IP 216.73.216.36, am 19.01.2026, 02:19:31. © Urheberrechtlich geschützter Inhalt. Ohne gesonderte Erlaubnis ist jede urheberrechtliche Nutzung untersagt, insbesondere die Nutzung des Inhalts im Zusammenhang mit, für oder in KI-Systemen, KI-Modellen oder Generativen Sprachmodellen.

to be performed and evaluated at least manually by a test engineer. If a test automation is planned for these test cases, then an automation script for execution shall be implemented which will be performed on the desired test environment. The execution step is followed by the evaluation where the measurement files are evaluated according to the test fit criteria manually or automatically. Finally, the test fit criteria are presented in a report document. Each step is controlled and reviewed. In case of an error in test design or implementation, the previous step may be carried out again. In case of a change in system requirements, the test case must be changed respectively. In such a complex process, it is difficult to carry on with single implementation of automated test run for each test case. Moreover, these implementations shall be easily adapted to other projects and test environments. The solution to those, lies in a test specification written in a generically developed language which:

- can be understood by non-testers, i.e. developers (HW, SW, MECH), system engineers, and customers. (comprehensible)
- can be readable by both the testers -manual run- and the automation system -automated run-. (human/machine readable)
- is reconfigurable against changes in requirement parametrization. (flexible)
- enables the reusability of test cases between different projects. (reusability & adaptability)

This solution approach was realized by taking into consideration keyword-driven testing. The keyword driven testing approach enables test engineers to design their test cases and evaluations step by step (sequential) combining a defined set of vocabulary according to the rules set by the language. The automation execution and evaluation functions are represented in the test step described in the generic language format, which is parameterizable by language-defined aggregations against requirement parametrization changes and differences in signal names between different projects. These test steps are parsed by the automation tool and mapped to the project or test environment specific functions. Following this solution, with one test specification written by the human/machine readable generic language, one can:

- carry out manual test executions and evaluations,
- carry out automated test executions and evaluations,
- easily adapt test case to changes in requirement parameters,
- easily share and adapt test cases from one project to another, and
- easily share and run the test case with other test environments.

It must be taken into account that the abstraction of automation functions has to be achieved in order to enable sharing and reproducibility of the automation test scripts, which is time consuming and requires high expertise in test automation area.

https://doi.org/10.51202/9783181023549 - Generiert durch IP 216.73.216.36, am 19.01.2026, 02:19:31. © Urheberrechtlich geschützter Inhalt. Ohne gesonderte Erlaubnis ist jede urheberrechtliche Nutzung untersagt, insbesondere die Nutzung des Inhalts im Zusammenhang mit, für oder in KI-Systemen, KI-Modellen oder Generativen Sprachmodellen.

Language Structure and Rules

As stated in the previous section, the principles of the key driven testing approach are followed during development of the language. In that sense, the HEV testing vocabulary were grouped as follows:

Nouns:

- Actuators: are the names of all control elements of the test environment devices. The actuator syntax has the prefix “act_”. Examples: act_hv_voltage, act_lv_voltage, act_dyno_speed, act_dyno_torque, etc.
- Measurements: are the names of measured signals. The measurement syntax has the prefix “meas_”. Examples: meas_hv_voltage_bat, meas_hv_voltage_dc-link, meas_lv_voltage_IGN, meas_dyno_speed, meas_dyno_torque, etc.
- Signals: are the names of input output signals for control algorithm software. The signal syntax – signal name is defined between two $ characters. Examples: $ExtIn_TqSpEm1$, $ExtOut_OpsDcdcCom$, etc. **Note:** The signals are generic and mapped to their corresponding project specific names.

Verbs:

- Operators: are verbs, conjunctions and logicals to be combined with nouns and adverbs to define simple sentences. Examples: set, ramp, wait until, step, check if, is/are equal to, is below, reaches, etc.

Adverbs:

- Parameters: have generic names and project specific values. The parameter syntax – parameter name is defined between two @ characters. Examples: @ParAppl_Dly_TimeoutOnCsInvalidSignals@, @ParAppl_FreewheelingFactor@, etc.

These sets of vocabulary are combined to together to build up test execution or test fit criteria sentences according to the rules, which are defined in the language manual.

Here are some test execution sentence rule examples:

- set {Actuator/$Signal$} to @Parameter@
- ramp {Actuator/$Signal$} to @Parameter@ within @Parameter@
- wait until {Measurement/$Signal$} reaches @Parameter@ with tolerance +/- @Parameter@
- set inverter torque_control working point at @Parameter@ and @Parameter@

Built-up test execution sentences:

- set $ExtIn_TqSpEm1$ to @ ParST_Torque_FDR_nom@

https://doi.org/10.51202/9783181023549 - Generiert durch IP 216.73.216.36, am 19.01.2026, 02:19:31. © Urheberrechtlich geschützter Inhalt. Ohne gesonderte Erlaubnis ist jede urheberrechtliche Nutzung untersagt, insbesondere die Nutzung des Inhalts im Zusammenhang mit, für oder in KI-Systemen, KI-Modellen oder Generativen Sprachmodellen.

- ramp act_dyno_speed to @ParST_Speed_FDR_nom@ within @ParST_Time_Ramp_FDR_nom@
- wait until $ExtOut_VoltLpfDcLink$ reaches @ParAppl_Volt_HVL1_DCDC@ with tolerance +/- @ParAppl_Volt_HVL1_DCDC_Tol_ST@
- set inverter torque_control working point at @ParST_Speed_FDR_nom@ and @ParST_Torque_FDR_gen_nom@

Here are some test fit criteria sentence rule examples:

- check if {Measurement/$Signal$} LogicalOperator {@Parameter@/Measurement/$Signal$}
- check if time duration LogicalOperator @Parameter@ until {Measurement/$Signal$} LogicalOperator @Parameter@

Built-up test fit criteria commands:

- check if meas_hv_voltage_dc_link is greater than @ParAppl_Volt_HVL1_DCDC@
- check if meas_dyno_torque is lower or equal to $ExtOut_TqMaxAvlDer$
- check if time duration is lower than @ParConst_T_Discharge_Active@ until meas_hv_voltage_dc_link is lower than @ParAppl_Volt_HVDC_PrechargeOn@

As seen from the above examples, the test execution and fit criteria sentences are always defined using parameters and generic signals.

The Test Workflow

As mentioned in the previous section, the generic test specification consists of vocabulary sets. These sets can be grouped into two according to their scope:

- Parameters are mapped to their values; generic signals are mapped to their project specific names.
- Actuators, Measurements, and Operators are global. These definitions are valid for each test environment and project. They are defined and documented in their single corresponding documents.

In order to organize the project specific configurations and separate execution and evaluation definitions (one execution for multiple evaluations possible); the following file types were defined:

- TCD (Test Case Definition) File: File for generic test execution specification.
- TFC (Test Fit Criteria) File: File for generic test evaluation specification.
- Parameter Files: Parameter definition files. Parameters are mapped to their values with units. Parameter mapping example: PhysLimit_Volt_HvMeas1_HiRangeUp = 220 [V]

https://doi.org/10.51202/9783181023549 - Generiert durch IP 216.73.216.36, am 19.01.2026, 02:19:31. © Urheberrechtlich geschützter Inhalt. Ohne gesonderte Erlaubnis ist jede urheberrechtliche Nutzung untersagt, insbesondere die Nutzung des Inhalts im Zusammenhang mit, für oder in KI-Systemen, KI-Modellen oder Generativen Sprachmodellen.

- Signal Files: Signal mapping files. Generic signal names are mapped to their project specific correspondences. Signal mapping example: ExtIn_TqSpEm1 = EmTorqueReq

The test workflow with these files is shown in the Figure 9:

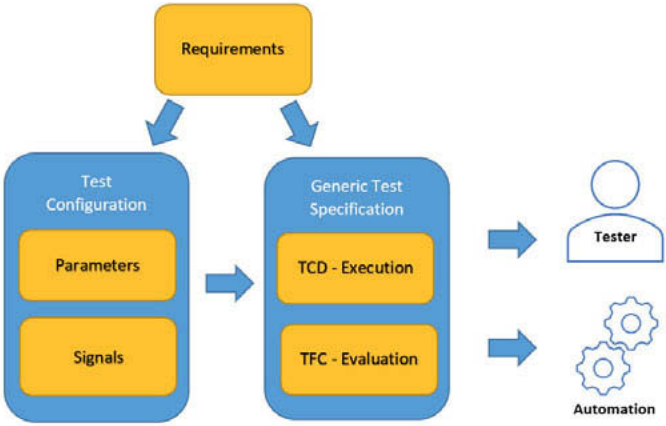


Fig. 9: Test workflow

As seen in Figure 9, for each TCD file (execution) there must be a TFC file (evaluation). The parser tool replaces the parameter and generic signals with their project specific values and signal names, so that the test specifications can be comprehended, executed and evaluated by both the tester or the automation tool. The workflow in Figure 10 is followed for an automated use case:

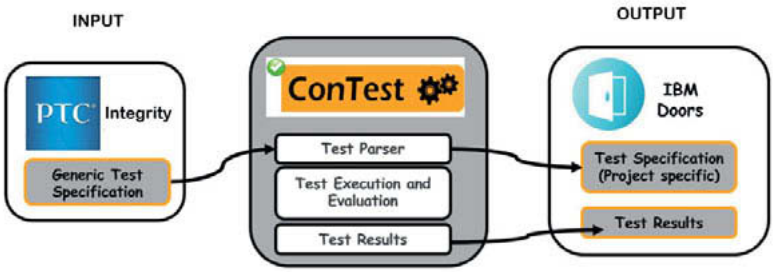


Fig. 10: Test Automation Workflow

https://doi.org/10.51202/9783181023549 - Generiert durch IP 216.73.216.36, am 19.01.2026, 02:19:31. © Urheberrechtlich geschützter Inhalt. Ohne gesonderte Erlaubnis ist jede urheberrechtliche Nutzung untersagt, insbesondere die Nutzung des Inhalts im Zusammenhang mit, für oder in KI-Systemen, KI-Modellen oder Generativen Sprachmodellen.

The work flow contains:

- **INPUT:** The generic test specification related files (TCD, TFC, parameter, and signal) are stored and versioned by file version control tool (PTC Integrity).
- **Test Automation (TA) Tool** (ConTest): The generic parameters and signals are replaced with their project specific values and names by the Test Parser. After this test execution and result evaluation is performed automated. Moreover, the TA tool generates reports, supports result review process, and finally exports the final test results into the test management tool.
- **OUTPUT:** In test management tool (IBM Doors) the following are stored:
    - Final verdict including review comments.
    - Link to detailed report. And measurement files.

The Standardized Test Setup

To achieve abstraction of automation functions, there must be a standardized test setup for each test environment. As seen in Figure 11, TA tool interacts with:

- Gateway: is responsible for sending commands to system under test (SUT) via $ExtIn_*Signals*$ and to the test environment via actuators (act_*XXX*) and receiving feedback signals $ExtOut_*Signals*$ from SUT and measurements (meas_*XXX*) from the test environment.
- Measurement & Calibration (MC) Tool: is responsible for changing the software calibrations $IntCal_*Signals*$ and measuring internal software variables $Int_*Signals*$ of the electric control unit (ECU).

The communication between Gateway and all test environment types (Dyno, HiL, and Emulator) is established via the standardized protocol. The standardized test setup ensures the execution of a TCD on each of these test environment types, although the control systems on each test environments are different.

https://doi.org/10.51202/9783181023549 - Generiert durch IP 216.73.216.36, am 19.01.2026, 02:19:31. © Urheberrechtlich geschützter Inhalt. Ohne gesonderte Erlaubnis ist jede urheberrechtliche Nutzung untersagt, insbesondere die Nutzung des Inhalts im Zusammenhang mit, für oder in KI-Systemen, KI-Modellen oder Generativen Sprachmodellen.

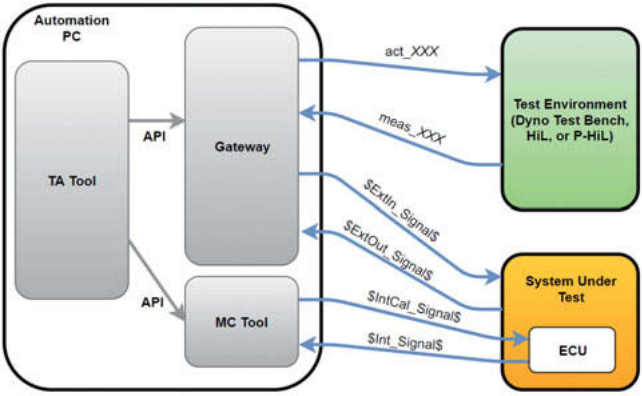


Fig. 11: Standardized test setup

Automation Library Structure for Test Execution

Each execution command defined in TCD is mapped to its corresponding TA tool execution function. For every command there is a standard function. Due to the differences in project software functionality (e.g. system initialization) and test environment setups, special functions must be implemented. In this case the standard function will be overloaded by its special implementation. In addition, each command can be configured as a manual action (in case full automation is not possible). Each command is configured to above mentioned modes with a command status matrix. There are four implementation status for each command:

1. Standard: function is implemented in standard form.
2. Special: function implementation differs from the standard form for each project and environment combination. **Important:** The special implementation must have the same outcome as the standard.
3. Manual: The test execution requires tester interaction. TA tool interacts with the tester by a Message Box.
4. Not Available: function cannot be executed for this project and test environment combination. In this case TA tool excludes related test case from test run.

The command status matrix is essential to keep tracking of automated execution maturity. The following questions can be answered by using the command status matrix **- advanced test preparation & execution planning**:

- Which test cases can be performed on which test environment? - **Not Available functions**

https://doi.org/10.51202/9783181023549 - Generiert durch IP 216.73.216.36, am 19.01.2026, 02:19:31. © Urheberrechtlich geschützter Inhalt. Ohne gesonderte Erlaubnis ist jede urheberrechtliche Nutzung untersagt, insbesondere die Nutzung des Inhalts im Zusammenhang mit, für oder in KI-Systemen, KI-Modellen oder Generativen Sprachmodellen.

- Which test cases can be run without tester presence – full automated runs (night or weekend runs)? **- Manual functions**
- How much effort is necessary to transfer the test packages to other projects or test environments? **- Special functions**

Automated Offline Test Evaluations

Evaluations are performed offline (after test execution) and command driven. The most significant profits of this approach are:

- Offline evaluations save time spent on test environments.
- Multiple command driven evaluations allow the tester to define test fit criteria flexible.
- Set of evaluations can be easily extended allows introduction of new evaluation methods.

Conclusions

The most important outcomes of above described approach can be summarized as following:

- Human/machine readable language designed for HEV drivetrain testing using keyword driven testing approach.
- Generic test specifications easily sharable between different projects using configuration files.
- Standardized test setup ensuring the test execution on every test environment with different control systems.

References

[1]:https://www.continental-automotive.com/en-gl/Passenger-Cars/Drivetrain/Electrification/Hybrid-Electric-Vehicles/Axle-Drive

[2]:https://www.continental-automotive.com/en-gl/Passenger-Cars/Drivetrain/Electrification/Hybrid-Electric-Vehicles/Power-Electronics

[3]:https://www.continental-automotive.com/en-gl/Passenger-Cars/Drivetrain/Electrification/48-Volt-Mild-Hybrid/48-Volt-belt-driven-starter-generator

https://doi.org/10.51202/9783181023549 - Generiert durch IP 216.73.216.36, am 19.01.2026, 02:19:31. © Urheberrechtlich geschützter Inhalt. Ohne gesonderte Erlaubnis ist jede urheberrechtliche Nutzung untersagt, insbesondere die Nutzung des Inhalts im Zusammenhang mit, für oder in KI-Systemen, KI-Modellen oder Generativen Sprachmodellen.

https://doi.org/10.51202/9783181023549 - Generiert durch IP 216.73.216.36, am 19.01.2026, 02:19:31. © Urheberrechtlich geschützter Inhalt. Ohne gesonderte Erlaubnis ist jede urheberrechtliche Nutzung untersagt, insbesondere die Nutzung des Inhalts im Zusammenhang mit, für oder in KI-Systemen, KI-Modellen oder Generativen Sprachmodellen.

Impact of hybridization on functional safety for Low voltage eMotors

Impact of electrical and hybrid architectures (P2... P4) on the ASIL of electrical machines (eMotors)

Magali Maillard, **Ludovic Laurenty**, **Stéphane Chretien**,
VALEO Powertrain Systems, Créteil, France

Abstract

One of the first steps in vehicle hybridization came with the launch of VALEO's 12V iStARS (BSG12) micro hybrid solution on the market in 2010. This generation of electrical machines was the first to implement ISO26262 functional safety automotive standard, applicable since November 2011.

Since then, the increasing needs of the manufacturers to reduce the consumption of their vehicles in CO^2 emission led to the evolution of the electrical and mechanical vehicle architectures. In addition, VALEO has improved the electrical and dynamic performances of its electrical machines. These changes make the requirements of functional safety for our products more stringent.

In this paper we will explain how, depending on the different electrical architectures, the definition of safety goals allocated to our products can be greatly impacted. The interface held by the DC / DC between the 12V and 48V networks, the replacement of lead-acid batteries by li-ion batteries, are all criteria that can make the safety mechanisms more severe or more complex to implement.

Similarly, the mechanical interfaces for the transmission of torque electrical machines to the wheels have evolved from the Front Engine Accessory Drive, through the gearbox, and now directly on the rear axle. We will then explain how the maximum potential torque transmitted by the electrical machine to the wheels and the possibility of mechanically disconnecting the wheels in a safe way have an impact on the severity of the dynamic safety objectives assigned to the electrical machines.

.

https://doi.org/10.51202/9783181023549 - Generiert durch IP 216.73.216.36, am 19.01.2026, 02:19:31. © Urheberrechtlich geschützter Inhalt. Ohne gesonderte Erlaubnis ist jede urheberrechtliche Nutzung untersagt, insbesondere die Nutzung des Inhalts im Zusammenhang mit, für oder in KI-Systemen, KI-Modellen oder Generativen Sprachmodellen.

Remind about ASIL definition (from ISO26262)

The Automotive Safety Integrity Level (ASIL) allocated to a subsystem is defined in the Preliminary Hazard Analysis (PHA) done at vehicle level based on subsystem main functions failure analyses. For each vehicle lifecycle and each failure, the vehicle effect is evaluated for Potential Severity (S), Probability of Exposure in the driving and operating situations (E), and Controllability by the driver (C). Theses 3 criteria are then used to evaluate the ASIL for each unexpected event of the subsystem.

- **Estimation of potential severity (S)**
- S1: Light and moderate injuries
- S2: Severe and life-threatening injuries (survival probable)
- S3 : Life-threatening injuries (survival uncertain), fatal injuries

- **Estimation of the probability of exposure in the driving and operating situations (E)**
- E1 : Extremely low probability
- E2 : Low probability
- E3 : Medium probability
- E4 : High probability

- **Estimation of controllability (C)**
- C1 : Simply controllable
- C2 : Normally controllable
- C3 : Difficult to control or uncontrollable

Table 1: ASIL definition based on S, E, C criteria

		C1	C2	C3
S1	E1	QM	QM	QM
	E2	QM	QM	QM
	E3	QM	QM	A
	E4	QM	A	B
S2	E1	QM	QM	QM
	E2	QM	QM	A
	E3	QM	A	B
	E4	A	B	C
S3	E1	QM	QM	A
	E2	QM	A	B
	E3	A	B	C
	E4	B	C	D

https://doi.org/10.51202/9783181023549 - Generiert durch IP 216.73.216.36, am 19.01.2026, 02:19:31. © Urheberrechtlich geschützter Inhalt. Ohne gesonderte Erlaubnis ist jede urheberrechtliche Nutzung untersagt, insbesondere die Nutzung des Inhalts im Zusammenhang mit, für oder in KI-Systemen, KI-Modellen oder Generativen Sprachmodellen.

Evolutions of electrical and mechanical vehicle architectures related to hybridization and impact on functional safety

The main changes between Belt systems (micro hybrid and mild hybrid) and the eMotors (hybrid) on the electrical and mechanical interfaces within the vehicle architecture will be described to understand the impact on functional safety.

Impact on electrical risks:
Impact of Hybridization on electrical architectures:
Before hybridization, the main electrical vehicle architectures are the one described below:

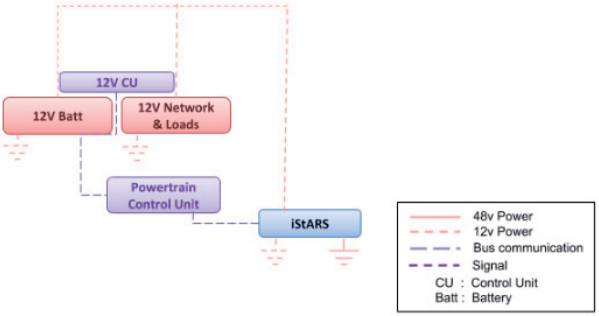


Fig. 1: Micro hybrid System vehicle electrical architecture

Since mild hybrid generation and for all low voltage hybrid architectures, the following electrical vehicle architectures are the one described below:

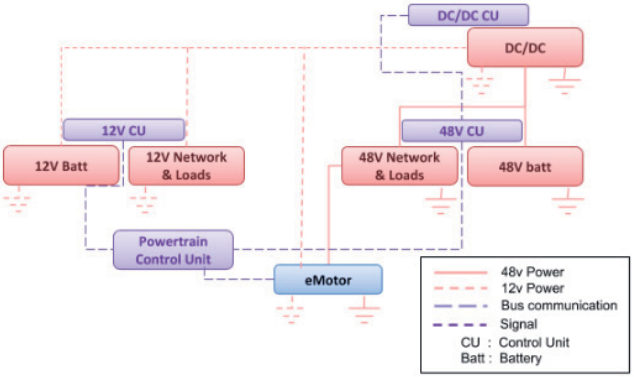


Fig. 2: Mild hybrid and eMotors System vehicle electrical architecture

https://doi.org/10.51202/9783181023549 - Generiert durch IP 216.73.216.36, am 19.01.2026, 02:19:31. © Urheberrechtlich geschützter Inhalt. Ohne gesonderte Erlaubnis ist jede urheberrechtliche Nutzung untersagt, insbesondere die Nutzung des Inhalts im Zusammenhang mit, für oder in KI-Systemen, KI-Modellen oder Generativen Sprachmodellen.

The DC/DC subsystem is in the interface between the 12V and 48V networks.

Hypothesis is that Safety loads are present on 12V only, not on 48V.

Impact on ASIL electrical unexpected events:
According to VALEO Preliminary Hazard Analysis based on eMotor main functions and the effect of their failures on the vehicle, the electrical unexpected events are:

- **Overvoltage** (due to internal eMotor failure)
- **Undervoltage** (due to internal eMotor failure)
- **Loaddump** (due to battery disconnection)

Hazard	Powertrain Electrical Systems			
	P0 : Belt machine		P1, P2, P3, P4: eMotors	IMPACT
	iStARS (BSG12)	iBSG (BSG48)	xMG (eMotor)	
Overvoltage	From QM to ASIL B	ASIL B	ASIL B	No impact
Undervoltage	ASIL A	ASIL A	ASIL A	No impact
Loaddump	QM	From QM to ASIL B (*)	From ASIL B to C (*)	MAJOR impact

Table 2: Powertrain Electrical Systems ASIL on mechanical risks

(*) : depends on ASIL decomposition with DC/DC and Li-Ion Battery

https://doi.org/10.51202/9783181023549 - Generiert durch IP 216.73.216.36, am 19.01.2026, 02:19:31. © Urheberrechtlich geschützter Inhalt. Ohne gesonderte Erlaubnis ist jede urheberrechtliche Nutzung untersagt, insbesondere die Nutzung des Inhalts im Zusammenhang mit, für oder in KI-Systemen, KI-Modellen oder Generativen Sprachmodellen.

Impact on mechanical risks:

Remind of hybridization mechanical architectures panel:
Hybrids power trains have different very well-known architectures, so called “P1, P2, P3, P4”, differences that we won’t develop in this paper. We will focus here on impact for functional safety for electrical machines (eMotors).

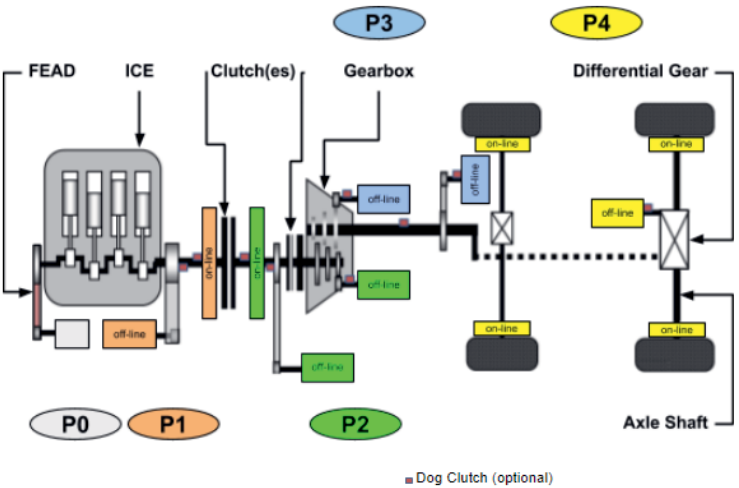


Fig. 3: Belt Systems & eMotors System position/ integration in vehicle mechanical architecture

Located in P0: Belt System is linked to ICE [1]’s FEAD [2]. Located in P1/ P2/ P3/ P4: eMotor System is linked to a shaft or a pinion. Different subsystems can disengage the eMotor to the powertrain chain. It can be a dig clutch for P1/ P2/ P3/ P4 configuration, it can be the gearbox for P3 configuration, and it can be the differential gear for P4 configuration. There may also be a configuration without any disengagement system. Let’s call this disengagement system a decoupling function.

Powertrain Electrical Systems mechanical performances range:
The table below shows the impact on hybridization on the Powertrain Electrical Systems mechanical performances.

https://doi.org/10.51202/9783181023549 - Generiert durch IP 216.73.216.36, am 19.01.2026, 02:19:31. © Urheberrechtlich geschützter Inhalt. Ohne gesonderte Erlaubnis ist jede urheberrechtliche Nutzung untersagt, insbesondere die Nutzung des Inhalts im Zusammenhang mit, für oder in KI-Systemen, KI-Modellen oder Generativen Sprachmodellen.

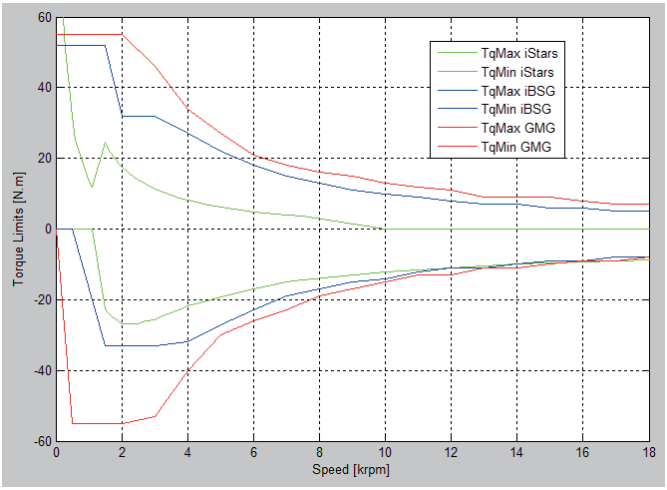


Fig. 4: Belt Systems & eMotors System mechanical performances

Table 3: Powertrain Electrical Systems performances ranges

Vehicle Architecture	Hybrid steps	Products		Decoupling function
P0 : Belt Systems	**Microhybrid**		iStARS (BSG12)	No
	Mildhybrid		iBSG (BSG48)	No
P1, P2, P3, P4 : eMotors	**Hybrid**		xMG (eMotor)	YES (optional)

https://doi.org/10.51202/9783181023549 - Generiert durch IP 216.73.216.36, am 19.01.2026, 02:19:31. © Urheberrechtlich geschützter Inhalt. Ohne gesonderte Erlaubnis ist jede urheberrechtliche Nutzung untersagt, insbesondere die Nutzung des Inhalts im Zusammenhang mit, für oder in KI-Systemen, KI-Modellen oder Generativen Sprachmodellen.

The table 2 and Figure 3 above shows that hybridization leads to increase the mechanical performance level of the eMotor. This can increase the impact of the eMotor on dynamic behaviour of the vehicle. But it is depending also on the transmission performance between the eMotor and the wheels as well as the weight of the vehicle and the ability of the system to disconnect the eMotor in a safe way.

Impact on ASIL mechanical unexpected events:
According to VALEO Preliminary Hazard Analysis based on eMotor main functions and the effect of their failures on the vehicle, the mechanical unexpected events are:

- **Wrong torque generation at low speed** (unexpected movement of the vehicle at low speed, no vehicle movement at low speed)
- **Wrong torque generation at high speed** (over torque positive or negative, Loss of torque, no torque, under torque positive or negative)

Table 4: Powertrain Electrical Systems ASIL on mechanical risks

Hazard	**Powertrain Electrical Systems**			
	P0 : Belt machine		**P1, P2, P3, P4 : eMotors**	**IMPACT**
	iStARS (BSG12)	**iBSG (BSG48)**	**xMG (eMotor)**	
Unexpected torque at low speed	**ASIL B**	**ASIL B**	**ASIL B**	**No impact**
No torque at low speed	**ASIL A**	**ASIL A**	**ASIL A**	**No impact**
Wrong Torque	**QM**	**From ASIL A to B (*)**	**From ASIL B to C (*)**	**MAJOR impact**

(*): depends on vehicle mechanical architecture, vehicle weight, eMotor mechanical performances

The main impact of hybridization remains on **Wrong Torque generation** which was not applicable for micro hybrid application and maximum ASIL B for iBSG (BSG48).

https://doi.org/10.51202/9783181023549 - Generiert durch IP 216.73.216.36, am 19.01.2026, 02:19:31. © Urheberrechtlich geschützter Inhalt. Ohne gesonderte Erlaubnis ist jede urheberrechtliche Nutzung untersagt, insbesondere die Nutzung des Inhalts im Zusammenhang mit, für oder in KI-Systemen, KI-Modellen oder Generativen Sprachmodellen.

Impact on Safety mechanism complexity:

- Safe state managed at eMotor level: ASC and Shut off

At vehicle level, during traction mode, the main safe state is ASC mode (Active Short Circuit). The ASC mode prevents the machine to convert mechanical energy into electrical energy to the DC link. ASC can be done with Low side MOSFETs or High side MOSFETs.
During ASC mode, the resistive torque at high speed is quite low, it is almost inversely proportional to the speed (Figure 4). The sensation is a "freewheel", the driver can control its deceleration with the mechanical brake. At low speed, a resistive torque peak appears.

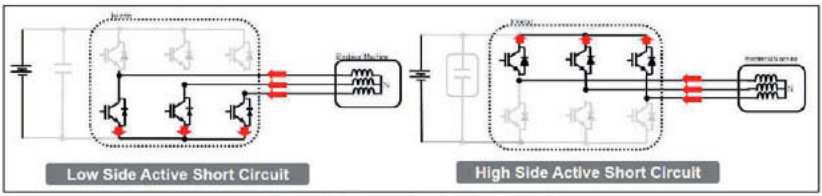


Fig. 5: Types of active short circuits

Due to the technology PMSM (Permanent Magnet Synchronous Motor) when the eMotors runs empty, it behaves as a dynamo and generates a back electromotive force (EMF). Thus the eMotor can't just always be shutdown (passive safe state, MOSFET off) to be in free wheel. The EMF level is proportional to motor speed and the effect to the powertrain systems depends on the load level of the traction battery. The back EMF has to be controlled to avoid overvoltage. The safe state at eMotor level has to be an active one to control the energy and with to ASC of Free Wheel.

https://doi.org/10.51202/9783181023549 - Generiert durch IP 216.73.216.36, am 19.01.2026, 02:19:31. © Urheberrechtlich geschützter Inhalt. Ohne gesonderte Erlaubnis ist jede urheberrechtliche Nutzung untersagt, insbesondere die Nutzung des Inhalts im Zusammenhang mit, für oder in KI-Systemen, KI-Modellen oder Generativen Sprachmodellen.

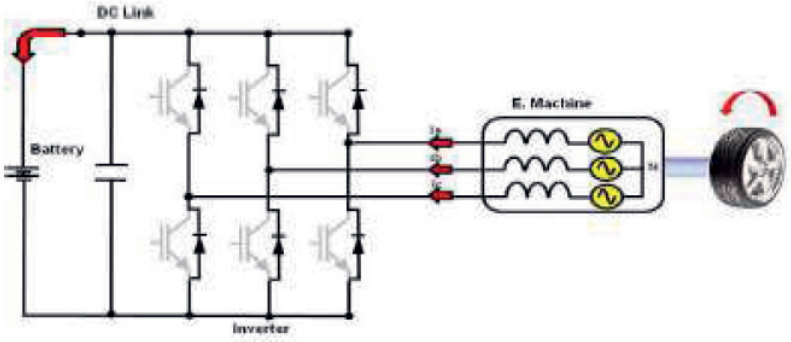


Fig. 6: Back EMF

- Safe state managed at vehicle system level: Disconnection of e-Motors (optional)

In case of eMotor failure the powertrain system disconnect the eMotor from the wheels to avoid unexpected movement of the vehicle. This safe state can be activated thanks to a CAN signal sent by the eMotor or thanks to the supervision of the eMotor signals and behavior.

Conclusion

The increasingly short development times and the increasing complexity of the products and systems in which they are integrated require automotive suppliers, their partners and OEMs to increasingly collaborate for the definition, the implementation and the integration in the vehicle architecture of the safety mechanisms to cover the electrical and dynamic risks since the very beginning of projects at least since RFI/RFQ phase.

Acronyms :
ICE = Internal Combustion Engine
FEAD = Front Engine Accessory Drive
QM = Quality Management
iStARS = integrated StArter Reversible System (for 12V Network)
iBSG = integrated Belt Starter Generator (for 48V Network)
BSG = Belt Starter Genenator

https://doi.org/10.51202/9783181023549 - Generiert durch IP 216.73.216.36, am 19.01.2026, 02:19:31. © Urheberrechtlich geschützter Inhalt. Ohne gesonderte Erlaubnis ist jede urheberrechtliche Nutzung untersagt, insbesondere die Nutzung des Inhalts im Zusammenhang mit, für oder in KI-Systemen, KI-Modellen oder Generativen Sprachmodellen.

https://doi.org/10.51202/9783181023549 - Generiert durch IP 216.73.216.36, am 19.01.2026, 02:19:31. © Urheberrechtlich geschützter Inhalt. Ohne gesonderte Erlaubnis ist jede urheberrechtliche Nutzung untersagt, insbesondere die Nutzung des Inhalts im Zusammenhang mit, für oder in KI-Systemen, KI-Modellen oder Generativen Sprachmodellen.

AUTOSAR Adaptive Platform – The standardized software framework for safe and intelligent e-mobility

Michael Niklas,
Continental Corporation, Regensburg;
Dr. **Günter Reichart**,
AUTOSAR Partnership, Munich

Zusammenfassung

Die AUTOSAR-Entwicklungspartnerschaft umfasst heute mehr als 270 Partnerunternehmen. Die erste Spezifikation der AUTOSAR Classic Platform wurde vor mehr als zwölf Jahren veröffentlicht. AUTOSAR hat auf der Grundlage etablierter Qualitätsstandards, ausgereifter Prozesse und starker Kommunikationskanäle innerhalb dieser Organisation einen völlig neuen Ansatz entwickelt, um den anspruchsvollen Markttrends in der Automobilindustrie zu begegnen, wie dem Internetzugang in Autos und dem hochautomatisierten Fahren, sowie der Fahrzeug zu Fahrzeug Kommunikation. Das Ergebnis dieser Aktivitäten der letzten 4 Jahre ist ein intelligenter und flexibler Software-Standard, die AUTOSAR Adaptive Platform genannt wird. Diese Platform läuft auf performanten Hardwarearchitekturen und unterstützt die parallele Verarbeitung auf vielen Multicore-Systemen und GPUs. AUTOSAR hat seine Wurzeln in der Automobilindustrie und die Unterstützung von Safety und Security Features hat einen hohen Stellenwert. Ebenso ist die Kompatibilität zur etablierten AUTOSAR Classic Platform eine Grundvoraussetzung für eine zukunftsorientierte E/E Systemgestaltung, die zur Umsetzung auch von elektrifizierten Antriebssträngen befähigt.

Abstract

The AUTOSAR community has grown to over 270 partner companies since the first AUTOSAR Classic Platform specification was released more than twelve years ago. Based on the well-established high-quality standards, mature processes and strong communication channels inside this organization, AUTOSAR has been developing a completely new approach to cope with the challenging market trends in the automotive industry such as internet access in cars, highly automated driving and vehicle to vehicle communication. The result of these activities of the last 4 years is an intelligent and flexible software infrastructure which therefore is named AUTOSAR Adaptive Platform. The software platform runs on high-end computing hardware and supports parallel processing on many core systems and GPUs. Since AUTOSAR has its

https://doi.org/10.51202/9783181023549 - Generiert durch IP 216.73.216.36, am 19.01.2026, 02:19:31. © Urheberrechtlich geschützter Inhalt. Ohne gesonderte Erlaubnis ist jede urheberrechtliche Nutzung untersagt, insbesondere die Nutzung des Inhalts im Zusammenhang mit, für oder in KI-Systemen, KI-Modellen oder Generativen Sprachmodellen.

roots in the automotive field, the partnership's prioritization of safety and security features is as self-evident as the compatibility to systems based on the AUTOSAR Classic Platform. A suitable software framework for safe and secure electric drive and other applications is now available.

1. Introduction

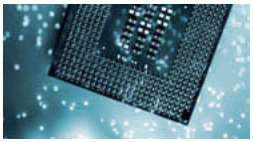
Automotive vehicles continue to turn into real cyber physical systems – just connecting to the internet and exchanging data with smartphones is state of the art. Future vehicles will be connected to almost everything: roadside infrastructure, vehicles around them and smart homes – they become a part of the internet of things.



Highly automated driving



IoT and cloud services



New processor technologies

Fig 1: Use cases driving the further development of the AUTOSAR Standard

In addition to increasing connectivity, another trend is the vision of autonomous driving. Further enhancements of today's driver assistance systems like Adaptive Cruise Control pave the way towards highly automated driving and autonomous parking, see Figure1.

The realization of these new features adds new requirements on the software platforms hosting these functionalities. To realize autonomous vehicles, the software architecture must support the existing functional safety and security requirements along with system capabilities such as hardware with high-end embedded computing power, updates-over-the-air, communication with backend-systems, dynamic deployment of applications, as well as reliability. An evaluation by AUTOSAR showed that these new requirements could not be realized by today's software architectures, given the internal communication is done via a deeply embedded controller to meet OEM requirements such as start-up-times or functional safety. In general, a much more flexible software architecture was required, one that is highly available and capable to adapt itself to specific application requirements at a given point in time. An extension of AUTOSAR's software architecture for deeply embedded systems was not feasible and sustainable. Consequently, present architectures will be complemented by a new platform that comes with operating systems designed for high-performance computing enhanced by dependability

https://doi.org/10.51202/9783181023549 - Generiert durch IP 216.73.216.36, am 19.01.2026, 02:19:31. © Urheberrechtlich geschützter Inhalt. Ohne gesonderte Erlaubnis ist jede urheberrechtliche Nutzung untersagt, insbesondere die Nutzung des Inhalts im Zusammenhang mit, für oder in KI-Systemen, KI-Modellen oder Generativen Sprachmodellen.

features like e.g. safety, availability, security or real-time. Nevertheless, the well-known characteristics of deeply embedded system will remain. The combination of these trends results in a revolution of current E/E architectures.

2. Key aspects of the new E/E architecture

The following three key aspects characterize tomorrow's E/E architectures:

A Integration of heterogeneous software platforms

Networking architectures of modern cars can be clustered into different domains for infotainment and connectivity versus chassis, powertrain, etc. Infotainment ECUs are typically using Linux or commercial general-purpose operating systems while the AUTOSAR Classic Platform is the standard for deeply embedded ECUs. With new use cases and the increasing demand from deeply embedded applications for computing power, a third type of ECUs arises with different characteristics that must be interconnected with existing E/E architectures.

B Service-oriented and signal-based communication

The traditional automotive communication is based on the idea of ECUs broadcasting signals to other ECUs. This paradigm fits very well for control data of limited size in cyclic communication technologies. Advanced applications like highly automated driving with higher payload demands e.g. to exchange dynamic length lists of objects detected by various sensor sources and Ethernet based technologies using sophisticated communication protocols. The concept of service-oriented communication is based on software applications providing a service on the communication system and other applications subscribing to this service. The data will only be sent to the subscribers. The efficient combination of service-oriented communication with the existing signal-based paradigm is the second key aspect of future E/E architectures and a demanding challenge from a methodological point of view.

AUTOSAR as the global standardization consortium for automotive software architectures aims to adopt to these trends and to provide a consistent standard for these aspects.

C New standard defined

The AUTOSAR Classic Platform will remain the first choice for deeply embedded systems realizing typical power train and chassis functionalities. Such applications are characterized by high demands on safety, real-time and determinism while running on low cost hardware. For these applications, AUTOSAR provides a well-proven and mature software platform including a widely used methodology which supports all of today collaboration models.

https://doi.org/10.51202/9783181023549 - Generiert durch IP 216.73.216.36, am 19.01.2026, 02:19:31. © Urheberrechtlich geschützter Inhalt. Ohne gesonderte Erlaubnis ist jede urheberrechtliche Nutzung untersagt, insbesondere die Nutzung des Inhalts im Zusammenhang mit, für oder in KI-Systemen, KI-Modellen oder Generativen Sprachmodellen.

To support dynamic software deployment of customer application software, dependable applications and to provide a software framework for applications that require high-end computing power, AUTOSAR is currently standardizing a second software platform, the AUTOSAR Adaptive Platform. Based on existing standards, the idea is to benefit as much as possible from developments in other areas (e.g. consumer electronics, automation industry), while still considering automotive-specific requirements such as functional safety and diagnostics.

3. The AUTOSAR Adaptive Platform

Figure 2 depicts the overall architecture of this new software platform. One of the main goals for the AUTOSAR Adaptive Platform is to provide application developers a stable programming interface, the so-called AUTOSAR Runtime for Adaptive Applications (ARA).

The interface consists of a standardized interface for accessing operating system functionalities and a communication middleware, which allows data exchange with local and remote applications as well as to the Adaptive AUTOSAR Services. The second goal is a smooth configuration to integrate the software platform into existing E/E architectures based on Ethernet technologies.

To achieve this goal, the following functional clusters are specified: The core of the AUTOSAR Adaptive Platform is the operating system based on POSIX. The OS can be used by the application software via a subset of POSIX according to IEEE1003.13 [1], namely PSE51 and provides the application developer commonly used functionality such as signals, timers, semaphores and thread handling. If an application restricts itself to the use of this subset it shall be portable to any AUTOSAR Adaptive Platform. From the functional point of view, the operating system defines some of the essential differences of the AUTOSAR Adaptive Platform compared to the AUTOSAR Classic Platform. Applications are no longer bound to a very strict and static scheduling and memory management but are free (within well-defined boundary conditions) to create and destroy threads and to allocate memory depending on their current needs.

https://doi.org/10.51202/9783181023549 - Generiert durch IP 216.73.216.36, am 19.01.2026, 02:19:31. © Urheberrechtlich geschützter Inhalt. Ohne gesonderte Erlaubnis ist jede urheberrechtliche Nutzung untersagt, insbesondere die Nutzung des Inhalts im Zusammenhang mit, für oder in KI-Systemen, KI-Modellen oder Generativen Sprachmodellen.

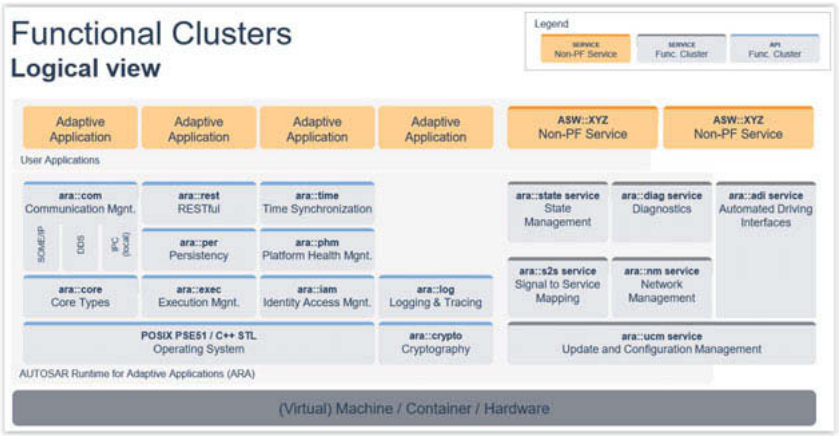


Fig 2: Logical Architecture of the AUTOSAR Adaptive Platform

Functional clusters are grouped into either API or Service Interfaces. APIs for functional clusters are specified in software specifications and they depend on the used programming language. The Service Interface of a Functional cluster is generated according to an ara::com specification.

The functional cluster e.g. Execution Management is responsible for startup and shutdown of the ECU and the applications by maintaining the application and ECU states. Together with the Platform Health Management it ensures availability of ECU resources for applications. Each ECU relies on its Platform Health strategy to provide robust runtime behaviour and being prepared for a critical situation.

Furthermore, the communication middleware realizes and abstracts the service-oriented communication between local applications as well as to applications residing on other ECUs. This includes the interaction with the AUTOSAR Adaptive Services.

As communication protocols ara:com provides SOME/IP and DDS. The SOME/IP protocol enables applications on the AUTOSAR Adaptive Platform to establish communication relationships with ECUs running the AUTOSAR Classic Platform. Additionally, it paves the ground to use service-oriented communication for intra ECU communication.

Adaptive Platform's current release also contains Log and Trace features for debugging of an AUTOSAR Adaptive ECU as well as Persistency. Furthermore, porting of the most important

https://doi.org/10.51202/9783181023549 - Generiert durch IP 216.73.216.36, am 19.01.2026, 02:19:31. © Urheberrechtlich geschützter Inhalt. Ohne gesonderte Erlaubnis ist jede urheberrechtliche Nutzung untersagt, insbesondere die Nutzung des Inhalts im Zusammenhang mit, für oder in KI-Systemen, KI-Modellen oder Generativen Sprachmodellen.

Diagnostics features to POSIX increases the Automotive Software flavour of Adaptive Platform.

The goal of release 18-10, to initiate first series development using AUTOSAR Adaptive Platform was mainly achieved. For the following releases of the Adaptive Platform a roadmap of major additional features is available. This includes support for fail-operational systems, enhanced safety and security features and the integration of V2X communication protocols. Obviously, Adaptive Platform will add use cases and features to convince software platform and application software developers for future challenges in Automotive software development.

4. Support for the integration of heterogeneous platforms

The methodology defined by AUTOSAR is the only standardized solution available today, which allows describing the software architecture together with the network topology in a unified machine-readable format. Up to now, this concept considered only the ECUs based on the AUTOSAR Classic Platform and the principle of signal-based communication. For the future, the most important challenge is to support a seamless integration process of different platforms. With the introduction of Ethernet and a service-oriented communication paradigm based on SOME/IP in the earlier Release 4.1.1 of the Classic Platform, AUTOSAR already made a big step to support this use case. In terms of SOME/IP, a service can be seen as the functional representation on the bus independent of the underlying software and hardware platform. Therefore, a formal description of a service has to be independent of a specific platform, be it the AUTOSAR Classic Platform, the AUTOSAR Adaptive Platform or a non-AUTOSAR platform, see figure 3. The key point is that each software platform realizes the service in the same way with regard to its behaviour and the representation in the wire protocol format. This means that AUTOSAR has to provide answers for the following aspects:

- Description of the relevant communication relationships on software level.
- Provisioning of standardized communication protocols.

https://doi.org/10.51202/9783181023549 - Generiert durch IP 216.73.216.36, am 19.01.2026, 02:19:31. © Urheberrechtlich geschützter Inhalt. Ohne gesonderte Erlaubnis ist jede urheberrechtliche Nutzung untersagt, insbesondere die Nutzung des Inhalts im Zusammenhang mit, für oder in KI-Systemen, KI-Modellen oder Generativen Sprachmodellen.

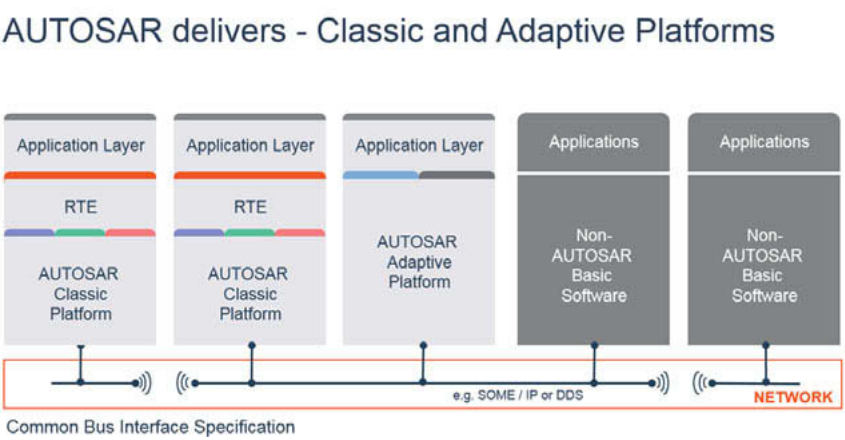


Fig 3: Integration of different platforms

The main difference between platforms supported by AUTOSAR and other platforms is the support of a methodology and templates, which enables tool vendors to provide automated configuration of ECUs running a software stack complying with the standard.

5. AUTOSAR standards and timeline

To keep the standard manageable, useable and to enable flexibility, AUTOSAR decided to split up its results into several standards for different feature sets. An AUTOSAR standard is now defined as a consistent set of AUTOSAR deliverables, which are released at the same time. AUTOSAR deliverables can but are not limited to be of the following types: textual explanations, textual specifications, test specification, source code, other formal or semi-formal textual formats (e.g. ARXML, UML models, XML Schema, .json).

The approach of structuring AUTOSAR's deliverables into standards also opens the new possibility to deal with future use cases and to establish the new AUTOSAR Adaptive Platform alongside the AUTOSAR Acceptance Test and the AUTOSAR Classic Platform. Common parts of these standards such as bus protocols and common aspects of the methodology are released as a separate standard called the AUTOSAR Foundation.

An overview of the currently planned timeline for their main AUTOSAR standards is represented in Figure 4, in line with an anticipation of level 3-5 autonomous vehicle introductions.

https://doi.org/10.51202/9783181023549 - Generiert durch IP 216.73.216.36, am 19.01.2026, 02:19:31. © Urheberrechtlich geschützter Inhalt. Ohne gesonderte Erlaubnis ist jede urheberrechtliche Nutzung untersagt, insbesondere die Nutzung des Inhalts im Zusammenhang mit, für oder in KI-Systemen, KI-Modellen oder Generativen Sprachmodellen.

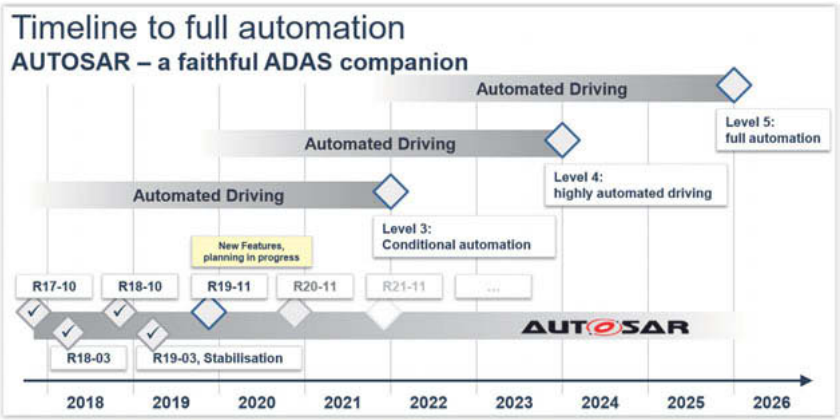


Fig 4: AUTOSAR Release Schedule

The AUTOSAR Classic Platform release R4.4.0 includes, among others, an extended serialization for Data Structures in SOME/IP with tag, length and value encoding (TLV). It simplifies the communication and improves the compatibility between the AUTOSAR Classic and Adaptive Platform. Moreover, a Transport Layer Security (TLS) allows the use of well-established services in non-vehicle domains.

One of the major achievements featured in the AUTOSAR Adaptive Platform Release R18-10 is the support of the Internet Protocol Security (IPSec) to secure data communication allowing a more secure communication between Adaptive platforms and their surrounding platforms. Advanced support for Diagnostics over Internet Protocol (DoIP) is in accordance with ISO 13400-x. In addition, release R18-10 includes the specification of the network binding to support the Data Distribution Service (DDS) protocol.

Most important, release R18-10 comprises the harmonization of Classic Platform and Adaptive Platform enabling the Network Management protocol to utilize network management across platforms. Moreover, a unique time base shared among all entities of both platforms has been introduced through the first step of the Time Sync harmonization.

For its spring release in 2019, R19-03, AUTOSAR improved the quality of the Adaptive Platform and the Foundation. R19-03 as new baseline for Adaptive Platform features enhances features like Diagnostics or Time Synchronization by robust extensions and supports further development.

https://doi.org/10.51202/9783181023549 - Generiert durch IP 216.73.216.36, am 19.01.2026, 02:19:31. © Urheberrechtlich geschützter Inhalt. Ohne gesonderte Erlaubnis ist jede urheberrechtliche Nutzung untersagt, insbesondere die Nutzung des Inhalts im Zusammenhang mit, für oder in KI-Systemen, KI-Modellen oder Generativen Sprachmodellen.

Therefore, the AUTOSAR experts were focusing on resolving the identified bugs and filling the gap of missing functionalities. Further synchronised releases of the three AUTOSAR standards shall continuously improve a holistic approach with a newly-defined joint methodology to apply AUTOSAR in modern E/E architectures. Besides that, the working group organization was harmonized in 2019 to achieve backward and forward compatibility of the Classic and Adaptive standards by joint work groups.

6. Conclusion

A suitable software framework for safe and secure applications is now available The AUTOSAR Classic and the Adaptive Platform pave the way for a large variety of automotive use cases. This includes the application of AUTOSAR to electric drive vehicles.

Upcoming demands and new functionalities will pose further challenging requirements on future E/E architectures.

ACKNOWLEDGMENT

This work was supported by the members of the AUTOSAR Steering Committee and the AUTOSAR Project Leader Team.

7. REFERENCES

[1] http://www.autosar.org

[2] IEEE1003.13; IEEE Standard for Information Technology - Standardized Application Environment Profile (AEP) - POSIX® Realtime and Embedded Application Support

[3] Slansky, Lorenz Daimler AG, Scharnhorst, Thomas, AUTOSAR Development Partnership, AUTOSAR für intelligente Fahrzeuge. HANSER automotive Special 2017.

https://doi.org/10.51202/9783181023549 - Generiert durch IP 216.73.216.36, am 19.01.2026, 02:19:31. © Urheberrechtlich geschützter Inhalt. Ohne gesonderte Erlaubnis ist jede urheberrechtliche Nutzung untersagt, insbesondere die Nutzung des Inhalts im Zusammenhang mit, für oder in KI-Systemen, KI-Modellen oder Generativen Sprachmodellen.

https://doi.org/10.51202/9783181023549 - Generiert durch IP 216.73.216.36, am 19.01.2026, 02:19:31. © Urheberrechtlich geschützter Inhalt. Ohne gesonderte Erlaubnis ist jede urheberrechtliche Nutzung untersagt, insbesondere die Nutzung des Inhalts im Zusammenhang mit, für oder in KI-Systemen, KI-Modellen oder Generativen Sprachmodellen.

A modular Concept for EMI Shielding of Thermoplastic Housings for E-Cars

An innovative Approach to support Weight Saving and Function Integration

Dipl.-Ing. **Volker Schroiff**,
Freudenberg Sealing Technologies GmbH & Co. KG, Weinheim

Zusammenfassung

Im Zuge des Wandels in der Automobilindustrie hin zur Elektromobilität gilt es, nicht mehr nur Systeme gegen Ölaus- und Schmutzeintritt abzudichten, sondern auch „Abdichtmaßnahmen" gegen unerwünschte elektromagnetische Strahlung zu realisieren. Anhand des entwickelten modularen Konzeptes können beide Abdichtaufgaben nach Bedarf wirkungsvoll miteinander kombiniert werden.

Das Konzept basiert zunächst auf einer Definition und Bewertung der technologischen Stoßrichtungen für die Abschirmung auf Basis der geltenden Normen und Kundenanforderungen. Für den mittleren Frequenzbereich des elektrischen Antriebsstranges spielt der Skin-Effekt eine entscheidende Rolle. Aufgrund der geringen Eindringtiefe der Strahlung besteht das Konzept aus einem Kunststoffgehäuse in Kombination mit einer hochleitfähigen Oberfläche und einer Dichtung, die auch zur Abschirmungsleistung betragen kann, falls dies erforderlich ist. Die Messungen der Abschirmwirkung zeigen je nach Werkstoffkombination befriedigende bis sehr gute Ergebnisse.

Aufbauend auf den Messergebnissen wurde ein Produktionskonzept erarbeitet für die Applizierung der funktionalen Oberfläche in Serie, wobei verschiedene Produktabmessungen und geometrische Komplexitätsgrade berücksichtigt wurden.

Abstract

Due to the change in the automotive industry towards electromobility, it is no longer only necessary to seal systems against leakage, but also to implement measures against unwanted electromagnetic radiation. Based on the developed modular concept, both sealing tasks can be effectively combined as needed.

https://doi.org/10.51202/9783181023549 - Generiert durch IP 216.73.216.36, am 19.01.2026, 02:19:31. © Urheberrechtlich geschützter Inhalt. Ohne gesonderte Erlaubnis ist jede urheberrechtliche Nutzung untersagt, insbesondere die Nutzung des Inhalts im Zusammenhang mit, für oder in KI-Systemen, KI-Modellen oder Generativen Sprachmodellen.

The concept is based initially on a definition and evaluation of the technological directions for shielding based on norms and customer requirements. For the middle frequency range of the electrical drive train the skin effect plays an important role. Due to the low penetration depth of the radiation, the main concept consists of a plastic housing in combination with a highly conductive functional surface and optionally a seal, which can also contribute to the shielding performance if needed. The measurements of the shielding effect show, depending on the combination of materials, sufficient to very good results.

Based on the measurement results a production concept was developed for the serial application of the functional surface taking different product sizes and design complexities for into consideration.

1 Introduction

The increasing complexity of electronic systems, e.g. in e-mobility, aerospace and medicine leads to high challenges for the parties involved. In electric vehicles, for example, electric drives with high performances are integrated in a very limited space and controlled by electronic assemblies. The individual devices may disturb each other by emitting interfering electromagnetic radiation. In order to improve the so-called electromagnetic compatibility, it has been known since a long time period to dampen electromagnetic interference by means of shielding housings. The first activities were started in the early 1960s in the military sector.

The term electromagnetic compatibility (EMC) is defined, for example, according to DIN VDE 0870 as the ability of an electrical device to operate satisfactorily in its environment without unduly affecting that environment, which may include other devices. Thus, the EMC must meet two conditions, the shielding of the emitted radiation and immunity to other electromagnetic radiation. The avoidance of electromagnetic "leakage" by shielding thus represents a comparable task as the seal against media loss, dirt and water penetration. However, it is based on completely different physical principles. However, shielding and sealing can be combined in a particularly approach.

https://doi.org/10.51202/9783181023549 - Generiert durch IP 216.73.216.36, am 19.01.2026, 02:19:31. © Urheberrechtlich geschützter Inhalt. Ohne gesonderte Erlaubnis ist jede urheberrechtliche Nutzung untersagt, insbesondere die Nutzung des Inhalts im Zusammenhang mit, für oder in KI-Systemen, KI-Modellen oder Generativen Sprachmodellen.

2 Basic Shielding Mechanism of electromagnetic Radiation

Electromagnetic waves usually have electrical and magnetic field components. The waves emitted by electronic components can lead to mutual electromagnetic interference. Due to the advances in semiconductor technology, electronic components have become increasingly smaller and their number has significantly increased within electronic devices. The frequency range relevant for EMI shielding is generally between 0 Hz and 100 GHz. The attenuation achieved by shielding of electromagnetic wave is generally composed of reflection and absorption (figure 1). By absorption, the electromagnetic wave loses energy which is converted to heat energy. The absorption depends on the wall thickness of the shielding material. Reflection, on the other hand, is less dependent on the thickness of the material in certain frequency ranges and for conductive types of material, and can occur at the front, back and inside of the material. The non-reflected and unabsorbed radiation components form the transmitted wave which shall be minimized in a suitable way.

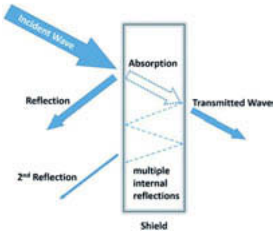


Fig. 1: Shielding of electromagnetic waves by reflection and absorption

The SE value in the unit [dB] has already been established as a measure of the shielding effect for some time. The SE value is calculated from the ratio of the electrical (or magnetic) field strength before (Ev) and after (En) the screen:

$$SE\ [dB] = 20 \log (Ev / En)$$

The relationship between the SE value and the ratio of the electric or magnetic field strength is thus strongly non-linear.

https://doi.org/10.51202/9783181023549 - Generiert durch IP 216.73.216.36, am 19.01.2026, 02:19:31. © Urheberrechtlich geschützter Inhalt. Ohne gesonderte Erlaubnis ist jede urheberrechtliche Nutzung untersagt, insbesondere die Nutzung des Inhalts im Zusammenhang mit, für oder in KI-Systemen, KI-Modellen oder Generativen Sprachmodellen.

3 Requirements and physical Background

The standard CISPR 25, jointly updated by the OEMs in 2016, essentially describes the requirements for the shielding quality in the middle frequency range of 150 kHz to 108 MHz, which is particularly relevant for the electric powertrain. The curves shown in Figure 2 show the required shielding quality for different grades A1 – A5 depending on the frequency in a simple-logarithmic scale [1].

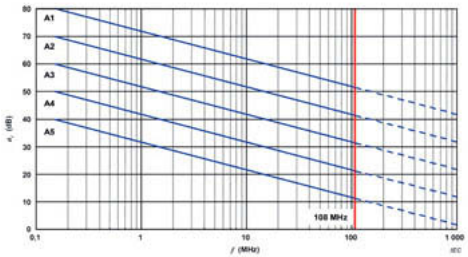


Fig. 2: Norm CISPR 25: Shielding requirements for different quality levels

In this frequency range, the shielding takes place predominantly through the process of reflection. For this purpose, the highest possible electrical conductivity of the materials is a basic requirement for shielding. As a rough value, it can be assumed that a conductivity above approx. 5000 S / m leads to a significant shielding effect. However, the conductivity alone is not completely sufficient as a criterion.

At present, predominantly metal housings - mostly made of aluminum - are used to shield electromagnetic radiation in electrically driven vehicles. Due to the high conductivities of aluminum very good shielding attenuation is achieved in this area. However, the use of purely metal shielding housings is associated with various disadvantages, including the existing but limited lightweight properties of aluminum and the relatively high production costs of components made of die-cast aluminum with increasing quantities. Also, the design freedom is somehow limited for metal materials.

https://doi.org/10.51202/9783181023549 - Generiert durch IP 216.73.216.36, am 19.01.2026, 02:19:31. © Urheberrechtlich geschützter Inhalt. Ohne gesonderte Erlaubnis ist jede urheberrechtliche Nutzung untersagt, insbesondere die Nutzung des Inhalts im Zusammenhang mit, für oder in KI-Systemen, KI-Modellen oder Generativen Sprachmodellen.

For the reasons mentioned above, the automotive industry is currently endeavoring to increasingly use plastic housings in the future (lightweight construction, functional integration, cost reduction). However, since most plastics are electrical insulators, the plastic housing components must be suitably imparted with conductivity. Therefore some technologies are in use.

For example, it is a common technology to coat plastic parts with metals after molding. For this purpose, a good adhesion of the conductive layer on the plastic surface is required. It is also a well-known and matured technology to use plastic compounds or composites for the production of electromagnetic shields. In this case the conductivity can be achieved by the compounding of a corresponding filler system into the polymeric matrix [2], [3].

In conjunction with electromagnetic shielding, the skin effect is of particular importance.

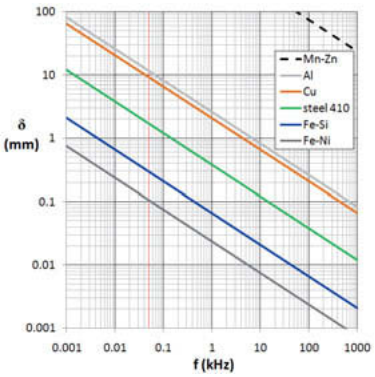


Fig. 3: Skin effect in dependency of frequency and kind of material (source: [7])

Simplified and related to the electromagnetic shielding can be said that the penetration depth of electromagnetic radiation into a conductive material decreases with increasing frequency and conductivity. At a frequency of, for example, 1 MHz, the penetration depth of the radiation in aluminum is less than 0.1 mm (Figure 3). This means that the shield in this frequency range relevant for the electric drive train is predominantly a task of the material surface. In the low-frequency range, on the other hand, e.g. at 100 Hz, the penetration depth in the housing material

https://doi.org/10.51202/9783181023549 - Generiert durch IP 216.73.216.36, am 19.01.2026, 02:19:31. © Urheberrechtlich geschützter Inhalt. Ohne gesonderte Erlaubnis ist jede urheberrechtliche Nutzung untersagt, insbesondere die Nutzung des Inhalts im Zusammenhang mit, für oder in KI-Systemen, KI-Modellen oder Generativen Sprachmodellen.

is several millimeters. Furthermore, magnetic fields often play a role here. Thus, it will be apparent that other physical shielding mechanisms must be used in this frequency range. However, this topic cannot be discussed in detail.

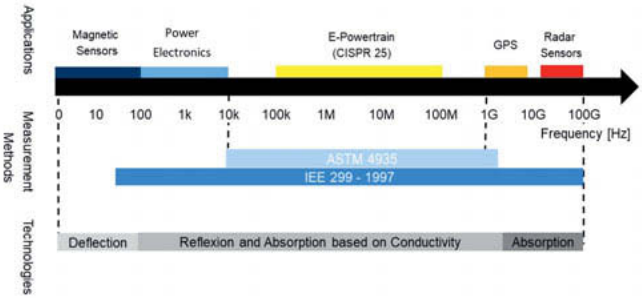


Fig. 4: Possible applications, test procedures and shielding mechanism for the relevant range of frequencies

Figure 4 summarizes the above mentioned statements and compares possible applications, measuring methods and potential shielding mechanisms as a function of the frequency. It becomes clear that a very broad frequency range of 11 orders of magnitude is relevant for the shielding. Different requirements and physical principles exist in the different frequency ranges. Thus, it is obvious that not only one shielding technology can cover the complete set of requirements optimally, but a certain technology portfolio is necessary.

4 **In the following the newly developed modular shielding concept will be described which is mainly focused on the medium range of frequencies covered by the CISPR 25. Never the less innovative solutions for low-frequency magnetic fields and for the absorption of radar waves were developed and successfully integrated into the modular concept of Freudenberg Sealing Technologies [5], [6].**

5 The modular Concept for Shielding and Sealing of Freudenberg Sealing Technologies

Based on the state of the art briefly described above, Freudenberg Sealing Technologies follows the technological approaches shown in Figure 5 as part of a strategic innovation project. The basis is the evaluation of the relevant customer requirements and the applicable standards for e-mobility and autonomous driving. The technological directions include the electromagnetic shielding, as well as the thermal conductivity and the selection of suitable test methods.

https://doi.org/10.51202/9783181023549 - Generiert durch IP 216.73.216.36, am 19.01.2026, 02:19:31. © Urheberrechtlich geschützter Inhalt. Ohne gesonderte Erlaubnis ist jede urheberrechtliche Nutzung untersagt, insbesondere die Nutzung des Inhalts im Zusammenhang mit, für oder in KI-Systemen, KI-Modellen oder Generativen Sprachmodellen.

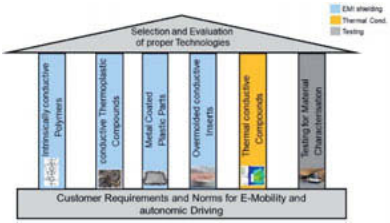


Fig. 5: Technological approaches at Freudenberg Sealing Technologies

As a test method for the electromagnetic shielding, the standard ASTM 4935-99 offers some benefits for a basic R&D project. With this method, different material combinations and technologies can be compared with each other in a comparatively simple way. In this method, the specimen is clamped between two flanges, which are equipped with a special transmitter and receiver technology. From the difference of the signals the shielding attenuation in the unit [db] can be calculated [4].

As already mentioned, the CISPR 25 describes the frequency range in which many units of the electric drive train work and emit electromagnetic radiation or react sensitively to the radiation of other devices. In addition, the skin effect plays an important role in this middle frequency range. Specifically for applications in this range, Freudenberg Sealing Technologies has developed the shielding concept shown basically in Figure 6.

The concept initially includes a housing made of a plastic chosen to meet the further requirements for later use (e.g. temperature and media resistance, mechanical properties, etc.). The actual shielding effect will be generated - according to the skin effect – by a highly conductive surface on the inside or outside or on both sides. Depending on the requirements, this functional surface can be both a conductive coating based on a polymeric matrix and a purely metallic coating. In principle, also conductive inserts can be overmolded with the housing material. Such inserts may also include conductive films, woven or nonwoven fabrics.

https://doi.org/10.51202/9783181023549 - Generiert durch IP 216.73.216.36, am 19.01.2026, 02:19:31. © Urheberrechtlich geschützter Inhalt. Ohne gesonderte Erlaubnis ist jede urheberrechtliche Nutzung untersagt, insbesondere die Nutzung des Inhalts im Zusammenhang mit, für oder in KI-Systemen, KI-Modellen oder Generativen Sprachmodellen.

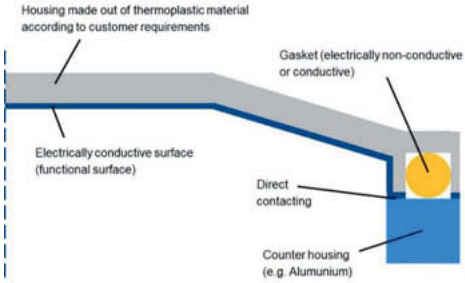


Fig. 6: Schematic sketch of the developed basic concept for shielding in the medium range of frequencies

Of course, the concept can be supplemented with a static and / or dynamic seal if necessary. Depending on the contact with the counter housing, the gasket must be designed to be electrically conductive or non-conductive. In case of direct contact of the functional surface usually no conductivity of the seal is required.

An important basic requirement for the function of the developed concept is a sufficient adhesion of the conductive surface on the housing material under the given boundary conditions in the application and over the required service life. For this purpose, appropriate validations must be scheduled. Due to the numerous possible combinations of materials, this concept offers the possibility of adaptation to a wide range of requirements and thus has a very modular character. Due to the functional separation in housing and conductive surface, a high degree of cost-effectiveness of the concept can be achieved by means of an appropriate material and process selection.

6 Results of Shielding Measurements

According to the concept idea, numerous test specimens for measuring the shielding effect according to standard ASTM 4935-99 were produced from different material combinations and measured by an external laboratory. The preparation of the specimens was carried out in a process that should correspond as far as possible to the later serial process. As a housing material for the overmolding a Polyamide 6.6 with 30% glass fibers has been used. Figure 7 shows an excerpt from the measurement results of the screen attenuation in [dB] for different material classes as a function of the frequency. In addition, as a comparison, the A1 class of the CISPR 25 is shown in red.

https://doi.org/10.51202/9783181023549 - Generiert durch IP 216.73.216.36, am 19.01.2026, 02:19:31. © Urheberrechtlich geschützter Inhalt. Ohne gesonderte Erlaubnis ist jede urheberrechtliche Nutzung untersagt, insbesondere die Nutzung des Inhalts im Zusammenhang mit, für oder in KI-Systemen, KI-Modellen oder Generativen Sprachmodellen.

It became obvious that aluminum and copper coated and overmolded nonwovens cannot meet the requirements of the CISPR 25. They are particularly suitable for simple shielding tasks with comparatively low requirements. Significantly better results are provided by the aluminum and copper meshes, which are commercially available and were also overmolded with PA 6.6 as the housing material. However, the best results were achieved by far by the self-developed functional surface, which has a very high conductivity. The patenting of this functional surface has already been initiated at the Patent Office.

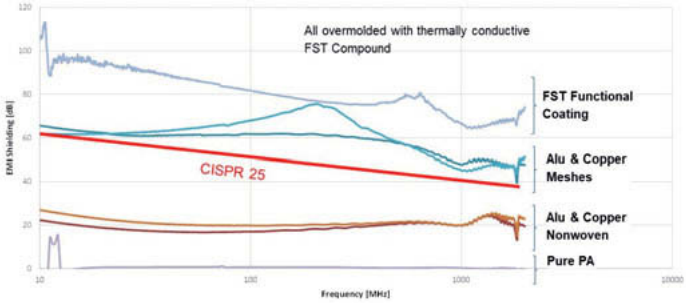


Fig. 7: Results of the shielding measurements for different material combinations according ASTM 4935-99

7 Serial Production Concept

Furthermore a production concept was developed for the serial application of the functional surface [8]. Different technologies were investigated and theoretically as well as practically evaluated by measuring of shielding performance and bonding behavior. Hereby different product sizes and design complexities for various application areas were taken into consideration.

https://doi.org/10.51202/9783181023549 - Generiert durch IP 216.73.216.36, am 19.01.2026, 02:19:31. © Urheberrechtlich geschützter Inhalt. Ohne gesonderte Erlaubnis ist jede urheberrechtliche Nutzung untersagt, insbesondere die Nutzung des Inhalts im Zusammenhang mit, für oder in KI-Systemen, KI-Modellen oder Generativen Sprachmodellen.

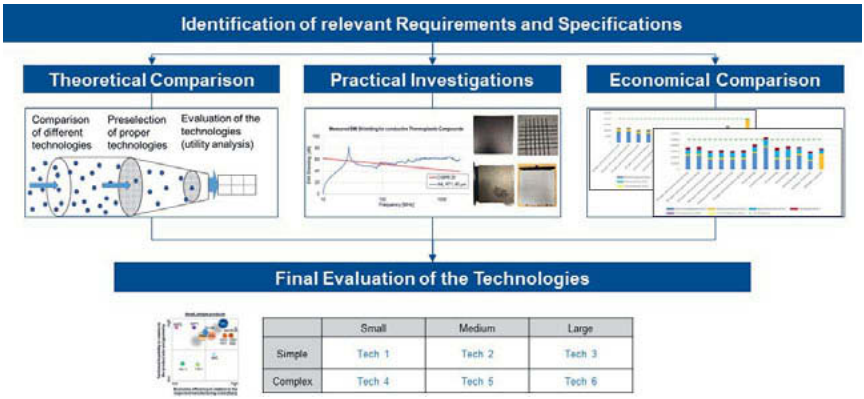


Fig. 8: Procedure to identify proper technologies for the application of the functional surface on plastic housings

https://doi.org/10.51202/9783181023549 - Generiert durch IP 216.73.216.36, am 19.01.2026, 02:19:31. © Urheberrechtlich geschützter Inhalt. Ohne gesonderte Erlaubnis ist jede urheberrechtliche Nutzung untersagt, insbesondere die Nutzung des Inhalts im Zusammenhang mit, für oder in KI-Systemen, KI-Modellen oder Generativen Sprachmodellen.

Literature

[1] CISPR 25, International Electrotechnical Commission, 1995-11, S. 1 – 49

[2] S. Geetha et al., Journal of Applied Polymer Science, Bd. 112, 2073 - 2086 (2009) N, N., *International Sealing Conference Stuttgart 2016*,

[3] K. Jagatheesan et al., Indian Journal of Fibre & Textile Research, Bd. 39, 329 - 342 (2014)

[4] ASTM 4935-99, Test Method for Measuring the Electromagnetic Shielding Effectiveness of Planar Materials (Withdrawn 2005)

[5] Mühlpfort R., Entwicklung eines Systems zur Abschirmung statischer und niederfrequenter Magnetfelder
Unveröffentlichte Bachelorarbeit an der Hochschule Mannheim,
Betreuer: Prof. Dr. M. Rädle (HS Mannheim), Volker Schroiff (FST)
Januar 2019

[6] Dehler V., Entwicklung und Validierung von Technologien zur elektromagnetischen Schirmung automobiler Radarsysteme über Kunststoffgehäuse unter Berücksichtigung technischer und wirtschaftlicher Aspekte
Unveröffentlichte Masterarbeit an der Hochschule Mannheim
Betreuer: Prof. Dr. J. Steffen (HS Mannheim), Volker Schroiff (FST)
März 2019

[7] https://de.wikipedia.org/wiki/Skin-Effekt

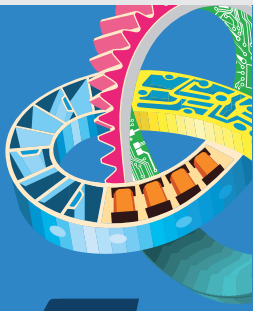
[8] Fasser K., Produktionskonzept zur Herstellung elektromagnetisch abschirmender Oberflächen für die Elektromobilität
Unveröffentlichte Masterarbeit an der Hochschule Mannheim
Betreuer: Prof. Dr. M. Hauth (HS Mannheim), Volker Schroiff (FST)
März 2019

https://doi.org/10.51202/9783181023549 - Generiert durch IP 216.73.216.36, am 19.01.2026, 02:19:31. © Urheberrechtlich geschützter Inhalt. Ohne gesonderte Erlaubnis ist jede urheberrechtliche Nutzung untersagt, insbesondere die Nutzung des Inhalts im Zusammenhang mit, für oder in KI-Systemen, KI-Modellen oder Generativen Sprachmodellen.

https://doi.org/10.51202/9783181023549 - Generiert durch IP 216.73.216.36, am 19.01.2026, 02:19:31. © Urheberrechtlich geschützter Inhalt. Ohne gesonderte Erlaubnis ist jede urheberrechtliche Nutzung untersagt, insbesondere die Nutzung des Inhalts im Zusammenhang mit, für oder in KI-Systemen, KI-Modellen oder Generativen Sprachmodellen.

https://doi.org/10.51202/9783161023549 - Generiert durch IP 216.73.216.36, am 19.01.2026, 02:19:31. © Urheberrechtlich geschützter Inhalt. Ohne gesonderte Erlaubnis ist jede urheberrechtliche Nutzung untersagt, insbesondere die Nutzung des Inhalts im Zusammenhang mit, für oder in KI-Systemen, KI-Modellen oder Generativen Sprachmodellen.

VDI Wissensforum



EDritev

International Conference
EDrive

ISBN 978-3-18-092354-3

https://doi.org/10.51202/9783181023549 - Generiert durch IP 216.73.216.36, am 19.01.2026, 02:19:31. © Urheberrechtlich geschützter Inhalt. Ohne gesonderte Erlaubnis ist jede urheberrechtliche Nutzung untersagt, insbesondere die Nutzung des Inhalts im Zusammenhang mit, für oder in KI-Systemen, KI-Modellen oder Generativen Sprachmodellen.

VDI Wissensforum

VDI-Berichte 2354



Dritev

6th International VDI-Conference

Drivetrain Solutions for Commercial Vehicles

July 10 and 11, 2019, Bonn

Main topics:

- E-Fuels: Varieties, costs and perspectives of synthetic fuels
- Electrification concepts for light and medium duty vehicles
- Potentials of gas powered heavy vehicles
- Hydrogen mobility for heavy duty trucks
- Advanced simulation methods for new drivetrains

https://doi.org/10.51202/9783181023549 - Generiert durch IP 216.73.216.36, am 19.01.2026, 02:19:31. © Urheberrechtlich geschützter Inhalt. Ohne gesonderte Erlaubnis ist jede urheberrechtliche Nutzung untersagt, insbesondere die Nutzung des Inhalts im Zusammenhang mit, für oder in KI-Systemen, KI-Modellen oder Generativen Sprachmodellen.

https://doi.org/10.51202/9783161023549 - Generiert durch IP 216.73.216.36, am 19.01.2026, 02:19:31. © Urheberrechtlich geschützter Inhalt. Ohne gesonderte Erlaubnis ist jede urheberrechtliche Nutzung untersagt, insbesondere die Nutzung des Inhalts im Zusammenhang mit, für oder in KI-Systemen, KI-Modellen oder Generativen Sprachmodellen.

VDI-BERICHTE
Herausgeber:
VDI Wissensforum GmbH

https://doi.org/10.51202/9783181023549 - Generiert durch IP 216.73.216.36, am 19.01.2026, 02:19:31. © Urheberrechtlich geschützter Inhalt. Ohne gesonderte Erlaubnis ist jede urheberrechtliche Nutzung untersagt, insbesondere die Nutzung des Inhalts im Zusammenhang mit, für oder in KI-Systemen, KI-Modellen oder Generativen Sprachmodellen.

Bibliographische Information der Deutschen Nationalbibliothek
Die Deutsche Nationalbibliothek verzeichnet diese Publikation in der Deutschen Nationalbibliographie; detaillierte bibliographische Daten sind im Internet unter www.dnb.de abrufbar.

Bibliographic information published by the Deutsche Nationalbibliothek (German National Library)
The Deutsche Nationalbibliothek lists this publication in the Deutsche Nationalbibliographie (German National Bibliography); detailed bibliographic data is available via Internet at www.dnb.de.

© VDI Verlag GmbH · Düsseldorf 2019
Alle Rechte vorbehalten, auch das des Nachdruckes, der Wiedergabe (Photokopie, Mikrokopie), der Speicherung in Datenverarbeitungsanlagen und der Übersetzung, auszugsweise oder vollständig.

Der VDI-Bericht, der die Vorträge der Tagung enthält, erscheint als nichtredigierter Manuskriptdruck.
Die einzelnen Beiträge geben die auf persönlichen Erkenntnissen beruhenden Ansichten und Erfahrungen der jeweiligen Vortragenden bzw. Autoren wieder. Printed in Germany.

ISSN 0083-5560
ISBN 978-3-18-092354-3

https://doi.org/10.51202/9783181023549 - Generiert durch IP 216.73.216.36, am 19.01.2026, 02:19:31. © Urheberrechtlich geschützter Inhalt. Ohne gesonderte Erlaubnis ist jede urheberrechtliche Nutzung untersagt, insbesondere die Nutzung des Inhalts im Zusammenhang mit, für oder in KI-Systemen, KI-Modellen oder Generativen Sprachmodellen.

Markets and Fuels

Drivetrain trend of truck of Asian market and new technology drive train for HD truck 1
S. Sudo, T. Maeda, R. Kobayashi, Hino Motors Limited, Tokyo Japan

Zero-Emission Driveline

New powertrain concepts for heavy duty commercial vehicles 9
R. Dold, Daimler Trucks, Stuttgart

Electric driveline adaptation from passenger-car application to Light & Medium Truck application – A competitive, efficient, compact and light solution 19
T. Basbous, Valeo, Cergy, France;
J. Mortal, Valeo, Saint-Quentin Fallavier, France

Emission Optimized Driveline

Dedicated hybrid transmission for commercial vehicle applications – Mechanical layout, system analysis and simulation of a dedicated hybrid transmission for commercial vehicles 29
C. Schoerghuber, I. Müller, H. Wiener,
AVL Commercial Driveline & Tractor Engineering GmbH, Steyr, Austria

Gas powered heavy duty vehicles from Scania: Current program and future potential 49
M. Lindström, Scania CV, Södertälje, Sweden

Diverse requirements, one product family – The HV Kit for LCV from MAGNA 55
R. Nasdal, Getrag Ford Transmissions, Köln;
K. Masser, MAGNA Engineering Center Steyr, St. Valentin, Austria

https://doi.org/10.51202/9783161023549 - Generiert durch IP 216.73.216.36, am 19.01.2026, 02:19:31. © Urheberrechtlich geschützter Inhalt. Ohne gesonderte Erlaubnis ist jede urheberrechtliche Nutzung untersagt, insbesondere die Nutzung des Inhalts im Zusammenhang mit, für oder in KI-Systemen, KI-Modellen oder Generativen Sprachmodellen.

Conventional Transmissions

Benefits of the new Allison 9-speed fully automatic – Medium duty commercial transmission 61
S. Kluemper, Conrad Rockey, Allison Transmission, Inc., Indianapolis, IN, USA

Mechatronic transmission control module for agile AMT Transmission actuation in commercial vehicles 75
S. Johnsen, Powertrain and Chassis, Kongsberg Automotive, Kongsberg, Norway;
R. Wexenberger, Powertrain and Chassis, Kongsberg Automotive GmbH, Hallbergmoos

Advanced Simulation Methods

Simulation of load cycles for commercial vehicle drivelines based on statistical reasoning . . 85
M. Scherpelz, J. Bernhardt, ZF Friedrichshafen AG, Friedrichshafen;
T. Weyh, M. Lübke Fraunhofer ITWM, Kaiserslautern

https://doi.org/10.51202/9783181023549 - Generiert durch IP 216.73.216.36, am 19.01.2026, 02:19:31. © Urheberrechtlich geschützter Inhalt. Ohne gesonderte Erlaubnis ist jede urheberrechtliche Nutzung untersagt, insbesondere die Nutzung des Inhalts im Zusammenhang mit, für oder in KI-Systemen, KI-Modellen oder Generativen Sprachmodellen.

Many thanks to the Gold-Sponsors of the Congress:



www.iot.bosch.com



www.castrol.com/de



www.gkndriveline.com



www.magna.com



www.daimler.de



www.zf.com

https://doi.org/10.51202/9783161023549 - Generiert durch IP 216.73.216.36, am 19.01.2026, 02:19:31. © Urheberrechtlich geschützter Inhalt. Ohne gesonderte Erlaubnis ist jede urheberrechtliche Nutzung untersagt, insbesondere die Nutzung des Inhalts im Zusammenhang mit, für oder in KI-Systemen, KI-Modellen oder Generativen Sprachmodellen.

https://doi.org/10.51202/9783161023549 - Generiert durch IP 216.73.216.36, am 19.01.2026, 02:19:31. © Urheberrechtlich geschützter Inhalt. Ohne gesonderte Erlaubnis ist jede urheberrechtliche Nutzung untersagt, insbesondere die Nutzung des Inhalts im Zusammenhang mit, für oder in KI-Systemen, KI-Modellen oder Generativen Sprachmodellen.

Drivetrain trend of Truck of Asian Market and New technology drive train for HD Truck

Dipl.-Ing. **Shinya Sudo**, Dipl.-Ing. **Tsuyoshi Maeda**,
Dipl.-Ing. **Ryoya Kobayashi**,
Hino Motors Limited, Tokyo Japan

Abstract

Hino Motors is producing commercial vehicles for about 90 countries. Our major markets are Japan and Asian countries. There are different demands to vehicle each country, therefore there are different drivers for engineering transmissions.
CO2 reduction is very important driver for engineering of drive train system. Hino Motors developed new hybrid system for heavy duty long haul trucks that will be released in Japan at first.

Asian Market

Hino Motors major market countries are Indonesia and Thailand, there are up-rising countries. There are different points to developed countries, social environment, infrastructure, regulation, culture and so on. Also operation conditions are different.
Operation conditions in Asian countries; heavy over load, narrow and rough road, steep hill, so muddy road after heavy rain…. etc.
Demands from customer and operation condition in Asian countries; cost, durability, reliability, toughness, easy to repair…etc.
(reference developed country, Japanese customer demands; Fuel economy, safety, comfortable, cost…. etc.)

Key driver of transmission development for Asian markets;
Cost: consider minimize power train configuration. Small displacement engine and minimum number of speed manual transmission, this configuration will have big impact to drive train durability because operation time in low gear will be long.
Reliability, Durability; Have to consider with heavy over loaded, steep hill and rough load…Increase load on each component.

https://doi.org/10.51202/9783181023549 - Generiert durch IP 216.73.216.36, am 19.01.2026, 02:19:31. © Urheberrechtlich geschützter Inhalt. Ohne gesonderte Erlaubnis ist jede urheberrechtliche Nutzung untersagt, insbesondere die Nutzung des Inhalts im Zusammenhang mit, für oder in KI-Systemen, KI-Modellen oder Generativen Sprachmodellen.



Fig1: Typical operation conditions in East Asian countries (Left: Semi trailer on public road, Right: Tipper in mountain area)

Transmission for Asian market

Hino Motors developed a couple of transmissions for Medium and Heavy duty trucks in Asian markets, there are MX06/07 (6/7speed) and M009 (9speed) transmissions.
Main drivers of development are durability, reliability and cost. Introduce some features in these transmission in this paper.

Table1: Basic specification of Transmission

Series Name	Torque Capacity	No. of Speed	Ratio
MX06	1000Nm	6 Speed	6.52 – 0.70
MX07	1000Nm	7 Speed	6.52 – 0.58
M009	1600Nm	9 Speed	10.18 – 0.72

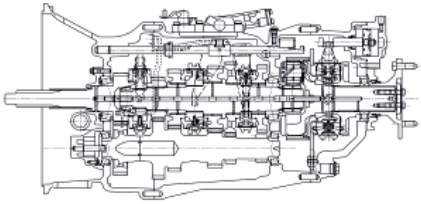


Fig2: Cross section of M009 transmission

https://doi.org/10.51202/9783181023549 - Generiert durch IP 216.73.216.36, am 19.01.2026, 02:19:31. © Urheberrechtlich geschützter Inhalt. Ohne gesonderte Erlaubnis ist jede urheberrechtliche Nutzung untersagt, insbesondere die Nutzung des Inhalts im Zusammenhang mit, für oder in KI-Systemen, KI-Modellen oder Generativen Sprachmodellen.

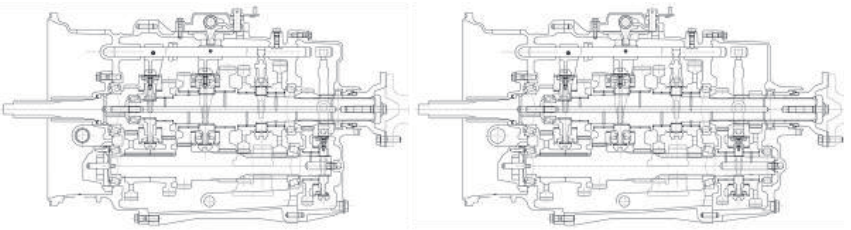


Fig3: Cross section of MX06(Left) and MX07 transmission

1. Module design

MX06/07 transmission is adopting for a lot of applications. There are some sections, main module, front module, rear module and control module.

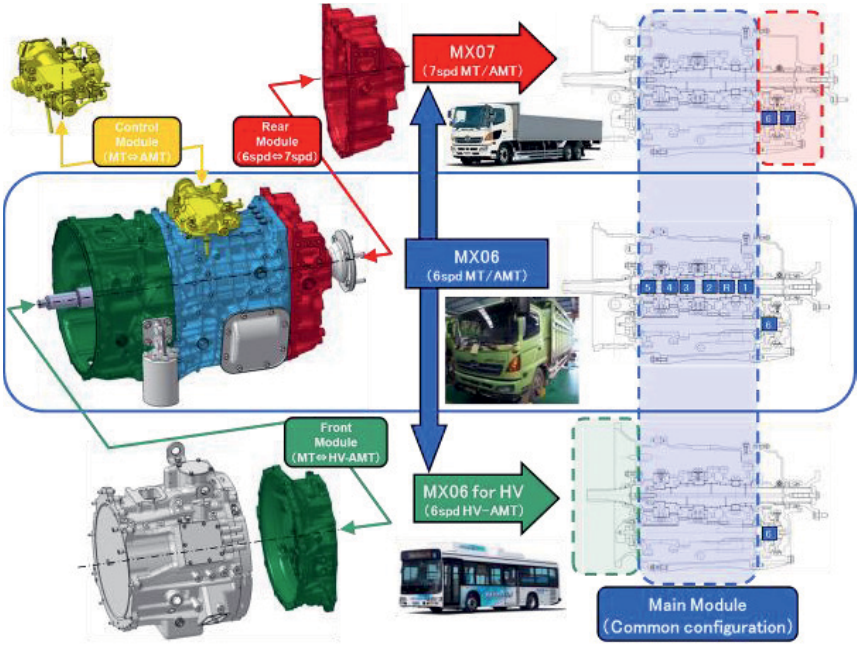


Fig4: Module design image of MX06/07 for each application

https://doi.org/10.51202/9783181023549 - Generiert durch IP 216.73.216.36, am 19.01.2026, 02:19:31. © Urheberrechtlich geschützter Inhalt. Ohne gesonderte Erlaubnis ist jede urheberrechtliche Nutzung untersagt, insbesondere die Nutzung des Inhalts im Zusammenhang mit, für oder in KI-Systemen, KI-Modellen oder Generativen Sprachmodellen.

2.Short shift stroke of transmission (MX06/07)

Shift stroke of transmission is 20% shorter than previous transmission that could increase 20% ratio between shift lever and transmission. Therefore, MX06/07 could remove air servo shift cylinder, but shift force on shift lever in cabin is same as previous transmission.

3.Carbon friction material synchronizer (M009)

Carbon friction material has very good effect synchronizer performance and durability. PV (Pressure of synchronizer surface – Velocity) limitation is 2.5 times higher than Mo-spray synchronizer. It has enough capacity for skip shifting in actual operation condition.



Fig5: Carbon friction material

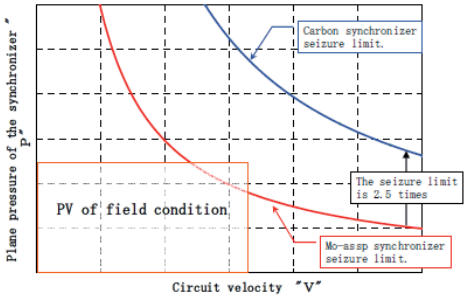


Fig6: PV chart of Carbon friction material

4.Definition durability target of each component by load cycle simulation

Calculate load cycle of each component by simulation virtual vehicle model with actual running data and road data. we could know which component or country will be severe in earlier stage in development.

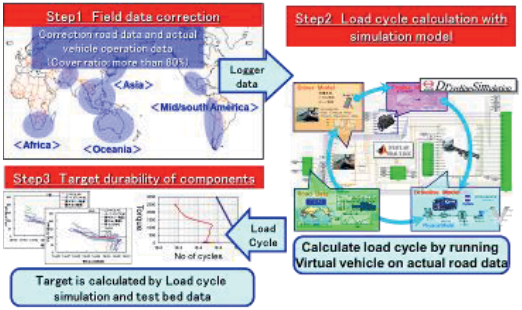


Fig7: process of definition of target durability of component

https://doi.org/10.51202/9783181023549 - Generiert durch IP 216.73.216.36, am 19.01.2026, 02:19:31. © Urheberrechtlich geschützter Inhalt. Ohne gesonderte Erlaubnis ist jede urheberrechtliche Nutzung untersagt, insbesondere die Nutzung des Inhalts im Zusammenhang mit, für oder in KI-Systemen, KI-Modellen oder Generativen Sprachmodellen.

Hino Motors' Environmental Technologies

Trucks and buses are made to transport large numbers of people or goods over relatively long distances, and fuel and energy are needed to do that. As a result, emission of CO2, a greenhouse gas, is inevitable.

Unique aspects of trucks and buses include their comparatively large size and loading capacities, the long distances they travel, and their wide array of uses and places where they are used. Taking into account these varying conditions, Hino Motors considers what types of environmental technologies are most suitable. By providing users with optimally equipped vehicles, the Company hopes to help curb global warming

Next Generation Vehicle

Hino Motors capitalizes on the unique benefits of electric vehicles such as clean exhaust gas emissions and quietness of ride to create next-generation vehicles that meet customers' and society's needs.

Hino primarily pursues development for applications in urban areas such as light-duty trucks and buses and route buses.

Hino will continue to develop vehicles along with related technologies including batteries, while seeking to reinforce

social infrastructure, such as charging facilities and hydrogen stations, in cooperation with relevant organizations. The ultimate goal is to offer electric or hydrogen power options on all models.

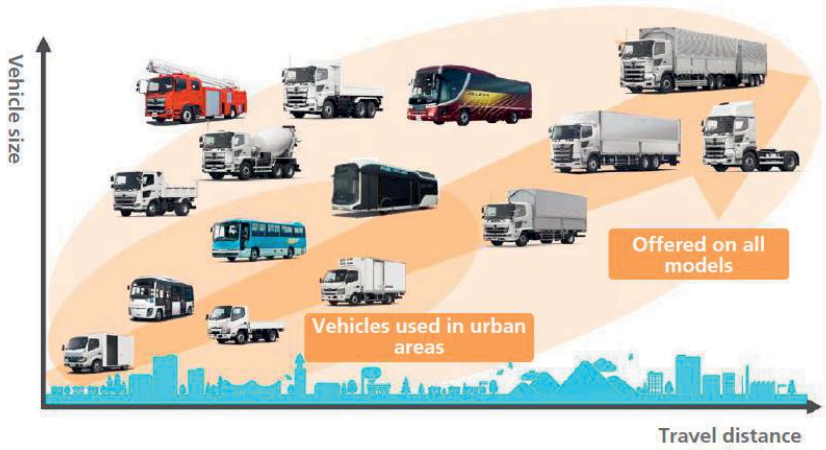


Fig.8: Image of Vehicle size and Travel Distance of commercial vehicle

https://doi.org/10.51202/9783181023549 - Generiert durch IP 216.73.216.36, am 19.01.2026, 02:19:31. © Urheberrechtlich geschützter Inhalt. Ohne gesonderte Erlaubnis ist jede urheberrechtliche Nutzung untersagt, insbesondere die Nutzung des Inhalts im Zusammenhang mit, für oder in KI-Systemen, KI-Modellen oder Generativen Sprachmodellen.

Evolution of the Hybrid Vehicle

Ever since Hino Motors commercialized and sold the world's first hybrid bus in 1991, the Company has constantly led the industry in environmentally friendly products. Hino Motor's environmentally friendly products continue to be loved by customers around the world. Among these products, cumulative sales of hybrid vehicles surpassed 15,000 as of the end of fiscal 2017.

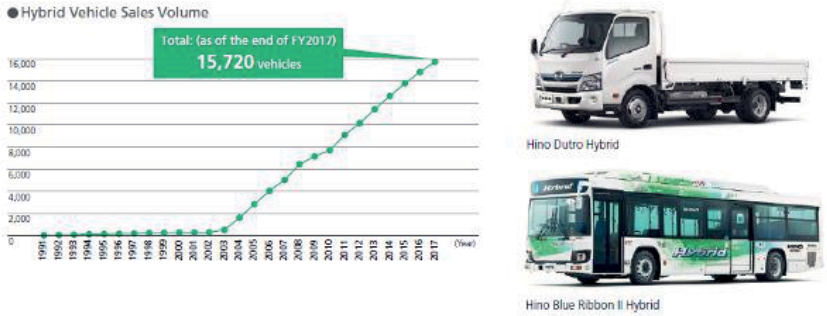


Fig9: Hino hybrid vehicle sales volume and pictures of hybrid commercial vehicles

Hino Motors will produce the Hino Profia Hybrid, an innovative heavy-duty hybrid truck that combines high level advanced performance and safety technology.
Thanks to hybrid control that pre-reads the road gradient using artificial intelligence (AI), Hino Motors has achieved the world's first hybrid system with fuel economy even in vehicles that run at high speeds, a feat considered difficult until now.
The system maintains the same fundamental performance and ease of use as offered by a diesel vehicle, reduces fuel consumption by about 15% (based on internal data), and is expected to cut vehicle operating costs.
The large-capacity lithium-ion battery in the truck can be used as an external emergency power supply. Moreover, noise and vibration are reduced during vehicle operation, which helps to alleviate driver fatigue.

https://doi.org/10.51202/9783181023549 - Generiert durch IP 216.73.216.36, am 19.01.2026, 02:19:31. © Urheberrechtlich geschützter Inhalt. Ohne gesonderte Erlaubnis ist jede urheberrechtliche Nutzung untersagt, insbesondere die Nutzung des Inhalts im Zusammenhang mit, für oder in KI-Systemen, KI-Modellen oder Generativen Sprachmodellen.



Fig10: Hybrid heavy duty long haulage truck for Japanese market

Hybrid power train configuration is P2 type <Engine (9litter/6Cyl) – Clutch – E-motor – Transmission (12speed AMT)>. There is no clutch between E-motor and Transmission. Transmission is MZ12 that is Hino motors in-house transmission. It has three main gear steps, two split steps and 2 range steps (2x3x2). Main section has no synchronizer, synchronize during shift change by E-motor. Shift time is shorter than conventional synchronized transmission due to short time and high accuracy synchronize by E-motor.

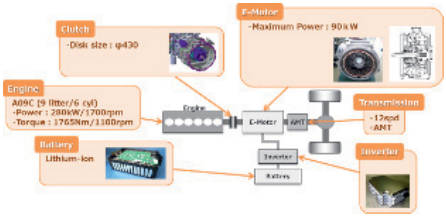


Fig11: Component configuration of new Hybrid system for Heavy Duty truck

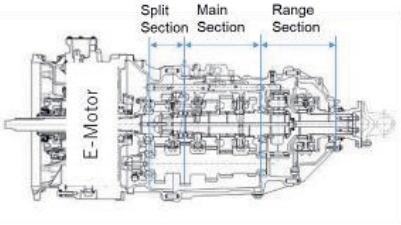


Fig12: Cross section of MZ12 transmission with E-Motor for Hybrid

[1] Hino sustainability report 2018: Hino Motors limited, 2018

[2] Development of New 9speed Transmission (M009) for Heavy-duty Commercial Vehicle, Noboru Yamazaki, Hino Motors Limited, 2012 JSAE symposium

https://doi.org/10.51202/9783181023549 - Generiert durch IP 216.73.216.36, am 19.01.2026, 02:19:31. © Urheberrechtlich geschützter Inhalt. Ohne gesonderte Erlaubnis ist jede urheberrechtliche Nutzung untersagt, insbesondere die Nutzung des Inhalts im Zusammenhang mit, für oder in KI-Systemen, KI-Modellen oder Generativen Sprachmodellen.

https://doi.org/10.51202/9783181023549 - Generiert durch IP 216.73.216.36, am 19.01.2026, 02:19:31. © Urheberrechtlich geschützter Inhalt. Ohne gesonderte Erlaubnis ist jede urheberrechtliche Nutzung untersagt, insbesondere die Nutzung des Inhalts im Zusammenhang mit, für oder in KI-Systemen, KI-Modellen oder Generativen Sprachmodellen.

New powertrain concepts for heavy duty commercial vehicles

Roland Dold, Daimler Trucks, Stuttgart

Current situation: Game Changer and Trends

The world is changing fast: growing cities and intensifying traffic require Zero Emission solutions for urban distribution.

Urbanization and growing population in the cities, climate change as well as changes in mobility behaviour are Megatrends which are influencing the whole world, especially Germany. Quality of life in cities will become more important. Increasing requirements with regard to freshness and quick availability give rise to more frequent deliveries.

Zero emission vehicles categorization

To fulfil upcoming CO2 regulations Daimler Trucks focusses on development of Zero Emission Vehicles (ZEV) for different Truck applications (Light Duty Trucks (LDT), Medium Duty Trucks (MDT), and Heavy Duty Trucks (HDT)):

https://doi.org/10.51202/9783181023549 - Generiert durch IP 216.73.216.36, am 19.01.2026, 02:19:31. © Urheberrechtlich geschützter Inhalt. Ohne gesonderte Erlaubnis ist jede urheberrechtliche Nutzung untersagt, insbesondere die Nutzung des Inhalts im Zusammenhang mit, für oder in KI-Systemen, KI-Modellen oder Generativen Sprachmodellen.

LDT	MDT	HDT
		 First demonstration for urban distribution @ IAA 2016
 eCanter: First LDT worldwide with SOP 2017	 eM2: First MDT for US Market demonstrated	 First demonstration for HD Class 8 Truck for US Market in 2018
		 eActros Gen1 Customer Demo Fleet

Table 1: Zero emission vehicles categorized after LDT, MDT or HDT

https://doi.org/10.51202/9783181023549 - Generiert durch IP 216.73.216.36, am 19.01.2026, 02:19:31. © Urheberrechtlich geschützter Inhalt. Ohne gesonderte Erlaubnis ist jede urheberrechtliche Nutzung untersagt, insbesondere die Nutzung des Inhalts im Zusammenhang mit, für oder in KI-Systemen, KI-Modellen oder Generativen Sprachmodellen.

Truck requirements for Zero Emission Vehicles

Requirements for truck zero emission vehicles are very different compared to passenger car requirements:

- Regarding the range: high volumetric energy density is necessary, which is equivalent to approx. 800 km/day.
- Regarding the payload: high gravimetric energy density is necessary.
- Regarding the lifetime: Long life is required for 1.2 Mio km and more than 10 years lifespan.
- Regarding the total cost of ownership: low purchase costs are needed.

For current Medium Duty Truck applications PHEV type cells acceptable compromise due to high power and relatively high cycle life.

Technical description and configuration of the Mercedes-Benz Electric Truck

For an integration of an electric drivetrain concept, the following characteristics should be fulfilled: clean, silent, highly efficient and suited to daily use.
The Truck is mainly build from Battery system, E-axle and chassis.
At first sight at the chassis, you notice that the Electric Truck has been designed from scratch and has consequently been designed as an electrically powered vehicle.

Instead of a central engine, it features an **electrically powered rear axle** with electric motors close to the wheel hubs. The powerful lithium-ion batteries with 212 kilowatt-hours in total are placed safely within the chassis. This design allows for a payload of 12.8 tons and for a range of up to 200 kilometres, which is comparable with diesel trucks of the same size.

https://doi.org/10.51202/9783181023549 - Generiert durch IP 216.73.216.36, am 19.01.2026, 02:19:31. © Urheberrechtlich geschützter Inhalt. Ohne gesonderte Erlaubnis ist jede urheberrechtliche Nutzung untersagt, insbesondere die Nutzung des Inhalts im Zusammenhang mit, für oder in KI-Systemen, KI-Modellen oder Generativen Sprachmodellen.

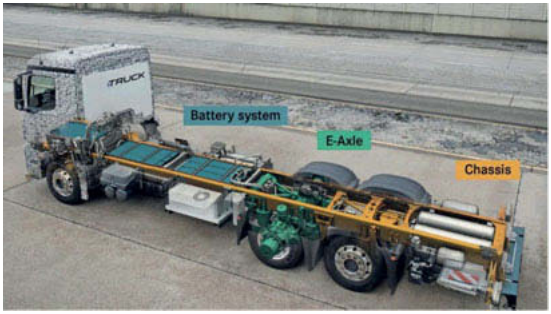


Fig. 1: Mercedes-Benz Electric Truck

The technical starting position is a **Mercedes-Benz chassis** for a flatbed vehicle in heavy-duty distribution operations. The chassis is a so-called 6x2 NLA, i.e. a 3-axle vehicle with 4,900 mm wheelbase and a steered trailing axle. This ensures maximum manoeuvrability in city traffic - it is still fully liftable to further reduce rolling resistance during an empty run.

The **battery system** includes 3 battery packs, which are placed inside the frame. Due to the fact that the centre of gravity is lowered, an increase in rolling stability is assured. Proven lithium-ion battery technology is used for safety reasons and weight reduction.

Charging concept: a direct current (DC) charging is located next to the battery system with an external station. The Electric Truck is chargeable up to 150 kW. It is rapidly charging, which is extremely important for heavy duty trucks. An external charging unit offers several advantages: it is saving vehicle weight, costs for customers and a standardized charging connector is adapted, that means no adapter is needed (Combo-Standard, Type 2, European Standard IEC 62196). The communication with the charging station also makes the Electric Truck flexible: it can also be charged with lower kW values than the maximum value of 150 kW - bandwidth

https://doi.org/10.51202/9783181023549 - Generiert durch IP 216.73.216.36, am 19.01.2026, 02:19:31. © Urheberrechtlich geschützter Inhalt. Ohne gesonderte Erlaubnis ist jede urheberrechtliche Nutzung untersagt, insbesondere die Nutzung des Inhalts im Zusammenhang mit, für oder in KI-Systemen, KI-Modellen oder Generativen Sprachmodellen.

from 20 kW to 150 kW. The downward compatibility also means that customers can adapt charging infrastructure to their specific conditions and implement requirements cost-effectively, for example, if charging takes place overnight, cheaper charging stations with lower capacity are sufficient. This leads to intelligent charging: for example, five vehicles can share a 100 kW charging station - and each can charge 20 kW overnight.

HD trucks: Mileage, Alternative fuels & drivetrains

Future transportation studies indicate growing HD Truck mileage: The forecast on future annual driven mileage from Prognos for EU28 market results in an increase of annual mileage for more than 20 t by approx. 25-30%.

Based on today‘s driving and rest periods the legislation allows 4,5 hours of driving, 45min rest period and again 4,5 hours of driving. Therefore HD Longhaul (LH) trucks need to fulfil the customer requirements to enable a daily range of 800km within the given time frame. If energy storage on board does not cover 800km range, a refuelling within 45 min has to be guaranteed. Based on current transport tasks and forecasts for EU28 the transport effort of HD LH trucks will increase heavily. High transportation efficiency with high payload, high transportation speeds and long ranges are required.

There are different options for future alternative truck fuels and drivetrains for HD LH transportation to meet the expected CO2 targets (see Figure 2).

https://doi.org/10.51202/9783181023549 - Generiert durch IP 216.73.216.36, am 19.01.2026, 02:19:31. © Urheberrechtlich geschützter Inhalt. Ohne gesonderte Erlaubnis ist jede urheberrechtliche Nutzung untersagt, insbesondere die Nutzung des Inhalts im Zusammenhang mit, für oder in KI-Systemen, KI-Modellen oder Generativen Sprachmodellen.

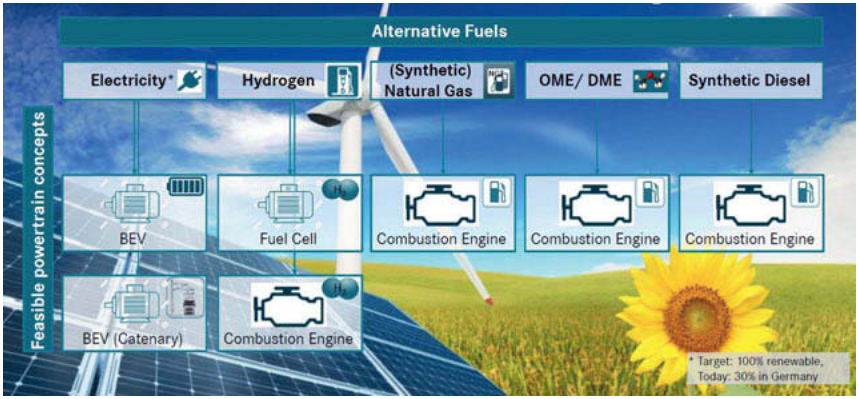


Fig. 2: Alternative powertrain concepts for HD trucks

Figure 3 shows a comparison of energy densities of possible alternative fuels.

For a HD LH specific range weight and volume of current batteries are too high to package enough batteries on a tractor or rigid.

A potential candidate for zero emission vehicle in the HD LH segment is Hydrogen. Considering zero emission potential and generation of fuels with usage of Hydrogen, fuel cell powered trucks will be the most promising solution for HD LH segment.

https://doi.org/10.51202/9783181023549 - Generiert durch IP 216.73.216.36, am 19.01.2026, 02:19:31. © Urheberrechtlich geschützter Inhalt. Ohne gesonderte Erlaubnis ist jede urheberrechtliche Nutzung untersagt, insbesondere die Nutzung des Inhalts im Zusammenhang mit, für oder in KI-Systemen, KI-Modellen oder Generativen Sprachmodellen.

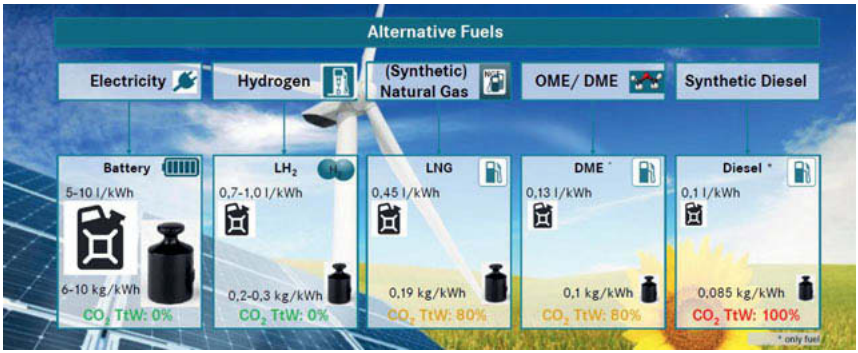


Fig. 3: Comparison of energy densities

Another option is the Catenary HD LH application, for which tests are planned in Germany (Route 1 on A5, Route 2 on A1 and Route 3 on B462) within a collaborative project of Sweden and Germany. Daimler Trucks sees more potential in battery and hydrogen electrified trucks than catenary trucks because the built-up and service of the infrastructure for catenary trucks is linked to high costs.

Built-up of a charging (Battery electric vehicles (BEV)) infrastructure and a tank (Fuel cell electric vehicles (FCEV)) infrastructure is way easier to perform than the built-up of a catenary infrastructure because the catenary has to be built-up on every single street throughout Germany/Europe.

https://doi.org/10.51202/9783181023549 - Generiert durch IP 216.73.216.36, am 19.01.2026, 02:19:31. © Urheberrechtlich geschützter Inhalt. Ohne gesonderte Erlaubnis ist jede urheberrechtliche Nutzung untersagt, insbesondere die Nutzung des Inhalts im Zusammenhang mit, für oder in KI-Systemen, KI-Modellen oder Generativen Sprachmodellen.

Hydrogen as feasible option for ZEV HDT

Today's hydrogen economy is producing 30 Mio. Tons H_2 per year.

The requirements to run all HD LH trucks worldwide with Hydrogen would be approx. 210 Mio. Tons of H_2 per year and 7.000 TWh per year. For Germany approx. 6 Mio. Tons of H_2 per year and 200 TWh per year are necessary to secure the upcoming H_2 demand for trucks.

To cover the worldwide consumption of Hydrogen (210 Mio tons Hydrogen equal 7.000 TWh per year) a solar space with a square length of 136.900 km^2 (for example in the outback of Australia) would be needed.

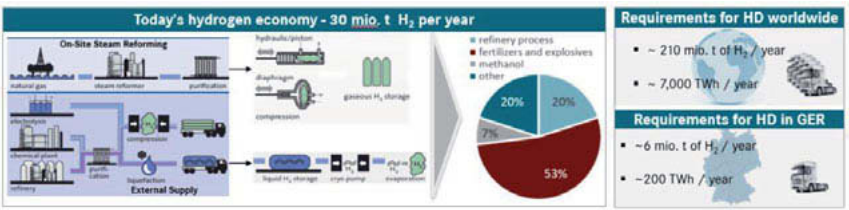


Fig. 4: Economy and Requirements of Hydrogen

A first Hydrogen production plant on industrial scale is worked out for a 400 MW plant with 176 electrolysers and 4.000 plants worldwide (approx. 100 for Germany).

Other Industry branches are pushing for usage of H_2, where the transportation segment can profit.

https://doi.org/10.51202/9783181023549 - Generiert durch IP 216.73.216.36, am 19.01.2026, 02:19:31. © Urheberrechtlich geschützter Inhalt. Ohne gesonderte Erlaubnis ist jede urheberrechtliche Nutzung untersagt, insbesondere die Nutzung des Inhalts im Zusammenhang mit, für oder in KI-Systemen, KI-Modellen oder Generativen Sprachmodellen.

First it is important enabling the renewable energy system with large-scale renewables integration and power generation as well as distribution of energy across sectors and regions, then decarbonizing end uses like transportation, e.g. train industry, like the hydrogen train from Alstom. Starting point therefore is right now.

H2 infrastructure will be build up stepwise and to be cost-efficient.

Conclusion for Truck Zero Emission Technology

Summarizing all aspects, which has been shown here, regarding Zero emission vehicles it can be concluded that for applications with limited ranges and energy needs, it is easier and cheaper to use battery electric vehicles (Passenger car, Van, Light/Medium Duty Trucks).
Fuel cells with hydrogen are the better solution for applications that require higher ranges and energy requirements and where payloads play a role (Heavy and Medium Duty Trucks).

https://doi.org/10.51202/9783181023549 - Generiert durch IP 216.73.216.36, am 19.01.2026, 02:19:31. © Urheberrechtlich geschützter Inhalt. Ohne gesonderte Erlaubnis ist jede urheberrechtliche Nutzung untersagt, insbesondere die Nutzung des Inhalts im Zusammenhang mit, für oder in KI-Systemen, KI-Modellen oder Generativen Sprachmodellen.

Sources:

- Daimler AG, Internal Documents

- Pictures and Figures from Daimler AG

- Shell Wasserstoffstudie 2017,
  https://www.shell.de/medien/shell-publikationen/shell-hydrogen-study.html

- Catenary field test from German Government,
  http://www.bmub.bund.de/fileadmin/Daten_BMU/Download_PDF/Verkehr/feldversuche_o_lkw_bf.PDF

https://doi.org/10.51202/9783181023549 - Generiert durch IP 216.73.216.36, am 19.01.2026, 02:19:31. © Urheberrechtlich geschützter Inhalt. Ohne gesonderte Erlaubnis ist jede urheberrechtliche Nutzung untersagt, insbesondere die Nutzung des Inhalts im Zusammenhang mit, für oder in KI-Systemen, KI-Modellen oder Generativen Sprachmodellen.

Electric driveline adaptation from passenger-car application to Light & Medium Truck application

A competitive, efficient, compact and light solution

Dr. Eng. **Thomas Basbous,** Valeo, Cergy, France;
Eng. **Jerrome Mortal**, Valeo, Saint-Quentin Fallavier, France

INTRODUCTION

With around 60% of urban population by 2030 [Frost and Sullivan], urban air pollution is one of the most challenges facing the world, not only for greenhouse gas emissions, but also for health damaging pollutants, namely NOx, Particle, HC and CO. This will heavily impact the transportation sector as one of the biggest contributors to urban pollution. Regions, countries and cities are looking for options to improve air quality in their communities through electrification. Whilst emission standards at a national level drive much of the move to electrification, an add-on factor is what local authorities are doing to strengthen further the pollution and noise constraints [https://www.interactanalysis.com/electric-commercial-truck-market]. The so called “diesel gate” that occurred in 2015 has increased public awareness about diesel engines real emissions and generated pressure to ban diesel vehicles. Megacities like London, Paris and Shanghai down to smaller, regional urban areas are looking to ban the diesel-fueled and even the combustion vehicles from their roads within the next five to ten years. Not only passenger cars have to comply with these restrictions, but also commercial vehicles while these have a very high diesel take rate.

On the other hand, the proliferation of e-commerce with a share of e-retail sales booming from 7% in 2015 to more than 25% by 2025 [3], results in a dramatic increase of the number of parcels delivered worldwide. For instance in 2014, 45 billion parcels were delivered, while this number has increased to 65 billion in 2016 and is expected to reach 100 billion in 2020 [source: e-delivery.net]. Consequently, more and more delivery trucks will be needed, but these will have to be electric as cities are not likely to give them any exemption.

However, regulation is not the only driver to trucks electrification, economics are also a part of the decision making process of fleet owners. The TCO (Total Cost of Ownership) is what drives

https://doi.org/10.51202/9783181023549 - Generiert durch IP 216.73.216.36, am 19.01.2026, 02:19:31. © Urheberrechtlich geschützter Inhalt. Ohne gesonderte Erlaubnis ist jede urheberrechtliche Nutzung untersagt, insbesondere die Nutzung des Inhalts im Zusammenhang mit, für oder in KI-Systemen, KI-Modellen oder Generativen Sprachmodellen.

the fleet operators. In spite of electric trucks being more expensive to purchase than diesel ones the lower operating cost due to cheaper energy cost and maintenance makes, for some specific usages, a positive business case. For example, an urban delivery electric truck could reach, provided an adequate battery sizing, a payback of 3 years versus a diesel one today. Furthermore, the price gap between diesel and electric is decreasing quickly due to fast drop of batteries to around 100 € per kWh by 2025 which will bring the payback time down to less than 2 years. This will boost the adoption of EV trucks even in the areas that have low or no regulatory push towards electrification.

We have seen in the recent years accelerated announcements of electric truck launches, going further towards higher weight categories as seen in Fig. 1.

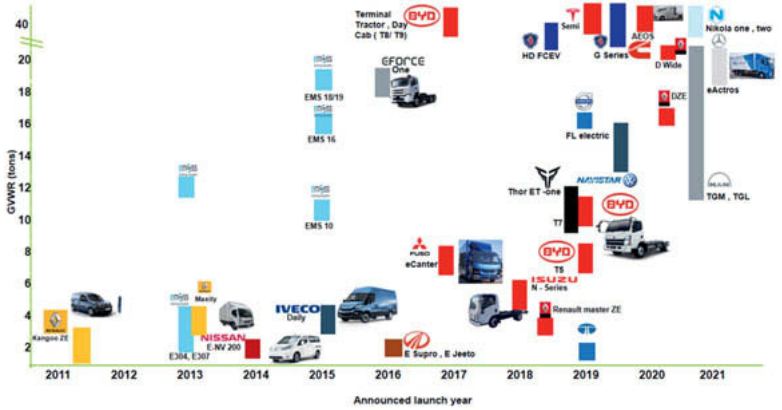


Fig. 1: Electric truck announced launches (not exhaustive list)

Based on these facts, Valeo estimates the market of electric trucks worldwide to around 4 million units per year by 2030, i.e. ~25% of total truck market, excluding autonomous droids. The truck makers that will succeed the BEV market introduction are those who will offer the most accessible electric trucks in order to shorten the payback time to their customers, or customer's customers, i.e. the fleet operators.

Carrying-over technologies from high-volume production passenger cars is one way to achieve these cost targets, as opposed to developing dedicated truck products that would be automatically less competitive due to lower scale effect. The carry-over is never straightforward though

https://doi.org/10.51202/9783181023549 - Generiert durch IP 216.73.216.36, am 19.01.2026, 02:19:31. © Urheberrechtlich geschützter Inhalt. Ohne gesonderte Erlaubnis ist jede urheberrechtliche Nutzung untersagt, insbesondere die Nutzung des Inhalts im Zusammenhang mit, für oder in KI-Systemen, KI-Modellen oder Generativen Sprachmodellen.

since the requirements of trucks are very different from those of passenger cars, especially in terms of performance, durability and driving pattern. This paper shows an adaptation of a passenger car electric drive to such specific requirements of a light/medium truck and illustrates the positive impact of doing so in terms of cost saving, weight reduction, and efficiency improvement.

TARGET TRUCK USED FOR THIS DEMONSTRATION

For this exercise, we have considered a medium truck having the characteristics expressed in Fig. 2:

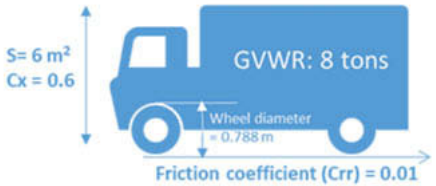


Fig. 2: Truck characteristics used for this study

The total losses (L) due to friction and aerodynamics, that characterize this truck are expressed as: $F = 784.8 + 0.1 \times V + 0.1667 \times V^2$, Where V is the speed in km/h and L is the losses in N.

As a base performance for this truck, we have considered the following:

- Maximum speed with full load:
  - 3% slope: 90 km/h
  - 8% slope: 50 km/h
- Acceleration at full load at 0% slope:
  - 0-50 km/h: < 10 sec
  - 0-90 km/h:< 30 sec

SIMULATION MODEL AND DRIVING CYCLE

The simulation model used for this study, illustrated in Fig. 4, was developed with AMESim using 0-D/1-D components. It comprises sub-models representing the vehicle, the electric drive (motor, inverter and reducer) performance and efficiency, the battery (a 300 kWh battery has been computed), and a PID controller to follow the driving pattern to be studied.

https://doi.org/10.51202/9783181023549 - Generiert durch IP 216.73.216.36, am 19.01.2026, 02:19:31. © Urheberrechtlich geschützter Inhalt. Ohne gesonderte Erlaubnis ist jede urheberrechtliche Nutzung untersagt, insbesondere die Nutzung des Inhalts im Zusammenhang mit, für oder in KI-Systemen, KI-Modellen oder Generativen Sprachmodellen.

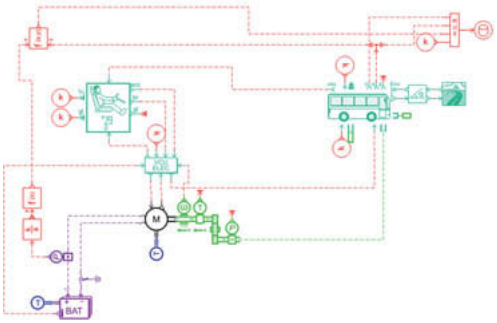


Fig. 4: Functional representation of the AMESim model used for this study

The model has been used to evaluate the performance and the electric consumption on an urban delivery cycle (from VECTO), as shown in Fig. 5.

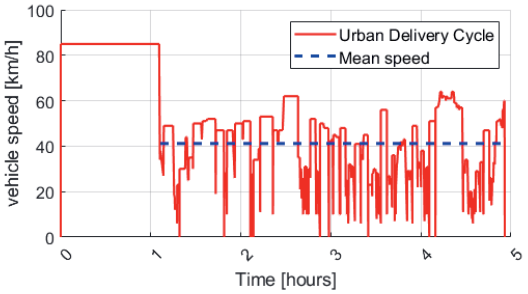


Fig. 5: Urban delivery cycle (VECTO)

COMPARING PASS-CAR MOTOR AND TRUCK DEDICATED TYPICAL MOTOR

When looking at the market power range as a function of the weight class (Fig. 6), we can see that an average 8 tons truck has a permanent power of around 120 kW.

https://doi.org/10.51202/9783181023549 - Generiert durch IP 216.73.216.36, am 19.01.2026, 02:19:31. © Urheberrechtlich geschützter Inhalt. Ohne gesonderte Erlaubnis ist jede urheberrechtliche Nutzung untersagt, insbesondere die Nutzung des Inhalts im Zusammenhang mit, für oder in KI-Systemen, KI-Modellen oder Generativen Sprachmodellen.

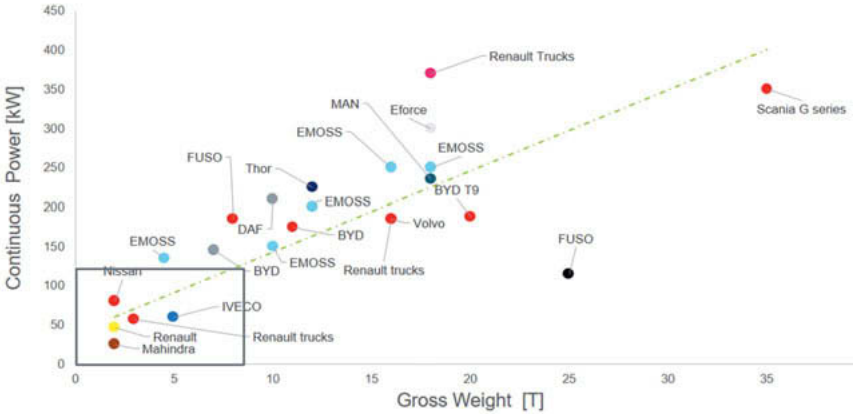


Fig. 6: Permanent Power as a function of Truck GVWR as seen in the market (not exhaustive list)

This choice is confirmed by simulation for top speed achievable at different slopes. As shown in Fig. 7, a ~115 kW motor allows a maximum speed of 90 km/h until 3% slope and 50 km/h until 8% slope as expressed in Paragraph 2.

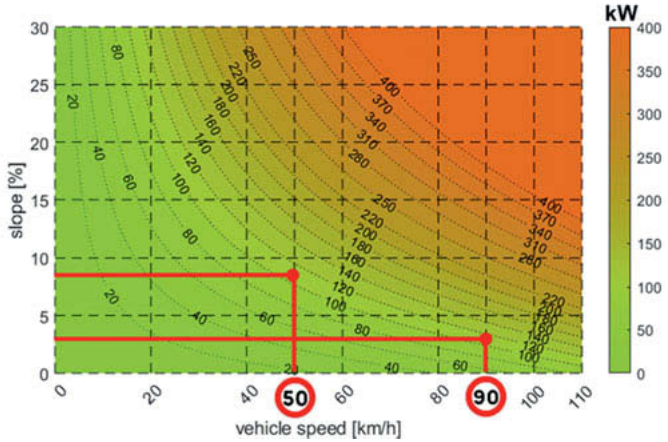


Fig. 7: Power required as a function of vehicle speed and slope for the 8-ton truck

https://doi.org/10.51202/9783161023549 - Generiert durch IP 216.73.216.36, am 19.01.2026, 02:19:31. © Urheberrechtlich geschützter Inhalt. Ohne gesonderte Erlaubnis ist jede urheberrechtliche Nutzung untersagt, insbesondere die Nutzung des Inhalts im Zusammenhang mit, für oder in KI-Systemen, KI-Modellen oder Generativen Sprachmodellen.

A current motor as seen in the market for such a medium trucks is a 115 kW continuous low-speed (~2500 RPM) high-torque (~3000 N.m) permanent magnet motor, with deported/stand-alone inverter as shown in Fig. 8. The base speed (maximum power reached) is around 700 RPM. Conversely, a typical passenger-car electric drive as proposed by Valeo is a 118 kW continuous, high-speed (~16000 RPM) permanent magnet motor with integrated inverter and reducer as shown in Fig. 9. The base speed is around 3200 RPM.



Fig. 8: Current truck low-speed high-torque motor and inverter 115 kW



Fig. 9: Valeo passenger-car high-speed integrated electric drive 118 kW

The Fig. 10 illustrates the continuous and peak performance of both motors as a function of the rotational speed.

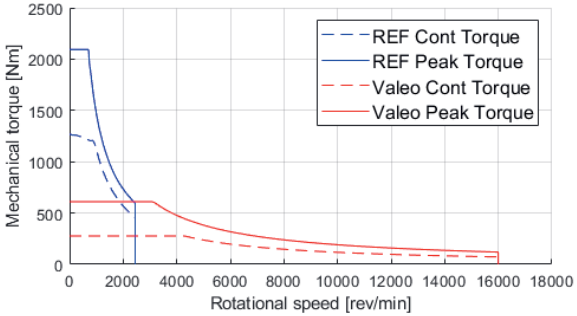


Fig. 10: Performance comparison between low-speed motor (REF) and Valeo high speed-motor

https://doi.org/10.51202/9783181023549 - Generiert durch IP 216.73.216.36, am 19.01.2026, 02:19:31. © Urheberrechtlich geschützter Inhalt. Ohne gesonderte Erlaubnis ist jede urheberrechtliche Nutzung untersagt, insbesondere die Nutzung des Inhalts im Zusammenhang mit, für oder in KI-Systemen, KI-Modellen oder Generativen Sprachmodellen.

The problem to solve in this paper is to compare both solutions above in terms of performance, electric consumption and weight on a typical urban delivery application.

Simulation results

1. Matching the right gear ratio

Assuming a single gear, the optimal ratio has to consider the best compromise between performance, gradability and efficiency. For this exercise, Valeo has used losses maps measured on its high speed eMotor, and on one competitor's low-speed motor (REF). For the low speed eMotor. The ratio offering best consumption on cycle is a ratio of 2.6, as shown in Fig. 11.

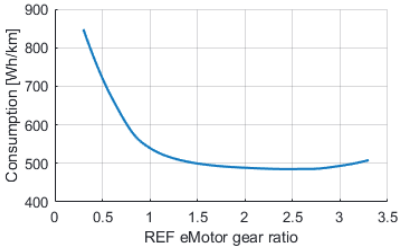


Fig. 11: Consumption with low-speed motor (REF) depending on Gear ratio

As for the high-speed eMotor, we have chosen a reducer ratio of 12 in order to match the same maximum speed with the Valeo eMotor, as illustrated in Fig. 12 (see continuous power curves).

https://doi.org/10.51202/9783181023549 - Generiert durch IP 216.73.216.36, am 19.01.2026, 02:19:31. © Urheberrechtlich geschützter Inhalt. Ohne gesonderte Erlaubnis ist jede urheberrechtliche Nutzung untersagt, insbesondere die Nutzung des Inhalts im Zusammenhang mit, für oder in KI-Systemen, KI-Modellen oder Generativen Sprachmodellen.

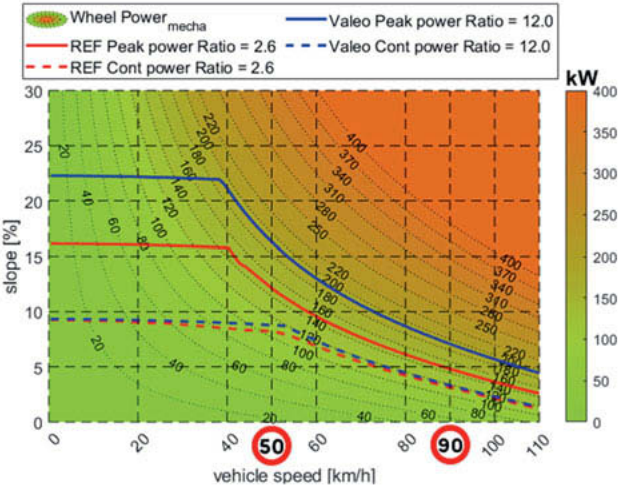


Fig. 12: Performance MAP with REF eMotor (ratio 2.6) and Valeo eMotor (ratio 12)

2. Comparing other features:

Table 1 below compares the behavior improvement that can be expected by using Valeo high-speed eMotor rather than a low-speed one. The first benefit in terms of acceleration potential is significant (less 2.4 seconds to reach 50 km/h, and less 6.2 seconds to reach 90 km/h at 0% slope). This is due to the fact that peak to continuous power ratio power ratio is around 1.3 for the low-speed motor and about 1.6 for the high-speed motor (limited by software with possibility to extend up-to 2.5 depending on application).

Also, the high-speed e-drive can bring an improvement of ~5% in terms of average efficiency on cycle which translates into around 22 Wh/km less electric consumption. To explain this improvement, we have plotted in Fig.s 13 and 14 the operating points on the efficiency MAPs of each eMotor with the selected reducer.

https://doi.org/10.51202/9783181023549 - Generiert durch IP 216.73.216.36, am 19.01.2026, 02:19:31. © Urheberrechtlich geschützter Inhalt. Ohne gesonderte Erlaubnis ist jede urheberrechtliche Nutzung untersagt, insbesondere die Nutzung des Inhalts im Zusammenhang mit, für oder in KI-Systemen, KI-Modellen oder Generativen Sprachmodellen.

Table 1: Comparison of behavior on vehicle cycle, between low-speed motor (REF) and high-speed (VALEO) motor

	Low-speed eMotor *REF*	High-speed eMotor *VALEO*
Cost	REF	Significant cost saving *More than 50% expected (indicative, not contractual)*
0-50 km/h *at 0% slope*	9.4 s	7 s
0-90 km/h *at 0% slope*	24.8 s	18 s
Avg. efficiency *on urban cycle*	80.2 %	85.8 %
Elec. consumption *on urban cycle*	484.6 Wh/km	462.3 Wh/km
Weight *including reducer*	~350 kg	~150 kg

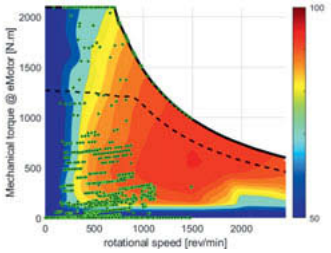


Fig. 13: Operating points plot on efficiency MAP with REF eMotor and a reducer ratio of 2.6.

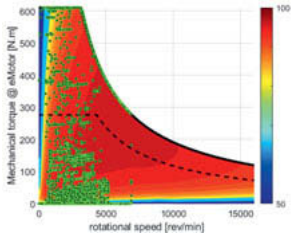


Fig. 14: Operating points plot on efficiency MAP with VALEO eMotor and a reducer ratio of 12.

Finally, having a higher power density, it brings weight reduction of around 200 kg, which could be translated directly into higher load capacity which is valuable for the fleet operators.

https://doi.org/10.51202/9783181023549 - Generiert durch IP 216.73.216.36, am 19.01.2026, 02:19:31. © Urheberrechtlich geschützter Inhalt. Ohne gesonderte Erlaubnis ist jede urheberrechtliche Nutzung untersagt, insbesondere die Nutzung des Inhalts im Zusammenhang mit, für oder in KI-Systemen, KI-Modellen oder Generativen Sprachmodellen.

Conclusion

Valeo believes passenger-car eMotors should find their path into light and medium truck market as they will bring scale economy as well as improved performance. This carry-over can be achieved provided some specific adaptations such as increased voltage (800V instead of 400V), extended CAN communication protocol (J1939) and increased board-net supply voltage (24V instead of 12V), and also dedicated transmission with a single gear reducer as demonstrated in this article, or even a multi-speed gearbox for further improvement in terms of efficiency and gradeability. Valeo Special Vehicles Application (SVA) team is already investigating several concepts and is willing to support truck customers who wish to explore such opportunities.

Sources

[1] Frost & Sullivan
[2] Interact Analysis
[3] E-Marketer
[4] e-Delivery

https://doi.org/10.51202/9783181023549 - Generiert durch IP 216.73.216.36, am 19.01.2026, 02:19:31. © Urheberrechtlich geschützter Inhalt. Ohne gesonderte Erlaubnis ist jede urheberrechtliche Nutzung untersagt, insbesondere die Nutzung des Inhalts im Zusammenhang mit, für oder in KI-Systemen, KI-Modellen oder Generativen Sprachmodellen.

Dedicated Hybrid Transmission for Commercial Vehicle Applications

Mechanical layout, system analysis and simulation of a dedicated hybrid transmission for commercial vehicles

Dr. **Christoph Schoerghuber**, Dipl.-Ing. **Ingomar Müller**,
Ing. **Herbert Wiener**,
AVL Commercial Driveline & Tractor Engineering GmbH, Steyr, Austria

Zusammenfassung

In diesem Beitrag wird ein neues dediziertes Hybridgetriebe für verschiedene Nutzfahrzeuganwendungen vorgestellt, welches die AVL im Rahmen eines Kundenprojekts entwickelt. Dieses neue Hybridgetriebe nutzt als Antriebsquellen einen Verbrennungsmotor und zwei hochintegrierte, hochdrehende E-Motoren. Mit Hilfe eines ausgeklügelten, aber vergleichsweise einfachen Getriebekonzeptes werden hohe Wirkungsgrade bei geringen Produktkosten und einfache Anpassbarkeit an unterschiedliche Nutzfahrzeuganwendungen erreicht. Die hohe Effizienz des Antriebsstrangs und das perfekt abgestimmte Zusammenspiel der drei Antriebssysteme sorgen für hohe Kraftstoffeinsparungen, ohne dabei auf höchsten Fahrkomfort verzichten zu müssen. Insbesondere bei dynamischen Lastprofilen, wie beispielsweise üblich bei Stadtbusanwendungen, wird dies über einen Betriebsmodus mit elektrischer Leistungsverzweigung und einem reinen elektrischen Betrieb erreicht. Darüber hinaus ermöglicht ein Overdrive-Betriebsmodus eine effiziente Fahrweise bei konstanten und hohen Fahrzeuggeschwindigkeiten auf der Autobahn. Dabei wird über einen mechanischen Leistungsfluss mit parallel hybrid Funktion ein hoher Getriebewirkungsgrad und ein optimaler Betriebsbereich für den Verbrennungsmotor sichergestellt. Der optimale Betriebsmodus wird auf Basis einer ausgereiften Hybridstrategie gewählt. Basierend auf den Ergebnissen einer Fahrzeugsimulation kann mit dem neuen dedizierten Hybridgetriebe eine deutliche Kraftstoffeinsparung gegenüber modernen, konventionellen Nutzfahrzeugantrieben erreicht werden.

Abstract

This Paper presents a new dedicated hybrid transmission for various commercial vehicle applications, which AVL is developing as part of a customer project. This new hybrid transmission uses a combustion engine and two highly integrated, high-speed e-motors as its drive sources. With the help of a sophisticated but comparatively simple transmission con-

https://doi.org/10.51202/9783181023549 - Generiert durch IP 216.73.216.36, am 19.01.2026, 02:19:31. © Urheberrechtlich geschützter Inhalt. Ohne gesonderte Erlaubnis ist jede urheberrechtliche Nutzung untersagt, insbesondere die Nutzung des Inhalts im Zusammenhang mit, für oder in KI-Systemen, KI-Modellen oder Generativen Sprachmodellen.

cept, high efficiencies, low product costs and a transmission design which is adaptable to different commercial vehicle applications are achieved. The high efficiency of the drive train and the perfectly coordinated interaction of the three drive systems ensure high fuel savings without compromising drivability and driving comfort. This is achieved, in particular with dynamic load profiles as they are usual for city bus applications, via power-split and pure electric vehicle operation mode. In addition, an overdrive operating mode enables efficient driving at constant and high vehicle velocities for highway applications. Thereby, an optimum operating range for the combustion engine is achieved via a mechanical power flow and parallel hybrid function. The operating mode is selected on the basis of a well-developed hybrid strategy. Based on the results of a vehicle simulation, the new dedicated hybrid transmission can achieve significant fuel savings compared to modern, conventional commercial vehicle powertrains.

1. Introduction

The development of highly efficient powertrains for commercial vehicles is subject of ongoing research and development activities all over the world. However, achieving highest efficiencies together with low product costs as well as adaptability to different applications usually leads to conflicting targets. Exactly these conflicts must be solved within state-of-the-art powertrain development to meet today's customer expectations and legislation requirements. Therefore, a dedicated hybrid transmission (DHT) with tailored functions for commercial vehicle applications is definitely a solution. The development of different DHT's was performed already by a couple of passenger car manufacturers in the past. First and foremost, Toyota with their Prius has brought a DHT into series production since 1997 and sold quite well. A good overview of different DHT concepts and descriptions can be found in [1] and [2]. There are also some DHT's already developed in the field of commercial vehicles, see [3], [4].

Reduction of fuel consumption is typically the main driver for hybridization of commercial vehicle powertrains. Hybrid powertrains typically have their biggest benefit in terms of fuel consumption when driving on highly dynamic driving cycles with dynamic speed and/or load profiles including high recuperation potential. This is typical for applications like city buses, regional delivery trucks or garbage trucks. But next to the achievement of highest fuel consumption benefits, one of the main targets for the development of a dedicated hybrid transmission (DHT) is the flexibility to apply the transmission to different commercial vehicle applications. Target applications for the DHT development are city buses but also highway coaches and medium duty trucks such as concrete mixers, cranes or delivery trucks. Thus, the powertrain must achieve high system efficiencies for city as well as overland and high-

https://doi.org/10.51202/9783181023549 - Generiert durch IP 216.73.216.36, am 19.01.2026, 02:19:31. © Urheberrechtlich geschützter Inhalt. Ohne gesonderte Erlaubnis ist jede urheberrechtliche Nutzung untersagt, insbesondere die Nutzung des Inhalts im Zusammenhang mit, für oder in KI-Systemen, KI-Modellen oder Generativen Sprachmodellen.

way driving and must be adaptable to different maximum vehicle velocity and gradeability requirements. Also, a PTO unit is required for some of these applications.

Within a customer project, AVL has developed a new DHT which exactly fulfills these demands. Via electric power split and further transmission modes this new DHT enables lowest fuel consumption for all target applications. Due to its modular and comparatively simple design the transmission can be adapted to the different commercial vehicle applications with moderate product costs.

The paper is organized as follows: First the mechanical layout of the DHT is presented and a system as well as a power flow description are given. Afterwards, the properties of the mechanical layout in relation to the different applications and a mathematical model of the DHT is presented. Finally, the sizing of the transmission is described, and simulation results of a fuel consumption analysis for a city bus application are shown.

2. Mechanical layout of the DHT

In Fig. 1 the layout of the new developed DHT including all required powertrain elements is depicted.

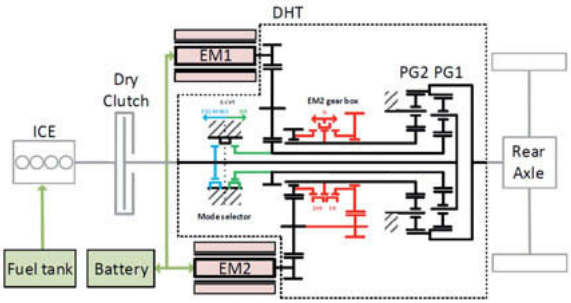


Fig. 1: Schematic layout of a powertrain including the new developed DHT (limp-home and PTO unit not depicted)

The powertrain consists of the engine (ICE), 2 electric motors (e-motors), a battery, a dry clutch, the DHT and the rear axle. The DHT consists of the input shafts for the e-motors and the engine, gear boxes for speed reduction of the e-motors, a mode selector unit (green and blue parts in Fig. 1), 2 planetary gear sets including (hollow) shafts, the transmission output shaft and a limp-home and PTO unit (not depicted in Fig. 1).

https://doi.org/10.51202/9783181023549 - Generiert durch IP 216.73.216.36, am 19.01.2026, 02:19:31. © Urheberrechtlich geschützter Inhalt. Ohne gesonderte Erlaubnis ist jede urheberrechtliche Nutzung untersagt, insbesondere die Nutzung des Inhalts im Zusammenhang mit, für oder in KI-Systemen, KI-Modellen oder Generativen Sprachmodellen.

The e-motor 1 (EM1) is connected to the sun gear of planetary gear set 1 (PG1). In between there is a gear box with fixed gear ratio. The ICE is connected to the dry clutch which then is connected to the carrier of PG1. The e-motor 2 (EM2) is connected to the sun gear of planetary gear set 2 (PG2). In between there is a shift able gear box with 2 gears as well as a neutral position (red parts in Fig. 1). The carrier of planetary gear set 2 (PG2) is fixed to the housing of the DHT. The rings of both planetary gear sets are connected to the transmission output shaft. Thus, there is a fixed ratio between sun and ring gear at PG2, and EM2 is always connected to the transmission output shaft with since a gear is engaged at EM2 gear box. PG1 is acting as power split or summation device enabling a CVT operation of the transmission (CVT-mode). Furthermore, the transmission consists of a mode selector unit where either the sun gear or the carrier of PG1 can be blocked to the housing. Thus, additionally to the CVT-mode a pure electric vehicle mode (EV-mode) and a direct ICE mode with overdrive gear ratio (OD-mode) can be selected. If there is a failure within the high voltage system, the vehicle can be operated via engine only utilizing the limp-home function (not depicted in Fig. 1). The dry clutch is used to cut the engine from the powertrain and to perform vehicle start-up in limp-home mode.

3. DHT power flow

For better understanding the operation modes of the transmission, the power flow within the powertrain for the different DHT modes is described below. Furthermore, the resulting degrees of freedom for the hybrid controller for optimization of system efficiency are explained.

3.1. Power flow in EV-mode

If EV-mode is selected the carrier of PG1 and thus the engine shaft is blocked to the housing of the DHT. As with PG2, PG1 has a fixed ratio between sun and ring gear in EV-mode and thus EM1 is always connected to the transmission output shaft with a fixed gear ratio. Because of limited battery capacity the EV-mode is typically used for low vehicle velocities. The power flow in EV-mode is depicted in Fig. 2.

https://doi.org/10.51202/9783181023549 - Generiert durch IP 216.73.216.36, am 19.01.2026, 02:19:31. © Urheberrechtlich geschützter Inhalt. Ohne gesonderte Erlaubnis ist jede urheberrechtliche Nutzung untersagt, insbesondere die Nutzung des Inhalts im Zusammenhang mit, für oder in KI-Systemen, KI-Modellen oder Generativen Sprachmodellen.

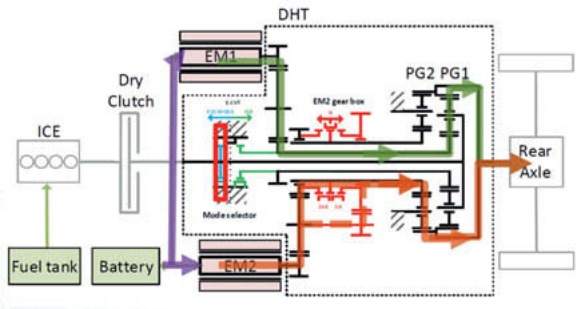


Fig. 2: Power flow in EV-mode for vehicle propulsion.

The energy for vehicle propulsion is provided by the battery to both e-motors. The requested transmission output power in general is provided by both e-motors as sum of the individual power values for vehicle propulsion and recuperation. Both e-motor speeds are depending on the vehicle velocity. The required transmission output torque generated by both e-motors can be shifted between EM1 and EM2. Thus, there is one degree of freedom for the hybrid controller for the optimization of system efficiency.

3.2. Power flow in OD-mode

If the sun gear of PG1 is connected to the housing, EM1 input shaft is blocked and thus EM1 is not used. In this so-called OD-mode there is a fixed ratio between ICE and transmission output shaft with an overdrive gear ratio. Due to the resulting engine operating points at small engine speed regions the OD-mode is enabling high system efficiencies for highway driving. If EM2 gear box is switched to neutral the vehicle is driven by the ICE only. If a gear is selected at EM2 gear box, additionally EM2 is connected to the transmission output shaft and the powertrain is operated as parallel hybrid. The OD-mode can only be used for higher vehicle velocities because the engine's idle speed is limiting the minimum vehicle velocity. The power flow in OD-mode is depicted in Fig. 3.

https://doi.org/10.51202/9783181023549 - Generiert durch IP 216.73.216.36, am 19.01.2026, 02:19:31. © Urheberrechtlich geschützter Inhalt. Ohne gesonderte Erlaubnis ist jede urheberrechtliche Nutzung untersagt, insbesondere die Nutzung des Inhalts im Zusammenhang mit, für oder in KI-Systemen, KI-Modellen oder Generativen Sprachmodellen.

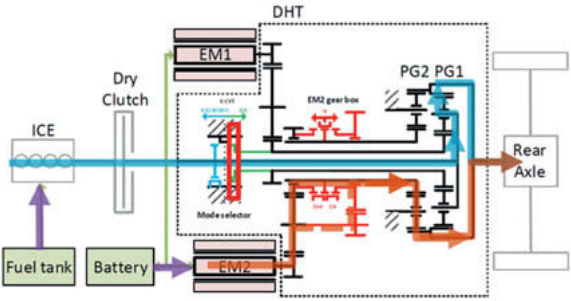


Fig. 3: power flow in OD-mode for vehicle propulsion.

The energy for the vehicle drive is supplied by the ICE and, if operated in a parallel hybrid, also by EM2. The requested transmission output power in general is provided by the ICE and EM2 as sum of the individual power values. Thus, this mode can be used for both vehicle propulsion and recuperation. Both ICE and EM2 speeds are depending on the vehicle velocity. The required transmission output torque can be shifted between ICE and EM2 resulting in typical parallel hybrid operations, i.e. load point shifting or boosting. Thus, there is one degree of freedom for the hybrid controller for the optimization of system efficiency.

.

3.3. Power flow in CVT-mode

If neither PG1 sun gear nor PG1 carrier are blocked, the DHT is operated in CVT-mode as continuous variable transmission, i.e. the ratio between transmission output and transmission input shaft can be adjusted between 0 and a certain finite value continuously. The speeds of EM1, ICE and transmission output shaft are coupled via the so called “Willi’s equation” defined for planetary gear sets, see e.g. [5]. If e.g. ICE speed is defined, EM1 speed is derived as function of transmission output shaft speed. Thus, the selection of ICE speed is representing the first degree of freedom in CVT-mode. The power flow in CVT-mode is depicted in Fig. 4.

https://doi.org/10.51202/9783181023549 - Generiert durch IP 216.73.216.36, am 19.01.2026, 02:19:31. © Urheberrechtlich geschützter Inhalt. Ohne gesonderte Erlaubnis ist jede urheberrechtliche Nutzung untersagt, insbesondere die Nutzung des Inhalts im Zusammenhang mit, für oder in KI-Systemen, KI-Modellen oder Generativen Sprachmodellen.

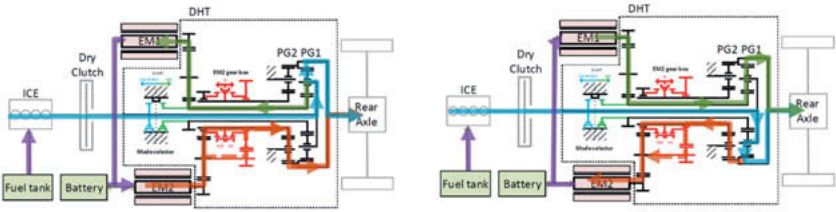


Fig. 4: Power flow in CVT-mode for vehicle propulsion. Left hand side: Possible power flow for low velocities. Right hand side: Possible power flow for high velocities.

The requested transmission output power is provided by the ICE, EM1 and EM2 as sum of the individual power values. Because of the power split operation, the power value of one e-motor can also be negative during vehicle acceleration, as it is depicted in Fig. 4. Thereby, PG1 is acting as power split and summation device. The required energy for vehicle propulsion is supplied from the fuel tank to the ICE and from the battery to the e-motors. The power split between ICE power and power from battery can be freely selected within certain limits. Thus, it can be defined whether the battery is charged, discharged or even operated in neutral mode which represents the second degree of freedom in CVT-mode for the hybrid controller for optimization of system efficiency.

4. Properties of the mechanical layout of the DHT

The mechanical layout of the DHT including the arrangement of the planetary gear sets, the shift able gear box at EM2 and the 2 e-motors are chosen very carefully to achieve positive properties for the transmission. The e-motors including inverters have the highest impact on product costs compared to the rest of the DHT (see Fig. 5). Some existing DHT layouts for commercial vehicle applications are using e-motors which are arranged concentrically to the main (hollow) shafts of the transmission resulting in big diameters for the stators and rotors of the e-motors [3], [4]. Because the centrifugal force is increasing with increasing diameter the maximum speeds of such big e-motors are limited to relatively small values. In general, if standard bearings can be used the costs of e-motors are decreasing with decreasing the geometrical size and thus the mass of active mechanical parts such as magnetic materials, iron lamination and copper. Via using high-speed e-motors (with reduced maximum torque and size) same power values compared to low-speed e-motors with high torque and geometrical sizing are possible. To enable the usage of high-speed e-motors they are arranged in parallel to the main (hollow) shafts of the transmission. For the DHT development, perma-

https://doi.org/10.51202/9783181023549 - Generiert durch IP 216.73.216.36, am 19.01.2026, 02:19:31. © Urheberrechtlich geschützter Inhalt. Ohne gesonderte Erlaubnis ist jede urheberrechtliche Nutzung untersagt, insbesondere die Nutzung des Inhalts im Zusammenhang mit, für oder in KI-Systemen, KI-Modellen oder Generativen Sprachmodellen.

nent magnet synchronous motors (PSM) with a maximum speed of 15000 rpm are selected, resulting in low product costs and good packaging properties.

Via the shift able gear box at EM2 with two gears the transmission output torque is significantly increased during vehicle start-ups. Thus, it is possible to reduce the power of EM2 and to achieve main vehicle requirements, e.g. maximum vehicle velocity and gradeability, with identical e-motor power for EM1 and EM2. Product costs can be further reduced because of a duplicated number of identical e-motor quantity. An estimated cost comparison between a DHT without and with shift able gear box at EM2 is depicted in Fig. 5.

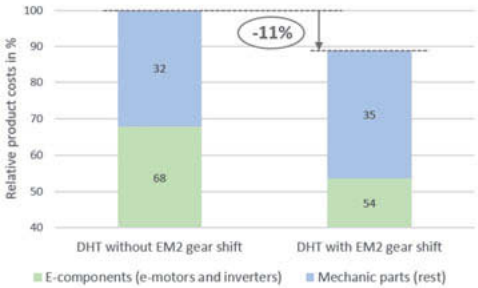


Fig. 5: Estimated cost comparison between a DHT without and with shift able gear box at EM2.

Thereby the costs of electric components including e-motors and inverters as well as all other mechanic parts are considered separately. As can be seen the electric components result in about two thirds of the overall product cost and therefore it is important to reduce the power of the electric components if possible. With the help of a shift able gear box at EM2 with two gears the overall product cost can be decreased by about 11%.

Within EM2 gear box, dog clutches are used as shifting elements again positively influencing product costs compared to using e.g. synchronizations. Despite there is an interruption of power flow from EM2 during shifting there is no complete torque interruption at the transmission output shaft because of the ongoing continuous torque flow via ICE and/or EM1.

The arrangement of PG1 within the DHT is resulting in an overdrive gear ratio between ICE and transmission output shaft if OD-mode is selected. Thus, if the vehicle is driving with high velocities, the engine is operated in the optimum speed range with low fuel consumption.

Via adaption of e-motor and ICE power as well as rear axle ratio it is possible to adapt the powertrain to different maximum velocity and gradeability requirements for different applications without changing the mechanic design of the DHT. If higher e-motor power is required

https://doi.org/10.51202/9783181023549 - Generiert durch IP 216.73.216.36, am 19.01.2026, 02:19:31. © Urheberrechtlich geschützter Inhalt. Ohne gesonderte Erlaubnis ist jede urheberrechtliche Nutzung untersagt, insbesondere die Nutzung des Inhalts im Zusammenhang mit, für oder in KI-Systemen, KI-Modellen oder Generativen Sprachmodellen.

an e-motor with same diameter but increased length is selected. The e-motors are arranged as separate modules close to the gearbox housing, which allows simple replacement of the e-motors. Since both e-motors are arranged on engine side of the gearbox, disassembly is further simplified. Thus, the idea is to develop a transmission family where the same mechanical DHT with same gear ratios is used for all applications, but ICE, e-motors and rear axle are adapted for achieving the different vehicle requirements.

Depending on the application the OD-mode and the PTO function are not required and therefore designed optionally. E.g. for a city bus application, the transmission is equipped with EV- and CVT-mode only. Since the city bus is not driving on the highway the OD-mode is not applied. Furthermore, no PTO function is used for a city bus application. For a highway coach the DHT is equipped with all DHT-modes but without PTO function. Some truck applications require PTO function as well as typically all DHT-modes. In further consequence the paper focuses on the city bus application.

5. Mathematical model of the DHT for a city bus application

Due to the complexity of the DHT a mathematical model is used to do the sizing of the transmission and the powertrain elements as well as to perform a fuel consumption analysis. For this purpose, the DHT model is based on stationary relations of torque, speed and power, hence no transient behaviour of the rotating shafts and the mode selection of the DHT are modelled. Each transmission mode is modelled separately, and the different model descriptions are switched depending on the desired DHT mode. The basis for modelling of the DHT are the torque and speed relations of a planetary gear set, see [5].

The model of the DHT for a city bus application consists of the mathematical equations for EV- and CVT-mode which are described separately. The transmission scheme for deriving torque, speed and power relations in EV-mode is depicted in Fig. 6.

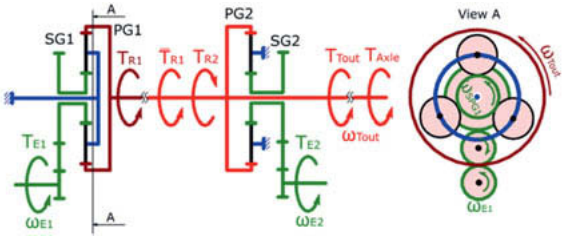


Fig. 6: Torque and speed scheme of the DHT in EV-mode

https://doi.org/10.51202/9783181023549 - Generiert durch IP 216.73.216.36, am 19.01.2026, 02:19:31. © Urheberrechtlich geschützter Inhalt. Ohne gesonderte Erlaubnis ist jede urheberrechtliche Nutzung untersagt, insbesondere die Nutzung des Inhalts im Zusammenhang mit, für oder in KI-Systemen, KI-Modellen oder Generativen Sprachmodellen.

In EV-mode both planetary gear sets are operated with fixed carriers. Thus, the ring torques T_{R1} and T_{R2} are calculated via

$$T_{R1} = -T_{E1} i_{SG1} \eta_{SG1} i_{PG1} \eta_{PG1}$$

and

$$T_{R2} = -T_{E2} i_{SG2} \eta_{SG2} i_{PG2} \eta_{PG2}$$

where T_{E1} and T_{E2} are the mechanical e-motor torques, i_{SG1} and i_{SG2} are the spur gear ratios of the e-motor gear boxes (i_{SG2} is changing according to the selected gear), η_{SG1} and η_{SG2} are the efficiencies of the spur gears, i_{PG1} and i_{PG2} are the fixed carrier ratios of the planetary gear sets and η_{PG1} and η_{PG2} are the fixed carrier efficiencies of the planetary gear sets. The transmission output torque T_{Tout} is calculated as sum of the ring torques

$$T_{Tout} = T_{R1} + T_{R2} = -T_{E1} i_{SG1} \eta_{SG1} i_{PG1} \eta_{PG1} - T_{E2} i_{SG2} \eta_{SG2} i_{PG2} \eta_{PG2}$$

The speeds of the e-motors ω_{E1} and ω_{E2} are calculated based on Willi's equation [5] with zero carrier speed via

$$\omega_{E1} = i_{SG1} i_{PG1} \omega_{Tout}$$

and

$$\omega_{E2} = i_{SG2} i_{PG2} \omega_{Tout}$$

where ω_{Tout} is the speed of the transmission output shaft. The required battery power is calculated as negative sum of both electrical e-motor power values

$$P_{Bat} = -P_{E1} - P_{E2} = -T_{E1} \omega_{E1} \eta_{E1} - T_{E2} \omega_{E2} \eta_{E2}$$

Where η_{E1} and η_{E2} are the efficiency values of the e-motors.

The transmission scheme for deriving torque, speed and power relations in CVT-mode is depicted in Fig. 7.

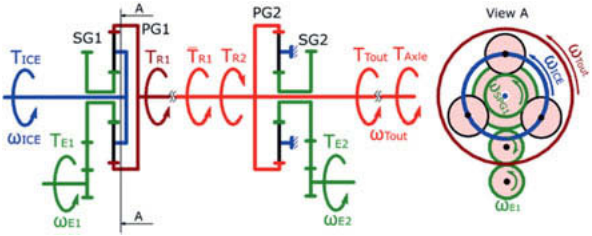


Fig. 7: Torque and speed scheme of the DHT in CVT-mode

https://doi.org/10.51202/9783181023549 - Generiert durch IP 216.73.216.36, am 19.01.2026, 02:19:31. © Urheberrechtlich geschützter Inhalt. Ohne gesonderte Erlaubnis ist jede urheberrechtliche Nutzung untersagt, insbesondere die Nutzung des Inhalts im Zusammenhang mit, für oder in KI-Systemen, KI-Modellen oder Generativen Sprachmodellen.

Planetary gear set 2 is operated with fixed carrier. Thus, the ring torque T_{R2} is calculated via

$$T_{R2} = -T_{E2} i_{SG2} \eta_{SG2} i_{PG2} \eta_{PG2}$$

Planetary gear set 1 is operated as power split device. Based on the basic torque relations of a planetary gear set, see e.g. [5], the ring torque T_{R1} can be calculated via

$$T_{R1} = -T_{E1} i_{SG1} \eta_{SG1} i_{PG1} \eta_{PG1}$$

The required ICE torque to fulfil static determination at PG1 results as

$$T_{ICE} = -T_{E1} i_{SG1} \eta_{SG1} (i_{PG1} \eta_{PG1} - 1)$$

The transmission output torque T_{Tout} is calculated as sum of the ring torques

$$T_{Tout} = T_{R1} + T_{R2} = -T_{E1} i_{SG1} \eta_{SG1} i_{PG1} \eta_{PG1} - T_{E2} i_{SG2} \eta_{SG2} i_{PG2} \eta_{PG2}$$

The speeds of ICE and EM1 are coupled based on Willi's equation. If the speed of ICE is selected in a way to operate the engine at e.g. best fuel consumption point, the EM1 speed ω_{E1} is calculated as function of ω_{ICE} and speed of transmission output shaft ω_{Tout} via

$$\omega_{E1} = i_{SG1} [i_{PG1} \omega_{Tout} + \omega_{ICE} (1 - i_{PG1})]$$

The speed of EM2 ω_{E2} is calculated via

$$\omega_{E2} = i_{SG2} i_{PG2} \omega_{Tout}$$

The required battery power is calculated as negative sum of both electrical e-motor power values

$$P_{Bat} = -P_{E1} - P_{E2} = -T_{E1} \omega_{E1} \eta_{E1} - T_{E2} \omega_{E2} \eta_{E2}$$

Depending on the desired DHT mode the appropriate model descriptions are used. To use this model e.g. for a fuel consumption analysis, a controller is required to define output torque and power, the desired mode, the desired E2 gear, as well as to define the degrees of freedom of the transmission for the different modes.

6. Sizing of the DHT and all powertrain components

The sizing of the powertrain components ICE, EM1 and EM2 as well as the gear ratios of the transmission and rear axle is done via calculations based on the presented model equations. The sizing of the battery is mainly depending on the drive cycle of the vehicle and thus is performed separately with the help of vehicle simulations. As the mechanical part of the DHT including all gear ratios is designed identical as transmission family for each application and some of the parameters are acting coupled, the sizing is performed within several loops to achieve all vehicle requirements for the different applications. Consequently, only the main relations for sizing of the components are described in this section.

First the basic considerations for sizing of the mechanic DHT including the gear ratios of PG1 and PG2 as well as the gear ratios of the e-motor gear boxes are described. Afterwards the selection of ICE- and e-motor-power as well as the rear axle ratio is described. The fixed

https://doi.org/10.51202/9783181023549 - Generiert durch IP 216.73.216.36, am 19.01.2026, 02:19:31. © Urheberrechtlich geschützter Inhalt. Ohne gesonderte Erlaubnis ist jede urheberrechtliche Nutzung untersagt, insbesondere die Nutzung des Inhalts im Zusammenhang mit, für oder in KI-Systemen, KI-Modellen oder Generativen Sprachmodellen.

carrier ratio of PG1 together with the rear axle ratio are defining the operating points of the engine in OD-mode. Thus, the fixed carrier ratio of PG1 is selected in a way to operate the engine speed at best fuel consumption region for the most common vehicle velocity when driving on the highway. Due to the blocked carrier at PG2, there is a fixed ratio between sun and ring gear and thus EM2 is always connected to the transmission output shaft with a fixed overall gear ratio depending on the selected gear at EM2 gear box. The overall gear ratio with engaged gear 2 at EM2 gear box is selected in a way to not exceed the maximum speed of EM2 when driving at maximum vehicle velocity. Mechanical limitations of the gears are defining the split between fixed carrier ratio of PG2 and the gear ratio of gear 2 at EM2 gear box. The gear ratio of gear 1 at EM2 gear box is selected based on gradeability requirements for vehicle start-up. In EV-mode as with EM2, EM1 is always connected to the transmission output shaft with a fixed gear ratio due to the blocked carrier of PG1. Thus, the ratio of EM1 gear box is selected to not exceed maximum speed of EM1 when driving at highest vehicle velocity required in EV-mode.
The maximum torque of EM2 and thus also the maximum power as well as the rear axle ratio are defined via gradeability requirements during vehicle start-up. Therefore, a traction force diagram in EV- and CVT-mode is considered. In OD-mode the DHT is mainly operated via the ICE at high vehicle velocities. If the vehicle is driving on the highway the average traction power must be provided by the engine due to limited battery capacity. Thus, maximum vehicle velocity as well as maximum gradeability at maximum velocity in OD-mode must be achieved via ICE operation. The resulting driving resistance at maximum vehicle velocity is defining the required ICE power. The sizing of EM1 power is done via consideration of CVT-mode. To operate the ICE with full torque during vehicle start-up in CVT-mode the EM1 must provide a defined counter torque at relatively high EM1 speed (see EM1 operating point at zero vehicle velocity in Fig. 8). The resulting operating point of EM1 is defining the maximum EM1 power.

Exemplarily, the sizing and the resulting traction torque, speed and power characteristics of the DHT for a city bus application are considered. The main vehicle requirements for the city bus application are summarized in table 1.

https://doi.org/10.51202/9783181023549 - Generiert durch IP 216.73.216.36, am 19.01.2026, 02:19:31. © Urheberrechtlich geschützter Inhalt. Ohne gesonderte Erlaubnis ist jede urheberrechtliche Nutzung untersagt, insbesondere die Nutzung des Inhalts im Zusammenhang mit, für oder in KI-Systemen, KI-Modellen oder Generativen Sprachmodellen.

Table 1: Main vehicle requirements for a city bus application used for sizing of the DHT and the powertrain components.

Parameter	**Value**
Gross vehicle weight	18000 kg
Maximum vehicle velocity	70 kph
Maximum e-motor speed	15000 rpm
Maximum gradeability at 15 kph	15 %
Maximum gradeability at 70 kph	3,1 %

The sizing of the powertrain for achieving these requirements is done based on the described way. In Fig. 8 the torque, speed and power characteristics of a city bus application equipped with the DHT are depicted. Thereby, the power values are positive if the power is going into the considered system and negative if the power is going out of the system. No losses are considered in the calculations used for generating these diagrams.

https://doi.org/10.51202/9783181023549 - Generiert durch IP 216.73.216.36, am 19.01.2026, 02:19:31. © Urheberrechtlich geschützter Inhalt. Ohne gesonderte Erlaubnis ist jede urheberrechtliche Nutzung untersagt, insbesondere die Nutzung des Inhalts im Zusammenhang mit, für oder in KI-Systemen, KI-Modellen oder Generativen Sprachmodellen.

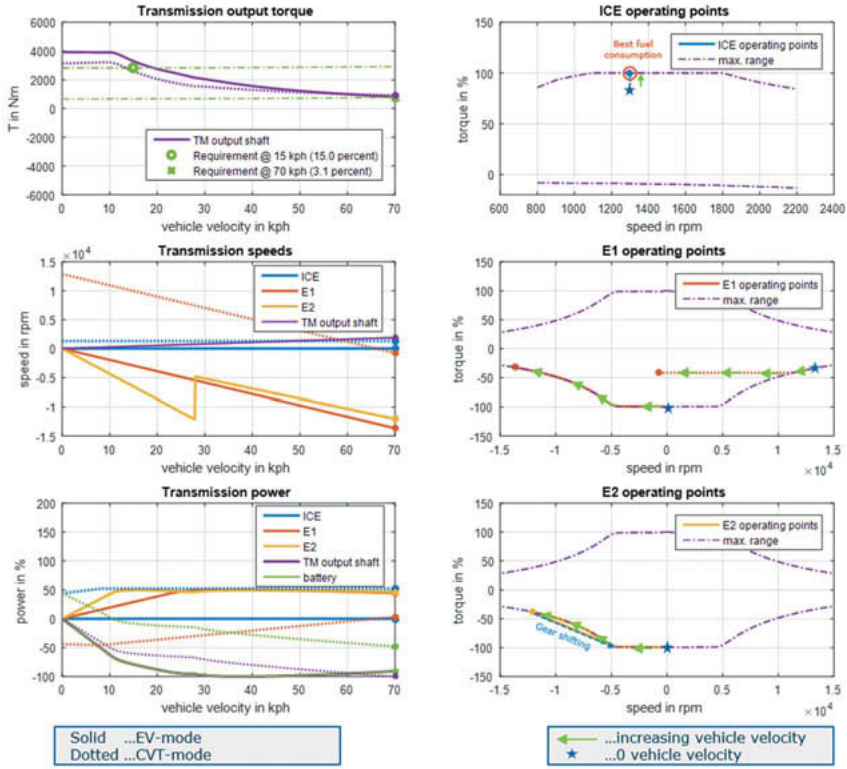


Fig. 8: Torque, speed and power characteristics resulting in maximum transmission output torque in EV- and CVT-mode for a city bus application.

The torque, speed and power diagrams (Fig. 8, left hand side) are based on the vehicle velocity from 0 to 70 kph. The operating point diagrams (Fig. 8, right hand side) show the behaviour of ICE and e-motors for achieving the presented output power and torque. Thereby, the solid lines represent the calculated values for achieving highest transmission output torque in EV-mode and the dotted lines for achieving highest transmission output torque when ICE is operated mainly at best point in CVT-mode.

As can be seen in the “Transmission output torque” diagram the resulting maximum output torque in EV-mode is higher compared to CVT-mode. The required transmission output torque at low vehicle velocity (15 kph) is achieved in EV-mode only whereas at maximum

https://doi.org/10.51202/9783181023549 - Generiert durch IP 216.73.216.36, am 19.01.2026, 02:19:31. © Urheberrechtlich geschützter Inhalt. Ohne gesonderte Erlaubnis ist jede urheberrechtliche Nutzung untersagt, insbesondere die Nutzung des Inhalts im Zusammenhang mit, für oder in KI-Systemen, KI-Modellen oder Generativen Sprachmodellen.

vehicle velocity is achieved for both EV- and CVT mode. The speeds of EM1 and EM2 are for each mode within its limits of 15000 rpm. There are different reasons for not achieving the limits exactly, e.g. the limits must be fulfilled for each application considering overspeed and reverse driving, too. In EV-mode the speeds of both e-motors are proportional to vehicle velocity (except during gear shifting of EM2 gear box). In CVT-mode the speed of EM2 is identical as in EV-mode. The speed of EM1 is relatively high for vehicle start-up and decreases with decreasing vehicle velocity to negative values. In EV-mode the power values of both e-motors are positive and battery power is negative as usual for pure electric vehicles. The resulting transmission output power equals the battery power as no losses are considered in Fig. 8. In CVT-mode the EM1 power is starting at high negative values resulting in generator operation. Same as in EV-mode the EM2 operated as motor with positive power. At zero vehicle velocity the mechanical EM2 power is zero even if operated at maximum torque. Thus, the ICE is providing exactly the EM1 power at zero vehicle velocity and the battery is charged resulting in positive battery power values during vehicle start-up. For increasing vehicle velocities, the EM1 power is decreasing to slightly negative values. Hence, also battery power is changing from positive to negative values resulting in battery discharging for higher vehicle velocities (>10 kph). The resulting transmission output power is decreasing to negative values where the absolute power value for maximum vehicle velocity is higher compared to the absolute power value achieved in EV-mode.

As can be seen in the operating diagrams both e-motors are operated at their torque limits in EV-mode. In CVT-mode EM2 is still operated at its torque limit, whereas EM1 is only operated at its torque limit for small vehicle velocities. For higher vehicle velocities EM1 is operated with constant torque (and decreasing speed) in CVT-mode. The ICE is operated at its torque limit only for higher vehicle velocities. For small vehicle velocities the maximum torque is not achieved. The reason therefore is the static torque relation at PG1 which must be fulfilled, i.e. either EM1 or ICE is limiting the transmitted torque to the ring of PG1. For small vehicle velocities EM1 is limiting the torque of ICE and for high velocities ICE is limiting the torque of EM1. The ICE speed is chosen for achieving best fuel consumption.

7. Fuel consumption simulation of a city bus with DHT

For estimation of fuel consumption benefits which are achievable with the DHT an overall vehicle simulation of an 18-ton city bus is performed. The vehicle simulation is done with AVL Cruise based on longitudinal dynamics of the vehicle. The powertrain model is split into engine (including 0,5 kW constant mechanic auxiliaries), DHT (including e-motors), battery (including battery management and 1 kW constant electric auxiliaries) and rear axle. For vehi-

https://doi.org/10.51202/9783181023549 - Generiert durch IP 216.73.216.36, am 19.01.2026, 02:19:31. © Urheberrechtlich geschützter Inhalt. Ohne gesonderte Erlaubnis ist jede urheberrechtliche Nutzung untersagt, insbesondere die Nutzung des Inhalts im Zusammenhang mit, für oder in KI-Systemen, KI-Modellen oder Generativen Sprachmodellen.

cle simulation of a powertrain with DHT, additionally to the mechanical parts of the powertrain also the transmission and hybrid controller must be considered. The DHT and the required controllers are modelled in Simulink and implemented as dynamic link libraries into the powertrain model in AVL Cruise. In Fig. 9 the controlled DHT model as it is implemented in Simulink is depicted.

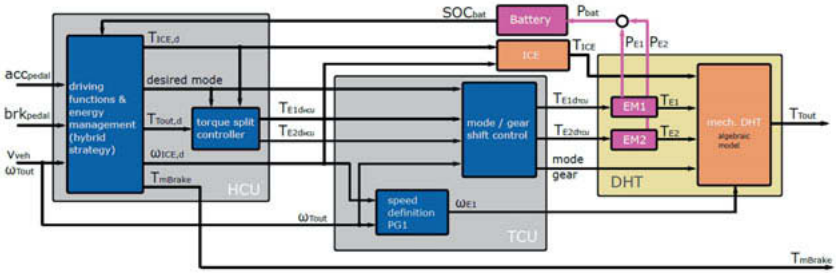


Fig. 9: Controlled DHT model including HCU and TCU for simulation purpose.

As DHT model the mathematic equations presented for EV- and CVT-mode are used and selected according to the desired DHT mode. The controller is split into hybrid control unit (HCU) and transmission control unit (TCU). The main inputs into the HCU are the driver demands, i.e. acceleration and brake pedal as well as the measured signals vehicle velocity and speed of transmission output shaft. Within the HCU the driving functions and the energy management as well as the torque split controller are implemented. For achieving highest powertrain efficiency, within the energy management the ICE operating point is selected, and the transmission mode is switched between EV- and CVT-mode based on e.g. battery state of charge. The torque split controller distributes the torque between EM1 and EM2 in a way to achieve the desired transmission output torque with the desired ICE torque and to fulfil the static relations at PG1 under consideration of actuator limitation. Due to the reason of using a simplified DHT model with switching algebraic torque, speed and power equations based on the desired DHT mode the TCU functions are simplified, too. In the TCU part the selection of the E2 gear depending on transmission output shaft speed is performed. Furthermore, the speed of EM1 is defined depending on the desired ICE and current output shaft speed according to the PG1 speed relation.

To perform a fuel consumption comparison an additional simulation of the same city bus with identical engine (including mechanic auxiliaries) and rear axle but with automatic transmis-

https://doi.org/10.51202/9783181023549 - Generiert durch IP 216.73.216.36, am 19.01.2026, 02:19:31. © Urheberrechtlich geschützter Inhalt. Ohne gesonderte Erlaubnis ist jede urheberrechtliche Nutzung untersagt, insbesondere die Nutzung des Inhalts im Zusammenhang mit, für oder in KI-Systemen, KI-Modellen oder Generativen Sprachmodellen.

sion (AT) and torque converter is performed. Thereby, a state-of-the-art AT transmission, a torque converter with lock-up clutch and an engine with start-stop function are modelled. Both Cruise vehicle models can be seen in Fig. 10.

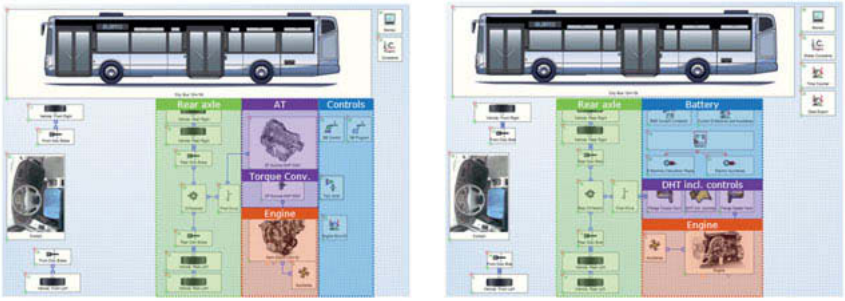


Fig. 10: AVL Cruise vehicle simulation of a city bus. Left hand side: Conventional city bus powertrain with torque converter and AT; Right hand side: city bus powertrain with DHT.

For fuel consumption comparison, both vehicles are simulated driving on the Chinese city bus cycle (CCBC). The resulting engine operating points for both powertrain models are depicted in Fig. 11.

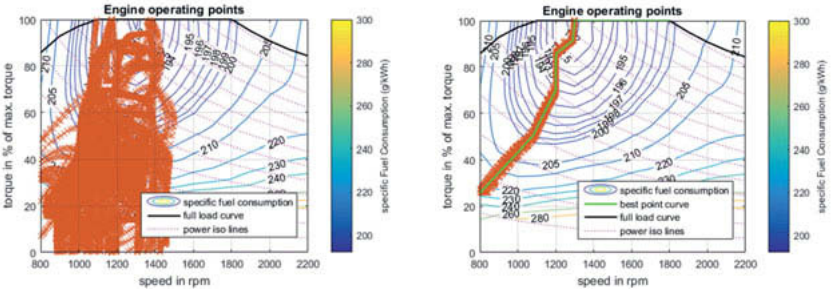


Fig. 11: Engine operating points of a city bus vehicle simulation driving on CCBC drive cycle. Left hand side: City bus powertrain with torque converter and AT; Right hand side: City bus powertrain with DHT.

https://doi.org/10.51202/9783181023549 - Generiert durch IP 216.73.216.36, am 19.01.2026, 02:19:31. © Urheberrechtlich geschützter Inhalt. Ohne gesonderte Erlaubnis ist jede urheberrechtliche Nutzung untersagt, insbesondere die Nutzung des Inhalts im Zusammenhang mit, für oder in KI-Systemen, KI-Modellen oder Generativen Sprachmodellen.

As can be seen the engine operating points of the conventional powertrain are located in a big region below about 1500 rpm. Whereas the engine operating points of the powertrain with DHT (in CVT-mode) are located at the best point curve, connecting the best fuel consumption points depending on engine power. The resulting fuel consumption benefit is depicted in Fig. 12.

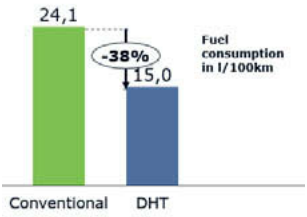


Fig. 12: Simulated fuel consumption results of an 18t city bus driving on CCBC drive cycle with conventional and DHT powertrain.

The fuel consumption results of the powertrain with DHT are based on a balanced state of charge of the battery where battery energy at beginning and end of the simulation is identical. With the DHT equipped powertrain a fuel consumption benefit of about 38% can be achieved. This benefit is a result of operating the engine at best point curve, recuperation of braking power, engine start-stop and driving purely electrically utilizing the recuperated battery power.

8. Summary and conclusion

A new hybrid powertrain based on a dedicated hybrid transmission (DHT) for commercial vehicle applications was presented in this paper. The described powertrain consists of an engine, two e-motors, a battery, the mechanic DHT and the rear axle. Based on a mathematical model the calculations for sizing of the gear ratios and the powertrain components (ICE, e-motors, rear axle) as well as a fuel consumption analysis are performed. The simulation results show the big benefits in terms of fuel consumption compared to conventional state-of-the-art powertrains, i.e. the fuel consumption can be reduced by 38% with the help of the DHT. The carefully developed gear arrangement results in many positive characteristics for different commercial vehicle applications. The mechanical layout is comparatively simple and offers the use of high-speed e-motors, resulting in optimum packaging and low product costs. With the help of a mode selector unit the new developed DHT combines and improves the

https://doi.org/10.51202/9783181023549 - Generiert durch IP 216.73.216.36, am 19.01.2026, 02:19:31. © Urheberrechtlich geschützter Inhalt. Ohne gesonderte Erlaubnis ist jede urheberrechtliche Nutzung untersagt, insbesondere die Nutzung des Inhalts im Zusammenhang mit, für oder in KI-Systemen, KI-Modellen oder Generativen Sprachmodellen.

advantages of serial and parallel hybrids as well as pure electric vehicle powertrains. Via a power split operation mode with continuous variable transmission function (CVT-mode) the engine can be operated at best fuel consumption point. In addition, an engine direct drive mode with overdrive gear ratio and parallel hybrid function (OD-mode) allows the engine to operate in areas with highest efficiency, resulting in lowest fuel consumption even when driving on highway cycles. Furthermore, an electric vehicle mode (EV-mode) is used to drive with zero emission and to utilize the recuperated battery power. The DHT can be equipped with a power take-off (PTO) and limp-home module. The PTO can be operated mechanical and purely electrical which is quite interesting for a lot of commercial vehicle applications. The limp-home function ensures a safe trip even in electric failure mode of the DHT. AVL is already industrializing such DHT's for its truck & bus customers. The first start of production is scheduled within the next 18 months.

[1] Fischer, R.: Dedicated Hybrid Transmissions (DHT). A New Category of Transmissions. 14th International CTI Symposium. Berlin. December 2015

[2] Nisewanger, J.: Revenge of the Two-Mode-Hybrid. Auto alternatives for the 21st century. November 5. 2015

[3] EP-0967102A2

[4] CN-203766482U

[5] Müller, H.: Die Umlaufgetriebe. Springer 1998

https://doi.org/10.51202/9783181023549 - Generiert durch IP 216.73.216.36, am 19.01.2026, 02:19:31. © Urheberrechtlich geschützter Inhalt. Ohne gesonderte Erlaubnis ist jede urheberrechtliche Nutzung untersagt, insbesondere die Nutzung des Inhalts im Zusammenhang mit, für oder in KI-Systemen, KI-Modellen oder Generativen Sprachmodellen.

https://doi.org/10.51202/9783181023549 - Generiert durch IP 216.73.216.36, am 19.01.2026, 02:19:31. © Urheberrechtlich geschützter Inhalt. Ohne gesonderte Erlaubnis ist jede urheberrechtliche Nutzung untersagt, insbesondere die Nutzung des Inhalts im Zusammenhang mit, für oder in KI-Systemen, KI-Modellen oder Generativen Sprachmodellen.

Gas powered Heavy Duty vehicles from Scania: Current program and future potential

Dr. **Mikael Lindström**, Scania CV, Södertälje, Sweden



Abstract

Scania has a long history of producing gas powered heavy vehicles. Scania sees a growing demand for such vehicles and sees biogas operation as an important part of reducing CO2-emissions. Currently Scania produces four different gas engine versions for vehicle use. These are Euro 6 engines in the power range 280 – 410 hp for use in trucks, buses, coaches and BRT-systems. Scania also produces gensets powered by gas engines for electricity production. Biogas is a high quality fuel which is possible to produce locally from waste products such as sewage and other waste products. This makes it possible to operate fleets of trucks and buses in a sustainable way.

https://doi.org/10.51202/9783181023549 - Generiert durch IP 216.73.216.36, am 19.01.2026, 02:19:31. © Urheberrechtlich geschützter Inhalt. Ohne gesonderte Erlaubnis ist jede urheberrechtliche Nutzung untersagt, insbesondere die Nutzung des Inhalts im Zusammenhang mit, für oder in KI-Systemen, KI-Modellen oder Generativen Sprachmodellen.

Introduction

Scania is dedicated to producing trucks and buses which are as sustainable as possible. Scania has an extensive program of alternatively fuelled vehicles, both in production and in development. This includes electric vehicles, hybrid vehicles, biodiesel, bioethanol and biogas powered vehicles.

Increasing demand

Traditionally the total amount of gas powered vehicles has been fairly small but recently there has been a rapidly growing demand for biogas powered vehicles. The driving forces includes the benefit of significant CO2-reduction when operating on biogas. Another customer benefit is the fact the a gas powered vehicle can be made to operate quieter than a corresponding diesel vehicle. All Scania gas vehicles which are currently in production have the low noice PIEK certificate which makes it legal to operate them during the night in cities and areas where that is otherwise not allowed. Night deliveries is an effective way of reducing congestion in cities, see E. Devin [1]. In most markets the price for gas fuel is also significantly lower than that of diesel and recently the gas powered vehicles has been exempt from the German road toll, the LKW-MAUT. These factors makes gas vehicle operation financially beneficial, see F.C. Barbosa. [2]

Using biogas as a fuel

Often there is a conception that biofuels are of a lesser quality than the more traditional corresponding fossil fuel. In the case of gas powered vehicles the biogas is in fact of higher quality than typical natural gas. The reason for this is that biogas is refined during the production process which gives it a high methane content. High quality biogas consists of about 98 % methane whereas typical natural gas also contains heavies hydrocarbons such as propane and butane. Methane is better suited for use in spark ignited engines since it has a higher resistance to autoignition than heavier gases and much higher than that of gasoline. This has made it possible for Scania's spark ignited gas engines to have an efficiency and low rpm torque characteristics which is similar to a diesel engine. There are many examples of cities and municipalities which operate a fleet of Scania buses and refuse collection trucks using biogas that are produced locally from waste products, thus making the operation of the fleet of vehicles sustainable.

https://doi.org/10.51202/9783181023549 - Generiert durch IP 216.73.216.36, am 19.01.2026, 02:19:31. © Urheberrechtlich geschützter Inhalt. Ohne gesonderte Erlaubnis ist jede urheberrechtliche Nutzung untersagt, insbesondere die Nutzung des Inhalts im Zusammenhang mit, für oder in KI-Systemen, KI-Modellen oder Generativen Sprachmodellen.

Historical Background

Scania has developed and manufactured gas powered internal combustion engines since the early 1980's. The first engines were the 11 litre ON11 and OL11 6-cylinder engines which were used for electricity production at off-shore oil drilling rigs. They were powered by natural gas that would otherwise have been flared off. Scania has also met an emerging market demand for heavy vehicles powered by gas. Subsequently Scania has developed and marketed six generations powered vehicle engines beginning in the early 1990's.

During the early 1990's a series of 9 and 11 litre 5- and 6-cylinder engines for use in trucks and buses were developed and marketed. Fig. 1 shows one of about 100 Scania CNG powered city buses which were delivered to Sydney, Australia in 1994, many of which are still in use.



Fig. 1: Scania CNG bus used in Sydney.

The current engine program

The previous Scania gas engines in the Eu3-5 emission ratings were lean burn combustion concepts while all previous and current Eu6 engines are stochiometric and utilizes three-way catalysts.

Currently there are four versions of Scania gas engines in production. These are the 5-cylinder OC09 engines which are available as 280, 320 and 340 hp versions and the 6-cylinder 410 hp OC13 engine. All four versions share the basic concept of combining diesel like low end torque and efficiency with Otto engine advantages such as low noise and biogas compatibility. The 5-

https://doi.org/10.51202/9783181023549 - Generiert durch IP 216.73.216.36, am 19.01.2026, 02:19:31. © Urheberrechtlich geschützter Inhalt. Ohne gesonderte Erlaubnis ist jede urheberrechtliche Nutzung untersagt, insbesondere die Nutzung des Inhalts im Zusammenhang mit, für oder in KI-Systemen, KI-Modellen oder Generativen Sprachmodellen.

cylinder OC09 engines are mostly used in buses, refuse collection and distribution trucks whereas the 6-cylinder OC13 101, (see Fig. 2 and 3) is mostly used for long haulage.

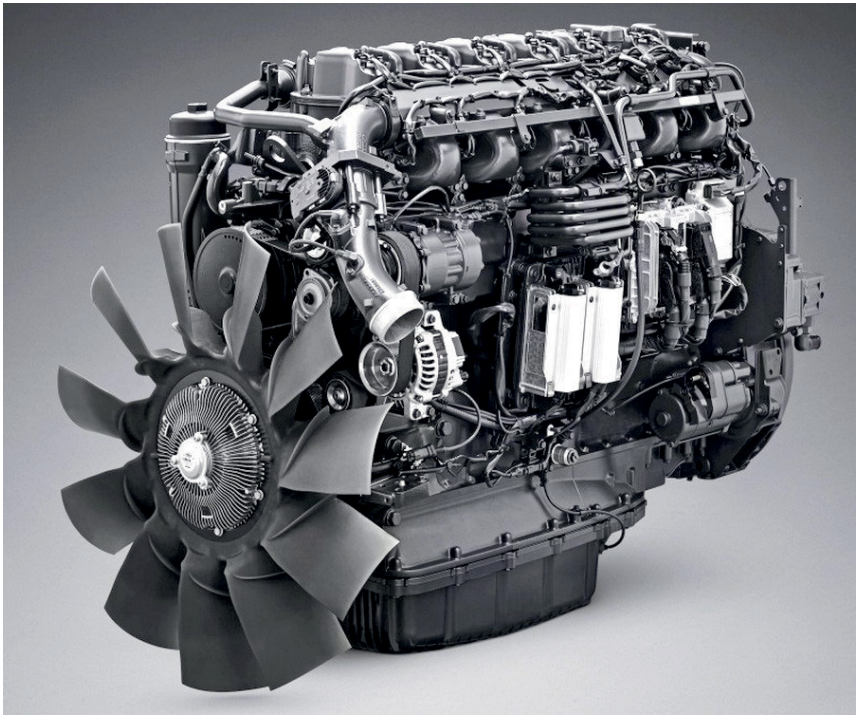


Fig. 2: Scania OC13 101 6-cylinder gas engine, cold side.

All the currently produced Scania 5- and 6-cylinder engines are spark ignited turbocharged stochiometric Euro 6 engines using a three-way catalyst. They also utilize cooled EGR as a means of reducing turbine inlet temperature and to increase part load efficiency as the EGR reduces the need for throttling and thus the pumping losses. The EGR-system can be seen on the hot side of the engine in Fig. 3.

https://doi.org/10.51202/9783181023549 - Generiert durch IP 216.73.216.36, am 19.01.2026, 02:19:31. © Urheberrechtlich geschützter Inhalt. Ohne gesonderte Erlaubnis ist jede urheberrechtliche Nutzung untersagt, insbesondere die Nutzung des Inhalts im Zusammenhang mit, für oder in KI-Systemen, KI-Modellen oder Generativen Sprachmodellen.

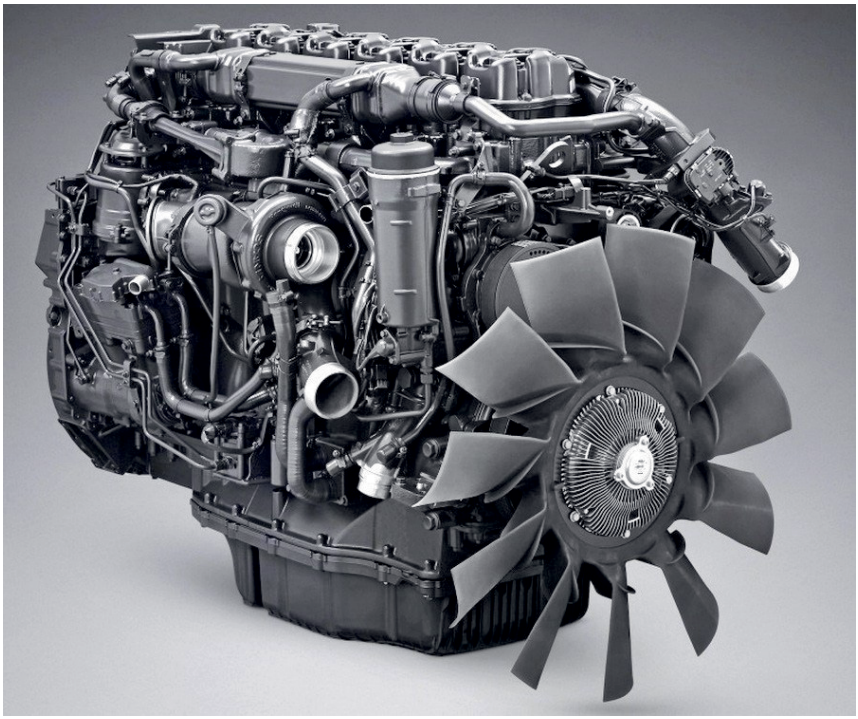


Fig. 3: Scania OC13 101 6-cylinder gas engine, hot side.

These engines can be operated using CNG, LNG or biogas without the need to modify the engine. Electronic fuel injection and lambda control using dual oxygens sensors allows the three-way catalyst to achieve emission levels which are far below the legal limits for Euro 6. Scania gas powered vehicles are available with either an automatic transmission with a torque converter or with Scania Opticruise. The Scania Opticruise is an automated mechanical gearbox with electro-hydraulic clutch control. This transmission allows the engine to operate with an optimized gear change strategy, further improving the vehicle overall efficiency.

BRT Systems

One interesting application for Scania's gas engines is in so called BRT-systems. A Bus Rapid Transfer, BRT-system offers a transportation capability similar to that of a train- or subway system at a much lower investment cost and construction time. With up to 300 passengers per bus and the possibility to use a traffic light priority system a high transportation capability is

https://doi.org/10.51202/9783181023549 - Generiert durch IP 216.73.216.36, am 19.01.2026, 02:19:31. © Urheberrechtlich geschützter Inhalt. Ohne gesonderte Erlaubnis ist jede urheberrechtliche Nutzung untersagt, insbesondere die Nutzung des Inhalts im Zusammenhang mit, für oder in KI-Systemen, KI-Modellen oder Generativen Sprachmodellen.

achieved. A BRT system can combine operation on regular roads, bus lanes and dedicated roads. They can also use platform based embarking and disembarking of passengers for time efficient station stops. Fig. 4 shows one of 740 BRT buses powered by 340 hp Scania OC09 engines that has been ordered by the city of Bogota, Colombia.



Fig. 4: A Bi-articulated BRT bus used by the city of Bogota, Colombia.

Conclusions

Scania has a long history of producing gas powered trucks and buses. As the demand for sustainable transports is increasing Scania considers vehicles powered by biogas to be an important part of the solution. A growing part of sold Scania vehicles are powered by gas, there is also a rapidly growing availability of CNG, LNG and biogas fuelling stations which makes gas vehicle operation possible in more and more areas. As gas powered vehicles can combine environmental benefits with financial benefits for its operators they are a vital part of a future sustainable transportation system.

[1] E. Devin. “Toward a certification of night delivery in urban freight transport“, ICR 2011

[2] F.C. Barbosa. “Evaluation of Biogas Use in Transit Bus Fleets”, SAE paper 2015-36-0227, 2015

https://doi.org/10.51202/9783181023549 - Generiert durch IP 216.73.216.36, am 19.01.2026, 02:19:31. © Urheberrechtlich geschützter Inhalt. Ohne gesonderte Erlaubnis ist jede urheberrechtliche Nutzung untersagt, insbesondere die Nutzung des Inhalts im Zusammenhang mit, für oder in KI-Systemen, KI-Modellen oder Generativen Sprachmodellen.

Diverse requirements, one product family

The HV Kit for LCV from MAGNA

Dipl.-Ing. **Roland Nasdal**, Getrag Ford Transmissions, Köln;
Dr. **Karl Masser**, MAGNA Engineering Center Steyr, St. Valentin, Austria

Abstract

Light commercial vehicles have a wide scope of use cases to cover: Transfer of passengers, transport of materials, box vans or parcel delivery vans. What they all have in common: In case the drivers must have unlimited access to cities, the vehicles need at least a certain level of electrification. This leads to diverse requirements concerning how much electric power needs to be installed and how much battery capacity is needed to fulfil the pure EV mode requirements.

Magna offers flexible solutions for every demand: Pure EV eDrive units with 90kW up to 280kW of power each. The combination of more than just one offers AWD function or torque vectoring if needed. Such systems can also be delivered in axle frame structures as complete “active axle”.

For the combination of uncompromised long distance fuel economy and EV mode for cities, two different kind of hybrid drive trains are offered: The rear axle eDrive unit to be combined with the untouched ICE powertrain in the front of the vehicle. This solution is easy to install and can be used as an AWD system in hybrid mode. The second solution is the fully integrated hybrid transmission 5BHT425 with an e-motor integrated in the base manual transmission. This solution offers full AT functionality with uncompromised fuel efficiency in EV mode and ICE mode. This is enabled by the two separate part transmissions for each function, which allows to set the unused part of the powertrain to fully idle. Additionally, the full automatic function allows significant fuel economy improvements in hybrid mode. This is enabled by the full automatic control over the combustion engine state and the integrated battery SOC management.

For both hybrid variants, the e-motor power can be scaled to the demand of the customer, equally the battery capacity to allow the best payload to EV range ratio.

https://doi.org/10.51202/9783181023549 - Generiert durch IP 216.73.216.36, am 19.01.2026, 02:19:31. © Urheberrechtlich geschützter Inhalt. Ohne gesonderte Erlaubnis ist jede urheberrechtliche Nutzung untersagt, insbesondere die Nutzung des Inhalts im Zusammenhang mit, für oder in KI-Systemen, KI-Modellen oder Generativen Sprachmodellen.

Future Challenges in Various Markets

Fleet Emission Targets have been reduced all over the main markets in the world. In the next years we will get even more challenging targets with further reduced CO2 Emissions. For example, current EU Proposal for 2030 is to reduce Fleet Emissions by 30%. Other main markets have similar relative targets but slightly less challenging in absolute target values. To fulfil these targets the OEMs will get under pressure.

As a consequence, powertrain electrification is growing in the near future. Traditional ICE concepts including micro-hybrids are diminished. From 2025 to 2030 Magna is estimating a significant drop in ICE Powertrains by half (from 34% to 18%) and micro-hybrid share reduces from almost half of all powertrains to a third. On the other hand mild-hybrid will drastically increase in sales volume to 41% in 2030. Completely electrified powertrains are expected to grow very fast, but will still have only a fourth in sales volume by 2030. However, Magna is focused on all these powertrain evolutions.

Extremely diverse Requirements for LCVs

LCVs are driving on highway routes, on rural construction sites and they enter cities with diesel drive-prohibition zones, e.g. for parcel delivery. LCVs can have chassis for dropsides, tippers and box vans. The customers have many different jobs: Transport of material, transfer of parcels between logistic centres, pick up travellers in the city and take them to the airport or shuttle services for a car rental station. In all regions the etelligentDrive™ of Magna offers solutions for efficient driving:

- Hybrid mode.
- Combustion engine mode with CO2-reduction.
- Full electric driving mode for diesel low emission zones.
- Various driver assistance situations like traffic jam assistance, autonomous parking.

Magna Simulation Tools

Looking at the fundamental details driving transmission efficiency we find that MT transmissions always have the best overall efficiency as only few components are contributing to losses in transmission system. These are mainly gears, bearings and splashing. Looking at DCT's efficiency, they consist of the same subsystems and additionally have the need for some actuation system resulting in only a small offset of efficiency compared to manual transmissions. Torque-Converter Automatics use the same components but in addition a power-consuming

https://doi.org/10.51202/9783181023549 - Generiert durch IP 216.73.216.36, am 19.01.2026, 02:19:31. © Urheberrechtlich geschützter Inhalt. Ohne gesonderte Erlaubnis ist jede urheberrechtliche Nutzung untersagt, insbesondere die Nutzung des Inhalts im Zusammenhang mit, für oder in KI-Systemen, KI-Modellen oder Generativen Sprachmodellen.

launch-device. And last but not least, CVT are those transmissions typically having the lowest efficiency as they require additional energy for the clamping of chain/belt.

All powertrain variants need enhanced control software, if they are combined with an electric motor to form a hybrid configuration (e.g. P0, P2, P3, P4). During the design phase, Magna has developed a Hybrid Manager together with the University of Stuttgart. This tool takes control of the torque split between ICE, EM and brake torque. The battery manager is responsible for the charge sustaining strategy during fuel efficiency drives (identical state of charge at test start and test end). Furthermore, the battery limits are monitored continuously. The software also controls the transmission output torque to avoid wheel slip (adaptive μ control for real world drive conditions), as these events are a total waste of energy.
All these tools are used to predict CO2 emissions of future hybrid powertrain variants, using the old NEDC cycle, which is still valid in China and in the new WLTP cycle:

Simulations for NEDC (B-Car, 1.0l engine, 6MTT215, 15KW)

- Base (2020): 92 g/km (B-Car 125PS, MX65)
- P0 without eclutch: 79 g/km
- P3 with eclutch and stop/start in drive mode: 72 g/km (=22% saving)

New simulations for WLTP end up in a more realistic CO2 reduction of ~9% up to 12%.

Modular Powertrain Concepts

Magna offers three modular powertrain concepts, which can be adapted to the various requirements of the different customers.

- Concept 1: ICE plus automated hybrid transmission and eDrive LOW up to 65kW
- Concept 2: Conventional drivetrain plus electric rear axle eDrive LOW up to 90kW
- Concept 3: Battery electric truck with eDrive MID on front axle up to 140kW

All concept are designed for pure eDrive, eParking, significant CO2 savings, admission to low/zero emission zones. Concept 2 additionally offers AWD driving, while Concept 3 guarantees lowest maintenance cost.

https://doi.org/10.51202/9783181023549 - Generiert durch IP 216.73.216.36, am 19.01.2026, 02:19:31. © Urheberrechtlich geschützter Inhalt. Ohne gesonderte Erlaubnis ist jede urheberrechtliche Nutzung untersagt, insbesondere die Nutzung des Inhalts im Zusammenhang mit, für oder in KI-Systemen, KI-Modellen oder Generativen Sprachmodellen.

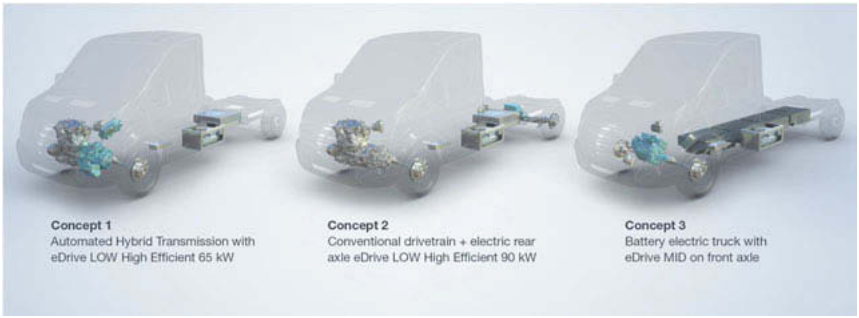


Fig. 1: Overview of electrification options; source: Magna

The newest technology is the fully scalable and customizable Hybrid powertrain based on the 5BHT425. It uses two separate part transmissions, which allows to set the unused part of the powertrain to fully idle. The 5BHT425 consists of a manual transmission based 5 speed gearset for the internal combustion engine, a 2 speed gearset for the e-machine and a coupling device to connect the e-machine with the inputshaft to allow the engine start and charge mode at vehicle standstill. In Fig.2 the powerflow through the transmission is shown for the 2nd e-drive ratio combined with the 5th speed on combustion engine side. There is no added torque other than at the differential, hence there is no limitation for the e-motor torque. The shift elements are actuated via shift drum technology as known from DCT products, the e-drive gears can be actuated independent from the ICE transmission side. Fig.2 shows a sectional view of the transmission. Due to the full AT functionality combined with dedicated gearsets for each source of torque, it offers uncompromised fuel efficiency in EV mode and ICE mode. Due to the full control of combustion engine state and the integrated battery SOC management the 5BHT425 allows significant fuel economy improvements in hybrid mode. The 2-speed e-drive gearset allows the e-machine to be connected at the entire speed range of the vehicle to enable charging during highway travel. On the other end, the vehicle is launched with the electric drive in 1st e-drive ratio, which allows pure e-

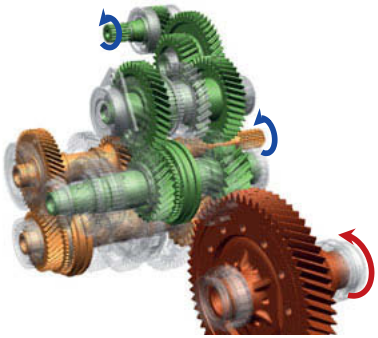


Fig. 2: Powerflow of 2nd e-speed and 5th speed for ICE in parallel; source: GETRAG Ford Transmissions GmbH

https://doi.org/10.51202/9783181023549 - Generiert durch IP 216.73.216.36, am 19.01.2026, 02:19:31. © Urheberrechtlich geschützter Inhalt. Ohne gesonderte Erlaubnis ist jede urheberrechtliche Nutzung untersagt, insbesondere die Nutzung des Inhalts im Zusammenhang mit, für oder in KI-Systemen, KI-Modellen oder Generativen Sprachmodellen.

drive up to 70 kph without gearshift. This enables uncompromised zero emission drive in cities. All other special hybrid modes are on board, like e.g. extended sailing, boosting, generator mode, load-shift, charge at standstill, restart of combustion engine after sailing. Generally, the degree of automation determines the available functionality, as can be seen in the table below.

Table 1: Functions depending on use of automation components in manual transmission based hybrid concepts

	Function definition	Base	48V		380V	
Added components			2-speed and decoupling	Clutch by wire	Shift by wire	3-way coupling
			MT operation		AT operation	
Added features						
3-pedal use	A	x	x	x		
2-Pedal use (e.g. BI6)	B					
2-pedal use (e.g. BI8)	C				x	x
sailing	D			x	x	x
recuperation	E		x	x	x	x
boost	F		x	x	x	x
load shift	G		x	x	x	x
e-Launch and Reverse	H			weight limit	x	x
e-Drive (in MT with special shifter position)	I			weight limit	x	x
Combined Hybrid Mode	J			weight limit	x	x
autonomous parking with eDrive	K		x	x	x	x
engine start / charge at standstill	L					x
FE benefit (SOC neutral)			10-12%	12-15%	25-30%	25-30%

Function explanation	
A	Clutch pedal determins the torque at wheel, regardless of the drive mode. In case of e-Drive, the clutch pedal is limiting the motor torque, corresponding to a slipping clutch.
B	Full automatic shifting, Shift quality better than AMT but limited torque fill due to limited eDrive power.
C	Full automatic shifting, Shift quality comparable to AT due to torque fill with high eDrive power.
D	In coast condition, the clutch will open and allow the ICE to be switched off. At low throttle position, the eDrive may support constant speed driving.
E	In coast condition with light brake pedal actuation, the eDrive will generate electric energy to re-charge the battery.
F	In drive condition, the eDrive will support the ICE and fill up torque above the ICE capability, reduce turbo-lag etc.
G	In drive condition, the ICE will deliver more torque than requested by the driver to allow the eDrive to act as generator to re-charge the battery during drive condition.
H	The vehicle will launch in eDrive mode per default and start the ICE at higher speeds.
I	pure eDrive without use of ICE and with open clutch to ICE or T/M in N gear selection
J	The ICE will be shutt off in certain load conditions and re-start automatically in each gear. Driver is using transmission as usual.
K	The autonomous parking function can be handled by the eDrive for forward and reverse and no driver interaction is needed
L	The ICE can be coupled with the eDrive via the transmission and the battery can be charged additionally at standstill of the vehicle. The starter can be deleted and the eDrive can start the ICE.

As the 5BHT425 is derived from Manual Transmission, no energy is required for clutch actuation & cooling during in-gear operation. This is an advantage compared to other hybrid transmissions based on planetary transmissions or DCT. The second energy efficiency contributor

https://doi.org/10.51202/9783181023549 - Generiert durch IP 216.73.216.36, am 19.01.2026, 02:19:31. © Urheberrechtlich geschützter Inhalt. Ohne gesonderte Erlaubnis ist jede urheberrechtliche Nutzung untersagt, insbesondere die Nutzung des Inhalts im Zusammenhang mit, für oder in KI-Systemen, KI-Modellen oder Generativen Sprachmodellen.

is the P3 hybrid concept, allowing the use of a main transmission that is designed for the torque level of the combustion engine only, since the e-motor power is directly transferred through the final drive.



Fig. 3: Section view of 5BHT425 hybrid transmission for light commercial applications (source: Getrag Ford Transmissions GmbH)

Conclusion

LCVs are the workhorses of the modern world. The requirements to these type of vehicles are extremely diverse. And they need to have access to the zero emission zones in the cities. The powertrain concepts introduced in this presentation were developed on this background. From pure ICE drive to Hybrid Drive to pure eDrive: The customer has the full flexibility to decide for optimum operation mode. The new technologies are designed to drive the vehicle with lowest CO2 emissions in the various traffic situations.

[1] M. Bahne; U. Frey: Transmission Technology Contribution to CO2 Roadmap - A Benchmark, VDI Wissensforum (2018)

[2] F. Casimir: Light Commercial Vehicle, IAA (2018)

https://doi.org/10.51202/9783181023549 - Generiert durch IP 216.73.216.36, am 19.01.2026, 02:19:31. © Urheberrechtlich geschützter Inhalt. Ohne gesonderte Erlaubnis ist jede urheberrechtliche Nutzung untersagt, insbesondere die Nutzung des Inhalts im Zusammenhang mit, für oder in KI-Systemen, KI-Modellen oder Generativen Sprachmodellen.

Benefits of the New Allison 9-Speed Fully Automatic Medium Duty Commercial Transmission

Scott Kluemper, **Conrad Rockey**,
Allison Transmission, Inc., Indianapolis, IN, USA

ABSTRACT

Allison Transmission's new patented medium duty 9-Speed builds on the proven durability platform of Allison's 2000 series 6-speed product, providing a cost effective power shift 9-Speed transmission that can deliver improved fuel savings to the end user while not sacrificing performance. This paper discusses how Allison Transmission has been able to leverage an existing transmission platform and add key features and capabilities to an already proven design. These capabilities enable an OEM to improve both fuel efficiency and performance while still delivering the proven reliability and durability of the Allison Transmission brand.

High level design requirements focused the design team to improve the 9-speed in all aspects over the current proven 6-speed product. Increased capabilities with respect to fuel efficiency, performance, ratings, and integration have all been designed into the product. Target applications were established with the new capabilities of the new 9-speed in mind.

The architecture discussion of the new 9-speed shows how components are added to achieve the design requirements of the new product while leveraging as much content as possible from the current 6-speed product. A brief discussion on the advantages of the torque converter as a launch device is covered. New optional hardware content for the new 9-speed product is shown. For the hydraulic controls, an all-new design was pursued in order to take full advantage of the new 9-speed's capabilities improving both fuel efficiency and performance characteristics. Finally, all of Allison's current control algorithm capabilities have been leveraged to better optimize the new 9-speed transmission.

https://doi.org/10.51202/9783181023549 - Generiert durch IP 216.73.216.36, am 19.01.2026, 02:19:31. © Urheberrechtlich geschützter Inhalt. Ohne gesonderte Erlaubnis ist jede urheberrechtliche Nutzung untersagt, insbesondere die Nutzung des Inhalts im Zusammenhang mit, für oder in KI-Systemen, KI-Modellen oder Generativen Sprachmodellen.

The benefits discussion provides additional insight into the enhanced capabilities of the new 9-speed. Fuel efficiency improvements are discussed, including simulation findings and Greenhouse Gas regulation credits.

INTRODUCTION

The new 9-Speed transmission is Allison Transmission's new entry in the medium duty commercial truck market. The transmission continues Allison's highly successful approach of providing full power shifting in combination with torque converter launch to deliver Allison's Continuous Power Technology™. When integrated with Allison's FuelSense® 2.0 technology, the new 9-Speed delivers a dynamic package of productivity and fuel efficiency for the medium duty truck market.

DESIGN REQUIREMENTS

The design team was challenged to deliver a product that is able to meet the ever increasing demands in the marketplace while leveraging content from the current Allison 2000 series 6-speed platform. The following is the list of the high level design requirements.

- Leverage Proven Reliability and Durability of the Allison 2000 Series
- Incorporate Features that Deliver GHG Regulation Credits
- Improve Performance and Fuel Efficiency
- Increase Torque and Weight Rating Capabilities

The new 9-Speed has also been designed to cover a wide range of markets in a variety of applications as shown in Figure 1. The 9-Speed will be offered in vehicle classes 3 thru 8.

https://doi.org/10.51202/9783181023549 - Generiert durch IP 216.73.216.36, am 19.01.2026, 02:19:31. © Urheberrechtlich geschützter Inhalt. Ohne gesonderte Erlaubnis ist jede urheberrechtliche Nutzung untersagt, insbesondere die Nutzung des Inhalts im Zusammenhang mit, für oder in KI-Systemen, KI-Modellen oder Generativen Sprachmodellen.



Figure1: New 9-Speed Target Applications

NEW 9-SPEED ARCHITECTURE - HARDWARE

The new 9-Speed architecture is a significant evolution from the current proven reliable Allison 2000 series 6-Speed architecture. The 6-Speed product has proven its reliability and durability as demonstrated by the fact it has been sold into approximately 4 million vehicles with an estimated 300 billion miles+ of successful commercial and heavy duty pickup operation. The 6-Speed has been able to successfully meet the severe duty cycle demands of the commercial duty market as well as the refined expectations of the heavy duty pickup market. This DNA is built into and improved upon with the new 9-Speed transmission. Figure 2 shows how the addition of a 4th planetary and an additional stationary clutch enables the 6-Speed to be transformed into the 9-Speed gearbox.

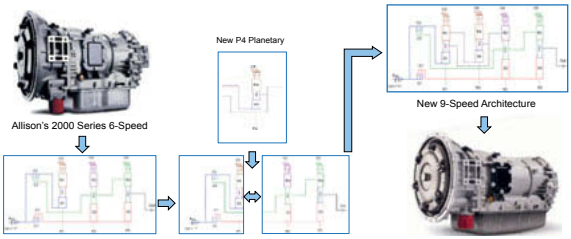


Figure 2: 9-Speed architecture derived from the Allison 2000 series 6-Speed architecture

Incorporating a 4th planetary enables the 9-Speed to deliver 50% more ratio coverage as compared to the Allison 2000 series 6-Speed product as shown in Figure 3. This added ratio

https://doi.org/10.51202/9783181023549 - Generiert durch IP 216.73.216.36, am 19.01.2026, 02:19:31. © Urheberrechtlich geschützter Inhalt. Ohne gesonderte Erlaubnis ist jede urheberrechtliche Nutzung untersagt, insbesondere die Nutzung des Inhalts im Zusammenhang mit, für oder in KI-Systemen, KI-Modellen oder Generativen Sprachmodellen.

coverage enables both improved fuel economy and performance. It provides small ratio steps that enable 1st range lock-up, smooth range transitions, and improved drivability. In addition to smaller steps the new 9-Speed is able to leverage the dual ratio offerings of the 6-Speed to provide similar flexibility in the 9-Speed product. This flexibility enables an OEM to better optimize their vehicle system by picking the optimal gear ratio coverage and range step sizes.

	2000 Series 6-Speed				New Medium Duty 9-Speed			
Gear Ratio	CR	CR Step	WR	WR Step	CR	CR Step	WR	WR Step
1st	3.10	-	3.51	-	4.20	-	4.82	-
2nd	1.81	1.71	1.90	1.85	3.10	1.36	3.51	1.36
3rd	1.41	1.28	1.44	1.32	2.61	1.19	2.85	1.22
4th	1.00	1.41	1.00	1.44	1.81	1.44	1.90	1.51
5th	0.71	1.41	0.74	1.36	1.41	1.29	1.44	1.32
6th	0.61	1.16	0.64	1.14	1.00	1.41	1.00	1.44
7th	-	-	-	-	0.71	1.41	0.74	1.36
8th	-	-	-	-	0.61	1.16	0.64	1.14
9th	-	-	-	-	0.54	1.15	0.57	1.14
Reverse	-4.49	-	-5.09	-	-4.49	-	-5.09	-
Ratio Coverage	5.05	-	5.46	-	7.78	-	8.46	-
TC Stall Torque Ratio (4 models)	1.58 - 2.05	-	1.58 - 2.05	-	1.58 - 2.05	-	1.58 - 2.05	-
Effective Ratio Coverage w/ Torque Converter	8.03 - 10.42	-	8.67 - 11.24	-	12.29 - 15.94	-	13.36 - 17.33	-

Figure 3: Comparison of 2000 series ratio coverage and steps to the new 9-Speed product

After the kinematic architecture was established the design team was able to analyse the structure and determine the strategic areas that needed to be enhanced in order to extend the torque and weight rating capabilities of the gear box. These enhancements have resulted in the ability to rate the new 9-speed in the medium duty commercial market up to 1200 Nm input torque and 26,000 kgs GCW.

In addition to the basic architecture a number of additional fuel savings technologies are included in the new 9-Speed architecture. Technologies incorporated include optimized lube, low drag seal rings, fully modulated main pressure, and low drag clutches.

The new medium duty 9-speed product will continue to utilize a torque converter as the launch device due to the many benefits it provides over a starting clutch equipped transmission. The benefits of a torque converter over a starting clutch are listed below;

- Multiplies engine torque thereby increasing a transmission's overall effective ratio coverage. See Figure 3 for actual effective ratios for the new 9-Speed. A high ratio coverage transmission is able to achieve both low speed gradeability and lower engine speeds at cruise thereby improving fuel efficiency of the vehicle.

https://doi.org/10.51202/9783181023549 - Generiert durch IP 216.73.216.36, am 19.01.2026, 02:19:31. © Urheberrechtlich geschützter Inhalt. Ohne gesonderte Erlaubnis ist jede urheberrechtliche Nutzung untersagt, insbesondere die Nutzung des Inhalts im Zusammenhang mit, für oder in KI-Systemen, KI-Modellen oder Generativen Sprachmodellen.

- Provides immediate, smooth torque at launch improving driveability and performance.
- Enables superior low speed manoeuvrability.
- Operates with high efficiency when in lockup due to no slip across the converter.

The one drawback that is typically discussed about the use of a torque converter is the reduced fuel efficiency that results from operating in converter mode. For the new medium duty 9-speed these losses have been minimized by the introduction of 1st lockup which is made possible due to the smaller ratio step between 1st and 2nd range.

To quantify the benefits of 1st lockup, a launch analysis of wasted energy due to the torque converter slip was calculated to be approximately 0.5% of the energy required to accelerate a vehicle from 0 – 80 km/hr. Figure 4 shows the torque converter lockup up in 1st range at an output speed of 190 rpm which is approximately 6 km/hour. Based on this analysis the price to pay for torque converter operation is a very small when all of the benefits of the torque converter are considered.

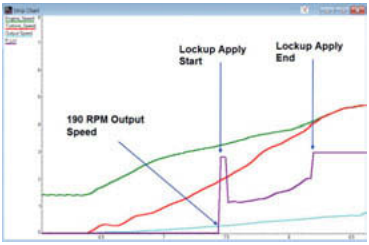


Figure 4: Lockup in 1st range at approximately 190 rpm (6 km/hour)

Another benefit that the new 9-Speed provides is the ability to do full power shifts. Power shifting benefits are clear when considering vehicle performance, in that they offer continuous power flow to the wheels even during a shift as opposed to lengthy power interrupts – particularly in commercial vehicles. However, power shifts also have significant fuel efficiency and emission benefits as compared to the power interrupt shifts of an AMT or manual transmission.

https://doi.org/10.51202/9783181023549 - Generiert durch IP 216.73.216.36, am 19.01.2026, 02:19:31. © Urheberrechtlich geschützter Inhalt. Ohne gesonderte Erlaubnis ist jede urheberrechtliche Nutzung untersagt, insbesondere die Nutzung des Inhalts im Zusammenhang mit, für oder in KI-Systemen, KI-Modellen oder Generativen Sprachmodellen.

Prior to diving into the details of each point it is important to provide a basic understanding of an engine Brake Specific Fuel Consumption (BSFC) plot. Figure 5 shows a simplified representation of a BSFC plot. It shows that all combustion engines have areas of high efficiency and areas of low efficiency.

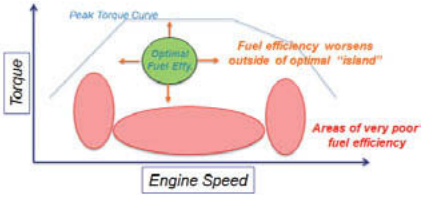


Figure 5: Fundamental Characteristics of an Engine BSFC Plot

The first point of emphasis for the advantage of power shifting is the loss of vehicle speed when the power is interrupted which actually results in an increased effective ratio step for an AMT or manual transmission as shown in Figure 6. The result is an AMT or manual transmission is not be able to lower shift points as far as a power shift transmission because the vehicle actually slows during a power interrupt shift. This limits the ability of an engine to take full advantage of down speeding as a solution to the increasingly stringent fuel economy demands from greenhouse gas regulations and ultimately the customer.

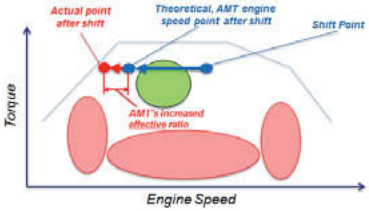


Figure 6: Total effective ratio step of a power interrupt shift

The other point to consider is the undeniable transient operation of a power interrupt shift. This results in the transmission causing the engine to travel in a very inefficient path as it changes from one ratio step to the next. Figure 7 illustrates this point. Prior to the shift the engine can be operating in the most fuel efficient or near the most fuel efficient point. The power interrupt will require the engine to move through some very inefficient operating points during the shift.

https://doi.org/10.51202/9783181023549 - Generiert durch IP 216.73.216.36, am 19.01.2026, 02:19:31. © Urheberrechtlich geschützter Inhalt. Ohne gesonderte Erlaubnis ist jede urheberrechtliche Nutzung untersagt, insbesondere die Nutzung des Inhalts im Zusammenhang mit, für oder in KI-Systemen, KI-Modellen oder Generativen Sprachmodellen.

This results in increased CO2 and NOx engine emissions. Contrast this with a power shift which would merely move on the blue path through the most efficient point of operation of the engine and the benefits are easy to understand.

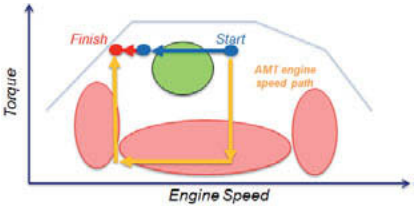


Figure 7: The transient engine operation of an AMT's power interrupt shift

NEW 9-SPEED ARCHITECTURE: HYDRAULIC CONTROLS

The new 9-Speed is being introduced with an all new hydraulic control's architecture. The system was designed to support both shift-by-wire or shift-by-cable interfaces to improve integration flexibility for an OEM. In both cases an integral engine stop start electric pump is able to be packaged internally as shown in Figure 8.



Figure 8: Hydraulic controls shown with optional park-by-cable and ES-S capabilities

The controls architecture has been designed to minimize leakage via employing low leakage solenoids, optimized valve geometry, and efficient diagnostic switches. From a diagnostic perspective, the architecture enables multi-range limp home capability to enable improved drivability in certain failure mode events. Finally the architecture is also able to deliver skip shift capability as shown in Figure 9. This additional capability improves fuel efficiency, drivability, durability, and performance by enabling the transmission to quickly transition to the optimal range as determined by the control algorithms.

https://doi.org/10.51202/9783181023549 - Generiert durch IP 216.73.216.36, am 19.01.2026, 02:19:31. © Urheberrechtlich geschützter Inhalt. Ohne gesonderte Erlaubnis ist jede urheberrechtliche Nutzung untersagt, insbesondere die Nutzung des Inhalts im Zusammenhang mit, für oder in KI-Systemen, KI-Modellen oder Generativen Sprachmodellen.

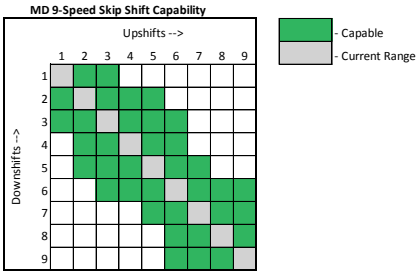


Figure 9: Medium duty 9-speed skip shift capability

NEW 9-SPEED ARCHITECTURE: ELECTRONIC CONTROLS AND SHIFT ALGORITHMS

The new 9-speed is being introduced with Allison Transmission's 6th Generation controls system. 6th Generation controls will support both 12 and 24 volt vehicle electrical systems. It will support multiple CAN and CAN-FD communication protocols and baud rates. It will provide Cyber Security and Functional Safety capability.

To optimize the fuel efficiency and performance of the new 9-Speed transmission, Allison Transmission is integrating numerous fuel savings and productivity enhancing control algorithms into the transmission system package. This set of features has been named FuelSense® 2.0. To provide some idea of the effectiveness of these strategies, Allison has conducted fleet testing of this feature set. The results can be quite dramatic with improvements of up to 6% fuel economy gains over baseline controls strategies that previously favoured performance operation. The set of controls algorithms can be categorized into the following areas.

DynActive™ Shifting

DynActive™ Shifting is a continuously-variable method of shift scheduling. Instead of using a shift point table with defined points, DynActive™ Shifting chooses the most efficient shift points based on the current environmental and vehicle conditions.

https://doi.org/10.51202/9783181023549 - Generiert durch IP 216.73.216.36, am 19.01.2026, 02:19:31. © Urheberrechtlich geschützter Inhalt. Ohne gesonderte Erlaubnis ist jede urheberrechtliche Nutzung untersagt, insbesondere die Nutzung des Inhalts im Zusammenhang mit, für oder in KI-Systemen, KI-Modellen oder Generativen Sprachmodellen.

Neutral at Stop

Neutral at Stop is a feature that reduces or eliminates the load on the engine while the vehicle is stopped, reducing fuel usage and emissions. It provides an output lock feature to eliminate vehicle rollback while on grades.

- Neutral at Stop Standard allows transmission shifts to a partial neutral condition as the vehicle comes to a stop with service brakes engaged.

- Neutral at Stop Premium provides full neutral as the vehicle comes to a stop with service brakes engaged and is available with Coast Mode to provide early activation at low speeds when the vehicle is braking to a stop.

Acceleration Rate Management

Acceleration Rate Management is an engine management function that can help prevent aggressive driving practices by automatically controlling engine torque and limiting the vehicle acceleration to a calibrated rate. Five levels of control are offered to provide more precision by limiting vehicle acceleration to a customized rate.

While the above features were highlighted, Allison will also offer the extensive controls features list that is available today on the 6-speed product with the new 9-speed product. Integration with multiple systems on the vehicle such as ABS, traction control, cruise control including adaptive cruise, engine brakes, engine management, hill hold, reverse warning, road speed limit, and prognostics are just a few of the integration features offered. This feature set is very long and is beyond the scope of this paper so please refer to Allison Transmission technical data if interested.

NEW 9-SPEED ARCHITECTURE: OPTIONAL FEATURES

A number of new features beyond what have already been highlighted are being designed for the new medium duty 9-speed. Here is the list of exciting new capabilities the new 9-speed is able to bring to the market.

https://doi.org/10.51202/9783181023549 - Generiert durch IP 216.73.216.36, am 19.01.2026, 02:19:31. © Urheberrechtlich geschützter Inhalt. Ohne gesonderte Erlaubnis ist jede urheberrechtliche Nutzung untersagt, insbesondere die Nutzung des Inhalts im Zusammenhang mit, für oder in KI-Systemen, KI-Modellen oder Generativen Sprachmodellen.

- An integral retarder without having to increase transmission length reducing integration efforts and vehicle cost
- An optional integral cooler to ease integration into the vehicle. The transmission will also be able to interface with a remote cooler if that is a desired capability of the OEM.
- A shallow sump design to improve ground clearance while reducing fluid fill requirements
- Lifetime fluid fill via a redesigned filtration system
- Cooler bypass to improve fuel efficiency
- Hybrid capable via integration with P2 or other mild hybrid systems

NEW 9-SPEED: GREENHOUSE GAS REGULATION BENEFITS

This paper has already touched on a number of benefits of the new medium duty 9-speed product as the architecture of the product was being discussed. What has not been covered up to this point is the benefit it provides to the regulatory environment of greenhouse gas emissions regulation. Greenhouse gas regulations are causing the commercial truck industry to innovate further and faster. The new 9-Speed is designed to provide OEM's the tools to help meet these ever increasing regulatory requirements.

The new 9-Speed is being designed to serve the global commercial truck market and will be subject to different regulations across the globe. In Europe, the European Commission is developing the Vehicle Energy Consumption Calculation Tool (VECTO) for Heavy Duty Vehicle CO2 certification purposes. The United States has taken a similar approach with respect to using a simulation platform to evaluate the effectiveness of different technologies on the ability to reduce greenhouse gas emissions. The paper discusses the benefits the new 9-Speed is able to deliver in both simulation platforms.

For the VECTO analysis the new Medium Duty 9-Speed was compared against a 6-Speed AMT with a 4 cylinder engine in a typical distribution truck configuration. Both vehicles were evaluated on a typical distribution truck duty cycle. In the VECTO analysis the new Medium Duty 9-Speed delivered 4.9% fuel savings over the 6-Speed AMT transmission. A second evaluation was run comparing the new Medium Duty 9-

https://doi.org/10.51202/9783181023549 - Generiert durch IP 216.73.216.36, am 19.01.2026, 02:19:31. © Urheberrechtlich geschützter Inhalt. Ohne gesonderte Erlaubnis ist jede urheberrechtliche Nutzung untersagt, insbesondere die Nutzung des Inhalts im Zusammenhang mit, für oder in KI-Systemen, KI-Modellen oder Generativen Sprachmodellen.

Speed to 8-Speed AMT running behind a 6 cylinder engine for a typical distribution truck running on a typical distribution cycle. In this VECTO analysis the new 9-Speed outperformed the 8-Speed AMT by delivering a 2.9% fuel savings.

The US greenhouse gas regulations utilize the Greenhouse Gas Emissions Model (GEM) to evaluate a vehicle's greenhouse gas emissions. Figure 10 shows how the new 9-Speed can provide significant fuel efficiency advantages over traditional commercial products on a variety of duty cycles. In addition, other FuelSense® 2.0 features although not currently recognized by the Greenhouse Gas Emission Model, do provide additional test benefit when exercising the option to submit powertrain test data with production shift schedules in the United States (i.e. DynActive™ shifting and Acceleration Rate Management). In addition to the GHG credits accrued by the OEM, significant added fuel efficiency improvements are realized by the customer.

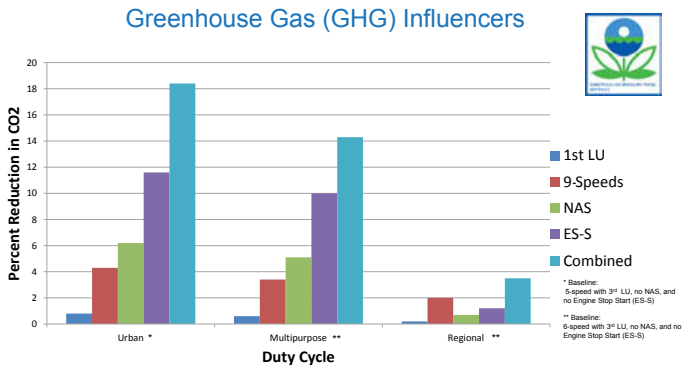


Figure 10: Greenhouse Gas Emission Model (GEM) Simulation Results

NEW 9-SPEED: FUEL EFFICIENCY AND PEFORMANCE BENEFITS

Analysis of the new 9-Speed has shown an improvement in both performance and fuel efficiency as compared to the current 6-Speed product. To prove this point, both transmissions were analysed on a high density stop start P&D cycle. Both 6-Speed and 9-Speed vehicles were set-up identically with identical control features like Neutral at Stop. Figure 11 illustrates

https://doi.org/10.51202/9783181023549 - Generiert durch IP 216.73.216.36, am 19.01.2026, 02:19:31. © Urheberrechtlich geschützter Inhalt. Ohne gesonderte Erlaubnis ist jede urheberrechtliche Nutzung untersagt, insbesondere die Nutzung des Inhalts im Zusammenhang mit, für oder in KI-Systemen, KI-Modellen oder Generativen Sprachmodellen.

improved fuel efficiency for a range of axles with the largest delta increase for any one axle being approximately 10% better fuel economy.

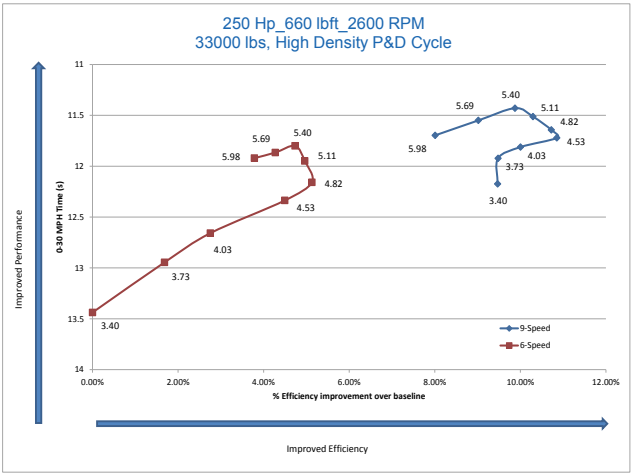


Figure 11: 9-Speed Fuel Efficiency Improvement

The same data set can also illustrate a performance improvement. All 9-Speed data points with the same axle selection performed better than the 6-Speed with the largest delta for any one axle being approximately 10% faster to 30 mph.

The final interesting point revealed in the data is fuel economy and performance sensitivity to axle ratio selection is reduced with the 9-Speed transmission. Axle ratio selection becomes less critical with the 9-Speed product as compared to the 6-Speed product. This demonstrates the 9-Speed is better suited to handle the variation in duty cycles while still delivering on the promise of increased fuel efficiency and performance.

SUMMARY

In closing, the new Allison Medium Duty 9-Speed delivers on its design requirements.

- Leverage Proven Reliability and Durability of the Allison 2000 Series
    - Significant re-use of 6-speed content

https://doi.org/10.51202/9783181023549 - Generiert durch IP 216.73.216.36, am 19.01.2026, 02:19:31. © Urheberrechtlich geschützter Inhalt. Ohne gesonderte Erlaubnis ist jede urheberrechtliche Nutzung untersagt, insbesondere die Nutzung des Inhalts im Zusammenhang mit, für oder in KI-Systemen, KI-Modellen oder Generativen Sprachmodellen.

- Incorporate Features with GHG Regulations GEM benefits
  - 9-Speeds, 1st lockup, Neutral At Stop, Engine Stop-Start
- Improved Performance and Fuel Efficiency
  - FuelSense® 2.0 control features in combination with 9-Speeds, 1st lockup, Neutral at Stop and Engine Stop-Start
- Increased Torque and GCW Rating Capability
  - Commercial vehicle ratings up to 1200 Nm input torque and up to 26,000 kgs GCW

The product was derived from the highly successful power shift Allison 2000 series 6-speed architecture. Its many new fuel efficiency features deliver impressive fuel savings potential while improving performance. Ease of use, drivability, reliability/durability, ease of integration and a world class service support network, which are synonymous with the Allison Transmission name, are all baked into this product.

The new 9-speed is currently undergoing extensive testing. Component level, system dyno level, vehicle level, and OEM evaluation testing are all being conducted. Production readiness activities are in process and production timing is being finalized. Allison Transmission looks forward to working with interested OEMs to bring this exciting new product to market.

https://doi.org/10.51202/9783181023549 - Generiert durch IP 216.73.216.36, am 19.01.2026, 02:19:31. © Urheberrechtlich geschützter Inhalt. Ohne gesonderte Erlaubnis ist jede urheberrechtliche Nutzung untersagt, insbesondere die Nutzung des Inhalts im Zusammenhang mit, für oder in KI-Systemen, KI-Modellen oder Generativen Sprachmodellen.

https://doi.org/10.51202/9783181023549 - Generiert durch IP 216.73.216.36, am 19.01.2026, 02:19:31. © Urheberrechtlich geschützter Inhalt. Ohne gesonderte Erlaubnis ist jede urheberrechtliche Nutzung untersagt, insbesondere die Nutzung des Inhalts im Zusammenhang mit, für oder in KI-Systemen, KI-Modellen oder Generativen Sprachmodellen.

Mechatronic transmission control module for agile AMT Transmission actuation in commercial vehicles

Dipl.-Ing. (TU) **Steffen Johnsen**,
Powertrain and Chassis, Kongsberg Automotive, Kongsberg, Norway;

Dipl.-Ing. (FH) **Robert Wexenberger**,
Powertrain and Chassis, Kongsberg Automotive GmbH, Hallbergmoos



Figure 1 ATrAct™ transmission actuation unit with ExAct™ external clutch actuator with bi-directional self-adjustment

Abstract

The development of the ATrAct™ transmission actuation unit and the built-in ExAct™ external clutch actuator with self-adjustment was performed by Kongsberg Automotive and the Eaton Cummins JV as a co-development. The development process was highly efficient, lasting only 3.5 years from start until SOP. Providing highly competitive performance in terms of actuation speed and precision, the self-adjusting clutch actuator drastically improves system agility whilst also reducing overall air consumption and making the unit suitable to work with a wide range of clutch characteristics due to the increase in natural frequency of the clutch and clutch-actuation system.

1. Introduction

During the last decade the market share of Automated Manual Transmissions (AMT) constantly increased and this transmission technology became the preferred choice for Heavy Duty and Medium Duty commercial vehicles in most of the markets. In this segment (44to down to 7,5to) you normally have pneumatic air on board, because air pressure is needed for breaking while commercial vehicles (lower than 7,5 to) use hydraulic

https://doi.org/10.51202/9783181023549 - Generiert durch IP 216.73.216.36, am 19.01.2026, 02:19:31. © Urheberrechtlich geschützter Inhalt. Ohne gesonderte Erlaubnis ist jede urheberrechtliche Nutzung untersagt, insbesondere die Nutzung des Inhalts im Zusammenhang mit, für oder in KI-Systemen, KI-Modellen oder Generativen Sprachmodellen.

brakes.
When this project development started, Kongsberg Automotive saw a high increase in demand of AMT solutions for the future, both in developed and emerging markets (see figure 2). With Kongsberg Automotive product and development knowledge base from hydraulic and pneumatic gear actuation systems we had the best starting point for our ATrAct™ transmission actuation system which was co-developed and launched for a dedicated customer.

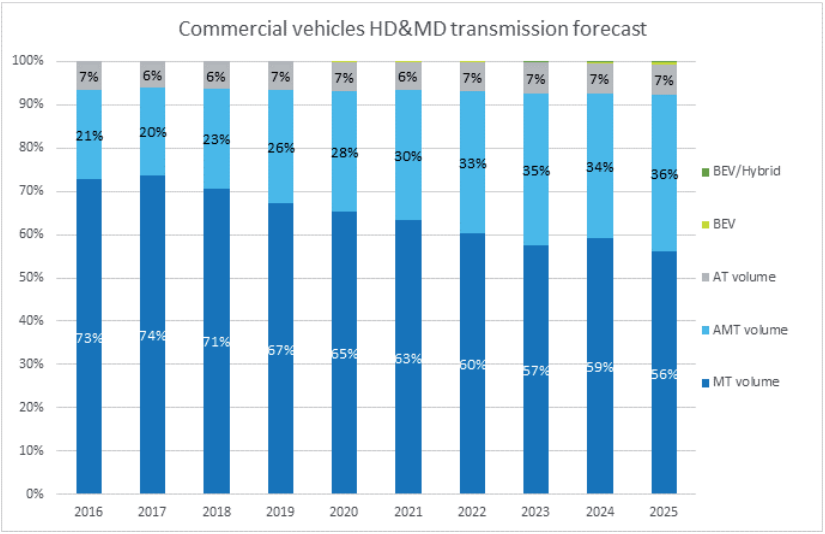


Figure 2 Global Commercial Vehicle Forecast LMC 2018-Q4, updated with KA background information

2. Clutch and gear actuation integrated in one transmission control unit, whilst obtaining serviceability through modularity

The Kongsberg Automotive ATrAct™ transmission actuation unit features three individual shift rails for actuation of the split, main box and range, in addition to an integrated clutch actuator and bolt-on control electronics. The main housing of the ATrAct™ is based on a mono-block design with internal air channels and interfaces to other parts and sub-systems. The external clutch actuator being fully integrated directly into the main housing is a particularly novel feature contributing to cost, performance and serviceability improvements. Located in a position accessible without dropping the transmission or removing significant parts from the truck make field-service possible. A new clutch actuator may be installed in a matter of minutes, as the position sensor does not require pairing or calibration. Poka-yoke assembly features ensures the actuator is assembled in the right angular orientation, while a bi-directional air supply channel is opened to atmosphere upon unbolting of the actuator avoiding dangerous situations if the actuator is removed when pressurized.

https://doi.org/10.51202/9783181023549 - Generiert durch IP 216.73.216.36, am 19.01.2026, 02:19:31. © Urheberrechtlich geschützter Inhalt. Ohne gesonderte Erlaubnis ist jede urheberrechtliche Nutzung untersagt, insbesondere die Nutzung des Inhalts im Zusammenhang mit, für oder in KI-Systemen, KI-Modellen oder Generativen Sprachmodellen.

The position, pressure and speed sensors are assembled directly onto the ATrAct™ monoblock, not requiring additional assembly or stretch of wires across the transmission. Except for the speed sensor, all sensors and connectors are sealed off from oil to simplify service and improve ingress protection. With a modular build-up, the control unit, shift actuators, valve banks, wire harness and sensors may be serviced individually to further lower the total cost of ownership through simplified maintenance.

3. Technical principles for securing agile clutch control through the KA pneumatic self-adjusting clutch actuator

The main intention with the self-adjustment is to reduce the dead volume necessary to comply with installation tolerances and clutch wear. As the clutch disc wears, the release bearing moves as the angle of the diaphragm spring changes. This is valid for both push and pull type clutches, meaning the actuator principle may be used for all clutch variants. A self-adjusting clutch actuator transfers (pneumatic) force in one direction as a stiff body, whilst providing dual direction compliance for the displacement of the release bearing when the clutch is worn, or if the clutch impose movement from the non-actuating direction. This movement may be observed during installation, cyclic thermal expansion and contraction and after installing a new clutch.

Self-adjustment mechanisms are inherently more complicated than standard pneumatic clutch actuators, however the improved system agility and ability to comply with a wide range of clutch types and clutch characteristics justify the added complexity. As shown in a later section, the reduced dead volume increases the stiffness of the “air spring” and the natural resonance frequency of the mass-spring system, increasing the achievable closed loop control bandwidth of the system. Among others, the ECJV Endurant™ “*urge to move*” – creep mode is made possible by the improved controllability and accuracy. When adjusting for both the clutch wear and installation tolerances, the self-adjustment may typically reduce the dead volume by as much as 80%, pending properties of the particular system in question. The improved speed makes it possible to complete a full disengage stroke in approximately 100 ms (5.5 barg, 22 mm stroke, 5500N max. force). The improved clutch actuator agility results in improved comfort and acceleration as well as a 50 % reduction in air consumption to operate the clutch, saving fuel.

Developing a self-adjustment mechanism, several parameters must be considered; if the adjustment mechanism is normally open or closed, the total stroke as the sum of the release stroke and the adjustment stroke, stroke redundancy, speed of adjustment, how to handle residual loads, etc. Self-adjustment mechanisms may be categorized into two domains; incremental adjustment or full range adjustment in a continuous motion. Kongsberg Automotive’s ExAct™ patented external clutch actuator is adjusting the length between the pneumatic piston and push rod, and is capable of full range bi-directional adjustment, as this fits the widest range of applications.

The selected self-adjustment mechanism for the ExAct™ external clutch actuator is based on a lead screw and nut. The relative axial translation of the nut along the screw is prohibited if the rotation of both nut and screw is simultaneously prohibited. The selective engagement of a locking feature to either allow or stop the rotation of the screw element is the main working principle. Providing a position dependent, non-load carrying un-locking element, the locking element opens to provided adjustability when the pneumatic piston is in the rearmost

https://doi.org/10.51202/9783181023549 - Generiert durch IP 216.73.216.36, am 19.01.2026, 02:19:31. © Urheberrechtlich geschützter Inhalt. Ohne gesonderte Erlaubnis ist jede urheberrechtliche Nutzung untersagt, insbesondere die Nutzung des Inhalts im Zusammenhang mit, für oder in KI-Systemen, KI-Modellen oder Generativen Sprachmodellen.

position. The locking element, embodied as a friction clutch, automatically locks when a pneumatic pressure above a certain threshold is applied, overcoming the preload spring force.
With the intention to lower overall system weight, the Kongsberg Automotive self-adjustment mechanism and gear shift rails uses reinforced engineering polymers to transfer cyclic, bi- and unidirectional load to the clutch push rod and shift forks. Long experience with engineering polymers and associated fatigue limits ensure safe operation and good tribological properties in sliding interfaces. To save material cost and reduce processing, the lead screw nut is cast as a stand-alone component and over-molded in a second operation. The nut itself is made of a particularly high strength polymer and is used in its as-cast state. When lubricated, friction properties have been proven to remain stable over the lifetime of the actuator. Nuts made of metallic alloys show significant larger variations in friction and high wear rates on both the nut and lead screw, as can be seen in Fig. 2.

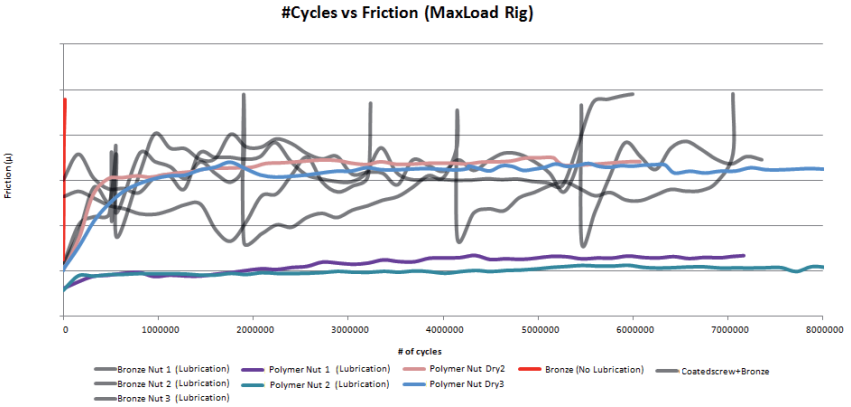


Figure 3 Friction properties of lead screw nuts with various materials and lubrications

4. Basic calculations of locking

Proper function of the self-adjustment requires sufficient friction to lock but also to adjust freely when the system is not pressurized. The locking capacity of the self-adjustment is evaluated as a combination of friction coefficients in the system and their associated band widths to ensure function. The clutch enables continuous locking without discrete steps, however a certain piston movement without locking (dead volume) is required to ensure a minimum separation of the clutch and ability to handle clutch wobbling impulses. Because the full vehicle clutch release load is transferred to the clutch through the lead screw, the locking capacity is designed to be load-independent, as shown in the following equation. However, as described in the following section, one must consider that the locking of the self-adjustment is also dependent on the dynamic response to vibration.

https://doi.org/10.51202/9783181023549 - Generiert durch IP 216.73.216.36, am 19.01.2026, 02:19:31. © Urheberrechtlich geschützter Inhalt. Ohne gesonderte Erlaubnis ist jede urheberrechtliche Nutzung untersagt, insbesondere die Nutzung des Inhalts im Zusammenhang mit, für oder in KI-Systemen, KI-Modellen oder Generativen Sprachmodellen.

$$\mu_{min} = \frac{P_{lead-screw-pitch} * \sin(\alpha_{half-cone-angle})}{\pi * d_{effective-cone-clutch}}$$

5. Self-adjustment dynamics

To predict the theoretically safe and unsafe operating conditions and design parameters of the self-adjustment, an idealized mathematical model describing its dynamic behavior was developed by Kongsberg Automotive employee Dr. Christian Hebert [1].
The self-adjustment mechanism consists of three moveable assemblies; however, the model assumes contact in the clutch, giving equal displacement and acceleration of the pneumatic piston and the cone/lead screw. The model also assumes proportionality of torque transferred to the cone clutch to the axial load and that the cone clutch provides full locking capacity when contact is obtained. Note that the actuator preload spring acts as a force to separate the two masses and reduce the cone clutch contact force. The derived system of equations to be solved may be written in simplified form as in the formulas below. Peak axial vibration level, vibration angular velocity, stiffness of springs, masses of bodies, pressures and forces further describe the individual terms in the formula, but are omitted for simplicity in this paper.

$$(m_p + m_{ctl})x`` = F_g - F_l + f_s$$

$$x_p`` = x_{ctl}`` = x``$$

Assuming a linear clutch characteristic at the onset of the push rod movement and an isentropic gas spring behavior, a set of non-dimensional parameter groups have been developed to better understand the physics of operation:

1) The ratio of the minimum dynamic contact force that exists at the cone clutch interface and the static adjusted contact force. **The main interest of the analysis, as the ratio may describe the boundary between safe and unsafe operation.**

$$\frac{F_{c_{min}} + F_{pl}}{F_{c_0} + F_{pl}} = \frac{Minimum\ adjusted\ contact\ force}{Static\ adjusted\ contact\ force}$$

2) The ratio of the driving vibration frequency to the natural mechanical resonance frequency of the system.

$$\frac{(m_p + m_{ctl}) * \omega^2}{|K_{g_0}| + |K_l|} = \frac{\omega}{\omega_r}$$

3) A measure of the relative influence of static loads over dynamic loads.

$$\frac{F_{c_0} + F_{pl}}{(m_p + m_{ctl})a} = \frac{Static\ loads}{Dynamic\ loads}$$

https://doi.org/10.51202/9783181023549 - Generiert durch IP 216.73.216.36, am 19.01.2026, 02:19:31. © Urheberrechtlich geschützter Inhalt. Ohne gesonderte Erlaubnis ist jede urheberrechtliche Nutzung untersagt, insbesondere die Nutzung des Inhalts im Zusammenhang mit, für oder in KI-Systemen, KI-Modellen oder Generativen Sprachmodellen.

4) The ratio of masses of the piston compared to the rest of the moveable mechanical system.

$$\frac{m_p}{m_{ctl}} = Mass\ ratio$$

5) The ratio of spring comparing the clutch spring stiffness to the gas spring

$$\frac{|K_l|}{|K_{go}|} = Spring\ stiffness\ ratio$$

A baseline simulation with given acceleration, frequency range, spring stiffness, forces and masses results in the system response shown in Fig. 3.

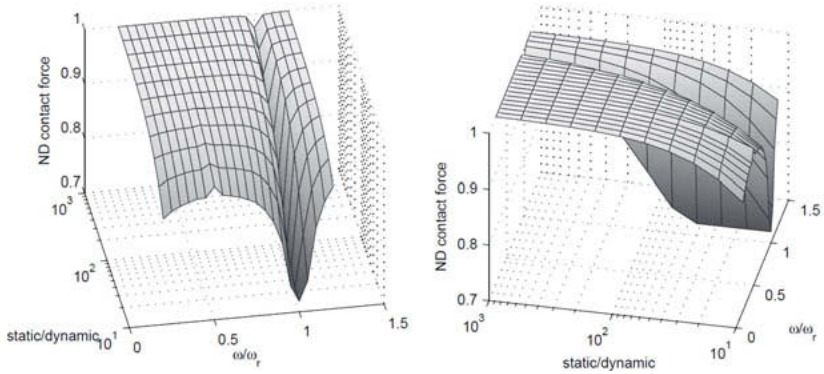


Figure 4 Baseline Non-Dimensional system response.

When dynamic loads due to system accelerations become dominant relative to static loads, the normalized, non-dimensional cone clutch contact force ratio decreases over the entire frequency spectrum. This indicated that effort should be made to keep the total sprung mass as low as possible, hence the extensive use of aluminium and composite materials. As expected, there is also a local dip in clutch contact ratio at the mechanical resonance frequency. Simulations performed with different mass ratios indicate the preferred mass distribution to reduce the impact of the resonance.

Changing the spring stiffness ratio between the clutch spring and the gas spring (Fig. 4) shows that the mechanism is performing at its best when the two are equally stiff, or the gas spring somewhat stiffer.

https://doi.org/10.51202/9783181023549 - Generiert durch IP 216.73.216.36, am 19.01.2026, 02:19:31. © Urheberrechtlich geschützter Inhalt. Ohne gesonderte Erlaubnis ist jede urheberrechtliche Nutzung untersagt, insbesondere die Nutzung des Inhalts im Zusammenhang mit, für oder in KI-Systemen, KI-Modellen oder Generativen Sprachmodellen.

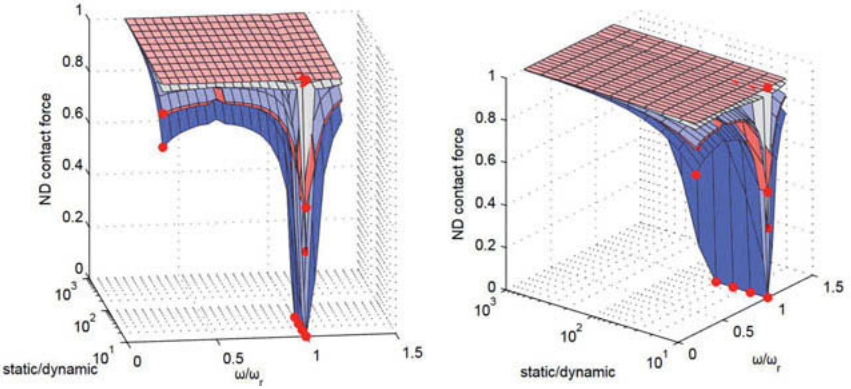


Figure 5 Spring stiffness ratio effects (two different angles). Dark red: |Kt|/|Kg0| = 0.2, light red: |Kt|/|Kg0| = 0.6, grey: |Kt|/|Kg0| = 1.0, light blue: |Kt|/|Kg0| = 1.7, dark blue: |Kt|/|Kg0| = 5.0

6. Pneumatics 101 – Stiffness calculations

By reducing the distance between the pneumatic piston and the rear wall of the cylinder, the dead volume of the actuator is reduced, leading to an increase in system natural frequency and response, both directly linked to the increased performance of the actuator. A gas piston is as a device often considered in terms of the thermodynamic properties of the gas it contains, namely the pressure P, temperature T and density ρ. The operation of a piston is generally formulated as a state process, in which the time dependent heat transfer to/from the gas to its surroundings becomes difficult to account for. However, a fully integrated differential formulation considering the conservation of mass and energy through simultaneous integration is not necessary to quantify the improved system stiffness and stability.

$$m = m_0 + \int_{t_0}^{t} \dot{m}\, dt$$

$$U = U_0 + \int_{t_0}^{t} \dot{U}\, dt$$

$$\dot{U} = \dot{Q} - P\dot{V} + C_p T_f \dot{m}$$

$$m_0 = \rho_0 V_0$$

$$P = (\gamma - 1)\frac{U}{V}$$

$$T = \frac{U}{mC_v}$$

$$\rho = \frac{m}{V}$$

https://doi.org/10.51202/9783181023549 - Generiert durch IP 216.73.216.36, am 19.01.2026, 02:19:31. © Urheberrechtlich geschützter Inhalt. Ohne gesonderte Erlaubnis ist jede urheberrechtliche Nutzung untersagt, insbesondere die Nutzung des Inhalts im Zusammenhang mit, für oder in KI-Systemen, KI-Modellen oder Generativen Sprachmodellen.

Resonance frequency analysis and plant linearization of a system using a gas piston requires knowledge of the stiffness of the piston at any given operating point. The stiffness of a spring being defined as $K = \frac{dF}{dx}$. Applying the state equations above and simplifying for a constant-bore piston, the pressure formulation of the air spring stiffness may be calculated with the formula below given a specific piston position including the initial dead volume $V = V_{stroke} + V_{dead}$. As seen in the formula, the derived air spring stiffness is shown to be inverse proportional to the total volume at a specific piston position.

$$K = -(\gamma - 1)\left(\frac{A}{V}\right)^2 \left(PV + \frac{PV}{\gamma - 1}\right)$$

$$= -\frac{\gamma P A^2}{V}$$

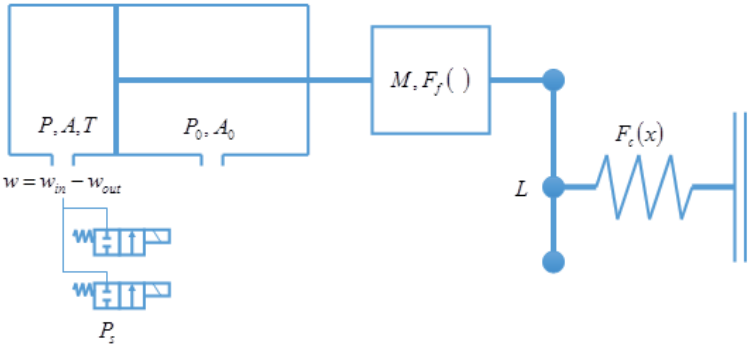


Figure 6 Simplified representation of clutch actuator and clutch system

Representing the system by a controlled dashpot, equivalent mass and lever (Fig. 5), the effective clutch spring stiffness may be described as $\frac{K_l}{L^2}$ for a push clutch [2]. This gives a system stiffness of $K_g + \frac{K_l}{L^2}$ and the important undamped natural frequency of the system described in the equation below. Observe that $x + x_0$ replaces the expression for the volume and that the A is no longer squared.

$$f_N[Hz] = \frac{1}{2\pi}\sqrt{\left(\frac{nPA}{x + x_0} + \frac{K_l}{L^2}.\right)}$$

The undamped natural frequency is proportional to the open loop bandwidth and achievable closed loop control bandwidth of the system, hence reducing x_0 with a up to 80% may increase the initial natural frequency in the beginning of the stroke by a factor of 1.5 or more

https://doi.org/10.51202/9783181023549 - Generiert durch IP 216.73.216.36, am 19.01.2026, 02:19:31. © Urheberrechtlich geschützter Inhalt. Ohne gesonderte Erlaubnis ist jede urheberrechtliche Nutzung untersagt, insbesondere die Nutzung des Inhalts im Zusammenhang mit, für oder in KI-Systemen, KI-Modellen oder Generativen Sprachmodellen.

(pending the particular system properties). This relation mathematically expresses the improved performance obtained by integrating the ExAct™ self-adjustment mechanism.

7. System stability and momentum balance argument

A static system is at force equilibrium when $F_{gas} - F_{load} = 0$. System stability is given when looking at the rate of change of these forces with respect to the position as illustrated by the equation below:

$$\left(\frac{dF_{gas}}{dx} - \frac{dF_{load}}{dx}\right)dx = F_{net}$$

If the piston is disturbed positively forward, the clutch load should increase more than the load from the pressurized air, and the opposite when the piston is disturbed negatively backwards. Given that the applied disturbance in either positive or negative direction is removed, the piston will return to the same position it had prior to the disturbance. The rate of increase or decrease of force from the clutch diaphragm spring load or pneumatic force from the pressurized piston is mathematically expressed as the stiffness K of each of the two. As we know from previously calculating the inversely proportional stiffness of the air spring, this will always be true for any pneumatic system working towards a clutch with linear characteristics.

Clutch characteristics are rarely linear, often degressive and at some point, exhibit a distinct negative stiffness after passing the maximum clutch force. If the rate at which the clutch load stiffness is decreasing faster with regards to a positive piston displacement than the air spring stiffness, the system will not be stable from a controls perspective, and vice versa. In other terms, a positive clutch load stiffness (increasing force with increasing position) is not necessary to insure stability, i.e. the clutch load can decrease with increasing piston position, if the gas force decreases even more to satisfy $K_{load} > -\frac{\gamma P A^2}{V}, \forall x$. This formulation is based on a simplification of the fully integrated formulation by assuming an adiabatic process with no heat transfer to or from the pneumatic cylinder. In this case $\eta = \gamma = \frac{c_p}{c_v} = 1.4$ for normal air. Implementing a self-adjustment shifts the operating range of the pneumatic piston, providing a stiffer system with greater stiffness gradient. The bigger the variation in gas spring stiffness through the operating range of the pneumatic piston, the more likely that the system will be unconditionally stable and suitable to fit a wider range of existing clutches with variable clutch characteristics.

8. Kongsberg AS success factors for obtaining efficient co-development of integrated system

The development of the Kongsberg Automotive ATrAct™ (Automated Transmission Actuation) was performed in close collaboration with our customer and development partner, with a mission to challenge the established AMT truck transmission market. High performance, durability and serviceability were key elements to make an impact. The co-

https://doi.org/10.51202/9783181023549 - Generiert durch IP 216.73.216.36, am 19.01.2026, 02:19:31. © Urheberrechtlich geschützter Inhalt. Ohne gesonderte Erlaubnis ist jede urheberrechtliche Nutzung untersagt, insbesondere die Nutzung des Inhalts im Zusammenhang mit, für oder in KI-Systemen, KI-Modellen oder Generativen Sprachmodellen.

development was completed in very limited time, with the development lasting only 3.5 years from the first conceptual discussions to the launch of serial production.
The intention with this paper is to describe success factors to obtain efficient co-development of integrated systems and explain the main features of the ATrAct™, as well as demonstrate how introducing a mechanical self-adjustment mechanism drastically improves clutch control agility.
Working in parallel with the development of the transmission and the actuation unit, both KA and our development partner front loaded the project with competent people. Key success factors to achieve the development in time included use of highly involved and experienced project managers, early sub-system testing, and selection of strategic suppliers based on feasibility tests to early kick off long lead time tools. Additionally, a local resident engineer from Kongsberg Automotive was assigned at our development partner in the US throughout the program to ensure flow in communication and efficient problem solving. Parallel validation phases further enabled quick design iterations and design corrections. Using the KA Knowledge Based Development – New Product Introduction process to guide the development and the DFMEA as an important tool to plan the development, the project early focused on high severity and RPN items and developed the Design Analysis Plan and Design Validation Plan accordingly. Mutual sharing of CAD-models multiple times per week and co-development of the requirement specification further secured alignment between the two teams leading to the successful SOP in late 2017. In particular, the time difference between the continents was beneficial as teams would quickly review work and provide feedback iteratively, utilizing more of the limited time available per day.

9. Summary

Kongsberg Automotive has effective developed and started successful series delivery of ATrAct™ transmission actuation. This system is prosperous implemented in a new AMT transmission and HD Truck Generation. With Kongsberg Automotive knowledge base in automotive pneumatics/ sensorics/ electrical actuators/ system integration and powertrain Kongsberg Automotive is focused for future market needs.
Especially for the new challenges and requests in accordance to the E-Mobility needs for future Commercial Vehicle solutions, Kongsberg Automotive is a professional development and series production partner for powertrain actuation components and systems.

References

[1] Hebert, Christian (2013), *ExAct™ Vibration Simulation Results*, Kongsberg Automotive
[2] Vestgård, Bård (2015), *Pneumatics 101*, Kongsberg Automotive
[3] Global Commercial Vehicle Forecast LMC 2018-Q4, with KA back ground information

https://doi.org/10.51202/9783181023549 - Generiert durch IP 216.73.216.36, am 19.01.2026, 02:19:31. © Urheberrechtlich geschützter Inhalt. Ohne gesonderte Erlaubnis ist jede urheberrechtliche Nutzung untersagt, insbesondere die Nutzung des Inhalts im Zusammenhang mit, für oder in KI-Systemen, KI-Modellen oder Generativen Sprachmodellen.

Simulation of load cycles for commercial vehicle drivelines based on statistical reasoning

M.Sc. **Morten Scherpelz**, Dipl.-Ing. **Jürgen Bernhardt**,
ZF Friedrichshafen AG, Friedrichshafen;
Dipl.-Ing. **Thorsten Weyh**, Dipl.-Math.oec. **Michael Lübke**
Fraunhofer ITWM, Kaiserslautern

Abstract

The assessment of the fatigue strength and service life of commercial vehicle drivelines in the new areas of application is a recurring challenge for product development departments. Especially for commercial vehicles, due to their high diversity, the boundary conditions (e.g. legislation and road conditions) and the target usage play an important part.

This paper explains the steps taken at ZF Friedrichshafen AG in order to solve this challenge. At first, the region of interest needs to be analyzed and a set of represented routes has to be found. To reduce the cost and timing issues, instead of classical, now virtual measurement campaigns are used to simulate the new load cycles. Afterwards, damage calculations are executed for the main components. Considering the estimated customer usage, load distributions will be created with the help of Monte-Carlo-Simulations. At the end, the results regarding to the new application can be compared to the original one and the boundary conditions for a product approval can be defined.

Introduction

One main characteristic of the commercial vehicle segment is the high variability from classical long haul trucks via a delivery and parcel service to specialized garbage trucks. Furthermore, considering passenger transport systems, this spectrum can expanded by coach, country and city buses. For the product release of commercial vehicle drivelines, this means that all the potential applications must be analyzed and evaluated. Taking international usage into account, additional challenges arise. It quickly becomes clear that the classical product approval with measurements reaches its limit because in Asia and South America the usage, tonnages and driveline combinations differ to those in Central Europe.

Therefore, computer-assisted virtual methods are needed to support the product approval for new applications bringing calculation of load cycles via simulations to a higher level. Statistically validated methods are essential to ensure that a broad spectrum can be tested.

https://doi.org/10.51202/9783181023549 - Generiert durch IP 216.73.216.36, am 19.01.2026, 02:19:31. © Urheberrechtlich geschützter Inhalt. Ohne gesonderte Erlaubnis ist jede urheberrechtliche Nutzung untersagt, insbesondere die Nutzung des Inhalts im Zusammenhang mit, für oder in KI-Systemen, KI-Modellen oder Generativen Sprachmodellen.

Product approval of commercial vehicle drivelines for new applications

For the product approval of commercial vehicle drivelines, detailed analysis of load cycles for a large number of different vehicle types and their application variance are essential. The classical way is to evaluate vehicle measurements of selected and application-representative reference routes. Afterwards, it is possible to derive a corresponding load cycle. If these reference routes are well known and validated, the required load cycles can also be determined by driveline simulations. Therefore, a virtual vehicle will be put on a route of a digital map, following the principles of driving physics.

Inputs are a speed profile and an altitude profile, both either from real or virtual measurements. The virtual vehicle moves forward depending on the available engine power. The current driving conditions (i.e. power requirement for the corresponding time step) depend on the total driving resistance, consisting of air, rolling, climbing and acceleration resistance (see Fig. 1). These need to be calculated in each time step. Using a company specific driveline simulation software provides detailed results by considering product specific properties, control algorithms and strategies, e.g. shifting strategy of the transmission (see [6]).

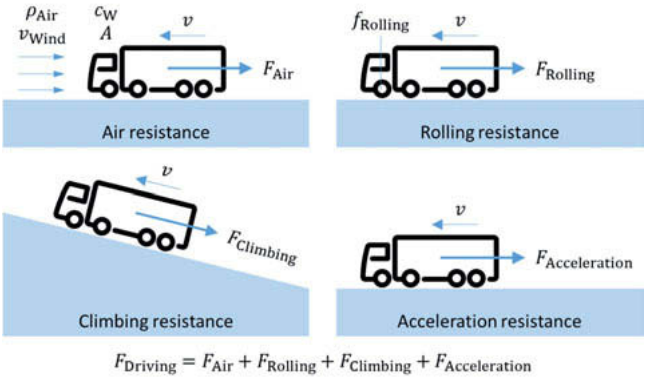


Fig. 1: Overview of general driving resistances

Similarly, stage of charge (SoC) and temperature cycles for electrified drivelines cannot yet be mapped with the software VMC (Virtual Measurement Campaign, Fraunhofer ITWM). From the results, the gear distribution and the load cycles for the main components can be derived. By considering the well-known damage mechanisms and material-specific SN-curves, damage calculations can be carried out for individual components from which a service life prognosis can be carried out.

https://doi.org/10.51202/9783181023549 - Generiert durch IP 216.73.216.36, am 19.01.2026, 02:19:31. © Urheberrechtlich geschützter Inhalt. Ohne gesonderte Erlaubnis ist jede urheberrechtliche Nutzung untersagt, insbesondere die Nutzung des Inhalts im Zusammenhang mit, für oder in KI-Systemen, KI-Modellen oder Generativen Sprachmodellen.

The challenge with new areas of application (e.g. long haul traffic in China) lies in their characteristic description: "How does my new application behave in comparison to my design cycle?" is a typical question that cannot be answered easily.
Under these conditions, it seems more appropriate to redefine the new application area by means of suitable reference routes. The load cycles required for the damage calculation can then be determined with reference to these new routes. A comparison with the original design cycle is possible and new service life forecasts can be derived. The workflow of this method, described in detail in the following chapters, is shown in Fig. 2.

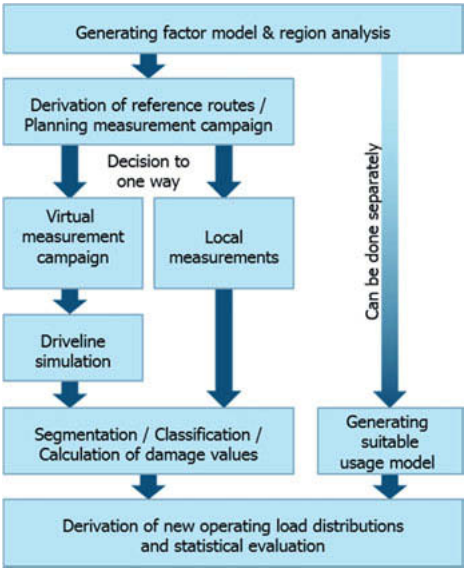


Fig. 2: Overview of the total method

The process starts with the definition of a suitable factor model of relevant influence factors and their levels. The factor model will be used to generate a suitable usage model for the target customer groups in the new market. Independent of the usage model creation, a regional analysis has to be carried out. Based on the results, a sub-region for the (virtual) measurement campaign can be chosen. Within this sub-region, a measurement campaign is planned using the VMC method “representative road selection” (RRS).
Depending on the actual situation, a virtual vehicle- and driveline simulation or real measurements may be more appropriate. In both cases, the results need to be cut into segments and

https://doi.org/10.51202/9783181023549 - Generiert durch IP 216.73.216.36, am 19.01.2026, 02:19:31. © Urheberrechtlich geschützter Inhalt. Ohne gesonderte Erlaubnis ist jede urheberrechtliche Nutzung untersagt, insbesondere die Nutzung des Inhalts im Zusammenhang mit, für oder in KI-Systemen, KI-Modellen oder Generativen Sprachmodellen.

classified with respect to the factor model. For each segment and measured channel corresponding damage values are calculated. This applies to load cycles coming from local measurements as well as to corresponding driveline simulations. The measurement data and the customer usage models will be combined via Monte-Carlo-Simulation to extrapolate loads to derive design targets and reference customers. This can be done with the software U·Sim (Usage-Simulation, Fraunhofer ITWM).

Basic concepts of geo-referenced analysis and usage simulation

The classical way to test new product developments to gain information about the variability of field loads, OEMs perform (real) measurement campaigns with instrumented vehicles. To measure realistic field loads, the vehicle should operate under ordinary field conditions. Since the measurement equipment of a prototype is a cost and time intense project, which requires an already existing prototype, the measured load data channels are only valid for this specific vehicle. A real measurement campaign is not suitable in every case. On the other side, a lot of information about the environment e.g. the road network, topographic and climate data can be obtained from various other data sources. To combine the best things of both worlds Fraunhofer ITWM has developed the concept of the Virtual Measurement Campaign (VMC) [3].

The fundamental layers of the VMC database is the worldwide available road network, a map of all roads and connections worldwide, supplemented by legislation data such as driving rules and speed limits as well as traffic lights, crossings etc. (see Fig. 3).

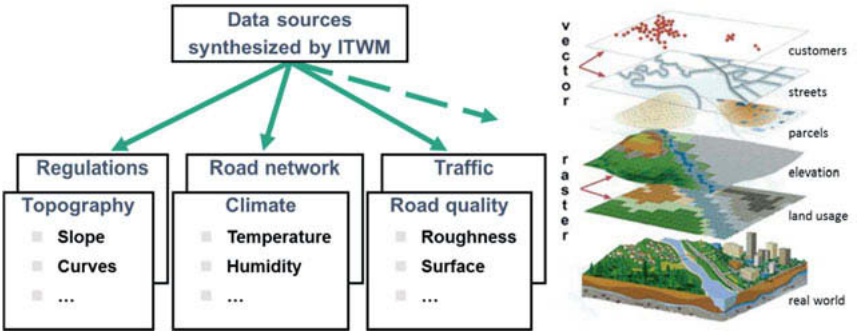


Fig. 3: Data sources in VMC (Virtual Measurement Campaign, Fraunhofer ITWM)

Additionally, land-use information for instance residential, industrial and agricultural areas are given. This part of the database is provided by the non-profit organization Open Street Map

https://doi.org/10.51202/9783181023549 - Generiert durch IP 216.73.216.36, am 19.01.2026, 02:19:31. © Urheberrechtlich geschützter Inhalt. Ohne gesonderte Erlaubnis ist jede urheberrechtliche Nutzung untersagt, insbesondere die Nutzung des Inhalts im Zusammenhang mit, für oder in KI-Systemen, KI-Modellen oder Generativen Sprachmodellen.

Foundation (see http://wiki.openstreetmap.org), which is permanently growing and has reached a very good quality level.

For all analysis, the entire road network of a region is split up into VMC road segments. A VMC road segment contains the road geometry as well as a unique road type and a unique identifier or name. In addition, the land-use information is evaluated to distinguish between urban and rural road parts. Since geo-referenced properties such as the amount of slopes and curves may change along a road, VMC will split the roads into shorter segments depending on the road type (typically 10 km on motorways, 5 km on country roads and 2 km in cities). All analyzing methods can also be applied on imported routes (e.g. reference or specific customer routes) and compared with a region of interest to highlight similarities or differences.

Besides the statistical analysis of the segments of regions and routes, there are also driver, traffic, and vehicle models available in order to simulate speed profiles of a vehicle traveling along a route under certain traffic conditions with a specified driver behavior [9]. To simulate a speed profile, the properties of the vehicle, driver and the traffic models have to be combined with the topography of the route and legislation restrictions (e.g. speed limits). Regarding the vehicle, a set of parameters such as engine and braking power, mass, aerodynamic resistance, rolling resistance, maximum lateral acceleration etc. have to be included. The driver's influence is modeled by thresholds for longitudinal and lateral accelerations including stochastic variations as well as on tolerance factors for following the legal speed limits. Some recent enhancements deal with the introduction of more detailed driveline parameters such as transmission ratios and engine maps, which were used in the project, but will not be described in detail.

Usage Simulation (U·Sim), an additional software developed by Fraunhofer ITWM, is used to model the usage variability of a large number of different customers and to determine reference loads for these customers. The customers are generated according to usage models by Monte-Carlo-Simulation and are represented by real measurement data. This results in empirical distributions for each measurement channel for all simulated customers. The quantile customers (e.g. 95% customer), in combination with safety factors and special maneuvers (e.g. curb crossings, emergency braking), define a design target that is explicitly linked to conditions in the field.

The U·Sim approach is to separate the measurement of different operating states ("What can happen?") and the combination of these measurements to virtual customers based on the usage model ("How often does something happen?"). Fig. 4 gives a process overview. Input data for the customer simulation are measurements in defined operational states for which a scalar value in each measurement channel (e.g. pseudo-damage value) is available. In addition, a

https://doi.org/10.51202/9783181023549 - Generiert durch IP 216.73.216.36, am 19.01.2026, 02:19:31. © Urheberrechtlich geschützter Inhalt. Ohne gesonderte Erlaubnis ist jede urheberrechtliche Nutzung untersagt, insbesondere die Nutzung des Inhalts im Zusammenhang mit, für oder in KI-Systemen, KI-Modellen oder Generativen Sprachmodellen.

usage model for the customers is specified. This includes the distribution of operational states, as well as the variability within each state. For further details, see [1] and [2].

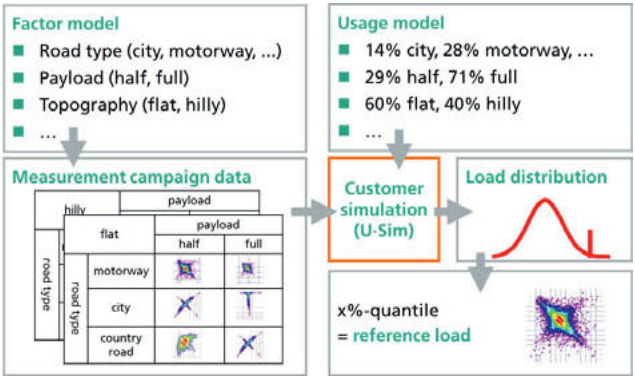


Fig. 4: Process overview of U·Sim (Usage Simulation, Fraunhofer ITWM)

Creating a factor model and geo-referenced analysis for new markets

At first, all relevant operation conditions for the vehicle and its application at hand needs to be defined. This can be done based on factor models by listing the relevant influence quantities and their levels, e.g. road type (motorway, rural road, city road), payload (full, empty) or topography factors like hilliness (hilly, flat), curviness (curvy, strait) or total variation of altitude (low, high) of a specific road (see Fig. 5).

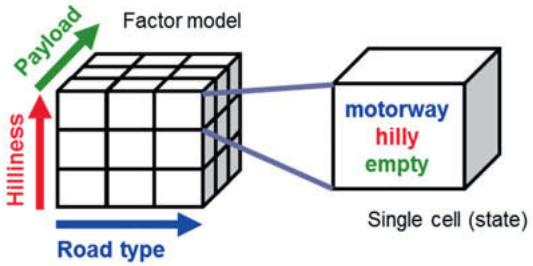


Fig. 5: Scheme of the factor model

It is necessary to classify all road segments of a given measurement campaign with respect to all defined factors. Additionally it is important to know the distribution of the operational states

https://doi.org/10.51202/9783181023549 - Generiert durch IP 216.73.216.36, am 19.01.2026, 02:19:31. © Urheberrechtlich geschützter Inhalt. Ohne gesonderte Erlaubnis ist jede urheberrechtliche Nutzung untersagt, insbesondere die Nutzung des Inhalts im Zusammenhang mit, für oder in KI-Systemen, KI-Modellen oder Generativen Sprachmodellen.

in the new market and the customer groups of interest. The later aspect is addressed by usage modeling (see next section).

If particularly large regions have to be analyzed, it is advisable to reduce the size of the target region, e.g. by choosing only one province of China. This sub-region needs to be as representative as possible. Therefor all provinces of china are analyzed separately and compared to China as a whole. For each factor and its levels, the relative deviations of the factor-level distribution of the province compared to the complete region China are aggregated.

First, in Fig. 6 the relative size of the single region is listed. While the five factor deviations should be as small as possible, the relative size of the province should not be too small. The green color signals a particularly good and the red color a worse correlation with total target region. The last column shows the average deviation of all five factors between the province and China.

As a result, “Province 25” shows the best correlation with a total deviation of only 2.7% and a good relative size. All examples in the next sections will refer to this region.

The next step is an in-depth analysis of the selected “Province 25” w.r.t. customer behavior and the derivation of a usage model for the application “long haul truck in China”.

Usage modeling of a customer group in a new target market

The decisive question that a development department is confronted with on a daily basis is the question of customer usage. If there is little or no information on customer usage available, meaningful assumptions must be made which ideally are close enough to actual customer behavior. However, it would be desirable to have a methodology that could provide statistically verified models for different customer types.

Fraunhofer ITWM has been conducting intensive research in this area for several years and has created the basis for modelling customer usage within the framework of various development and research projects (see [4] and [5]). The goal of the usage simulation lies in the generation of a huge amount of representative customer routes for long haul truck users in China. The routes will be generated automatically on basis of a small questionnaire, which describes the behavior of this specific user group. In this paper, the focus will lie on the usage model for long haul trucks. Nevertheless, models are also available for several other customer groups (e.g. delivery service, craftsman, sales and distribution).

https://doi.org/10.51202/9783181023549 - Generiert durch IP 216.73.216.36, am 19.01.2026, 02:19:31. © Urheberrechtlich geschützter Inhalt. Ohne gesonderte Erlaubnis ist jede urheberrechtliche Nutzung untersagt, insbesondere die Nutzung des Inhalts im Zusammenhang mit, für oder in KI-Systemen, KI-Modellen oder Generativen Sprachmodellen.

Province	relative size	road type deviation	hilliness deviation	curviness deviation	uad* deviation	dad** deviation	total deviation
Province 1	0.76	1.67	2.15	10.25	8.87	7.91	6.17
Province 2	0.90	1.99	9.67	16.73	11.43	12.93	10.55
Province 3	0.93	2.73	36.36	17.91	35.87	35.92	25.76
Province 4	1.05	3.34	33.68	14.71	27.81	27.65	21.44
Province 5	1.21	2.76	19.90	1.47	12.61	12.96	9.94
Province 6	1.79	4.36	16.08	4.54	9.90	10.56	9.09
Province 7	1.84	3.15	45.89	32.02	44.51	44.51	34.02
Province 8	2.14	2.95	4.00	10.47	8.19	9.41	7.00
Province 9	2.29	3.63	49.38	33.49	47.87	47.43	36.36
Province 10	2.47	2.86	26.32	18.91	25.64	26.02	19.95
Province 11	2.55	10.19	24.28	24.20	19.58	17.03	19.06
Province 12	2.68	3.18	20.62	15.97	24.45	24.03	17.65
Province 13	2.81	3.86	13.56	0.33	13.23	12.93	8.78
Province 14	2.85	4.12	13.39	5.76	8.19	8.34	7.96
Province 15	3.00	3.07	5.42	2.53	5.35	5.76	4.43
Province 16	3.01	2.03	17.18	19.74	23.97	23.56	17.30
Province 17	3.11	2.61	13.30	11.34	10.66	10.74	9.73
Province 18	3.15	2.85	6.10	13.34	10.30	10.75	8.67
Province 19	3.27	3.21	25.96	15.34	26.53	26.47	19.50
Province 20	3.55	2.79	18.20	15.30	16.37	16.07	13.75
Province 21	3.83	2.62	20.74	14.60	21.55	20.58	16.02
Province 22	3.85	1.23	23.10	11.83	21.98	22.05	16.04
Province 23	3.98	2.65	41.29	39.12	39.55	39.60	32.44
Province 24	4.13	2.89	23.79	17.92	25.39	24.76	18.95
Province 25	4.80	1.79	0.10	6.51	2.76	2.44	2.72
Province 26	4.90	1.21	28.90	25.81	29.09	29.06	22.81
Province 27	5.28	4.35	21.45	22.25	20.64	20.50	17.84
Province 28	5.46	2.02	17.12	24.15	19.66	18.73	16.34
Province 29	5.96	2.07	6.70	6.05	16.93	16.88	9.73
Province 30	6.44	2.15	36.11	14.73	31.22	31.02	23.05
Province 31	6.52	3.19	23.52	21.13	25.49	25.30	19.73

Fig. 6: Comparison of the single provinces with whole China in %
(*uad: upward altitude difference, **dad: downward altitude difference, see next section for a description of uad and dad)

To generate the customer usage model, the start and end position of the route have to be defined. Typically, the route will start on a company site, can contain several stopovers and will end on the site of the customer. In a first step, the customer usage algorithm will pick a location (GPS coordinate) on the digital map as starting point. Regarding the stored customer model a first via point will be selected within a circle in a certain airline distance. This location is also a part of a company side. Bit by bit more GPS locations will added to the route, depending on the number of selected via destinations. The final ending point of the route will complete the route. Based on several investigations, two fundamental route classes can be identified: a star and a circuit-based shape (see Fig. 7). Routes with several stopovers are created using a “travelling sales man algorithm”.

https://doi.org/10.51202/9783181023549 - Generiert durch IP 216.73.216.36, am 19.01.2026, 02:19:31. © Urheberrechtlich geschützter Inhalt. Ohne gesonderte Erlaubnis ist jede urheberrechtliche Nutzung untersagt, insbesondere die Nutzung des Inhalts im Zusammenhang mit, für oder in KI-Systemen, KI-Modellen oder Generativen Sprachmodellen.

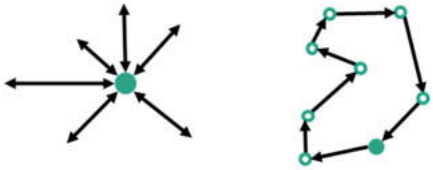


Fig. 7: The basic driving patterns (left: star shaped, right: circuit shaped)

Since the creation process is highly automated, several tens of thousands of customer routes can be generated. All routes will be analyzed using the same VMC methods as those used for the region. The basic customer usage result will be a table, filled with percentages for road types, hilliness and curviness values. These numbers will be used as input for the following U·Sim process (extrapolation of measured data).

Planning a representative virtual measurement campaign

Planning a virtual measurement campaign in a given region is not exactly the same task as planning a real local measurement campaign. The selected routes need not be close to each other. One can ignore traffic and other constraints that make an actual measurement difficult or impossible. A virtual measurement campaign can purely focus on covering all relevant operational states, i.e. considering all factor-level-combinations in a sufficient manner. The main goal is to find representative roads (or road segments) within a given region with some dedicated properties needed for the factor model.

In this paper, the focus is on driveline applications. Therefor uphill and downhill segments are important as well as the road type. The VMC measures “Upward Altitude Difference” and “Downward Altitude Difference” are well suited to describe segments with driveline applications (see [8]).

The problem of a representative road selection (RRS) can be solved for each road type individually. For every road out of one road type in the given region, one has to decide whether it is in the selection or not. This can be modeled as a linear integer optimization problem. The score values of the measure are classified into a certain amount of classes (i.e. 20) and for each class a minimum number of segments is defined that need to be in the selection. This parameter controls how extensive the selection will be.

The solution of that optimization problem is a subset of roads of the entire region with segments covering all possible score values of the measure for the given road type. This process can be

https://doi.org/10.51202/9783181023549 - Generiert durch IP 216.73.216.36, am 19.01.2026, 02:19:31. © Urheberrechtlich geschützter Inhalt. Ohne gesonderte Erlaubnis ist jede urheberrechtliche Nutzung untersagt, insbesondere die Nutzung des Inhalts im Zusammenhang mit, für oder in KI-Systemen, KI-Modellen oder Generativen Sprachmodellen.

repeated for each road type and if required for further measures. The result is a minimal set of routes covering all operational states of interest.

Fig. 8 shows a possible solution for the region “Province 25”, road type “motorway” and the measure “Upward Altitude Difference” (UAD). For this example, 21 classes for the measure “UAD” were defined the minimum number of required segments was one for the first 20 classes. The last class is reserved for implausible values and hence should not be used. The solution consists of four roads with a total length of 265 km. These 265 km of motorway roads were chosen out of approximately 10.000 km of motorway roads in the region “Province 25”.

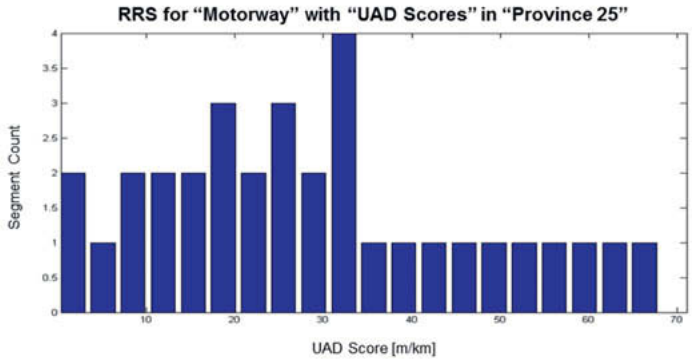


Fig. 8: RRS (representative road selection) classing for road type motorway and upward altitude difference in “Province 25”

Some classes are overachieved. This is due to the fact that a road is always completely selected if it contains a desired segment. By doing so, longer roads are preferred, which has some advantages for the following virtual measurement on those roads.

Virtual measurement and geo-referenced load data analysis

A key feature of VMC is the speed profile generation. Inputs are a driver model, a vehicle model, traffic data and the digital map data itself.

The driver model includes some basic parameters like maximal lateral and longitudinal accelerations the driver will accept, the degree of willingness to ignore legal speed limits and parameters to create a stochastic behavior for braking and acceleration events.

The vehicle model consists of standard parameters like mass, air and rolling resistance coefficients, etc. Additional advanced driveline parameters like transmission ratios, a consumption

https://doi.org/10.51202/9783181023549 - Generiert durch IP 216.73.216.36, am 19.01.2026, 02:19:31. © Urheberrechtlich geschützter Inhalt. Ohne gesonderte Erlaubnis ist jede urheberrechtliche Nutzung untersagt, insbesondere die Nutzung des Inhalts im Zusammenhang mit, für oder in KI-Systemen, KI-Modellen oder Generativen Sprachmodellen.

matrix, etc. are important if signals like engine speed, engine torque or gear should be computed.

The traffic model is a stochastic model using varying average traffic densities and a safe distance rule. Finally, the digital road network is used to get traffic lights, traffic regulations, and the road geometry, including slopes and curvature.

All this data is combined in VMC and speed profiles are computed using optimal control algorithms. The result is a set of simulated signals such as lateral and longitudinal forces and accelerations, driving resistances, engine speed, torque and gear, speed, GPS position, altitude, slope, stop events etc. (see [9] for further details).

These simulation results will be used as input for the geo-referenced load data analysis (GeoLDA) with VMC GeoLDA. Alternatively, one can use real measurement data as input for VMC GeoLDA as long as GPS positions are available along with the other channels.

Using the GPS position the data is projected via map matching to the digital map. The digital road will split into shorter segments depending on length and road type (see Fig. 9). These segments are classified w.r.t. relevant topographical factors (e.g. curviness, upward altitude difference etc.).

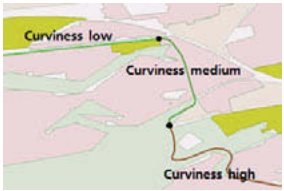


Fig. 9: Segmented road with three segments classified w.r.t. factor curviness

By classifying each segment, it is assigned to its operational state of the factor model. Cutting a measurement into segments provides also sliced time series data. For all relevant measurement channels, one can compute pseudo-damage values for each segment. This data will be the second main input for usage simulation besides the already generated usage model.

Customer simulation and reference loads

The last step to new reference loads is the customer simulation. Input for the Monte-Carlo-Simulation of many virtual customers are all categorized measurement data and the usage models for each customer group. Within the simulation, each customer has an individual vehicle usage, i.e. the distribution of operational states is randomized according to the usage

https://doi.org/10.51202/9783181023549 - Generiert durch IP 216.73.216.36, am 19.01.2026, 02:19:31. © Urheberrechtlich geschützter Inhalt. Ohne gesonderte Erlaubnis ist jede urheberrechtliche Nutzung untersagt, insbesondere die Nutzung des Inhalts im Zusammenhang mit, für oder in KI-Systemen, KI-Modellen oder Generativen Sprachmodellen.

model. Within a specific operational state, each customer gets randomly assigned measurement data up to a certain mileage limit modeled via a parameter called variability. This parameter controls if a customer uses a wide range of different roads or operates more locally.
It is important for the complete process that the measurement database is rich enough, i.e. each operational state is covered by a certain amount of measurements. The actual required amount depends largely on the variance of damage values in this operational state. This request can be analyzed in detail with ANOVA (analysis of variance) methods (see [7]). Fig. 10 shows an example factor model with three factors and a typical database size.

	Factor	Level	Number of measurements	Mileage
1	Roadtype	City Expressway	76	114.269
2		Country Expressway	93	382.53
3		City Major	73	114.502
4		City Minor	183	259.825
5		Country Minor	113	503.364
6		Country Major	105	480.536
7		Motorway	57	544.283
8	DownwardAltitudeDifference	low	471	1453.73
9		high	229	945.582
10	UpwardAltitudeDifference	low	494	1623.34
11		high	206	775.971

Fig. 10: Example for a measurement data set for usage simulation with three factors

The main result of the customer simulation is a large amount of virtual customers, e.g. 50.000. Each customer is represented by a set of measurements with its collection of time signals, Rainflow matrices or damage values. Given the damage values, the set of measurements and the desired target lifetime of a vehicle or component, one can compute the total damage value of each measured channel for each virtual customer. The result is a non-parametric empirical load distribution for each measured channel (see Fig. 11).
Now, by picking any high quantile in a load distribution (e.g. 90%, 95% or 99%), one will receive a specific simulated customer with the exact quantile damage value in that channel including time series data, Rainflow matrices etc. A quantile customer matching the 95% damage quantile for one channel (e.g. longitudinal acceleration) does not necessarily match the 95% damage quantile in another channel (e.g. lateral acceleration).

https://doi.org/10.51202/9783181023549 - Generiert durch IP 216.73.216.36, am 19.01.2026, 02:19:31. © Urheberrechtlich geschützter Inhalt. Ohne gesonderte Erlaubnis ist jede urheberrechtliche Nutzung untersagt, insbesondere die Nutzung des Inhalts im Zusammenhang mit, für oder in KI-Systemen, KI-Modellen oder Generativen Sprachmodellen.

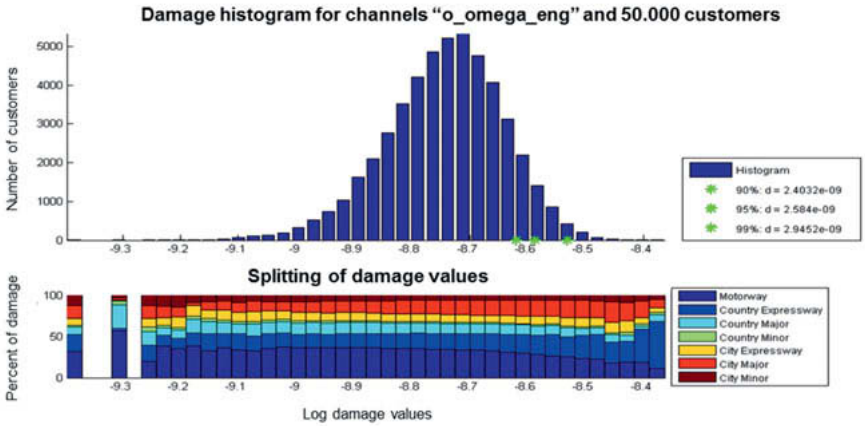


Fig. 11: Damage histogram for channel "Engine Speed" including damage contribution w.r.t. road type (data anonymized)

Fig. 12 shows an artificial example with four quantile-customers w.r.t. four channels and their corresponding damage values in each channel. Note that the 100% level on the y-axis marks the 95% quantile value (the target). The figure shows that the virtual 95% customer for longitudinal acceleration (channel "o_a") is only at approx. 30% of the 95% level for the lateral acceleration (channel "o_a_y").

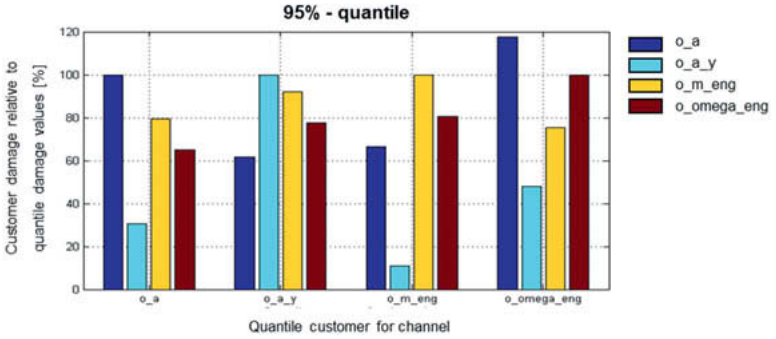


Fig. 12: 95% quantile customers for four different channels without considering the other three channels ("o_a", "o_a_y", "o_m_eng" and "o_omega_eng" denote longitudinal acceleration, lateral acceleration, engine torque and engine speed resp.)

https://doi.org/10.51202/9783181023549 - Generiert durch IP 216.73.216.36, am 19.01.2026, 02:19:31. © Urheberrechtlich geschützter Inhalt. Ohne gesonderte Erlaubnis ist jede urheberrechtliche Nutzung untersagt, insbesondere die Nutzung des Inhalts im Zusammenhang mit, für oder in KI-Systemen, KI-Modellen oder Generativen Sprachmodellen.

In typical applications, it is required to find one customer, i.e. one mix of the measurement data that matches a certain quantile in as many channels as possible. Even in the small example with four channels and four possible customers, it is not obvious which one to choose.
This problem can be solved by setting up and solving a linear optimization problem for each potential quantile customer. The solution is a linear combination of many simulated customers (e.g. 20 or even 50) ensuring that the original quantile damage value is preserved while the other channels are improved. The solution of four optimization problems is shown in Fig. 13. In this example, the first customer-mix for channel “o_a” would be a very good candidate.

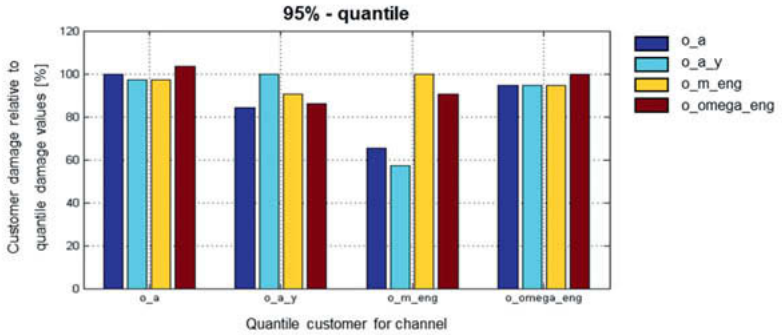


Fig. 13: 95% quantile customers for four different channels with optimized results for the other three channels

The selected reference customer serves as design load for further development steps, e.g. the assessment of components on test rigs or vehicles on proving grounds. Since it consist of a mixture of measured data segments, one can compute Rainflow matrices or even refer to the underlying time signals for spectral analysis or other specific evaluations.

https://doi.org/10.51202/9783181023549 - Generiert durch IP 216.73.216.36, am 19.01.2026, 02:19:31. © Urheberrechtlich geschützter Inhalt. Ohne gesonderte Erlaubnis ist jede urheberrechtliche Nutzung untersagt, insbesondere die Nutzung des Inhalts im Zusammenhang mit, für oder in KI-Systemen, KI-Modellen oder Generativen Sprachmodellen.

Conclusion and outlook

The method used in this paper shows the possibility to use statistically secured reasoning for the product approval. Using the example of the new application “long haul traffic in China”, it was shown how to systematically get a customer specific load distribution starting from a white paper. In this case, the definition of the reference routes plays a decisive role.

One main benefit of this method is the unnecessity of real hardware in the form of products or prototypes for real local measurements. That is why it can be used even in early stages of the product development. Nevertheless, all simulation methods need to be calibrated with real measurements periodically. This guarantees a high simulation quality and an increasing explanatory power of the results.

This method allows defining boundary conditions with which a product approval for new applications is possible. In case the new application has higher loads than the original design cycle, restrictions for mileage or warranty claims can be derived. Similarly, customer or usage specific maintenance intervals can be developed.

Furthermore, this method is not only limited to load cycles. Because the Monte-Carlo-Simulation can analyze any integrable quantity, range statements for electrified drivelines can be handled as well. Considering usage models, it is possible to analyze customer specific range distributions. Therefore, the results will support the development of suitable concepts for electro mobility significantly.

https://doi.org/10.51202/9783181023549 - Generiert durch IP 216.73.216.36, am 19.01.2026, 02:19:31. © Urheberrechtlich geschützter Inhalt. Ohne gesonderte Erlaubnis ist jede urheberrechtliche Nutzung untersagt, insbesondere die Nutzung des Inhalts im Zusammenhang mit, für oder in KI-Systemen, KI-Modellen oder Generativen Sprachmodellen.

References

[1] Dreßler, K., Speckert, M., Müller, R., Weber, C.: Customer Loads Correlation in Truck Engineering. In: FISITA World Automotive Congress, vol. 3 Testing & Simulation. Springer Automotive Media (2008).

[2] Eckstein, C.: Ermittlung repräsentativer Lastkollektive zur Betriebsfestigkeit von Ackerschleppern, Dissertation TU Kaiserslautern, (2017).

[3] Speckert, M., Dreßler, K., Ruf, N., Halfmann, T., Polanski, S.: The Virtual Measurement Campaign (VMC) concept: A Methodology for Geo-referenced Description and Evaluation of Environmental Conditions for Vehicle Loads and Energy Efficiency. In: Berns, K., Schindler, C., Dreßler, K., Jörg, B., Kalmar, R., Zolynski, G. (eds.) 3rd Commercial Vehicle Technology Symposium 2014, pp. 88–98. Shaker, Aachen (2014).

[4] Weyh, T.; Speckert, M.; Opalinski, A.; Wagner, M.: Planning a measurement campaign in Eastern Europe using Fraunhofer VMC („Virtual Measurement Campaign“). In VDI-Tagung „Nutzfahrzeuge 2015 - Truck, Bus, Van, Trailer “, Eindhoven, VDI-Berichte Nr. 2247, VDI-Verlag GmbH Düsseldorf, (2015).

[5] Biedinger, C., Weyh, T., Opalinski, A., Wagner, M.: Simulation of customer-specific vehicle usage. In: Berns, K., Dreßler, K., Fleischmann, P., Ilsen, R., Jörg, B., Kalmar, R., Nagel, T., Schindler, C. Stephan, N. (eds.) 4th Commercial Vehicle Technology Symposium 2016, pp. 523–532. Shaker, Aachen (2016).

[6] Scherpelz, M.; Plieske, M.; Gottwald, A.; Halfmann, T.; Weyh, T.: Use of virtual measurement campaigns in transmission development, Proceedings of the 5th Commercial Vehicle Technology Symposium (CVT 2018), Springer Vieweg, 129-139, (2018).

[7] Speckert, M.; Dreßler, K.; Lübke, M.; Halfmann, T.: Automatisierte und um GEO-Daten angereicherte Auswertung von Messdaten zur Herleitung von Beanspruchungsverteilungen, DVM Bericht 143, 165-180, (2016).

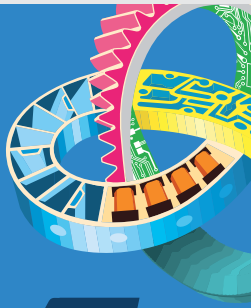
[8] Speckert, M.; Lübke, M.; Wagner, B.; Anstötz, T.; Haupt, C.: Representative Road Selection and Route Planning for Commercial Vehicle Development, Proceedings of the 5th Commercial Vehicle Technology Symposium (CVT 2018), Springer Vieweg, 117-128, (2018).

[9] Sandmann, K.; Leyendecker, T.; Burger, M.; Speckert, M.: Ableitung von feldrelevanten Lastkollektiven mittels Stochastischer Verkehrssimulation, DVM Bericht 145 - Effiziente Auslegung und Absicherung in der Betriebsfestigkeit, DVM, Berlin, (2018).

https://doi.org/10.51202/9783181023549 - Generiert durch IP 216.73.216.36, am 19.01.2026, 02:19:31. © Urheberrechtlich geschützter Inhalt. Ohne gesonderte Erlaubnis ist jede urheberrechtliche Nutzung untersagt, insbesondere die Nutzung des Inhalts im Zusammenhang mit, für oder in KI-Systemen, KI-Modellen oder Generativen Sprachmodellen.

https://doi.org/10.51202/9783161023549 - Generiert durch IP 216.73.216.36, am 19.01.2026, 02:19:31. © Urheberrechtlich geschützter Inhalt. Ohne gesonderte Erlaubnis ist jede urheberrechtliche Nutzung untersagt, insbesondere die Nutzung des Inhalts im Zusammenhang mit, für oder in KI-Systemen, KI-Modellen oder Generativen Sprachmodellen.

VDI Wissensforum



6th International VDI-Conference
Drivetrain Solutions for Commercial Vehicles

ISBN 978-3-18-092354-3

https://doi.org/10.51202/9783181023549 - Generiert durch IP 216.73.216.36, am 19.01.2026, 02:19:31. © Urheberrechtlich geschützter Inhalt. Ohne gesonderte Erlaubnis ist jede urheberrechtliche Nutzung untersagt, insbesondere die Nutzung des Inhalts im Zusammenhang mit, für oder in KI-Systemen, KI-Modellen oder Generativen Sprachmodellen.